NUCLEAR STRUCTURE

DUBNA SYMPOSIUM 1968

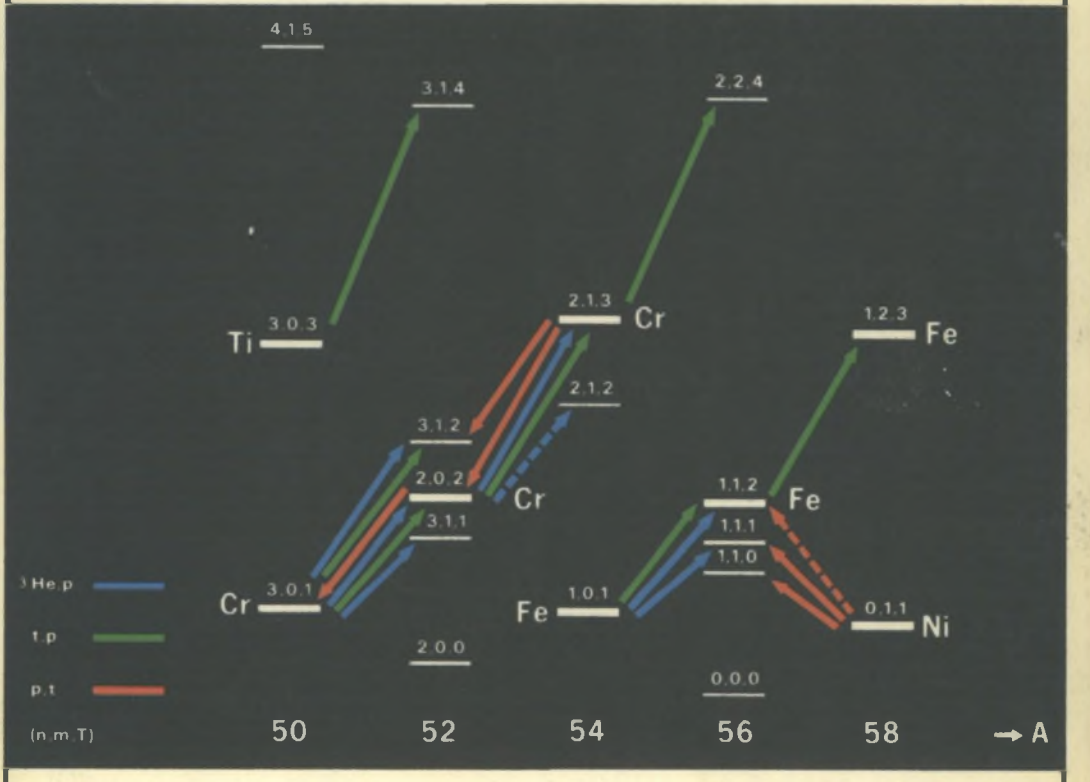

INVITED PAPERS
from the International Symposium organized by the Joint Institute for Nuclear Research, Dubna, 4-11 July, 1968
SUPPORTED BY IUPAP AND IAEA

INTERNATIONAL ATOMIC ENERGY AGENCY, VIENNA, 1968

NUCLEAR STRUCTURE:
DUBNA SYMPOSIUM 1968

PROCEEDINGS SERIES

NUCLEAR STRUCTURE

DUBNA SYMPOSIUM 1968

INVITED PAPERS FROM
THE INTERNATIONAL SYMPOSIUM ON NUCLEAR STRUCTURE
ORGANIZED BY THE
JOINT INSTITUTE FOR NUCLEAR RESEARCH, DUBNA,
AND HELD IN DUBNA, 4-11 JULY 1968

Supported by:
The International Union of Pure and Applied Physics
and The International Atomic Energy Agency

INTERNATIONAL ATOMIC ENERGY AGENCY
VIENNA, 1968

NUCLEAR STRUCTURE: DUBNA SYMPOSIUM 1968
(Proceedings Series)

ABSTRACT. Invited papers of a Symposium organized by the Joint Institute for Nuclear Research, Dubna, supported by IUPAP and IAEA, and held in Dubna from 4 to 11 July 1968. The meeting was attended by about 450 scientists from 30 countries. The volume contains the invited papers, all by distinguished scientists, and the discussions and short contributions that followed the presentation of these papers.

Contents: I. Nuclear structure at low excitations (15 papers); II. Nuclear structure at high excitations (6 papers): III. Open problems in nuclear physics (3 papers); IV. Equilibrium deformations (6 papers); V. General properties of nuclei (6 papers); VI. Closing remarks; List of contributions; List of seminar papers; List of participants; Author index.

All papers, discussions and short contributions are in English; the abstracts are in English and Russian, which were the working languages of the Symposium.

(642 pp., 16 × 24 cm, paper-bound, 250 figures; 1968) Price: US $15.00; £6.5.0

The diagram on the cover shows the 0^+ excited states in the pairing scheme of Bohr, and the corresponding two-nucleon transfer reactions in the mass region A = 50 - 58. For purposes of illustration, the energies of the states are not shown rigorously to scale.

NUCLEAR STRUCTURE:
DUBNA SYMPOSIUM 1968
IAEA, VIENNA, 1968
STI/PUB/189

Printed by the IAEA in Austria
December 1968

FOREWORD

The International Symposium on Nuclear Structure, held in Dubna from 4 to 11 July 1968, was organized by the Joint Institute for Nuclear Research, Dubna, and supported by the International Union of Pure and Applied Physics and by the International Atomic Energy Agency.

About 450 scientists from 30 countries participated. This alone is an indication of the great interest of scientists in the problems of nuclear structure.

The present volume contains the invited papers, all by distinguished authors, and the discussions that followed the presentation of these papers. Some of the discussions contain short contributions included because of their relevance. The two working languages of the symposium were Russian and English. All the abstracts are printed in both languages, but the papers, discussions and short contributions are entirely in English.

The symposium was preceded by an IAEA Panel on the Future of Nuclear Structure Studies. This panel discussed not only the principal problems of nuclear physics but also the possibilities of small and developing countries participating in research on nuclear structure. The main results of the panel meeting were reported to the symposium by Professors V.F. Weisskopf, G.N. Flerov and D.H. Wilkinson, and these talks formed the first session of the symposium. The Chairman of this session was Professor N.N. Bogolyubov, Director of the Joint Institute for Nuclear Research. However, as the proceedings of the IAEA Panel are being published in the IAEA Panel Proceedings Series as a separate book under the title "The Future of Nuclear Structure Studies", the material of the first session of the symposium is not included in the present volume.

Approximately 200 contributions containing results of original investigations, each about 400 words long, were also presented to the symposium. These were collected into a small book, Dubna publication D-3893, for the participants before the meeting; a list of the titles is included here. A number of seminars, devoted to the detailed discussion of special problems, were also held during the period of the symposium; a list of these presentations is also given in the present volume.

These proceedings contain much new scientific information and instructive reviews of the latest work. It is hoped that they will contribute greatly to a better understanding of the structure of atomic nuclei.

CONTENTS

I. NUCLEAR STRUCTURE AT LOW EXCITATIONS

II. NUCLEAR STRUCTURE AT HIGH EXCITATIONS

III. OPEN PROBLEMS IN NUCLEAR PHYSICS

IV. EQUILIBRIUM DEFORMATIONS

V. GENERAL PROPERTIES OF NUCLEI

VI. CLOSING REMARKS

I

NUCLEAR STRUCTURE AT LOW EXCITATIONS

Chairmen	Secretaries
H. NIEWODNICZAŃSKI	V.G. CHUMIN
J. SCHINTLMEISTER	R. ARLT
R.F. BELL	V.K. LUKYANOV
B.S. DZHELEPOV	M. ADAM
N. SODNOM	V.A. KARNAUKHOV
A.S. DAVYDOV	B.N. KALINKIN
Zh. ZHELEV	I.Z. PETKOV
G. RASMUSSEN	S. REVAI

ONE-PARTICLE MOTION IN SPHERICAL NUCLEI

B.L. COHEN
UNIVERSITY OF PITTSBURGH,
PITTSBURGH, PA., UNITED STATES OF AMERICA

Abstract — Аннотация

ONE-PARTICLE MOTION IN SPHERICAL NUCLEI. *New information on locations of single-particle states as determined by single-nucleon transfer reactions and elastic proton scattering through isobaric analogue states is summarized. The situation with neutron single particle states is reasonably satisfactory although there is considerable uncertainty about the particle states in N = 83 nuclei. Information on proton single-particle states has accumulated rapidly recently. The single-particle level structure is very similar for neutrons and protons in nuclei of the same mass number A, more so than for either one at very different A. The principal A-dependence is that high-j states move downward rapidly relative to low-j states with increasing A, for well understood reasons. Information on imperfect major shell closure at "magic numbers" is summarized, and it is pointed out that it is not unexpected. The only really good closed shell nuclei are those near* ^{208}Pb. *The significance of deep-lying hole states found in (e, e' p) reactions is mentioned. Information on neutron single quasiparticle states in the 28-50 and 50-82 shells is reviewed. Experiments are now available on non-single-closed shell nuclei in the latter region; fragmentation of single quasiparticle states is somewhat larger than heretofore encountered, but there is generally one nuclear state that contains a large fraction of their strength. An important difficulty is encountered in the* $g_{7/2}$ *and* $h_{11/2}$ *states where results from stripping and pick-up reactions differ greatly in nuclei between Mo and In. Plots of the "degree of emptiness",* U_j^2 *, and of single quasiparticle energies,* E_j*, are given for all single-particle states for nuclei with N = 28-82, and comparisons are made with pairing theory predictions. In general, the agreement is good although there are several difficulties that are discussed.*

ОДНОЧАСТИЧНОЕ ПЕРЕДВИЖЕНИЕ В СФЕРИЧЕСКИХ ЯДРАХ. *Дается обзор новых данных о положении одночастичных состояний, определяемых из однонуклонных реакций передачи и упругого рассеяния протонов на изобарических аналоговых состояниях. Положение с нейтронными одночастичными уровнями весьма удовлетворительно, хотя и имеются значительные неясности в вопросе одночастичных состояний в ядрах с* $N \approx 83$. *В последнее время быстро накапливается информация по одночастичным протонным состояниям. В ядрах с одинаковым массовым числом А структура одночастичных уровней протонов и нейтронов весьма схожа, и даже больше схожа, чем структура какой-либо одной системы для ядер с сильно отличающимися А. Главным в зависимости структуры одночастичных уровней от А является то, что с ростом А состояния с большими моментами понижаются быстрее, чем состояния с малыми моментами, по хорошо понятным причинам. Дается обзор данных о нарушении в заполнениях оболочек при "магических числах" и указывается, что это не является неожиданным. Единственными ядрами с хорошо замкнутыми оболочками являются ядра в районе* ^{208}Pb. *Упоминается важность низколежащих (глубоких) дырочных состояний, обнаруженных в (e, e' p) реакциях. Дается обзор информации об одночастичных нейтронных состояниях в области оболочек* $28-50$ *и* $50-82$. *В настоящее время получены экспериментальные результаты в последней указанной выше области для ядер с неодночастичной замкнутой оболочкой. Размывание одноквазичастичных состояний несколько больше, чем до сих пор считалось, однако имеется, в основном, одно состояние с большим весом этого состояния. Возникло серьезное затруднение в объяснении* $g_{7/2}$ *и* $h_{11/2}$ *состояний, когда результаты, полученные от реакций стрипинга и подхвата, значительно отличаются по ядрам между Mo и In. Графики вероятностей "дырочных состояний"* U_j^2 *и одноквазичастичные энергии* E_j *приведены для всех одночастичных состояний с* $N \approx 28-82$, *и проведено сравнение с предсказаниями теории парных корреляций. В основном, согласие хорошее, хотя имеются некоторые трудности, которые требуют объяснения.*

NEUTRON SINGLE PARTICLE STATES

The best method for determining locations of single particle states is by studies of single nucleon transfer reactions on closed shell nuclei (or their equivalent by elastic scattering through isobaric analogue states). By this method, one not only determines the angular momentum and parity of nuclear states, but also checks that the spectroscopic factors sum to the proper value which assures that all nuclear states containing appreciable fractions of the single particle state are included. The energy of the single particle state is then taken as the centre of gravity of the nuclear states, weighting each by its spectroscopic factor.

A few years ago, the information on neutron states seemed to be fairly complete [1] but there were several uncertainties and a few missing points. Work on the missing points has proceeded well in the past year. Yagi [2] has located the $g_{7/2}$ and $d_{5/2}$ hole states in the N = 81 nucleus ^{139}Ce; he found the previous estimates [1] to be rather poor. Fou et al. [3] and Bassani et al. [4] have located the $p_{3/2}$ and $f_{5/2}$ hole states in N = 50 nuclei. The only single particle or single hole states in adjacent shells still not located in this way are the $i_{13/2}$ and $h_{11/2}$ single particle states in N = 82 and N = 50 nuclei respectively. We have recently searched for the latter again with the ^{92}Mo (d, p) reaction [5], and have found an important component at 2.3 MeV, but its spectroscopic factor is only about $\frac{1}{3}$ of that expected for the single particle state.

With the recent availability of much improved accelerators and detectors, there has been a great deal of work in checking previous determination of energies of single particle states; in many cases the earlier experiments were crude and left reasonable doubts. Rather extensive work [6] has been done on locating the single particle states in N = 83 nuclei where previous studies were made before the availability of distorted wave Born approximation (DWBA). It has been found that sums of spectroscopic factors fall considerably short of unity for all but the $f_{7/2}$ and $h_{9/2}$ states. The locations of the $p_{1/2}$, $p_{3/2}$ and $f_{5/2}$ states must therefore be considered to be very questionable, and further studies of this would be highly desirable.

The most complete checking has been done in the shells adjacent to ^{208}Pb. In Table I, the spectroscopic factors for the previously assigned single particle states in ^{209}Pb are shown according to determinations with (d, p) reactions at several bombarding energies at Michigan [7], isobaric analogue studies at Texas [8], and (t, d) reactions at Los Alamos [9]. In all cases, the simple theory predicts unity. This is typical of the general type of agreement one usually gets. An optimist points to the fact that DWBA calculations are uncertain by about 20% at best and can sometimes be much worse, and is therefore satisfied with the results. Where discrepancies are large as for the $g_{7/2}$ in (d, p) and the $j_{15/2}$ in (t, d), he can point to the fact that other experiments give more favourable results. A pessimist can often find reasons to argue that the DWBA uncertainties are smaller in cases giving unfavourable results like the $j_{15/2}$ where the (t, d) measurement is remarkably intensitive to the choice of optical model parameters.

A similar disagreement exists over the $h_{9/2}$ hole state in ^{207}Pb where (p, d) work [2] indicates that the 3.6 MeV level contains almost all of the $h_{9/2}$ strength while $^{3}He, \alpha$) studies [10] indicate that it contains only a little more than half. In both this case and the $j_{15/2}$ case discussed above, it is

TABLE I. SPECTROSCOPIC FACTORS FOR SINGLE PARTICLE STATES IN ^{209}Pb BY VARIOUS METHODS

S.P. State	(d,p) [7]	Analogue [8] (p,p)	(t,d) [9]
$2g_{9/2}$	0.67	0.97	0.93
$1i_{11/2}$	0.94		1.05
$1j_{15/2}$	1.13		0.51
$3d_{5/2}$	1.00	0.85	0.86
$4s_{1/2}$	0.93	0.90	0.86
$2g_{7/2}$	1.17	0.84	0.90
$3d_{3/2}$	1.17	0.86	0.83

not difficult to explain fragmentation of the single particle state into several nuclear states, but no one has found any of the other fragments.

It has long been contended by nuclear structure theorists (see, for example, Ref. [11]) that the shell model picture of single particle states is only about 85% correct. The sum of spectroscopic factors should therefore be only about 0.85 instead of 1.0; the remaining 15% of the strength should be scattered over tens of MeV. The uncertainty in DWBA analyses is easily large enough to adjust all previous data for this, and few would argue that there is experimental evidence to dispute the point. Interest in this matter has recently been revived by the new stripping theory of Butler, Hewitt, May and McKellar [12], which seems to be much less parameter-sensitive than DWBA in determinations of absolute spectroscopic factors. It consistently finds spectroscopic factors much less than unity for states that have long been considered to be good single particle states. While very few calculations have been made with this theory and there have been no checks on its consistency when applied to different reactions, it should be viewed as a hopeful development. The uncertainties in absolute determinations of spectroscopic factors are a much more serious problem than is widely realized, and any theory that would substantially reduce them would be extremely welcome.

In spite of the new developments, the previous analysis [13] of locations of neutron single particle states is not appreciably altered. These locations can be explained [13] by properly taking into account [14] special neutron-proton interactions when they are in states with strongly overlapping wave-functions, self-binding energy (i.e. a single particle state moves down in energy as it fills owing to extra strong interactions among the particles in it), a spin-orbit force of the form $r^{-1}(dV/dr)$, a velocity dependence corresponding to an effective mass of about 1.3 times the nucleon mass, and a symmetry energy of the type known from the optical model.

PROTON SINGLE PARTICLE STATES

The most important recent development in the area under discussion has been the cataloguing of proton single particle states principally with (^{3}He, d) and (d, ^{3}He) reactions. As a result of work from Oak Ridge [15], Aldermaston [16], Tokyo [17], Saclay [18], Moscow [19], Argonne [20], Pennsylvania [21], and Los Alamos [22], studies are now available on both particle and hole states at each closed shell. Unfortunately, however, there seems to be more fragmentation here [17, 22] than was present in the study of neutron states, so the accurate determination of single particle state locations is not always easy.

The best information is for the Z = 50-82 and the Z = 82-126 shells This is shown and compared with related neutron results in Fig. 1a. In that figure, the results are arranged in order of increasing A, without regard to whether they are neutron or proton single particle states. The neutron states in the Sn region deduced from studies of the fullness of single quasiparticle states [23] are included.

Nearly all the changes in relative energies in Fig. 1a are shifts downward with increasing A for high angular momentum (j) states by amounts which increase with j (or equivalently, upward shifts of low j states). This may be explained by realizing that high-j nucleons interact more strongly with other high-j nucleons that with low-j nucleons because of the better overlap in their wave-functions – they have the same n quantum number and are pushed outward by similar angular momentum barriers. Thus, as high-j states fill, the energy of other high-j states is lowered. This effect is larger for high-j states because of the large number of nucleons they contain.

An especially notable feature of Fig. 1a is the similarity between proton and neutron single particle states in the same shell and in the same nuclei. There are examples of this in Fig. 1a for the 82-126 states in the Pb region and for the 50-82 states in the Sn region. This similarity is far stronger than that between the same neutron states, or between the same proton states, at different values of A. This implies that single particle level structure is determined principally by what other states are occupied, and does not depend much on whether we are dealing with neutrons or protons.

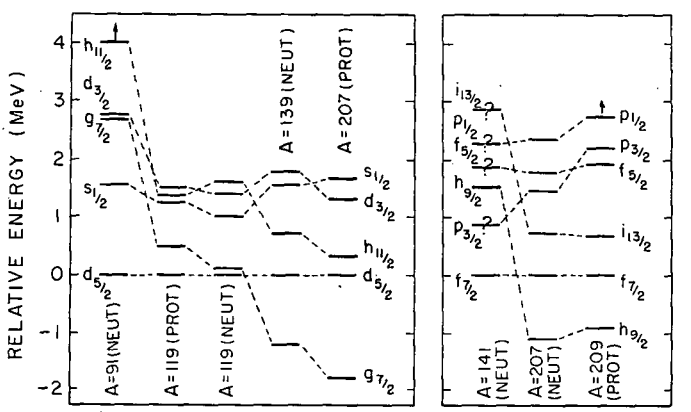

FIG. 1a. Energies of single particle states in the 50-82 and 82-126 shells.

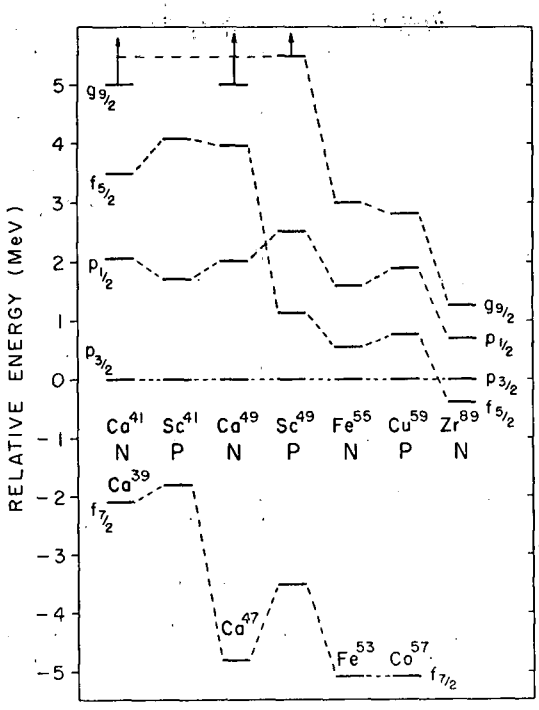

FIG. 1b. Energies of single particle states in the 20-50 shells.

The situation in the 20-50 shells is shown in Fig. 1b. For neighbouring nuclei ^{55}Fe and ^{59}Cu, and again for ^{41}Ca and ^{41}Sc, the similarity between proton and neutron single particle states in neighbouring nuclei persists. However in ^{49}Ca and ^{49}Sc, it fails rather badly. Still it seems significant that in four of the five cases where comparisons can be made, including the three of highest mass, there is much greater similarity between neutron and proton single particle states at the same mass than there is between neutron single particle states at different masses. The old custom of giving different single particle level diagrams for neutrons and protons is misleading; it would be much better to give such diagrams as a function of A, with the stipulation that it is only valid along the "line of beta stability."

IMPERFECT MAJOR SHELL CLOSURE AT "MAGIC NUMBERS"

It has long been realized that major shell closure is not perfect in nuclei with "magic numbers" of neutrons or protons. Several years ago, Blair [22] found that well-known $7/2^-$ states in Cu isotopes were excited in (^{3}He, d) reactions on Ni with a spectroscopic factor indicating that the $f_{7/2}$ proton single particle state lacks being full by about 0.8 particle. Fulmer et al. [24] found by a combination of (d, p) and (d, t) reactions that the $f_{7/2}$ neutron single particle states lack being full in ^{58}Ni and ^{60}Ni by about 0.36 and 0.28 particles even though these nuclei contain 30 and 32 neutrons respectively. By similar methods, Jolly [25] found that there is already

0.2 $2f_{7/2}$ neutrons in the 78 neutron nucleus, ^{130}Te. Lin [26] found similar evidence that there are about 0.6 neutrons in the $2d_{5/2}$ state in the 44, 46, and 48 neutron nuclei ^{78}Se, ^{80}Se, and ^{82}Se. Evidence of this type has expanded rapidly in the past year. Peterson [27] reported that ^{48}Ca has about 0.9 2p neutrons. Zeidman's [28] experiments showed that Fe nuclei, which have only 26 protons, already have 0.2-0.5 $p_{3/2}$ protons; this number increases with the neutron number. Heidelberg [28] and Argonne [20] work indicates imperfect shell closure at the "magic number" 20: ^{40}Ca already has 0.8 neutrons and 0.8 protons in the $f_{7/2}$ single particle states. Purser et al. [29] found that the ground state of ^{16}O may be written approximately as

$$\psi_{16} = \sqrt{0.68}\ p^{12} + \sqrt{0.23}\ p^{10}\ d^2 + \sqrt{0.09}\ p^{10}\ s^2$$

The 0.46 d-particles and 0.18 s-particles are mostly protons, but some are neutrons.

To the best of my knowledge there is no evidence for imperfect shell closure in ^{208}Pb for either neutrons or protons. This region has been studied very thoroughly, and they seem to be the best closed shells we have.

There is, of course, nothing very surprising about imperfect shell closure. Separations between single particle energies in different major shells are not infinite, and the amount of mixing across shells is of about the magnitude expected from our knowledge of residual interactions.

DEEP-LYING HOLE STATES

All the previous discussion has dealt with states near the top of the "Fermi Sea". Single particle states deep down in the Fermi Sea – two or three shells below the top – have been studied with (p, 2p) reactions, and more recently and successfully, with (e, e'p) reactions [30]. The binding energies of these states greatly exceed 50 meV, the approximate depth of a static shell theory potential; this requires a velocity dependence corresponding to an effective mass considerably less than the nucleon mass in agreement with nuclear matter theory but in contrast to the value above the nucleon mass encountered near the top of the Fermi Sea. This velocity dependence was pointed out by G. E. Brown several years ago, but its experimental confirmation is welcome.

SINGLE QUASIPARTICLE STATES

Studies of single quasiparticle states – including determinations of their energy E_j and the ratio of their particle and hole natures, usually expressed as the fullness of the single particle states, V_j^2 – have been going on for many years using single nucleon transfer reactions. In heavy nuclei, these studies were formerly limited to nuclei near closed shells, but since higher energy precision accelerators with attached spectrographs have become available in the past few years, virtually any nucleus in the periodic table is now open to such studies. Much of this work has been done on non-spherical nuclei and will be discussed in other papers at this meeting.

At our laboratory we have been concentrating rather on spherical nuclei in an effort to follow single quasiparticle states through entire major shells and observe how they gradually shift from purely particle to purely hole states. Fig. 2 shows an example [31] of the type of data obtained; it is from the ^{108}Pd (d, p) reaction. Vertical lines show the locations of nuclear levels which contain components of the neutron single quasiparticle state in whose row they are shown, and the heights of these lines are the spectroscopic factors which measure the fraction of their wave-function that is the single quasiparticle state. The sum of spectroscopic factors is U_j^2, the degree to which the single particle state is empty, and the centre of gravity of the components, shown by the ⊗, is E_j, the energy of the single quasiparticle state.

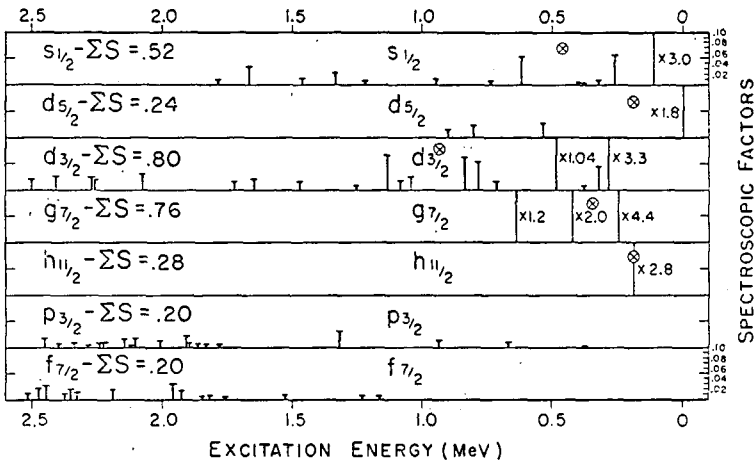

FIG. 2. Energies, J^π assignments, and spectroscopic factors of nuclear states excited in ^{108}Pd (d, p) ^{109}Pd reactions. Also shown are summed spectroscopic factors for each single particle state, which are U_j^2 in Fig. 3, and the "centres of gravity" of states for each j, which are E_j in Fig. 4.

Fig. 3 shows the value of U_j^2 for all nuclei studied in the N = 50-82 shell. It includes some data from Argonne on Ru [32] as well as experiments on Zr, Nb, Mo, Pd, Cd, In, Sn, Te, Ba and Ce from our laboratory [33]. The two curves show the predictions of simple pairing theory for the single particle energies at the beginning and at the end of the shell. For the $g_{7/2}$ and $h_{11/2}$ states in Pd and Cd, two sets of points are shown, one for determinations from (d, p), and the other for determinations from (d, t) reactions. The lack of agreement between these is the strangest phenomenon the author has ever encountered in many years of studies of this type; he believes it is due to a break-down in basic assumptions of stripping reaction theory [34].

An optimist can find much reason to be satisfied by the results of Fig. 3, especially if he ignores the $g_{7/2}$ and $h_{11/2}$ results from Pd, Cd, and Ru (d, p) reactions (the lower points for $h_{11/2}$ and the higher points for $g_{7/2}$). Near the ends of the shell, the results are close to the prediction lines, and in the middle of the shell they lie between the predictions. This is as expected from the monotonic and relatively smooth shifting of levels with A seen in Fig. 1. On the other hand, there are several disturbing features. The low values for the $s_{1/2}$ states in Ru and Pd, the high values

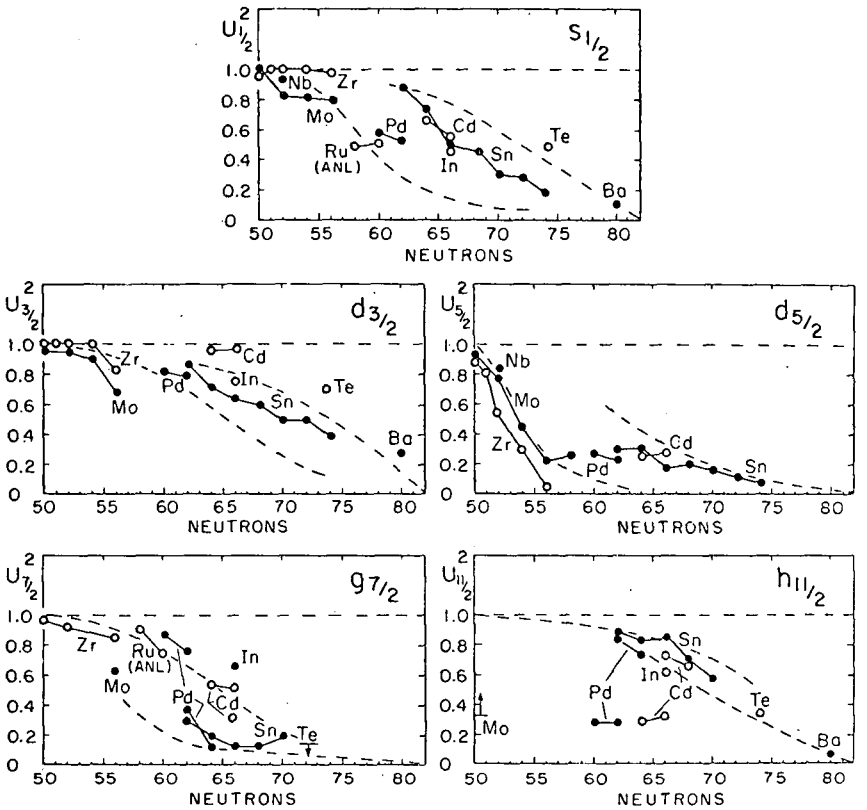

FIG. 3. "Emptiness", U_j^2, for each single particle state versus neutron number in the 50-82 shell. The dashed lines are predictions of pairing theory. Those starting at the left and right are based on single particle energies in 51 and 81 neutron nuclei respectively.

for the $d_{3/2}$ states in Te and Ba, and the generally erratic behaviour of the $g_{7/2}$ states are examples. These problems can generally be eliminated by judicious assumptions about energies of single particle states if one does not require their variation with A to be smooth. However, the author feels that uncertainties due to difficulties with reaction theories should first be reduced before jumping to such conclusions. We are therefore in the process of making further studies with (d, t) reactions.

The single quasiparticle energies E_j found in these studies are shown in Fig. 4, along with pairing theory predictions on the same basis as those in Fig. 3. Here again there is a considerable area of agreement with theory, but there are still some discrepancies. In the case of E_j, there is little chance of error in the analysis of experiments, but pairing theory predictions are not reliable. For example, the quadrupole force has long been known to produce large shifts in energies of nuclear states.

Figs 5 and 6 show similar but less elaborate studies from our laboratory on the N = 28-50 shell [35]. The data are for Ni, Ge and Se, and the pairing theory calculations are based on the single particle energies in ^{55}Fe and ^{89}Zr. The latter are shown at the right in Fig. 6. The single

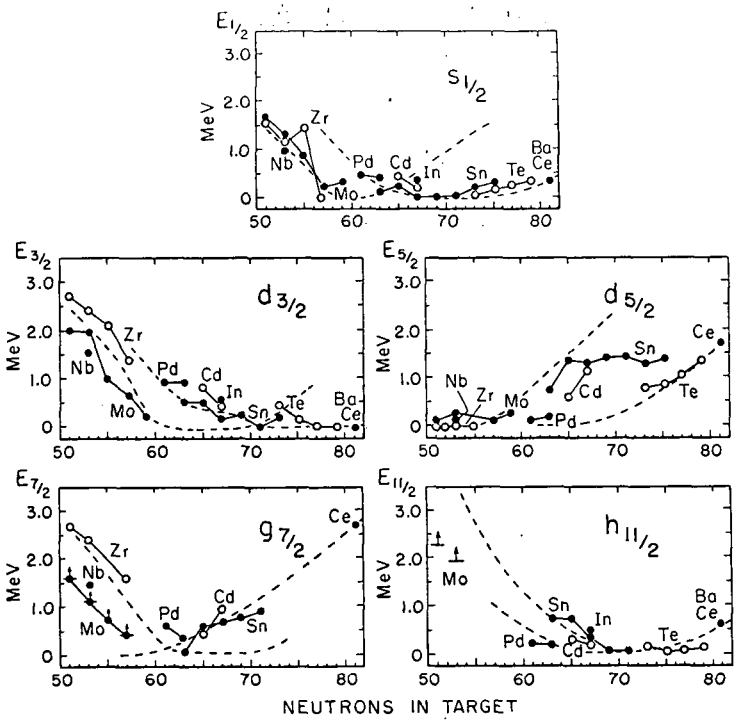

FIG.4. Energy of single quasiparticle states versus neutron number in the 50-82 shell. Dashed lines are pairing theory predictions as described in caption for Fig.3.

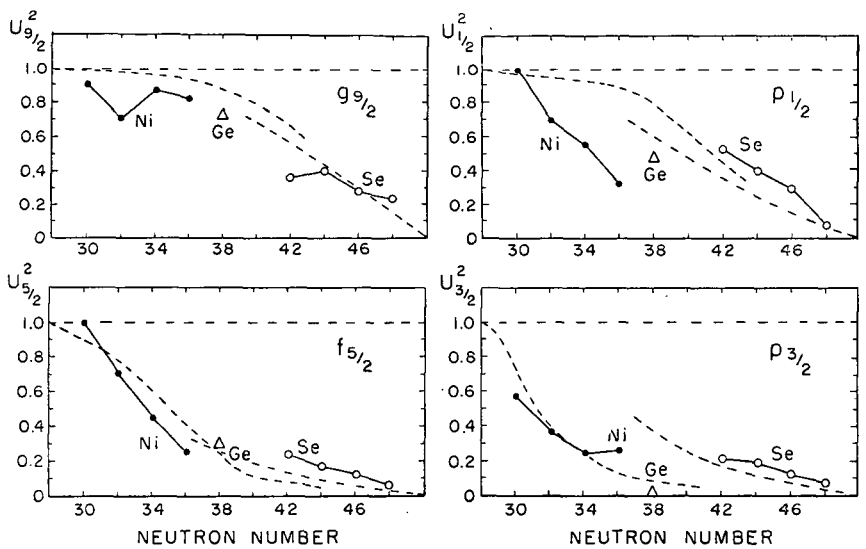

FIG.5. "Emptiness", U_j^2, for each single particle state versus neutron number in the 28-50 shell. The dashed lines are predictions of pairing theory. Those starting at left and right are based on single particle energies in 29 and 49 neutron nuclei respectively.

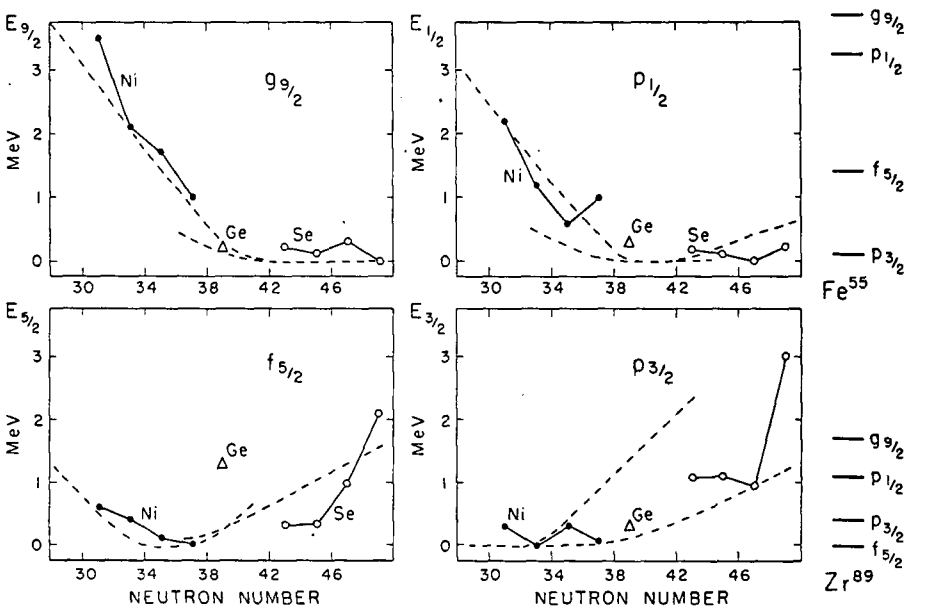

FIG.6. Energy of single quasiparticle states versus neutron number in the 28-50 shell. Dashed lines are pairing theory predictions as described in caption for Fig.5.

particle energies do not change as much here as they do in the N = 50-82 shell, so the two calculations do not vary greatly.

In general, the measured U_j^2 agree well with the theory except for the $p_{1/2}$ states in the heavy Ni isotopes. The measured single quasiparticle energies also agree reasonably well with the theory except for the $f_{5/2}$ state in Ge.

In summary, studies of single quasiparticle states with stripping reactions give large areas of agreement with theory, but there are many anomalies.

REFERENCES

[1] COHEN, B.L., FULMER, R.H., McCARTHY, A.L., MUKHERJEE, P., Rev. Mod. Phys. 35 (1963) 332.
[2] YAGI, K., ISHIMATSU, T., SAJI, Y., ISHIZAKI, Y., Tokyo Conf. on Nuclear Structure (1967) Paper 4.87.
[3] FOU, C.M., ZURMUHLE, R.W., JOYCE, J.M., Phys. Rev. 155 (1967) 1248.
[4] BASSANI, G., PICARD, J., SAUNIER, N., SOUCHERE, G., Tokyo Conf. on Nuclear Structure (1967) Paper 4.80.
[5] MOORHEAD, J.B., MOYER, R.A., Bull. Am. phys. Soc. 13 (1968) 119.
[6] WIEDNER, C.A., et al., Nucl. Phys. A103 (1967) 433.
HARNEY, H.L., et al., Phys. Lett. 26B (1968) 204.
MOORE, P.A., et al., Bull. Am. phys. Soc. 13 (1968) 658; 12 (1967) 1188.
[7] MUEHLLEHNER, G., POLTORAK, A.S., PARKINSON, W.C., BASSEL, R.H., Phys. Rev. 159 (1967) 1039.
[8] ZAIDI, S.A.A., DARMADJO, S., Phys. Rev. Lett. 19 (1967) 1446
[9] IGO, G.J., BARNES, P.D., FLYNN, E.R., ARMSTRONG, D.D., (Los Alamos, USA), to be published.
[10] ALFORD, W.P., BURKE, D.G., (Univ. of Rochester, N.Y.) to be published.

[11] BROWN, G.E., Tokyo Conf. on Nuclear Structure (1967), Discussion.
[12] BUTLER, S.T., HEWITT, R.G.L., McKELLAR, B.H.J., MAY, R.M., Ann. Phys. 43 (1967) 282.
[13] COHEN, B.L., Am. J. Phys. 33 (1965), 1011; Phys. Rev. 130 (1963) 227.
[14] DE-SHALIT, A., GOLDHABER, M., Phys. Rev. 92 (1953) 1211.
[15] WILDENTHAL, B.H., PREEDOM, B.M., NEWMAN, E., CATES, M.R., Phys. Rev. Lett. 19 (1967) 960.
NEWMAN, E., HIEBERT, J.C. (Oak Ridge, USA) to be published.
[16] HINDS, S., MIDDLETON, R., BJERREGAARD, J.H., HANSEN, O., NATHAN, O., Nucl. Phys. 83 (1966) 17.
[17] ISHIMATSU, T., YAKI, K., OHMURA, H., NAKAJIMA, Y., NAKAGAWA, T., ORIHARA, H., Nucl. Phys. A104 (1967) 481.
[18] CONJEAUD, M., HARAR, S., BASSANI, G., CASSAGNOU, Y., PICARD, J., Tokyo Conf. on Nuclear Structure (1967) Paper 4.86.
BRUGE, G., BUSSIERE DE NERCY, A., CONJEAUD, M., FAIVRE, J.C., HARER, S., THURIERE, E., Compte Rendu d'Activité, Dept. de Physique Nucléaire, Saclay (1967) 32.
[19] TOLCHENKOV, D.L., Inst. Theor. Exp. Phys. Report No. 597 (1968); OKOROKOV, V.V., et al., Ibid, No. 595 (1968) (Moscow).
[20] ZEIDMAN, B., private communication.
[21] PULLEN, D.J., ROSNER, B., (University of Pennsylvania, USA) to be published.
[22] BLAIR, A.G., Phys. Rev. 140 (1965) B648; Phys. Lett. 9 (1964) 37.
[23] SCHNEID, E.J., PRAKASH, A., COHEN, B.L., Phys. Rev. 156 (1967) 1316.
COHEN, B.L., PRICE, R.E., Phys. Rev. 121 (1961) 1441.
[24] FULMER, R.H., DAEHNICK, W.W., Phys. Rev. 139 (1965) B579.
COHEN, B.L., FULMER, R.H., McCARTHY, A.L., Phys. Rev. 126 (1962) 698.
[25] JOLLY, R.K., Phys. Rev. 136 (1964) B683.
[26] LIN, E.K., Phys. Rev. 139 (1965) B340.
[27] PETERSON, R.J., (Princeton University, USA) to be published.
[28] BOCK, R., DAHM, H.H., STOCK, R., Phys. Lett. 18 (1965) 61.
[29] PURSER, K.H., ALFORD, W.P., CLINE, D., FULBRIGHT, H.W., GOVE, H.E., KRICK, M.S., University of Rochester Nuclear Physics Laboratory Annual Report (1967).
[30] AMALDI, Jr., U., et al., Phys. Lett. 22 (1966) 593.
[31] COHEN, B.L., MOORHEAD, J.B., MOYER, R.A., Phys. Rev. 161 (1967) 1257.
[32] NOLEN, J.A., FORTUNE, H.T., KIENLE, P., MORRISON, G.C., Bull. Am. phys. Soc. 13 (1968) 584.
[33] COHEN, B.L., CHUBINSKY, O.V., Phys. Rev. 131 (1963) 2184.
HJORTH, S.A., COHEN, B.L., Phys. Rev. 135 (1964) B920.
MOORHEAD, J.B., COHEN, B.L., MOYER, R.A., Phys. Rev. 165 (1968) 1287.
GOLDMAN, L.H., KREMENEK, J., Bull. Am. phys. Soc. 13 (1968) 120.
COHEN, B.L., FINK, C.L., HINDS, S., Phys. Rev. 157 (1967) 1114.
FULMER, R.H., McCARTHY, A.L., COHEN, B.L., Phys. Rev. 128 (1962) 1302.
See also Refs [5], [23], [25], and [31].
[34] COHEN, B.L., MOYER, R.A., MOORHEAD, J.B., GOLDMAN, L.H., DIEHL, R.C., Phys. Rev. (in press).
[35] FULMER, R.H., McCARTHY, A.L., Phys. Rev. 131 (1963) 2133.
FULMER, R.H., McCARTHY, A.L., COHEN, B.L., MIDDLETON, R., Phys. Rev. 133 (1964) B955.
GOLDMAN, L.H., Phys. Rev. 165 (1968) 1203.
See also Ref. [26].

DISCUSSION

H. MELDNER: Don't you agree that your mass differences or differences in total binding energy for different occupation functions should not simply be identified with eigenvalue spacings in potential wells - even if pairing is negligible? In other words, that rearrangement can well have the same order of magnitude as the so-called level differences?

I would like to mention here recent self-consistent calculations [Nuovo Cim. 53B (1968) 195] indicating an order of 10^{-3} or MeV's of orbital rearrangement energies for medium nuclei. Therefore, the tentative conclusions - which you mentioned - of a very anomalous effective mass at the Fermi surface are quite questionable.

B.L. COHEN: This is a question for theorists.

V. GILLET: It seems that double closed shell nuclei are very closed for the experimentalists and quite open for the theoreticians. In fact, departures from a pure H-F shell model ground state are very large, whether they are computed in the RPA framework or by admixing 2 particle-hole configurations. In these calculations (Brown and Jacob, Goswamy and Pal, Agassi-Gillet and Lumbroso, Bonches) ^{16}O, ^{40}Ca and ^{208}Pb appear to be only half of the time in a pure closed shell state. However, the average number of excited nucleons is small, generally inferior to unity. Consequently, the quantities the experimentalists measure, i.e. the particle and hole occupation numbers, are small.

TWO- AND THREE-QUASIPARTICLE STATES IN SPHERICAL NUCLEI

K.F. ALEXANDER
JOINT INSTITUTE FOR NUCLEAR RESEARCH,
DUBNA, UNION OF SOVIET SOCIALIST REPUBLICS

Abstract — Аннотация

TWO- AND THREE-QUASIPARTICLE STATES IN SPHERICAL NUCLEI. From the experimental study of two- and three-quasiparticle states in spherical nuclei useful information can be obtained on the residual interaction between quasiparticles. Such states can be assumed to be relatively pure, if they have the maximum possible spin value. Experimental data on several maximum spin states are discussed. Possible causes for the hindrance of electromagnetic transitions de-exciting 2qp and 3qp states are pointed out. A further tool to investigate the quasiparticle structure of excited states is the analysis of allowed beta decay. This is demonstrated, for example, with the 4^+ states of the even Sn isotopes. The residual proton-neutron interaction can considerably shift 3 qp states if strongly interacting proton and neutron orbitals are involved. This effect is studied in detail for states in which the structure $(\pi g_{9/2} \nu g_{7/2})_{1+}$ is present.

ДВУХ- И ТРЕХКВАЗИЧАСТИЧНЫЕ СОСТОЯНИЯ В СФЕРИЧЕСКИХ ЯДРАХ. Экспериментальным изучением двух- и трехквазичастичных состояний в сферических ядрах можно получить полезную информацию об остаточном взаимодействии между квазичастицами. Можно предполагать, что состояния являются относительно чистыми, если они имеют максимально возможное значение спина. Обсуждаются экспериментальные данные о нескольких состояниях такого рода. Указывается на возможные причины замедления электромагнитных переходов, разряжающих двух- и трехквазичастичные уровни. Другой способ изучения квазичастичной структуры возбужденных состояний – анализ разрешенного бета-распада. Это доказывается на примере уровней 4^+ в четных изотопах Sn. Остаточное протон-нейтронное взаимодействие может передвигать существенно трехквазичастичные уровни, если участвуют сильно взаимодействующие протонные и нейтронные орбиты, а этот эффект изучается детально для состояний, в которых принимает участие структура $(\pi g_{9/2} \nu g_{7/2})_{1+}$.

1. INTRODUCTION

Two- and three-quasiparticle excitations are the simplest configurations that allow us to study the residual interaction between quasiparticles. The experimental identification of such states is important if we want to test calculations which go beyond the simple pairing force scheme. We know that this simple type of residual interaction works rather well in the region of strongly deformed nuclei. This is because the main part of the long-range residual interaction is absorbed into the deformed Hartree-Fock potential, giving rise only to rotational collective motion. Furthermore, the deformation destroys the degeneracy of the shell model levels, thus severely limiting the number of quasiparticles that can participate in a given excitation. Thus 2qp and 3qp states predicted by the superfluid model for deformed nuclei [1] are generally in good agreement with experimental findings.

In spherical nuclei the situation is more complicated. Here there is no such clear-cut difference between collective and single-particle excitations as in deformed nuclei. In addition to the truly collective states

there are many possibilities for constructing excited states above the gap in which several pairs of quasiparticles participate. One should expect pure two-quasiparticle states when there is only one possibility of forming them from the quasiparticle states available in the energy region considered. Most other states, if not truly collective, can be thought of as being a mixture of several 2qp excitations, if the possibility of excitations with higher seniority (e.g. 4qp excitations) is for the moment neglected. This also applies, correspondingly, to the 3qp excitations of odd-mass spherical nuclei.

2. MAXIMUM-SPIN STATES

Very often, only the excitation energy, spin, and parity of an excited state are known from experiment. These data can be sufficient to identify a 2qp or 3qp state if one is sure that there is only one possibility of constructing such a state from the quasiparticles available in the mass and energy region concerned. States of this kind will have the maximum possible spin value and can, therefore, sometimes be identified as isomeric states. As already shown by Kisslinger and Sorensen [2], in this case the simple pairing scheme gives a fair estimate of the excitation energy. As an example, Fig. 1 shows the two-neutron state $(d_{3/2}h_{11/2})_{7^-}$ which occurs systematically in the mass region between Sn and Nd.

The highest spin value for a 2qp excitation with positive parity in this mass region is 10^+ from the $(h_{11/2})^2$ configuration. It seems very probable

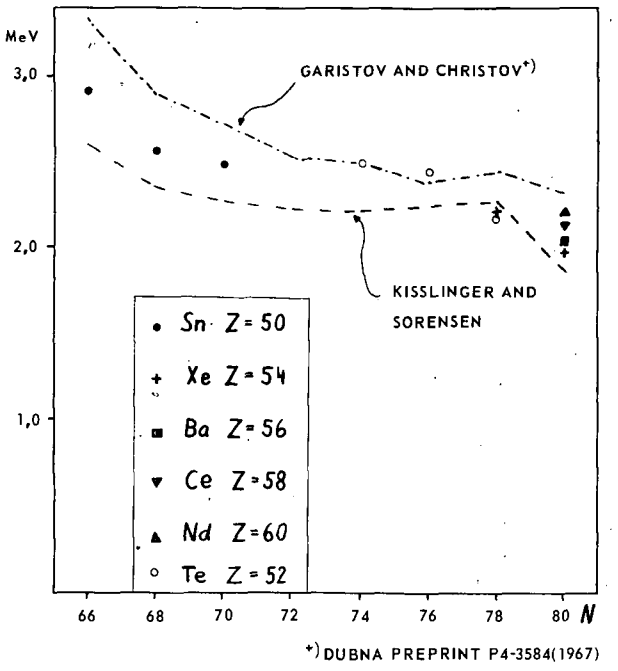

FIG. 1. Excitation energy of the 2qp state $(h_{11/2}d_{3/2})_{7^-}$ as a function of neutron number.
○ Data on tellurium by courtesy of L.K. Peker.

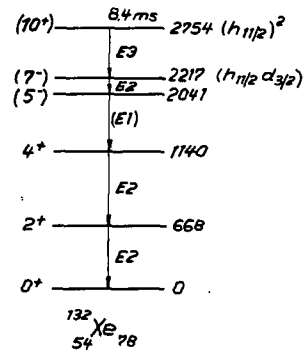

FIG.2. 2qp isomeric state in ^{132}Xe after Brinckmann et al. [4].

that this state is responsible for the isomerism in ^{132}Xe, recently reported by Brinckmann et al.[3]. New measurements of conversion electrons [4] confirmed the decay scheme as given in Fig.2. This interpretation implies that the state 10^+ of the $(h_{11/2})^2$ multiplet lies below or at least very near to the 8^+ state. This is to be expected if one takes into account only the quadrupole-quadrupole interaction between the quasiparticles. In the more neutron-deficient Xe isotopes the 8^+ states are found at lower excitation energies [5]; this can be explained by the tendency to develop a "quasi-rotational" level structure for nuclei farther off from closed shells. As the present analysis shows, the nucleus $^{132}_{54}Xe_{78}$ does not belong to this type, but can well be described as spherical.

Yamazaki et al.[6] reported the excitation of new isomeric states in the even tin isotopes via the Cd(α, xn) reaction which they also interpret as due to the $(h_{11/2})^2_{10^+}$ configuration. Fig.3 is taken from this work. The nanosecond isomeric states in the lighter even Sn isotopes are ascribed to the $(g_{7/2})^2_{6^+}$ states which are maximum spin states in this region.

3. ELECTROMAGNETIC TRANSITION PROBABILITIES

The isomeric transition in ^{132}Xe is hindered in comparison to a single-particle E3 transition by a factor of about 100. As the transition between the configurations $(h_{11/2})^2_{10^+}$ and $(d_{3/2}h_{11/2})_{7^-}$ is j-forbidden, such a hindrance is to be expected.

Generally, electromagnetic transitions between 2qp and 3qp states should often be slower compared to the single-particle estimate. The hindrance is to be expected on one or several of the following grounds: (i) the influence of the pairing factor which can reduce electrical transitions seriously, (ii) a necessary recoupling of the angular momenta of the quasiparticles, and (iii) the impossibility of realizing the transition as a one-particle transition (j- and F-forbiddenness). In Table I are listed several E2 and E3 transitions which de-excite known 2qp states in the region $64 \leq N \leq 80$ [7]. The slowing-down of the E2 transitions between the states $(d_{3/2}h_{11/2})_{7^-}$ and $(s_{1/2}h_{11/2})_{5^-}$ is probably caused by the pairing factor $(U_iU_f - V_iV_f)^2$ because the states $d_{3/2}$ and $s_{1/2}$ are near the Fermi surface. The hindrance of the E3 transitions seems to be connected with the degree of collectivization of the final state. So the transitions which go to the collective first 2^+ state are already faster than the single-particle estimate,

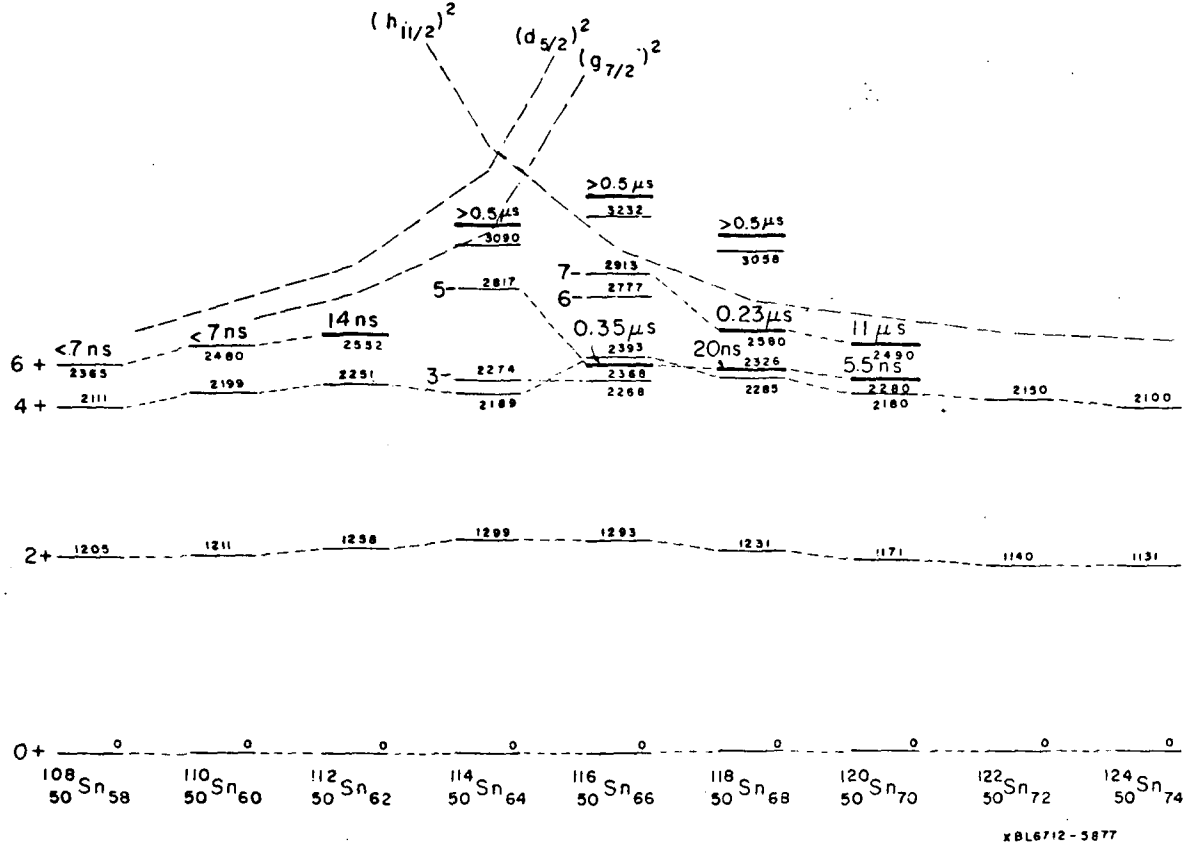

FIG.3. 2qp states in the even Sn isotopes after Yamazaki et al. [6].

TABLE I. ELECTROMAGNETIC TRANSITION PROBABILITIES

Nuclide	J_i	J_f	Transition energy (MeV)	$T_{1/2}$ (partial)	Multipolarity	F
(i) decay of 2qp states						
^{112}Sn	6^+	4^+	0.302	14 ns	E2	2
^{118}Sn	7^-	5^-	0.253	0.23 μs	E2	10
^{120}Sn	7^-	5^-	0.200	11 μs	E2	20
^{132}Xe	10^+	7^-	0.537	8.4 ms	E3	100
^{136}Ba	7^-	4^+	0.164	0.32 s	E3	4
^{138}Ce	7^-	4^+	0.303	9.2 ms	E3	3
^{140}Nd	7^-	4^+	0.435	0.6 ms	E3	3
^{116}Sn	5^-	2^+	1.06	0.6 μs	E3	0.6
^{118}Sn	5^-	2^+	1.09	0.3 μs	E3	0.4
^{120}Sn	5^-	2^+	1.12	0.5 μs	E3	0.8
(ii) decay of 3qp states						
^{53}Fe	$19/2^-$	$11/2^-$	0.702	2.6 min	E4	4
^{93}Mo	$21/2^+$	$13/2^+$	0.264	6.9 h	E4	1
^{109}In	$19/2^+$	$13/2^+$	0.678	0.2 s	M3	1000
^{135}Cs	$19/2^+$	$11/2^+$	0.840	53 min	M4	800

the transitions to the 4^+ states are only slightly hindered, whereas the transition between pure 2qp states in ^{132}Xe is strongly slowed down.

Transitions of the j-forbidden type can also be observed between 2qp levels in odd nuclei. The 2.5 ms isomeric transition in $^{208}_{83}Bi_{125}$, for instance, was recently interpreted [8] as a j-forbidden E3 transition (F = 3200) between the configurations $(\pi h_{9/2}\nu i_{13/2})_{10^-}$ and $(\pi h_{9/2}\nu f_{5/2})_{7^+}$. In ^{114}In and ^{116}In a strong enhancement of the thermal neutron activation cross-sections for the second isomeric states with structure $(\pi g_{9/2}\nu h_{11/2})_{8^-}$

TABLE II. POSITON DECAY $_{51}Sb \rightarrow {}_{50}Sn$

	Experimental data				Interpretation	
A	J_i	J_f	E_f (MeV)	log ft	Initial state	Final state
115	$5/2^+$	$3/2^+$	0.494	4.7	$\pi d_{5/2}$	$\nu d_{3/2}$
116	8^-	7^-	2.90	4.6	$(\pi d_{5/2} \nu h_{11/2})_{8^-}$	$(\nu d_{3/2} \nu h_{11/2})_{7^-}$
117	$5/2^+$	$3/2^+$	0.158	4.9	$\pi d_{5/2}$	$\nu d_{3/2}$
118	8^-	7^-	2.572	5.0	$(\pi d_{5/2} \nu h_{11/2})_{8^-}$	$(\nu d_{3/2} \nu h_{11/2})_{7^-}$

was observed. This could be explained by the j selection rule which directs the γ-ray cascade through the multiplet $(\pi g_{9/2}\nu h_{11/2})_{1^-\ldots 10^-}$ to its lowest-lying member, i.e. the isomeric state [9].

An interesting case is the E4 decay of the 6.9 h isomer of $^{93}_{42}Mo_{51}$. The isomer has the spin $21/2^+$; it is the maximum spin state of the multiplet $(\pi g_{9/2})^2 \nu d_{5/2}$ and decays to a $13/2^+$ state of the same multiplet, no other configurations being available. In this case none of the possible causes hindrance applies, and the observed transition has indeed single-particle speed. The same argument can be used for the 2.6 min isomeric state in ^{53}Fe reported by Eskola [10]. Here the isomeric E4 transition connects the states $19/2^-$ and $11/2^-$ of the multiplet $(\pi f_{7/2})^2 \nu f_{7/2}$ and has also about single-particle speed.

In contrast, the M3 transition de-exciting the 0.2 s isomer of ^{109}In and the M4 transition de-excitating the 53 min isomer of ^{135}Cs are both delayed by a factor of about 10^3. In both cases, the isomeric states are not maximum-spin states and may have, therefore, a more complicated structure. Then the hindrance will be caused by the recoupling of angular momenta and/or the cancellation of matrix elements.

4. BETA DECAY PROBABILITIES

Beta decay probabilities can sometimes be used effectively to determine the quasiparticle structure of certain levels [11]. In many spherical nuclei in the regions of $N = 50$, $Z = 50$ and $N = 82$ we find allowed unhindered beta transitions. For these transitions, having log ft values < 5.5, we can formulate the following rules: (i) the decay is of pure Gamov-Teller type as Fermi-transitions are isotopic spin forbidden, (ii) the decay connects always one-particle states with the same orbital momentum ℓ. The regular occurrence of fast beta transitions below $A = 140$ is caused by the spin-orbit splitting of shell model levels, so that a state with $j = \ell + 1/2$ is found near the Fermi surface of the proton system while at the same time its spin-orbit partner $j = \ell - 1/2$ lies near the Fermi surface of the neutron system. If such a case is realized the reduced transition probability can be written

$$(ft)^{-1} \sim R \cdot S \cdot |\langle j \,||\, \sigma \,||\, j' \rangle|^2$$

using the reduced matrix element of an allowed GT transition between the orbitals j' and j. Here R is the correction factor for pairing correlations, and S a statistical factor which depends on the angular momenta and the kind of transition (1qp → 1qp, 1qp → 3qp, 2qp → 2qp, 2qp → 0 etc.). Using this formula we can compare different transitions which involve the same orbitals j', j, for instance transitions between 1qp states with transitions between 2qp states. If we compare analogous transitions in neighbouring nuclei for which the pairing factor R can be assumed to be approximately equal, then the conclusions about the structure of the states involved are rather precise. In Table II are listed some transitions between 2qp states (decay of even mass nuclei) and their analogous 1qp transitions (decay of odd mass nuclei) for the case where not only the pairing factors but also the statistical factors are equal [7]. The equality of the measured log ft values confirms the assumed internal structure and the resulting spin to

TABLE III. BETA DECAY TO THE 4^+ STATES OF ^{116}Sn, ^{118}Sn AND ^{120}Sn; NEGATON DECAY $_{49}In \rightarrow {}_{50}Sn$

Experimental data						a_i^2	$\Sigma a_i^2 E_i$ (MeV)	2qp (MeV)
A	J_i	J_f	E_f (MeV)	log ft	log $\bar{ft}$*			
116	5^+	4^+	2.38	5.2		0.22		
			2.52	5.1		0.26		
			2.80	5.1	4.5	0.26	2.69	2.7
			3.05	5.1		0.26		
117	$9/2^+$	$7/2^+$	0.73	4.5	4.5			
118	5^+	4^+	2.28	5.6		0.08		
			2.48	5.7	4.5	0.07	2.87	3.1
			2.96	4.6		0.85		
119	$9/2^+$	$7/2^+$	0.84	4.4	4.4			
120	5^+	4^+	2.18	5.6		0.09		
			2.65	6.0		0.03		
			3.06	4.8		0.54		
			3.17	5.6	4.5	0.09	3.15	3.4
			3.39	5.7		0.07		
			3.54	5.9		0.04		
			3.78	5.4		0.14		

* $(\bar{ft})^{-1} = \Sigma (ft_i)^{-1}$

which the particles are coupled in the 2qp states. This argument applies, of course, only for pure 2qp states without admixtures.

The beta decay probability can, however, also be used to explore the structure of mixed states if only one of the components of the mixture can be excited via an allowed GT transition [11]. Here the transition probability should be proportional to the squared amplitude a^2 of this component in the given state. How this method works can be seen from the example of the 4^+ states in ^{116}Sn, ^{118}Sn and ^{120}Sn, which are excited by beta decay of the 5^+ isomeric states of indium [7]. Adding together the transition probabilities to all the 4^+ states in each case we get exactly the transition probability of the analogous $\pi g_{9/2} \rightarrow \nu g_{7/2}$ transition in the neighbouring odd-mass nuclei (see Table III). It is concluded that the transitions in the even mass chains are of the type $(\pi g_{9/2}\, \nu s_{1/2})_{5^+} \rightarrow (\nu g_{7/2}\, \nu s_{1/2})_{4^+}$, assuming that the initial state is a rather pure 2qp state and the final state is spread over several states with a mixed structure. The centre of mass $\Sigma a_i^2 E_i$ gives us an experimental value for the excitation energy of the pure 2qp state without residual quasiparticle interaction. As is seen from Table III the theoretical values of Kisslinger and Sorensen are quite well reproduced, but the experimental amplitudes do not agree with the calculated values of Arvieu [12].

The same method can be applied to 1qp→3qp transitions. In the odd-mass isotopes ^{111}In and ^{117}In certain highly excited states are populated by fast beta transitions [7, 12, 13]. Fig.4 shows the decay scheme ^{117g,m}Cd → ^{117}In, recently published by Pandharipande [13], where several transitions with log ft < 5.5 are observed. Here the structures which can be reached by allowed GT transitions are $(\pi g_{9/2} \nu g_{7/2})_{1^+} \nu s_{1/2}$ and $(\pi g_{9/2} \nu g_{7/2})_{1^+} \nu h_{11/2}$. Their centres of mass (obtained in the same manner as for the 4^+ states in Sn) lie at 2.20 and 2.33 MeV, respectively. The

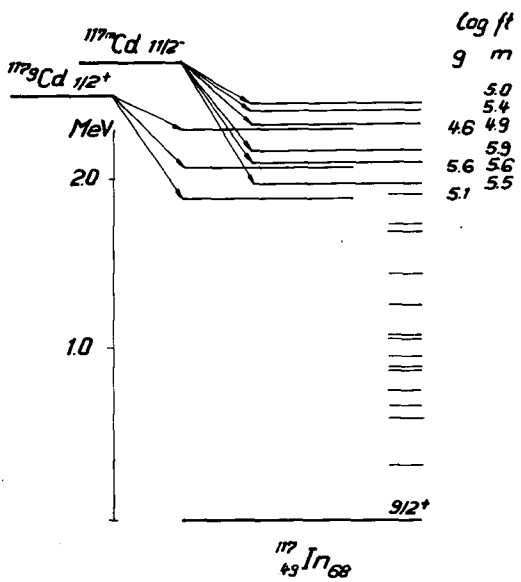

FIG.4. Fast beta transitions in the decay of ^{117g,m}Cd after Pandharipande [13]. Only transitions with log ft < 6.0 are shown.

summed transition probabilities give in both cases log ft = 4.5, in excellent agreement with the analogous transition $^{118}Cd(0^+) \rightarrow {}^{118}In(1^+)$ for which log ft = 4.6 is observed [7].

5. EVIDENCE FOR NEUTRON-PROTON INTERACTION

The residual proton-neutron interaction between quasiparticles will show up if we compare the excitation energy of the 3qp states with the energy of the corresponding 2qp "parent" states in the neighbouring even-mass nuclei. Thus, the $21/2^+$ state in ^{93}Mo is composed of a $d_{5/2}$ neutron coupled to the $(g_{9/2})^2_{8^+}$ state of the even core which is observed in ^{92}Mo at 2.795 MeV, that is 0.367 MeV higher than the isomeric state in ^{93}Mo. As was already shown by Auerbach and Talmi [14], the lowering of the 3qp state is caused by the residual proton-neutron interaction which for the states $g_{9/2}$ and $d_{5/2}$ is especially strong if the orbital momenta and the spins of proton and neutron are aligned, thus leading to the observed "spin gap". Based on such considerations, more general rules to determine the lowest-lying member of a 3qp multiplet were discussed by Peker [15].

The 3qp state in ^{117}In with the structure $(\pi g_{9/2} \nu g_{7/2})_{1^+} \nu s_{1/2}$ which was identified in beta decay is shifted for about 0.7 MeV against the parent state $(\nu g_{7/2} \nu s_{1/2})_{4^+}$ in ^{118}Sn. The exceptionally strong interaction seems to be connected with the structure $(\pi g_{9/2} \nu g_{7/2})_{1^+}$ which can be observed in several other nuclei of this mass region as a 2qp state (in odd nuclei) or as a part of 3qp states. In many odd nuclei this configuration forms the ground state as is predicted by the "strong" Nordheim rule.

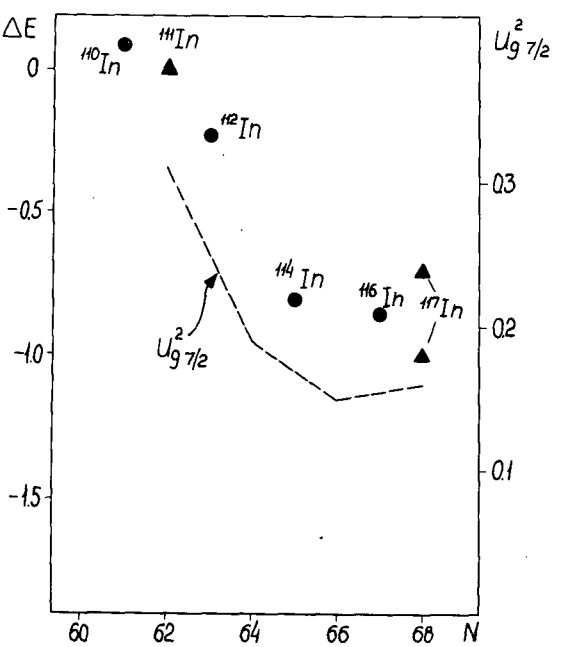

FIG. 5. Strength of proton-neutron interaction for the 2qp structure $(\pi g_{9/2} \nu g_{7/2})_{1^+}$.

The residual neutron-proton interaction which is effective here should strongly depend on the occupation numbers of the levels involved. For instance, a simple δ-force interaction leads to a strong lowering of the state $[\pi(\ell+1/2)\nu(\ell-1/2)]_{1^+}$ relative to the other members of the 2qp multiplet if both quasiparticles are preferentially particles or preferentially holes. If this condition is fulfilled the interaction is of the same order of magnitude as for the $J=0$ state of two like particles sitting on the same orbital. Fig.5 shows the energy gain which is caused by coupling a neutron and a proton quasiparticle to the structure $(\pi g_{9/2}\nu g_{7/2})_{1^+}$ for several 2qp and 3qp states in indium isotopes. In the even-mass isotopes this state is the ground state, in the odd-mass isotopes it is part of the 3qp states which are seen in beta decay. The energy gain ΔE was calculated by using experimentally known 1qp and 2qp excitations in the neighbouring nuclei. At the same time the "emptiness" of the orbital $\nu g_{7/2}$ is shown which was experimentally obtained by (d, p) reactions on the isotopes of tin by Schneid et al.[16]. This confirms qualitatively the assumption that the interaction is strongest if both quasiparticles are mainly holes. In other cases where such conditions are not fulfilled, the 3qp state is not shifted away so much from the excitation energy we expect without taking into account neutron-proton interaction. This applies, for instance, to the new isomeric state in ^{207}Bi just reported to the author by the Stockholm group [17] (see Fig.6).

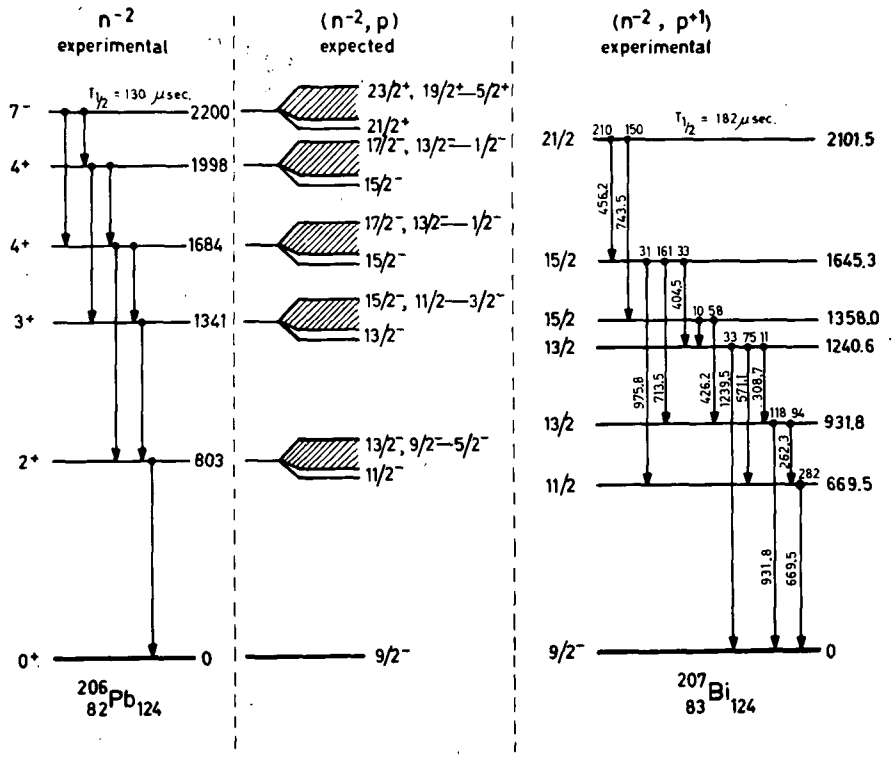

FIG.6. 3qp isomeric state in ^{207}Bi after Bergström et al. [17].

Having probably the structure $[(\nu i_{13/2}\ \nu p_{1/2})_{7^-}\ \pi h_{9/2}]_{21/2^+}$, it is supposed to be built on the 7^- 2qp state of ^{206}Pb and is found only 0.1 MeV lower than this parent state.

REFERENCES

[1] GALLAGHER, C.J., SOLOVIEV, V.G., Mat. Fys. Skr. Dan. Vid. Selsk. 2 No.2 (1962); SOLOVIEV, V.G., Zh. eksp. teor. Fiz. 43 (1962) 246.
[2] KISSLINGER, L.S., SORENSEN, R.A., Mat. Fys. Medd. Dan. Vid. Selsk. 32 No.9 (1960); Rev. Mod. Phys. 35 (1963) 853.
[3] BRINCKMANN, H.F., HEISER, C., FROMM, W.D., Nucl. Phys. A96 (1967) 318.
[4] BRINCKMANN, H.F. et al., Contribution No.20 to this symposium.
[5] BERGSTRÖM, I. et al., (Forskningsinstitutet för Atomfysik, Stockholm) personal communication; BRINCKMANN, H.F. et al., Zentralinstitut für Kernphysik, Rossendorf, Dresden, Preprint ZfK-137 (1968).
[6] YAMAZAKI, T., EWAN, G.R., Phys. Lett. 24B (1967) 278; YAMAZAKI, T. et al., (Univ. of Tokyo, Bunkyo-ku, Tokyo) personal communication.
[7] LEDERER, C.M., HOLLANDER, J.M., PERLMAN, I., Table of Isotopes, Sixth Ed., New York (1967).
[8] BONITZ, M., KANTELE, J., SIGURD HANSEN, N.J., Nucl. Phys. (in press).
[9] ALEXANDER, K.F. et al., Nucl. Phys. A112 (1968) 474.
[10] ESKOLA, K., Phys. Letters 23 (1966) 471; Annls Acad. Sci. Fenn. Ser. A/VI, Nr. 261 (1967).
[11] ALEXANDER, K.F., Preprint JINR P6-3785, Dubna (1968).
[12] DA COSTA, N.L., et al., Nuovo Cim. 50B (1967) 345.
[13] PANDHARIPANDE, V.R. et al., Nucl. Phys. 109A (1968) 81.
[14] AUERBACH, N., TALMI, I., Phys. Lett. 9 (1964) 153.
[15] PEKER, L.K., Yadernaya Fiz. 4 (1966) 27.
[16] SCHNEID, E.J., PRAKASH, A., COHEN, B.L., Phys. Rev. 156 (1967) 1316.
[17] BERGSTRÖM, I. et al., (Forskningsinstitutet för Atomfysik, Stockholm) personal communication.

QUASIPARTICLES AND NUCLEAR VIBRATIONAL STATES

R.A. SORENSEN
CARNEGIE-MELLON UNIVERSITY, PITTSBURGH, PA.,
UNITED STATES OF AMERICA

Abstract — Аннотация

QUASIPARTICLES AND NUCLEAR VIBRATIONAL STATES. The level structure associated with various nuclear vibrations is described. It is shown how these vibrations are described in terms of particle or quasiparticle excitations by means of the harmonic random phase approximation. Vibrations corresponding to different modes of excitation are compared. Motions corresponding to the enhancement of three different simple operators are considered: (a) the E2 one-body operator, (b) the operator causing the removal or addition of a like, zero-coupled pair of nucleons from the nucleus, and (c) the operator for allowed beta decay which changes one proton to a neutron or one neutron to a proton.

КВАЗИЧАСТИЦЫ И ВИБРАЦИОННЫЕ СОСТОЯНИЯ ЯДЕР. Дается описание структуры уровней, связанных с различными ядерными колебаниями. Показано, как такие вибрации могут быть описаны с помощью частичных и квазичастичных возбуждений в гармоническом приближении метода случайных фаз. Сравниваются колебания, соответствующие различным типам возбуждений. Рассматриваются движения, соответствующие увеличению трех различных простых операторов: а) одночастичный оператор E2-перехода, в) оператор поглощения или порождения спаренных нуклонов с нулевым моментом, с) оператор разрешенного β-распада, заменяющий протон на нейтрон или нейтрон на протон.

This paper discusses the description of collective nuclear vibrations in terms of single particle or quasiparticle excitations. It is assumed that a lowest order description of an even-even nucleus can be made, in which the nuclear ground state is the lowest state of an approximate Hamiltonian of the form of a sum of one-body interactions. This allows the possibility of a spherical or deformed Hartree-Fock solution, and if all bilinear combinations of creation and destruction operators are included as one-body interactions, it allows also a superconducting solution of the Bardeen, Cooper, Schrieffer type.

If this approximate ground state has a lower symmetry than the full Hamiltonian, the ground state and corresponding excited states must be obtained by projecting the approximate ground state on states with good quantum numbers corresponding to the full symmetry. Such excitations (for example, a rotational band) are collective in the sense that their excitation involves a change in many particles, but they are not the vibrations under discussion.

For this paper, collective vibrations are states other than those just discussed, for which the matrix element to the even-even ground state is strongly enhanced above the single particle value, for some simple one-body type of operator. These vibrational states will be described in terms of single particle and particle-hole excitations built on the ground state of the approximate one-body Hamiltonian.

Such collective vibrational states of low energy will occur whenever two different approximate ground states, of the type discussed in the first

paragraph, can be found with roughly the same total energy. For then the lowest approximate ground state may not be a very good approximation to the true state, as the nucleus will make relatively large excursions toward the other of the two approximate ground states. Excitations corresponding to this type of motion include 2^+ quadrupole vibrations of a spherical nucleus, where the second approximate ground state is one with a quadrupole deformation. The quadrupole transition operator $r^2Y_{2\mu}$ is strongly enhanced for such a state. These vibrations are distinguished from rotations by the fact that in addition to the 2^+ one-phonon state strongly connected by $r^2Y_{2\mu}$ to the ground state, there is also a two-phonon state at approximately twice the excitation energy strongly connected to the one-phonon state by $r^2Y_{2\mu}$.

Pairing vibrations are of the same type. The enhanced operator in this case is the pair transfer operator $[a_j^+ a_j^+]_0$ or its Hermitian conjugate. The competing approximate ground states are the normal and superconducting states. Since all but magic nuclei are in the superconducting state, such vibrations are expected only at magic numbers or in nuclei with a small or vanishing superconducting gap. The one-phonon states corresponding to the 0^+ ground state of the even-even nucleus (Z, N) will be the 0^+ ground states of (Z±2, N) and (Z, N±2). The pair transfer operator strongly connects (Z, N) to these one-phonon states. If there are real pairing vibrations there will also be two-phonon states strongly connected to the one-phonon states by the pair transfer operator. These will include excited 0^+ states of (Z, N). Thus pairing vibrations are characterized by strong transitions of the pair transfer operator from (Z, N-2) to both the ground state and an excited 0^+ state of (Z, N). This is in contrast to the BCS situation for which only ground state to ground state transitions would be enhanced.

The lowest approximate ground state (solution of the approximate one-body Hamiltonian) does not contain those correlations which would be introduced by that part of the true force which favours the second, nearby, approximate ground state. The effect of that part of the force is to lower the energy of certain of the independent particle excitations built on the lowest approximate ground state, and to collect the transition strength for the operator associated with the motions toward the second approximate ground state, so that a large fraction of that transition strength will appear in the lowest of these excited states. This lowest state is then called the phonon. At the same time, the lowest approximate ground state will acquire some ground state correlations.

Collective nuclear vibrations can also occur at relatively high excitation. This will be the case if there are force components not utilized by the approximate ground state, which resist the formation of a certain correlation. The effect of such a force component is to raise the energy of the corresponding independent particle excitations built on the approximate ground state, and to push them to higher energies, and perhaps collect the corresponding transition strength. The state or states receiving the transition strength will be called the phonon. Examples of this situation include the giant dipole state for the E1 operator, the analogue state associated with the $\tau_\pm$ operator, and the Gamov-Teller super multiplet states associated with the $\sigma\tau_\pm$ operator.

The only widely used treatments of all of these vibrations are the Tam Dancoff Approximation (TDA) or its extension to include the ground state

correlations, the Random Phase Approximation (RPA) [1]. The RPA treats all vibrations as harmonic and thus has the disadvantage that anharmonicities already apparent from the data cannot easily be treated. The proper treatment of such anharmonicities is one of the most interesting problems in theoretical nuclear physics today. However, RPA has the advantage of great simplicity, and in the rest of this paper only the structure of TDA and RPA for various possible modes of vibration will be discussed.

The approximate even-even ground state (solution of the one-body interactions) is $|0\rangle$, and the normalized, boson-like independent particle excitations built on it are specified by

$$|\nu\rangle = A^{\dagger}_{\nu}|0\rangle$$

$$A_{\nu}|0\rangle = 0$$

The operator $A^{\dagger}$ may create particle-hole excitations (or two quasiparticle excitations) in the same nucleus as that represented by $|0\rangle$, or it may create or destroy a pair of particles, producing a state in a neighbouring nucleus, or it might for example create a proton and destroy a neutron producing a state in an odd-odd nucleus. The Hamiltonian will not connect the states $|\nu\rangle$ and $|0\rangle$, since they will have different conserved quantum numbers for the modes considered.

Then within the zero and one "boson" space the only matrix elements are

$$H_{\mu\nu} = \langle 0|A_{\mu} H A^{\dagger}_{\nu}|0\rangle = \rho_{\mu\nu} + \delta_{\mu\nu}\langle 0|H|0\rangle \qquad (1)$$

where

$$\rho_{\mu\nu} = \langle 0|[A_{\mu}, H]\, A^{\dagger}_{\nu}|0\rangle \qquad (2)$$

Thus diagonalization of the Hamiltonian (1) referred to as TDA consists of diagonalizing the Hermitian matrix ρ of Eq. (2) to obtain the approximate energies and wave-functions.

The widely-used extension of TDA, namely RPA, is most easily obtained by considering the commutator in Eq. (2). If the commutator is expressed in terms of $A^{\dagger}$ and A and other normal ordered operators relative to $|0\rangle$ we obtain

$$[A_{\mu}, H] = \sum_{\nu} \rho_{\mu\nu} A_{\nu} + \sum_{\nu} \sigma_{\mu\nu} A^{\dagger}_{\nu} \quad + \text{other terms} \qquad (3a)$$

$$[A^{\dagger}_{\mu}, H] = -\sum_{\nu} \rho^{*}_{\mu\nu} A^{\dagger}_{\nu} - \sum_{\nu} \sigma^{*}_{\mu\nu} A_{\nu} \quad + \text{other terms.} \qquad (3b)$$

Eq. (3b) is simply the Hermitian conjugate to (3a). The definition of $\rho_{\mu\nu}$ is Eq. (2) while $\sigma_{\mu\nu}$ is defined by

$$\sigma_{\mu\nu} = -\langle 0|[A^{\dagger}_{\mu}, H]\, A^{\dagger}_{\nu}|0\rangle^{*} \qquad (4)$$

RPA consists of dropping the other terms in Eq. (3). Then if matrix elements of (3) are taken between the actual correlated nuclear ground state $\langle\psi_0|$ and the excited state $|\psi_W\rangle$ of energy W, one obtains

$$W\, r_\mu^W = \sum_\nu \rho_{\mu\nu}\, r_\nu^W + \sum_\nu \sigma_{\mu\nu}\, s_\nu^W \tag{5a}$$

$$W\, s_\mu^W = -\sum_\nu \sigma_{\mu\nu}^*\, r_\nu^W - \sum_\nu \rho_{\mu\nu}^*\, s_\nu^W , \tag{5b}$$

where

$$r_\mu^W = \langle\psi_0 | A_\mu | \psi_W\rangle \tag{6a}$$

$$s_\mu^W = \langle\psi_0 | A_\mu^\dagger | \psi_W\rangle \tag{6b}$$

The equations (5), linear and homogeneous in r and s, have non-trivial solutions only for values of W which are eigenvalues of the non-Hermitian matrix M where

$$M = \begin{bmatrix} \rho & \sigma \\ -\sigma^* & -\rho^* \end{bmatrix} \tag{7}$$

The RPA matrix elements, transition rates associated with the operators $A^\dagger$ and A, and approximate wave-functions are easily expressed in terms of r_μ^W and s_μ^W of Eq. (6). In particular one can write

$$|\psi_W\rangle = B_W^\dagger |\psi_0\rangle, \quad B_W |\psi_0\rangle = 0,$$

where

$$B_W^\dagger = \sum_\mu r_\mu^W\, A_\mu^\dagger - \sum_\mu s_\mu^W\, A_\mu$$

$$A_\mu^\dagger = \sum_W r_\mu^W\, B_W^\dagger + \sum_W s_\mu^W\, B_W$$

if Bose commutation relations are assumed for B and A. The correlated ground state can be written [2]

$$|\psi_0\rangle = \exp\left(\sum_{\mu\nu} \tfrac{1}{2}\, c_{\mu\nu}\, A_\mu^\dagger\, A_\nu^\dagger\right) |0\rangle$$

where $c = r^{-1}\, s$ or $s_\mu^W = \sum_\nu r_\nu^W\, c_{\nu\mu}$.

Different modes of vibration may now be treated by considering the structure of the $\rho_{\mu\nu}$ and $\sigma_{\mu\nu}$ matrices, Eqs (2) and (4), associated with the corresponding transition operators.

First consider quadrupole, low-energy vibrations. The analysis is the same for octupole vibrations. The transition operator is the quadrupole operator

$$Q = \sum_{ij} \langle i | r^2 Y_2 | j \rangle a_i^\dagger a_j$$

which creates particle hole excitations. To allow for a diffuse Fermi surface this may be written in terms of quasiparticles

$$Q = \sum_{\mu} q_\mu (A_\mu^\dagger + A_\mu) \tag{8a}$$

where

$$q_\mu = 5^{-\frac{1}{2}} \langle i \| r^2 Y_2 \| j \rangle (U_i V_j + U_j V_i) \tag{9a}$$

and the basic excitations are

$$A_\mu^\dagger = (\alpha_i^\dagger \alpha_j^\dagger)_{2^+} \tag{10a}$$

The $\alpha^\dagger$ are quasiparticle creation operators $\alpha_i^\dagger = U_i a_i^\dagger - V_i a_i$, and quasiparticle scattering terms of the form $\alpha^\dagger \alpha$ have been omitted. The factor $(U_i V_j + U_j V_i)$ represents the fact that particle-hole excitations are involved; it is small unless one member of the ij pair is more or less particle-like, $V \ll U$, and the other hole-like, $V \gg U$. The particle-hole or two quasiparticle excitation energy is $\mathscr{E}_\mu = E_i + E_j$ where E_i is the quasiparticle energy. That part of the force capable of causing quadrupole deformations and thus low-energy quadrupole vibrations is the quadrupole force

$$H_Q = -\tfrac{1}{2} \chi Q \cdot Q \tag{11a}$$

From Eqs (2), (4), (8a) and (11a) it follows at once that

$$\rho_{\mu\nu} = \delta_{\mu\nu} \mathscr{E}_\nu - \chi q_\mu q_\nu \tag{2a}$$

$$\sigma_{\mu\nu} = -\chi q_\mu q_\nu \tag{4a}$$

Each matrix is simply separable. It is easy to show that the eigenvalues of ρ are obtained from the dispersion equation

$$\text{TDA: } \frac{1}{\chi} = \sum_{\nu} \frac{q_\nu^2}{\mathscr{E}_\nu - W} \tag{12a}$$

while those of M, Eq. (7), are given by [3]

$$\text{RPA: } \frac{1}{\chi} = \sum_{\nu} \frac{2 q_\nu^2 \mathscr{E}_\nu}{\mathscr{E}_\nu^2 - W^2} \tag{13a}$$

The structure of levels given by Eq. (13a) is shown on Fig. 1. The RPA contains in addition to each positive root W, an equal negative spurious root. As χ increases to $\chi_{crit.}$, the lowest positive root of (13a) decreases to zero, and for larger χ values there are imaginary roots to (13a). Simple algebraic expressions may also be obtained for r_μ^W and s_μ^W and thus for the transition rates.

For pairing vibrations [4] let $|0\rangle$ represent a shell model wave-function with no pairing. The pair transfer operator is

$$\begin{aligned} P &= \sum_\nu \Omega_\nu A_\nu^\dagger \qquad \text{for empty states} \\ &= \sum_\nu \tilde{\Omega}_\nu A_\nu^\dagger \qquad \text{for full states} \end{aligned} \tag{8b}$$

where the sum on ν is over both particle and hole states but

$$\begin{aligned} \Omega_\nu &= (j_\nu + \tfrac{1}{2})^{\frac{1}{2}} \text{ for empty states, zero otherwise} \\ \tilde{\Omega}_\nu &= (j_\nu + \tfrac{1}{2})^{\frac{1}{2}} \text{ for full states, zero otherwise} \end{aligned} \tag{9b}$$

The basic excitations are

$$\begin{aligned} A_\nu^\dagger &= [a_{j_\nu}^\dagger \; a_{j_\nu}^\dagger]_0 \qquad \text{for empty states} \\ A_\nu^\dagger &= [a_{j_\nu} \; a_{j_\nu}]_0 \qquad \text{for full states.} \end{aligned} \tag{10b}$$

The energies of the basic excitations depend on the choice of zero for the single particle spectrum. If the zero is chosen to lie somewhere between the full and empty levels and if e_ν is the absolute magnitude of the energy difference between this zero of energy and the filled or empty single particle energy in question, the excitation energy of the basic excitations will be $\mathscr{E}_\nu = 2e_\nu$, a positive quantity for either particle or hole excitations. Finally, that part of the force capable of causing pairing deformations and thus also pairing vibrations is the pairing force

$$\begin{aligned} H_p &= -G \sum_{jj'} (j + \tfrac{1}{2})^{\frac{1}{2}} \; (j' + \tfrac{1}{2})^{\frac{1}{2}} \; [a_j^\dagger \; a_j^\dagger]_0 \; [a_{j'} \; a_{j'}]_0 \\ &= -G \sum_{\mu\nu} (\Omega_\mu A_\mu^\dagger + \tilde{\Omega}_\mu A_\mu)(\Omega_\nu A_\nu + \tilde{\Omega}_\nu A_\nu^\dagger) \end{aligned} \tag{11b}$$

From Eqs (2), (4), (8b), (10b), (11b) we obtain

$$\rho_{\mu\nu} = \delta_{\mu\nu} \mathscr{E}_\mu - G(\Omega_\mu \Omega_\nu + \tilde{\Omega}_\mu \tilde{\Omega}_\nu) \tag{2b}$$

$$\sigma_{\mu\nu} = -G(\Omega_\mu \tilde{\Omega}_\nu + \tilde{\Omega}_\mu \Omega_\nu) \tag{4b}$$

Since $\Omega_\nu \tilde{\Omega}_\nu = 0$, the $\rho_{\mu\nu}$ matrix is block diagonal and each of the two blocks is a separable form. These blocks simply describe the pairing of two

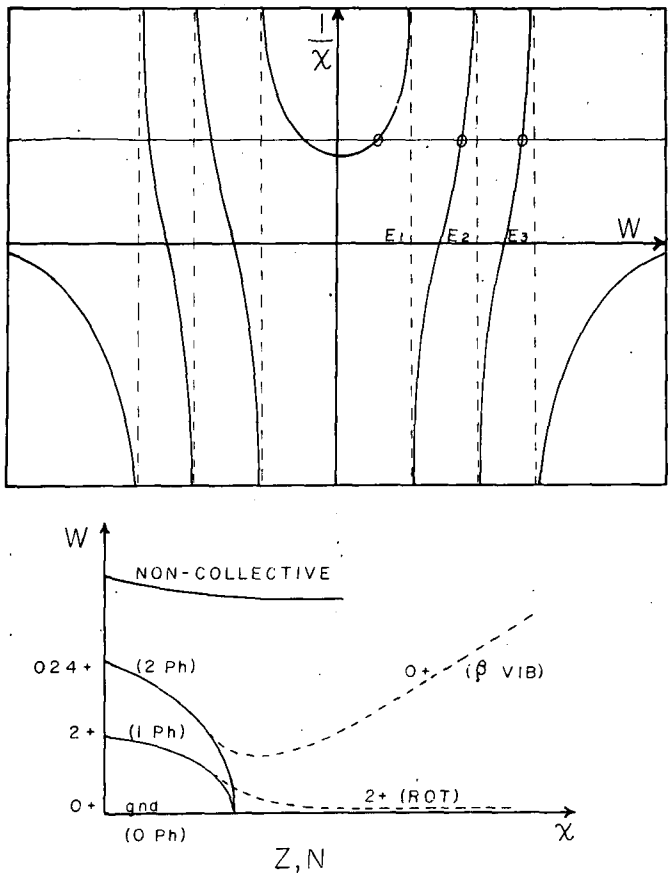

FIG. 1. Quadrupole vibrations. The structure of Eq.(13a) is shown by the solid lines of the upper figure. The solutions for a fixed value of χ are shown as circles and are seen to be shifted downward in energy from the original excitation energies $\mathscr{E}_i$. The solid lines of the lower figure show the 0, 1, and 2-phonon collective states and a non-collective state as given by the RPA, and the dashed lines follow the excited 2^+ and 0^+ levels as the coupling becomes so strong as to cause a stable quadrupole deformation. For χ near the value for which W goes to zero in RPA, there are large quadrupole matrix elements connecting the zero to one-phonon (Ph) states and the one- to two-phonon states.

particles in the empty levels of $|0\rangle$ and of two holes in the full levels of $|0\rangle$. The $\sigma_{\mu\nu}$ matrix connects the particle and hole spaces. Diagonalization of ρ gives

$$\text{TDA:}\quad \left[\sum_{\mu} \frac{\Omega_\mu^2}{\mathscr{E}_\mu - W} - \frac{1}{G}\right]\left[\sum_{\nu} \frac{\tilde{\Omega}_\nu^2}{\mathscr{E}_\nu - W} - \frac{1}{G}\right] = 0 \qquad (12b)$$

while the eigenvalues of M, Eq. (7), are given by

$$\text{RPA:}\quad \left[\sum_{\mu}\left(\frac{\Omega_\mu^2}{\mathscr{E}_\mu - W} + \frac{\tilde{\Omega}_\mu^2}{\mathscr{E}_\mu + W}\right) - \frac{1}{G}\right]\left[\sum_{\nu}\left(\frac{\tilde{\Omega}_\nu^2}{\mathscr{E}_\nu - W} + \frac{\Omega_\nu^2}{\mathscr{E}_\nu + W}\right) - \frac{1}{G}\right] = 0 \qquad (13b)$$

In (12b), setting the first square bracket to zero gives the two particle energies with pairing while the second gives the paired two-hole energies. In (13b), the second bracket gives the negatives of the roots of the first bracket so that one need solve only the first bracket equal to zero. The structure of this RPA solution from (13b) is shown in Fig. 2. However, the desired non-spurious roots are then the absolute values of the solutions so obtained.

The zero of energy for the single particle states may be chosen between the filled and empty states such that the lowest hole and particle excitations will decrease to zero at the same value of $G=G_{crit}$ beyond which imaginary roots of (13b) appear.

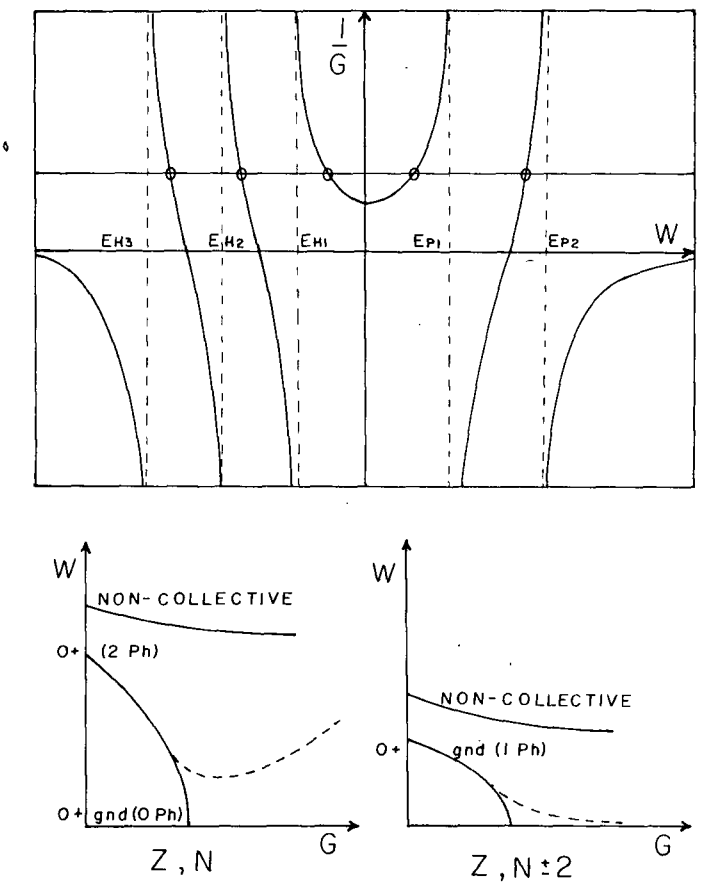

FIG. 2. Pairing vibrations. The structure of Eq. (13b) is shown by the solid lines of the upper figure together with their reflection (not shown) through the vertical axis. For a fixed value of G, the distances of the circles to the right (left) of the vertical axis from that axis represent the energies of 0^+ states in the nucleus Z, N+2(Z, N-2) relative to the ground state of Z, N. The solid lines of the lower figures show the zero-and two-phonon energies of Z, N and the one-phonon state of Z, N ± 2 as given in RPA, while the dashed curves show the development of those levels when G is strong enough to produce a superconducting solution. For G near the value for which W goes to zero in RPA, the two-particle transfer operator has large zero-to one-and one- to two-phonon matrix elements.

The relation between pairing and quadrupole vibrations should now be apparent. As χ increases from zero, the one-phonon state (2^+) becomes lower in energy and more collective going to W=0 at χ_{crit} in RPA, but in fact becoming a rotational excitation in actual nuclei (Project J=2 from deformed state). Likewise, as G increases, the one-phonon energy of the $A \pm 2$, ground states (0^+) decrease to zero at G_{crit} in RPA eliminating the closed shell gap,

$$\Delta E = \tfrac{1}{2} [E(A - 2) + E(A + 2)] - E(A)$$

At the same time the matrix element of the transfer operator increases. For $G > G_{crit}$ a pairing deformation exists and these states in $A \pm 2$ are actually obtained by projecting $|BCS\rangle$ on states of definite $N=A\pm2$.

The two-phonon energy also decreases in RPA. As χ passes χ_{crit}, the two-phonon quadrupole vibration goes over into a beta vibration of the deformed nucleus and subsequently rises in energy as χ increases and the deformed shape becomes more stable. Likewise, as G passes G_{crit}, the two-phonon pairing vibration, which is an excited 0^+ state of the A system itself, goes over into a two quasiparticle excitation in A, which rises in energy as G increases since it must lie above the pairing energy gap, 2Δ, which increases with G.

The same formalism may also be used to describe vibrations in which n, p transfer is involved. As an example, consider the operator for allowed Gamov-Teller beta transitions [5] (the identical equations can be used to discuss Fermi transitions if σ_μ is everywhere replaced by 1). As in (8b), two beta decay operators must be defined:

$$\beta^- = \sum_{pn} \langle p|\vec{\sigma}|n\rangle \, a_p^\dagger \, a_n$$

$$\beta^+ = \sum_{pn} \langle n|\vec{\sigma}|p\rangle \, a_n^\dagger \, a_p$$

To allow for a diffuse Fermi surface due to separate pairing of protons and neutrons, this can be expressed in terms of quasiparticles. Omitting quasiparticle scattering terms, we have

$$\begin{aligned} \beta^- &= \sum_\mu (\sigma_\mu \, A_\mu^\dagger - \tilde{\sigma}_\mu \, A_\mu) \\ \beta^+ &= \sum_\mu (\tilde{\sigma}_\mu \, A_\mu^\dagger + \sigma_\mu \, A_\mu) \end{aligned} \tag{8c}$$

where

$$\begin{aligned} \sigma_\mu &= 3^{-\frac{1}{2}} \langle p \| \vec{\sigma} \| n \rangle \, U_p \, V_n \\ \tilde{\sigma}_\mu &= 3^{-\frac{1}{2}} \langle p \| \vec{\sigma} \| n \rangle \, V_p \, U_n \end{aligned} \tag{9c}$$

and the basic excitation

$$A_\mu^\dagger = [\alpha_p^\dagger \, \alpha_n^\dagger]_{1^+} \tag{10c}$$

is from the even-even ground state to 1^+ states of the neighbouring odd-odd nuclei. These would be 0^+ for Fermi beta decay. The excitation energy $\mathscr{E}_\mu$ is just the sum of the proton and neutron quasiparticle energies $E_p + E_n$.

The excitations of interest are proton particle, neutron hole, or the opposite as seen from the factor $U_p V_n$, $V_p U_n$. Owing to the diffuse Fermi surface, a given pair of states (p, n) in an odd-odd nucleus will be able to execute both β^+ and β^- decay to $|0\rangle$, although, except for both p and n near their respective Fermi surfaces, the transition will be predominantly of one type. Thus in contrast to (9b), there are a number of excitations for which $\sigma_\mu \tilde{\sigma}_\mu \neq 0$.

The force component specific for shifting the Gamov-Teller strength is

$$H_{GT} = +X\, \vec{\sigma}\cdot\vec{\sigma}\ \vec{\tau}\cdot\vec{\tau}$$

the pertinent part of which can be written

$$H_{GT} = X \sum_{\mu\nu} (\sigma_\mu A^\dagger_\mu - \tilde{\sigma}_\mu A_\mu)\,(\tilde{\sigma}_\nu A^\dagger_\nu - \sigma_\nu A_\nu) \tag{11c}$$

Then

$$\rho_{\mu\nu} = \delta_{\mu\nu}\, \mathscr{E}_\mu + X(\sigma_\mu \sigma_\nu + \tilde{\sigma}_\mu \tilde{\sigma}_\nu) \tag{2c}$$

and

$$\sigma_{\mu\nu} = -X(\sigma_\mu \tilde{\sigma}_\nu + \tilde{\sigma}_\mu \sigma_\nu) \tag{4c}$$

Diagonalization of ρ yields

$$\text{TDA:} \left[\sum_\mu \frac{\sigma_\mu^2}{\mathscr{E}_\mu - W} + \frac{1}{X}\right]\left[\sum_\nu \frac{\sigma_\nu^2}{\mathscr{E}_\nu - W} + \frac{1}{X}\right] - \left[\sum_\mu \frac{\sigma_\mu \tilde{\sigma}_\mu}{\mathscr{E}_\mu - W}\right]^2 = 0 \tag{12c}$$

while diagonalization of M yields

$$\text{RPA:} \left[\sum_\mu \left(\frac{\sigma_\mu^2}{\mathscr{E}_\mu - W} + \frac{\tilde{\sigma}_\mu^2}{\mathscr{E}_\mu + W}\right) + \frac{1}{X}\right]\left[\sum_\nu \left(\frac{\tilde{\sigma}_\nu^2}{\mathscr{E}_\nu - W} + \frac{\sigma_\nu^2}{\mathscr{E}_\nu + W}\right) + \frac{1}{X}\right]$$

$$- \left[\sum_\mu \sigma_\mu \tilde{\sigma}_\mu \left(\frac{1}{\mathscr{E}_\mu - W} + \frac{1}{\mathscr{E}_\mu + W}\right)\right]^2 = 0 \tag{13c}$$

Eq. (13c) differs from (13b) by the last term of the former, due to the non-vanishing terms $\sigma_\mu \tilde{\sigma}_\mu$, and by the sign of the interaction, attractive for pairing vibrations, and repulsive for Gamov-Teller vibrations. The root structure of (13c) is shown in Fig. 3.

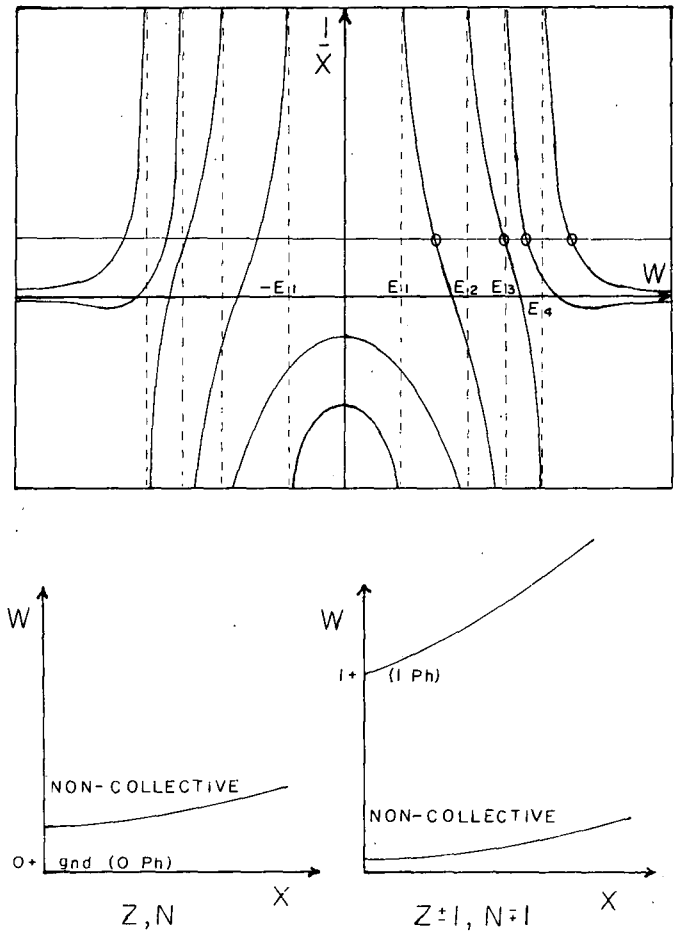

FIG.3. Gamov-Teller vibrations. The solid lines of the upper figure show the structure of Eq.(13c). The solutions for a fixed X, shown as circles, are raised from their unperturbed values. The lower figure shows that the top level rises indefinitely in energy and becomes the phonon. The two-phonon state of Z, N is too high in energy to be of interest. For strong coupling for heavy nuclei with a neutron excess, the beta decay operator will only connect the no-phonon ground state of Z, N with the one-phonon state of Z+1, N-1, its supermultiplet partner (or its isobaric analogue partner for the Fermi case).

For weak coupling (small X, G or X) RPA becomes TDA which is equivalent to a perturbation approximation. For strong coupling RPA yields imaginary solutions for the quadrupole and pairing vibrations at such a coupling strength that the original ground state $|0\rangle$ becomes unstable. In contrast, the repulsive pn force in strong coupling puts all the transition strength in the top level. In the limit of strong coupling this odd-odd state has an even-even ground state matrix element of the β transition operator identical with that to the super-multiplet state generated by H_{GT}. The analogous odd-odd state associated with Fermi transitions is the isotopic analogue state of $|0\rangle$. Thus the n, p RPA is correct in both weak and strong coupling.

The RPA has had great success in describing quadrupole vibrations in both odd and even nuclei, although it fails to yield the observed anharmonicities of excited states. For pairing vibrations there are some very interesting, but less conclusive results. For β decay, this formalism is able to help in explaining the retardation of allowed transitions between low states of heavy nuclei. With this formalism, it has been possible to gain considerable insight into the connection between the individual particle and collective vibrational motions of nuclei.

REFERENCES

[1] THOULESS, D.J., Nucl. Phys. 22 (1961) 78.
[2] SORENSEN, R.A., Nucl. Phys. 25 (1961) 674.
[3] BARANGER, M. Phys. Rev. 120 (1960) 957.
[4] BES, D.R., BROGLIA, R.A., Nucl. Phys. 80 (1966) 290.
[5] HALHLEIB, J.A., SORENSEN, R.A., Nucl. Phys. A98 (1967) 542.

ON EXCITED STATES WITH SMALL SPINS IN EVEN-EVEN DEFORMED NUCLEI

B.S. DZHELEPOV
V.G. KHLOPIN INSTITUTE OF RADIUM
AND
S.A. SHESTOPALOVA
D.I. MENDELEEV INSTITUTE OF METROLOGY
LENINGRAD, UNION OF SOVIET SOCIALIST REPUBLICS

Abstract — Аннотация

ON EXCITED STATES WITH SMALL SPINS IN EVEN-EVEN DEFORMED NUCLEI. The properties of 0_1^+, 2_1^+, 1^- and 1^+ states in even-even deformed nuclei of average weight ($150 < A < 194$) are discussed. All available information is used, but the paper is based mainly on information on the numerous excited states of these types occurring in the nucleus of ^{170}Yb. Attention is drawn particularly to the fact that several 0^+ states in the 1-2 MeV range can be detected in a number of nuclei (for example, in ^{164}Er there are five; in ^{170}Yb there are four; in ^{178}Hf there are three). The existing theories and hypotheses on the origin of 0^+ states are examined. At the present time it is not clear how observed and theoretical states can be compared, since no criteria have yet been developed for this purpose. In this study, a summary is made of all that is known of these criteria and an attempt is made to classify certain 0^+ states.

Data are adduced on twelve ^{170}Yb states with $I^\pi = 1^-$ and the transitions between them.

From seven states of the 1^+ type in ^{170}Yb, a single rotational pair of levels 1^+ and 2^+ is detected.

О ВОЗБУЖДЕННЫХ СОСТОЯНИЯХ С МАЛЫМИ СПИНАМИ В ЧЕТНО-ЧЕТНЫХ ДЕФОРМИРОВАННЫХ ЯДРАХ. Обсуждаются свойства состояний 0_1^+, 2_1^+, 1^- и 1^+ в четно-четных деформированных ядрах среднего веса ($150 < A < 194$). Используются все имеющиеся сведения, но основным материалом являются сведения о многочисленных возбужденных состояниях этих типов, имеющихся в ядре ^{170}Yb. Особое внимание обращено на факт обнаружения в ряде ядер нескольких состояний 0^+ в интервале 1 – 2 Мэв (например, в ^{164}Er их 5; в ^{170}Yb – 4; в ^{178}Hf – 3). Рассмотрены существующие теории и гипотезы о происхождении состояний 0^+. В настоящее время неясно, как сопоставлять наблюдающиеся и теоретические состояния, так как не разработаны еще критерии для сравнения. Суммировано то, что известно об этих критериях, и сделана попытка классифицировать некоторые 0^+ состояния. Приведены данные о 12 состояниях ^{170}Yb с $I^\pi = 1^-$ и переходах между ними. Среди 7 состояний типа 1^+ в ^{170}Yb обнаружена одна ротационная пара уровней 1^+ и 2^+.

This paper deals with the properties of states with $I^\pi = 0^+$, 2^+, 1^- and 1^+ in even-even deformed nuclei of average weight ($150 < A < 194$). All available information is used but the paper is based mainly on information on the numerous excited states of these types occurring in the nucleus of ^{170}Yb [1-3].

1. ON 0^+ STATES

Before 1955 no excited states of 0^+ type were known for even-even deformed nuclei of average weight, although in other regions of the periodic table such states had been known for some time. When 0^+ levels were first found for deformed nuclei, this caused no particular surprise; at excitation

energies greater than 1 MeV, nucleon pairs may be broken apart and the two free nucleons thus formed may produce two-particle states with widely differing I^{π}, including $I^{\pi} = 0^+$. It was also assumed that 0^+ states could occur in the event of radial vibrations of nuclear matter. In 1952 A. Bohr [4] studied the longitudinal and transverse quadrupole surface vibrations of a deformed axially-symmetrical nucleus, giving them the name by which they are still known, i.e. beta and gamma vibrations, and introducing the vibrational quantum numbers n_β and n_γ. In ensuing studies [5, 6] these concepts were developed, and in Ref. [6] (for the first time apparently) β and γ bands were represented. Over the last few years the amount of information on 0^+ states has increased considerably. So far these states are known to exist for 26 deformed nuclei of average weight. We do not know much about the properties of these states, but at least we no longer think that all these states are of the same type and can all be classified as 0^+_β states. The reason for this lies in the fact that in three nuclei, those of ^{164}Er, ^{170}Yb and ^{178}Hf, several 0^+ states have been detected in the 1-2.2 MeV range: in ^{164}Er there are five (1245.5, 1698.0, 1766.1, 2170.5 and 2185.0 keV); in ^{170}Yb there are four (1069.14, 1228.40, 1479.54 and 1565.98 keV); and in ^{178}Hf there are three (1199, 1434 and 144 keV). It is possible that this plurality of 0^+ levels is not a specific peculiarity of these three nuclei but a general rule, and it is merely that conditions are particularly favourable for detecting these levels in the case of these three nuclei; all three nuclei are obtained by beta-decay of nuclei with very small spins – 0^+ (^{170}Lu) and 1^+ (^{164}Tm and ^{178}Ta) – and at large decay energies.

The existence of a large number of low-lying 0^+ states raises the question of how are they to be classified. There are many theories and hypotheses on the origin of 0^+ states, possibly too many, but it is not clear how observed and theoretical states should be compared, since no criteria have been developed for this purpose. In the following paragraphs we shall summarize what we know of these criteria and attempt to classify certain 0^+ states.

2. MEASURABLE VALUES

Apart from the excitation energy of states, the following values are determined experimentally.

(1) Moments of inertia J_0

(2) X values:

$$X_0 = \frac{B(E0; 0_i^+ \to 0_g^+)}{B(E2; 0_i^+ \to 2_g^+)} \qquad X_2 = \frac{B(E0; 2_i^+ \to 2_g^+)}{B(E2; 2_i^+ \to 0_g^+)}$$

(3) Values r_2 and r_4:

$$r_2 = \frac{B(E2; 2_i^+ \to 2_g^+)}{B(E2; 2_i^+ \to 0_g^+)} \qquad r_4 = \frac{B(E2; 2_i^+ \to 4_g^+)}{B(E2; 2_i^+ \to 0_g^+)}$$

(4) The value $B(E2; 0_g^+ \to 2_i^+)$

(5) The values ρ_0^2, ρ_2^2, ρ_4^2 ...:

$$\rho_0^2 = \frac{1}{e^2 R_0^4} B(E0;0_i^+ \to 0_g^+) \qquad \rho_2^2 = \frac{1}{e^2 R_0^4} B(E0;2_i^+ \to 2_g^+)$$

In the following paragraphs the values J_0, X_0 and $B(E2;0_g^+ \to 2_i^+)$ will be considered; later we hope to consider the remainder. For 1^- and 1^+ states, measurements have been made for the ratios

$$R = \frac{B(L1;1 \to 2)}{B(L1;1 \to 0)}$$

where L1 represent E1 or M1, and the lower levels belong either to the 0_g^+ band (R_g) or to other 0_i^+ bands (R_i). In two cases the rotational pairs $1^+ - 2^+$ are known and for these the moment of inertia J_1 has been determined.

3. THEORIES CONCERNING 0^+ STATES

In order to interpret the accumulated information, theories are essential. At the time of writing, there are already a number of theories. We shall divide them into two groups.

(i) Theories describing collective motions – rotations and quadrupole vibrations in nuclei

A few studies, notably those of Davydov et al. [7, 8], Belyak and Zaikin [9] and Faessler, Greiner and Sheline [10], were devoted to the consideration of small quadrupole vibrations in weakly deformed nuclei. In this connection certain questions can be solved analytically [7-9], while for others, in particular the question of mixing the wave-functions of various states, numerical methods are appropriate [10].

In the article by Davydov and Chaban [11] no assumptions were made concerning the weak deformability of the nucleus. However, the non-axiality parameter γ of the nucleus was fixed (on the supposition that it has an effective value). Many of the quantitative deductions made in these studies differ a great deal, but they are in agreement on the main point, namely the general character of the sequence of excited states. In Fig. 1 excited states are represented for a "conventional" nucleus with $E_\gamma = E_\beta = 50\ \epsilon$ (parameters of the RV theory [10]), which must have properties very similar to those of the nucleus of ^{170}Yb. (For this nucleus $\epsilon = 24.6$ keV and theory predicts $E(0_\beta^+) \cong 1230$ keV, $E(2_\beta^+) \cong 1260$ keV and $E(2_\gamma^+) \cong 1330$ keV, while the observed values are $E(2_\gamma^+) = 1138.27$ keV and $E(0_i^+) = 1069.14$, 1228.40, 1479.54 and 1565.98 keV.) The energy of excited states in small vibration theories is expressed by the formula:

$$E = E_0 + n_\beta E_\beta + \left(2n_\gamma + \frac{K}{2}\right) E_\gamma + \{I(I+1) - K^2\} \cdot \frac{1}{2}\epsilon$$

where E_0 is the ground-state energy;
n_β and n_γ are vibrational quantum numbers equal to 0, 1, 2, ...;
E_β, E_γ, ϵ are parameters of the RV theory;
$I = 0, 2, 4 \ldots$ when $K = 0$, and $I = K, K+1, K+2 \ldots$ when $K \neq 0$.

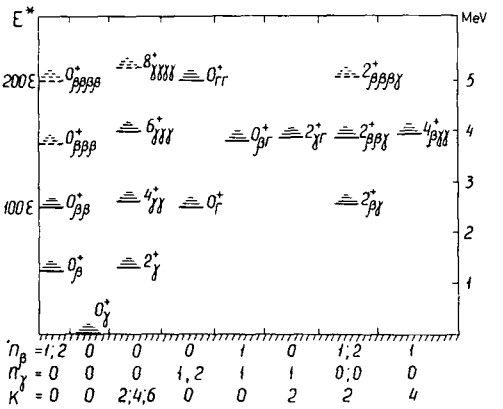

FIG. 1: System of collective levels of positive parity in an even-even deformed nucleus. Only the lower states of rotational bands are represented: the bands themselves are represented conventionally in a highly reduced form. The relative position of the bands depends on the ratio between the parameters E_β/ϵ and E_γ/ϵ in the RV theory or μ and Γ in the theory described in Ref. [36]. The case of $E_\beta = E_\gamma = 50\epsilon$ is represented, approximating to what should be the position in the nucleus of ^{170}Yb; the scale on the right-hand side in MeV is indicative only. Quantum numbers used in the energy formula are indicated under each band. Each figure β denotes energy $E_\beta = E(0^+_\beta)$ and spin 0; each γ denotes energy $E_\gamma + \epsilon = E(2^+_\gamma)$ and spin 2; each Γ denotes energy $2E_\gamma$ and spin 0. These are the energies of the levels if wave-function mixing is disregarded.

The states form rotational bands; the lower state of each band has I = K. The number of lower states is unlimited; for ^{170}Yb in the region up to 5 MeV there must be about 15; Fig. 1 clearly shows that for nuclei similar to ^{170}Yb, in the range from $E(0^+_1)$ to $2E(0^+_1)$, that is to say, practically in the range from 1 MeV to 2 MeV, there should be no other collective states of the 0^+ type. This deduction contradicts the experimental data for ^{164}Er, ^{170}Yb and ^{178}Hf.

In theories describing collective motions, transition intensities are also calculated. There are corresponding formulae in the small-vibration theory and in the theory of M. G. Davydov and Chaban. In their wave-function calculations, Faessler et al. took into account 13 states which are marked by means of thick lines in Fig. 1; here

$$\Psi = \sum_{i=1}^{13} C_i \psi_i$$

However, when states with small spins are considered, only three lower bands (g, β and γ) emerge. A table of energies and the coefficients C_g, C_β and C_γ is given in Ref. [10]. From this it is possible to calculate B(E0), B(E2), J_β, J_γ, r_2, r_4, etc. The results of calculations made of these values, both for the small vibration theory of Faessler et al. [10] and for the work of Davydov and Chaban [11], are discussed in the following paragraphs.

(ii) Microscopic theories

In microscopic theories, assumptions are initially made about the behaviour of separate nucleons within the nucleus. In order to describe

the properties of 0^+ states in a nucleus consisting of many nucleons, it is necessary to sum, in one way or another, the contributions made by separate nucleons. In this process some types of 0^+ states are noted which perhaps do not even exist in a 'pure' form, but which may be theoretically conceived in a pure form:

(a) Beta-vibrations caused by the superposition of a large number of two-quasiparticle states and residual quadrupole-quadrupole interactions. 0^+_{QQ} states are, as a general rule, low-lying and are characterized by relatively high B(E2) values, exceeding single-particle values, and X_0 values in the neighbourhood of 0.3. Calculations were made by Bes [12] and Soloviev et al. [13, 14] on the basis of Nilsson single-particle functions, taking into account pairing and quadrupole-quadrupole interactions. Calculations of the energy of the lower 0^+_{QQ} state have been made for 29 nuclei of the category under review [14], and in all cases the energy lies in the 0.8-1.7 MeV range. Calculations of the second 0^+_{QQ} state were made for only two nuclei and gave an energy 0.3 MeV higher than for the lower 0^+_{QQ} state;

(b) It is possible to find 0^+_π states in which the pairs are not broken apart and each pair is on its own level, excitation of the nucleus being explained by pair vibrations. These states must lie higher than 1.4 MeV. They were considered by Bohr and Mottelson in 1964 [15] and further studied by Bes and Broglia [16], Soloviev [13] and Kuliev and Pyatov [17];

(c) Belyaev [18] considered a particular kind of pair vibration, formally differing from those mentioned above in the parity of the time inversion operator. He called them 'coherent pairing fluctuations', bearing in mind that in the pair vibrations of Bohr and Mottelson, the contributions from particle and hole excitations were of different signs but in the states under consideration the contributions were all of the same sign. For 0^+_σ states of this type there must be a high probability of E0-transition to the ground state and often low values of B(E2);

(d) Spin-quadrupole excitations of the type 0^+ are due to the superposition of states in which at least one pair is broken apart and quasiparticles can be found at various levels. States of this type, which we shall hereinafter designate $0^+_{\sigma Q}$ states, were examined by Pyatov et al. [17, 19 - 21]. They may be low-lying but must have low values of $X \ll 1$ and B(E0). Kuliev and Pyatov [17] point out that "$0^+_{\sigma Q}$ states with structures resembling two-quasiparticle states must have particularly low X values if quasiparticles can be found at various levels of one and the same shell". Kuliev and Pyatov calculated B(E0), B(E2) and X_0 for $0^+_{\sigma Q}$ states in a number of deformed nuclei in rare earths.

4. MOMENTS OF INERTIA J_0

Moments of inertia of 0^+_i states are determined by the formula:

$$J_0 = \frac{E(2^+_g)}{E(2^+_i) - E(0^+_i)} J_g$$

where J_g is the moment of inertia of the ground state of the nucleus. There is information on 19 0_i^+ states (see Table I).

The experimental values of J_0/J_g lie in the 0.70 - 1.55 range. Since the energies can usually be determined with a high degree of precision,

TABLE I. EXPERIMENTAL VALUES OF J_0/J_g

The sign ↓ indicates that level 2_γ^+ is higher than level 2_β^+ so that taking their mutual repulsion into account may reduce J_0/J_g; the sign ↑ indicates that the 2_γ^+ level is below 2_β^+

1	2	3	4	5	6
Nucleus	Energy level in keV			J_0/J_g	References
	0_i^+	2_i^+	2_g^+		
^{152}Sm	685.0	810.7	121.78	0.968 ↓	[23, 24]
^{154}Gd	680.6	815.7	123.07	0.911 ↓	[25]
^{156}Dy	675.80	828.9	137.80	0.898 ↓	[26]
^{158}Dy	986.1	1085.0	98.90	1.00 ↑	[27]
^{160}Dy	1263	1350	86.8	0.998 ↑	[32]
^{164}Er	1245.5	1334	91.4	1.033 ↑	[30]
^{164}Er	1698	1789	91.4	1.004 ↑	[30]
^{168}Yb	1150	1233	87.9	1.059 ↑	[28]
^{168}Yb	(1156)	1233	87.9	(1.14) ↑	[22]
^{170}Yb	1069.14	1145.42	84.26	1.105 ↑	[3]
^{170}Yb	1228.4	1306.03	84.26	1.086 ↑	[3]
^{170}Yb	1479.54	1534.16	84.26	1.542 ↑	[3]
^{170}Yb	1565.98	1648.2	84.26	1.027 ↑	[3]
^{172}Yb	1045	1116	78.7	1.11 ↓	[28]
^{174}Hf	827	899	91.0	1.26 -	[22]
^{174}Hf	(1241)	1330	91.0	1.02 -	[22]
^{178}Hf	1199	1276	93.17	1.275 ↑	[31]
^{180}W	(908)	1008	103.6	1.036 ↑	[22]
^{188}Os	1086	1306	155.03	0.705 -	[29]

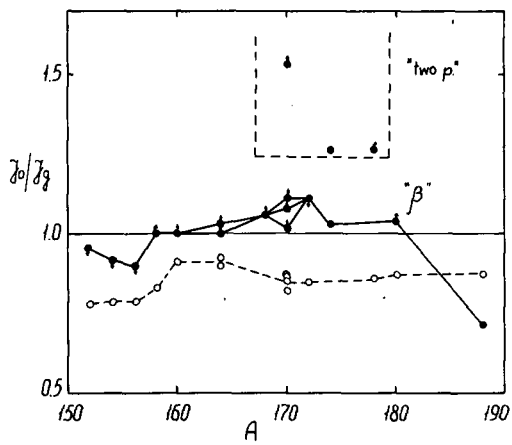

FIG. 2. Moments of inertia of 0_1^+, 2_1^+ bands; "β" merely indicates that 0_1^+, 2_1^+ states behave as β-bands; "two p." denotes two-particle states.

the differences in J_0/J_g are clearly not due to measuring errors but to 'internal' reasons (in most cases the error is less than the size of the points in Fig. 2). The arrangement of the points in Fig. 2 is such that it is necessary to divide them into two groups:

a group in which J_0 differs from J_g by no more than ± 11%;

a group of three points (1479.54 keV for ^{170}Yb, 827 keV for ^{174}Hf and ^{178}Hf) in which J_0 is considerably higher than J_g.

The first group evidently includes 0_β^+ states (thus this group is marked "β" in Fig. 2) but since for certain nuclei this group includes a number of points yet there is only one 0_β^+ state, we can only affirm that the group includes various states resembling 0_β^+ in regard to their moment of inertia. The second group evidently includes two-particle 0^+ states (and this group is marked "two p." in Fig. 2).

We shall begin by studying the first group. Within the group a spread of points can be observed, which even if not large, cannot be explained by simple experimental errors.

It was possible to surmise that the vibrations in J_0/J_g were caused by repulsion of the levels 2_1^+ and 2_γ^+; for levels 2_β^+ and 2_γ^+ this could actually be observed. If the 2_γ^+ level is located higher than 2_1^+ (Fig. 3a), the repulsion should reduce the distance between 2_1^+ and 0_1^+, that is increase J_0/J_g; if 2_γ^+ is lower than 2_1^+, the repulsion should decrease J_0/J_g. In Table I and Fig. 2 arrows are placed by the values for J_0/J_g, showing how J_0/J_g should change if repulsion is excluded. Judging by the direction of the arrows, taking repulsion into account does not bring the points closer to any sort of smooth curve. It is strange that the point for ^{170}Yb, for which the energies $E(2_1^+) = 1145.42$ keV and $E(2_\gamma^+) = 1138.27$ keV are in close proximity, thus giving rise, one would think, to a strong anomaly, gives $J_0/J_g = 1.105$. Allowing for repulsion in this case should increase J_0/J_g even more, that is move the point away from a smooth curve.

The theory of small quadrupole vibrations of weakly deformed (μ, $\Gamma < 0.3$), axially symmetrical ($\gamma_0 = 0$; $\beta_0 \neq 0$) nuclei is set out in the book by Davydov [11]. From formula (14.38) of Ref. [11] it follows that in this theory 'in the zero approximation' $J_0/J_g = 1$. In the theory of Davydov and

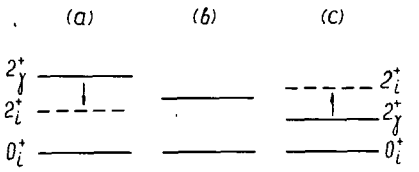

FIG. 3. Change in the $2^+_i - 0^+_i$ spacing under the influence of level 2^+_γ.
(a) Level 2^+_γ slightly higher than level 2^+_i; because of their repulsion, levels 2^+_i and 0^+_i are drawn together and J_0/J_g become higher;
(b) Level 2^+_γ remote from level 2^+_i; the distance between 2^+_i and 0^+_i is not distorted;
(c) Level 2^+_γ is lower than 2^+_i and repulsion results in J_0/J_g becoming lower.

Chaban (β vibrations for fixed γ) at low μ values $J_\beta/J_g = 1 - 3\mu^2$ (see Davydov [11], p. 125). For the μ values encountered in reading (between 0.15 and 0.38) this formula does not always hold true; in this case J_β/J_g may easily be obtained by interpolating for μ and Γ Davydov's Table 24. The calculated values for J_β/J_g are represented by open rings in Fig. 2. Similar results are given by the theory of Faessler, Greiner and Sheline (RV-theory). This is clear from Table II.

The majority of nuclei in Table I fall within the E_β/ϵ and E_γ/ϵ range covered by Table II. Thus the RV theory predicts that for all nuclei J_β/J_g must be within the 0.73-0.90 range; in this respect it agrees with the theory of Davydov and Chaban. Both theories correctly predict a certain reduction of J_β/J_g for low-lying level 0^+ (for example, in ^{152}Sm, ^{154}Gd, ^{156}Dy). However, J_β/J_g for both theories is always less than 1 (by 10 to 20%) and in this respect they contradict experiment.

For the time being there is nothing to be said about the second group of points. An odd particle usually increases the moment of inertia (sometimes by 100% in comparison to the neighbouring even-even nuclei). Hence it is not surprising that two quasiparticles may considerably increase the moment of inertia — for example by 54% of J_g for the 1479.54 keV level in ^{170}Yb.

TABLE II. VALUES OF $J_\beta/J_g = \dfrac{E(2^+_g)}{E(2^+_i) - E(0^+_i)}$ ACCORDING TO THE RV THEORY

E_β/ϵ	E_γ/ϵ = 30	50	70
20	0.75	0.73	0.73
30	0.79	0.80	0.80
50	0.87	0.86	0.86
70	0.86	0.90	0.89

5. VALUES OF $X_0 = B(E0;0_i^+ \rightarrow 0_g^+)/B(E2;0_i^+ \rightarrow 2_g^+)$

Values for X_0 are listed in Table III. The values were calculated by the formula

$$X_0 = \frac{2.54\times10^9 A^{4/3} E_\gamma^5 \alpha_K^{E2}}{\Omega_K} \cdot \frac{K(0^+ \rightarrow 0^+)}{K(0^+ \rightarrow 2^+)} \qquad (1)$$

Most X_0 values lie in the 0.10 - 1.0 range. However, there are also very low – 0.0037 – and very high – 5.56 – values. At all events, this is indicative of the fact that the 0_i^+ levels encountered in Table I differ in respect of their physical nature.

TABLE III. VALUES OF $X_0 = B(E0;0_i^+ \rightarrow 0_g^+)/B(E2;0_i^+ \rightarrow 2_g^+)$

1	2	3	4	5
Nucleus	0_i^+ energy (keV)	X_0	References	X_0 for $0^+_{\sigma Q}$ [17]
^{152}Sm	685.0	0.10 ± 0.03	[23, 24]	0.20
^{154}Gd	680.6	0.30 ± 0.18	[33]	0.20
^{156}Gd	1010	0.89 ± 0.31	[34]	0.20
^{164}Er	1245.5	0.15 ± 0.03	[30]	0.13
^{164}Er	1698.2	0.39 ± 0.06	[30]	0.34
^{164}Er	1766.1	0.78 ± 0.11	[30]	0.87
^{164}Er	2170.5	1.76 ± 0.25	[30]	0.08
^{164}Er	2185.0	5.56 ± 1.84	[30]	0.03
^{168}Yb	1197	>1.1; 0.51	[22]	0.13
^{168}Yb	1543	>3.1; 0.76	[22]	0.13
^{170}Yb	1069.14	0.0025 ± 0.0005	[3]	0.14
^{170}Yb	1228.4	0.094 ± 0.012	[3]	0.29
^{170}Yb	1479.54	0.94 ± 0.07	[3]	0.05
^{170}Yb	1565.98	0.51 ± 0.12	[3]	
^{178}Hf	1199	0.18 ± 0.04	[31]	0.18
^{178}Hf	1434	0.10 ± 0.02	[31]	0.30
^{178}Hf	1444	0.38 ± 0.08	[31]	0.24

The X_0 values for 0^+ states may be computed using both 'macroscopic' theories, allowing only for collective motions – vibrations and rotations – and 'microscopic' theories, in which the calculations are based on the motion of individual nucleons.

Among macroscopic studies mention must be made first of the work of Rasmussen [35] who obtained the following formula for the longitudinal vibrations of a uniformly charged ellipsoid of revolution:

$$X_0 = 4\beta^2$$

where β is a parameter of axial deformation. For the majority of nuclei under consideration, β lies between 0.2 and 0.3, and therefore X_0 must lie between 0.16 and 0.36. For a few nuclei X_0 actually has a value near to this.

Further development of the theory allowed for longitudinal and transverse vibrations, and 0^+_β and 0^+_Γ states were discovered (we shall introduce the symbol 0^+_Γ for the ground states of transverse vibrational states). Calculations of the energy of these states and the corresponding B(E0) and X values were carried out by Davydov, Rostovsky and Chaban [36] for small quadrupole vibrations. The calculations showed that 0^+_β states had the least energy. The excitation energy of 0^+_Γ states is approximately double (see for example Fig. 1). It is conceivable, of course, that for some reason or other the 0^+_Γ level may fall. For 0^+_β states Davydov et al. obtained:

$$X(0^+_\beta) = 4\beta^2\left[1+\frac{E(2^+_g)}{E(2^+_\gamma)}\right] \qquad (2)$$

Inasmuch as $E(2^+_\gamma)$ is usually about 10 times higher than $E(2^+_g)$, the second term is a small correction to the Rasmussen value $4\beta^2$ and is sometimes written in this way: $X(0^+_\beta) \cong 4.4\beta^2$).

The 0^+_Γ levels must have a significantly higher X_0 value. According to Davydov:

$$X(0^+_\Gamma) = 36\beta^2\left[1-\left(\frac{E(0^+_\beta)}{E(2^+_\gamma)}\right)^2\right]^{-2} \qquad (3)$$

(see Ref. [36], p. 181). Without the second multiplier, $X(0^+_\Gamma) = 36\beta^2$, that is 9 times higher than $X(0^+_\beta)$, and as a rule, $X(0^+_\Gamma)$ must be greater than 1. The additional multiplier increases $X(0^+_\Gamma)$ even more, and it may be very large. Clearly, significance should not be given to the resonance aspect of this multiplier, that is, to the fact that it tends to infinity when $E(0^+_\beta) \to E(2^+_\gamma)$: the given formula is only an approximate one.

Theoretical predictions for the value of X_0 in microscopic theories are extremely vague; this is partly due to the fact that X is equal to the ratio between B(E0) and B(E2), and each of these quantities may have widely differing values. In microscopic theories of beta vibrations the value obtained for X_0 is about 0.3.

Kuliev and Pyatov [17] calculated the X values for 0^+ states of two other types: pair vibrations and spin-quadrupole excitation (see section 3). Pair vibrations in deformed nuclei of average weight produce 0^+_Π states with energies larger than 1.45 MeV; probably the lowest 0^+ states observed experimentally are of a different nature. Pair vibrations are charac-

terized by pronounced fluctuations in B(E0) and B(E2) and as a result the values of X_0 for different nuclei may differ by a factor of 10 000 or more (from 0.002 to 54).

In $0^+_{\sigma Q}$ states resulting from spin-quadrupole interactions, B(E0), B(E2) and X fluctuate sharply for different states. If we limit ourselves only to the lowest $0^+_{\sigma Q}$ states, the range of X_0 values is small: from 0.13 to 0.20. However, if we consider the two to three lowest states, the range of X_0 values becomes considerably larger – from 0.001 to 4.7 – and covers almost all experimental values.

In a paper by Belyaev and Rumyantsev [37], it was shown that 0^+_σ states must have an energy of 1.2 - 1.5 MeV, values of $B(E0;0^+_\sigma \to 0^+_g)$ similar to 0^+_{QQ} states, and values of $B(E2;0^+_\sigma \to 2^+_g)$ three to four times lower, that is to say X_0 values, three to four times higher, than 0^+_{QQ} states.

In a paper presented in Moscow, March 1968, Belyaev pointed out that estimates for ^{152}Sm have B(E2) values of about 4×10^{-5}, and ρ^2 values of 0.8 (consequently, very large X values).

To sum up, the following conclusion may be drawn: whereas macroscopic theories predict for all nuclei $X(0^+_\beta)$ values in the range 0.2 - 0.4 and $X(0^+_\gamma) \geq 2$, microscopic theories make it possible in principle to explain both very low (~0.001) and very high (~50) X_0 values. For the time being, however, it is scarcely possible to identify specific states in terms of their X_0 values, because of the simplified method of describing nucleon motion, which underlies microscopic theories.

6. VALUES OF s

The value of $s = \dfrac{\{B(E0)/B(E2)\}2^+_i}{\{B(E0)/B(E2)\}0^+_i} = \dfrac{X_2}{5X_0}$ must be equal to 1 if the states 0^+_i and 2^+_i are completely identical in their internal structure, have a good quantum number K and differ only in their rotation. It may differ slightly from 1 if small 'alien' components appear in the wave-functions of the states 0^+_i and 2^+_i. It may be expected that in $(0^+_i 2^+_i)$, $(0^+_j 2^+_j)$, ..., pairs differing completely in nature (and therefore having completely different X_0 and X_2, etc.) the value of s will not differ greatly from 1: it is essential that the main wave-function components of the states of one pair should be the same and the small components from the admixtures sufficiently small. The best method of checking that the levels 0^+_i and 2^+_i actually form a rotational pair is by directly determining s from experimental data. All 0^+ and 2^+ pairs should be checked in this way, but at the moment there are

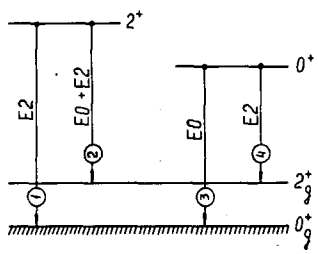

FIG.4. Diagram showing transitions to formula (5).

data for only four pairs. The value of s is determined from experimental data by the formula:

$$s = \frac{1}{5}\frac{K_2K_4}{K_1K_3}\frac{\Omega_{3K}}{\Omega_{2K}}\left(\frac{E_1}{E_4}\right)^5\frac{(\alpha_K^{E2})_1}{(\alpha_K^{E2})_4}\left\{1 - \frac{10}{7}\frac{K_1}{K_2}\left(\frac{E_2}{E_1}\right)^5\frac{(\alpha_K^{E2})_2}{(\alpha_K^{E2})_1}\right\} \quad (5)$$

The meaning of the symbols is clear from Fig. 4. K_n denotes the conversion line intensities.

The following s values are known:

^{170}Yb	0^+: 1228.4 keV	$s = 0.67 \pm 0.17$ [3]
	0^+: 1479.54 keV	$s = 1.50 \pm 0.18$ [3]
^{178}Hf	0^+: 1197 keV	$s = 0.8 \pm 0.3$ [31]
	0^+: 1434 keV	$s = 1.2 \pm 0.5$ [31]

They are all actually close to 1. In the RV theory, s depends on the parameters E_β/ϵ and E_γ/ϵ. Belenky computed s for several pairs of parameters; the results are listed in Table IV. For almost all cases of interest $s = 1.4 \pm 0.2$. We should note that the s value in each column is minimum when $E_\beta = E_\gamma$, due to the proximity of the $\beta\gamma$-resonance; if this is so, perhaps s is near to this resonance and less than 1.4.

TABLE IV. VALUES OF s

E_β/ϵ	E_γ/ϵ = 30	50	70
30	1.57	2.13	2.09
50	1.48	1.29	1.60
70	1.34	1.34	1.20

7. VALUES OF $B(E2;0_g^+ \rightarrow 2_i^+)$

2_i^+ rotational levels are now known for 25 0_i^+ nuclear states. Their detection is facilitated by the possibility of Coulomb excitation $0_g^+ \rightarrow 2_i^+$, and their identification (decay characteristics) by the strong E0-components in the $2_i^+ \rightarrow 2_g^+$ transition and the relative intensity of the $2_i^+ \rightarrow 4_g^+$ transition. The Coulomb excitation of 2^+ levels was studied by Sheline et al. [38], Gangrsky et al. [39] and Yoshizawa et al. [40]. From the $B(E2;0_g^+ \rightarrow 2_i^+)$ values determined by them, $T_{\frac{1}{2}\text{ part.}}$ values for $(2_i^+ \rightarrow 0_g^+)$ have been calculated:

$$T_{\frac{1}{2}\text{ part.}}(2_i^+ \rightarrow 0_g^+) = \frac{283}{\{E(2_i^+)_{\text{keV}}\}^5 B(E2;0_g^+ \rightarrow 2_i^+)}\ \text{sec} \quad (6)$$

These values are listed in Table V. They are all in the range (2 - 13) $\times 10^{-12}$ sec. In order to determine the half-life $T_{\frac{1}{2}}$ of level (2_i^+), it is necessary to take into account all discharge channels:

$$T_{\frac{1}{2}}(2_i^+) = \frac{\lambda(2_i^+ \to 0_g^+)}{\Sigma\lambda} T_{\frac{1}{2}\ \text{part.}}\ (2_i^+ \to 0_g^+) \qquad (7)$$

In most cases this can only be done approximately, since the relative intensities of all three transitions – to 0_g, 2_g and 4_g – have not been measured.

The channel $2_i^+ \to 0_g^+$ is responsible for approximately one-fifth of the decay events affecting the state 2_i^+, therefore $T_{\frac{1}{2}}(2_i^+) = 1/5\ T_{\frac{1}{2}\ \text{part.}}\ (2_i^+ \to 0_g^+)$ and amounts to approximately 1 picosecond (10^{-12} sec).

This low value for $T_{\frac{1}{2}}(2_i^+)$ in the first place practically excludes all methods of measuring $T_{\frac{1}{2}}$ other than by means of Coulomb excitation, and

TABLE V. VALUES OF $B(E2;0_g^+ \to 2_i^+)$ AND LIFETIMES OF 2_i^+ LEVELS

Nucleus	Energy of 2_i^+ level in keV	$B(E2;0_g^+ \to 2_i^+)$ in b^2e^2	$T_{\frac{1}{2}}$ part. for $2_i^+ \to 0_g^+$ in 10^{-12} sec (formula (6))	$B(E2;0_g^+ \to 2_i^+)$calc. Davydov (formula (8))	Soloviev [c] [14]
^{150}Nd	840 [32]	0.12 ± 0.03 [32]	5.6 ± 1.4	0.216	0.13
^{152}Sm	810.7	0.07 ± 0.02 [34] 0.065 ± 0.025 [35] 0.061 ± 0.014 [32]	13 ± 3	0.271	0.11
^{154}Sm	1180 [32]	0.030 ± 0.007 [32]	4.1 ± 1.0	0.302	0.074
^{154}Gd	815.7	0.12 ± 0.08 [32]	6 ± 4	0.179	0.25
^{156}Gd	1130 [32]	0.07 ± 0.03 [32]	2.2 ± 1.0	0.209	0.070
^{158}Dy	1083	0.0076 [7]	< 2.5	0.163	
^{164}Er	1308 [a]	0.0013 [7]	< 57	0.189	0.013
^{168}Yb	1233	0.028 [7]	~ 3.5		
^{174}Yb	(1400) [b]	0.015 [32]	> 3.5		
^{174}Hf	899	0.12 [7]	< 4		
^{186}Os	-	0.231 [33]			
^{188}Os	-	0.245 [33]			
^{190}Os	-	0.243 [33]			
^{192}Os	-	0.180 [33]			

[a] According to Ref. [30] there is no such level.

[b] The state 0^+ was introduced by Wilson and Pool, and states 2^+ and 4^+ by De Boer et al.; not yet confirmed.

[c] The data given in Ref. [14], Table 13, in the column headed "B(E2) from level $I^\pi K = 2^+$ 0, experiment" probably relate to the transition to the level $I^\pi K = 2^+$ 0, i.e. give the value $B(E2; 0_g^+ \to 2_i^+)$.

in the second place, makes it very difficult to observe the intra-band transition $2_i^+ \to 0_i^+$ for which $T_{\frac{1}{2}\text{ part.}}$ $(2_i^+ \to 0_i^+)$ is about 10^{-9} sec, and consequently the $\gamma(2_i^+ \to 0_i^+)$ intensity is approximately one thousand times less than for $\gamma(2_i^+ \to 0_g^+)$. So far the intra-band transitions $2_i^+ \to 0_i^+$ and $4_i^+ \to 2_i^+$ have never been observed, although there is no doubt about their existence or about the correspondence between their intensity and theory. Comparing the values for $T_{\frac{1}{2}\text{ part.}}$ $(2_i^+ \to 0_g^+)$ listed in Table V, we may note that they all lie in a relatively narrow range from 2 to 13 picoseconds. This shows that the properties of these states are similar to those of E2 transitions to the g-band.

In the theories describing small quadrupole vibrations of ellipsoids of revolution, the values of $T_{\frac{1}{2}}(2_i^+ \to 0_g^+)$ should not differ widely for different nuclei. In Davydov's book [11] we find the formula:

$$B(E2;2_\beta^+ \to 0_g^+) = \frac{1}{2q}\left(1 - \frac{1}{S_\gamma}\right)\frac{Q_0^2}{16\pi} \qquad (8)$$

where

$$S_\gamma = \frac{E(2_\gamma^+)}{E(2_g^+)} \qquad \text{and} \qquad q = \frac{E(0_\beta^+)}{E(2_g^+)}$$

Substituting in this the energies of states 2_g^+, 0_β^+ and 2_γ^+ and the quadrupole moments Q_0 from Ref. [41], we find values for $B(E2; 0_g^+ \to 2_\beta^+)_{\text{calc.}}$; and these are given in Table V. The calculated values exceed $B(E2;0_g^+ \to 2_\beta^+)_{\text{exp.}}$ by $1\frac{1}{2}$ to 6 times. Allowing for the simplicity of the theory such agreement can be regarded as attesting its unqualified success. Unfortunately, the experimental data mainly relate only to one extremity of the deformed-nuclei region. In the microscopic model developed by Soloviev [14] (Nilsson functions, pairing and quadrupole forces), the values of $B(E2;0_g^+ \to 2_{QQ}^+)$ were calculated with constants obtained from power engineering; they are listed in Table V and differ from the experimental ones by a factor of approximately two (the difference is less than in the theory of small quadrupole vibrations).

8. STATES WITH $I^\pi = 1^-$

Theory predicts the possible existence of four types of states with $I^\pi = 1^-$:

(1) Octupole vibrations of nuclear matter with K = 0 and spin sequence 1^-, 3^-, 5^-...

(2) Mixed octupole-quadrupole vibrations $(3^- + 2^+)$ with K = 1 and spin sequence 1, 2, 3 ...

(3) Two-particle states with $I^\pi = 1^-$ 1 with normal spin sequence 1^-, 2^-, 3^-, 4^- ...

(4) Two-particle states with K = 0 and split band 0^-, 2^-, 4^- ... and 1^-, 3^-, 5^- ..., the two parts of which may be at a considerable distance from each other (in particular, because the first may lie much higher than the second and thus have low excitation).

In the region of deformed nuclei of average weight, states of the 1^- type are seldom found: in the decay schemes of 1963 there were only nine.

But now 12 states with $I^{\pi} = 1^-$ have been found in the ^{170}Yb nucleus (Fig. 5). Unfortunately, not one of them has yet been found with a rotational level: for the sequence 1^-, 3^-, 5^- this is too much to hope for, but for the sequence 1^-, 2^-, 3^- the 2^- level could have manifested itself.

Figure 5 also gives the ratios of the probabilities (as cited in the literature) for transitions to the rotational band of the ground state (R_g) and to the band of other 0_i^+ levels (R_i). The possibility of an M2 admixture in transitions $1^- \rightarrow 2^+$ was not taken into account: conversion coefficient measurements are not sufficiently accurate for this admixture to be detected.

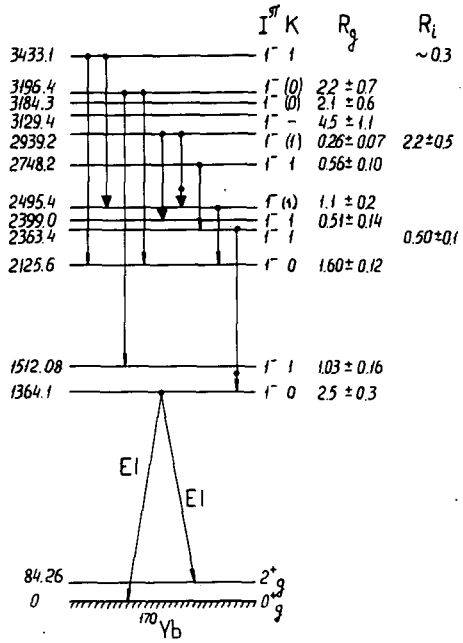

FIG. 5. ^{170}Yb states with $I^{\pi} = 1^-$ and transitions between them. $R_g = \frac{B(E1; 1^- \rightarrow 2^+_g)}{B(E1; 1^- \rightarrow 0^+_g)}$; R_i is the corresponding ratio for transitions to other 0_i^+, 2_i^+ pairs. Transitions for which $\alpha_K^{exp.} > \alpha_K^{M1}$ are marked with thick arrows. Transitions which may also be located elsewhere are marked with a dot.

According to Alaga's laws, the values of R must be equal to 2 when K = 0 and to 0.5 when K = 1. R values near to these are observed more often than others, but intermediate R values are also met; it is possible that intermediate R values are induced by M2 impurities or the pronounced mixing of wave-functions of 1^- states in close proximity to each other.

The presence of a large number of $I^{\pi} = I^-$ levels is to some extent unexpected. The octupole vibration theory predicts the existence of only one level of this type; another 1^- level may appear as the result of the superposition of octupole and quadrupole vibrations. However, a considerably large number of 1^- levels is observed; obviously they must be related to the two-particle type. It is strange that for a few levels K = 0; the supposition that all these levels, apart from one, are rotational states $I^{\pi} = 1^-$ 0 of two-particle levels 0^- 0 with sharply split bands cannot be refuted, although it does not appear to fit in too well with the general theory.

The calculations of Soloviev and Gallagher predicted 0^- 0 two-quasiparticle levels for ^{170}Yb at energies:

2.0 MeV: $p[523]\uparrow + p[404]$

and 2.3 MeV: $p[633]\uparrow + n[514]$

Later calculations, taking into account octupole-octupole interaction, reduced the energies of analogous levels in ^{168}Yb and ^{172}Yb by 0.3 MeV; if the same reduction is made in the case of ^{170}Yb, it can be expected that the first two-quasiparticle 0^- states have an energy of about 1700-2000 keV. Unfortunately, attempts to find 0^- states which would correspond to the observed 1^- levels are hampered by the fact that it is not known what the energy difference between 0^- and 1^- levels should be. Transitions may be observed among the levels $I^\pi = 1^-$, seven of which have a unique position in the decay scheme (these are the transitions with no dots on the arrows in Fig. 5). These transitions may have the multipole order E0 + M1 + E2. If $\alpha_K^{exp.} > \alpha_K^{E2}$ and $> \alpha_K^{M1}$, then it is almost certain that the E0 component is present. This creates a new method of comparing K values; for if there is an E0 component, then the K values are identical.

9. STATES WITH $I^\pi = 1^+$

Theory does not predict the existence of collective states of the 1^+ type — these are the only characteristics which are not to be found in any collective state. It must be assumed that all states of this type are two-quasiparticle states. They are very seldom found and usually lie above 1 MeV. In the decay schemes of 1963 there was sufficient evidence to attest the existence of only two levels of the 1^+ type, namely 1966 keV in ^{156}Gd and 1430 keV in ^{178}Hf.

Up to 1967, none of the $I^\pi = 1^+$ states were found to have rotational levels, nor were any of their properties determined. In 1967 Burke and Elbek found for ^{172}Yb the rotational band $I^\pi = 1^+, 2^+, 3^+, 4^+$, based on a level with the probable characteristics:

$$1^+\left\{\frac{5^-}{2}[512] - \frac{3^-}{2}[521]\right\} \text{ (2008 keV)}$$

For this band, $J(2008)/J_g = 1.39$, i.e. much more than 1, which is not surprising for a two-quasiparticle level.

In ^{170}Yb seven levels of the 1^+ type have been successfully identified (Fig. 6). Detection of a large number of 1^+ levels in ^{170}Lu was facilitated by the decay characteristics of this nuclide, which has $I^\pi = 0^+$. The allowed decay of ^{170}Lu could excite 0^+ and 1^+ levels, but isobaric forbidding reduces several thousandfold the probability of decay to 0^+ levels, so that allowed decay only occurs to 1^+ levels. These levels are high-lying and become manifest only because of the very high decay energy of ^{170}Lu.

The authors of Ref. [3] detected a rotational pair of levels 1^+ and 2^+, namely the level 1775.92 keV(1^+) and 1831.26 keV(2^+). For these levels: $J(1775)/J_g = 1.015 \pm 0.007$.

For five levels of the $I^\pi = 1^+$ type the ratio $B(M1; 1^+ \rightarrow 2_g^+)/B(M1; 1^+ \rightarrow 0_g^+)$ can be determined according to the ratio of intensities of K-conversion

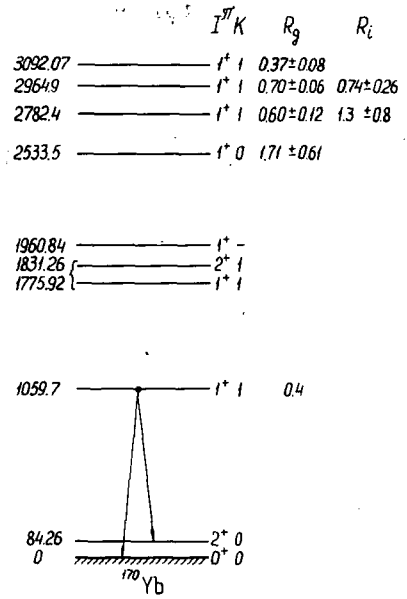

FIG.6. ^{170}Yb states with $I^{\pi} = 1^{+}$.

lines and compared with Alaga's laws (assuming that we are concerned with pure M1 transitions). These ratios and the K values obtained from them are given in Fig.6. However, on analysing 1^{+} level decay, it is impossible to be sure that the transition $1^{+} \rightarrow 2^{+}$ does not include an E2 component, which would raise the experiment ratio R_g or R_i.

REFERENCES

[1] DZHELEPOV, B., TER-NERSESYANTS, V., SHESTOPALOVA, S., Izv. Akad. Nauk SSSR, Ser. fiz. 31 (1957) 1633.

[2] BONCH-OSMOLOVSKAYA, N., VRZAL, Ya., GRIGOREV, E., ZAITSEVA, N., LIPTAK, Ya., TISHIN, V., URBANETS, Ya., JINR preprint P6-3452 (1967).

[3] BALALAEV, V., DZHELEPOV, B., MEDVEDEV, A., TER-NERSESYANTS, V., UCHEVATKIN, I., SHESTOPALOVA, S., Proc. XVIIIth Conf. Nuclear Spectroscopy (Riga 1968) p.82; Izv. Akad. Nauk SSSR, Ser. fiz. 32 (1968) 75.

[4] BOHR, A., Danske Mat-Fys. Med. 26 14 (1952).

[5] BOHR, A., MOTTELSON, B., Danske Mat-Fys. Med. 27 16 (1955).

[6] ALDER, K., BOHR, A., HUUS, T., MOTTELSON, B., WINTHER, A., Rev. mod. Phys. 28 (1956) 432.

[7] DAVYDOV, A. et al., Nucl. Phys. 24 (1961) 682; 27 (1961) 134; Vest. Mosk. Univ., Ser. fiz. 3 (1961) 66.

[8] DAVYDOV, A., ROSTOVSKY, V., Nucl. Phys. 60 (1964) 529.

[9] BELYAK, V., ZAIKIN, D., Izv. Akad. Nauk SSSR, Ser. fiz. 25 (1961) 1663; Nucl. Phys. 30 (1962) 142.

[10] FAESSLER, A., GREINER, W., SHELINE, R., Nucl. Phys. 70 (1965) 33.

[11] DAVYDOV, A., CHABAN, A., Nucl. Phys. 20 (1960) 499; DAVYDOV, A., Vozbuždennije Sostojanija Atomnih Jader (Excited States of Atomic Nuclei), Atomizdat (1967), § 12.

[12] BES, D., Nucl. Phys. 49 (1963) 544.

[13] SOLOVIEV, V., Nucl. Phys. 69 (1965) 1.

[14] SOLOVIEV, V., JINR preprint P-1973 (1965).

[15] BOHR, A., Congrès Internat. de Physique Nucléaire 1 (Paris 1964) 487.
[16] BES, D., BROGLIA, R., NORDITA preprint (Sept. 1965).
[17] KULIEV, A., PYATOV, N., JINR preprint P4-3576 (1967).
[18] BELYAEV, S., Nucl. Phys. 64 (1955) 17; USSR Academy of Sciences (Siberian Section), Nuclear Physics Institute, Preprint No.25 (1966).
[19] ZHELEZNOVA, K., PYATOV, N., CHERNEI, M., Izv. Akad. Nauk SSSR, Ser. fiz. 31 (1967) 550.
[20] PYATOV, N., Proc. Symp. Lysekil, Sweden (1966).
[21] KULIEV, A., PYATOV, N., JINR preprint P4-3171 (1967).
[22] GRAETZER, R., HAGEMAN, G., HAGEMAN, K., ELBEK, B., Nucl. Phys. 76 (1966) 1.
[23] MARKLUND, I., NATHAN, O., NIELSSEN, O., Nucl. Phys. 15 (1960) 199.
[24] DZHELEPOV, B., ZHUKOVSKY, N., MALAYAN, A., Yadernaya Fiz. 1 (1965) 945; 3 (1966) 785.
[25] DZHELEPOV, B., DMITRIEV, A., ZHUKOVSKY, N., MALOYAN, A., Izv. Akad. Nauk SSSR, Ser. fiz. 30 (1966) 1265.
[26] MUKHTASIMOV, F., Author's abstract for doctoral thesis, Tashkent State University (1967).
[27] ABDURAZAKOV, A., VRZAL, Ya., GROMOV, K., ZHELEV, M., KALINNIKOV, V., LIPTAK, Ya., LI SAN SHEEN, MUKHTASIMOV, F., NAZAROV, U., URBANETS, Ya., JINR preprint P6-3464 (1967).
[28] BURKE, D., ELBEK, B., Kong. Danske Vid. Sel. Mat.-Fys. Med. 36 6 (1967).
[29] STEPHENS, Phys. Rev. Lett. 12 (1964) 225.
[30] VRZAL, Ya., GROMOV, K., LIPTAK, Ya., MOLNAR, F., MOROZOV, V., URBANETS, Ya., CHUMIN, V., JINR preprint P-2820 (1966) Izv. Akad. Nauk SSSR, Ser. fiz. 31 (1967) 604.
[31] NIESEN, H., WILSKY, K., ŽYLICZ, J., SPRENSEN, G., Nucl. Phys. A 93 (1967) 385.
[32] BONCH-OSMOLOVSKAYA, N., VRZAL, Ya., GRIGOREV, E., LIPTAK, Ya., PFREPPER, G., URBANETS, Ya., KHRISTOV, D., Izv. Akad. Nauk SSSR, Ser. fiz. 32 (1968) 98.
[33] Cited in [17].
[34] GROSHEV, L., DEMIDOV, A., IVANOV, V., LUTSENKO, V., PELEKHOV, V., Izv. Akad. Nauk SSSR, Ser. fiz. 26 (1962) 1119.
[35] RASMUSSEN, J., Preprint UCRL-9084 (1960).
[36] DAVYDOV, A., ROSTOVSKY, V., CHABAN, A., Vest. Mosk. Univ. 3 (1961) 66 or DAVYDOV, A., Vozbuždenije Sostojanija Atomnih Jader (Excited States of Atomic Nuclei) Atomizdat (1967) 181.
[37] BELYAEV, S., RUMYANTSEV, B., Int. Conf. Nuclear Structure, Tokyo (1967) 100.
[38] SHELINE, R., NIELSEN, H., SPERDUTO, A., Nucl. Phys. 16 (1960) 578.
[39] GANGRSKY, Yu., LEMBERG, I., NABICHVRISHVILI, V., Yadernaya fiz. 3 (1966) 794.
[40] YOSHIZAWA, Y., ELBEK, B., HERSKIND, B., OLESEN, M., Nucl. Phys. 73 (1965) 273.
[41] DZHELEPOV, B., "Struktura Složnih Jader" (Structure of Complex Nuclei) Atomizdat (1966) 199.

DISCUSSION

V.G. SOLOVIEV: To investigate the structure of the 1^+ levels, many of which have been observed in ^{170}Yb, it will be necessary to perform direct nucleon reaction studies in addition to the $\beta-\gamma$ measurements. The study of the (d, p), (d, t), (^{3}He, d) and other nuclear reactions allows us to determine the mixture of different two-quasiparticle states in the states in question.

A.S. DAVYDOV: When you spoke about collective excitations you did not mention γ-vibrations with spin 0.

B.S. DZHELEPOV: In such nuclei as ^{170}Yb these states probably lie higher than 2 MeV (see Fig. 1 in our paper).

V.G. SOLOVIEV: I should like to make two comments. First, the difficulties of the theory are particularly great when studying states with $K^\pi = 0^+$. The structure of all the $K^\pi = 0^+$ states cannot be described consistently. The different methods explain the features only of a few 0^+ states. The consistency description of the 0^+ states in the framework of uniform theory is a very topical problem.

Second, the non-collective states with energies up to 2.5 MeV in the even-odd deformed nuclei are described well in the framework of the model of independent quasiparticles. The energies of the two-quasiparticle states and their properties are in surprisingly good agreement with those calculated by us more than five years ago. However, with increasing excitation energy the two-quasiparticle structure of the states becomes more and more complicated. Because of the interaction between the quasiparticle and the phonons two-quasiparticle states are spread over some levels. Such a type of 1^+ level has been demonstrated by B.S. Dzhelepov.

ANALYSIS OF QUADRUPOLE AND OCTUPOLE COLLECTIVE STATES IN EVEN-EVEN NUCLEI

P. VOGEL
NUCLEAR RESEARCH INSTITUTE,
ŘEŽ NEAR PRAGUE, CZECHOSLOVAKIA

Abstract — Аннотация

ANALYSIS OF QUADRUPOLE AND OCTUPOLE COLLECTIVE STATES IN EVEN-EVEN NUCLEI. The collective vibrational states of even-even nuclei are investigated. The mathematical technique used is the quasiparticle random phase approximation.

In the first part information on the residual interaction obtained by the analysis of the calculations is discussed. The interaction constants of the residual multipole-multipole interaction used in different calculations are compared. Their closeness seems to indicate that a rather universal multipole-multipole force especially suitable for treatment of the vibrational states exists. The multipole-multipole force and the other schematic force – the surface delta interaction (SDI) – are compared. It is suggested that the main characteristics of the collective states (energy, $B(E\lambda)$ value) are insensitive to the radial form of the residual interaction. Calculations of the octupole states in the spherical nuclei with the multipole-multipole force, the SDI and the usual δ-force seem to support this assumption.

In the second part, results of new calculations of the vibrational states in rare-earth deformed nuclei are reported. The deformed Woods-Saxon potential instead of the Nilsson one was used. The description of the $K^{\pi} = 2^{+}$ states is satisfactory while agreement between simple theory and experiment for the octupole states is not so good.

АНАЛИЗ КВАДРУПОЛЬНЫХ И ОКТУПОЛЬНЫХ КОЛЛЕКТИВНЫХ СОСТОЯНИЙ В ЧЕТНО-ЧЕТНЫХ ЯДРАХ. Исследуются коллективные колебательные состояния четно-четных ядер. В качестве математической техники применяется метод случайных фаз. В первой части обсуждается информация об остаточном взаимодействии, получаемая при анализе расчетов. Сравниваются константы остаточного мультиполь-мультипольного взаимодействия, применяемые в различных расчетах. Их близость указывает на существование сравнительно универсальной мультиполь-мультипольной силы, очень удобной для изучения колебательных состояний. Сравниваются две схематические силы: мультиполь-мультипольная и поверхностное δ-взаимодействие. Предполагается, что главные характеристики коллективных состояний (энергия, величины $B(E\lambda)$) не чувствительны к радиальной форме остаточного взаимодействия. Расчеты октупольных состояний сферических ядер с мультиполь-мультипольными силами, поверхностным δ-взаимодействием и обычной δ-силой подтверждают это предположение. Во второй части приводятся результаты новых вычислений колебательных состояний редкоземельных деформированных ядер. Вместо потенциала Нильссона применяется деформированный потенциал Вудса-Саксона. Описание состояний с $K^{\pi} = 2^{+}$ является удовлетворительным. В случае октупольных состояний согласие простой теории с экспериментом не столь хорошее.

1. INTRODUCTION

The "microscopic" theories of collective excitations have been used by many authors in the study of quadrupole and octupole vibrations of the spherical and deformed even-even nuclei. In such theories usually the particles are supposed to move in a shell-model potential, interacting by a pairing interaction of the superfluid type and by a residual interaction (particle-hole interaction). This means that the Hamiltonian is of the form

$$H = H_{\text{shell model}} + H_{\text{pairing}} + H_{\text{residual}} \qquad (1)$$

It is well known that there is no simple and straightforward method for obtaining the residual interaction from, for example, the scattering data of free nucleons. Therefore — and for simplicity as well — different simple residual interactions are widely used. Using such schematic forces, it is possible to explain basic properties (energies, transition probabilities) of the low-lying collective states in the mass region including spherical as well as deformed nuclei.

In the first part (sections 2-4) the schematic forces are analysed. An attempt is made to answer such questions as: Does really unique multipole-multipole interaction exist? Can one obtain some information on the radial form of the residual interaction from the calculations of the collective states? If not, is there any connection between the interaction constants of the forces with different radial dependence?

In the second part of the paper the collective states in deformed rare-earth nuclei are discussed. The new results obtained in Dubna by means of the deformed Wood-Saxon potential are compared with new experimental data.

The mathematical technique usually used in calculations is the quasi-particle Random Phase Approximation (RPA) or a similar one. Since the theory is well known [1, 2], only the basic definitions and equations are given here, in order to see which parameters are needed for the actual numerical calculations.

The system of equations for the density matrix is schematically as follows:

$$\begin{aligned}\omega Z^{-}_{12} &= (E_1 + E_2)\, Z^{+}_{12} + (u_1v_2 + v_1u_2) \sum_{34} \langle\, 14 \,|\, \Gamma \,|\, 23 \,\rangle (u_3v_4 + v_3u_4)\, Z^{+}_{34} \\ \omega Z^{+}_{12} &= (E_1 + E_2)\, Z^{-}_{12} + (u_1v_2 - v_1u_2) \sum_{34} \langle\, 14 \,|\, \Gamma \,|\, 23 \,\rangle (u_3v_4 - v_3u_4)\, Z^{-}_{34}\end{aligned} \tag{2}$$

Here the quantity $(u_1v_2 \pm v_1u_2)\, Z^{\pm}_{12}$ is that part of the density matrix which is even (odd) under the time conjugation. $E_1 = \sqrt{(\epsilon_1^2 + \Delta^2)}$ is the quasi-particle energy. The symbols ϵ_1, ϵ_2 denote the single-particle energies, counted off the chemical potential,

$$u_1^2 = 1 - v_1^2, \qquad v_1^2 = \tfrac{1}{2}\left(1 - \frac{\epsilon_1}{E_1}\right)$$

The index 1 designates all the relevant single-particle quantum numbers including τ_z. The quantities $\langle 14 \,|\, \Gamma \,|\, 23 \,\rangle$ are the matrix elements of the residual interaction. When the $Z^{\pm}_{12}$ are properly normalized then the matrix element of EJ transition is

$$M(EJ) = \sum_{12} e_{12} V_{12} (u_1v_2 + v_1u_2)\, Z^{+}_{12} \tag{3}$$

where V denotes the multipole operator EJ and e_{12} the corresponding charge.

In Eqs (2) there are two groups of parameters. The first contains the characteristics of the average field; they affect the single-particle

energies ϵ_1 and the single-particle wave-functions used for the calculation of the matrix elements. The other group of parameters is connected with the residual interaction and includes the functional form of the interaction and the interaction constants. The choice of the pairs of states 1, 2, which form the collective state, is a "hidden" parameter. If only a restricted set of states is taken a modified residual interaction and effective charges must be used.

2. MULTIPOLE-MULTIPOLE FORCE

It is well known that considerable progress has been achieved in explaining the main characteristics of the collective vibrational states using the multipole-multipole force as the residual interaction (see, for example, Refs [3-8]). In such a case the operator Γ in Eq. (2) has the form

$$\Gamma = (\kappa + \kappa' \vec{\tau}_1 \vec{\tau}_2)\, r_1^\lambda \cdot r_2^\lambda \cdot Y_{\lambda\mu}(\vartheta_1) \cdot Y_{\lambda\mu}(\vartheta_2) \tag{4}$$

($\lambda = 2$ for the quadrupole states, $\lambda = 3$ for the octupole ones). When the antisymmetrization of the matrix element $\langle 14 \,|\, \Gamma \,|\, 23 \rangle$ is disregarded (as is usually the case) a relatively simple dispersion equation is obtained and no matrix diagonalization is needed. This enables us to use Eqs (2) even with the deformed nuclei, where otherwise the order of matrices is too large.

The quantity κ' in Eq. (4) has little influence on the properties of the low-lying states. In practical calculations κ' is usually set equal to zero (i.e. $\kappa_{nn} = \kappa_{pp} = \kappa_{np} \equiv \kappa$). Thus, with the parameters describing the average field already fixed or taken from other experiments, only the interaction constant κ remains as an unspecified parameter.

In Table I the quadrupole-quadrupole and octupole-octupole interaction constants used by different authors are collected. In columns 2 and 4 the quantities k ($\kappa = k/A^{5/3}$ MeV), obtained in calculations with a restricted set of single-particle states (one or two shells) are given. In columns 3 and 5 the values of $k^{(2)}$ and $k^{(3)}$ without renormalization are shown. The values in the table come from somewhat different sources. The numbers in lines 1-3 come from the calculations of the spectra of spherical nuclei, in lines 4-7 from the spectra of deformed nuclei and in lines 8-9 from calculations of the equilibrium deformations. Finally, in line 10 there is an estimation

$$\kappa^{(\lambda)} = \frac{4\pi}{2\lambda + 1} \frac{M\omega_0^2}{A\langle r^{2\lambda-2} \rangle} \tag{5}$$

from Ref. [2]. Sometimes a dependence of κ on A different from $\sim A^{-5/3}$ was used. In such a case the κ values were extrapolated to A = 165.

It is seen that the numbers in the respective columns are close to each other (the β-vibrations being a special and difficult problem). The renormalization gives a reasonable factor of 2-3. The results shown in

TABLE I. QUADRUPOLE AND OCTUPOLE INTERACTION CONSTANTS USED BY DIFFERENT AUTHORS. THE QUANTITIES $k^{(\lambda)} = \kappa^{(\lambda)} \cdot A^{5/3}$ MeV ARE SHOWN

	Col.1	Col.2	Col.3	Col.4	Col.5
	References	$k^{(2)}_{renorm.}$	$k^{(2)}_{unrenorm.}$	$k^{(3)}_{renorm.}$	$k^{(3)}_{unrenorm.}$
Line 1	Yoshida [3]		100		
Line 2	Kisslinger-Sorensen [4]	200-300			
Line 3	Veje [11]				15
Line 4	Soloviev [8]	340		26	
Line 5	Soloviev et al. [12]	270		19	
Line 6	Bes, β-vibrations [6]	150			
Line 7	Bes et al., γ-vibrations [7]	320	160		
Line 8	Bes-Szymanski [9]		100		
Line 9	Kumar-Baranger [10]	280			
Line 10	Bohr-Mottelson [2]		100		12

the table seem to support the assumption of the existence of rather universal multipole-multipole interaction, specially suitable for calculation of the collective states.

3. SURFACE DELTA INTERACTION AND THE MULTIPOLE-MULTIPOLE INTERACTION

The other widely used schematic force, the Surface Delta Interaction (SDI), is even simpler than the multipole-multipole one. Its operator form (i.e. the Γ in Eq.(2)) is

$$\Gamma(r_{12}) = - \frac{2F}{(R_0 u_0)^4} \delta(\cos\vartheta_{12} - 1)\, \delta(r_1 - R) \cdot \delta(r_2 - R). \qquad (6)$$

Here R_0 is the nuclear radius, u_0 the amplitude of the single-particle wavefunction on the nuclear surface, and F the interaction constant.

The matrix elements of the SDI are separable. Moreover, the SDI contains all multipoles and in principle it could describe all the correlation effects [13] (pairing properties, vibrations). Extensive numerical calculations made by Faessler and Plastino [14, 15] have shown that the results with the SDI are as close to experiment as earlier results with the multipole-multipole force.

Thus two forces, with rather different radial dependence, can explain an extensive experimental material. This seems to mean that only

very general features of the residual interaction (e.g. mean value of the radial matrix element) are important for the determination of the basic (coherent) properties of the collective states.

If this is the case, the ratio of the respective interaction constants should be equal to the mean radial matrix element. This is really so, as is seen from Table II. The dispersion of values in columns 3 and 4 is quite small. Note that the similarity of the results with the SDI and the multipole-multipole interaction could be understood from another point of view too. In the radial matrix element

$$\int_0^\infty u_1(r)\, r^\lambda\, u_2(r)\, r^2\, dr$$

the integrand has a sharp maximum around $r = R_0$ and is therefore similar to the $\delta(r - R_0)$ function.

4. OCTUPOLE COLLECTIVE STATES IN Sn AND Zr ISOTOPES

An attempt was made to estimate the importance of the residual interaction radial dependence for the collective states of spherical nuclei too. For this purpose, we have calculated the energies of the octupole states and the transition probabilities using the octupole-octupole force, the SDI and the usual δ - force [16]. Thus, the $H_{residual}$ in Eq.(1) or the operator Γ in Eq.(2) had the form

$$H_{residual} = (f + f'\vec{\tau}_1\vec{\tau}_2)\, V(\vec{r}_1, \vec{r}_2) \qquad (7)$$

with $V(\vec{r}_1, \vec{r}_2)$ equal to

$r_1^3 \cdot r_2^3 \cdot Y_{3\mu}(\vartheta_1) \cdot Y_{3\mu}(\vartheta_2)$ for octupole-octupole force

$\delta(\vec{r}_1 - \vec{r}_2) \cdot \delta(r_1 - R_0)$ for the SDI

$\delta(\vec{r}_1 - \vec{r}_2)$ for the δ-force

We took $f'/f = -0.5$, which corresponds approximately to the interaction of the Serber type. The constants were fitted so as to obtain the same energy for the first $I^\pi = 3^-$ state in ^{116}Sn. All the other parameters were taken from Ref. [11].

The results for the Sn isotopes are shown in Fig. 1, the results for Zr being very similar. It is seen that with different types of residual interaction we obtained practically the same energies and even the corresponding transition probabilities within rather narrow limits.

Thus, from the point of view of the calculated states all mentioned interactions are equivalent. This means that the strengths of the inter-

TABLE II. THE MEAN RADIAL MATRIX ELEMENT (COL. 2), THE QUANTITY A·F, F BEING THE SDI INTERACTION CONSTANT (COL. 3), AND THE QUANTITY $F' = A \cdot \kappa \cdot \bar{R}^2_{ij}/4\pi$ (COL. 4)

Col. 1	Col. 2	Col. 3	Col. 4
	$\bar{R}_{ij}$	F(MeV)	F'(MeV)
Rare-earths, quadrupoles	5.7	27.5	29.6
Rare-earths, octupoles	15.5	34.0	36.0
Actinides, quadrupoles	6.4	29.4	34.5
Actinides, octupoles	18.0	33.5	29.0

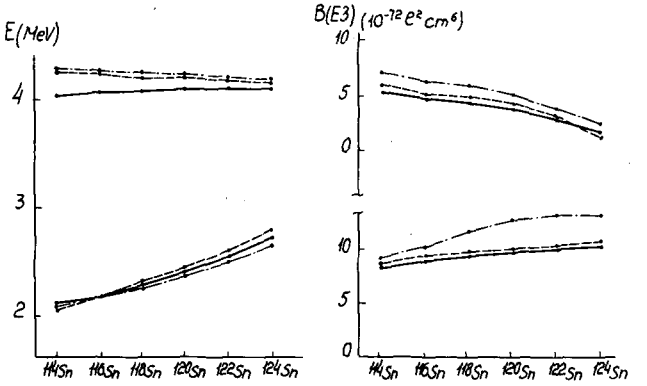

FIG. 1. The energies of the first and second collective states in Sn isotopes (left) and the corresponding B(E3) values (right).
Notation: ———— δ - force
---------- surface delta interaction
-·—·—·— octupole-octupole force

TABLE III. INTERACTION CONSTANTS (IN $\hbar\omega_0^0$) FOR DIFFERENT FORCES

	Interaction	f	f'	$f\bar{V}_R$
Sn	δ-function	-2.63	1.31	0.130
	SDI	-0.128	0.064	0.125
	oct-oct	-7.4×10^{-4}	3.7×10^{-4}	0.115
Zr	δ-function	-2.21	1.10	0.130
	SDI	-0.121	0.06	0.120
	oct-oct	-8.4×10^{-4}	4.2×10^{-4}	0.110

action and the energies of the low-lying two-quasiparticle states have the decisive effect.

The interaction constants used in the calculations are collected in Table III. They are close (within 20% limit) to those used by other authors. In the last column the quantities fV_R ($\bar{V}_R$ is the mean value of the radial matrix element) are given. The similarity of these values illustrates once more that the results are independent of the radial form of the residual interaction.

In the author's opinion, the similarity is also the connection that has been sought between different interactions and a criterion for the "right" residual interaction as well.

5. COLLECTIVE VIBRATIONAL STATES IN THE RARE-EARTH DEFORMED NUCLEI

Recently many new experimental data, based mostly on the (d, d') experiments done at the Niels Bohr Institute [18], have become available. Thanks to these experiments one's knowledge of the energies and corresponding B(E2) values for the $K^\pi = 2^+$ γ-vibrational states is almost complete. The only exception is the B(E2) values in Hf, W and Os isotopes, where only two experimental points exist nowadays. The experimental evidence of the negative parity states is less complete. Nevertheless, the energies and the B(E3) values of $I^\pi = 3^-$ states have been measured for many nuclei in the region considered. Unfortunately, the K-values are known only exceptionally. The rotational bands, based on the octupole states, are often distorted or, if they follow the I(I + 1) rule, their momenta of inertia are considerably larger than the momenta of the rotational bands based on the ground states or quadrupole vibrations. This seems to mean that some other interaction (e. g. coriolis coupling) is important in this case and we cannot expect very close agreement between experiment and simple theory.

The author would like to describe here briefly the results of recent calculations made in Dubna [12] and to compare them with the experimental information just mentioned.

The Nilsson potential was used as the average field in the previous calculations [8]. However, the Wood-Saxon potential, with its proper asymptotic behaviour of the wave-functions, should be closer to the "right" average field. The simple method of calculating energy levels and wave-functions in a deformed Wood-Saxon well suggested in Ref. [17] permits such a potential to be used for practical calculations.

In Figs 2-4 the results of the calculations are collected and compared with the experiments. During the calculations the mass-number A dependence of the Wood-Saxon potential as well as the change of the deformation from nucleus to nucleus were properly taken into account. The multipole-multipole interaction constants $\kappa^{(\lambda)}$ are practically independent of the form of the average field, provided the quantity $\langle r^2 \rangle$ has the right value. Note that there is no substantial difference between the results obtained with the Wood-Saxon and Nilsson potentials. Let us shortly comment on the particular results.

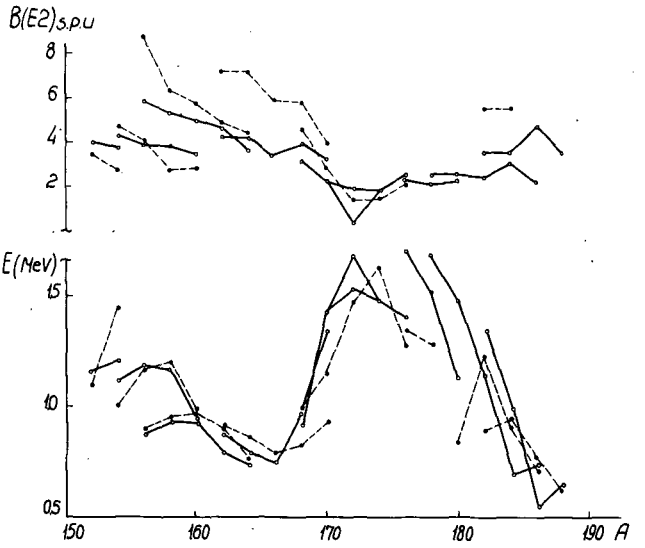

FIG.2. The energies (bottom) and the B(E2) values (above) of the $K^{\pi} = 2^{+}$ states. Isotopes of the same elements are connected.
Notation: theory; experiment

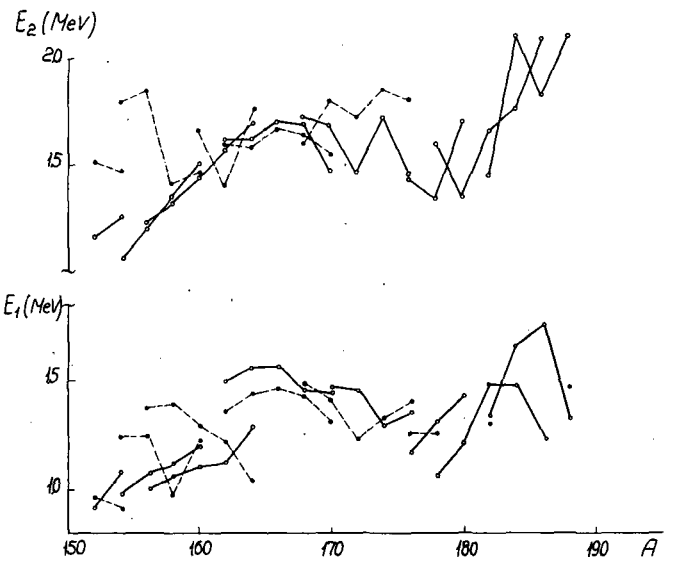

FIG.3. The energies of the first (bottom) and second (above) octupole states. Notation as for Fig.2.

The $K^{\pi} = 2^{+}$ γ-vibrations

As is seen from Fig. 2, very satisfactory agreement between theory and experiment is achieved. Not only the general behaviour but even the

change from one isotope to another is properly described. However, the predicted increase of the energy of the $K^{\pi} = 2^{+}$ states after A = 166 is faster than the experimental one. Similarly, the B(E2) values for Er isotopes are lower than the measured values. For nuclei with N = 106 the experimental decrease of the energy is not obtained in the calculations. In ^{172}Yb, as in previous calculations, two low-lying $K^{\pi} = 2^{+}$ states are predicted: a collective one and a two-quasiparticle n512↑-n521↓ state.

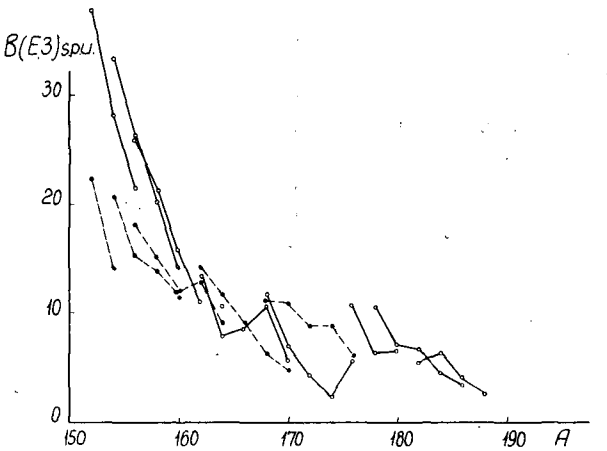

FIG.4. The sum of the B(E3) values for the octupole $K^{\pi} = 0^{-}$, 1^{-}, 2^{-} states. Notation as for Fig.2.

Octupole states

The energies of the first and second octupole states are shown in Fig. 3. The experimental values correspond to the $I^{\pi} = 3^{-}$ states [18], while the calculated energies correspond to the basis of the rotational bands. Therefore, the theoretical points should lie 100-150 keV below the experimental ones. In the calculations one predicts, of course, the K-value for each of the states. Thus, in Sm isotopes the lowest are K = 0 states and the K = 1 ones are higher. In Gd and Dy isotopes the first states have K = 2 and the second K = 0. In Er and Yb the order is K = 2, K = 1. Finally, in some of the heavier nuclei the order is K = 2, K = 1, while in others it is K = 1, K = 2. Overall agreement is obtained; however, a lot of details need further explanation (e. g. the energies in the Dy isotopes).

As has already been mentioned, it is assumed that the octupole states are not very pure. Therefore we compare only the full calculated B(E3) strength with the experimental value (Fig. 4). It is seen that the agreement is rather good. Let us note that the expected increase of the ΣB(E3) [18] at the end of the considered region is not confirmed in the calculations.

6. CONCLUSIONS

Let us divide the quantities describing the collective vibrational states of even-even nuclei into two categories. The first includes "integral" quantities (energy, $B(E\lambda)$-value, α-transition probability); they are coherent sums of all the collective state components. In the second category there are "differential" quantities (spectroscopic factors, log (ft) values, non-collective γ-transition rates, etc.) usually proportional to one component of the collective state.

In the first part of this paper it was shown that the integral quantities are practically independent of the radial form of the residual interaction, provided that the mean radial matrix element has the prescribed value. Probably only a very careful analysis of many "differential" quantities can select the "right" residual interaction.

The second part of the paper shows the successes as well as the limitations of our understanding of the vibrational states in the rare-earth deformed nuclei. Careful calculations give satisfactory agreement with experiment for the $K^{\pi} = 2^{+}$ γ-vibrational states. For the octupole states, although general agreement is obtained, many details need further explanation.

REFERENCES

[1] LANE, A.M., Nuclear Theory, Benjamin, N.Y. (1964).
[2] BOHR, A., MOTTELSON, B.R., Lectures on Nuclear Structure and Energy Spectra (to be published).
[3] YOSHIDA, S., Nucl. Physics 38 (1962) 380.
[4] KISSLINGER, L.S., SORENSEN, R.A., Rev. Mod. Phys. 35 (1963) 853.
[5] MARSHALEK, E.R., RASMUSSEN, J.O., Nucl. Phys. 43 (1963) 438.
[6] BES, D.R., Nucl. Phys. 49 (1963) 544.
[7] BES, D.R., FEDERMAN, P., MAQUEDA, E., ZUKER, A., Nucl. Phys. 65 (1965) 1.
[8] SOLOVIEV, V.G., Atom. Energy Rev. 3 (1965) 117.
[9] BES, D.R., SZYMANSKI, Z., Nucl. Phys. 28 (1961) 42.
[10] KUMAR, K., BARANGER, M., Nucl. Phys. 110A (1968) 529.
[11] VEJE, C.J., Mat. Fys. Medd. Dan. 35 1 (1966).
[12] KORNEICHUK, A.A., MALOV, L.A., SOLOVIEV, V.G., FEDOTOV, S.I., SCHULTZ, H., Contribution No. 77 to this Symposium; MALOV, L.A., SOLOVIEV, V.G., FAINER, U.M., Contribution No. 78 to this Symposium.
[13] GREEN, I.M., MOSZKOWSKI, S.A., Phys. Rev. 139 (1965) B790.
[14] FAESSLER, A., PLASTINO, A., Nucl. Phys. A94 (1967) 580.
[15] FAESSLER, A., PLASTINO, A., Z. Phys. 203 (1967) 333.
[16] ŘIZEK, J., VOGEL, P., Preprint UJV 2024, Řež, Czechoslovakia (1968).
[17] GAREEV, F.A., IVANOVA, S.P., KALINKIN, B.N., Preprint R4-3451, Dubna (1967).
[18] ELBEK, B., GROTDAL, T., NYBO, K., TJOM, P.O., VEJE, E., Paper 4.90, Int. Conf. on Nucl. Structure, Tokyo (1967).

DISCUSSION

V. GILLET: You have shown excellent agreement for the octupole states of single closed shell nuclei. Was your calculation limited to 2-quasiparticle excitations of the outer shell or did you include particle-hole excitations of the core? Did you use any effective charge?

P. VOGEL: We used all the particle-hole states with an energy $1\hbar\omega_0$. The effective charge $e_{eff} = 0.1$ e comes from the states with energy $3\hbar\omega_0$. It has already been calculated by Veje.

A.S. DAVYDOV: Did you take rotational collective states into account?

P. VOGEL: No, the rotational states were not taken into account.

A.S. DAVYDOV: You have mentioned gamma-vibrations with spin 2^+. In these states the rotational states cannot be separated from vibrational ones.

P. VOGEL: I think the energies and absolute B(E2) values are not very sensitive to rotational admixtures.

A.S. DAVYDOV: Collective excitations are related to the variations of the self-consistent field. In all microtheories the calculations are made in the constant self-consistent potential. In the consistent theory one should take into consideration the variations of the self-consistent potential due to collective excitations. Have you taken this effect into account?

P. VOGEL: No, this effect was not taken into account. I agree that in a very consistent theory it should be taken into account.

B.L. BIRBRAIR: On what basis (perhaps you had special reasons for this) have you not taken into account residual interaction in the particle-particle channels in the state 2^+? For instance, in the case of the first 2^+ level in magic isotopes (e.g. in Sn isotopes) just this interaction is of special importance. According to our recent results, the particle-hole interaction does not affect either the energy or B(E2) in this case.

P. VOGEL: We did not calculate the 2^+ states in Sn, but the 3^- states. However, I do not understand how the interaction in the particle-particle channel can enhance the B(E2).

B.L. BIRBRAIR: In Sn isotopes no such enhancement is observed. In these isotopes B(E2) does not exceed five one-particle units. At the same time there are about thirty B(E2) (in the same units) in neighbouring double non-magic nuclei.

KRISHNA KUMAR: I would like to comment on your statement concerning the radial dependence of the quadrupole interaction. This radial dependence is perhaps not very important if one includes only a few states near the Fermi surface in the calculation. However, the matrix-elements connecting states far away from the Fermi surface, for example those of the shell above and below the major one and the $N = 2$ matrix elements, are quite sensitive to the radial dependence. These matrix elements are particularly important for the transitional nuclei.

P. VOGEL: I do not think so. Matrix elements are usually included in the sums over all transitions. Thus, some averaging takes place and the radial dependence is not shown distinctly.

A. BOHR: The different interactions considered, surface delta and volume delta, although generally similar, differ significantly in the ratios of particle-particle interaction (pairing) and particle-hole interaction (field effect). The collective states are expected to be rather sensitive to these ratios.

P. VOGEL: In the calculation, different forces were used only in the particle-hole channel. For pairing force the standard approximation $G = \text{const.}$ was used in all cases.

S.T. BELYAEV: In the quadrupole and octupole states considered the interaction in the particle-hole channel predominates. However, for quantitative calculations, analogous interactions in the particle-particle channel must be taken into account. The calculations performed by Belyaev and

Rumyantsev show that taking them into account results in an effective variation of the quadrupole constant from nucleus to nucleus (up to 25%) and in a still more appreciable change of transition probabilities.

P. VOGEL: We hope that this effect could be included, at least partly, in a renormalization of the interaction constant. In the mentioned calculations the latter is a free parameter.

M. GMITRO: At ICTP in Trieste we have compared the results of 2-quasiparticle and 4-quasiparticle theories (including correlations with the ground state) of tin isotopes. Reasonable stability of the lowest part of the spectrum against the inclusion of 4 qp excitation has only been found in the case of residual interaction deduced from a realistic potential (Tabakin, Yale). On the other hand, spectroscopic results in the case of non-realistic (quadrupole-quadrupole and Gaussian forces in our experience) residual interactions could be rather sensitive to the inclusion of 4 qp excitation.

P. VOGEL: As I understand it, you have included only neutrons in the open shell. So your 2 qp configuration space is very restricted. I do not think that the sensitivity you have mentioned occurs in calculations with less restricted 2 qp configuration space as in our case.

V.G. SOLOVIEV: I would like to remark that, as has been shown by the calculations of Jolos, Zheleznova, Fainer and myself for strongly deformed nuclei, the admixtures of two-phonon components to one-phonon states are rather small.

As regards the accuracy in calculating one-phonon states, this is greatly restricted by the very approximate description of the mean field. The need to go beyond the quasi-boson approximation framework is most noticeably seen when describing states with energies much lower than the first pole of the corresponding secular equation.

EXPERIMENTAL DECOMPOSITION OF THE WAVE-FUNCTIONS OF DEFORMED NUCLEAR STATES INTO THEIR COMPONENTS

R.K. SHELINE
FLORIDA STATE UNIVERSITY,
TALLAHASSEE, FLA., UNITED STATES OF AMERICA

Abstract — Аннотация

EXPERIMENTAL DECOMPOSITION OF THE WAVE-FUNCTIONS OF DEFORMED NUCLEAR STATES INTO THEIR COMPONENTS. Increasing experimental and theoretical evidence for the complexity of low-lying states in deformed nuclei suggests the need for a variety of experimental approaches. The available experimental methods are summarized with particular emphasis on multi-reaction spectroscopy as a method of separating various components in the structure of deformed nuclear states. Level structures and other experimental parameters of ^{162}Dy, ^{177}Hf, ^{175}Lu and ^{177}Lu agree well with the Nilsson Model and the calculations of Soloviev as is typical of the most strongly deformed nuclei. In this paper emphasis is placed on nuclei in the transition region between spherical and deformed nuclei where experiment is expected to test the theory most severely. Experimental data on ^{153}Sm, ^{155}Gd, ^{186}Re and ^{181}Hf indicate the presence of strong coriolis coupling, of mixing of principal harmonic oscillator shells ($\Delta N=2$ mixing) and of complex phonon admixtures in low-lying states which probably require more sophisticated theoretical analysis.

ЭКСПЕРИМЕНТАЛЬНЫЙ АНАЛИЗ ВОЛНОВЫХ ФУНКЦИЙ СОСТОЯНИЙ ДЕФОРМИРОВАННЫХ ЯДЕР ПО ИХ КОМПОНЕНТАМ. Возрастание экспериментальной и теоретической информации о сложности низколежащих состояний в деформированных ядрах требует разнообразия экспериментальных подходов. Резюмируются развитые для этого экспериментальные методы, и в частности, выделяется спектроскопия реакций многонуклонных передач как метод выделения различных компонент в структуре состояний деформированных ядер. Структура уровней и другие экспериментальные параметры ^{162}Dy, ^{177}Hf, ^{175}Lu и ^{177}Lu хорошо согласуются с моделью Нильссона и расчетами Соловьева, что является характерным для большинства сильно деформированных ядер. Заостряется внимание на ядрах переходной области, от сферических к деформированным, где ожидается, что эксперимент подвергнет теорию наиболее строгому испытанию. Экспериментальные данные по ^{153}Sm, ^{155}Gd, ^{186}Re и ^{181}Hf указывают на сильную кориолисову связь, смешивание главных оболочек гармонического осциллятора ($\Delta N = 2$ смешивание) и сложные фононные примеси в низколежащих состояниях, что потребует, по-видимому, более кардинального теоретического анализа.

I. INTRODUCTION

In the last two decades there has been an explosive development in both our experimental and theoretical understanding of the spectroscopy and structure of nuclei. This development has been particularly spectacular for deformed nuclei as a direct outgrowth of the research of Bohr and Mottelson [1] and the Copenhagen School. From knowledge of one or a few states in a few nuclei our experimental efforts have led to knowledge of literally hundreds of states in the first two or three MeV of many nuclei. Often the states are quite complex. To a very considerable extent the theory has kept pace with experiment - first through the Nilsson Model [2], then through a pairing plus quadrupole model developed in detail by Kisslinger and Sorensen [3] and finally through the detailed application of the microscopic model to the deformed region by Soloviev and collaborators [4], and by Bès and Yi-Chung [5].

We will attempt to understand how the experimentalist uses the tools at his disposal to categorize complex nuclear states. After describing the methods and their uses, a few cases of nuclear spectra are presented, where considerable agreement between experiment and theory has been found. However, the main aim of this paper is to show the "growing edges" and, therefore, many of the remaining difficulties in our study of the spectroscopy and structure of deformed nuclei. Accordingly, we will attempt to deal with those regions where experiment and theory are not in the best agreement. We will emphasize with our experimental data those aspects of the nuclear theory which may not be satisfactory. We will choose those regions of the nuclear periodic table - particularly in the transition region between spherical and deformed nuclei in which the deformation is not so well developed - where nuclear models are expected to have the most difficulty. It should, however, be kept clearly in mind that for the most part we have chosen to neglect the large body of nuclear data which is in excellent agreement with nuclear theory and already at this time stands as one of the outstanding edifices of man's ability to understand nature.

II. EXPERIMENTAL METHODOLOGY

(1) The problem

A very wide variety of spectroscopic information determines the characteristics of any one nuclear state. For even-even nuclei there are the possibilities of 0, 2, 4 ... quasiparticle states. For odd-A nuclei, there are 1, 3, 5 ... quasiparticle states. For odd-odd nuclei 2, 4, 6 ... quasiparticle states. In addition, there is a wide variety of neutron and proton state combinations possible in each case. There is the particle-hole nature of the state. Superimposed on each intrinsic state is a rotational band, although in the transition region this rotational band may be so disturbed and mixed as to be almost unidentifiable. There are also vibrational states - quadrupole, such as the β and γ shape vibrations, the pairing vibrations, octupole vibrations and higher multipole vibrations which obviously exist, but have not yet been observed. In the microscopic model these vibrations can be described in terms of a super-position of higher quasiparticle states.

Finally, many of these different kinds of states may be (and almost always are) mixed in some degree. Different intrinsic states with the same number of quasiparticles may mix via coriolis coupling, for example. The vibrations mix with intrinsic states. In the case of an odd-A nucleus, one often finds a 1 quasiparticle intrinsic state with considerable admixture of a K-2 gamma vibration which may be thought of as an admixture of various 3 quasiparticle states into the 1 quasiparticle state. In higher energy states in particular, it is common that there will be several components in a particular state. The question to which we now address ourselves is: How can we systematically study this complexity?

(2) Decay scheme methods

Traditionally, the spectroscopy of nuclear states has been studied by decay scheme methods. These have included the various types of beta decay, alpha decay, and gamma decay following isomerism, alpha or beta decay. In spite of the fact that decay scheme methods, because of selection rules, populate relatively few states in a nucleus, the method continues to have considerable value because of the detailed information which can be obtained from the states which are populated. For example, the observation of an "allowed unhindered" (au) beta decay with its accompanying low log ft value can clearly indicate even a small component of a particular state related to the decaying state. There are many examples of this phenomenon including at least one presented to this conference by Bunker and colleagues [6]. Gamma transition probability ratios or absolute transition rates can clearly indicate K values or mixed K values, coriolis coupling, or vibrational components in a state. Low hindrance factors in alpha decay also indicate the presence of components in directly populated states which are similar to the alpha decaying state. Because several examples of the use of decay scheme spectroscopy for identifying components of nuclear wave-functions will be presented to this conference, no specific examples will be presented in this paper.

(3) Nuclear reactions

Table I presents some of the possible nuclear reactions on various targets together with the type of states which can be populated. It is clearly obvious that a large variety of different quasiparticle states can be populated, particularly where a wide variety of nuclear reactions are used. On the other hand, often higher quasiparticle states cannot be populated. It should also be noted that it is often necessary to use several reactions even to populate the fewer numbered quasiparticle states. In addition, Table I indicates the importance of Coulomb excitation and inelastic scattering in studying collective states related to the ground state of the target nucleus. Probably the most powerful advantage of nuclear reactions in studying the detailed nature of deformed states comes about because of the patterns of (d, p) and (d, t) cross-sections which are so unique and follow so closely the theory [7]. The formalism is different for each of the different types of targets presented in Table I. The following general formulas give the cross-section for (d, p) or (d, t) population of a state made up of the target ground state and a Nilsson orbital, q:

$$\frac{d\sigma}{d\omega} = \frac{2I_f + 1}{2I_i + 1}\, g \sum_{jl} \Theta_j^2 \quad \phi_{jl},$$

where $g = 2$ if K_i or $K_f = 0$

$g = 1$ otherwise,

$$\Theta_j = \sqrt{\frac{2I_i+1}{2I_f+1}} \cdot P \left\langle j \pm \Omega_q I_i \pm K_i \,\middle|\, I_f K_f \right\rangle \cdot C^q_{jl} \begin{Bmatrix} U_q \\ V_q \end{Bmatrix}$$

TABLE I. NUCLEAR REACTIONS USED FOR STUDYING DEFORMED NUCLEI

	Nuclear Reaction Producing Particles	Targets			Nuclear Reactions Producing Holes
		Even-even	Odd A	Odd-odd	
		Give following states			
One Neutron Transfer	(d,p)	1 quasi particle	0 quasi particle g.s. and 2 quasi particle (proton)	1 quasi particle g.s. and 3 quasi particle	(p,d) (d,t)
One Proton Transfer	(He^3,d) (He^4,t)	1 quasi particle	0 quasi particle g.s. and 2 quasi particle (proton)	1 quasi particle g.s. and 3 quasi particle	(d,He^3) (t,α)
Two Particle Transfer	(t,p)	Neutron pairing vibrations; vib states, states related to target. 0 or 2 quasi particle	1 or 3 quasi particle	2 or 4 quasi particle	(p,t)
	(He^3,p) (He^4,d)	2 quasi particle	1 or 3 quasi particle	2 or 4 quasi particle	(p,He^3) (d,He^4)
	Coulomb excitation (pp'),(dd'),(αα'),(O^{16},O^{16}')	Rotational & vibrational states; states related to the g.s.			

and

$P = 1$ if $K_f = K_i + \Omega_q$,

$P = (-1)^{I_f+K_f}$ if $K_f = \Omega_q - K_i$,

$P = (-1)^{j+\Omega_q}$ if $K_f = K_i - \Omega_q$, and

I_i, K_i and I_f, K_f refer to the target and residual nuclear spins and their projection on the symmetry axis respectively,

ϕ_{jl} is the DWBA single-particle cross-section [8] with angular momentum transfer, j,

the C^q_{jl} are the coefficients of the expanded state, q, in terms of spherical eigen-states, and the U^2_q (V^2_q) are the probabilities that the state is unoccupied (occupied) in the target nucleus.

Agreement between the experimental and theoretical relative intensities in a rotational band, with absolute experimental intensities in a rotational band, with absolute experimental intensities less than theoretical, indicates the presence of admixtures in the band which are not populated in the (d, p) or (d, t) reaction. Failure to observe the relative intensity pattern predicted by the theory indicates the admixture of two or more components both of which are populated in the reaction under study. This method of separating out components by studying the intensity patterns in rotational bands is just beginning to be important and will obviously gain greatly in importance in the years ahead.

(4) Thermal neutron capture

The study of high- and low-energy gamma rays and electrons following thermal neutron capture is proving to be an increasingly important method of studying the complexity of nuclear states. High-energy gamma rays directly populate a sub-set of the states observed in other nuclear reactions. Thus they put limits on the spins which are valuable to spectroscopists. Furthermore, there is an amazing correspondence between the states directly populated in deformed nuclei following thermal neutron capture and those populated in the (d, p) reaction. The failure of the (n, γ) reaction to directly populate excited proton states in ^{166}Ho and ^{170}Tm appears to indicate a unique nature in the neutron capture process which was not previously envisaged. It should, however, be pointed out that excited proton states have been directly populated in ^{94}Nb [9], ^{90}Y [10], and recently in ^{186}Re [11] and ^{177}Lu [12]. Even so, in view of the very few examples of direct population observed in the deformed nuclei, we are led to believe in a "direct" mechanism playing some part in the (n, γ) reaction.

Low-energy (n, γ) and (n, e) spectroscopy may be thought of in the same terms as decay scheme spectroscopy and has the same advantages. However, because a larger number of gamma rays are observed and a larger number of states populated, the quantity of information obtained is greater.

(5) Analogue state spectroscopy

One of the clearly exciting prospects for future spectroscopy in deformed nuclei is the use of the analogue state (see, for example, Ref. [13]). This type of spectroscopic study is unusually well suited to the study of complex states. Commonly in this type of study, elastic and inelastic proton scattering is used to produce analogues of the same states observed in the (d, p) reaction. With this technique the relationships between the ground state (in the case of the (p, p) reaction) and the excited states (in the case of (p, p') reactions) and the analogue states can be intimately studied. Thus the study of a wide variety of partial compositions of states is available to the spectroscopist. A further advantage of this type of spectroscopy, which has not yet been utilized for deformed nuclei, is a comparison of the energy systematics of the states observed in the (d, p) reaction with the analogue states. In those cases where deformation changes between intrinsic bands, one would expect to see energy differences between the levels observed in the (d, p) reaction and the corresponding analogue states.

III. EXAMPLES

(1) The level structure of ^{162}Dy

At Florida State we have been involved in what has jokingly been called by some an "International Cartel". We feel, however, in all seriousness that the type of co-operation that has evolved, crossing national boundaries, is the future way of experimental low-energy nuclear physics. It allows scientists the potential of approaching nuclear structure problems from a multi-reactional point of view. For the most part, the wide variety of techniques would be unavailable in a single laboratory. As an example of this type of co-operation, we present our work [14] on ^{162}Dy. Conversion spectroscopy following thermal neutron capture was done at Studsvik in Sweden. High-resolution low-energy gamma spectroscopy at Risø in Denmark by German physicists. The high energy (n, γ) spectroscopy was done at Los Alamos, New Mexico, and the charged particle reaction spectroscopy was done at Florida State University. Calculations using the microscopic model for the interpretation of this nucleus were done here in Dubna. Whereas it is already clear from a number of these collaborations that there are often considerable differences of opinion which seriously slow publication and often require successful arbitration, the end result in our opinion is clearly worth the effort. In Figs 1-4, we show the low-energy (n, e), low-energy (n, γ), high-energy (n, γ) and charged-particle reaction spectra. The high-energy (n, γ) picks out a certain sub-set of states populated in the charged-particle reaction. To a large extent these two sets of experiments define the states. The low-

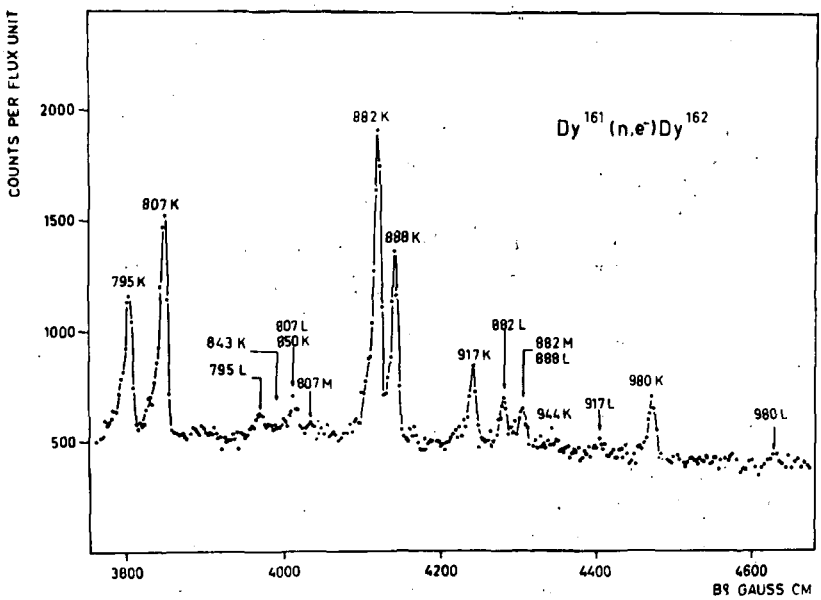

FIG.1. A partial internal conversion spectrum from the reaction ^{161}Dy (n, γ) ^{162}Dy obtained with the Studsvik beta spectrometer.

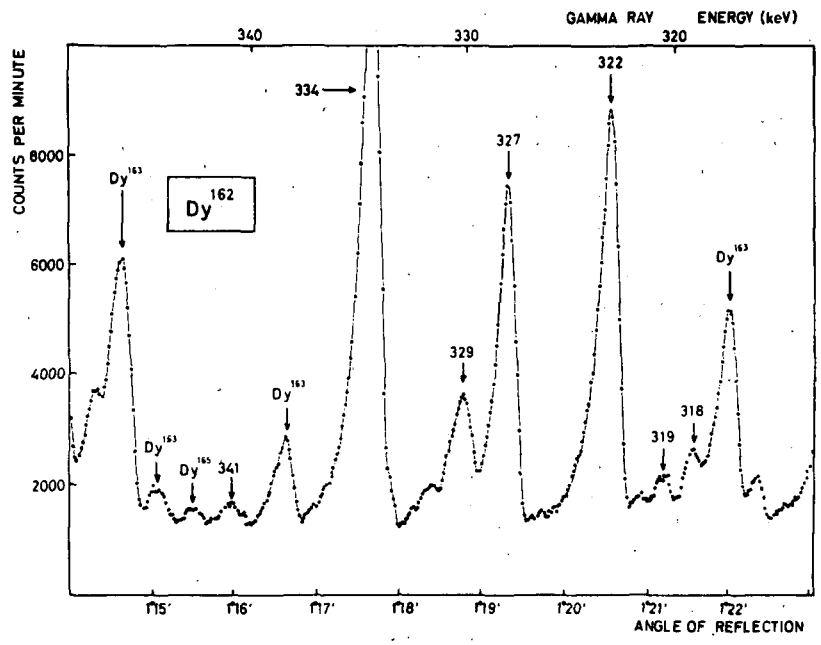

FIG.2. Partial low-energy gamma-ray spectrum for the reaction ^{161}Dy (n, γ) ^{162}Dy obtained with the Risø bent crystal spectrometer in the third order of reflection.

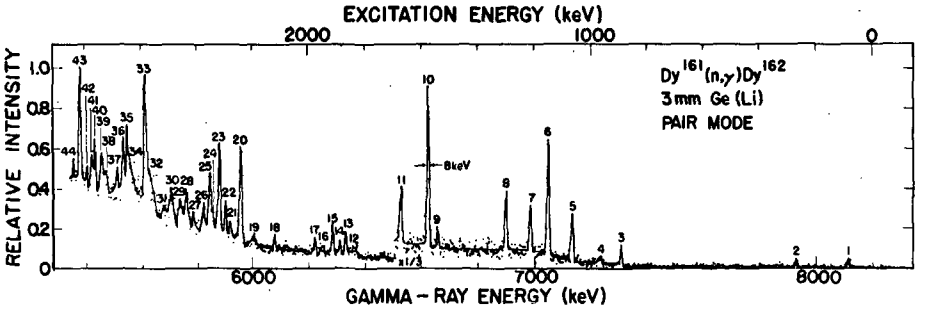

FIG.3. High-energy gamma spectra from the reaction ^{161}Dy (n, γ) ^{162}Dy obtained with a Ge(Li) spectrometer at Los Alamos.

energy (n, γ) and (n, e) spectroscopy determine multipolarity and energy of transitions between states. Through the use of all these data one obtains the level scheme shown in Fig. 5. There is clear evidence for a ground state rotational band with spin parities from 0^+ to spin 8^+ of the K=2 gamma vibrational band from spin 2^+ to spin 6^+ or 7^+ of a K=0 octupole vibrational band with two or possibly three members and of a tentative beta vibrational band. In addition, there is evidence for two sets of 2-neutron quasiparticle rotational bands, and one rotational band which has been interpreted as a 2-proton quasiparticle band. Comparison with the calculations of Soloviev [15] are shown in Table II. The agreement is very satisfactory.

(2) Levels in ^{177}Hf

Using (d, p) and (d, t) reactions [16], together with detailed angular distributions, it is possible to obtain the level scheme shown in Fig. 6 for ^{177}Hf. Heavy bars from the right show the (d, p) cross-section; heavy bars from the left, the (d, t). Comparison of the level structure with the Nilsson Model clearly indicates a large number of low-lying states which cannot be explained by the Nilsson Model and, therefore, probably have vibrational character. Absolute cross-section measurements are also in agreement with this hypothesis. Comparison with the microscopic model calculations of Soloviev is shown in Table III. Although there are many examples in which Soloviev's calculations are closer to experiment, the agreement in this case is quite satisfactory.

(3) Levels in ^{175}Lu and ^{177}Lu

One of the more exciting tests of the theory is the attempt to populate 3 quasiparticle states by beginning with an odd-odd target. This has been done for ^{175}Lu and ^{177}Lu by beginning with the relatively stable odd-odd nucleus ^{176}Lu, the reactions being ^{176}Lu (d, t) ^{175}Lu and ^{176}Lu (d, p) ^{177}Lu [12]. The triton spectrum resulting from the (d, t) reaction on ^{176}Lu is shown in Figure 7. A large number of 3 quasiparticle states is observed. Experimental analysis is thus far incomplete. The 1 quasiparticle ground state band is clearly observed from the 7/2 ground state through the 17/2 state with some slight evidence also for a 19/2 state. The analogous proton spectra resulting from the (d, p) reaction

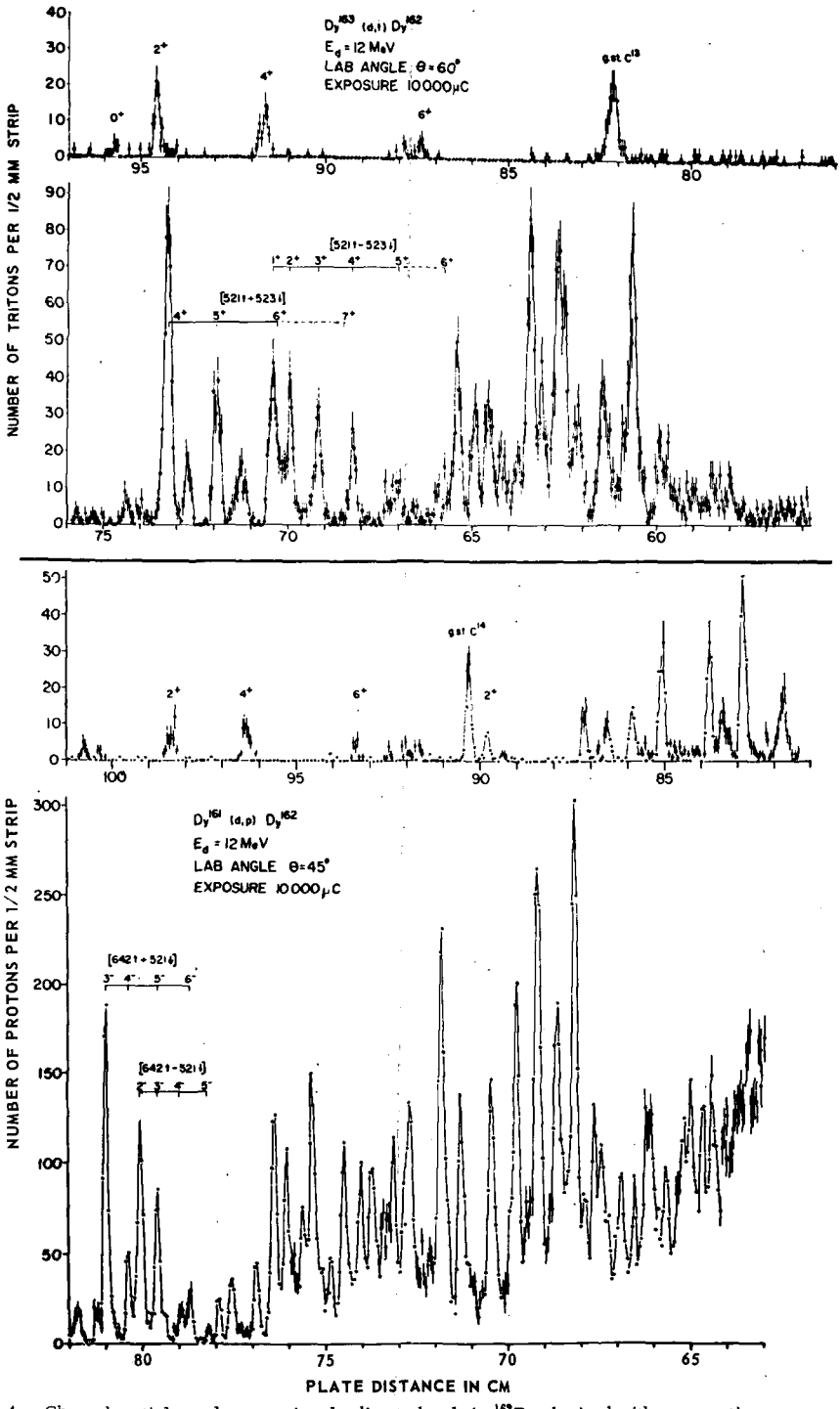

FIG.4. Charged particle nuclear reactions leading to levels in ^{162}Dy obtained with a magnetic spectrograph and the Tandem Van de Graaff at Florida State University. Reaction conditions are given in the figure.

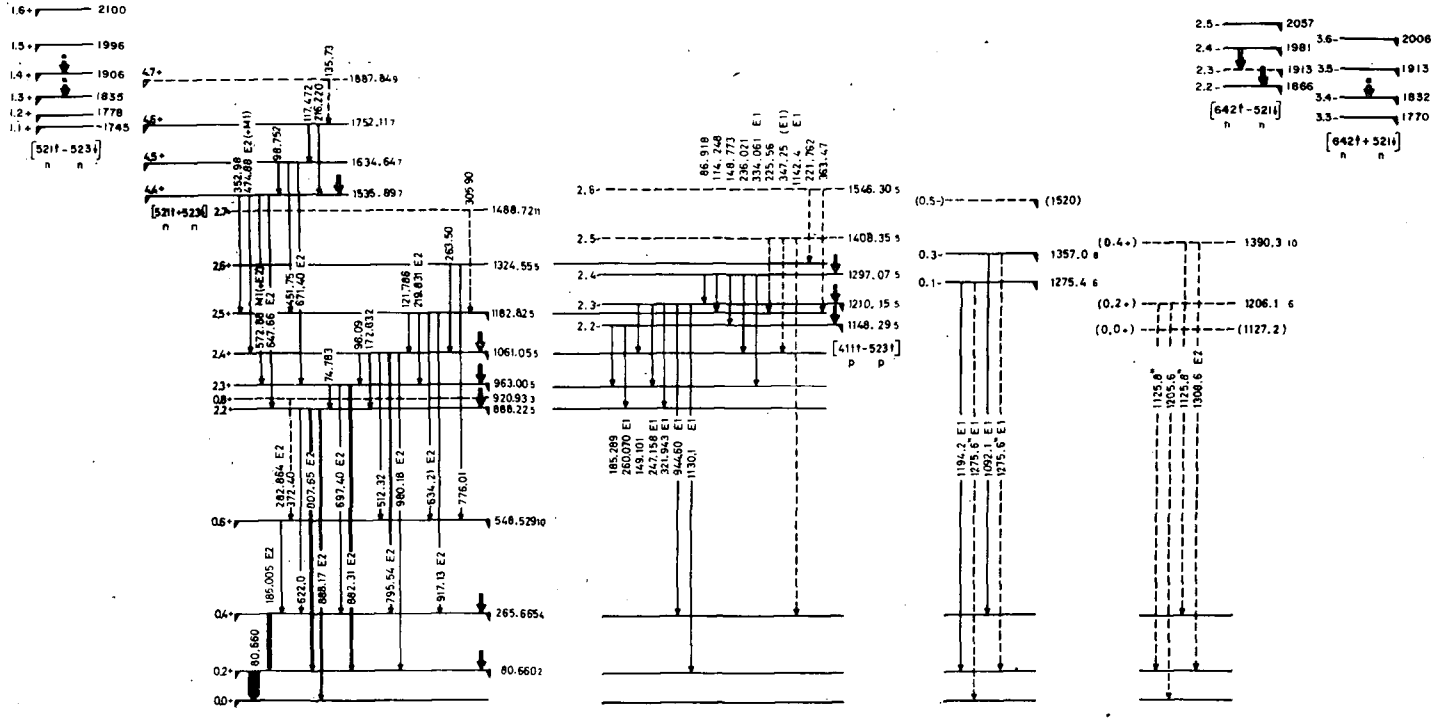

FIG. 5. The level scheme of ^{162}Dy obtained by a combination of experimental methods. The quantum numbers $K\pi^{\pi}$ and the energy in keV are given for each level. A thick arrow indicates direct high energy (n, γ) population. A triangle to the left side of a level indicates a (d, t) populated level and a triangle to the right, a (d, p) populated level.

TABLE II. COMPARISON OF THE CALCULATIONS OF SOLOVIEV [15] WITH THE EXPERIMENTALLY OBSERVED EXCITED BANDS IN ^{162}Dy BELOW 2 MeV

Class of State	State	Kπ	Energy (keV) Expt.	Calc.	Structure
Collective	See Structure	2+	888.2	830	pp 411↑+411↓ 35%; pp 413↑-411↓23%; nn 523↑-521↓ 14%; nn 521↑+521↓12% nn 633↑-651↓ 3%; nn 642↑-660↑ 2%
		0+	(1127)	1400	nn 523↑-523↓ 63%; nn 642↑-642↓21% pp 523↑-523↓ 2%
		2-	1148.3	1200	pp 523↑-411↑ 95%; nn 633↑-521↑ 2%
		0-	1275.4	1100	nn 642↑-523↓ 31%; nn 770↑-660↓12% pp 514↑-404↓ 6%; nn 651↑-521↓ 6% nn 642↑-512↑ 6%; pp 660↑-550↓ 4%
		0+		1600	nn 523↑-523↓ 32%; nn 642↑-642↓36% pp 523↑-523↓ 10%
Two Quasi-Particle Neutron Levels	N N+1 505↑ 523↓	8+ 3+		1700	
	N-1 N+1 642↑ 523↓	5- 0-	1485 Coll.	1710	
	N-2 N+1 521↑ 523↓	4+ 1+	1535.9 1745	1800	
	N-1 N+3 642↑ 521↓	3- 2-	1770 1866		
Two Quasi-Particle Proton Levels	P P+1 411↑ 523↓	2- 5-	1148.3	1670	

TABLE III. CALCULATED AND EXPERIMENTAL LEVELS IN $^{177}_{72}Hf_{105}$

K^{π}	Energy (keV) exper.	calcul.	STRUCTURE					
7/2 −	0	0	514↓ 96%					
5/2 −	504	230	512↑ 97%					
9/2 +	324	440	624↑ 99,5%					
1/2 −	567	600	510↑ 80%;	512↓ + $Q_1(22)$	9%;	512↑ + $Q_1(22)$	5%	
1/2 −	560	720	521↓ 90%;	523↓ + $Q_1(22)$	4%;	521↑ + $Q_1(22)$	4%	
3/2 −	804	750	512↓ 68%;	514↓ + $Q_1(22)$	20%;	510↑ + $Q_1(22)$	11%	
7/2 +	851	1100	633↑ 91%;	633↑ + $Q_1(20)$	5%			
7/2 −	1058	1100	503↑ 82%;	501↑ + $Q_1(22)$	8%;	503↑ + $Q_1(20)$	5%	
1/2 +		1350	651↓ 76%;	651↓ + $Q_1(20)$	14%;	651↓ + $Q_2(20)$	7%	
5/2 −		1450	523↓ 28%;	521↓ + $Q_1(22)$	68%			
3/2 −		1500	521↑ 19%;	521↓ + $Q_1(22)$	80%			
1/2 −	(1882)	1550	510↑ 4%;	512↑ + $Q_1(22)$	95%			
1/2 −	(1634)	1650	521↓ 1%;	521↓ + $Q_1(20)$	99%			
3/2 −	1666	1660	512↓ 11%;	514↓ + $Q_1(22)$	75%;	510↑ + $Q_1(22)$	12%	
3/2 −	1434	1700	501↑ 26%;	503↑ + $Q_1(22)$	40%;	501↓ + $Q_1(22)$	15%	
3/2 −	(1502)	1750	501↑ 30%;	503↑ + $Q_1(22)$	35%;	501↓ + $Q_1(22)$	10%	

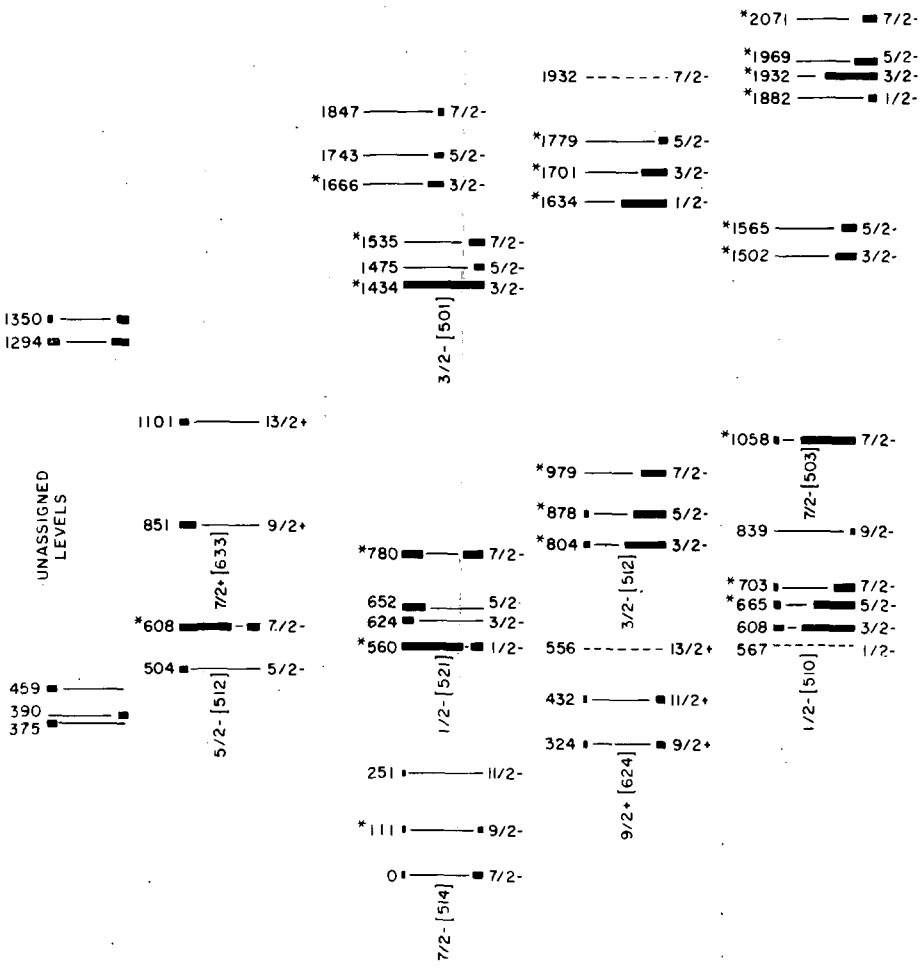

FIG. 6. The level structure of ^{177}Hf. Solid bars from the right indicate relative (d, p) cross-sections and from the left, the (d, t) cross-sections. Asymptotic quantum numbers are listed under each of the bands. Asterisks beside the energy of levels indicate that the measured angular distributions are in agreement with the assignments.

on ^{176}Lu are shown in Fig. 8. Here the ground state band is very weak. However, there are obviously some extremely strongly populated 3 quasiparticle rotational bands. A summary of the interpretation is shown in Fig. 9. The strong 3 quasiparticle states can be interpreted as the configuration $p_{7/2}[404] + n_{7/2}[514] \pm n_{1/2}[510]$. Unfortunately, the appropriate microscopic model calculations for these three quasiparticle states have not yet been made. However, in this case we can test the interpretation using the cross-sections and assuming that the ground state rotational and 3 quasiparticle rotational bands have the pure Nilsson Model configurations. This comparison between experiment and theory is shown in Fig. 10. The agreement is surprisingly satisfactory. Furthermore, this figure allows us to check certain sum rules. More

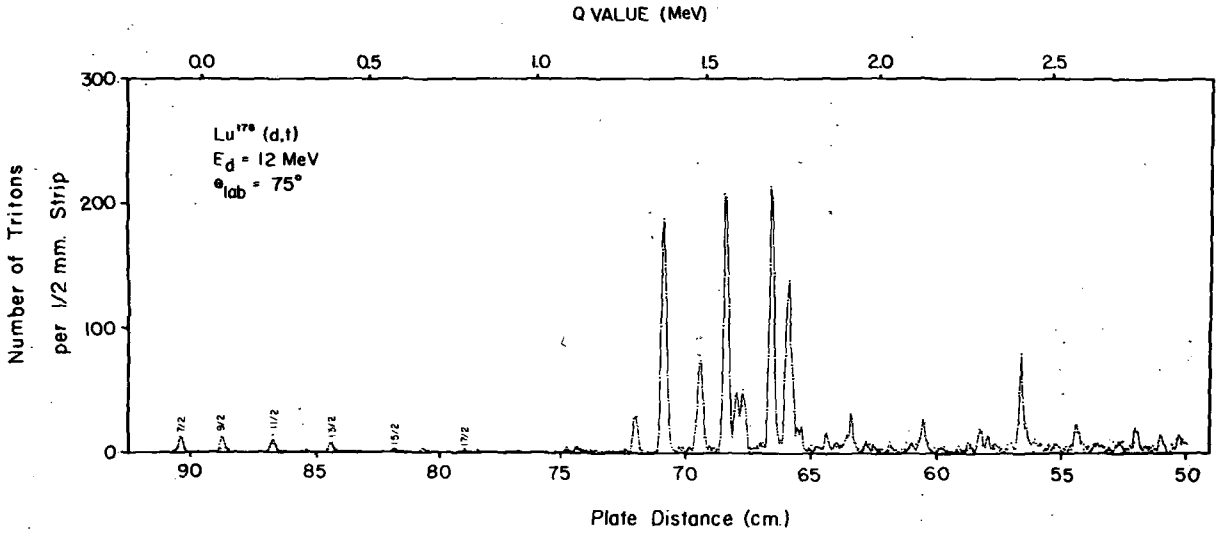

FIG. 7. The triton spectrum resulting from the reaction ^{176}Lu (d, t) ^{175}Lu. The 1 or 3 quasiparticle spectrum is clearly observed. The ground state band is observed from the $7/2^-$ through the $17/2^-$ members.

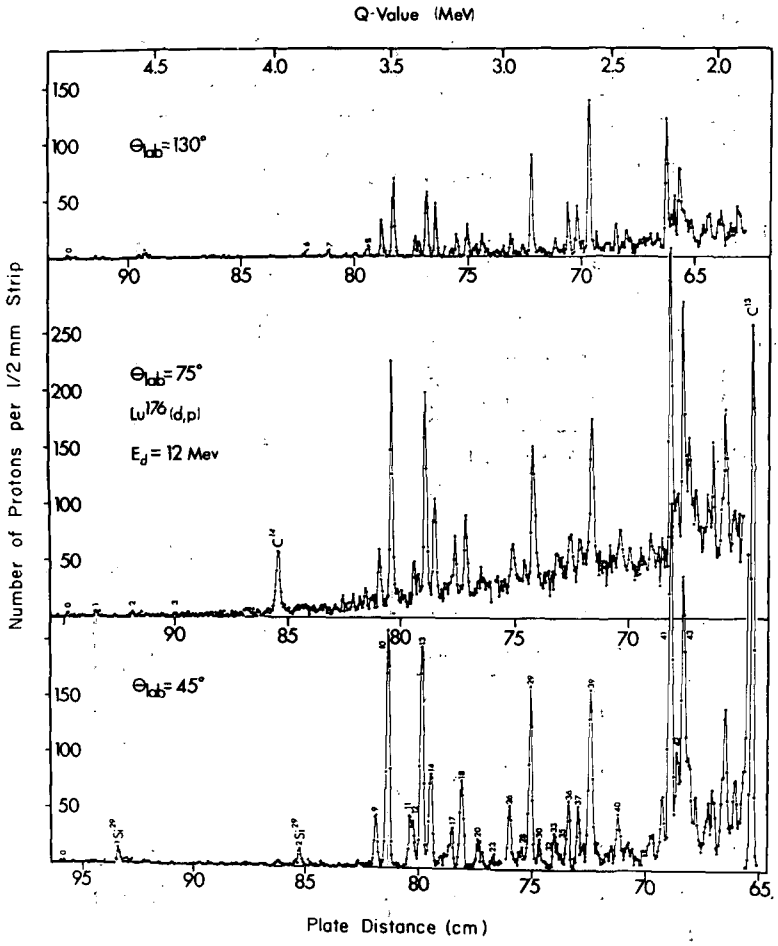

FIG. 8. The proton spectrum resulting from the reaction ^{176}Lu (d, p) ^{177}Lu. The 1 or 3 quasiparticle nature of the spectrum is obvious.

specifically, the summed cross-section to the 15/2 and 13/2 3 quasiparticle bands is expected to be the same and the sum of the strength to both of these bands can be compared to the summed strength of the $1/2^-$ [510] band in the isobaric neighbouring nucleus, ^{177}Yb. These sum rules are in amazingly satisfactory agreement with theory. Thus it seems probable that for a number of 0, 1, 2 and even 3 quasiparticle states, the Nilsson Model or the microscopic calculations of Soloviev using the Nilsson Model are able to successfully predict the spectroscopy of the nuclei and the complex nature of the states. We will now proceed to consider cases in which the Nilsson Model is more severely tested.

(4) Levels in ^{181}Hf

As one approaches the transition region in which the nuclear shape is less rigid and the bottom of the potential well less curved, although

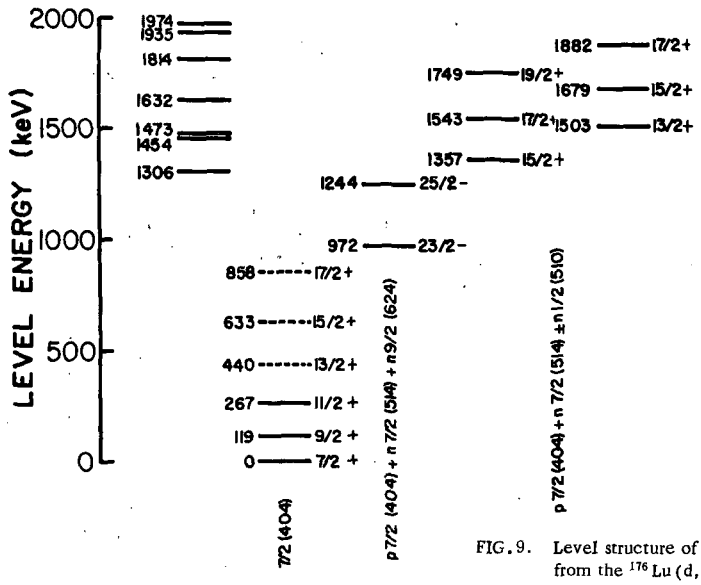

FIG. 9. Level structure of ^{177}Lu as deduced from the ^{176}Lu (d, p) ^{177}Lu reaction.

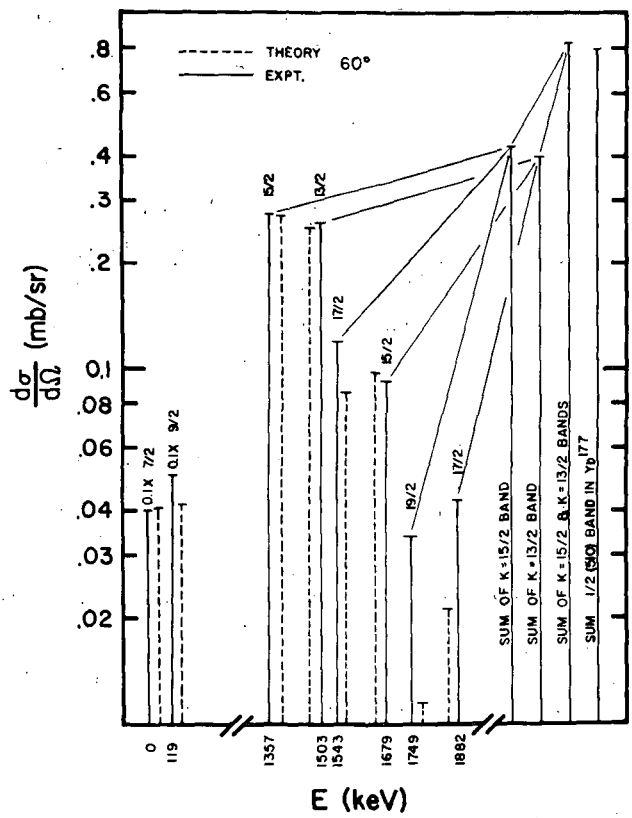

FIG. 10. Comparisons between experiment and theory for the cross-sections observed in the reaction ^{176}Lu (d, p) ^{177}Lu.

nuclei are still deformed at least in their ground state, the validity of the Nilsson Model and the microscopic calculations derived from it is less secure. For example, we have recently completed (d, p) spectroscopy including detailed angular correlation measurements on ^{180}Hf [16]. The level scheme is shown in Fig. 11. For the most part the level structure above 1 MeV cannot be assigned to simple Nilsson states nor reproduced with microscopic model calculations. In particular, I would like to draw your attention to the 1/2⁻ rotational band beginning at 1406 keV. Its "fingerprint" pattern is very similar to that of the ground state 1/2⁻ [510]. Detailed microscopic calculations using the Nilsson Model have been made by Soloviev. A comparison is shown in Table IV. Unfortunately, there is a relatively poor correlation between experiment and theory for states above 1 MeV. In particular, the complex low spin rotational bands perdicted do not agree with experiment. The 1/2⁻ band beginning at 1406 keV, experimentally, is a good example of the failure of the theory. We believed, at the time these experiments were completed, on the basis of absolute (d, p) intensities, that the large number of low spin rotational bands would ultimately be explained in terms of a

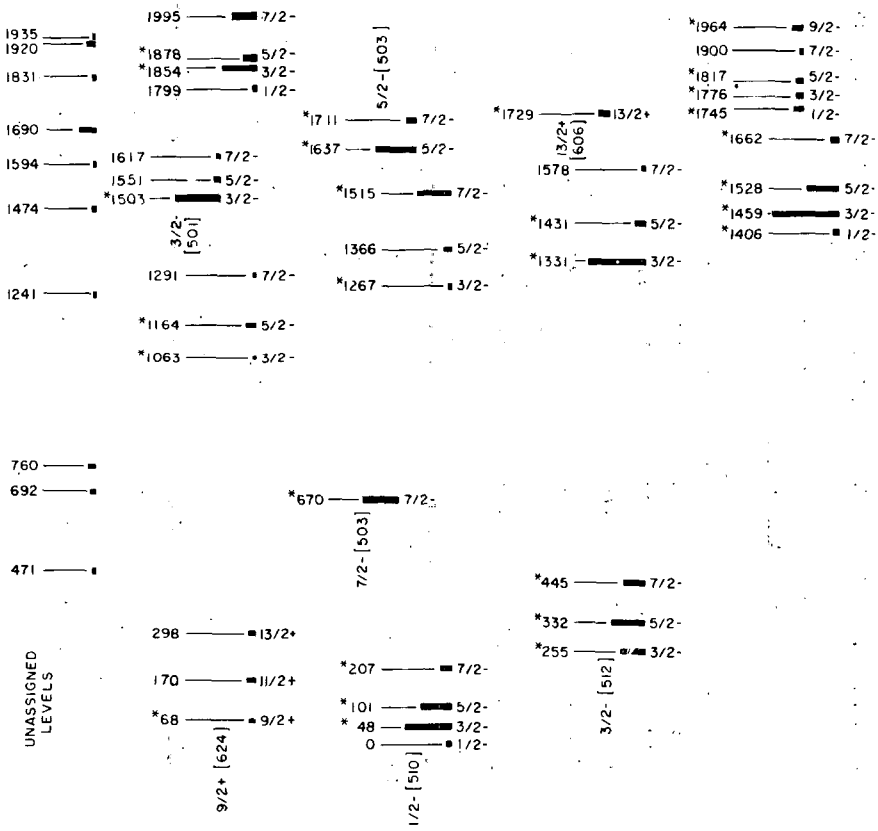

FIG. 11. The level scheme of ^{181}Hf. Heavy bars from the right correspond to (d, p) cross-sections. Asymptotic quantum numbers are given under each of the appropriate rotational bands. Asterisks beside the energy of levels indicate that the measured angular distributions are in agreement with the assignments.

TABLE IV. CALCULATED AND EXPERIMENTAL LEVELS IN $^{181}_{72}Hf_{109}$ (δ = 0.2)

K^{π}	Energy (keV) Exper.	Calcul.	STRUCTURE					
1/2 −	0	0	510↑ 94%;	512↓ + $Q_1(22)$	3%			
3/2 −	255	290	512↓ 91%;	510↑ + $Q_1(22)$	6%			
9/2 +	68	370	624↑ 97%					
9/2 −		460	505↓ 93%;	503↓ + $Q_1(22)$	2%;	505↓ + $Q_1(20)$	2%	
7/2 −	670	610	503↑ 92%;	501↑ + $Q_1(22)$	3%;	503↑ + $Q_1(20)$	3%	
3/2 −	1503	800	501↑ 90%;	503↑ + $Q_1(22)$	7%;	501↓ + $Q_1(22)$	2%	
7/2 −		820	514↓ 97%					
5/2 −		1050	512↑ 86%;	510↑ + $Q_1(22)$	5%			
11/2 +		1100	615↑ 94%;	615↑ + $Q_1(20)$	2%			
1/2 −		1200	521↓ 90%;	523↓ + $Q_1(22)$	3%;	521↑ + $Q_1(22)$	3%	
7/2 +		1350	633↑ 89%;	633↑ + $Q_1(20)$	4%			
1/2 +		1350	651↓ 81%;	651↓ + $Q_1(20)$	7%			
5/2 −		1600	512↑ 4%;	510↑ + $Q_1(22)$	90%			
5/2 −	1637	1650	503↓ 36%;	505↓ + $Q_1(22)$	62%			
3/2 −		1700	512↓ 6%;	510↑ + $Q_1(22)$	92%			
3/2 −		1800	521↑ 49%;	521↓ + $Q_1(22)$	37%;	514↓ + $Q_1(22)$	4%	
1/2 −		1850	501↓ 32%;	501↓ + $Q_1(22)$	58%			
13/2 +	1729	1900	606↑ 88%;	624↑ + $Q_1(22)$	8%			

wide variety of vibrational admixtures. Included are beta, gamma, pairing and octupole vibrations. Since the completion of this experiment a beautiful confirmation of this hypothesis has been obtained by Allan, Britt and Rickey at Los Alamos [17]. These results are shown in Figs 12 and 13, in which the resonance structures obtained from the reaction (p, p) and (p, p') on ^{180}Hf are shown. In Fig. 12, the relationship of various ^{181}Hf states to the ground state of ^{180}Hf is shown. There is a strong isolated $\ell = 3$ resonance at approximately 12.28 MeV which can clearly be associated with the isolated $7/2^-$ band head of the [503] band observed in

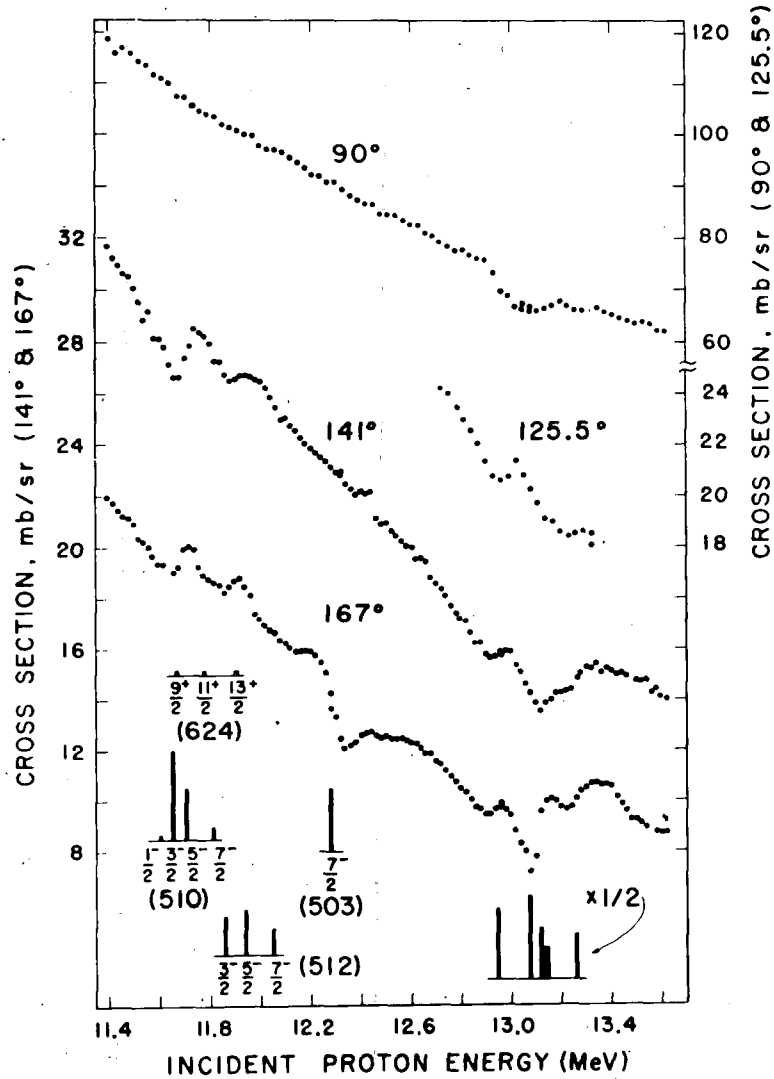

FIG. 12. *Elastic scattering cross-sections for the reaction* ^{180}Hf(p, p)^{180}Hf at 90°, 125.5°, 141°, and 167°. Insets show levels observed in ^{180}Hf(d, p)^{181}Hf (Ref. [16]) where the heights of the bars are proportional to the (d, p) cross-sections at 90°.

the (d,p) reaction at 670 keV. The estimated width of this band is 70 keV and the Coulomb energy shift [^{181}Ta - ^{181}Hf] is measured as 17.24 ± 0.05 MeV compared with the value at 17.40 MeV predicted from the systematics [18]. These data give the first measurement of an isolated resonance width and the first absolute Coulomb energy shift for a deformed nucleus. Of more specific interest in understanding the spectroscopy of ^{181}Hf analogues and ^{180}Hf is the relationship between the 2^+, 4^+ and 1215 keV states of ^{180}Hf and the ^{181}Hf analogue states shown in Fig. 13. The excitation function for the 1215 keV state shows two strong resonances at approximately 12.97 and 13.3 MeV which correspond most closely with the 1331 and 1637 keV states in ^{181}Hf. One of these states (1331 keV) was unassigned and believed to contain large vibrational components. It is now clear that it is closely related to the 1215 keV state in ^{180}Hf and that probably both of these states have considerable gamma vibrational components. It is interesting to note in passing that the analogue experiment does not give absolute information on complex spectroscopic assignments. Instead it relates states. It is, therefore, important to have detailed experimental assignments and microscopic model calculations on both members of the pair being studied (in this case ^{180}Hf and ^{181}Hf analogues).

(5) Levels in ^{186}Re

As we move closer to spherical nuclei, we find that even the ground state rotational band is difficult to explain in terms of the Nilsson Model. The level structure for the odd-odd nucleus, ^{186}Re, is shown in Fig. 14. This research also was done by the "International Cartel" [11], and although the assignments shown are the best which can be made, comparison between the calculated and experimental cross-sections shown in Fig. 15 clearly indicate that the ground state $K=1^-$ band in ^{186}Re is not pure. Coriolis coupling calculations with admixtures of one additional band improve the situation considerably, but do not give an adequate agreement with experiment.

(6) Levels in ^{153}Sm and ^{155}Gd

If we consider the other transition region in rare-earth deformed nuclei — namely, the region in which the neutron number is 91 — we find even more deviations from the simple Nilsson Model. Figs 16 and 17 present the level structure of ^{153}Sm and ^{155}Gd, both 91 neutron nuclei. The level scheme in ^{153}Sm represents a combination of the experimental work of Smither and colleagues [19] at Argonne and charged particle spectroscopy and additional (n,γ) work at Los Alamos and Florida State [20]. The ^{155}Gd nucleus is one of the most thoroughly studied and one of the least understood. The level scheme presented in Fig. 17 results from experimental work at Florida State [21] and was strongly influenced by the coriolis coupling calculations of Bunker and Reich [22]. Several points should be made regarding the spectroscopy of each of these nuclei. In the first place, strong coriolis coupling is playing a very important role. This is most evident in the positive parity bands where even the grouping into bands is highly arbitrary and where some of the states are an almost equal mixture of three different

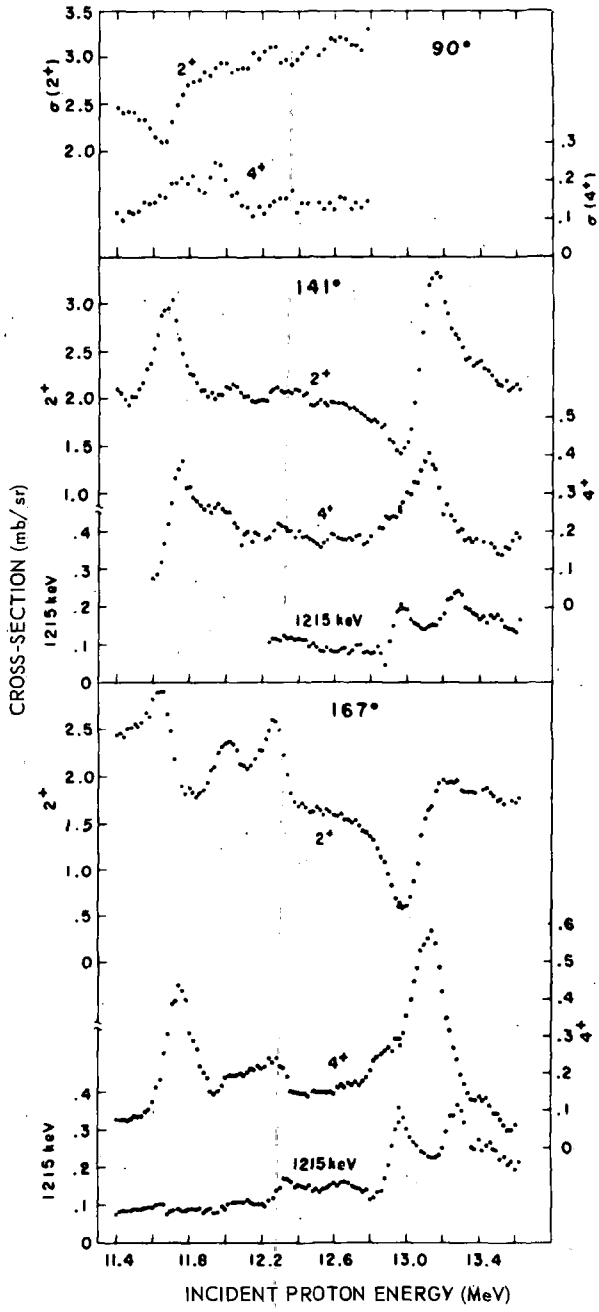

FIG. 13. Cross-sections for inelastic proton scattering to the 2^+, 4^+ and 1215 keV states in ^{180}Hf at 90°, 141° and 167°.

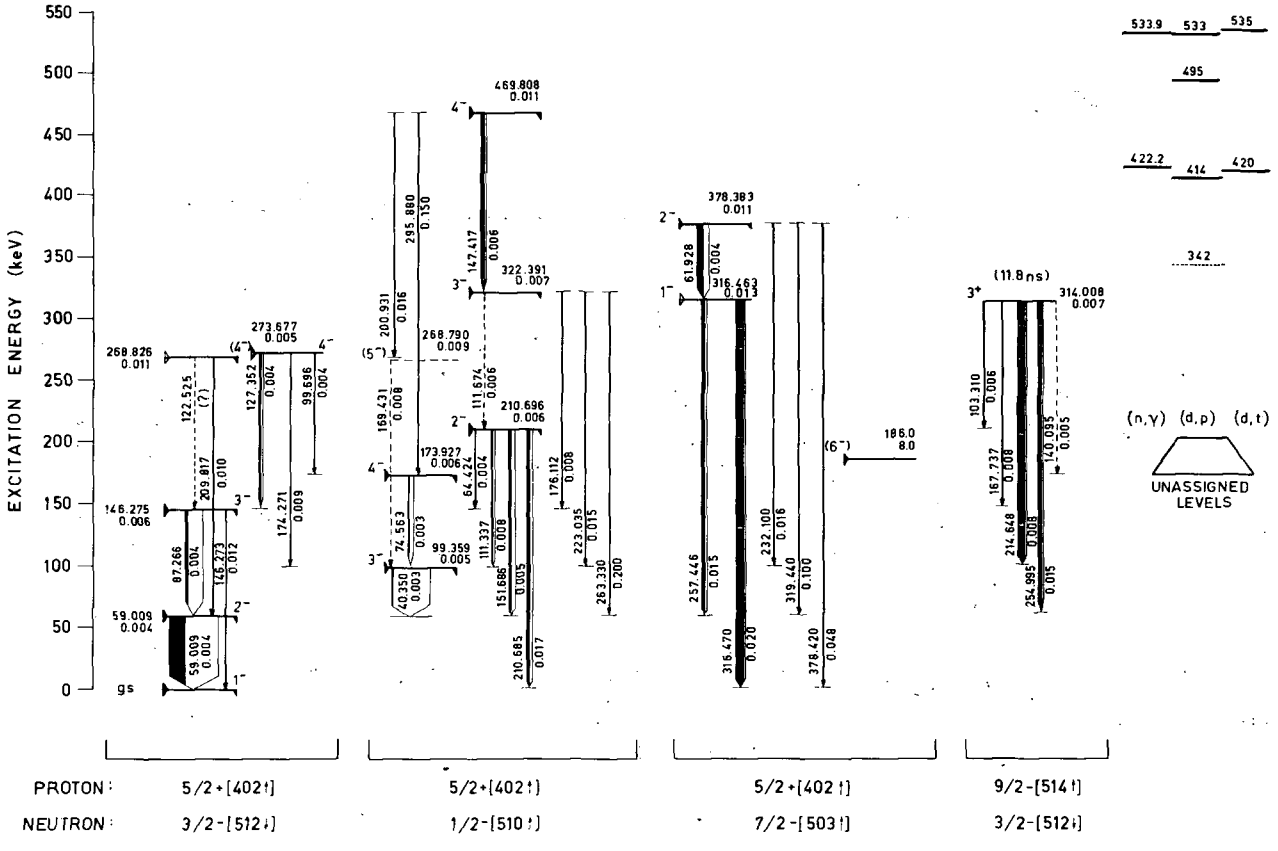

FIG. 14. The level structure in ^{186}Re. Nilsson assignments are shown below the levels. Triangles above the level to the left represent (d, p) population and below, (d, t). Small arrows to the right represent direct high energy (n, γ) population.

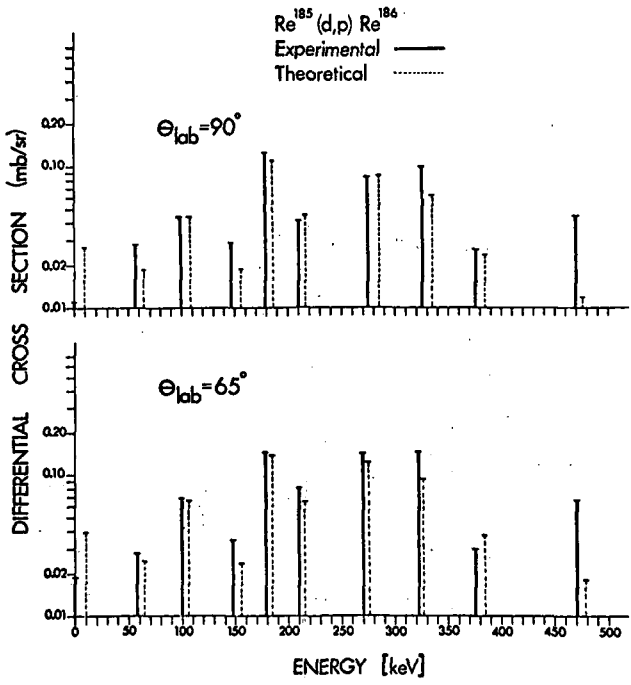

FIG. 15. Comparison between the experimentally calculated and theoretically observed (d, p) cross-sections in the reaction ^{185}Re (d, p) ^{186}Re.

rotational bands. This results in a breakdown of the usual energy sequences, which is clearly evident from the level diagrams themselves. Although the coriolis coupling is considerably less in the negative parity bands it is by no means negligible and in particular the coriolis coupling between the $1/2^-$ [530] and $3/2^-$ [521] band in ^{153}Sm can clearly be observed as an alternation in energy spacings in the $3/2^-$ band. Another interesting anomaly observed both in ^{153}Sm and ^{155}Gd is the presence of two $3/2^+$ rotational bands both of which are populated in the (d, p) and (d, t) reactions quite contrary to expectations from the Nilsson Model. The Nilsson Model predicts that there should be two $3/2^+$ bands with asymptotic quantum numbers [651] and [402]. The band head of the former should not be populated in the (d, p) or (d, t) reactions, whereas the band head of the latter should be extremely intensely populated. In fact, both bands are populated. In ^{155}Gd the total population of both band heads is approximately that expected for the $3/2^+$ [402] band head and indicates approximately a 40-60 mixing of these bands. In ^{153}Sm the total cross-section is somewhat less than expected and the mixing is also less. This phenomenon has been called $\Delta N = 2$ mixing. The type of mixing experimentally observed is shown schematically in Fig. 18. It should be pointed out that the Nilsson Model predicts a much more narrow region of interaction for the two $3/2^+$ bands and a much smaller splitting than that experimentally observed. It seems probable at the present time that the Saxon-Woods diffuse potential gives a reasonable

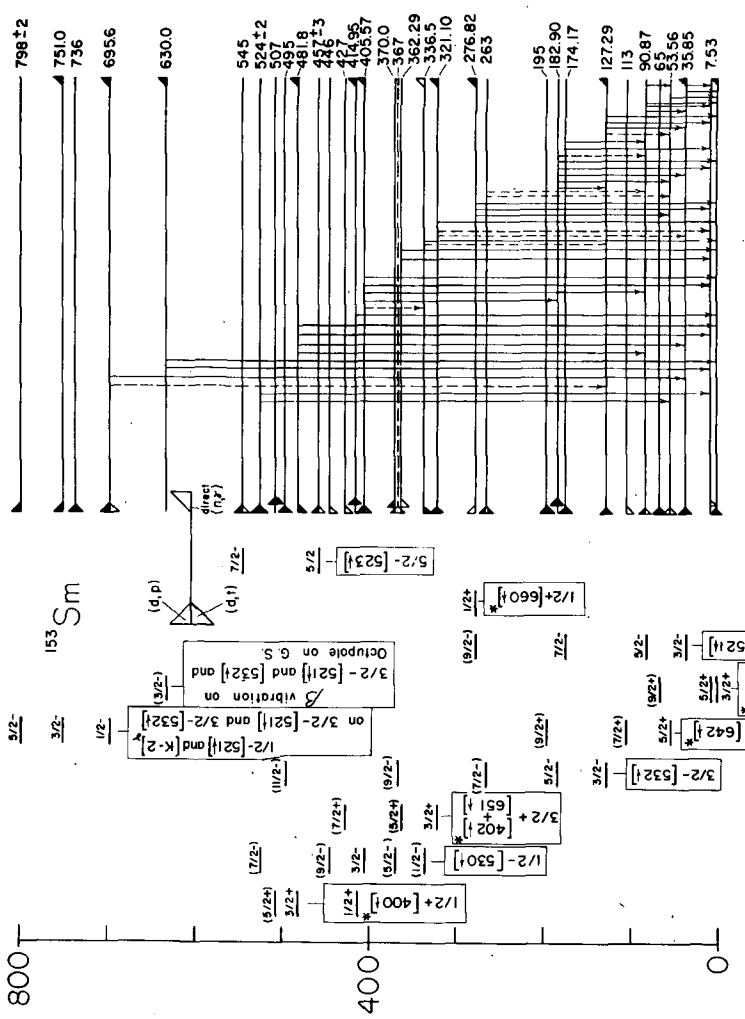

FIG. 16. The level structure of ^{153}Sm. Experimental observations are shown on the right and theoretical interpretation in terms of bands on the left. The (d, p), (d, t) and direct (n, γ) population symbols are shown on the graph. Asterisks indicate highly mixed bands.

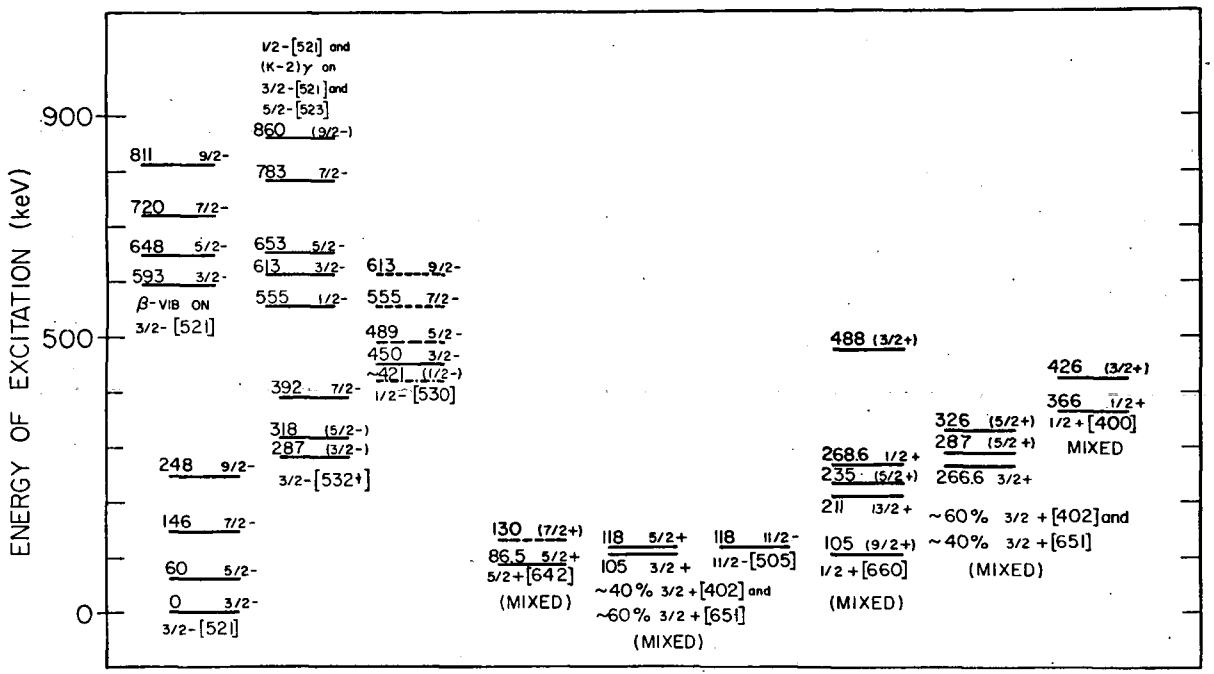

FIG. 17. The level structure of ^{155}Gd. Rotational bands are given Nilsson assignments although, particularly in the positive parity bands, the states are so mixed that the Nilsson assignments are an indication in many cases of only the major component.

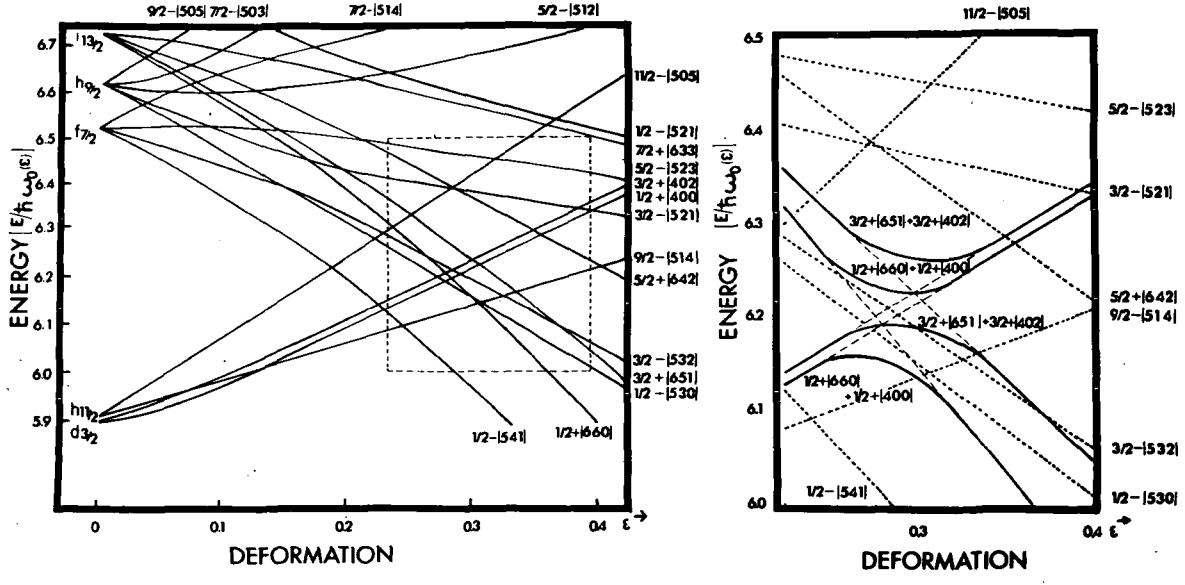

FIG. 18. A schematic representation of $\Delta N=2$ mixing in the region of the Nilsson levels appropriate to the spectroscopy of ^{153}Sm and ^{155}Gd.

account of $\Delta N = 2$ mixing. In any case, however, the ^{153}Sm and ^{155}Gd level schemes clearly illustrate the considerable distortion in the usual level systematics which occurs as one approaches the transition between spherical and deformed nuclei.

IV. CONCLUSIONS

It is becoming increasingly evident that the complex wave-functions of deformed nuclei require considerable variety in the experimental approach. One of the most reasonable ways of obtaining a multi-reactional approach to the study of nuclear levels involves collaboration between a number of laboratories each of which is an expert in one or at most a few experimental methods. It seems probable that this type of collaborative experimental approach will increase in importance in the years ahead.

Without dealing with the large body of strongly deformed nuclei which fit experimental data exceedingly well, we have attempted in this paper to view nuclei which test most severely current nuclear models. It seems that, in the future, calculations will be refined to fit strongly deformed nuclei even more satisfactorily than at present. However, new theoretical approaches may be necessary, particularly in the transitional region between deformed and spherical nuclei. If these new types of theoretical approaches are successful, they may well prove extremely important in studying a large number of nuclei which are not normally considered deformed, but which may, in fact, be more susceptible to a deformed model approach than a shell model approach with considerable configuration interaction. In addition, the new experimental phenomenon of $\Delta N = 2$ mixing needs to be studied theoretically. It seems probable that a Saxon-Woods potential will be necessary in this study. Finally, a wide variety of additional microscopic model calculations, of the type which Soloviev has already made, needs to be carried out. These include calculations of 3 and 4 quasiparticle states in addition to somewhat more sophisticated calculations for 0, 1, and 2 quasiparticle states for a wide variety of nuclei in the strongly deformed region.

ACKNOWLEDGEMENTS

The author wishes to express his appreciation of the help of all the members of the "International Cartel" whose collaboration was essential in much of the information presented in this paper.

REFERENCES

[1] BOHR, A., MOTTELSON, B.R., Dan. Matt. Fys. Medd. 27 16 (1953).
[2] NILSSON, S.G., Dan. Matt. Fys. Medd. Dan. Vid. Selsk. 29 16 (1955).
[3] KISSLINGER, L.S., SORENSEN, R.A., Matt. Fys. Medd. Dan. Vid. Selsk. 32 9 (1960).
[4] SOLOVIEV, V.G., VOGEL, P., JUNGCLAUSSEN, G., Izv. Akad. Nauk SSSR (ser. fiz.) 31 (1967) 518.
[5] BES, D.R., CHO YI-CHUNG, Nucl. Phys. 86 (1966) 581.
[6] BUNKER, M.E., BERZINS, G., STARNER, J.W., Contribution No.35 to this Symposium.

[7] SATCHLER, G.R., Ann. Phys. (N.Y.) 3 (1958) 275.
[8] RASSEL, R.H., DRISKO, R.M., SATCHLER, G.R., ORNL Report No.3240 (1962) unpublished.
[9] JURNEY, E.T., MOTZ, H.T., SHELINE, R.K., SHERA, E.B., VERVIER, J., accepted for publication in Nucl. Phys. (1968).
[10] SHELINE, R.K., JURNEY, E.T., MOTZ, H., (Florida State University) unpublished data.
[11] LANIER, R.G., SHELINE, R.K., MAHLEIN, H.F., VON EGIDY, T., KAISER, W., KOCH, H.R., GRUBER, U., MAIER, B.P.K., SCHULT, O.W.B., HAFEMEISTER, D.W., SHERA, E.B., to be submitted to Phys. Rev.
[12] MINOR, M., SHELINE, R.K., Proc. Int. Conf. on Nuclear Structure, Tokyo (1967).
[13] ANDERSON, J.D., WONG, C., Phys. Rev. Lett. 7 (1961) 250; FOX, J.D., MOORE, C.B., ROBSON, D., Phys. Rev. Lett. 12 (1964) 198.
[14] BÄCKLIN, A., SUAREZ, A., SCHULT, O.W.B., MAIER, B.P.K., GRUBER, U., SHERA, E.B., HAFEMEISTER, D.W., SHELTON, W.N., SHELINE, R.K., Phys. Rev. 160 (1967) 1001.
[15] SOLOVIEV, V.G., (JINR) private communication (1968).
[16] RICKEY, F.A., SHELINE, R.K., accepted for publication in Phys. Rev. (1968).
[17] ALLAN, D.L., BRITT, H.C., RICKEY, F.A., Jr., accepted for publication in Phys. Lett. (1968).
[18] ANDERSON, J.D., WONG, C., McCLURE, J.W., Phys. Rev. 138 (1965) B615.
[19] SMITHER, R.K., BEIBER, E., VON EGIDY, T., KAISER, W., WIEN, K., Bull. Am. phys. Soc. 12 7 (1967) 1065.
[20] SHELINE, R.K., SHIDA, Y., BENNETT, M., (1968) in preparation.
[21] SHELINE, R.K., SHIDA, Y., Phys. Lett. 26B (1968) 210.
[22] BUNKER, M.E., REICH, C.W., Phys. Lett. 25B (1967) 396.

DISCUSSION

KRISHNA KUMAR: In your Table IV there seemed to be a large difference between one experimental energy (68 keV) and the corresponding calculated value (370 keV). Is it a misprint or is this the actual difference?

R.K. SHELINE: This is not a misprint, but is the actual difference between experiment and theory. The difference is somewhat larger than usual but there are several cases of differences this large.

G.K. BACKENSTOSS: I should like to comment on the question of determining the r.m.s. radius of deformed nuclei, their deformation and diffuseness. The study of muonic X-ray spectra (2p-1s and 3d-2p transitions) yields information on the r.m.s. radius, the deformation and the diffuseness. Three years ago at CERN we performed measurements on deformed nuclei and, as I have just learnt from Mrs. Wu, there are also new measurements from Columbia University. There are also data available from the group at the Carnegie Institute of Technology.

R.K. SHELINE: It is of course important to understand the different effects from nuclear shape and diffuseness. Much more data and systematics are obviously necessary.

P. HUBER: What would be the use of polarized particles in getting a new insight into this field?

R.K. SHELINE: There is no doubt that the use of polarized targets, polarized beams or both is an exceptionally important tool. These, of course, are already being used and perhaps I should have mentioned them in my paper. I could mention the very beautiful work of Prof. F.L. Shapiro here at Dubna with polarized targets and beams. These are difficult experiments, but they will obviously become more important in the future.

I.S. SHAPIRO: I would like to note that at present there is neither theoretical nor experimental information allowing one to consider (t, p) or (^{3}He, n) reactions as mainly transfer reactions. These reactions can (and

should) have a more complex mechanism since the separation energy of two transferred nucleons turns out to be too high. (The singularities of the simplest diagrams are, therefore, too remote from the physical region). For this reason, one can hardly use (t, p) and (^{3}He, n) reactions at present to reconstruct the wave-function of complex nuclei.

A. BOHR: I agree with Professor I.S. Shapiro that the analysis of the particle transfer reactions requires profounder studies. However, it is remarkable how well the simple model of a transfer of two particles, as a unit, in a definite state of relative motion works. It is especially significant that this model not only reproduces the angular distributions, but also, rather well, the relative cross-sections. Thus, one sees directly from the experimental data that the states involving the addition of two particles with spatial correlations of the type assumed are populated with strongly enhanced transition amplitudes.

N.K. GLENDENNING: In many cases you are looking at the effects of the deformed field on the bound particle states. However, in the analysis of the experiments, the effect of the deformed field on the scattered particle is neglected. I wonder if you would comment on how important a correction these effects might be.

R.K. SHELINE: We have been interested in the signatures or fingerprints as a spectroscopic tool and have not been concerned so much with the DWBA single-particle cross-sections. Perhaps at least in part this results because this spectroscopic method was first developed at Florida State. Others, such as Dr. Erskine, have been interested in the problem mentioned by Dr. Glendenning. Perhaps Dr. Erskine would like to comment.

J.R. ERSKINE: Our experience at Argonne National Laboratory with (d, p) and (d, t) reactions on various rare-earth and actinide nuclei has shown that agreement between measured cross-sections to deformed single-particle levels and calculated cross-sections is no better than a factor of two, both in absolute cross-section and in relative cross-section for the various levels within a rotational band. Presumably the DWBA theory of the reaction mechanism must be improved with the addition of inelastic scattering effects.

R.K. SHELINE: We too find differences between experiment and theory for (d, p) and (d, t) reactions at Florida State University. The differences are greater for (d, t) reactions than for (d, p) and also greater for states with low cross-section where experiment is uniformly higher than theory.

P. von BRENTANO: You mentioned that there has been recent interest in work trying to measure nuclear deformations from changes in the Coulomb displacement energies. Such differences were recently seen in the deformed nuclei by Mme. Papineau at Saclay, and Wurm and Solf in Heidelberg found a systematic change in the Coulomb displacement energies of the g state analogues of ^{143}Nd to ^{151}Nd. This can be interpreted as due to increasing deformation. However, Lindner has recently pointed out in Zeitschrift für Physik that the Coulomb energy really depends on the r.m.s. radius $\langle R^2 \rangle$. Therefore ΔE_c depends sensitively both on the diffuseness a and the deformation parameter δ. And one needs additional information if one wants to separate these two effects on the Coulomb energy ΔE_c.

J.O. RASMUSSEN: Has there been observation, in (d, p) or (d, t) reactions on even nuclei, of population of rotational members with spin

higher than expected from simple Nilsson wave-functions? Such observations might shed light on the possible importance of extranuclear quadrupole coupling in altering the stripping rotational signatures.

R.K. SHELINE: Such states have been observed by Rickey at Los Alamos. It is felt, however, that the more probable explanation is $\Delta N = 2$ mixing between $N = 6$ and $N = 8$ states.

R.R. CHASMAN: Which is the Nilsson state involved in the $\Delta N = 2$ mixing which Rickey has observed?

M.E. BUNKER: I believe it is the $1/2^+$ [631] state, which is very near the ground state.

J.R. ERSKINE: The (^{3}He, α) reaction has recently been used to measure very high spin states in odd-A uranium nuclei at the University of Rochester. This reaction strongly enhances the yield of high l-value transitions, and therefore may be very useful in finding the components with high j in the deformed wave-functions, which Professor Rasmussen previously asked about.

D. BURKE: I have been involved in the (^{3}He, α) reactions at Rochester. Since this reaction can transfer large amounts of angular momentum we have tried to populate the 17/2 member of the $7/2^+$ [633] rotational band in ^{171}Yb. The calculations of Nemirovsky et al. suggest this state should have a spectroscopic factor of 3 or 4%. A weak population of the state is observed but it is not yet possible to decide whether this is due to an $N = 8$ admixture into the $7/2^+$ [633] state or to an inelastic excitation in the reaction process. There is some hope of distinguishing these two effects because the latter is expected to be enhanced at backward angles. An angular distribution has not been measured.

INTERACTION OF QUASIPARTICLES WITH PHONONS IN DEFORMED NUCLEI

V.G. SOLOVIEV
JOINT INSTITUTE FOR NUCLEAR RESEARCH,
DUBNA, UNION OF SOVIET SOCIALIST REPUBLICS

Abstract — Аннотация

INTERACTION OF QUASIPARTICLES WITH PHONONS IN DEFORMED NUCLEI. The effect of the interaction of quasiparticles with phonons on the structure of the ground and excited non-rotational states of deformed nuclei is investigated. It is noted that both the lowest-lying quasiparticle and one-phonon states are pure enough. The admixture of the two-phonon components to the one-phonon states increases in nuclei of the transition regions as compared to the strongly deformed nuclei. It is shown that with increasing excitation energy the structure of quasiparticle states becomes more complex, i.e. the role of the admixtures becomes more important. The 1-, 2- and 3-quasiparticle components are distributed among a number of non-rotational nuclear levels. As a result, at an excitation energy of 2 MeV and still higher, the number of non-rotational states observed should be greater than that which follows from the independent quasiparticle model. To find the structures of these states a complex experimental study combining alpha, beta and gamma spectroscopy with direct nuclear reactions is needed.

ВЗАИМОДЕЙСТВИЕ КВАЗИЧАСТИЦ С ФОНОНАМИ В ДЕФОРМИРОВАННЫХ ЯДРАХ. Исследовано влияние взаимодействия квазичастиц с фононами на структуру основных и возбужденных неротационных состояний деформированных ядер. Отмечено, что наиболее низкие квазичастичные, а также однофононные состояния являются достаточно чистыми. Примеси двухфононных компонент к однофононным состояниям возрастают в ядрах переходных областей по сравнению с сильно деформированными ядрами. Показано, что с ростом энергии возбуждения происходит усложнение структуры квазичастичных состояний, т.е. увеличивается роль примесей. Одно-, двух- и трехквазичастичные компоненты распределяются по ряду неротационных уровней ядер. В результате, при энергиях возбуждения 2 Мэв и выше должно наблюдаться количество неротационных состояний, большее по сравнению с тем, которое следует из модели независимых квазичастиц. Для нахождения структуры таких состояний необходимо проводить комплексное экспериментальное изучение, сочетающее альфа-, бета- и гамма-спектроскопию с прямыми ядерными реакциями.

I

An investigation is made of the properties of the ground and excited states of deformed nuclei in the framework of the model which takes into account the superconducting pairing correlations and the multipole-multipole interactions.

We perform the Bogolyubov canonical transformation and pass from particles to quasiparticles. The independent quasiparticle model describes well a large assembly of the non-collective states of deformed nuclei. The success of this model is due to the fact that the parameters of the Nilsson and Woods-Saxon potentials, which describe the average field of deformed nuclei, are chosen so that they completely reflect the interactions among all nucleons. It may be said that the average field taken for the ground state of each deformed nucleus is such that it corresponds to the case when the density matrix is actually diagonal. That is why the lowest quasiparticle states are very pure. The potentials used in the calculations describe the average field better in deformed nuclei than in spherical ones.

The collective vibrational states are treated by the approximate second quantization method (Random Phase Approximation). To describe these states we introduce the phonon operators $Q_i(\lambda\mu)$ of multipolarity $\lambda\mu$:

$$Q_i(\lambda\mu) = \frac{1}{2}\sum_{qq'}\left\{\psi_{qq'}^{\lambda\mu i}\, A(q,q') - \varphi_{qq'}^{\lambda\mu i}\, A^+(qq')\right\} \tag{1}$$

The operators

$$A(q,q') = \sum_{\sigma} \sigma \alpha_{q'\sigma}\alpha_{q-\sigma} \qquad \left(\text{or} = \frac{1}{\sqrt{2}}\sum_{\sigma}\alpha_{q\sigma}\alpha_{q'\sigma}\right) \tag{2}$$

$$B(q,q') = \sum_{\sigma} \alpha_{q\sigma}^{+}\alpha_{q'\sigma} \qquad \left(\text{or} = \sum_{\sigma}\sigma\alpha_{q-\sigma}^{+}\alpha_{q'\sigma}\right) \tag{3}$$

are expressed in terms of the quasiparticle operators $\alpha_{q\sigma}$; $q\sigma$ denote the quantum numbers of the average field levels, $\sigma = \pm 1$.

The collective non-rotational states are treated as one-phonon, two-phonon and so on states with wave functions

$$Q_i^+(\lambda\mu)\Psi_0,\ Q_{i_1}^+(\lambda_1\mu_1)Q_{i_2}^+(\lambda_2\mu_2)\Psi_0 \ldots \text{ where } Q_i(\lambda\mu)\Psi_0 = 0$$

The energies of the one-phonon states $\omega_i^{\lambda\mu}$ are the solutions of the secular equation

$$1 = 2\kappa^{(\lambda)}\sum_{qq'}\frac{(f^{\lambda\mu}(qq'))^2 u_{qq'}^2 (\epsilon(q)+\epsilon(q'))}{(\epsilon(q)+\epsilon(q'))^2 - (\omega_i^{\lambda\mu})^2} \tag{4}$$

Here $\kappa^{(\lambda)}$ is the interaction constant of multipolarity λ, $f^{\lambda\mu}(qq')$ is the matrix element of the multipole-moment operator $\lambda\mu$, $\epsilon(q) = \sqrt{C^2 + \{E(q)-\lambda\}}$, $u_{qq'} = u_q v_{q'} + u_{q'} v_q$ (in this case $u_q^2 + v_q^2 = 1$), $u_q^2 = \frac{1}{2}\left\{1 + \frac{E(q)-\lambda}{\epsilon(q)}\right\}$ where C is the correlation function, λ is the chemical potential, E(q) are the energies of the average field one-particle levels. The roots of (4) are denoted as $i = 1, 2, \ldots$

After performing the Bogolyubov canonical transformation introducing the phonon operators and finding the roots of (4), the most essential part of the interaction Hamiltonian can be written as follows:

$$H = \sum_q \varepsilon(q) B(q,q) - \frac{1}{4}\sum_{\lambda,\mu>0}\sum_{ii'}\frac{1}{2\kappa^{(\lambda)}}\frac{(Q_i(\lambda\mu)^+ + Q_i(\lambda\mu))(Q_{i'}^+(\lambda\mu)+Q_{i'}(\lambda\mu))}{\sqrt{Y^i(\lambda\mu)\,Y^{i'}(\lambda\mu)}}$$

$$-\frac{1}{4}\sum_{\lambda\mu i}\frac{1}{\sqrt{Y^i(\lambda\mu)}}\sum_{qq'} f^{\lambda\mu}(qq')\, v_{qq'}\left\{B(qq')(Q_i^+(\lambda\mu)+Q_i(\lambda\mu)) + (Q_i^+(\lambda\mu) + \right.$$

$$\left. + Q_i(\lambda\mu))\, B(qq')\right\} \tag{5}$$

Here

$$Y^i(\lambda\mu) = \sum_{qq'} \frac{(f^{\lambda\mu}(qq'))^2 u_{qq'}^2 \omega_i^{\lambda\mu}(\varepsilon(q)+\varepsilon(q'))}{[(\varepsilon(q)+\varepsilon(q'))^2 - (\omega_i^{\lambda\mu})^2]^2}, \quad v_{qq'} = u_q u_{q'} - v_q v_{q'} \quad (6)$$

The theoretical and experimental information on the one-phonon states is summarized in Ref.[1]. The one-phonon state components, the values of $\omega_i^{\lambda\mu}$ and $Y^i(\lambda\mu)$, calculated with the wave functions of the Nilsson potential are given in Ref.[2].

It should be noted that, as is shown in Ref.[3], the lowest one-phonon states in strongly deformed nuclei (i.e. in nuclei outside the transition regions) are fairly pure, i.e. the two-phonon state admixtures to them are very small.

As is known, there are two main reasons for the appearance of admixtures to quasiparticle and phonon states: (i) the coupling between the internal and rotational motions of the nucleus as a whole, and (ii) the interaction of quasiparticles with phonons. We shall investigate the effect of the quasiparticle-phonon interaction on the structure of quasiparticle and one-phonon states in deformed nuclei.

We should bear in mind that the presence of quasiparticles leads to some change in phonons. However, as a rule this change is not large and is neglected by us.

II

Let us investigate what the quasiparticle-phonon interaction in odd-mass deformed nuclei leads to. Following Ref.[4], the wave function of an odd-mass nucleus with a given K^π value is written as

$$\Psi(K^\pi) = \frac{1}{\sqrt{2}} C_\rho \sum_\sigma \left\{ \alpha_{\rho\sigma}^+ + \sum_{\lambda\mu i\nu} D_{\rho\nu\sigma}^{\lambda\mu i} \alpha_{\nu\sigma}^+ Q_i^+(\lambda\mu) \right\} \Psi_0 \quad (7)$$

with the normalization condition

$$C_\rho^2 \left\{ 1 + \frac{1}{\sqrt{2}} \sum_{\lambda\mu i} \sum_{\nu\sigma} (D_{\rho\nu\sigma}^{\lambda\mu i})^2 \right\} = 1 \quad (8)$$

Here by ρ we denote the average field level with a given K^π.

We find the average value of H over $\Psi(K^\pi)$ and from the condition of the energy minimum, taking into account Eq.(8), we get a secular equation and the quantities C_ρ, $D_{\rho\nu\sigma}^{\lambda\mu i}$ in the form

TABLE I. DISTRIBUTION AND MIXING OF THE ONE-QUASIPARTICLE COMPONENTS

Nuclei	K^{π}	ρ_1	$\epsilon(\rho_1)$ (MeV)	ρ_2	$\epsilon(\rho_2)$ (MeV)	η_j (MeV)	$c_j^2(\rho_1)$ (%)	$c_j^2(\rho_2)$ (%)	Poles (MeV) (β_0)
^{177}Yb	$1/2^-$	510 ↑	1.11	521 ↓	2.34	0.93	91.0	10^{-3}	
						2.12	2×10^{-3}	88.0	
						2.92	0.1	8.2	
^{167}Yb	$5/2^-$	523 ↓	1.13	512 ↑	2.06	0.86	90.0	2.0	
						1.44	2.4	76.0	1.868
						1.90	2.0	3.3	
^{165}Dy	$5/2^-$	523 ↓	1.34	512 ↑	1.65	0.98	25.0	58.0	
						1.17	69.0	23.0	2.967
						3.14	0.1	4.9	
	$3/2^-$	521 ↑	1.64	532 ↓	3.35	1.23	79.0	1.0	1.821
						1.85	2.3	0.1	1.977
						2.00	12.5	4.5	
						2.65	0.4	51.0	
^{159}Dy	$3/2^+$	402 ↓	1.62	651 ↑	1.42	0.76	1.0	83.0	(β=0.30)
						1.03	85.0	1.3	
			1.40		1.55	0.78	16.0	65.0	(β=0.33)
						0.85	72.0	16.0	
^{157}Dy	$5/2^-$	523 ↓	1.42	512 ↑	3.05	0.85	72.0	4.0	
						1.74	11.0	14.0	1.769
						1.98	0.8	2.0	
						2.21	1.8	47.0	

$$\varepsilon(\rho) - \eta_j - \frac{1}{4}\sum_{\lambda\mu i}\sum_{\nu}\frac{v_{\rho\nu}^2}{Y^i(\lambda\mu)}\frac{(f^{\lambda\mu}(\rho\nu))^2}{\varepsilon(\nu)+\omega_i^{\lambda\mu}-\eta_j} = 0 \qquad (9)$$

$$C_\rho^{-2} = 1 + \frac{1}{4}\sum_{\lambda\mu i}\sum_{\nu}\frac{v_{\rho\nu}^2}{Y^i(\lambda\mu)}\frac{(f^{\lambda\mu}(\rho\nu))^2}{(\varepsilon(\nu)+\omega_i^{\lambda\mu}-\eta_j)^2} \qquad (10)$$

$$D^{\lambda\mu i}_{\rho\nu\sigma} = \frac{1}{2}\frac{v_{\rho\nu}}{\sqrt{Y^i(\lambda\mu)}}\frac{f^{\lambda\mu}(\rho\nu)}{\varepsilon(\nu)+\omega_i^{\lambda\mu}-\eta_j} \qquad (11)$$

The quantity C^2 determines the contribution of the one-quasiparticle component, the quantity $1/2C_\rho^2 \sum_\sigma (D^{\lambda\mu i}_{\rho\nu\sigma})^2$ that of the component with a quasiparticle in the ν-state and the phonon $\lambda\mu i$.

For each value of K^π and ρ there is an equation of the type (9), whose solution $\eta_1, \eta_2, \ldots$ gives the state energies. As is known, in the scheme of the average field levels there are several states with a given K^π. In Ref.[4] the general case is considered when several states $\rho_1, \rho_2, \ldots \rho_n$ with a given K^π are taken into account. The case when two states are taken into account is studied in detail in Ref.[5].

The interaction of quasiparticles with phonons leads to the appearance of admixtures in the one-quasiparticle states, to collective non-rotational states and to the appearance of the complex structure states. It affects spectroscopic factors, decoupling parameters, etc. The role of the interaction of quasiparticles with phonons in odd-A deformed nuclei was investigated in detail in Refs.[5-8].

Using an equation such as Eq.(9), which takes into account simultaneously the two one-quasiparticle states ρ_1 and ρ_2, we calculate the admixtures of one state to the other due to the interaction through phonons. The investigations performed show that in the overwhelming majority of cases the mixing of two states with given K^π's is fairly small. A considerable mixing of two one-quasiparticle components occurs in the two cases: when one or both $\epsilon(\rho_1)$ and $\epsilon(\rho_2)$ are larger than the first pole of Eq.(9) and when both the average field levels with identical K^π are very close to each other, e.g. in the quasi-intersection of one-particle states from different principal oscillator shells ($\Delta N = 2$ mixing).

The effect of mixing of ρ_1 and ρ_2 in comparatively high-excited states is shown in Table I, where $C_j^2(\rho_1)$ and $C_j^2(\rho_2)$ determine the contribution of the components ρ_1 and ρ_2 to the state with a given η_j. It is seen from Table I that in most cases the mixing is not large. The states which contain a noticeable contribution of both components ρ_1 and ρ_2 can be found experimentally. When ρ_1 is a hole and ρ_2 is a particle state removed from the Fermi surface, this level will be excited simultaneously in the (dp) and (dt) reactions, i.e. (dp) will go through ρ_2, and (dt) through ρ_1. The first experimental evidence for these states is available [9, 10].

It should be noted that the results of Tables I and II are calculated with the one-particle state energies and the wave-functions of the Woods-Saxon potential [11-12], the phonons being calculated in Refs [13, 14]. The one-particle states are denoted by the Nilsson potential quantum numbers $Nn_z\Lambda\Sigma$; $Nn_z\Lambda\uparrow$ labels the state with $K = \Lambda + \Sigma$ and $Nn_z\Lambda\downarrow$ the state with $K = \Lambda - \Sigma$.

As is known, the states with identical K^{π} and with quantum numbers N and $N \pm 2$ must be mixed. In Ref.[11] it is shown that in the case of the one-particle states of the Woods-Saxon potential, such a mixing occurs near the quasi-intersection of levels, but for a very narrow range of the deformation values. Experimental data, giving evidence of the mixture of the N and $N \pm 2$ states, are obtained in Refs [15, 16]. It is clear that this effect can be observed only when the range of the deformation parameter values is not too narrow so that this range includes the equilibrium deformation of an odd-mass nucleus. The quasiparticle-phonon interaction leads to an enlargement of the deformation range where the mixing of the two states occurs. This effect is shown in Table I where for ^{159}Dy we give the mixing of the $402\downarrow$ and $651\uparrow$ states for $\beta = 0.30$ and 0.33; the quasi-intersection of these levels occurs at $\beta = 0.32$.

III

The quasiparticle-phonon interactions result only in small admixtures in the ground and lowest-lying states of odd-mass deformed nuclei, states with large K being purer. With increasing excitation energy the admixtures become more important. The interactions of quasiparticles with phonons cause the one-quasiparticle states of the Nilsson or Woods-Saxon potentials to be distributed over a number of non-rotational levels with given K values. With increasing excitation energy the one-quasiparticle component is distributed, as a rule, over a still increasing number of levels. Table II gives examples of this distribution.

The study of the odd-mass deformed nucleus structure performed in Refs [10, 17-19] with the aid of the (dp) - and (dt)-reactions has shown that the number of non-rotational states with a given K^{π} found in experiments is much larger than that given by the Nilsson scheme although the total excitation intensity agrees with the estimates obtained with the Nilsson wave-functions. These experiments prove the conclusions about the distribution of the one-quasiparticle components over many non-rotational levels.

Three-quasiparticle components must be distributed over many levels to a still larger extent. Among the purest three-quasiparticle states are states with largest K or those which cannot form the combination quasiparticle plus phonon with $\lambda = 2$ or $\lambda = 3$.

The distribution of some three-quasiparticle components over several levels can be detected in the allowed-unhindered (au) beta decay. For example, in Ref.[20] fast beta-transitions from the $p411\uparrow$ state in ^{163}Tb to some ^{163}Dy levels are found. They may be explained as transitions to the three-quasiparticle configuration $n523\downarrow$, $p523\uparrow$, $p422\uparrow$, i.e. the au beta decay proceeds between the $n523\downarrow$ and $p523\uparrow$ states. It should be noted that the $pp523\uparrow$-$411\uparrow$ states enter the composition of the phonon $\lambda = 3$, $\lambda = 2$.

At excitation energies of 2-3 MeV or higher, the process of the distribution of the one- and three-quasiparticle components over the non-rotational levels in odd-mass nuclei is expected to be essentially intensified as compared with lower excitation energies. Information on the structure of such states in deformed and spherical nuclei is very poor. Interesting qualitative results proving this distribution are obtained in Ref. [21]. The spectrum of

TABLE II. DISTRIBUTION OF THE ONE-QUASIPARTICLE COMPONENTS OVER THE LEVELS

Nuclei	K^{π}	ρ	$\epsilon(\rho)$ (MeV)	j	η_j (MeV)	$c_j(\rho)^2$ (%)	Poles (Eq. (9)) (MeV)
^{167}Yb	$7/2^+$	633 ↑	1.17	1	1.00	94.0	2.34
				2	2.38	2.3	2.59
	$1/2^-$	521 ↓	1.30	1	1.17	93.0	2.06
				2	2.10	2.6	2.18
				3	2.19	1.3	2.46
				4	2.48	2.5	2.59
	$5/2^-$	512 ↑	2.06	1	1.42	79.0	1.87
				2	1.88	2.8	2.21
					5.06	14.0	
	$9/2^+$	624 ↑	2.38	1	1.94	59.0	2.15
				2	2.22	15.0	2.51
				3	2.56	8.0	2.98
				4	2.99	0.3	3.37
^{157}Dy	$3/2^-$	532 ↓	2.06	1	0.97	61.0	1.67
				2	1.72	1.5	1.75
				3	1.79	3.6	1.82
^{155}Gd	$5/2^+$	642 ↑	1.28	1	0.94	86.0	2.02
				2	2.09	4.5	2.34
				3	-	-	2.41
				4	2.44	1.6	2.71
	$3/2^-$	532 ↓	2.06	1	1.13	70.0	1.99
				2	-	-	2.37
				3	2.38	0.3	2.44
	$9/2^-$	514 ↑	3.27	1	2.27	24.0	2.36
				2	2.44	6.7	2.47
				3	2.60	42.0	3.14
				4	3.15	0.4	3.65
				5	3.66	0.5	3.68
				6	4.51	23.0	

delayed protons produced as a result of the β^+ decay of ^{111}Te to the ^{111}Sb levels is studied there. The complex structure of the proton spectrum may be understood if the one- and three-quasiparticle components are assumed to be distributed over many ^{111}Sb levels.

IV

We consider the admixtures of the two-phonon states to the lowest one-phonon states in even-even deformed nuclei. Following Ref.[3], the wave function describing the state with a given K^π (corresponding to λ_0, μ_0, i_0) is written in the form

$$\Psi_{i_0}(K^\pi) = C_{i_0}(\lambda_0\mu_0)\Big\{Q^+_{i_0}(\lambda_0\mu_0) + \sum_{\substack{\lambda\mu i\\ \lambda'\mu' i'}} \Delta^{\lambda\mu i}_{\lambda'\mu' i'}(\lambda_0\mu_0 i_0) Q^+_i(\lambda\mu) Q^+_{i'}(\lambda'\mu')\Big]\Psi_0 \qquad (12)$$

with the normalization condition

$$C^2_{i_0}(\lambda_0\mu_0)\Big\{1 + 2\sum_{\substack{\lambda\mu i\\ \lambda'\mu' i'}} \big(\Delta^{\lambda\mu i}_{\lambda'\mu' i'}(\lambda_0\mu_0 i_0)\big)^2\Big\} = 1 \qquad (13)$$

We find the average value of H over $\Psi(K^\pi)$ and then from the condition of the energy minimum we find $C_{i_0}(\lambda_0\mu_0)$ and $\Delta^{\lambda\mu i}_{\lambda'\mu' i'}(\lambda_0\mu_0 i_0)$. The secular equation determining the excited state energies ζ_j is obtained in the form

$$\omega^{\lambda_0\mu_0}_{i_0} - \zeta_j = \frac{1}{2}\sum_{\substack{\lambda\mu i\\ \lambda'\mu' i'}} \frac{\big[U^{\lambda\mu i}_{\lambda'\mu' i'}(\lambda_0\mu_0 i_0)\big]^2}{\omega_i^{\lambda\mu} + \omega_{i'}^{\lambda'\mu'} - \zeta_j} \qquad (14)$$

where

$$U^{\lambda\mu i}_{\lambda'\mu' i'}(\lambda_0\mu_0 i_0) = \frac{1}{2}\sum_{qq'q_2} v_{qq'}\Big\{\frac{\rho^{\lambda\mu}_{qq'}}{\sqrt{Y^i(\lambda\mu)}}\big(\psi^{\lambda_0\mu_0 i_0}_{q_2 q}\psi^{\lambda'\mu' i'}_{q_2 q'} + \varphi^{\lambda_0\mu_0 i_0}_{q_2 q}\varphi^{\lambda'\mu' i'}_{q_2 q'}\big) +$$
$$+ \frac{\rho^{\lambda'\mu'}_{qq'}}{\sqrt{Y^{i'}(\lambda'\mu')}}\big(\psi^{\lambda_0\mu_0 i_0}_{q_2 q}\psi^{\lambda\mu i}_{q_2 q'} + \varphi^{\lambda_0\mu_0 i_0}_{q_2 q}\varphi^{\lambda\mu i}_{q_2 q'}\big) + \qquad (15)$$
$$+ \frac{\rho^{\lambda_0\mu_0}_{qq'}}{\sqrt{Y^{i_0}(\lambda_0\mu_0)}}\big(\psi^{\lambda\mu i}_{q_2 q}\varphi^{\lambda'\mu' i'}_{q_2 q'} + \psi^{\lambda'\mu' i'}_{q_2 q}\varphi^{\lambda\mu i}_{q_2 q'}\big)\Big\}$$

Further,

$$C^2_{i_0}(\lambda_0\mu_0) = 1 + \frac{1}{2}\sum_{\substack{\lambda\mu i\\ \lambda'\mu' i'}} \frac{\big[U^{\lambda\mu i}_{\lambda'\mu' i'}(\lambda_0\mu_0 i_0)\big]^2}{\big(\omega_i^{\lambda\mu} + \omega_{i'}^{\lambda'\mu'} - \zeta_j\big)^2} \qquad (16)$$

$$\Delta^{\lambda\mu i}_{\lambda'\mu' i'}(\lambda_0\mu_0 i_0) = \frac{1}{2}\,\frac{U^{\lambda\mu i}_{\lambda'\mu' i'}(\lambda_0\mu_0 i_0)}{\omega_i^{\lambda\mu} + \omega_{i'}^{\lambda'\mu'} - \zeta_j}\,. \qquad (17)$$

The energy shifts of the lowest vibrational states and the contributions of the one-phonon components are calculated by means of Eqs (14) and (16) in Refs [3, 22]. The calculations are carried out with the one-particle level scheme and the Nilsson potential wave functions, the parameters of which are given in Ref.[23]. In calculating the Nd, Sm, Dy, Er, Th and U isotopes the following two-phonon admixtures $(\lambda\mu i)$, $(\lambda'\mu' i')$ are taken into account: for the one-phonon states $K^\pi = 0^+$ - (201), (201); (221), (221); (301), (301); (311), (311) and (321), (321); for the one-phonon states $K^\pi = 2^+$ - (221), (201); (321), (301) and (311), (311). In calculating the first $K^\pi = 2^+$ states in the W and Os isotopes only the admixtures (221)(201) are taken into account. A part of the calculation results is given in Table III.

It is seen from the table that for strongly deformed nuclei the admixtures of the two-phonon components to the one-phonon states are very small. The exception is the case of the $K^\pi = 0^+$ state in ^{166}Er where the (201) one-phonon state energy is close to the (221) (221) two-phonon pole.

The calculations show that the lowest two-phonon states of strongly deformed nuclei are very pure. Therefore the splitting energy of the two-phonon multiplets in them is expected to be lower than in the spherical nuclei. It is interesting to detect these states experimentally. For example, the two-phonon $K^\pi = 4^+$ (221)(221) states in the Dy and Er isotopes must have an energy of (1.5-2.0) MeV.

It is seen from Table III that for the nuclei of the transition region the anharmonic effects increase slightly. For example, in ^{152}Sm and ^{150}Nd the admixtures of the two-phonon states to the gamma vibrational ones are very small. However, the admixtures to the beta vibrational states are large and they increase rapidly from ^{158}Dy to ^{152}Sm and especially in ^{150}Nd. This appears to be due to a strong change of the deformation in the transition from $N = 90$ to $N = 88$.

In the region of the W and Os isotopes the inverse picture is observed. The admixtures of the two-phonon components to the one-phonon $K^\pi = 0^+$ states are very small. The admixtures of the two-phonon components to the first one-phonon $K^\pi = 2^+$ states are somewhat larger; they grow in the transition from the W to Os isotopes, and they increase in these isotopes with increasing number of neutrons. The magnitude of the admixtures also increases with decreasing deformation. In other words, in the W and Os isotopes the gamma vibration anharmonicity increases when approaching the boundary of the region of non-spherical nuclei. However, the anharmonicity is not large and can be taken into account by perturbation theory. It is interesting to compare this result with the smooth decrease of the equilibrium deformations of nuclei in the considered region.

It should be noted that the two-phonon states in nuclei of the transition region, the first experimental evidence for which is given in Ref.[24], are not so pure as in strongly deformed nuclei.

Thus, the performed investigations show that anharmonic effects in even-even nuclei in the regions $150 < A < 190$ and $228 < A < 256$ are very small and in the overwhelming majority of cases may be neglected. This conclusion agrees with the calculated dependence [25, 26] of the total energy of strongly deformed nuclei on β and γ deformations which is the parabola near its minimum. The situation essentially differs in nuclei of the new deformation region containing neutron-deficient isotopes of barium, cerium and others. As is shown in Ref.[27], the nuclei of this region are very soft

TABLE III. ENERGY SHIFTS $\Delta\omega_1^{\lambda_0\mu_0} = \omega_1^{\lambda_0\mu_0} - \zeta_1$ AND THE CONTRIBUTIONS OF THE ONE-PHONON COMPONENTS $C_1(\lambda\mu)^2$ TO THE $K^\pi = 0^+$ AND 2^+ STATES

Nuclei	β_0	$K^\pi = 0^+$		$K^\pi = 2^+$	
		$\Delta\omega_1^{20}$ (keV)	$C_1(20)^2$ (%)	$\Delta\omega_1^{22}$ (keV)	$C_1(22)^2$ (%)
^{159}Nd	0.30	357	76.40	0.05	99.98
^{152}Sm	0.30	46.1	95.40	0.05	99.989
^{158}Dy	0.30	16	98.40	-	-
^{166}Er	0.30	2	94.60	3	99.50
^{184}W	0.23	-	-	0.01	99.99
	0.20	-	-	0.02	99.99
^{186}W	0.23	-	-	0.2	99.99
	0.20	-	-	1.8	99.87
^{184}Os	0.20	-	-	0.001	99.99
	0.17	-	-	1.1	99.89
^{186}Os	0.20	-	-	0.13	99.99
	0.17	-	-	10.3	99.07
^{188}Os	0.20	-	-	3.0	99.73
	0.17	-	-	32.1	97.31
^{190}Os	0.20	-	-	32.7	95.52
	0.17	-	-	82.7	93.40

against gamma deformations. The coupling between rotations and oscillations in them is expected to be strong and anharmonic corrections to be large.

V

We consider here the effect of the interaction of quasiparticles with phonons on the two-quasiparticle states in even-even deformed nuclei and the problem as to how complicated the structure of these states becomes with increasing excitation energy.

Since Eq.(12) is valid for all $\lambda\mu i$ values it contains the limiting cases too, when one or two phonon operators transform into two-quasiparticle operators. If we consider only phonons with $\lambda = 2$, $\mu = 0, 2$ and $\lambda = 3$, $\mu = 0, 1, 2$ (in Ref.[28] it is shown that the states with $\lambda = 3$, $\mu = 3$ are practically two-quasiparticle ones), then Eq.(12) can be written as follows:

$$\Psi(K^{\pi}, \rho_1, \rho_2) = C(\rho_1\rho_2)\Big\{\sum_{\sigma_1\sigma_2} a_{\sigma_1\sigma_2}\Big[\alpha^{+}_{\rho_1\sigma_1}\alpha^{+}_{\rho_2\sigma_2} + \sum_{\substack{\lambda\mu i \\ q_1 q_2}} D^{\lambda\mu i}_{q_1 q_2 \sigma_1\sigma_2}(\rho_1\rho_2)\alpha^{+}_{q_1\sigma_1}\alpha^{+}_{q_2\sigma_2}Q_i^{+}(\lambda\mu)\Big] + \sum_{\substack{\lambda\mu i \\ \lambda'\mu' i'}} \Delta^{\lambda\mu i}_{\lambda'\mu' i'}(\rho_1\rho_2)Q_i^{+}(\lambda\mu)Q_{i'}^{+}(\lambda'\mu')\Big\}\Psi_0 \qquad (18)$$

where all $\psi^{\lambda\mu i}_{q_1 q_2} = 0$, $a_{\sigma_1\sigma_2} = \delta_{\sigma_1\sigma_2}$, if $K = K_{\rho_1} + K_{\rho_2}$ and $a_{\sigma_1\sigma_2} = \sigma_1\delta_{\sigma_1,-\sigma_2}$, if $K = |K_{\rho_1} - K_{\rho_2}|$.

We find the average value of the Hamiltonian (5) over (18) and using the variation principle we get the secular equation in the form

$$\varepsilon(\rho_1) + \varepsilon(\rho_2) - \lambda_j - \frac{1}{8}\sum_{\lambda\mu i}\sum_{\nu}\frac{1}{Y^2(\lambda\mu)}\Big\{\frac{(f^{\lambda\mu}(\rho_1\nu))^2 v^2_{\rho_2\nu}}{\varepsilon(\nu) + \varepsilon(\rho_2) + \omega_i^{\lambda\mu} - \lambda_j} + \frac{(f^{\lambda\mu}(\rho_2\nu))^2 v^2_{\rho_1\nu}}{\varepsilon(\rho_1) + \varepsilon(\nu) + \omega_i^{\lambda\mu} - \lambda_j}\Big\} - \frac{1}{2}\sum_{\substack{\lambda\mu i \\ \lambda'\mu' i'}}\frac{(U^{\lambda\mu i}_{\lambda'\mu' i'}(\rho_1\rho_2))^2}{\omega_i^{\lambda\mu} + \omega_{i'}^{\lambda'\mu'} - \lambda_j} = 0 \qquad (19)$$

where $U^{\lambda\mu i}_{\lambda'\mu' i'}(\rho_1\rho_2)$ is easily obtained from (15). From the normalization condition we find

$$C(\rho_1\rho_2)^{-2} = 1 + \sum_{\lambda\mu i}\sum_{q_1 q_2 \sigma}\left(D^{\lambda\mu i}_{q_1 q_2 \sigma, \pm\sigma}(\rho_1\rho_2)\right)^2 + 2\sum_{\substack{\lambda\mu i \\ \lambda'\mu' i'}}\left(\Delta^{\lambda\mu i}_{\lambda'\mu' i'}(\rho_1\rho_2)\right)^2 \qquad (20)$$

$$D^{\lambda\mu i}_{q_1 q_2 \sigma, \pm 6}(\rho_1\rho_2) = \frac{1/4}{Y^L(\lambda\mu)} \frac{\delta_{\rho_2 q_2} v_{\rho_1 q_1} f^{\lambda\mu}(\rho_1 q_1) + \delta_{\rho_1 q_1} v_{\rho_2 q_2} f^{\lambda\mu}(\rho_2 q_2)}{\varepsilon(q_1) + \varepsilon(q_2) + \omega_i^{\lambda\mu} - 3j} \qquad (21)$$

$$\Delta^{\lambda\mu i}_{\lambda'\mu' i'}(\rho_1\rho_2) = \frac{1}{2} \frac{U^{\lambda\mu i}_{\lambda'\mu' i'}(\rho_1\rho_2)}{\omega_i^{\lambda\mu} + \omega_{i'}^{\lambda'\mu'} - 3j} \qquad (22)$$

For the $K > 4$ states $U^{\lambda\mu i}_{\lambda'\mu' i'}(\rho_1\rho_2) = 0$ and Eq.(19) takes on the form obtained in Ref.[29].

Eqs (19) have been solved for $U^{\lambda\mu i}_{\lambda'\mu' i'}(\rho_1\rho_2) = 0$ and the structure of non-collective states of even-even deformed nuclei has been investigated. The results of calculations are given in Tables IV and V, the two-quasiparticle state energies being calculated without taking the blocking effect into account.

The analysis performed has shown that the lowest two-quasiparticle states, the first poles of (19) of which are essentially higher than the two-quasiparticle energies, are fairly pure. Table IV gives the states where the admixtures are less than 2%. Somewhat higher two-quasiparticle states, the first poles of which exceed the two-quasiparticle energy by 0.5 MeV and more, are also sufficiently pure; the admixtures do not exceed 5%.

When the first pole in (19) is close to $\epsilon(\rho_1) + \epsilon(\rho_2)$ or even smaller than this value, then such states can no longer be considered to be two-quasiparticle states. In these cases the considered two-quasiparticle configuration is distributed over several levels. States of this kind are shown in Table V. The energies of these states as a rule exceed 3 MeV in the range $150 < A < 190$.

This distribution effect can be observed experimentally in beta decay and direct nuclear reactions when the number of the discovered states with a given K^π will be larger than the number of corresponding two-quasiparticle states available. Apparently, the distribution of such a type occurs in a number of cases. For example, in Ref.[30] several $K^\pi = 4^+$ levels have been observed in ^{158}Dy; in Ref.[31] several $K^\pi = 1^+$ and 1^- levels have been detected in ^{160}Dy, and, as is shown in Refs [32, 33] an especially large number of $K^\pi = 1^+$, 1^- and 0^- levels have been found in ^{170}Yb. The observed increase of log ft in the transitions to these states as compared to the majority of transitions of the type ah and 1u is an additional argument in favour of the two-quasiparticle component distribution.

Thus, the overwhelming majority of the two-quasiparticle states up to an energy of 3 MeV are fairly pure. However, with increasing energy the structure of the states becomes more complicated, the admixtures to the two-quasiparticle component increase and in some cases are predominant, and the two-quasiparticle configurations are distributed over a number of levels.

Let us investigate the problem as to how strongly the interaction of quasiparticles with phonons mixes the two-quasiparticle states with identical K^π. The wave function is taken in the form

TABLE IV. STRUCTURE OF THE TWO-QUASIPARTICLE STATES

Nuclei	K^{π}	ρ_1	ρ_2	$\epsilon(\rho_1)+\epsilon(\rho_2)$ (MeV)	j	ζ_j (MeV)	$C_j(\rho_1\rho_2)^2$ (%)	Poles (Eq. (19)) (MeV)
^{178}Hf	8^-	n514↓,	n624↑	1.88	1	1.86	99.0	3.10
	8^-	p514↑,	p404↓	1.82	1	1.80	99.8	3.10
^{170}Yb	5^-	p411↓,	p514↑	2.33	1	2.24	94.1	2.91
					2	2.93	2.6	3.12
					3	3.28	2.7	
	5^+	p411↑,	p404↓	2.84	1	2.77	94.6	3.35
					2	3.37	3.6	3.75
	3^+	n521↓,	n512↑	2.57	1	2.54	96.6	3.04
					2	3.05	0.3	3.38
					3	3.40	1.8	3.42
					4	3.43	0.9	3.50
					5	3.51	0.2	
	5^+	n523↓,	n512↑	2.95	1	2.92	97.3	3.53
					2	3.54	0.2	3.64
					3	3.65	1.2	
^{166}Er	5^-	n642↑,	n523↓	2.26	1	2.22	97.3	3.34
					2	3.35	0.1	3.36
					3	3.37	0.8	3.53
					4	3.54	0.1	4.30
^{164}Dy	6^+	n642↑,	n633↑	2.57	1	2.52	96.8	3.37
					2	3.39	1.3	3.50
					3	3.51	0.4	3.63
^{160}Dy	4^-	n521↑,	n642↑	2.37	1	2.30	97.6	3.21
					2	3.22	0.2	3.34
					3	3.35	0.5	3.48

$$\Psi(K^{\pi};\rho_1\rho_2\rho_3\rho_4) = \frac{1}{\sqrt{2}} \sum_{\sigma_1\sigma_2} a_{\sigma_1\sigma_2} \{C'(\rho_1\rho_2)\alpha^+_{\rho_1\sigma_1}\alpha^+_{\rho_2\sigma_2} + \quad (23)$$

$$+C'(\rho_3\rho_4)\alpha^+_{\rho_3\sigma_1}\alpha^+_{\rho_4\sigma_2} + \sum_{\substack{\lambda\mu i\\ q_1q_2}} D^{\lambda\mu i}_{q_1q_2\sigma_1\sigma_2}(\rho_1\rho_2\rho_3\rho_4)\alpha^+_{q_1\sigma_1}\alpha^+_{q_2\sigma_2}Q^+_i(\lambda\mu)\}\Psi_0$$

We find the average value of H over this state and on the basis of the variational principle we get a secular equation. After solving this equation

TABLE V. DISTRIBUTION OF THE TWO-PARTICLE CONFIGURATIONS OVER THE LEVELS

Nuclei	K^{π}	ρ_1	ρ_2	$\epsilon(\rho_1)+\epsilon(\rho_2)$ (MeV)	j	ζ_j (MeV)	$C_j(\rho_1\rho_2)^2$ (%)	Poles (Eq. (19)) (MeV)
^{170}Yb	3^+	p411↓,	p402↑	2.78	1	2.65	78.3	2.91
					2	2.96	13.0	3.12
					3	3.28	8.2	
	7^-	n633↑,	n514↓	3.19	1	2.94	24.0	3.01
					2	3.23	73.8	3.56
	3^+	n512↓,	n514↓	3.37	1	3.23	51.8	3.04
					2	3.42	1.8	3.43
					3	3.48	13.4	3.51
					4	3.54	32.0	
^{166}Er	5^+	n523↓,	n512↑	3.02	1	2.95	88.0	3.14
					2	3.25	0.9	3.52
					3	3.59	10.4	
^{160}Dy	5^-	n521↑,	n633↑	3.30	1	3.17	61.4	3.21
					2	3.23	18.5	3.25
					3	3.37	15.9	3.48

TABLE VI. MIXING OF THE TWO-QUASIPARTICLE $K^{\pi} = 1^{+}$ STATES IN ^{162}Dy

ρ_1 ρ_2	$\epsilon(\rho_1)+\epsilon(\rho_2)$ (MeV)	ρ_3 ρ_4	$\epsilon(\rho_3)+\epsilon(\rho_4)$ (MeV)	j	ζ_j (MeV)	$C_j^{\prime}(\rho_1\rho_2)^2$ (%)	$C_j^{\prime}(\rho_3\rho_4)^2$ (%)
n523↓, n521↑	2.28	n642↑, n633↑	2.83	1	2.25	83.0	0.4
				2	2.81	0.16	91.0
n523↓, n512↑	2.28	n642↑, n651↑	2.74	1	2.25	97.5	0.05
				2	2.71	0.2	92.3
n523↓, n521↑	2.28	p523↑, p532↑	2.83	1	2.25	98.0	0.04
				2	2.82	0.01	95.0
p411↑, p411↓	2.815	p523↑, p532↑	2.83	1	2.78	63.0	33.0

we find the energies ζ_j and using the normalization condition we determine the contributions of the two-quasiparticle components $C'(\rho_1\rho_2)^2$ and $C'(\rho_3\rho_4)^2$. A part of the results is given in Table VI. It is seen that in the overwhelming majority of cases this mixing is small; the exceptions are a few cases when the two-quasiparticle state energies are close to each other.

In the framework of the model with pairing and multipole-multipole forces, the effect of the interaction of quasiparticles with phonons on the complication of the state structure of deformed nuclei with increasing excitation energy has been considered. This complication is also due to the coupling with rotations, and to the occurrence of such interactions which either lead to, for example, spin splitting, or which are considered by Bochnacki and Ogaza [34]. It is interesting to study the structure of excited states for the interactions of quasiparticles by the Migdal theory of finite Fermi systems [35]. The available experimental data suggest that this complication of the structure with increasing excitation energy actually occurs. It is not quite clear how reliably and completely the above model describes the structure of the states at an energy of 1-2 MeV and higher in odd-A and at 2-3 MeV and higher in even-even deformed nuclei. With increasing excitation energy new features of the internuclear interactions should certainly be revealed and we may hope that the experimental information going beyond the framework of the considered model would help to single out and formulate some additional important components of nuclear forces. The most important conclusions of the model are related to the symmetry properties of the interaction rather than to the explicit form of the nuclear forces (e.g. to their radial dependence).

Since the structure of the deformed nuclear states becomes complicated with increasing excitation energy, a complex experimental study of these states is needed which will combine β and γ spectroscopy with direct nuclear reactions.

ACKNOWLEDGEMENTS

The author wishes to thank R.V.Jolos, A.A.Korneichuk, L.A.Malov, S.I.Fedotov, U.M.Fainer and G.Jungclaussen for their help and discussions.

REFERENCES

[1] SOLOVIEV, V.G., Atom. Energy Rev. 3 (1965) 117.
[2] ZHELEZNOVA, K.M., KORNEICHUK, A.A., SOLOVIEV, V.G., VOGEL, P., JUNGCLAUSSEN, G., Preprint JINR D-2157 (1965).
[3] JOLOS, R.V., SOLOVIEV, V.G., ZHELEZNOVA, K.M., Phys. Lett. 25B (1967) 393.
[4] SOLOVIEV, V.G., Phys. Lett. 16 (1965) 308.
[5] SOLOVIEV, V.G., VOGEL, P., Nucl. Phys. A92 (1967) 449.
[6] BES, D.R., CHUNG, Cho Yi, Nucl. Phys. 86 (1966) 581.
[7] SOLOVIEV, V.G., VOGEL, P., Dokl. Akad. Nauk SSSR 171 (1966) 69.
[8] SOLOVIEV, V.G., VOGEL, P., JUNGCLAUSSEN, G., Izvestiya Akad. Nauk SSSR, ser. fiz. 31 (1967) 518.
[9] FRIEDMAN, A.M., (Argonne National Laboratory, USA) private communication.

[10] BURKE, D.G., ZEIDMAN, B., ELBEK, B., HERSKIND, B., OLESEN, M., Mat. Fys. Dan. Vid. Selsk. 35 (1965) N2.
[11] GAREEV, F.A., IVANOVA, S.P., KALINKIN, B.N., Preprint JINR P4-3451 (1967).
[12] GAREEV, F.A., IVANOVA, S.P., KALINKIN, B.N., SLEPNEV, S.K., GINSBURG, M.G., Preprint JINR P-4-3607.
[13] KORNEICHUK, A.A., MALOV, L.A., SOLOVIEV, V.G., FEDOTOV, S.I., SHULZ, H., Contribution No.77 to this Symposium.
[14] MALOV, L.A., SOLOVIEV, V.G., FAINER, U.M., Contribution No.78 to this Symposium.
[15] SHELINE, R.K., BENNETT, M.J., DAWSON, J.M., SHIDA, Y., Phys. Lett. 26B (1967) 14.
[16] BUNKER, M.E., (Los Alamos, New Mexico, USA) private communication.
[17] TJØM, P.O., ELBEK, B., Mat. Fys. Medd. Dan. Vid. Selsk. 36 (1967) N8.
[18] RICKEY, F.A., SHELINE, R.K., Phys. Rev. Lett. 17 (1966) 1057.
[19] BRAID, T.H., CHASMAN, R.R., ERSKINE, J.R., FRIEDMAN, A.M., Phys. Lett. 18 (1965) 149.
[20] FUNKE, L., GRABER, H., KAUN, K.H., SODAN, H., GESKE, G., FRANA, J., Nucl. Phys. 84 (1966) 424.
[21] BOGDANOV, D.D., DAROTSI, Sh., KARNAUKHOV, V.A., PETROV, L.A., TER-AKOPYAN, G.M., Yadernaya Fiz. 6 (1967) 893.
[22] JOLOS, R.V., FEINER, U.M., SOLOVIEV, V.G., ZHELEZNOVA, K.M., Preprint JINR P4-3898 (1968).
[23] MALOV, L.A., SOLOVIEV, V.G., KHRISTOV, I.D., Yadernaya Fiz.6 (1967) 1186.
[24] MEYER, R.A., Preprint UCRL-70672 (1967).
[25] BARANGER, M., KUMAR, K., Nucl. Phys. A110 (1968) 529.
[26] ARSENJEV, D.A., MALOV, L.A., PASHKEVITCH, V.V., SOLOVIEV, V.G., Izvestiya Akad. Nauk SSSR, ser. fiz. 32 (1968) N5.
[27] ARSENJEV, D.A., MALOV, L.A., PASHKEVITCH, V.V., SOBICHEVSKI, A., SOLOVIEV, V.G., Preprint JINR E4-3816 (1968).
[28] SOLOVIEV, V.G., VOGEL, P., KORNEICHUK, A.A., Izv. Akad. Nauk SSSR, ser. fiz. 28 (1964) 1599.
[29] SOLOVIEV, V.G., Phys. Lett. 21 (1966) 320.
[30] ABDURAZAKHOV, A.A., VRSAL, Ya., GROMOV, K.Ya. et al. Preprint JINR P6-3464 (1967).
[31] BONCH-OSMOLOVSKAYA, N.A., GRIGORIJEV, E.P., VRSAL, N.A. et al., Izv. Akad. Nauk SSSR, ser. fiz. 32 (1968) 99.
[32] DZHELEPOV, B.S., SHESTOPALOVA, S.A., these Proceedings.
[33] BONCH-OSMOLOVSKAYA, N.A., VRSAL, Ya., GRIGORIJEV, E.P. et al. Preprint JINR P6-3452 (1967).
[34] BOCHNACKI, Z., OGAZA, S., Nucl. Phys. 69 (1965) 186; 83 (1966) 619.
[35] MIGDAL, A.B., Theory of Finite Fermi Systems and Properties of Atomic Nuclei, Nauka, Moskow (1965).

DISCUSSION

V. GILLET: For these heavy nuclei is there a simple way to justify the neglect of the Pauli principle between the quasiparticles and the phonons?

V.G. SOLOVIEV: In the quasiparticle plus phonon system the Pauli principle is partly taken into account only in the case of a beta-rotational phonon. In the overwhelming majority of cases, taking the Pauli principle into account leads to small corrections due to the fact that phonons consist of a rather large number of two-quasiparticle components.

J.J. GRIFFIN: When large phonon admixtures are obtained in a calculation one wonders whether there might exist a better zero-order Hamiltonian which would diagonalize some of these effects. (For example, one might consider whether the quasiparticles, by "blocking" the coherent pairing in the ground state, could decrease the stability of the nucleus against anaxial deformations.) Are there any specific features of your calculations which could distinguish such an adjustment of the

self-consistent field from the phonon-quasiparticle admixtures which you considered?

V.G. SOLOVIEV: The ground and low-lying non-collective states of deformed nuclei are quasiparticle states with small admixtures. With a growth of excitation energy admixtures increase. An explanation could probably be found in which the density matrix is practically diagonal for a given excited state. However, for another state the explanation may be different. The interpretation of the structure of such states becomes ever more complicated. Actually, by describing excited states on the same basis we obtain some states that are, say, quasiparticle ones, and others that are the superposition of two quasiparticle states.

Z. SZYMANSKI: Could you comment on the influence of the second-order coriolis coupling that would essentially produce the same effects as those discussed in your lecture?

V.G. SOLOVIEV: The coriolis interactions are very important in deformed nuclei. They should be taken into account in calculations. They will result in a further complication of the state structure.

S.T. BELYAEV: In calculating small admixtures in single-particle states one should be careful about restricting oneself to only a few three-quasiparticle or phonon single-particle configurations. Although the admixture in each individual configuration appears to be small, their number rapidly increases (their conglomeration determines, fundamentally, the quasiparticle effective mass). The state quasiparticle - phonon is well determined when the contribution of a certain configuration of such a type predominates.

V.G. SOLOVIEV: For deformed nuclei the average nuclear field is such that it corresponds to the density matrix, being practically diagonal. In this case, the ground and low-lying states are quasiparticle ones with small admixtures. The available experimental data confirm this, which is reflected, for example, in the rules of selecting by analytical quantum numbers in β-decay from the experiments on (d, p) and (d, t) reactions, etc.

The model considered in the report shows that with a growth of the excitation energy the state structure becomes more complex. This fact was qualitatively confirmed by the available experimental data. In a number of cases the contribution of different components of quasiparticle plus phonon is appreciable.

SYSTEMATIC FEATURES OF NON-ROTATIONAL STATES IN THE ODD-A DEFORMED NUCLEI*

C.W. REICH
NATIONAL REACTOR TESTING STATION,
IDAHO NUCLEAR CORPORATION, IDAHO FALLS, IDAHO,
AND
M.E. BUNKER
LOS ALAMOS SCIENTIFIC LABORATORY, LOS ALAMOS, N.MEX.,
UNITED STATES OF AMERICA

Abstract — Аннотация

SYSTEMATIC FEATURES OF NON-ROTATIONAL STATES IN THE ODD-A DEFORMED NUCLEI. Some results are presented of a comprehensive survey of the experimental data concerning the non-rotational states of the odd-A deformed nuclei in the rare-earth region. The ordering and relative energy spacings of the one-quasiparticle states in these nuclei are in quite good agreement with the predictions of the Nilsson model. It is shown, however, that the observed spacings of these states are smaller by a factor of ≈ 2 than those calculated from this model. At energies of only a few hundred keV, strong mixing is found between the one-quasiparticle states and states of vibrational character. This phenomenon, which is more pronounced in the odd-neutron nuclei than in the odd-proton nuclei, exhibits systematic features that are exemplified by the observed behaviour of the $K \approx 1/2$ states of complex structure. Other types of mixing that complicate the analysis of the level structures in this region are (1) mixing of states arising from different major shells (N-mixing) and (2) mixing induced through coriolis coupling. For those aspects of N-mixing that are discussed, it is shown that the Nilsson model seriously underestimates the magnitude of this effect. The ground-state rotational band of ^{161}Dy and the positive-parity states of ^{155}Gd are used as examples where the effects of coriolis coupling are especially striking. Cases where discrepancies between the predicted magnitudes of the coriolis-coupling matrix elements and those obtained empirically are pointed out. Difficulties in making detailed configurational assignments to the higher-lying (> 0.5 MeV) states of these nuclei are illustrated in terms of the well-studied case of ^{163}Dy.

СИСТЕМАТИЧЕСКИЕ СВОЙСТВА НЕВРАЩАТЕЛЬНЫХ СОСТОЯНИЙ В НЕЧЕТНЫХ ДЕФОРМИРОВАННЫХ ЯДРАХ. Представлены некоторые результаты большого обзора экспериментальных данных по невращательным состояниям в нечетных деформированных ядрах в редкоземельной области. Порядок и относительные энергетические расстояния одноквазичастичных состояний в этих ядрах находятся в хорошем согласии с предсказаниями модели Нильссона. Однако показано, что наблюдаемые энергетические расстояния между этими состояниями меньше на фактор ≈ 2, чем вычисленные из этой модели. Только при энергиях нескольких сотен кэв найдено сильное смешивание одноквазичастичных вибрационных состояний. Это явление, которое по сравнению с протонно-нечетными ядрами более явно выражено в нейтронно-нечетных ядрах, проявляет систематические особенности. Последние иллюстрируются примером наблюдаемого поведения состояний с $K = 1/2$ сложной структуры. Другими типами смешивания, которые усложняют анализ структуры уровней в этой области, являются: 1) смешивание состояний, возникающих из различных главных оболочек (N-смешивание) и 2) смешивание состояний, индуцированное кориолисовым взаимодействием. Показано, что в рассматриваемом аспекте в модели Нильссона недооценивается величина эффекта N-смешивания. Вращательная полоса над основным состоянием ^{161}Dy и состояния положительной четности в ^{155}Gd использовались в качестве примера, где эффекты кориолисового взаимодействия особенно существенны. Указаны случаи расхождений предсказанных величин матричных элементов кориолисового взаимодействия и экспериментально полученных величин. Трудности определения конфигураций для высоколежащих (> 0,5 Мэв) состояний этих ядер иллюстрируются на примере ^{163}Dy.

* Work supported by the U.S. Atomic Energy Commission.

I. INTRODUCTION

The past few years have witnessed a great increase in the general understanding of the structure of the energy states of the odd-mass deformed nuclei. Through the combined efforts of the theorists [1-3] and experimentalists, it is now apparent that many of the observed states below 1 MeV are not of simple single-particle character, but have highly complex configurations.

We have recently performed a critical evaluation of the experimental data currently available on the energy levels of the deformed odd-mass nuclei in the rare-earth region. This paper is concerned with some results of this study which have relevance to certain mixings which exist among nuclear states. In general, we shall use the notation and terminology of the Nilsson [4] model, which, in spite of its conceptual simplicity, has been highly successful in describing the occurrence and properties of the single-particle states of these nuclei.

II. STATES OF THE AVERAGE FIELD

The identification and characterization of those states of the deformed odd-mass nuclei which are predominantly of "single-particle"[1] character is a matter of great importance to both theorists and experimentalists. First, these provide information on the average-field potential itself. Second, since the energies of the states of the average potential enter as essential parameters in more sophisticated nuclear structure calculations, such as those mentioned above [1-3], knowledge of the actual location of these states should help eliminate some of the uncertainty in these calculations.

Those states of the odd-Z nuclei which appear to be predominantly one-quasiparticle in nature are shown in Fig. 1. On this plot only the positions of the band heads are shown. Ground states are represented by filled circles and excited states are represented by empty circles. Hole states are plotted below their respective ground states, while particle states are plotted above. The relative positions of the ground states of adjacent-Z nuclei have been determined by empirical adjustment so that the shifts of the various orbitals will be as small as possible. The band heads are labelled by their respective K^{π} values. With the data arranged in this fashion, the systematic occurrence of the various states throughout the mass region is made more apparent. In ^{159}Tb, two low-lying $K^{\pi} = 1/2^{+}$ states are observed and in ^{169}Tm there is evidence for two states with $K^{\pi} = 3/2^{+}$. Each set of states is connected with a vertical dashed line. They are presumably of mixed single-particle plus vibrational character, although the current experimental data do not clearly indicate to what extent these modes of excitation are mixed. We shall return to this point in the discussion of the $K = 1/2$ states that have complex structure (see Sect. III.A).

At the left in Fig. 1 we show the single-particle energies predicted by the Nilsson model for a deformation of $\delta = 0.3$ (using the revised parameters of Ref. [5]), except that the theoretical energy scale has been

[1] In this discussion we use the terms "single-particle" and "one-quasiparticle" interchangeably.

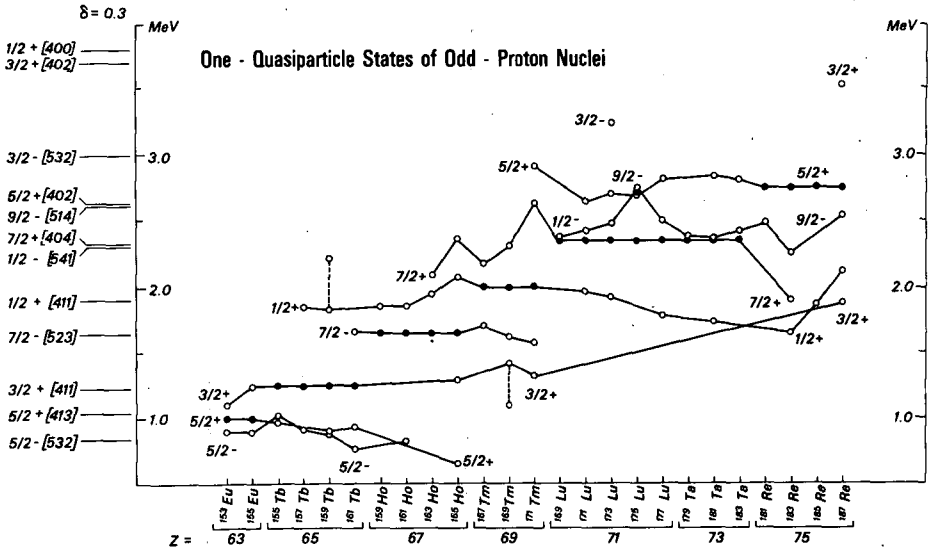

FIG. 1. Energy systematics of the one-quasiparticle states in the odd-proton nuclei. For the method of plotting, see the text.

compressed by a factor of ≈ 1.9. The agreement with respect to both the level ordering and the empirical energy spacing is seen to be quite impressive. The fact that the spacings between the single-particle levels are smaller than those predicted by the model has been mentioned previously [6]. This presumably arises [7] from the short-range residual interaction, which is not included in the average-field potential. The factor of 1.9 is in good agreement with estimates of the magnitude of this effect.

Systematics similar to those shown in Fig. 1 also have been worked out for the odd-neutron nuclei. The situation in these nuclei appears to be somewhat more complicated than that for the odd-proton nuclei, the effects of mixing among the various low-lying configurations being in general more pronounced. This added complication is partially offset by the fact that a wider variety of experimental data are available for the odd-N nuclei (very few single-particle transfer reaction data currently exist for the odd-Z nuclei). As with the odd-proton nuclei, the energy spacing of odd-neutron states is lower (by a factor of ≈ 2) than that predicted by the Nilsson model.

III. CONFIGURATION MIXING

The general complexity of the make-up of the energy states of these nuclei has been mentioned above. We now consider briefly some of these mixings. The three to be discussed are the following: (1) mixing of single-particle and vibrational degrees of freedom; (2) mixing of states arising from different major oscillator shells (primarily $\Delta N = \pm 2$); and (3) mixing induced through coriolis coupling.

A. Coupling of single-particle and vibrational motion

The existence of mixing between single-particle and vibrational degrees of freedom is by now a well-established feature of the level structures of the deformed odd-mass nuclei. There is strong experimental evidence for vibrational excitations of several different multipolarities; however, the overwhelming bulk of data which we have at present involves collective 2^+ excitations. For this reason, we shall restrict our discussions to these latter states, known as "gamma vibrations".

As a first approximation, one can think of a particular gamma-vibrational state in an odd-mass nucleus as arising from the coupling of the base-state orbital and the 2^+ vibrational state of the even-even core. Thus, if the odd particle is on the orbital $|K_0\rangle$, this coupling gives rise to two vibrational states with K values of $K_0 + 2$ and $|K_0 - 2|$. A few states have been found which appear to be fairly pure vibrational states of this type. In general, however, these vibrational configurations are found to be spread over several intrinsic states. This mixing of one-quasiparticle states and $|K_0 - 2|$ phonon excitations, concerning which there is now a large amount of experimental data, is observed to exhibit certain regularities, which appear to be rather well described by the current theories [1-3]. Among these regularities we include the following.

(1) Mixing of a $(K_0 - 2)$ vibrational excitation and a particular one-quasiparticle state $|K'\rangle$ is especially important if the one-quasiparticle state and the base state of the vibration are connected with a large E2 matrix element. This occurs when the asymptotic quantum numbers of the base state are related to those of the admixed one-quasiparticle state in the following manner: $\Delta N = \Delta n_z = 0$, $\Delta\Lambda = \Delta K = \pm 2$. Furthermore, this mixing can be large even if the positions of the unperturbed states $|K'\rangle$ and $|K_0 - 2\rangle$ are separated by many hundreds of keV.

(2) The trend of the excitation energies of these mixed "particle-phonon" states resembles to a great extent that of the gamma-vibrational states of the corresponding even-even nuclei. In the regions where the gamma vibrations of the even-even nuclei lie especially low (Dy, Er) the effect of this mixing in the odd-mass nuclei is important at excitation energies as low as 0.3 - 0.4 MeV. Where the even-even vibrations occur at relatively high excitations (as in the Yb isotopes 172 and 174), one-quasiparticle states occur with a high degree of purity even up to excitation energies as high as $\approx$ 1 MeV. While the (K-2) states of the odd-mass nuclei occur systematically lower in energy than the 2^+ states in the even-even nuclei, the extent to which their excitation energies follow those of the even-even nuclei is quite striking (cf. Fig. 2).

There are several interesting groups of $K = 1/2$ excited states that exhibit mixed character. The dominant single-particle component in the lowest-lying $1/2^-$ bands in the region of neutron number from 91 through 97 is $1/2^-[521]$, a fact that is well established by (d, p) and (d, t) reaction studies [8, 9]. The cross-sections for exciting these bands are systematically smaller than those predicted for pure $1/2^-[521]$ bands, suggesting that collective configurations play an important role in the make-up of these states. This is in agreement with the calculations of Soloviev et al. [1, 2] which predict that the $1/2^-[521]$ single-particle component should comprise only (50-75%) of these states. The situation regarding

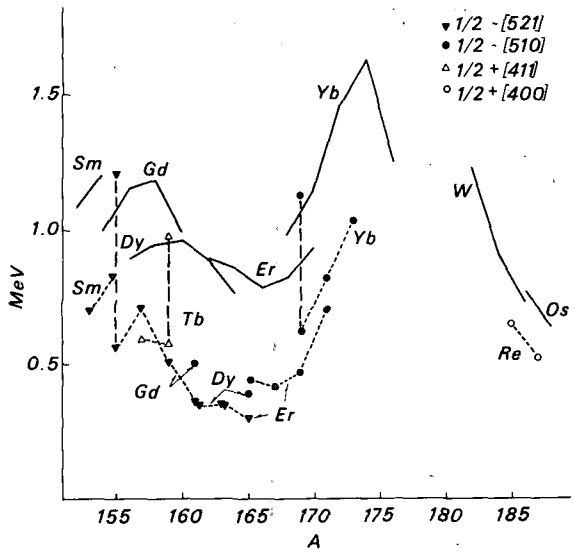

FIG. 2. Behaviour of several groups of K = 1/2 bands of mixed single-particle and (K_0 - 2) vibrational character. The energies plotted are those of the respective K = 1/2 band heads measured with respect to the energy of the state presumed to be the base state of the (K_0 - 2) vibration. The energies of the gamma-vibrational states in the even-even nuclei are shown connected with the solid lines.

vibrational admixtures is complicated by the fact that there exist two low-lying single-particle orbitals ($3/2^-$ [521] and $5/2^-$ [523]) in these nuclei which are connected to $1/2^-$ [521] by large E2 matrix elements; hence, important contributions to these K-2 states from the vibrational configurations[2] $\{3/2^-$ [521], $2^+\}$ and $\{5/2^-$ [523], $2^+\}$ are expected. In ^{155}Gd and ^{157}Gd, where the ground state is $3/2^-$ [521], the presence of a significant $\{3/2^-$ [521], $2^+\}$ component in the $1/2^-$ bands is established through the enhanced E2 transition probabilities observed in (d, d') experiments [10]. In ^{163}Dy, (ground state: $5/2^-$ [523]), an important $\{5/2^-$ [523], $2+\}$ component in the $1/2^-$ band is similarly established by the enhanced interband E2 transition probability [11]. Detailed comparisons of the make-up of these $1/2^-$ states with theory is difficult since the experimental data do not currently provide reliable estimates of the amount of each vibrational component present. The theoretical calculations [1, 2], however, suggest that roughly comparable amounts of the two vibrational configurations should be present, except for the N = 97 nuclei where the $3/2^-$ [521] band occurs close to the $1/2^-$ band and where, consequently, the contribution of $\{3/2^-$ [521], $2^+\}$ is predicted to be quite small ($\lesssim 3\%$).

The presence of $1/2^-$ [510] in the other set of $K^\pi = 1/2^-$ bands shown in Fig. 2 has been firmly established through (d, p) reaction studies [12]. For these bands, there should be only one strongly admixed vibrational component, namely $\{5/2^-$ [512], $2^+\}$. Here, the evidence for the presence of this vibrational component is rather indirect, being based largely

[2] The notation employed here for vibrational components is to specify the base-state orbital and the type of vibration, the latter being indicated by the K^π of the analogous excitation in the even-even core. For example, $\{[633\uparrow], 2^+\}$ indicates a gamma-vibrational excitation built on the Nilsson orbital [633↑] (i.e., $7/2^+$ [633]).

on the dramatic downward energy shift - with an accompanying dilution on the single-particle strength as reflected in reduced (d, p) cross-sections - which this band exhibits as one goes from the Yb isotopes to the Er and Dy isotopes where, as we have seen, the gamma vibrations occur at especially low energies. This behaviour is shown in Fig. 3, where the energy systematics of several one-quasiparticle states of the odd-neutron nuclei are shown. In the N = 105 and 107 nuclei, the $1/2^-$ [510] orbital behaves as an essentially pure one-quaisparticle state. With decreasing neutron number, however, the position of the state departs further below its expected position until, in ^{165}Dy, it occurs ≈ 900 keV below the expected position of $1/2^-$ [510].

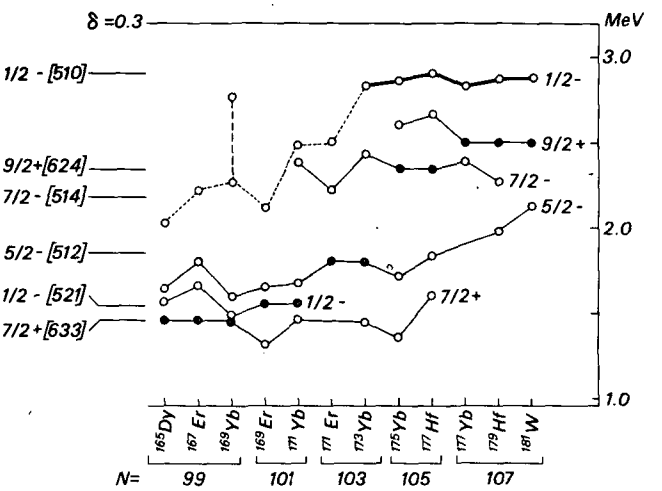

FIG. 3. Energy systematics of several intrinsic states of the odd-neutron nuclei, illustrating the sharp decrease in energy of the "$1/2^-$ [510]" state, presumably as a result of mixing of this orbital with the vibrational configuration $\{5/2^-[512], 2^+\}$. The method of plotting is the same as that of Fig. 1. At the left is a portion of the Nilsson [5] diagram at δ = 0.3, compressed by a factor of 2.0.

In the Tb isotopes, the situation with respect to $1/2^+$ [411] is similar to that of $1/2^-$ [521] in the odd-N nuclei; that is, there exist two orbitals, $3/2^+$ [411] and $5/2^+$ [413], which are connected to it with large E2 matrix elements. Consequently, one expects that the vibrational configurations $\{3/2^+[411], 2^+\}$ and $\{5/2^+[413], 2^+\}$ (particularly the former) will contribute significantly to the $1/2^+$ bands in these nuclei. In ^{159}Tb, which has a $3/2^+$ [411] ground state, two $1/2^+$ bands are observed (at 580 and 970 keV), and the presence of a component of the vibrational structure $\{3/2^+[411], 2^+\}$ in each of these bands is indicated by the enhanced B(E2↑) values (1.5 and 0.1 single-particle units,[3] respectively [13]). The relative amounts of single-particle and vibrational components in these bands, however, are uncertain. The larger B(E2) value to the lower band might at first suggest that this band contains the larger portion of the $\{3/2^+[411], 2^+\}$ excitation. This supposition appears to be supported by the magnitude of the decoupling parameters for the two bands;

[3] We use as our single-particle unit for E2 transition strengths the quantity $B(E2)_{sp} = 3 \times 10^{-5} A^{4/3}$ $e^2 \times 10^{-48}$ cm^4. This corresponds to five of the single-particle units as defined by Moszkowski [14].

that of the lower band is very small (+ 0.05) while that of the upper band (-0.81) is close to that observed for the $1/2^+$ [411] orbital in other odd-Z nuclei. If it is true that most of the single-particle strength is located in the upper band, this constitutes a serious disagreement with theory, since both Soloviev [1, 2] and Bès [3] predict that this state should be $\geq 50\%$ $1/2^+$ [411]. The fact that the B(E2) value to the lower-lying $1/2^+$ band is larger than that to the higher-lying one does not necessarily imply that the vibrational component $\{3/2^+$ [411], $2^+\}$ is dominant in the 580-keV band, as Bès and Cho [3] have pointed out. It is a feature of their treatment of the quasiparticle-vibration coupling that there exists a positive interference term for the quadrupole transition rate to the lower member of such a mixed pair of states, so that an enhanced E2 transition rate to the lower state is predicted even when this state is predominantly a one-quasiparticle excitation.

The ^{159}Tb case is not the only one where problems exist concerning decoupling parameters of "mixed" $K = 1/2$ bands. In ^{155}Gd, for example, $K^\pi = 1/2^-$ bands are observed at 557 keV and 1203 keV which are excited in (d, d') reactions with B(E2) values of ≈ 2.2 $B(E2)_{sp}$ and ≈ 2.6 $B(E2)_{sp}$, respectively [10]. The decoupling parameters of these two bands are + 0.34 and + 0.32, respectively (see Table I); and it is reasonable to suppose that these two bands contain significant components of $1/2^-$ [521] and $\{3/2^-$ [521], $2^+\}$, as discussed above. However, from the (d, p) reaction data, the upper band would appear to contain $\lesssim 2\%$ of the $1/2^-$ [521] orbital.

In the Re isotopes, important quasiparticle-phonon mixing should occur between $1/2^+$ [400] and $\{5/2^+$ [402], $2^+\}$. There is reason to believe that the well-known $1/2^+$ bands at 646 keV in ^{185}Re and at 512 keV in ^{187}Re involve this mixture. The quite large B(E2↑) values (3.6 $B(E2)_{sp}$ and 3.8 $B(E2)_{sp}$, respectively [15]) to these bands suggest that the vibrational configuration is dominant. On the other hand, the observed decoupling parameters for these bands (+ 0.39 and + 0.37, respectively) are both quite close to the value (+ 0.33) expected for a $1/2^+$ [400] orbital. The theoretical calculations predict that these states should be largely (50-75%) $1/2^+$ [400]. On the basis of current data, it is not possible to draw definite conclusions regarding the relative amount of one-quasiparticle and vibrational excitations present in these $K^\pi = 1/2^+$ states.

In spite of the complex nature of many of the $K = 1/2$ bands throughout this region, some of these states are relatively free of quasiparticle-phonon mixings. This is especially true in the Yb region, where the 2^+ states of the even-even nuclei lie especially high (see Fig. 2). An outstanding example of this is proved by the $1/2^-$ state at 399 keV in ^{173}Yb [6]. The E2 transition to the ^{173}Yb ground-state ($5/2^-$ [512]) is the slowest K-allowed E2 transition thus far reported, having a B(E2) value of only $\approx 6 \times 10^{-5}$ $B(E2)_{sp}$. Yet, this transition is hindered by a factor of only ≈ 5 with respect to the Nilsson estimate (including a correction for pairing) for a $1/2^-$ [521] → $5/2^-$ [512] transition. This demonstrates the smallness of the E2 matrix element between $1/2^-$ [521] and $5/2^-$ [512] and the absence of any significant amount of $\{5/2^-$ [512], $2^+\}$ in the $1/2^-$ band at 399 keV, the latter being well explained by the theoretical calculations [1, 3].

Table I. Energies and decoupling parameters for K = 1/2 bands of mixed particle-phonon character.

Nuclide	Energy (keV) Exp.	Energy (keV) Calculated Refs. [1,2]	Energy (keV) Calculated Ref. [3]	a Exp.	a Calculated Refs. [1,2]	a Calculated Ref. [3]	Single-Particle component
^{153}Sm	696	900		+0.31	0.50		
^{155}Sm	824	950		+0.32	0.58		
^{155}Gd	557	550		+0.34	0.36		
"	1203			+0.32			
^{157}Gd	704	700	776	+0.27	0.45	0.45	1/2-[521]
^{159}Gd	507			+0.48			a_{sp} = +0.89
^{161}Gd	356			+0.31			
^{161}Dy	368	450		+0.44	0.47		
^{163}Dy	351	300	386	+0.26	0.60	0.60	
^{163}Er	346	480		+0.47	0.49		
^{165}Er	298	340	409	+0.56	0.65	0.64	
^{161}Gd	1309			-0.12			
^{165}Dy	570	700		+0.05	0.05	0.03	
^{165}Er	920			+0.08			
^{167}Er	763	810		+0.12	0.05		
^{169}Er	562			+0.07			1/2-[510]
^{171}Er	701			+0.13			a_{sp} = +0.20
^{169}Yb	813	790	725	+0.01	0.06	0.08	
"	1317			(+0.12)			
^{171}Yb	945	630	934	+0.19	0.08	0.11	
^{173}Yb	1031	850	922	+0.20	0.12	0.14	
^{157}Tb	598	530		+0.05	-0.50		
^{159}Tb	580	430	595	+0.05	-0.47	-0.22	1/2+[411]
"	970	1150		(-0.81)	0		a_{sp} = -0.78
^{185}Re	646	400	750	+0.39	0.32	0.09	1/2+[400]
^{187}Re	512	400	683	+0.37	0.31		a_{sp} = +0.33

B. Mixing of states arising from different major oscillator shells

A number of recent experimental results on odd-A deformed nuclei point to mixing between Nilsson orbitals which originate from different major oscillator shells. These data come primarily from (d, p) and (d, t) reaction studies, although important supporting evidence is provided by Coulomb-excitation and β-decay studies.

In the original work of Nilsson [4] and, as the model is generally applied at present, the coupling between states of the same K^{π} but which differ in the radial quantum number N by 2 units is essentially neglected. One result of this simplification is that certain pairs of orbitals having the same K^{π} are predicted to cross. The "crossings" of particular interest here involve the orbital pairs $\{3/2^+ [651], 3/2^+ [402]\}$ and $\{1/2^+ [660], 1/2^+ [400]\}$. As shown in Fig. 4, these pairs are predicted to cross near $\delta = 0.3$, which is the approximate deformation of nuclei in this mass region. Experimentally, convincing evidence has been found in several nuclei that these respective orbital pairs are strongly mixed. The charged-particle spectroscopic data provide one of the most powerful arguments, since the N = 4 and N = 6 rotational bands are populated with quite different cross-section "fingerprints" (see Table 9, Ref. [8]).

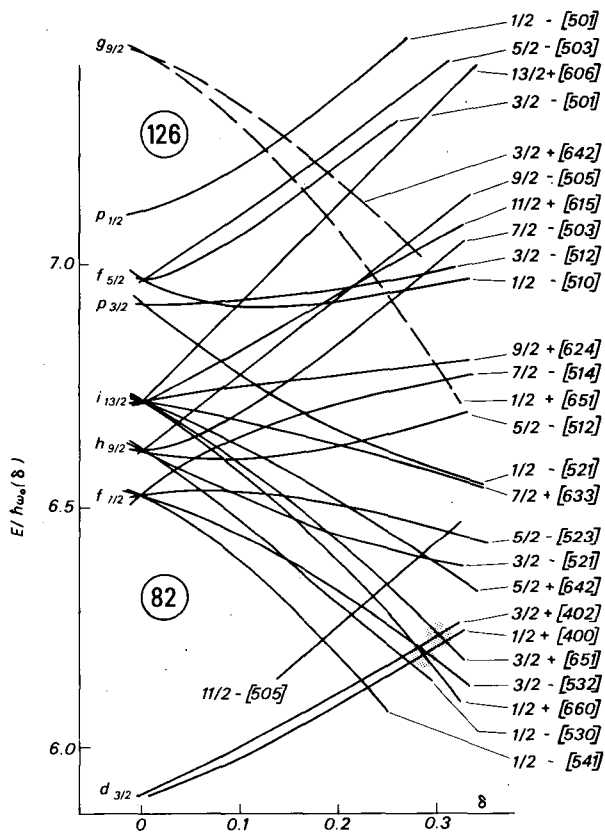

FIG. 4. Nilsson diagram for certain odd-N states of the rare-earth region, showing the crossing of the orbital pairs $1/2^+ [400]$, $1/2^+ [660]$ and $3/2^+ [402]$, $3/2^+ [651]$. The revised [5] model parameters were used.

In ^{161}Dy (see Fig. 5a) a $3/2^+$ state at 551 keV is excited in Coulomb excitation [16] with a $B(E2\uparrow)$ of $\approx 1.2\ B(E2)_{sp}$. The only reasonable way to explain this relatively large B(E2) is to assume that there exists strong coriolis coupling between this band and the ^{161}Dy ground state, which in turn implies that there is a large component of $3/2^+ [651]$ in the 551-keV

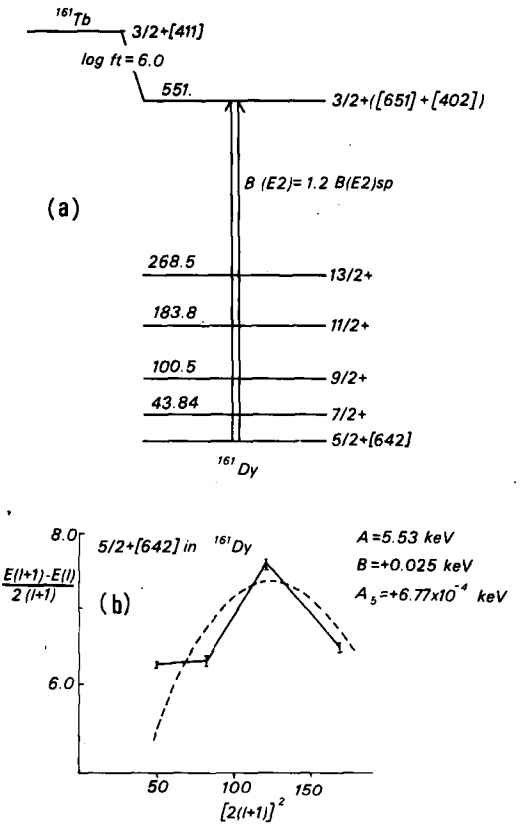

FIG.5. (a) Ground-state rotational band and $K^{\pi} = 3/2^+$ state of mixed [402↓] plus [651↑] character in ^{161}Dy. (b) Plot showing the alternating term presumably arising through coriolis coupling involving $1/2^+$ [660]. The solid curve results from a least-squares fit to the rotational band using A, B, and A_5 terms [23] with the values indicated. The dashed curve shows such a fit using A, B, and C terms.

state (see also Section III.C). On the other hand, this state is strongly excited in the (d,t) reaction [17], which means that there is a large ($\approx$ 50%) component of $3/2^+$[402] present. A higher-lying state, at 726 keV, also strongly excited in the (d,t) reaction, is presumed [17] to be the second member of the $3/2^+$ [402], $3/2^+$ [651] pair.

In the Gd, Dy and Er nuclei, other examples of a strong $\Delta N = 2$ mixing between the two $K = 1/2^+$ orbitals and the two $K = 3/2^+$ orbitals are reported [8, 17], In ^{155}Gd there are two low-lying $3/2^+$ bands (band heads at 105.3 and 266.6 keV) that are strongly excited in the ^{156}Gd (d,t) reaction [8]. The relative cross-sections for exciting these bands suggest that they contain $\approx$ 40% and $\approx$ 60%, respectively, of the $3/2^+$ [402] orbital strength. It is logical to assume that the remainder of these two states is largely $3/2^+$ [651], a supposition which finds support from the coriolis-coupling results discussed below. This strong mixing is significant because it indicates a deformation that is close to the virtual intersection of the $3/2^+$ orbitals, and so the energy difference of $\approx$ 160 keV is a rough measure of the actual "distance of closest approach" of these orbitals.

The 160-keV energy separation, together with the relative amounts of the two configurations present in the two bands, allows one to estimate the magnitude of the matrix element responsible for the mixing, and it turns out to be $\approx$ 80 keV. This value is essentially the same as that obtained (80 keV) from an analysis of the mixing of the $1/2^+$ [660], $1/2^+$ [400] configurations in ^{159}Gd [18].

Although Nilsson did not include N mixing in his calculations [4], he specified how to take it into account. In his model, the coupling between orbitals whose N values differ by 2 units arises through the $\Delta N = \pm 2$ matrix elements of an operator proportional to $r^2Y_2^0$, whose $\Delta N = 0$ matrix elements provide the deformation-dependent mixing among the spherical shell-model states. We have found that this model seriously underestimates the magnitude of the N-mixing phenomenon. It yields a value of $\approx$ 7 keV for the N-mixing matrix element between $3/2^+$[402] and $3/2^+$ [651], which is roughly an order of magnitude smaller than that observed experimentally.

Other data that suggest the presence of N-mixing are the log ft values for beta transitions between states having $\Delta N = 2$. Of particular interest are the ft values of the $7/2^+[404]_p \rightleftarrows 9/2^+[624]_n$ transitions, which are systematically smaller by a factor $\gtrsim 10$ than those of the $7/2^+ [404]_p \rightleftarrows 7/2^+ [633]_n$ transitions (see Table II). The $\Delta N = 2$ matrix elements of the operator $r^2Y_2^0$ have the selection rules in the asymptotic quantum numbers: $\Delta N = \Delta n_z = \pm 2$, $\Delta \Lambda = 0$. Consequently, through the action of this operator, appreciable amounts of $7/2^+[624]_p$ and $9/2^+ [404]_n$, respectively, are expected to be admixed into the states $7/2^+ [404]_p$ and $9/2^+ [624]_n$. Each of these admixed components can give rise to allowed-unhindered (au) beta transitions to the main component of the other state. This is not the case for the $7/2^+ [404]_p \rightleftarrows 7/2^+ [633]_n$ transitions, and so one expects them to be slower. Within the framework of the Nilsson model, however, our calculations indicate that there is far too little N-mixing to account for the speed of the $7/2^+ [404] \rightleftarrows 9/2^+ [624]$ transitions.

Table II. Log ft values of two groups of "N-forbidden" β transitions.

$7/2+[404]_p \overset{\leftarrow}{\rightarrow} 9/2+[624]_n$	log ft	$7/2+[404]_p \overset{\leftarrow}{\rightarrow} 7/2+[633]_n$	log ft
^{177}Lu (β^-) ^{177}Hf, 321.3	6.5	^{169}Yb (e.c.) ^{169}Tm, 316.2	$\lesssim$ 7.6
^{177}Ta (e.c.) ^{177}Hf, 321.3	8.4	^{173}Lu (e.c.) ^{173}Yb, 351.2	8.3
^{177}Yb (β^-) ^{177}Lu, 0	6.5	^{175}Ta (e.c.) ^{175}Hf, 207.4	$\gtrsim$ 6.7
^{179}Ta (e.c.) ^{179}Hf, 0	6.3	^{177}Ta (e.c.) ^{177}Hf, 746.1	8.1
^{179}Lu (β^-) ^{179}Hf, 0	7.0		
^{181}W (β^-) ^{181}Ta, 0	6.5		
^{183}Os (e.c.) ^{183}Re, 851.1	7.2		

Recently, the phenomena associated with the N-mixing have been the subject of extensive theoretical study, using a single-particle potential of Saxon-Woods shape [18-20]. In some respects, these calculations give much better agreement with experiment than does the harmonic oscillator potential used by Nilsson. One implication of this work is that when more complete data are available on these mixed states, theoreticians will gain valuable insight into critical features of the nuclear potential well.

C. Coupling between particle and rotational motion (coriolis coupling)

The coupling of particle and rotational motion in deformed nuclei has been well described theoretically [21, 22]. As the data concerning many nuclear properties have become more extensive and precise, the importance of coriolis coupling among nuclear states has become more apparent. In particular, it can profoundly affect the rates of beta- and gamma-ray transitions between nuclear states, the effective moments of inertia, and the energy spacings within rotational bands.

The operator which gives rise to the rotation-particle coupling connects states whose K values differ by one unit. Furthermore, the strongest couplings produced by this interaction involve single-particle orbitals which originate from the same spherical shell-model state. The strength of these "unhindered" couplings depends on the j-value of the spherical shell-model state from which the orbital originates, being larger for the larger j-values. The effects of coriolis coupling are, consequently, especially pronounced among the orbitals which originate from the $h_{11/2}$ and $i_{13/2}$ spherical shell-model states. These orbitals account, respectively, for the majority of the odd proton negative-parity states and the odd-neutron positive-parity states currently known in the rare-earth nuclei.

One consequence of this interaction is the large effective moments of inertia systematically observed for the N = 6 odd-neutron states which originate from $i_{13/2}$. Another effect, and one concerning which there is considerably less experimental evidence at present, is the existence of an alternating term in the energy spacings of the rotational bands built on these states. While such terms are expected on very general grounds [23] to occur in the rotational bands of all intrinsic states, for these particular states their effects should be especially large because of the very anomalous rotational spacing of the $1/2^+$ [660] band ($a_{th} \gtrsim +6.0$) and of the especially large coriolis-coupling matrix elements. These energy perturbations are quite pronounced in the $5/2^+$ [642] bands of ^{161}Dy and ^{163}Dy. This is illustrated by the ground-state band of ^{161}Dy as observed in Coulomb excitation [24] (see Fig. 5b). A least-squares fit to the level energies of this band was made using a function of the form $E_I = AI(I+1) + BI^2(I+1)^2 + (-)^{I+1/2} A_5(I+5/2)!/(I-5/2)!$. The results of this analysis, which gives an excellent fit to the experimental data, are shown in Fig. 5b. It is possible to fit these data rather well using a five-band coriolis-coupling calculation involving the K = 1/2 to K = 9/2 bands. However, because of the limited amount of data available on the other band members, no degree of uniqueness can be claimed for this fit.

In the application of coriolis-coupling ideas to the interpretation of the properties of nuclear states, a number of unsolved problems exist.

One of these deals with the magnitude of the coupling between orbitals for which the matrix elements are "unhindered" in the asymptotic quantum numbers. In the cases thus far studied, it appears that coupling strengths considerably smaller than the theoretical values (by approximately a factor of 2) are required. When the two orbitals involved are a hole state and a particle state (as in the case of the $5/2^-$ [532] and $7/2^-$ [523] orbitals in ^{161}Tb [25]), it has been proposed that this decrease in coupling strength may arise from an overestimate of the pairing factor (UU' + VV') which multiplies the coupling matrix element. For the lowest $i_{13/2}$ orbitals, $1/2^+$ [660] and $3/2^+$ [651], the situation is further complicated by the fact that these orbitals are observed to be "fragmented" through the effect of N-mixing and, consequently, one has somehow to take this into account in the calculations. In the known cases of "hindered" coriolis coupling, the coupling matrix elements deviate in both directions from the theoretical values. For example, in the extensively studied case of the $1/2^-$ [510] and $3/2^-$ [512] orbitals in ^{183}W, it has been found necessary to use a coupling matrix element that is a factor of $\sim$ 1.6 [21, 22] larger than that predicted theoretically. For the orbitals $5/2^-$ [523] and $3/2^-$ [521] in ^{161}Dy [26], however, it has been shown that a matrix element about one-half the theoretical value is required[4].

An extreme example of the effect of coriolis coupling is provided by the low-lying positive-parity states in ^{155}Gd. The nature of these states was unexplained until recently when it was shown [27] that they could be described in terms of coriolis coupling involving the orbitals $1/2^+$ [660], $3/2^+$ [651] and $5/2^+$ [642]. Our published calculations predicted a quadrupole moment for the 86.5-keV state which is larger than the subsequently measured values [28], although the two existing experimental measurements disagree significantly. We have since shown that slight modifications of the calculational parameters can be made which reproduce the small value of the quadrupole moment of this state while still preserving the good fit to the energy-level spectrum and radiative transition probabilities. From these calculations certain features have emerged which are worth noting.

The role of $1/2^+$ [660] is of fundamental importance in this picture. Because of its large decoupling parameter (as discussed above) and the fact that it occurs, together with $3/2^+$ [651] and $5/2^+$ [642], at a relatively low energy in ^{155}Gd, it is essentially impossible to recognize the rotational band structures of the positive-parity states. Some of the individual states are predicted to be more or less completely mixed so that the association of a given state with a particular band becomes meaningless. In fact, the lowest-lying positive-parity state, the $I^\pi = 5/2^+$ state at 86.5 keV, is predicted to contain essentially equal amounts of the three orbitals involved. Related to this is the fact that some of the states, as a result of the coupling, have been shifted by as much as 200-300 keV from their "unperturbed" position.

The nuclide ^{155}Gd has been a very revealing case in this regard since in it these states occur at low energies where they have been susceptible to detailed study with a wide variety of experimental techniques. The experience gained from the study of these levels in ^{155}Gd should serve to point out the extreme caution which must be exercised in attempting to

[4] The theoretical coriolis matrix element between $5/2^-$ [523] and $3/2^-$ [521] is $0.89\hbar^2/2\mathcal{I}$, rather than the value quoted in Ref. [26].

understand the properties of these states in other nuclei, where they occur at higher excitation energies and where, at present, the data concerning them are considerably less detailed.

D. Conclusion

The discussion above suggests that the agreement between theory and experiment regarding the low-lying states of the nuclei in this region is reasonably good. While in certain respects this is correct, the point needs to be emphasized that serious problems still exist and that much work remains to be done, particularly in the region above ≈ 0.5 MeV. The situation is perhaps best illustrated by reference to a specific case, for which we have selected the nuclide ^{163}Dy.

The ^{163}Dy level structure has been especially well investigated; concerning it there currently exist decay-scheme data [29] and the results of a co-operative experimental effort [30] that included (d, p) and (d, t) reaction studies, high- and low-energy (n, γ) studies, and conversion-electron measurements on the gamma-ray transitions associated with neutron capture. The intrinsic states of ^{163}Dy revealed by these studies are shown at the left in Fig. 6.

To the right in Fig. 6, we show the spectrum of intrinsic states calculated [2] for ^{163}Dy together with their predicted make-up. For clarity in the figure, we have listed for the states of complex structure only the largest two predicted constituents. For the states below ~ 0.8 MeV, there is a rather good correspondence between theory and experiment. Although the match of the level energies is not spectacular, the predicted structure of the observed states is well supported by the experimental data. Above $\approx$ 800 keV, however, it is no longer a simple matter to make a clear-cut correspondence between the experimental and the theoretical levels.

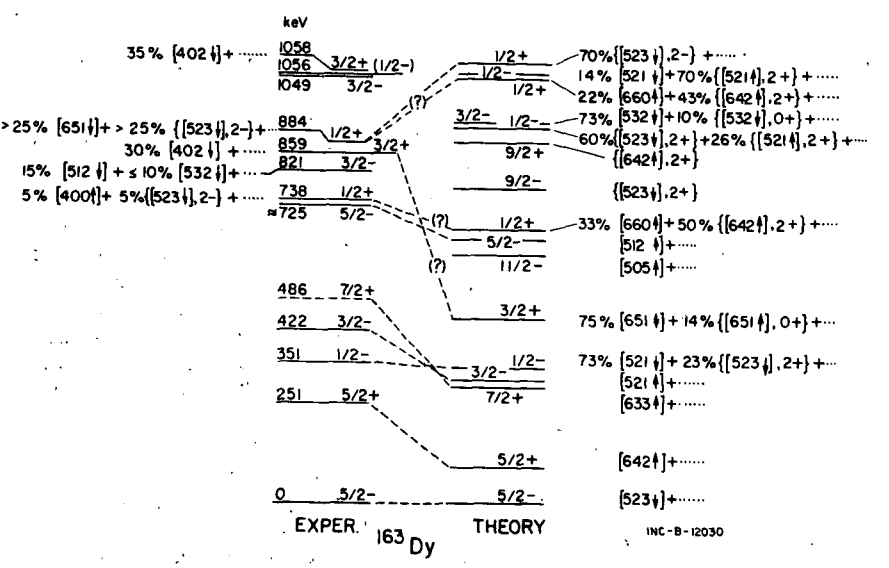

FIG. 6. Comparison of the known intrinsic states of ^{163}Dy with those calculated in Ref. [2]. The experimental wave functions for the states below 730 keV are in good agreement with theory; consequently, they are not listed at the left.

An interesting component in the 884-keV state is the three-quasiparticle configuration $\{3/2^+[411]_p, 7/2^-[523]_p, 5/2^-[523]_n\}$, which can be thought of as essentially a $K^\pi = 2^-$ octupole phonon coupled to the ^{163}Dy ground state ($5/2^-[523]$). This configuration is expected to be admixed into several of the lowest-lying $1/2^+$ states [2]. In certain other nuclei in this region, states at $\approx$ 1 MeV excitation have been found that appear to have admixtures of individual three-quasiparticle configurations that have no obvious relation to phonons. This phenomenon remains unexplained theoretically.

The overall situation in ^{163}Dy, which, as we have just described, is a very carefully studied nuclide, should serve as a cautionary reminder of the present problems inherent in making configurational assignments to states above $\approx$ 0.5 MeV in the deformed odd-A nuclei, particularly in cases where the experimental data are less extensive than those available for this nucleus.

REFERENCES

[1] SOLOVIEV, V.G., VOGEL, P., Nucl. Phys. A92 (1967) 449.
[2] SOLOVIEV, V.G., VOGEL, P., JUNGCLAUSSEN, G., Izv. Akad. Nauk SSSR, Ser. Fiz. 31 (1967) 518; Bull. Acad. Sci. USSR, Phys. Ser. 31 (1967) 515.
[3] BÈS, D.R., CHO YI-CHUNG, Nucl. Phys. 86 (1966) 581.
[4] NILSSON, S.G., Mat. Fys. Medd. Dan. Vid. Selsk. 29 16 (1955).
[5] GUSTAFSON, C., LAMM, I.L., NILSSON, B., NILSSON, S.G., *Lysekil Conference report (1966)*; Ark. Fys. (1967), in press.
[6] REICH, C.W., BUNKER, M.E., Izv. Akad. Nauk SSSR, Ser. Fiz. 31 (1967) 42; Bull. Acad. Sci. USSR, Phys. Ser. 31 (1967) 46.
[7] BAKKE, F.H., Nucl. Phys. 9 (1958/59) 670; WAHLBORN, S., Nucl. Phys. 37 (1962) 554; SOLOVIEV, V.G., in Selected Topics in Nuclear Theory (International Atomic Energy Agency, Vienna, 1963) 223.
[8] TJØM, P.O., ELBEK, B., Mat. Fys. Medd. Dan. Vid. Selsk. 36 8 (1967).
[9] KENEFICK, R.A., SHELINE, R.K., Phys. Rev. 139 (1965) B1479.
[10] ELBEK, B., (Niels Bohr Institute, Copenhagen) private commun.
[11] TVETER, A., (Niels Bohr Institute, Copenhagen) private commun.
[12] BURKE, D.G., ZEIDMAN, B., ELBEK, B., HERSKIND, B., OLESEN, M., Mat. Fys. Medd. Dan. Vid. Selsk. 35 2 (1966); HARLAN, R.A., SHELINE, R.K., Phys. Rev. 168 (1968) 1373; SHELINE, R.K., SHELTON, W.N., MOTZ, H.T., CARTER, R.E., Phys. Rev. 136 (1964) B351.
[13] DIAMOND, R.M., ELBEK, B., STEPHENS, F.S., Nucl. Phys. 43 (1963) 560.
[14] MOSZKOWSKI, S.A., "Alpha-, Beta-, and Gamma-Ray Spectroscopy" (SIEGBAHN, K., Ed.) North-Holland Publishing Co., Amsterdam, (1965), Chap. XV.
[15] BISGÅRD, K.M., VEJE, E., Nucl. Phys. A103 (1967) 545.
[16] EROKHINA, K.I., LEMBERG, I.Kh., NABICHVRISHVILI, V.A., Ivz. Akad. Nauk SSSR, Ser. Fiz. 29 (1965) 1103; Bull. Acad. Sci. USSR, Phys. Ser. 29 (1965) 1104.
[17] SHELINE, R.K., BENNETT, M.J., DAWSON, J.W., SHIDA, Y., Phys. Lett. 26B (1967) 14.
[18] ANDERSEN, B.L., Preprint, Niels Bohr Institute (1968).
[19] GAREEV, F.A., KALINKIN, B.N., PYATOV, N.I., CHERNEI, M.I., Preprint JINR-P4-3650 (1967) and references quoted therein.
[20] NEMIROVSKY, P.E., CHEPURNOV, V.A., Yadernaya Fiz. 3 (1966) 998; Sov. J. Nucl. Phys. 3 (1966) 730; FAESSLER, A., SHELINE, R.K., Phys. Rev. 148 (1966) 1003.
[21] KERMAN, A.K., Mat. Fys. Medd. Dan. Vid. Selsk. 30 15 (1956).
[22] BROCKMEIER, R.T., WAHLBORN, S., SEPPI, E.J., BOEHM, F., Nucl. Phys. 63 (1965) 102.
[23] BOHR, A., MOTTELSON, B.R., Atomnaya Energiya 14 (1963) 41; Soviet J. atom. Energ. 14 (1963) 36.
[24] HAGEMANN, G.B., TVETER, A., Phys. Lett. 26B (1968) 136.
[25] ŻYLICZ, J., HANSEN, P.G., NIELSEN, H.L., WILSKY, K., Nucl. Phys. 84 (1966) 13.
[26] HANSEN, P.G., NIELSEN, O.B., SIDENIUS, G., Paper 4.136, Contributions, Int. Conf. Nuclear Structure, Tokyo (1967) 181.
[27] BUNKER, M.E., REICH, C.W., Phys. Lett. 25B (1967) 396.

[28] BLUMBERG, H., PERSSON, B., BENT, M., Phys. Rev. (to be published); TOMBLIN, F.F., BARRETT, P.H., Int. Conf. Hyperfine Interactions Detected by Nuclear Radiation, Asilomar Conf. Grounds (1967).
[29] FUNKE, L., GRABER, H., SODAN, K.-H., GESKE, G., FRÁNA, J., Nucl. Phys. 84 (1966) 424.
[30] SCHULT, O.W.B., BUNKER, M.E., HAFEMEISTER, D.W., SHERA, E.B., JURNEY, E.T., STARNER, J.W., BÄCKLIN, A., FOGELBERG, B., GRUBER, U., MAIER, B.P.K., KOCH, H.R., SHELTON, W.N., MINOR, M., SHELINE, R.K., Phys. Rev. 154 (1967) 1146.

DISCUSSION

S. WAHLBORN: In connection with Dr. Reich's talk, I should like to report briefly on the evidence for a spin polarization term from the 482 keV M1 transition in ^{181}Ta. This proceeds between the intrinsic state $5/2^+$ [402] and the ground state $7/2^+$ [404] and has a retardation factor of $\sim 3 \times 10^6$. We have made a variety of calculations including coriolis coupling and vibrational admixtures. The M1 transition operator is assumed to have the form $t(M1)_m = (g_\ell - g_R)\ell_m + (g_s - g_R)s_m + k[\sigma Y^2]^1_m$, where k is considered as an empirical parameter. No other parameter occurs in the calculation. All necessary quantities can either be obtained from empirical information (as the g-factors) or be computed from the Nilsson model. Special attention has to be paid to the matrix elements

$$X \equiv \langle 7/2^+ | \ell_+ | 5/2^+ \rangle, \quad Y \equiv \langle 7/2^+ | s_+ | 5/2^+ \rangle$$

which form the most important part of the M1 amplitude, apart from the spin polarization term. With $k = 0$ it is found that $B(M1)$ consistently remains $\gtrsim 10^{-3}\, B(M1)_{s.p.}$. With $k > 0$, cancellation occurs. To accomplish $B(M1) \lesssim 10^{-6}\, B(M1)_{s.p.}$ we find the condition

$$k = 0.9 \pm 0.3$$

Previous authors have estimated k from spin-dependent central forces and found positive values of this order. Blomqvist recently carefully re-investigated the contribution due to pion exchange currents and found that this would correspond to $k_{pion} \approx -0.5$. Consequently, $k_{spin\ pol.}$ might be as large as ≈ 1.5. It should finally be mentioned that similar calculations have also been performed for ^{175}Lu where the results are less definite, allowing only a rough upper limit estimate for k, in agreement with the result for ^{181}Ta.

P.G. HANSEN: The ^{175}Lu and ^{181}Ta cases are very similar and the retarded M1 can in both cases be traced back to destructive interference from the coriolis interaction. The matrix elements are, however, somewhat different in the two cases: both the intrinsic M1 matrix element and the coriolis strength are smaller for ^{181}Ta.

S. WAHLBORN: Extensive calculations show that it is not possible to get sufficiently destructive interference from the coriolis interaction in the case of ^{181}Ta for any reasonable choice of the inertial parameter. I agree that the situation is somewhat different for the case of ^{175}Lu.

D.B. FOSSAN: If the magnetic-dipole operator contains the additional spin-polarization term as you suggested, would it be possible to

observe a manifestation of this term by an angular correlation measurement on the gamma rays?

S. WAHLBORN: No, I don't think so. On the other hand, it might be possible, for example, to trace an effect of this term in the analysis of high-energy electron scattering.

J.O. RASMUSSEN: On the troublesome factor of two by which one must reduce the large coriolis-mixing matrix elements, Nilsson remarked to me recently that the needed reduction below the simple BCS matrix element may naturally come out if one properly takes particle-number-conserving wave-functions. Dr. Chasman has made such calculations in rare earths. The reduction below BCS will be more important as the pairing gets weaker.

Short contribution

R.L. GRAHAM (Chalk River Nuclear Laboratories, Atomic Energy of Canada Ltd, Chalk River, Ontario, Canada): I should like to mention some new results which R.L. Graham, J.S. Geiger and M.W. Johns have obtained on the level structure of ^{171}Tm since we submitted Contribution No.44 to the conference.

We have carried out a new set of γ-γ coincidence measurements using two ~20 cm^3 coaxial Ge(Li) detectors. These studies provide evidence for new γ transitions making the total number 54, to be compared with 38 found by Megli et al.[1] and 40 reported by Raeside et al.[2]

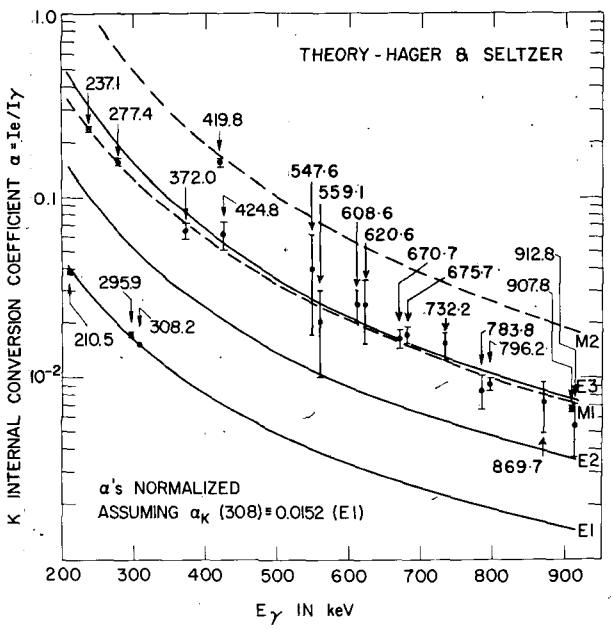

FIG. A. K internal coefficient values.

[1] MEGLI, D.G. et al., Nucl. Phys. A107, (1968) 217.

[2] RAESIDE, D.E. et al., Preprint, University of Michigan (May 1968).

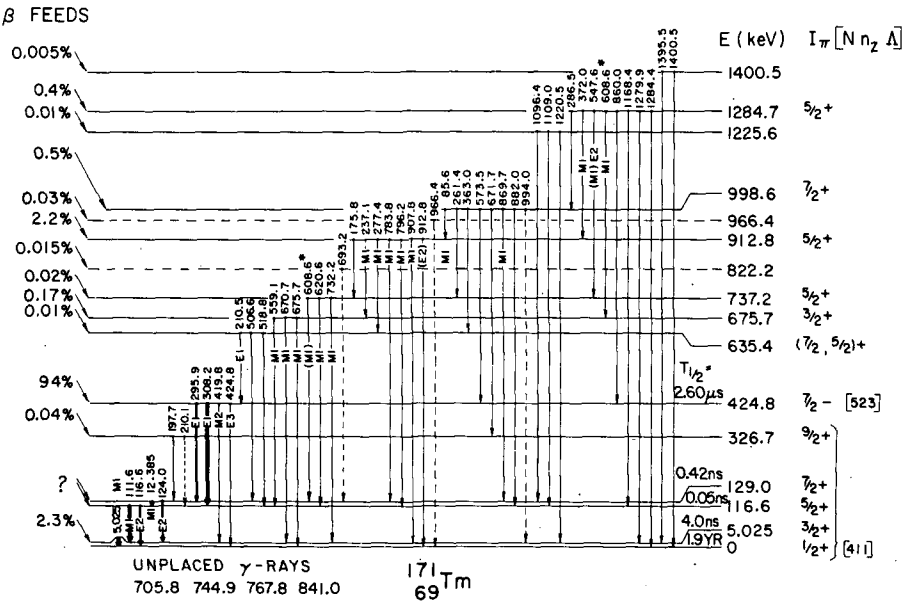

FIG.B. ^{171}Tm levels fed by ^{171}Er β decay.

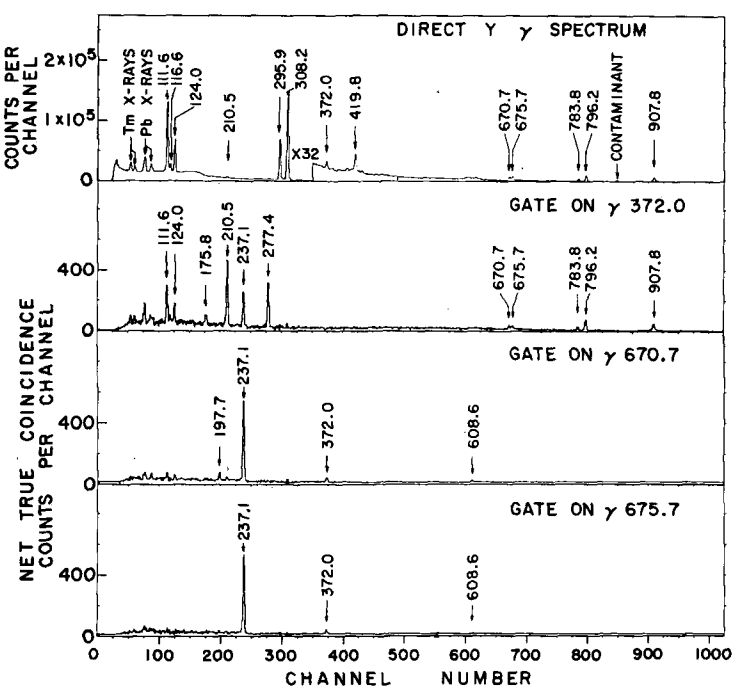

FIG.C. The coincidence γ372 spectrum.

We have obtained multipolarity information on 19 transitions by combining our K line and γ-ray quantum intensity data to yield the K internal coefficient values shown in Fig.A. The two intensity scales were normalized by assuming γ308.2 is pure E1. Most of the transitions are dominantly M1. These multipolarities make it possible to assign spins and parities to six of the higher energy levels in ^{171}Tm as shown in Fig.B.

This level scheme accounts for 50 of our 54 γ transitions. The levels at 635.4, 675.7, 737.2, 912.8, 998.6 and 1284.7 keV are now unambiguously established from our γ-γ coincidence studies. The 1225.6 and 1400.5 keV levels are based on the measured differences in γ-ray energies. The 966.4 keV level is introduced to account for γ966.4 which is not seen in γ-γ coincidence studies although it is of moderate intensity. Recent γ-γ coincidence studies fail to confirm the 1443.2 keV level tentatively proposed in our conference abstract.

Megli et al. do not have a level at 1284.7 keV but have introduced, instead, a level at 489 keV in order to account for the 372 keV γ transition. On our scheme one expects to see the family of γ-rays from the 912.8 keV level and their successors to be coincident with γ372.0. The γ spectrum in coincidence with γ372 is shown in Fig.C. It shows clearly that the predicted family of γ-rays have the relative intensity pattern expected from our direct γ-ray spectra.

Returning to Fig.B, both Megli et al. and Raeside et al. have proposed a level at 862 keV to account for the 732 and 745 keV γ-rays. On our level scheme γ732 de-excites the 737.2 keV level and γ745 is unplaced. The 737.2 keV level is populated by γ175.8. On our scheme we expect to see γ732.2 as well as γ608.6 and γ620.6 in coincidence with γ175.8. Our evidence for this is shown in Fig.D. Also shown on this figure is the γ spectrum coincident with γ124.0. There is no evidence for γ732.2 in this spectrum as predicted by the other workers. We do, however, note that γ671.7 and γ693.2 are in coincidence with γ124.8.

On Fig.B note that we have introduced the tentative level at 822.2 keV to account for the γ693.2 - γ124.0 coincidences. We believe that γ671.7 de-excites the 998.6 keV level and populates the previously unobserved $9/2^+$ member of the ground-state rotational band at 326.7 keV. This level decays by γ197.7 (previously unplaced) to the $3/2^+$ level at 129.0 keV and the weak γ210.1 (previously unobserved) to the $5/2^+$ level at 116.6 keV.

γ671.7 is very weak and is masked in the direct spectrum by the relatively intense γ-ray doublet of 670.7 and 675.7 keV. This doublet de-excites the 675.7 keV level. One expects to see identical spectra in coincidence with both γ-rays, the dominant peak being γ237.1. The lower portion of Fig.C shows these two coincidence spectra. As expected, both show a dominant γ237.1 peak. Note, however, that the γ670.7-gated spectrum has peaks at 197.7 and 210.1 keV which are not present in the lower spectrum. A more detailed analysis of our data has shown that the γ-ray coincident with γ 197.7 has an energy of 671.7 keV.

Some features of the presently known level structure of ^{171}Tm (Fig.B) have an obvious interpretation. Hatch and Boehm[3] were the first to study the properties of the K = 1/2 [411] ground-state rotational band. All studies to date agree on the properties of the 424.8 keV level and there seems little doubt that its assignment is the $7/2^-$ [523] Nilsson orbital. At this stage we hesitate in making definite Nilsson orbital assignments

[3] HATCH, E.N., BOEHM, F., Phys. Rev. 108 (1957) 113.

to the higher energy levels until our data are more fully analysed. However, one notes that Nilsson orbitals $7/2^+$ [404], $5/2^+$ [402] and $3/2^+$ [411] might be expected to appear at moderate excitation energies.

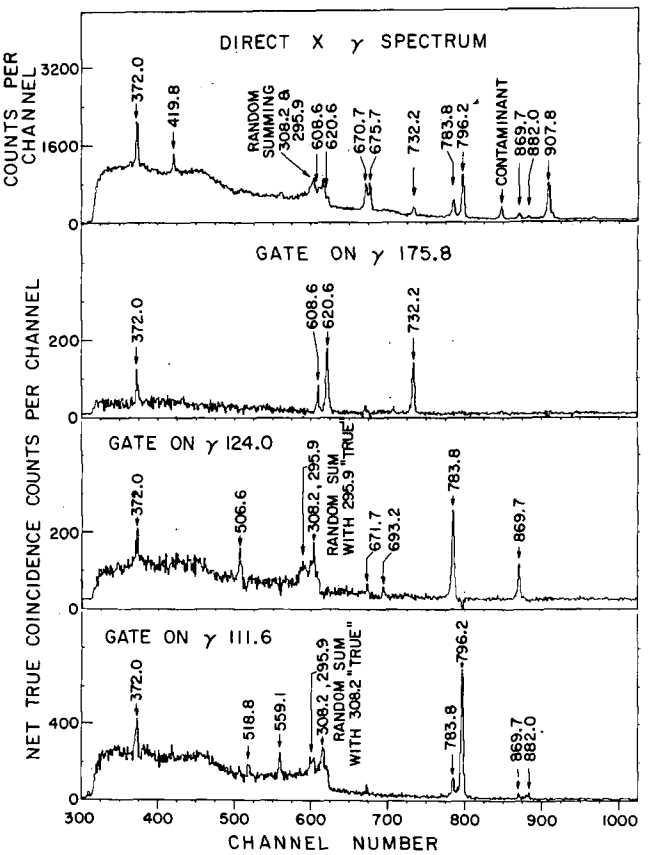

FIG.D. The coincidence γ 175.8 and γ 124.0 spectra.

The 998.6 keV $7/2^+$ level de-excites to the 912.8 keV $5/2^+$ level by γ 85.6 [M1 + ~ 5% E2] suggesting that these two levels are members of a $K = 5/2^+$ rotational band. The 675.7 and 737.2 keV levels may possibly be members of a $K = 3/2^+$ rotational band although we have no evidence, as yet, for a 61.5 keV M1 transition between them.

NUCLEAR DEFORMABILITY AND QUADRUPOLE MOMENTS

A.S. DAVYDOV
INSTITUTE FOR THEORETICAL PHYSICS,
UkrSSR ACADEMY OF SCIENCES,
KIEV, UNION OF SOVIET SOCIALIST REPUBLICS

Abstract — Аннотация

NUCLEAR DEFORMABILITY AND QUADRUPOLE MOMENTS. A survey of the present phenomenological theory of collective excited states in spherical and non-spherical even-even nuclei is made. It is shown that the character of excited states depends essentially upon the two parameters specifying the nuclear equilibrium shape in the ground state as well as two other dimensionless parameters specifying the longitudinal and transversal deformability of the nuclear surface. Relative to these parameters the nuclei are subdivided into rigid and soft nuclei. In the soft nuclei the rotations are not separated from the vibrations. The above parameters are computed from the data concerning energies of three excited levels. The reduced transition probabilities for E2-transitions between excited states are also expressed in terms of these parameters. Sum rules for reduced E2-transition probabilities and expectation values of quadrupole moments in excited states are discussed. It is shown that the theory of non-spherical deformable nuclei yields expectation values of the quadrupole electric moments of the first 2^+ excited state in good agreement with experimental data for isotopes of the nuclei Cd, Ba, Sm and Gd.

ДЕФОРМИРУЕМОСТЬ ЯДЕР И КВАДРУПОЛЬНЫЕ МОМЕНТЫ. Дается обзор современного состояния феноменологической теории коллективных возбужденных состояний сферических и несферических четно-четных ядер. Показано, что кроме двух параметров, характеризующих равновесную форму ядра в основном его состоянии, характер возбужденных состояний существенно зависит от двух других безразмерных параметров, характеризующих продольную и поперечную деформируемость поверхности ядра. По отношению к этим параметрам все ядра можно разделить на жесткие и мягкие. В мягких ядрах вращательные движения не отделяются от вибрационных. Значения этих параметров определяются на основании данных об энергиях трех возбужденных уровней. Через эти же параметры выражаются приведенные вероятности E2-переходов между возбужденными состояниями. Обсуждаются правила сумм для приведенных вероятностей E2-переходов и средних квадрупольных моментов в возбужденных состояниях. Показано, что теория несферических деформируемых ядер определяет средние значения квадрупольных электрических моментов первого 2^+ возбужденного состояния в изотопах ядер Cd, Ba, Sm и Gd при хорошем согласии с экспериментальными данными.

1. INTRODUCTION

The present survey deals with collective excitations of the quadrupole type, whose theory has so far been developed fairly completely. The quadrupole vibrations of the nuclear surface are described by five dynamical variables. In the co-ordinate system associated with the nuclear principal moments of inertia (the nuclear co-ordinate system) these five dynamical variables can be subdivided into two types, namely two intrinsic variables β and γ determining the instantaneous nuclear shape in the nuclear co-ordinate system and three Euler angles $\theta = \{\theta_1, \theta_2, \theta_3\}$ characterizing the orientation of the nuclear co-ordinate system with respect to the laboratory frame.

The potential energy of quadrupole vibrations $V(\beta, \gamma)$ depends on the intrinsic variables β and γ. The equilibrium shape of the nucleus in the

ground state is determined by the values β_0 and γ_0 which minimize the potential energy. The value $\beta_0 = 0$ corresponds to the spherical equilibrium shape. If $\beta_0 \neq 0$, the nuclear shape in the ground state is not spherical. The surface vibrations occur about equilibrium values $\beta_0 \neq 0$ and γ_0. When $\gamma_0 = 0$ or $\pi/3$ the equilibrium shape of the nucleus is axially symmetric.

2. QUADRUPOLE EXCITATIONS OF SPHERICAL NUCLEI

In spherical nuclei the spectrum of collective quadrupole excitations has the equidistant character shown in Fig. 1. The excited states are characterized by the wave-functions (see Sect. 6 of Ref. [1]).

$$\psi_{IMns}(\beta, \gamma, \theta_i) = \varphi_{ns}(\beta) \sum_{K \geq 0} |IMK\rangle A^{(s)}_{IK}(\gamma) \qquad (2.1)$$

where $I = 0, 2, 3, 4, \ldots$ is the total spin, $K = 0, 2, 4, \ldots$; $n = 0, 1, 2, \ldots$; $s = 1, 3/2, 2, 5/2$ are the quantum numbers of "intrinsic" collective excitations;

$$|IMK\rangle = \left[\frac{2I+1}{16\pi^2(1+\delta_{0K})}\right]^{1/2} \left\{D^I_{MK}(\theta) + (-1)^I D^I_{M,-K}(\theta)\right\} \qquad (2.2)$$

$D^I_{MK}(\theta)$ are generalized spherical functions depending on the three Euler angles θ_i; $A^{(s)}_{IK}(\gamma)$ are functions of the variable γ.

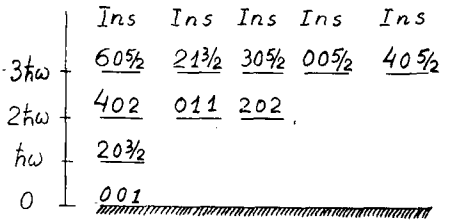

FIG. 1. The first quadrupole excited states of the spherical nucleus.

In the ground state of the nucleus $I = n = 0$, $s = 0$. The energy of excited states I, n, s is determined by

$$E_{ns}(I) = 2\hbar\omega(n + s - 1)$$

where ω is a parameter of the theory specifying a nucleus. In particular, the first excited state of zero spin (0, 1, 1) has energy $E_{11}(0) = 2\hbar\omega$ and its wave-function depends on the variable β. The second excited state of zero spin (0, 0, 5/2) has energy $E_{0,5/2}(0) = 3\hbar\omega$ and its wave-function depends on the variables β and γ. The excited states with spin $I \neq 0$ depend on five dynamical variables.

It is essential that the expectation values of electric quadrupole moments be equal to zero for all excited states of the quadrupole type in the spherical nucleus:

$$\langle \mathrm{Ins} | Q_2 | \mathrm{Ins} \rangle = 0 \qquad (2.3)$$

The quadrupole excited states of spherical nuclei and the probabilities of E2-transitions between them are determined by the values of $\hbar\omega$ and $\langle 0|\beta^2|0\rangle$ which should be considered as parameters of the theory.

It is known that twice-magical nuclei and those close to them have a spherical shape in the ground state. Their spectrum of excited states noticeably differs from the predictions of a simple theory (see Fig. 1) of *quadrupole vibrations of the surface of spherical nuclei*. For instance, the first excited state of some nuclei with magical number of either neutrons or protons (^{16}O, ^{72}Ge, ^{90}Zr) has spin equal to 0 rather than to 2. For the nuclei ^{42}Ca, ^{70}Ge, ^{140}Ce the energy of the zero spin level differs a little from that of the first excited state with spin 2 which is also in contradiction with theory. This inconsistency can be explained by a violation of the adiabatic assumption used in theory.

3. QUADRUPOLE EXCITATIONS OF "RIGID" NON-SPHERICAL NUCLEI

For non-spherical even-even nuclei the adiabatic conditions are satisfied much better since the energy of the first quadrupole excitations is less than that of single-nucleon excitations. In order to give a theoretical description of quadrupole excitations in non-spherical nuclei one should know, in addition to parameters $\beta_0 \neq 0$ and γ_0, two more parameters specifying the deformability of the nuclear shape. It is convenient to take as these parameters the following dimensionless quantities

$$\mu = \left\{ \frac{\langle 0|(\beta-\beta_0)^2|0\rangle}{\beta_0^2} \right\}^{1/2}, \quad \Gamma = \left\{ \langle 0|(\gamma-\gamma_0)^2|0\rangle \right\}^{1/2} \qquad (3.1)$$

where $\langle 0|(\beta-\beta_0)^2|0\rangle$ and $\langle 0|(\gamma-\gamma_0)^2|0\rangle$ are expectation values of the squared β- and γ-vibrations of the nuclear surface about equilibrium values β_0 and γ_0 in the nuclear ground state. The parameter μ characterizes the longitudinal or β-*deformability* of the nuclear surface. The parameter Γ characterizes the transversal or γ-deformability of the nuclear surface. The values $\mu = \Gamma = 0$ correspond to the perfectly rigid nucleus.

Thus in the phenomenological theory of non-spherical even-even nuclei the energies of quadrupole excitations as well as the probabilities of E2-transitions between them and the expectation values of electric quadrupole moments in excited states are in general expressed in terms of four parameters β_0, γ_0, μ and Γ. In the case of nuclei axially symmetric in the ground state, γ_0 is equal either to 0 or to $\pi/3$. Therefore the quadrupole excitations in these nuclei are expressed in terms of three independent parameters β_0, μ and Γ.

If the energy of excited quadrupole states is expressed in units of $\hbar^2/B\beta_0^2$, where B is the mass parameter, then the operator of potential energy can be written in the form

$$V(\beta,\gamma) = \frac{(\beta-\beta_0)^2}{(\mu\beta_0)^2} + \frac{\gamma^2}{4\Gamma^2} \qquad (3.2)$$

In the same units the operator of rotational energy has the form

$$H_{rot} = \left(4\beta^2\right)^{-1} \sum_{\lambda=1}^{3} \frac{I_\lambda^2}{\sin^2\left(\gamma - \frac{2\pi}{3}\lambda\right)} \tag{3.3}$$

If the parameter $\Gamma < 0.3$, the atomic nucleus is comparatively rigid under the action of transversal or γ-vibrations. Therefore the effective value $\gamma \ll 1$ when excitation energies are small. Then the operator (3.3) can be expanded in powers of γ

$$H_{rot} = H_{rot}^{(0)} + H_{rot}^{(1)} + \ldots \tag{3.4}$$

where

$$H_{rot}^{(0)} = \frac{I^2}{3\beta^2} + \frac{1}{4\beta^2}\left(\frac{1}{\gamma^2} - 1\right) I_3^2 \tag{3.5}$$

$$H_{rot}^{(1)} = \frac{2}{3\sqrt{3}\,\beta^2}\gamma\,(I_1^2 - I_2^2) \tag{3.6}$$

In the zero-order approximation, i.e. when only the first term is maintained in (3.4), the total Hamiltonian commutes with operator I_3, and the projection (K) of spin on the nuclear symmetry axis is an integral of motion. In this approximation the quadrupole excited states are characterized (see Sect. 14 of Ref. [1]), by the total spin I, its projection K and two quantum numbers ν_n, n_γ with n and n_γ running through the values 0, 1, 2, ... If the nucleus is rigid under longitudinal (β) vibrations as well (when $\mu < 0.3$), then the quantum numbers ν_n are close to integers:

$$\nu_n \approx n_\beta = 0, 1, 2, \ldots$$

With regard to the operator of vibration (3.6) the excited states are characterized by a superposition of states with different K. At small Γ only one term of this superposition is important. The value of K corresponding to it is an approximate integral of motion and can be used to characterize excited states.

Thus, in rigid nuclei (μ, $\Gamma < 0.3$) the spectrum of quadrupole excitations is split into a set of bands, part of which is shown in Fig. 2.

The first band with quantum numbers $n_\beta = n_\gamma = 0$ and $K \approx 0$ in the ground state corresponds mainly to the rotation of the nucleus around the axis perpendicular to its symmetry axis. It is called the ground rotational band. When

$$\mu^4 I(I+1) < 1 \tag{3.7}$$

the energies of excited states in this band obey approximately the interval rule

$$1 : 10/3 : 7 : 12 : 55/3 : 26 : 35 : \ldots \qquad (3.8)$$

With increasing μ and I a considerable deviation from this rule can be observed.

The second band with quantum numbers $n_\beta = n_\gamma = 0$, $K \approx 2$ is called the first anomalous rotational band. It corresponds to a complex combination of rotational and vibrational excitations.

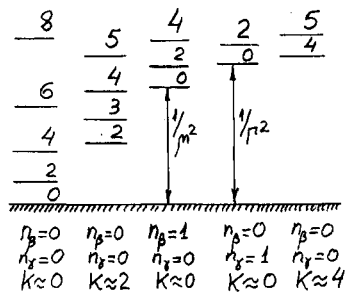

FIG.2. The first excited states of the "rigid" non-spherical nuclei.

The excited states with quantum numbers $n_\gamma = 0$, $n_\beta = 1$, $K = 0$, $I = 0, 2, 4, \ldots$ can be called the first rotational band of longitudinal vibrations. The excited states with quantum numbers $n_\beta = n_\gamma = 0$, $K \approx 4$, $I = 4, 5, 6$ form the second anomalous rotational band and so on.

A theory of nuclear quadrupole excited states based on the expansion of the Hamiltonian in powers of $(\beta-\beta_0)/\beta_0$ and γ in the space of five dynamic variables, which also takes into account the terms responsible for the mixing of rotational and vibrational motions by the usual perturbation theory method, has been developed in Refs [2-4]. In Refs [5-6] perturbation theory has been used taking into account 13 functions of the zero-order approximation operator. The results of all these considerations can be applied to the states with small spins ($I \leq 6$) in comparatively rigid nuclei.

4. QUADRUPOLE EXCITATIONS OF NON-SPHERICAL "SOFT" NUCLEI

With "soft" nuclei the parameters μ and Γ exceed 0.3. The values $\gamma_0 \neq 0$ are also possible. So far, there is no general theory of quadrupole excitations taking into account all the five dynamic variables. In the soft nuclei rotational motions are closely connected with intrinsic vibrations of the nuclear surface. Under rotation the nucleus is stretched, which leads to a change of the value β_0 characterizing the equilibrium shape of the stationary (motionless) nucleus. To account for this effect Davydov and Chaban [7] have developed a theory in which the variable γ is replaced by the effective value

$$\gamma_{\text{eff}} = \sqrt{\Gamma^2 + \gamma_0^2} \qquad (4.1)$$

whereas β remains free. In this theory the operator of quadrupole excitations is determined in the space of four dynamic variables β, θ_1, θ_2, θ_3. The energy of quadrupole excitations is expressed in terms of three parameters ω_0, μ and γ_{eff} by

$$E_{I\tau\nu} = \hbar\omega_0 \left\{ \left(\nu + \frac{1}{2}\right) \sqrt{1 + \frac{3}{2}\left(\frac{\mu}{p_{I\tau}}\right)^2} E^{(a)}_{I\tau}(\gamma_{eff}) \right. \tag{4.2}$$

$$\left. + \frac{1}{4}\left(\frac{\mu}{p_{I\tau}}\right)^2 E^{(a)}_{I\tau}(\gamma_{eff}) + (p_{I\tau} - 1)^2/\mu^2 \right\}$$

where $E^{(a)}_{I\tau}(\gamma_{eff})$ is the energy (in units of $\hbar^2/4B\beta_0^2$) of rotational states in the theory of rigid non-axial nuclei [8], I is the total spin of the state, τ is the number of the level of a given spin; the quantity $p_{I\tau}$ is determined for any pair of the quantum numbers I and τ by solving the equation

$$(P_{I\tau} - 1)\, P^3_{I\tau} = \frac{1}{2}\, \mu\, E^{(a)}_{I\tau}(\gamma_{eff})$$

The quantity ν is a root $(\nu_0, \nu_1, \ldots)$ of the completed equation (see Ref. [7]).

It follows from (4.2) that the ratios $R_{I\tau\nu_n}$ of the energies of excited states $E_{I\tau\nu_n}$ and that of the first excited level $E_{21\nu_0}$ are expressed in terms of two parameters μ and γ_{eff} for any nucleus. These parameters are uniquely determined if the experimental values for the energies of the three levels $E_{21\nu_0}$, $E_{22\nu_0}$ and $E_{21\nu_1}$ or of any other three levels are known.

In Figs 3 and 4 the experimental values for the ratios

$$\frac{E_{22}}{E_{21}} \equiv \frac{E_{22\nu_0}}{E_{21\nu_0}} \quad \text{and} \quad \frac{E_\beta(0)}{E_{21}} \equiv \frac{E_{21\nu_1}}{E_{21\nu_0}}$$

and the values for the parameters μ and γ_{eff} determined with the help of the tables [9, 1] are listed for the isotopes of the nuclei Sm and Gd.

We see that the isotopes of Sm with the number of neutrons equal to 84, 86, 88 and those of Gd with the neutron number equal to 88 are just soft nuclei. In these nuclei the collective excited states represent a complex "mixture" of rotational and vibrational motions. The ratios of energies of excited states differ widely from interval rule (3.8) of the adiabatic ($\mu = 0$) theory even in the ground rotational band with successive spins 2, 4, 6, ... For instance, in the nuclei with $\mu = 1$ and $\Gamma = 25°$ the following interval rule

$$1 : 2.05 : 3.10 : 4.16 : 5.24 : 6.32, \ldots$$

must hold rather than interval rule (3.8) which was previously considered as an indispensable condition of the nuclear rotational motion. Thus in this case the spectrum of excitations in the ground rotational band becomes almost equidistant. Earlier, an almost equidistant spectrum of excited states was considered as a direct indication of the spherical symmetry of the nucleus in the ground state since it was known (see Section 2) that the spherical nuclei were characterized by an equidistant spectrum. Such a conclusion, nevertheless, may be erroneous because soft non-spherical

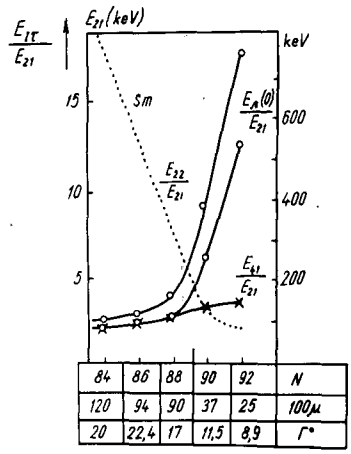

FIG.3. The values of parameters μ and Γ and ratios of the energies of excited quadrupole states in Sm isotopes as functions of the neutron number N (solid lines). The dashed line shows the energy change of the first excited level in keV (the right-hand scale).

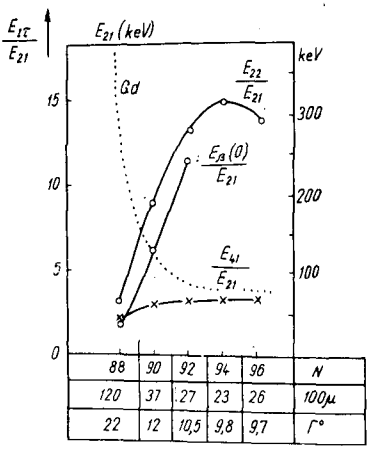

FIG.4. The same as Fig.3 for Gd isotopes.

nuclei can have the spectrum of collective excitations close to an equidistant one as well.

Figs 5 and 6 exhibit the values of parameters μ and γ_{eff} for a number of nuclei. It is seen that in the region of heavy and medium nuclei the "softness" of nuclei increases with the number of neutrons approaching the magic number. This is easily understood if one recalls that with the number of neutrons approaching the magic number the nuclear shape approaches the spherical one, i.e. β_0 decreases. Then μ increases according to the definition (3.1). The increase of parameter γ_{eff} is connected with that of parameter Γ under transition to the nuclei with a weak dependence of potential energy $V(\beta, \gamma)$ on γ. There is no such dependence in the spherical nuclei. To the rigid nuclei there correspond small values of μ and γ_{eff}.

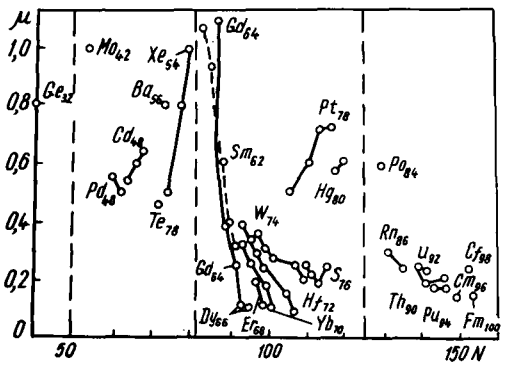

FIG.5. The parameter μ against the number of neutrons.

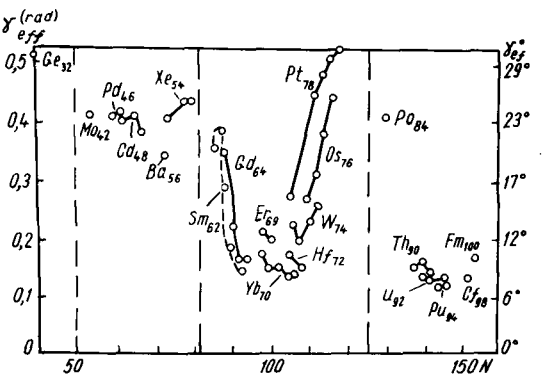

FIG.6. The parameter γ_{eff} against the number of neutrons.

With μ and $\gamma_{\text{eff}} < 0.2$ the theory of Davydov and Chaban [7] brings about the same results for the excited states of a small spin as the theory of rigid nuclei of Section 3 if one puts [2] $\gamma_{\text{eff}} = \Gamma$. The advantage of the theory [7] is that it does not rely on perturbation theory and takes into account the change of the nuclear equilibrium shape due to rotation. Thus the conclusions of the theory can be applied to the high-spin states too.

The equilibrium shape is characterized by the magnitude $\beta_{I\tau} = p_{I\tau}\beta_0$. The distortion of the equilibrium shape of nuclei with $\mu > 0.3$ is especially large for the states with high spins. Stephens, Lark, Dimond [10] have presented a convincing proof of a large deformability even of the nuclei possessing a pronounced rotational spectrum at small excitation. They obtained [9] nuclei in the excited states with high spins (up to $I = 16$). When examining conversion electrons and the γ-quanta emitted by these nuclei under the cascade transition to the ground state, the energy of excited states of the ground-rotational band has been measured with great accuracy (up to 0.3%). A comparison of the experimental data obtained with the theory of Davydov and Chaban developed in Ref. [7] has shown that for five nuclei the discrepancy with theoretical values is less than 0.3% and only for one of the nine nuclei (^{166}Hf) is the error about 1.45%.

The introduction of the parameter μ enables us not only to clarify the deviation from the interval rule in an arrangement of rotational levels but also to explain a number of excited states of positive parity, relating to the vibration and rotation-vibration type.

5. EXPECTATION VALUES OF QUADRUPOLE MOMENTS AND E2-TRANSITION PROBABILITIES IN NON-SPHERICAL NUCLEI

A theory of electric quadrupole transitions taking into account the deformation of even-even nuclei has been developed by Ovcharenko and Davydov [11, 12]. The reduced probabilities of electric quadrupole transitions between states $I\tau\nu$ and $I'\tau'\nu'$ in deformed nuclei are determined by

$$b(E2; I\tau\nu \to I'\tau'\nu') = b_a(E2;\ I\tau \to I'\tau')\, S^2_{I\tau\nu;\ I'\tau'\nu'} \qquad (5.1)$$

where $b_a(E2; I\tau \to I'\tau')$ is the reduced E2-transition probability (in units of $Q_0^2/16\pi$, $Q_0 = 3ZeR_0^2\beta_0/\sqrt{5\pi}$) of the adiabatic theory,

$$S_{I\tau\nu;\ I'\tau'\nu'} = \langle I'\tau'\nu' \left| \beta/\beta_0 \right| I\tau\nu \rangle \qquad (5.2)$$

is the factor responsible for the deformability of the nucleus and the vibrational mode change under the quantum transition $I\tau\nu \to I'\tau'\nu'$. The diagonal matrix element (5.2) determines the correction, arising at nuclear deformation, to the expectation value of the electric quadrupole moment in the state $I\tau\nu$. So

$$\langle Q_2 \rangle_{I\tau\nu} = \langle Q_2 \rangle^{(a)}_{I\tau}\, S_{I\tau\nu}$$

where

$$S_{I\tau\nu} \equiv S_{I\tau\nu;\ I\tau\nu}$$

$\langle Q_2 \rangle^{(a)}_{I\tau}$ is the expectation value of the electric quadrupole moment in the adiabatic theory [1, 8]. In particular, in the first excited state of the ground rotational band, the values (5.1) and (5.3) depend on three parameters Q_0, μ and γ_{eff} only. Table I presents experimental and theoretical values for $\langle Q_2 \rangle_{21\nu_0}$ calculated in Ref. [13]. Also, the values of parameters μ and γ_{eff} are indicated for the corresponding nuclei as well as the values for Q_0 obtained by making use of formula (5.1) from the experimental data concerning the probabilities of transitions from the ground state to the first excited spin 2 states. The asterisked experimental values were communicated to the author by de Boer at the International Conference on Nuclear Structure in Tokyo, 1967. The good agreement of theoretical values for $\langle Q_2 \rangle_{21\nu_0}$ with experimental ones indicates that the equilibrium shape of the nuclei of Table I has no spherical symmetry and that the theory of non-spherical nuclei [7] reflects the principal properties of the first excited states of even nuclei. In particular, the large expectation value of the electric quadrupole moment in the first 2^+ state of the nucleus ^{114}Cd shows that this nucleus is a soft ($\mu = 0.60$; $\gamma_{eff} = 23.8°$) non-spherical one.

TABLE I. AVERAGED QUADRUPOLE MOMENTS OF 2^+ STATE IN EVEN NUCLEI

Nucleus	μ	γ_{eff}	Q_0 ($e \cdot 10^{-24}$ cm^2)	$\langle Q_2 \rangle_{21\nu_0}$ ($e \cdot 10^{-24}$ cm^2)	
				Theoretical	Experimental
^{112}Cd	0.50	24.7	2.173	-0.456	-
^{114}Cd	0.60	23.8	2.101	-0.521	-0.49 ± 0.25 -0.6 ± 0.2 -0.7 ± 0.21
^{116}Cd	0.65	22.5	2.115	-0.600	-0.78 ± 0.14*
^{130}Ba	0.80	20	2.914	-1.029	-1.10 ± 0.34
^{148}Sm	0.94	22.4	2.115	-1.735	-1.73 ± 0.38
^{150}Sm	0.90	17	2.662	-1.087	-1.22 ± 0.22
^{152}Sm	0.37	11.5	5.858	-1.693	-1.8 ± 0.6*
^{154}Sm	0.25	8.9	6.799	-1.938	-
^{156}Gd	0.27	10.5	6.769	-1.916	-

* Communicated to the author by de Boer.

Table II exhibits experimental and theoretical values for the ratios of the reduced E2-transition probabilities for some states of the nucleus ^{114}Cd calculated in Ref. [11] by formula (5.1). The values for parameters μ and γ_{eff} indicated in Table I have been used for the calculation. Fig. 7 presents ratios of the reduced E2-transition probabilities calculated by Begzhanov, Belen'ky and Rakovitsky [14] for many nuclei on the basis of the theory of Faessler and Greiner [6] and the theory of Davydov and Ovcharenko [11, 12]. The available experimental values for the corresponding ratios are also listed there.

6. SUM RULES FOR REDUCED E2-TRANSITION PROBABILITIES AND EXPECTATION VALUES OF QUADRUPOLE MOMENTS

In the adiabatic theory of non-spherical nuclei [1, 8, 15] the reduced E2-transition probabilities and the expectation values of quadrupole electric moments obey a number of sum rules.

When the longitudinal deformability of the nucleus is taken into account these sum rules are replaced by [1, 2]

$$S^{-1}_{21\nu_0} \langle Q_2 \rangle_{21\nu_0} + S^{-1}_{22\nu_0} \langle Q_2 \rangle_{22\nu_0} = 0 \qquad (6.1)$$

$$S^{-2}_{21\nu_0;0} b(E2; 21\nu_0 \to 0) + S^{-2}_{22\nu_0;0} b(E2; 22\nu_0 \to 0) = 1 \qquad (6.2)$$

$$\frac{35}{2} \langle Q_2 \rangle^2_{21\nu_0} (S_{21\nu_0} Q_0)^{-2} + S^{-2}_{22\nu_0;21\nu_0} b(E2; 22\nu_0 \to 21\nu_0) = \frac{10}{7} \qquad (6.3)$$

The factors appearing in these sum rules are determined by relation (5.2). They can be calculated unequivocally [13] for any values of the two parameters μ and γ_{eff}.

TABLE II. RATIOS OF REDUCED PROBABILITIES OF E2-TRANSITIONS IN NUCLEUS ^{114}Cd

Ratios	Theoretical	Experimental
$\frac{b(E2; 22\nu_0 \to 21\nu_0)}{b(E2; 22\nu_0 \to 0)}$	16.4	69
$\frac{b(E2; 22\nu_0 \to 21\nu_0)}{b(E2; 21\nu_0 \to 0)}$	0.94	1.21 ± 0.25
$\frac{b(E2; 41\nu_0 \to 21\nu_0)}{b(E2; 21\nu_0 \to 0)}$	1.84	1.80 ± 0.23
$\frac{b(E2; 22\nu_0 \to 0)}{b(E2; 21\nu_0 \to 0)}$	0.057	0.015 ± 0.005

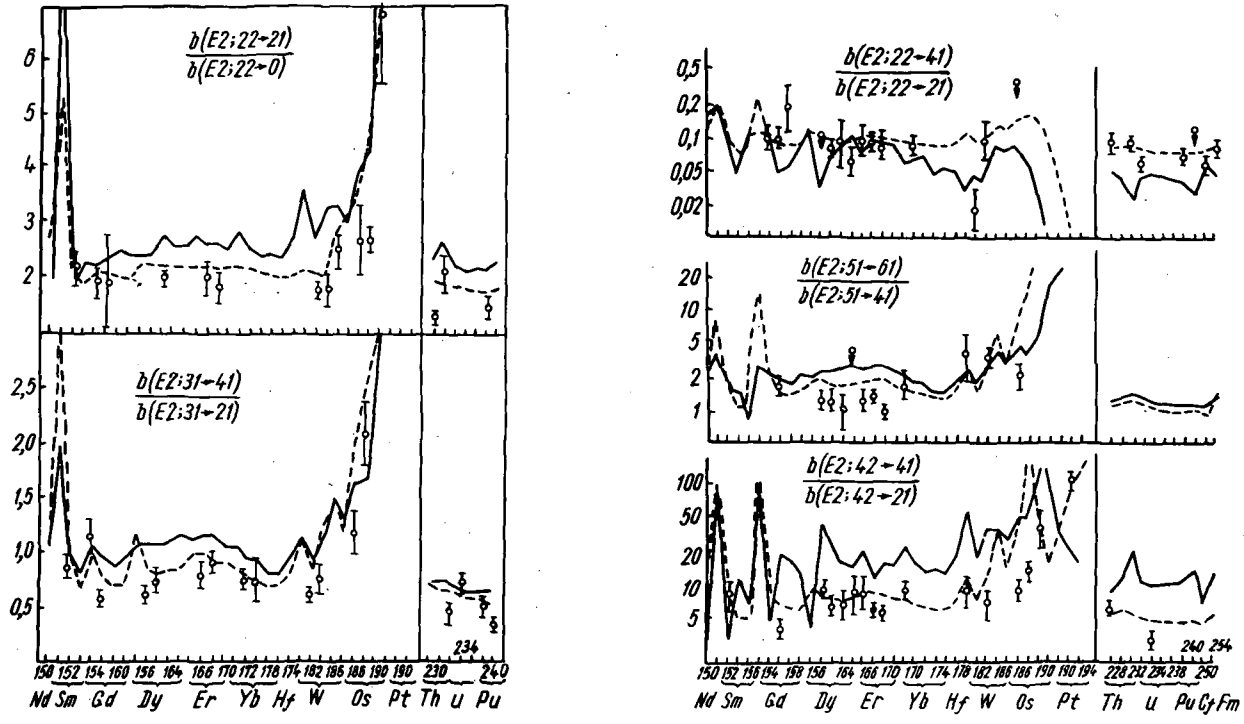

FIG. 7. Ratios of the E2-transition reduced probabilities. Solid lines represent theory of Faessler, Grainer; dashed lines represent theory of Davydov, Ovcharenko. Circles are experimental values for the ratios.

TABLE III. VERIFICATION OF SUM RULE (6.2)

Nucleus	μ	γ_{eff}	$\frac{b(E2;\, 21\nu_0 \to 0)}{S^2_{21\nu_0;\,0}} \simeq A$	$S^2_{21\nu_0;0}$	$\frac{b(E2;\, 22\nu_0 \to 0)}{S^2_{22\nu_0;0}} = B$	$S^2_{22\nu_0;0}$	A + B
^{112}Cd	0.50	- 24.7	0.955	1.14	0.019	1.17	0.974
^{114}Cd	0.60	23.8	0.947	1.29	0.017	1.32	0.964
^{116}Cd	0.65	22.5	0.938	1.34	0.035	1.40	0.973
^{152}Sm	0.37	11.5	0.965	1.03	0.032	1.01	0.997
^{154}Sm	0.25	8.9	0.977	1.01	0.014	1.00	0.991
^{156}Gd	0.27	10.5	0.970	1.01	0.013	1.02	0.983

The sum rules of the type (6.3) relating the expectation values of quadrupole moments to E2-transition probabilities are of especial interest. Table III presents the results of a check on the sum rule (6.2) for certain nuclei. We see that this sum rule is obeyed well for the comparatively rigid nucleus ^{154}Sm as well as for the soft Cd nuclei.

REFERENCES

[1] DAVYDOV, A.S., Vozbushdennye Sostoyaniya atomnykh Yader (Excited states of atomic nuclei), Atomizdat, Moscow (1967).
[2] DAVYDOV, A.S., ROSTOVSKY, V.S., CHABAN, A.A., Nucl.Phys., 27 (1961) 134.
[3] BELYAK, V.I., ZAIKIN, D.A., Nucl.Phys. 30 (1962) 142.
[4] DAVYDOV, A.S., ROSTOVSKY, V.S., Nucl.Phys. 60 (1964) 529.
[5] FAESSLER, A., GREINER, W., Z.Phys. 168 (1962) 425; 170 (1962) 105; 177 (1964) 190.
[6] FAESSLER, A., GREINER, W., SHELINE, R.K., Nucl.Phys. 70 (1965) 33.
[7] DAVYDOV, A.S., CHABAN, A.A., Nucl.Phys. 20 (1960) 499.
[8] DAVYDOV, A.S., FILIPPOV, G.F., Nucl.Phys. 8 (1958) 237.
[9] DAY, P.P., KLEMA, E.D., MALLMAN, C.A., Argonne National Laboratory Report ANL-6220 (Nov.1960).
[10] STEPHENS, F.S., LARK, N., DIMOND, R.M., Phys.Rev.Lett. 12 (1964) 225; Nucl.Phys. 63 (1965) 82.
[11] DAVYDOV, A.S., OVCHARENKO, V.I., Yadernaya Fiz. 3 (1966) 1011.
[12] DAVYDOV, A.S., OVCHARENKO, V.I., Dokl.Akad.Nauk SSSR 163 (1965) 329.
[13] DAVYDOV, A.S., OVCHARENKO, V.I., Preprint ITF-67-14, Kiev (1967).
[14] BEGZHANOV, R.B., BELENKY, V.M., RAKOVITSKY, S.L., Preprint ITF-68-7, Kiev (1968).
[15] OVCHARENKO, V.I., Yadernaya Fiz. 4 (1966) 30.

DISCUSSION

L. MÜNCHOW: You apply a simple form for the potential energy, doing the harmonic approximation. On the other hand, the microdescription, for example in Cd-isotopes, needs strong anharmonicities. Does that mean that anharmonicity, in the main, is equivalent to an effective deformation and non-axiality or does your formalism also need some anharmonicity?

A.S. DAVYDOV: We use the harmonic approximation in order to simplify theory. The introduction of anharmonic corrections will require including new parameters which have to be determined from the experimental data. Phenomenological theory with a large number of parameters has small practical value. We leave two independent parameters for each nucleus. This makes it possible to obtain a number of very interesting relations between experimental data. These relations will certainly be approximate.

B.L. BIRBRAIR: How do you explain in the framework of your model the lack of quadrupole states in double magic nuclei? In particular, does this imply that the parameters of the nucleus surface change considerably during the transition from a double magic nucleus to a "double magic nucleus plus two external nucleons"?

A.S. DAVYDOV: When the nucleus approaches a double magic one the energy of quadrupole excitations becomes comparable with the energy of single-nucleon states. Here, the adiabatic approximation becomes invalid. In other words, in double magic nuclei the excitations cannot be

divided into collective (quadrupole) and single-nucleon ones. Only in non-spherical nuclei is such a division justified for collective modes of excitation with an energy less than 2-3 MeV.

A. BOHR: The analysis of the response of the particle motion to the rotation of the field indicates that the deviation from the I(I + 1) term in the rotational energy is mainly due to the competition between rotation and pairing rather than to centrifugal stretching. The evidence on the coupling to beta-vibrations also indicates that the model considered by Professor Davydov may not be adequate on this point. A further test would be provided by measurements of E2 transition as a function of I.

Another point indicating more structure is the observation that mass parameters for the beta and gamma-vibrational motion are several times larger than for the rotational motion.

As to notation, it would appear convenient to refer to the lowest K=2 band in the deformed nuclei as a vibrational excitation (and give it the quantum numbers $n_\gamma = 1$, $n_\beta = 0$ rather than $n_\gamma = 0$, $n_\beta = 0$), since it is a mode of excitation which can be repeated (it is a quantum of excitation). It is also quite similar to other vibrations, such as octupole modes.

A.S. DAVYDOV: (1) *In our theory the coupling of rotation with* vibrations has been taken into account most completely. This coupling is seen both in the change of the I(I + 1) rule in the main rotational band as well as in the values of mean quadrupole momenta and the transition probabilities. The so-called microtheories take into account the rotational effect rather roughly at present. Therefore the conclusions on the relative role of the pairing and rotational effects obtained on the basis of the microtheory in its modern form is not, however, convincing.

(2) Excited states in hard non-spherical nuclei are defined as follows

$$E(I, K, n_\beta, n_\gamma) = E_{rot}(I, K) + E_{n_\gamma k} + E_{n_\beta}$$

where

$$E_{n_\gamma, k} = \sqrt{\frac{C_\gamma}{B}}\, \hbar\, (2n_\gamma + \tfrac{1}{2} K)$$

Hence, the first excited level with $K = 2$ and $n_\gamma = 0$ has the energy

$$E(2200) = \hbar\sqrt{\frac{C_\gamma}{B}} + \frac{\hbar^2}{3 B \beta_0^2}$$

This energy corresponds to a complex combination of the rotation and gamma-vibration. On the other hand, the energy of the first excited state with K=0 and $n_\gamma = 1$ is

$$E(0001) = 2\hbar\sqrt{\frac{C_\gamma}{B}}$$

This energy corresponds to "pure" gamma-vibrations.

I.N. MIKHAILOV: I should like to discuss the strength of arguments based on the fitting of the energies of wide rotational bands. It is well known that these energies follow nicely the prescriptions of the Harris formula containing only two parameters. Now, this formula may be derived from the general equations of statistical mechanics and may be supplemented by a whole spectrum of other formulas giving no worse fit of the energies.

The derivation based on statistical mechanics gives no indication as to the physical nature of the parameters. Thus the predicted value of the fitting of the energies is not as high as it appears, to judge by the large number of known states in the rotational bands.

A.S. DAVYDOV: Our theory does not only explain the change of energy ratios in the main rotational band as compared with the ratios of adiabatic theory. Using two parameters, μ and Γ, the relative probabilities of E2 transitions between all quadrupole excitations, the average values of quadrupole electric momenta in each excited state, the sum rules for energies, as well as the average quadrupole momenta and probabilities of E2-transitions, etc., are also explained. In the work of Harris just mentioned, two parameters are introduced exclusively to explain the spacing of levels in the rotational band, i.e. the particular problem is solved but the relation of these parameters with other properties of quadrupole excitations is not considered.

Yu.T. GRIN: The corrections to the energies of rotational states in deformed nuclei are determined, in general, by the interaction between rotation and the single-particle spectrum. On the other hand, a change in the mean square radius or quadrupole moment is determined by interaction between rotation and vibrational excitation.

In phenomenological theory both effects are defined by the same parameters μ and Γ. An explanation of the change of the mean square radius using known μ and Γ will be a possible test of this theory.

Dr. I. HAMAMOTO (Niels Bohr Institute, Copenhagen, Denmark) presented Contribution No.71 to the Symposium, by himself and T. Udagawa, and Dr. M. SAKAI (Institute for Nuclear Study, University of Tokyo, Tokyo, Japan) presented Contribution No.26 by Y. Gono, M. Ishihara and himself.

THE MICROSCOPIC MODELS OF COLLECTIVE EXCITATIONS
Present status and possible ways of improvement

S.T. BELYAEV
INSTITUTE OF NUCLEAR PHYSICS, NOVOSIBIRSK,
UNION OF SOVIET SOCIALIST REPUBLICS

Abstract — Аннотация

THE MICROSCOPIC MODELS OF COLLECTIVE EXCITATIONS: PRESENT STATUS AND POSSIBLE WAYS OF IMPROVEMENT. The paper analyses possible generalizations of the known collective excitation models in the following directions: (a) inclusion of other kinds of interactions, generating new types of oscillations, (b) improvement of the quasiboson approximation.

The classification of excitations according to the quantum numbers of correlate pairs provides the basis for the corresponding classification of the elementary interactions generating these excitations. For low excitations the number of important "generating interactions" is not large and practically all of them have been tested.

A special study is made of the particle-particle channel where "elementary interactions" can be introduced without any new parameters, if the hypothesis of gauge invariance of nucleon-nucleon interaction is used. Additional (to usual pairing) interaction in the particle-particle channel generates 0^+-states — "coherent pairing fluctuation" — having a uniquely large probability ratio of *E0* and *E2 transitions into the* ground band. The experimental identification of such states is of great interest.

The necessity to reject the quasiboson approximation is dictated by the complicated vibrational-*rotational structure of experimental nuclear spectra. The main difficulty of their theoretical description* is the absence of a consistent microscopic picture of rotational excitations. Only in very special models can the group theory be applied and show how rotation appears in the system of interacting particles. A method worked out by *Belyaev and Zelevinsky is considered, which gives* the possibility of a microscopic description of rotations. The proposed method includes some aspects of group theory approach that, together with the equations of motion for pair operators, allow the consideration of realistic models in a sufficiently *good approximation. The illustration* of the method serves to obtain the rotational spectrum for j^N configuration with a further generalization on an arbitrary number of levels (in the model with quadrupole interaction). The microscopic structure of rotational states obtained corresponds to the coherent contribution of all the j-levels in rotation and can be directly linked with a visual picture of a deformed nucleus. The wave-function found does not confirm the "stretch scheme" model of Danos and Gillet.

МИКРОСКОПИЧЕСКИЕ МОДЕЛИ КОЛЛЕКТИВНЫХ ВОЗБУЖДЕНИЙ: СОВРЕМЕННОЕ СОСТОЯНИЕ И ВОЗМОЖНОСТИ УСОВЕРШЕНСТВОВАНИЯ. Анализируются возможные *обобщения известных* моделей коллективных возбуждений в направлении: а) включения *других типов* взаимодействий, генерирующих новые типы колебаний, и б) обобщения квазибозонного приближения. Классификация возбуждений в соответствии с квантовыми числами коррелированных пар позволяет выделить соответствующие "элементарные взаимодействия", генерирующие эти возбуждения. Для низких возбуждений число этих "генерирующих взаимодействий", невелико, и практически все они рассмотрены. Специально исследуется канал частица-частица, где "элементарные взаимодействия" могут быть введены без каких-либо параметров, если использовать градиентную инвариантность нуклон-нуклонного взаимодействия. *Дополнительное (к обычному спариванию)* взаимодействие в канале частица-частица генерирует 0^+ состояния ("когерентные флуктуации спаривания"), имеющие уникально большое отношение вероятностей E0- и E2-переходов в основную вращательную полосу. Экспериментальное обнаружение таких состояний представляет большой интерес. Необходимость отказа от квазибозонного приближения диктуется сложной вращательно-колебательной структурой наблюдаемых ядерных спектров. Основная трудность единого теоретического описания таких спектров заключается в отсутствии последовательной микроскопической картины вращательных состояний. *Только в очень специальных моделях, при использовании* методов теории групп, можно *проследить появление* вращательных возбуждений в системе взаимо-

действующих частиц. Излагается метод микроскопического описания вращений, разработанный Зелевинским и автором. Метод содержит некоторые аспекты теоретико-группового подхода в сочетании с уравнениями движения для парных операторов и допускает рассмотрение реалистических моделей в достаточно хорошем приближении. Для иллюстрации метода рассматривается возникновение вращательного спектра в модели с квадрупольными силами для конфигурации j^N с дальнейшим обобщением на произвольное число уровней. Полученная микроскопическая структура вращательных состояний соответствует когерентному вкладу всех j-уровней и может быть непосредственно связана с наглядными представлениями о деформированном ядре. Найденная волновая функция не подтверждает модель "stretch scheme" Даноса и Жилле.

In recent years, owing to the progress made in experimental techniques, our knowledge of the spectrum of low-lying excited states of nuclei has significantly increased and become more precise. But the new data obtained make the classification and the quantitative description of even-even nuclei within the framework of traditional models increasingly difficult. We shall dwell on only some of the contradictions.

Classifying the nuclei into deformed and spherical according to their experimental characteristics becomes more and more conditional. "Strange" qualities are found in the traditionally spherical nuclei: large quadrupole moments in 2^+ states, rotational bands in higher excited states.

The multiformity of collective excitations, both in spherical and in deformed nuclei, turns out to be richer than foreseen by the model with five quadrupole collective degrees of freedom. Particularly unclear is the nature of a large number of collective 0^+ states, found in many nuclei in the region of 1-2 MeV.

These and similar anomalies necessitate a critical reappraisal of the arsenal of theoretical models and an analysis of the ways and means of improving and generalizing them.

I

Three groups of collective excitation models can be differentiated. Their main features are summed up in Table I.

While not belittling the euristic value of the first and third model groups, it must be admitted that the microscopic approach is the most consistent and fundamental. Its restrictions are connected with two "weak" points:

(a) Choice of effective interaction;
(b) Quasiboson approximation (or RPA, etc.).

These two circumstances are analysed in the following pages.

TABLE I. GROUPS OF COLLECTIVE EXCITATION MODELS

Phenomenological approach

Main supposition: adiabaticity of collective excitations.

Starting point: postulation of collective Hamiltonian $H_{coll} = T + U$.

Differences between models: collective variables, parameters and form of H_{coll}.

Aim: the description of the greater part of the spectrum by the least number of parameters.

Methods: the solution of the Schrödinger equation with H_{coll}.

Desirable feature: the establishment of general relations between various spectrum characteristics.

Comparison with experiment: a significant part of the spectrum, individual parameters for each nucleus.

Microscopic approach

Starting point: Hamiltonian of nucleons H_p with effective interaction V_{eff}.

Main suppositions: restrictions to (mainly) pair correlations.

Differences between models: choice of single particle functions; form of V_{eff}.

Method: RPA, two-particle Green functions, TDHF, quasiboson approximation, linearized equations of motion, Bogolyubov generalized transformations.

Aims: (a) calculation of phenomenological model parameters;
(b) calculation of H_{coll} for phenomenological models;
(c) definition of the characteristics of the first excited states (collective and 2-quasiparticle).

Comparison with experiment: change of characteristics of the lower levels from one isotope and element to another.

Specific microscopic models

Main suppositions: specially chosen interactions; restricted configuration j^N,$(sd)^N$, etc.).

Aim: precise solution or spectrum classification.

Method: group theory, exact diagonalizations of the Hamiltonian.

Comparison with experiment: only qualitative (for restricted nuclei groups when postulating pure configurations).

II

In the quasiboson approximation the collective excitations of nuclei are described as coherent superpositions of states of the particle-hole (ph) or particle-particle (pp) (hole-hole) type and are characterized: by the baryon quantum number [b = 0 for a pair of type (ph) and b = 2 for (pp) or (hh)], by the angular momentum λ, parity π, isospin τ [1], time-parity T [2] and a radial quantum number ν, numbering excitations of one type. The possibility of realizing one specific type and its characteristics is defined by corresponding components of effective interaction (V_{eff}).

As no fundamental theory exists, we are forced to be content with a phenomenological description (parametrization) V_{eff}, either choosing V_{eff} directly in the form of some potential or calculating V_{eff} in a certain approximation, proceeding from the "realistic forces" between the free nucleons or parametrizing V_{eff} within the framework of Fermi liquid theory. All these methods inevitably contain arbitrariness and very often lead to a complicated form of V_{eff}. Owing to these circumstances, the method representing V_{eff} in the form of a sum of separable "interactions" has become very widespread. Each "interaction" models only a definite group of properties V_{eff} – interaction of a pair of particles only in a definite quantum state. The pairing and quadrupole interaction model has proved very fruitful, explaining many regularities in the nucleus structure.

It is convenient to classify "elementary interactions" according to quantum numbers of corresponding pair states. Then the characteristic $b = 2$ [channels (pp), (hh)] $\lambda = 0$ can be assigned to pairing and $b = 0$, $\lambda = 2$ to quadrupole interaction. Moreover, the radial quantum number $\nu = 0$, defined as the number of nodes of the radial wave function $R(r)$ of the pair, can be assigned to both interactions $R(r)$ (to pairing $R \sim 1$, for quadrupole interaction $R \sim r^2$). Interaction in the channel particle-hole is also characterized by time parity. For quadrupole forces $T = +1$.

Within the framework of the pairing + quadrupole interaction model only a restricted class of collective excitations is described: quadrupole (β, γ) oscillations ($\nu b \lambda T = 002^+$) and "pair vibrations" (020^+) [3]. A more general model is needed to describe excitations of a different nature.

For the particle-hole channel ($b = 0$) we can first of all study higher angular momenta (e.g. actual interaction with $\lambda = 3$ [4]). If we restrict ourselves to quadrupole excitations only ($\lambda = 2$), then only T-odd forces (spin-quadrupole [5]) may be included. Studying the terms with $\nu > 0$ is of little interest, as it leads to too high excitations. It is worthy of note that the ability to generate 0^+ excitation in the particle-hole channel is very restricted as monopole forces ($\lambda = 0$) result only in high excitations.

In the channel particle-particle ($b = 2$) each type of interaction can generate two branches with different T-parity. Pairing ($\lambda = 0$; $\nu = 0$) in addition to "pair vibrations" can also generate the T-odd branch but the latter has zero energy and hence is a "ghost" excitation. It is only natural to study elementary interactions of the same nature ($\lambda = 0$) but with $\nu > 0$. As for interaction with $\lambda > 0$, for this the main factor is terms with $\nu = 0$. The author has studied the possibilities and the consequences of supple mentary "elementary interactions" in the particle-particle channel [2]. The latter, unlike interaction in the (ph)-channel, can be included without introducing additional free parameters if the gauge invariance of the nucleon-nucleon interaction is used.

By the gauge invariance of interaction we mean its non-changeability when transforming the moments of interacting particles $\vec{p}_{1,2} \to \vec{p}_{1,2} - \nabla\Lambda(\vec{x}_{1,2})$, where $\Lambda(\vec{x})$ is an arbitrary co-ordinate function. Potentials not depending on velocity, as well as spin orbital forces of the form

$$U_{ls} \sim (\vec{\sigma}_1 + \vec{\sigma}_2)\cdot(\vec{p}_1 - \vec{p}_2) \times \nabla\,\delta(\vec{x}_1 - \vec{x}_2)$$

have strict invariance. That is why the forces acting between free nucleons may, with good precision, be considered to be gauge-invariant. Though

the transition from the interaction of free nucleons V_0 to the effective interaction of nucleons inside the nuclei V_{eff} is a very complicated problem, we can still formulate the conditions on V_{eff} in the general form for gauge-invariant V_0. The usual pairing does not satisfy these conditions and must be supplemented by a number of other "elementary interactions" whose form is defined in a unique manner [2].

TABLE II. ENERGIES ω, PROBABILITIES OF E2-TRANSITIONS INTO THE GROUND ROTATIONAL BAND (IN SINGLE-PARTICLE UNITS), AND $\rho^2 = |(0|r^2|\omega)|^2 / R^4$ FOR THE FIRST TWO 0^+ STATES

The quadrupole interaction constant $\kappa = k\hbar\mathring{\omega}A^{-4/3}$, $k = 18.02$; $e_p = 1 + e_{eff}$, $e_n = e_{eff} = 1$.
(Parameters are taken from the nucleus ^{150}Nd: $\omega = 0.69$; $B(E2) = 5 \pm 1.3$).

	Theory			Experiment	
	ω (MeV)	$B(E2)/B_{sp}$	$\rho^2(E0)$	ω (MeV)	$B(E2)/B_{sp}$
^{152}Sm	0.81	3.6	0.14	0.685	2.5 ± 0.6
	1.69	3×10^{-4}	0.53	1.10	-
^{154}Sm	1.11	2.2	0.19	1.1	1.2 ± 0.3
	1.7	10^{-3}	0.48	1.22	-
^{154}Gd	0.95	2.7	0.08	0.68	4.8 ± 1.2
	1.68	10^{-3}	0.7	-	-
^{156}Gd	1.22	1.8	0.12	1.04	2.8 ± 1.2
	1.68	2×10^{-5}	0.67	-	-
^{156}Dy	1.05	2.2	0.04	0.68	-
	1.71	10^{-5}	0.85	-	-
^{158}Dy	1.29	1.43	0.07	0.99	> 0.3
	1.71	8×10^{-5}	0.84	-	-
^{164}Er	1.49	0.17	0.88	1.245	> 0.05
	1.5	0.16	0.17	1.698	-
^{166}Er	1.5	10^{-2}	0.96	1.46	-
	1.57	0.02	0.14	-	-
^{168}Yb	1.46	0.11	0.83	1.156	-
	1.57	0.01	0.25	1.196	-
^{170}Yb	1.25	10^{-4}	0.22	1.065	-
	1.46	0.11	0.92	-	-
^{174}Hf	1.22	0.08	0.24	0.85	-
	1.55	6×10^{-3}	8×10^{-3}	-	-
^{176}Hf	1.46	5×10^{-3}	0.14	1.25	-
	1.67	0.05	0.06	1.42	-

III

Rumiantsev and the author [6] calculated the collective 0^+ states for deformed nuclei with quadrupole interaction and gauge-invariant pairing (terms with $\lambda\nu$ = 00; 01; 20 were considered[1]). The role of supplementary terms in V_{eff} is as follows:

(a) New branches of collective 0^+ excitations appear, i.e. "coherent pairing fluctuations" [2].

(b) Because of the coupling with new excitations, β oscillations change their properties somewhat. The change of the latter can be represented by the dependence of the effective constant of the quadrupole interaction on energy. Taking this effect into account noticeably improves the agreement with experiment.

Some results of the calculations for the first two 0^+ states are given in Table II.

Especially noticeable is the striking difference of the B(E2) transition probabilities into the ground rotational band (except ^{164}Er). States having a larger B(E2) are slightly modified β oscillations. As a rule these states lie somewhat lower in energy (^{166}Er being an exception). Second states (mainly coherent pairing fluctuations) deserve special attention because of the uniquely large ratio[2] $X = \rho^2/B(E2)$. Finding these states experimentally is most interesting.

It is evident from the classification of pair states that coherent pairing fluctuations exhaust the new types of low-lying excited collective states in the framework of quasiboson approximations. Using a more exact form of V_{eff} can, of course, alter the quantitative characteristics, but it is doubtful whether it will change the qualitative scheme of excitations.

IV

Quasiboson approximation (and its equivalent RPA, etc.) gives one the possibility of considering only two quasiparticle states and their coherent superposition. Thus the results are applicable only to the first (single phonon) excitation. The highest excited states can be constructed out of several non-interacting or weakly interacting phonons. But an approximation of this kind turns out to be rather rough.

One means of improving the model is the simultaneous and equal consideration of two- and four-particle correlations [7]. This gives us the chance of improving the description of the two-phonon states, but an improvement of this sort is hardly worth the complication of the calculations. Further steps in this direction, namely the inclusion of higher states, can hardly be considered promising. A different approach, namely a fundamental change of the quasiboson approximation, seems to be much more promising.

---

[1] Especially important is the fact that supplementary "elementary interactions" are introduced with no new parameters. Their constants are uniquely defined by the demands of gauge invariance.

[2] It is worth mentioning that the too small values of B(E2) in Table II should be considered only as qualifiers as in this case the small corrections that are not considered may essentially change the quantitative result.

In the quasiboson approximation the spectrum of collective excitations is constructed of non-interacting phonons, in other words it is equidistant. It is evident that rotational states drop out of this description. That is why we are forced to describe β, γ oscillations and rotations of deformed nuclei under a microscopic approach separately and by different methods. On the other hand, the analysis of experimental data proves that there does not exist any considerable difference between the rotational and vibrational states. A sequence of nuclei can be chosen in which vibrational states gradually turn into rotational ones [8]. A similar transition can be seen, perhaps, in "spherical" nuclei along with the growth of the energy of excitation [9]. These circumstances force us to look for a unified description of both vibrational and rotational states.

Marumori et al. [10] tried to make the boson rules of commutation for pair quadrupole operators $[A^{(+)}_{2\mu}; A^{(-)}_{2\mu'}] = 2(-)^{\mu}\delta_{\mu,-\mu'}$ more complicated by considering the fact that the commutators of different components $A^{(+)}_{2\mu}$ (or $A^{(-)}_{2\mu}$) are proportional to the angular momentum operator $\hat{J}_{\lambda}$. Finally, the properties of the phonons (of the operator that raises the system one state higher) begin to depend upon the angular momenta of the initial (J) and final (J') states; this leads to the deviation of the spectrum from equidistance. The phonon energy, which is related to the energy of a two-quasiparticle transition (in an isolated j - level model), is equal to

$$\omega_{J'J} = \frac{1}{2}(1-\omega_0^2)\beta_{J'J} + \sqrt{\omega_0^2 + \frac{1}{4}(1-\omega_0^2)^2\beta^2_{J'J}} \qquad (1)$$

where $\beta_{J'J} = \text{const} \cdot [J'(J'+1) - J(J+1)]$ and ω_0 is the phonon energy in a quasiboson approximation, defined by the relation of the dimensionless quadrupole (κ) and pairing (g) interaction constants and by the occupation of the level $n = N/(2j+1)$:

$$\omega_0^2 = 1 - \frac{\varkappa}{g} 4n(1-n) \qquad (2)$$

When a change ω_0^2 in the interval from 1 to 0 takes place, the spectrum defined by Eq.(1) changes from equidistant to purely rotational. But it would be erroneous to think that we have obtained a unique description of both spherical and deformed nuclei as Eq.(1) has no sense in the extreme field of nuclei which are known to be deformed ($\kappa/g \to \infty$; $\omega_0^2 \to -\infty$).

V

The rotational bands of deformed nuclei present the main problem in unifying the microscopic description of nuclear spectra. As is known, when considering only quadrupole forces between nucleons in an oscillatory potential the rotational spectrum can be easily obtained from group properties [11]. But group theory methods turn out to be too complicated and have little prospect for real models of medium and heavy nuclei.

Zelevinsky and the author have studied the possibilities of deriving a rotational spectrum from particle dynamics by other methods; even if they are approximate, they allow a solution in realistic models.

Let us first study the nucleons on one j-level ($j \gg 1$) interacting through quadrupole forces

$$H(j) = -\frac{1}{2}\varkappa \sum_{\mu} (-)^{\mu} Q_{2-\mu}(j)\, Q_{2\mu}(j) \tag{3}$$

If we consider the angular momentum (neglecting the octupole) in the commutator of quadrupole operators

$$\left[Q_{2\mu}(j),\, Q_{2\mu'}(j)\right] = -\sqrt{30}\, \beta(j) \sum_{\lambda} (-)^{\lambda} \begin{pmatrix} 2 & 2 & 1 \\ \mu & \mu' & -\lambda \end{pmatrix} \hat{J}_{\lambda} \tag{4}$$

then the eight operators $Q_{2\mu}$ and $\hat{J}_{\lambda}$ included in Eqs (3) and (4) generate the group SU(3) and thus the problem becomes absolutely equivalent to the Elliott problem [11]. The system spectrum consists of a set of rotational bands (limited from above) that are characterized by the different values of the Casimir operator

$$C_j = \sum_{\mu} (-)^{\mu} Q_{2-\mu}(j)\, Q_{2\mu}(j) + \beta(j) \sum_{\lambda} (-)^{\lambda} \hat{J}_{-\lambda}\, \hat{J}_{\lambda} \tag{5}$$

The lower band has the following value of this quantity:

$$C_j^{\circ} = \frac{4}{3}\beta(j)\, \lambda_j (\lambda_j + 3) \tag{6}$$

where λ_j, the maximum possible value of the system angular momentum, is defined by the level occupation $n_j = N_j/(2_j + 1)$

$$\lambda_j = \frac{1}{2}(2j+1)^2 n_j (1-n_j) \tag{7}$$

The energies of the levels and the reduced matrix elements of Q in the ground band have the following form:

$$E(J) = E(0) + \frac{1}{2}\varkappa \beta(j)\, J(J+1) \tag{8}$$

$$(J \| Q(j) \| J') = \sqrt{C_j^{\circ}(2J+1)(2J'+1)} \begin{pmatrix} J & 2 & J' \\ 0 & 0 & 0 \end{pmatrix} \xi_{JJ'} \tag{9}$$

$$\xi_{JJ}^2 = 1 + \frac{9}{4\lambda_j(\lambda_j+3)}, \qquad \xi_{JJ+2}^2 = 1 - \frac{J(J+3)}{\lambda_j(\lambda_j+3)}$$

The factor ξ, when the angular momenta J are close to the maximum value, cuts non-diagonal matrix elements. If we restrict ourselves to the region $J \ll \lambda_j$, then the deviation of ξ from unity can be neglected[3]. In this case the matrix elements will satisfy Eq. (4) without the right-hand side. An approximation of this kind is fully consistent as the right-hand side of (4) is actually small ($b(j) \sim j^{-3}$).

VI

Let us now formulate a simple approximation method for solving the same problem which would be valid in the region $J \ll \lambda_j$.

(A) Let us neglect the right-hand side of (4) and consider for Q only matrix elements inside the band. We then obtain the whole of Eq. (9) (with $\xi = 1$) but only within the accuracy of the normalization constant.

(B) From Eq. (5), neglecting the last term, let us normalize Q through C_j^0.

(C) The value C_j^0 is obtained by calculating the expectation value of the Casimir operator in the state $J = \lambda_j$ when the last term in Eq. (5) has to be retained, while the non-diagonal matrix element of Q can be neglected.[4]

(D) In order to define the rotational level energies, let us make use of the equations of motion for Q:

$$(E_{J'} - E_J)(J\|Q(j)\|J') = \tfrac{1}{2}\varkappa\sqrt{30}\,\beta(j)\,(J\|(\hat{J}Q + Q\hat{J})_2\|J') \qquad (10)$$

from which Eq. (8) immediately follows.

VII

For the transition to realistic models the formulated method of approximation demands generalizations in two directions: one should not be restricted to one j-level and one should include other types of interaction. Let us start out from two postulates, physically evident for deformed nuclei:

(a) There exists a sequence of states with angular momenta $J = 0, 2, 4\ldots$ ("rotational band").

(b) The full quadrupole moment operator $Q_{2\mu}$ has large matrix elements inside the band (diagonal and non-diagonal), while the transitions into states of other types are relatively small.

As an illustration let us study an arbitrary number of j-levels with restriction to $Q \cdot Q$ interaction of the following kind

$$H_{QQ} = -\tfrac{1}{2}\varkappa \sum_{jj'\mu} (-)^{\mu} Q_{2-\mu}(j)\, Q_{2\mu}(j') \qquad (11)$$

---

[3] When $\xi = 1$ the relation between the matrix elements (9) is the same as in the case of the symmetrical rotator.

[4] Thus, having an explicit expression for the Casimir operator, we can relate the regions of small and extremely large angular momenta J.

Then the operations (A), (B), (C) given above lead to formulas (6), (7) and (9) for partial values (defined on each j-level). Equation (10) also remains valid provided that by Q on the right-hand side we understand a full quadrupole moment and by $\hat{J}_\lambda \equiv \hat{J}_\lambda(j)$ a partial angular momentum operator. If we assume $\hat{J}_\lambda(j)$ to be proportional to the operator of the total angular momentum of the system $\hat{J}_\lambda(j) = g(j)\,\hat{J}_\lambda^{tot}$ (inside the rotational band), then both the energy spectrum and the "Lande factor" g(j) are defined from (10):

$$E(J) = E(0) + \tfrac{1}{2}\varkappa \sum_j g(j)\beta(j)J(J+1),$$
$$g(j) = \frac{\lambda_j}{\sqrt{\beta(j)}}\left[\sum_{j'}\frac{\lambda_{j'}}{\sqrt{\beta(j')}}\right]^{-1} \qquad (12)$$

The result has a simple physical meaning. The partial momenta of j-levels sum coherently into a full angular momentum, the contribution of each level depending upon the occupation ($\lambda_j \sim n_j(1-n_j)$). The particle distribution among j-levels (n_j) can be defined by minimizing the energy of the ground state:

$$E(0) = \sum_j (2j+1)n_j\varepsilon_j - \tfrac{2}{3}\varkappa\left(\sum_j \lambda_j\sqrt{\beta(j)}\right)^2 \qquad (13)$$

The structure of the ground state can be clearly presented for the case of two j-levels. If their interaction $(Q(j_1)\cdot Q(j_2))$ is fully neglected then the lowest state (when the distribution of particles in levels is fixed) will be $|(j_1^{N_1})_{J_1=0}\ (j_2^{N_2})_{J_2=0}\rangle$. The higher angular momenta $J_1, J_2 > 0$ are not profitable because of the loss in the rotational energy. But the quadrupole interaction between levels covers this small effect, which is why coherent superposition turns out to be the most profitable combination[5]:

$$|J=0\rangle \sim \sum_{J'} |((j_1^{N_1})_{J'}\ (j_2^{N_2})_{J'})_0\rangle \qquad (14)$$

A similar result could be obtained by selecting wave-functions for each of the j-levels as a "deformed state", $|\vec{n}\rangle = \sum_{J'M'} Y_{J'M'}(\vec{n})\,|J'M'\rangle$, and projecting their product into the state with a definite total angular momentum. The microscopic states thus found actually correspond to the phenomenological suppositions about the deformed nuclei.

The authors have also studied a more realistic model with quadrupole interaction and pairing. In this case one has to take into consideration the operators with higher multipolarity ($Q_{k\mu}$, $k > 2$), as well as pair creation and annihilation operators ($A^\dagger_{k\mu}$, $A_{k\mu}$). In spite of the increase in the number of operators the problem can be treated in a similar manner, provided that

[5] It is worth noting that the given coupling scheme is in principle different from the "stretch scheme" [12] where instead of the coherent sum (14) there ought to be only the one term with a maximal angular momentum.

Eq.(5) is substituted by a more general Casimir operator. The dependence of the matrix elements on angular momenta J, J' inside the rotational band can be separated in the form similar to Eq.(9). Then one obtains, for the amplitudes of the matrix elements, equations of motion analogous to those in the deformed-nucleus model. The moment of inertia found exhibits reasonable dependence on pairing interaction strength. Details of the calculation will be published elsewhere. Results obtained allow one to hope for the successful solution of the last step of the problem: the unified description of both rotational and vibrational excitations.

Let me finish with a quite general remark. Irrespective of the success of the concrete approach described here, the author is positive that for the transition from the description of one elementary excitation (phonon) to the whole spectrum of nucleus excitation, it is necessary to introduce group methods into the traditional microscopic models. Coming back to the collective model classification, this idea can be formulated as follows: combinations of methods, approaches and aims typical for various classes of models are in fact the most promising.

REFERENCES

[1] BOHR, A., Congrès Intern. Phys. Nucl., Vol.1, Paris (1964).
[2] BELYAEV, S.T., Yadernaya Fiz. 4 (1966) 936.
[3] BES, D.R., BROGLIA, R.A., Nucl. Phys. 80 (1966) 289.
[4] SOLOVIEV, V.G., VOGEL, P., KORNEICHUK, A.A., Izvestia Akad. Nauk SSSR 28 (1964) 1599.
[5] CHERNEY, M.I., PYATOV, N.I., ZHELEZNOVA, K.M., Izvestia Akad. Nauk SSSR 31 (1967) 550.
[6] BELYAEV, S.T., RUMIANTSEV, B.A., Proc. Int. Conf. Tokyo (1967).
[7] OTTAVIANI, P.L., SAVOIA, M., SAWICKI, J., TOMASINI, A., Phys. Rev. 153 (1967) 1138.
[8] SHELINE, R.K., Rev. Mod. Phys. 32 (1960) 1.
SAKAI, M., Nucl. Phys. A104 (1967) 301.
[9] PEKER, L.K., Lectures at the 3rd winter school, Leningrad (1968).
[10] MARUMORI, T., SHONO, Y., YAMAMURA, M., TOKUNAGA, A., MIYANISHI, Y., Phys. Lett. 25B (1967) 249.
[11] ELLIOTT, J.P., Proc. Roy. Soc. 245 (1958) 128, 562.
[12] DANOS, M., GILLET, V., Phys. Rev. 161 (1967) 1034.

DISCUSSION

N.I. PYATOV: The numerical results which you have given for 0^+ states can be obtained from the usual model by including spin-quadrupole interactions. Spin-quadrupole interactions put the second 0^+ states below the energy gap, but small B(E2) and large values of X are characteristic of pairing vibrations. Can you definitely point to a feature by which one can distinguish coherent pairing fluctuations from other types of vibrations?

S.T. BELYAEV: I would prefer to put the question in a different way. In order to include spin-quadrupole forces, a new constant must be introduced. The additional interaction, which we considered, follows automatically from the principle of gauge invariance and we must take it into account. As regards spin-quadrupole forces, if any, they should be taken into consideration additionally.

S. SZPIKOWSKI: We know from the Elliott model that the SU(3) group is a proper group to treat the quadrupole-quadrupole forces. On the other hand, the pairing forces are governed by the orthogonal group in five dimensions (j-j coupling) or in eight dimensions (L-S coupling). From the group theory point of view one can do a simple thing in principle: take the operators of Q-Q forces that generate the SU(3) group, and the pairing operators that generate the O_5 (or O_8) group, and commute them to complete the set of generators which will generate the group to be found. Such a group will be a symmetry group of the interactions and would be just a group to diagonalize at the same time these interactions. Do you know anything about the realization of such a program?

S.T. BELYAEV: Exact diagonalization of a similar type is possible only for the simplest single-particle configuration. The generalization to a real scheme of single-particle levels and real forces is practically impossible. The main purpose of our approach is to develop an approximate method for the Elliott model which, however, will permit generalization. This is not a group theory method, although we have borrowed the Kasimir operator from the latter.

I.N. MIKHAILOV: Let me raise a question about the theoretical foundation of the principle of gauge invariance relative to effective forces. Could you give the reason for such an application?

S.T. BELYAEV: The assumption about the gauge invariance is made for the forces between free nucleons and not for the effective interaction of nucleons in a nucleus. But it follows as a consequence that there are certain limitations on the effective interaction.

V.G. SOLOVIEV: Important progress has been made in the many-body problem due to the development of methods in which some law or other is followed approximately. The mathematical basis for applying such methods was created by N.N. Bogolyubov in his paper on quasi-averages. As regards the physical problem, the task is to find such a mathematical method that would permit the most precise solution of the problem. In so doing, one has to restrict oneself by applying one or another conservation law only approximately or for some average values. Certainly, it is good if some conservation law or other is obeyed sufficiently accurately, i.e. gauge invariance takes place. However, the requirement of the fulfilment of gauge invariance in the many-body problem is not strict.

S.T. BELYAEV: I do not agree with the latter statement. Certainly, we are sometimes forced to violate rigorous conservation laws at a certain stage of solving the problem. We do this with the gauge principle, when solving a single-particle problem. (Another example is single-particle levels in the deformed well - the angular momentum is not conserved). However, the conservation laws and symmetry principles must be recovered at further stages of the calculation. Briefly, we must compensate for what we have violated in the single-particle picture (gauge invariance) by collective modes of excitations. These are just the excitations considered.

I.S. SHAPIRO: I would like to ask a simple question: what do you mean in this case by T-parity in the particle-particle system? I can imagine T-parity in the particle-hole system. But as regards the wave-function of two particles, it cannot pass into itself with time.

S.T. BELYAEV: The T-parity of excitation is determined by the relative phase of the contribution of two-particle and two-hole states to

the phonon wave-function, in other words, by the behaviour of the phonon wave-function with respect to the interchange of holes and particles.

I.N. MIKHAILOV: What is the reason for using realistic forces in the theories considered above (say, in the random phase approximation)?

S.T. BELYAEV: The conception of "realistic forces" is usually related to the interaction of free nucleons, whereas collective modes of excitation are determined by the effective interaction inside the nucleus. We used just the latter (certainly, in the form of a model).

B.L. BIRBRAIR: Is there any connection between the pairing coherent fluctuations and the nuclear analogue of ordinary sound? To obtain the latter it is sufficient to take into account the equation of continuity, which in itself is a condition for frequencies, but which does not explicitly include the interaction. Thus, for the sound as well as for the pairing coherent fluctuation there is no need to introduce new constants and therefore there should be a connection between these types of excitation.

S.T. BELYAEV: There actually exists some formal analogy between the sound waves in the superconductor and the excitations considered, although the difference in the systems is very important, which affects even formal results - the frequency of 0^+ vibrations depends on the pairing constant.

D.F. ZARETSKY: Are there vibrations of your type in spherical nuclei? If they do exist, how do they manifest themselves?

S.T. BELYAEV: Similar vibrations should exist in spherical nuclei. We did not calculate them because, in our opinion, the structure of spherical nuclei is not clear at present.

O. NATHAN: I would like to point out that the two second excited states of the Sm isotopes shown in your Table II have a very specific behaviour in double stripping and double pick-up. I would therefore suggest that you use your theory to calculate these (t, p) and (p, t) transition rates. This might test your theory more sensitively than the B(E2) values which are probably very difficult to measure precisely.

S.T. BELYAEV: I agree. At present we are doing such calculations although the results will probably only be qualitative due to the uncertainty of the operator generating (p, t) and (t, p) reactions.

I.N. MIKHAILOV: Is the use of operators of the interaction with the scattering amplitude dependent on density in the Migdal theory consistent with your principle?

S.T. BELYAEV: If the effective interaction depends only on space variables there are no restrictions.

A.S. DAVYDOV: The rotation considered in the Elliott model does not correspond to the nucleus rotation as we usually understand it - the rotation of the coordinate system associated with the directions of the main inertial moments. This is probably the quasiparticle rotation in relation to the coordinate system connected with a self-consistent field, i.e. internal rotation. I shall clarify my remark by an example from molecular theory. The motion of electrons in the field of nuclei of a molecule with a certain total momentum corresponds to their rotation around the molecule core. On the other hand, we can speak of the rotation of the molecule as a whole, i.e. the rotation of the nuclei in the molecule (of the field, in which electrons move).

S.T. BELYAEV: In the Elliott model internal motion and rotation as a whole are not separated. The problem is solved precisely and

self-consistently because both "deformation" (the average value of the total quadrupole moment) and the probabilities of E2-transitions and the energetic spectrum appear simultaneously.

N.I. PYATOV: In your classification of effective interactions in the particle-hole channel there is no interaction with $\lambda = 1$, say $(\vec{\sigma}_1 \cdot \vec{\sigma}_2)$-interactions which may lead to the core spin polarization and generate collective 1^+ states. Have you any particular arguments against the consideration of such effective forces?

S.T. BELYAEV: I have presented only the scheme of the classification, but have not, naturally, pointed out all the possibilities. The terms with $\lambda = 1$ also exist, in principle.

A. BOHR: Would not the gauge invariance put restrictions on effective two-particle forces that could be tested for configurations with two particles or holes outside closed shells?

S.T. BELYAEV: This is probably difficult because the gauge invariance gives rather weak restrictions. Thus arbitrary potentials $V(\vec{r})$ may be used.

A.S. DAVYDOV: Quasiparticles are determined by a self-consistent field. Vibrational modes are connected with a change of the self-consistent field. The consideration of the interaction of quasiparticles with the phonons of surface oscillations should reflect the effect of the change of the self-consistent field.

PROPERTIES OF SOME EXACT SOLUTIONS OF THE PAIRING FORCE PROBLEM*

J.O. RASMUSSEN†
UNIVERSITY OF CALIFORNIA, BERKELEY, CALIF.,
UNITED STATES OF AMERICA

Abstract — Аннотация

PROPERTIES OF SOME EXACT SOLUTIONS OF THE PAIRING FORCE PROBLEM. In this paper are considered the 0^+ ground and excited states of even systems of nucleons interacting by a pure pairing force. The lowest four roots of exact matrix diagonalization are calculated for the even tin nuclei. Among other things a remarkable behaviour of two-nucleon transfer probabilities near subshells, such as 64 neutrons, is found. Namely, only near subshells does collective enhancement of pair transfer occur to excited as well as ground states. For ^{114}Sn at the closed subshell this enhancement occurs for the first excited 0^+ state and this behaviour is the measure of the "pairing vibrational character". The enhancement moves unsymmetrically to higher roots for neighbouring nuclei on either side of the subshell.

Noting the strong dependence of nuclear properties on particle number near subshells, it is suggested that quasiparticle methods not conserving particle number may be unreliable when the Fermi energy is near irregularities in nucleon orbital spacing. Further theoretical studies using particle-number-conservation and realistic reaction-matrix interactions are much needed as well as further experimental information on excited 0^+ states and pair-transfer reactions.

СВОЙСТВА НЕКОТОРЫХ ТОЧНЫХ РЕШЕНИЙ ЗАДАЧИ О СИЛАХ СПАРИВАНИЯ. Рассматриваются основные и возбужденные 0^+ состояния четных систем нуклонов, взаимодействующих лишь силами спаривания. После точной диагонализации матрицы рассчитываются четыре нижайших корня в четных изотопах олова. Наряду с другими фактами, найдено интересное поведение вероятностей двухнуклонной передачи вблизи таких подоболочек, как, например, 64 нейтрона. Именно, только вблизи подоболочек происходит коллективное увеличение передачи пары на возбужденные состояния так же, как и на основные состояния. Для ^{114}Sn с заполненной подоболочкой это увеличение происходит для первого возбужденного 0^+ состояния, и такое поведение является мерой "парно-вибрационного характера" этих состояний. Увеличение смещается несимметрично к высшим корням для соседних ядер по обе стороны от подоболочки. Отмечая сильную зависимость ядерных свойств от числа частиц вблизи подоболочек, предполагаем, что квазичастичные методы, не сохраняющие число частиц, могут оказаться ненадежными, если энергия Ферми находится вблизи нерегулярностей в пространстве нуклонных уровней. Необходимы дальнейшие теоретические исследования с использованием методов, сохраняющих число частиц и матрицу реакции реалистического взаимодействия, наряду с дополнительной экспериментальной информацией о возбужденных 0^+ состояниях и реакциях двойной передачи.

The superfluid nuclear model has rapidly advanced our understanding of the important correlations in nuclear states. We owe this great progress in large measure to the pioneering work of Bogolyubov [1], of Bardeen, Cooper and Schrieffer [2], of Bohr, Mottelson and Pines [3], of Belyaev [4], and of many others.

I shall mostly limit myself here to discussing a very restricted class of states, namely, 0^+ states of even single-closed-shell nuclei. This limitation of states means that the only transitions we can treat are pair transfer between neighbouring nuclei and E0 transitions and monopole inelastic

* Research supported by U.S. Atomic Energy Commission, Contract AT(11-1)34.

† On leave at Yale University, New Haven, Connecticut.

scattering between states of a single nucleus. Even with this drastic truncation of subject matter, there is a bewildering array of alternative methods to survey.

Why not simply use large computers and make shell-model calculations? Such studies have indeed been made, but the number of configurations gets astronomically large for larger systems. Table I lists the shell-model configurations for 0^+ states with four identical nucleons in three active orbitals with j values of 5/2, 3/2, and 1/2. Calculations [5] on ^{60}Ni are such an example. There are five configurations with no unpaired nucleons (s = 0), the five different ways that two indistinguishable objects can be arranged in the three boxes of different sizes. There are five additional seniority-four configurations with nucleons pairwise coupled to 2 and the resultant vectors of J = 2 coupled to zero. A shell-model calculation with realistic reaction matrix elements here must diagonalize a 10×10 matrix, yielding 10 roots corresponding to 0^+ states. The matrix elements for this simple problem fall into two classes, (a) the pairing type, which conserves seniority, and (b) the quadrupole-quadrupole type, among which are matrix elements mixing the seniority-zero and -four configurations. If we are interested only in the lowest-lying states, we may truncate the shell-model space to take only seniority 0 [6]. This approximation is aided by the fact that the seniority-breaking matrix elements are generally smaller than the seniority-conserving and by the fact that the diagonal energies of the zero seniority configurations lie generally lower than the seniority four. The validity of lowest seniority truncation schemes is probably better for 0^+ states than for others, but needs further study. At any rate, we shall

TABLE I. LIST OF SHELL-MODEL CONFIGURATIONS FOR 0^+ STATES

Number of nucleons in orbitals			
of j = 5/2	3/2	1/2	
4	0	0	
2	2	0	
0	4	0	5 configurations of seniority zero
2	0	2	
0	2	2	
2'	2'	0	
2'	1	1	
3	1	0	5 configurations of seniority 4
1	2'	1	
2'	1	1	

Note: The prime (') denotes coupling to angular momentum of 2.

henceforth concern ourselves with only the seniority-zero subspace. I wish next to present results based on exact matrix diagonalizations within this subspace. Finally, we shall take these results as yardsticks for evaluation of various approximate methods based on the superfluid model. Results often depend crucially on the dimensionless ratio between the matrix element for promoting a pair across the Fermi surface and the shell-model energy for such promotion. Thus, the 0^+ spectra and wavefunctions of nuclei at closed subshells may be essentially different from neighbouring nuclei which develop stronger pairing correlation in ground. We thus frequently carry out calculations for a range of pairing force strengths, not just the one value that fits the odd-even mass difference.

Consider now the 64 neutron system of ^{114}Sn and the five orbitals between 50 and 82. The seniority-zero space now has 105 configurations. Fig. 1 shows the energy of the lowest four roots as a function of the pairing force matrix elements, here taken as constant. Note the minimum in first excited 0^+ energy at a certain value of the force strength. This critical value of minimum separation of the lowest two roots is about the critical value below which the superfluid BCS solution is lost. The ground-state and first-excited-state wave functions also exchange character near this closest approach of roots, as one can see in Fig. 2. Here are plotted as a function of pairing force strength the amplitudes for the lowest configuration in the ground and first excited 0^+ roots. For the calculations of Figs 1 and 2 we have used the single particle orbital energies deduced from experimental stripping cross-sections [7].

The next examples we consider are the other even tin nuclei, where again we calculate exact solutions in the seniority-zero subspace, now with one value of pairing force strength, G = 0.18 MeV. We adjusted the orbital energies and pairing force strength to nearly match the ^{117}Sn spectrum and odd-even mass difference.

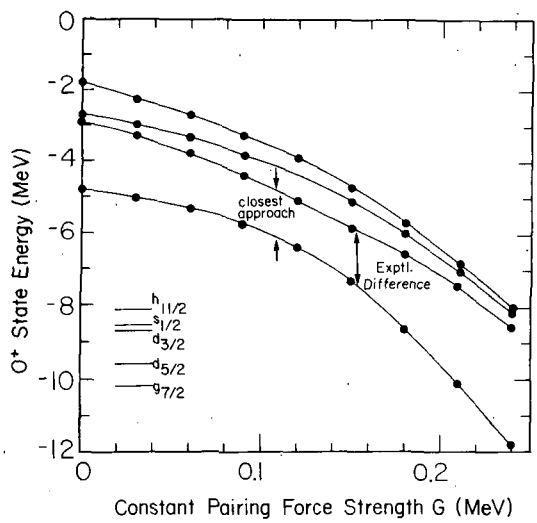

FIG. 1. Energies of ground and three lowest excited 0^+ roots for ^{114}Sn as a function of pairing force strength. The calculation considers neutron excitations in the space of seniority-zero. The inset on the lower left shows the assumed orbital energies from Ref. [7].

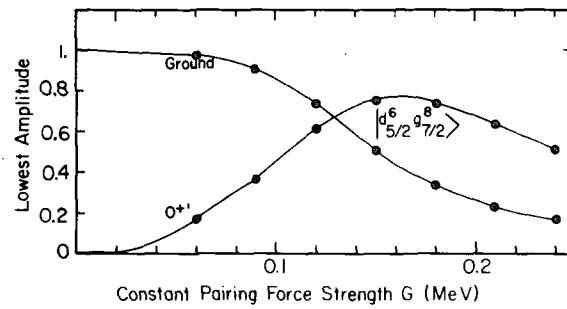

FIG.2. Amplitudes of the dominant shell-model configuration ($d^6_{5/2}$, $g^8_{7/2}$) in ground and first excited 0^+ roots as a function of pairing force strength.

It would be of the greatest value to have more experimental measurements of E0 transition rates among 0^+ states of single closed shell nuclei. The only reported value in the tin nuclei occurs from the lowest excited 0^+ state in ^{116}Sn to ground. The absolute rate is not known, and only a branching ratio between E0 and the E2 to the 2^+ state is reported. Thus we cannot directly confront theory; if we assume some effective charge for neutrons in monopole transitions, it is easy to use our exact wave-functions to calculate E0 rates. The largest rates for $0^{+\prime} \rightarrow 0^+$ should occur when the Fermi energy lies between orbitals of different parity, as is the case in ^{116}Sn, where the $4S_{1/2}$ orbital is just below and the $5h_{11/2}$ orbital is just above. We have good reason to believe that monopole effective charge renormalizations are large, mainly because E0 rate calculations by Oliver Johns and the author for ^{90}Zr show the need for a proton effective charge much reduced from unity ($e_{eff}^{mono} \cong 0.4e$). That is, the 28 closed core protons evidently are induced into radial density oscillations nearly cancelling the E0 contribution due to the 12 explicitly-treated open-shell protons. We must have more data to understand the E0 rate problem. Possibly inelastic electron or muon scattering can extract this information where states are not populated by radioactivity. As a general rule the 0^+ excited states do not seem to be very strongly excited by alpha and proton inelastic scattering. The microscopic theoretical calculations with our exact wave-functions will not be difficult given reliable form factors for scattering from nucleons in various shell model orbitals. Only to the extent that nucleons in orbitals just above and below the Fermi energy exhibit significant differences in scattering will there arise any monopole inelastic scattering. These differences are more likely to arise in proton or neutron scattering than in alpha or other complex particle scattering, since the latter, being strongly absorbed, only sample the tails of nucleon wave-functions where all orbitals look much the same.

One is familiar with the enhancement by the pairing force of processes transferring a pair of nucleons in a $J = 0$ state – processes such as alpha decay or (t, p), (p, t), (^{3}He, n) reactions. With BCS wave functions one gets a pairing enhancement (where finite size effects are neglected) of approximately $(\Delta/G)^2$, where Δ is the odd-even mass difference and G the pairing force strength.

Fig. 3 shows the ground-to-ground enhancement factors for 2-nucleon transfer among even ten nuclei with our model wave-functions. The results are very little different from what BCS would give, the dashed curve taking

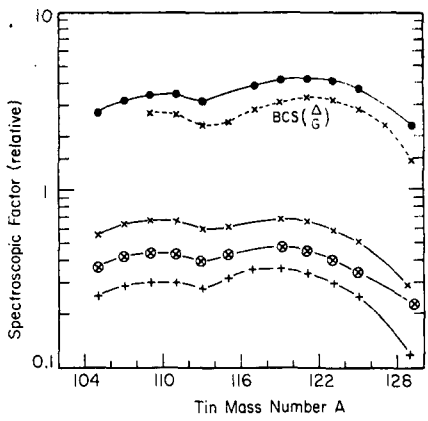

FIG. 3. Ground-to-ground enhancement factors for neutron-pair transfer between adjacent even tin nuclei. The uppermost curve used our exact wave functions, based on the simplest assumption that all orbitals have intrinsic spectroscopic factors that are equal. The dashed curve just below the top is the simplest BCS approximation based on calculations of Ref. [8]. The lowest three curves are based on our exact wave functions but with a Gaussian factor exp[$-C\ell(\ell+1)$] suppressing contributions of higher-ℓ orbitals analogous to finite-size corrections (C values were 0.06, 0.08, and 0.10, respectively).

values from Kisslinger and Sorensen [8]. The solid curves are based on our exact wave-functions. The top curve is the point nucleus approximation, and lower curves represent rough correction for increasing finite size by a Gaussian factor in angular momentum suppressing contributions of transfer from higher angular momentum orbitals.

There is a slight dip at 7 pairs, the sub-shell where pairing correlation is weaker than in adjacent nuclei.

The matrix diagonalization shows to best advantage for the calculation of properties of excited 0^+ states. Next, in Fig. 4, are shown the energies of the first three excited 0^+ states in our model. The arrows indicate the only excited states receiving any collective enhancement for pair transfer.

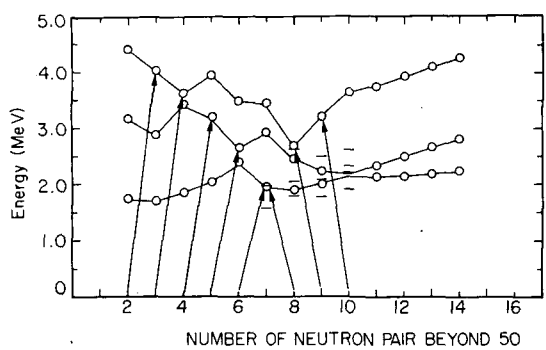

FIG. 4. Energies of excited 0^+ states in even tin nuclei. The solid bars are experimental values from Ref. [7]. The open circles are theoretical values in our exact seniority-zero scheme with constant pairing force ($G \approx 0.18$ MeV) and constant orbital spacing. The upward slanting arrows indicate the only excited states receiving pair-transfer enhancement.

Note that for ^{114}Sn at the subshell between the $g_{7/2}$ and the $s_{1/2}$ orbital the lowest excited 0^+ state receives pair transfer strength from either side; quantitatively we calculate the cross-sections to be about 20% of ground. We may thus say this state in ^{114}Sn has a pairing vibration character. This behaviour was not surprising but the pattern of collective enhancement for nuclei away from the subshell was an interesting surprise.

As we go away from the subshell, the collective enhancement moves to successively higher roots. Furthermore, the enhancement is unsymmetrical, showing itself only for pair transfer going toward the subshell. Perhaps Professor Bohr in the following paper will have something further to say on this matter. It seems likely that this behaviour is general for subshells with many levels either side of the shell gap.

The solid bars in Fig. 4 are experimental 0^+ energies, mostly from the stripping studies. While our model yields roots in the correct region of energy, a detailed correspondence is absent, and there seem to be too many experimental 0^+ states in ^{118}Sn for the model to explain.

It may be that the truncation to seniority-zero is too severe, and that the neglected seniority-four space gives rise to additional states and more complicated wave-functions. For example, we might surmise the possible importance of the seniority-four component arising from the 0^+ coupling of the lowest 2^+ excitation of the proton structure and the lowest 2^+ excitation of the neutron structure. A quadrupole-quadrupole neutron-proton force might greatly lower the diagonal energy of this configuration, such that it becomes an intruder state or mixes with the seniority-zero excited states we calculate. A state with this collective seniority-four character should exhibit a large E2 transition probability to the 2^+ first excited state, so perhaps double-coulomb excitation studies to 0^+ states could help answer these questions.

Another question about our calculations of the 0^+ states arises from our use of the constant-G pairing matrix elements. Either delta forces or finite range forces systematically give diagonal matrix elements larger than off-diagonal, except for large matrix elements between spin-orbit partners. We have made a few exploratory calculations with our seniority-zero model, using the matrix elements of a finite Gaussian force. Fig. 5 shows a comparison of excited 0^+ states for ^{116}Sn calculated by various approaches. The Gaussian force calculation is seen to bring down a higher density of excited states than the constant-G calculation. For the constant-G calculation a 17% lowering of pairing force causes the first two excited 0^+ states to drop sharply. The excited 0^+ state energies are sensitive to the form and strength of the residual force. Fig. 5 also shows Gmitro and Sawicki's [9] recent calculated values, using the Tabakin potential with core polarization corrections included; they used a quasiparticle Tamm-Dancoff calculation with no more than two quasiparticles in the basis (QTD2). We show also the Plastino, Arvieu, and Moszkowski calculations by QTD2 with their surface delta interaction [10].

It is not easy to isolate the reasons for the differences of one theoretical calculation from another. The unprojected quasiparticle theories have the particle number fluctuation problem such that there is a certain averaging over states of adjacent nuclei. Next to the subshell at 64 neutrons our exact seniority-zero calculations of Fig. 4 show a rapid shifting of excited state energy patterns with neutron number. We believe the quasiparticle methods must be regarded quite sceptically here where the Fermi energy

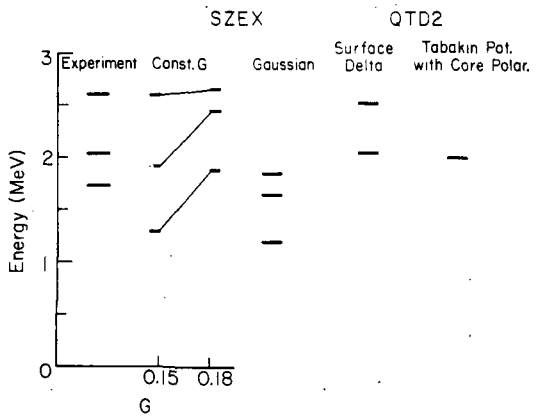

FIG.5. Experimental and theoretical excited 0^+ energies in ^{116}Sn. Experimental values are at the far left. Next are our exact calculations in the seniority-zero space (abbreviated SZEX) for two different strengths of pairing force (G = 0.15 and G = 0.18 MeV). Next are our exact seniority-zero calculations with non-constant matrix elements of a Gaussian force. The final calculations are from Refs [9] and [10] and are made by the quasiparticle Tamm-Dancoff method with two different sets of matrix elements.

is close to irregularities in orbital spacing. On the other hand, for the heavier tin nuclei, sufficiently removed from the 64 subshell, the excited state energy pattern and the wave functions vary only slowly with neutron number. This smooth variation should also hold in deformed nuclei, so that the QRP2 calculations of Soloviev and others [11] should be free of serious difficulties from number fluctuation except near subshells like 90, 142, or 152 neutrons. We underscore this remark by showing calculations on the 142 and 144 neutron systems. Fig. 6 shows the orbital spacings used in the tin calculations of Figs 3 and 4, and it also shows the actinide neutron orbital energies taken from Chasman's pairing force calculations [12] to fit experimental band-head energies in ^{235}U. Our calculations have used four and five pairs in the nine orbitals shown as solid lines, the matrix size being 126×126 (i.e. the order is a binomial coefficient $9!/(4!5!)$).

Fig. 7 shows the behaviour of excited 0^+ states as a function of energy for N = 142 at the subshell. The excited state energies are fairly flat functions of pairing force strength. The experimental 0^+ energies lie lower, probably a consequence of our neglecting quadrupole-quadrupole forces, which couple proton and neutron modes and depress a beta-vibrational collective root. Fig. 8 shows the drastically different behaviour of 0^+ roots for N = 144, one pair beyond the subshell. Obviously, particle number fluctuation in a quasiparticle method could introduce serious uncertainties near this subshell.

Chasman has also calculated [13] 0^+ excitation of neutrons in these deformed actinides using his special variational method and taking more orbitals. Neither he nor I take seriously these pure pairing force calculations of excited 0^+ states of deformed nuclei. We know that other force components play important roles in bringing down collective quadrupole vibrational character and thus coupling neutron and proton modes.

The past decade has seen a remarkable growth in our understanding of pairing correlation phenomena in nuclei. Much of this progress has

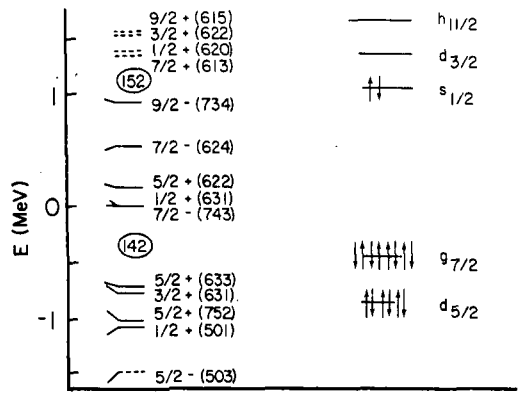

FIG.6. Single particle orbital spacing used in the calculations of 0^+ states presented in Fig.4 (spherical nuclei) and in Figs 7 and 8 (deformed nuclei). The solid lines on the left indicate the nine Nilsson orbitals used in the calculation. The dashed levels were not used. The slanting lines attached to the levels indicate the slope of the level on a Nilsson diagram, i.e. dependence of the energy on quadrupole deformation.

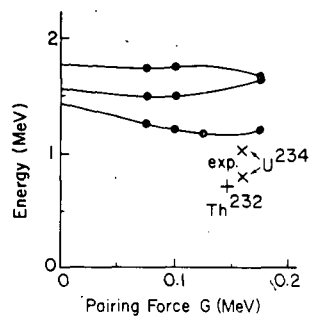

FIG.7. Theoretical 0^+ neutron-excitation states for the 142-neutron system as a function of pairing force strength. Experimental 0^+ energies in ^{232}Th and ^{234}U are shown.

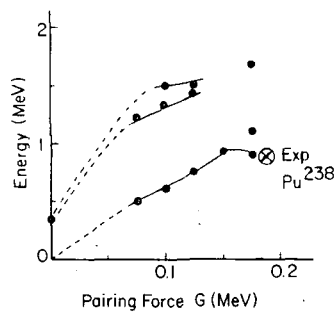

FIG.8. Theoretical 0^+ neutron-excitation states for the 144-neutron system as a function of pairing force strength. The experimentally known 0^+ energy in ^{238}Pu is indicated.

come with simple constant-G matrix element assumption and the Bogolyubov-Valatin transformation. Our knowledge of the structure of the lowest nuclear state of a given spin is now rather good, but the knowledge of states higher than these leaves much to be desired. Kuo and Brown especially have pointed the way to applying realistic reaction matrix elements [14], and we should use the methods to replace the simpler phenomenological forces. Theorists, furthermore, must devise and explore particle-number-conserving methods for excited states of practical nuclear systems. Finally, since nature has presented to us such complex situations in nuclei, it will be the new and better data on nuclear spectra that play a decisive role in further progress.

REFERENCES

[1] BOGOLYUBOV, N.N., Zh. eksp. teor. Fiz. (SSSR) 34 (1958) 58 and 73.
[2] BARDEEN, J., COOPER, L.N., SCHRIEFFER, J.R., Phys. Rev. 108 (1957) 1175.
[3] BOHR, A., MOTTELSON, B.R., PINES, D., Phys. Rev. 110 (1958) 936.
[4] BELYAEV, S.T., Mat. Fys. Medd. Dan. Vid. Selsk. 31 11 (1959).
[5] HSU, L.S., FRENCH, J.B., Phys. Lett. 19 (1965) 135.
HSU, L.S., Nucl. Phys. A96 (1967) 624.
AUERBACH, N., Phys. Lett. 21 (1966) 57.
LAWSON, R.D., MACFARLANE, M.H., KUO, T.T.S., Phys. Lett. 22 (1966) 168.
KERMAN, A.K., LAWSON, R.D., MACFARLANE, M.H., Phys. Rev. 124 (1961) 162.
[6] RHO, M., RASMUSSEN, J.O., Phys. Rev. 135B (1964) 1295.
[7] SCHNEID, E.J., PRAKASH, A., COHEN, B.L., Phys. Rev. 156 (1967) 1316.
[8] KISSLINGER, L.S., SORENSEN, R.A., Mat. Fys. Medd. Dan. Vid. Selsk. 32 9 (1960).
[9] GMITRO, M., SAWICKI, J., Preprint IC/68/4, Trieste (1968).
[10] PLASTINO, A., ARVIEU, R., MOSZKOWSKI, S., Phys. Rev. 145 (1966) 837.
[11] cf. SOLOVIEV, V.G., Atom. Energy Rev. 3 (1965) 117 (English translation of Dubna preprint P-1973 (Jan. 1965)).
[12] CHASMAN, R.R., (1967) private communication; see also BRAID, T.H. et al., Phys. Lett. 18 (1965) 149.
[13] CHASMAN, R.R., Phys. Rev. 138B (1965) 326.
[14] KUO, T.T.S., BROWN, G.E., Nucl. Phys. 85 (1966) 40 and A92 (1967) 481.

DISCUSSION

O. NATHAN: I would like to comment upon the experimental situation for 0^+ states in ^{114}Sn. We have preliminary data from the ^{112}Sn(t, p)^{114}Sn reaction which indicate the presence of two strong 0^+ states in ^{114}Sn near 2 MeV, separated by about 200 keV. Now, one of these may be identified with one of Professor Cohen's 0^+ states of ^{114}Sn. However, he has another 0^+ state at lower excitation energy which has a negligible cross-section in the (t, p) reaction. In fact, we do not see it at all. Would this state possibly be the neutron-proton, quadrupole-quadrupole state suggested in your talk? And if it is, is it reasonable that it appears so low in the excitation spectrum?

J.O. RASMUSSEN: Your results are most interesting. The lower-lying 0^+ state which is not populated by the (t, p) reaction could be a good candidate for the n-p quadrupole-quadrupole state. I have no idea how low it could come, but there will be quadrupole collective features that favour

considerable lowering below the region of four quasiparticles. The question of identifying the n-p quadrupole-quadrupole state calls for double Coulomb excitation or other experiments establishing the B(E2) value to the 2^+ first excited state.

R. A. SORENSEN: The monopole polarization effect or charge renormalization will probably be quite different from one j-level to another, so that in the absence of a real theory of this renormalization, the effective monopole charge is really unknown. Thus for wave-functions involving several j-values, the B(E0) simply cannot be calculated.

J. O. RASMUSSEN: I would be interested in learning more about your ideas on the charge renormalization. Certainly our ^{90}Zr calculations of the E0 rate, assuming unit charge for protons, considerably overestimate the rate, suggesting important renormalization effects of some kind.

S. SZPIKOWSKI: I have two questions. The first is a trivial one, but I would like to be sure whether I quite understand your lecture. Can your diagonalization be applied to the two kinds of particles? I mean to protons and neutrons together. Secondly, the seniority-four states lie so high compared to the seniority-zero states that their contribution to the low-lying 0^+ states is negligible. But in your table they were taken into account. Are they present in the calculation too?

J. O. RASMUSSEN: First, I agree that use of the matrix diagonalization approach away from single-closed-shell nuclei will not be simple. It should be possible soon to apply it to deformed nuclei, using the diagonalizations of neutron and proton systems separately to form a basic set for diagonalizing the quadrupole-quadrupole part of the neutron-proton force.

In answer to your second question, let me clarify. The table listed seniority-four configurations only to illustrate what we are neglecting by truncating to a seniority-zero space only. We have indeed never tried to include seniority-four, hoping that such configurations will not mix very much into the low-lying 0^+ states we are calculating.

S. SZPIKOWSKI: If you generalize your diagonalization to both protons and neutrons, a rather difficult problem arises. For the one kind of particle the two-particle isospin is necessarily one and this assures the proper symmetry of the wave-function. Both for two kinds of particles the contribution of the $T = 0$ state can be compared to the contribution of the $T = 1$ state, but they cannot be taken into account because of the limitation of the pairing forces to only $T = 1$ states.

BOHR: The effective nucleonic force in the $T = 1$ channel gives an especially strong binding in the $J = 0$ state, which leads to the pair correlations. In the $T = 0$ channel there is an attraction of a similar magnitude, but in (jj)-coupling it appears to act with similar strength in several J-states and therefore may not give rise to a pairing in $J = 1$ states.

S. SZPIKOWSKI: There is, however, the possibility of including the states of $T = 0$ within the pairing. If you take L-S coupling you have either $T = 1$, $S = 0$ for two-particle states or $T = 0$, $S = 1$. Both of them can be theoretically treated.

PAIR CORRELATIONS AND DOUBLE TRANSFER REACTIONS

A. BOHR
THE NIELS BOHR INSTITUTE,
UNIVERSITY OF COPENHAGEN,
COPENHAGEN, DENMARK

Abstract — Аннотация

PAIR CORRELATIONS AND DOUBLE TRANSFER REACTIONS. A discussion is given of the collective modes of excitation of the nuclear pairing field, on which experimental evidence from the two-nucleon transfer reactions is accumulating. In regions of closed shells, the excitations have a vibrational character. The neutron 0^+ pair vibrations around ^{208}Pb are considered in the harmonic approximation and with the inclusion of interaction effects between the quanta of excitation. The relation between the vibrational treatment of pair correlations and the treatment in terms of superfluidity (dynamic and static pairing) is compared with the relation between vibrational and rotational descriptions of shape oscillations. The role of the isospin of the pairs is discussed with special attention to the spectrum of 0^+ pairing modes based on ^{56}Ni. When the isospin degree of freedom is included, a static pairing (superfluidity) produces a deformation in isospace, with a resulting rotational spectrum in isospace. Finally, the coupling between particles and pair vibrational quanta is briefly discussed.

ПАРНЫЕ КОРРЕЛЯЦИИ И РЕАКЦИИ ПЕРЕДАЧИ ДВУХ ЧАСТИЦ. Обсуждаются коллективные возбуждения ядерного поля спаривания, экспериментальные данные о которых собраны на основе реакций передачи двух нуклонов. Для ядер в областях замкнутых оболочек возбуждения носят колебательный характер. Рассматриваются вибрации пары нейтронов 0^+ около ^{208}Pb в гармоническом приближении и с учетом эффектов взаимодействия между квантами возбуждения. Соотношение между рассмотрением парных корреляций с точки зрения вибрации и рассмотрением с точки зрения сверхтекучести (динамическое и статическое спаривание) сравнивается с соотношением между вибрационным и вращательным описаниями колебаний формы. Обсуждается роль изоспина пар, причем особое внимание уделяется спектру 0^+ с уровнями парной природы, основанными на ^{56}Ni. Когда учитывается изоспиновая степень свободы, статическое спаривание (сверхтекучесть) дает деформацию в изопространстве, в котором появляется вращательный спектр. Наконец, обсуждается взаимодействие частиц, а также парные вибрационные кванты.

In recent years, the study of double transfer reactions has developed into an important tool for nuclear spectroscopy. It enables us to explore new aspects of nuclear structure and in particular to study the collective modes associated with nuclear pair correlations. The following paper by Nathan [1] will give a survey of the experimental findings in this new field; the present report deals with some general features of the collective pairing modes. (Many of the basic properties of pair vibrations were considered by Bès and Broglia [2]).[1]

NEUTRON PAIRING VIBRATIONS IN THE REGION OF ^{208}Pb

We first consider the neutron pairing modes based upon the closed-shell configuration of ^{208}Pb. A two-neutron transfer reaction, by which

[1] The subjects considered in the present report will be discussed in more detail in a forthcoming treatise on nuclear structure by Ben R. Mottelson and the author.

two neutrons are added to ^{208}Pb in a $J^{\pi} = 0^{+}$ state, produces the ground state of ^{210}Pb with a cross-section which is strongly enhanced as a consequence of the strong spatial correlation of the two neutrons in the ground state of ^{210}Pb. A similar enhancement characterizes the (p, t) reaction leading to the ground state of ^{206}Pb.

We may therefore view the ground states of ^{210}Pb and ^{206}Pb as collective excitations of ^{208}Pb. The quanta of excitation of these "pair vibration" modes will be labelled by the quantum number, α, the nucleon transfer number. Thus, $\alpha = +2$ for the pair addition mode and $\alpha = -2$ for the pair removal mode. In first approximation, the pair vibrations create two particles in the major shell above $N = 126$ or remove two particles from the shell below, but the properties of the quanta are significantly affected by the ground-state correlations in ^{208}Pb, representing the virtual excitation of pairs of particles across the gap between the shells. In particular, this zero-point vibrational motion implies an enhancement of the two-particle transfer matrix elements. The effect is of a similar nature to the enhancement of the E2 matrix elements for the low-energy quadrupole mode with $\alpha = 0$, resulting from the virtual excitation of quasiparticle pairs in the nuclear ground state.

With the $\alpha = +2$ and $\alpha = -2$ quanta as building blocks, we can construct the pair vibrational spectrum. In Fig.1, the binding energies of the states are plotted relative to that of ^{208}Pb; for convenience, a linear term in N has been added, so as to give equal energies, $\hbar\omega_2 = \hbar\omega_{-2}$, for the $\alpha = +2$ and $\alpha = -2$ quanta. Adding two or more quanta of the same kind, we obtain states denoted by $(n_1, 0)$ and $(0, n_2)$. These states correspond to the ground states of the more distant Pb isotopes. The members of the vibrational spectrum with quantum numbers $(n_1, 1)$ and $(1, n_2)$ are expected to occur at excitations of the order of 5 MeV. So far, only a single member of this type, the (1, 1) level in ^{208}Pb, has been established [1, 3].

In the harmonic approximation, the energies of the vibrational excitations would equal $(n_1 + n_2)\hbar\omega$, as represented by the dotted lines in Fig.1. The observed deviations represent anharmonicity effects, which one may attempt to describe in terms of interactions between pairs of quanta. It is seen that two like quanta repel each other, while two unlike quanta exhibit a weak attraction. By determining the interaction from the states with

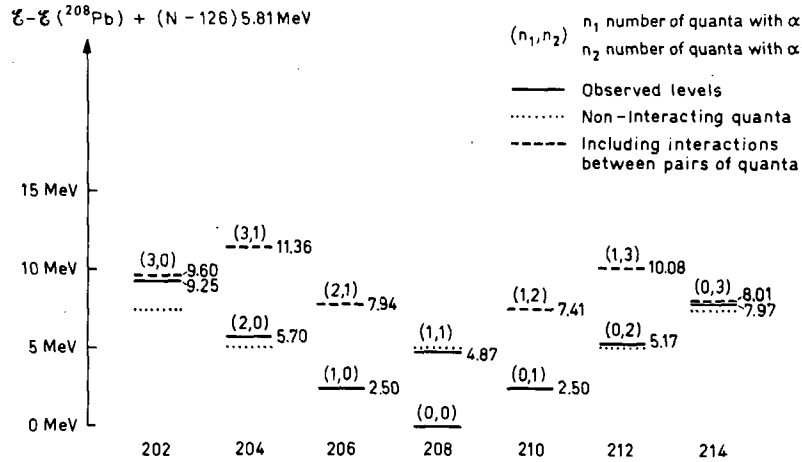

FIG. 1. Neutron pairing vibrations based on ^{208}Pb.

two quanta, one can estimate the energies of the states with more quanta (dashed lines in Fig.1), and for the observed levels, the agreement is fairly good.

The interactions between the quanta receive contributions from several components of the nuclear forces. Thus, a pairing force acting among the neutrons implies a repulsion of about 400 keV between like quanta and of about 200 keV between unlike quanta [4]. The nuclear symmetry potential, which is known to contribute to the N^2 dependence of the binding energy, gives a repulsion between like quanta of about 300 keV, and a similar attraction between unlike quanta. The observed energies show that additional interactions are present; in particular, the observed small interaction between $\alpha = +2$ quanta indicates that the above-mentioned repulsive effects are partially compensated by an attractive interaction. Such an attraction may arise from the quadrupole interactions, by which the quanta can make transitions from the 0^+ state to the 2^+ state, represented by the first excited state in ^{210}Pb, or ^{206}Pb. In Fig.2, the quanta are labelled by the J-value, and one sees that an additional 0^+ level in ^{208}Pb can be formed by coupling two quanta with $J = 2$ to a resultant angular momentum, $I = 0$. The two 0^+ states repel each other through the familiar quadrupole interaction in the $\alpha = 0$ channel. The matrix element is estimated to be about 0.5 MeV, which would give a repulsion of the order of 100 keV, but the estimate is somewhat uncertain owing to lack of information on the quadrupole transition probability for the $\alpha = 2$ quantum, and of the renormalized coupling constant for the quadrupole interaction. A similar effect occurs for the states (0, 2) and (2, 0) with two identical quanta, and the rather large attractive component in the interaction of two $\alpha = +2$ quanta might indicate that the quadrupole matrix element for these quanta is especially large; information on the B(E2) value for the excitation of ^{210}Pb and on the polarization charge for a neutron in ^{209}Pb would be of significance for

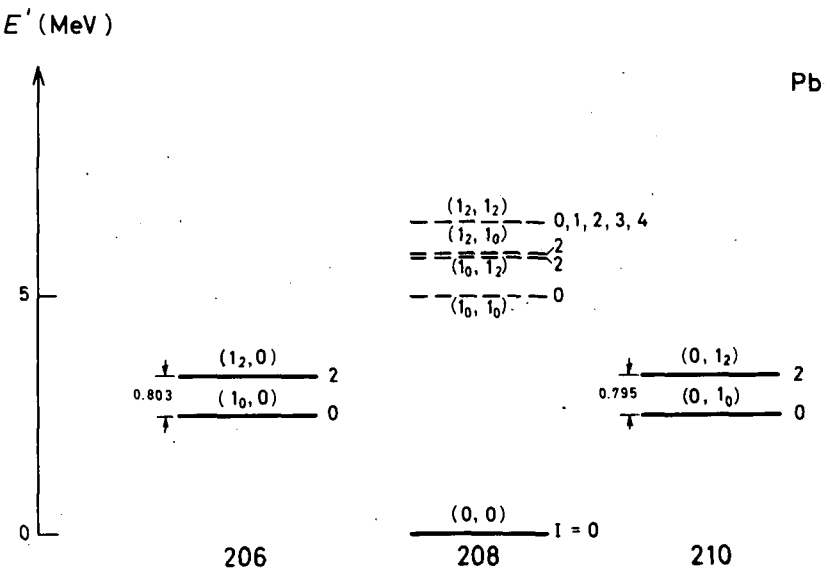

FIG.2. States in ^{208}Pb obtained by superposing quanta with $J = 0\,(1_0)$ and $J = 2\,(1_2)$.

testing this point. [There is a further structure in the 0^+ spectrum of the $\alpha = +2$ mode which may be of relevance in the present context. The calculations of the (t, p) transfer by Glendenning [5] and by Broglia and Riedel [6] predict the occurrence of a 0^+ state at about 3 MeV of excitation in ^{210}Pb with a cross-section even larger than for the ground state, and the experimental data do seem to show a very large transfer strength in this region of excitation. The occurrence of such a strong transition is connected with a subshell structure in the single particle spectrum together with the non-locality in the transfer process which gives especially strong weight to the nucleon orbits with small orbital angular momentum].

The admixing of the 0^+ states in Fig.2 also implies that the higher level can be excited by the reactions ^{206}Pb(t, p) and ^{210}Pb(p, t), and the strength of these transitions would give valuable information on the coupling.

Fig.2 also shows the two $I^\pi = 2^+$ states, which can be formed by exciting either of the quanta; the unperturbed positions of these states differ by only 8 keV and the states are therefore expected to be strongly mixed by the quadrupole interaction.

The essential property which joins the states in Fig. 1 into a collective family is the strong matrix element for two-particle transfer. In the harmonic approximation, the transition strength for the reaction $(n_1, n_2) \rightarrow (n_1+1, n_2)$ is proportional to (n_1+1). The interactions between the quanta, associated with the exclusion principle for the particles, are expected to somewhat reduce the transition strength; to first order, the correction factor has the form $(1 - \alpha n_1)$, with α a constant. The interactions also lead to a violation of the selection rule $\Delta n_1 = \pm 1$, $\Delta n_2 = 0$ or $\Delta n_1 = 0$, $\Delta n_2 = \pm 1$, and imply the occurrence of weaker transitions such as $(0, 0) \rightarrow (1, 2)$. Anharmonicity effects in the two-nucleon transfer matrix elements, for neutrons in the region of ^{208}Pb interacting by a pairing force, have been evaluated by Sørensen [4].

STATIC AND DYNAMIC PAIRING

The pair correlations in the Pb isotopes with neutrons outside closed shells can also be treated by considering the systems as superfluid. The relationship between the two approaches is like that of a vibrational and rotational treatment of shape oscillations; time permits me only briefly to indicate some of these general relations.

The key concept in the treatment of pair correlations as a collective mode is the pairing field. The pair correlations produce an average potential, acting on the nucleons, of the form

$$U_{pair} = \Delta \sum_{\nu>0} a^+(\bar{\nu}) a^+(\nu) \qquad (1)$$

which creates two nucleons in orbits conjugate under time reversal. The pairing potential is analogous to the deformed potentials associated with a distortion of the nuclear shape, which are proportional to a^+a. The quantity

Δ is the deformation parameter and represents the average value of the pairing density,

$$\Delta = G\langle \sum_{\nu>0} a(\nu)a(\bar{\nu}) \rangle \qquad (2)$$

which produces the potential (1).

The pairing potential violates particle number conservation just as the deformed potential violates angular momentum conservation, and the collective quantum number for the pairing modes is the particle number.

The pairing field operator is non-hermitian and Δ is therefore a complex quantity. The phase of Δ is the gauge angle, ϕ, which is conjugate to the particle number operator, and which corresponds to the orientation of the deformed nucleus.

In the ground state of ^{208}Pb, Δ oscillates about the value 0, and the excitations have a vibrational character. However, when many quanta are present, $|\Delta|$ has a mean value exceeding the fluctuations about this mean value, just as a two-dimensional oscillator in a state of large angular momentum has an amplitude whose magnitude exceeds the zero-point amplitude.

When the mean value of Δ exceeds the fluctuations, one can treat the system in terms of a static pairing field. The motion now separates into intrinsic motion, described in terms of quasiparticles (which correspond to the Nilsson particles in the deformed field), and collective motion of rotational type, the pair addition mode. The time derivative $\dot{\phi}$, which corresponds to the rotational frequency, is the chemical potential, λ, and the coriolis force is the familiar term $-\lambda N$ in the quasiparticle Hamiltonian. The gap equations for the superfluid system are the cranking formulae for the rotations in gauge space.

In the description based on a static pairing field, one neglects fluctuation effects in Δ; however, the treatment takes into account the anharmonicity in the vibrational motion, which becomes of major significance when the number of quanta is so large that the shift in λ is comparable with Δ. The pairing modes, with their especially simple structure, provide a favourable opportunity for studying the general problems associated with anharmonicity effects and transitions from vibrational to rotational spectra.

PAIRING MODES FOR Sn ISOTOPES

As an example of the structure of pairing modes in regions away from closed shells, Fig.3 illustrates the neutron pairing excitations for the Sn isotopes. The isotope ^{114}Sn marks the filling of the neutron subshell at $N = 64$, but the pairing is able to overcome this minor shell gap and establish a static pairing field. The collective transitions joining the ground states are thus of "rotational" type, and it is seen that the energies approximately follow a parabolic trajectory, rather than a linear variation as in the vibrational region around ^{208}Pb.

The dotted lines in the figure referring to the target nucleus ^{118}Sn indicate 0^+ excitations involving the degrees of freedom of the neutrons in the $50<N<82$ shell. The excitations represent two quasiparticle states

with the spurious degree of freedom removed, and the analysis of the two particle strengths is due to Broglia et al.[7]. These excitations are seen to carry a total (t, p) strength of a few percent and a (p, t) strength of about 20% of the ground-state transition, in accordance with the analysis presented by Rasmussen [8]. Thus the subshell structure gives rise to only rather weak pairing vibrations.

Stronger pairing vibrations are expected to be associated with $\alpha = 2$ transitions into the next higher shell ($N > 82$) and $\alpha = -2$ transitions from the lower shell ($N < 50$), as indicated by the dashed lines in Fig.3. The estimate of the position of these states is rather uncertain, but it is of considerable significance to establish whether major parts of the two-particle transfer strength into the more distant levels are concentrated in well-defined collective modes.

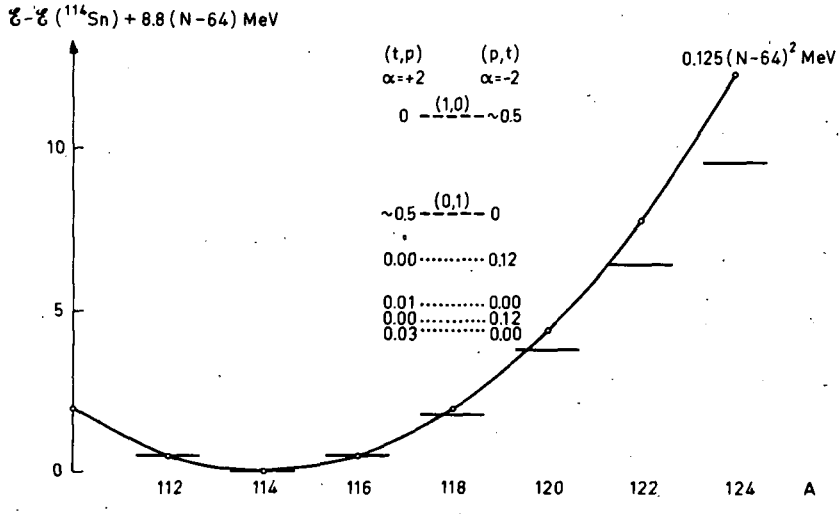

FIG.3. Neutron pair excitations in Sn isotopes. The solid lines represent ground states.

ISOSPIN OF PAIRING MODES: REGION OF A = 56

The correlated J = 0 pairs carry unit isospin and therefore involve three degrees of freedom, which gives a new dimension to the spectrum of pairing modes. We first consider the isospin structure of the pairing modes in the medium heavy nuclei with relatively small neutron excess. Taking ^{56}Ni with the closed neutron and proton shells (N = Z = 28) as a basis, the pair excitations again have vibrational character, and there are now six fundamental modes with $\alpha = \pm 2$, and $\mu_T = -1, 0, +1$. The one-quantum excitations have T = 1, and the $M_T = 1$ components (^{54}Fe and ^{58}Ni) are shown in Fig.4. Adding two quanta of the same type ($\alpha = +2$ or $\alpha = -2$), we obtain states with T = 0 and 2, while two unlike quanta give states of T = 0, 1 and 2. The T = 2, $M_T = 2$ component is the ground state of ^{56}Fe; the T = 0 and 1 levels of the configuration (1, 1) represent excited 0^+ states, which have recently been observed to be strongly populated in two-particle transfer reactions, as is discussed by Nathan [1].

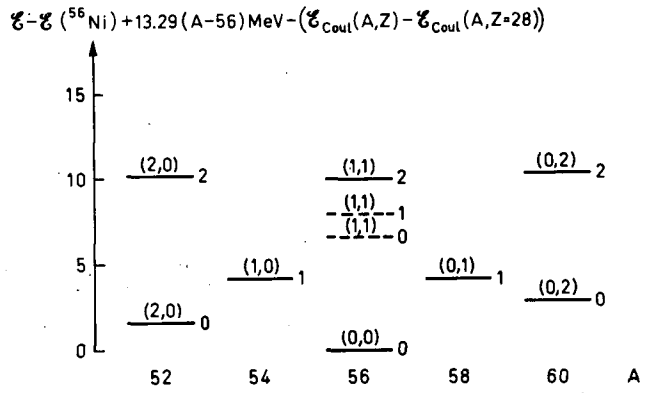

FIG.4. Pair excitations with one or two quanta added to ^{56}Ni. The quantum numbers labelling the levels are (n_1, n_2) and T.

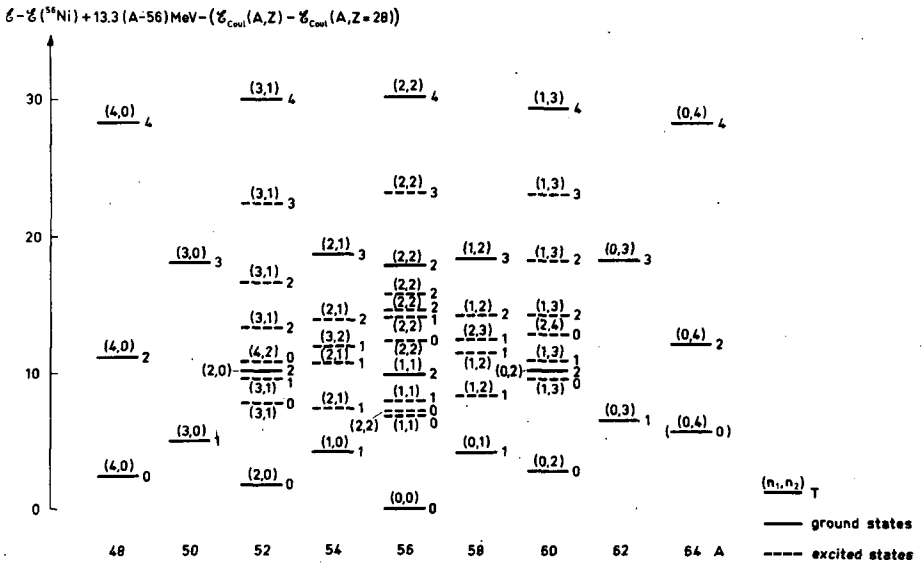

FIG.5. Schematic illustration of many-pair excitations based on ^{56}Ni.

The pattern of states obtained by superposing more quanta is illustrated schematically in Fig.5. Superposing n quanta of one type, we obtain the symmetric states T = n, n-2, ... 0 (or 1). These states have the relations of an SU(3) representation, and the various matrix elements, such as for double transfer reactions, can be expressed in terms of Clebsch-Gordan coefficients in SU(3). The $M_T = T$ components of the configurations $(n_1, 0)$ and $(0, n_2)$ correspond to ground states of even-even nuclei with $N < 28$, $Z < 28$, and $N > 28$, $Z > 28$, respectively.

If we add an $\alpha = 2$ quantum to a state $(n_1, 0)T_1$ with n_1 quanta of the $\alpha = -2$ type coupled to isospin T_1, we obtain states of the configuration $(n_1, 1)$ with $T = T_1 + 1$, T_1, $T_1 - 1$. The states with maximum alignment

of the isospin, i.e. with $T_1 = n_1$, $T = T_1 + 1$ and $M_T = T$ correspond to ground states of even-even nuclei with $N>28$ and $Z<28$. The additional members of the $(n_1, 1)$ configuration represent excited states. In this coupling scheme, the ratio of two-particle transfer matrix elements leading from the target $(n_1,0)T_1$ to the final states $(n_1, 1)T$ is given by the ratio of the vector addition coefficients $\langle T\ (M_T)_1\ \ 1\mu_T | T\ M_T\rangle$, where μ_T is the transferred isospin component [+1 for (t,p), 0 for (^{3}He, p) and -1 for (^{3}He, n)].

The energies of the dashed levels in Fig.5, representing excited states, are only intended for qualitative orientation. They have been estimated by assuming an interaction between unlike quanta consisting of an isoscalar component of 0.7 MeV, as indicated by the observed (1, 1) levels (see Fig.4), and an isovector component so constructed as to give the observed positions of the $(n_1, 1)$ states with $T = n_1 + 1$. The needed strength of this component varies somewhat with n_1, reflecting the presence of higher-order interaction effects. (An analysis of the observed interactions in terms of isoscalar, isovector and isoquadrupole components has been given by Damgård [9].) Similar considerations apply to the states of the configurations $(1, n_2)$. A few of the lowest $(n_1, 2)$ and $(2, n_2)$ states are also included in Fig.5.

The analysis of the family of collective excitations in Fig.5 involves at least three important interaction effects.

First, there is the pairing interaction, which can be treated by an extension of the analysis discussed for the neutron pairing mode. Thus, for few quanta, the anharmonicity effects can be expressed in terms of interactions between pairs of quanta. When many quanta are present, the anharmonicity may become large, but one can then employ a treatment in terms of a static pairing field. The isospin degree of freedom implies that we are dealing with a pairing field possessing a deformation in isospace. We must, therefore, treat the particle motion with respect to an intrinsic frame in isospace and the total system performs rotations in isospace as well as in the gauge space conjugate to the number operator, A. Thus, the $(n_1, 0)$ states [and $(0, n_2)$ states] can be viewed as forming a single rotational band with $K_T = 0$. Such a band comprises a sequence of states with even values of $T - A/2$. Moreover, one can evaluate the various matrix elements with the inclusion of rotational distortion effects in quite a similar manner as for the ordinary rotational spectra in I-space. (A charge-independent treatment of pair correlations, based on pairing in an intrinsic co-ordinate system in isospace, has been considered by Elliott and Lea [10]; the formalism has been further developed by Ginocchio and Weneser [11].)

Second, there is the symmetry potential (the isovector component in the average nuclear potential), which gives an energy proportional to $T(T+1)$, and which is responsible for a large part of the observed splitting of the states with given (n_1, n_2).

Third, there is the quadrupole interaction. Estimates of the quadrupole interaction matrix elements of the type considered for ^{208}Pb indicate that, in the $A=56$ region, these matrix elements are large compared with the energies for exciting the quanta to 2^+ states; therefore, the angular momentum quantum numbers of the individual quanta are not expected to be even approximately conserved. Indeed, it is likely that among the family of excitations in Fig.5, we encounter nuclei with stable shape deformations. Evidence for deformation effects in this region of nuclei have been considered by many authors. Large deformations may especially occur for

states with many quanta and low isospin. For example, it appears possible that the 0^+, 2^+, and 4^+ levels in ^{56}Ni at 4.97 MeV, 5.33 MeV, and 6.39 MeV, recently observed in the (p, t) reaction [12], may constitute a rotational band associated with the (2, 2)T = 0 configuration.

The occurrence of quadrupole interactions leading to instability of the spherical shape may strongly affect the pattern of the pairing modes. Thus, if abrupt changes in the nuclear shape occur with the addition of a pair of particles, the J = 0 double transfer strength may fractionate, as has been observed in the N = 90 region [13]. However, if the nuclear shape varies smoothly with A and T, the states joined together by strong J = 0 double transfer reactions may still form a pattern such as that illustrated in Fig.5.

For the establishment of the appropriate coupling scheme, it is of special significance to test the validity of the quantum numbers n_1 and n_2. If the deformations wash out the large gap in the single-particle spectrum at N = Z = 28, a static pairing field is established across this gap. In such a situation, the number of strong transitions is reduced, i.e. the pair vibrations become weak compared with the pair rotations, as illustrated by the pairing modes in the Sn isotopes (see Fig.3).

Another significant point is the degree of validity of the quantum numbers T_1 and T_2. In general, a configuration (n_1, n_2) may give rise to several states of given T, involving different values of (T_1, T_2). The extent to which these states become mixed by the interactions can be studied by testing the selection rules and intensity relations in double transfer reactions (such as discussed above), which characterize the coupling scheme in which T_1 and T_2 are constants of the motion.

The available evidence on strong J = 0 double transfer reactions in the region considered are reviewed by Nathan [1]. It is still very incomplete and much more data concerning transfer reactions with J = 2 as well as J = 0 will be needed to establish the appropriate coupling scheme. Also the evidence on quadrupole transitions in the $\alpha = 0$ channel (E2 transitions, inelastic scattering) must be brought into the analysis. The problem involves the familiar competition between pairing and quadrupole effects, which takes a new form for these nuclei because of the role of isospin. The development of two-particle transfer studies has given us a new powerful probe and a new way of thinking of these problems.

ISOSPIN OF PAIRING MODES: NUCLEI WITH LARGE NEUTRON EXCESS

When the isospin T is large, the coupling scheme in isospace can be treated in a "semiclassical" approximation by which the $M_T = T$ components are considered as having their intrinsic axis in isospace fully aligned in the direction of the z-axis in isospace. The pair correlation in the ground state can then be treated in terms of a pairing among neutrons and protons, separately. The modes of excitation can be characterized by the quantum number ν_τ representing the component of isospin along the intrinsic axis, and the excitations have $T = T_0 + \nu_\tau$, where T_0 is the isospin of the ground state or target nucleus.

The pairing excitations with $\nu_\tau = +1$ and -1 are the familiar ones associated with neutrons and protons, respectively, but in addition one

expects pairing vibrations with $\nu_\tau = 0$ and $T = T_0$. The matrix elements for exciting the various M_T components are proportional to the coefficient

$$\langle T_0\ M_T = T_0\ 1\mu_\tau \,|\, T_0 + \nu_\tau,\ M_T = T_0 + \mu_\tau \rangle \approx \begin{cases} 1 \\ (T_0)^{-\frac{1}{2}} \\ 2^{\frac{1}{2}}\ T_0^{-1} \end{cases} \qquad \mu_\tau = \begin{cases} \nu_\tau \\ \nu_\tau - 1 \\ \nu_\tau - 2 \end{cases} \tag{3}$$

The pairing modes with $\nu_\tau = 0$ and $T = T_0$ are, therefore, most strongly excited in reactions with the transfer of an (np) pair, but so far there appears to be no experimental evidence concerning these modes.

INTERACTION BETWEEN PARTICLES AND PAIRING VIBRATIONS

Additional evidence with a direct bearing on the structure of the pairing modes can be obtained from the study of the interaction between single particles and the quanta of the pairing vibrations. The fundamental interaction can be illustrated by the diagrams in Fig.6a. In the Pb region, the value of the matrix element m is estimated to be about 4 (a little smaller for $\alpha = -2$, a little larger for $\alpha = 2$) while G is close to 0.1 MeV.

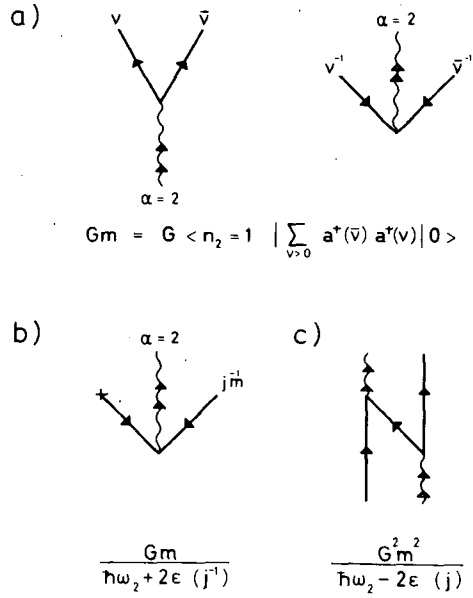

FIG.6. Diagrams illustrating the coupling between particles (or holes) and pair vibrational quanta.

First-order effects of the interaction can be studied in one-particle transfer reactions. An example is illustrated in Fig.6b; on account of the ground-state correlations in ^{208}Pb, a particle jm can be deposited in an empty orbit with the excitation of the state j^{-1} m, $n_2 = 1$ containing a hole and a quantum of the $\alpha = 2$ pairing vibration. The admixed amplitudes are of the

order of 0.1 and the cross-sections thus small compared with single-particle magnitude. However, the detection of the effect would be of considerable interest as a test of the assumed coupling. The study of similar reactions in the A = 56 region would also yield very significant information on the pairing modes. In second order, the coupling gives rise to energy shifts of the states involving a particle (or hole) and a quantum (see the example in Fig.6c), but for this order it is necessary also to consider the other interaction effects discussed above, which are found to play a role in the anharmonicity of the pair vibration mode.

REFERENCES

[1] NATHAN, O., Experimental status of two-neutron transfer reactions in medium and heavy nuclei, these Proceedings.
[2] BES, D.R., BROGLIA, R.A., Nucl. Phys. 80 (1966) 289.
[3] BJERREGÅRD, J.H., HANSEN, O., NATHAN, O., Nucl. Phys. 89 (1966) 337.
[4] SØRENSEN, B., Nucl. Phys. A97 (1967), 1 and private communication.
[5] GLENDENNING, N.K. (Berkeley, California) private communication.
[6] BROGLIA, R.A., RIEDEL, C. (Niels Bohr Institute, Copenhagen) private communication.
[7] BROGLIA, R.A., RIEDEL, C., SØRENSEN, B., UDAGAWA, T., Nucl. Phys., to be published.
[8] RASMUSSEN, J., Properties of some exact solutions of the pairing force problem, these Proceedings.
[9] DAMGÅRD, J., (Niels Bohr Institute, Copenhagen) private communication.
[10] ELLIOTT, J.P., LEA, D.A., Phys. Lett. 19 (1965) 291.
[11] GINOCCHIO, J.N. (Massachusetts Institute of Technology, Cambridge, USA), WENESER, J. (Brookhaven National Laboratory, N.Y., USA) Preprint.
[12] DAVIES, W.G., KITCHING, J.E., McLATCHIE, W., MONTAGUE, D.G., RAMAVATRAM, K., CHANT, N.S. Phys. Lett. 27B (1968) 363.
[13] BJERREGÅRD, J.H., HANSEN, O., NATHAN, O., HINDS, S., Nucl. Phys. 86 (1966) 145.

EXPERIMENTAL STATUS OF TWO-NEUTRON TRANSFER REACTIONS IN MEDIUM AND HEAVY NUCLEI

O. NATHAN
THE NIELS BOHR INSTITUTE,
UNIVERSITY OF COPENHAGEN,
COPENHAGEN, DENMARK

Abstract — Аннотация

EXPERIMENTAL STATUS OF TWO-NEUTRON TRANSFER REACTIONS IN MEDIUM AND HEAVY NUCLEI. The systematics of the strong L=0 transitions observed in two-nucleon transfer reactions in the mass regions near N=126 and N=28 is discussed within the framework of the pairing vibrational model of Bohr. Near ^{208}Pb, the evidence consists of (t, p) and (p, t) data for the even-even Pb nuclei, and for ^{209}Pb and ^{207}Tl. Near N=28, the pairing vibrational spectrum is expected to have a characteristic isospin structure. The evidence for this structure is reviewed on the basis of recent (p, t), (t, p) and (^{3}He, p) data, with particular emphasis on the mass-56, mass-52 and mass-48 nuclei, for which the data are most abundant. Tentative identifications of pairing vibrational 0^+ states are made for the nuclei ^{56}Ni, ^{56}Co, ^{52}Mn, ^{52}Cr, ^{50}Ti, ^{48}V, ^{48}Ti and ^{48}Ca. In the lighter Ca isotopes, the pairing vibrational strength seems to be fragmentated and the simple zero-order picture breaks down.

It is suggested that the model might be extended to comprise also 2^+ excitations built upon the pairing vibrational states. Possible candidates for such pairing-quadrupole states are indicated by (t, p) data for ^{48}Ca, ^{50}Ti, ^{52}Cr, and ^{209}Pb. The energies and intensities of these L=2 transitions are, however, in poor agreement with a zero-order picture and indicate the presence of considerable mixing effects.

The success of the model for the classification of strong L=0 and L=2 transitions in two-nucleon transfer reactions near closed shells cannot be assessed in detail from the present scanty data material. Further experiments, which emphasize the measurement of relative transition probabilities in two-nucleon transfer reactions, are strongly indicated. Evidence concerning pairing vibrational transitions near N=50 and N=82 would also be highly desirable.

СОСТОЯНИЕ ЭКСПЕРИМЕНТА ДЛЯ РЕАКЦИЙ ПЕРЕДАЧИ ДВУХ НЕЙТРОНОВ В СРЕДНИХ И ТЯЖЕЛЫХ ЯДРАХ. В рамках парной вибрационной модели Бора обсуждается систематизация сильных L= 0 переходов, обнаруженных в реакциях передачи двух нейтронов в области массовых чисел около N= 126 и N= 28. Около ^{208}Pb имеются данные по (t ,p) и (p,t) для четно-четных ядер Pb и для ^{209}Pb и ^{207}Tl. Около N= 28 предполагается, что спектр парных вибраций имеет характерную изоспиновую структуру. На основе последних данных по реакциям (p, t), (t ,p) и (^{3}He,p) делается обзор данных об этой структуре, причем особое внимание уделяется ядрам с массовыми числами 56, 52 и 48, для которых собрано наибольшее количество материала. Предварительная идентификация парных вибрационных 0^+ -состояний сделана для ядер ^{56}Ni, ^{56}Co, ^{52}Mn, ^{52}Cr, ^{50}Ti , ^{48}V, ^{48}Ti и ^{48}Ca. В более легких изотопах Ca сила парных вибраций распределяется по другим конфигурациям и простое описание оказывется неверным. Предлагается обобщение модели на возбуждения 2^+, построенные на парных вибрационных состояниях. Данные по (t ,p) для ^{48}Ca, ^{50}Ti, ^{52}Cr и ^{209}Pb указывают на существование таких парных квадрупольных состояний. Энергии и интенсивности этих L= 2 переходов, однако, плохо согласуются с картиной нулевого перехода и указывают на наличие значительных эффектов смешивания. Об успехе применения модели для классификации сильных L= 0 и L= 2 переходов в реакциях передачи двух нуклонов около замкнутых оболочек нельзя пока судить на основе имеющихся скудных данных. Указываются дальнейшие эксперименты, в которых особое внимание уделяется измерению вероятностей соответствующих переходов в реакциях передачи двух нуклонов. Весьма желательно также получить сведения о парных вибрационных переходах для ядер с N = 50 и N = 82.

In the past, most experimental studies of two-neutron transfer reactions have been done with light target nuclei and it is only recently that (t, p) and (p, t) reactions have been investigated systematically in the medium and heavy mass regions. Here, we shall discuss some of these recent results and especially those which have a bearing on the pairing model [1]. We shall assume throughout that the (t, p) and (p, t) reactions proceed by a direct, one-step transfer mechanism. For the main part, we shall be concerned with the systematics of the strong, collectively enhanced transitions rather than with the detailed spectroscopy of individual reactions.

1. PAIRING VIBRATIONAL L = 0 TRANSITIONS NEAR THE CLOSED SHELLS N = 126 AND N = 28

1.1. The Pb region

In the previous paper, by Bohr [1], the strong L = 0 transitions near closed shells were considered in terms of two elementary quanta, a pair addition quantum (0, 1), and a pair removal quantum (1, 0). The former quantum may be added in stripping, the latter in pick-up. Near N = 26, we consider ^{208}Pb(g. s.) as the state (0, 0) and the elementary quanta ('building blocks') may then be considered as reactions I and II of Fig. 1. The 0^+ pairing vibration of the closed shell ^{208}Pb is characterized as (1, 1) and is expected to be seen in the ^{206}Pb(t, p) reaction (reaction III of Fig. 1). If the interaction between the quanta is small, we expect reactions I and III to have nearly the same Q-value and the same cross-section. The available data [2, 3] test the first of these predictions; the ^{206}Pb(t, p) reaction, in fact, exhibits one strong 0^+ state at E_x = 4.87 MeV, which has approximately the expected Q-value (Fig. 1).

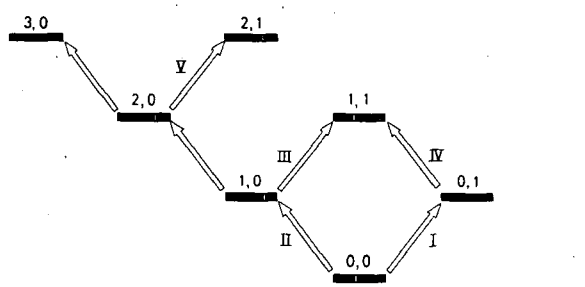

I	(0,0) → (0,1)	^{208}Pb (t,p)	$Q_{0,1}$ = 0,63 MeV
II	(0,0) → (1,0)	^{208}Pb (p,t)	$Q_{1,0}$ = -5,63 MeV
III	(1,0) → (1,1)	^{206}Pb (t,p)	Q = 0,75 MeV
IV	(0,1) → (1,1)	^{210}Pb (p,t)	NOT OBSERVED
V	(2,0) → (2,1)	^{204}Pb (t,p)	DATA INCONCLUSIVE
VI	$p_{1/2}^{-1}(0,0) \rightarrow p_{1/2}^{-1}(0,1)$	^{207}Pb (t,p)	Q = 0,66 MeV
VII	$s_{1/2}^{-1}(1,0) \rightarrow s_{1/2}^{-1}(1,1)$	^{205}Tl (t,p)	Q = 0,51 MeV

FIG. 1. Pair excitations with L=0 in the lead region. The diagram shows schematically the energies of some of the lowest pair excitations for the even-even lead isotopes, using the ^{208}Pb ground state as zero point (cf. the caption to Fig. 3).

One may note that the ^{208}Pb (1, 1) state should be important also in the pick-up reaction IV of Fig. 1. This reaction involves a target of radioactive ^{210}Pb (20 years) and is not yet observed.

When we go to ^{206}Pb, the pairing vibration is described as the state (2,1). It can be reached by the (t, p) reaction on ^{204}Pb (2, 0) but none of the two published experiments [4, 5] are conclusive concerning 0^+ states in the relevant region of excitation ($\approx$ 5.5 MeV).

According to the previous paper [1], there should exist simple intensity relations within a sequence of transitions involving the addition of successive quanta, provided that the anharmonicity effects are small. For the Pb isotopes, the intensity relations can be tested for the case of three successive quanta by considering the ground-state cross-section ratios $\sigma(0, 0 \rightarrow 1, 0) : \sigma(1, 0 \rightarrow 2, 0) : \sigma(2, 0 \rightarrow 3, 0)$. In a harmonic description, these ratios are 1 : 2 : 3. The relevant (p, t) experiments have been done [6] at E_p = 40 MeV and give the result 1 : 1.7 : 2.7 ($\pm$ 20%), indicating that anharmonicity effects are of moderate importance, even when three quanta are added.

The pairing vibrational mode is expected to play an important role also for odd mass nuclei near ^{208}Pb, where the corresponding states would appear as coupled particle-pairing vibrational excitations. Such states appear to have been identified in two recent (t, p) experiments leading to ^{209}Pb and ^{207}Tl, respectively.

In the first of these reactions [3], the ^{207}Pb target may be considered as a rather pure $p_{1/2}$ single-neutron hole state, which we may describe as $p^{-1}_{1/2}$ (0, 0). With a two-neutron capture of the (0, 1) type, we reach a state $p^{-1}_{1/2}$ (0, 1) which is the lowest (2p-1h) state of ^{209}Pb, having $j^\pi = 1/2^-$. Experimentally, one observes (Fig. 1) a strong L = 0 transition in the (t, p) reaction on ^{207}Pb, the Q-value being close to that of $Q_{0,1}$.

In the second reaction, ^{205}Tl(t, p)^{207}Tl, the target state is known to be somewhat more complicated (see Refs [7, 8]). For the main part (about 75%), it is an $s_{1/2}$ proton hole state coupled to the ^{206}Pb ground state (1, 0) but it also contains $d_{3/2}$ and $d_{5/2}$ holes coupled to the 2^+ quadrupole vibration of ^{206}Pb. In the (t, p) experiment [9], one observes two L = 0 transitions to excited states at 4.35 MeV and 4.53 MeV, respectively, the former transition (reaction VII, Fig. 1) being three times stronger than the latter. We interpret tentatively the transition to the 4.35 MeV state as a simple pairing vibrational excitation $s^{-1}_{1/2}(1, 0) \rightarrow s^{-1}_{1/2}(1, 1)$. This is reasonable from the point of view of intensity and Q-values (Fig. 1). We may then think of the second transition as proceeding via the core excitation in the target state, i.e. the L = 0 two-body transfer may connect the 2^+ collective quadrupole state of ^{206}Pb with a (2p-2h) state of 2^+ character in ^{208}Pb, which couples with the proton d hole to give a $1/2^+$ state of ^{207}Tl. It should be stressed, however, that the above arguments necessarily are incomplete. In a quantitative analysis, the mixing of the close $1/2^+$ states of ^{207}Tl probably will play an important role.

Fig. 2 shows the angular distributions observed at 12-13 MeV for reactions I, III, VI and VII. The L=0 transitions are seen to have a characteristic signature in the sharp angular distribution minimum at about 35°.

1.2. The region of N = 28

Whereas double transfer data unfortunately are still scarce near the closed shells of N = 82 and N = 50, the experimental situation is becoming

clearer in the mass region 40-60, near the closed shell N = 28. In the following, we attempt a classification of some strong L = 0 double transfer transitions in this region. Besides (t, p) and (p, t) data, we shall discuss also some closely related (^{3}He, p) results.

When discussing the lead experiments above, we neglected the isospin structure of the pairing modes. This is justified near N = 126 where the ground-state isospins are large, and all excited states considered have the same isospin as that of the ground state. In lighter nuclei, however, we must take into account the fact that the elementary quanta have isospin T = 1. Thus, for instance, in a closed-shell nucleus like ^{56}Ni with $T_z = 0$, the (1, 1) pairing mode has three components with T = 0, 1 and 2, respectively. This follows from the fact that the pairing vibration is obtained by the addition of two different quanta, each with T = 1. The theoretical consequences of the isospin structure of the pairing mode are discussed in the preceding talk [1].

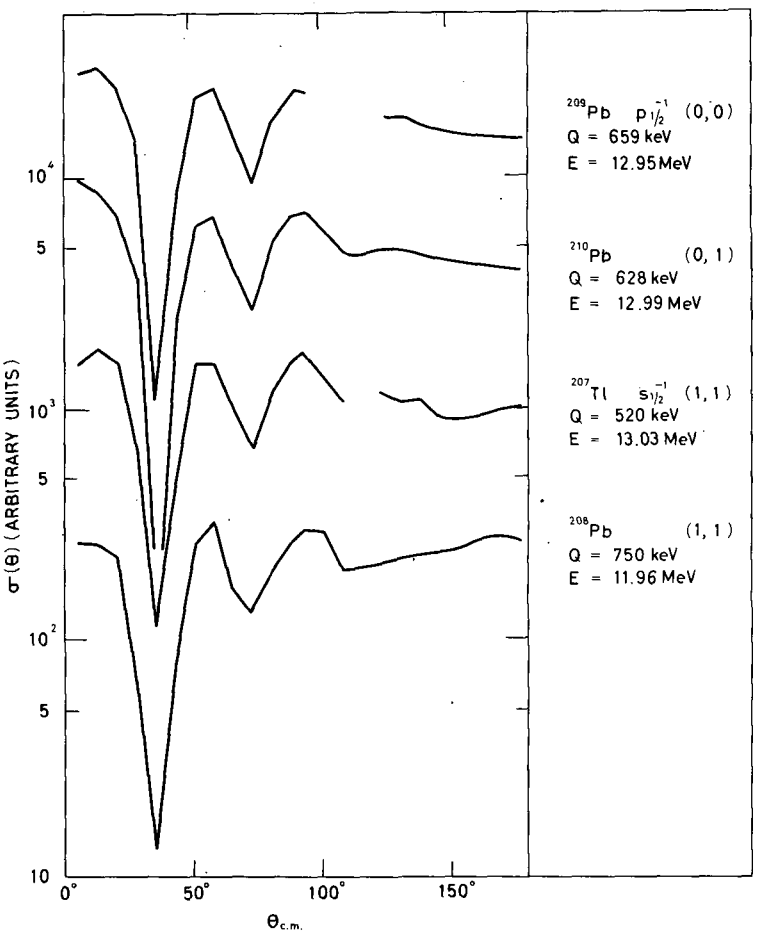

FIG.2. Experimental L=0 angular distributions for (t, p) transitions in the lead region. The final state is labelled by the quantum numbers (n, m) of the pairing scheme. The data are from Refs [2], [3] and [9].

A schematic diagram [1] of the situation in the Cr-Fe-Ni region is shown in Fig. 3, where we label the ^{56}Ni ground state (0, 0) T = 0 *or simply* (0, 0, 0), etc. In a very recent experiment [10] at E_p = 50 MeV, the structure of ^{56}Ni was investigated by the ^{58}Ni(p, t) reaction. 0^+ states were identified at 0 MeV (100%), 4.97 MeV (2%), 6.60 MeV (10%), and 7.93 MeV (10%). Now, the T = 2 analogue of the ^{56}Fe ground state which has the label (1, 1, 2) is expected to occur at $E_x \approx$ 10.0 MeV in ^{56}Ni: the spacing between the states (1, 1, 1) and (1, 1, 2) in the mass-56 system may be inferred to be about 2.12 MeV from a recent ^{54}Fe(^{3}He, p)^{56}Co experiment [11], in which these two states are seen as strong L = 0 transitions. Hence, we expect the (1, 1, 1) state in ^{56}Ni to occur at about 7.9 MeV and it seems reasonable to identify it with the 7.93 MeV state of Ref. [10]. The 6.62 MeV state of ^{56}Ni is then possibly the (1, 1, 0) component of the pairing vibration. The weak 4.97 MeV 0^+ state is not accounted for as a state of the (1, 1, T) type. Bohr [1] has pointed out that this state possibly can be associated with the (2, 2, 0) mode.

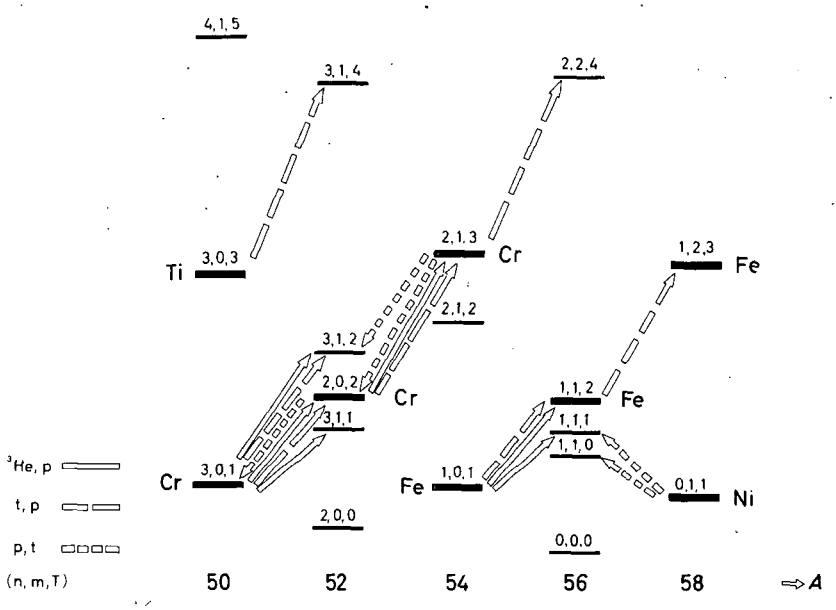

FIG. 3. Diagram of 0^+ excited states in the pairing scheme of Bohr [1] and corresponding two-nucleon transfer reactions in the mass region A=50-58. For illustrative purposes, the energies of the states are not shown rigorously to scale.

Each state is labelled by three quantum numbers (n, m, T), where (n, m) represents the number of pair removal quanta and pair addition quanta, *respectively, and T is the isospin of the state.* Thus, each state of the diagram represents (2T+1) nuclear states. (1, 0, 1), for instance, corresponds to the ground states of ^{54}Fe and ^{54}Ni, and to a 0^+ state of ^{54}Co. Stable ground states are indicated by solid lines.

The energies E of the states are shown (not to scale!) with the ^{56}Ni ground state (0, 0, 0) as zero point, using the following expression (cf. Ref. [1]):

$$E_{MeV} = E(A, Z) - E(^{56}Ni) + 13.3\,(A - 56) - \Delta E_c \{(A, Z) - (A, 28)\}$$

In this way, the states (1, 0, 1) and (0, 1, 1) appear at the same energy in the diagram.

The diagram shows mainly those states for which we have experimental evidence from two-body transfer reactions. The complete scheme [1] contains a number of additional states for which we have no evidence as yet.

According to the intensity rules of Bohr [1], the (p, t) intensities from ^{58}Ni to the T = 0, 1, 2 pairing vibrational triplet should be in the ratio $\langle 1\text{-}1\ 11 | 00 \rangle^2 : \langle 1\text{-}1\ 11 | 10 \rangle^2 : \langle 1\text{-}1\ 11 | 20 \rangle^2 = \frac{1}{3} : \frac{1}{2} : \frac{1}{6}$. For the observed states with T = 0 and 1, this prediction is close to the result of the experiment [10]. It should be emphasized, however, that the intensity rules of the model only concern the intrinsic transition probabilities. The actual yield ratios will be somewhat modified by the Q-dependence of the transfer cross-section.

In the ^{54}Fe(^{3}He, p)^{56}Co experiment (target (1, 0, 1)), it is possible to populate the two pairing excitations (1, 1, 1) and (1, 1, 2) in ^{56}Co (see Fig. 3). The intensity rules [1] predict a cross-section ratio of 1:1 for these two transitions. Experimentally [11], one finds two strong L = 0 transitions at E_x = 1.45 and 3.58 MeV, respectively, with similar intensities which probably correspond to the (1, 1, 1) and (1, 1, 2) states. The latter, of course, is just the IAS of the ^{56}Fe ground state. The model does not predict further strong L = 0 transitions for the ^{54}Fe(^{3}He, p) experiment. Higher pairing states of mass-56 nuclei may be excited in other types of experiments. Thus, for instance, the model predicts L = 0 transsitions in the ^{54}Cr(^{3}He, n)^{56}Fe process to states of the types (2, 2, 2), (2, 2, 3) and (2, 2, 4).

Two (t, p) reactions have been performed with the mass-56 system, namely the ^{54}Fe(t, p)^{56}Fe and ^{56}Fe(t, p)^{58}Fe reactions [12, 13]. No excited 0^+ states of strength comparable to that of the ground state are observed here, in agreement with the model prediction for (t, p) reactions with (1, 0, 1) and (1, 1, 2) targets (see Fig. 3). Since the two ground-state reactions involve the successive addition of two quanta (cf. the Pb(p, t) reactions, discussed above), the intensity rules [1] predict a cross-section ratio of $\sigma(1, 0, 1 \rightarrow 1, 1, 2) : \sigma(1, 1, 2 \rightarrow 1, 2, 3) = 1 : 2$. Experimentally [12, 13], one finds this ratio to be of the order of 1 : 1.6. Again, it should be noted that a stringent test of the model would require a full DW calculation.

We next consider the mass-52 system. The ^{52}Cr ground state has the quantum numbers (2, 0, 2) and the lowest pairing vibrational state in this nucleus is of the (3, 1, 2) type, formed by coupling a (0, 1, 1) quantum to the ^{50}Cr ground state (3, 0, 1). This coupling gives rise also to the states (3, 1, 1) and (3, 1, 0), but these modes do not occur in the ^{52}Cr nucleus (T_z = 2). Further pairing states in mass-52 nuclei labelled (3, 1, 2), (3, 1, 3) and (3, 1, 4) are formed by the coupling of a (0, 1, 1) quantum to the ^{50}Ti ground state (3, 0, 3). Thus, in ^{52}Cr, we expect two (3, 1, 2) states which we may denote ($_1$3, 1, 2) and ($_3$3, 1, 2), respectively. The ($_1$3, 1, 2) state is expected to occur below the ($_3$3, 1, 2) state and it should be populated in (t, p) as well as in (p, t). The higher-lying ($_3$3, 1, 2) state cannot be formed in the (t, p) reaction on ^{50}Cr, if we assume the pairing states to be pure. This state can be formed, however, in the (^{3}He, n) and (p, t) reactions leading to ^{52}Cr.

Experimentally, ^{52}Cr has been studied by the (t, p) process [14] as well as by the (p, t) reaction [15]. In both reactions, the dominant 0^+ state above the ground state is a state at 2.66 MeV, which probably may be identified with the above-discussed ($_1$3, 1, 2) excitation. The (p, t) experiment [15] is not conclusive concerning higher-lying 0^+ states, due to the relatively low bombarding energy employed (E_p = 17 MeV). In the (t, p) reaction [14], one observes additional, weaker 0^+ states in the 5 MeV region. If these states were associated with the ($_3$3, 1, 2) mode, their presence in the (t, p) reaction would indicate considerable mixing between the various 0^+ excitations.

In the ^{50}Cr(^{3}He, p)^{52}Mn reaction [16], three strong L = 0 transitions are seen at 2.64, 2.95 and 5.47 MeV, which may be interpreted as the ($_1$3, 1, 1),

(2, 0, 2) and ($_1$3, 1, 2) states of ^{52}Mn. The energy splitting of 2.52 MeV between the two latter states is close to the 2.66 MeV energy difference between the two corresponding states in ^{52}Cr. The (^{3}He, p) 'intrinsic' intensity ratio σ ($_1$3, 1, 2) : σ ($_1$3, 1, 1) as predicted[1] from the simple intensity rules [1] is 1 : 1, which may be compared with an experimental ratio [17] of about 0.8. The predicted 'intrinsic' cross-section ratio for the (^{3}He, p) and (t, p) transitions leading to the ($_1$3, 1, 2) state of ^{52}Mn and ^{52}Cr, respectively, is 1 : 2, but the available data cannot test this prediction.

In connection with Fig. 2, we finally note that the (^{3}He, p) reaction with a ^{52}Cr target should lead to two strong 0^+ states of ^{54}Mn, having quantum numbers (2, 1, 3) and (2, 1, 2), respectively, and an 'intrinsic' intensity ratio of 1 : 2. The preliminary results reported at this conference [18] do not show the presence of such a strong 0^+, T = 2 state in ^{52}Mn. A restudy of this reaction with higher energy resolution would seem desirable.

The situation in the mass region A = 46 - 50 is illustrated by Fig. 4, where the notation is the same as that of Fig. 3, i.e. ^{56}Ni(g.s.) is taken as the state (0, 0, 0). Most of the two-body transfer data in this region come from (t, p) studies, and in all of these experiments strong, excited 0^+ states are reported in the 3-6 MeV region of excitation. Thus, for instance, in the ^{46}Ca(t, p)^{48}Ca reaction, a very strong L = 0 transition (Q = 3.29 MeV) is observed [19], leading to a state at E_x = 5.46 MeV. We interpret this as the (5, 0, 3) → (5, 1, 4) transition and we note that the cross-section should be the same as that of the ^{48}Ca ground-state transition (4, 0, 4) → (4, 1, 5), which has Q = 3.01 MeV. The observed cross-sections [19] are, in fact, equal to within the 20% experimental uncertainty. Candidates for the corresponding pairing vibrational states can be identified in ^{48,50}Ti [20] and in the lighter Ca isotopes [19].

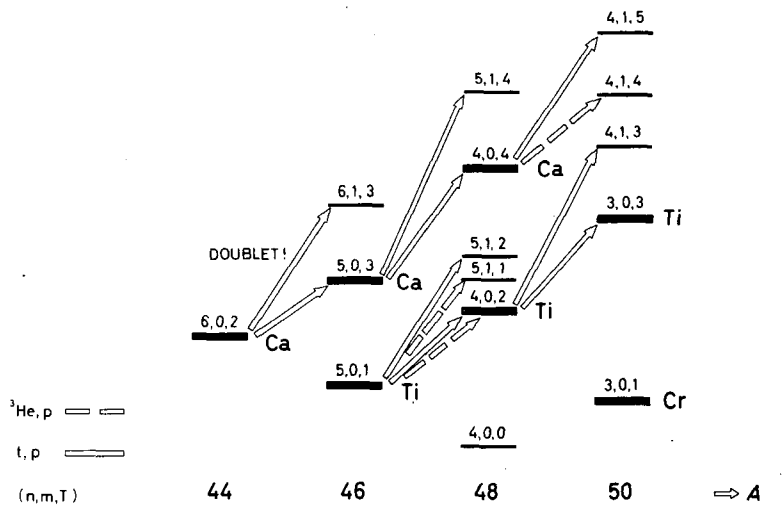

FIG. 4. The figure is a continuation of Fig. 3 for the mass region A=46-50. The notation is that of Fig. 3.

[1] If mixing between the ($_1$3, 1, 2) and ($_3$3, 1, 2) states is taken into account, the predicted ratio [16] drops to about 0.9.

In the ^{46}Ti(^{3}He, p)^{48}V reaction (target (5, 0, 1)), two strong L = 0 transitions are observed [23], leading to the analogue of the ^{48}Ti ground state (4, 0, 2) at E_x = 3.02 MeV and to a state at 3.70 MeV. The latter state is a possible candidate for the (5, 1, 1) excitation; the (5, 1, 2) state (cf. the ^{46}Ti(t, p)^{48}Ti reaction [20]) is expected at higher energy, but there are no (^{3}He, p) data available in this energy region as yet.

The ^{48}Ca(^{3}He, p)^{50}Sc reaction has been investigated recently by the Heidelberg group [22]. Only one 0^+ state is reported at E_x = 3.09 MeV. This is a possible candidate for the (4, 1, 4) state which is the only T = 4, 0^+ state expected from the pairing scheme. Further (^{3}He, p) studies in this region would be desirable.

From the examples considered in this section, summarized in Figs 1, 3 and 4, we conclude that the pairing vibrational scheme [1] meets with a certain success as regards the classification of strong L = 0 transitions in double transfer reactions. However, the experimental evidence is still scarce and it remains to be seen if the scheme will work further away from the closed shells and in the unexplored regions near N = 50 and N = 82. In the Ca region, the present data, in fact, indicate certain difficulties. The (t, p) data [19, 21] show a monotonic decrease by almost a factor of four in cross-section for the strong, excited 0^+ states, when going from ^{48}Ca to ^{42}Ca, and the (t, p) spectra contain several other 0^+ states of smaller, but not insignificant intensity. In ^{46}Ca, the (6, 1, 3) state is of doublet character, the doublet spacing being about 40 keV. This fragmentation of the pairing vibrational strength indicates that couplings to other degrees of freedom cannot be ignored.

As a further critical remark, it may be noted that the data [14, 19, 20] also indicate the presence in some N = 28 nuclei of 0^+ states which may not belong to the simple pairing coupling scheme. In ^{48}Ca, for instance, a 0^+ state at 4.28 MeV has a (t, p) yield equal to 40% of the (5, 1, 4) yield. The nature of the 4.28 MeV level is not clear at the present time.

2. PAIRING-QUADRUPOLE L = 2 TRANSITIONS

Above we have considered 0^+ excitations formed by the addition of two different types of 0^+ quanta. We shall now go one step further and tentatively consider quanta of 2^+ nature. The motivation for this is the occurrence of strong 2^+ states above the 0^+ pairing vibrations in ^{48}Ca [19], ^{50}Ti [20] and ^{52}Cr [14, 15].

Let us discuss, for instance, the case of ^{52}Cr. The T = 2 ground state is labelled (2, 0) and the (3, 1) T = 2 pairing vibration at 2.66 MeV is formed by the addition of a (1, 0) and a (0, 1) quantum to the ground state. Suppose we now replace the (0, 1) quantum by the (t, p) transition to the first excited 2^+ state of ^{54}Cr (E_x = 0.83 MeV). We then obtain a 2^+ state of ^{52}Cr, which we may describe by the notation $(2_0, 0)\ (1_0, 0)\ (0, 1_2)$, subscripts now denoting ordinary spin values. In zero'th order, this state should occur at 3.49 MeV; it should be strong in the ^{50}Cr(t, p) process and weak in the ^{54}Cr(p, t) reaction. On the other hand, if we instead replace $(1_0, 0)$ by $(1_2, 0)$, corresponding to the first excited state of ^{50}Cr (E_x = 0.79 MeV), we obtain the ^{52}Cr 2^+ state $(2_0, 0)\ (1_2, 0)\ (0, 1_0)$, which should occur at 3.45 MeV in zero'th order. This state should be strong in (p, t) and weak in (t, p).

A strong 2^+ state of ^{52}Cr in fact is observed both in pick-up [15] and in stripping [14], the reported level energies being (3.175 ± 0.015) MeV in (t, p) and 3.168 MeV in (p, t). Contrary to the zero order expectations, the data thus suggest that one and the same 2^+ state is involved in both processes. It is, of course, possible that a close doublet of 2^+ levels exists in ^{52}Cr, but a more likely explanation is to be found in the assumption of strong mixing between several (2p-2h) states of 2^+ character near 3 MeV.

In ^{48}Ca and ^{50}Ti, the double transfer data also show strong 2^+ states in the relevant region of excitation above the pairing vibrations. The most probable candidates are:

in ^{48}Ca: 6.33 MeV $(1_0, 0)(0, 1_2)$ [19]

6.79 MeV $(1_2, 0)(0, 1_0)$ [19]

in ^{50}Ti: 4.32 MeV $(1_0, 0)(0, 1_2)$ [20]

In both nuclei, energies and stripping intensities deviate from the zero order picture, indicating the presence of strong mixing effects.

In the Pb region, the ^{208}Pb data are inconclusive concerning 2^+ states but a set of L = 2 transitions are identified in the $^{207}Pb(t,p)^{209}Pb$ reaction [3], leading to states about 700 keV above the previously discussed $p^{-1}_{1/2}(0, 1_0)$ state at 2.15 MeV.

The situation is illustrated in Fig. 5. Part I of the figure shows the $p_{1/2}$, $f_{5/2}$, and $p_{3/2}$ single-hole states of ^{207}Pb. Part II shows the lowest (2p-1h) states of ^{209}Pb in zero'th order, i.e. the states $p^{-1}_{1/2}(0, 1_0)$, $f^{-1}_{5/2}(0, 1_0)$, $p^{-1}_{3/2}(0, 1_0)$, $\left[p^{-1}_{1/2}(0, 1_2)\right]_{J=5/2,3/2}$, and the states formed by coupling the $g_{9/2}$

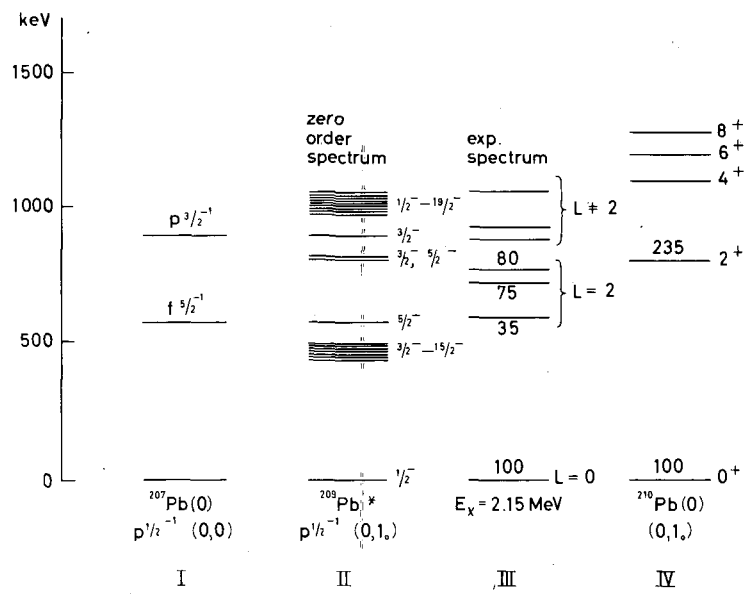

FIG. 5. The lowest two-particle one-hole states of ^{209}Pb seen in the (t, p) reaction on ^{207}Pb (see Ref. [3]). Also shown are the lowest one-hole states of ^{207}Pb and the lowest two-particle states of ^{210}Pb. The numbers on the levels in parts III and IV are relative (t, p) intensities.

ground state with the collective 3^- and 5^- states of ^{208}Pb. Parts III and IV show the relevant (t, p) data for ^{209}Pb and ^{210}Pb, respectively. If the zero order picture were correct, the only L = 2 transitions would go to the $\left[p^{-1}_{1/2}(0, 1_2)\right]_{J=5/2,3/2}$ doublet, which should be populated in the ratio 3:2. Instead, we find about 80% of the expected L = 2 intensity shared by three levels, indicating appreciable mixing with the $f^{-1}_{5/2}(0, 1_0)$ and possibly the $p^{-1}_{3/2}(0, 1_0)$ states, and probably also with higher-lying $3/2^-$ and $5/2^-$ states.

The examples considered here of pairing-quadrupole L = 2 transitions clearly show the inadequacy of the simple, zero order picture for this collective mode. Among the experiments that could illuminate the situation one may note especially the case of ^{208}Pb. It would be interesting to have ^{206}Pb(t, p) experiments with higher bombarding energy than previously employed to locate strong 2^+ states above the 4.87 MeV pairing vibration. The presence of such states is indicated by the data on ^{207}Tl, discussed in section 1.1.

REFERENCES

[1] BOHR, A., Pair correlations and double transfer reactions, these Proceedings.
[2] BJERREGAARD, J.H. et al., Nucl.Phys. 89 (1966) 337.
[3] BJERREGAARD, J.H. et al., Nucl.Phys. A113 (1968) 484.
[4] BJERREGAARD, J.H. et al., Nucl.Phys. A94 (1967) 457.
[5] FLYNN, E.R. et al., Phys.Rev.Lett. 19 (1967) 798.
[6] REYNOLDS, G.M. et al., Phys.Rev. 153 (1967) 1283.
[7] COVELLO, A., SARTORIS, G., Nucl.Phys. A93 (1967) 481.
[8] NATHAN, O. et al., Nucl.Phys. A109 (1968) 481.
[9] HANSEN, O. et al. (Niels Bohr Institute, Copenhagen) to be published.
[10] DAVIES, W.G., KITCHING, J.E., McLATCHIE, W., MONTAGUE, D.G., RAMAVATRAM, K., CHANT, N.S., Phys.Lett. 27B (1968) 363.
[11] BELOTE, T.A. et al., Nucl.Phys. A109 (1968) 666.
[12] COHEN, B.L. et al., Phys.Rev. 157 (1967) 1033.
[13] COHEN, B.L., MIDDLETON, R., Phys.Rev. 146 (1966) 748.
[14] HINDS, S. (Daresbury Nuclear Laboratories, Lancs, UK) private communication.
[15] WHITTEN, C.A., Jr., Phys.Rev. 156 (1967) 1228.
[16] DAMGÅRD, J. (Niels Bohr Institute, Copenhagen) private communication.
[17] RAPAPORT, J. et al., Nucl.Phys. A109 (1968) 657.
[18] GASTEBOIS, J. et al., Contribution No.3 to this Symposium.
[19] BJERREGAARD, J.H. et al., Nucl.Phys. A103 (1967) 33.
[20] HINDS, S., MIDDLETON, R., Nucl.Phys. A92 (1967) 422.
[21] WILLIAMS, D.C. et al., Phys.Rev. 164 (1967) 1419.
[22] SANTO, R. (Max Planck Institut für Kernphysik, Heidelberg) private communication.
[23] DORENBUSCH, W.E. et al., Nucl.Phys. A109 (1968) 649.

DISCUSSION

on the papers by A. Bohr and O. Nathan

V. G. NEUDACHIN: What mechanism of two-nucleon capture is assumed?

A. BOHR: It is assumed that the two nucleons are transferred as a unit in an S state of relative motion. The general pattern of the transfer probabilities does not depend on the further details of the process (wave-function of relative motion, the interaction by which the transfer takes place, motion of in- and out-going projectiles, etc.).

L. MÜNCHOW: You used the charge-independent pairing interaction in T = 1 states. Usually it is argued, however, that in nuclei of the considered region this interaction is not essential because of the difference of the chemical potentials.

A. BOHR: In the region of A = 56 the neutron excess is rather small and it is essential to include pairing. For large T the pairing correlations in the ground state can be described in terms of nn and pp correlations.

Krishna KUMAR: Since the value of the static energy gap is zero for a closed shell nucleus but non-zero for the neighbouring nuclei with two additional particles or holes, does it not imply that we are already in a transitional region?

A. BOHR: Already for states with a few pairs, the average value of $|\Delta|$ is non-zero and comparable with or greater than the zero-point fluctuations, and we are therefore in a transition region. However, for this transition the domain of n-values for which the vibrational and rotational treatments can be applied may overlap (n is the number of quanta).

R. A. SORENSEN: Why is it that you try to describe states of the light calcium isotopes in terms of pairing vibrations based on ^{56}Ni instead of basing them on ^{40}Ca or on ^{48}Ca if you do not like ^{40}Ca as a closed shell?

O. NATHAN: It appears that data concerning two-body pick-up from the s-d shell are still not sufficiently comprehensive to allow an analysis in terms of (0, 1) and (1, 0) quanta relative to a (0, 0)-^{40}Ca system. Such quanta would give rise to additional 0^+ states in the Ca region. I would like to stress that the experimental (p, t) and (t, p) data for the Ca region contain more 0^+ states than discussed here. Some of these states might possibly be related to pairing vibrations built on ^{40}Ca.

J. O. RASMUSSEN: If we are to understand the ground states of nuclei near ^{114}Sn as a rotational band in pairing, are we to understand the first excited state of ^{114}Sn as an analogue to a first beta-vibrational excitation? Is the approximately 20% strength we see in our calculations going to the first excited state to be thought of as measuring a ratio between pairing fluctuation and the stable pairing average?

A. BOHR: Yes, the 20% represents fluctuations in Δ associated with the orbits in the $50 < N < 82$ shell. Additional fluctuations are associated with the more distant shells.

S. T. BELYAEV: As far as I understood, your excited state corresponds to a transfer of two particles into the upper shell without considerable rearrangement. However, there are other ways of pairing excitation, in particular the rearrangement of the pair radial wave function.

Are there any reasons to think that your states are so advantageous that they occur in double transfer reactions?

A. BOHR: The pairing vibrations considered, for example, in the Pb region are similar to the ground-state transitions. They are associated with the total monopole moment $\Sigma a^+(\nu)a^+(\nu)$ of which the different components contribute coherently in the two-particle transfer reaction.

J.J. GRIFFIN: (1) You mentioned that in cases where a strong average pairing field exists the pairing vibrational spectrum goes over into a pairing "rotation". Could you elaborate on the differences between these pairing vibrational and pairing "rotational" spectra?

(2) Could you describe the creation operator for a pairing vibrational phonon in terms of particle creation and annihilation operators?

A. BOHR: (1) For vibrational spectra, the elementary modes of excitation are the quanta of vibration and individual particles and holes, which in first approximation can be simply superposed. For rotational spectra, the elementary modes are the particles moving in the deformed field (quasiparticles) on which is superposed a rotational motion of the whole system.

(2) The creation operator for a pairing vibrational quantum is of the form $\Sigma c(j)(a^+(j)a^+(j))_0$ for the 0^+ pairing mode in a spherical nucleus.

S. SZPIKOWSKI: I have three questions for Professor Bohr. The first is connected with the T = 0 pairing correlations. There is, as you said, no experimental evidence that such pairing takes place. On the other hand, there is, as far as I know, no theoretical paper on that problem. The lack of experimental evidence is possibly caused partly by the lack of theoretical work. What is your opinion? Secondly, if one is energetic one can take more and more correlated pairs of particles and space them over more and more one-particle levels, dealing in such a way with a wider and wider matrix. What restrictions were imposed on your calculations? Thirdly, what value of the G constant was adopted for the n-p, T = 1 pairing correlation?

A. BOHR: (1) One should be open-minded about particle-particle correlations in the T = 0 channel. The problem requires more study, both experimentally and theoretically.

(2) The considerations reported were of a phenomenological character, based on the concept of the pair vibrational quanta and their symmetry properties.

(3) The pairing interaction was taken to be charge-independent, and G thus the same for np as for nn and pp.

B. L. BIRBRAIR: From the viewpoint of the shell model the 0^+ excited state in ^{208}Pb is a two particle-two hole state. This state is formed by both the particle-particle interaction (in $0^+, 2^+$, etc. states) and the particle-hole interaction. Have you any arguments in favour of the fact that the particle-particle interaction in the 0^+ state plays the main role and all the other interactions give a small correction?

A. BOHR: The observed properties of the 0^+ excited state in ^{208}Pb indicate that the interaction between the two quanta is relatively small, and the estimates reported, which include both particle-particle and particle-hole effects, are consistent with this.

S. T. BELYAEV: In one and the same reaction both ground and excited states of an end nucleus may appear, say in ^{206}Pb(p, t)^{208}Pb. What is the difference in the structure of a pair of nucleons generating the ground and excited states?

A. BOHR: The pairing vibrations considered in the region of ^{208}Pb involve two types of pairs, in the shells above and below N = 126.

Short Contribution

T. UDAGAWA (Nordita, Copenhagen, Denmark): I should like to report some preliminary results on analysing the (t, p) reaction on even deformed nuclei, being particularly interested in the excitations of 0^+, 2^+ and 4^+ members of the ground-state rotational band. The experimental data available now are very limited but strong 0^+ and 2^+ excitations have been observed in a few cases of the Sm isotopes. The excitation of the 4^+ state is also observed in $^{154}Sm(t, p)^{156}Sm$.

In a rough approximation, we may say that the cross-sections are proportional to so-called multipole pairing strengths, namely the excitation of the λ^+ state,

$$\sigma(\lambda^+) \sim \left| \Sigma u_i v_i q_i^{(\lambda)} \right|^2$$

where $q_i^{(\lambda)}$ is the λ-pole moment of the Nilsson orbital i. Thus, we can obtain from the (t, p) data information on quadrupole and higher multipole phenomena in deformed nuclei.

In Table A are shown our results from a more elaborate DWBA analysis obtained by assuming zero-range approximation. The 0^+ cross-sections are arbitrarily normalized to 100. The numbers in the bracket for the 2^+ excitations are those obtained by neglecting the $\Delta N = 2$ mixing in the Nilsson single-particle wave function. The final calculated results, including $\Delta N = 2$ mixing effects, are somewhat larger than the experimental ones. However, we should remark that in estimating $\Delta N = 2$ mixing effects, we introduced an approximation which overestimates the effects. Considering this point, the agreement of our calculated results with experiments are not so bad for the 2^+ states.

The Nilsson model predicts a too small cross-section for the 4^+ state to explain the observed value. Thus, it would be necessary to take into account the Y_4-deformation. Our preliminary estimate requires $\beta_4 \sim 0.04$ to explain the experimental data, which is roughly equal to the value obtained in a (α, α') experiment by the Berkeley group. The work reported here was done in collaboration with R. Broglia and C. Riedel.

TABLE A. RESULTS FROM DWBA ANALYSIS

Final nucleus	Final state	Exp.	$\delta = 0.27$	$\delta = 0.30$
^{154}Sm	0^+	100	100	100
	2^+	34	47 (10)	55 (10)
	4^+		0.10	0.14
^{156}Sm	0^+	100	100	100
	2^+	33	50 (9)	69 (10)
	4^+	6	0.16	0.23

Short Contribution

A. A. OGLOBLIN (I. V. Kurchatov Institute of Atomic Energy, Moscow): I should like to mention some results on the excitation of alpha-particle states in (^{6}Li, d) and (^{7}Li, t) reactions.

Several-nucleon transfer reactions which permit both low and high levels to be excited are a most effective method of studying cluster states in nuclei. However, the mechanism of the nuclear interaction with heavy nuclei used for this purpose is usually rather complicated and ambiguous. In this respect the reactions induced by accelerated nuclei of lithium are unmatched. The situation is seen in Fig. A. Since the binding energy of

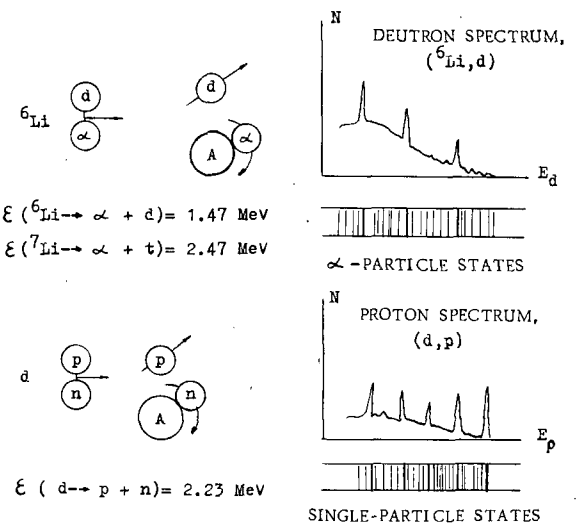

FIG. A. The mechanism of the reactions induced by accelerated ions of Li.

	E_{Li} (MeV)	TARGETS
1. ALPHA-PARTICLE TRANSFER		
(^{6}Li, d) -REACTION	25.8	^{12}C, ^{13}C, ^{14}N, ^{16}O, ^{24}Mg, ^{28}Si, ^{32}S
	35.5	^{12}C
(^{7}Li, t) -REACTION	28.2	^{12}C, ^{13}C, ^{16}O
	30.3	^{9}Be, ^{12}C, ^{13}C, ^{16}O, ^{20}Ne, ^{24}Mg, ^{28}Si, ^{32}S, ^{40}Ca
2. DEUTERON TRANSFER		
(^{6}Li, α) -REACTION	25.7	^{6}Li, ^{7}Li, ^{9}Be, ^{12}C, ^{13}C, ^{14}N, ^{16}O, ^{24}Mg
3. TRITON TRANSFER		
(^{7}Li, α) -REACTION	30.3	^{12}C

FIG. B. The main results of investigating reactions with ^{6}Li and ^{7}Li on the cyclotron of the I.V. Kurchatov Institute of Atomic Energy.

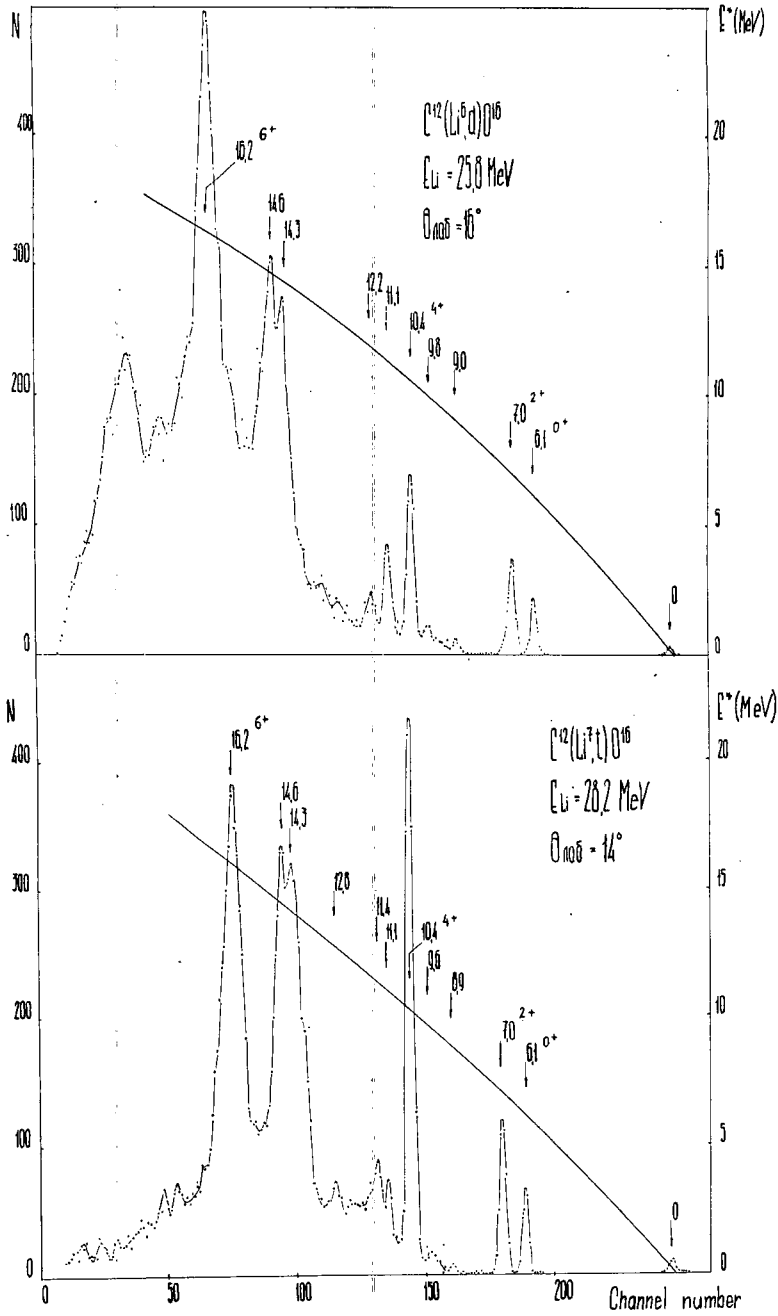

FIG.C. The spectra in the (^{6}Li, d) and (^{7}Li, t) reactions with ^{12}C.

lithium nuclei is very small, they should behave in nuclear reactions as deuterons do, i.e. the stripping process will be one of the most basic mechanisms. The only difference is that, instead of the nucleon transfer, the transfer of a deuteron, triton or α-particle takes place and instead of single-particle states the corresponding cluster states become excited with the greatest probability.

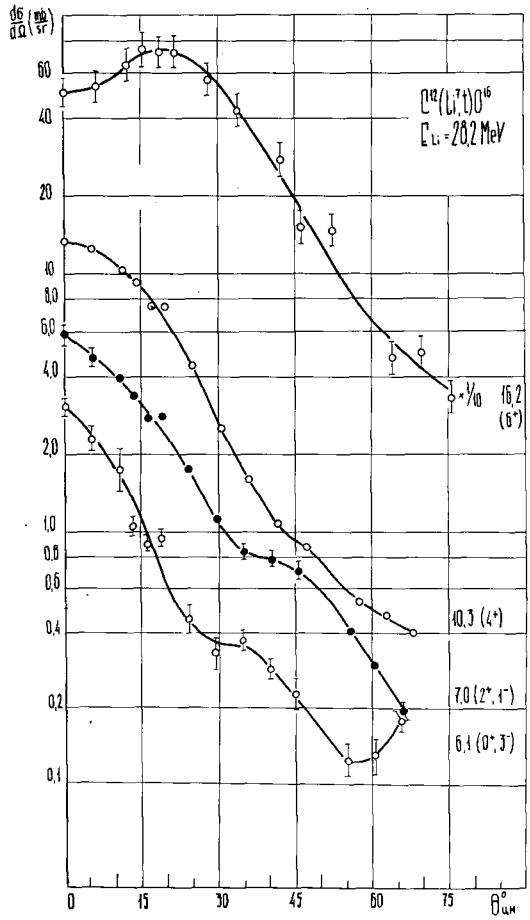

FIG. D. Angular distributions of tritons in the (^{7}Li, t) reaction with ^{12}C for transitions to the rotational states of the ^{16}O nucleus.

Because of the serious technical difficulties of the acceleration of lithium ions to sufficiently high energies (10 MeV and more), this has been hitherto done only on the cyclotron of the Kurchatov Institute. Only quite recently have lithium ion fluxes been obtained on the tandem accelerators in Heidelberg (GFR) and Pennsylvania University (USA).

Figure B shows the results of the investigation of the reactions with lithium ions on the IAE cyclotron. Alpha-particle transfer reactions are most interesting and they have been studied in greatest detail.

Figure C shows the spectra of deuterons and tritons in the (^{6}Li, d) and (^{6}Li, t) reactions with ^{12}C. The spectra of both reactions are very similar; this confirms the assumption that a simple mechanism of the alpha-particle transfer predominates in these reactions.

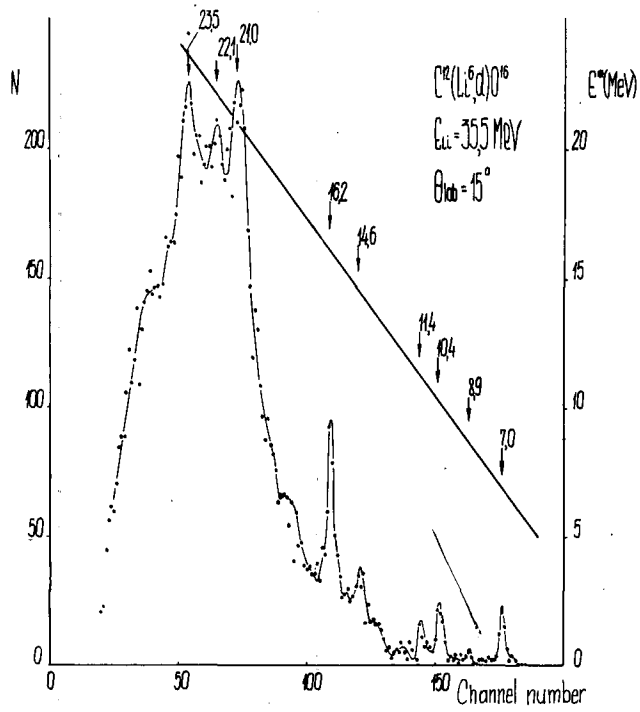

FIG. E. The spectrum of deuterons in the (^{6}Li, d) reaction with ^{12}C at an energy of 35.5 MeV.

In the above-mentioned reactions with ^{12}C the states of the nucleus of ^{16}O with the structure 4p-4h should be mainly excited. As is seen from Fig. C, in addition to the doublet at 14.3 - 14.6 MeV, the levels of the rotational band based on the state 6.05 (0^+): $0^+ - 2^+$(6.92 MeV) - 4^+ (10.35 MeV) - 6^+(16.2 MeV) get excited intensively. Angular distributions (Fig. D) are extended forward and in a number of cases permit conclusions as to the momentum transferred. It should be noted that for the energies in question the kinematics of reactions brings about an increase in the transitions to the states with greater spins.

The increase of the initial energy up to 35.5 MeV results in the intensive excitation of several states of the ^{16}O nucleus in the range 21 - 24 MeV (Fig. E).

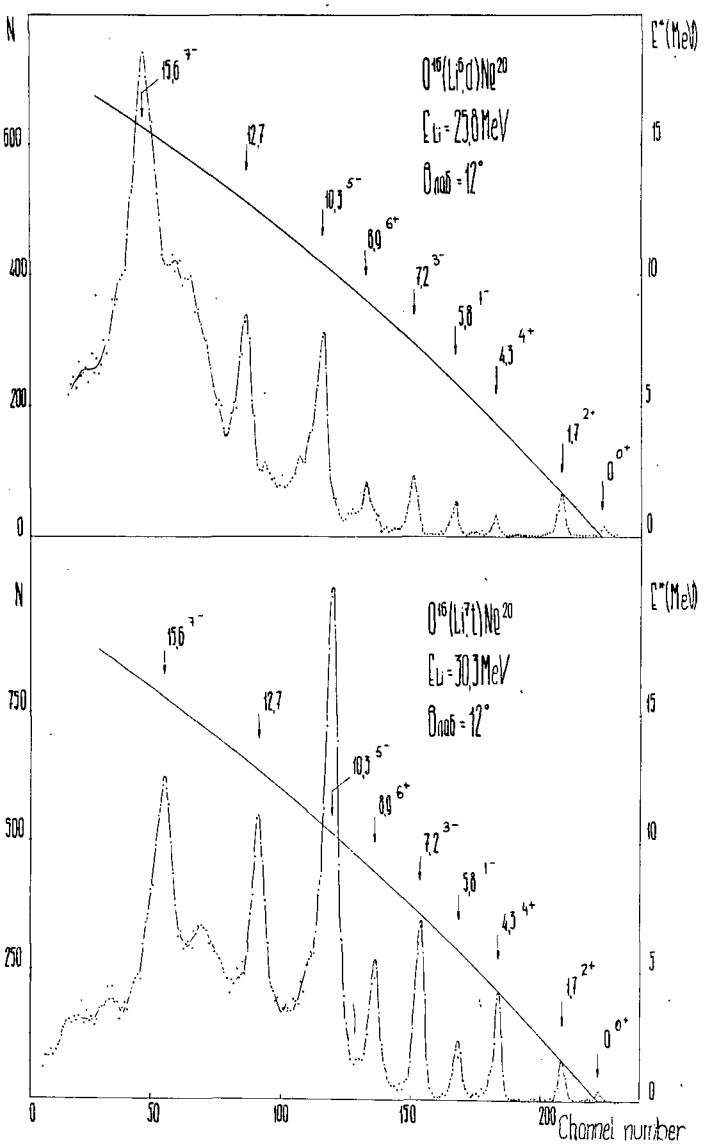

FIG.F. The spectra in the (^{6}Li, d) and (^{7}Li, t) reactions with ^{16}O.

Figure F shows the spectra of $^{16}O(^{6}Li, d)^{20}Ne$ and $^{16}O(^{7}Li, t)^{20}Ne$. Besides the 12.7 MeV energy level, two rotational bands of the ^{20}Ne nucleus become intensively excited: 0^+ (ground) - 2^+(1.7 MeV) - 4^+(4.25 MeV) - 6^+(8.9 MeV) and 1^-(5.80 MeV) - 3^-(7.17 MeV) - 5^-(10.3 MeV) - 7^-(15.5 - 15.6 MeV). At no angle was the 8^+ level (11.99 MeV) discovered.

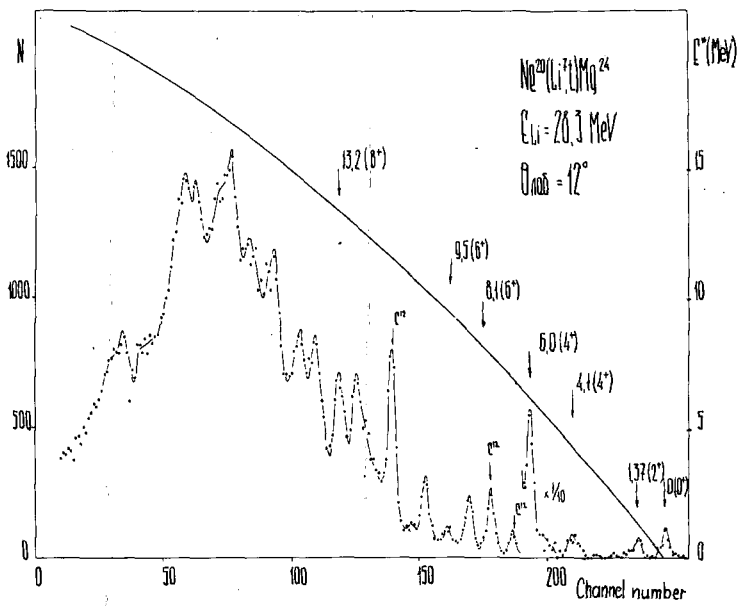

FIG.G. The spectrum of tritons in the ($^{7}Li, t$) reactions with ^{20}Ne.

Figure G shows the spectrum of tritons in the $^{20}Ne(^{7}Li, t)^{24}Mg$ reaction. The levels of the rotational band of the ground state of ^{24}Mg, 0^+ - 2^+(1.37 MeV) - 4^+(4.1 MeV) - 6^+(8.1 MeV), become excited very weakly. Compared with ^{16}O and ^{20}Ne, the cross-section absolute values are more than an order of magnitude smaller and another intensity relation of transitions to different levels of the band is observed. Of the low states the 6.0 MeV (4^+) level is excited most of all. The most intensive transitions fall into the region of an excitation energy of 10 - 15 MeV.

The results obtained for the ^{24}Mg target (residual nucleus of ^{28}Si) and the ones given in Fig. H are close to the preceding case. The rotational band of the ground state of ^{28}Si becomes excited as weakly as that of ^{24}Mg. This result causes us to suppose that the nature of the appearance of ^{16}O and ^{20}Ne nuclear deformation is very different from that of ^{24}Mg and ^{28}Si.

The results obtained for the other nuclei, ^{9}Be, ^{13}C, ^{28}Si, ^{32}S and ^{40}Ca, have in general the same character. The most intensive transitions lie above 10 MeV, and low states become excited relatively weakly. The measurements made with ^{40}Ca (Fig. I) allowed the data on the scheme of levels of the ^{44}Ti nucleus to be obtained for the first time. The preliminary analysis shows that a rotational band based on the ground state probably exists in ^{44}Ti.

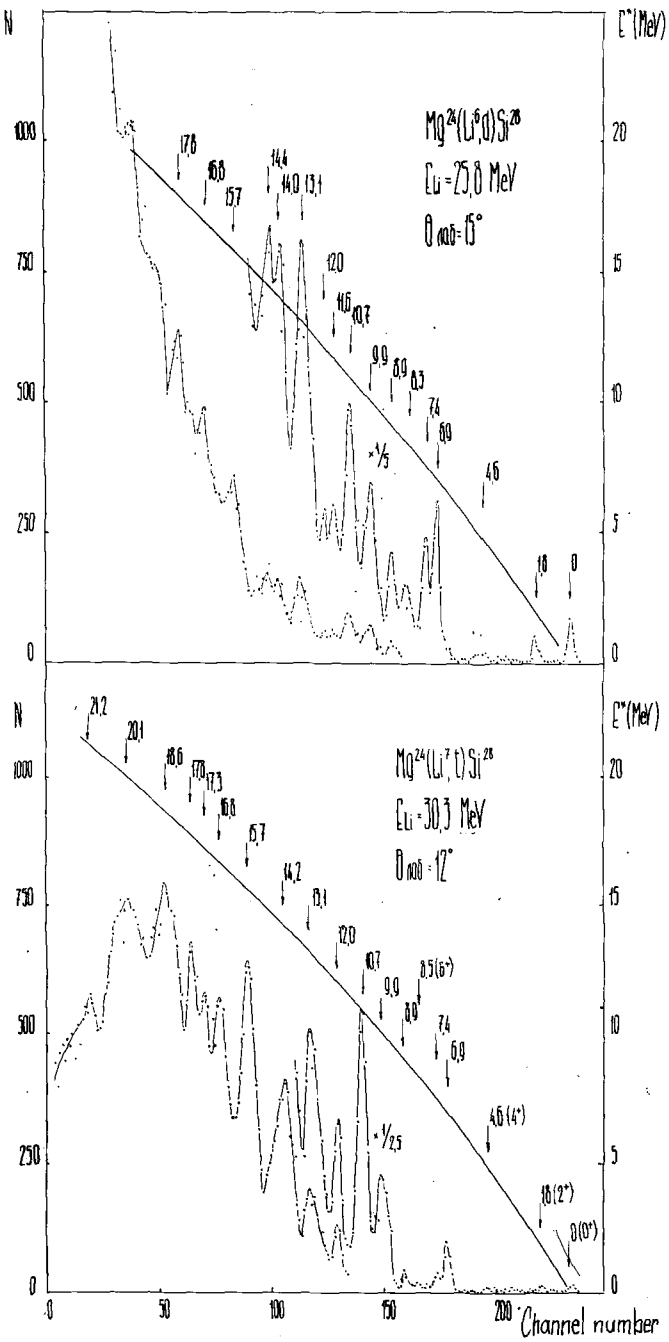

FIG. H. The spectra in the (^{6}Li, d) and (^{7}Li, t) reactions with ^{24}Mg.

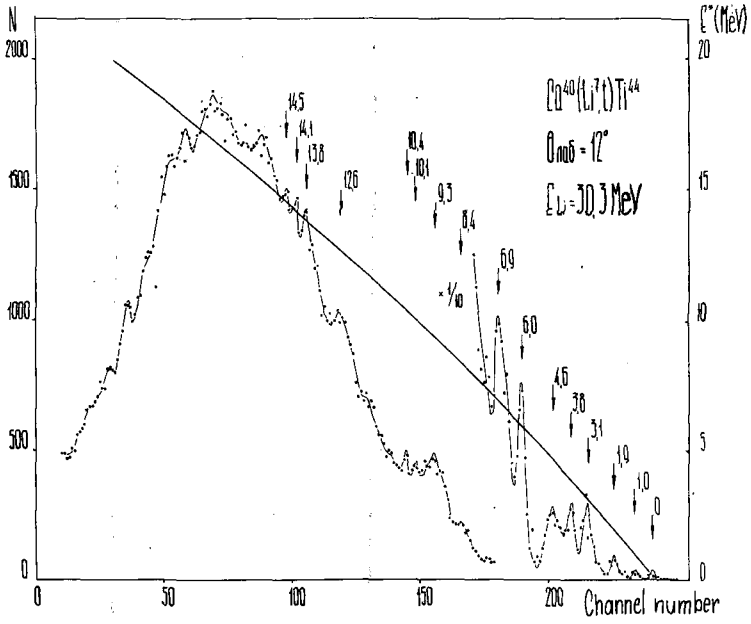

FIG.I. The spectrum of tritons in the (^{7}Li, t) reaction with ^{40}Ca.

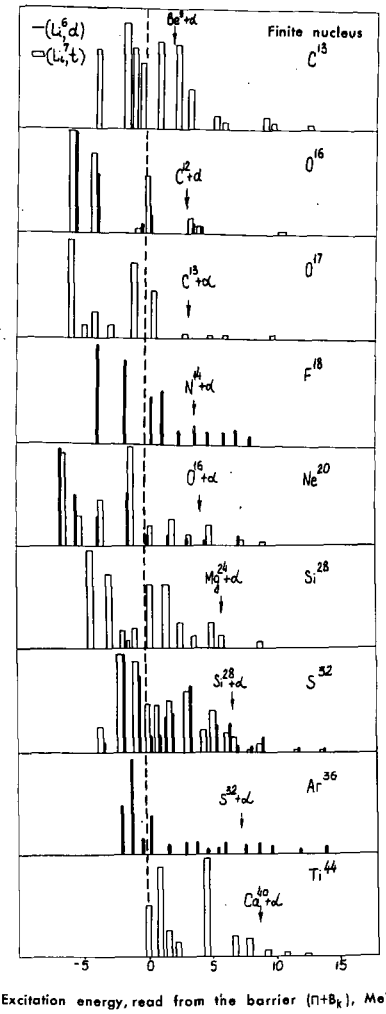

FIG. J. The transition intensity distribution in (^{6}Li, d) and (^{7}Li, t) according to the excitation energy of the residual nucleus.

The high states excited during (^{6}Li, d) and (^{7}Li, t) reactions reveal a characteristic feature: they are grouped around the value of $\Pi_\alpha + B_k$ where Π_α is the threshold of the residual nucleus integration into the target nucleus and α-particle, and B_k is the Coulomb barrier of this system. In Fig. J this quantity is taken as zero, and vertical cuts are proportional to the cross-sections. Starting from rather simple considerations about the symmetry of the wave-function outside the nucleus and inside it, it may be shown that the cluster states should occur at energies smaller than the value of $\Pi_\alpha + B_k$ (at the expense of the centrifugal barrier this value may be somewhat increased). Analogous grouping of the strongest transitions around the threshold plus the barrier takes place at the deuteron transfer.

INELASTIC SCATTERING OF NUCLEAR PARTICLES AND THE STRUCTURE OF VIBRATIONAL NUCLEI*

T. TAMURA†
OAK RIDGE NATIONAL LABORATORY, OAK RIDGE, TENN.,
UNITED STATES OF AMERICA

Abstract — Аннотация

INELASTIC SCATTERING OF NUCLEAR PARTICLES AND THE STRUCTURE OF VIBRATIONAL NUCLEI. Recent work on the scattering of nuclear particles by spherical nuclei is reviewed. The elastic scattering data have been used in fixing the optical parameters, but the recent tendency is to go one step further beyond the simple parametrization, and so far it has been done for the real part. Existence of some ambiguity in the strength W_D of the imaginary part is pointed out in connection with the one-step inelastic processes, and the importance of more basic theories is invoked. Excitation of the two-phonon states is discussed in some detail using data of Cd(p, p') and a lack of parallelism between the (p, p') process and the Coulomb excitation is stressed. It is also shown, however, that this parallelism may be recovered if the use of different W_D in different channels could be justified. Analyses of (p, p') data from odd-A spherical nuclei, and some recent work on inelastic processes from deformed nuclei, are also discussed. Finally, a brief account is given of the possible analyses of the (p, p') data via isobaric analogue resonance. An outline is given of such a theory based on the shell model approach to nuclear reactions.

НЕУПРУГОЕ РАССЕЯНИЕ ЯДЕРНЫХ ЧАСТИЦ И СТРУКТУРА ВИБРАЦИОННЫХ ЯДЕР. Дается обзор последних работ по рассеянию ядерных частиц сферическими ядрами. Данные по упругому рассеянию использовались до сих пор лишь для фиксации оптических параметров, но недавно появилась тенденция не ограничиваться простой параметризацией, что и было сделано для действительной части взаимодействия. Указывается существование некоторой неоднозначности в величине W_D мнимой части в связи с одноступенчатыми упругими процессами и говорится о важности развития более фундаментальной теории. Подробно обсуждается возбуждение двухфононных состояний с использованием данных по Cd(p,p') и подчеркивается отсутствие соответствия между процессом (p,p') и кулоновским возбуждением. Показано также, что это соответствие можно восстановить, если использование различных W_D в разных каналах будет оправдано. Обсуждается анализ данных по (p,p') на основе нечетных - A сферических ядер, а также несколько последних работ, посвященных неупругим процессам с деформированными ядрами. Наконец, приводится краткий перечень возможных способов анализа данных по (p,p') в сравнении с изобарическим аналоговым резонансом. Даются общие очертания такой теории, основывающейся на оболочечно-модельном подходе к ядерным реакциям.

This paper reviews from the theoretical point of view how the inelastic scattering of various nuclear particles serves as a tool to clarify the nature of the so-called vibrational nuclei. However, the technique of analysing the inelastic scattering data from vibrational nuclei can be extended to deformed nuclei with slight modifications; so I shall also briefly refer to a few recent developments along these lines. I have tried to refer to the most recent work, so some of my information is taken from preprints or private communications. My review may be heavily weighted with references to work done in the United States, and for this I apologize at the outset.

* Research sponsored by the U.S. Atomic Energy Commission under contract with Union Carbide Corporation.

† Present address: Center for Nuclear Study, University of Texas, Austin, Texas.

As is well known, there are two techniques fashionably used for the analyses of inelastic scattering processes where the direct process predominates: the distorted wave Born approximation (DWBA) [1] and the coupled channel calculations [2]. The former is usually easier to carry out than the latter but, in its standard form, its use is restricted to the one-step processes. It also gives less accurate information on the strength of the coupling between channels when this strength exceeds a certain value. The coupled channel calculations are free from these faults, but the technique is usually more involved than for DWBA. However, most of the practically needed calculations are within the capacity of the present-day computer. I must also emphasize that, if the calculations are restricted to one-step processes, the coupled channel calculations are by no means more involved than DWBA.

The main objective of analysing scattering data may be considered as twofold. One is to reveal the properties of nuclear matter, and the other is to extract information on the strucutre of individual levels in the target nucleus. In practice, the former is almost equivalent to finding the parameters of the optical potential. Therefore the major part of this objective can be achieved by analysing only the elastic scattering data.

It is safe to say that the possible ranges of values of the optical parameters for projectiles of mass one to four have been quite narrowed down, so that one can find a reasonable set of parameters for any of these projectiles with intermediate energies. Still, with the accumulation of more accurate and more systematic data, particularly those that include polarization, further refinement is still taking place, and this is leading to a deeper insight into the properties of nuclear matter.

For example, Greenlees et al. [3] started to go one step beyond the usual optical analysis, which has so far been almost entirely phenomenological. They put much emphasis on the meaning of the root mean square radius of the potential and considered a model in which this radius is written as the sum of matter and nuclear force mean square radii. Because of the short-range nature of the spin-orbit part of the nucleon-nucleon interaction, the radius of the spin-orbit potential was equated to the matter radius. Thus it is smaller than the radius of the central part of the optical potential. Taking the appropriate nuclear force radius, then the total radius, the depth and diffuseness parameters, etc., were sought, and a very good set of parameters was obtained. One interesting finding is that the matter radius is larger than the charge radius, which means that the neutrons are distributed further out of protons.

This and another work by Slanina and McManus [4], which may be considered as complementary to it, will certainly need more refinement but they nevertheless seem to give an important start towards putting more direct physical meaning at least into the real part of the optical potential. However, the imaginary part was treated in the conventional phenomenological way. We shall discuss the imaginary part later in connection with inelastic scattering. Incidentally, a smaller spin-orbit radius than the radius of the central potential seems to be required also for deuterons [5]. Such a potential nicely explains the elastic cross-section and polarization, and also the j-dependence of the (d, p) cross-section if used in DWBA [6].

The excitation of states that are excited by the one-step inelastic scattering process, particularly those of one-phonon states, is the simplest

process next to the elastic scattering and gives further information on the optical parameters as well as on the nature of these excited states.

Recently Kruse et al. [7] at Rutgers made a systematic investigation of this problem by bombarding isotopes of Cd, Sn and Te with 16 MeV protons. As an example the result for Cd isotopes is shown in Fig. 1. Both 2^+ and 3^- cross-sections decrease monotonically, and the elastic scattering cross-sections show less marked oscillation with increasing A. This feature is also true for Sn and Te isotopes. By fitting the elastic data with the optical model and then the inelastic data with DWBA, they extracted the β_2 and β_3 values or more precisely the deformation length $\delta = \beta \times r_0$. The results for Cd are illustrated in Fig. 2, where the δ values obtained from the Coulomb excitation are also shown for comparison. General agreement between these two is clearly observed, though they do not agree exactly. Note that two δ_2 values show different trends as a function of A.

It is not very clear to what extent one should take these discrepancies seriously. In extracting the δ values Kruse et al. took optical parameters in which the depths of the real and imaginary parts increase approximately linearly with A. The proportionality constants are in line with the values known from other works. Therefore these parameters seem reasonable, but the question is whether such a set of parameters is unique or not.

In Fig. 3 we show similar results for Sn isotopes also obtained by the Rutgers group [7]. As is seen, the discrepancy between the Coulomb excitation and (p, p') values of δ_2 is quite large. This strong A dependence

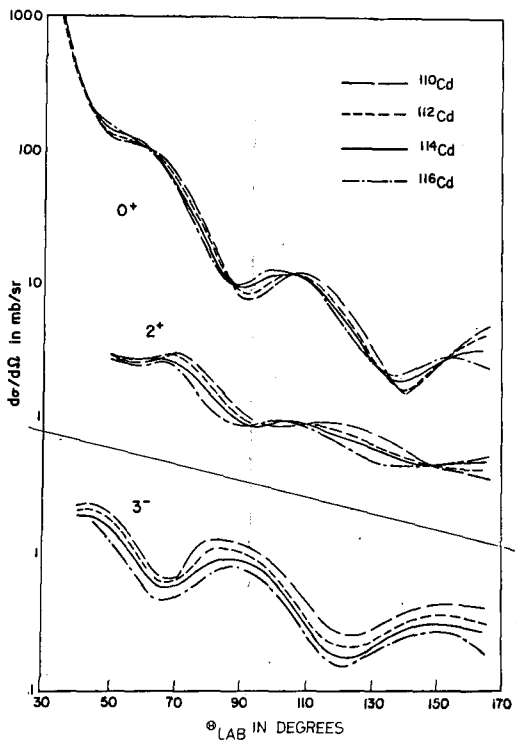

FIG. 1. Inelastic scattering cross-section of 16 MeV protons from Cd isotopes.

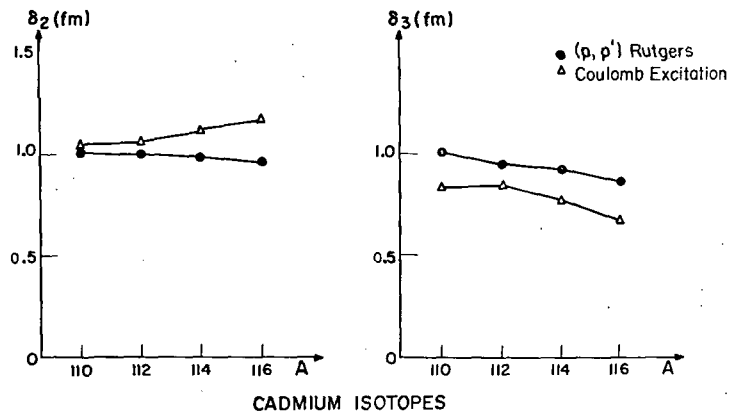

FIG.2. Deformation parameters δ_2 and δ_3 for Cd isotopes.

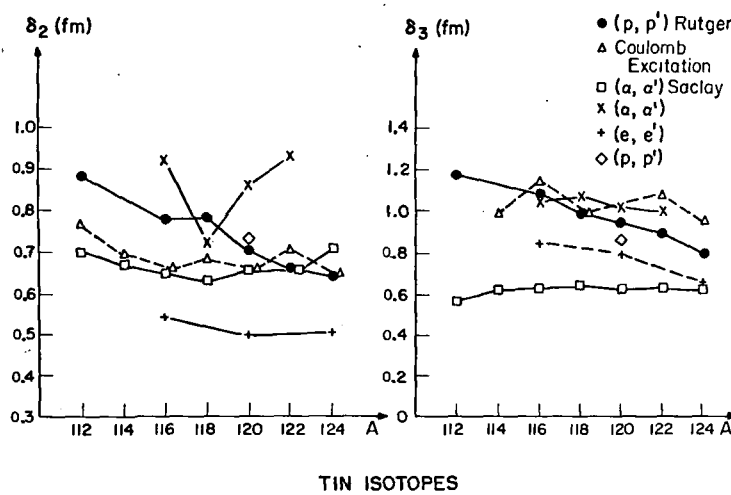

FIG.3. Deformation parameters δ_2 and δ_3 for Sn isotopes.

of δ_2 is necessary to explain the systematic decrease of the 2^+-state cross-section with increased A. However, if the imaginary potential is chosen to increase with A more rapidly than was chosen by the Rutgers group, the use of Coulomb excitation δ_2 values may still have explained the 2^+-state cross-section. Indeed, such a calculation was made by us previously [8].

Of course the range of the possible values of W is not unlimited, because the theoretical fit to the elastic as well as inelastic scattering data is always required. Nevertheless, W-δ ambiguity does seem to exist. Also it is not completely clear whether one should take exactly the same W-values for elastic and inelastic channels. This affects the inelastic cross-section without greatly affecting the elastic cross-section.

The existence of these ambiguities makes it difficult to say whether there exists a precise parallelism between the Coulomb excitation and the (p, p') processes. The microscopic approach to the (p, p') processes that has been developed may not yet be powerful enough to answer this question.

It seems that a microscopic theory which can derive the optical potential and the (p, p') cross-sections simultaneously from first principles is needed. We shall see later that a similar problem is observed also in the (p, p') processes from the two-phonon states.

Another systematic survey of inelastic scattering processes is the work on (α, α') processes done at Saclay by Mme. Faraggi and her co-workers [9]. This is a summary of 6 years' work of bombarding about 20 nuclei with 44-MeV α-particles. Most of the targets are either singly or doubly closed shell nuclei. The data are extensive and look as though they would be quite useful if they were analysed properly. However, the analysis has been made so far by using the Austern-Blair theory [10], which is quite handy but its accuracy is somewhat dubious. As for the one-step collective escitation, the angular distribution is fairly satisfactorily reproduced, as is seen in Fig. 4. However, the magnitude of the theoretical cross-section is overestimated, resulting in underestimation of the δ values. This is seen in Fig. 3. For the two-phonon transitions this theory gives angular distributions which are not steep enough compared with experiment, as is seen in Fig. 5, and thus meaningful extraction of the δ values does not seem possible. I hope the data are re-analysed by using either DWBA or coupled channel calculations. To show to what extent the coupled channel calculation works, I would like to present here a result of my old calculation [11] in Fig. 6. This is for ^{62}Ni(α, α') and the data are from Berkeley [12]. As is seen, quite nice fits can be obtained over a wide range of energy.

In passing, I should like to mention that a quite extensive experiment has been started at Los Alamos by Armstrong et al. [13] using a triton beam. Fig.7 shows the excitation of the one-phonon 2^+ states while Fig. 8

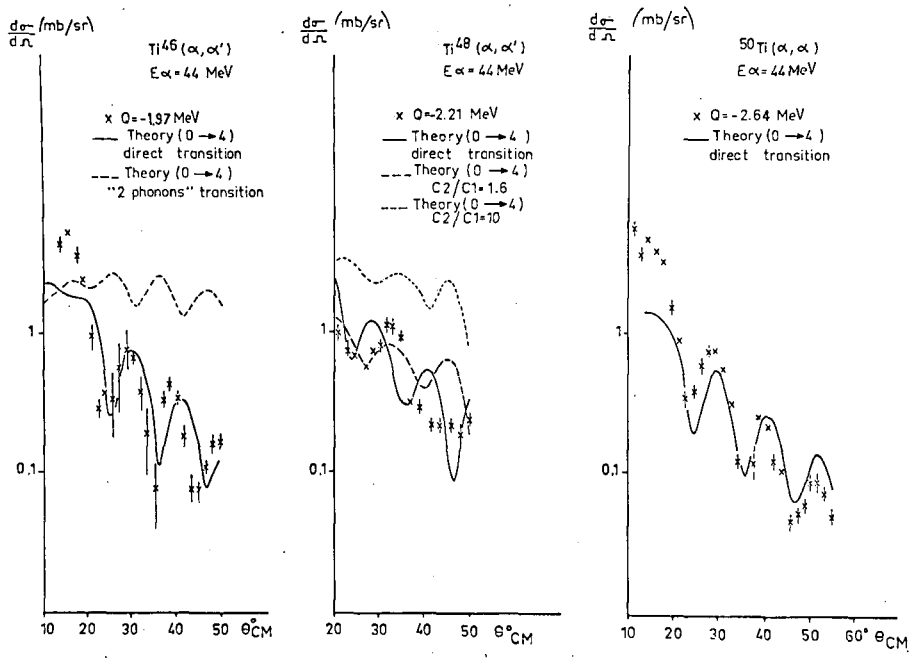

FIG.4. Examples of one-step (α, α') cross-sections. Curves are due to Austern-Blair theory.

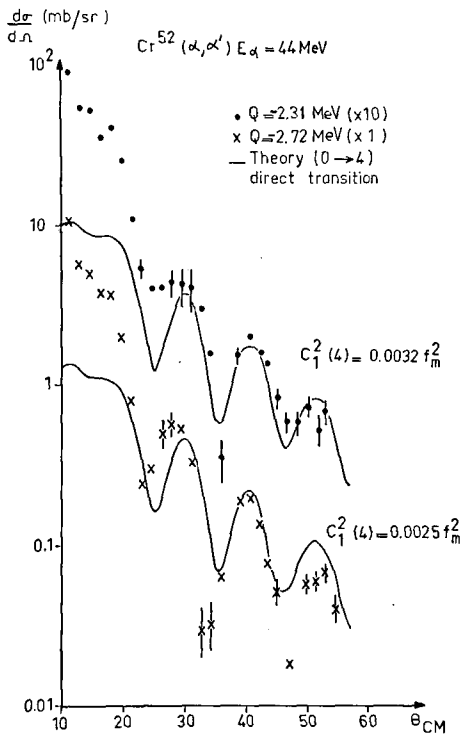

FIG. 5. Examples of two-step (α, α') cross-sections. Curves are due to Austern-Blair theory.

depicts that of 3^- states. The curves are DWBA results and the fit is seen to be good for all the angles. The extracted δ values are also in line with those obtained from other sources.

We shall now turn to the excitation of the two-phonon states. For obvious reasons the available data are few compared with those of one-phonon excitations. Nevertheless, an interesting analysis can be performed using existing data, and I present here an Oak Ridge study [14] of (p, p') processes from ^{112}Cd and ^{114}Cd. In the analysis a phenomenological vibrational model was used, and not the microscopic theory [15]. We then aimed at finding out to what extent the ideal vibrational model is destroyed. Such knowledge will be useful in attempting to perform microscopic structure calculations in the future. Anyway, the present lack of very reliable microscopic wave-functions, particularly for the two-phonon states, prevents one from carrying through the coupled-channel calculations with microscopic form factors.

Figure 9 shows the experimental cross-section of the 0^+, 2^+, and 4^+ two-phonon states for ^{114}Cd, together with the theoretical fits. The agreement is quite good, in particular as regards the 2^+ angular distributions. This agreement was obtained by assuming a fairly large admixture of the amplitude of the one-phonon 2^+ state into the dominant two-phonon amplitude. It is also seen that the phase of this admixture is definitely determined by this data fitting, because the theoretical angular distribution obtained by

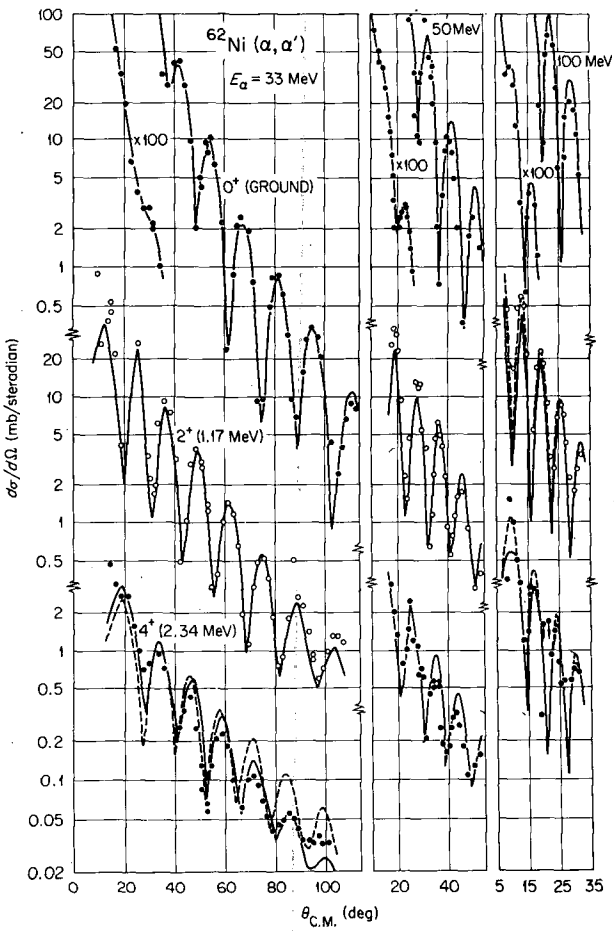

FIG. 6. Example of coupled-channels fit to (α, α') data.

changing the sign of this admixture is completely out of phase with experiment. The 0^+ and 4^+ angular distribution is quite structureless, which means that the admixture of one-phonon type amplitude into these states is not very large. Similar fits and conclusions were obtained for ^{112}Cd and also for ^{106}Pd and ^{108}Pd [16].

In obtaining these curves, good optical parameters were found first by fitting the elastic cross-section. The depth of the imaginary potential, W_D, fixed in this way is used in the excited channels, but a value 20% smaller is used in the elastic channel since we can keep fitting the elastic cross-section in this way.

Let us now look at the β values fixed in this way which are summarized in Table I. β_2 is in accord with the Coulomb excitation value. On the other hand, the values of β_{21}, which is the measure of the strengths of the coupling of the one-phonon 2^+ state and a two-phonon state of spin I, are all smaller than β_2. How small they are is a measure of the extent to which

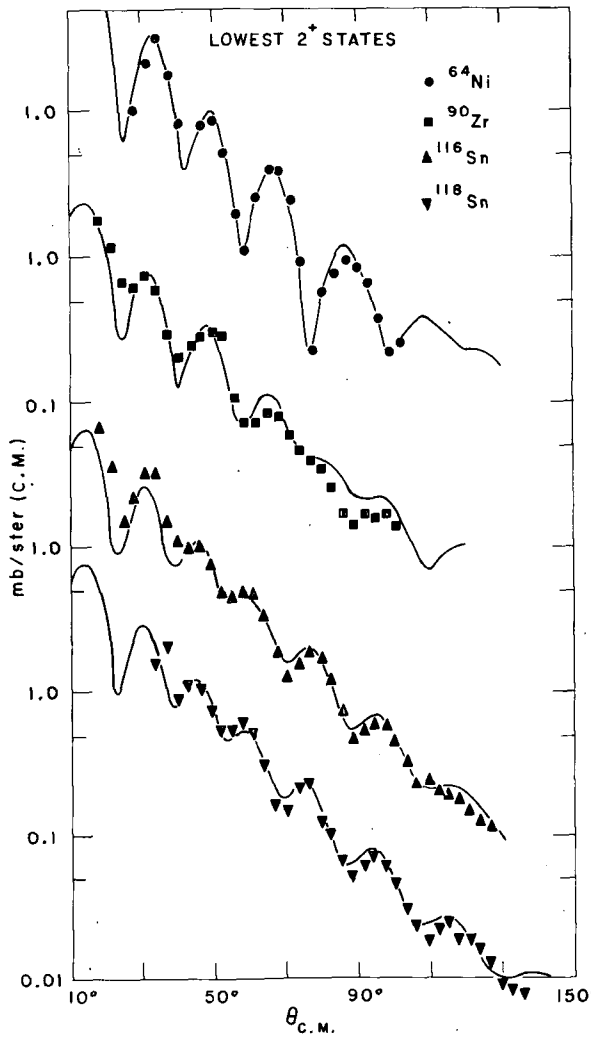

FIG. 7. Typical (t, t') data to 2^+ states and DWBA fit.

the ideal two-phonon description is destroyed. That β_{2I} are smaller than β_2 has been known for a long time from the Coulomb excitation analyses [17]. However, a surprising fact is that all the β_{2I} values obtained from the (p, p') fit are much smaller than the corresponding values of the Coulomb excitation, which are also shown in Table I. Thus if the (p, p') value is taken literally, it means that the two-phonon nature is much more destroyed than would have been thought from the results of Coulomb excitation.

One possible source of ambiguity in reaching this conclusion is again whether our choice of W_D was correct or not. If, somehow, larger values of W_D are to be used in the two-phonon channels, correspondingly larger values of β_{2I} are to be assumed to keep fitting the (p, p') data. In other words, one may ask how strong W_D has to be in the two-phonon channels,

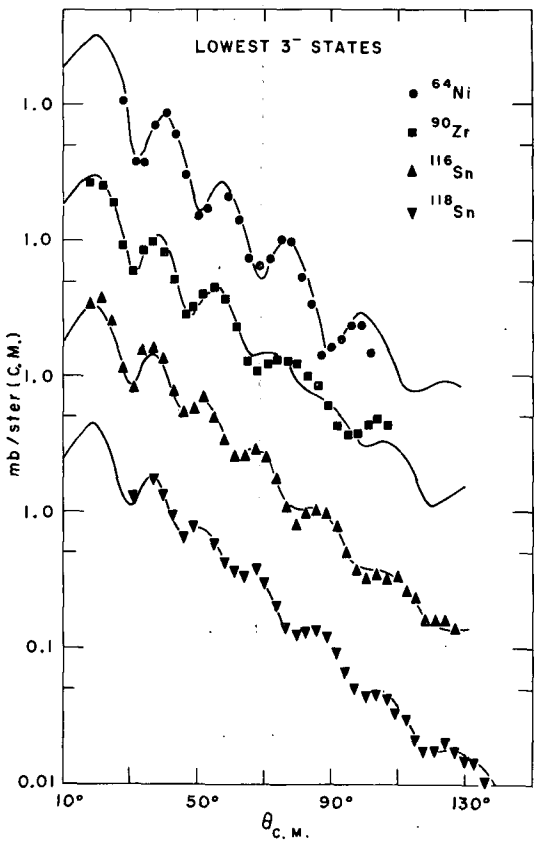

FIG. 8. Typical (t, t') data to 3^- states and DWBA fit.

if the Coulomb excitation β_{2I} were to be used. The quantity called C_I in Table I is the correction factor to be multiplied into the elastic channel value of W_D. As is seen, they are all of the order of 1.5 - 1.6 when the Coulomb excitation β_{2I} is used. This means that 20 or 30% stronger W_D must be assumed in the two-phonon channels than in the lower phonon channels.

In this way the present analysis presents the very challenging theoretical problem of describing the nature of vibrational nuclei in a microscopic way. Namely, we have to be able to explain either why the parallelism of the Coulomb excitation and the (p, p') process is destroyed to this large extent, or why W_D taken for the two-phonon channel is so large compared with W_D taken for lower channels.

Another point to be noted is that the value of β_{02}'' necessary for a good angular distribution of the second 2^+ cross-section is rather large, and, if it is taken literally in calculating the B(E2) from this 2^+ to the ground state, the latter is much too large compared with experiment. One possible way out of this difficulty might be to consider that a one-step transition with a spin-flip contributes to the (p, p') process. Whether such a conjecture is correct or not will again be answered only after accurate microscopic wave-functions are found for the excited states of vibrational nuclei.

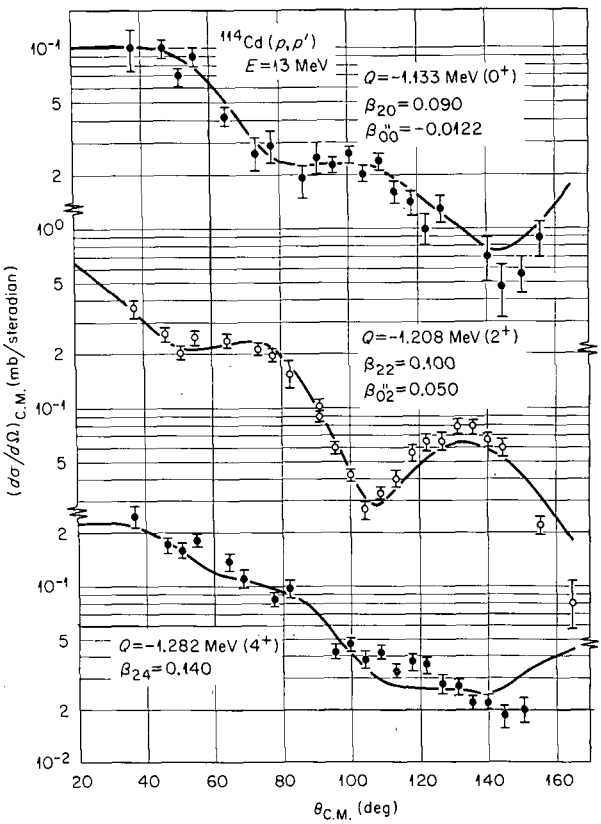

FIG. 9. Coupled-channels fit to (p, p') cross-section from two-phonon states in ^{114}Cd.

Another thing to be noted is that the sign of β''_{02} is definitely known to be positive for both ^{112}Cd and ^{114}Cd, and also for ^{106}Pd and ^{108}Pd. This fact seems to allow us to make an interesting comment on the extraction of the static quadrupole moment, Q_2, of the first 2^+ state of these nuclei. As is well known [18], the theoretical Coulomb excitation cross-section of the 2^+ state calculated up to second order consists of three terms: the first order term, the reorientation term and the interference term. The latter term comes from the process in which the second 2^+ state is excited and then de-excited to the first 2^+ state. The magnitude of this term can be determined rather accurately using the experimental cross-sections to excite the second 2^+ state, but the sign of this term is not determined this way. However, the value Q_2 extracted depends quite strongly on this sign. At present an ambiguity of about 30% is attached to Q_2 because of this ambiguity. This figure may be reduced to 10% or so, if the sign of the interference term is known.

If our model is taken literally, then a short calculation shows that the sign of this term is the same as that of β''_{02}. Since we know that β''_{02} is positive, the interference term is also positive. It should be noted that irrespective of the sign of this term the extracted Q_2 is always negative for the Cd and Pd isotopes, but its magnitude is concluded to be larger for positive sign of this term than otherwise.

TABLE I. β VALUES USED IN DATA FITTING.
For each nuclei, β's in the first column were obtained for a fixed value of $C_I = 1.2$, while in the second column β-values known from Coulomb excitation were used and C_I was searched for. C_I is defined such that W_D in channel of I^+ two-phonon state equals C_I times W_D in the elastic channel. For ^{112}Cd and ^{114}Cd, β_2 was taken as 0.20 and 0.18, respectively.

		^{112}Cd		^{114}Cd	
		β(pp')	$\beta_{C.E.}$	β(pp')	$\beta_{C.E.}$
	β_{20}	0.094		0.090	0.117
0^+	β''_{00}	-0.0097	No data for $\beta_{C.E.}$	-0.0122	-0.0122
	C_0	1.2		1.2	1.5
	β_{22}	0.100	0.173	0.100	0.140
2^+	β''_{02}	0.054	0.050	0.050	0.060
	C_2	1.2	1.65	1.2	1.6
	β_{24}	0.120	0.180	0.140	0.170
4^+	β''_{04}	0.010	0	0	0
	C_4	1.2	(1.6)	1.2	1.5

Since this statement is based on a completely phenomenological model, it is not certain how seriously it should be taken. Also, it is known that by bombarding a given target with different projectiles and different energies the sign of this term can be determined within the framework of the Coulomb excitation. Nevertheless, it is interesting to observe that the Coulomb excitation and the (p, p') process are interrelated in this way.

Concerning the vibrational nuclei, one interesting inquiry to be made is whether there exist states that can be called three- or four-quadrupole-phonon states. To my knowledge, so far no state has been definitely identified as such, although a few states in several nuclei may be considered as possible candidates [19]. Generally speaking, the detection of three-phonon states may not be so easy; this is because they cannot remain purely as such states since they are surrounded by a fairly high density of quasiparticle type levels of the same spin and parity. One possible exception may be the highest spin state for a given number of phonons, and (α, nx) type experiments have indeed detected 6^+ states in Cd and Te isotopes [20]. To analyse (p, p') data from such a state will be quite interesting.

Contrary to the three-quadrupole states, the two-phonon states that consist of one quadrupole-phonon and one octupole-phonon [21] may survive the admixture of other states, because the density of negative parity quasi-particle states is expected to be comparatively sparse, for excitation

energies of about 2 MeV, and there exists evidence that such states do exist. To confirm, however, the nature of these states, as well as that of the three-quadrupole-phonon states, (p, p') data must be combined with some other data in order to know, for example, the spin. Unfortunately, it does not appear that such combined work has been done for any nucleus.

In passing, I would like to refer to recent work by Mermaz et al. [22]. In Fig. 10 the data of ^{32}S(d, d') are presented and are compared with the theoretical prediction obtained by performing coupled-channel calculations. As is seen, the very different nature of the two 2^+-state angular distributions are nicely reproduced by this calculation. I am not completely certain whether this interpretation of the 4.29 MeV 2^+ state as a two-phonon state is unique, but if this is the case, it is an interesting example to show that nuclei as light as ^{32}S can have a two-phonon state with a high purity.

The (p, p') process has hitherto not been used very extensively to investigate the nature of odd-A vibrational nuclei, and perhaps the only example is the work on ^{107}Ag(p, p') performed at Oak Ridge [23]. As we have seen, the analysis of the (p, p') data from even nuclei is already fairly complicated, and it is generally expected that the situation gets worse for odd-A nuclei, because of the core-particle coupling. However, the spin of the ground state of ^{107}Ag is 1/2, i.e. the valence proton occupies the $p_{1/2}$ orbit, which makes the core-particle coupling equal to zero, unless the excitation of this valence proton into higher orbits occurs. Therefore,

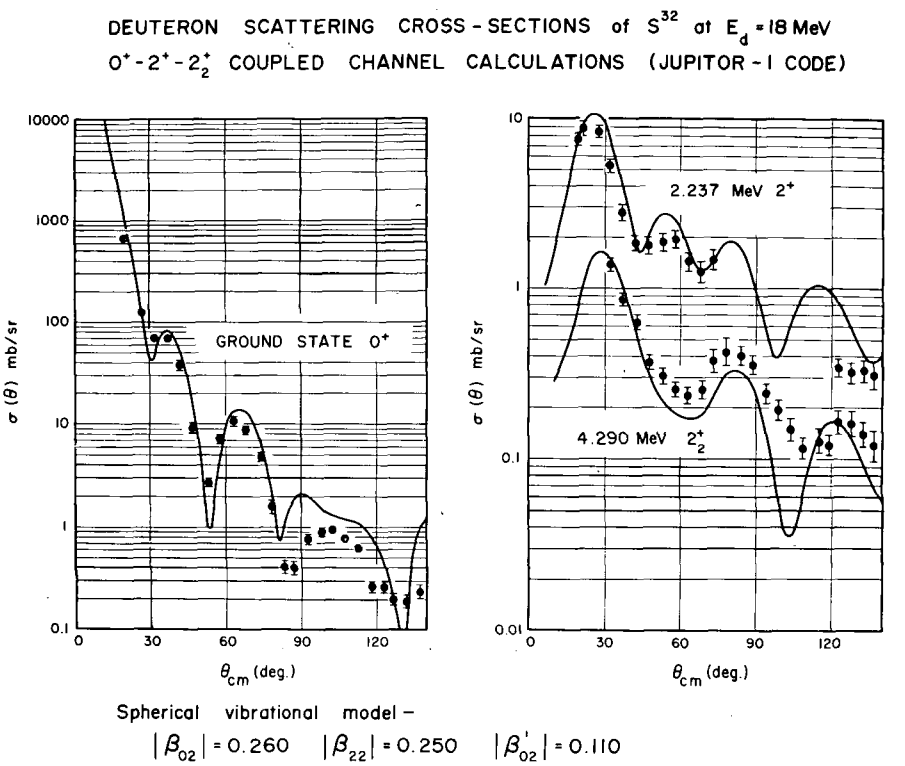

FIG. 10. Coupled-channels fit to (d, d') cross-sections from ground, one- and two-phonon states in ^{32}S.

one expects that the situation is comparatively simple and our results showed that this is in fact the case.

^{107}Ag is a nucleus which is bracketed by ^{106}Pd and ^{108}Pd in the periodic table. Thus we expect that its levels can be described in terms of the weak coupling model based on these nuclei as its core. Fig. 11 shows the levels of these three nuclei, and it is seen that the conjecture is correct to a good extent. In Fig. 12 we show as an example the angular distribution from the 950 keV level and the fit by coupled-channel calculations. We believe this level is described largely as $p_{1/2}$-proton coupled to the two-phonon 2^+ state in the core, and this conjecture may be supported by the fact that the angular distribution is remarkably similar to what we saw in the (p, p') cross-sections from two-phonon 2^+ states in Fig. 9. Similar results were obtained for states which are based on two-phonon 4^+ states.

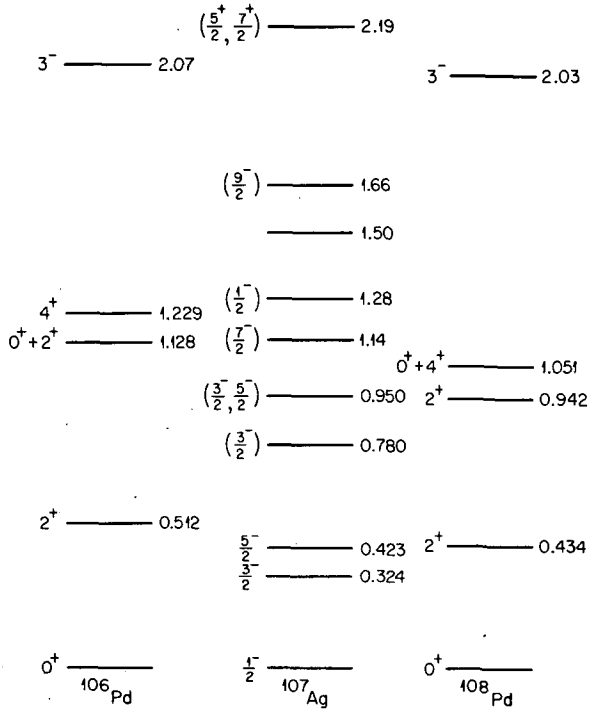

FIG. 11. Comparison of levels in ^{107}Ag and those in ^{106,108}Pd.

In this way we were able to parametrize the wave-functions of several levels of ^{107}Ag. These wave-functions were then used to calculate various γ-ray transitions, and fairly good agreement with experiment was obtained. Nevertheless, experimental facts exist which show that the valence proton does not occupy the $p_{1/2}$ orbit all the time. Thus the simple weak coupling model we used is too crude and the importance of the microscopic approach may again be invoked.

Much work has been reported on the microscopic analyses of inelastic scattering data [15], but generally speaking it is still in its infancy, in

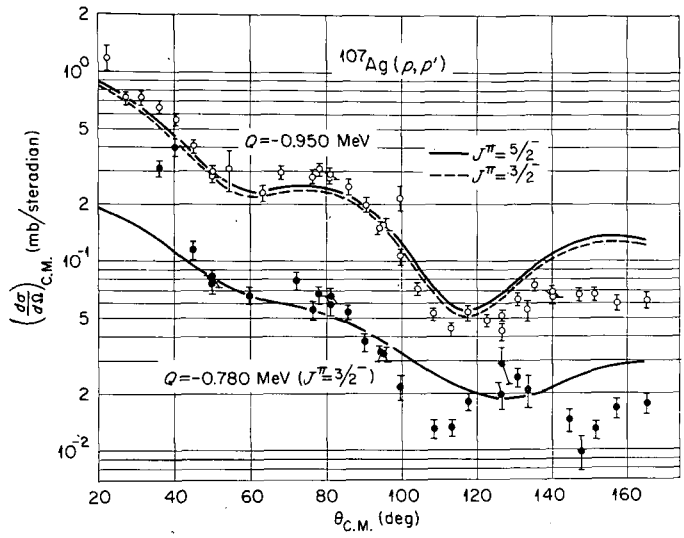

FIG. 12. Coupled-channels fit to (p, p') data from 950 keV state in ^{107}Ag.

particular in the sense that effort is still being put into clarifying its reaction mechanism rather than for using it to investigate nuclear structure. In many cases successful calculations were made for the one-step collective transitions, probably because many particle-hole transitions add up coherently in this case, and thus the resulting amplitude is insenstitive to various parameters involved in the theory. Success was also obtained in describing the excitation of almost pure one-particle-one-hole type states. However, if the excitation, for example, of a two-phonon-like state is concerned, the situation is not very good; here the lack of the knowledge of either or both good microscopic wave-functions and effective two-body interactions shows up badly. It should be noted that this is just where good microscopic theory is most urgently needed. A similar statement to the one I have made about the microscopic approach could also be made about the analyses of the (p, p') process based on the distorted wave impulse approximation (DWIA). One interesting finding recently made by Haybron [24] is that the theoretical (p, p') cross-section obtained by DWIA gets too small if the proton energy is less than 100 MeV or so. Since DWIA is known to be good at very high energy, such a result is not necessarily very surprising. Nevertheless it clearly indicates the importance of higher-order corrections, either in the reaction mechanism or in the evaluation of the two-body t-matrix elements, and thus seems to present an interesting theoretical problem.

I would like to touch very briefly on the scattering of nuclear particles from deformed nuclei. One noticeable piece of work done in the past year or so is the finding by the Berkeley group of the P_4-type deformation in rare-earth nuclei from the analysis of (α, α') data [25]. This, however, will be discussed in later sessions devoted to the structure of deformed nuclei, and I shall not go into it here.

Another piece of work which I want to refer to is the measurement of the total cross-section σ_t of neutrons from ^{165}Ho [26]. The neutron energy ranged from 2 to 135 MeV, and Fig. 13 shows the results. The Cd and Pb

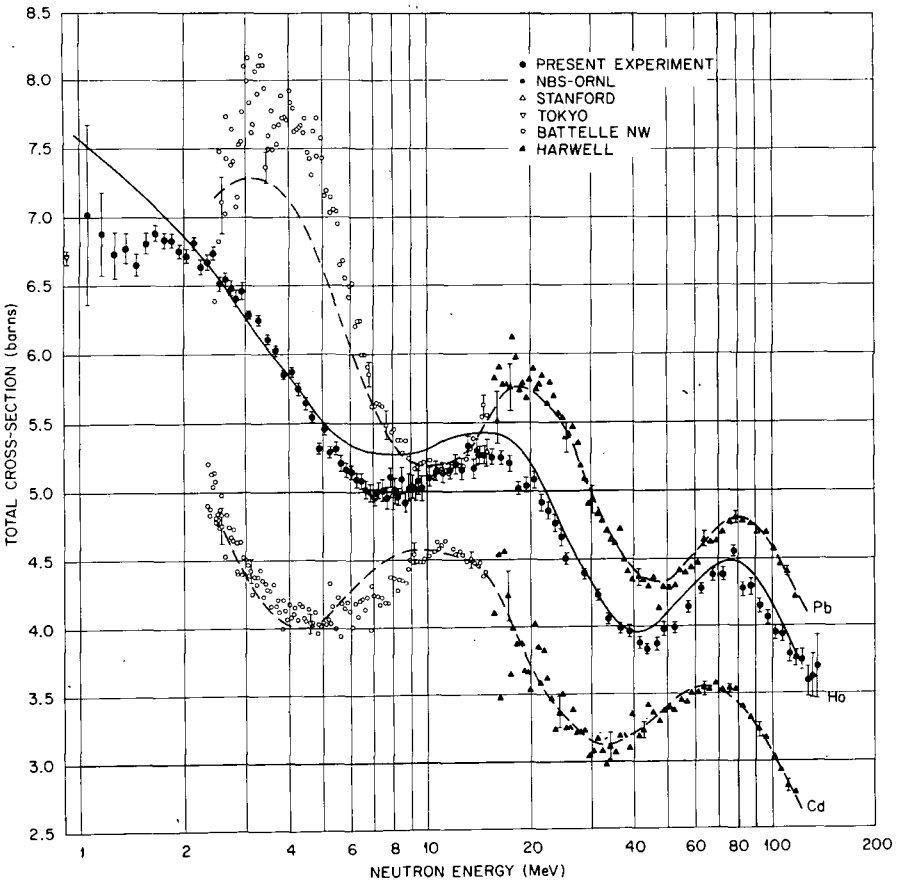

FIG. 13. Total cross-section of Cd, Pb, and ^{165}Ho for neutrons.

data were obtained by a Harwell group some time ago [27]. The theoretical fit to them is Perey's calculation, which he kindly made for us. There V, W and W_D were assumed to vary linearly with energy. Using Perey's parameters, σ_t was calculated for ^{165}Ho by using the adiabatic coupled-channel calculations [28], assuming that $\beta_2 = 0.33$. The fit is good except at around 10 MeV. The measurements and calculations of σ_t were also made for an oriented target, and the difference of this σ_t and that for an unoriented target, which we call the deformation effect, is shown in Fig. 14. The agreement between theory and experiment is very good.

To get an insight into what is happening, the same data were studied from the point of view of the nuclear Ramsauer effect. According to this [29], σ_t oscillates with energy because the product of the path length (which is the nuclear radius along the beam direction) times the difference of the wave numbers inside and outside the nucleus periodically becomes equal to integer multiples of π. If the target is oriented, the effective path length is changed from what it was for the unoriented target. Therefore the oscillatory nature of σ_t is modified, and this difference of the effective path

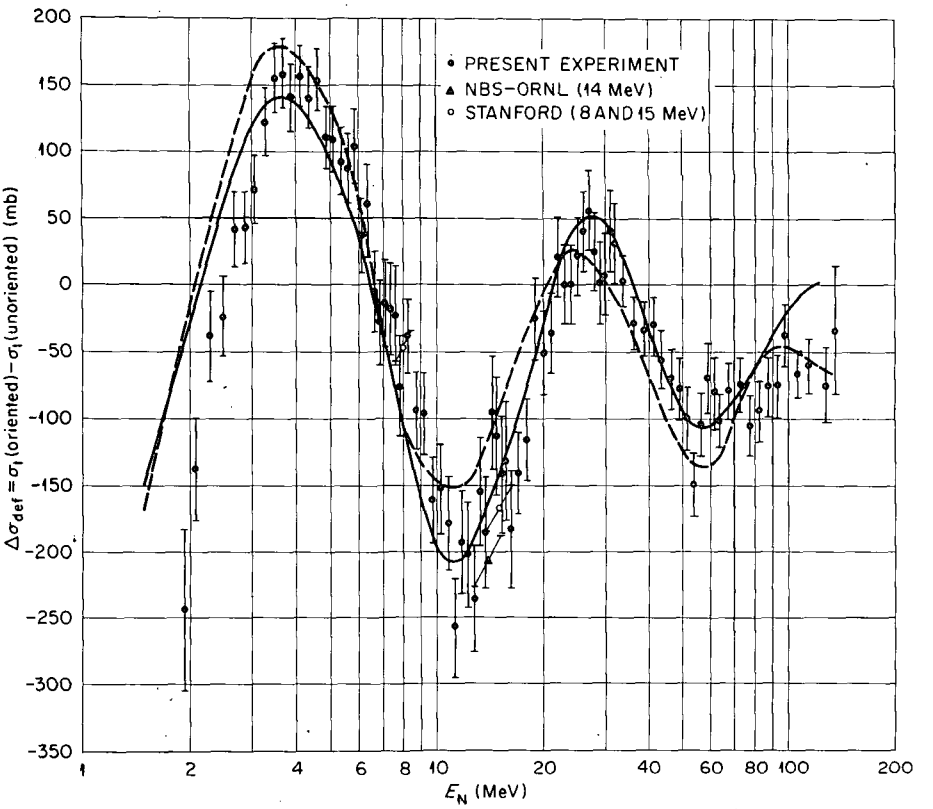

FIG. 14. Deformation effect in the total neutron cross-section for ^{165}Ho.

length gives rise to the deformation effect. With this fact in mind and then making a simple geometrical assumption on the target area, it is easy to to derive a formula which allows one to calculate the deformation effect from the known experimental σ_t for unoriented target. The dotted line in Fig. 14 is obtained in this way and, as is seen, it also reproduces the experiment quite nicely.

In reviewing the inelastic scattering problem, one thing that should not be excluded is the (p, p') process via the isobaric analogue resonance (IAR). Since the problems related to the analogue states are to be reviewed by Professor Temmer later in this Symposium, I shall only briefly summarize what is the present theoretical status of the analysis of IAR, as far as I understand it.

As is well known, the analysis of the (p, p') process via IAR can in principle give spectroscopic information on the excited states of the target. In particular, it is believed to give direct information on the particle-hole structure of these states. Already some intuitive arguments have been made along these lines, e.g. by Moore et al. [30], and it has been shown that such a conjecture is true. However, the construction of theories which allow detailed numerical analysis of the excitation functions and then the extraction of spectroscopic factors is still underway, and at present a large amount of experimental data are being left unanalysed. Nevertheless,

useful theoretical techniques have now been developed quite extensively, and it seems that we are almost ready to start detailed numerical calculations.

There are several possible approaches to this problem. One is the R-matrix theory [31]. This theory was used successfully by Robson [32] in his earliest paper on the (p, p_0) process via IAR. This theory has often been criticized, however, because it introduces a matching radius a, and the extracted spectroscopic factors are functions of it. This dependence on a can be removed in principle if the complete set of states defined in the internal region is included in all steps of the calculation, but clearly such a calculation is impossible. Recently Lane and Robson [33] invented a technique in which only a few eigenstates in the internal region are used, and the a dependence of the final result is largely removed. We expect that the application of this technique to IAR will be reported shortly by them.

Another method is the so-called shell-model approach to reactions, which was initiated by Fano [34] and may be considered as a special realization of Feshbach's general theory of nuclear reaction [35]. Many people have worked along these lines, but the most extensive development was made by Weidenmüller and his collaborators [36]. Unfortunately, however, Weidenmüller's work seems to have been based on a misconception of the behaviour of the proton in IAR, and thus many of the resulting formulas are useless, though not all.

In the shell-model approach, one first divides the total Hamiltonian into two parts: the one-body potential H_0, and the residual interactions V. It should be noted that this division is not unique, since a part of the one-body potential in the original Hamiltonian can be included in the residual interaction if this is found to be convenient.

In describing the IAR, the most ideal way to start is to write down the wave-function of the parent analogue state, and then operate the T_- operator resulting in the so-called 'ideal' analogue state. Since this T_- operator operates only on the isospin part of the wave-function, the spatial behaviour of the protons in the ideal analogue states must be the same as that of the corresponding neutrons in the parent analogue state. This means that at this stage the one-body potential to be used for protons must be the same as that used for neutrons. We know, however, that in addition to the fact that the Coloumb interaction exists for protons, the nuclear part of the one-body potential is much deeper for protons than for neutrons. (In fact, I believe that this is the reason why we get $T_>$ analogue states higher than the corresponding $T_<$ antianalogue states.) Thus in this approach the p-n potential difference plus the Coulomb interaction must be part of the residual interaction.

The ideal analogue state is a bound state by construction, its energy being equal to that of the parent analogue state if only H_0 is considered. We now take into account the residual interaction to re-evaluate the eigenenergy of this analogue state; then clearly it becomes higher than the eigenenergy of the parent analogue state just by Δ_C, the Coulomb energy for a proton. We thus get a bound state embedded in the continuum, which is a typical situation in Fano's theory.

We finally consider the coupling of this bound analogue state with the continuum via the residual interaction defined previously. The matrix element of this interaction between the continuum and the analogue state wave-functions gives the reduced width which we want to evaluate.

I have found that the formalism given by MacDonald and Mekjian [37], based on the K-matrix approach, is quite suitable for formulating the program I have just described, so I have taken their formulas as our starting point. Since the mathematical structure of the K-matrix theory is very much the same as that of the R-matrix theory, the derivation of the S-matrix elements from the K-matrix can be done fairly easily following the technique developed for the R-matrix theory by Lane and Thomas [31]. The final expression of the S-matrix is given in such a way as to allow a description of most of the important features known for IAR, such as the asymmetric nature of the resonance, and the fine structure superimposed on it. Also, the spectroscopic factor can be defined in exactly the same way as is done in DWBA for (d, p) processes. The (p, p') processes can be treated completely in parallel with the (p, p_0) process.

I said previously that the reduced width was defined as the matrix element of the residual interaction. I made this statement for simplicity, but it is not in fact correct. Since the residual interaction includes part of the one-body interaction, the so-called continuum-continuum interaction must be considered all the time, even if the original residual interaction had no two-body interaction. Consideration of the continuum-continuum interaction then forces us to introduce an effective interaction which should replace the original residual interaction in the evaluation of the reduced width. In this way the derivation of the effective interaction becomes the central problem of the numerical calculations in this approach.

The evaluation of the effective interaction is shown to be equivalent to evaluating a kind of Neuman series. In a paper treating the elastic scattering of neutrons by ^{15}N, Weidenmüller et al. [38] showed that such a problem can be handled by using a technique developed by Weinberg [39]. I thus reformulated this technique so as to make it applicable to our problem of IAR and thus the effective interaction was obtained. A computer program to perform numerical calculations along these lines has been written and tested in all but the very last stage. I thus hope we can begin to extract the spectroscopic factors very shortly.

REFERENCES

[1] See e.g., BASSEL, R.H., SATCHLER, G.R., DRISKO, R.M., ROST, E., Phys. Rev. 110 (1958), 1080.

[2] See e.g., TAMURA, T., Rev. Mod. Phys. 37 (1965), 679; TAMURA, T., Proc. Int. Conf. on Nuclear Structure, Tokyo (1968), 288.

[3] GREENLEES, G.W., PYLE, G.J., TANG, Y.C., Phys. Rev., to be published.

[4] SLANINA, D., McMANUS, H., Phys. Rev., to be published.

[5] SCHWANDT, P., HAEBERLI, W., Nucl. Phys. A110 (1968), 585.

[6] ROBSON, B.A., Phys. Lett. 26B (1968), 501.

[7] MAKOFSKE, W., SAVIN, W., OGATA, H., KRUSE, T.H., Phys. Rev., to be published.

[8] MAKOFSKE, W., SLAGOWITZ, M., SAVIN, W., OGATA, H., KRUSE, T.H., TAMURA, T., Phys. Lett. 25B (1967), 322.

[9] BRUGE, G., FAIVRE, J.C., FARAGGI, H., Nucl. Phys., to be published.

[10] AUSTERN, N., BLAIR, J.S., Ann. Phys. (N.Y.) 33 (1965), 15.

[11] TAMURA, T., Nucl. Phys. 73 (1965), 81.

[12] MERIWETHER, J.R., BUSSIERE DE NERCY, A., HARVEY, B.G., HOREN, D.J., Phys. Lett. 11 (1964), 299.

[13] ARMSTRONG, D.D., FLYNN, E.R., BLAIR, A.G. (Los Alamos), private communication.

[14] STELSON, P.H., ROBINSON, R.L., FORD, J.L.C., Jr., WONG, C.Y., TAMURA, T., Nucl Phys., to be published.
[15] GLENDENNING, N.K., Lectures of Varenna Summer School (1967), to be published; DICKENS, J.K., EICHLER, E., SATCHLER, G.R., Phys. Rev. 168 (1968) 1355; AGASSIANA, D., SCHAEFFER, R., Phys. Lett. 26B (1968), 703.
[16] ROBINSON, R.L., FORD, J.L.C., Jr., STELSON, P.H., SATCHLER, G.R., Phys. Rev. 146 (1966), 816.
[17] See e.g. McGOWAN, F.K., ROBINSON, R.L., STELSON, P.H., FORD, J.L.C., Jr., Nucl. Phys. 66 (1965), 97.
[18] ALDER, K., BOHR, A., HUUS, T., MOTTELSON, B., WINTHER, A., Rev. Mod. Phys. 28 (1965), 432; deBOER, T.J., EICHLER, H., Advances in Nuclear Physics 1 (1968), 1.
[19] YOSHIZAWA, Y., Phys. Lett. 2 (1962), 261; PRAMILA, G.C., MIDDLETON, R., TAMURA, T., SATCHLER, G.R., Nucl. Phys. 61 (1965), 448.
[20] LARK, N.L., MORINAGA, H., Nucl. Phys. 63 (1965), 466; BERGSTRÖM, I., HERRLANDER, C.J., KEREK, A., LUUKKO, A., Contribution to Tokyo Conf. (1967), 4-116; YAMAZAKI, T., Lectures of Varenna Summer School (1967), to be published.
[21] SAKAI, M., TAMURA, T., Phys. Lett. 10 (1964), 323; BABA, C.V.K., EWAN, G.T., SUAREZ, J.F., Nucl. Phys. 43 (1963), 264, 285; METZGER, F.R., Phys. Rev. 137 (1965), B1415; BHATT, K.H., Phys. Lett. 17 (1965), 282; LIPAS, P.O., Nucl. Phys. 82 (1966), 91.
[22] MERMAZ, M.C., WHITTEN, C.A., BROMLEY, D.A. (Yale Univ.), private communication.
[23] FORD, J.L.C., Jr., WONG, C.Y., TAMURA, T., ROBINSON, R.L., STELSON, P.H., Phys. Rev. 158 (1967), 1194.
[24] HAYBRON, R.M. (Oak Ridge), private communication.
[25] HENDRIE, D.L., GLENDENNING, N.K., HARVEY, B.G., JARVIS, O.N., DUHM, H.H., SANDINOS, J., MAHONEY, J., Phys. Lett. 26B (1968), 127.
[26] MARSHAK, H., LANGSFORD, A., WONG, C.Y., TAMURA, T., Phys. Rev. Lett. 20 (1968), 555; also, to be submitted to Phys. Rev.
[27] BOWEN, P.H., SCANLON, J.P., STAFFORD, G.H., THRESHER, J.J., HODGSON, P.E., Nucl. Phys. 22 (1961), 640.
[28] DROZDOV, S.I., J.E.T.P. 1 (1955), 588 and 591; BARRET, B.C., Nucl. Phys. 51 (1964), 27.
[29] PETERSON, J.M., Phys. Rev. 125 (1962), 955.
[30] MOORE, C.F., KULLECK, J.G., von BRENTANO, P., RICKEY, F., Phys. Rev. 164 (1967), 1559; see also BONDORF, J.P., von BRENTANO, P., RICHARD, P., Phys. Lett. 27B (1968), 5; LIEB, K.P., KENT, J.J., MOORE, C.F., Nucl. Phys., to be published.
[31] WIGNER, E.P., EISENBUD, L., Phys. Rev. 72 (1947), 29; LANE, A.M., THOMAS, R.G., Rev. Mod. Phys. 30 (1958), 257.
[32] ROBSON, D., Phys. Rev. 137B (1965), 535.
[33] LANE, A.M., ROBSON, D., Phys. Rev., to be published.
[34] FANO, V., Phys. Rev. 124 (1961), 1866.
[35] FESHBACH, H., Ann. Phys. (N.Y.) 5 (1958), 357; 19 (1962), 287.
[36] WEIDENMÜLLER, H.A., Nucl. Phys. A99 (1967), 269, 289.
[37] MacDONALD, W., MEKJIAN, A., Phys. Rev. 160 (1967), 730.
[38] GLÖCKLE, W., HÜFNER, J., WEIDENMÜLLER, H.A., Nucl. Phys. A90 (1967), 481; EBENHÖH, W., GLÖCKLE, W., HÜFNER, J., WEIDENMÜLLER, H.A., Z. Phys. 202 (1967), 301.
[39] WEINBERG, S., Phys. Rev. 131 (1963), 440.

DISCUSSION

A. BOHR: A possible reason for the different β-values obtained from the excitation of 2^+ and 3^- vibrations in different processes such as (p, p'), (α, α') and Coulomb excitation might be the isovector component in the deformed potentials. The strength of this component could be obtained from the studies of the excitation of the isobaric states in (p, n) reactions.

T. TAMURA: I see, but my main concern is in the ratio of β_{21}/β_2. For example, Coulomb excitation gives this ratio close to unity, while my (p, p') value is about half.

V. GILLET: From a microscopic point of view the surprising fact is not that there are differences between the β-values extracted from (p, p') data and those extracted from (e, e') scattering or Coulomb excitation, but that these are so similar in some of the cases you have presented. These processes involve quite different parts of the nuclear wave-function. For example, for Cd isotopes, the E-M excitations involve the 2-proton hole core components only, while (p, p') involve also the neutrons of the open shell.

T. TAMURA: I know that if you take microscopic description you would get different β-values for different projectiles. What I would like to see is somebody explaining the difference in a convincing, clear-cut way.

J. BANG: When the β_λ-values measured by Coulomb excitation and by inelastic scattering at higher energies are compared it is necessary for the charge distribution assumed in the calculations of Coulomb excitation to be realistic. This is trivial and so is the fact that the point is particularly important for the higher multipoles, but uniform distributions are in effect often used in the calculations.

T. TAMURA: I think your question is essentially the same as that of Dr Gillet, so my answer to him applies also to your question.

COLLECTIVE STATES IN CONTINUUM

V.V. BALASHOV
INSTITUTE OF NUCLEAR PHYSICS,
MOSCOW STATE UNIVERSITY,
UNION OF SOVIET SOCIALIST REPUBLICS

Abstract — Аннотация

COLLECTIVE STATES IN CONTINUUM. An analysis of the state of theory describing collective excitations of nuclei in the region of the continuous spectrum is given. Isobaric analogue resonance in heavy nuclei is considered as a special case of a collective state. The accuracy of the approximate methods used to calculate the nucleon resonance widths is estimated by the method of strong coupling of channels.

КОЛЛЕКТИВНЫЕ СОСТОЯНИЯ В НЕПРЕРЫВНОМ СПЕКТРЕ. Дан анализ состояния теории, описывающей коллективные возбуждения ядер в области непрерывного спектра. Как особый случай коллективного состояния рассматривается изобарический аналоговый резонанс в тяжелых ядрах. С помощью расчетов по методу сильной связи каналов оценивается точность приближенных методов, используемых для расчета нуклонной ширины резонансов.

The problem of collective states in continuum is handled under three main headings:

(1) Classification of collective states and the means for their excitation and study.

(2) Damping of collective excitations as an effect of coupling with states of a different nature.

(3) Collective states in continuum as an effect of the strong coupling of channels; the decay involving particle emission.

I

The classification of states is not difficult. This may be done on a simple formal basis, according to the rank of the spatial, spin and isospin parts of operators which excite these states when acting on the ground states of a nucleus:

$$\hat{Q}_{kl}(sq) = \sum_i \rho_l(r_i) \sum_q [Y_e(i) \times \sigma^s(i)]_k \cdot \tau^q(i); \quad s = 0; 1; \quad q = 0; 1; \quad \vec{k} = \vec{l} + \vec{s}$$

(for example, q = 0 are the isoscalar excitations; q = 1 are the isovector excitations; s = 1 are the processes with spin flipping, etc.). The general structure of operators

$$\hat{Q}_{kl}(sq) = \sum_{i=1}^{A} \hat{Q}_{kl}^{(i)}(sq)$$

is determined by the additive character of outer perturbations with respect to the nucleons of a nucleus ("impulse approximation"). When discussing

such processes we confine ourselves to the collective states where excitations of the particle-hole type form the basis.

The best known and most important example of such states is the dipole giant resonance of photoabsorption [1]. For a long time photonuclear reactions were practically the only means of studying the collective excitations of nuclei in continuum. But at present the idea of the giant resonance is widely used in other fields, both close to photonuclear reactions and a long way from them. It is interesting that the problems of high-energy nuclear physics are now among the main stimuli in investigating the structure of various giant resonances. In what ways can these investigations be promoted?

First, the excitation and decay of collective states are of particular importance for the processes of nuclear disintegration in elementary particle absorption. Here the excitation and decay compete strongly with the "direct" mechanism of disintegration. The relation between the direct and resonance mechanisms of disintegration is one of the main problems of the μ-capture theory [2]. Several questions of weak interaction theory depend on the solution of this problem. The same problem is involved in such theories as the π-meson radiation capture theory [3] and the π-meson photoproduction theory [4].

There is a certain analogy between the processes of μ-capture and the photodisintegration of nuclei. This analogy, however, makes it possible to establish certain quantitative relations between the probabilities of the two processes only in some specific cases (in practice these are only the lightest "alpha-particle" nuclei). In dealing with medium and heavy nuclei, the states excited in the photoeffect and μ-capture only partially overlap — the less so with increasing A [5]. Even the dipole portion of the transitions in μ-capture does not correspond to the whole dipole giant resonance of photodisintegration but to its upper weak branch with isospin which exceeds the isospin of the ground state by unity: $T = T_> = T_0 + 1$ (see Fig.1).

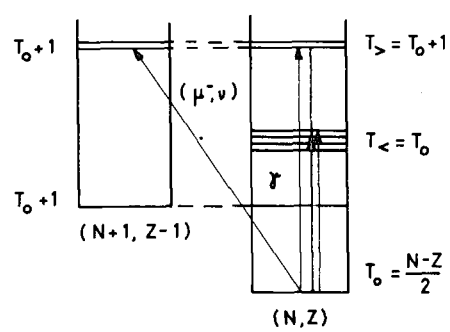

FIG.1. Schematic relation between dipole transitions in muon capture and photoeffect.

Thus, the use of the idea of the giant resonance in μ-capture theory and in other similar processes has inspired the search for direct ways of finding the appropriate collective states.

Another urgent problem of high-energy nuclear physics involves a similar program. I have in mind the prospects of using complex nuclei as a selector of individual mechanisms (amplitudes of elementary particle

interaction with nucleons). The special purpose of such an approach is to test various one-boson exchange models for describing the amplitudes of elementary particle scattering [6, 7]. From this viewpoint, the collective excitation of various types is associated with the exchange of various intermediate bosons. The excitation structure determines the structure of the corresponding vertex parts which, for the impulse approximation, may be directly expressed through the matrix elements of the transitions.

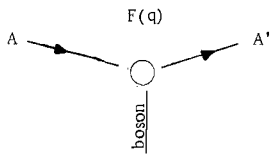

$$\longrightarrow \quad \langle \Psi_{A'} | \sum_{i=1}^{A} Q_{kl}^{(i)}(sq) \, | e^{i\vec{q}\vec{r}_i} | \, \Psi_A \rangle$$

Thus the problem of the collective excitation of a nucleus is added to the problem of "complete experiment" for determining the characteristics of a nucleus as an "elementary particle" [8].

The most obvious way of exciting and studying collective states in continuum is the inelastic scattering of electrons and protons. In either case the dipole giant resonance is strongly excited but at this resonance the levels of the spin-wave resonance are also excited in the same region. These levels correspond in the even-even nuclei to the states 0^-, 1^- (with spin flip) and 2^-. The excitation of these levels in the case of electron and proton scattering has been repeatedly discussed within the framework of the shell particle-hole approach [9] and it has been shown that this excitation may be described on the same basis and with about the same accuracy as the usual dipole excitation. No special problems are seen here at present.

The study of highly excited collective states in medium and heavy nuclei presents much greater difficulties. In this case the data on inelastic electron scattering are absent altogether (only quite recently have the first theoretical calculations been performed [10]). As regards the photoeffect, even in this problem, which has been much studied, the important questions remain unsolved: a reliable way of investigating the quadrupole absorption of γ-quanta has not been evolved; the overlapping character of the main branches of the dipole oscillation with $T = T_0$ and $T = T_0 + 1$ is obscure; it is not clear to what extent the overtones of the dipole oscillations are important. These questions were discussed in detail in 1967 at the First International Conference on Electromagnetic Interactions at Dubna but no great progress has been noted since then.

Just recently, the first experiments were carried out [11] bearing on the charge exchange (n, p) reaction. The use of neutrons with high energies (higher than hundreds of MeV) at high (of the order of 1 MeV) monochromaticity of the beam lends great value to this reaction from the viewpoint of the above-mentioned "complete experiment". This reaction is of special importance as an addition to inelastic scattering reactions in order to separate individual types of collective excitations in the medium and heavy nuclei corresponding to different values of isospin. In the absence of strong spin-flip effects the (n, p) reaction might be a direct means of studying the upper branch of the dipole oscillations in heavy nuclei which, according to present opinions, is associated with the maximum of the (γ, p) cross-section. However, this may unfortunately

not be true. In the Moscow State University, Karapetyan, Korenman and Yadrovsky recently estimated [12] the (n, p) reaction on the ^{90}Zr nucleus for neutrons with energies of 150 MeV. The excitation spectra of the ^{90}Y residual nucleus, calculated in the framework of the impulse approximation for small angles of proton escape, show (see Fig.2) that in this reaction the spin-flip transitions will be most strongly excited including the levels 1^- whose analogues in the target nucleus are not the levels of the dipole excitation but the spin-wave resonance $J = 1^-$; $T = T_0 + 1$, which is 3 MeV higher than the maximum of the (γ, p) reaction.

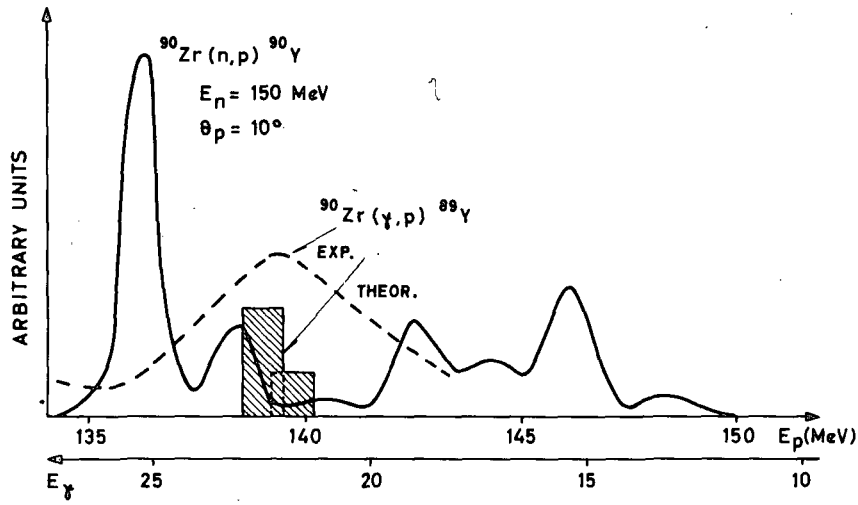

FIG.2. Calculated excitation spectrum in the $^{90}Zr(n,p)^{90}Y$ reaction at 150 MeV compared with experimental data for the $^{90}Zr(\gamma,p)^{89}Y$ reaction and theoretical calculations for the dipole excitation in zirconium with isospin $T_>$.

Virtually, study of complex giant resonances in medium and heavy nuclei has not yet started. It is hardly likely that their explanation will require a theory differing from the theory of the photoabsorption giant resonance. In any case, experiments are urgently needed.

II

Let us turn now to the theoretical problems. The main trend of recent theoretical studies in the field under consideration is the inclusion of the specific character of the formation of collective excitations in continuum which is due to the presence of a number of open channels. For this purpose, various methods were used for solving the general equations of the many-channel scattering problem. These equations were simplified by using a limited set of channels with the help of general ideas of the shell model. With such an approach the resonances for the reactions, including more intensive resonances corresponding to the collective excitations, appear "automatically" as an effect of the channel coupling. One usually considers the particle-hole excitations in the continuum of double magic nuclei ^{12}C, ^{16}O, ^{40}Ca. Despite the variety of approaches, the common

problems are solved. These are the scattering and charge exchange of nucleons on the "hole" nuclei (in practice on ^{15}N) [13, 14], the dipole photoeffect [15-18], and the excitation of the dipole giant resonance by electrons [19, 20]. The calculations of nuclear disintegration at μ-capture [21] are also involved here. We have just finished work on a unified description of the quasielastic (with nucleon knock-out) and inelastic (with excitation of many-particle resonances) scattering of high-energy electrons [22].

As regards the long-term (4-5 years) activity of various groups in this field, it is of interest now to go back to the original sources.

The main stimulus for the development of the modern theory of collective states in continuum was the absence of a unified description of the direct and resonance processes in reactions. In addition, some dissatisfaction was caused by the fact that within the framework of the shell particle-hole approach, generally accepted earlier, the interpretation of highly excited states of a collective nature in no way differed from the consideration of low (for example quadrupole) collective states. In such an approach, the one-particle functions of an infinite well (infinite rectangular well, Nilsson functions) were often used, which was especially inadmissible when describing states in the region of continuum. In particular there were objections to the combination of the reduced width method for calculating the decay of states and the diagonalization method of configuration mixing in continuum.

An analysis of the results obtained within the framework of the new approach shows that in some cases this approach to some extent refines the old shell approach and brings the results of the calculation closer to experiment. This statement concerns the form-factors of inelastic electron scattering and the probability of μ-capture. The new approach makes it possible to include more naturally the mixing of individual dipole levels for the isospin, which results in an additional structure of the giant resonance, etc. However, in the light of the most urgent problems relating to the nature of the collective states these improvements may not seem so important. Of greater importance is the fact that the new calculations roughly repeat the results of the simpler old shell-model approach, thereby substantiating it to a certain extent. These calculations give almost the same position of resonances as the old approach and the widths of the resonances appear to be in qualitative agreement with what may be obtained by using the diagonalization procedure and reduced width method. In this case the disagreement with experiment is still much greater than the difference between the theoretical results (it will be noted once more that these conclusions are drawn from calculations for light nuclei).

It becomes more and more obvious that the main defect of the classical particle-hole approach to the description of collective states in continuum does not lie in the fact that the specific character of formation of these excitations, due not only to the close channels but also to the open ones, was not taken into account. The particle-hole excitations are strongly coupled with other states of a more complex nature (two particles - two holes, etc.). This coupling destroys the coherence of motion of individual nucleons, thus resulting in a complex structure of the collective resonance and an increase in its width. Of course, in the case of a strict approach these states should also be considered by taking the specific character of continuum into account. Such generalizations of the theory of particle-

hole excitations in continuum have been made by Gillet et al. [23] and by the author and colleagues in the Moscow State University [24]. It seems to me, however, that such a technically subtle procedure diverts attention from the main difficulties of the theory. The difficulties arise not from the techniques of including individual complex states but from the fact that it is not quite clear which states determine the spread of the collective excitation, at what frequencies they are located, and (which is of greatest importance) whether an especially strong successive coupling of the two holes - two particles states with even more complex states takes place.

The microscopic theory of the damping of collective particle-hole excitations in nuclei was based on estimates of the coupling between the dipole and quadrupole (surface) oscillation [25]. At present Greiner's group has used great skill in calculating this coupling and has calculated the cross-section of the dipole photoabsorption in a number of nuclei using the method of direct diagonalization of the collective Hamiltonian in the space of the states which contain a large number of quadrupole phonons [26]. Much work on the theory of damping of collective states is being done by Yudin's group [27]. In particular, this group has shown that not only quadrupole oscillation but also other collective states with a higher multipolarity (of the types 3^- and 5^-) may strongly affect the form of the dipole resonance. Investigation of the connection between various modes of collective nucleon motion in nuclei has become a widespread problem of microscopic theory. This trend, as applied to the photoeffect, cannot be estimated until the energy distributions of the photoproducts and the relation of the branches of the main reactions (γ, n) and (γ, p) are considered on this microscopic basis. The spectra of the photoprotons and photoneutrons calculated within the framework of the particle-hole model appear to be too hard. It is clear that the widening of the dipole absorption curve causes a softening of these spectra and draws their form closer to the statistical one which is characteristic for the evaporation models.

III

The problems of describing the real (with nucleon emission) decay of collective dipole states are closely associated with the problem of their damping - spread over states of a different nature. One would imagine that the two main questions are also strongly interlinked with the problem of quadrupole resonance, giant resonances of spin-wave excitation, etc. To study the problem of the decay of collective states in a pure form one should seek examples of those selection rules which break the coupling of these states with the background of states of a different nature which surround them. At present, we know only one such example: the isobaric analogue states of the ground and lower excited levels of heavy nuclei which are located in these nuclei much higher than the threshold of their nucleon decay.

Isobaric resonances of such a type are an excellent example of the collective state with typical effects of the coherent contribution of various particle-hole excitations - in this case, excitations of the "neutron hole - proton" type. This aspect of the problem has been dealt with very little in the many works on analogue states and therefore I shall discuss it at

greater length. I repeat once more that I am interested in analogue resonances as a unique opportunity to study, in the pure form, the general problem of the decay widths of collective states in heavy nuclei. The microscopic (many-particle) theory of these resonances has gone through several stages. Let us consider them briefly using the classical example, namely the analogue of the ground state of the ^{208}Pb nucleus which may be observed during proton scattering on the ^{207}Pb nucleus as a narrow (of the order of 250 keV in width) resonance of the compound nucleus ^{208}Bi (see Fig.3).

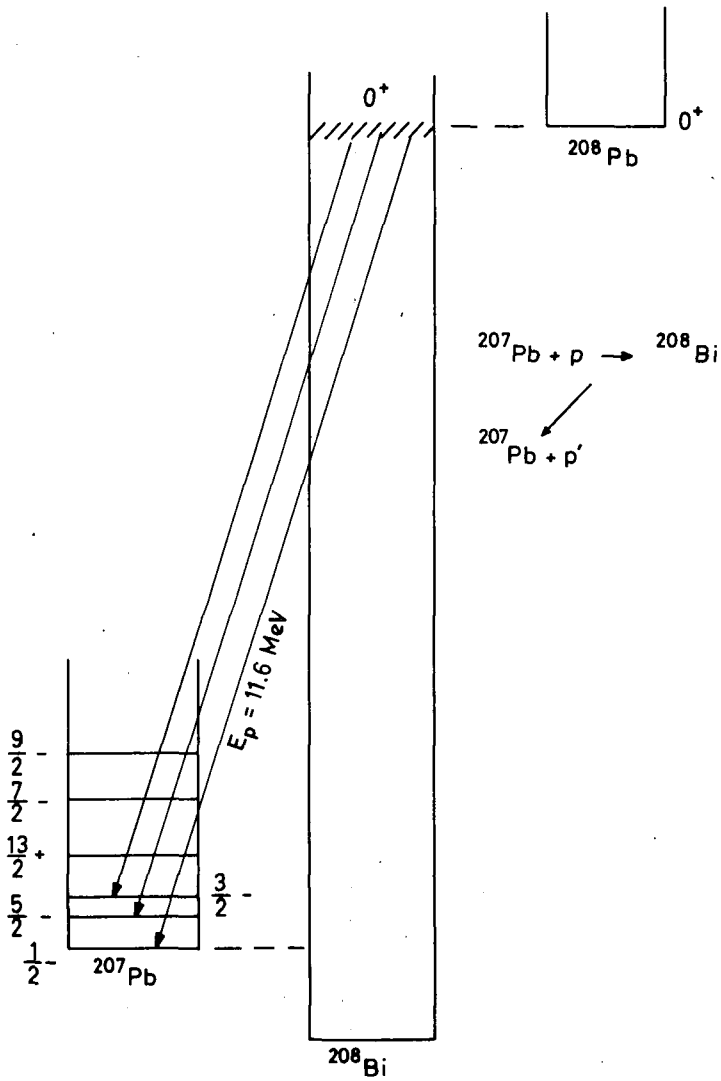

FIG.3. Schematic diagram of excitation of the analogue of the ground state of ^{208}Pb in elastic and inelastic scattering for ^{207}Pb + p.

Assuming from the very beginning that the isospin is conserved, the simplest way is to construct the wave function of the ^{208}Bi nucleus in the isospace:

$$\Psi\,(^{208}\mathrm{Bi};\ 0^+) \sim \hat{T}^{(-)}\ \Psi\,(^{208}\mathrm{Pb};\ 0^+)$$

With such an approach the problem of the energy position of the analogue resonance is absent: it is completely determined by the Coulomb shift; this fact agrees with experiment. The wave function $\Psi\,(^{208}\mathrm{Bi};\ 0^+)$ appears to be entirely determined by the superposition of elementary particle-hole excitation:

$$\Psi\,(^{208}\mathrm{Bi};\ 0^+) = \sum_j \sqrt{\frac{2j+1}{2\,T_0}}\ \left| j^{-1}(n)\, j\,(p) : 0^+ \right\rangle$$

According to the method of construction, this function absorbs the whole sum of the transitions caused by the charge exchange operator $T^{(-)} = \sum_j a_j(n)\, a_j^{\dagger}(p)$ and in this sense it is a function of the collective excitation with respect to this operator. The latter expression immediately gives the reduced widths of the proton decay into various hole levels of the target nucleus ^{207}Pb:

$$\theta_p = \sqrt{\frac{2j+1}{2\,T_0}}$$

If the one-particle widths of the decay $\Gamma_j^{(0)}$, which depend on the penetration factors, the channel radius, etc., are known one may obtain the decay widths:

$$\Gamma_j = \Gamma_j^{(0)} \cdot \theta_p^2$$

Such a procedure was adopted by Anderson et al. [28] and resulted in qualitative agreement with experiment.

The next step [29] was the rejection of the initial assumption about the conservation of the isospin in the excited state and the usual diagonalization calculation of the whole spectrum of bound quasistationary states 0^+ in the ^{208}Bi nucleus on the basis of configurations $\left| j^{-1}(n)\, j\,(p) : 0^+ \right\rangle$. To zero approximation the particle-hole levels occupy a narrow band in the range of 3.0-4.5 MeV. The inclusion of the particle-hole interaction $\hat{V}_{ph}$ results in an anomalous escape of one of the states from this range. This is a typical Brown-Bolsterly effect [30]. The matrix elements of the particle-hole interaction are properly correlated with the matrix elements of the excitation operator:

$$\left\langle j_1^{-1}(n)\, j_1\,(p) : 0^+ \left| \hat{V}_{ph} \right| j_2^{-1}(n)\, j_2\,(p) : 0^+ \right\rangle \sim \sqrt{2j_1+1} \cdot \sqrt{2j_2+1}$$

The collective level absorbs more than 98% of the total intensity of the transitions $^{208}Pb - ^{208}Bi$ and it is natural that the reduced widths relating to this level prove to be close to those calculated in the scheme of pure isospin (Table I).

Now as regards the problem of finding the one-particle proton widths $\Gamma_j^{(0)}$: in the work by Anderson et al. [28] these widths were calculated using an artificial technique the reliability of which is difficult to estimate. We have not found another method for calculating them correctly except by confining the whole problem within the framework of the strict mathematical problem of the coupling of channels in scattering [31]. With such an approach another defect of the old description (separation of the inner and outer regions of a nucleus) may also be avoided.

The total wave function of the system $^{207}Pb + p$ is sought at each energy value in the form of the expansion

$$\Psi_E = \sum_j \varphi_j (r_h) \cdot f_j (E, r_p)$$

where $\varphi_j (r_h)$ are the functions of the holes and $f_j(E, r_p)$ are the sought wave functions of a proton in the appropriate channels. All the channels are open and this fact determines the asymptotic form of the functions $f_j^{(i)}$:

$$f_j^{(i)} (E, r_p) \Big|_{r_p \to \infty} \longrightarrow [G(k_j r_p) - iF(k_j r_p)] \delta_{ij} - S_{ij} (E) [G(k_j r_p) + iF(k_j r_p)]$$

where G(kr) and F(kr) are the Coulomb functions. For the functions $f_j(E, r_p)$ we obtain the system of coupled linear equations. Of course, this system is reduced according to the total angular momentum of the system $^{207}Pb + p$. For the state 0^+ we arrive at a system of six coupled differential equations, according to the number of hole levels of the ^{207}Pb nucleus: $3p_{1/2}$, $2f_{5/2}$, $3p_{3/2}$, $1i_{13/2}$, $2f_{7/2}$, $1h_{9/2}$.

$$[\hat{H}_j - (E - \epsilon_j)] f_j (E, r_p) = -\sum_k V_{jk} (r_p) \cdot f_k (E, r_p)$$

TABLE I. CALCULATIONS OF REDUCED WIDTHS FOR 0^+ ANALOGUE RESONANCE IN ^{205}Bi

θ_p	Diagonalization calculation [29]	$\sqrt{\frac{2j+1}{2T_0}}$
$p_{1/2}$	0.22	0.21
$f_{5/2}$	0.40	0.37
$p_{3/2}$	0.32	0.30

The Woods-Saxon one-particle potential is used as $\hat{H}_j$ (in this calculation it is without an imaginary part, as in Anderson's calculation).

It can be seen that this is the usual problem of channel coupling which has been developed in detail, for example, for application to nucleon scattering on deformed nuclei. A peculiarity of the case under consideration is the appearance high in the spectrum (10 MeV higher than the threshold and resonances of potential scattering) of a narrow collective resonance which is solely due to the coupling of the open channels between each other. In the calculation according to the method of distorted waves it is absent at all the channels; at a fixed (sufficiently high) coupling amplitude the resonance is successively shifted towards higher energies when new channels are included (see the scheme in Fig.4 for one of the inelastic scattering channels). To explain the shift qualitatively one may easily generalize the Brown-Bolsterly schematic model taking the asymptotic of the open channels into account.

By fitting the amplitude of the particle-hole interaction (it corresponds to the amplitude of δ-interaction $g = 1350$ MeV $\cdot$ fm^3 with exchange parameter $\alpha = 0.13$) one can obtain agreement on the position of this resonance with experiment. The curves of the cross-section of inelastic scattering with excitation of various levels of ^{207}Pb for the vicinity of the analogue

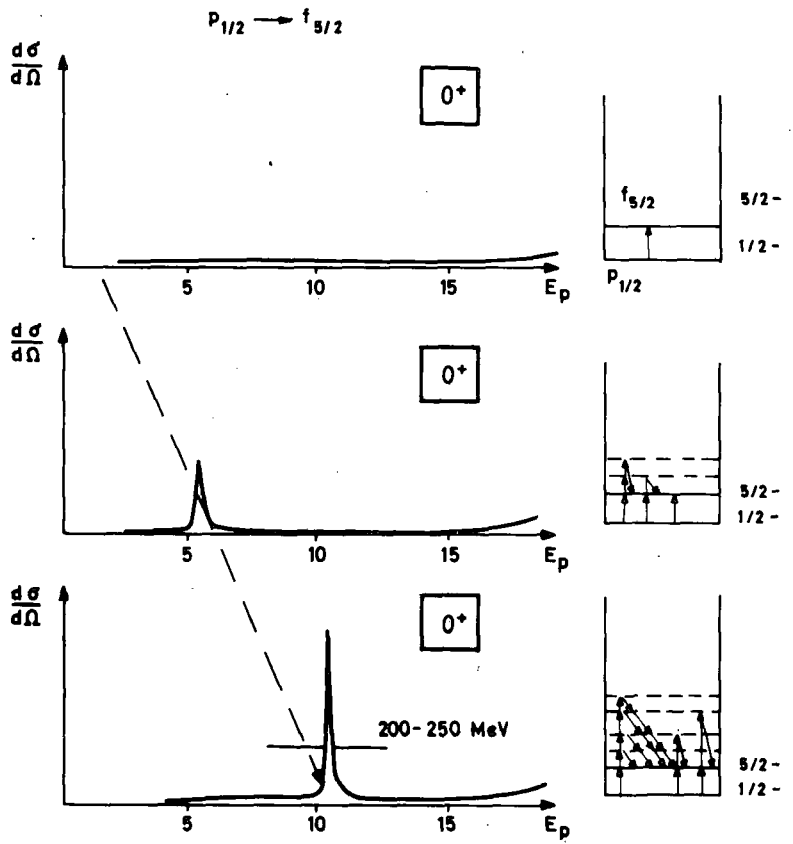

FIG.4. Effect of the number of the coupled channels in forming the collective resonance: schematic.

resonance are shown in Fig.5. In almost all the channels the resonance has an asymmetrical form. The resonance widths are mostly included in the calculation as parameters but if one approximates the resonance by the Breit-Wigner formula it is possible to obtain the proton widths Γ_j and the total width Γ_t, which, within the framework of this calculation, is the sum of the proton widths from the curves $\Gamma_p = \sum_j \Gamma_j$. The values of the widths as well as the experimental data and the results of calculation by Anderson et al. [28] are presented in Table II.

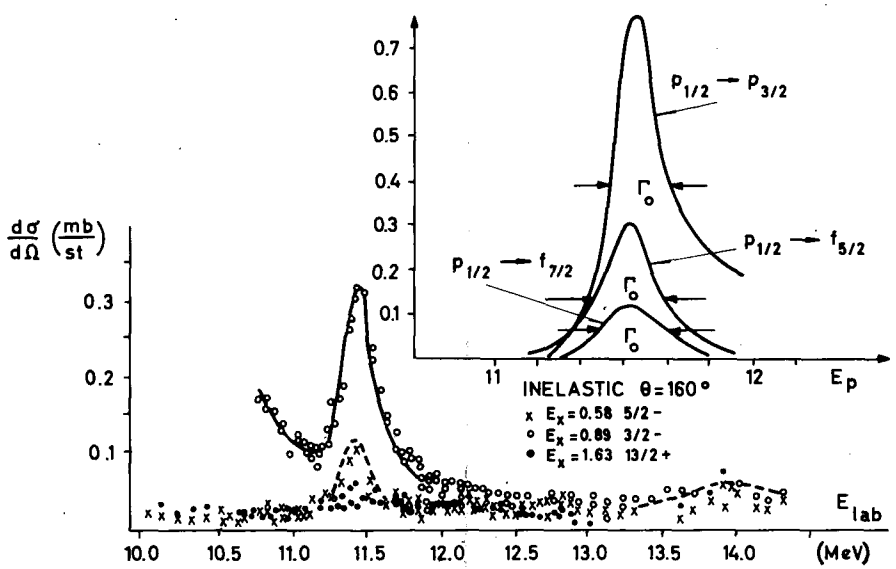

FIG.5. Inelastic cross-sections of the reactions $^{207}Pb(p, p')^{207}Pb^*$ in the region of analogue resonance 0^+. Upper diagram: close coupling calculations [31]. Lower diagram: experiment [33].

The calculated values of the proton widths are overestimated (on average by a factor of 2) in comparison with experiment. Similarly as in the calculations by Hill and Buck of the photoeffect in light nuclei [32], an imaginary part can be included in the Woods-Saxon proton potential; this would result in diminishing the proton widths. However, there is fundamentally some uncertainty about the use of the one-particle complex potential in the problem of particle-hole interaction.

A comparison of the above calculation with that by Anderson et al. and, to an even greater degree, with the diagonalization calculation [29], is especially important. The general agreement between these results (on an average within 50%) substantially confirms the validity of the simple diagonalization approach to the description of collective resonances even at such great shifts (of the order of 10 MeV) which are characteristic for heavy nuclei.

If one turns now to the most difficult problem of the spread of collective states in continuum over states of a complex nature, it might be suggested that when solving this problem one hardly needs to fear the specific effects of continuum.

TABLE II. PROTON PARTIAL WIDTHS FOR 0^+ ANALOGUE RESONANCE IN ^{208}Bi

^{207}Pb		Γ_j (keV)			
E^*	J^π	Experiment [26]	Pure isospin [26]	Diagonalization [29]	Close coupling [31]
0	$\frac{1}{2}^-$	66	60	60.3	81
0.57	$\frac{5}{2}^-$	19	16	17.3	38
0.89	$\frac{3}{2}^-$	44	74	79	92
1.63	$\frac{13}{2}^+$	-	0.4	0.3	7
2.34	$\frac{7}{2}^-$	-	8.8	9.5	15
3.63	$\frac{9}{2}^-$	-	-	-	0.3
	Γ_p	129	159	166	233
	Γ_t	220			

The microscopic approach to the calculation of the isobaric resonances, outlined above, might be considered as an alternative to another method based on the solution of the related Lane equations for the closed neutron and open proton channels. The optical $(\hat{T} \cdot \hat{t})$ Lane potential is good for solving the problem of the direct charge exchange (p,n). However, its application to the problem of analogue resonance excitation requires a special foundation. Neglecting antisymmetrization for all the nucleons of the system inherent in this method may result in spurious states which are strictly forbidden because of simple group considerations. In particular, this may put one on a false track, in looking for "antianalogue" states (i.e. states with mostly $T_<$) in cases where they just do not exist.

REFERENCES

[1] Proc. Int. Conf. Low and Intermediate Energy Electromagnetic Interactions (Dubna, 1967) Vol.3, Moscow (1967).

[2] BALASHOV, V.V., ERAMZHYAN, R.A., Atom. Energy Rev. 5 (1967) 3.

[3] DAVIES, H., MUIRHEAD, H., WOULDS, J.N., Nucl. Phys. 78 (1966) 673.

[4] KORENMAN, G.Ya., Thesis, Moscow State University (1967).

[5] FALLICOOS, S., HUGHES, T.A., GOULARD, B., Proc. Williambury Conf. (1966) 743.

[6] STODOLSKY, L., Phys. Rev. 144 (1966) 1145.

[7] VEILLET, J.J., Topical Conf. High-energy Collisions of Hadrons, CERN, Geneva (Jan. 1968).

[8] PRIMAKOFF, H., Proc. 2nd Int. Conf. High-energy Physics and Nuclear Structure, Rehovoth (1967), North-Holland, Amsterdam (1967).

[9] GILLET, V., "Enrico Fermi" International School, Varenna (1965).

[10] TUAN, S.T., WEBER, H.J., WEIGHT, L.E., Phys. Rev. 167 (1968) 939.
[11] MEASDAY, D.F., PALMICRI, J.N., Phys. Rev. 161 (1967) 1071.
[12] KARAPETYAN, V.V., KORENMAN, G.Ya., YADROVSKY, E.L., Phys. Lett. (to be submitted).
[13] LEMMER, R.H., SHAKIN, C., Ann. Phys. 27 (1964) 13.
[14] BALASHOV, V.V., DOLESHAL, D., KORENMAN, G.Ya., KOROTKIKH, V.L., FETISOV, V.N., Yadernaya Fiz. 2 (1965) 643.
[15] EICHLER, J., Nucl. Phys. 56 (1964) 577.
[16] WEISS, M.S., Phys. Lett. 19 (1966) 393.
[17] KABACHNIK, N.M., KOROTKIKH, V.L., UNGER, H., Yadernaya Fiz. 6 (1967) 973.
[18] DELSANTO, P.P., WAHSWEILER, H.S., GREINER, W., (preprint).
[19] FRIAR, J.L., Nucl. Phys. 84 (1966) 150.
[20] KABACHNIK, N.M., Yadernaya Fiz. 7 4 (1968).
[21] BALASHOV, V.V., KORENMAN, G.Ya., KOROTKIKH, V.L., FETISOV, V.N., Nucl. Phys. B1 (1967) 158.
[22] BALASHOV, V.V., KABACHNIK, N.M., MARKOV, V.I., Nucl. Phys. (in press).
[23] GILLET, V., MELKANOFF, M.A., RAYNAL, J., Nucl. Phys. A97 (1967) 631.
[24] BALASHOV, V.V., KABACHNIK, N.M., Phys. Lett. 25B (1967) 316.
[25] BALASHOV, V.V., CHERNOV, V.M., Zh. eksp. teor. Fiz. 43 (1962) 227; Nucl. Phys. 40 (1963) 93.
[26] WEBER, H.J., HUBER, M.G., GREINER, W., Z. Phys. 190 (1966) 25; 192 (1966) 182.
[27] ZHIVIPISTSEV, F.A., MOSKOVKIN, V.M., YUDIN, N.P., Proc. Int. Conf. Low and Intermediate Energy Electromagnetic Interactions, Dubna (1967).
[28] ANDERSON, B.L., BONDORF, I.P., MADSEN, B.S., Phys. Lett. 22 (1966) 651.
[29] BALASHOV, V.V., YADROBSKY, E.L., Phys. Lett. 25B (1967) 67.
[30] BROWN, G.E., BOLSTERLY, M., Phys. Rev. Lett. 3 (1959) 472.
[31] BALASHOV, V.V., GRISHANOVA, S.I., Phys. Lett. (to be submitted).
[32] BUCK, B., HILL, A.D., Nucl. Phys. A95 (1967) 271.
[33] SLIV, L.A., Proc. 2nd Nuclear Structure School, Leningrad (1967).

DISCUSSION

J. J. GRIFFIN: I just want to mention that one's attempts to learn about nuclear excitations at high excitation energy might proceed from two directions. The one is from our knowledge of low excited bound states towards a description of the similar states which occur in the continuum. This approach enables us to use theoretical knowledge to obtain a detailed description of certain states in the continuum, as has been discussed here.

On the other hand, one might also imagine that new kinds of excitation could exist at high excitation energy which could result in structure not easily predictable from our knowledge of low-lying bound states. Then one can proceed in the opposite direction (from the limit where bound states are very complicated and close together and lead in first approximation to smooth cross-sections) and search in the data for systematic deviations from the appropriate smooth statistical description. The latter viewpoint might recommend itself especially to experimentalists.

P. von BRENTANO: Can you say how much the wave-function for the ground state analogue of $^{208}Bi(0^+)$, which you have calculated, differs from the wave-function of $T_- |^{208}Pb(0^+)\rangle$?

V. V. BALASHOV: This difference has two aspects. First, the functions differ in a certain 'integral' manner, which is revealed as a difference in the ratio of partial proton widths calculated using the above method. This can be seen from Table II. Second, a more detailed difference, concerning

the form of the proton radial wave-function in the resonance, should be mentioned. In spite of the high barrier, the shape of the proton function does not coincide with that of the neutron function in the ground state of ^{208}Pb.

D. F. ZARETSKY: In the second calculation you did not take into account the coupling between the simple configurations and complicated states of the compound nucleus. Are your calculations stable against including this coupling? What is the effect of isospin non-conservation upon your calculations?

V. V. BALASHOV: The coupling you were speaking about has been taken into account neither in the simple diagonalization nor in the coupled channels calculation. This coupling is important but its treatment goes beyond the scope of the problem for which our calculation has been performed.

II

NUCLEAR STRUCTURE AT HIGH EXCITATIONS

Chairmen	Secretaries
P. HUBER	V.I. FURMAN
J. URBANEC	F. BEČVÁŘ
I.M. FRANK	N. IANEVA

ANALOGUE STATES AND RESONANCES*

G.M. TEMMER**
RUTGERS, THE STATE UNIVERSITY,
NEW BRUNSWICK, N.J., UNITED STATES OF AMERICA

Abstract — Аннотация

ANALOGUE STATES AND RESONANCES. A review is given of recent experiments on isobaric analogue resonances (IAR), especially near closed shells, with examples in ^{208}Pb and ^{118}Sn where high-resolution inelastic-scattering data are now available. The use of polarized beams in the study of IAR is discussed. Several extensions of resonance experiments into the region of deformed and transition nuclei have revealed interesting structural information, although the question of the deformation dependence of Coulomb displacement energies has not been answered as yet in view of complications. The use of (p, n) reactions with resolved neutron groups via IAR for nuclear spectroscopy seems promising. Many new results are available on gamma decay of IAR, especially for those with isospin-fobidden particle-decay channels, observed mainly in the p-shell and ds-shell nuclei. The question of the isobaric spin splitting of the giant dipole resonance (mainly in ^{90}Zr) is under active investigation. Useful connections have been pointed out between El decay of IAR and corresponding first-forbidden beta transitions. Another class of gamma transitions recently observed are those de-exciting residual excited states following inelastic proton scattering through IAR, shedding light on the particle-hole structure of excited states. The difference between "allowed" (conventional) and "forbidden" IAR is discussed, and the current situation for T=3/2 states in $T_z = -1/2$ nuclei is summarized in the light of recent successful analyses of these resonances to extract partial and total widths. We also present the status of T=2 states in $T_z = 0$ nuclei. The role of T-allowed particle-transfer reactions in establishing the properties of these T-multiplets is emphasized. Finally, a number of open problems in these areas are presented, such as stripping to isospin-forbidden states, the use of neutrons in the study of IAR, and two – or more – particle transfer reactions in the heavy nuclei to excite additional members of T-multiplets. It is pointed out that our theoretical understanding of such problems as the widths of these T-fobidden IAR, or the structural Coulomb displacement energy shifts found between multiplet members, is generally still lacking, although precise experimental values, and the ingredients for calculations, are available.

АНАЛОГОВЫЕ СОСТОЯНИЯ И РЕЗОНАНСЫ. Дается обзор последних экспериментов по изобарическим аналоговым резонансам (ИАР) вблизи, главным образом, замкнутых оболочек. В качестве примера приводятся ^{208}Pb и ^{118}Sn, для которых в настоящее время имеются данные о неупругом рассеянии с высокой степенью разрешения. Обсуждается использование поляризованных пучков для изучения ИАР. Некоторые случаи распространения резонансных экспериментов на область деформированных и переходных ядер позволяют получить интересную информацию о структуре ядра, хотя вопрос о зависимости кулоновского сдвига в энергиях от деформации остается не решенным из-за возникающих осложнений. Использование (p,n)-реакций через ИАР с разрешенными нейтронными группами для ядерной спектроскопии представляется перспективным. Получено много новых результатов по γ распаду ИАР, особенно для ИАР с запрещенными по изоспину частичными каналами распада, наблюдаемому, главным образом, в ядрах p-оболочки и dS-оболочки. Исследуется вопрос об изоспиновом расщеплении гигантского дипольного резонанса (главным образом в ^{90}Zr). Указано на полезную связь между E1-распадом ИАР и соответствующим запрещенным в первом порядке бета-переходом. Недавно наблюдался другой класс гамма-переходов, разряжающих остаточные возбужденные состояния после неупругого рассеяния протона через ИАР. Это проливает свет на частично-дырочную структуру возбужденных состояний. Обсуждается разница между "разрешенными" (обычными) и "запрещенными" ИАР, а также рассматривается современное положение для $T = 3/2$ состояний в ядрах с $T_z = -1/2$ в свете последних успешных анализов этих резонансов, проведенных с целью извлечения точной парциальной и полной ширины. Приводятся данные о положении $T = 2$ состояний в ядрах с $T_z = 0$. Подчеркивается роль T-разрешенных реакций по передаче частицы в выявлении свойств таких T-мультиплетов. Наконец, указан ряд нерешен-

* Supported in part by the National Science Foundation, and the Ford Foundation.

** Rutgers Research Council Faculty Fellow, at present at the Niels Bohr Institute, Copenhagen, Denmark.

ных в этой области проблем, как, например, стриппинг на запрещение по изоспину состояния, использование нейтронов в изучении ИАР, реакции передачи двух или более частиц в тяжелых ядрах с возбуждением добавочных членов Т-мультиплета. Указано, что теоретическое понимание таких проблем, как ширина данных Т-запрещенных ИАР или структурный энергетический сдвиг благодаря кулоновскому смещению, обнаруживаемый между членами мультиплета, все еще страдает недостатками, хотя имеются как точные экспериментальные данные, так и возможности для вычислений.

1. INTRODUCTION

As is customary, this survey paper must begin by deploring the limited time available for its presentation, as well as the abundance of recent excellent research results from laboratories other than my own which merit mention. I shall limit myself mainly to new and unusual aspects of the vast field which has grown out of the realization that isobaric spin symmetry usefully applies to all nuclei, light and heavy. This exciting new horizon we owe without a doubt to the direct (p, n)-reaction experiments of Anderson and collaborators [1] in 1961, and to the new approach to resonance reactions by Fox, Robson and their co-workers in 1964 [2]. In all this, the early theoretical considerations of French and Macfarlane [3] and Lane [4] were essential. My paper will of necessity emphasize the experimental aspects of the subject, and by preference the isobaric analogue resonances, since they have contributed most of the recent material (and I have been involved with them personally). Also, in spite of a number of advances in the theoretical approach [5, 6], I believe that experiments have held the lead, and to a large extent pointed the way recently.

2. NEW DEVELOPMENTS WITH CONVENTIONAL ANALOGUE RESONANCES

(a) Elastic and inelastic scattering: Many additional nuclei have been studied, the preference clearly being for even-even targets, the more magic the better. The region of lead, perhaps more than any other, has yielded a rich assortment of new results bearing on nuclear spectroscopy. Rutgers [7], Seattle [8], Texas [9] and Yale [10] have extended the range of target nuclei (Z = 82 - 76, A = 208 - 188) [7], as well as the bombarding-energy range to above 20 MeV [10], and the inelastic proton excitation range to about 7 MeV [8 - 10]. Striking examples of the selective excitation of successively higher excited target states in ^{208}Pb with increasing proton bombarding-energy are shown in Fig. 1a and 1b [8, 9], revealing very clearly the construction of the low-lying excited states of doubly-magic ^{208}Pb in terms of their particle-hole excitations. Much work of this type remains to be done with high-resolution magnetic spectrographs; in Fig. 2 we show a more complicated but beautiful example in ^{118}Sn [11] with inelastic proton spectra obtained every 100 keV in excitation energy ^{119}Sb. Additional information on certain of the particle-hole states in the residual nuclei can be obtained from their gamma decay, to be discussed below.

Polarization measurements are becoming very popular, especially with the increasing availability of polarized accelerator beams. Fig. 3 shows more recent results on ^{124}Sn [12] using the older and more heroic double-scattering method with a carbon analyser. In Fig. 4 we give a recent asym-

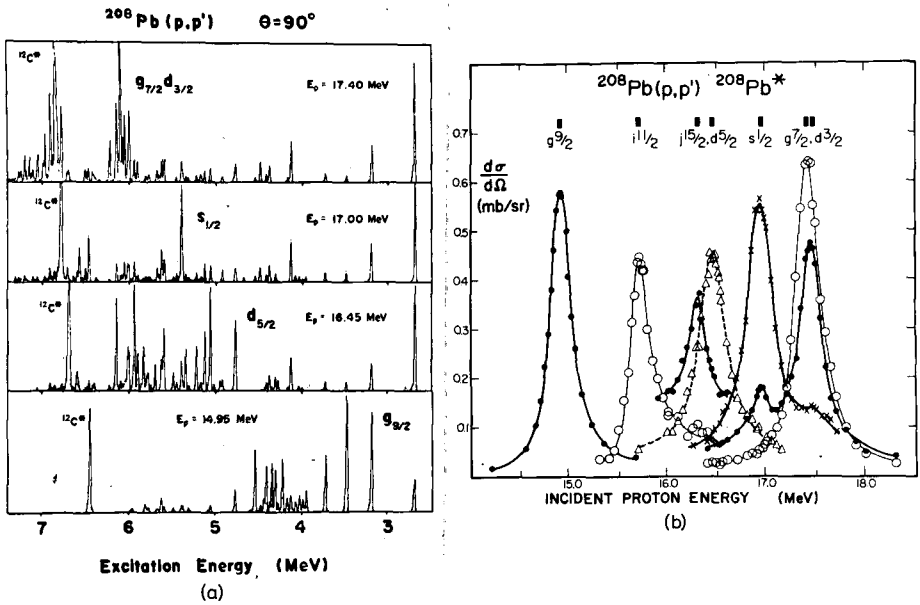

FIG.1. (a) Inelastic proton spectra from ^{208}Pb at four bombarding energies corresponding to successive single-particle analogue states of ^{209}Pb. Excitation energy increases from right to left. (From Ref. [9]). (b) Excitation functions for various inelastic proton groups from ^{208}Pb, mostly at 90 degrees; peaks correspond to analogue states listed in the figure, and excitation of states in ^{208}Pb ranges from 3.469 MeV (first peak) to 5.914 MeV (last peak). (From Ref. [8]).

metry excitation curve of ^{140}Ce +p [13] covering several analogue resonances, using a polarized ion source, and conclusively determining the j-value of each of the resonances, including one unexpected $1/2^-$ state, just as in ^{138}Ba [13] and ^{144}Sm [14]. These intense polarized beams will soon allow the study of the asymmetry of the weaker inelastic proton groups from analogue resonances, a rich potential source of nuclear coupling scheme information.

In the last year, deformed nuclei in the rare-earth region and beyond have come under scrutiny via analogue resonance experiments. Some of us [15 - 17] had the hope that, in addition to pursuing Nilsson spectroscopy in the way described by Sheline at this Symposium, one might detect deformation effects in the Coulomb displacement energies ΔE_c [18]. Because of the close spacing of states in the parent nuclei, and the intrinsic widths (~100keV) of their analogues, it is usually difficult to locate corresponding states with sufficient accuracy. The expected decrease if ΔE_c for deformations encountered in the rare earths is about 100 keV relative to spherical nuclei. It is controversial as to how to establish ΔE_c for zero deformation from the systematics, and how to separate the shifts which are known to exist due to structural (orbital) differences between states. The most direct approach to this problem would be to compare ΔE_c for deformed and spherical states with the same ℓ-value in the same nucleus.

Figure 5 shows an example of elastic and inelastic excitation curves for ^{192}Os, illustrating another effect which becomes particularly pronounced for nuclei with collective 2^+ states [15, 16, 19]; their enhanced B(E2) values lead to Coulomb-excitation cross-sections which account for most of the

non-resonant yield between analogue resonances. Since this inelastic process is well understood (especially below the Coulomb barrier), its interference with the resonant amplitudes is amenable to theoretical treatment [20], and may help in our quantitative understanding of inelastic scattering through analogue resonances in more complicated situations.

(b) Progress in (p, n) reactions through analogue resonances: Since the initial discovery of isobaric analogue resonances through this isospin-forbidden reaction channel [2] without discrimination as to neutron energy, several groups have begun to study outgoing neutron spectra [21 - 23]. The decay of these highly excited states takes place in the usual statistical (Hauser-Feshbach) manner through the so-called $T_<$ component; the only

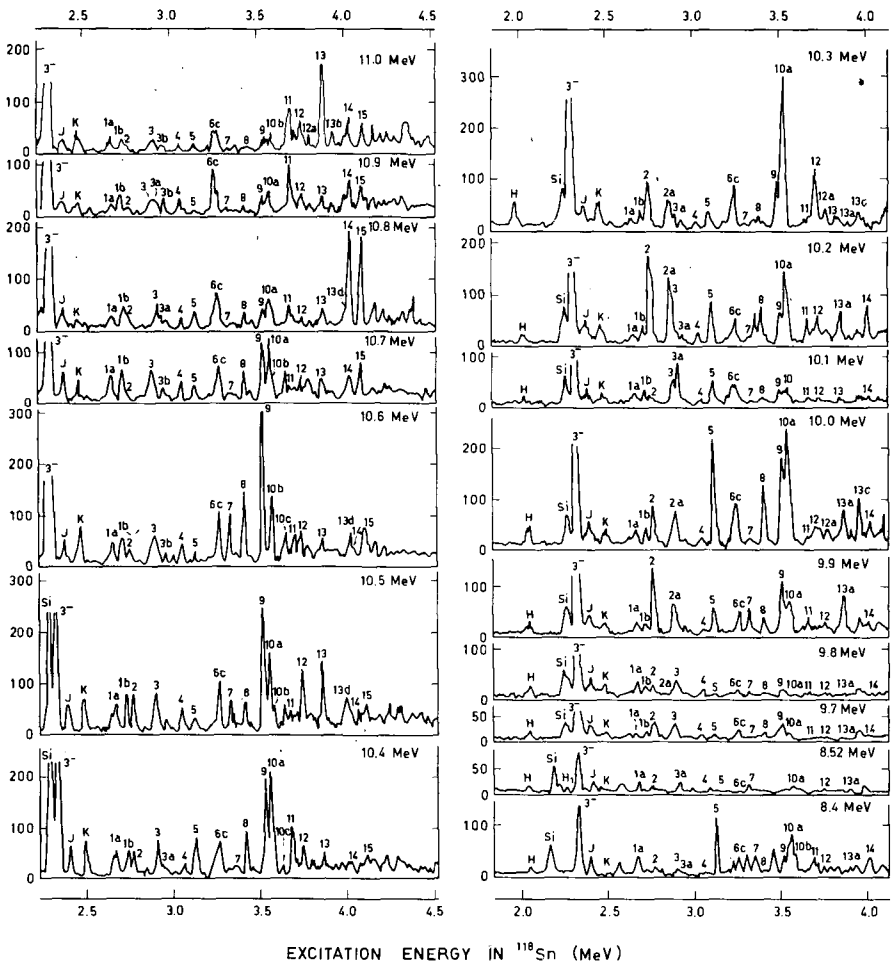

FIG.2. Inelastic proton energy spectra taken at 100-keV intervals of bombarding energy for ^{118}Sn. Excitation energy increases from left to right, and bombarding energy from lower right to upper left. Changes in inelastic emphasis are more complicated than in Fig.1. (From Ref. [11]).

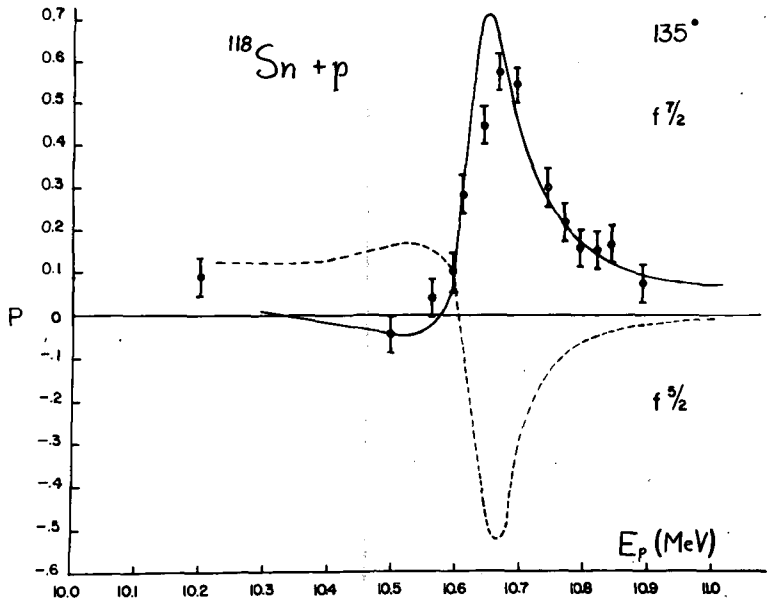

FIG.3. Asymmetry excitation curve for ^{118}Sn + p from double scattering, using a carbon second scatterer, over the region of the $\ell = 3$ analogue state of ^{119}Sn in ^{119}Sb. Dashed curve is theoretical prediction for $j = 5/2^-$; solid curve for $j = 7/2^-$. (From Ref. [12]).

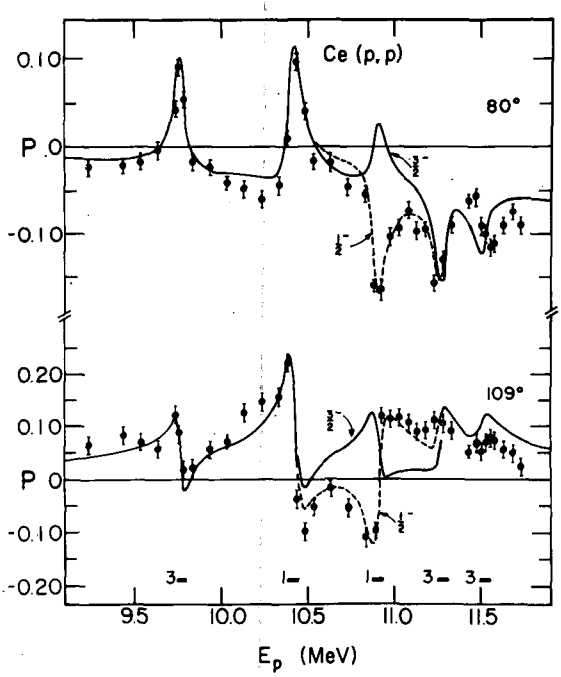

FIG.4. Asymmetry excitation curves for ^{140}Ce at two angles, using a polarized ion source, traversing five analogue resonances in ^{141}Pr whose ℓ-values are indicated at the bottom. Solid curve is calculated for a given set of choices for the various j-values, which are correct except for 10.9-MeV resonances where dashed curve ($j = 1/2^-$) gives correct behaviour. (From Ref. [13]).

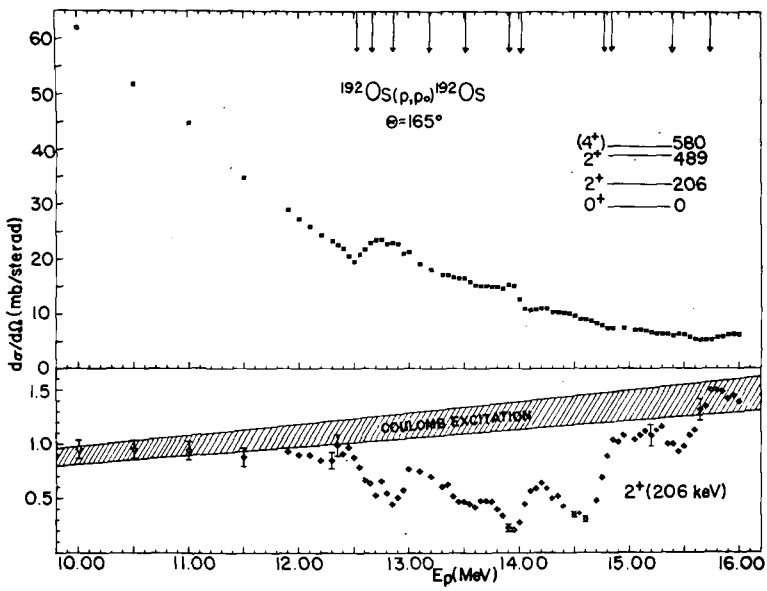

FIG. 5. Elastic and inelastic (2^+) excitation curves for protons on ^{192}Os. Cross-hatched band indicates Coulomb excitation cross-section as calculated from the B(E2) value; agrees perfectly with observed 2^+ excitation at the lowest energies (below the Coulomb barrier) where elastic scattering is pure Rutherford. Arrows along top indicate states observed in corresponding $^{192}Os(d,p)^{193}Os$ reaction. (From Ref. [15]).

special use being made of their location within isobaric analogue-resonances lies in the enhancement of their reduced widths, and our knowledge of their unique spin and parity, which often allows the determination of the spins of the residual states from neutron angular-distribution measurements. Fig. 6 shows an example of outgoing neutron spectra, taken on and off the 0^+ analogue resonance of ^{120}Sn in ^{120}Sb [22].

(c) Gamma decay of isobaric analogue states: In the lighter nuclei, especially in the ds-shell, the beautiful work of the groups at Utrecht (see for example, Ref. [24]) and Dayton (USA) [25] has for some time revealed very systematic behaviour in the gamma transitions connecting $T_>$ analogue states with their lower-lying $T_<$ homologues (often called anti-analogues) which proceed by strong M1 transitions of the order of the Weisskopf unit, in agreement with theoretical expectations [26].

Another class of gamma transitions involve the giant dipole resonance, studied especially in ^{90}Zr. The question of the splitting of this resonance into $T_>$ and $T_<$ components [27 - 29] is under active investigation in various laboratories [30, 31], and by no means clear-cut.

Very recently, the direct E1 gamma transition from an isobaric analogue resonance ($2f_{7/2}$) to the ground state ($2d_{5/2}$) [32] of the compound nucleus ^{141}Pr was observed, using Ge(Li) detectors. This transition can be directly related to the first-forbidden beta transition $^{141}Ce \rightarrow {}^{141}Pr$ as illustrated in Fig. 7; there is promise of valuable spectroscopic information from the hindrance factors obtained in this way.

Finally, isobaric analogue resonances, which are made up to a large extent of 2p-1h configuration, have been used to populate neutron p-h states

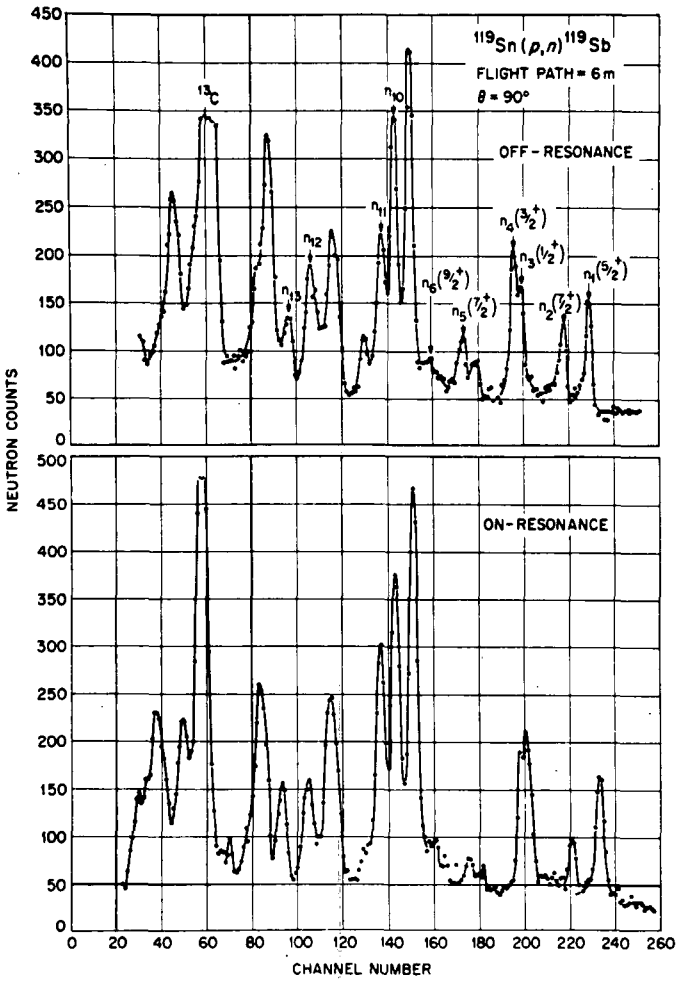

FIG.6. Neutron time-of-flight spectra (flight time increasing with increasing channel number) taken on the 0^+ ground-state analogue resonance of ^{120}Sn in ^{120}Sb (E_p = 4.642 MeV) and off resonance (E_p = 4.709 MeV) showing 13 residual neutron groups leading to low-lying states of ^{119}Sb. Resonant enhancements can be used to deduce spins and parities of residual states. (From Ref. [22]).

in ^{140}Ce [33] and ^{208}Pb [34] via inelastic proton scattering; the E1 gamma decay of these states to the 0^+ ground state has been identified from the angular distributions, leading to unique 1^- spin assignments for eight states between 5 and 7 MeV excitation in ^{208}PB, as illustrated in Fig. 8.

3. RECENT DEVELOPMENTS IN ISOSPIN-FORBIDDEN RESONANCES

Figure 9 shows the basic difference between a conventional isobaric analogue resonance for a nucleus with neutron excess (bottom), and an isospin-forbidden resonance with no allowed channels (top). The Coulomb field produces mixing in both cases, involving the $T_<$ states of the same spin and parity as the resonance, the mixing coefficient being given by the

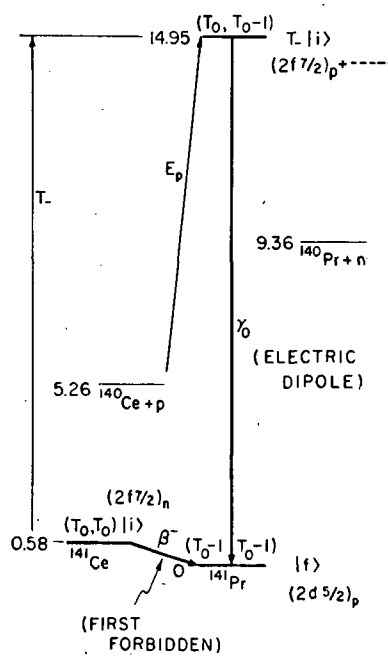

FIG. 7. Relation between the E1 gamma decay connecting the $2f_{7/2}$ analogue state and $2d_{5/2}$ ground state of ^{141}Pr, and the first-forbidden beta decay of ^{141}Ce to the same ground state. (From Ref. [32]).

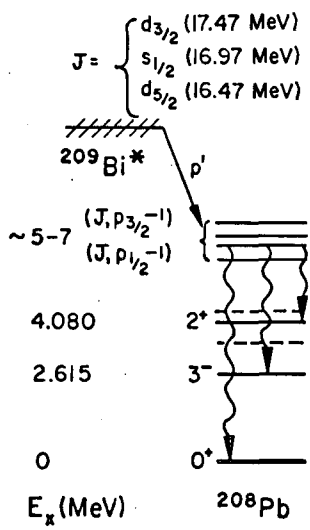

FIG. 8. Excitation of 1^- particle-hole states in ^{208}Pb between 5 and 7 MeV, and their subsequent gamma decay, following the inelastic proton emission from various analogue resonances in ^{209}Bi. (From Ref. [34]).

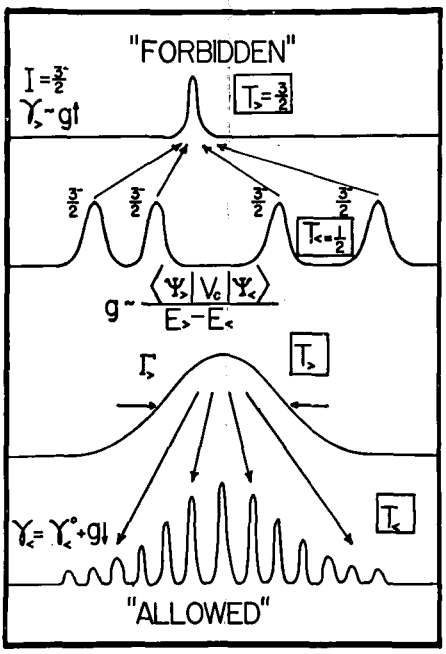

FIG. 9. Schematic comparison of "allowed" and "forbidden" isobaric analogue resonances with respect to Coulomb mixing. For detailed description, see text.

perturbation expression in the centre of the figure. The fundamental difference lies in the fact that, in the former case, the analogue resonance has a residual proton width even in the absence of Coulomb mixing, and this width is then shared with the large density of $T_<$ states (downward arrows); in the latter (iso-forbidden) case, on the other hand, there is no "primordial" proton width (Coulomb interaction switched off), but the few neighbouring $T_<$ resonances contribute proton width via Coulomb mixing (upward arrows), the width being then a direct measure of the degree of isospin impurity.

(a) Elastic and inelastic proton scattering: $T = 3/2$, $T_z = -1/2$ resonances have now been observed for ^{13}N [35], ^{17}F [35, 36], ^{21}Na [38], ^{25}Al [39], ^{29}P [39], ^{37}K [40], and ^{41}Sc [41], thus completing the 4n series of stable nuclei with the exception of ^{33}Cl. In all these cases, isospin-allowed (p,t) and/or (^{3}He, n) reactions, as well as delayed-proton decays have located these states within certain error limits (~40-100 keV) given by the respective instrumental resolutions. Their widths were determined from elastic scattering experiments at Rutgers [35, 39], Caltech [38, 40], and Rice [41]. We present a summary of the results for ground-state analogue resonances in these nuclei in Table I; we list the bombarding energies E_p(lab), excitation energies E*, spin-parity I, total widths Γ, and partial elastic proton widths Γ_{p_0}; we also indicate the isospin-allowed transfer reactions and delayed-proton decays ($\bar{p}$) leading to these states, and their references. We show two examples of the analysis of these narrow resonances, which illustrate how one can account for the characteristic resonant signatures at various angles by having a sufficient phase-shift description

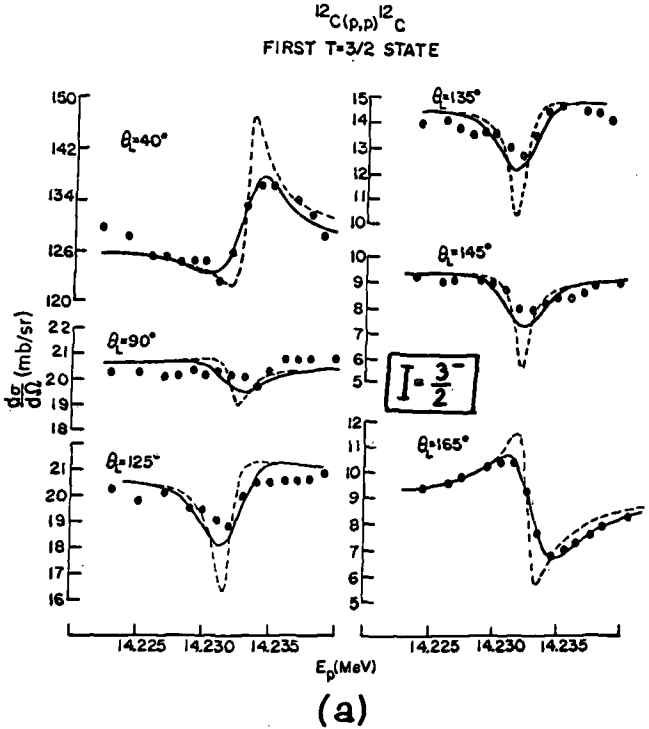

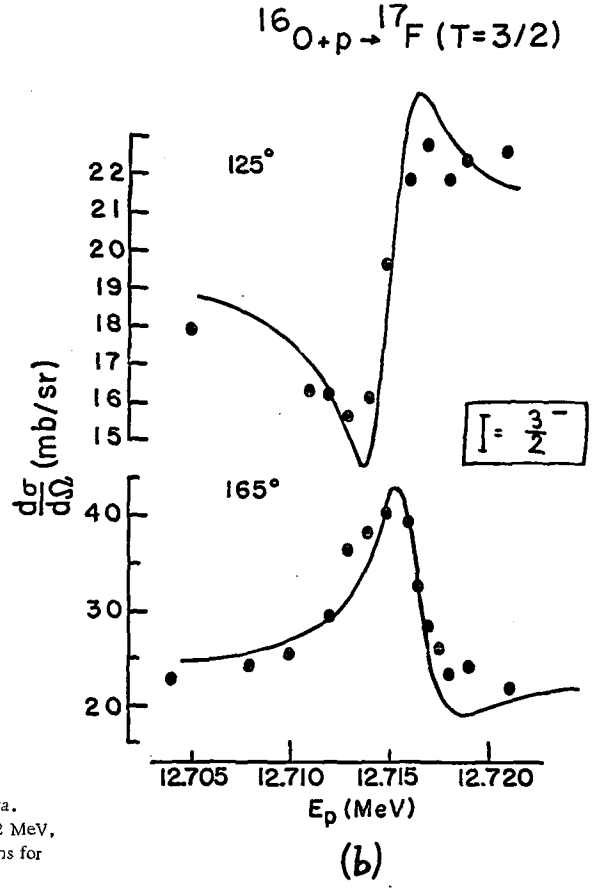

FIG. 10. (a) Ground-state analogue resonance of ^{13}B in ^{13}N as observed in twice T-forbidden elastic scattering. Dashed curves are theoretical predictions for ideal conditions; solid curves include finite beam spread and target thickness effects, at six angles of observation. Solid dots are experimental data. (From Ref. [35]). (b) Resonance associated with the analogue of the first-excited state of ^{17}N at 1.32 MeV, observed in ^{17}F via twice-forbidden elastic scattering, at two angles. Curves are theoretical predictions for $I = 3/2^-$, which was previously unknown. (From Ref. [35]).

TABLE I. SUMMARY OF RESONANCE PARAMETERS FOR LOWEST T = 3/2, T_z = -1/2 STATES.
Energies in MeV; widths in eV. For definitions, see text.

Nucleus	E_p(lab)	E^*	I	Γ	Γ_{po}	References			
						Resonance	(^{3}He, n)	(p, t)	$\bar{p}$
^{13}N	14.233	15.068	$3/2^-$	1550	280	[35]	[61]	[55]	-
^{17}F	11.270	11.196	$1/2^-$	~500	~50	[35, 37]	[62]	-	[63]
^{21}Na	6.872	8.973	$5/2^+$	<1500	~300	[38]	[64]	[65]	[66]
^{25}Al	5.866	7.916	$5/2^+$	~100	~17	[39]	-	[67]	[68]
^{29}P	5.840	8.376	$5/2^+$	~170	~140	[39]	-	[67]	[69]
^{37}K	3.249 3.280	5.018 5.048	$3/2^+$	600 40	600 40	[40]	-	[65]	[70]
^{41}Sc	4.899	5.865	$3/2^+$	2600	2600	[41]	-	-	[70]

of the non-resonant background amplitude, plus a resonant amplitude having the appropriate ℓ and j. Fig. 10a gives the $3/2^-$ analogue resonance [35] of the ground state of ^{13}B, where the dashed lines represent the ideal curves, and the solid lines include the effects of beam spread and target thickness. Fig. 10b presents similar results for the analogue of the first-excited state of ^{17}N, establishing $j = 3/2^-$ for this isospin quartet whose parent spin was not known.

Having all these widths available, it is now of great interest to relate them to isospin impurities. Very little progress has been made on this theoretical problem. Recently, Yoshida and Arima at Rutgers undertook a detailed and essentially exact calculation of the elastic width for the ^{13}N case, using available p-shell wave functions. Unfortunately, at our present state of knowledge of nuclei, a different model has to be used for each of the above cases. A closely related problem concerns the isotope shifts in the Coulomb-displacement energies, for which very precise values are now available; we believe that the solution of these problems will shed considerable light on the reliability of wave functions, as well as on our ideas as to the origins of isospin impurities.

(b) Gamma decay of isospin-forbidden resonances: This isospin-allowed decay channel has been studied for some time in the T = 3/2 cases A = 13 [42], A = 25 [43], A = 29 [44], and A = 37 [40]. For A = 25, a more detailed recent study [45] has given interesting spectroscopic information in the form of branching ratios to the ground-state rotational band of this deformed nucleus; the isospin question of the capturing state is incidental, serving only to single out a well-defined initial state with simple radiative properties, in the continuum.

Much proton-capture activity has centered on the lowest T = 2, T_z = 0, $I = 0^+$ states in the 4n -type nuclei ^{20}Ne [46][1], ^{24}Mg[48], ^{28}Si [49], and ^{32}S [50][1]. Moreover, the next higher T = 2 state in ^{20}Ne (2^+) has been found as a resonance in ^{19}F + p, as observed in the outgoing elastic pro-

[1] Twice-forbidden resonant elastic scattering was also observed [47] for ^{20}Ne, and [50] for ^{32}S.

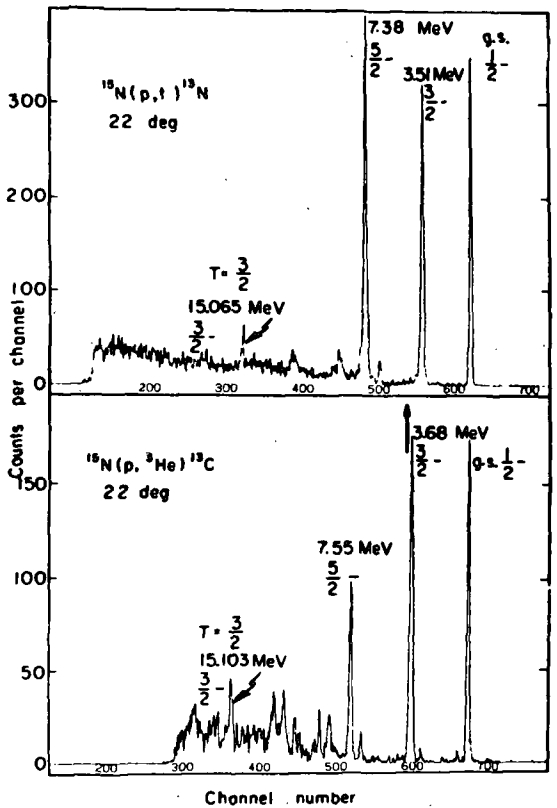

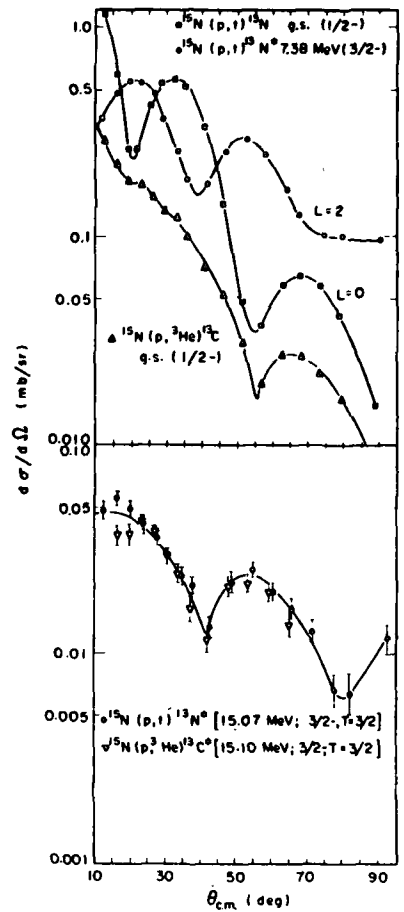

FIG.11. (p, t) and (p, ^{3}He) reactions on ^{15}N, leading to T = 3/2 states in ^{13}N and ^{13}C by T-allowed process. Left-hand graphs illustrate t and ^{3}He spectra showing the lowest T = 3/2 states; right-hand graphs show angular distributions to various mirror states; upper portion to T = 1/2 states with no similarity in shape; lower portion to corresponding T = 3/2 states superimposed after correction for isospin-coupling factor (two-nucleon transfer has $\Delta T = 1$ only) and slight Q-value difference. (From Ref. [55]).

ton channel, alpha[2] channels to the first three states of ^{16}O, a gamma channel [51], as well as in some neutron groups [52]. The gamma decay of these states was found to occur by two-step cascades via one or more known T = 1 states of low spin, located about midway between the T = 2 states and the 0^+ ground states. Because of the 0 - J - 0 nature of these cascades, the angular correlations are very pronounced and permit definite spin 0 assignments for the T = 2 resonances.

We wish to make special mention here of the extensive work on two-nucleon (and even three- and four-nucleon) transfer reactions at Berkeley (mainly (p,t) and (p, ^{3}He) [53] and Caltech (mainly (^{3}He, n) and (^{3}He, p) [54]) which located all T = 3/2 and T = 2 states by isospin-allowed paths, without which the search for these forbidden resonances would have been hopeless. Moreover, the identical angular distributions, and simple Clebsch-Gordan ratios of relative intensities for the pairs of mirror transfer reactions mentioned provide the strongest evidence for the analogue relationship between the states reached. A beautiful illustration of this is shown in Fig. 11, where the left-hand side gives the spectra of the mirror nuclei ^{13}N and ^{13}C, while the lower right-hand side shows the angular distributions to the lowest T = 3/2 states superimposed after correcting for phase space and isospin coupling [55].

4. OPEN PROBLEMS

(a) Higher isospin-forbidden resonances: It is of great interest to have very accurate locations for $T > T_z$ states in nuclei so as to be able to check some of the semi-empirical isobaric mass formulae more stringently, and to predict the masses of as yet undiscovered nuclear species. At present, only T = 3/2 states in $T_z = \pm 1/2$ nuclei, and T = 1 and 2 states in $T_z = 0$ nuclei have been located. We have attempted to form T = 5/2 resonances in the $T_z = 1/2$ nucleus ^{43}Sc, using the $T = T_z = 1$ target ^{42}Ca [56], the lightest nucleus for which the necessary information is available from allowed transfer reactions. The same degree of forbiddenness ($\Delta T = 1$) is involved as in the reactions previously discussed. Preliminary results are not encouraging in view of the very complicated structure found in the appropriate continuum region of ^{43}Sc. The next available stable targets for escalation in isospin are the T = 3/2 nuclei ^{37}Cl, ^{41}K, and ^{45}Sc, leading to forbidden T = 3, 0^+ compound resonances in the $T_z = 1$ nuclei ^{38}Ar, ^{42}Ca and ^{46}Ti, respectively. In the first of these cases, the T = 3 state has been located by allowed $^{40}Ar(p,t)^{38}Ar$ [57]. Of course, in all these isospin-forbidden resonances the paramount consideration is whether they will be narrow; this depends upon whether all possible decay channels are isospin-forbidden; specifically, whether the lowest state having isospin one unit greater than the ground state of the target, is energetically accessible or not. A systematic examination of this question was made by Jähnecke [58].

(b) Stripping to isospin-forbidden states: The possibility exists of exciting, say, T = 3/2 states in the (d, p) reaction on T = 0 targets. It is expected that these states, in spite of their exceedingly small spectroscopic factors ($\sim 10^{-4}$ or less) would nevertheless show characteristic

[2] Note that here only the iso-tensor part of the Coulomb perturbation can produce the necessary mixing in first order.

stripping angular distributions, whereas ordinarily, states with $S < 0.1$ do not show such patterns. On the other hand, second-order processes such as virtual target or deuteron (singlet-state) excitation may make themselves felt here. A number of the cases discussed in section 3 could be so investigated.

(c) Neutron excitation of analogue resonances: Since (p, n) reactions have proved very effective in revealing isobaric analogue resonances, the possibility of using the inverse reaction exists in those cases where an important branch of the (p, n) reaction would in fact lead to the ground state. A great many nuclei never before accessible to analogue resonance study might be available through this channel. One might also consider the excitation of the isospin-forbidden $T = 3/2$ and $T = 2$ states discussed in section 3, using neutrons instead of protons, and leading to the mirror nuclei of those considered earlier. A few favourable cases exist where high-resolution, low-energy neutron sources might reach the appropriate states. The main interest here would be in the elucidation of the role of the charge of the projectile in the broadening (isospin-mixing) process of these resonances.

Another variation in the use of neutrons is in the excitation of unbound parent states of isobaric analogue resonances. One such case has apparently already been observed in $^{89}Y + n$, exciting one of the $T_>$ 1^- components of the giant dipole resonance, in the parent nucleus ^{90}Y whose analogue states in ^{90}Zr were mentioned earlier.

(d) Two-nucleon transfer reactions in heavy nuclei: The extension of these studies to heavy nuclei with the high-resolution, higher-energy accelerators now coming into use is clearly of special interest since they can reveal an additional ($T_z = T - 2$) member of the isospin multiplets which, until now, are only known through their $T_z = T$ and $T - 1$ members. For instance, the $T = 23$, $T_z = 21$ state in ^{206}Pb can be formed via $^{208}Pb(p, t)^{206}Pb^*$ or $^{204}Hg(^3He, n)^{206}Pb^*$, being the third member (spin 0^+) of the 47-plet whose parent is the ground state of ^{206}Hg, which can be studied in turn via the $^{204}Hg(t, p)^{206}Hg$ reaction. When we recall that three-nucleon [59], and four-nucleon [60] transfers have also been observed recently, the possibilities for climbing the isospin ladder are virtually unlimited.

5. CONCLUSION

The great variety of experiments carried out over the past 7 years as a result of the rather unexpected applicability of the isospin concept throughout the periodic table, have greatly enriched our appreciation of nuclear spectra and of relationships between nuclei. There seems to be no end in sight to the kinds of approaches that have been and can be tried in this field. The existence of this slightly broken symmetry in nuclear physics, with the presumption of an understanding of what causes the breaking, constitutes a challenge to which the experimentalists seem to have amply responded. However, many theoretical problems raised by these experiments have been neglected and even ignored; it is to be hoped that this situation will improve, perhaps in time for the next International Nuclear Physics Conference.

REFERENCES

[1] ANDERSON, J.D., WONG, C., McCLURE, J.W., Phys. Rev. 126 (1962) 2170.
[2] FOX, J.D., MOORE, C.F., ROBSON, D., Phys. Rev. Lett. 12 (1964) 198.
[3] FRENCH, J.B., MACFARLANE, M.H., Nucl. Phys. 26 (1961) 168.
[4] LANE, A.M., Nucl. Phys. 35 (1962) 676.
[5] ROBSON, D., Phys. Rev. 137B (1965) 535.
[6] WEIDENMÜLLER, H.A., Nucl. Phys. A99 (1967) 269 and 289.
[7] LENZ, G.H., TEMMER, G.M., Nucl. Phys. A112 (1968) 625.
[8] von BRENTANO, P., et al., Phys. Lett. 26B (1968) 666.
[9] MOORE, C.F., et al., Phys. Rev. 164 (1967) 1559; ZAIDI, S.A.A., et al., Phys. Rev. 165 (1968) 1312.
[10] STEIN, N., WHITTEN, C.A., Jr., BROMLEY, D.A., Phys. Rev. Lett. 20 (1968) 113.
[11] ALLAN, D.L., Nucl. Phys., in press.
[12] GONSIOR, B., ARKING, R., LOMBARDI, J., ROBBINS, A.B., Bull. Am. phys. Soc. 13 (1968) 562.
[13] VEESER, L., ELLIS, J., HÄBERLI, W., Phys. Rev. Lett. 18 (1967) 1063.
[14] FAIRMAN, S., MICHELMAN, L., ROBBINS, A.B., Bull. Am. phys. Soc. 13 (1968)
[15] WIESEN, M. et al., Bull. Am. phys. Soc. 12 (1967) 597.
[16] ADAM, A., et al., Phys. Lett. 25B (1967) 122.
[17] ALLAN, D.L., BRITT, H.C., RICKEY, F.A., to be published.
[18] MACFARLANE, M.H., Isobaric Spin in Nuclear Physics (FOX, J.D., ROBSON, D., eds.) Academic Press, N.Y. (1966) p. 383.
[19] WIESEN, M., SCHNEID, E.J., TEMMER, G.M., Bull. Am. phys. Soc. 13 (1968) 563.
[20] GRIFFY, T.A., BIEDENHARN, L.C., Nucl. Phys. 32 (1962) 273.
[21] LIGHTBODY, D.B., SAYRES, A., MITCHELL, G.E., Phys. Rev. 153 (1967) 1214.
[22] KIM, H.J., et al., Phys. Rev. Lett. 19 (1967) 325.
[23] FINCKH, E., JAHNKE, U., WIRSICH, J., Isobaric Spin in Nuclear Physics, (FOX, J.D., ROBSON, D., eds.) Academic Press, N.Y. (1966) p. 713, and to be published.
[24] ENDT, P.M., Nuclear Structure (HOSSAIN, A., et al., eds.) North-Holland, Amsterdam (1967) p. 58.
[25] WATSON, D.D., MANTHURUTHIL, J.C., LEE, F.D., Phys. Rev. 164 (1967) 1399, and references therein.
[26] ERNE, F.C., Nucl. Phys. 84 (1966) 91; MARIPUU, S., submitted to Nucl. Phys. (1968).
[27] PIAZZA, A., WAHSWEILER, H.G., GREINER, W., Phys. Lett. 25B (1967) 579.
[28] MACFARLANE, M.H., Isobaric Spin in Nuclear Physics, (FOX, J.D., ROBSON, D., eds.) Academic Press, N.Y. (1966) p. 383.
[29] FALLIEROS, S., GOULARD, B., VENTER, R.H., Phys. Lett. 19 (1965) 398.
[30] AXEL, P., et al., Phys. Rev. Lett. 19 (1967) 1343; also HANNA, S.S., private communication.
[31] VAN BREE, R., TEMMER, G.M., Bull. Am. phys. Soc. 13 (1968) 584.
[32] EJIRI, H., et al., to be published.
[33] von BRENTANO, P., et al., Phys. Lett. 26B (1968) 448.
[34] CRAMER, J.G., et al., to be published.
[35] TEMMER, G.M. et al., Proc. Int. Conf. Nuclear Structure (Tokyo, 1967) p. 318; VAN BREE, R., TEMMER, G.M., Phys. Rev., to be published.
[36] HARDIE, G., DANGLE, R.L., OPPLIGER, L.D., Phys. Rev. 129 (1963) 353.
[37] PATTERSON, J.R., WINKLER, H., ZAIDINS, C.S., Phys. Rev. 163 (1967) 1051.
[38] McDONALD, A.B., PATTERSON, J.R., WINKLER, H., Bull. Am. phys. Soc. 13 (1968) 652.
[39] TEITELMAN, B., TEMMER, G.M., Phys. Lett. 26 (1968) 371; Phys. Rev. (in press).
[40] GOOSMAN, D.R., KAVANAGH, R.W., Phys. Rev. 161 (1967) 1156.
[41] YOUNGBLOOD, D.H., WILDENTHAL, B.H., CLASS, C.M., to be published; ENDT, P.M., VAN DER LEUN, R., Nucl. Phys. A105 (1967) 1, Table 41.12 on p. 340.
[42] DIETRICH, F.S., et al., Phys. Rev. 168 (1968) 1169.
[43] MORRISON, G.C., et al., Proc. Int. Conf. Nuclear Structure (Tokyo, 1967) p. 143.
[44] YOUNGBLOOD, D.H., MORRISON, G.C., SEGEL, R.E., Phys. Lett. 22 (1966) 625.
[45] SEGEL, R.E., Bull. Am. phys. Soc. 13 (1968) 577, and to be published.
[46] KUAN, H.M., et al., Phys. Lett. 25B (1967) 217.
[47] BLOCH, R., PIXLEY, R.E., TRUÖL, Phys. Lett. 25B (1967) 215.
[48] RIESS, F., et al., Phys. Rev. Lett. 19 (1967) 367.
[49] KUAN, H.M., et al., Los Alamos Meeting, American Physical Society, June 1968.
[50] HEIKKINEN, D.W. et al., Los Alamos Meeting, American Physical Society, June 1968.

[51] LATSCHAW, G.L., et al., Los Alamos Meeting, American Physical Society, June 1968.
[52] ADELBERGER, E.G., Los Alamos Meeting, American Physical Society, June 1968.
[53] Cf. review by CERNY, J., Ann. Rev. nucl. Sci. 18 (1968) to be published.
[54] BARNES, C.A., and co-workers, Proc. Int. Conf. Nuclear Physics, Gatlingburg (ZUCKER, A., ed.), Academic Press, N.Y. (1967) p. 884.
[55] CERNY, J., et al., Phys. Lett. 20 (1966) 35.
[56] OGATA, H., VAN BREE, R., TEMMER, G.M., unpublished.
[57] BRUNNADER, H., HARDY, J.C., CERNY, J., to be published.
[58] JÄHNECKE, J., Proc. Third. Int. Conf. Atomic Masses, Winnipeg, Canada (1967).
[59] CERNY, J., et al., Phys. Lett. 13 (1964) 726.
[60] CERNY, J., et al., Phys. Lett., 16 (1966) 469.
[61] ADELBERGER, E.G., BARNES, C.A., Bull. Am. phys. Soc. 10 (1965) 1195.
[62] ADELBERGER, E.G., BARNES, C.A., Phys. Lett. 23 (1966) 474.
[63] ESTERLUND, R.A., et al., Phys. Rev. 156 (1967) 1094.
[64] McDONALD, A.B., ADELBERGER, E.G., Phys. Lett. 26B (1968) 380.
[65] BUTLER, G.W., et al., Phys. Rev. 166 (1968) 1096.
[66] McPHERSON, R., HARDY, J.C., Can. J. Phys. 43 (1965) 1.
[67] HARDY, J.C., SKYRME, D.J., Bull. Am. phys. Soc. 11 (1966) 627; Isobaric Spin in Nuclear Physics (FOX, J.D., ROBSON, D., eds.) Academic Press, New York (1966) p. 701.
[68] REEDER, P.L., et al., Phys. Rev. 147 (1966) 781.
[69] HARDY, J.C., VERRALL, R.I., BELL, R.E., Nucl. Phys. 81 (1966) 113.
[70] POSKANZER, A.M., et al., Phys. Rev. 152 (1966) 995.

DISCUSSION

D. F. ZARETSKY: Are there any data on the (p, n) reactions in the heavy nuclei region (e. g. Pb)?

G. M. TEMMER: We tried to observe ^{207}Pb(p, n)^{207}Bi without success. As far as I know, Sm is the heaviest nucleus for which the (p, n) reaction has been observed.

D. F. ZARETSKY: What is known about the difference between the total width of the analogue resonance and the total proton width?

G. M. TEMMER: This is a question which should be answered by a theoretician.

P. von BRENTANO: Concerning Professor Zaretsky's question on the spreading width in heavy nuclei, we have measured these spreading widths for five analogue resonances in ^{209}Bi at the University of Washington. We measured the total width Γ of a resonance and also the inelastic proton decay width $\Gamma^{p'}$ to various final states from the resonance. Then we obtain $\omega = \Gamma - \sum_{\alpha} \Gamma^{p'}_{\alpha}$. We found values $\omega \sim 100$ keV for the $g_{9/2}$ resonance and $\omega \sim 150$ keV for the $d_{5/2}$ analogue resonance. I would like to mention the very interesting idea of Dr. Bondorf, who claims that we can determine the spreading width $W^{sp}(J)$ due to a single particle J only by comparing the spreading width of the single-particle resonance in ^{209}Bi with spin J - W(J, 209) with the spreading width of the ground-state analogue in ^{208}Bi(0^+) - W(0^+, 208). $W^{sp}(J) \cong W(J, 209) - W(0^+, 208)$. The values found for $W^{sp}(J)$ are about 50-100% of the elastic widths.

Ya. A. SMORODINSKY: How do you know the values of the isotopic spins? In what cases are several members of the same isotopic family known?

G. M. TEMMER: In this game, one never really has sufficient conditions for determining the value of the isospin. Most experimenters agree with each other on the values of T. To state it naively, any resonance

observed on heavier nuclei (below the Coulomb barrier) will have a value $T_>$ simply because it is observed, i.e. it is simple enough to have a large overlap with the target + proton channel.

V.I. MANKO: What are the specific features of the gamma decay from the analogue and double analogue states?

G.M. TEMMER: In the s-d shell many cases of transitions from $T_>$ to $T_<$ states with the same spin and parity, via strong M1 transitions, have been observed (see Refs [24] and [25] of my paper). Also Professor Hanna will discuss some aspects of this process in his contribution which will follow. There is also the question of the isospin splitting of the giant E1 resonance (see Refs [27] to [31] of my paper).

V.I. GOLDANSKY: Are there any direct comparisons for the analogue states arising in various nuclear reactions and in the emission of delayed protons in the decays

$$\underset{T\,=\,3/2}{{}^{A=2Z-3}_{Z}M_{N=Z-3}} \xrightarrow{\beta^+} \underset{T\,=\,3/2}{\left[{}^{A=2Z-3}_{Z-1}M_{N=Z-2}\right]^*} \longrightarrow \underset{T\,=\,1/2}{p} + \underset{T\,=\,0}{\left[{}^{A=2Z-4}_{Z-2}M_{N=Z-2}\right]}$$

(e.g. in the decay of ^{21}Mg, ^{25}Si, ^{29}S, ^{33}Ar, etc.)?

Is it possible by studying analogue states in nuclear reactions to make any definite assumptions regarding the β^+-decay mechanism and energies in lighter emitters of the delayed protons of the type

$$\underset{T\,=\,2}{{}^{A=2Z-4}_{Z}M_{N=Z-4}} \xrightarrow{\beta^+} \underset{T\,=\,2}{\left[{}^{A=2Z-4}_{Z-1}M_{N=Z-3}\right]} \longrightarrow \underset{T\,=\,1/2}{p} + \underset{T\,=\,1/2}{\left[{}^{A=2Z-5}_{Z-2}M_{N=Z-3}\right]}$$

(e.g. in the decay of ^{20}Mg, ^{24}Si, ^{28}S, ^{28}Ar, etc.)?

Are there any experimental results for similar analogue states?

G.M. TEMMER: For the odd nuclei you mention in the first part of your question we have used the delayed proton results very much indeed (see Refs [63], [66], [68], [69] and [70] of my paper). As to the even nuclei, I have no information on any results to date.

P. AXEL: In answer to the question about the (p, n) reaction in Pb, one could learn about the width of the analogue state and about the branching ratio of protons by observing the distinctive decay protons emitted after the analogue state is formed in a (p, n) reaction.

G.M. TEMMER: I agree with you.

M.G. URIN: Do you know any recent data on the fine structure of the analogue states in nuclei heavier than ^{48}Ca?

G.M. TEMMER: Fox and his co-workers have studied ^{92}Mo + p, as you know. That is the heaviest element in which any evidence for fine structure was found. Heavier elements around Sm and Nd have been examined with ~5 keV resolution without revealing any structure. We at Rutgers are working hard to reduce the spread of our beam to about 100 eV (it is now about 500 eV) to study this problem.

P. von BRENTANO: You mentioned the new work in which the neutron decay of analogue resonances to various final states was measured. There is a quite definite prediction from analogue states theory, namely that the ratios of the cross-sections $\sigma_{pn}(i)$ to two final states i and j, $\sigma_{pn}(i)/\sigma_{pn}(j)$, should be independent of the incident energy, that is they should not vary

over the resonance. Does this check out? I think this is a very important check on the theory.

G. M. TEMMER: Both Refs [22] and [23] of my paper discuss the type of comparison you suggest. So far as I know, the ratios are in agreement with the Hauser-Feshbach theory and so are the angular distributions.

Dr. P. von BRENTANO presented Contribution No. 55 to the Symposium, by P. von Brentano, P. Richard and W. Wharton (University of Washington, Seattle, USA).

Short contribution

S. S. HANNA: I should like to make some remarks on the subject of T = 2 levels in ^{20}Ne as compound-nucleus resonances, work done by S. S. Hanna, F. Riess, W. J. O'Connell, K. A. Snover, H. M. Kuan, D. W. Heikkinen, G. L. Latshaw, E. Adelberger, and A. V. Nero (Stanford University, Stanford, California, USA).

The T = 2 resonances in $T_z = 0$ nuclei are observed by means of the isospin cascade $T = 2 \rightarrow 1 \rightarrow 0$ in (p, $\gamma\gamma$) reactions. For the lowest T = 2 levels, the spin cascade is $J^\pi = 0^+ \rightarrow 1^+ \rightarrow 0^+$ which produces the γ - γ correlation $1 + \cos^2\theta$. These resonances are also observed in the reactions (p, p_0), (p, p_1)... (p, α_0), (p, α_1)... and (p, n_0), ... In general the $T = 2 \rightarrow 1$, $T_z = 0$ transitions are gamma ray analogues of observed $T_z = 2 \rightarrow 1$ beta transitions.

The lowest T = 2 level in ^{20}Ne is observed as a resonance in ^{19}F(p, $\gamma\gamma$)^{90}Ne. The T = 2 state cascades through a 1^+, T = 1 level for which all particle channels are closed. The resonance was located by observing the yield of the second γ-ray of higher energy. The primary transition is the gamma analogue of the beta transition from the ground state of ^{20}O to the analogue 1^+ level of ^{20}F. The resonance occurs at $E_p = 4.090 \pm 0.005$ MeV or $E_x = 16.728 \pm 0.005$ MeV in ^{20}Ne. The angular distribution of the 11.2-MeV γ-ray relative to the proton beam is isotropic, which is consistent with J = 0 for the T = 2 state. The particle groups from the reaction were observed at several angles. The T = 2 state appears as a sharp anomaly in the elastic scattering at all angles. The curves are consistent with $\ell = 0$, $J^\pi = 0^+$, $\Gamma \leq 2$ keV, and $\Gamma_p/\Gamma \approx 0.1$. The unresolved group $\alpha_1 + \alpha_2$ shows a striking anomaly at the backward angles. At 154° the α_2 group was resolved and shows that the anomaly can be attributed principally to the transition to the 3^- level of ^{16}O with $\Delta\ell = 3$ and $\Delta T = 2$. The α_0 group shows similar but less pronounced anomalies. From the γ-ray data it is estimated that $\Gamma_p\Gamma_\gamma/\Gamma \approx 0.5$ eV. Thus $\Gamma_\gamma \approx 5$ eV. The Weisskopf estimate is 3.4 eV.

The second T = 2 level in ^{20}Ne was observed in ^{19}F(p, p_0), (p, α_0), (p, α_1) and (p, α_2) at $E_p = 5.880 \pm 0.005$ MeV, $E_x = 18.427$ MeV, with $\Gamma_{lab} = 11 \pm 3$ keV, and $\Gamma_p/\Gamma \approx 0.2$ (for $J^\pi = 2^+$). In ^{19}F(p, γ)^{20}Ne the gamma-rays γ_0, γ_1, γ_2, γ_3, γ_4 and γ_5 are not resonant but the resonance is observed for a 10.6-MeV γ-ray, identified as the second γ-ray of a cascade through a T = 1 level at $E_x = 12.26$ MeV to the 2^+, 1.63-MeV level. The resonance curve gives $\Gamma_p\Gamma_\gamma/\Gamma \approx 0.055$ eV. Hence $\Gamma_\gamma \approx 0.3$ eV. In the ^{19}F(p, n)^{19}Ne reaction, strong anomalies were observed for n_0 and $n_1 + n_2$ at backward and forward angles with a pulsed-beam, time-of-flight spectrometer.

Short contribution

S. S. HANNA: I should also like to report on work done by M. Hasinoff, H. M. Kuan, S. S. Hanna and G. A. Fisher (Stanford University, Stanford, California, USA) on E1 analogue states in the $T_>$ region of ^{90}Zr from the ^{89}Y + p reactions.

The reaction $^{89}Y(p, \gamma_0)^{90}Zr$ was studied from E_p = 10.0 - 17.4 MeV corresponding to E_x = 18.2 - 25.6 MeV in ^{90}Zr. In addition to the previously observed resonance at E_x = 21.0 MeV,[1] a narrower resonance at E_x = 19.5 MeV was observed. The widths are 0.7 and 0.2 MeV, respectively. Angular distributions taken at E_x = 19.2, 19.6, 19.85, 20.4, 20.75, 20.85, 21.10 and 21.75 MeV indicate a dipole distribution consistent with $J^\pi = 1^-$ for both levels. These two states are presumably the theoretically predicted[2] T = 6 analogue states in ^{90}Zr at E_x = 19.7 and 21.2 MeV (corresponding to predicted states at E_x = 6.3 and 8.0 MeV in ^{90}Y). The (p, n) yield in this region was also measured and no strong structure was observed; this supports the suggestion that these resonances are part of the $T_>$ dipole strength. Elastic and inelastic proton scattering at several angles in the region E_p = 10.5 - 13.5 MeV indicate weak resonances in (p, p_0) at E_p = 11.25 MeV and 12.6 MeV in agreement with the gamma-ray data. The shapes of the (p, p_0) excitation curves are consistent with $\ell = 0$ capture to 1^- states. Preliminary analysis of the inelastic data shows no resonance structures.[3]

V. I. MANKO: What is known about alpha-decay from analogue and double analogue resonances?

G. M. TEMMER: This α-decay must involve the iso-tensor component of the Coulomb field in first order which, according to Hecht of the University of Michigan, may not be much smaller than the iso-vector component. The curvature of the isobaric mass parabola shows another effect produced by the iso-tensor component.

S. S. HANNA: We have not yet obtained values for the reduced alpha particle width for these T = 2 resonances. However, our work and the work of the Berkeley group indicate that the alpha widths may be comparable to the proton widths. Thus the alpha widths could be of the order of 10% of the total width.

Short Contribution

M. G. URIN (Moscow Physical Engineering Institute, Moscow, USSR): I should like to present some results by Yu. N. Deviatko, D. I. Zaretsky and myself on the proton width of analogue resonances.

Professor Temmer touched upon the problems concerning analogue resonance. I would like to dwell upon one of these problems, namely, the theoretical interpretation of the mechanism of the proton decay of analogue states in heavy nuclei. I shall give a brief account of the results on some partial proton widths for the case of resonance (pp)-scattering on ^{207}Pb, ^{208}Pb nuclei.

---

[1] AXEL, P., DRAKE, D.M., WHETSTONE, S., HANNA, S.S., Phys. Rev. Lett. 19 (1967) 1348.

[2] FALLIEROS, S., private communication.

[3] VAN BREE, R., TEMMER, G.M., Bull. Am. phys. Soc., Washington, D.C. (1968).

TABLE A. CALCULATED PROTON PARTIAL WIDTHS (IN keV)

		E_K(MeV)	$\xi = 0.15$	$\xi = 0.2$	W = 15 MeV	Γ_{exp}
	$\frac{1}{2}^-$	11.4	58	39	61	61± 15[a]
^{207}Pb	$\frac{5}{2}^-$	10.9	26	18	24	17± 4[a]
	$\frac{3}{2}^-$	10.6	74	51	80	50± 11[a]
	0^+	14.9	25(ξ = 0.18)	17(ξ = 0.24)	18.5 (W = 18 MeV)	17± 4[a]
^{208}Pb	4^-	11.4	26	18	27	24[b]
	5^-	11.7	32	21	34	23[b]

Note: E_K is the proton kinetic energy, ξ the imaginary part of the optical potential versus the real one for volume absorption, W the force of the surface absorption.

(a) LENZ, G.H., TEMMER, G.M., Nucl. Phys. A112 (1968)625.
(b) RICHARD, P. et al., Phys. Lett. 26B (1967)8.

The decay of the analogue state with proton emission results from nuclear interaction. The matrix element determining the decay width is

$$M = \langle f | \hat{F} | a \rangle.$$

Here $|a\rangle \sim T^{(-)} |0\rangle$ is a wave-function of the analogue state. F is an irreducible amplitude of scattering in the particle-hole channel which in the coordinate representation has the form

$$\hat{F} = F \sum_{ik} \tau_i \tau_k \delta(\vec{r}_i - \vec{r}_k)$$

The value of the strength constant F is related to such nuclear characteristics as the position of the giant dipole resonance, symmetry energy, Lane's potential value, etc.

Consider the proton decay of the excited state ^{208}Bi*, which is an analogue state of ^{208}Pb with excitation of hole states in ^{207}Pb. In this case the matrix element M can be related to the diagram

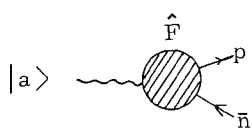

Simple calculation gives the following expression for the partial proton width

$$\Gamma \sim \left| F \int R^{(-)}_{kj\ell}\ n(r) R_{nj\ell}\ r^2\, dr \right|^2$$

Here $R^{(-)}_{kj\ell}$ is a proton radial wave-function in a continuous spectrum which is determined from the optical model, $R_{nj\ell}$ is a neutron-hole wave-function, n(r) the density of excess neutrons.

In a similar way, the elastic and inelastic widths for the proton decay of the ^{209}Pb ground state analogue resonance have been calculated by taking into account the excitation of the particle-hole levels of ^{208}Pb levels with spin and parity values equal to 4^- and 5^-. The results of calculations are in satisfactory agreement with experimental data (see Table A).

G.E. BROWN: This is a very special case where you have calculated only the width for decay. In general, the width arises also from mixing into compound states, etc., and the situation is much more complicated.

M.G. URIN: We do not state that the sum of partial proton widths for the decay of an analogue state should be equal to the total resonance width. Indeed, the analogue state can also decay at the compound-nucleus level. In the case of heavy nuclei the width for this decay is likely to coincide with the resonance neutron width.

FINE STRUCTURE AND QUASIBOUND STATES

V. GILLET
CENTRE D'ETUDES NUCLEAIRES DE SACLAY,
GIF-SUR-YVETTE, FRANCE

Abstract — Аннотация

FINE STRUCTURE AND QUASIBOUND STATES. With the exception of single-particle resonances, or of the gross structure of the giant resonance, the nature of unbound nuclear states is still largely unexplored. However, this field of research is becoming rapidly a most promising one. This is due on one hand to the extension of shell model concepts and techniques to the microscopic description of nuclear modes above particle emission threshold, and on the other hand to the recent development of the technology of cluster transfer reactions (i.e. reactions where a number of nucleons are added to a target nucleus).

The fine structure of nuclear continuum states is interpreted in the framework of the shell model as the result of coupling unbound configurations to many particle - many hole quasibound states. The density of the resonances is linked to the density of shell model quasibound states which can be formed while the widths of the peaks are related to the overlap between the wave-functions of the quasibound states and of the unbound configurational states. This description is amenable to experimental verification. For example an interference shape in the cross-section curve for a process induced by a one body operator may be attributed to a n particle - n hole quasibound state when a resonance in the excitation cross-section via the transfer of a n-p cluster to a n-h target occurs at the same energy.

As an illustration the present experimental situation for the ^{16}O continuum is reviewed.

ТОНКАЯ СТРУКТУРА И КВАЗИСВЯЗАННЫЕ СОСТОЯНИЯ. За исключением одночастичных резонансов и грубой структуры гигантского резонанса, природа несвязанных ядерных состояний остается в значительной степени неизученной. Однако, эта область исследований становится в настоящее время одной из наиболее обещающих. С одной стороны, это происходит благодаря распространению принципов и методов оболочечной модели на вопросы, связанные с микроскопическим описанием ядерных свойств выше порога эмиссии нуклонов. С другой стороны, это происходит благодаря новейшему достижению в области осуществления реакций с передачей кластеров (т.е. реакций, когда несколько нуклонов добавляется к ядру мишени). Тонкая структура ядерных состояний в непрерывном спектре интерпретируется в рамках модели оболочек как результат связи с многочастичными – многодырочными квазисвязанными состояниями. Плотность таких резонансов связана с плотностью квазисвязанных состояний, которые могут быть построены в модели оболочек, а их ширины определяются перекрыванием, существующим между волновыми функциями квазисвязанных состояний и несвязанных конфигураций. Такое описание подлежит экспериментальной проверке. Например, интерференционная форма кривой сечения для процессов, вызываемых одночастичным оператором, может быть приписана к n-частичному – n-дырочному квазисвязанному состоянию, если при той же энергии расположен резонанс в сечении возбуждения этого состояния при передаче n – p-частичного кластера n – h-дырочному ядру мишени. В качестве иллюстрации рассматривается современное состояние эксперимента для непрерывного спектра ^{16}O.

INTRODUCTION

With the exception of single particle resonances, or of the gross structure of the giant resonance, the nature of unbound nuclear states is still largely unexplored. However, this field of research is becoming rapidly a most promising one. This is due on the one hand to the extension of shell model concepts and techniques to the microscopic description of nuclear modes above the particle emission threshold, and on the other

hand to the recent development of the technology of cluster transfer reactions (i.e. reactions where a number of nucleons are added to a target nucleus).

Experimental and theoretical results are still very scarce. Accordingly, this paper will be limited to general considerations about the mechanism for the continuum fine structure when looked at from a shell model viewpoint. This brings in the notion of "quasibound" states. They play exactly the role of the Bohr compound nucleus in the microscopic theory of nuclei with, however, the major simplification that only a very few nucleons can be excited in the compound state due to the existence of a large Hartree-Fock energy gap. We shall review the theoretical and experimental situation in ^{16}O, which is the only nucleus for which a fairly complete set of data exists.

NATURE OF QUASIBOUND STATES

According to the compound nucleus model of Bohr, the existence of a rapidly varying structure in the continuum is attributed to long-lived compound states in which the available excitation energy exceeding the threshold is shared among many nucleons, none of which has enough of it to escape. The transposition of this concept into a shell model framework leads to considerable simplification by restricting the number of nucleons which can be excited in the compound state due to the large energy gap between filled and unfilled shell-model orbitals. Thus, considering a double closed shell nucleus for simplicity, the configurations to be considered can be classified according to their number of particle-hole pairs, namely (1p-1h), (2p-2h), (3p-3h), (4p-4h), ..., (np-nh). It is true that the number of configurations increases rapidly with n, as well as their shell model energies. However, as we discuss below, there are a few particular coherent superpositions of these configurations which undergo sufficient energy shift to yield in the intermediate energy region, i.e. between the particle emission threshold and the giant resonance, n particle - n hole (np-nh) states wherein all excited nucleons are bound. Assuming the ground state of the system to be a pure closed shell state, these discrete bound (np-nh) states can decay or be excited in a reaction only because of their coupling to the unbound configurations. If this coupling is small, the coherent (np-nh) states are long lived, and thus they play exactly the role of compound states in a shell model framework and are called quasibound states [1].

The mechanism responsible for the existence of np-nh quasibound states at energies much lower than the shell model energy jump needed for creating the n-particle n-hole pair is simple. It may be sketched in a schematic two-level model: a level j completely filled with protons and neutrons representing the double closed shell and an empty level k at energy ϵ above level j. Raising n nucleons from j to k requires an energy $n\epsilon$, i.e. which varies linearly with the number of excited nucleons. On the other hand there will be a gain of potential energy, which will increase quadratically with the number of excited nucleons (i.e. it is proportional to the number of bound states); this gain is proportional to $V = V_1 + V_2$, where V_1 is the potential energy of two holes and V_2 the potential energy of two particles. This quadratic behaviour is subject to a very important

restriction without which the gain of potential energy for some n value would always overcome the shell model excitation energy: two nucleons mutually interact strongly only when in a symmetric (space) bound state and much less so in an antisymmetric (space) bound state. We may schematize this effect by setting the potential energy of two nucleons in an antisymmetric space state equal to zero. The resulting quasibound state spectrum is shown in Fig. 1. The lowest state at energy $x = 4\epsilon - 6V > 0$ is a 4p-4h one, then, in succession, 3p-3h, 1p-1h, 2p-2h.... It is seen that an 8p-8h quasibound state may appear below the 1p-1h one if x is small enough. If $x < 0$ the chosen shell model ground state is unstable. Detailed calculations show indeed that such a mechanism is already responsible for the existence of bound many particle - many hole states [2].

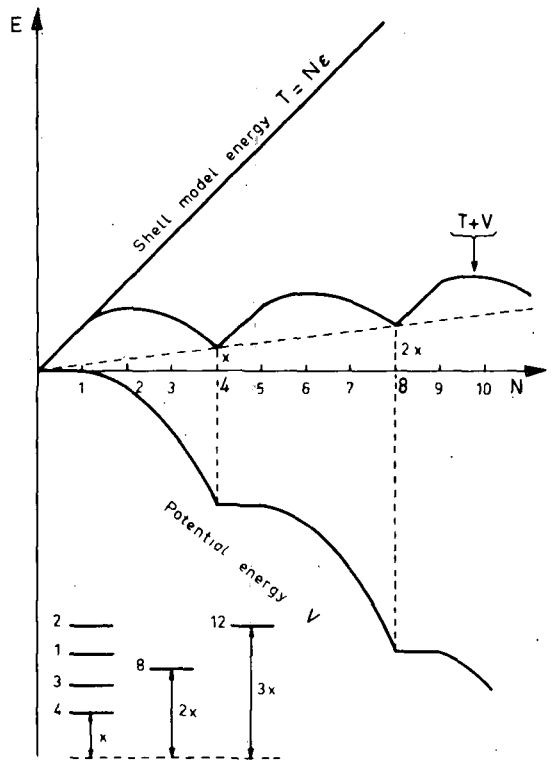

FIG. 1. The energy E = T + V of the 2-level schematic model as a function of the number N of particle-hole excited pairs.

The complete structure of the continuum is obtained from the coupling of the quasibound states to the unbound shell model configurations. Thus in this microscopic shell model description of continuum states, the density of the structure is linked to the density of shell model quasibound states which can be formed, while the widths of the peaks are related to the overlap between the wave-functions of the quasibound states and the wave-functions of the unbound configurational states.

Unbound configurations in the energy region under consideration are generally simple, for example (1p-1h), and their overlap with the shell

model quasibound states will decrease rapidly as the complexity of the latter increases. This permits the peaks in the structure to be classified according to their widths into a hierarchy linked to the (1p-1h), (2p-2h), (3p-3h), etc...., quasibound states [1].

GENERAL FORMALISM

The correct theoretical treatment of the fine structure is out of reach for the shell modellists. In a unified microscopic theory the treatment of np-nh quasibound states, where all n excited particles are bound, would require the treatment on the same footing of up to n unbound nucleons. It is well known that all present continuum theories are limited to states with at most one unbound particle in order to avoid the formidable mathematical difficulties which appear as soon as two nucleons are in the continuum.

An approximate procedure [3] has been used which neglects the coupling with the np ($n > 1$) continuum and only retains the coupling between the quasibound states and the 1p-1h continuum. The treatment is carried out in two steps. Step 1: Diagonalization of the shell model residual interaction over the space of the eigenstates of H_0 which involve configurations of more than 1 particle - 1 hole excitations, yielding a number of quasibound states $|\lambda\rangle$ at energy E_λ. Here the calculation is done for simplicity with the discrete states of an harmonic oscillator, which is quite justified since finite edge effects upon bound state wave-functions are small. Furthermore, all appropriate approximations for treating configuration mixing in the np-nh space ($n > 1$) can be used, such as interacting phonons in weak coupling [3] or the deformed orbital method with J projection [2], etc..... Step 2: Treatment of the residual interaction over the extended space consisting of the bound and unbound 1p-1h configurations of H_0 and the quasibound states $|\lambda\rangle$ obtained in Step 1. Here the bound and unbound 1p-1h configurations are calculated in the proper finite (real) well. The method of solution of the Schrödinger equation for positive energy $E > 0$ can be one of the many recently proposed, such as the Coupled Channel Equations [4] in coordinate representation, the Eigenchannel Method [5] or the K-matrix Method [6] in the energy representation. For example, in the latter method the complete nuclear wave-function is given by the expansion

$$\Psi^{(n)}(E) = \sum_\alpha \int d\epsilon \; a_\alpha^{(n,E)}(\epsilon) \; |\alpha,\epsilon\rangle + \sum_\lambda a_\lambda^{(n,E)} \; |\lambda\rangle$$

where (n) denotes the order of degeneracy of the 1p-1h continuum (i.e. the number of independent sets of discrete quantum numbers α), and $|\alpha,\epsilon\rangle$ are Slater determinants of orthonormalized single particle states with one unbound particle of energy ϵ. The mixing coefficients $a_\alpha^{(n,E)}(\epsilon)$ and $a_\lambda^{(n,E)}$ are obtained by resolving the set of equations resulting from the application of H to the above form of $\Psi^{(n)}$ [3, 6].

This wave-function $\Psi^{(n)}(E)$ can only be used for evaluating processes which lead to at most one particle in the continuum (γ-absorption, p, p', e, e', γ, n etc...) although it includes the effect of the quasibound states. For these processes, the absolute values of the cross-sections cannot be correct since coupling with unbound many-particle channels is neglected;

however, the relative variation with E should not be affected by this coupling which varies slowly and smoothly with E.

For example, given a complete set of wave-functions $\Psi^{(n)}(E)$, the γ-absorption rate at energy E is given by

$$T(E) = \frac{2\pi}{\hbar} \sum_{n} \left| \sum_{\alpha} \int d\epsilon \langle \alpha\epsilon \, | \mathcal{O} | 0 \rangle \, a_{\alpha}^{(n,E)}(\epsilon) \right|^2$$

where $|0\rangle$ denotes the shell model ground state and $\mathcal{O}$ the one-body transition operator. In this expression it should be noted that while the matrix elements are solely functions of the (1p-1h) configurations, the effect of the quasibound states $|\lambda\rangle$ *is felt through the mixing coefficients* $a_{\alpha}^{(n,E)}(\epsilon)$ since these are obtained by solving equations where the $|\lambda\rangle$'s appear explicitly [7]. This is shown in Fig. 2. The coupling of a discrete np-nh quasibound state to a smoothly varying 1p-1h continuum yields a rapidly varying structure in the cross-sections of processes produced by one-body operators (p, p', α, α', (p, γ), (γ, n) etc...). If a cluster np is transferred to a target represented by n-holes, both with the appropriate space symmetry as discussed above, we may expect a resonance shape (Fig. 2),

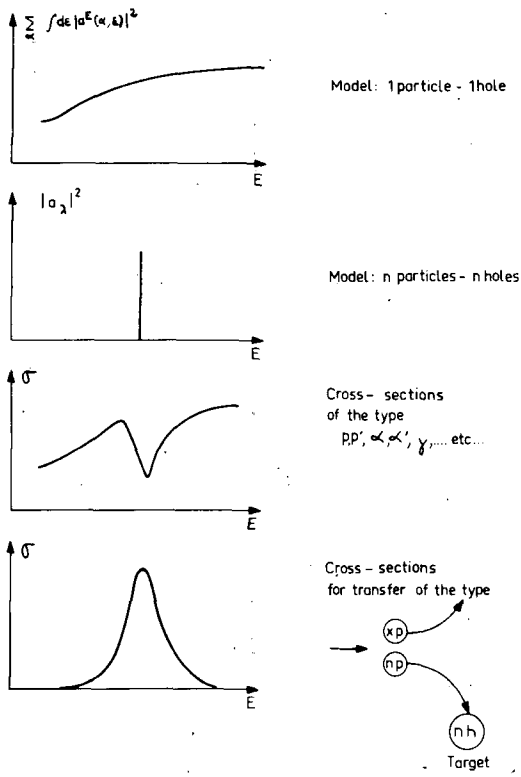

FIG.2. Effect of the mixing of an np-nh quasibound state with the 1p-1h continuum on cross-sections via a one-body operator (i.e. p, p', α, α', p, γ, γ, n, etc.) and on cross-sections for a cluster transfer reaction (incoming projectile np + xp, target nh).

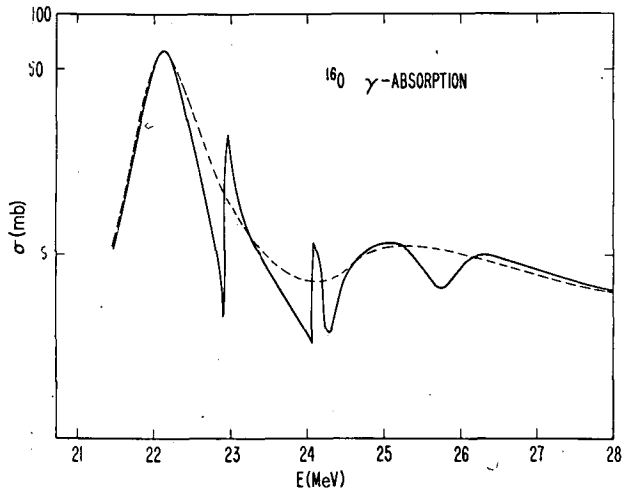

FIG.3. The giant resonance of ^{16}O in a one-particle one-hole continuum model without (dashed curve) or with coupling with 2p-2h quasibound states [3].

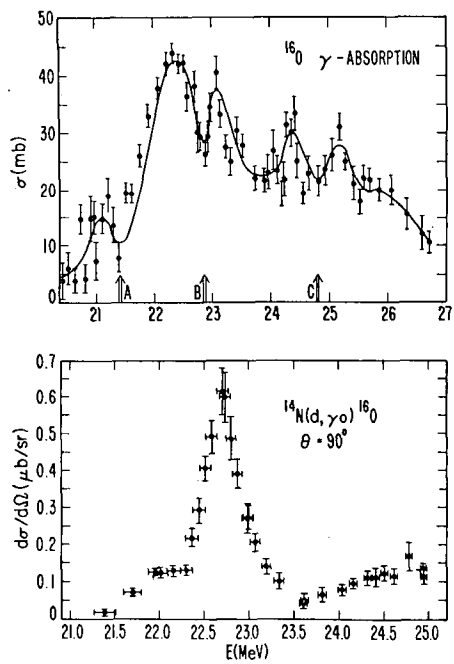

FIG.4. Upper curve: total photoabsorption cross-section in ^{16}O (from Ref. [9]). Lower curve: the reaction ^{14}N(d, γ)^{16}O (from Ref. [11]).

corresponding to the spreading of the quasibound state by its coupling with the continuum.

The result of a calculation [3] carried out on these lines is shown in Fig. 3. It represents the total photo-absorption cross-section in ^{16}O

calculated in the 1p-1h continuum alone (dashed curve) and with the coupling to 2p-2h quasibound states (solid curve). This coupling yields a definite fine structure in spite of the fact that the quasibound states are not coupled directly to the ground state (taken as a pure shell model state) by a one-body operator.

REVIEW OF THE EXPERIMENTAL DATA IN ^{16}O

As an illustration of these considerations, we discuss now the experimental situation for the continuous spectrum of ^{16}O. This is the only nucleus for which there exists at present a fairly complete set of data.

The data can be divided into three groups. Group 1: Excitations via one-body operators, such as γ-absorption, $^{16}O(\gamma, n)^{15}O$, $^{15}N(p,\gamma)^{16}O$, $^{16}O(p,p')$, $^{16}O(e,e')$, etc. Group 2: Photo-capture of clusters such as $^{14}N(d,\gamma)^{16}O$, $^{13}C(^3He,\gamma)^{16}O$, $^{12}C(^4He,\gamma)$, etc. Group 3: Cluster transfer reactions such as $^{14}N(^3He,p)^{16}O$, $^{12}C(^6Li,d)^{16}O$, etc. In the absence of theoretical results, it is the systematic study of the correlations between these cross-sections which may shed some light on the origin of the observed fine structures.

We discuss first the processes of group 1 in the region of the giant resonance.

Under poor energy resolution the photo-absorption cross-section exhibits two peaks around 22 and 25 MeV, having widths of 2 to 3 MeV.

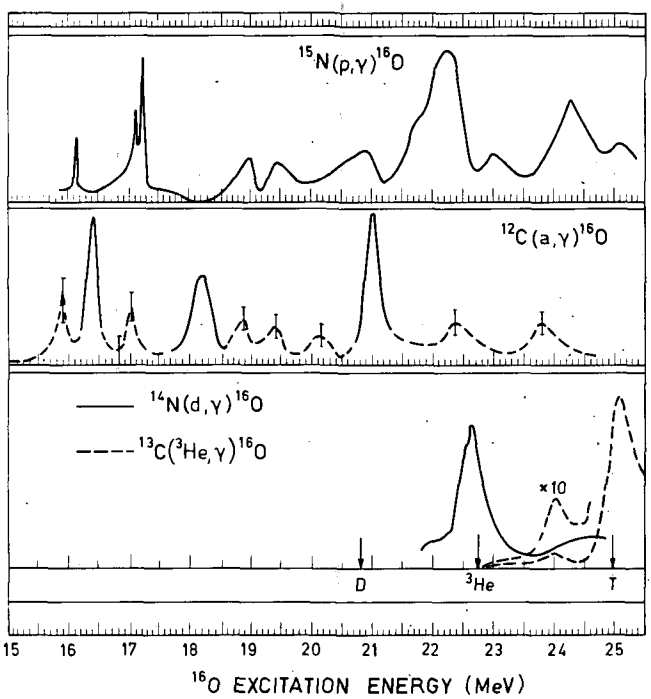

FIG.5. Comparison between $^{15}N(p,\gamma)^{16}O$ [10], $^{12}C(\alpha,\gamma)^{16}O$ [12], $^{13}C(^3He,\gamma)^{16}O$ [14] and $^{14}N(d,\gamma)^{16}O$. The diagram is by courtesy of M. Suffert.

The position and widths are well explained by coupling 1p-1h quasibound states to the 1p-1h continuum [8], while the calculated sum rule is wrong by a factor of 4 too much. More recent higher resolution photo-absorption experiments [9] reveal a fine structure with dips at 21.05 MeV, 22.7 MeV and 24.7 MeV (arrows A, B and C in Fig. 4) having smaller widths (200-300 keV). This fine structure is not accounted for by the one particle - one hole model.

A similar fine structure is observed in (p, γ) experiments [10] (Fig. 5).

The origin of this fine structure is partly explained by the results of the processes of group 2. The reactions of the type $^{14}N(d,\gamma)^{16}O$ and $^{12}C(\alpha,\gamma)^{16}O$ have T = 0 in the entrance channel. However, the dipolar nature of the emitted γ is experimentally well established [11, 12]. Accordingly, these reactions are only possible because of the isospin impurities of the wave-function. The parity of the emitted γ is not known; in what follows we adopt the working hypothesis of negative parity.

The $^{14}N(d,\gamma)^{16}O$ experiment [11] (Fig. 4, lower part) yields a peak at 22.7 MeV, exactly where the interference dip shows in the γ-absorption curve (arrow B, Fig. 4, upper part). This situation is similar to that of Fig. 2. This would mean that a 2p-2h quasibound state 1^- T = 1 is responsible for the fine structure shown there by the processes of group 1, although these do not couple directly the 2p-2h excitations to the ground state. Some support for this interpretation is given by the calculation of Fig. 3, where the 22.7 MeV dip is reproduced by the coupling of a 2p-2h quasibound state to the 1p-1h continuum.

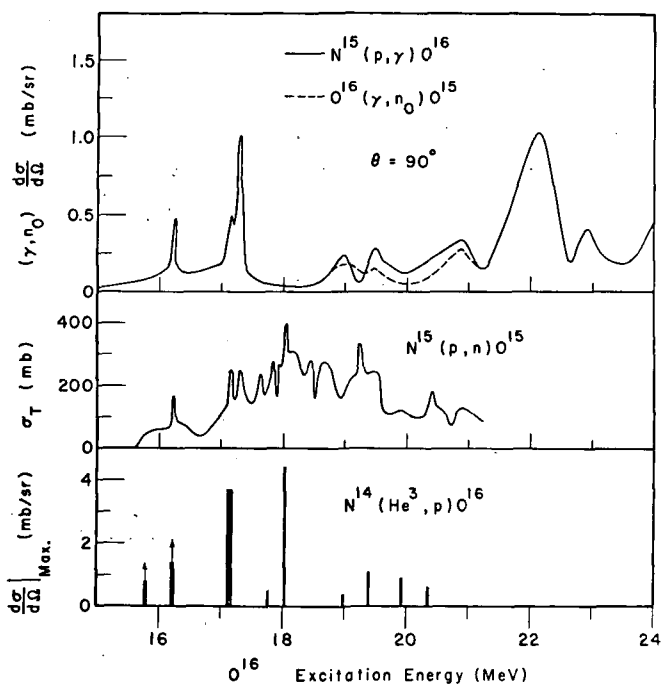

FIG. 6. Comparison between $^{14}N(^3He,p)^{16}O$ [15], $^{15}N(p,\gamma)^{16}O$ [10] and $^{15}N(p,n)^{15}O$ [19]. The diagram is from Ref. [15].

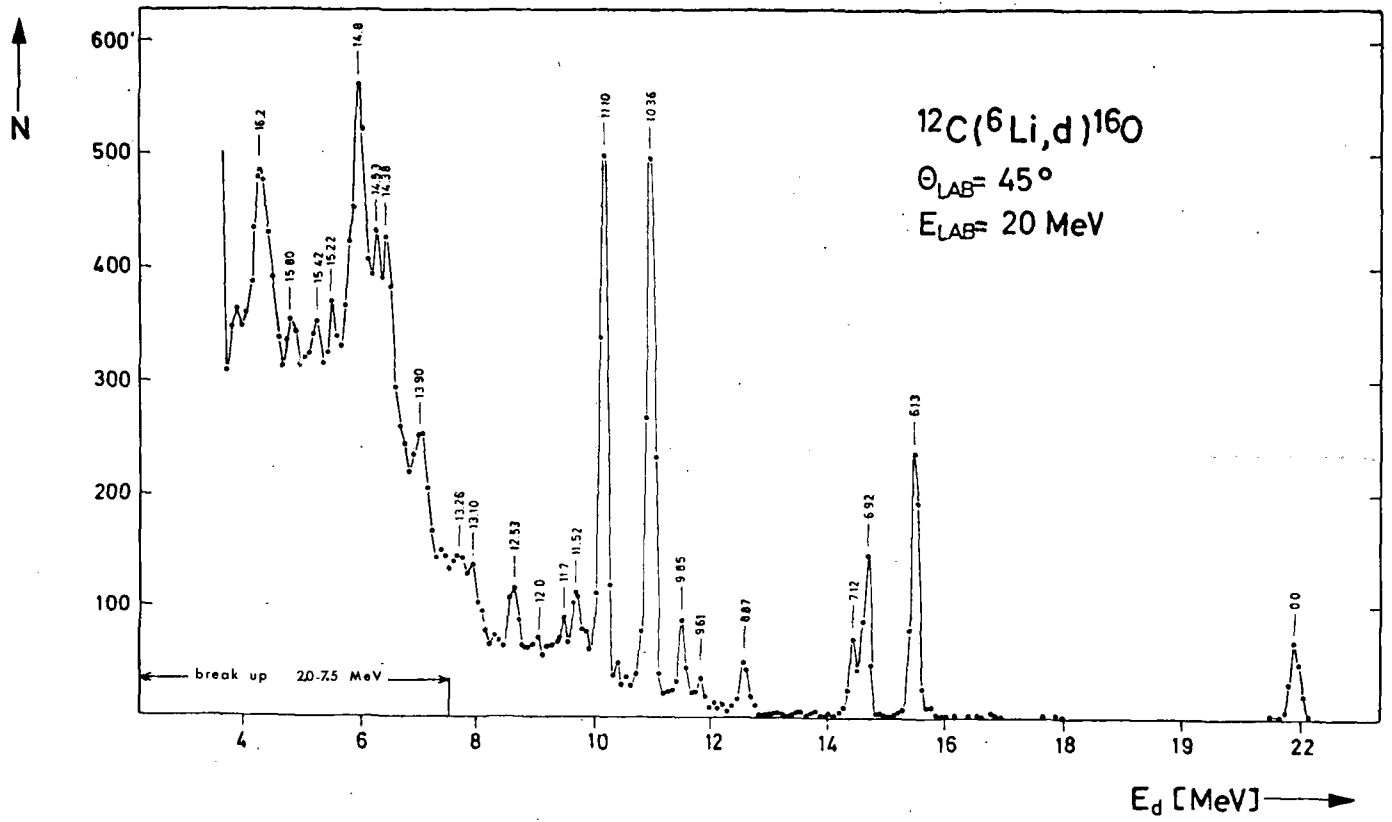

FIG. 7. The ^{12}C (^{6}Li, d) ^{16}O reaction [16].

Similarly $^{12}C(\alpha,\gamma)^{16}O$ [12] yields a narrow dipolar peak exactly where the processes of group 1 yield a dip at 21.05 MeV (Fig. 5). The γ is dipolar, hence T = 1 [12], and with our hypothesis of negative parity a 4p-4h quasibound state would thus appear responsible for the giant resonance structure at that energy.

The nature of the structure around 24.7 MeV is more uncertain. The $^{14}N(d,\gamma)^{16}O$ experiment carried out up to 25 MeV [13] gives some evidence of a peak in that region. However, the $^{13}C(^3He,\gamma)^{16}O$ [14] experiment also gives a resonance in the same energy region. The structure would thus appear as the result of coupling 2p-2h and 3p-3h quasibound states (see Fig. 5).

Other correlations, at lower energy, can be seen in Fig. 5 between the processes of group 1 and group 2.

The processes of group 3 are more difficult to interpret since they are not limited to the selection rules brought in by the γ signature. For example, most of the states seen in $^{14}N(^3He,p)^{16}O$ [15] are not correlated with the dipole states (for example, seen in p,γ) but with others seen for example in (p,n) (Fig. 6). Comfort et al. [15] conclude from a comparison with $^{14}N(t,p)^{16}N$ that most of the excitations obtained in $^{14}N(^3He,p)^{16}O$ are T = 1, even parity and 2p-2h; this may be an indirect technique for parity, isospin and spin assignment of the 1p-1h states seen in (p,n), according to whether they interfere or not with the identified 2p-2h components. Likewise, $^{12}C(^6Li,d)^{16}O$ [16] yields many more 4p-4h states in ^{16}O than $^{12}C(\alpha,\gamma)^{16}O$, which was predominantly 1^- T = 1. Some results, carried out only up to 16 MeV, are given in Fig. 7. More complicated processes involving 8p-8h excitations, as in $^{12}C(\alpha,^8Be)^8Be$ [18], have been studied, which show a definite strong structure below 20 MeV.

CONCLUSION

In conclusion, it appears that in order to improve our understanding of the structure of the continuum it is necessary to carry out comparative experimental studies of various cluster transfer reactions such as $(^6Li,d)$, $(^3He,p)$, $(^{16}O,^{12}C)$, (d,γ), $(^4He,\gamma)$, leading directly to the possible np-nh quasibound states. A very precise calculation of the position of such (np-nh) states is at present not possible owing to the very large energy shifts involved and the inherent uncertainties of shell model calculations. Accordingly, the identification of the cluster nature of the quasibound states responsible for the structure of continuum states rests with the experimentalists.

REFERENCES

[1] BLOCH, C., Proc. Enrico Fermi School, Varenna, Session 36, Academic Press, N. Y. (1966).
[2] RIPKA, G., in: Advances in Nuclear Physics, (BARANGER, VOGT, Eds.) Vol. 1, Plenum Press, N. Y. (1967).
[3] GILLET, V., MELKANOFF, M., RAYNAL, J., Nucl. Phys. A97 (1967) 631.
[4] BUCK, B., HILL, A. D., Nucl. Phys. A95 (1967) 271.
[5] DANOS, M., GREINER, W., Phys. Rev. 138 (1965) 877B.
[6] BLOCH, C., GILLET, V., Phys. Lett. 16 (1964) 62.

[7] GILLET, V., BLOCH, C., Phys. Lett. 18 (1965) 58.
[8] RAYNAL, J., MELKANOFF, M., SAWADA, T., Nucl. Phys. A101 (1967) 369.
[9] BURGOV, N. A., DANILYAN, G. V., DOLBILKIN, B. S., LAZAREVA, L. E., NIKOLAEV, F. A., Soviet Phys. JETP 16 (1963) 50.
[10] TANNER, N. W., THOMAS, G. C., EARL, E. D., Nucl. Phys. 52 (1964) 8869.
[11] SUFFERT, M., Nucl. Phys. 75 (1965) 226.
[12] SUFFERT, M., FELDMAN, M., (work done at Stanford Univ., USA) private communication.
[13] SUFFERT, M., (work done at Strasbourg and at Stanford Univ., USA) private communication.
[14] PUTTASWAMY, N. G., KOHLER, D., Phys. Lett. 20 (1966) 288.
[15] COMFORT, J. R., BAGLIN, J. E. E., THOMSON, M. N., Preliminary report presented at the American Physical Society meeting, Washington (1968).
[16] MEIER-EWERT, K., BETHGE, K., PFEIFFER, K. O., Nucl. Phys. A110 (1968) 142.
[17] CHEVALLIER et al., Proc. Conf. Nuclear Structure, Max-Planck Institute, Heidelberg (1966).
[18] BARNETT, A. R., Isobaric Spin in Nuclear Physics (FOX, T. D., ROBSON, D., Eds.) Academic Press, N. Y. (1966) p. 774.
[19] FIRK, F. W. K., WU, C., PHILLIPS, T. (1968) unpublished work quoted in Ref. [15].

DISCUSSION

B. N. ZAKHARIEV: I want to make a remark about one of the difficulties of unified theories of nuclear reactions. It is concerned with the continuous part of the expansion of the wave-function Ψ and it leads to complicated integral or integro-differential equations. This is due to the fact that Ψ differs from zero in an infinite region and its expansion involves a generalized Fourier integral (instead of a sum). This difficulty can be overcome[1] if we subtract from Ψ its known asymptotic part ϕ and expand only $\chi = \Psi - \phi$ which is different from zero in a finite region. The expansion of χ contains only a discrete sum (and no integral).

V. GILLET: Another method, along the same lines, has been recently proposed by Lane and Robson. Their method is also based on the remark that the unbound nucleon scattering wave-function is needed, when setting up the Green's function matrix, only in the interior region. Consequently, instead of using a continuous expansion which would yield the scattering wave-function in the whole space, they use a finite expansion over discrete harmonic oscillator functions. This basis is totally wrong in the external region but it gives rapidly convergent results in the inner region and provides a convenient representation of limited dimensions for inverting the nuclear matrix.

S. SZPIKOWSKY: My question concerns the simple two-level model. Here you take into account only the potential energy of the nucleons in the higher level. The results might be quite different if you took into account the interaction in the lower level too.

V. GILLET: The interaction in the lower level is taken into account. More precisely, as pointed out by Dr. Ripka, by definition in the present simple model the shell energy jump ϵ is equal to the breaking energy of three nuclear bounds in the lower level. On the other hand, when creating 1, 2, 3, 4 particle-hole pairs you lose in the lower level 3, 2, 1, 0 bounds, each equal to V_1, and gain 0, 1, 2, 3 bounds, equal to V_2 in the upper level. Introducing a loss of shell energy equal to $N\epsilon \equiv 3NV_1$, this leads to a gain of potential energy $[N(N-1)/2]V$, where $V = V_1 + V_2$. In other words, the potential energy of two holes adds up to the potential energy of two particles.

[1] EFIMENKO, T. G., ZAKHARIEV, B. N., ZIGUNOV, V. P., Ann. Phys. 47 (1968) 275.

C. F. CLEMENT: It would be nice if there were more experimental work on a fourth class of experiments which would be a valuable tool for investigating collective states in the continuum. These are capture reactions which lead to excited states of nuclei. Because these states can be chosen to have particular particle-hole properties relative to the ground state, transition from the continuum would examine corresponding particle-hole or multiparticle-multihole states in the continuum which may have collective properties. For example, final states selected could be vibrational or rotational 2^+ states.

V. GILLET: I quite agree. May I give another example: in the calculation of the fine structure of ^{16}O, the interference dip at 22.7 MeV appears as due to a 2p-2h quasibound state, whose main component is the two-phonon vector $\{(ph)\,0^+;\,(ph)1^-\}$. The 0^+ p-h phonon, in a spherical basis, has energy ~ 11 - 12 MeV while the dipole phonon is the 13 MeV state. Observation of a dipole γ, of about 13 MeV energy, leading to an excited 0^+ state around 11 MeV, would confirm this interpretation.

S. S. HANNA: As a comment on Dr. Clement's remark, I should like to mention that the giant dipole resonances built on excited states of nuclei are being studied in several laboratories, e. g. Argonne and Stanford. Quite detailed information is now available for several nuclei. The observations cover several light and medium nuclei up to ^{90}Zr. The case of ^{16}O is especially difficult experimentally because the excited states lie at rather high excitation energies. However, this experiment is planned and it is hoped results will be obtained soon.

THE STUDY OF ATOMIC NUCLEI USING NEUTRON SPECTROSCOPY METHODS
Some results and prospects

F.L. SHAPIRO
JOINT INSTITUTE FOR NUCLEAR RESEARCH,
DUBNA, UNION OF SOVIET SOCIALIST REPUBLICS

Abstract — Аннотация

THE STUDY OF ATOMIC NUCLEI USING NEUTRON SPECTROSCOPY METHODS: SOME RESULTS AND PROSPECTS. The results of some investigations performed recently on the pulsed reactor of the Laboratory of Neutron Physics, Dubna, are presented. The experiments on the (n,α) reaction in resonances with ^{143}Nd, ^{145}Nd, ^{147}Sm, ^{149}Sm, ^{95}Mo and some others as targets are discussed in greatest detail. The results of measuring variations of the neutron average number ν per fission event in neutron resonances of ^{235}Pu and ^{235}U are presented; these experiments yield information on the dependence of ν on the spin of a fissionable nucleus. The gamma-spectra study of neutron radiative capture in resonances and also the future prospects of applying polarized neutrons and oriented nuclear targets in neutron spectroscopy are given briefly.

ИССЛЕДОВАНИЯ АТОМНЫХ ЯДЕР МЕТОДАМИ НЕЙТРОННОЙ СПЕКТРОСКОПИИ. НЕКОТОРЫЕ РЕЗУЛЬТАТЫ И ПЕРСПЕКТИВЫ. Представлены результаты некоторых исследований, выполненных в последнее время на импульсном реакторе Лаборатории нейтронной физики. Наиболее подробно обсуждаются эксперименты по изучению реакций (n,α) в резонансах, проведенные с мишенями ^{143}Nd, ^{145}Nd, ^{147}Sm, ^{149}Sm, ^{59}Mo и некоторыми другими. Излагаются результаты измерений вариаций среднего числа нейтронов ν на акт деления в нейтронных резонансах ^{239}Pu и ^{235}U; эти опыты дают сведения о зависимости ν от спина делящегося ядра. Кратко рассматриваются исследования гамма-спектров радиационного захвата нейтронов в резонансах, а также перспективы использования в нейтронной спектроскопии поляризованных нейтронов и ориентированных ядерных мишеней.

1. INTRODUCTION

In approximately twenty years of intense development, slow neutron spectroscopy has enriched nuclear physics with important information on the properties of highly excited nuclei. These include direct data on energy level densities, distributions of level spacings and their widths, and neutron strength functions. These data helped to improve the optical and statistical models and confirmed the validity of their predictions within an accuracy, which may, in general, be considered satisfactory if one takes into account that the models themselves are only crude approximations. From the viewpoint of the above-mentioned theoretical models neutron spectroscopy has to a considerable extent accomplished its mission. This is probably what is responsible for the opinion that it is difficult to expect much from the further study of neutron resonances and that it would possibly be useful only as far as the requirements of nuclear energetics are concerned.

This may be argued from the most general conceptions of the ways of scientific development. At present, however, the need for such argument has passed since a new and promising trend has already been outlined in

neutron spectroscopy. Perhaps it manifests itself most clearly in the recent discovery which will be discussed in detail in the invited papers by Lynn and by Strutinsky and Bjørnholm in this Symposium — the discovery of two different systems of highly excited states in many fissionable nuclei.

The presence of two systems of levels implies that the compound nucleus has a structure which is general and simple enough to be of interest for both experimental and theoretical studies. It could hardly be doubted that this peculiarity is characteristic not exclusively of fissionable nuclei. More probably, the presence of a channel greatly simplifies the observations of structure connected with large nuclear deformation.

Another feature of this promising trend is the great deal of information becoming available on the properties of the capture state and of many low-lying levels; this information is provided by measurements of γ-ray spectra of resonance neutron capture using germanium detectors.

Indications as to the non-statistical character of γ-ray spectrum variations from resonance to resonance are especially interesting. The Harwell group, which observed such an anomaly in the target nucleus of mercury-198, considered it as evidence of the structure of a compound nucleus analogous to that observed in fissionable nuclei [1].

In the end, progress in the experimental technique has been the basis of the new trend. This progress has made it possible to pass to high-resolution neutron spectrometry experiments, yielding new information as compared with the measurements of total neutron cross-sections, which were the only ones available a few years ago.

In the present report some of these more complicated experiments on neutron resonances, which are being conducted or planned in Dubna, are considered.

2. (n,α) REACTION IN THE RESONANCE ENERGY REGION

The study of the (n,α) reaction in neutron resonances was begun by Popov and Kvitek about 2 years ago [2].

The experiments are very difficult owing to the smallness of the (n,α) reaction cross-sections caused by the low α-particle penetrability of the Coulomb barrier. They were made possible thanks to the development of gas scintillation and ionization multilayer chambers with low (less than 10^{-8}) efficiency for gamma-rays, which enabled one to operate with layers of investigated substance having an area of 2000-6000 cm^2. So far, Popov and co-workers have obtained positive results for the isotopes of neodymium-143, neodymium-145, samarium-147, samarium-149 and molybdenum-95. The lower part of Fig.1 presents the yield of the reactions ^{143}Nd (n,α) ^{140}Ce versus neutron energy measured by the time-of-flight spectrometer of the Laboratory of Neutron Physics, JINR (IBR reactor with a microtron injector). The main curve is measured with a resolution of 100 ns/m over 75 hours.

The inset diagram shows the results of measurements with a resolution of 30 ns/m (exposure 140 hours); the target consisted of a thin layer of neodymium oxide enriched in neodymium-143 to 73.2%, the total weight of the target being about 20 g. The upper part of the curve represents the yield of radiative capture gamma-rays for the same target, obtained

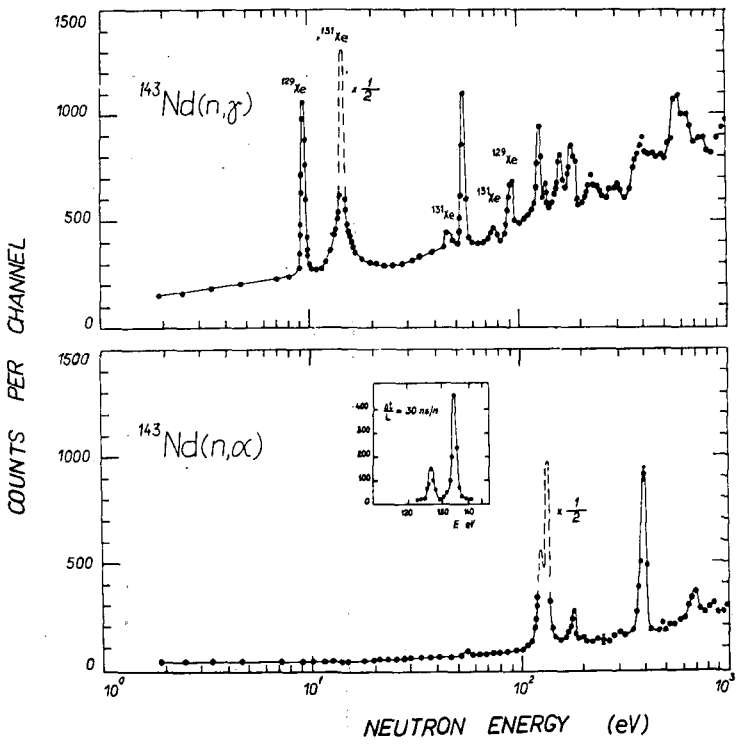

FIG.1. The curves of α-particle and γ-ray yields for the ^{143}Nd target.

with the same resolution, 100 ns/m. A comparison of the areas of the corresponding peaks on the curves of α-particle and γ-ray yields gives the α-particle widths of the resonances Γ_α, since their radiation widths Γ_γ are well known. Here the absolute calibration is obtained by measurements in the thermal energy region, where the cross-sections of both reactions (n,α) and (n,γ) are known for some isotopes. The data on the alpha-widths of neodymium-143 resonances are given in Table I. The 55.8 eV, 157 eV and 190 eV resonances are characterized by a much smaller α-width than the other resonances. The difference may be explained by the decay scheme of a compound nucleus of neodymium-144 (Fig.2). Capture of an s-wave neutron by neodymium-143 leads to excitation of levels of neodymium-144 with spin and parity 3^- and 4^-. The conservation of parity forbids the α-decay of 4^- states into the 0^+ ground state of the even-even product-nucleus of cerium-140. Decay into the 2^+ level with excitation energy 1.6 MeV is possible.

A decrease of α-particle energy by 1.6 MeV results in a decrease of the Coulomb barrier penetrability by two orders of magnitude. Therefore the α-widths of resonance with spin 4 should be smaller than those of resonances with spin 3 by a factor of several hundreds. Thus, in Table I spin 3 is assigned to strong resonances, whereas spin 4 is most probable for weak resonances.

The situation is analogous for the other isotopes investigated. However, for them the first excited level of a product-nucleus is not so high

TABLE I. Γ_α FOR ^{143}Nd RESONANCES

Resonance energy (eV)	Resonance spin	Γ_α (μeV)	Resonance spin from the value of Γ_α
-6	3	5.6 ± 1.3	
55.8		≤0.1	(4)
128		7 ± 1	3
138		36 ± 3	3
157		≤0.2	(4)
184		2 ± 0.4	3
190		≤0.5	(4)
410		14 ± 3.5	3
713		17 ± 8	3

as for the magic cerium-140, so that the dependence of the α-widths on the resonance spin is less pronounced. Fig.3 represents the curve of the α-particle yield from the samarium-149 target (enrichment 94.6%). The largest number of α-widths is determined for this nucleus; their integral distribution for 15 resonances is represented as a histogram in Fig.4. For five samarium-149 resonances with known spin 4^-, the average value of an α-width is equal to $\bar{\Gamma}_\alpha(4^-) = 5.3 \times 10^{-2}$ μeV. If the number of resonances is assumed to be proportional to $2J + 1$, $\bar{\Gamma}_\alpha(3^-) = 0.41$ μeV may be found. In Fig.4 the solid curve gives the sum of two χ^2 distributions with the number of degrees of freedom $\nu = 2$ (i.e. two exponents) and the average values given above. As is seen, the solid curve fits the experimental data sufficiently well.

The spread of α-particle widths of ^{143}Nd 3^- levels corresponds to the number of degrees of freedom $\nu_{eff} = 1.8 \pm 1$, whereas, in this case, if the Porter-Thomas theory is valid for α width distributions, it would be expected that $\nu = 1$.

For samarium-149, where transitions to the excited level, to which several orbital momenta contribute, are appreciable, ν should be about 2. Thus, with a very low accuracy of the experimental estimation of ν it can be preliminarily concluded that the observed distribution of α-widths is consistent with the Porter-Thomas theory.

Fig.5 presents the curve of the α-particle yield obtained with a chamber in which neodymium-143 and molybdenum-95 targets (enrichment 82.4%) were placed simultaneously. Apart from the neodymium-143 resonances, three peaks corresponding to the molybdenum-95 resonances are distinctly seen. These resonances also appeared in the measurements with only a molybdenum target. A very strong resonance of molybdenum-95 at 45 eV did not occur. It may thus be concluded that spin 3^+ is probable for this level, whereas the 553 eV, 899 eV and 1145 eV levels have spin 2^+.

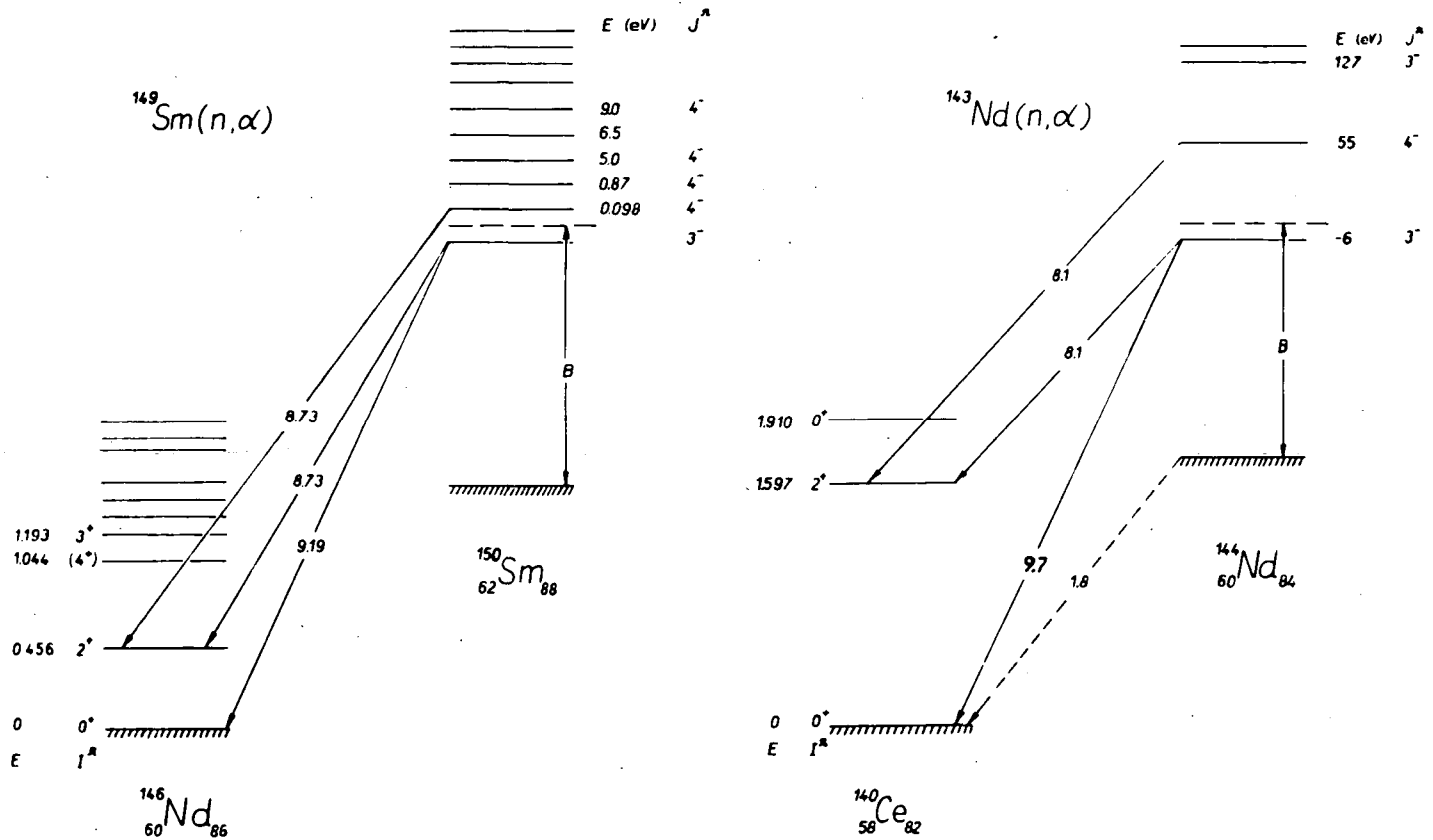

FIG.2. The level schemes for α-decay of ^{144}Nd and ^{150}Sm compound nuclei. B is the neutron binding energy.

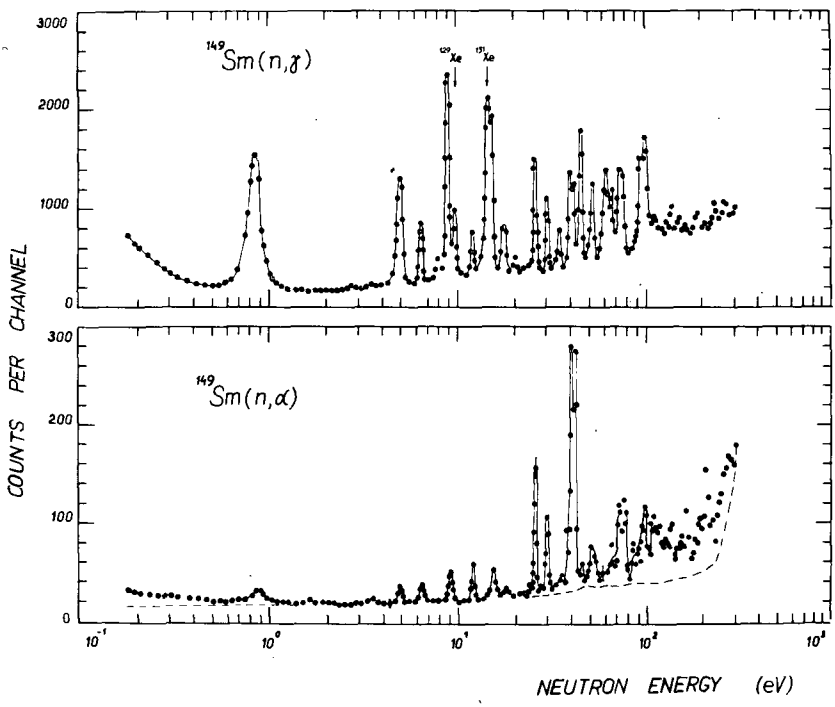

FIG.3. The curves of α-particle and γ-ray yields for the ^{149}Sm target.

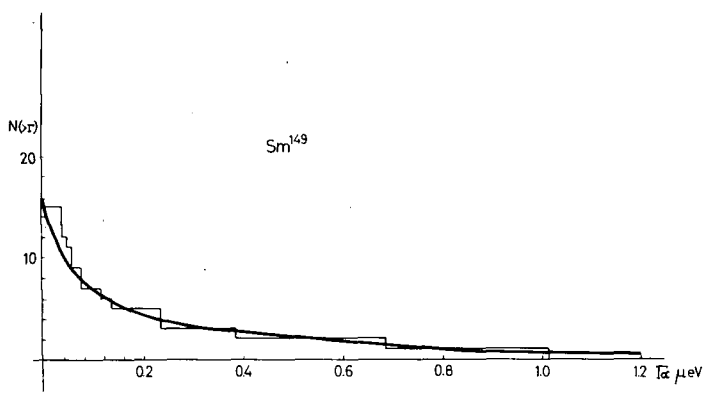

FIG.4. Integral distribution of α-widths of ^{149}Sm neutron resonances (histogram). The solid curve is the sum of two χ^2 distributions with the number of degrees of freedom $\nu = 2$. ($N(>\Gamma_\alpha) = 7 \exp[-\Gamma_\alpha/0.41] + 9 \exp[-\Gamma_\alpha/0.053]$).

The data on the average α-widths for the isotopes investigated by Popov et al. are summarized in Table II. The same table gives the values of α-widths calculated from the well-known formula of statistical theory:

$$\bar{\Gamma}_\alpha = \frac{D}{2\pi} \sum_{\ell,i} T_{\ell i}$$

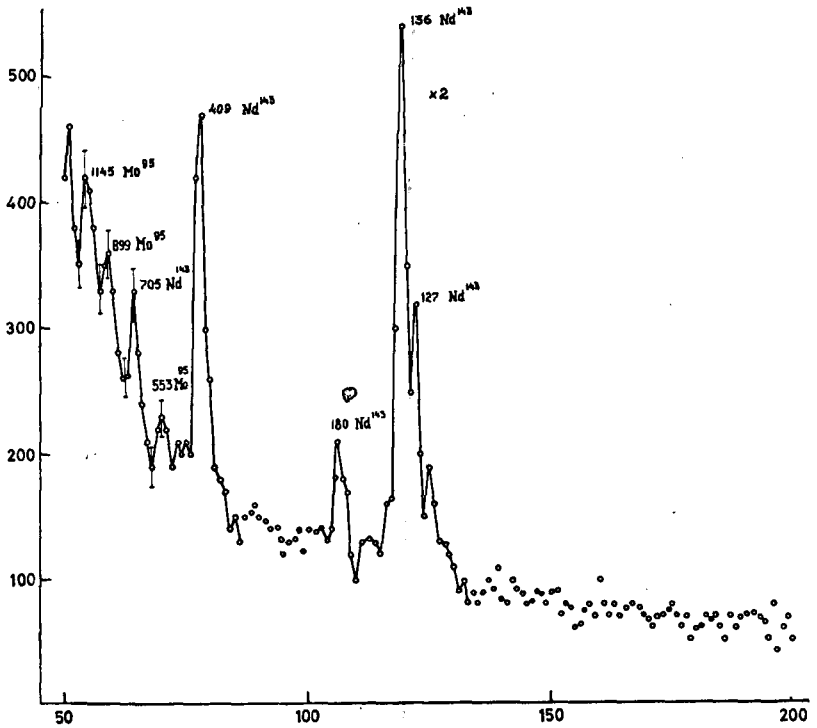

FIG.5. The curve of α-particle yield in resonances of ^{143}Nd and ^{95}Mo.

where D is the average distance between resonances with given spin and parity, $T_{\ell i}$ is the barrier penetrability for a partial wave with orbital momentum 1 for transition to the i-th level of the finite nucleus.

The penetrability was calculated in the quasi-classical approximation. Though the experimental data are characterized by large errors due primarily to the small number of isotopes under investigation, still, the general impression is that the observed average α-widths are smaller than those predicted by statistical theory (Fig.6). The discrepancy is especially large for molybdenum-95. It is difficult at present to say anything definite about the nature of the hindrance of the α-decay of the compound nuclei investigated. Measurements of α-particle spectra should yield valuable additional information. Such measurements for thermal neutron capture are being made successfully by several groups and measurements for resonance capture have been begun by Popov' s group.

Figure 7 presents the α-particle spectra for the ^{147}Sm 3.4 eV and 18.3 eV resonances obtained with an IBR plus microtron set-up using a grid ionization chamber [3].

Data on partial α-transition widths per level of a finite nucleus, averaged over levels with excitation energy below or above the pairing energy, are tabulated in Table III. As is seen in the statistical theory estimates are reached for transitions to the levels above the pairing energy and this is not so for transitions to the levels below the pairing energy. This difference may be understood in the following way. When

TABLE II. AVERAGE VALUES OF Γ_α

Compound nucleus	D (eV)	Spin and parity	Number of levels	$\bar{\Gamma}_\alpha$ (μeV)	
				Experiment value	Statistical theory
^{144}Nd	80	3^- 4^-	6 3	13 < 0.3	36 0.1
^{146}Nd	38	3^- 4^-	3	0.4	0.4 $2.2.10^{-2}$
^{148}Sm	14	3^- 4^- $3^- + 4^-$	2 1 8	1.2 0.34 0.6	8.1 1.1 4.6
^{150}Sm	6	3^- 4^-	10 5	0.41 0.053	1.2 0.16
^{96}Mo	280	2^+ 3^+	3 1	6.4 $< 1.10^{-2}$	360 6.4
^{130}Xe	80	1^+ 2^+	1 1	$< 2.10^{-3}$ < 0.1	4.10^{-3} 0.3
^{106}Pd	27	$2^+, 3^+$	3	$< 3.10^{-2}$	> 0.1
^{190}Os	10	$1^-, 2^-$	3	$< 3.10^{-3}$	0.3

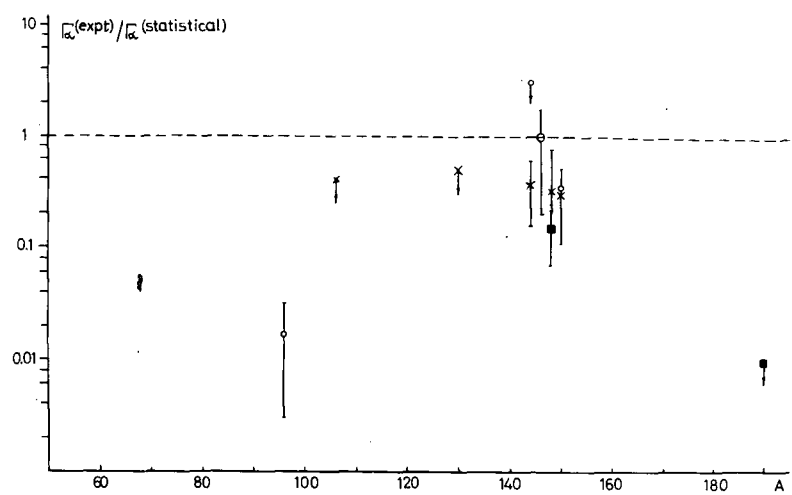

FIG. 6. The ratio of experimental values of resonance α-widths to the theoretical values estimated from statistical theory (see Table II).

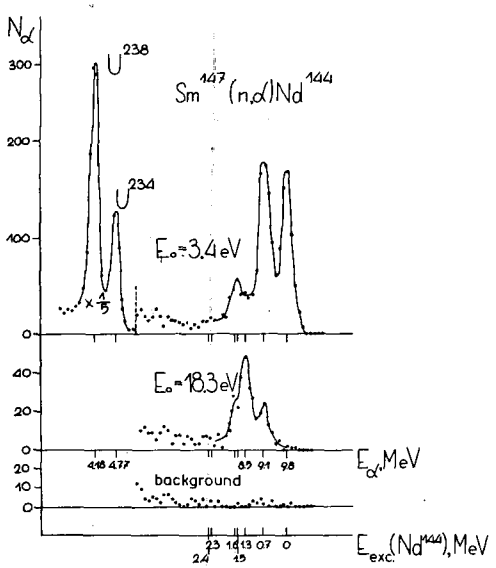

FIG. 7. The α-particle spectra of the $^{147}Sm(n,\alpha)$ reaction for resonances with an energy of 3.4 eV ($J^\pi = 3^-$) and 18.3 eV ($J^\pi = 4^-$). In the upper plot the α-particle spectrum of the uranium source, which was used to calibrate the apparatus, is also shown.

TABLE III. AVERAGE REDUCED α-PARTICLE WIDTHS

Compound nucleus	δ^2(eV)			Remarks
	Statistical theory $\delta^2 = D$	Experimental values		
		For levels below pairing energy	For levels above pairing energy	
^{146}Nd	38	5	40 - 80	Resonance 4.37 eV
^{148}Sm	14	7	100 ± 80	Resonance 3.4 eV
		3.7	26 ± 22	Resonance 18.3 eV
^{150}Sm	6	1	5.3	Measurements with thermal neutrons [14]
^{144}Nd	80	20	140	" " [15]

an α-particle is formed in a hot compound nucleus two or more unpaired nucleons are left in the residual nucleus. The structure of this state is very different from that of a finite nucleus state situated below the pairing energy and in this connection additional forbiddenness appears. Total α-widths (Table II) are practically entirely determined by the partial widths of transition to the ground or first excited state of a finite nucleus. Therefore, from the above point of view, they should be lower than the statistical value, as is actually observed. The preliminary data given in

Table II on the upper limits of palladium-105, osmium-189 and xenon-129 resonance α-widths for which the reaction (n,α) has not yet been observed, confirm this conclusion.

Pikelner et al. have attempted to evaluate the α-widths of neptunium-237 resonances characterized by very large fission widths. Since the latter is assumed to be due to the great deformation of a compound nucleus, it would be of interest to see if the deformation can also cause acceleration of α-decay.

At present, it may only be stated that for neptunium-237 resonances with energy of 40 eV and 205 eV, Γ_α/Γ_f is < 0.1 and ≤ 1, respectively. The statistical theory, when applied to Γ_α, gives a value many orders of magnitude smaller.

3. THE YIELD OF PROMPT FISSION NEUTRONS VERSUS RESONANCE SPIN IN PLUTONIUM-239 AND URANIUM-235.

The number ν of prompt neutrons emitted during fission is a measure of the excitation energy transferred to fragments in the process of fission. As Andreev [4] supposed, the excitation energy may to some extent be dependent on the parameters of a fission channel.

Since the fission channels for the levels of a compound nucleus with spin $J = i + 1/2$ and $J = i - 1/2$ (i is target-nucleus spin) are different, the excitation energy of fragments and neutron yield may also vary for these levels. Larger level density, corresponding to a greater spin, should facilitate the energy transfer to internal degrees of freedom at the moment of nuclear fission, which may be another reason for spin dependence. From both points of view, a stronger spin dependence of ν should be expected for plutonium-240 than for uranium-236. The energies of the fission channels ($J = 0^+$ and 1^+) are farther apart for both spins of plutonium-240 than for uranium-236 ($J = 3^-$ and 4^-); the ratio of the statistical weights of two spin states is also much more in the case of plutonium.

Variations of ν in the resonances of the nuclei mentioned above have been measured by Ryabov, So Don Sick, Chickov and Ivaneva in the Laboratory of Neutron Physics, Dubna [5]. A 500-litre liquid scintillation detector, which permitted registration of the number of neutrons per fission events, was used. Fig.8 presents the values of ν for a number of plutonium-239 resonance related to the average value of $\langle \nu \rangle$.

The levels, which according to Ref.[6] have spin 1, are marked with circles, and the levels with spin 0 are marked with squares.

The measurements were made with three samples of metallic plutonium of various thickness. The results for all the samples agree within statistical error. As is easily seen, resonances with spin 1 are characterized by a larger neutron yield than resonances with spin 0. The difference accounts for $\Delta\nu/\langle \nu \rangle = (5.8 \pm 1)\%$. It is known that as the kinetic neutron energy increases, ν increases linearly at a rate $d\nu/dE = 0.14$ MeV^{-1}. If we take the dependence between ν and the excitation energy of fission fragments to be the same, the difference in excitation energies for fission of plutonium-240 with spin 1 and spin 0 is 1.2 ± 0.2 MeV. This value is close to the expected difference between the energies of 1^+ and 0^+ states in the saddle point of a heavy even-even nucleus [7].

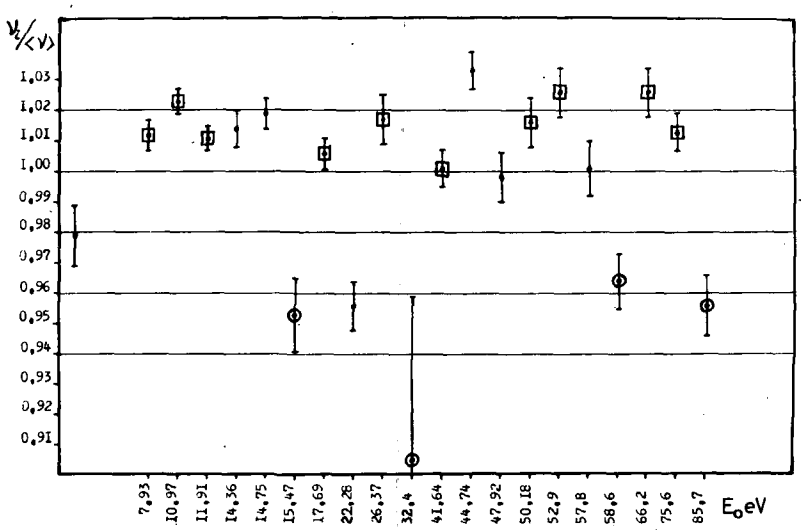

FIG. 8. The average number of neutrons per fission event for the resonances of ^{239}Pu (relative units). Circles represent the resonances with spin and parity $J^{\pi} = 0^{+}$; squares indicate those with $J^{\pi} = 1^{+}$; dots mean that reliable data on the resonance spin are lacking.

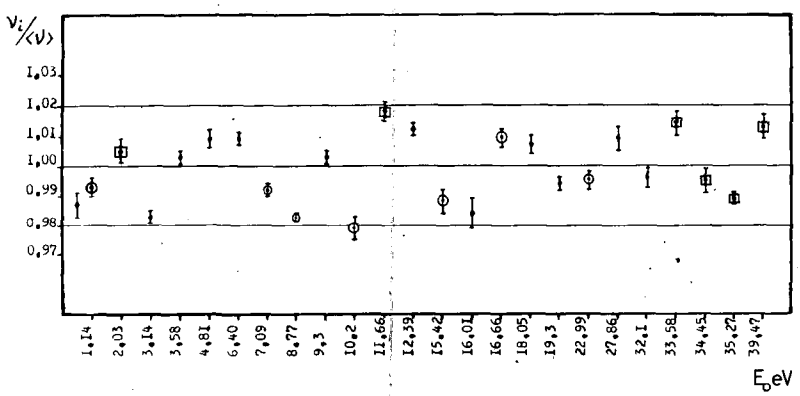

FIG. 9. The average number of neutrons per fission event for the resonances of ^{235}U (relative units). Circles represent the resonances with a probable value of $J^{\pi} = 3^{-}$; squares indicate those with a probable value of $J^{\pi} = 4^{-}$; dots mean that reliable data on the resonance spin are lacking.

Figure 9 shows the uranium-235 data of the same group. From Ref. [8] definite spins (3^{-} and 4^{-}) may be assigned, with certain probability, to thirteen of the investigated resonances. The measurements were made on several samples and also with a fission chamber connected in coincidence with the liquid scintillation detector. The results of various measurements agreed within statistical accuracy. On the average, resonances with higher spin have a larger value of ν:

$$\Delta\nu / \langle \nu \rangle = (1.6 \pm 0.6)\%$$

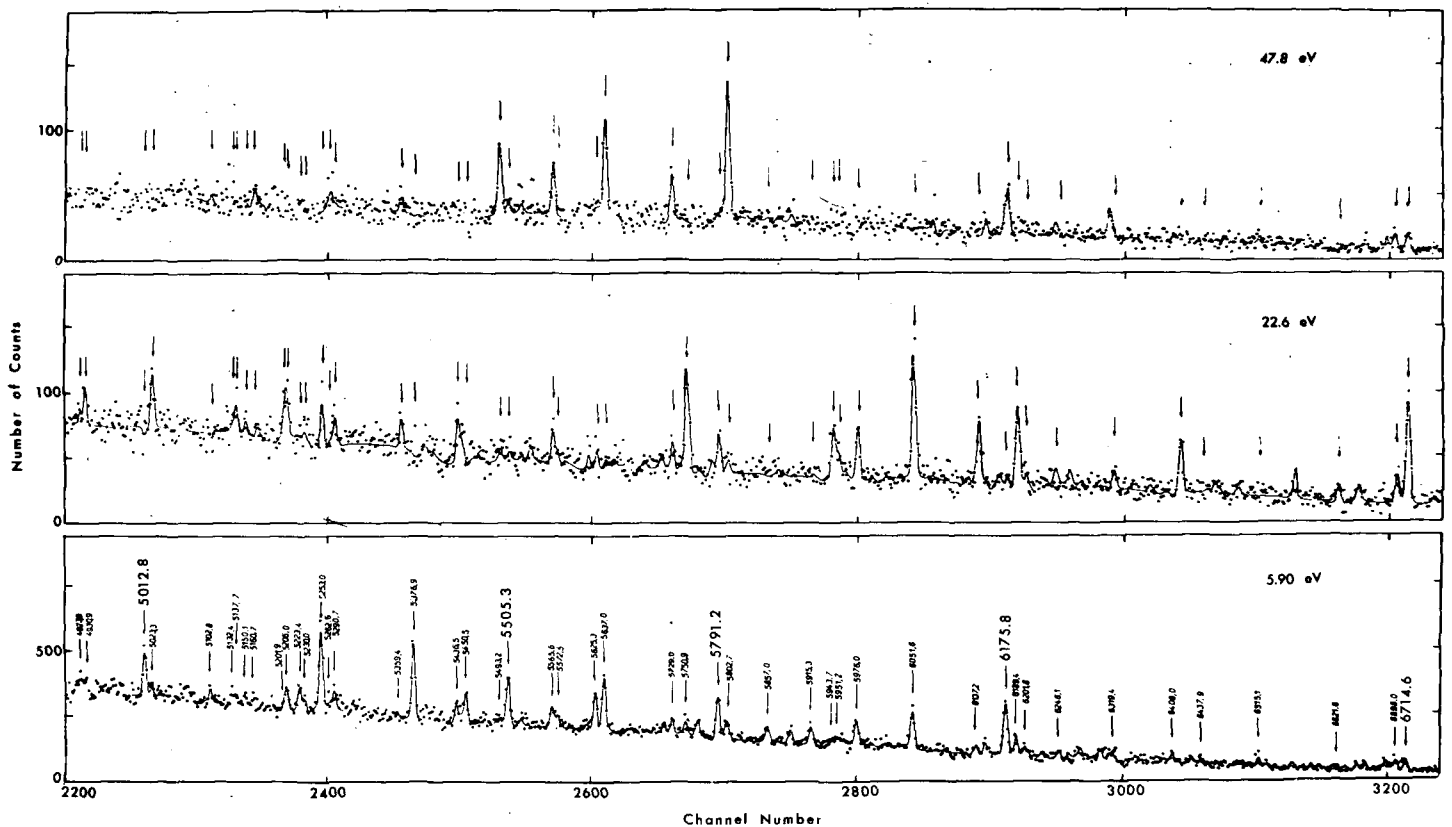

FIG.10. The gamma spectra for neutron capture at three resonances of ^{133}Cs. The gamma-ray energy is given in keV above the lines.

The error is determined from the spread of the values of ν for seven resonances with spin 3 and six resonances with spin 4 around the corresponding average values. This result does not agree with the data in a recent paper by Weinstein and Bloch [9] using a similar technique. In the latter paper the values of ν were obtained for 30 resolved resonances of uranium-235 in an energy region up to 40 eV. Points are contained in an interval of ν about 1.7% and are not split into groups according to the two spin states. The authors draw the conclusion that within an accuracy of ± 0.25% all the resonances are characterized by one value of ν. The reason for the discrepancy of the results of the two papers remains to be seen. The only conclusion that can at present be drawn is that the change of ν versus spin is within 1.5%. Consequently, a change in the excitation energy of fragments does not exceed 0.3 MeV. Thus for uranium-235 the spin dependence of ν, if any, is at any rate much weaker than that for plutonium-239, as expected.

The summated kinetic energy of fission fragments should be changed in the inverse direction to the change of their excitation energy and of ν. Experiments on the study of variations of fission fragment kinetic energy from resonance to resonance were carried out by Bochvarov, Dermendzhiev and Koshukeev. The indirect method was used: the yields of fission fragments from a uranium layer were compared for low and high energy thresholds of registration in a grid ionization chamber. Available data for ^{235}U indicate that the difference in the total kinetic energy for the 1.14 eV, 7.09 eV and 8.78 eV levels ($J = 3^-?$) and that for the 2.03 eV level ($J = 4^-?$) is 0.6 ± 1.2 MeV. Within normal error, this result is consistent with the preceding one.

4. GAMMA-SPECTRA OF NEUTRON RESONANCE CAPTURE

Measurements of gamma-spectra are being made by Urbanec, Bečvář et al. at Dubna. They use germanium-lithium coaxial detectors with a volume of 12-30 cm^3; the neutron energy resolution is about 80 ns/m. Caesium-133, barium-135, praseodymium-141 [10] and quite recently iodine-127 have been investigated. I shall consider only two features of the results obtained.

(a) The experiment indicates the existence of γ-ray spectrum fluctuations exceeding those which may be expected from the Porter-Thomas statistical theory. Figure 10 shows a solid part of the gamma-spectrum for three resonances of caesium-133. The spectra are dissimilar. The spectrum of the 47.8 eV resonance, characterized by five strong transitions with an energy in the interval 5493-5803 keV and with a strongly reduced intensity of almost all the other transitions, is especially interesting. The total intensity of 5 lines of 5493-5803 keV for the 47.8 resonance may be compared with the average intensity of these transitions for all caesium-133 resonances of energy up to 625 eV. The probability of the observed fluctuation for χ^2 distribution with five degrees of freedom amounts to only 3.5×10^{-3}. Analogous peculiarities are observed in the spectra obtained for barium-135 and iodine-127 resonances. However, additional data are required to clarify the situation.

(b) For barium-135 an anomalously high intensity of M1 transitions is observed. It is difficult to understand this phenomenon as a result of

the influence of a giant M1 resonance, since in neighbouring nuclei no very high intensity of M1 transitions was observed. The reason for the increase of such transitions in barium-135 remains to be studied.

5. EXPERIMENTS WITH POLARIZED NEUTRONS AND ORIENTED NUCLEAR TARGETS

In the Laboratory of Neutron Physics, Dubna, there is a polarized beam of resonance neutrons with 65% polarization in the region from 1 eV to some tenths of 1 keV. The polarization is achieved by transmitting the neutron beam through a dynamically polarized proton target. The polarizator transmission is approximately 0.15, and its area is 22 cm^2. This beam was used in experiments to determine the spins of holmium-165 neutron resonances using a statically polarized nuclear target of holmium-165 [11]. It was also used to study the spin dependence of neutron-deuteron scattering lengths [12]. The latter experiment was recently repeated in better experimental conditions and confirmed that the real set of neutron-deuteron scattering lengths is that for which the doublet length is smaller than the quadruplet one. Later on, the polarized neutron beam will be used to determine the spins of neutron resonances of rare earths and some other nuclei and to study the spin dependence of cross-sections in the energy region where individual resonances are not resolved. The polarization of nuclei will be achieved at the expense of internal magnetic fields while cooling the samples to a temperature of a few hundredths of °K. To obtain such temperatures the method of dissolving helium-3 in helium-4 was used.

To separate the interaction of neutrons with orbital momenta different from zero, experiments with unpolarized neutrons and aligned nuclei [13] will be useful. Measurements of angular gamma-ray anisotropy, for neutron capture by an oriented target, may yield vast information on the multipolarity of gamma-rays of resonance capture and on quantum numbers of low-lying levels.

Measurements of magnetic dipole moments of compound nuclei are also being planned. The method is based on using a small shift in the neutron resonance energy due to the hyperfine interaction of a compound nucleus [13]. This means measuring changes in the counting rate on the slope of the resonance curve by some tenths of one percent. Estimates show that such an experiment is possible, which seems of interest since it will yield quite a new type of information on the levels of a compound nucleus.

It may then be possible to go on to measurements of electrical quadrupole moments, which is especially interesting in relation to new data on the existence of states of a compound nucleus with large deformation. However, in this case the effects are expected to be smaller by an order of magnitude.

REFERENCES

[1] MAXON, M.C. et al., Paper UK/22, UK/USSR Seminar, Dubna (June 1968).

[2] KVITEK, I., POPOV, Yu.P., Phys. Lett. 22 (1966) 186; KVITEK, I., POPOV, Yu.P., Pis'ma Zh.eksp. teor. Fiz. 5 (1967) 365.

[3] POPOV, Yu.P., STEMPINSKI, M., Preprint P6-3605, Dubna (1967).
[4] ANDREEV, V.N., Contributions to the Meetings on Atomic Nuclear Fission, Akad. Nauk USSR, Leningrad (1961).
[5] RYABOV, Yu.V., SO DON SICK, CHICKOV, N., IANEVA, N., Contribution No.88 to this Symposium.
[6] SAUTER, G.D., BOWMAN, C.D., Phys. Rev. Lett. 15 (1965) 761, ASGHAR, M., Report EANDC (UK) 70 "S" (1966): COWAN, G. et al., Phys. Rev. 144 (1966) 3.
[7] LYNN, J.E., in Nuclear Structure Study with Neutrons, North-Holland, Amsterdam (1966).
[8] SAILOR, V., et al., Bull. Am. phys. Soc., 11 (1966) 29, COWAN, G. et al., Phys. Rev. 130 (1963) 2380; POORTMANS, F. et al., Conf. Neutron Cross Section Technology, Washington, 1966, TID 4500, p.755; ASGHAR, M. et al., Phys. Lett. 26B (1968) 664.
[9] WEINSTEIN, S., BLOCK, R.C., Rensselaer Polytechnic Institure paper PPI-328-311 (1968).
[10] BEČVÁŘ, F., VRZAL, J., LIPTÁK, J., URBANEC, J., Preprint P3-3969, and P3-3697, Dubna (1968).
[11] ALFIMENKOV, V.P. et al., Yadernaya Fiz. 3 (1966) 55; Preprint P3-3208, Dubna (1967).
[12] ALFIMENKOV, V.P. et al., Phys. Lett. 24B (1967) 151.
[13] SHAPIRO, F.L., in Polarized Targets and Ion Sources, Proc. Saclay Conference, Dec.5-9, 1966.
[14] OAKEY, N.S., McFARLANE R.D., Phys. Lett. 24B (1967) 142.
[15] ANDREEV, V.N., SIROTKIN, C.M., Yadernaya Fiz. 1 (1965) 252.

DISCUSSION

T. KROGULSKI: Have you measured the energy spectrum of neutrons emitted during the fission of ^{240}Pu?

F. L. SHAPIRO: No, because the efficiency of the neutron counter did not depend on the energy of neutrons and therefore the results presented mean simply that the average number of neutrons for both spin states differs by ~6%.

T. KROGULSKI: In this situation, can we conclude that the excitation energy of fragments differs really for both modes of fission of ^{240}Pu?

F. L. SHAPIRO: The difference in the excitation energy of the fragments for the two spin states is about 1.2 MeV.

A. BOHR: In the statistical estimate of Γ_α were the transmission factors calculated on the basis of an optical model?

F. L. SHAPIRO: The transmission factors were calculated semi-classically.

SIMPLE NUCLEAR EXCITATIONS DISTRIBUTED AMONG CLOSELY SPACED LEVELS

P. AXEL
UNIVERSITY OF ILLINOIS,
URBANA, ILL., UNITED STATES OF AMERICA

Abstract — Аннотация

SIMPLE NUCLEAR EXCITATIONS DISTRIBUTED AMONG CLOSELY SPACED LEVELS. A review is given of the limited information available about the correct description of simple nuclear excitations when they are mixed with more complicated excitations to form the quasi-stationary highly excited states of nuclei. Examples are given which illustrate the energy region over which a simple excitation appears, the existence of local variations or intermediate structure with a characteristic energy of about 100 keV, and correlations which might exist between two different simple excitations. The types of simple excitations considered are single-particle states, analogue states, and electric dipole excitation.

There is little quantitative information about the gross spreading of single-particle strength despite the successes of the optical model and the popularity of transfer reactions. There may be some evidence for intermediate structure in reported variations of neutron scattering cross-sections, but the interpretation is ambiguous. A convincing and educational example of a single-particle "doorway" is given by the Monahan and Elwyn analysis of s-wave neutron resonances in Fe.

The fragmentation of an analogue state among the $T_<$ states is another interesting example of experimentally observable spreading of strength. Additional information on the spreading of strength in highly excited states (e.g. in ^{90}Y) can be obtained by studying the more easily seen corresponding analogues (e.g. in ^{90}Zr).

Information on the spreading of electric dipole strength can be obtained directly from gamma-ray interaction cross-sections. The non-statistical neutrons emitted from the giant dipole resonance provide guidance for the theoretical description of the resonance. At energies well below the giant resonance there is evidence for substantial intermediate structure. In the same energy region comparisons between (γ, γ) and (γ, p_0) cross-sections are particularly sensitive to correlations.

Many more relevant experiments will be needed before the spreading of strength and the correlations between different simple excitations are understood.

ПРОСТЫЕ ЯДЕРНЫЕ ВОЗБУЖДЕНИЯ, РАСПРЕДЕЛЕННЫЕ МЕЖДУ БЛИЗКО РАСПОЛОЖЕННЫМИ УРОВНЯМИ. Приводится обзор ограниченной в настоящее время информации о правильном описании простых ядерных возбуждений, когда они смешаны с более сложными возбуждениями при образовании квазистационарных сильно возбужденных состояний ядер. Приводятся примеры, иллюстрирующие в области энергий, в которой появляется простое возбуждение, существование промежуточной структуры с характерной энергией около 100 кэв и корреляции, которые, возможно, существуют между двумя различными простыми возбуждениями. Рассмотрены простые типы возбуждений: одночастичные состояния, аналоговые состояния, электрическое дипольное возбуждение. Несмотря на успехи применения оптической модели и популярность реакций передачи, в настоящее время имеется лишь незначительная количественная информация об основных чертах распределения силы одночастичной конфигурации. Наличие вариаций в приведенных сечениях рассеяния нейтронов можно рассматривать как некоторое указание на существование промежуточной структуры, но такая интерпретация носит неоднозначный характер. Убедительный и поучительный пример одночастичного "doorway" состояния дается Монаханом и Эльвином при анализе s-волновых нетронных резонансов в Fe. Другим интересным примером наблюдаемого экспериментально распределения силы одночастичного резонанса является расщепление аналогового состояния на $T_<$ состояния. Дополнительная информация о разбросе силы в сильно возбужденных состояниях (например, в ^{90}Y) может быть получена посредством изучения соответствующих аналогов их состояний, которые наиболее легко наблюдать (например, в ^{90}Zr). Информацию о разбросе электрической дипольной силы можно получить прямо из сечений взаимодействия гамма-квантов. Нестатистические нейтроны, испущенные в области гигантского дипольного резонанса, служат основой для теоретического описания резонанса. При энергиях, намного меньших энергии гигантского резонанса, имеются данные о существенной

промежуточной структуре. В той же области энергий сравнения между сечениями (γ, γ) и (γ, p_0) особенно чувствительны к корреляциям. Потребуется провести еще много экспериментов, прежде чем разброс силы одночастичных резонансов и корреляции между различными простыми возбуждениями будут поняты.

1. INTRODUCTION

1.A. Gross structure, intermediate structure, and correlations

One of the major unsolved problems in nuclear physics is the description of simple nuclear excitations when they are mixed with many more complicated excitations to form the numerous quasi-stationary states found above several MeV of excitation in medium and heavy nuclei. The qualitative importance of this problem merits emphasis because many nuclear physicists are too pessimistic to recognize the simplicity of the questions involved, while others are so optimistic as to believe the questions have been answered.

To make the questions clear, let us consider only the 1^- states in the ^{90}Zr nucleus at an excitation energy near 11 MeV. A 1 MeV energy interval might contain about 3000 of these 1^- states. If one were to try to explain these using an independent particle model, one would be faced with the task of listing at least 3000 zero-order 1^- states that are expected near 11 MeV due to the excitation of one or more individual nucleons. Even if one had the fortitude to list these zero-order states, it would be necessary to add a residual interaction and diagonalize the resulting matrix to obtain the mixed wave-functions for the actual 1^- states. The pessimistic nuclear physicist would correctly point out that we are very far from being able to carry out such a calculation with sufficient reliability to trust it; even more important, no one really wants that much detailed information about the 1^- states in ^{90}Zr. However, the qualitative questions which physicists should be able to answer do not involve the exact wave-functions of the individual levels; instead, the important questions are concerned with the average distribution of a particularly simple excitation. For example, one might concentrate on the extent to which the 1^- states contain the excited proton configuration $(2p^{-1}_{1/2}, 3s_{1/2})$ relative to the ^{90}Zr ground state. If a particular simple configuration is selected, three qualitative questions can be asked:

1. Over what energy region in ^{90}Zr does the simple configuration appear?
2. If one averages over enough levels to smooth out expected statistical fluctuations, is the simple configuration distributed smoothly in energy or is it concentrated in some energy intervals?
3. Is the simple configuration correlated with some other simple excitation? For example, is this proton particle-hole state correlated with the gamma-ray decay width to the ground state?

These questions and the fragmentary answers available at this time can be illustrated with examples involving the three simple excitations about which most information is available: single particle excitations, analogue states, and the one particle - one hole excitations activated by

electromagnetic excitations. The notation needed to discuss the examples can be introduced by reviewing some well-known relations between widths of isolated energy levels and cross-sections.

1. B. Level widths, average cross-sections, and strength functions

The amount of mixing in highly excited states is usually inferred from experimental measurements which determine partial decay widths. The total width of the i^{th} excited state, $(\Gamma_t)_i$, is the sum of partial widths, $(\Gamma_{yf})_i$, where y denotes the type of emitted radiation and f specifies the final state in the appropriate residual nucleus:

$$(\Gamma_t)_i = \sum_y \sum_f (\Gamma_{yf})_i \tag{1}$$

The subscripts p, n, and γ will be used in place of y for proton, neutron and photon decay. For example, $(\Gamma_{n0})_i$ represents the partial width for neutron decay from the i^{th} excited state in (Z, A) to the ground state in (Z, A-1). The cross-section for the production of an isolated state resonant at neutron energy, E_i, by a neutron of energy E is:

$$\sigma_a(E)_i = g(I_i)\,\pi\lambda\!\!\!^{-2}\,\frac{(\Gamma_{n_0})_i}{(\Gamma_t)_i}\,\frac{1}{\left[\frac{2}{\Gamma_t}(E - E_i)\right]^2 + 1} \tag{2}$$

where

$$g(I_i) = 4g'(I_i) = 4\,\frac{2I_i + 1}{2(2I_0 + 1)} = \frac{2(2I_i + 1)}{2I_0 + 1} \tag{3}$$

and

$$E = \frac{\hbar^2 k^2}{2M} = \frac{\hbar^2}{2M\lambda\!\!\!^{-2}} \tag{4a}$$

Note that Eqs (2) and (3) hold for gamma ray absorption as well as neutron absorption if $(\Gamma_{\gamma 0})_i$ replaces $(\Gamma_{n0})_i$, and if the wavelength of the gamma ray is used:

$$\lambda\!\!\!^{-} = \hbar c/E_\gamma \tag{4b}$$

The cross-section integrated over the resonance is

$$\int_i \sigma_a(E)\,dE = \frac{\pi^2\lambda\!\!\!^{-2}}{2}\,g(I_i)\,(\Gamma_{n0})_i \tag{5}$$

The simple form of the integrated cross-section in Eq.(5) leads to a correspondingly simple average cross-section $\langle \sigma_a \rangle$ for an energy interval ΔE which contains n levels of the same spin I_i:

$$\langle \sigma_a \rangle = \frac{1}{\Delta E} \sum_i \int_i \sigma_a \, dE = \frac{\pi^2 \lambda\!\!\!^{-2}}{2} g(I_i) \frac{1}{\Delta E} \sum_i (\Gamma_{n0})_i = \frac{\pi^2 \lambda\!\!\!^{-2}}{2} g(I_i) \frac{n \langle \Gamma_{n0} \rangle}{\Delta E} \quad (6)$$

If n is large enough, $\langle \Gamma_{n0} \rangle$ is independent of n or ΔE; similarly, if n is large enough, a meaningful average level spacing, $D(I_i) = \Delta E/n$, can be defined independent of ΔE and n.

$$\langle \sigma_a \rangle = \frac{\pi^2 \lambda\!\!\!^{-2}}{2} g(I_i) \frac{\langle \Gamma_{n0} \rangle}{D} \quad (7)$$

Note that $\langle \sigma_a \rangle$, $\langle \Gamma_{n0} \rangle$ and D all correspond to a particular value of I_i; if resonances of more than one spin value participate, each contributes a partial cross-section such as appears in Eq.(7).

If the partial width $\langle \Gamma_{y0} \rangle$ is governed by a simple configuration, the ratio $\langle \Gamma_{y0} \rangle / D$, which is the amount of partial width per energy interval in the excited nucleus, is proportional to the amount of simple configuration per unit energy. Because of the theoretical treatment which will be mentioned below, we shall give the name "strength function" to the amount of simple configuration per unit energy. One can obtain the strength function, and its energy dependence, from $\langle \Gamma_{y0} \rangle / D$ if the energy dependence of Γ_{y0} is known. For example, the energy dependence of the partial gamma decay width to the ground state, Γ_{y0}, is well known; for dipole radiation it is:

$$(\Gamma_{\gamma 0})_i \propto E_\gamma^3 \, |\langle i \, | z \, | 0 \rangle|^2 \quad (8)$$

Therefore, the amount of dipole matrix element per unit excitation energy or the dipole strength function is:

$$\text{dipole strength function} \propto \frac{\langle \Gamma_{\gamma 0} \rangle}{D} \frac{1}{E_\gamma^3} \propto \frac{\langle \sigma_a \rangle}{E_\gamma} \quad (9)$$

(The strength function should not be confused with the oscillator strength frequently mentioned in photoreactions; the oscillator strength is defined proportional to $E_\gamma |\langle i \, | z \, | 0 \rangle|^2$, and hence is E_γ times the strength function).

For neutrons, the transition matrix element is more obscure than it is for gamma rays, but the strength function can be inferred from measured partial widths by extracting the neutron penetrability, P_ℓ, which depends on the angular momentum, ℓ, carried away by the neutron:

$$\text{neutron strength function} \propto \frac{\langle \Gamma_{n0} \rangle}{D} \frac{1}{P_\ell} \quad (10)$$

The ratio of the neutron width to the penetrability, Γ_{n0}/P_ℓ, is called the reduced neutron width. For s-wave neutrons, the penetrability is proportional to $E_n^{\frac{1}{2}}$. The reduced s-wave width, $\Gamma_{n0}^0 = \Gamma_{n0}\,(1\text{ eV}/E_n)^{\frac{1}{2}}$, is commonly used; another frequently used reduced width is $\lambda\Gamma_{n0}/2$ which is 2.28×10^{-10} cm Γ_{n0}^0.

The neutron strength function should in principle also be obtainable from transfer reactions which deposit a neutron into the nucleus. The quantity proportional to $(\Gamma_{n0})_i/P_\ell$ is simply the spectroscopic factor, S_i. As is well known, it has not yet been feasible to extract spectroscopic factors, S_i, for very complicated energy levels such as those usually found when the level density is high. It is also possible, in principle, to obtain information about the neutron strength function by studying the proton decay of the analogues of the dense nuclear levels whose neutron strength function is of interest. If either transfer reactions or analogue decays could be used to obtain spectroscopic factors, the sum of spectroscopic factors per unit energy would give the desired strength function.

1.C. The theoretical interpretation of the strength function and the spreading of strength

1.C.1. The theory of resonances

The mixing of a simple excitation with more complicated excitations has been accepted as a universal property of closely spaced nuclear energy levels ever since Niels Bohr [1] introduced the concept of the "compound nucleus" (produced by the rapid exchange of energy between nucleons) to explain neutron interactions and the sharp resonances observed with slow neutrons. The ratio $\langle\Gamma_{n0}\rangle/D$, whose experimental importance for non-overlapping resonances is displayed in Eq.(7), also plays a central role in the theory of resonances. Early theoretical descriptions [2] related $\langle\Gamma_{n0}\rangle/D$ to the "sticking probability"; the forerunners of modern theory stressed the relations between $\langle\Gamma_{n0}\rangle/D$ and the transmission coefficient [3,4]. The term "strength function" was introduced by Wigner [5] during the development of the R-matrix theory of nuclear resonances. Lane, Thomas and Wigner [6] discussed the mixing of a simple excitation over a limited energy range with more complicated excitations in terms of a "giant resonance" of this strength function. The theory of resonances has been reviewed, interpreted, and amplified in too many works to list here; the partial list given [7-13] includes many additional significant references. There is no difficulty in formulating a satisfactory theoretical framework which relates the strength function to the average cross-section for levels whose spacing is much greater than the total level widths; more ambiguity arises [13] for levels whose widths are equal to or greater than the spacing.

It is important to recognize that although the elegant theory of nuclear resonances provides an interpretation of the strength function and a framework for treating resonances, it does not include the physical content necessary to make any predictions about either the energy dependence of the strength function or the correlations which may exist between simple excitations.

1.C.2. The spreading of strength

The modern nuclear models which are related to the spreading of strength evolved in three stages. The first stage followed from Bohr's original compound nucleus picture [1] which entailed very strong interactions and corresponded to a uniform spreading of strength. This uniform spreading is implicit in the continuum model [3,4,14] which predicts an average neutron cross-section which is a smooth monotonic function of energy and mass number A.

The experimentally observed systematic variations of the average neutron cross-section led Feshbach, Porter and Weisskopf [15] to introduce an optical model potential with moderate absorption. In its original square well form, the optical model prediction for the spreading of the strength function was particularly simple; the spreading is characterized by a width, $\Gamma = 2W$, where W is the imaginary part of the potential. The numerous refinements and successes of the optical model are well known, and relevant references can be found in a recent review [16]. However, it should be remembered, as emphasized by McVoy [17], that the peaks in the neutron interaction cross-sections due to giant resonances of the strength function are generally obscured by non-resonant contributions to the cross-section. Thus, the general success of the optical model does not imply that the concentrations of the strength functions predicted by the model have been checked sensitively by experiments.

The third stage in the evolution of reaction theories involves an attempt to obtain a more refined description of the mixing of a simple configuration than is given by the imaginary part of the optical potential. The "doorway state" was introduced [18] to describe the first step in the process of energy sharing by an incoming nucleon; on encountering a nucleon within the nucleus, the incoming nucleon can scatter, creating a particle-hole pair. The resulting "doorway" for an incident nucleon is therefore a 2 particle - 1 hole state; if the incoming nucleon scattered as a result of producing a coherent particle-hole excitation, the doorway could be described as a particle coupled to a phonon.

It has been suggested [19] that doorway states are responsible for the intermediate structure observed in experimental cross-sections, and a theory of intermediate resonances has been developed [20]. Intermediate structure in cross-sections had also been interpreted with a partial equilibrium model [21]. Many of the experimental manifestations of an intermediate structure model have been given [20], but the degree to which observable intermediate structure might be anticipated at different energies in different nuclei remains quite uncertain. One aid to the identification of intermediate structure will be the recent calculations [22-26] which describe the distribution of intermediate structure strength among the underlying nuclear energy levels.

1.D. Statistical fluctuations and correlations

The large fluctuations of the reduced partial widths, $(\Gamma^0_{n0})_i$, from level to level are well known, and generally seem describable by the

Porter-Thomas distribution [27], which is appropriate to one degree of freedom and non-overlapping levels:

$$P(x)\,dx = \frac{e^{-x/2}}{(2\pi x)^{\frac{1}{2}}}\,dx \tag{11a}$$

or

$$P(y)\,dy = \frac{2e^{-y^2}}{\pi^{\frac{1}{2}}}\,dy \tag{11b}$$

where

$$2y_i^2 = x_i = (\Gamma_{n0}^0)_i / \langle \Gamma_{n0}^0 \rangle \tag{12}$$

The fluctuations implied by this distribution are responsible for the large errors due to finite sample size which are associated with experimental values of strength functions.

The effects of the Porter-Thomas distribution on average branching ratios are less well known even though they were discussed [28] for neutron capture, were put into the convenient numerical form of a single integral by Moldauer [29], and applied to average gamma-ray cross-sections [30]. These branching ratio effects can be understood qualitatively when it is recognized that many levels have reduced widths much less than the mean, $\langle \Gamma_{n0}^0 \rangle$. There are 10% of the levels whose reduced width is less than 1.7% of the mean, 30% whose width is less than 15%, and only 31% whose width is greater than the mean. At the same time, the less than 13% of the levels whose widths are more than 2.3 times the mean carry half of the total absorption strength. In the extreme case when only two uncorrelated Porter-Thomas channels are open, elastic scattering can be favoured by a huge factor compared to what might be expected from the average widths. For example, consider the case in which only the partial neutron width, Γ_{n0}, and the partial gamma-ray width to the ground state, $\Gamma_{\gamma 0}$, compete:

$$\frac{\langle \sigma_{\gamma\gamma} \rangle}{\langle \sigma_{\gamma n} \rangle} = \frac{\langle \Gamma_{\gamma 0} \rangle}{\langle \Gamma_{n0} \rangle} + 2\left(\frac{\langle \Gamma_{\gamma 0} \rangle}{\langle \Gamma_{n0} \rangle} \right)^{\frac{1}{2}} = \frac{\langle \Gamma_{\gamma 0} \rangle}{\langle \Gamma_{n0} \rangle} \left[1 + 2\left(\frac{\langle \Gamma_{n0} \rangle}{\langle \Gamma_{\gamma 0} \rangle} \right)^{\frac{1}{2}} \right] \tag{13}$$

This implies that for $\langle \Gamma_{\gamma 0} \rangle / \langle \Gamma_{n0} \rangle$ as small as 0.01, $\langle \sigma_{\gamma\gamma} \rangle / \langle \sigma_{\gamma n} \rangle = 0.21$ if $(\Gamma_{\gamma 0})_i$ and $(\Gamma_{n0})_i$ are completely uncorrelated; of course, if they were completely correlated, the cross-section ratio would be only 0.01. Although this enhancement of the elastic cross-section is reduced if a third Porter-Thomas channel is open, or if each level has a constant gamma-ray width for decay to all levels except the ground state, large enhancements persist which probably make the average elastic gamma-ray scattering cross-section a particularly sensitive indication of local correlations in appropriate cases.

Correlations between partial widths of non-overlapping levels can be thought of as the low energy forerunner of the "resonant-direct" [31] photoneutrons emitted from the giant dipole resonance. In both energy intervals, gamma rays might produce more photoneutrons than would be implied by statistical considerations because the wavefunctions favoured by gamma rays are related to those responsible for nucleon emission. It should be emphasized that neither resonant-direct photonucleons nor correlations are related to a direct process which might exist independently, and be non-resonant.

2. THE CURRENT STATUS AND THE CHALLENGE

A brief summary of this type can neither be comprehensive nor do justice to the fine relevant work that has been done by many physicists. Although the coverage given below will obviously be severely limited, it should be emphasized that the omitted material, valuable though it is, does not change the main qualitative conclusion. Surprisingly little is known about the energy dependence of the strength function, the existence of intermediate structure, or correlations between channels.

The examples given below were chosen mainly to define and to illustrate the problems; some examples may indicate the promise of future answers. The work with which I was personally associated is overemphasized disproportionately because the data were easily available; these data illustrate the questions, and should not be misinterpreted as meriting attention because they provide answers.

2.A. Single particle strength

2.A.1. The gross spreading of strength seen in transfer reactions

In view of the amount of information available about single particle strength, as indicated in Professor Cohen's talk, it is surprising how little consideration has been given to the energy range over which a particular single particle strength has been spread. Professor Cohen and his group are among the very few who seem to consider this problem, and even they maintain the crude qualitative approach they introduced [32] in 1962. They often show, together with the experimentally observed fragmentation, a line extending $E_c/3$ on either side of the centre-of-strength energy, E_c. This extension was originally chosen because for a square well volume absorption optical model, $\Gamma = 2W$, and because Professor Cohen inferred that $W = E_c/3$ was a reasonable approximation to the data available in 1962.

Although there is some indication that as E_c increases, the single particle strength appears more fragmented and spread over a larger energy region, the value of $\Gamma = 2E_c/3$ has not been shown to represent the data particularly well by even a semiquantitative analysis. From a theoretical point of view, it is not at all clear that this choice of Γ is consistent with the modern optical model and its surface absorption [33]. The surface absorption might imply both an energy and an angular momentum dependence because different bound-state wave-functions sample the region of the nuclear surface differently. Furthermore, if the spreading

of strength among bound states is indeed related to the imaginary part of the optical potential, there must be some very interesting physics in the relation between the optical potential and such nuclear structure features as pairing, shell closure, vibrations, and configuration mixing.

One recent experimental paper which seemed particularly interesting [34] concerned itself with the identification of the $p_{1/2}^{-1}\, d_{3/2}$ configuration in ^{90}Zr. Although the aim of this study was to find an empirical value for the nuclear symmetry energy, it incidentally extended the extraction of strength function information to higher energy than usual and also gave information about a particle-hole rather than a single particle strength. The authors infer [34] that the strength is mainly confined to an energy interval of about 1.5 MeV even though the centre-of-strength excitation energy is 5.8 MeV.

2.A.2. Information from reduced neutron widths

Although the main discussion about reduced neutron widths will occur later in the conference, there are two aspects which should be mentioned during this review of the spread of strength as a function of energy. Because the energy variation of the strength function is difficult to obtain experimentally, optical model analyses often concentrate on the variation with A of the strength sampled by very low energy neutrons, as defined in Eq.(10). A typical plot of $\langle \Gamma_{n0}^{0} \rangle / D$ as a function of A can be found in a recent compilation [35]. The experimental values fall between a maximum of 5×10^{-4} just below A = 60 and a minimum of 0.2×10^{-4} near A = 120. Although this A dependence of the slow neutron "strength function" has been discussed qualitatively [9-11] in terms of the Lane, Thomas and Wigner [6] giant resonance model, the detailed agreement does not inspire confidence in the position, or spacing, or spreading of single particle strength. The qualitative interpretations [9-11] are usually given in terms of "size" resonances which imply 40 MeV energy spacings between s-wave single particle levels; this spacing is about twice that implied by usually accepted shell model oscillator spacings. In addition, values of Γ between 2 and 10 MeV have been quoted [9-11] as being representative. The fringe surface absorption model of Moldauer [36] seems to account for the absorption of low energy neutrons but it obscures any nuclear structure concept such as "single particle strength" in the nuclear interior.

The A dependence of the s-wave neutron "strength function" can provide some indication about intermediate structure if one assumes, as seems reasonable, that the neutron binding energy is uncorrelated with the energy of doorway states. If the neutron strength function varied greatly with energy, the amount of strength found near zero neutron energy would indiscriminately sample the variation. Although the experimental uncertainties are large, and some modulation of the strength function might exist, the experimental points are not as erratic as one would expect if the single particle strength were generally clustered in peaks that were separated by deep valleys. Individual points rarely deviate from the neighbouring average by as much as a factor of 2.

2.A.3. Energy dependence and intermediate structure

Although many experimental results have been interpreted in terms of intermediate structure, we still have extremely little systematic information about possible clustering of strength. Total neutron interaction cross-sections up to energies of about 600 keV revealed 10-20% variations which had correlation widths of 50-100 keV [37]. Several experiments [38] suggest a possible rapid energy dependence of the neutron strength function; although these effects may not be statistically significant because of the Porter-Thomas distribution, they may equally well hint at large intermediate structure effects near the magic nucleon numbers. In several cases involving light nuclei, angular distributions of both alpha particles [39] and neutrons [40] indicate that particular partial waves resonate at energy intervals corresponding to intermediate rather than gross structure. On the other hand, when the elastic and inelastic scattering of neutrons with energies from 400 keV to 1.6 MeV were studied using Ta, Re, and Pt targets [41] no intermediate structure effects were noted. It has also been noted [42] that total neutron cross-sections at higher energy (4.5-7.5 MeV) do not fluctuate by as much as 1% for 10 elements between Co and Ta. For eight other samples (which were mainly lighter elements but included Pb) cross-section variations were found [42], but could be explained by a statistical fluctuation analysis without invoking intermediate structure. These measurements indicate that for medium and heavy nuclei away from magic numbers, the superimposed intermediate structure of many partial waves does not modulate the total neutron cross-section enough to be detected. In addition, for the targets in which fluctuations were seen, the total cross-sections could not be used to distinguish intermediate structure from statistical fluctuations. It has also been shown [43] that statistical fluctuations can often appear to have the form of intermediate structure so that peaks of anomalous width in cross-sections are not necessarily intermediate structure.

2.A.4. Intermediate structure revealed by an analysis of fine structure

A convincing example of intermediate structure and an appreciation of its significance can be obtained from a recently published analysis by Monahan and Elwyn [44] of the neutron scattering cross-section of ^{56}Fe. The total cross-section obtained with 20 keV resolution [45] is shown in the upper part of Fig.1. A phase shift analysis of "poor resolution" differential cross-sections and polarization implied an s-wave door-way state at E_D = 360 keV which had a total width of about Γ = 145 keV, a neutron escape width, $\Gamma\uparrow$ = 50 keV, and hence a $\Gamma\downarrow$ of 95 keV [44]. The same total cross-section taken with 1 keV resolution by Dr. A.B. Smith of Argonne is shown in the bottom part of Fig.1. Similar data had already been analysed by a multilevel fit [46] which gave the energies, E_λ, and reduced widths $(\Gamma^0_{n0})_\lambda$ of 14 s-wave levels between 186 and 645 keV.

A reinterpretation of these level parameters in terms of an extreme single doorway state formalism [26] seeks to learn whether the nuclear

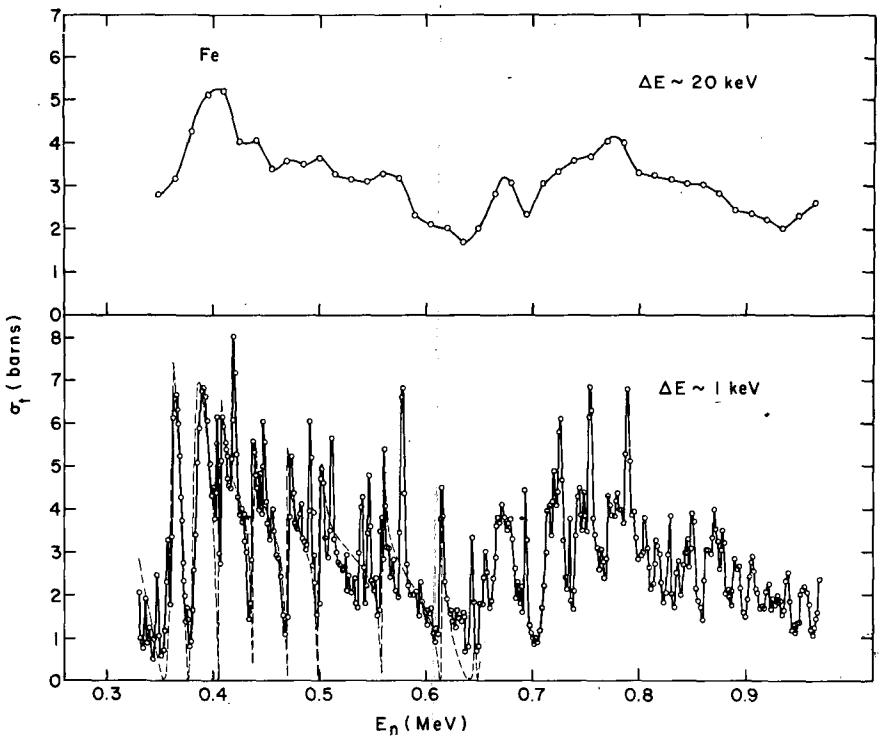

FIG.1. The total neutron scattering of Fe in moderate and good energy resolution. The upper portion of the curve shows the total cross-section taken with 20 keV resolution [45]. With the aid of differential scattering and polarization studies, the s-wave contribution can be analysed to give [44]: ϵ_d = 0.36 MeV, Γ = 145 keV, and $\Gamma\uparrow$ = 50 keV. The lower part of the figure shows the same energy region when studied with much better resolution by Dr. A.B. Smith; the dashed curve shows a detailed fit to the s-wave levels obtained from similar data [46]. When the detailed level parameters were reinterpreted with a doorway state analysis [44], values of ϵ_d = 0.36 MeV, $\Gamma\uparrow$ = 46 keV, and Γ = 132-151 keV were obtained. See section 2.A.4 and Ref. [44] for more details.

structure of these levels would be more transparent if one used a model in which a single state with the entire neutron width,

$$(\Gamma^0_{n0})_d = \sum_{\lambda=1}^{N} (\Gamma^0_{n0})_\lambda$$

mixes with (N - 1) background states, each of which have zero reduced neutron width before the mixing. Monahan and Elwyn selected 13 states (omitting the one at 645 keV) and transformed the 26 parameters (E_λ and $(\Gamma^0_{n0})_\lambda$) [46] into the 26 doorway parameters which consist of the doorway state unperturbed energy, ϵ_d, its reduced width, $\Gamma^0\uparrow = (\Gamma^0_{n0})_d$, and 24 parameters associated with the 12 background levels. Each background level, q, has an unperturbed energy, E_q, and a matrix element squared, V^2_q, which represents the coupling between the doorway state

and state q. There are several criteria for evaluating the usefulness of the doorway state parametrization. First, for the parameters to be acceptable, the doorway damping width, $\Gamma\downarrow$, which is defined to depend on E and an averaging interval, I, should actually be relatively independent of E and I provided that the averaging interval is larger than the average level spacing and smaller than the total width $\Gamma\uparrow + \Gamma\downarrow$. The ^{56}Fe data satisfy this condition [44]. (This condition is related to the sensitivity of the parameters to the number of levels, λ, used in the analysis.) In addition, the doorway state parametrization may be tested by comparing the derived parameters E_q and V_q^2 with statistical theories. If the E_q values and the V_q^2 values are distributed statistically (e.g. if the V_q^2 values follow the Porter-Thomas distribution of Eq.(11)), the E_λ and $(\Gamma_{n0}^0)_\lambda$ will not be distributed statistically. In particular, there will be large reduced widths $(\Gamma_{n0}^0)_\lambda$ for levels with E_λ near E_d; these widths would be governed by proximity of background levels to the doorway state rather than the size of matrix elements whose randomness was assumed to derive the Porter-Thomas width distribution. Finally, an important nuclear structure question associated with the doorway parametrization is whether the values of $\Gamma\uparrow$ associated with different doorways can be interpreted microscopically.

2.B. Analogue states and intermediate structure

Although Professor Temmer has already given this conference a review of the impressive nuclear structure information obtained from analogue state studies, their usefulness in teaching us about the spreading of strength should also be stressed. It is clear from the classic high resolution studies at Duke [47] that analogue states in the region of non-overlapping compound nuclear resonances provide excellent examples from which parameters such as $\Gamma\uparrow$ and $\Gamma\downarrow$ should be extracted and understood. As a by-product of such studies, the spin dependence of the compound nuclear level spacings should be obtainable by examining the fine structure associated with analogue states of different spin. At higher energies, where level widths exceed spacings, fine structure may teach us about the spin dependence of level widths. Whether or not the fine structure associated with analogue states can be observed, it would be extremely worthwhile to obtain systematic data about the spreading width of analogue states.

The widths of some analogues observed in the nucleus $_{Z+1}A$ can also give valuable information about the spreading of strength in the corresponding parent states in $_ZA$. For example, consider the 1^- analogue state near 21 MeV in ^{90}Zr which was recognized [48] because it had been predicted as a $T_>$ component of the giant dipole resonance in ^{90}Zr [49]. The corresponding energy region in ^{90}Y is about 7.9 MeV above the ground state where the 1^- level spacing is probably about 1 keV; because this is about 1 MeV above the neutron separation energy, the level widths are probably an appreciable fraction of the spacing. Therefore, if the peak observed near 21 MeV in ^{90}Zr can be thought of as the analogue of a "state" in ^{90}Y, it must be the analogue of at least one 1^- doorway state near 7.9 MeV in ^{90}Y. The observed 600 keV width of the 1^- analogue in ^{90}Zr must include some analogue state damping width and some proton emission width in addition to the $\Gamma\uparrow + \Gamma\downarrow$ doorway width

characteristic of the 1^- strength in ^{90}Y. The 1^- analogue state in ^{90}Zr will have the additional complication of a possible interference between the isospin allowed and the isospin forbidden neutron emission to states in ^{89}Zr near 9 MeV of excitation. The 1^- doorway in ^{90}Y should be observable in studies of 1 MeV neutron scattering from ^{89}Y; preliminary differential cross-sections and polarization studies seem to show an anomaly [50], but no definite information is available. There is also evidence for another 1^- analogue in ^{90}Zr at about 19.6 MeV [51]; the observed width of about 200 keV [51] provides an upper limit on the width of the corresponding 1^- doorway near 6.5 MeV in ^{90}Y.

2.C. Gamma-ray interactions and intermediate structure

2.C.1. The giant dipole resonance

The enhancement of the gamma-ray strength function at the giant dipole resonance is extremely well known, but the degree to which this resonance could be considered as a "simple" intermediate resonance was not tested in detail until recently [52]. Photoneutron spectra from ^{209}Bi were obtained at different gamma-ray energies throughout the giant dipole resonance region. It was found that a crude model in which the entire giant dipole resonance was treated in terms of an electric dipole doorway state could account for the data if $\Gamma\downarrow$ was allowed to have an energy dependence. This interpretation of the giant dipole resonance is incomplete at this stage partly because $\Gamma\uparrow$ (i.e. the nucleon emission from the dipole doorway) cannot be predicted accurately, and partly because the entire energy dependence of the gamma-ray absorption cross-section has not received a reliable interpretation.

2.C.2. The distribution of dipole strength below the giant dipole resonance

The energy distribution of the electric dipole strength function seems to be a particularly confusing one for many nuclear physicists. The well-known proportionality between the gamma-ray decay width and E_γ^3 for a given matrix element (Eq.(8)) seems to lead to the misconception that the observed widths of nuclear transitions are expected to be proportional to E_γ^3. This proportionality could be expected, as shown in Eq.(9), only if the gamma-ray strength function or the sum of the squares of the dipole matrix element per unit energy in the nucleus were independent of the excitation energy. There is neither experimental nor theoretical support for this radical, obviously incorrect, energy-independent strength function. The quantities $\Gamma_{\gamma 0}/E_\gamma^3$ and $\langle\Gamma_{\gamma 0}\rangle/DE_\gamma^3$ contain, as Eqs (8) and (9) show, very interesting nuclear structure information, but they are not expected to be independent of E_γ or A. There is little theoretical guidance about the spreading of dipole strength. The experimentally known systematic behaviour of the giant dipole resonance can provide excellent estimates in the energy region of this resonance (Eq.(9)), but there is little conclusive evidence for higher or lower energy regions.

The little that is known about the average low-energy dipole strength seems to be consistent with an extrapolation of the giant dipole resonance [30]. Professor Bollinger will show some interesting capture gamma-ray results which add support to this extrapolation procedure. On a finer

energy scale, there is definite evidence [53] for significant clustering of electric dipole strength at least in ^{209}Bi, ^{206}Pb, Sn, and ^{90}Zr, all of which have magic numbers. The photon scattering data obtained with a Zr target will be discussed below.

2.C.3. Correlations between particle and photon widths

The possibility of finding correlations can be made plausible by considering $(\Gamma_{p0})_i$ and $(\Gamma_{\gamma 0})_i$ for 1^- levels in ^{90}Zr. A large proton emission width would be expected for ^{90}Zr states which are very similar to an s-wave proton and ^{89}Y (which can be thought of as ^{90}Zr and a $p_{1/2}$ proton hole). If the gamma-ray transition probability depended only on a single particle-hole configuration, a 1^- level which had a large component of $|^{90}\mathrm{Zr}\, p_{1/2}^{-1}\, s_{1/2}\rangle$ would also have a particularly large gamma-ray transition rate because the dipole operator could move the excited proton from the $s_{1/2}$ to the $p_{1/2}$ single particle level. This physical argument favouring correlations is weakened considerably because the main electric dipole transition strength due to individual single particle - single hole states is shifted up in energy to form the giant dipole resonance. The same mixing which provides a coherent combination of particle-hole states in the giant dipole resonance region mixes the configurations of the other unshifted one particle - one hole states in just the way necessary to cancel most of the dipole transition strength. As a result, it is not clear whether one should or should not expect to find correlations between particle and gamma-ray partial widths; experiment must decide.

A positive correlation between neutron reduced widths $(\Gamma_{n0})_i$ and partial gamma decay widths $(\Gamma_{\gamma f})_i$ was reported for some neutron resonances in the $^{169}_{69}$Tm + n reaction [54]. Only 8 neutron resonances were included in the analysis (i.e. i = 1, 2, ... 8), but data were obtained for gamma ray transitions to 15 final states in ^{170}Tm (i.e. f = 1, 2, ... 15). The possible correlation mentioned in the previous paragraph would correspond to testing each of the 8 resonances for one particular final state, f. However, to improve the statistical accuracy, the correlations were averaged over all final states. Despite this averaging, a significant correlation was obtained. There are, however, two features of this interesting report which might justify scepticism. First, a major part of the apparent correlation is probably due to the lowest resonance (at 3.9 eV) which has both the largest neutron reduced width and almost twice the average number of high-energy gamma-rays. In addition, the final levels whose gamma-ray transitions seem most correlated with reduced neutron widths are not the same levels that are most strongly populated in a (d, p) reaction [55].

The final example of strength spreading, intermediate structure, and correlations is shown in Fig.2. The line marked extrapolated absorption represents the total gamma-ray absorption expected for ^{90}Zr from data [56] in the giant resonance region. The experimental points are the elastic gamma-ray scattering cross-section observed with about 100 keV energy resolution [53, 57]; the cross-section assumes that only ^{90}Zr is contributing to the elastic scattering above 8.7 MeV because all other Zr isotopes can emit neutrons. Although the elastic scattering cross-section would be expected to be below the absorption cross-section due to inelastic gamma-ray scattering (below 11 MeV) and proton emission (above

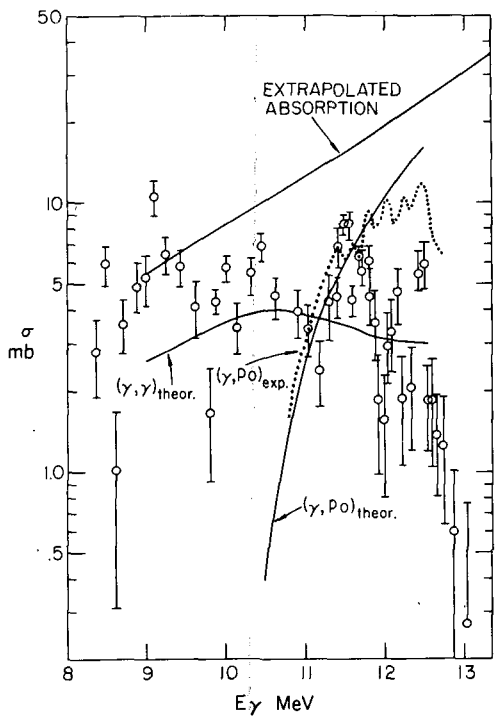

FIG.2. The elastic gamma-ray scattering and ground-state photoproton cross-sections for ^{90}Zr. The experimental points correspond to the total elastic gamma-ray scattering cross-section assuming only the isotope ^{90}Zr contributes above 8.7 MeV. The uppermost curve is the extrapolation of the measured [56] total absorption cross-section of ^{90}Zr in the giant resonance region. The experimental values of (γ, p_0) are 10 times the 90° differential cross-section obtained with a poor resolution average of (p, γ_0) results [58, 59]. The theoretical curves for (γ, γ) and (γ, p_0) were obtained by using the extrapolated cross-section to calculate $\langle\Gamma_{\gamma_0}\rangle/D$, and optical model parameters [60] to calculate $\langle\Gamma_{p_0}\rangle/D$. The other parameters required for the calculation were chosen as D(10.8 MeV) = 440 eV, T = 1.2 MeV, and a constant inelastic gamma-ray width of 0.2 eV. The theoretical curves emphasize the presence of intermediate structure in the gamma-ray strength function. Some of the correlated finer structure in the (γ, p_0) and (γ,γ) yields might also be due to correlations between $(\Gamma_{\gamma_0})_i$ and $(\Gamma_{p_0})_i$. See section 2.C.3 for more details.

11 MeV), the elastic scattering cross-section should vary smoothly with energy as illustrated by the curve marked $(\gamma, \gamma)_{theor.}$. Despite the large statistical errors, it is clear that the dipole strength varies significantly with energy, and shows intermediate structure. The sharp rise in the scattering from 11.2 to 11.5 MeV is particularly striking.

The dotted curve, labelled $(\gamma, p_0)_{exp.}$, is inferred from a 100 keV resolution average of the p, γ_0 data reported [58, 59] for ^{89}Y + p. The sharp rise in the (γ, p_0) cross-section near 11 MeV is dominated by the rise in proton transmission coefficient, as can be seen from the theoretical curve, labelled $(\gamma, p_0)_{theor.}$, which assumes a proton strength function given by the optical model using Los Alamos parameters [60]. The gamma-ray strength function used for the theoretical calculation is obtained from the extrapolated absorption cross-section as in Eq.(7) or (9). According to these calculations $\langle\Gamma_{p0}\rangle = \langle\Gamma_{\gamma 0}\rangle$ at 10.8 MeV. The absolute widths

depend on the value assumed for the 1^- level spacing, D. D was chosen as about 440 eV and a constant nuclear temperature of about 1.2 MeV was used to obtain the level spacing at other energies; this choice implied $\langle \Gamma_{p0} \rangle = \langle \Gamma_{\gamma 0} \rangle = 53 \times 10^{-3}$ eV at 10.8 MeV. A constant inelastic width of 200×10^{-3} eV was also assumed for every compound nuclear level.

Both $(\Gamma_{p0})_i$ and $(\Gamma_{\gamma 0})_i$ were assumed to be independent uncorrelated Porter-Thomas distributions. The theoretical cross-sections do not become equal until $\langle \Gamma_{p0} \rangle = 4 \langle \Gamma_{\gamma 0} \rangle$. Because it is difficult to summarize the effects which correlations would have, one example will have to suffice. At 12 MeV, where the inelastic, elastic and proton widths are 15.6%, 3.1% and 81.3% respectively, the corresponding percentages of the cross-sections with no correlations are 30.6%, 15.8%, and 53.6%. If the elastic gamma widths and the proton widths were completely correlated these percentages would change to about 12%, 3%, and 85%. The experimental cross-section fluctuations in both the elastic scattering and the photoproton cross-section may well represent a delicate interplay between intermediate structure and correlations, and we do not yet understand them.

This entire review has had a sufficiently consistent theme to permit its summary section to be short. Strength is spread in nuclei but we have very little experimental information about this spreading. There are some examples of intermediate structure, and many more can be found. Our task is not only to find peaks or identify them as doorways, but also to learn enough about the processes to establish the character of at least some of these doorways. Widths or strength functions for different processes may be correlated; they may share the same doorways. This entire field of nuclear physics presents an exciting challenge to which more nuclear physicists will respond.

REFERENCES

[1] BOHR, N., Nature, Lond. 137 (1936) 344.
[2] BETHE, H.A., Rev. mod. Phys. 9 (1937) 69.
[3] FESHBACH, H., PEASLEE, D.C., WEISSKOPF, V.F., Phys. Rev. 71 (1947) 145.
[4] BLATT, J.M., WEISSKOPF, V.F., Theoretical Nuclear Physics (John Wiley and Sons (1952)).
[5] WIGNER, E.P., Proc. Cambridge phil. Soc. 47 (1951) 790.
[6] LANE, A.M., THOMAS, R.G., WIGNER, E.P., Phys. Rev. 98 (1955) 693.
[7] LANE, A.M., THOMAS, R.G., Rev. mod. Phys. 30 (1958) 257.
[8] BREIT, G., Encyclopedia of Physics, Volume XLI/1 (FLUGGE, S., Ed.) Springer-Verlag (1959).
[9] BROWN, G.E., Rev. mod. Phys. 31 (1959) 893; BROWN, G.E., Unified Theory of Nuclear Models, North-Holland (1964).
[10] FESHBACH, H., Nuclear Spectroscopy, Part B (Ajzenberg-Selove, F., Ed.) Academic Press (1960).
[11] VOGT, E., Rev. mod. Phys. 34 (1962) 723; VOGT, E., Advances in Nuclear Physics, Vol.1, (BARANGER, M., VOGT, M., Eds.) Plenum Press (1968).
[12] LANE, A.M., ROBSON, D., Phys. Rev. 151 (1966) 774.
[13] MOLDAUER, P.A., Phys. Rev. 157 (1967) 907.
[14] FESHBACH, H., WEISSKOPF, V.F., Phys. Rev. 76 (1949) 1550.
[15] FESHBACH, H., PORTER, C.E., WEISSKOPF, V.F., Phys. Rev. 96 (1954) 448.
[16] HODGSON, P.E., Ann. Rev. nucl. Sci. 17 (1967) 1.
[17] McVOY, K.W., Ann. Phys. (N.Y.) 43 (1967) 91; McVOY, K.W., HELLER, L., BOLSTERLI, M., Rev. mod. Phys. 39 (1967) 245.
[18] BLOCK, B., FESHBACH, H., Ann. Phys. (N.Y.) 23 (1963) 47.

[19] KERMAN, A.H., RODBERG, L.S., YOUNG, J.E., Phys. Rev. Lett. 11 (1963) 422.
[20] FESHBACH, H., KERMAN, A.K., LEMMER, R.H., Ann. Phys. (N.Y.) 41 (1967) 230.
[21] IZUMO, K., Progr. theoret. Phys. 26 (1961) 807; IZUMO, K., Nucl. Phys. 62 (1965) 673.
[22] FALLIEROS, S., FERRELL, R.A., Phys. Rev. 154 (1967) 921.
[23] MAHAUX, C., WEIDENMULLER, H.A., Nucl. Phys. A94 (1967) 1.
[24] MacDONALD, W., MEKJAN, A., Phys. Rev. 160 (1967) 730.
[25] ROBSON, D., LANE, A.M., Phys. Rev. 161 (1967) 982.
[26] KERMAN, A.K., DE TOLEDO PIAZ, A.F.R., Ann. Phys. (N.Y.), to be published.
[27] PORTER, C.E., THOMAS, R.G., Phys. Rev. 104 (1956) 483.
[28] LANE, A.M., LYNN, J.E., Proc. phys. Soc. A70 (1957) 557.
[29] MOLDAUER, P.A., Phys. Rev. 123 (1961) 968.
[30] AXEL, P., Phys. Rev. 126 (1962) 671.
[31] WILKINSON, D.H., Physica 22 (1956) 1039.
[32] COHEN, B.L., FULMER, R.H., McCARTHY, A.L., Phys. Rev. 126 (1962) 698.
[33] MOLDAUER, P.A., Phys. Rev. Lett. 10 (1963) 525.
[34] VOURVOPOULOS, G., FOX, J.D., Phys. Lett. 25B (1967) 543.
[35] SETH, K.K., Nucl. Data 2 (1966) 299.
[36] MOLDAUER, P.A., Nucl. Phys. 47 (1963) 65.
[37] SETH, K.K., Phys. Lett. 16 (1965) 306.
[38] GOOD, W.M., PAYA, D., WAGNER, R., TAMURA, T., Phys. Rev. 151 (1966) 912; GOOD, W.M., KIM, H., Phys. Rev. 165 (1968) 1329; WYNCHANK, S., GARG, J.B., HAVENS, Jr., W.W., RAINWATER, J., Phys. Rev. 166 (1968) 1234.
[39] SINGH, P.P., WATSON, B.A., KROEPFL, J.J., MARVIN, T.P., Phys. Rev. Lett. 17 (1966) 968.
[40] MONAHAN, J.E., ELWYN, A.J., Phys. Rev. 153 (1967) 1148.
[41] SMITH, A.B., GUNTHER, P.T., WHALEN, J.F., Phys. Rev. 168 (1968) 1344.
[42] CARLSON, A.D., BARSCHALL, H.H., Phys. Rev. 158 (1967) 1142.
[43] SINGH, P.P., HOFFMAN-PINTHER, P., LANG, D.W., Phys. Lett. 23 (1966) 255.
[44] MONAHAN, J.E., ELWYN, A.J., Phys. Rev. Lett. 20 (1968) 1119.
[45] ELWYN, A.J., MONAHAN, J.E., Bull. Am. phys. Soc. 12 (1967) 1186.
[46] BOWMAN, C.D., BILPUCH, E.G., NEWSON, H.W., Ann. Phys. (N.Y.) 17 (1962) 319.
[47] KEYWORTH, G.A., KYKER, G.C., Jr., BILPUCH, E.G., NEWSON, H.W., Nucl. Phys. 89 (1966), 590; Phys. Lett. 20 (1966) 281.
[48] AXEL, P., DRAKE, D.M., WHETSTONE, S., HANNA, S.S., Phys. Rev. Lett. 19 (1967) 1343.
[49] FALLIEROS, S., GOULARD, B., VENTNER, R.H., Phys. Lett. 19 (1965) 398.
[50] ELWYN, A.J., COX, S.A., private communication.
[51] HASINOFF, M., KUAN, H.M., HANNA, S.S., FISCHER, G.A., Bull. Am. phys. Soc. 13 (1968).
[52] KUCHNIR, F.T., AXEL, P., CRIEGEE, L., DRAKE, D.M., HANSON, A.O., SUTTON, D.C., Phys. Rev. 161 (1967) 1236.
[53] AXEL, P., MIN, K., STEIN, N., SUTTON, D.C., Phys. Rev. Lett. 10 (1963) 299.
[54] BEER, M., LONE, M.A., CHRIEN, R.E., WASSON, O.A., BHAT, M.R., MUETHER, H.R., Phys. Rev. Lett. 20 (1968) 340.
[55] SHELINE, R.K., WATSON, C.E., MAIER, B.P., GRUBER, U., KOCH, R.H., SCHULT, O.W.B., MOTZ, H.T., JURNEY, E.T., STRUBLE, G.L., Phys. Rev. 143 (1966) 857.
[56] BERMAN, B.L., CALDWELL, J.T., KELLY, M.A., BRAMBLETT, R.L., FULTZ, S.C., Phys. Rev. 162 (1967) 1098.
[57] AXEL, P., MIN, K.K., SUTTON, D.C., to be published.
[58] OBST, E., RAUCH, F., ROSSLE, E., Phys. Lett. 21 (1966) 50.
[59] OBST, E., RAUCH, F., WAHNSWEILER, H.G., Nucl. Phys. A103 (1967) 17.
[60] ROSEN, L., BEERY, J.G., GOLDHABER, A.S., AUERBACH, E.H., Ann. Phys. (N.Y.) 34 (1965) 96.

DISCUSSION

G. BARTHOLOMEW: I would like to make the point that analyses of (n, γ) spectra have gone beyond the point of assuming a constant strength function. I refer in particular to the analyses of Starfelt and Bergqvist on γ-ray spectra following fast neutron capture. In some mass regions one

gets a best fit by assuming that the strength function is given by an extrapolation of the tail of the giant resonance; for other mass regions, for example elements between Ta and Pb, one must also assume a second peak (or pigmy resonance) at about 5.5 MeV to fit the data. Recent (d, pγ) measurements at Chalk River also give information on this question.

Yu. P. POPOV: The identification of processes which proceed through a doorway state is often made by looking for deviations from the predictions of statistical models. However, this procedure is not always unambiguous. It would be useful to identify doorway states by studying the product particles. For example, gamma-ray spectra should show evidence of the doorway states.

P. AXEL: I agree. I tried to emphasize the same idea by pointing out that it is very important to observe the doorway state in more than one channel. There must be correlations between the partial widths associated with the main decay modes of each doorway state.

G. M. TEMMER: I have heard that someone has already seen the parent state of the 1^- analogue state in ^{90}Zr which you mentioned with neutrons of about 1 MeV on ^{89}Y, but unfortunately I do not know the authors.

P. AXEL: The only work of which I am aware is the preliminary work by Elwyn and Cox, which is mentioned in my paper as Ref. [50]. In a private communication to me Elwyn indicated that there is an anomaly in the scattering by ^{89}Y of neutrons of about 1 MeV. However, the data have not yet been analysed; it would be premature to claim that there is direct evidence about the 1^- parent in ^{90}Y.

M. G. URIN: What can you say about the theoretical estimates of spreading widths for doorway states?

P. AXEL: I do not know of any recent calculations; the early estimates of about 100 keV - 300 keV for spreading widths remain our only theoretical guide.

S. S. HANNA: I would like to confirm what Dr. Axel said about the experiment of Elwyn et al. on $^{89}Y(n, n)^{89}Y$. I have seen those data and believe they show structure which could be indicative of the analogue resonance in ^{90}Y. However, I do not think the authors believe the evidence is conclusive. I might add that we are attempting to observe the analogue resonances by means of the reaction $^{89}Y(d, p)^{90}Y$.

RADIATIVE TRANSITIONS FROM HIGHLY EXCITED NUCLEAR STATES*

L.M. BOLLINGER
ARGONNE NATIONAL LABORATORY, ARGONNE, ILL.,
UNITED STATES OF AMERICA

Abstract — Аннотация

RADIATIVE TRANSITIONS FROM HIGHLY EXCITED NUCLEAR STATES. The experimental characteristics of radiative transitions from the highly excited states formed by slow-neutron capture are summarized. The partial radiation widths obtained from the refined spectra measured with Ge-diode γ-ray spectrometers are in good agreement with the Porter-Thomas distribution. Both the absolute values and the energy dependence of the widths for E1 transitions are in quantitative agreement with what is expected from the presence of the electric-dipole giant resonance at a higher energy. Various kinds of nuclear-structure effects for E1 radiation are examined critically. For relatively light nuclides there is convincing evidence for a correlation between the strengths for (n, γ) and (d, p) transitions, as is expected if the single-particle component of radiative capture is significant. For the typical heavy nucleus, recent measurements show that the radiation width is independent of the character of the final state to a high degree of refinement. However, two experiments seem to indicate that single-particle effects are significant in the reaction ^{169}Tm (n, γ)^{170}Tm, since they give convincing evidence for a correlation between radiation and neutron widths. However, the expected correlation between (n, γ) and (d, p) strengths for this reaction are not observed. Evidence concerning hard-sphere capture is described. The reduced widths for M1 transitions are summarized. They are found to be considerably larger than expected. Also, there is some indication that the reduced widths for ^{136}Ba and perhaps some tin isotopes are abnormally large. The reduced widths for M1 transitions in ^{136}Ba exhibit a strong energy dependence.

РАДИАЦИОННЫЕ ПЕРЕХОДЫ С ВЫСОКОВОЗБУЖДЕННЫХ ЯДЕРНЫХ СОСТОЯНИЙ. Приведены экспериментальные характеристики радиационных переходов с высоковозбужденных состояний, образованных захватом медленных нейтронов. Парциальные радиационные ширины, полученные из точных спектров, измеренных с помощью γ-спектрометров на германиевых диодах, находятся в хорошем согласии с распределением Портера-Томаса. Как абсолютные величины, так и энергетическая зависимость ширин для E1-переходов, находятся в качественном согласии с тем, что ожидается из наличия электрического дипольного гигантского резонанса при высокой энергии. Проверены разного рода эффекты ядерной структуры для E1-переходов. Для относительно легких изотопов есть убедительное доказательство, как и ожидается, существования корреляций между силами (n, γ) и (d, p) переходов, если одночастичная компонента радиационного захвата значительна. Для типичного тяжелого ядра последние измерения показывают, что радиационная ширина не зависит от структуры конечного состояния в высшей степени точности. Однако представляется, что два эксперимента указывают на то, что одночастичные эффекты значительны в реакции ^{169}Tm (n, γ) ^{170}Tm, так как в них обнаружены явные корреляции между излучением и нейтронными ширинами. Однако, ожидаемая корреляция между (n, γ) и (d, p) сечениями для этой реакции не замечена. Описаны данные, касающиеся прямого захвата. Систематизированы приведенные ширины для M1-переходов. Они оказались значительно большими, чем ожидалось. Имеются также некоторые указания на то, что приведенные ширины для ^{136}Ba и, вероятно, для некоторых изотопов олова аномально велики. Приведенные ширины для M1-переходов в ^{136}Ba сильно зависят от энергии.

* Work performed under the auspices of the U.S. Atomic Energy Commission.

1. INTRODUCTION

This paper attempts to summarize the present state of experimental knowledge about radiative transitions from a particular set of highly excited nuclear states – the states formed by capture of slow neutrons. The level spacings and neutron widths of these states have provided one of our best sources of information about the statistical characteristics of nuclear energy levels, but until recently the data on radiative transitions from these same states have been quite crude. This situation is now changing rapidly because of the advent of the Ge-diode γ-ray spectrometer, the availability of more intense neutron sources, and the development of new methods of measurement. Thus the data now being accumulated may be expected not only to provide a good description of the statistical behaviour of the high-energy transitions, but also to elucidate the degree to which the radiation widths deviate from a simple statistical description because of the influence of nuclear structure.

A good example of the kind of raw material with which we will be concerned here is provided by the spectrum for the reaction $^{113}Cd(n, \gamma)^{114}Cd$, as given in Fig. 1. Here one sees that the spectrum has three characteristic regions of energy – a high-energy region in which individual γ-ray lines are well resolved, an intermediate region in which a broad maximum is formed by a very large number of unresolved lines, and a low-energy region of resolved lines. We will be concerned only with the high-energy γ-ray lines, which are formed by primary transitions from the initial state to low-energy states in the compound nucleus. Typically, the initial state is so complex that its characteristics cannot be understood in detail, whereas the final states are relatively simple.

The high-energy transitions observed in three kinds of measurements will be considered. The first of these is the measurement of spectra

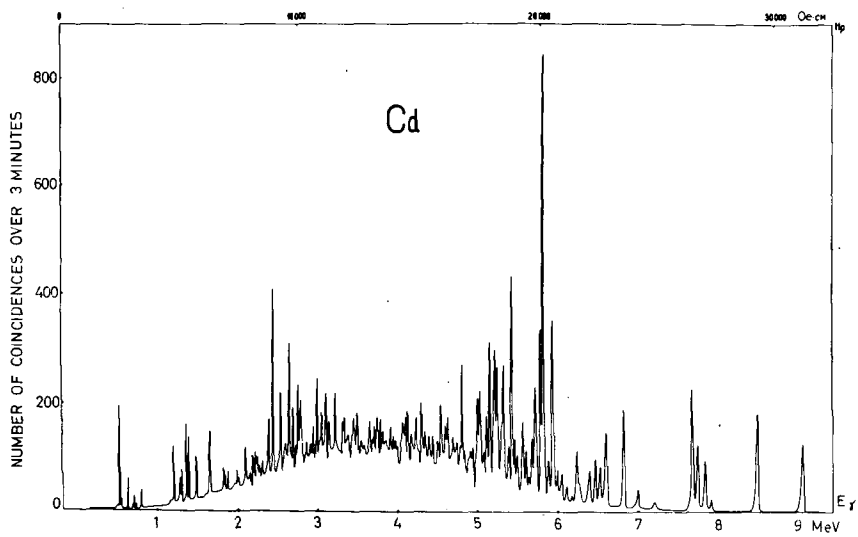

FIG. 1. Gamma-ray spectrum for the reaction $^{113}Cd\ (n, \gamma)\ ^{114}Cd$ (Groshev [1]).

formed by the radiative capture of thermal neutrons. The second type is the observation of spectra for a variable, well-defined neutron energy, usually at neutron resonances. Such measurements are usually made with a Ge-diode γ-ray spectrometer at a time-of-flight neutron spectrometer. Because of the low intensity of time neutrons, spectra of this kind are usually of poor quality technically, but potentially they can give the most information. The third class of measurements is the newly developed neutron-filter technique in which the measured spectrum is formed by the capture of neutrons in a band of energy that is broad enough to contain many resonances — typically hundreds. These spectra give a direct measure of average widths of radiative transitions.

2. DISTRIBUTION OF PARTIAL RADIATION WIDTHS

One of the most intensively studied characteristics of the high-energy transitions has been the distribution of partial widths for E1 transitions. The starting point for a discussion of this topic is the familiar analysis by Porter and Thomas [2] of the distribution of reduced neutron widths. They showed that the extremely broad distribution of neutron widths is a result of the complexity of the wave functions of the highly excited states formed by neutron capture. Reasonable assumption about the nature of the complexity leads to the expectation that, for a reaction that proceeds by way of a single exit channel, the distribution of the width Γ is of the form $x^{-1/2}\ e^{-x/2}$, where $x = \Gamma/\bar{\Gamma}$. And if this form is valid for a single-channel process, the distribution of widths for a reaction that proceeds by way of ν exit channels of the same mean width must be a χ^2 distribution with ν degrees of freedom, i.e. a distribution of the form

$$\rho(x) = \left[\Gamma\left(\frac{\nu}{2}\right)\right]\left(\frac{\nu}{2}x\right)^{(\nu/2)-1}\ e^{-\nu x/2} \qquad (1)$$

where $\Gamma(\nu/2)$ is the usual Γ function. Eq. (1) is written in such a form that the mean value of x is unity and the variance is $2/\nu$.

Many experimenters have shown that the reduced neutron widths are in excellent agreement with the Porter-Thomas distribution ($\nu = 1$). Since a radiative transition from a highly excited state also appears to be a reaction that proceeds by way of a single exit channel and since the initial states are the same ones involved in neutron emission, the distribution of partial radiation widths is also expected to obey the Porter-Thomas distribution. In any case, it has been customary for experimenters to analyse their measured distribution of radiation widths on the assumption that the widths are drawn from a χ^2 population, and the results have been summarized by giving the range of values of ν that are consistent with the data. The main point of the analysis is to determine whether or not the data are consistent with the value $\nu = 1$ expected from the statistical model. If not, the result indicates the influence of some nuclear-structure effect.

The results reported over the years for the distribution of partial radiation widths have been varied and conflicting, with values of ν ranging from 1 to 100! It now seems almost certain that many of these early results were caused by the use (or misuse) of a NaI scintillator as the γ-ray spectrometer. The results now being obtained with Ge-diode

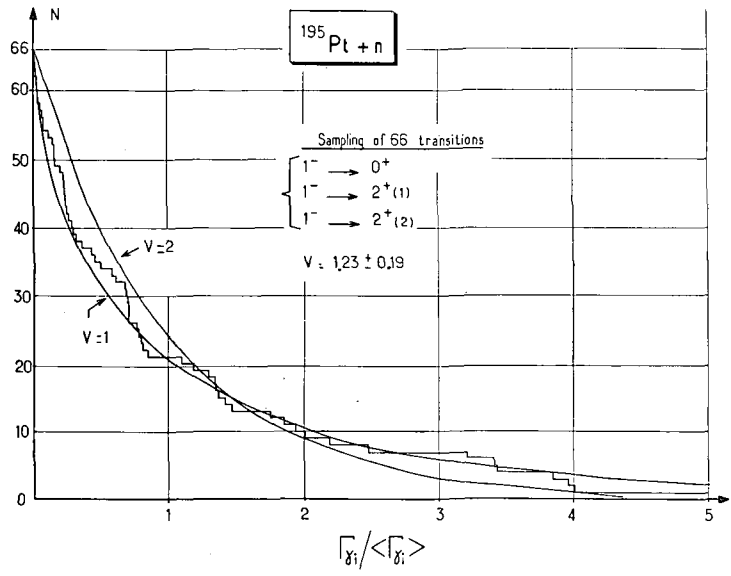

FIG. 2. Integral distribution of partial radiation widths for the reaction ^{195}Pt(n, γ) ^{196}Pt (Jackson et al. [3]).

spectrometers are all consistent with the Porter-Thomas distribution. Perhaps the most refined result reported yet is that obtained at Saclay by Jackson et. al. [3] for the reaction ^{195}Pt(n, γ) ^{196}Pt. They measured the transitions to three low-energy states in the spectra from 22 resonances with J = 1 and from these 66 transitions obtained the value $\nu = 1.23 \pm 0.19$. This result is shown graphically in Fig. 2.

Although the question of the distribution of partial radiation widths for a compound nucleus reaction in the typical heavy nucleus has been settled, it is perhaps worth keeping in mind that there may be special cases for which the distribution deviates significantly from the Porter-Thomas distribution because of nuclear-structure effects.

From the point of view of most of the remaining subject matter to be covered in this paper, an important practical implication of the broad distribution of widths for individual transitions is the difficulty it causes in the determination of average values of the widths. Specifically, the value $\nu = 1$ implies that the relative error of an average determined from n widths is

$$\frac{\Delta\overline{\Gamma}}{\overline{\Gamma}} = \sqrt{\frac{2}{n}} \qquad (2)$$

Thus, since for most nuclides only 5 or 10 resonances can be studied individually with a neutron spectrometer, average widths determined from measurements on individual resonances are typically uncertain by 50% or more.

3. GIANT-RESONANCE DESCRIPTION OF E1 TRANSITIONS

The most widely-used relationships for the widths of high-energy transitions are those obtained from the single-particle model [4]. Specific-

ally, the widths for the transitions that are strong enough to be detectable in the neutron-capture γ-rays are

$$\Gamma_{\gamma ij}\,(E1) = 6.8 \times 10^{-2}\, A^{2/3}\, E_\gamma^3\, D_i/D_0 \tag{3a}$$

$$\Gamma_{\gamma ij}\,(E2) = 4.9 \times 10^{-8}\, A^{4/3}\, E_\gamma^5\, D_i/D_0 \tag{3b}$$

$$\Gamma_{\gamma ij}\,(M1) = 2.1 \times 10^{-2}\, E_\gamma^3\, D_i/D_0 \tag{3c}$$

where $\Gamma_{\gamma ij}$ is in eV, E_γ is the γ-ray energy in MeV, A is the nucleon number, and D_i is the spacing at the initial state i of levels with the same spin and parity as the radiating state. The subscript j designates the final state. The quantity D_0 is a spacing that is characteristic of the separation between major shell-model shells. Both D and D_0 are in MeV. The value of D_0 originally suggested by Weisskopf was 0.5 MeV. However, recently it has been customary to use a value of about 15 MeV. The numerical constants in Eq.(3) are those given by Wilkinson [5].

An alternative approach to an understanding of the behaviour of the E1 transitions is one in which the transitions observed in the neutron-capture reaction are assumed to result from the same physical processes that form the familiar dipole giant resonance observed in photonuclear reactions. Several years ago Axel [6] explored the implication of this hypothesis under the assumption that the giant resonance is describable by a classical Lorentzian line shape and that this shape is valid down to the 6-8 MeV range of interest for the neutron-capture γ rays, well beyond the range in which the Lorentzian shape has been verified experimentally for most nuclides. Under these assumptions the width $\Gamma_{\gamma 0}$ for the ground-state transition is

$$\frac{\Gamma_{\gamma 0}}{D_i} = 1.13 \times 10^{-6}\, A\, \frac{E_\gamma^4\, \Gamma_g}{(E_g^2 - E_\gamma^2)^2 + E_\gamma^2 \Gamma_g^2} \tag{4}$$

where E_γ and also the giant-resonance energy E_g and width Γ_g are in MeV; A is the atomic weight.

To obtain a relationship that is applicable to a wide range of nuclides, Axel used the approximate values $\Gamma_g = 5$ MeV and $E_g = 80\, A^{-1/3}$ MeV. Then in the range 6-8 MeV Eq.(4) reduces to the simple approximate relationship

$$\frac{\Gamma_{\gamma 0}}{D_i} = 6.1 \times 10^{-15}\, E_\gamma^5 A^{8/3} \tag{5}$$

Here $\Gamma_{\gamma 0}$ and D are in the same units and E_γ is in MeV.

Eqs (4) and (5) are relationships for the ground-state transition whereas in the capture γ-ray spectra one is usually concerned with transitions to excited states. However, if a giant resonance with a universal shape is built on each excited state, then it is easily shown that Eqs (4) and (5) describe the energy dependence of the radiation width, independent of whether the energy of the initial or final state is varied. Let us proceed to examine the experimental data to see whether they support this hypothesis.

We start our discussion of data by attempting to determine whether the energy dependence is consistent with the E_γ^5 dependence of Eq.(5).

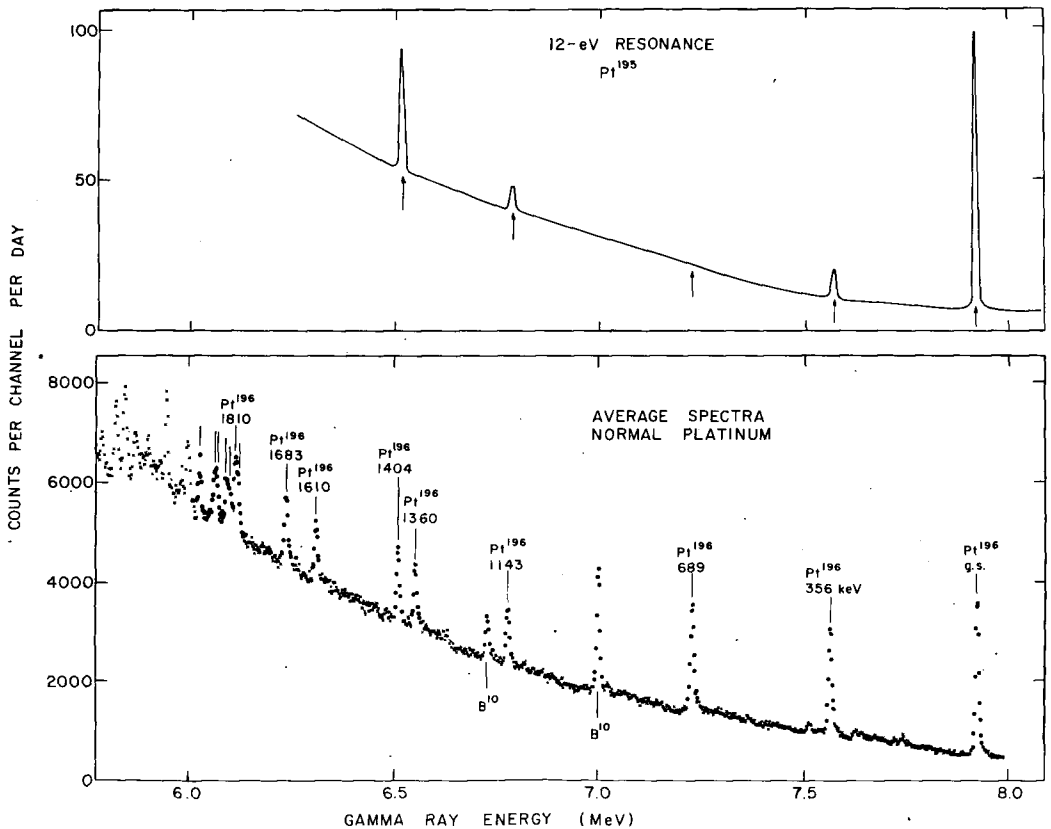

FIG. 3. Average resonance-capture spectrum for platinum (Bollinger and Thomas [7]).

Because the capture γ-ray spectra for heavy nuclides can be resolved only over a range of 1 or 2 MeV, the average widths must be determined accurately if one is to distinguish between an E_γ^5 dependence and some other such as E_γ^3. The main experimental difficulty is caused by the Porter-Thomas distribution, which results in an uncertainty given by Eq.(2). This kind of uncertainty is too large to permit much to be learned about the energy dependence of radiation widths from measurements at individual neutron resonances. However, the problem of Porter-Thomas fluctuations can be diminished greatly by the new technique in which one measures directly the average spectrum formed by capture of neutrons in a band of energy that is broad enough to contain many resonances. This approach has been used by Bollinger and Thomas [7] at Argonne in a study of the energy dependence of high-energy transitions in ^{196}Pt.

An example of an average resonance-capture spectrum is given in Fig. 3. Notice the high degree of uniformity of the intensities of the γ-ray lines, in contrast to the wide fluctuations in intensity of the spectrum for a single resonance, as given in the top part of the figure. The energy dependence of the measured intensities are given in Fig. 4. The error bars on the data points give the rms uncertainties caused by Porter-Thomas fluctuations. The data are seen to be entirely consistent with an E_γ^5 dependence and quite inconsistent with an E_γ^3 dependence. Assuming that the width is proportional to E_γ^α, a least-squares fit gives $\alpha = 4.9 \pm 0.5$.

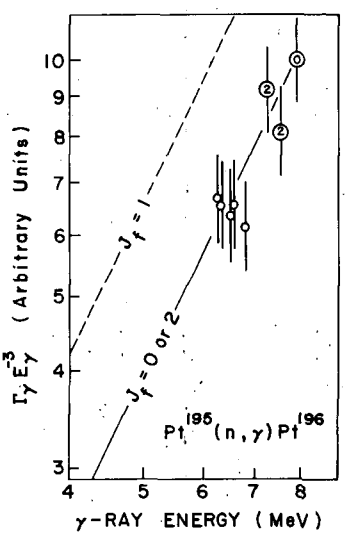

FIG. 4. Energy dependence of radiative transitions in ^{196}Pt (Bollinger and Thomas [7]).

The relationship of the data to the Lorentzian shape is shown in Fig. 5. Similar measurements [8] on ^{166}Ho, ^{168}Er, ^{170}Tm, ^{178}Hf, ^{182}Ta, ^{184}W, and ^{190}Os all give results similar to those for ^{196}Pt, although less accurate. Thus, the widths in a number of nuclides exhibit the energy dependence that is expected from the suggestion that a giant resonance with a universal shape is built on each excited state.

Another check on Eq.(5) would be a determination of the dependence of $\Gamma_{\gamma ij}$ on A. However, the data that are now available from the neutron

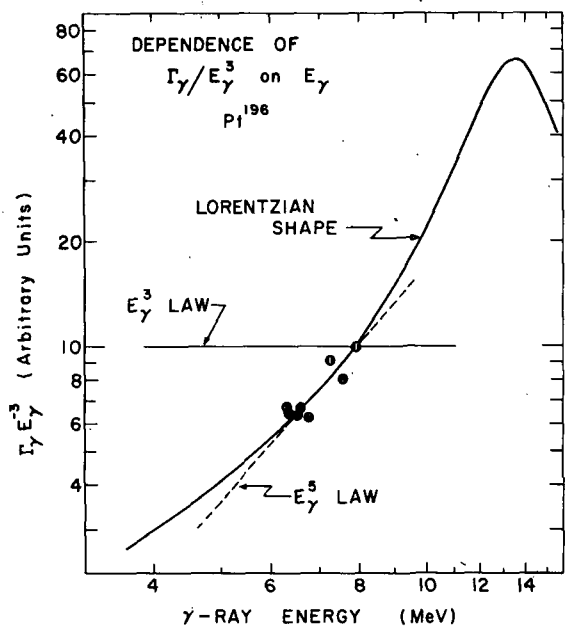

FIG. 5. Energy dependence of radiative transitions in ^{196}Pt (Bollinger and Thomas [7, 8]).

capture γ-rays are not accurate enough to allow one to distinguish with certainty between an $A^{8/3}$ dependence and the $A^{2/3}$ dependence that is expected from the single-particle model. On the other hand, at the somewhat higher energy of 10.8 MeV Hurst and Donahue [9] showed by a measurement of the (γ, n) cross-section that the quantity $\Gamma_{\gamma 0}/D$ is in good agreement with the $A^{8/3}$ dependence for a set of targets ranging from ^{75}As to ^{209}Bi.

The smooth variation of $\Gamma_{\gamma ij}$ with E_γ in Fig. 4 and similar data for many other nuclides pose two interesting questions. First, why is the radiation width so highly independent of the character of the final state? And second, how does one justify theoretically the idea that a giant resonance with a universal shape is built on each excited state? Rosenzweig [10] has considered both of these questions in terms of a hydrodynamic model of the radiation process. In this treatment the fundamental physical assumption is that electric-charge vibrations of the entire nucleus play the dominant role in electric dipole radiation. Under this assumption the dipole absorption integral is shown to be effectively the same for all excited states and the mean energy of the giant resonance associated with an excited state is higher than the mean energy for the ground-state resonance by an amount that is exactly equal to the excitation energy. These two characteristics of the giant resonance make it entirely plausible that the giant resonance built on an excited state has the same shape as the resonance built on the ground state and that this universal shape is displaced in energy by an amount equal to the excitation energy.

Up to this point, we have been concerned only with the manner in which the radiation widths vary. However, the absolute values are also of interest. The most extensive study of the widths was made by Carpenter [11] in a study of resonance capture. In all, 121 well-understood transitions were

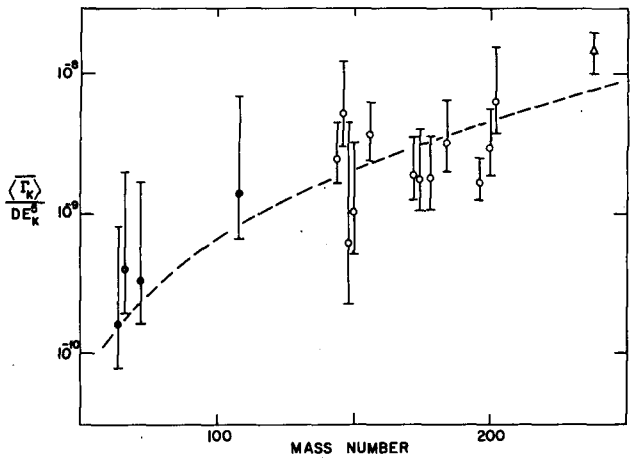

FIG.6. Dependence of average radiation widths on A (Carpenter [11]).

observed in 12 nuclides ranging from ^{144}Nd to ^{202}Hg. When interpreted in terms of the single-particle model, his average value for the reduced width $\bar{k}_{E1} = \Gamma D^{-1} E_\gamma^3 A^{2/3} = 4.0$; another way of expressing the same result is that $D_0 = 16.5$ MeV in Eq.(3). When interpreted in terms of the giant-resonance model, the data are as given in Fig.6, and the best fit to the data is

$$\bar{\Gamma}_{\gamma ij} = 3.2 \times 10^{-15} D_i E_\gamma^5 A^{8/3} \qquad (6)$$

where Γ_γ and D are in eV and E_γ is in MeV. The constant 3.2×10^{-15} is considered to be in satisfactory agreement with the value 6.1×10^{-15} obtained from the photonuclear data, in view of the errors in the data and the approximations made in deriving Eq.(5).

Rosenzweig [10] has examined the particular case of transitions in ^{196}Pt to determine whether or not the absolute values of the widths are quantitatively consistent with what would be inferred from detailed balance by extrapolating the measured photoabsorption cross-sections for ^{196}Pt to low energies. He finds that there is agreement within the experimental uncertainty of about 50%. Also, this more detailed treatment of the photoabsorption data shows that in ^{196}Pt the widths are expected to be proportional to $E_\gamma^{5.5}$ rather than E_γ^5 at energies near the neutron binding energy.

4. NUCLEAR STRUCTURE EFFECTS

As was seen in the preceding section, the neutron capture γ-rays for many nuclides are accurately describable by a statistical model in which the γ-ray strength function $(\Gamma_{\gamma ij}/D)$ is a smooth function $f(E_\gamma)$ of γ-ray energy, independent of the nuclear structure of the final state. However, during the past 10 years there have been a number of suggestions, both theoretical and experimental, that nuclear-structure effects do play a significant role in the radiative capture of slow neutrons. Let us examine the more recent evidence of this kind.

The theory of radiative capture developed by Lane and Lynn [12] has been an important stimulus to most of the recent experimental efforts to find evidence for nuclear-structure effects. This theoretical treatment takes into account not only the usual compound-nucleus formation leading to an initial radiative state of great complexity but it also includes processes in which dipole radiation is emitted while the incident s-wave neutron in the field of the target nucleus undergoes a single-particle transition to a final state with a large component of p-wave orbital. In the resonance region of neutron energy, the amplitude for radiative emission to a given final state is found to be made up of three parts – the usual "internal" compound-nucleus resonance part, an "external" or "channel" resonance part, and a "hard-sphere" part. The internal resonance contribution exhibits the familiar statistical behaviour that is insensitive to nuclear structure whereas both channel resonance and hard-sphere capture depend on the single-particle character of the final state. The channel resonance part exhibits the same kind of resonance behaviour as the internal resonance part, which makes it hard to separate the two in any straightforward way; however, in principle the presence of channel-resonance capture can be recognized either by the anomalously large intensity of a transition or by a dependence of its radiation width on the reduced neutron width. Hard-sphere capture, which has a non-resonance behaviour, also results in anomalously strong transitions and in addition it may be recognized by a characteristic neutron-energy dependence for the γ-ray intensity; interference between the amplitude for resonance and hard-sphere capture produces asymmetries of the same kind as are observed in the neutron scattering cross-section.

The three experimental characteristics that are of interest to the Lane and Lynn theory (the γ-ray intensity, the correlation with neutron width, and the neutron-energy dependence) provide a convenient way to classify the experimental results, whether or not the data are thought to be interpretable in terms of the theory.

(1) Anomalously strong transitions. The transition intensity is the only kind of information about nuclear-structure effects that can be obtained from thermal-neutron capture spectra. Perhaps the most widely discussed indication of a dependence of these spectra on nuclear structure is what appears to be the anomalously large strengths of certain high-energy transitions in the spectra for nuclides in the range $24 < A < 70$. As pointed out by Lane and Lynn [12], these strong transitions appear to be associated with final states that have a large component of p-wave neutron orbital.

A quantitative way to study the non-statistical behaviour of the capture γ-rays is to compare the strengths of (n, γ) transitions with the strengths of the corresponding (d, p) transitions, for which the intensity depends on the single-particle character of the final state in a well understood way. Groshev and Demidov [13] have recently summarized results of this kind for 11 light nuclides ranging from ^{25}Mg to ^{67}Zn. Fig. 7 shows the striking degree of correlation between the strengths for (n, γ) transitions and (d, p) transitions with orbital angular momentum $\ell_n = 1$, a correlation that provides strong support for the reality of single-particle effects in the radiative transitions in light nuclides. However, the data do not tell us whether hard-sphere capture or channel resonance capture is the dominant process.

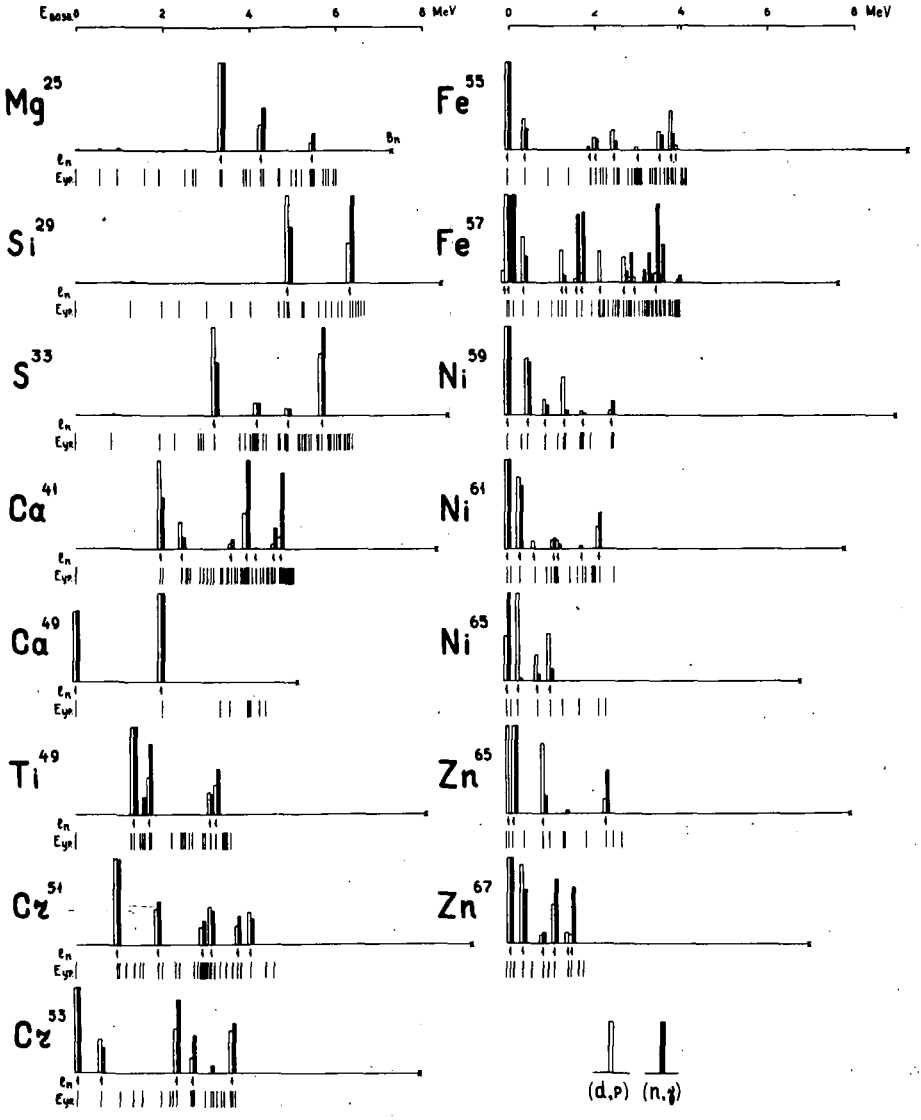

FIG. 7. Correlation between strengths for (n,γ) and (d, p) transitions (Groshev and Demidov [13]).

A comparison between the spectra for thermal-capture and resonance-capture can give some indication about the nature of the radiation. Good data of both kinds are available for the reaction $^{63}Cu(n,\gamma)\,^{64}Cu$, and the two kinds of spectra are found to be strikingly different. In thermal capture 43% of the capture proceeds by way of high-energy transitions to three low-energy states [14]. In contrast, the transitions to these three low-energy states are no stronger than many other transitions in the average resonance-capture spectrum formed by the capture of neutrons in the keV range of energy [15]. This striking difference between thermal

and resonance capture suggests that the strong lines in thermal capture are formed by hard-sphere capture rather than by channel resonance capture.

When the level spacing of the compound nucleus is small enough to permit γ-ray spectra to be measured at several resonances, in principle somewhat more complete information about the reaction mechanism can be obtained. The reaction ^{55}Mn (n, γ) ^{56}Mn and ^{59}Co (n, γ) ^{60}Co have been actively studied with this aim. Prestwich and Coté [16] found that the (n, γ) strengths in both thermal and resonance capture in ^{55}Mn exhibit a significant correlation with the (d, p) strengths. And in ^{59}Co (n, γ) ^{60}Co they find that the (n, γ) transitions to states fed by (d, p) transitions with $\ell_n = 3$ are only 0.126 ± 0.08 times as strong as (n, γ) transitions to states with $\ell_n = 1$. This dependence on ℓ_n is what is expected from single-particle effects, since only the $\ell_n = 1$ transitions are associated with final states that have a strong component of p-wave.

Comfort [17] has refined the analysis of the ^{55}Mn (n, γ) ^{56}Mn data by taking into account j-j coupling in the direct-capture model of Bockelman [18]. In this treatment the ratio of (n, γ) to (d, p) reduced widths is expected to depend on the total angular-momentum transfer j_n as well as on the orbital angular momentum ℓ_n; in particular, the ratio is proportional to $(2j_n + 1)$. The measured reduced-width ratios for the Mn data form a pattern that is consistent with this expectation, but the prediction cannot be tested fully because the spins of many of the final states are not known.

Turning now to heavier substances, one of the most widely discussed indications of a nuclear-structure effect is the presence of an anomalous "bump" in the unresolved spectra of some heavy nuclides such as gold. This phenomenon, which was originally pointed out by Groshev [19], has been investigated intensively by Bergqvist and Starfelt [20], who have shown that the bump is inconsistent with a simple statistical description of the capture γ-ray spectra and also is inconsistent with the Lane and Lynn model. One would hope that the more highly-resolved spectra now obtainable with Ge-diode spectrometers will soon provide an explanation for the anomalous bump.

Unexpected regularities in the easily resolved portion of the gamma-ray spectra from thermal-neutron capture in several deformed even-even heavy nuclides have recently excited interest. The first evidence of this kind came from studies of thermal capture in ^{176}Hf and ^{178}Hf by Namenson et al. [21] and capture in ^{182}W, ^{184}W and ^{186}W by Martin et al. [22]. The evidence has been reviewed by Namenson and Bolotin [23]. In these data, high-energy transitions to the $1/2^-$ and $3/2^-$ states of the $1/2^-$ [510] Nilsson band and to the $3/2^-$ state of the $3/2^-$ [512] band are observed. The arresting feature of the data is that for all five nuclides the high-energy transitions to the $1/2^-$ [510] band are very much stronger than the transitions to the $3/2^-$ [512] band, as is shown in their Table IV; also, except in ^{187}W, the $1/2^-$ state of the $1/2^-$ [510] Nilsson band is fed more strongly than the $3/2^-$ state of the same band. A somewhat similar pattern was observed by Prestwich and Coté [24] for the reaction ^{166}Er (n, γ) ^{167}Er. It is not surprising that this unusual degree of regularity was for a time considered to be convincing evidence for a specific nuclear-structure effect. Direct capture does not explain the data, since the (n, γ) intensities are not correlated with the (d, p) transition strengths.

Namenson and Bolotin [23] suggested that the observed intensity pattern might result from the Λ selection rule that, in the collective model, would govern transitions from an initial state in which the incident $s_{1/2}$ neutron is strongly coupled to the 0^+ deformed even-even target.

Several studies of resonance capture have been carried out in an effort to check the intensity pattern observed in thermal capture. These experiments throw considerable doubt on the significance of the regularity in the thermal spectra, since not all of the resonance spectra exhibit the intensity pattern found in the thermal spectra. Moreover, average spectra from resonance capture were measured [25] for targets of ^{182}W, ^{184}W, and ^{186}W. In all of these average spectra, the transitions to the $1/2^-$ [510] and $3/2^-$ [512] Nilsson bands are of equal intensity within an experimental uncertainty of about 30%, as is shown in Table I. Thus, until a convincing alternative explanation is offered, one must conclude that the regularities observed in the thermal spectra result from an uninteresting statistical fluctuation.

Before closing this discussion of the influence of nuclear structure on the intensities of high-energy radiative transitions, let us inquire to what extent the transitions may be independent of the character of the final state. The most refined experimental answer to this question is being provided by the average resonance-capture spectra of Bollinger and Thomas [7, 8, 26, 27]. The results presented earlier for ^{196}Pt are a good example. When the widths of transitions to eight low-energy states are assumed to vary as E_γ^α, the rms deviation of the measured widths from a least-squares fit is only 9% and this is consistent with the 11% deviation that is expected on the basis of the number of resonances that contribute to the average. Thus, the widths for the high-energy transitions in ^{196}Pt are very insensitive indeed to the character of the final state. Other compound nuclides whose widths depend smoothly on E_γ to a similar degree are ^{166}Ho, ^{168}Er, ^{178}Hf and ^{190}Os. Also, the widths of the other 11 even-even nuclides that have been studied are all consistent with a smooth dependence on E_γ, although the uncertainties from Porter-Thomas fluctuations are somewhat greater. In contrast, the widths for the odd-odd nuclides ^{170}Tm and ^{182}Ta exhibit fluctuations that are much greater than can be accounted for in terms of Porter-Thomas fluctuations. This difference in behaviour is not understood.

(2) Correlation with the neutron width. As mentioned earlier, in the Lane and Lynn [12] theory the amplitude for channel resonance capture is expected to be proportional to the reduced neutron-width amplitude. The detection of the predicted correlation between radiation width and reduced neutron width is a hard experimental problem because the systematic dependence on neutron widths is obscured by the random fluctuation in the dominant compound-nucleus component of the radiation amplitude. As a result, until recently no statistically significant correlations were found.

This uninteresting situation has changed during the past year, however, since Beer et al. [28] at Brookhaven have reported the detection of a statistically significant positive correlation between the reduced neutron width and the radiation widths in the reaction $^{169}Tm(n, \gamma)^{170}Tm$. They studied 15 high-energy transitions in the spectra of seven resonances and found the coefficient of correlation between Γ_n^0 and $\Gamma_{\gamma j}$ to be $R = +0.27$, where the correlation coefficient R is defined in the usual way so that its possible values range from -1 to +1.

TABLE I. RELATIVE INTENSITIES OF HIGH-ENERGY RADIATIVE TRANSITIONS IN THE ISOTOPES OF TUNGSTEN

Emitting nucleus	Final State			Relative Intensity	
	Energy (keV)	Nilsson band	J^{π}	Thermal[a] capture	Resonance[b] capture
	0	$\frac{1}{2}^-[510]$	$\frac{1}{2}^-$	100	100 ± 25
^{183}W	47	$\frac{1}{2}^-[510]$	$\frac{3}{2}^-$	34	99 ± 25
	209	$\frac{3}{2}^-[512]$	$\frac{3}{2}^-$	< 1	63 ± 25
	0	$\frac{3}{2}^-[512]$	$\frac{3}{2}^-$	10	90 ± 25
^{185}W	23	$\frac{1}{2}^-[510]$	$\frac{1}{2}^-$	100	100 ± 25
	93	$\frac{1}{2}^-[510]$	$\frac{3}{2}^-$	16	77 ± 25
	0	$\frac{3}{2}^-[512]$	$\frac{3}{2}^-$	5	75 ± 35
^{187}W	147	$\frac{1}{2}^-[510]$	$\frac{1}{2}^-$	100	100 ± 30
	205	$\frac{1}{2}^-[510]$	$\frac{3}{2}^-$	139	138 ± 30

[a] Martin et al. [22]
[b] Bollinger and Thomas [25]

To determine the statistical significance of the observed positive correlation, the Tm data were interpreted in terms of the theory of Lane and Lynn by assuming that the radiation amplitude is made up of a channel-resonance term and a compound-nucleus term, so that

$$\Gamma_{\gamma ij}^{\frac{1}{2}} = A_j \Gamma_{\gamma i}^{0\frac{1}{2}} + \Gamma_{cij}^{\frac{1}{2}} \qquad (7)$$

where A_j is a parameter independent of the initial state i and $\Gamma_{cij}^{\frac{1}{2}}$ is a random compound-nucleus amplitude with a mean value of zero. Defining ρ_j as the coefficient of correlation between $\Gamma_{\gamma ij}^{\frac{1}{2}}$ and $\Gamma_{ni}^{\frac{1}{2}}$, a Monte Carlo technique was used to show that the experimental value $R = +0.27$ implies that $0.2 < \bar{\rho} < 0.7$ with 80% confidence and that there is only a 0.1% probability that the data are consistent with no correlation. This convincing demonstration of a positive correlation between Γ_n^0 and $\Gamma_{\gamma ij}$ was cited as evidence for the detection of channel resonance capture.

A somewhat disturbing feature of the Brookhaven data is that the non-zero correlation is caused entirely by the influence of one resonance – one with the largest radiation width. In an attempt to remove this source of doubt, Jackson and Bollinger [29] at Argonne have extended the correlation study to other resonances that have large neutron widths. In these measurements it was necessary to have good neutron-energy resolution and consequently the neutron intensity was not large enough to permit the use of a Ge diode as the γ-ray spectrometer. Instead, a large NaI scintillator was used. Since the effective resolution width of this detector is about 300 keV, the measured intensities were formed by transitions to several final states. However, this is no handicap if the objective of the experiment is to measure the average intensity of transitions to many final states.

The significance of an average intensity of transitions to many final states may be understood by squaring both sides of Eq.(7) and averaging over final states to obtain

$$\langle \Gamma_{\gamma i} \rangle_j = \langle A^2 \rangle_j \Gamma_{ni}^0 + \langle \Gamma_{ci} \rangle_j \pm \langle A \Gamma_{ni}^{0\frac{1}{2}} \Gamma_{ci}^{\frac{1}{2}} \rangle_j \qquad (8)$$

Here we see that there is a linear dependence of $\langle \Gamma_{\gamma i} \rangle_j$ on Γ_{ni}^0, but superimposed upon this systematic dependence are two randomly fluctuating terms. Nevertheless, the dependence of $\langle \Gamma_{\gamma i} \rangle_j$ on Γ_{ni}^0 would be revealed, if the parameter $\langle \rho^2 \rangle_j = \langle A^2 \rangle_j \langle \Gamma_n^0 \rangle_i / \langle \Gamma_\gamma \rangle_{ij}$ is large enough.

In spite of the relatively poor resolution of the NaI γ-ray spectrometer used in the Argonne experiment [20], it is good enough to permit the determination of the average intensity of transitions to approximately the same final states as were studied in the Brookhaven experiment [28]. The dependence of this average intensity on Γ_n^0 is shown in Fig. 8. From these data it seems qualitatively obvious that the radiation width is not independent of Γ_n^0 and this conclusion is confirmed by a χ^2 analysis, which shows that there is less than a 0.1% probability that Porter-Thomas fluctuations could cause the measured intensities to deviate from a constant value as much as they do. Thus, it seems quite certain for the reaction ^{169}Tm(n, γ) ^{170}Tm, at least, that there is a correlation between the radiation and neutron widths. Measurements on other targets are in progress.

Since the amplitude for channel resonance capture depends on the single-particle character of the final state, when channel resonance capture

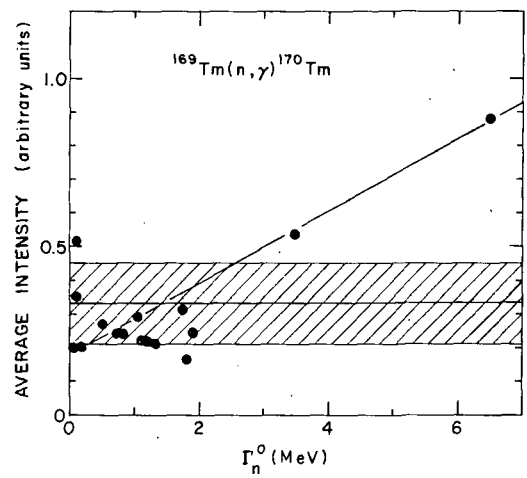

FIG. 8. Dependence of average radiation width on reduced neutron width Γ_n^0 (Jackson and Bollinger [29]). The slope of the line drawn through the data points corresponds to $\rho^2 \approx 0.3$.

is significant the radiation widths are expected to be correlated with the intensities of (d, p) transitions as well as with the reduced neutron widths. The expected relationship is contained in the parameter A_j in Eq. (7), which should be proportional to the $\ell_n = 1$ amplitude of the (d, p) transition. Thus, under the channel-resonance-capture interpretation of the ^{169}Tm(n, γ)^{170}Tm data, there should be a positive correlation between the strengths for (n, γ) and (d, p) transitions to the final states for which a non-zero value of $\rho_j^2 = A_j^2 \langle \Gamma_n^0 \rangle_i / \langle \Gamma_{\gamma j} \rangle_i$ was measured. Bollinger and Thomas [30] have attempted to test this idea by using a neutron-filter technique to obtain accurate values of the average widths of radiative transitions from many initial states to individual final states in ^{170}Tm. No correlation between the (n, γ) and (d, p) intensities was observed, even though the final states of the transitions compared were the same as those involved in the transitions that exhibit a correlation with the neutron widths. This negative result suggests strongly that the correlation between radiation and neutron widths in ^{169}Tm(n, γ) ^{170}Tm does not result from channel resonance capture. On the other hand, this inference may be premature, in view of doubts raised by the complexity of the nuclear reaction and the incompleteness of the (d, p) data involved. In any case, the general question of the extent to which channel resonance capture is significant for most nuclides is still an unsolved experimental problem.

(3) Interference effects. When the possibility of hard-sphere capture is taken into account [12], the cross-section $\sigma_j(E)$ for a primary radiative transition to a final state j varies with the neutron energy E according to a relationship of the form

$$\sigma_j(E) \propto \frac{1}{\sqrt{E}} \left| a_j + \sum_i \frac{(\Gamma_{ni}^0 \Gamma_{ij})^{\frac{1}{2}}}{E_i - E + \frac{1}{2} i \Gamma_i} \right|^2 \qquad (9)$$

where a_j is the amplitude for hard-sphere direct capture and the terms in the summation are amplitudes for resonance capture; the quantities Γ_i,

Γ_{ni}^{0}, Γ_{ij}, and E_i are, respectively, the total width, the reduced neutron width, the width for a radiative transition to a state j, and the resonance energy for an initial state i. It is assumed that the spacing between the levels is much greater than the widths. The hard-sphere and resonance amplitudes add constructively and destructively to form a capture cross-section σ_j with an asymmetric interference pattern of the kind that is familiar from neutron scattering.

In principle the observation of the expected interference effect in the neutron-energy dependence of the cross-section for individual radiative transitions should provide an unambiguous measure of the amplitude for the hard-sphere part of direct capture. However, in practice such measurements are difficult and usually the data are not very sensitive to a small cross-section for direct capture, since the interference effects associated with hard-sphere capture are obscured by the ordinary resonance-resonance interference. The uncertainty caused by resonance-resonance interference is especially hard to remove because nuclear levels below the binding energy, about which we have little information, can have a large influence on the cross-section above the binding energy.

The Brookhaven group have been especially active in the search for evidence of hard-sphere capture and they have reported that the energy dependence in the reactions $^{59}Co(n,\gamma)\,^{60}Co$ and $^{238}U(n,\gamma)^{239}U$ both exhibit interference effects that cannot be explained in terms of resonance-resonance interference [31, 32]. Let us consider what seems to the author to be the more convincing case, the reaction $^{238}U(n,\gamma)^{239}U$. The neutron-energy dependence of the cross-sections for the 4059-keV and 3982-keV γ-rays were measured [32] over the energy range 0-21 eV, a range that contains the prominent resonances at 6.7 and 21 eV. Both cross-sections show a sharp departure from the shape described by a sum of single-level Breit-Wigner terms. The data for the 3982-keV γ-ray can be explained in terms of the interference between nearby resonances; but the energy dependence of the cross-section for the 4059-keV transition cannot be explained in terms of known resonances unless hard-sphere capture is assumed to be present. As is shown in Fig. 9, the best fit is obtained for a hard-sphere-capture cross-section of 0.0016 barns at 1 eV, a value that is an order of magnitude smaller than is calculated from the theory of Lane and Lynn [12]. This direct-capture interpretation is reinforced by the fact that the state fed by the 4059-keV transition is known to have a strong p-wave single-particle component whereas the state fed by the 3982-keV transition has little if any single-particle character. However, from a strictly experimental point of view, the lack of information about the influence of states below the neutron binding energy would seem to be a source of uncertainty.

5. M1 TRANSITIONS

This is a poor time at which to attempt to summarize the data on M1 transitions, because the results now available are still quite fragmentary and at the same time new experimental information is being rapidly accumulated. Thus anything said now will soon be outdated.

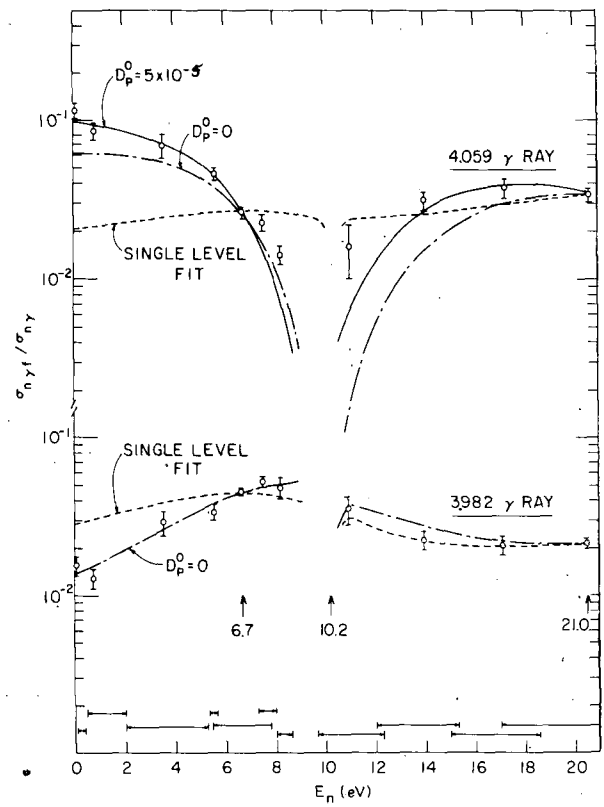

FIG. 9. Evidence for direct capture in ^{238}U (n,γ) ^{239}U (Chrien et al.[32]). The vertical axis gives the fractional intensity of the indicated γ-ray as a function of neutron energy E_n.

Much of what we know about high-energy M1 transitions is summarized in Table II. The average reduced width $\bar{k}_{M1}$ for M1 transitions, the quantity of interest in the table, is defined by Bartholomew [33] to be

$$\bar{k}_{M1} = \bar{\Gamma}_{\gamma ij} D^{-1} E_\gamma^{-3} \tag{10}$$

where $\bar{\Gamma}_{\gamma ij}$ is in eV, and both D and E_γ are in MeV. In the calculation of the reduced widths given in the table, experimental values of the average width $\bar{\Gamma}_{\gamma ij}$ were obtained by averaging over transitions from several initial states i and/or transitions to several final states j, depending on what data are available.

For all the transitions used in the table, the M1 character of the radiation was inferred from the known spins and parities of the initial and final states under the assumption that transitions of higher multipolarity (especially E2 transitions) may be neglected. Not enough is known about E2 radiation to be sure that this assumption is valid for all the data, although average resonance-capture measurements [8, 27] have shown that E2 transitions are much weaker than M1 transitions in ^{96}Mo, ^{98}Mo, ^{106}Pd, ^{136}Ba, ^{166}Ho, and ^{168}Er.

TABLE II. SUMMARY OF AVERAGE VALUES OF REDUCED WIDTHS $\bar{k}_{M1}$ FOR M1 TRANSITIONS.

Under spectra, the symbols T, R, and A stand for data obtained from spectra formed by capture of thermal neutrons, capture in individual resonances, and average resonance capture, respectively.

Emitting Nucleus	$\bar{k}_{M1} \times 10^{-3}$	Spectra	Uncertainty Factor	E_γ (MeV)	Ref.
^{92}Zr	8	R	2	7.7	a
^{96}Mo	10	T	2.5	7.6	b
^{106}Pd	17	T	2	8.3	c
^{106}Pd	18	A	2	8.6	d
^{114}Cd	18	T	2	7.8	e
^{117}Sn, ^{119}Sn	150	R	3	6.6	f,g
^{118}Sn	31	T	2	7.8	h
^{118}Sn	17	A	2	7.5	d
^{124}Te	8	T	2	7.9	i
^{136}Ba	49	R	2	8.0	j
^{136}Ba	52	A	2	8.3	d
^{166}Ho	7	T	2.5	6.0	k
^{168}Er	6	T	2	7.0	l
^{168}Er	21	A	2	6.8	d
^{170}Tm	22	A	2	5.9	d
^{178}Hf	24	A	2	6.5	m
^{182}Ta	12	A	2	5.8	d
^{239}U	30	R	2	4.7	n,o

a Jackson [37]
b Kinsey and Bartholomew [38]
c Groshev et al. [39]
d Thomas and Bollinger [8,27]
e Smither [40]
f Harvey et al. [34]
g Slaughter et al. [35]
h Harvey et al. [41]
i Chaturvedi et al. [42]
j Becvar et al. [36]
k Motz et al. [43]
l Groshev et al. [44]
m Buss and Smither [45]
n Bergqvist [46]
o Jackson [47]

Two quite different kinds of information are used in the table. One kind is the absolute intensities of M1 transitions observed in the spectra formed by capture of thermal neutrons or capture of neutrons in individual resonances. These absolute intensities (usually expressed as photons per neutron capture) are combined with the total radiation width and the level spacing at the initial state in an obvious way to obtain values of $\bar{k}_{M1}$. The second class of information is the ratio $\bar{\Gamma}(E1)/\bar{\Gamma}(M1)$ of average widths for E1 and M1 transitions obtained from average resonance-capture spectra. An example of a result of this kind is given in Fig. 10, where the measured intensities for the reaction $^{167}Er(n,\gamma)^{168}Er$ are given as a plot of

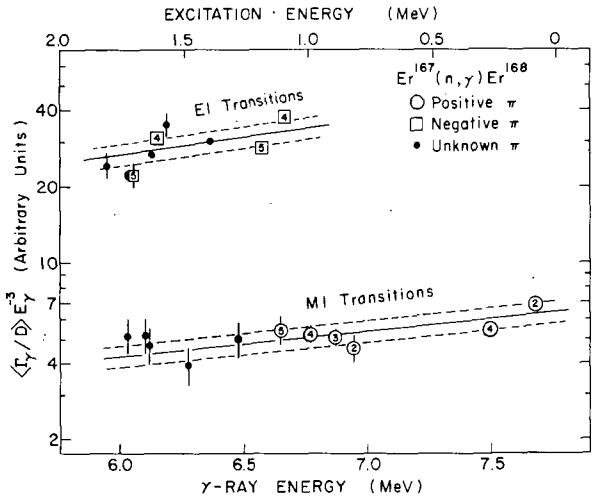

FIG. 10. Data used to determine the ratio $\bar{\Gamma}(E1)/\bar{\Gamma}(M1)$ for ^{167}Er (n, γ) ^{168}Er (Bollinger and Thomas [26]). The numbers within the data points give known spins of final states.

$\bar{\Gamma}_{\gamma ij} E_\gamma^{-3}$ versus E_γ. The ratio $\bar{\Gamma}(E1)/\bar{\Gamma}(M1)$ is immediately apparent from this plot. Aside from the uncertainties caused by Porter-Thomas fluctuations (indicated by the dashed lines) and counting statistics (given by error bars), the only source of error is the possible influence of p-wave capture. However, for the data in the figure and for many other data, p-wave capture has been shown to be negligible. The value of $\bar{k}_{M1}$ is calculated from the ratio $\bar{\Gamma}(E1)/\bar{\Gamma}(M1)$ under the assumption that $\bar{\Gamma}(E1)$ is given by Eq. (6), the summary of Carpenter's experimental results.

In the table, the entries under "uncertainty factor" give the factor by which the $\bar{k}_{M1}$ values are believed to be uncertain (in the spirit of a standard statistical error). Porter-Thomas fluctuations are a major source of uncertainty for the data obtained from thermal capture or from the spectra for capture in individual resonances, since in all cases the average $\bar{\Gamma}_{\gamma ij}$ is obtained from a rather small number of transitions – typically 6 or 8. In addition, the uncertainty in the level spacing D is often a significant source of uncertainty in $\bar{k}_{M1}$. For the average resonance capture data, the main source of uncertainty comes from the assumption that the width for E1 transitions is given by Eq. (6).

The $\bar{k}_{M1}$ values of Table II are plotted in Fig. 11 as a function of A. In view of the large uncertainties associated with all the data points, the results obtained from the various kinds of measurements appear to be consistent. Although in published discussions of M1 transitions there has been frequent mention of abnormally strong transitions that give evidence for an M1 giant resonance, one sees from the figure that, with the possible exception of transitions in ^{117}Sn, ^{119}Sn and ^{136}Ba, all the data are consistent with a constant value of $\bar{k}_{M1} \cong 20 \times 10^{-3}$. This value is somewhat greater than that inferred previously by Bartholomew [33] from thermal-capture data and it is very much larger than the value calculated from the single-particle model — Eq. (3c). Thus, the frequent observation in the literature that an M1 transition is anomalously strong because it is an order of magnitude greater than the single-particle estimate is seen to be misleading.

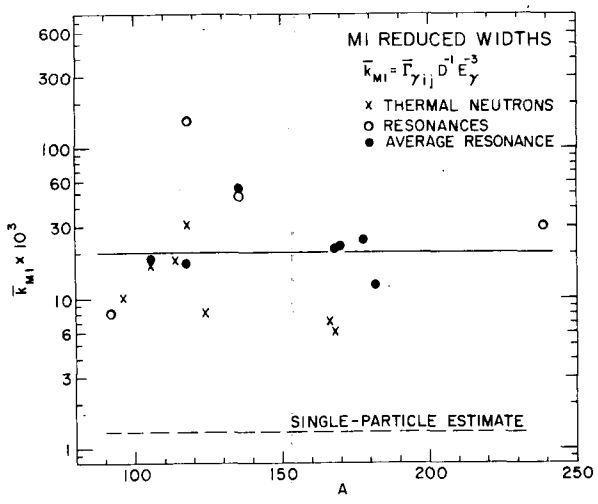

FIG.11. Summary of reduced widths for M1 transitions.

The relatively large values of $\bar{k}_{M1}$ in Table II and Fig.11 have the important practical implication that E1 and M1 transitions are not as easily distinguishable on the basis of their intensities as seems to have been generally thought to be the case. If one assumes that the average width for E1 transitions is given by Eq.(6) and that the average width for M1 transitions is given by the value $\bar{k}_{M1} = 20 \times 10^{-3}$, then the ratio of E1 to M1 widths is

$$\frac{\bar{\Gamma}(E1)}{\bar{\Gamma}(M1)} \approx 1.7 \left(\frac{E_\gamma}{7}\right)^2 \left(\frac{A}{100}\right)^{8/3} \qquad (11)$$

Although this relationship may be in error by as much as a factor of 3 for some nuclides, it shows clearly that the intensities for E1 and M1 transitions are of the same order of magnitude under conditions that are frequently encountered with neutron-capture γ-rays. Eq.(11) is intended to be meaningful only over the limited energy range from about 6-8 MeV and for $A > 90$.

Since the large values of $\bar{k}_{M1}$ for ^{117}Sn and ^{119}Sn and for ^{136}Ba would be interesting, if true, let us briefly consider the nature of the experimental evidence. The data [34, 35] for the Sn isotopes consists of just four transitions, two each for one resonance in ^{116}Sn(n,γ) ^{117}Sn and one resonance in ^{118}Sn(n,γ)^{119}Sn. Since the Porter-Thomas fluctuations associated with a sample of four can be quite large and since there are other possible sources of error, it appears to the author that the large value of $\bar{k}_{M1}$ for ^{117}Sn and ^{119}Sn cannot be accepted as reliable until other transitions in these nuclides are observed to exhibit a similar behaviour.

Two kinds of data seem to indicate that the value of $\bar{k}_{M1}$ for ^{136}Ba is exceptionally large. Becvar et al. [36] used the Dubna pulsed reactor to measure the spectra for six resonances of ^{135}Ba, in which they observed a total of 13 M1 transitions. The probability that the value $\bar{k}_{M1} = 49 \times 10^{-3}$ deduced from their data is consistent with the more typical value 20×10^{-3} is small – roughly 5%, taking into account all sources of uncertainty.

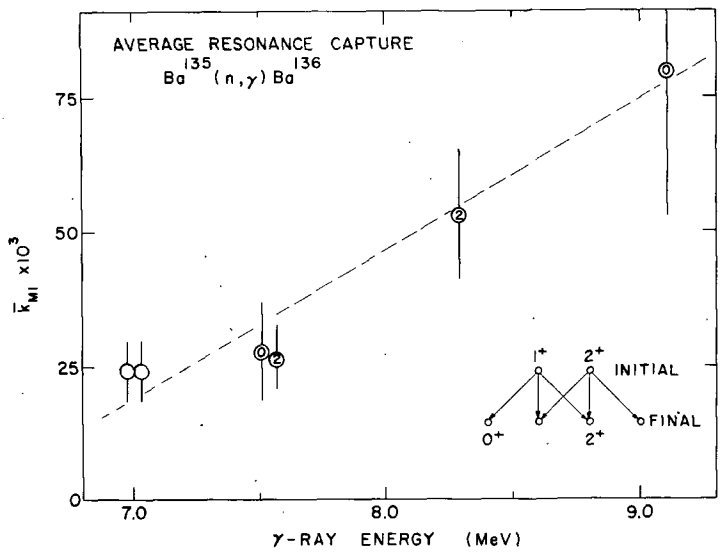

FIG. 12. Energy dependence of reduced widths for M1 transitions in ^{135}Ba (n,γ)^{136}Ba (Bollinger and Thomas[8]). The numbers within the data points give known spins of final states.

The second piece of evidence for an abnormally large value of $\bar{k}_{M1}$ for ^{136}Ba comes from the average resonance-capture spectra measured at Argonne [8, 27]. In these experiments the quantity measured is the ratio $\bar{\Gamma}(E1)/\bar{\Gamma}(M1)$, where the E1 width is that associated with transitions to the 3^- state at 2532 keV. The major source of uncertainty in the $\bar{k}_{M1}$ value is the need to use Eq. (6) to calculate $\bar{\Gamma}(E1)$. Again, the probability that the result could be consistent with the value $\bar{k}_{M1} = 20 \times 10^{-3}$ is thought to be less than 10%. Attempts now being made to measure $\bar{k}_{M1}$ directly by means of the average resonance-capture technique are expected to give a much more refined result.

For a plot such as Fig. 11 to be meaningful requires that $\bar{k}_{M1}$ should not depend markedly on the γ-ray energy. The average resonance-capture data [8, 27] provide an experimental answer to this question. The result for ^{167}Er (n,γ)^{168}Er, as given in Fig. 10, is typical of the data for most of the nuclides that have been studied; the data indicate that $\bar{k}_{M1}$ depends somewhat on E_γ, but the variation is relatively small over the limited range of energies available for study. However, there are three exceptions – ^{118}Sn, ^{120}Sn, and ^{136}Ba – and for these the value of the reduced width seems to vary by a factor of 3 within the energy range E_γ = 7-9 MeV. The data for ^{136}Ba are given in Fig. 12, where $\bar{k}_{M1}$ is seen to increase rapidly with increasing energy. The observed energy dependence is probably real, since a statistical analysis shows that there is less than a 1% chance that random fluctuations could cause the data points to deviate from a constant value as much as they do. Unfortunately, there are no published theoretical treatments of M1 radiation that take into account the nuclear-structure effects needed to explain the observed energy dependence.

REFERENCES

[1] GROSHEV, L.V., Proc. Int. Conf. Nuclear Structure, Kingston, Canada, University of Toronto Press, Toronto, Canada (1960) p.568.
[2] PORTER, C.E., THOMAS, R.G., Phys. Rev. 104 (1956) 483.
[3] JACKSON, H.E., JULIEN, J., SAMOUR, C., BLOCH, A., LOPATA, C., MORGENSTERN, J., MANN, H., THOMAS, G.E., Phys. Rev. Lett. 17 (1966) 656.
[4] BLATT, J.M., WEISSKOPF, V.F., Theoretical Nuclear Physics, John Wiley & Sons, N.Y. (1952).
[5] WILKINSON, D.H., Nuclear Spectroscopy, Part B. (Ajzenberg-Selove, F., Ed.) Academic Press, N.Y. and London (1960) p.852.
[6] AXEL, P., Phys. Rev. 126 (1962) 671.
[7] BOLLINGER, L.M., THOMAS, G.E., Phys. Rev. Lett. 18 (1967) 1143.
[8] BOLLINGER, L.M., THOMAS, G.E. (1968) to be published.
[9] HURST, R.R., DONAHUE, D.J., Nucl. Phys. A91 (1967) 365.
[10] ROSENZWEIG, N., submitted to Nucl. Phys.
[11] CARPENTER, R.J., Argonne National Laboratory Report ANL-6589.
[12] LANE, A.M., LYNN, J.E., Nucl. Phys. 17 (1960) 563; Nucl. Phys. 17 (1960) 586.
[13] GROSHEV, L.V., DEMIDOV, A.M., Yadernaya Fiz. 4 (1966) 785.
[14] GROSHEV, L.V., DEMIDOV, A.M., LUTSENKO, V.N., PELEKHOV, V.I., Atlas of γ-Ray Spectra from Radiative Capture of Thermal Neutrons, English edition Pergamon Press, London (1958).
[15] ALLEN, B.J., Nucl. Phys. A111 (1968) 1.
[16] PRESTWICH, W.V., COTE, R.E., Phys. Rev. 155 (1967) 1223.
[17] COMFORT, J.R., Phys. Rev. Lett. 20 (1968) 941.
[18] BOCKELMAN, C.K., Nucl. Phys. 13 (1959) 205.
[19] GROSHEV, L.V., DEMIDOV, A.M., LUTSENKO, V.N., PELEKHOV, V.I., Int. Conf. peaceful Uses atom. Energy (Proc. Conf. Geneva, 1958) 15 UN, New York (1958) 138.
[20] STARFELT, N., Nucl. Phys. 53 (1964) 397.
[21] NAMENSON, A.I., JACKSON, H.E., SMITHER, R.K., Phys. Rev. 146 (1966) 844.
[22] MARTIN, M.J., HARVEY, J.A., SLAUGHTER, G.C., Bull. Am. phys. Soc. 11 (1966) 336.
[23] NAMENSON, A.I., BOLOTIN, H.H., Phys. Rev. 158 (1967) 1206.
[24] PRESTWICH, W.V., COTE, R.E., Phys. Rev. 162 (1967) 1112.
[25] BOLLINGER, L.M., THOMAS, G.E., Bull. Am. phys. Soc. 12 (1967) 105.
[26] BOLLINGER, L.M., THOMAS, G.E., Bull. Am. phys. Soc. 12 (1967) 1200; also in Argonne National Laboratory Report ANL-7405 (1967) p.1.
[27] THOMAS, G.E., BOLLINGER, L.M., Bull. Am. phys. Soc. 13 (1968) 721.
[28] BEER, M., LONE, M.A., CHRIEN, R.E., WASSON, O.A., BHAT, M.R., MUETHER, H.R., Phys. Rev. Lett. 20 (1968) 340.
[29] JACKSON, H.E., BOLLINGER, L.M., (1968) to be published.
[30] BOLLINGER, L.M., THOMAS, G.E., Bull. Am. phys. Soc. 13 (1968) 722.
[31] WASSON, O.A., BHAT, M.R., CHRIEN, R.E., LONE, M.A., BEER, M., Phys. Rev. Lett. 17 (1966) 1220.
[32] CHRIEN, R.E., PRICE, D.L., WASSON, O.A., BHAT, M.R., LONE, M.A., BEER, M., Phys. Lett. 25B (1967) 195.
[33] BARTHOLOMEW, G.A., Ann. Rev. nucl. Sci. 11 (1961) 259.
[34] HARVEY, J.A., MARTIN, M.J., SLAUGHTER, G.G., in Slow-Neutron Capture Gamma-Ray Spectroscopy, Argonne National Laboratory Report ANL-7282 (1966).
[35] SLAUGHTER, G.G., MARTIN, M.J., HARVEY, J.A., in Slow-Neutron Capture Gamma-Ray Spectroscopy, Argonne National Laboratory Report ANL-7282 (1966).
[36] BECVAR, F., VRZAL, J., LIPTAK, J., URBANEC, J., JINR Preprint P3-3696.
[37] JACKSON, H.E., Phys. Rev. 131 (1963) 2153.
[38] KINSEY, B.B., BARTHOLOMEW, G.A., Can. J. Phys. 31 (1953) 537.
[39] GROSHEV, L.V., DEMIDOV, A.M., SHADIEV, N., Izv. Akad. Nauk SSSR, Ser. Fiz. 29 (1965) 760.
[40] SMITHER, R.K., (Argonne) (1968) private communication.
[41] HARVEY, J.A., SLAUGHTER, G.G., MARTIN, M.J., Oak Ridge National Laboratory Report ORNL P-1353 (1965).
[42] CHATURVEDI, R.R., BUSHNELL, D., SMITHER, R.K., Bull. Am. phys. Soc. 12 (1967) 1064.
[43] MOTZ, H.I., et al., Phys. Rev. 155 (1967) 1265.
[44] GROSHEV, L.V., DEMIDOV, A.M., IVANOV, V.A., LUTSENKO, V.N., PELEKHOV, V.I., SHADIEV, N., Izv. Akad. Nauk SSSR, Ser. Fiz. 29 (1965) 772.

[45] BUSS, D.J., SMITHER, R.K., (Argonne) (1968) private communication.
[46] BERGQVIST, I., Nucl. Phys. 74 (1965) 15.
[47] JACKSON, H.E., Phys. Rev. 134 (1964) B931.

DISCUSSION

K. F. ALEXANDER: Could you comment on the strong anticorrelation effects between (n,γ) and (d,p) strengths found in several nuclei?

L. M. BOLLINGER: I have treated this subject only briefly in my paper because it seems to me that the published reports on the anticorrelation have not made a convincing case that the anticorrelations actually exist. This is not to say that I believe that the anticorrelations do not exist. I merely mean that I will reserve judgment until I see a more quantitative discussion of the subject.

W. RUDOLPH: There are many anticorrelations in the mass region $A \approx 40-60$, especially in odd-odd nuclei. These anticorrelations show clearly the influence of the special structure of the final and also of the capture state, I think.

L. M. BOLLINGER: My reply to this comment is the same as my previous one.

W. RUDOLPH: We calculated the low-energy level scheme of ^{52}V and found strong admixtures of excited target states in most of the states. Taking into account the admixture of the first excited target state and assuming that this configuration is also mixed into the capture state, it was possible to describe the measured intensities better than by the direct capture. Also it is not possible to explain the strong γ-rays to levels with $\ell_n = 3$ in ^{40}K and ^{46}Sc by the direct capture.

R. E. CHRIEN: It is unfortunate that Professor Bollinger did not have time in his short presentation to describe an interesting aspect of the theory of Lane and Lynn, namely the potential or hard sphere capture. At Brookhaven, the Fast Chopper Group has presented convincing evidence for this effect in $^{59}Co\,(n,\gamma)^{60}Co$, $^{238}U\,(n,\gamma)^{239}U$ and $^{169}Tm\,(n,\gamma)^{170}Tm$. The effect has been studied by the interference of the smooth amplitude for potential capture with the fluctuating amplitude for compound nucleus formation.

L. M. BOLLINGER: This subject is treated in my written paper.

G. M. TEMMER: When you make your comparison with the giant E1 Lorentzian tail, does your sample contain only target spins $\frac{1}{2}^-$ so that $\frac{1}{2}^- + (\text{s-wave neutron}) \rightarrow (0^-)$ or 1^- in the capture state, decaying by pure E1 transition to the 0^+ ground state?

L. M. BOLLINGER: In the illustration I gave on $^{195}Pt\,(n,\gamma)^{196}Pt$ the target spin is $\frac{1}{2}^-$ and we observe E1 transitions not only to the 0^+ ground state but also to 0^+ and 2^+ excited states. However, other targets we have studied do not have spin $\frac{1}{2}$. This causes no difficulty, however, if one knows the spins and parities of the final states.

H. T. MOTZ: The odd-odd nucleus ^{166}Ho, like ^{170}Tm mentioned by Dr. Chrien, shows a strong intensity correlation between (d,p) and thermal (n,γ). In the simplest view, since the states excited by primary transitions are almost identical, the only states excited by capture in ^{166}Ho are 'neutron-excited' states. We observe no proton-excited states. Therefore,

one may say that the compound nucleus remembers the initial target (^{165}Ho) proton state. This appears inconsistent with a purely statistical concept for the compound nucleus.

L. M. BOLLINGER: I have read your papers on this subject and, frankly, I do not understand your confidence that the high-energy thermal-neutron-capture γ-rays in ^{166}Ho and ^{170}Tm are so very non-statistical.

J. URBANEC: I would like to ask about the energy dependence of primary transition probabilities. It seems to me that in a proper experiment the transitions feeding the final states of the same structure must be taken into account. Indeed, the dependence of the transition probability on the final state structure may cause a distortion of the probability dependence of the primary transitions. Did you try to compare the transition probabilities of primary transitions which are going to final states of the same structure as two particle states or so?

L. M. BOLLINGER: One of the main points I have been trying to make is that the radiation widths for many nuclides do not seem to depend on the character of the final state. The evidence for this is that the width varies smoothly with γ-ray energy over an energy range that contains states that must have quite different characteristics. A good example of this is the data I showed for ^{167}Er $(n,\gamma)^{168}$Er, where the final states involved are known to be associated with at least four different rotational bands.

R. K. SHELINE: I would like to enlarge on the comment of Dr. Motz. We have looked in considerable detail at the low-lying levels in ^{170}Tm and ^{166}Ho both with (d, p) and (n, γ) reactions. We see no case in which a level populated in the (n, γ) reaction is not also populated in the (d, p) reaction. In each case these populated states are neutron states since the (d, p) reaction cannot populate excited proton states. Yet we know from the detailed studies of Dr. Bunker and Dr. Reich that the density of proton and neutron states in the rare earth nuclei is very similar (200-400 keV spacing). It is therefore virtually inconceivable that there are no excited proton states in the first 750-1000 keV of either ^{170}Tm or ^{166}Ho which (from the point of view of spin and parity only) would not be populated in the (n, γ) reaction. The fact that they are not populated should probably be ascribed to a nuclear structure effect.

L. M. BOLLINGER: As I understand your comment and your papers, your argument that there must be low-energy proton states in ^{166}Ho and ^{170}Tm is based entirely on nuclear-model considerations. Is it not possible that the proton states are raised in energy by 100 or 1000 keV? In view of the high degree to which the resonance-average radiation width is independent of the character of the final state under many other circumstances, I simply cannot accept your argument that there are E1 transitions that we do not see at all because of some nuclear-structure effect. I will issue a challenge — you show me a low-energy proton state and I will show you a radiative transition to it!

G. V. DANILYAN: I should like to comment on that part of Professor Bollinger's report which treats of the partial radiation width distributions. A few years ago we investigated the γ-ray spectra averaged on a very large quantity of resonances from the capture of neutrons in nuclei of ^{103}Rh, ^{181}Ta and ^{197}Au. The results were so unexpected that we have not published them yet. (The preliminary results were presented at the Annual Nuclear Spectroscopy and Nuclear Structure Meeting, Moscow, 1966). The neutron spectrum was sufficiently large and a very high number of resonances

contributed to the reaction but nevertheless the fluctuations of partial radiation widths were very great. Assuming the Porter-Thomas distribution, these fluctuations would correspond to the contribution in the reaction of only three-four resonances which is obviously not the case. It is important to underline that all investigated nuclei are odd-odd.

W. RUDOLPH: There are also strong primary transitions to excited proton states in ^{46}Sc at about 600 keV. These states are excited very weakly in the (d, p) but strongly in the ^{47}Ti(d, ^{3}He)^{46}Sc and in the (n, γ) reaction. Further, in the mass region A = 40-60 strong mixing of excited proton and neutron states can be expected.

Short contribution

R. E. CHRIEN (Brookhaven National Laboratory, Upton, N. Y., USA): I should like to make some observations on the anomalies in the statistical properties of radiative widths in slow neutron capture.

In the usual interpretation of the decay of the highly excited states formed by slow neutron capture, a statistical picture is adopted. Following the plausible assumption that the compound state is highly complex, and using the central limit theorem, one is led to a Gaussian distribution of width amplitudes with zero mean. A Porter-Thomas or chi-square distribution with one degree of freedom is thereby obtained for the widths. In this picture, no correlation between width amplitudes is expected.

Recently, evidence has been accumulating that this simple picture is not valid for all nuclides. I would like to present additional evidence indicating the breakdown of the statistical assumptions, and indicating the presence of simple structures in the capturing states. In the reaction ^{169}Tm(n, γ)^{170}Tm, the Brookhaven Fast Chopper Group have demonstrated a correlation between partial radiative widths and reduced neutron widths. In this recently published work[1] an average correlation coefficient of +0.27 was found for 15 final states from 8 resonances. The positive correlation indicates that the γ-rays tend to be stronger from resonances with large neutron widths. Taking advantage of an extension of the Chopper flight path to 48.87 metres, and an improved detector geometry, the Brookhaven group have extended their data to several hundred electron volts, including a large resonance at 153 eV, with a reduced width almost twice as large as the largest width in the previously published work. Table A shows the γ-ray intensities, as recorded with a 10 cm^3 Ge(Li) detector of 8 keV resolution, for the 15 final states in ^{170}Tm, as recorded in the 153 eV resonance. The resonance, indeed, shows strong radiative transitions. The summed intensity for these 15 lines exceeds that on any previously recorded resonance in thulium. The correlation coefficient has been calculated for 10 J = 1 resonances, including the 153 eV resonances. The result is +0.26, which confirms the previously reported value. Such non-zero correlations have also been established for ^{182}W(n, γ)^{183}W and ^{186}W(n, γ)^{187}W.

---

[1] BEER, M., LONE, M. A., CHRIEN, R. E., WASSON, O. A., BHAT, M. R., MUETHER, H. R., Phys. Rev. Lett. 20 (1967) 340-343.

[2] HUGHES, D. J., PALEVSKY, H., BOLOTIN, H. H., CHRIEN, R. E., Proc. Int. Conf. Nuclear Structure (BROMLEY, D. A., VOGT, E. W., Eds), Univ. of Toronto Press, Toronto, Ontario, Canada (1960) 771; CORGE, C., HUYNH, V. D., JULIEN, J., MORGENSTERN, J., NETTER, F., J. Phys. Rad. 22 (1961) 722-723; JACKSON, H. E., Phys. Rev. 134B (1964) 931.

TABLE A. SUMMARY OF Tm DATA.

E_0 = 153 eV, Γ_n^0 = 6.5 MeV

E_γ	I_γ (photons/1000 cap.)
6594	1.86 ± 0.49
6556	1.02 ± 0.48
6445	3.39 ± 0.41
6389	< 0.47
6375	< 0.44
6356	2.61 ± 0.58
6003	4.04 ± 0.70
5945	6.57 ± 0.75
5911	< 0.44
5900	< 0.64
5809	8.30 ± 0.79
5736	< 0.65
5730	3.12 ± 0.71
5684	0.85 ± 0.68
5518	1.56 ± 0.72

Considerable interest in the distribution of partial radiative widths was engendered by early results[2] on ^{238}U taken with NaI detectors. These results indicated a distribution of widths with a relative variance much smaller than possessed by the Porter-Thomas distribution. Recent data of much higher resolution are at present available, and it is of interest to re-examine ^{238}U γ-rays to see if the departure from the Porter-Thomas distribution is a real effect. Contrary to expectations, the small relative variance is confirmed by the high resolution data. Figure A shows the cumulative probability distribution for 90 partial widths (5 resonances and 18 final states) from ^{238}U. The transitions have been normalized to the same γ-ray energy, 4.059 MeV, by applying an E^3 normalization factor. Known E2 and M1 transitions have been omitted from the sample. The maximum likelihood value of ν lies between 4 and 5. A detailed Monte Carlo analysis shows that the data is inconsistent with ν = 1 or 2. Clearly the (n,γ) reaction mechanism in ^{238}U is different from ^{195}Pt, whose consistency with the Porter-Thomas distribution is well established.[3] The distribution of partial widths for several nuclides is under investigation.

[3] JACKSON, H.E., JULIEN, J., SAMOUR, C., BLOCH, A., LOPATA, C., MORGENSTERN, J., MANN, H.M., THOMAS, G.E., Phys. Rev. Lett. 17 (1966) 656.

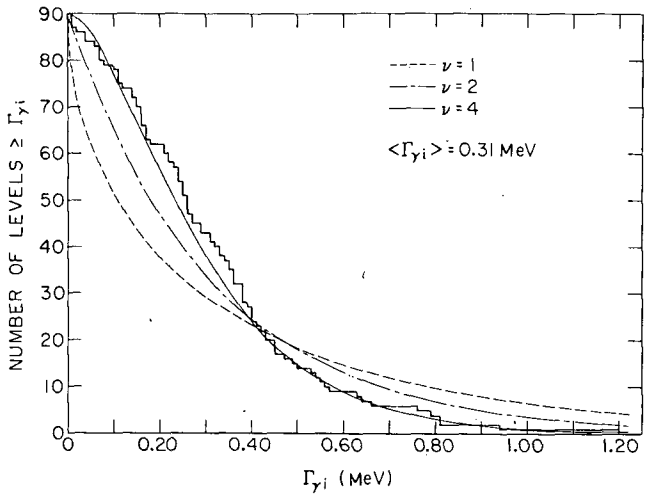

FIG. A. Cumulative probability distribution for 90 partial widths from ^{238}U.

Short Contribution

G. A. BARTHOLOMEW (Atomic Energy of Canada Ltd, Chalk River, Ontario, Canada): I should like to introduce a γ-ray effect not well covered in earlier talks in this session. This is a gross structure effect that has been known for many years in thermal neutron capture γ-ray spectra studied in the Soviet Union, Canada and elsewhere. It has been more recently studied in fast-neutron capture γ-ray spectra by Bergqvist and Starfelt in Sweden and we are currently studying the same effect using the (d, pγ) reaction at Chalk River. My colleagues in the latter work are I. Bergqvist, E. D. Earle, and A. J. Ferguson.[1]

The main features of the effect are as follows:

(1) It is observed in elements in the mass ranges $110 < A < 140$ and $180 < A < 208$. The effect is strongest in the latter region and, to conserve time, I will discuss only those elements.

(2) The gross structure is centred at ~5 MeV and appears as a bump or peak with width about 1.5 MeV. The peak remains at ~5 MeV regardless of the excitation energy E_x. In fast neutron capture, for example, the 5 MeV bump is observed for all neutron energies up to E_n = 4 MeV. In the (d, pγ) experiment we observed the γ-ray spectra in coincidence with 240 keV-wide bands of protons feeding constructive bands of levels from E_x = 0.8 MeV up to ~1.2 MeV above the neutron binding energy. Throughout the range, the gross structure bump remained at ~5 MeV.

(3) The spectrum shape cannot be reproduced with a statistical theory involving a smoothly varying level density, E_γ^3 energy dependence, and a constant, or monotonically varying, γ-ray strength function.

(4) In the particular case of the $^{199}Hg(n, \gamma)^{200}Hg$ reaction with thermal neutrons, where it has been possible to make multipolarity assignments by polarization correlations, the bump is known to be at least 85% E1 radiation.

---

[1] BARTHOLOMEW, G. A., EARLE, E. D., FERGUSON, A. J., BERGQVIST, I., Phys. Lett. 24B (1967) 47.

(5) The radiation is mostly primary, i.e. emitted first in the γ-ray cascade. This has been shown for a large number of the bump γ-rays in ^{200}Hg by coincidence measurements. One can also make an argument that the bump is primary from the intensity of the bump observed for E_x only 400 keV or so above the bump energy. If the bump were secondary it would have to be preceded by ~400 keV primary radiation in this case, which seems inconsistent with the observed normal bump intensity.

(6) The bump does not appear to be a direct-capture effect. The cross-section is, in some cases, an order of magnitude or more larger than the cross-sections for direct capture predicted by Lane and Lynn. If the γ-rays in the bump fed a special group of low-lying levels, e.g. p-states, E_γ would change with E_x, which is not observed.

Figure (i) shows the bump in the spectra of Pt and Ir as observed by Groshev and co-workers. These spectra are compared with the spectra of higher elements which contain no bumps.

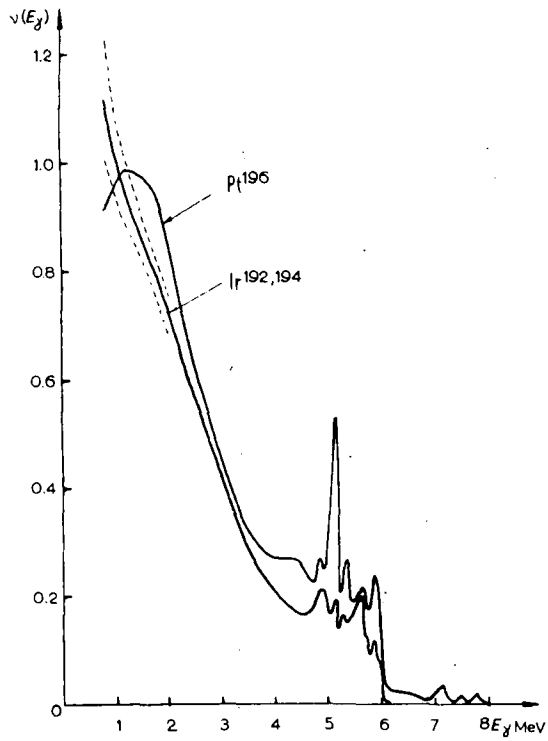

FIG.(i). Neutron capture γ-ray spectra of ^{196}Pt and ^{192,194}Ir showing gross structure bump at 5.5 MeV. From GROSHEV, L.V., et al., Nucl. Phys. 16 (1960) 645.

Figure (ii) contains thermal neutron capture γ-ray spectra from the $180 < A < 208$ region smoothed to remove all but the major gross structure features. This figure shows clearly how the bump diminishes as one proceeds away from the closed shell.

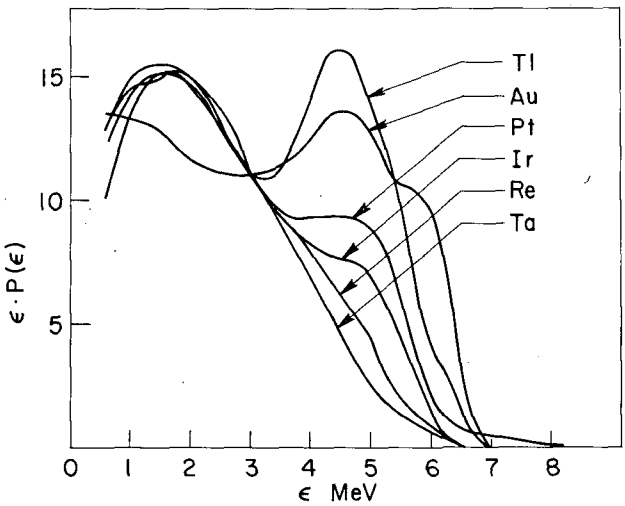

FIG. (ii). Gross spectral distributions from a NaI detector of gamma rays from the (n, γ) reaction with thermal neutrons. The ordinates, in units of counts per channel times channel energy, are normalized at 3 MeV.

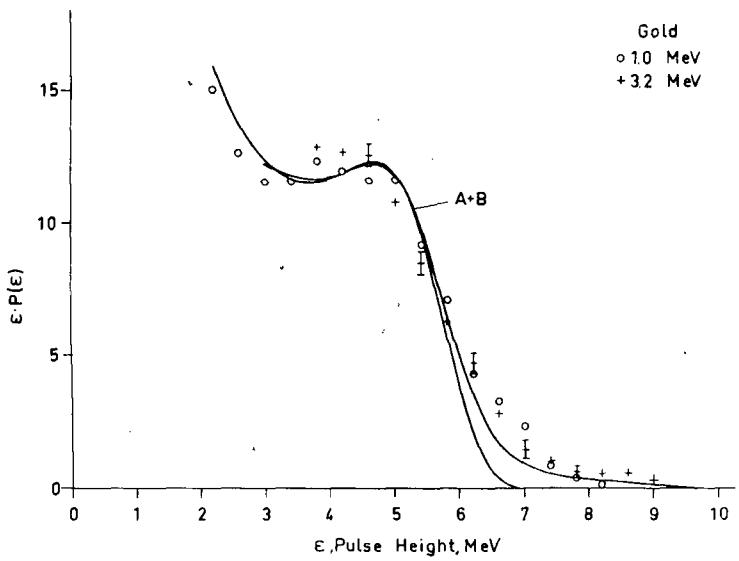

FIG. (iii). As in Fig. (ii) but for fast neutron capture in Au at neutron energies shown. From LUNDBERG, B., STARFELT, N., Nucl. Phys. 67 (1965) 321.

Figure (iii) shows the γ-ray spectrum following fast-neutron capture in gold as observed with a NaI detector by Bergqvist and Starfelt. The bump is clearly evident at the same energy for E_n = 1.0 and 3.2 MeV.

Figure (iv) contains spectra from our recent (d, pγ) results smoothed to remove all but the gross structure features. The spectra were obtained

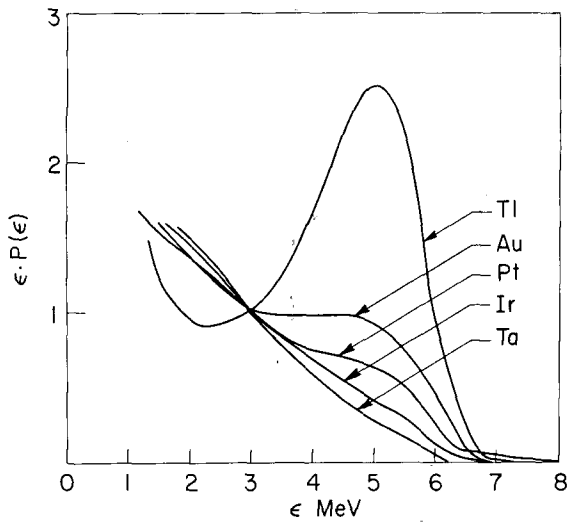

FIG. (iv). Gamma rays from the (d, pγ) reaction at excitation energy equal to the neutron binding in the product nucleus. Ordinates as in Fig. (ii).

at an excitation energy near the neutron binding energy. Similar curves were obtained at other excitation energies.

As a possible explanation, we suggest that the incoming neutron excites a neutron particle-hole configuration of the type $f^{-1}g$, $p^{-1}d$, $p^{-1}s$, etc. The subsequent E1 decay then competes with other processes open to this "doorway state". At higher excitations the particle-hole may be coupled to other particle excitations forming, for example, two particle-two hole configurations in the product nucleus, or it might be coupled to a collective excitation. The spacing between shells of opposite parity differing by 1 unit is just about 5 MeV near Pb. One could also have spin-flip M1 neutron transitions, $i_{13/2}$ to $i_{11/2}$, for which the splitting is also about 5 MeV, and also proton particle-hole excitations.

This picture requires that some of the E1 strength remain at 5 MeV and is not pushed up into the giant dipole resonance. In ^{197}Au (n, γ)^{198}Au the spectrum shape can be accounted for by assuming a strength function with a 'resonance' at 5 MeV with 2% of the giant dipole strength (as shown by Starfelt[2]). From the successive spectra of our (d, pγ) experiment in Au one can deduce, assuming a certain level distribution, a strength function with a 5 MeV resonance similar to that obtained by trial-and-error fitting by Starfelt.

We have tried recently to excite individual levels giving rise to the bump in ^{206}Pb (d, pγ)^{207}Pb but low intensity in the experiment has so far defeated these attempts.

[2] STARFELT, N., Nucl. Phys., 53 (1964) 397.

DENSITIES OF NUCLEAR LEVELS AND STRENGTH FUNCTIONS AT EXCITATION NEAR THE NEUTRON BINDING ENERGY

L.B. PIKELNER
JOINT INSTITUTE FOR NUCLEAR RESEARCH,
DUBNA, UNION OF SOVIET SOCIALIST REPUBLICS

Abstract — Аннотация

DENSITIES OF NUCLEAR LEVELS AND STRENGTH FUNCTIONS AT EXCITATION NEAR THE NEUTRON BINDING ENERGY. A review is given of some recent work on neutron spectroscopy of non-fissionable nuclei, performed on the pulsed reactor, Dubna.

Neutron transmission and radiative capture were measured for separated isotopes of rare earths – neodymium, gadolinium and erbium – and for isotopes of germanium and selenium. Parameters of the considerable number of levels of these isotopes were obtained, by which strength functions, average level spacings, and single-particle state density near the Fermi energy were calculated.

Strength functions of rare earths have a weak maximum at $A \simeq 160$, in addition to two main peaks at $A \simeq 145$ and $A \simeq 180$ associated with nuclear deformation in this mass number region. Strength functions of germanium and selenium isotopes are in satisfactory agreement with the calculations from the optical model, which take into account nuclear dynamic deformation.

The detailed experimental data on nuclear level density in the rare earth region made it possible to determine reliably a peak of the density g of single-particle states near the Fermi level at $A \simeq 150$. As was shown by the calculations of Furman and Popov, the experimental results are in satisfactory agreement with theoretical $g_{shell}(N)$ calculated from single-particle level schemes in the deformed well.

Level spacings versus neutron excess in a nucleus (N - Z) in the region of light nuclei are discussed and comparison is made with the experimental data.

ПЛОТНОСТИ УРОВНЕЙ И СИЛОВЫЕ ФУНКЦИИ ЯДЕР ВБЛИЗИ ЭНЕРГИИ СВЯЗИ НЕЙТРОНА. Дается обзор работ по нейтронной спектроскопии неделящихся ядер, выполненных в последнее время на импульсном реакторе ОИЯИ. Измерения пропускания и радиационного захвата нейтронов были проведены для разделенных изотопов редкоземельных элементов неодима, гадолиния и эрбия, а также для изотопов германия и селена. Получены параметры значительного числа уровней этих изотопов, по которым рассчитаны силовые функции, средние расстояния между уровнями, плотность одночастичных состояний вблизи энергии Ферми. Силовые функции редкоземельных элементов имеют слабо выраженный максимум при $A \simeq 160$, помимо двух основных пиков при $A \simeq 145$ и $A \simeq 180$, связанных с деформацией ядер в этой области массовых чисел. Силовые функции изотопов германия и селена удовлетворительно согласуются с расчетами по оптической модели, в которых учитывается динамическая деформация ядер. Подробные экспериментальные данные о плотности уровней ядер в области редкоземельных элементов поволили надежно проследить пик плотности g одночастичных состояний вблизи поверхности Ферми при $A \simeq 150$. Как показали расчеты Попова и Фурмана, экспериментальные результаты удовлетворительно согласуются с теоретически полученной $g_{обол}(N)$, вычисленной из схем одночастичных уровней в деформированной яме. Обсуждается зависимость плотности уровней от избытка нейтронов в ядре (N – Z) в области легких ядер и проводится сравнение с экспериментальными данными.

INTRODUCTION

Neutron spectroscopy is one of the oldest branches of nuclear studies; however, the subject is far from being exhausted and intensive development work is continuing. This development is on the following lines: improving spectrometer energy resolution, refining detection apparatus, and using enriched isotopes as samples.

Nuclear information obtained by neutron spectroscopy methods comprises such data as strength functions (primarily for S-wave neutrons), level density and average radiation width. The high resolution of the present-day spectrometers permits parameters to be obtained of up to hundreds of levels for an individual isotope. Hence, the detailed investigation of distributions of widths and level spacings becomes possible.

In this paper I review some recent work on the neutron spectroscopy of non-fissionable nuclei, performed in the Laboratory of Neutron Physics at JINR.

The microtron, which provided a short burst of bremsstrahlung, made it possible to improve the neutron spectrometer resolution considerably [1]. At present, the spectrometer has the following characteristics: electron pulse duration: 1.5-2 μs; neutron multiplying constant for the reactor: 200; integral neutron output: $(3\text{-}4) \times 10^{13}$ neutrons/s, neutron pulse half-width: 3 μs. Work was recently carried out at a resolution of up to 3 ns/m for transmission and 12 ns/m for radiative capture.

A liquid methyl borate scintillation detector with an area of 800 cm^2 analogous to that described earlier [2] was used. Radiative capture was measured by a liquid scintillation detector, which consisted of two tanks with a total volume of about 500 litres [3].

The Laboratory Measuring Centre comprises 4096-channel time analysers, used in the measurements. The data from the analysers were conveyed to a computer for subsequent treatment.

For the transmission data processing we applied the area method, and in a number of cases the form method was used [4].

For the radiative capture data processing the following relation was used [5]:

$$C = \frac{\sum_i N_i}{\Pi(E)\epsilon_\gamma} = \frac{\Gamma_\gamma}{\Gamma} A \qquad (1)$$

where $\sum_i N_i$ is the sum of counts under a resonance, $\Pi(E)$ the number of neutrons impinging on the total sample area during the measurement, ϵ_γ the detection efficiency for a radiative capture event, Γ_γ, Γ the radiation and total level widths, and $A = \int [1 - \exp(-n\sigma_t)]\, dE$ a function of the sample thickness and level parameters, having the meaning of the area of the dip in the transmission curve.

Expression (1) allows Γ_γ and Γ_n to be deduced from the experimental value of C according to the relation between them. It may be illustrated most clearly for the case of a thin sample. It may then be written in the form

$$C = \frac{\Gamma_\gamma}{\Gamma} 2\pi^2 \lambda^2 n g \Gamma_n \qquad (2)$$

where λ is the neutron wave length at the resonance energy and g the statistical factor.

As is easily seen, for $\Gamma_n \gg \Gamma_\gamma$, C is determined by the product $g\Gamma_\gamma$, and for $\Gamma_n \ll \Gamma_\gamma$, C depends only on $g\Gamma_n$. In the intermediate case, C is a function of both widths. These properties vary slightly for the more general expression (1). Thus, the radiative capture measurements per-

mit Γ_γ to be obtained for resonances with a large neutron width, Γ_n for $\Gamma_n \ll \Gamma_\gamma$ and in the intermediate case they complement considerably the data obtained in transmission measurements. In a number of cases level spins can be determined.

Neutron cross-section measurements were performed recently in JINR for two groups of nuclei: rare earths and nuclei of mass number A = 70 to A = 80. In all the cases, enriched isotopes were used as samples.

Rare earths with even Z have a large number of isotopes in natural mixture and their investigation is impossible until separated isotopes are available. The data on these nuclei were very scarce. Only quite recently the results of measurements by the Brookhaven [6] and Kiev [7] groups were reported, but they were obtained with worse resolution than in JINR.

The data on germanium and selenium isotopes were also rather modest. They consist primarily in the results of Good et al. [8] and also the data of the Saclay [9] and Argonne [10] groups for selenium in a rather narrow energy range.

The main results obtained in JINR are discussed below.

RARE EARTHS

The first measurements of rare-earth cross-sections were performed on the pulsed reactor with praseodymium, terbium and ytterbium as the nuclei investigated [11, 12]. Holmium [4] and erbium, neodymium and gadolinium isotopes [13, 14, 15] were investigated after the reconstruction of the spectrometer and the transition to work under microtron-reactor conditions. Transmission and radiative capture measurements were made for all of them. As a result, the parameters of a considerable number of levels were obtained for the investigated isotopes, from which the averaged characteristics summarized in Table I were then calculated. Here the energy region indicated the neutron energy range, which contains the investigated levels, D_{obs} is the observed average level spacing, S_0 the strength function for S-neutrons, $\bar{\Gamma}_\gamma$ the average radiation width and a the single-particle state density parameter near the Fermi level.

A comparison of the data from Table I with recent results [6, 7] points to satisfactory agreement between them.

Better resolution of the JINR spectrometer made it possible to measure resonance parameters in a wider neutron energy region. This, in particular, permitted an explanation of the discrepancy in values of S_0, deduced from the resonance parameters and averaged cross-sections for ^{167}Er given in Ref. [6]. The higher value of S_0 found by the resonance parameters is due to some strong levels, primarily the strong 26 eV level, which appreciably affect the strength function taken in a small energy range.

Figure 1 presents the experimental data on the strength functions for S-neutrons in the rare-earth region. The maximum at A ≃ 145 is evident. The second peak at A ≃ 180 is less distinct. In addition, at A ≃ 165 a weak local maximum is observed, which was noticed in Ref. [13].

The splitting of the peak of the strength function in the rare-earth region due to nuclear deformation was calculated from the optical model in Refs [16, 17]. More recent calculations by Jain [28], the results of which are presented as a curve in Fig. 1, fit well the experimental data in the region of maxima. However, near A ≃ 160 the curve is markedly below the experi-

TABLE I. AVERAGE PARAMETERS OF RARE-EARTH NUCLEI

Target nucleus	Energy region (keV)	D_{obs} (eV)	$S_0(10^{-4})$	$\bar{\Gamma}_\gamma$ (meV)	a (MeV^{-1})
^{142}Nd	0 - 10	1000 ± 250	$1.0^{+1.2}_{-0.5}$	-	18.5 ± 0.5
^{143}Nd	0 - 1	39 ± 6	4.3 ± 1.4	76 ± 11	17.7 ± 0.3
^{144}Nd	0 - 14	520 ± 70	$4.5^{+3.1}_{-1.8}$	78 ± 12	19.4 ± 0.4
^{145}Nd	0 - 1	19 ± 3	3 ± 0.7	58 ± 8	20.3 ± 0.4
^{146}Nd	0 - 7	310 ± 43	$4.6^{+3.2}_{-1.6}$	55 ± 8	24.4 ± 0.5
^{148}Nd	0 - 9	200 ± 21	$3.5^{+1.7}_{-1.1}$	96 ± 14	26.9 ± 0.5
^{150}Nd	0 - 4	230 ± 28	$1.8^{+1.1}_{-0.6}$	84 ± 12	27.4 ± 0.5
^{152}Gd	0 - 0.23	15 ± 2	$4.0^{+2.6}_{-1.5}$	57 ± 15	25.3 ± 0.4
^{154}Gd	0 - 0.23	15.5 ± 2.3	$2.1^{+1.5}_{-0.7}$	63 ± 15	25.2 ± 0.4
^{155}Gd	0 - 0.18	1.8 ± 0.3	2.10 ± 0.35	100 ± 10	22.6 ± 0.4
^{156}Gd	0 - 1.2	47 ± 4	$1.6^{+0.8}_{-0.5}$	82 ± 12	22.8 ± 0.3
^{157}Gd	0 - 0.3	5.6 ± 0.7	2.16 ± 0.45	86 ± 10	21.6 ± 0.3
^{158}Gd	0 - 2	85 ± 9	$1.4^{+0.7}_{-0.4}$	89 ± 13	22.2 ± 0.4
^{160}Gd	0 - 2.5	170 ± 21	$2.7^{+1.7}_{-0.9}$	98 ± 15	22.1 ± 0.4
^{165}Ho	0 - 0.5	5.5 ± 0.5	1.9 ± 0.3	73 ± 3	20.8 ± 0.2
^{164}Er	0 - 0.6	23 ± 4	$1.2^{+0.9}_{-0.4}$	-	22.4 ± 0.4

TABLE I (cont.)

Target nucleus	Energy region (keV)	D_{obs} (eV)	$S_0(10^{-4})$	$\bar{\Gamma}_\gamma$ (meV)	a (MeV^{-1})
^{166}Er	0 - 1.4	52 ± 7	$1.8^{+0.9}_{-0.4}$	87 ± 13	21.1 ± 0.4
^{167}Er	0 - 0.32	4.6 ± 0.7	1.8 ± 0.4	92 ± 3	20.0 ± 0.4
^{168}Er	0 - 1.5	110 ± 16	$1.6^{+1.0}_{-0.5}$	81 ± 10	21.2 ± 0.4
^{170}Er	0 - 3	170 ± 24	$1.3^{+0.8}_{-0.5}$	-	21.3 ± 0.4

mental points. Elagin et al. [18] noticed that taking into account the spin-orbital interaction for the nuclei with static deformation results in additional splitting of the strength function and the appearance of a weak maximum in the region A ≈ 160. If this brings about an appreciable increase of the strength function, the theoretical curve will fit the strength function in the rare-earth region well enough (within experimental accuracy). It should

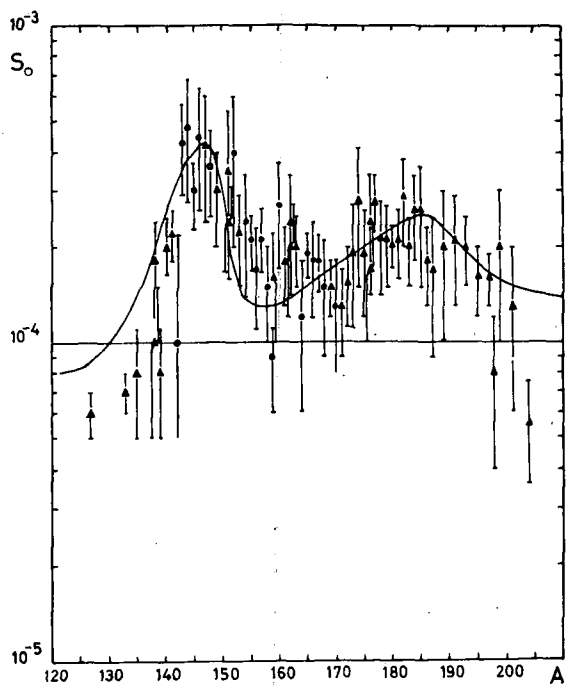

FIG.1. The strength function S_0 for S-neutrons in the region 130 < A < 200. ‡ - the data of JINR, ‡ - the data of others. The curve has been calculated from the optical model (rotational model with surface absorption) by Jain [28].

be noted here that the accuracy of the experimental value of S_0 calculated by individual levels is estimated in different ways by different authors. In our opinion, the most rigorous approach is given in Refs [19, 20]. Though the frequently used expression $\Delta S_0/S_0 = (2.5/n)^{1/2}$, where n is the number of levels used to obtain the strength function, takes into account neutron width and level spacing distributions, it does not fit the case of a small number of levels ($n < 10$) and gives an appreciable underestimation of the error. Therefore it is desirable that the methods presented in Refs [19, 20] be used in the experimental data processing.

Let us consider the nuclear level density at excitation of the order of the neutron binding energy. This is usually described in the framework of the Fermi gas model by the Bethe formula:

$$\rho(U, J) = \frac{2J + 1}{24\sqrt{2}\, a^{1/4} U^{5/4} \sigma^3} \exp\left[2\sqrt{aU} - \frac{J(J+1)}{2\sigma^2}\right] \qquad (3)$$

where U is the excitation energy corrected for the nucleon pairing effect and a the single-particle state density parameter near the Fermi level.

A spin cut-off factor σ is determined by the relationship

$$\sigma^2 = \frac{6}{\pi^2} \langle m_j^2 \rangle (aU)^{1/2} \qquad (4)$$

where $\langle m_j^2 \rangle$ is the average square of the projection of the total angular momentum for the states around the Fermi level. $\langle m_j^2 \rangle = KA^{2/3}$ is a satisfactory approximation for it. The value of the constant K is usually taken as 0.146 [21], however in Ref. [22] it is indicated that the value 0.24 is more exact. Neutron cross-section measurements permit the level density to be obtained for a large number of nuclei and the parameter a to be calculated using expressions (3) and (4). Figure 2 gives the experimental values of a calculated in this way. The data obtained in JINR [4, 13-15] are marked with crosses, the rest is borrowed from the tables in Ref. [22]. In Fig. 2, in addition to the known structure associated with magic nuclei,

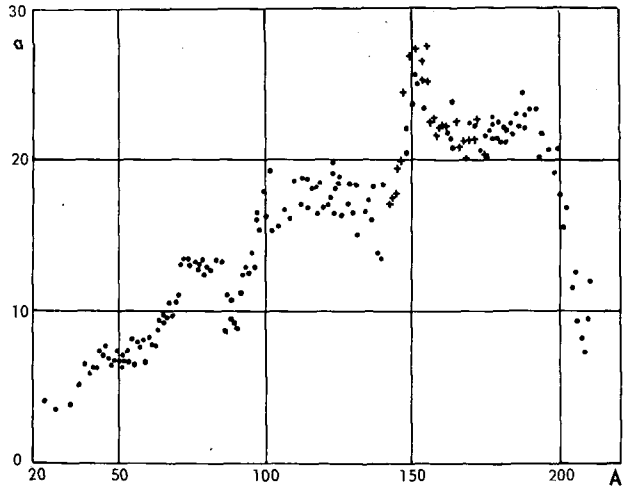

FIG. 2. The experimental data on the parameter a. + the data of JINR, • the data from Ref. [22].

attention is attracted to the peak at A ≃ 150. A satisfactory interpretation of a versus A was first given by Newton [23], assuming that

$$a = 2\alpha (\bar{j}_Z + \bar{j}_N + 1)\, A^{2/3} \qquad (5)$$

$\bar{j}_Z$ and $\bar{j}_N$ being the averages of proton and neutron momenta for the states near the Fermi level, and α = const.

As a result of calculating $\bar{j}_Z$ and $\bar{j}_N$ the values of a were obtained, which reproduced a regular course of a and the presence of minima for magic nuclei.

In Ref. [22] the experimental dependence of a on the neutron number N was compared with the value $a_{shell}(N) = (\pi^2/6)\, g_{shell}(N)$ calculated by Strutinsky [24] (g_{shell} is the shell level density near the Fermi level).

In the range N = 20 to 150 there is a general correlation between theory and experiment. However, a peak around N ≃ 90, determined definitely in

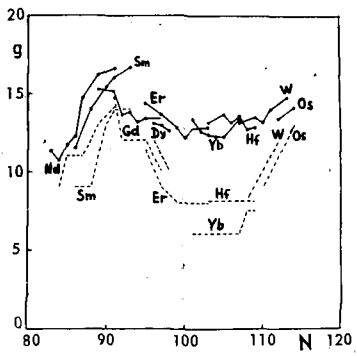

FIG. 3. The density g of single-particle states near the Fermi level as a function of the neutron number N. The solid lines connect the experimental points for isotope groups of an element. The dashed lines represent the theoretical values of g_{shell} for isotope groups.

JINR investigations [14, 15], is not discussed in Ref. [22]. The influence of the nuclear shell structure on the level density for isotope groups in the indicated mass number region was considered by Furman and Popov [30]. In Fig. 3 the values of $g_{shell}(N)$ for the isotope groups are represented by dashed lines, calculated from the single-particle level schemes in the deformed hole with diffused edge, obtained in JINR [29]. The solid line corresponds to the values of g_{exp} for the isotope groups. As can be seen, g_{shell} reproduces satisfactorily the behaviour of g_{exp}, in particular the presence and position of the peak at N = 90, though the quantitative disagreement is considerable. As is seen from Fig. 3, the experimental points are always above the calculated ones. It may be said roughly that a rise of g(N) in the intermediate region A ≲ 155 is determined by the increase of g_{shell} due to the mixing of subshells at small deformations ($\beta \simeq A^{-2/3}$). A drop of g_{shell} and its further trend are determined by the transition to greater deformations ($\beta \simeq A^{-1/3}$) resulting in rarefications in the level schemes for the middle of the neutron shell.

As to the σ in formula (3) it should be noted that if one uses expression (4), the values obtained for σ for the rare-earth nuclei are about 7. This disagrees very much with the experimental values obtained in Refs [6, 12],

where σ was close to 2.8. The reason for such a discrepancy is not clear. It may be due to the fact that σ may be derived from the experiment only under some assumptions about a. In particular, in Refs [6, 12] the values of a were assumed to be the same for the investigated nuclei in order to find the parameter σ from Eq.(3) by leaving it only in the exponent, and in the term before the exponent replacing it according to Eq.(4). In so doing, it should be borne in mind that in the exponent $2\sqrt{aU} \gg J(J+1)/2\sigma^2$, so that a decrease of a or U by 10% compensates for the increase of σ from 3 to infinity.

GERMANIUM AND SELENIUM

The results of investigating all stable isotopes of germanium and selenium are given in Refs [25, 26]. Transmission and radiative capture measurements permitted parameters to be obtained for about 200 levels for all the isotopes, on which Table II was based, giving the average parameters of the investigated isotopes. The symbols here are the same as in Table I.

TABLE II. AVERAGE PARAMETERS OF GERMANIUM AND SELENIUM NUCLEI

Target nucleus	Energy region (keV)	D_{obs} (eV)	$S_0(10^{-4})$	$\bar{\Gamma}_\gamma$ (meV)	a (MeV^{-1})
^{70}Ge	0 - 30	1330 ± 210	$2.3^{+1.0}_{-0.9}$	162 ± 25	11.9 ± 0.3
^{72}Ge	0 - 30	1550 ± 270	$1.0^{+0.6}_{-0.4}$	160 ± 25	13.4 ± 0.4
^{73}Ge	0 - 9	62 ± 7	$2.0^{+0.7}_{-0.6}$	197 ± 29	13.2 ± 0.3
^{74}Ge	0 - 30	3900 ± 770	$1.3^{+1.1}_{-0.6}$	195 ± 40	13.0 ± 0.6
^{76}Ge	0 - 30	4200 ± 835	$2.3^{+2.1}_{-1.0}$	120 ± 25	14.2 ± 0.7
^{74}Se	0 - 7	370 ± 70	$2.6^{+3}_{-0.9}$	290 ± 50	14.1 ± 0.5
^{76}Se	0 - 13	700 ± 150	$1.7^{+1.1}_{-0.5}$	230 ± 40	14.3 ± 0.4
^{77}Se	0 - 4	120 ± 20	J = 0 $1.4^{+1.6}_{-0.5}$ J = 1 $1.1^{+0.6}_{-0.3}$	390 ± 70	14.1 ± 0.3
^{78}Se	0 - 20	1000 ± 270	$1.9^{+1.3}_{-0.5}$	220 ± 45	14.0 ± 0.5
^{80}Se	0 - 23	1200 ± 380	$2.0^{+2}_{-0.7}$	220 ± 50	14.7 ± 0.7

The values of the strength function for all the germanium and selenium isotopes do not differ very much, as is seen from Fig. 4, and give satisfactory agreement with the theoretical curve obtained by Buck and Perey from the optical model taking nuclear dynamic deformation into account [27]. Attention should be drawn to the values of the strength function of ^{77}Se for different spins J. In Ref. [9], where the level parameters in the energy range up to 1.5 keV were measured, it was concluded that the strength function of ^{77}Se for J = 0 is 7 times as large as S_0 for J = 1. In Ref. [26] the energy range over which the strength function was calculated was widened to 4 keV, the values of J being obtained for all the strong levels from the measurements of the radiative capture cross-section. In so doing, the radiation widths were assumed to be the same for the levels of both spins; this was in agreement with the spin values obtained in Refs [9, 10]. As a result, the values of S_0 were found for both spins; and the difference between them did not exceed the error. Thus the difference between S_0 (observed in Ref. [9]) for two spin states was not confirmed, but was a result of fluctuation in neutron width distributions due to the small number of investigated levels. During radiative capture measurements a large number of levels was discovered, the neutron widths of which accounted for 10^{-2} to 10^{-3} of the average width for a given isotope. The estimations showed that this agrees with the expected widths of P-wave resonances in this region. In this connection such resonances were not taken into account in the calculations of S_0 and D_{obs} given in Table II. For the isotopes with odd A, D_{obs} was determined for the mixture of two spin states.

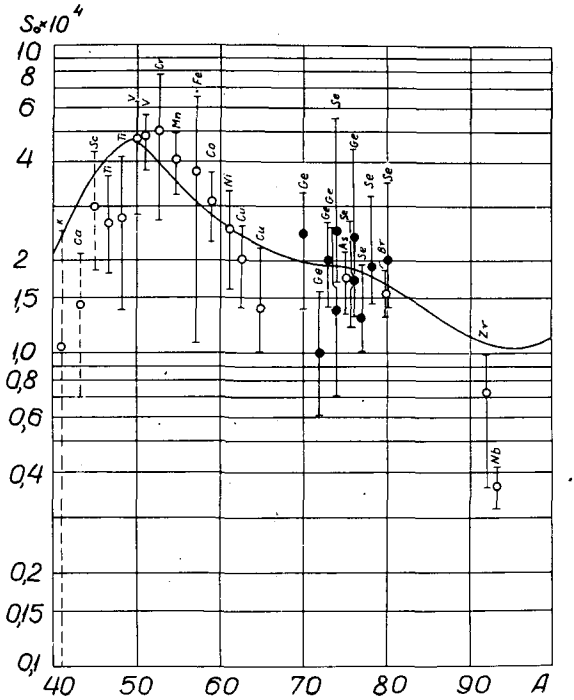

FIG. 4. The strength function S_0 for S-neutrons in the region $40 < A < 90$. ▮ - the data of JINR, ▯ - the data of other authors. The curve is the calculation from the optical model, taking nuclear dynamic deformation into account, by Buck and Perey [27].

The found average level spacings permitted the values of the parameter a to be determined from expressions (3) and (4). In the region of mass numbers from 70 to 80 the behaviour of a versus A has a smooth character.

It seems of interest to consider one more dependence of the parameter a, which was indicated by Malishev et al. [31]. They found that a depends on the difference N-Z and this dependence may be expressed by the semi-empiric formula for the coefficient α entering Eq. (5):

$$\alpha = \alpha_0 - \beta \sin\left\{\frac{\pi}{20}\,\frac{A}{1+\frac{\gamma(A-A_0)}{2}}\right\} \cos\left\{\frac{\pi}{20}\,\frac{\left(1-\frac{\gamma A_0}{2}\right)(N-Z)}{\left[1+\frac{\gamma(A-A_0)}{2}\right]^2}\right\} \quad (6)$$

Here $\alpha_0 = 0.0380$, $\beta = 0.0125$, $\gamma = \begin{cases} 0 \text{ at } A < 80 \\ 6.7 \times 10^{-3} \text{ at } A \geq 80, \end{cases}$ $A_0 = 80$. This dependence results in the modulation of the parameter a so that in the region $A < 60$ the points representing the behaviour of $a/A^{2/3}$ versus A are higher with greater values of N-Z and in the region $80 > A > 60$ the effect changes its sign.

Figure 5 gives the experimental points for the region with A between 40 and 80. The spread of the points is too great to speak of an explicit dependence, although a tendency to the above-mentioned distribution of points may be observed.

In conclusion, it may be noted that although the experimental data on strength functions are, in general, fitted satisfactorily by the optical model theory, further progress is required both in experiment and in theory. In experimental investigations it is essential not only to increase the accuracy, but also to obtain the values of the strength functions in a wider energy range. This is of interest from the viewpoint of the doorway state concept, and also to clarify the question as to whether the strong fluctuations in strength functions, observed for a number of nuclei (^{53}Cr [32], ^{76}Ge [25] and some

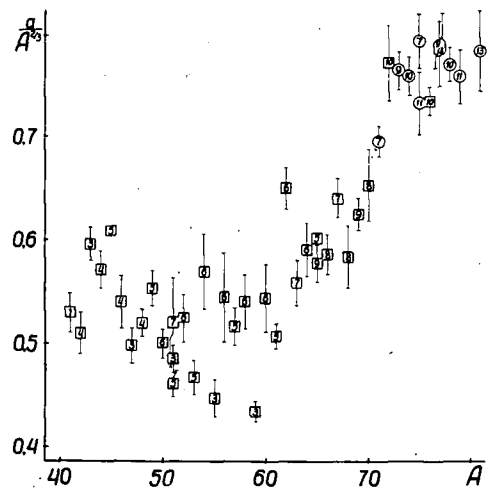

FIG. 5. The experimental values of $a/A^{2/3}$ in the region $40 < A < 80$. ✦ is the data of JINR, ✦ is the data of others. The numerals are the values of N-Z for a compound nucleus.

others), are accidental. In addition, the problem of the spin dependence of strength functions is not quite clear.

The optical model does not fit sufficiently well the experimental data in the region of mass numbers from 100 to 120 and from 155 to 170.

As regards level density, recent theoretical papers have satisfactorily reproduced the main peculiarities of a versus A obtained in experiment, although quantitative agreement is not yet sufficient.

The quantity σ remains to be studied both theoretically and experimentally.

REFERENCES

[1] PIKELNER, L.B., RUDENKO, V.T., in Research Applications of Nuclear Pulsed Systems (Proc. Panel Dubna, 1966), IAEA, Vienna (1967) 165.

[2] VIZI, I., ZHUKOV, G.P., ZABIYAKIN, G.I. et al., in Nuclear Electronics (Proc. Conf. Belgrade 1961) 1, IAEA, Vienna (1962) 27.

[3] PIKELNER, L.B., PSHITULA, M.I., KIM HI SAN, CHEN LIN-YAN, SHARAPOV, E.I., Pribory Tekh. Eksp., No.2, (1963) 48.

[4] KARZHAVINA, E.N., POPOV, A.B., YAZVITSKI, Yu.S., EFIMOV, B.H., SHIRIKOVA, N.Yu., Yadernaya Fiz. 5 (1967) 471.

[5] ZELIGER, D., ILIESKU, N., KIM HI SAN et al., Zh. eksp. teor. Fiz. 45 (1963) 1294.

[6] MUGHABGHAB, S.F., CHRIEN, R.E., BHAT, M.R., Phys. Rev. 162 (1967) 1130; CHRIEN, R.E., MUGHABGHAB, S.F., BHAT, M.R., JAIN, A.R., Preprint BNL 11327.

[7] VERTEBNI, V.P., GNIDAK, N.L. et al., Ukr. fiz. Zh. 13 (1968) 679.

[8] GOOD, W.M., NISHIMURA, K., MÜNZER, H., in BNL-325 (2nd Edn).

[9] JULEN, J., CORGE, C. et al., Phys. Lett. 3 (1962) 67.

[10] COTE, R.E., BOLLINGER, L.M., THOMAS, G.E., Phys. Rev. 136 (1964) B703.

[11] VAN NAI-YAN, ILIESKU, N., KARZHAVINA, E.N. et al., Zh.eksp. teor. Fiz. 47 (1964) 43.

[12] VAN NAI-YAN, KARZHAVINA, E.N., POPOV, A.B., YAZVITSKI, Yu.S., YAO CHI-CHUAN, Yadernaya Fiz. 3 (1966) 48.

[13] KARZHAVINA, E.N., POPOV, A.B., YAZVITSKI, Yu.S., Yadernaya Fiz. 7 (1968) 225.

[14] KARZHAVINA, E.N., NGUEN NGUEN FONG, POPOV, A.B., TASKAEV, A.I., Preprint JINR P3-3564 (1967).

[15] KARZHAVINA, E.N., NGUEN NGUEN FONG, POPOV, A.B., Preprint JINR P3-3882, Dubna (1968).

[16] MARGOLIS, B., TROUBETZKOY, E., Phys. Rev. 106 (1957) 105.

[17] CHASE, D.M., WILETS, L., EDMONS, A.R., Phys. Rev. 110 (1958) 1080.

[18] ELAGIN, Yu., LYULKA, L., NEMIROVSKI, P., Zh. eksp. teor. Fiz. 41 (1961) 959.

[19] MURADYAN, H.W., ADAMCHUK, Yu.V., Nuclear Structure Study with Neutrons, North Holland Publ. Co., Amsterdam (1966) 569.

[20] SLAVINSKAS, D., KENNETT, T., Nucl. Phys. 85 (1966) 641.

[21] MALISHEV, A.V., Zh. eksp. teor. Fiz. 45 (1963) 316.

[22] FACCHINI, U., SAETTA-MINICHELLA, E., Energia Nucleare 15 (1968) 54.

[23] NEWTON, T.D., Can. J. Phys. 34 (1956) 804.

[24] STRUTINSKY, V.M., Nucl. Phys. A95 (1967) 420.

[25] MAŁECKI, H., PIKELNER, L.B., SALAMATIN, I.M., SHARAPOV, E.I., Atomn. Energ. 24 (1968) 173.

[26] MAŁECKI, H., PIKELNER, L.B., SALAMATIN, I.M., SHARAPOV, E.I., Contribution No.125 to this symposium.

[27] BUCK, B., PEREY, F., Phys. Rev. Lett. 8 (1962) 444.

[28] JAIN, A.P., Nucl. Phys. 50 (1964) 157.

[29] GAREEV, A.F., KALINKIN, B.N., IVANOVA, S.P. et al., Preprint JINR, P4-3607, Dubna (1967).

[30] FURMAN, V.I., POPOV, A.B., Preprint JINR P4-3925.

[31] SHUBIN, Yu.N., MALISHEV, A.V., STAVINSKI, V.S., Contr. CN-23/106, Paris Congress on Nuclear Data (1966).

[32] GOOD, W.M. et al., Phys. Rev. 151 (1966) 912.

DISCUSSION

R. L. HAHN: Several papers have appeared in the literature over the last few years in which the experimental variation of the level density parameter 'a' (ρ (U) $\sim \exp\sqrt{aU}$) with mass number A has been analysed. The results in general have shown that 'a' varies in a linear way with A, as is expected for the degenerate Fermi gas. Could you discuss this conclusion since you take 'a' to be proportional to $A^{2/3}$ in your analysis?

L. B. PIKELNER: In the evaluation of the parameter 'a' from the experimental data we did not use its dependence on A. As far as comparison with theory is concerned, it seems to me that the proportionality of a to $A^{2/3}$, which has been taken in the work of Newton and some more recent work, does not need to be changed on the basis of experimental data.

P. DECOWSKI: I should like to make a remark about the σ^2 value. It is known that the pairing correlations play a very important role which can be seen in the decrease of the σ parameter in the excitation energy range lower than critical energy, i. e. $\sim$15 MeV for medium and heavy nuclei. This fact can explain the disagreement between experimental σ^2 values and those predicted on the basis of the Fermi gas model.

A. V. IGNATYUK: For experimental data processing by the excited state density in order to pass to the level density parameter 'a' it is necessary to introduce the effective excitation energy $U_{eff} = U - \delta$. Theoretical calculations of the condensation energy, taking into account pairing correlations, give a value which in the majority of cases greatly exceeds the experimental value of δ. When U_{eff} is taken into account more accurately, this greatly affects the values of the parameter 'a', and the dependence a(U) obtained from the calculations for low excitation energies may appear to be considerable due to the decrease of U_{eff} to several MeV in the case of neutron resonances. Therefore, the direct study of the level spacing $\overline{D}$ seems to be more to the purpose at present than the study of 'a'.

M. V. PASECHNIK: My comment is on the level density in close binding energy excitations. The data on the level density obtained in neutron transmission experiments provide valuable information about the properties of single-particle levels (degree of degeneracy, level spacing, population, etc.). It was interesting to study the variation of level density at the same excitation energy for a large number of isotopes, particularly for slightly distributed isotopes for which data were not available.

In our laboratory data have been obtained on $^{152, 154}$Cd, $^{156, 158, 160}$Dy, $^{162, 164, 166-168}$Er and $^{130, 132}$Ba levels in the energy region of 0-100 eV with a resolution of 50 ns/m. Using our data and that published in the literature from Dubna, the Kurchatov Institute and other laboratories, we calculated the level spacing ($D_{red.}$) referring to the same excitation energy (U = 6 MeV). Figure A shows the dependence of $D_{red.}$ on the neutron number. It has been established that:

(1) $D_{red.}$ increases in the vicinity of the neutron number to magic numbers.

(2) The minima of $D_{red.}$ are at neutron numbers N $\sim$ 90 and N $\sim$ 115.

(3) There is considerable disagreement between the calculated and experimental data for ^{130}Ba (20 and 140 eV).

It seems to us that the isotopic dependence of $D_{red.}$ is more significant for the structure effects than the constant a, especially in the report. We are continuing to work on the isotopic dependence of $D_{red.}$.

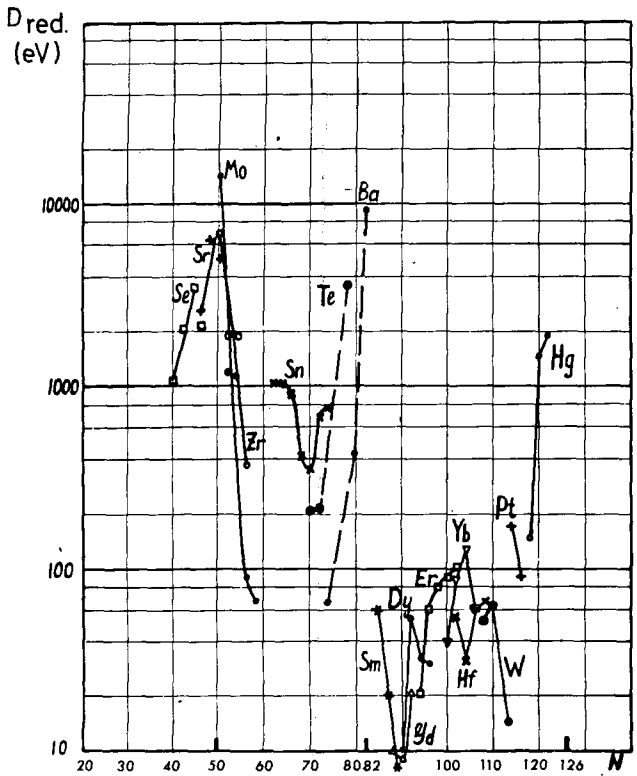

FIG. A. Isotopic dependence of reduced level spacings.

Short Contribution

C. SAMOUR (Centre d' études nucléaires de Saclay, France): The improvements made in experimental apparatus at Saclay have allowed detailed examination of resonance neutron capture gamma-ray spectra. Time-of-flight experiments were performed at the 2 kW Saclay Linac with two flight paths: 29 m (for which the resolution was 30 ns/m at 100 eV and 10 ns/m at 700 eV); and 15 m (60 ns/m at 100 eV). The gamma-rays were detected in an 8 cm^3 Ge(Li) detector with a resolution of 15 keV at 7 MeV. Spectra were recorded with a 24-digit two-parameter tape-recording system.

The distribution of partial radiation widths was determined in the framework of the Porter-Thomas description. Such a distribution is given by the χ^2-distribution for ν degrees of freedom. The ν parameter may be interpreted as the reaction channel number. Then the distribution of Γ_{γ_i}, which corresponds to only one exit channel, should be expected to have $\nu = 1$. The ^{196}Pt compound nucleus is a very favourable case for such a study: a large number of 1^- resonances are available (22 resonances between 10 and 700 eV) and there are three distinct intense E1 transitions to the ground state and the two first excited states, giving an experimental sample of 66 widths.

The experimental histograms of reduced widths $\chi_i = \Gamma_{\gamma i} / \langle \Gamma_{\gamma_i} \rangle$ are shown in Fig. (i). χ^2 square distributions for $\nu = 1$ and 2 are also drawn; our data appear consistent with $\nu = 1$ rather than an exponential function ($\nu = 2$). We have developed a statistical treatment based on a two-dimensional Monte Carlo method, in which the experimental threshold is introduced and which takes into account the fact that our experimental sample is a random sample. In this method both experimental sample and simulated samples are characterized by two parameters, the number of degrees of freedom and the number of widths less than the experimental threshold. This method gives the best estimate:

$$\nu = 1.25 \begin{matrix} + 0.35 \\ - 0.27 \end{matrix}$$

The partial radiative capture for platinum can be considered as a one-exit channel reaction and we have an a posteriori justification of the extension of the channel notion to reactions with gamma emission.

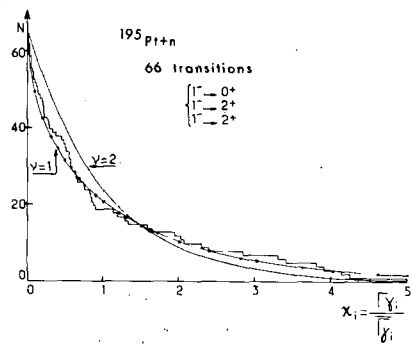

FIG.(i). Distribution of 66 partial radiative widths $\Gamma_{\gamma i}$ in ^{195}Pt + n and comparison with χ^2-function.

To investigate the possibility of correlation between two partial radiative widths relative to transitions going to very close energy states, one may examine the distribution of their sums, which must be a χ^2- distribution with $\nu = 2$ if the two transitions are to be independent. We have investigated the two E1 transitions going to the fundamental state and the first excited state of ^{184}W. This nucleus is very interesting to study because it is a deformed nucleus and the two preceding levels belong to the same rotational band (K = 0, I = 0, 2). Figure (ii) shows the experimental distribution for thirteen 1^- resonances from 7 to 360 eV. Our data are consistent with χ^2 functions with $\nu = 2$. The Monte Carlo analysis gives

$$\nu = 2.5 \begin{matrix} + 1.6 \\ - 1.2 \end{matrix}$$

in agreement with the previous value and we can conclude that there is no appreciable correlation between these two transitions. However, it would be very interesting to study resonances of highest energy to increase the statistical precision. This is possible now with separated isotopes.

The variation of partial capture cross-sections with neutrons allows an interference effect to be put in evidence. For instance, we have found a negative interference in ^{196}Pt for the transition of 7920 keV going to the fundamental of this nucleus between 12 and 19 eV 1^- resonances. This

effect is shown in Fig. (iii), where we have plotted the relative intensity of this transition versus neutron energy. Curve 1 is obtained without interference effect, curve 2 with positive interference and curve 3 with negative interference. Curve 4 is like 3 except that we have taken into account four other 1^- or 0^- resonances up to 120 eV.

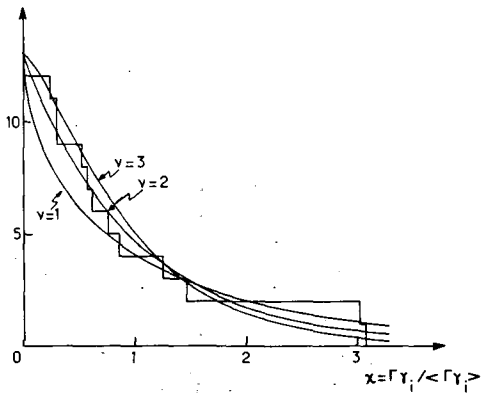

FIG. (ii). Distribution of the sum of two $\Gamma_{\gamma i}$ in $^{183}W + n$, corresponding to the 2 dipolar electric transitions going to the ground state and first excited state of ^{184}W.

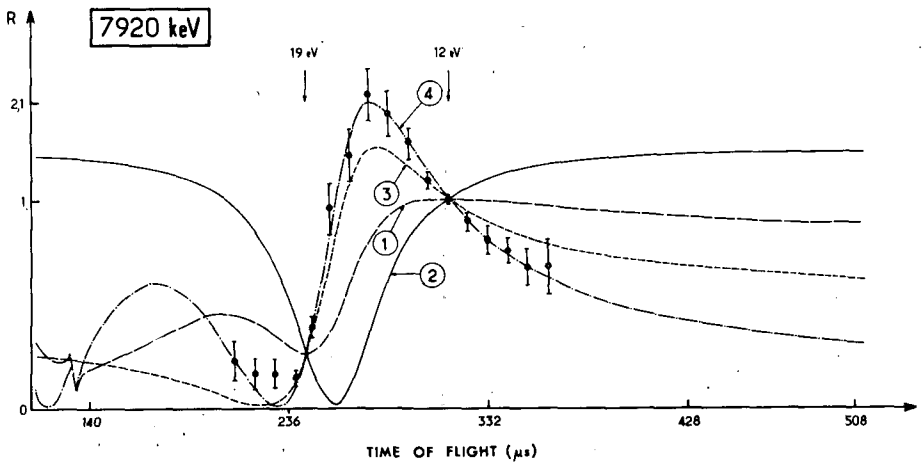

FIG. (iii). Interference effect in $^{195}Pt + n$, for the transitions of 7920 keV going to the ground state of ^{196}Pt.

The study of these gamma-ray spectra has allowed us to compare the intensities of dipolar electric and dipolar magnetic transitions. A transmission measurement made at Saclay allowed the ℓ value to be evaluated for several resonances. We have found 6 s-waves and 3 p-waves from 39 to 200 eV. We have estimated the intensities of 12 E1 and 12 M1 transitions in five different isotopes. We have supposed with Harvey that the two highest energy transitions in 62 eV resonance represent 65% of the total radiative width. The analysis of the spectra shows very strong M1 transitions. We have obtained the mean values $\langle \Gamma^{E1}_{\gamma i} \rangle$ = 28 MeV and $\langle \Gamma^{M1}_{\gamma i} \rangle$ = 5 MeV.

Detailed level schemes can be obtained from gamma-ray emission following resonance neutron capture. Such a study presents several advantages in connection with thermal neutrons: enhancement of transitions because Γ_{γ_i} obeys a Porter-Thomas distribution, spin assignments when many resonances are available, the unambiguous assignment of level schemes to different isotopes.

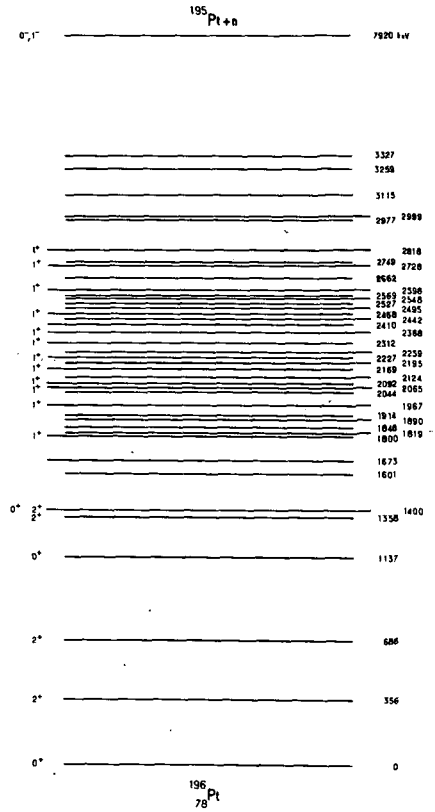

FIG. (iv). Level scheme of ^{196}Pt obtained from 30 neutron resonances (22 resonances with $J^{\pi} = 1^-$ and 8 resonances with $J^{\pi} = 0^-$); 40 excited states are obtained, 12 having $J^{\pi} = 1^+$.

I shall give only one example. We have obtained a detailed level scheme for ^{196}Pt from 22 1^- resonances and eight 0^- resonances. Forty excited states have been found up to 3500 keV. Twelve levels have spin 1^+, corresponding ones being observed in 1^- and 0^- resonances (Fig. (iv)). Other levels are probably 0^+ or 2^+. We have also studied the β-decay of ^{196}Au. So it is interesting to compare the experimental level sequence of ^{196}Pt with the predictions of the vibrational harmonic model. The second excited state 2^+ at 356 keV can be considered as a pure 2-phonon state. But the separation of the three excited states 2^+, 4^+ and 0^+ at 686, 876 and 1137 keV is too high to allow these three states to be considered as the three components of the 2-phonon triplet. On the other hand, an intermediate state 3^+ appears at 1015 keV and we observe two other levels at 1358 keV ($J = 2^+$) and 1400 keV ($J = 0^+$ or 2^+). Here the level sequence would be explained rather by a very anharmonic vibration mode.

III

OPEN PROBLEMS IN NUCLEAR PHYSICS

Chairman

A. BOHR

Secretary

L.A. MALOV

ISOTOPE SHIFTS AND ISOMER SHIFTS IN MUONIC ATOMS*

C.S. WU
COLUMBIA UNIVERSITY,
NEW YORK, UNITED STATES OF AMERICA

Abstract — Аннотация

ISOTOPE SHIFTS AND ISOMER SHIFTS IN MUONIC ATOMS. Recent results on isotope shifts ($^{142-146,148,150}$Nd, $^{92,95-97}$Mo, $^{50,52-54}$Cr) and isomer shifts (^{182,184,186}W) are summarized in this paper. First, the merits and disadvantages of the three different isotope shift methods (optical h.f.s. spectra, electronic X-rays and muonic X-rays) are briefly outlined. The sensitivities of model dependence of the observed isotope shifts by these three methods are also introduced and discussed. The main emphasis of the paper is to show and to explain how the muonic isotope shift results may be used to normalize the optical isotope shift results and obtain the specific mass corrections occurring in optical results. The energy shifts of nuclear gamma rays as the result of the dynamic E2 interactions in several deformed nuclei have been precisely measured. The calculated shifts of the centre of gravity of the unresolved magnetic doublet are first applied to the observed shifts. The remaining shifts may be interpreted as the isomer effects, i.e. the effect of charge distribution on the transition energy. A comparison of the isomer effects by the muonic atom method and by the Mössbauer technique is included.

ИЗОТОПИЧЕСКИЕ И ИЗОМЕРНЫЕ СДВИГИ В МЮ-МЕЗОННЫХ АТОМАХ. Представлены последние результаты исследований по изотопическим сдвигам ($^{142-146,148,150}$Nd, $^{92,95-97}$Mo, $^{50,52-54}$Cr) и изомерным сдвигам (^{182,184,186}W). Дается краткое описание достоинств и недостатков трех различных методов изотопических сдвигов (оптические спектры сверхтонкой структуры, электронные гамма-кванты и мю-мезонные гамма-кванты). Представлены и обсуждаются данные о чувствительности модельной зависимости наблюдаемых изотопических сдвигов при использовании этих трех методов. Показывается и объясняется, как можно использовать результаты мю-мезонного изотопического сдвига для нормализации результатов оптического изотопического сдвига и получения поправок на изменение удельной массы, которое не учитывается в оптических результатах. Точно измерены энергетические сдвиги ядерных гамма-квантов как результат динамических E2-взаимодействий в нескольких деформированных ядрах. Расчетные сдвиги центра тяжести неразрешенного магнитного дублета впервые применяются по отношению к наблюдаемым сдвигам. Остальные сдвиги можно интерпретировать как изомерные эффекты, т.е. влияние распределения заряда на энергию перехода. Приводится сравнение изомерных эффектов с помощью метода мю-мезонных атомов и метода Мессбауэра.

It is well known that, since the rest mass of the muon is 207 times larger than that of the electron, a "K-shell" muon will be about 200 times nearer the nucleus than a "K-shell" electron. The close proximity of the "K-shell" muon in the Coulomb field of a nucleus, and particularly its exceedingly weak interaction with nucleons, allow the muon to spend an appreciable fraction of its lifetime (10^{-7} - 10^{-6} s) within the nucleus itself and serve as an ideal probe for the distribution of nuclear charge and nuclear moments inside the nucleus. The pioneer work in muonic X-rays in the early period of 1953-1954 demonstrated [1, 2] quite clearly some of these remarkable attributes of the muon as a nuclear probe. Since the introduction in 1964 of the high resolution Ge(Li) detector [3] into the experimental technique of muonic X-ray studies, most of the fine structure and hyperfine structure of the muonic X-ray spectra can now be resolved

* Partially supported by the US Atomic Energy Commission and the National Science Foundation.

and analysed. The progress made so far in the field has been most encouraging.

Because the time allotted to this paper is short, it is impossible to try to touch on all the interesting results obtained in the field of the muonic atom. I shall present only our recent work on isotope shifts and isomer shifts in muonic atoms. The muonic isotope shift results not only reveal the variation of nuclear charge distribution between neighbouring isotopes in a vivid manner (the line shifts can be detected by the unaided eye), but also illustrate a possible approach in relating our understanding of the muonic isotope shifts to optical isotope shifts. The last part of the paper will be on nuclear isomer shifts in which it will be shown that the isomer shifts of deformed nuclei can be determined by the muonic atom method as well as by the Mössbauer technique. Furthermore, their results are in substantial agreement.

I. THE ISOTOPE SHIFT

A. Introduction

The isotopic shift can be studied by using either optical h.f.s. spectra, electronic X-rays, or muonic X-rays.

The optical isotope shift [4] has been continuously studied for nearly four decades and recognized as an important source of information on the changes of nuclear charge distribution and the fine variations of nuclear structure between isotopes. However, calculations of electron energy levels in an atom are complicated by not only the screening effects, but also the specific mass effects which are due to the correlation of motions of the electrons in an atom. I will explain this in more detail later.

The electronic X-ray measurement of isotope shift has been developed into a fine art only recently through the valiant efforts of the two experimental groups headed by Dr. O. I. Sumbaev of the Ioffe Institute [5] and Dr. F. Boehm of Cal. Tech. [6]. The interpretations of the electronic X-ray results on isotope shifts are relatively free from the limitations existing in the optical method. However, because of the Doppler line-broadening, which is generally several hundred times larger than the line-shift expected, and furthermore, because of its extreme sensitivity to chemical composition and crystalline structure, the experimental precision seems to be the only major limitation on its effectiveness as a sensitive tool at the present moment. Both optical and electronic X-ray isotope shift studies are limited to medium and heavy atoms with $Z \gtrsim 40$.

B. Model dependence

The results from both optical and electronic X-ray methods are relatively insensitive to the detailed model of nuclear charge distribution. This is because the wave-length of the electron is long compared to the nuclear dimension; therefore the electron wave-function can be considered to be constant over the nuclear volume. In other words, one can extract from these shifts only information on the change of r.m.s. radius $\Delta\langle r^2\rangle$.

Because of its simple hydrogen-like structure, the binding energies of the various levels of a muonic atom can be calculated accurately if the

charge distribution is known. However, for light and medium nuclei, even the muonic X-rays are rather model-independent. Therefore one again measures only the r.m.s. radius in these muonic atoms. For nuclei of atomic number $Z \geq 60$, in principle it is possible to determine two parameters in a charge distribution if the absolute energies of K and L X-rays are determined to an accuracy equal to or better than 1 and 0.1 keV, respectively. Under such favourable conditions, the isotope shift results should be applied to a Fermi charge distribution model or other appropriate models and the pair of variations Δc and Δt or $\Delta\langle r^2\rangle$ and Δt can thus be deduced. The $\Delta\langle r^2\rangle$ thus obtained in muonic atoms may then be compared with that obtained from optical and electron X-ray results.

In short, the optical and electronic X-ray isotope shift results yield only $\Delta\langle r^2\rangle$. In heavy muonic atoms, the isotope shifts may yield information on the charge distribution by a pair of quantities such as $\Delta\langle r^2\rangle$ and Δt only if high precision in the L X-ray energy measurements (better than 100 eV) is attained. However, there are other uncertainties involved other than the experimental precision which will be discussed later.

C. Major contributing terms in optical isotope shifts

Before presenting the experimental results, I will first write down the important terms which contribute to the observed optical isotope shifts. Generally, the I.S. effect[1] comes from two major sources

$$(\Delta E)_{\text{I.S.}} = (\Delta E)_{\text{Mass Effect}} + (\Delta E)_{\text{Field Effect}}$$

where the mass effect can be divided into normal mass and specific mass effect and the field effect is contributed by both volume changes and deformation effect. Therefore

$$(\Delta E)_{\text{I.S.}} = (\Delta E)_{\text{Normal Mass}} + (\Delta E)_{\text{Specific Mass}} + (\Delta E)_{\text{Volume}} + (\Delta E)_{\text{Deformation}}$$

The origin of the two mass terms can be shown by writing the non-relativistic Hamiltonian of an atom with n electrons in the centre of mass system

$$H = \frac{1}{2\mu}\sum_{j=1}^{n}(\vec{p}_j)^2 + \frac{1}{2M}\sum_{j\neq i}(\vec{p}_j\cdot\vec{p}_i) + V$$

where μ (reduced mass) $= m_e M_N/(m_e + M_N)$. Therefore the transition energy is larger for the heavier isotopes due to the normal mass effect alone.

The specific mass effect originates from correlations in the motion of the electrons in an atom $\sum_{j\neq i}(p_j\cdot p_i)$. Naturally, this effect vanishes in the hydrogen atom or one-electron ions. It also does not exist in

[1] Conventionally, the isotope shift is expressed as $\delta(\Delta E)$. ΔE represents the line shift due to the finite size effect (the effects on levels other than s electrons are generally neglected) and $\delta(\Delta E)$ is the shift between isotopes. However, for simplicity, we use ΔE for the isotope shift $\delta(\Delta E)$.

muonic atoms. From the Hamiltonian expression shown above, it can be seen that the specific mass term is inversely proportional to the nuclear mass (1/M); therefore its contribution to the isotope shift $(\Delta E)_{L.S.}$ should vary as $1/M^2$ and it has been construed that this effect is negligible in heavy atoms in the past. However, recent experimental evidence [4, 17] indicates that this term does vary with $1/M^2$ but C/M^2 is by no means negligible. Theoretically, there are no extensive calculations of this effect in the medium and heavy atoms. Nevertheless, several serious attempts have been initiated in this direction and the calculated results are comparable to those observed [7].

The deformed volume effect was first suggested by Brix and Kopfermann [8] in 1947 to account for the anomalously large isotope shifts observed in some of the rare earth isotopes. It is easy to see that nuclei which have non-spherical shapes appear (after averaging over angles) to be more extended radially than spherical nuclei of the same volume. It is possible, therefore, to obtain a change in the r.m.s. charge radius between isotopes by merely allowing the shapes of the nuclei to vary, even when the volume remains constant. To lowest order in β, one may express the relation:

$$\langle r^2 \rangle_\beta^{\frac{1}{2}} = \left(1 + \frac{5}{8\pi}\beta^2\right) \langle r^2 \rangle_{\text{spherical}}^{\frac{1}{2}}$$

The normal volume effect comes from the assumption that heavier nuclei are larger according to the $A^{\frac{1}{3}}$ law so that the electron orbits penetrate more deeply into the nucleus and thus move in a weaker field. This naturally results in a decrease in binding energy.

Actually, although the radii of the nuclei on the line of maximum stability in general vary with the $A^{\frac{1}{3}}$ law, this does not imply that the variation of radius between isotopes of the same element must also follow the $A^{\frac{1}{3}}$ law. Let us imagine that we take two neutrons and add them to a nucleus. Since the Coulomb repulsion is diluted in adding two neutrons, the last protons become more strongly bound and, therefore, the protons distributed on the outer surface probably get pulled towards the centre of the nucleus. The r.m.s. charge radius actually becomes smaller than that predicted from the $A^{\frac{1}{3}}$ law. This was pointed out for the first time by Wilets et al. [9] on the basis of the theory of nuclear compressibility and later was further extended in its application to isotope shift effect by Bodmer [10]. This proton binding energy effect is actually related to the isospin dependent term in the nuclear optical potential as suggested by Lane [11]

$$V = V_0 + \frac{\vec{t} \cdot \vec{T}}{A} V_1$$

where $\vec{t}$ is the isospin of the "added" neutron and $\vec{T}$ is the isospin of the "target" nucleus. Perey and Shiffer [12] and Elton and Swift [13] have shown that by choosing Woods-Saxon potentials for both V_0 and V_1 and by adjusting parameters to give the correct binding energies for the outer shell protons, the isotope shifts in $^{40-44}$Ca and $^{40-48}$Ca become smaller than that expected from the $A^{\frac{1}{3}}$ law.

Magic shell effect

This deviation from the $A^{\frac{1}{3}}$ law manifests itself in a striking fashion when two added neutrons happen to complete the magic shells of 20, 28, or 50 neutrons. The $\langle r^2 \rangle$ of the neutron magic nuclei of mass number A compared with that of the lighter isotope (A-2) not only increases much less than expected from the $A^{\frac{1}{3}}$ law, it actually decreases [14, 15]. In other words, the charge radii of nuclei A with neutron magic shells of n = 20, 28, and 50 are smaller than those of the corresponding (A-2) nuclei. The presence of the shell effect was first detected in the studies of optical isotope shifts in Ba, Ce (n=82). Because there was no simple way to calculate accurately on the correction of the specific mass effect, the shell-closure effect is somewhat masked by it and appeared less striking than that in muonic data.

II. EXPERIMENTAL RESULTS

Our muonic atom experiments were carried out on the Columbia synchrocyclotron at Nevis Laboratory. The detailed description of our experimental set-up can be found in recent literature [16]. In this paper, only the results on Nd, Cr, and Mo will be presented.

Nd

The muonic K and L X-ray line shifts among the seven isotopes $^{142-146,148,150}_{60}$Nd have been measured. This is a particularly interesting sequence of isotopes to study. Firstly, the isotopes begin from nearly spherical shape with neutron magic number (n=82), then proceed to the last member with 90 neutrons which is known to behave as a soft rotator with the characteristics of permanent deformation. Secondly, the isotope shifts of Nd isotopes have been precisely and extensively studied by the optical method [17] and also, recently, by the electronic X-ray method [5, 6]. In these isotopes, the isotope shifts due to the normal volume effects are reinforced by the deformation effect, that is deformation increases with increase of neutron number; the observed isotope shifts are much larger than those predicted by the $A^{\frac{1}{3}}$ law. The shifts between two adjacent (even-even) isotopes are generally of the order of tens of keV, and can be easily seen from Fig. 1. Furthermore, the line shapes of the odd isotopes are much more complicated than those of the even ones because of the presence of the static quadrupole hyperfine structure. The ground state of ^{143}Nd has spin 7/2 and a positive static quadrupole moment. The interaction of the muon and the nuclear quadrupole moment causes the $2p_{3/2}$ muon state to split into four components (it does not affect the $2p_{1/2}$ state). Below the experimental spectrum of ^{143}Nd in Fig. 1 we have shown schematically the position of these four components, as well as two components due to isotopic impurities. The calculated line width agrees roughly with the measured value. The shift between ^{148}Nd and ^{150}Nd is nearly twice as large as that from other (e-e) pairs. Particularly, the dynamic quadrupole hyperfine structure appears suddenly in the spectrum of the deformed ^{150}Nd isotope in contrast to the spectrum of ^{148}Nd.

In Fig. 2, the upper portion (2a) shows the positions of the observed $K_{\alpha 1}(2p_{3/2} \longrightarrow 1s_{1/2})$ and $K_{\alpha 2}(2p_{1/2} \longrightarrow 1s_{1/2})$ lines from various Nd isotopes. The unusually large difference in the splitting of the $2p_{3/2}$ and $2p_{1/2}$ levels between ^{148}Nd and ^{150}Nd is mostly due to the large difference in the dynamic quadrupole excitation which perturbs the two p levels differently in these two nuclei. However, these perturbations on the various levels of a muonic atom can be calculated accurately using Wilets' or Jacobsohn's formulation. The optical isotope shifts of the lines (5621 Å and 4945 Å) from the Nd isotopes measured by Hansen, Stendel and Walther [17] are reproduced in Fig. 2b. The general similarity between the muonic and the optical isotope shifts is apparent.

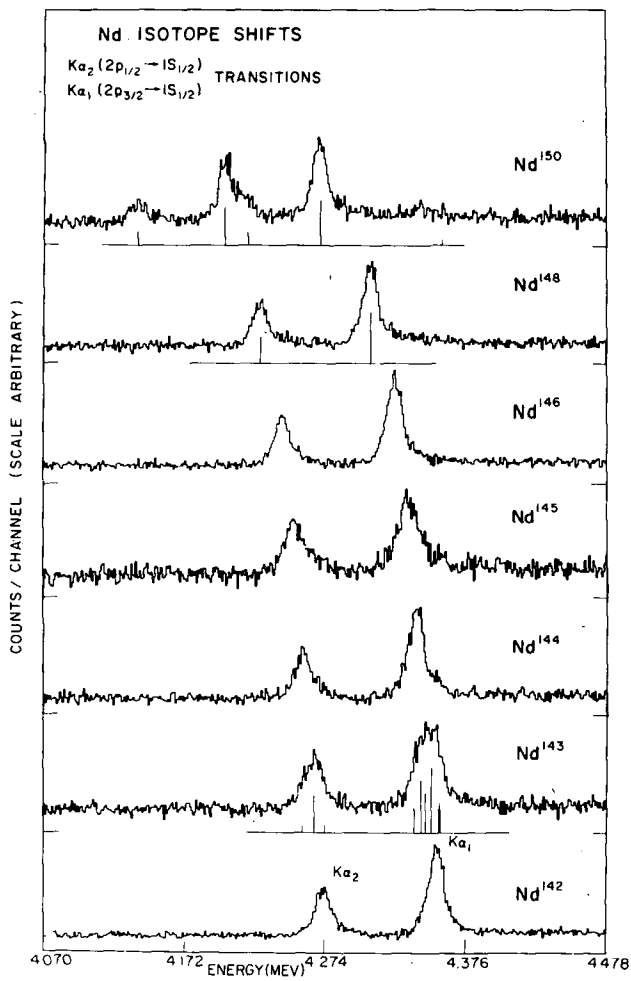

FIG. 1. Experimental muonic K X-ray spectra of $^{142-146,148,150}$Nd isotopes. Note the broadening of the lines in the odd isotopes and the dynamic h.f.s. structure in ^{150}Nd. The vertical lines under the peaks of ^{143}Nd represent the calculated position and relative intensities of the various hyperfine components and two impurity lines due to ^{142}Nd and ^{144}Nd.

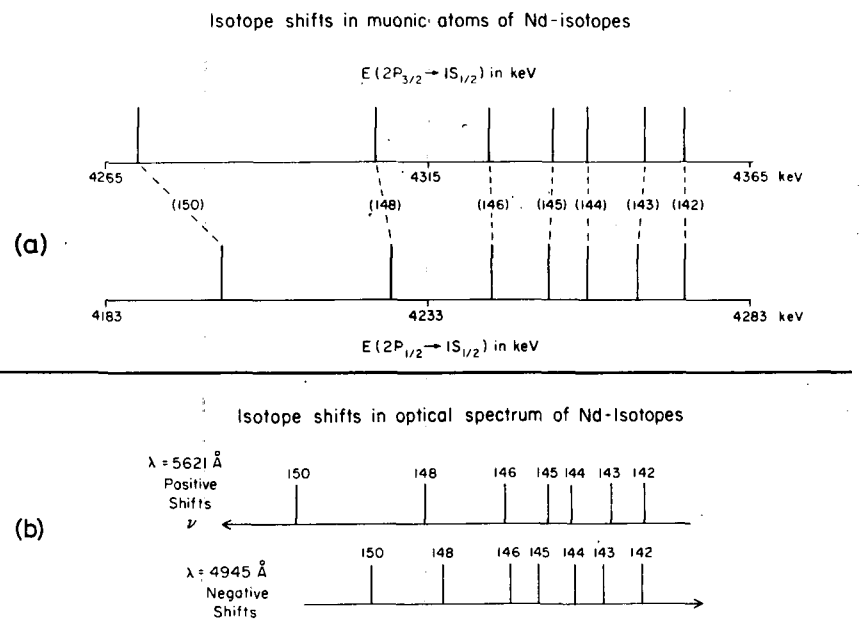

FIG. 2a. Relative positions of the $K_{\alpha 1}$ and $K_{\alpha 2}$ lines in the Nd isotopes. The unusually large isotope shift between ^{148}Nd and ^{150}Nd is due to both the dynamic E2 interaction and the deformation effect.

2b. Isotope shifts in optical spectra of Nd isotopes [17]. The large shift between ^{148}Nd and ^{150}Nd is due to the deformation effect. The similarities between the muonic and optical isotope shifts can be seen.

Figure 3 shows the 2p fine structure separations observed in the muonic K and L lines in Nd-isotopes before and after the correction for the dynamic E2 perturbation. The corrected values are plotted in open circles and uncorrected data in solid dots. The theoretically calculated variation of the fine structure splitting for a Fermi charge distribution with $c \sim A^{\frac{1}{3}}$ and $\Delta t = 0$ in Nd isotopes is shown in dotted curves. The agreement between the experimental results and the theoretical calculations for $\Delta t = 0$ is rather good.

Cr

The four isotopes $^{50, 52-54}_{24}$Cr were studied. The closing of the $n = 28$ shell in ^{52}Cr makes the isotope shifts in chromium particularly interesting. The fine structure in the K_α lines was too small to be completely resolved. The shifts of the 1s levels in muonic atoms are shown in Fig. 4a. The isotope shift between ^{50}Cr and ^{52}Cr is reversed in direction; this implies that the 1s level in muonic atoms of ^{52}Cr actually lies deeper than in ^{50}Cr or the r.m.s. charge radius of ^{52}Cr is smaller than that of ^{50}Cr. This reversal of the shift is partly due to the shell-closure effect and partly due to the change of deformation from $\beta(50) = 0.31$ to $\beta(52) = 0.23$. The latter alone cannot account for the reversing of the effect observed. ^{53}Cr lies closer to ^{52}Cr than ^{54}Cr. This is known as odd-even staggering effect.

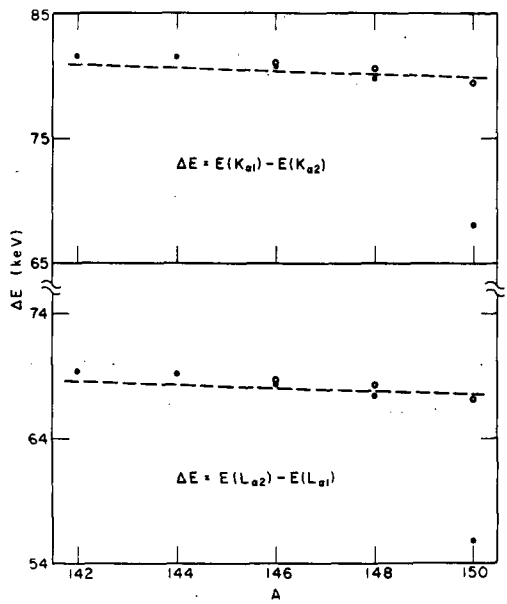

FIG. 3. Fine structure splitting of the muonic K and L lines versus mass number for the Nd isotopes. The solid dots denote experimentally observed values; the open circles represent the same data after the correction of the dynamic E2 effects. The dotted line indicates the behaviour expected for a change of c only in a Fermi distribution.

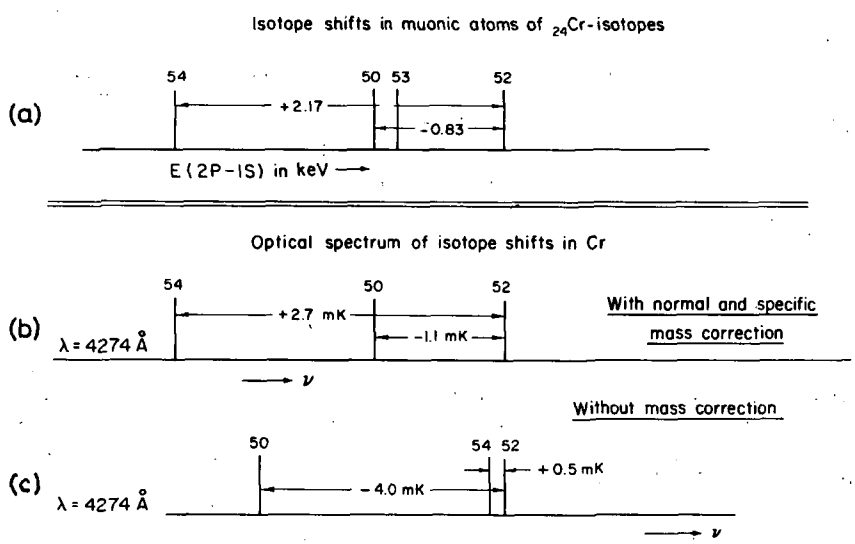

FIG. 4a. Muonic isotope shifts in $^{50,52-54}_{24}Cr$ isotopes.

4b. Optical isotope shifts in $^{50,52,54}_{24}Cr$ isotopes with the correction of mass effects.

4c. Observed isotope shifts in Cr isotopes [18].

The staggering parameter γ_N which is conventionally defined as

$$\gamma_N = \frac{[E(N-1) - E(N)]}{1/2[E(N-1) - E(N+1)]}$$

is equal to $\gamma_N = 0.65$.

The optical isotope shifts on Cr have been measured recently by Heilig and Wendlandt [18]. They have investigated transitions of the type $3d^5 4s - 3d^5 4p$. The observed isotope shifts in the optical spectrum for the line $\lambda = 4274$ Å before applying the specific mass correction are shown in Fig. 4c and show no resemblance to the shifts observed in muonic atoms. When the specific mass correction, as calculated by normalizing the optical data with muonic isotope shifts, is applied, the corrected optical shifts are as shown in Fig. 4b; for comparison the muonic results are shown in Fig. 4a.

Mo

The four isotopes $^{92,95-97}_{42}$Mo were studied. The optical results of Hughes [19] for the line at 5793 Å and those of Arroe and Cornwall [20] for the line at 6032 Å will be compared.

III. INTERPRETATION AND DISCUSSION

One of the strong motivations of study of isotope shifts is to extract information concerning the variations of charge distribution between isotopes. Since the optical and electronic X-ray results are model-independent, only one quantity which is proportional to the change of r.m.s. charge radius $\Delta\langle r^2 \rangle$ can be obtained. For muonic isotope shifts in heavy nuclei ($Z \geqslant 50$), the interpretation is more involved because it is model-dependent and, therefore, depends on the variations of two or more parameters in a given charge distribution. For instance, if the phenomenological Fermi charge distribution is used, the isotope shifts should depend not only on the variation of $c(\Delta c)$ but also on the variation of $t(\Delta t)$. As a matter of fact, the recently proposed modified charge distributions [21, 22] indicate that even a third parameter may be required to modify the Fermi distribution. However, let us suppose that the K and L X-rays of muonic atoms could be determined to very high accuracy ($\ll 100$ eV). To deduce the parameters c and t separately and uniquely, one must also know very accurately several other quantities. As was mentioned before, the nuclear polarization correction due to virtual excitations on 1s and 2p levels must be evaluated to an accuracy better than 1 and 0.1 keV, respectively, which is beyond the precision limits given to these quantities at the present moment. Particularly, the skin thickness is extremely sensitive to the 3d - 2p L X-ray. A correction of 2 keV in the L X-ray energies of muonic atoms in the rare earth region can affect a change in skin thickness of (25-35)% (see Ref. [23]). In interpreting the isotope shift results, the difference of the nuclear polarization between isotopes must also be taken into account. In general, this fractional change in nuclear polarization between (e-e) isotopes may be assumed to be in proportion to the fractional

change in nuclear volume; therefore $\delta(\Delta E)_{N.P.} \sim (\Delta E)_{N.P.} \times \delta V/V = (\Delta E)_{N.P.} \times \delta A/A$. For Nd, $(\Delta E)_{N.P.}$ is calculated to be around 6 keV [24-27]; $\delta(\Delta E)_{N.P.} \sim 6 \times 2/150 \sim 0.1$ keV, which is small in comparison with the experimental uncertainty. No correction for the difference in nuclear polarization has been applied in our interpretation of the muonic isotope shift results. However, where abrupt changes in nuclear configuration should occur between the adjacent isotopes, the above assumption may not apply. Secondly, the deformation parameter β^2 derived from other experiments such as Coulomb excitation must be known accurately to better than 1%. This is also beyond the reach of the present technique.

The variation of t between the adjacent (e-e) isotopes

Now, let us see how the variations Δc and Δt can affect the isotope shift ΔE observed. Taking into account the first order terms only, then

$$\Delta E = \left(\frac{\delta E}{\delta c}\right)_t \Delta c + \left(\frac{\delta E}{\delta t}\right)_c \Delta t$$

The coefficients $(\delta E/\delta c)_t$ and $(\delta E/\delta t)_c$ vary with Z and very slightly with A and can be obtained from the calculated muon level energies.

For example, in Nd, where Z = 60 and A = 142 - 150,

$$\left(\frac{\delta E}{\delta c}\right)_t \cong -390 \text{ keV/F}; \quad \text{and} \quad \left(\frac{\delta E}{\delta t}\right)_c \cong -150 \text{ keV/F}.$$

For $\Delta A = 2$, $\Delta c \cong 0.03$F from the $A^{\frac{1}{3}}$ law, if the variation in t between two isotopes is as large as $\Delta t/t = 5\%$, then the contributions from Δt and Δc are about equal.

The pertinent question here, then, is: What evidence do we have concerning the variation of t between isotopes? Unfortunately, our knowledge of this is rather limited. Elton [28] has shown that with a constant t (2.35 F), the electron scattering results and muonic transition energies can be fitted over a wide range of A. Of course, this does not really imply that it is also true for variation of t between isotopes. The only experimental information on the variation of t between isotopes came from the interpretation[2] of recent results [29] of electron scattering on $^{40, 44, 48}$Ca. Both ^{40}Ca and ^{48}Ca are doubly magic nuclei and ^{44}Ca is in-between. The results could be interpreted as $\Delta c = 2.2\%$ and $\Delta t = -1.7\%$ between ^{40}Ca and ^{44}Ca and $\Delta c = 4.1\%$ and $\Delta t \sim -12\%$ between ^{40}Ca and ^{48}Ca. The Δt between ^{40}Ca and ^{48}Ca is probably $\sim -10\%$. Therefore the assumption that the variation of t between (e-e) isotopes of Nd with neutron difference of 2 is no more than 5% is not unreasonable. On the other hand, there is a better way to obtain some information concerning this pertinent question of variation of skin thickness t between isotopes in heavy nuclei. This is to study the behaviour of the ratios of isotope shifts among several isotope pairs of a given element measured by both optical and muonic methods. The following sections will be devoted mostly to this type of comparison and its conclusions.

[2] In interpreting the electron scattering data, no account has been taken of nuclear polarization.

The $(\Delta E)_{\text{Field Effect}}$ in muonic, optical and electronic isotope shifts

If Δt is a considerable fraction of t and also fluctuates from one adjacent (e-e) isotope pair to another, then the ratio of $(\Delta E)_{\text{Field Effect}}$ in muonic isotope shifts to that of optical or electronic X-ray shifts should vary irregularly among the adjacent pairs because the former is model-dependent while the latter two are not. Fortunately, the isotope shifts between the adjacent (e-e) isotopes in a long sequence of $^{142, 144, 146, 148, 150}$Nd have been measured accurately by both the muonic[30, 31] and the optical method [17]. The electronic X-ray shifts of Nd isotopes have also been reported recently by two separate studies [5, 6]. In Fig. 5 the muonic shifts[3] [31] are plotted against the optical shifts [17] measured for the two lines at $\lambda = 5621$ Å and $\lambda = 4945$ Å. A perfectly straight line can be drawn through all the points representing either one of these two optical lines. Although the remarkable linearity of these plots cannot be construed as evidence for $\Delta t = 0$, there is no evidence of large variations of Δt. Figure 6 shows the same linear plot in Mo. Here the statistics are not as good as in Nd isotopes.

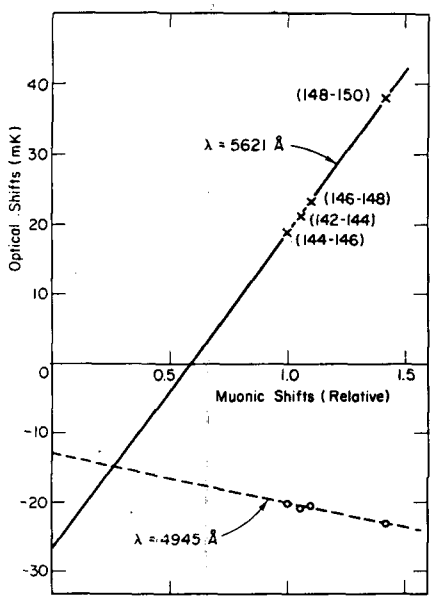

FIG. 5. Plot of the muonic isotope shifts versus the optical isotope shifts per two neutrons in Nd. The optical data include the total mass effect and are taken from Ref. [17].

The same relation was also plotted for muonic [30, 31] and electronic isotope shifts [5, 6] in Nd. Although a straight line can be drawn through the points within the uncertainty limits, unfortunately the uncertainties in the electronic X-ray shifts were so large that no firm conclusions

[3] Our muonic shifts represent the energy shifts of 1s levels in muonic atoms. This is determined by $[(K^{A}_{\alpha 1} + L^{A}_{\alpha 1}) - (K^{A+\Delta A}_{\alpha 1} + L^{A+\Delta A}_{\alpha 1})]$ or analogously for the $K_{\alpha 2}$ and $L_{\alpha 2}$ lines. The shift of 3d level is only a few eV and therefore negligible.

concerning the question of Δt between isotopes could be reached. More precise measurements of the electronic isotope shifts in Nd isotopes are highly desired.

Specific mass effect in optical isotope shifts and 1s energy terms in muonic atoms

It has been frequently emphasized in the literature that the muonic isotope shifts can be used to normalize the optical isotope shifts. To obtain the field effect term $(\Delta E)_{\text{Field Effect}}$ in optical shifts, one must first subtract the mass effect term $(\Delta E)_{\text{Mass Effect}}$ from the observed effect $(\Delta E)_{\text{obs}}$.

$$(\Delta E)_{\text{Field Effect}} = (\Delta E)^{\text{opt.}} - (\Delta E)_{\text{Specific Mass}}$$

where $(\Delta E)^{\text{opt.}} = (\Delta E)^{\text{opt.}}_{\text{obs.}} - (\Delta E)_{\text{Normal Mass}}$. The calculation of $(\Delta E)_{\text{Normal Mass}}$ is trivial. $(\Delta E)_{\text{Specific Mass}}$ may be expressed in terms of $mC(N_2 - N_1)$, where mC is the specific mass effect per nucleon $m = 1/(A^i \cdot A^{i+2})$, and $(N_2 - N_1)$ = neutron difference. The $(\Delta E)_{\text{Field Effect}}$, due to a small change in the nuclear charge distribution, may be expressed as

$$(\Delta E)_{\text{Field Effect}} \sim |\psi(0)|^2 \Delta \langle r^2 \rangle$$

where $\psi_e(0)$ is the wave-function of the electron involved in the transition at the nucleus. $|\psi_e(0)|^2$ represents the electron density at the nucleus.

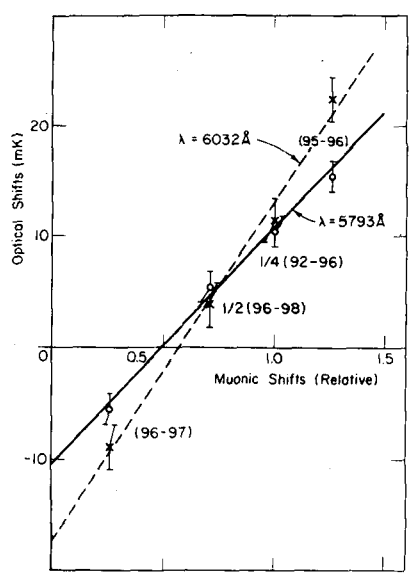

FIG. 6. Plot of the muonic isotope shifts versus the optical isotope shifts per neutron in Mo. The data for $\lambda = 6032$ Å is taken from Ref. [19] and $\lambda = 5793$ Å is from Ref. [20].

The change of nuclear charge distribution is proportional to $\Delta\langle r^2\rangle$. Therefore

$$|\psi_e(0)|^2 \Delta\langle r^2\rangle \sim (\Delta E)^{\text{opt.}} - mC(N_2 - N_1).$$

In muonic isotope shifts, at first the specific mass term does not exist. However, the 1s muonic energy also depends on higher order terms $\langle r^{2n}\rangle$ as well as the $\langle r^2\rangle$ term. This arises from the 1s muonic wave-function not being a constant over the nuclear volume. The $(\Delta E)_{\text{Field Effect}}$ could be expressed as

$$(\Delta E)_{\text{Field Effect}} \sim |\psi_\mu(0)|^2 [\Delta\langle r^2\rangle + a_2\Delta\langle r^4\rangle + a_3\Delta\langle r^6\rangle + a_4\Delta\langle r^8\rangle + \ldots].$$

The ratio of the sum of the higher moments $\sum_{n\geq 2} a_n\Delta\langle r^{2n}\rangle$ to the $\Delta\langle r^2\rangle$ term depends on the charge distribution used but is not very sensitive to it.

However, when the isotope shifts between two or more pairs of isotopes have been measured by both muonic and optical methods, then, in the optical case, we have the ratio:

$$\frac{(\Delta E)^{\text{opt.}}_{N_1, N_2} - mC(N_2 - N_1)}{(\Delta E)^{\text{opt.}}_{N_3, N_4} - mC(N_4 - N_3)} = \frac{\Delta\langle r^2\rangle_{N_1, N_2}}{\Delta\langle r^2\rangle_{N_3, N_4}}.$$

In the corresponding muonic case, we have

$$\frac{(\Delta E)^{\mu}_{N_1, N_2}}{(\Delta E)^{\mu}_{N_3, N_4}} = \frac{\left[\Delta\langle r^2\rangle_{N_1, N_2} + \sum_{n\geq 2} a_n\Delta\langle r^{2n}\rangle_{N_1, N_2}\right]}{\left[\Delta\langle r^2\rangle_{N_3, N_4} + \sum_{n\geq 2} a_n\Delta\langle r^{2n}\rangle_{N_3, N_4}\right]}$$

The electron density $|\psi_e(0)|^2$ and the muon density $|\psi_\mu(0)|^2$ are assumed to be the same for the two pairs of isotopes involved and therefore cancel in the ratio.

The ratio of the sum of the higher moments $\sum_{n\geq 2} a_n\Delta\langle r^{2n}\rangle$ to the $\Delta\langle r^2\rangle$ term was investigated by using a non-relativistic muon wave-function and assuming a Fermi charge distribution. It gives the ratio

$$\frac{\sum_{n\geq 2} a_n\Delta\langle r^{2\mu}\rangle}{\Delta\langle r^2\rangle} \cong 0.19 \pm 0.02$$

for Nd isotopes and neutron difference = 2. Furthermore, the ratio is very constant and varies only about (1-2)% between the successive pairs and if $\Delta t < 20\%$ is assumed. Therefore, the ratio of the $(\Delta E)_{\text{Field Effect}}$

in muonic isotope shifts can be expressed again approximately in terms of $\langle r^2 \rangle$:

$$\frac{(\Delta E)^{\mu}_{N_1, N_2}}{(\Delta E)^{\mu}_{N_3, N_4}} = \frac{\Delta\langle r^2 \rangle_{N_1, N_2}}{\Delta\langle r^2 \rangle_{N_3, N_4}} = \frac{(\Delta E)^{opt.}_{N_1, N_2} - mC(N_2 - N_1)}{(\Delta E)^{opt.}_{N_3, N_4} - mC(N_4 - N_3)}$$

From the above relation, the value of the mass effect per two nucleons can be first roughly estimated from the intercept of the linear plot on the ordinate axis of Figs 5 and 6. Then the more accurate value of C is obtained by taking into consideration the proportionality factor: $m = 1/(A^i \cdot A^{i+2})$.

The specific mass constants C obtained from the normalization method as described above are listed in Table I. The percentage in the parenthesis indicates the possible uncertainty in the determination where both the uncertainties in the measurements as well as that from the analysis are approximately taken into account. The $(\Delta E)_{\text{Normal Mass}}$ per two nucleons is listed in the last column. The specific mass effect $(\Delta E)_{\text{Specific Mass}}$ per two nucleons can be calculated by

$$(\Delta E)_{\text{Specific Mass}} = 2mC = \frac{2C}{A^i \cdot A^{i+2}}$$

which is usually expressed in mK ($cm^{-1} \times 10^{-3}$). For instance, $(\Delta E)^{5621\text{Å}}_{\text{Specific Mass}} = -23.55$ mK ($^{142-144}$Nd) and $(\Delta E)^{4945\text{Å}}_{\text{Specific Mass}} = -10.72$ mK ($^{142-144}$Nd).

From the optical isotope shift analysis, a relation between the mass effect for a transition line "a" to that of another line "b" can be obtained by plotting the observed isotope shifts for line "a" to that of line "b". This is known as King's method. Hansen, Steudel and Walther [17] made a thorough investigation of this method and obtained such a relation for the two lines $\lambda_a = 4945$ Å and $\lambda_b = 5621$ Å from Nd isotopes (see Eq. (4) of Ref. [17]). The values of C for Nd isotopes as listed in Table I fit that relation beautifully.

Heilig and Wendlandt [18] compared the optical shifts in Cr isotopes of three optical lines and can conclude only that the minimum specific mass effect of any one of these lines must be greater than 4.4 mK. This is again in accord with our determination of 6.6, 7.1, and 7.05 mK for the lines 4254Å, 4274Å and 4289Å in $^{50-52}$Cr respectively.

It is most encouraging to see that the specific mass effect due to the correlation motion of electrons in an atom as complicated as Nd can be now determined with the help of muonic isotope shifts in such a simple way.

Bauche [7] used non-relativistic Hartree-Fock wave-function to calculate the specific mass effect for the transition $4f^3\ 5d\ 6s^2\ ^5L - 4f^4\ 6s^2\ ^5I$ in Nd and $\Delta A = 2$ and obtained a value for $(\Delta\nu)_{\text{Specific Mass}} \cong -18$ mK, which is indeed comparable to what was observed (-23.55 ± 1) mK for $^{142-144}$Nd. These observations should reinforce strongly the statement that the specific mass effects even in heavy nuclei could be comparable to the observed shift and therefore cannot be neglected in general.

TABLE I. THE SPECIFIC MASS EFFECTS EXTRACTED FROM THE OPTICAL ISOTOPE SHIFT DATA WITH THE HELP OF MUONIC ISOTOPE SHIFT RESULTS.

		Specific Mass Constant $C_{S.M.}$ in cm^{-1}	$(\Delta E)_{Normal\ Mass}$ in mK
Nd	λ = 5621Å	-240 (±5%)	-0.95
	= 4945Å	-110 (±5%)	-1.08
Mo	λ = 5793Å	-85 (±10%)	-2.0
	= 6032Å	-148 (±10%)	-1.9
Cf	λ = 4254Å	+8.58 (±10%)	-9.9 (50-52) -9.2 (52-54)
	= 4274Å	+9.23 (±10%)	-9.9 (50-52) -9.2 (52-54)
	= 4289Å	+9.16 (±10%)	-9.9 (50-52) -9.2 (52-54)

IV. ISOMER EFFECTS IN MUONIC ATOMS

In a highly deformed nucleus, the electronic quadrupole interaction between the muon and the nucleus is comparable to the energies of the low-lying rotational levels and the fine structure splitting of the muonic 2p doublets. Therefore the E2 interaction mixes the nuclear ground state I_0 with various excited states I_1, I_2 ... and also the various muon states. This dynamic E2 h.f.s. spectrum has been observed and closely studied in most of the deformed nuclei.

Now let us turn to discuss the observed energy shift of the nuclear gamma ray in muonic states. In the dynamic E2 interaction in the (e-e) nuclei as just described, the probability that the nucleus will be left in the $I = 2^+$ state is high. The subsequent de-excitation of the nuclear state, which has a lifetime of about 10^{-9}s, takes place in the presence of the 1s muon, since the muon capture lifetime from the 1s state is about 10^{-7}s in the rare earth region. If the charge distribution of the excited state is different from that of the ground state, then an energy shift is expected which is known as the isomer effect, i.e. the effect of charge distributions on the transition energy:

$$\Delta E_\mu = \frac{2\pi}{5} Ze^2R^2 \left|\psi_\mu(0)\right|^2 \langle R^2_{ex} \rangle - \langle R^2_{Gd} \rangle$$

An analogous case in electronic atoms is the measurement of energy shift by Mössbauer effect through the difference of electron density produced in different chemical environments at the nucleus.

The gamma-ray energy shifts expected in muonic atoms are generally less than 1 keV. Measurements of such small energy differences were carried out by directly and simultaneously comparing the energy of the nuclear gamma ray in coincidence with a stopped muon with that of the unshifted gamma ray following $\beta^{\pm}$ decay from a Z ± 1 nucleus in the same detector and electronic system. The general layout of the experimental set-up is shown in Fig. 7.

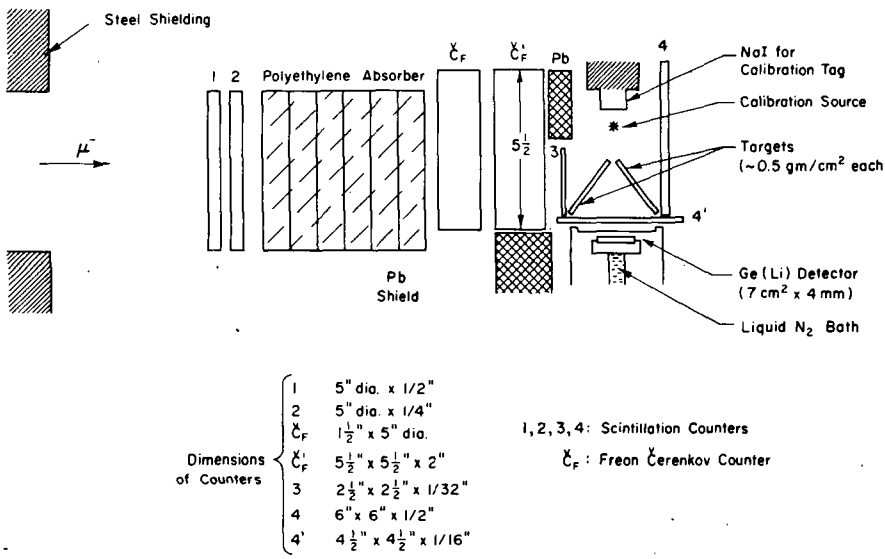

FIG.7. Schematic diagram of beam telescope and Ge(Li) detector arrangement.

Our first observation of the gamma ray energy shift in ^{152}Sm was reported [32] in 1967. Since then, we have completed the energy shift measurements [33] also in ^{150}Nd, ^{154}Gd, ^{166}Er, ^{182}W, ^{184}W and ^{186}W, and CERN [38] has reported their gamma ray shifts in muonic ^{152}Sm, ^{182}W, ^{184}W, ^{186}W, ^{188}Os, ^{190}Os and ^{192}Os. The agreements between these two groups are excellent [33, 38]. The nuclear gamma ray shifts in muonic ^{152}Sm and ^{184}W are shown in Fig. 8. The measured energy shifts are listed in Table II and the last four nuclei are all with negative signs. If the observed effect is all due to the difference of nuclear radii between the excited and ground states, then the negative value could imply that the r.m.s. radius of the excited state is smaller than that of the ground state, $\langle r^2_{ex} \rangle < \langle r^2_{Gd} \rangle$.

Recent theoretical investigations by Gal, Grodzins and Hüfner [34] have shown that the negative shifts could have resulted from the shift of the centre of gravity of the unresolved magnetic doublet. They pointed out that the F = 5/2 state decays mainly to the F = 3/2 state via a strong Auger transition, and not directly to the ground state (F = 1/2). This intense M1 interdoublet transition has the effect of lowering the observed

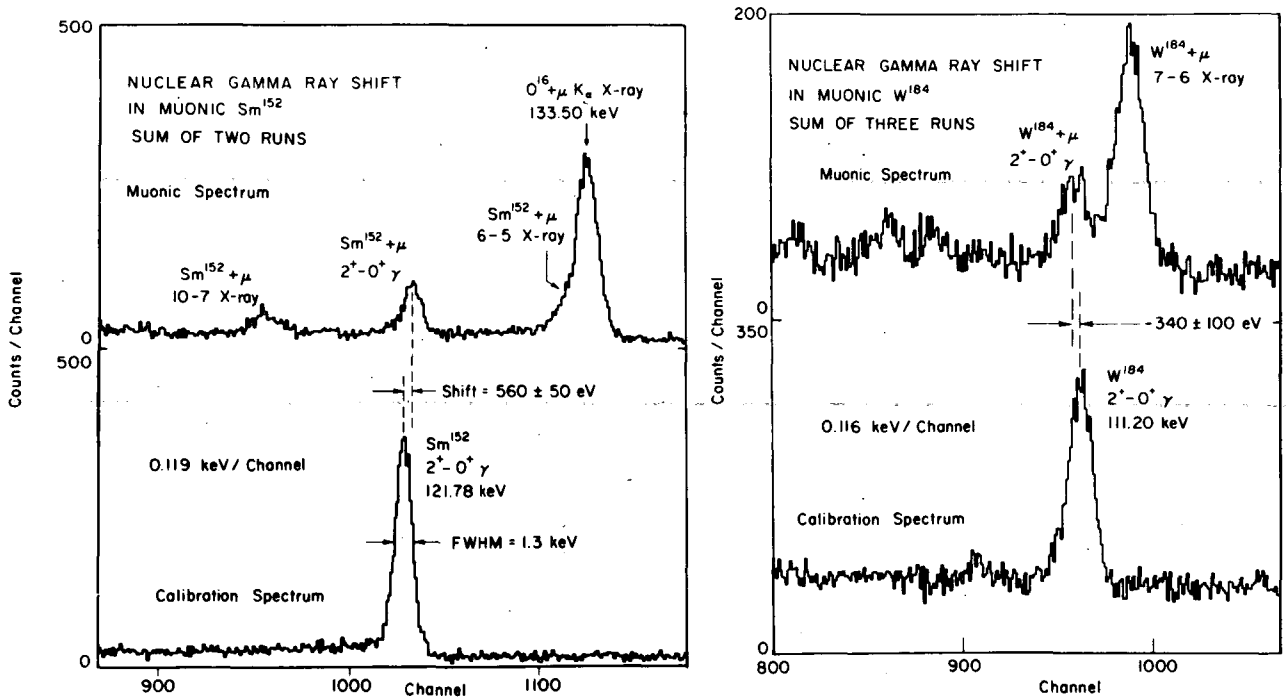

FIG. 8. The shifts in the energies of the first rotational nuclear gamma rays of ^{152}Sm and ^{184}W due to the 1s muon. The upper spectra show the de-excitation gamma rays ($2^+ \rightarrow 0^+$) in the presence of the muon. The lower spectra exhibit the corresponding ($2^+ \rightarrow 0^+$) gamma rays from radioactive sources.

TABLE II. A COMPARISON OF $\Delta\langle r^2\rangle/\langle r^2\rangle$ AS OBTAINED WITH MUONIC ATOMS AND MÖSSBAUER TECHNIQUES

Isotope	$2^+ \rightarrow 0^+$ energy (keV)	Comparison Source	Exp. Energy Shift ($\Delta E_{obs.}$) (eV)	Centre of Gravity Shift [a] ($\Delta E_{c.g.}$) (eV)	ΔE_{isomer} (eV)	$\frac{\Delta\langle r^2\rangle}{\langle r^2\rangle} \times 10^4$ Muonic	$\frac{\Delta\langle r^2\rangle}{\langle r^2\rangle} \times 10^4$ Mössbauer
$^{150}_{60}$Nd	130.17	Coulomb excitation [b]	+570±120	-270	+840±120	+5.8±0.8	No measurement
$^{152}_{62}$Sm	121.78	^{152}Eu(β^+ E.C.)	+560±60	-360 -240	+920±70 +800±70	+5.9±0.4 +5.1±0.4	+3.7 [6] +4.8 [c]
$^{154}_{64}$Gd	123.07	^{154}Eu(β^-)	+670±150	-310	+980±150	+5.9±0.8	No measurement
$^{166}_{68}$Er	80.56	^{166}Ho(β^-)	-350±150	-320	- 30±150	-0.16±0.8	No measurement
$^{182}_{74}$W	100.10	^{182}Ta(β^-)	-320±100	-290 -240	- 30±100 - 80±100	-0.13±0.5 -0.33±0.5	+0.15 [6] +1.2 [5]
$^{184}_{74}$W	111.20	^{184}Re(E.C.)	-340±100	-315 -250	- 25±100 - 90±100	-0.11±0.5 -0.40±0.5	+0.8
$^{186}_{74}$W	122.57	^{186}Re(E.C.)	-350±100	-340 -250	- 10±100 -100±100	-0.04±0.5 -0.50±0.5	No measurement

[a] The values of the centre of gravity shift for ^{152}Sm, ^{166}Er, ^{182}W, ^{184}W, ^{186}W are taken from Ref. [34]. Those for ^{150}Nd and ^{154}Gd are calculated by Hüfner (private communication) using the value 0.2 for the feeding factor. The uncertainty is estimated to be ±10%.

[b] The Coulomb excitation on ^{150}Nd was carried out in the 8 MeV He^{++} beam of the Pegram Van de Graaff accelerator by E. Greenbaum, F. Hsu, Z. Y. Chow and R. Howes. The calibration lines used were the 137.16 and 122.6 keV lines of ^{186}Re.

[c] From Ref. [39]. Recently Hüfner has measured the 5f shielding effect in solids by observing the isotope shifts of ^{151}Eu and ^{153}Eu in CaF and found an increase of the electron density by a factor of 2.09 compared with the free atom. Hence $\Delta\langle r^2\rangle/\langle r^2\rangle = (+10 \times 10^{-4})/2.09 = +4.8 \times 10^{-4}$.

energy, since most of the radiative de-excitation takes place from the F = 3/2 substate. Since Dr. Grodzins will report on their work later in this Symposium, I will show you only our measured energy shifts with the corrections for the calculated magnetic shifts (Table II). The fractional changes of $\Delta\langle r^2\rangle/\langle r^2\rangle$ are calculated assuming only c changes and plotted against mass number A as shown in Fig. 9. It is very striking to see that all three nuclei, $^{150}_{60}$Nd, $^{152}_{62}$Sm, and $^{154}_{64}$Gd, known as soft rotators, have approximately equal large stretchings. The isomer effect of the rest nuclei, which are known as rigid rotators, drops down an order of magnitude from that of the soft rotators. The observed values of $\Delta\langle r^2\rangle/\langle r^2\rangle$ of these rigid rotators are only a small fraction of the value ($\sim 4\times 10^{-4}$) estimated in the framework of the rotation-vibration coupling model [35]. For the more detailed discussions, readers are referred to Refs [33], [36], and [37].

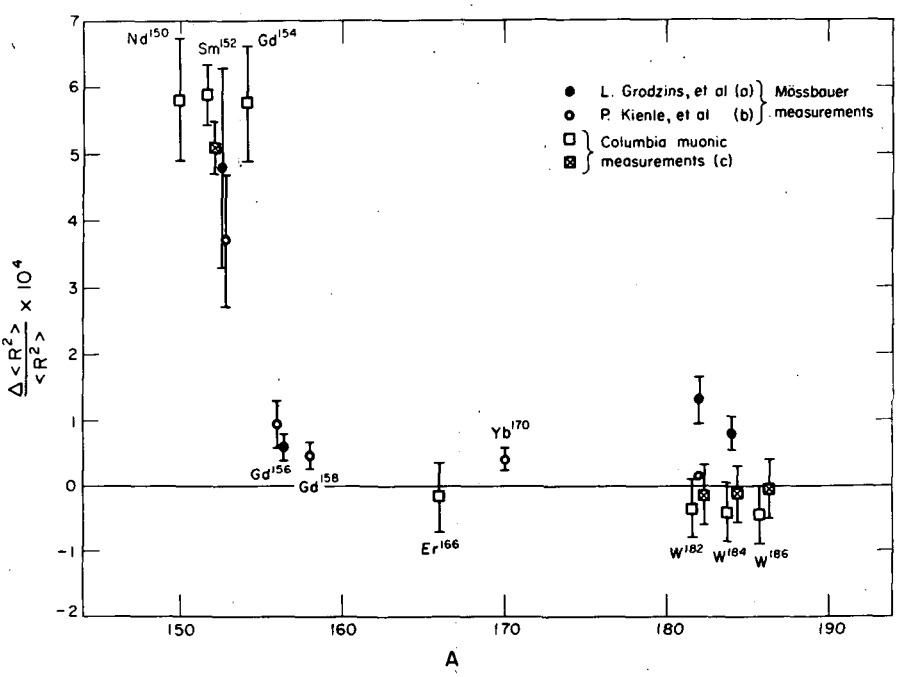

FIG. 9. $\Delta\langle r^2\rangle/\langle r^2\rangle$ plotted against mass number A for several even-even nuclei in the rare earth region. (a) Table II and Refs [35] and [37]; (b) Ref. [36]; (c) The two values of $\Delta\langle r^2\rangle/\langle r^2\rangle$ shown for ^{152}Sm represent two values of $\Delta E_{c.g.}$ corresponding to two different measurements of the g factor of the 2^+ state. The two values of $\Delta\langle r^2\rangle/\langle r^2\rangle$ shown for each of the W isotopes represent two values of $\Delta E_{c.g.}$ corresponding to N_I or O_I electron shell conversion ([7]).

The isomer effects observed by the Mössbauer technique are also plotted on the same figure for comparison (Fig. 9). It is gratifying to see that the agreement between them is good within the limits of experimental precision.

ACKNOWLEDGEMENTS

I wish to express my gratitude to the following members of the group, who made major contributions to the work discussed in this talk: E. R. Macagno D. Hitlin, R. Barrett (present address: Surrey University, London, U. K.), S. Bernow, I. Duerdoth, J. W. Kast, W. Y. Lee, K. Runge (present address: CERN, Geneva, Switzerland), S. Devons, J. Rainwater.

REFERENCES

[1] WHEELER, J. A., Phys. Rev. 92 (1953) 812; Rev. mod. Phys. 21 (1949) 133.
[2] FITCH, V. L., RAINWATER, J., Phys. Rev. 92 (1953) 789.
[3] TAVENDALE, A. J., Ann. Rev. nucl. Sci. 17 (1967) 73.
[4] KOPFERMANN, H., Nuclear Moments, Academic Press, New York (1958); BRIX, P., KOPFERMANN, H., Rev. mod. Phys. 30 (1958) 517; STACEY, D. N., Reports on Progress in Physics 29 Part 1 (1966) 171; GOLOVIN, A. F., STRIGANOV, A. R., Soviet Phys. Uspelski Translation 10 (1968) 658.
[5] SUMBAEV, O. I., PETROVICH, E. V., ZYKOV, V. S., RYLINKOV, A. S., GRUSHKO, A. I., Trans: Sov. J. nucl. Phys. 5 (1967) 387 (Nd Isotope Shifts); SUMBAEV, O. I., MEZENTSEV, A. F., Soviet Phys. J. E. T. P. 22 (1966) 323.
[6] CHESLER, R. B., BOEHM, F., BROCKMEIER, R. T., Phys. Rev. Lett. 18 (1967) 953; CHESLER, R. B., BOEHM, F., Phys. Rev. 166 (1968) 1206; BHATTACHERJEE, S. K., BOEHM, F., LEE, P., Phys. Rev. Lett. 20 (1968) 1295 (Nd isotope shifts).
[7] BAUCHE, J., C. r. hebd. Séanc. Acad. Sci., Paris 263 (1966) 685.
[8] BRIX, P., KOPFERMANN, H., Z. Phys. 126 (1949) 344.
[9] WILETS, L., HILL, D. L., FORD, K. W., Phys. Rev. 91 (1953) 1488.
[10] BODMER, A. R., Nucl. Phys. 9 (1958) 371.
[11] LANE, A. M., Phys. Rev. Lett. 8 (1962) 161.
[12] PEREY, F. G., SCHIFFER, J. P., Phys. Rev. Lett. 17 (1966) 324.
[13] ELTON, L. R. B., SWIFT, A., Williamsburg Conf. Intermediate Energy Physics (1966) 731.
[14] EHRLICH, R. D., FRYBERGER, D., JENSEN, D. A., NISSIM-SABAT, C., POWERS, R. J., TELEGDI, V. L., HARGRAVE, C. K., Phys. Rev. Lett. 18 (1967) 959; Phys. Rev. Lett. 19 (1967) 344 Erratum.
[15] MACAGNO, E. R., BERNOW, S., DEVONS, S., DUERDOTH, I., HITLIN, D., KAST, J. W., RAINWATER, J., RUNGE, K., WU, C. S., Proc. Int. Conf. Electromagnetic Sizes of Nuclei, Ottawa (May 1967) 71.
[16] BARDIN, T. T., COHEN, R. C., DEVONS, S., HITLIN, D., MACAGNO, E. R., RAINWATER, J., RUNGE, K., WU, C. S., BARRETT, R. C., Phys. Rev. 160 (1967) 1043; Progress Report of Pegram Nuclear Physics Laboratories, 1966 (NYO-GEN-72-28); 1967 (NYO-GEN-72-132), and 1968 (NYO-GEN-72-191).
[17] HANSEN, J. E., STENDEL, A., WALTHER, H., Z. Phys. 203 (1967) 296 (most extensive and precise); also DONTSOV, Yu. P., MAROZOR, V. A., STRIGONOV, A. R., Optics Spectrosc. 8 (1960) 391; NOLDEKE, G., STENDEL, A., Z. Phys. 137 (1954) 632; MURAKAWA, K., Phys. Rev. 96, 1543 (1954); GERSTENKORN, S., HELBERT, J-M., CHABBAL, R., C. r. hebd. Séanc. Acad. Sci. Paris 261 (1965) 1232.
[18] HEILIG, K., WENDLANDT, D., Phys. Lett. 25A (1967) 277.
[19] HUGHES, R. H., Phys. Rev. 121 (1961) 499.
[20] ARROE, H., CORNWALL, J. M., Phys. Rev. 117 (1960) 748.
[21] HOFSTADTER, R., Proc. Int. Conf. Nuclear Structure, Tokyo, (Sept. 1967).
[22] BETHE, H., ELTON, L. R. B., Phys. Rev. Lett. 20 (1968) 745.
[23] HITLIN, D., (Columbia University) private communication.
[24] CHEN, M. Y., Nuclear Polarization in Muonic Atoms, THESIS, Ph. D., Palmer Phys. Lab., Princeton University, Technical Report PUC-937-291 (Jan. 1968).
[25] SCHECK, F., Z. Phys. 172 (1963) 239.
[26] PIEPER, W., GREINER, W., Phys. Lett. 24B (1967) 377.
[27] COLE, R. K., Jr., Phys. Lett. 25B (1967) 178; also preprint ITP-306, Stanford University (Aug. 1968).
[28] ELTON, L. R. B., Nuclear Sizes, Oxford University Press, London (1961).

[29] VAN OOSTRUM, K.J., HOFSTADTER, R., NÖLDEKE, G.K., YEARIAN, M.R., CLARK, B.C., HERMAN, R., RAVENHALL, D.G., Phys. Rev. Lett. 16 (1966) 528.
[30] MACAGNO, E., BARRETT, R., BERNOW, S., DEVONS, S., DUERDOTH, I., HITLIN, D., KAST, J.W., RAINWATER, J., RUNGE, K., WU, C.S., Proc. Int. Conf. Electromagnetic Sizes of Nuclei, Ottawa (May 1967); also Progress Report of Pegram Nuclear Physics Laboratories, Columbia University, 1967 (NYO-GEN-72-132).
[31] BARDIN, T., BARRETT, R., COHEN, R., DEVONS, S., HITLIN, D., MACAGNO, E.R., NISSIM-SABAT, C., RAINWATER, J., RUNGE, K., WU, C.S., Phys. Rev. Lett. 16 (1966) 718.
[32] BERNOW, S., DEVONS, S., DUERDOTH, I., HITLIN, D., KAST, J.W., MACAGNO, E.R., RAINWATER, J., RUNGE, K., WU, C.S., Phys. Rev. Lett. 18 (1967) 787.
[33] BERNOW, S., DEVONS, S., DUERDOTH, I., HITLIN, D., KAST, J.W., LEE, W.Y., MACAGNO, E.R., RAINWATER, J., WU, C.S., Phys. Rev. Lett. 21 (1968) 457.
[34] GAL, A., GRODZINS, L., HÜFNER, J., Phys. Rev. Lett. 21 (1968) 453.
[35] MARSHALEK, E.R., Phys. Rev. Lett. 20 (1968) 214.
[36] KIENLE, P., HEMING, W., KAINDL, G., KÖRNER, H.J., SCHALLER, H., WAGNER, F., Proc. Int. Conf. Nuclear Structure, Tokyo, Japan (Sept. 1967) p. 207.
[37] GRODZINS, L., these proceedings
[38] BAADER, R., BECKE, H., ENGFER, R., HESSE, K., KANKELEIT, E., SCHRÖDER, U., WALTER, H.K., WIEN, K., Phys. Lett. 27B (1968) 425; ^{152}Sm (+0.50 ± 0.07), ^{182}W (-0.29±0.09), ^{184}W (-0.35 ± 0.07) ^{186}W (-0.40 ± 0.07), ^{188}Os (-0.41 ± 0.07), ^{190}Os (-0.47 ± 0.07), and ^{192}Os (-0.61 ± 0.07).
[39] GRODZINS, L., et al. Phys. Rev. Lett. 18 (1967) 791.

DISCUSSION

G.M. TEMMER: Could you comment on the present status of your knowledge of the shape of the nuclear charge distribution in deformed nuclei?

C.S. WU: For ^{182}W and ^{184}W a negative value of β' in the modified deformed Fermi charge distribution is required in order to obtain the calculated values of $Q_0(0, 2)$ comparable to that obtained from Coulomb excitation. When β' is negative, it implies that the skin thickness of the deformed Fermi distribution is thicker in the equatorial plane than at the poles. However, we have measured the E2 h.f.s. spectra of ^{150}Nd, ^{152}Sm, $^{162, 164}$Dy, $^{166, 170}$Er and ^{238}U; not all of them need negative β'. To reach any definite conclusion, one must try to interpret the results with different charge distribution with slight alterations of the density at the centre or at the shoulder as suggested by Bethe's recent papers.

D.F. ZARETSKY: 2p-1s transitions in the muonic atom with deformed nuclei are accompanied by excitement of the nucleus levels. The magnetic interaction of the muon with excited nuclei causes the hyperfine splitting of the nucleus levels (the estimate gives a value of about a few keV). Have you observed such splitting?

C.S. WU: The magnetic h.f.s. of the 2^+ level in deformed nuclei of the rare earth region is about 500 eV to 1 keV. Such a splitting has not been resolved and therefore has not been directly observed. However, its presence seems to have been observed in the negative shift of the isomer effect. Since I had no time to go into detail on this interesting subject, Dr. Grodzins will discuss this magnetic h.f.s. of the 2^+ level in his paper.

V.I. GOLDANSKY: Values of $\Delta\langle R^2\rangle/\langle R^2\rangle$ for a few isotopes of tungsten (^{182}W, ^{184}W, ^{186}W) have been obtained both from muonic experiments and the Mössbauer effect. The absolute values are small but they differ in sign; these values are positive in the Mössbauer experiments and negative in the muonic experiments. Are there any suggestions con-

cerning the reasons for the possible disagreement of the Mössbauer and the muonic interpretation of this problem?

C. S. WU: If one takes into account the asymmetries of the unresolved magnetic hyperfine structure of the gamma-rays, the negative shifts seem to disappear and the isomer shift results from the muonic method and Mössbauer technique can be reconciled.

A. FAESSLER: I would like to comment on the decrease of the root mean square radius in tungsten (W) as seen by the Mössbauer effect and by μ-mesonic atoms. This may be due to an anharmonicity in the β-vibrational potential. Baranger and Kumar did show that this potential is steeper for deformations larger than the equilibrium deformation than on the side for smaller deformations. If the nucleus is excited, the equilibrium will shift therefore to smaller values.

NUCLEON-NUCLEUS FORWARD DISPERSION RELATIONS

T.E.O. ERICSON AND M.P. LOCHER
EUROPEAN ORGANIZATION FOR NUCLEAR RESEARCH (CERN),
GENEVA, SWITZERLAND

Abstract — Аннотация

NUCLEON-NUCLEUS FORWARD DISPERSION RELATIONS. Elastic forward dispersion relations are illustrated by n-α scattering and preliminary results are given. Exchange effects are of great importance at low energies. This conclusion should be generally valid for light nuclei.

СООТНОШЕНИЯ ПРИ РАССЕЯНИИ ВПЕРЕД НУКЛОНА НА ЯДРЕ. Показываются соотношения при упругом рассеянии вперед с помощью n-, α-рассеяния и приводятся предварительные результаты. При низких энергиях важное значение имеют обменные эффекты. Обычно этот вывод справедлив для легких ядер.

Stimulated by our previous results [1] on the effective π-nucleus coupling constant in $T = \frac{1}{2}$ nuclei, we are at present applying forward dispersion relations (FDR) to nucleon-nucleus elastic scattering. Since total cross-sections are very similar above 20 MeV for all light elements we have chosen the technically simplest case of n-α scattering to demonstrate the method [one amplitude (spin and isospin zero), no negative energy resonances in the compound state, no Coulomb effects]. Our main conclusion is that the nucleus behaves like an elementary particle at high energies, whereas at low energies very important contributions come from the exchange channel, especially from the exchange of deeply bound systems (in the particular case of n-α scattering from ^{3}He exchange).

The once subtracted dispersion relation[1] for the forward n-α laboratory scattering amplitude is[2]

$$\mathrm{Re}\, f(E) = \mathrm{Re}\, f(0) + \frac{G^2 E}{(E_0 - E)E_0} - \frac{E}{\pi} P \int_{-2m}^{E_b} dE' \frac{\mathrm{Im}\, f(E')}{(E'-E)E'} + \frac{k^2}{2\pi^2} \int_0^\infty dk' \frac{\sigma(k')}{k'^2 - k^2}$$

$$- \frac{E}{4\pi^2} \int_0^\infty dE' \frac{[\bar{\sigma}(E') - \sigma(E)]k'}{(E'+E+2m)(E'+2m)} \qquad (1)$$

This exact formula is relativistic and completely general except for the pole term. For non-relativistic approximations one can neglect the last term($\sim \bar{\sigma} - \sigma$).

---

[1] For comparison with NN scattering see Ref.[2].

[2] Notation: E is the laboratory kinetic energy of the neutron (mass m), $k = (E^2 + 2mE)^{\frac{1}{2}}$ its momentum, f and $\bar{f}$ the n-α and $\bar{n}$-α amplitudes, σ and $\bar{\sigma}$ the corresponding total cross-sections, E_0 the ^{3}He pole position, G the pole residue, E_b the branch point of the unphysical cut. $\mathrm{Re}\, f(0) = (1 + m/m_{^4\mathrm{He}}) \times$ (scattering length), $d\sigma/d\Omega(0^0) = |f|^2$; $c = 1$.

The singularity structure of the unphysical region for n-α scattering is as follows:

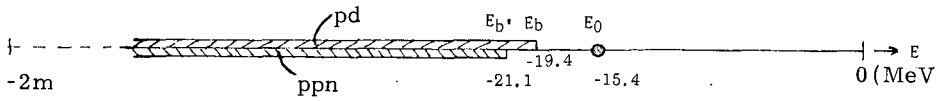

The pole term corresponds to ^{3}He exchange, with a position $E_0 = -15.4$ MeV. The sign of the pole is characteristic of the positive parity of ^{3}He.

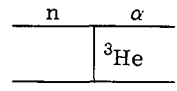

(In an elementary particle treatment of $n(\frac{1}{2}^+)\,^3He\,(\frac{1}{2}^+)\,^4He\,(0^+)$ the pole is analogous to that in Kp scattering [3]. Note that the correspondence is to pseudoscalar Kp scattering, because ^{3}He is a negative energy intermediate state. Our definition of G^2 includes the mass factors that are responsible for this sign dependence on parity.)

The exchange of more than one particle leads to cuts. The nearest branch point coming from pd exchange starts at $E_b = -19.4$ MeV. The exchange of ppn begins at $E_{b'} = -21.1$ MeV, whereas the cut corresponding to ^{3}He π^0 exchange starts at -120 MeV.

A number of accurate phase shift analyses [4] being available for $0 < E < 50$ MeV, we have studied Eq. (1) mainly in this energy region. To show the importance of the unphysical region, we have compared the dispersion integral from the physical region only, including the subtraction constant (dashed line in Fig. 1) to the real part of the amplitude from phase shift analysis [4] (solid line).

The total cross-sections are taken from Ref. [5]. The integral dependent on $(\bar{\sigma} - \sigma)$ has been neglected since it contributes less than 1% for $E < 50$ MeV under all reasonable parametrizations (note the suppression due to the large denominator > 4 m^2). The difference Δ (= solid minus dashed line) is very large and is shown in Fig. 2. If the ^{3}He pole of Eq. (1) is the dominating singularity, we expect the quantity E/Δ to be linear in E. Indeed, the linearity is striking (dashed line). Comparison with the pole term in (1) fixes the parameters as:

$$E_0 = -10 \text{ MeV} \qquad G^2 \cong 1.3 \qquad \text{or} \quad \frac{G^2}{E_0} \cong 25\text{F}$$

Note that the sign of G^2 is characteristic of the exchange of a particle of positive parity (cf. the remark further above). The shift of the pole position by 5 MeV, if it is a real effect, could be due to a negative contribution from the nearby cut. A comparatively large cancellation of the order of 50% would then be necessary.

An evaluation of Re f around 100 MeV, pole term included, still indicates missing contributions of the order of -4F which vary slowly with E. These

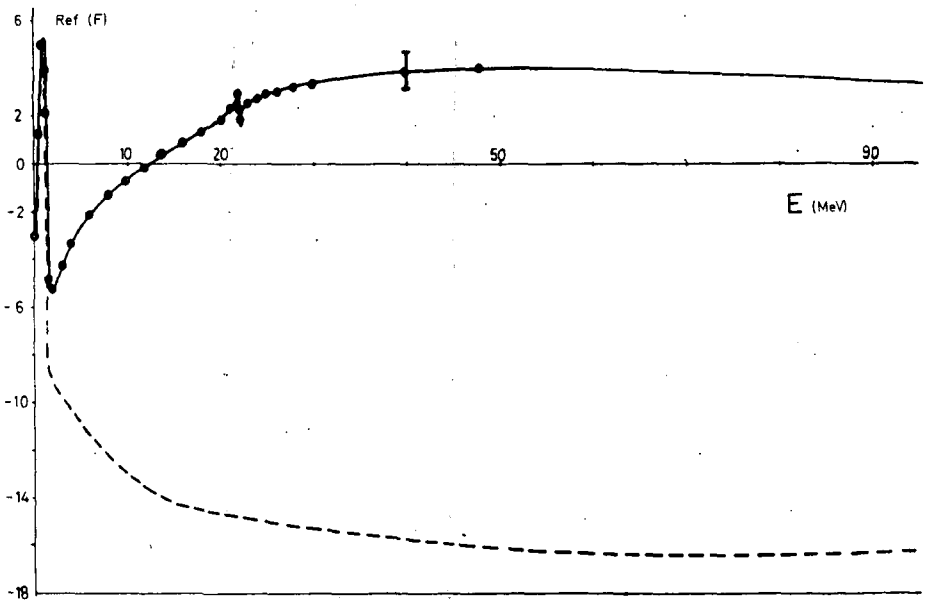

FIG. 1. The full points are Re f in n-α scattering from phase shifts [4]. The solid line is a smooth interpolation. The error bar is the estimated systematic error at 40 MeV. It is less at lower energies. The dashed line is the contribution to Re f from the physical region (see text) with Re f(0) = -3.04 F.

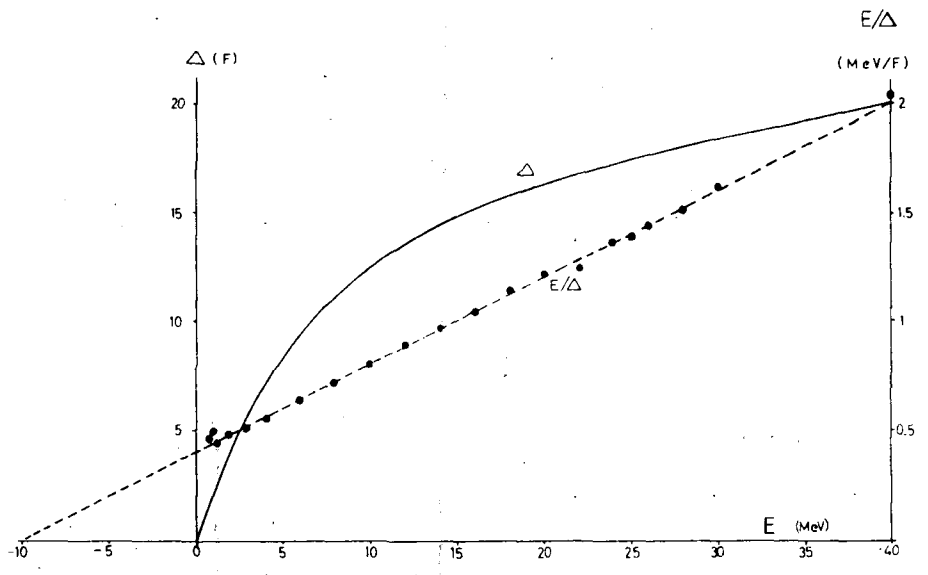

FIG. 2. The derived exchange amplitude Δ and the function E/Δ versus the kinetic energy E. Full points are directly related to phase shift analysis, while the dashed line is the pole extrapolation described in the text.

presumably come from more distant singularities like exchange of ^{3}He π, ^{3}He ρ (or ω or φ) etc. and are of the expected magnitude and sign. However, the experimental real part begins to be unreliable at these energies. In addition, the physical region of antiparticle cross-sections begins to contribute a few per cent to the dispersion integral. Therefore these statements must remain qualitative.

The exchange amplitude from ^{3}He of about 25F can be related to the reduced width for $^4\text{He} \to n + {}^3\text{He}$. With an interaction radius $R \cong 2F$ this is compatible with a reduced width $\gamma^2 \sim 1$; it should be noted, however, that the exponential penetration factor $\exp[\kappa R]$ is very large.

Since the total cross-sections have similar shape as for ^{4}He in other light elements, similar dispersion integrals occur leading to the general conclusion of very important exchange terms in nucleon-nucleus forward scattering amplitudes. It is interesting to ask how this is reconcilable with ordinary potential scattering. The explanation is the following theorem: scattering from an external real potential with some bound states occupied is identical to that from an unoccupied well, provided that the incident particle is identical to the bound ones and that the particles are non-interacting. Thus, the exchange contribution is exactly the contribution from the states which are occupied and hence blocked.

To establish the corresponding importance of exchange for other light nuclei, we are at present investigating n-^{12}C scattering, which has the additional complication of a few negative energy compound states.

REFERENCES

[1] ERICSON, T.E.O., FORMÁNEK, J., LOCHER, M.P., Phys.Lett. 26B (1967) 91.

[2] GOLDBERGER, M.L., NAMBU, Y., OEHME, R., Ann.Phys. 2 (1957) 226; SÖDING, P., Phys.Lett. 8 (1964) 285.

[3] AMATI, D., VITALE, B., Nuovo Cim. 7 (1958) 190.

[4] HOOP, B., BARSCHALL, H.H., Nucl.Phys. 83 (1966) 65; DAVIES, B.W. et al., Nucl.Phys. 97A (1967) 241; CROMER, A.H., PALMIERI, J.N., Ann.Phys. 30 (1964) 32.

[5] STEHN, J.R. et al., Brookhaven National Laboratory, BNL 325, Suppl. 2 (1964); MEASDAY, D.F., PALMIERI, J.N., Nucl.Phys. 85 (1966) 129; PALMIERI, J.N., GOLOSKIE, R., Nucl.Phys. 59 (1964) 253; RIDDIFORD, L., WILLIAMS, A.W., Proc. R. Soc. A257(1966) 316; IGO, G.J., et al. Nucl.Phys. B3 (1967) 181. For energies above 100 MeV, nucleon-^{12}C total cross-sections with scaling factors have also been used.

DISCUSSION

H. MELDNER: Since all your results depend on the assumed analyticity, I would like to ask about justifications. I understand from your paper that you are led to this particular assumption from its similarity to the NN amplitude analyticity via Glauber-type multiscattering approximations. However, taking the NN case as the single scattering term in this sense, you get the full amplitude as an infinite series of convolution integrals involving single terms. This way you generate a rather complicated cut structure. I wonder how you instead get this simple CDD pole plus cut? Another technical point: did you compute the integrals (up to infinity) as in the FESR game?

T.E.O. ERICSON: We have not been led to the analyticity structure by multiple scattering approximations. The structure of the dispersion relation is obtained directly from an analysis of the singularity structure of the amplitude. Of course, we do not pretend that the nucleon-nuclear and pion-nuclear dispersion relations are rigorous in the sense of axiomatic field theory, but even in high-energy physics dispersion relations are rarely proven, although they are extremely plausible. As far as nuclear physics is concerned, we can consider them to be exact.

The Glauber approximations enter only in an extremely minor way in the numerical evaluation of unmeasured high-energy total cross-sections awaiting direct experiments. There is ample evidence that the approximation is quite sufficient for our purpose since we could have approximated the high-energy cross-sections even more crudely. In the high-energy region we invoke that $\bar{\sigma}(E)$ and $\sigma(E)$ become equal (Pomeranchuk theorem), as everybody does.

Finally, I want once more to insist on the great simplification introduced in the analytical structure by considering only forward dispersion relations.

V.M. KOLYBASOV: If you neglect the contribution of the cut in the non-physical region and leave only the contribution of the pole, you obtain an excellent extrapolated straight line, but the pole position is strongly removed from the right one. However, we see the cut begins very close to the pole. It might happen that the conclusion you probably come to concerning the dominant contribution of the pole term in the non-physical region is not correct, and the cut gives the contribution comparable with or larger than the pole, but the extrapolated curve comes close to a straight line owing to the already-mentioned short distance between the cuts and the pole.

A.K. KERMAN: It is not surprising that your extrapolation did not come to the expected 15 MeV in view of the large distance to the pole. However, it may still be interesting to see the residue. Does it agree with what one expects for the tail of the single particle wave-function in ^{4}He?

T.E.O. ERICSON: This is exactly our conclusion. The exchange amplitude Δ is determined experimentally and simply plotted so as to give it a chance to display a single pole if there is one. The excellent straight line to a point where there manifestly is no pole should be a lesson to pologlogists. There should clearly be an important ^{3}He pole at -15 MeV. My statement was that we can 'explain' the absence of curvature to the eye between 0 and 40 MeV as well as the apparent pole at -10 MeV by introducing an additional pole to describe the cut. Its sign must be typical of negative parity exchange; its position can be anywhere from -20 MeV to -120 MeV, if parameters are chosen corresponding to 0 to 100 MeV excitation of ^{3}He. The problem is that ^{4}He structure is well understood and there is not much place for such rather strong negative parity strength in the cut. There is no evidence at all of an enhancement of any kind or even of any strength in the cut in knockout reactions of a proton from ^{4}He (i.e. p, 2p experiments) in the first 20 MeV of the continuum. This is why it is a challenge to find out the origin of the continuum ^{3}He contribution.

C.F. CLEMENT: In connection with the use of dispersion relations in nuclear physics it is important to ask the question whether they can be derived from the conventional potential theory used to describe nuclear reactions. Alternatively, we can ask whether the theories are equivalent

and, if not, in what respect they differ. One of the reasons why dispersion relations have not been used successfully in the past in nuclear reactions is that it has been found difficult to show that they can reproduce such characteristic features as strong absorption.

T.E.O. ERICSON: Absorption is directly included in the dispersion relations by the total cross-sections so that its effects in the forward Re f appears immediately. The dispersion theory should be more general than potential theory, which represents a special case. Even so, the two approaches differ in the kinematical recoil effects associated with the bound state scattering as compared to exchange effects in the dispersion relation (the difference is small for heavy elements but not for ^{4}He).

It should be added that we do not even attempt to describe diffraction scattering produced by strong absorption at present. These phenomena involve non-forward scattering. For a loosely bound system new singularities called anomalous thresholds then appear. The study of these effects is extremely interesting although much more difficult and ambitious. We believe it is important to first understand the simplest situations in full detail before tackling this more ambitious problem.

Gy. BENCZE: Lipperheide at Berlin has recently investigated the analytical properties of the generalized optical potential and by assuming causality has obtained a dispersion relation between the real and imaginary parts of the potential. This relationship was then used to check the consistency of optical model potentials obtained from phenomenological analyses. Now my question is, what is the advantage of your using the scattering amplitude rather than the generalized optical potential? Does not the study of the generalized optical potential reveal more features of reaction mechanisms in nuclear physics?

T.E.O. ERICSON: While it is interesting to study the dispersive properties of an optical potential it must be clearly realized that this potential is a theoretical object derived under specific assumptions. I doubt whether Lipperheide's potentials include relativistic effects exactly. Furthermore, you have the difficulty of uniquely determining this potential from experiments without highly specific additional assumptions. The advantage of the scattering amplitude is that it is a directly measurable physical quantity. The lack of ambiguity here seems to me an enormous advantage.

HYPERFINE MAGNETIC FIELDS ON MOVING ATOMS IN FERROMAGNETIC MEDIA

L. GRODZINS
MASSACHUSETTS INSTITUTE OF TECHNOLOGY,
CAMBRIDGE, MASS., UNITED STATES OF AMERICA
AND
A. WINTHER
THE NIELS BOHR INSTITUTE,
UNIVERSITY OF COPENHAGEN,
COPENHAGEN, DENMARK

Abstract — Аннотация

HYPERFINE MAGNETIC FIELDS ON MOVING ATOMS IN FERROMAGNETIC MEDIA. Strong transient magnetic fields have been shown to act on moving ions during slowing down in ferromagnetic materials. A summary of the experimental evidence is given together with a short description of a theoretical model.

ВЛИЯНИЕ МАГНИТНЫХ ПОЛЕЙ НА ДВИЖУЩИЕСЯ АТОМЫ В ФЕРРОМАГНИТНЫХ СРЕДАХ. Показано влияние сильных переходных магнитных полей на движущиеся ионы при их замедлении в ферромагнитных материалах. Приводятся результаты экспериментов вместе с кратким описанием теоретической модели.

In this report we describe some of the recent observations of hyperfine fields on moving ions in ferromagnetic media and summarize the first-order theory which seems to account for many of the properties of the observed magnetic fields. The shortness of this report is justified by the extensive descriptions of these experiments published early in 1968 [1-3], as well as by the forthcoming papers describing recent developments in theory [4] and experiment [5, 6].

The experiments at the University of Wisconsin Tandem Accelerator were carried out on isotopes from iron to mercury using the technique (IMPAC) of Coulomb excitation with heavy ions and consequent implantation of the recoiling nuclei into various backings. The schematic drawing of the apparatus shown in Fig. 1 has been displayed many times. An oxygen beam of approximately 35 MeV strikes a thin target which has been evaporated onto an appropriate backing, the back-scattered oxygen particles being detected in a surface barrier heavy-ion detector. The γ-rays from states Coulomb excited by these back-scattered oxygen particles are detected in four movable co-planar counters. For ferromagnetic foils a magnetizing field perpendicular to the counter plan is provided.

Typical precession results, again well-described in the literature [7], are shown in Fig. 2, for the 334 keV, 0.07 ns state of ^{150}Sm in polarized Fe, Ni, Co, and Gd backings. The data are fitted by theoretical curves, assuming that there is no attenuation of the gamma ray other than that from a single-values magnetic field. Such results as those of Fig. 2 give confidence that the IMPAC technique is reliable for states living as short as a few tenths of a nanosecond.

For nuclear states of shorter lifetimes, one generally determines the Larmor precession angle, $\omega_L\tau$, from the effect of magnetic field flip at the maximum anisotropy of the gamma-ray angular distribution since the attenuation of the angular distributions, being proportional to $[1+(\omega\tau)^2]^{-1}$, is negligible. For such short-lived states a comparison of the precession angles, $(\omega_L\tau)_{IMPAC}$, with the corresponding values now measured by using radioactive sources in iron is given in Fig. 3. The references to the radioactivity data may be found in Ref. [2]. The radioactivity precession angles do not agree with those observed by IMPAC. (For states living longer than nanosecs, however, the agreement is good [2].)

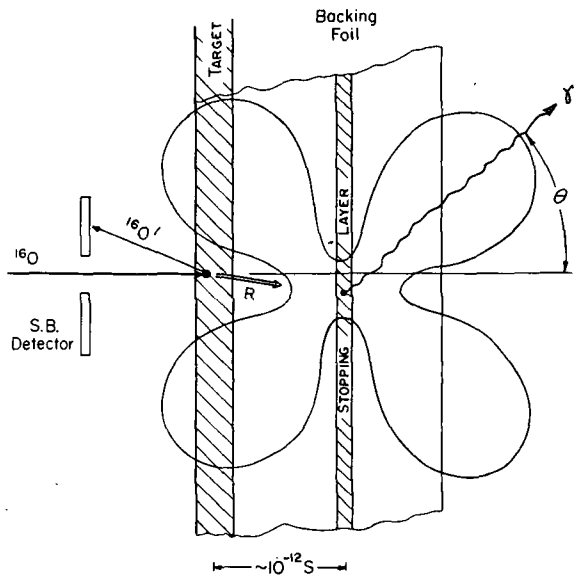

FIG. 1. Schematic diagram of IMPAC technique apparatus.

Many features of the anomalous hyperfine field are evident in the precession results for 2^+ states of ^{70,72,74,76}Ge (see Fig. 4 [6]). The values of $(\omega_L\tau)_{IMPAC}$ are essentially independent of the lifetimes of the states. Moreover, the precessions in Fe backings are uniformly greater in magnitude than those in Ni backings. The static magnetic fields [8], $H_{Ge}(Fe) = +70 \pm 3$ kG and $G_{Ge}(Ni) = +30 \pm 3$ kG, are small and result in negligible precessions for the 1.8 ps, 2^+ state of ^{70}Ge. Clearly, then, we are dealing with a transient magnetic field which takes place in less than 1.8 ps. Moreover, the evidence of Fig. 4 corroborates previous evidence [9] that the transient hyperfine field is proportional to the host magnetic moment (or to the conduction electron polarization).

In Ref. [1], a series of sandwich target experiments were described which showed quite clearly that there is a velocity dependence to this transient hyperfine field and that much of the effect occurs at low velocity. Rather than repeat this description, we describe a particularly elegant experiment now being carried out at the Niels Bohr Institute Tandem Accelerator by Herskind and co-workers [5], wherein the transient hyperfine field

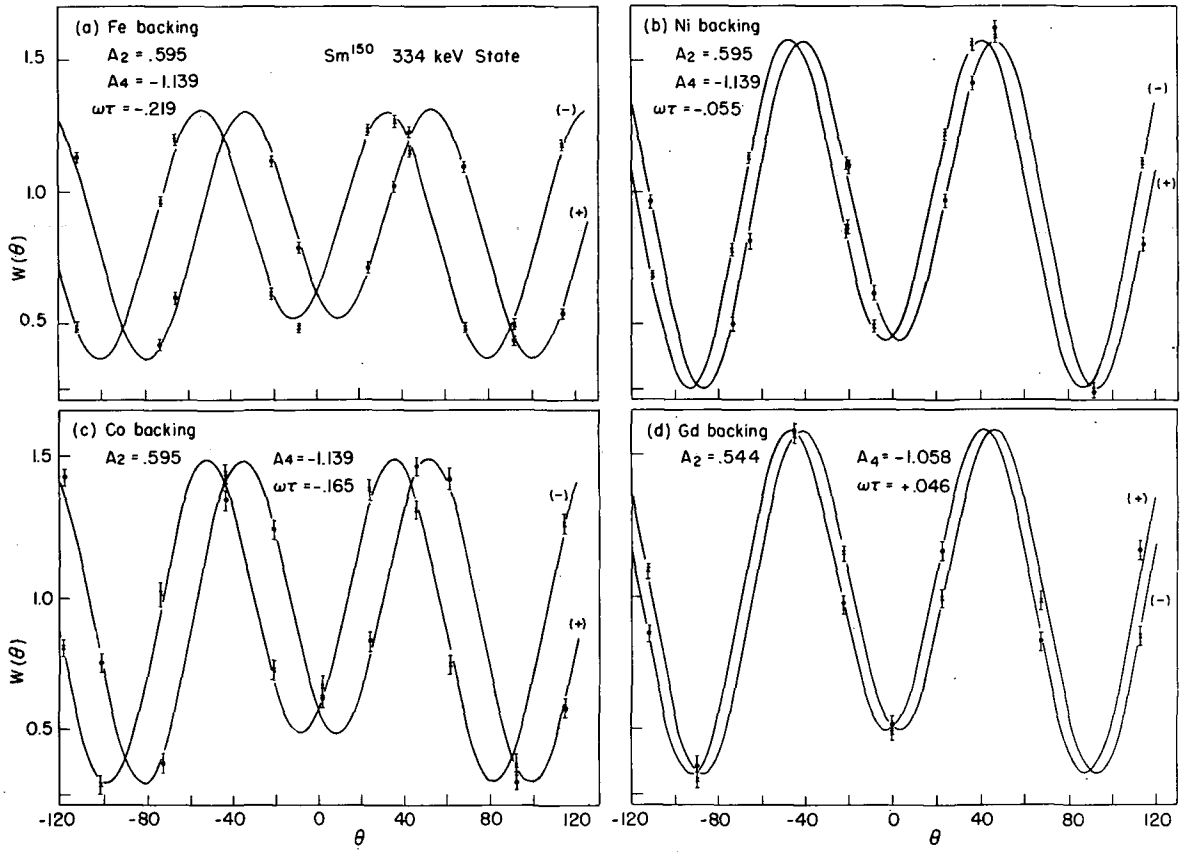

FIG. 2. Typical precession results for the 334 keV, 0.07 ns state of ^{150}Sm in polarized Fe, Ni, Co, and Gd backings.

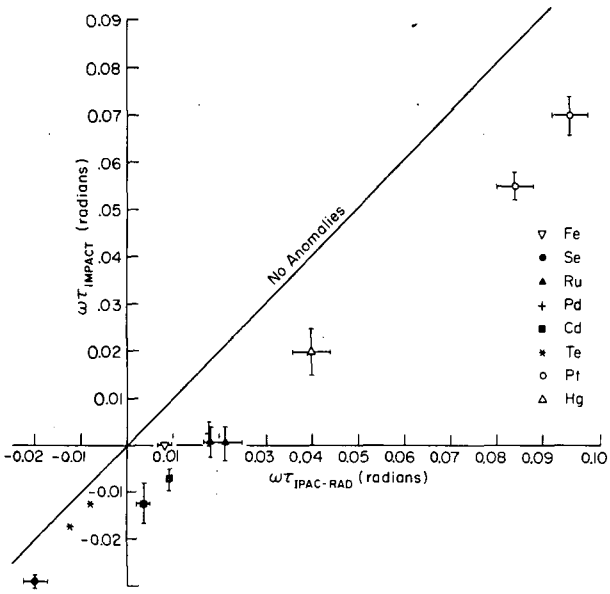

FIG. 3. Comparison of precession angles $(\omega_L \bar{\tau})_{IMPAC}$ with the corresponding values measured by using radioactive sources in iron.

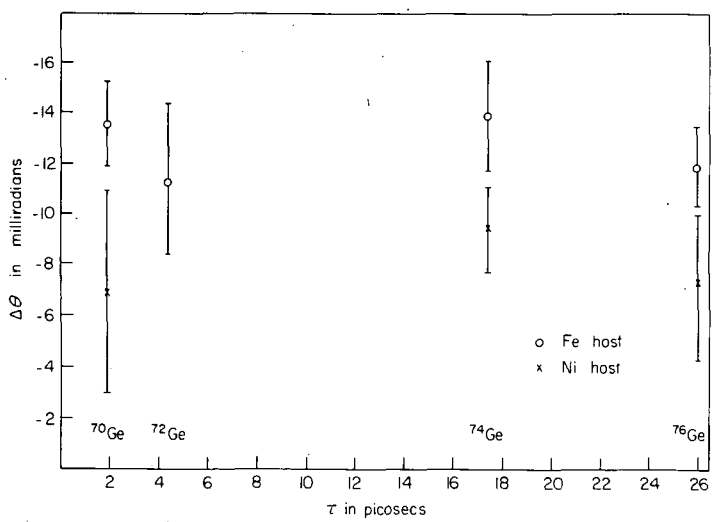

FIG. 4. $\Delta\theta$ data for Fe and Ni hosts.

on ^{56}Fe recoiling through an iron lattice is being isolated and measured. The preliminary results presented here have already been confirmed by Borchers et al. [10].

A series of experiments [3, 11, 12] have shown that the transient precession for the 10 ps, 856 keV state of ^{56}Fe recoiling in Fe is, accidentally, just equal and opposite to the static precession. Thus, unless the recoil velocity is very small [11], the observed precession is essentially zero. To isolate the transient hyperfine field, Herskind et al. [5] used a rolled 2.8 mg/cm^2 iron target onto which a Cu backing of ~3 mg/cm^2 was evaporated. Herskind made use of the fact that the energy of the back-scattered oxygen particles reflects the depth at which the Coulomb excitation takes place in the iron target, thus making it possible, in one experiment, to sort and measure the precession of recoils which stop in the Fe target itself (created in the front of the Fe layer) from those created nearer to the Fe-Cu interface, and thus spending the last portion of their flight in copper. The early results are shown in Fig. 5. The negative values of $\omega\tau$ correspond to positive hyperfine fields. One sees that the maximum of the transient precession occurs at very low velocities where the Fe recoils just stop in the Cu by the Fe-Cu interface. Similar experiments are in progress on other elements.

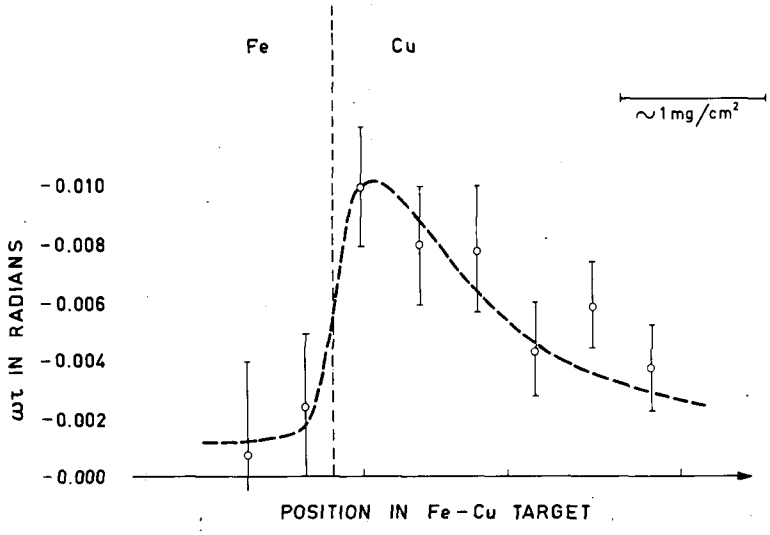

FIG. 5. Total rotation angle as a function of stopped ^{56}Fe recoils in Fe-Cu target. (Preliminary data of Herskind et al.).

We shall now summarize the systematics obtained on the transient hyperfine magnetic field by Borchers, Bronson, Grodzins, Heestand, Herskind, Kalish and Murnick at the Wisconsin accelerator.

1. The transient field is always positive. Independent of whether the static field is positive or negative, the transient field is in the direction of the applied field.
2. The transient field acts primarily on the moving ion.
3. The magnitude of the transient field may be expressed by the equation $H\tau \simeq 0.2\,Z$ megagauss-picoseconds. From the sandwich experiments

above, it is reasonable to conclude that the time over which the transient field acts is approximately a third of a picosecond so that $H_T \simeq 0.6\,Z$ megagauss.

4. The transient field is roughly proportional to the atomic magnetic moment of the host. The data are also consistent with the transient field being proportional to the polarization of the conduction electrons.
5. A transient hyperfine field exists when the backing foil is Gd though the transient precession is smaller than that with Ni [12]. This too is in keeping with the idea that the transient field is proportional to the conduction electron polarization.
6. The possible existence of a transient precession when rare earths are recoiled into Fe is a completely open question at the present time.

Finally, a few comments on the theory of transient fields as suggested by Lindhard [13].

A heavy ion which moves through a solid with moderate velocities is subject to two types of collisions: nuclear collisions where momentum and energy are transferred to the atoms as a whole, and electronic collisions where electrons are excited or ejected from the atoms along the path. For low velocities, the nuclear collisions are responsible for the main part of the rather constant specific energy loss.

An essential feature in the description of these processes is the average field surrounding the ion. The field is a screened Coulomb field where the screening is partly due to electrons bound by the ion and partly to electrons which are scattered by the ion. The field is a rather smooth function of the velocity which, at small velocities, approaches the Thomas-Fermi field of a free atom with a screening radius of

$$a \simeq a_0 / Z_1^{1/3}$$

where a_0 is the Bohr radius and Z_1 is the ion charge.

The ions with an energy larger than, say, 10 keV move rather freely in the lattice, and atomic electrons except the strongly bound ones will be scattered in the field. In this scattering, the electron density at the ion will be amplified as compared to the average electron density by a factor of the order

$$\zeta = \frac{2\pi\eta}{1 - e^{-2\pi\eta}} \simeq 2\pi\eta = \frac{2\pi Z_1 e^2}{\hbar v_r}$$

where v_r is the relative velocity of electron and ion. This estimate, which is accurate for a plane wave scattered in a pure Coulomb field, may not be too bad since the K-radius a_0/Z_1 is much smaller than a.

For low ion velocities, $\langle 1/v_r \rangle$ may be of the order of $1/v_0$; the amplification factor is of the order of several hundred. Since the magnetic field at the ion is approximately proportional to the density of polarized electrons at the nucleus, the average magnetic field in iron of, say, 2×10^4 G may be amplified to several megagauss.

To calculate in detail the precession of the nucleus during slowing down, we must evaluate the average Larmor precession and integrate it over the stopping time until the ion is so slow that it cannot penetrate into the polarized 1d electrons in the ion lattice. The result of rather preliminary estimates shows reasonable agreement with the above-mentioned experimental results both in regard to the absolute magnitude and to the dependence on ion charge, lifetime, and range.

REFERENCES

[1] BORCHERS, R.R., HERSKIND, B., BRONSON, J.D., GRODZINS, L., KALISH, R., MURNICK, D.E., Phys. Rev. Lett. 20 (1968) 424.
[2] GRODZINS, L., Hyperfine Structure and Nuclear Radiations (MATTHIAS, E., SHIRLEY, D., Eds) North-Holland, Amsterdam (1968) 607.
[3] HERSKIND, B., BORCHERS, R.R., BRONSON, J.D., MURNICK, D., GRODZINS, L., KALISH, R., Hyperfine Structure and Nuclear Radiations (MATTHIAS, E., SHIRLEY, D., Eds) North-Holland, Amsterdam (1968) 735.
[4] LINDHARD, J., WINTHER, A., to be published.
[5] HERSKIND, B., HAGEMANN, K.A., MURNICK, D., to be published.
[6] HEESTAND, G., BORCHERS, R., HERSKIND, B., GRODZINS, L., KALISH, R., MURNICK, D., to be published.
[7] MURNICK, D.E., GRODZINS, L., BRONSON, J.D., HERSKIND, B., BORCHERS, R.R., Phys. Rev. 163 (1967) 254.
[8] MORGENSTERN, J., private communication.
[9] MURNICK, D., GRODZINS, L., KALISH, R., BORCHERS, R.R., BRONSON, J., HERSKIND, B., Hyperfine Structure and Nuclear Radiations (MATTHIAS, E., SHIRLEY, D., Eds) North-Holland, Amsterdam (1968) 503.
[10] BORCHERS, R., private communication.
[11] MURNICK, D., MacDONALD, J.R., BORCHERS, R., HEESTAND, G., HERSKIND, B., Proc. R. Soc., to be published.
[12] KALISH, R., KOSSLER, W.J., Phys. Rev. Lett. 20 (1968) 271.
[13] LINDHARD, J., Proc. Meeting on Ion Implantation and Hyperfine Interactions, Royal Society London (May 1968).

IV

EQUILIBRIUM DEFORMATIONS

Chairmen	Secretaries
S. GORODETZKY	V.V. PASHKEVICH
G.N. FLEROV	V.A. DRUIN
L.N. USACHEV	Yu.P. GANGRSKY

EQUILIBRIUM DEFORMATIONS OF THE GROUND AND EXCITED STATES IN NUCLEI

Z. SZYMANSKI
INSTITUTE FOR NUCLEAR RESEARCH
AND
UNIVERSITY OF WARSAW, POLAND

Abstract — Аннотация

EQUILIBRIUM DEFORMATIONS OF THE GROUND AND EXCITED STATES IN NUCLEI. The deformations of atomic nuclei, i.e. the deviations of their shape from the spherical one, are discussed. An attempt is made to understand the origin and nature of deformation. Various aspects of the problem such as axial symmetry, higher multipole (hexadecapole) components, deformations of the excited states, potential and kinetic energy in the fission process, etc. are discussed.

РАВНОВЕСНЫЕ ДЕФОРМАЦИИ ОСНОВНЫХ И ВОЗБУЖДЕННЫХ СОСТОЯНИЙ ЯДЕР. Рассматриваются деформации атомных ядер, т.е. отклонения их формы от сферической. Сделана попытка понять причину и природу деформаций. Обсуждаются различные аспекты проблемы, как, например, аксиальная симметрия, высшие мультипольные (гексадекапольные) компоненты, деформации возбужденных состояний, потенциальная и кинетическая энергия в процессах деления и др.

1. INTRODUCTION

A great amount of experimental data confirms the assumption that the spatial distribution of nucleons in some atomic nuclei differs appreciably from a spherical distribution. The well-known rotational properties of the spectra in these nuclei seem to be a good criterion for the existence of the nuclear equilibrium deformation from a sphere. The Coulomb excitation experiments as well as the hfs measurements of the atomic spectra are the main evidence used for the quantitative determination of the magnitude of nuclear deformation. The "classical" regions of the deformed nuclei such as the rare earth, actinide, and light element regions ($A \sim 24$) have been well established. The quadrupole (or ellipsoidal) character of the nuclear shape has been concluded, as also the axial symmetry and the positive sign of the deformation parameter (prolate shape). The equation for the nuclear surface (or the equipotential surface)

$$R = R_0 (1 + \beta_2 Y_{20} + \beta_4 Y_{40} + \dots) \qquad (1)$$

serves as a definition of deformation parameters β_2, $\beta_4 \dots$ (Another parametrization is defined by Eq. (2)). The non-axial quadrupole deformation parameter γ is usually introduced by adding a term $(1/\sqrt{2})\, \beta_2 \sin\gamma\, (Y_{22} + Y_{2-2})$ to the right-hand side of Eq. (1) and at the same time by replacing β_2 by $\beta_2 \cos\gamma$.

In recent years great progress in the experimental investigation of nuclear shapes has been made. Completely new techniques such as the X-ray measurements of μ-mesic atoms or inelastic scattering of particles have been employed. The amount of information has been considerably

enriched. Moreover, a large number of new problems related to nuclear shape have been attacked. The behaviour of nuclei in the transition regions; the existence of non-axial and oblate deformations; the other than quadrupole (P_2) components in nuclear deformation, especially the hexadecapole component (P_4); the new regions of deformed nuclei lying off the stability line; the extension of the investigations into very large deformation regions (related to fission); these are all examples of the new lines of investigation.

Let us briefly recall the basic theoretical assumptions and methods used in the deformation calculation. The proper calculation should be based on the nuclear two-body force. Unfortunately, such a calculation would be too complicated as it would require the solution of the many-body problem. Therefore, the existing calculations are mainly confined to the framework of the independent particle assumption. The average nuclear deformed potential is then introduced and the nuclear wave-function can be determined from the equation of motion. Finally, the spatial shape of the density distribution can be found. In the state of equilibrium the deformation of the calculated density should overlap with the deformation of the potential assumed initially. Such a condition of self-consistency can thus be used for the determination of the equilibrium state in the nucleus. The method of calculation described above proves, however, very inefficient in practice, as it turns out that the self-consistency condition is approximately valid almost in the whole region of reasonable deformations. Thus, the determination of the equilibrium from the self-consistency condition becomes very inexact. A simple method commonly used is one that consists in the summation of the single-particle energies for each deformation. The total energy calculated in this way can then be minimized with respect to deformation. In this method, however, the potential energy, and in particular the part of it that depends on deformation, is counted twice as the true nuclear potential energy has a two-body character. Bohr and Mottelson have elucidated this point in their book [1]. Their conclusion is that the minimum in the single-particle energy curve really corresponds to the self-consistent point under the condition that the nuclear potential fulfils the requirements of a constant volume, i.e. the equipotential surface should enclose regions of constant volume for any deformation.

The method of summing up the single-particle energies with the constant volume condition has been used in the pioneer work of Mottelson and Nilsson [2]. In this work the anisotropic harmonic oscillator single nucleon potential, completed by the $\vec{l} \cdot \vec{s}$ and $\vec{l}^2$ term, has been used [3] (see Eq. (2)). Later on, the effect of the short-range residual nuclear interaction has been included in the considerations [4, 5]. Such short-range pairing forces tend to couple nucleons in pairs with total angular momentum equal to zero. It turns out that they are more effective in the spherical nuclei than in the deformed ones. Thus pairing forces restore spherical symmetry in nuclei with only few nucleons outside closed shells while they reduce appreciably the deformation energy (i.e. the difference in total energy between the spherical and equilibrium case) in nuclei with pronounced deformation.

The calculations with the 1955 Nilsson potential [3] including pairing forces have led to a serious difficulty [4]. In the transition region, for example the vicinity of the Sm isotopes, it has proved impossible to get reasonable results for the equilibrium deformation. This is illustrated in Fig. 1. To avoid the monotonic decrease of the total nuclear energy with deformation an illegitimate procedure of shifting the major harmonic oscillator shells has been used [4] to restore the existence of equilibrium.

In 1966 Gustafson et al. [6] noticed that the presence of the negative $\vec{l}^2$ term in the old 1955 Nilsson potential leads to the artificial condensation of the major harmonic oscillator shells. The appropriate shell distance can be restored when the $\vec{l}^2$ term is corrected by the subtraction of a constant term $\langle \vec{l}^2 \rangle_{av}$, the average value being taken over each major shell separately. The calculations made with this new potential proved to be much more satisfactory, although the results for deformation appeared somewhat on the lower side (see Fig. 1).

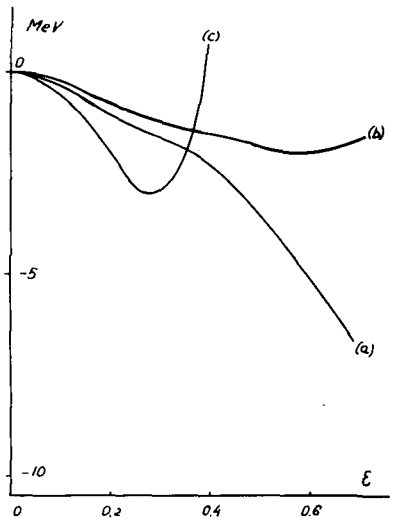

FIG. 1. Total energy for the ^{152}Sm nucleus plotted against deformation parameter ϵ. For the definition of the parameter ϵ see Eq. (2). Curve (a) corresponds to the 1955 Nilsson potential [3] without any modifications. Curve (b) includes also the level shifts [4]. Curve (c) corresponds to the new Nilsson potential [6]. Pairing interactions have been included in all three cases.

An alternative procedure for overcoming this difficulty has been suggested by Baranger and Kumar [5]. By comparing the matrix elements of the quadrupole force to the more realistic ones they conclude that the summation of the contributions to the total energy should be limited to a certain number of states lying not too far from the Fermi surface.

Another possible way of improving the calculations in the transition region consists in using the projected BCS functions corresponding to a fixed number of particles [7]. Of course the use of more realistic (as compared with the harmonic oscillator) potentials should be investigated in the deformation problem. For example, a deformed Saxon-Woods potential has been suggested. Preliminary attempts have been made in this direction [8].

The development of experimental techniques in nuclear reactions such as inelastic scattering permits the investigations to be extended to other than P_2-components of deformation. In particular, the experimental determination of the P_4-component (hexadecapole) is now possible. Rough estimates of the P_4 deformations can be obtained from precise experiments on the Coulomb excitation of the rotational states in deformed nuclei. For the pure quadrupole deformation, only the first state (2^+) in the rotational

band can be excited. The second state (4^+) can only be reached by a double Coulomb excitation. However, the existence of a hexadecapole component in the nuclear shape permits direct excitation of the 4^+ state. Hence, the exact balance of the single and double excitations enables the determination of the existing P_4 deformation [9].

Similar arguments were used in the recent experiments by Hendrie et al. [10] on inelastic alpha particle scattering on deformed nuclei. Here, the method consisted in the measurement of the differential cross-section and appeared to be much more efficient as the alpha particles carry high enough momentum for direct transfer of large units of angular momenta to be possible. The calculation of nuclear equilibrium in both the quadrupole and hexadecapole components has been recently performed [11]. The calculation uses the Nilsson potential completed by the addition of a new term proportional to P_4. This potential is then given by the following expression:

$$V = \tfrac{1}{2}\hbar\omega_0(\epsilon,\epsilon_4)\rho^2(1 - \tfrac{2}{3}\epsilon P_2 + 2\epsilon_4 P_4)$$

$$- 2\kappa\hbar\mathring{\omega}_0[\vec{l}_t\cdot\vec{s} + \frac{\mu}{2}(\vec{l}_t^{\,2} - \langle\vec{l}_t^{\,2}\rangle_N)] \qquad (2)$$

where $\rho^2 = \xi^2 + \eta^2 + \zeta^2$ and $\vec{l}_t$ as well as the arguments of P_2 and P_4 are defined in the "stretched co-ordinate" system of Ref. [3]:

$$\xi = x\sqrt{\frac{M\omega_0}{\hbar}(1+\frac{1}{3}\epsilon)}; \quad \eta = y\sqrt{\frac{M\omega_0}{\hbar}(1+\frac{1}{3}\epsilon)}; \quad \zeta = z\sqrt{\frac{M\omega_0}{\hbar}(1-\frac{2}{3}\epsilon)}$$

and the dependence of $\hbar\bar{\omega}_0(\epsilon, \epsilon_4)$ on ϵ and ϵ_4 is fixed by the condition that equipotential surfaces enclose a space of constant volume independent of deformation. The P_4 term couples the major harmonic oscillator shell N to N ± 2. The polarization of the states due to this coupling turns out to be important so that no perturbation treatment of the P_4 term seems to be valid.

Thus, the diagonalization of the single-particle Hamiltonian involves all the harmonic oscillator shells up to a certain N_{max} value used to cut off the rank of matrices. Figs 2 and 3 present the results of the calculation for the rare earth and actinide regions, respectively. Fig. 2 contains in addition the experimental determinations taken from Ref. [10]. It can be seen that the agreement is quite satisfactory.

The possibility of the existence of the octupole (P_3) component in nuclear equilibrium shape has also been the subject of recent considerations [12].

The dependence of nuclear energy on the non-axial deviation in the quadrupole deformation as well as the question of the possible choice between a prolate and oblate shape has also been the subject of recent discussions. Calculations by Arseniev et al. [13] show that the total nuclear energy in the rare earth region plotted against deformation exhibits two minima (Fig. 4) for the positive and negative deformation parameters, a result in line with previous investigations [5]. However, the oblate minimum does not seem to be a stable one as no significant barrier in energy appears when going from one minimum to the other via gamma deformation (Fig. 5). In other regions, however, for example the region of non-stable

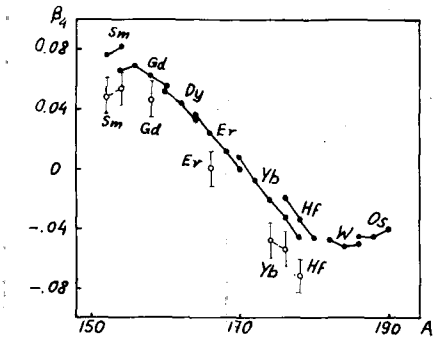

FIG.2. The equilibrium hexadecapole deformations for nuclei in the rare earth region. The solid line with black circles refers to the theoretical results [11]. Open circles correspond to the experimental values obtained by Hendrie et al. [10]. The figure is taken from Ref. [11].

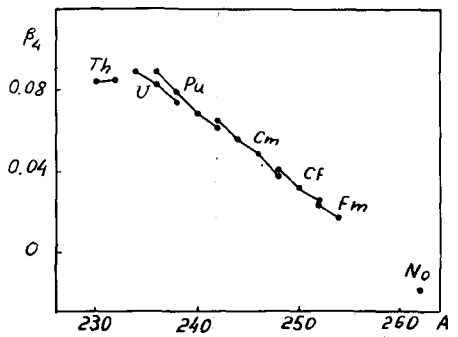

FIG.3. Theoretical results [11] for the equilibrium hexadecapole parameters for the actinide region. The figure is taken from Ref. [11].

nuclei with both N and Z lying between 50 and 82, the existence of an oblate deformation does not seem to be excluded [14].

An interesting question is: how does the nuclear shape change when the nucleus itself is excited? For example, the last odd particle in the odd-A nuclei can be shifted from the lowest available orbit to one of the next orbits. Then, the calculated change of nuclear deformation seems to be of the order of a few percent of the ground-state deformation in the well-deformed region [15]. Slightly lower deformation changes of the order of a few per mille (‰) are expected for the collective rotational excitations of nuclei [16]. The isotope shift studies are a valuable source of experimental information on this kind of nuclear deformability [17]. In the region of transition between spherical and deformed nuclei, where the curve of total nuclear energy plotted versus deformation becomes very flat, appreciable changes in nuclear shape are not excluded for the excited states. This could be a possible explanation of the existence of shape isomers in some nuclei [14]. The shape isomers can also occur in the middle of the deformed region if the nuclei are soft enough with respect to non-axial distortion [14].

The well-known phenomenon of nuclear fission is connected with a drastic change in nuclear shape, leading finally to the scission of the

nucleus into two or more parts. Investigations of the fission threshold in various nuclear reactions permit the determination of the height of the barrier of the nuclear potential energy, i.e. the total nuclear energy minus the kinetic energy of the collective motion in the fission channel.

On the other hand, the measurements of the life-time for spontaneous fission characterize the dynamics of the process. This characteristic is closely connected with the kinetic energy involved in the rate of change in nuclear distortion.

The main problem in the investigation of the nuclear potential energy consists in the proper extrapolation of the single-particle potential parameter into the region of very large distortions, possibly involving several components of various multipolarities. The well-known potentials, such as the Nilsson potential given by Eq. (2), that fit very well almost all the data in the equilibrium region, may behave very violently when extended over the large distortion region. Let us first consider a very simple potential of the anisotropic harmonic oscillator. The behaviour of the potential energy of the heavy nucleus is presented in Fig. 6. The curves show first of all the pronounced asymmetry with respect to the prolate and oblate sides. The very steep decrease of the energy for large positive deformations is found to result mainly from the influence of Coulomb energy in accordance with the expectations of the role of electric repulsion in fission. The addition of the $\vec{l}^2$ term to the harmonic oscillator potential changes the situation completely. The energy curve increases very rapidly with the deformation so that there is no possibility of explaining fission with the potential containing an $\vec{l}^2$ term.

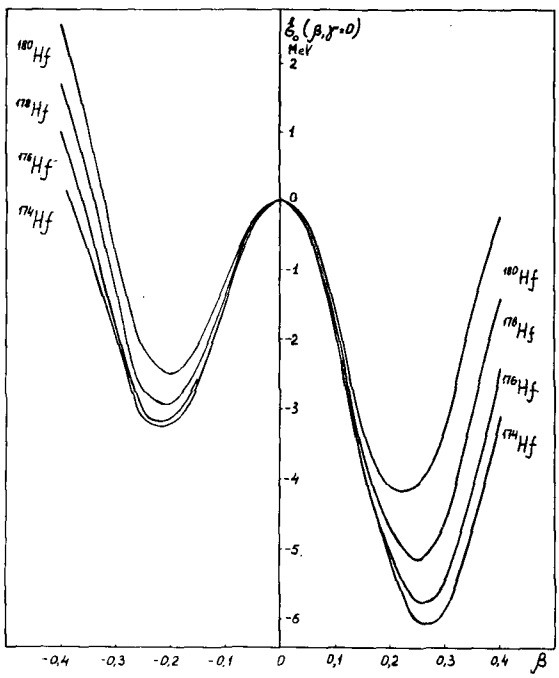

FIG. 4. Total energy curves plotted for some nuclei for negative and positive values of the deformation parameter $\beta = \beta_2$. The figure is taken from Ref. [13].

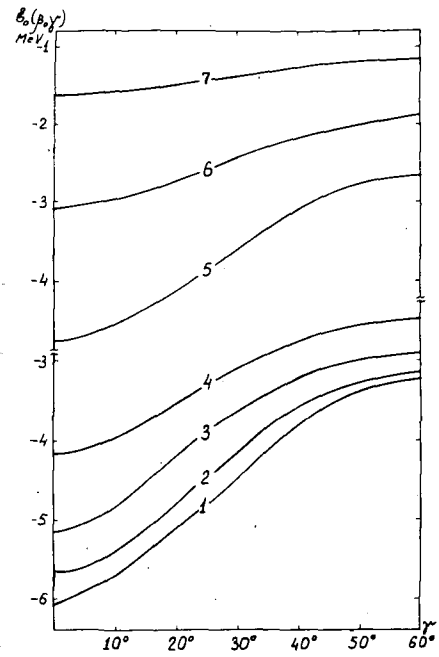

FIG.5. Total energy plotted against non-axial deformation parameter γ for some nuclei. Curves 1 - 7 correspond to the nuclei ^{174}Hf, ^{176}Hf, ^{178}Hf, ^{180}Hf, ^{156}Gd, ^{154}Gd, ^{152}Gd respectively. The figure is taken from Ref. [13].

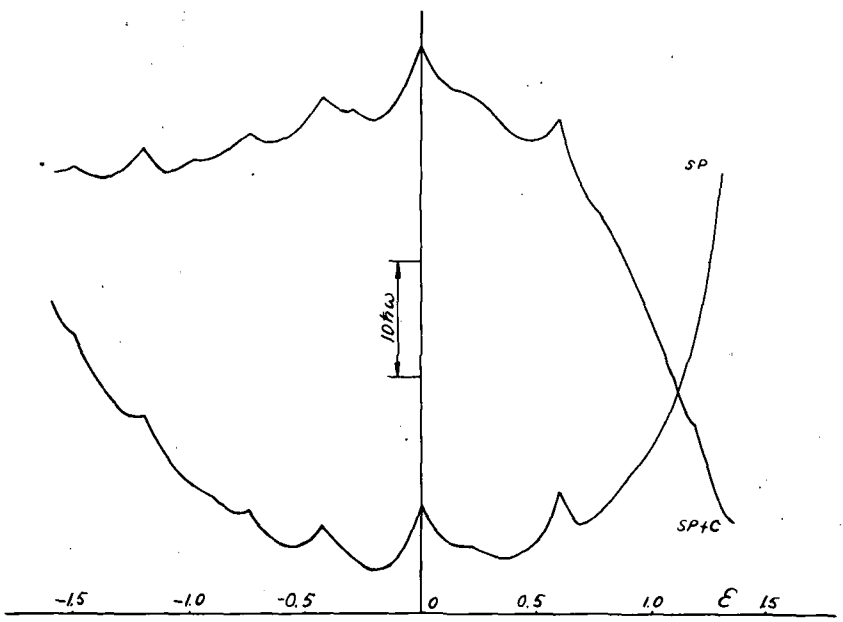

FIG.6. Energy diagram based on a pure harmonic oscillator for a nucleus with Z=100 and N=154. The curve marked SP represents the sum of single-particle energies. The curve SP + C includes in addition the Coulomb energy calculated for the uniformly charged ellipsoid.

Up to now, no nuclear potential has been presented that reproduces correctly the equilibrium properties of nuclei and at the same time allows a proper extrapolation into the region of large deformations. Perhaps a deformed Saxon-Woods potential [8] will fulfil these requirements. On the other hand, the liquid-drop model is believed to reproduce fairly correctly the general behaviour of nuclear energy with respect to deformation. Here, the surface tension appears as the main factor tending to restore the spherical shape of the nucleus. The deformation dependence of the surface energy seems to be much more reasonable than the behaviour of the $\vec{l}^2$ term added to the harmonic oscillator potential. In order to include both the liquid-drop general behaviour and at the same time the single-particle shell effects, Strutinsky [18] has introduced a new method in the calculation of nuclear deformation. It is a further development of the approaches of Myers and Swiatecki [19] and Johansson [20]. The single-particle energy, including also the pairing interaction, is renormalized by the subtraction of its averaged value, the average being taken over an interval of energy large enough compared to the single level distance. The result is then added to the background liquid-drop energy. In the equilibrium region the Strutinsky method gives almost the same results as compared to the approaches that attempt to sum the single-particle energies. On the other hand, this method, as applied to the large deformations, seems to reproduce fairly correctly the behaviour of the potential energy. Obviously, the detailed results substantially depend on the parametrization. For example, the more multipole components P_2, P_4, P_6 ... taken into account, the better the results that should be expected. Recently, Nilsson's group [21] have performed extensive calculations of the potential energy as a function of two deformation parameters ϵ and ϵ_4. A typical example of the results is shown in Fig. 7. The location of the saddle point in the energy surface, as well as the position of the equilibrium deformation, can be seen from this figure.

In addition to the P_2, P_4 ... components in the nuclear shape parametrization, odd multipoles can also appear. In particular, the octupole deformation, P_3, most probably plays an important role in explaining the asymmetry in the mass distribution of the fission fragments.

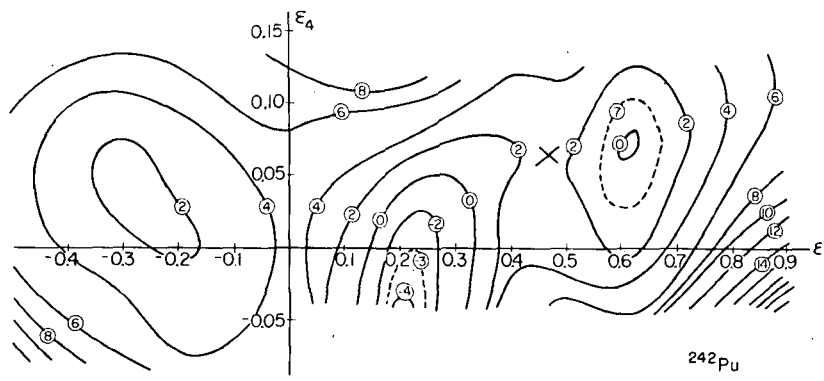

FIG. 7. Topographical diagram for ^{242}Pu total intrinsic energy. The calculation [21] has been performed using the Strutinsky method [18]. Parameters ϵ and ϵ_4 are defined by Eq. (2). The figure is taken from Ref. [21].

TABLE I. ESTIMATES OF THE SADDLE-POINT POSITION

First column identifies the nuclide; second column lists the calculated difference between the saddle-point deformation ϵ_s and the equilibrium deformation ϵ_{eq}.

^{232}Th	0.40	^{242}Cm	0.36
^{234}U	0.39	^{244}Cm	0.36
^{236}U	0.39	^{246}Cm	0.39
^{238}U	0.40	^{248}Cm	0.39
^{236}Pu	0.34	^{246}Cf	0.34
^{238}Pu	0.37	^{248}Cf	0.37
^{240}Pu	0.39	^{250}Cf	0.38
^{242}Pu	0.38	^{252}Cf	0.37
^{244}Pu	0.41	^{254}Fm	0.36
^{240}Cm	0.35		

The behaviour of the potential energy characterizes the purely static properties of nuclei. On the other hand, the evidence from the measurements of the spontaneous fission life-time is connected rather with the dynamic properties of nuclei. The nuclear kinetic energy of deformation,

$$T = \frac{1}{2} \sum_{\lambda\kappa} B_{\lambda\kappa} \dot{\epsilon}_\lambda \dot{\epsilon}_\kappa \tag{3}$$

is characterized by the inertial parameters $B_{\lambda\kappa}$ of the nuclear collective motion. Here the summation is extended on the various multipoles. The effective inertial parameter B in the fission channel, together with the potential energy, determines the probability of penetration into the fission barrier as a quantum tunnelling effect. The values of B calculated by a microscopic method [22] prove to be typically of the order of (6-10) of the B_{irr}, the mass parameter calculated for the deformed liquid drop.

Using the knowledge of the observed life-times for spontaneous fission together with the experimental estimates for the fission barrier heights, one can attempt to estimate the effective width of the barrier and thus the location of the saddle point in the potential energy curve. The calculation involves the theoretical values of B [22] and is based on the WKB method in the computation of the probability of barrier penetration. The results are shown in Table I. The saddle-point deformation is then expected to lie in the region of $\epsilon \sim 0.6$ according to this estimate.

REFERENCES

[1] BOHR, A., MOTTELSON, B.R., Lectures on Nuclear Structure and Energy Spectra, Monograph, to be published.

[2] MOTTELSON, B.R., NILSSON, S.G., Dan. Vid. Selsk. Mat. Fys. Skr. 1 8 (1959).

[3] NILSSON, S.G., Dan. Vid. Selsk. Mat. Fys. Medd. 29 16 (1955).

[4] BES, D.R., SZYMANSKI, Z., Nucl. Phys. 28 (1961) 42 and SZYMANSKI, Z., Nucl. Phys. 28 (1961) 63.

[5] DAS GUPTA, S., PRESTON, M.A., Nucl. Phys. 49 (1963) 401; BARANGER, M., KUMAR, K., Nucl. Phys. 62 (1965) 113, and A110 (1968) 490 and 529.

[6] GUSTAFSON, C., LAMM, I.L., NILSSON, B., NILSSON, S.G., Ark. Fys. 36 (1967) 613.

[7] SOBICZEWSKI, A., Nucl. Phys. A93 (1967) 501; A96 (1967) 258.

[8] GAREJEV, F.A., IVANOVA, S.P., KALINKIN, B.N., Preprint JINR P4-3451 Dubna (1967).

[9] ELBEK, B., KREGAR, M., VEDELSBY, P., Nucl. Phys. 86 (1966) 385.

[10] HENDRIE, D.L., GLENDENNING, N.K., HARVEY, B.G., JARVIS, O.N., DUHM, H.H., SAUDINOS, J., MAHONEY, J., Phys. Lett. 26B (1968) 127.

[11] MÖLLER, P., NILSSON, B., NILSSON, S.G., SOBICZEWSKI, A., SZYMANSKI, Z., WYCECH, S., Phys. Lett. 26B (1968) 418.

[12] VOGEL, P., Preprint JINR E4-3629, Dubna (1967); see also papers quoted in this reference.

[13] ARSENIEV, D.A., MALOV, L.A., PASHKEVICH, V.V., SOLOVIEV, V.G., Preprint JINR E4-3703, Dubna (1968).

[14] ARSENIEV, D.A., MALOV, L.A., PASHKEVICH, V.V., SOBICZEWSKI, A., SOLOVIEV, V.G., Contribution No. 92 to this Symposium; ARSENIEV, D.A., MALOV, L.A., SOBICZEWSKI, A., SOLOVIEV, V.G., Contribution No. 93 to this Symposium; see also BARANGER, M., KUMAR, K., Phys. Rev. Lett. 42 (1964) 73.

[15] SOLOVIEV, V.G., Phys. Lett. 21 (1966) 331 and Progress in Nuclear Physics (1967); SZUMANSKI, K., private communication.

[16] KRUMLINDE, J., NILSSON, S.G., Proc. Contribution 4.51 to Int. Conf. Nuclear Structure Tokyo (1967); BES, D.R., LANSDOWNE, S., MARISCOTTI, Preprint, Carnegie Mellon University, Pittsburgh, and Brookhaven National Laboratory, Upton, New York.

[17] See the experimental papers quoted in Ref. [16] and in MARSHALEK, E.R., Phys. Rev. Lett. 20 (1968) 214.

[18] STRUTINSKY, V.M., Nucl. Phys. A95 (1967) 420, Yadernaya Fiz. 3 (1966) 614.

[19] MYERS, W.P., SWIATECKI, W.J., Ark. Fys. 36 (1967) 343.

[20] JOHANSSON, S.A.E., Nucl. Phys. 22 (1961) 529.

[21] NILSSON, S.G., NIX, J.R., private communication; NILSSON, S.G., NIX, J.R., SOBICZEWSKI, A., SZYMANSKI, Z., WYCECH, S., GUSTAFSON, C., MÖLLER, P., to be published.

[22] GUSTAFSON, C., MÖLLER, P., NILSSON, B., NILSSON, S.G., NIX, J.R., SOBICZEWSKI, A., SZYMANSKI, Z., WYCECH, S., to be published.

DISCUSSION

H. MELDNER: You mentioned the problem due to double counting of potential energies in your calculations. If you do this right for local Nilsson-type potentials you will get binding energies wrong by at least an order of magnitude. However, your model provides another major logical problem. Since you do not have self-consistency you cannot, as you should, minimize the Hamiltonian minus a set of Lagrangian multipliers times a set of multipole moments, i.e. $H - \vec{\lambda} \cdot \vec{Q}$, for the calculation of potential energy surfaces as shown in your figures.

Z. SZYMANSKI: I agree that the procedure of summing up the single-particle levels does not seem to be sufficiently justified. However, I can refer you here to the theorem proved recently by Bohr and Mottelson according to which this procedure is equivalent to finding the minimum from the more appropriate two-body force. This holds, providing the nuclear potential fulfils the volume conservation condition.

H. MELDNER: That might work at one point. But how about all the other points on your calculated energy surfaces?

Z. SZYMANSKI: In principle, there are two points where the two approaches seem to be equivalent: equilibrium and saddle point. However, I agree that at the saddle point the Bohr-Mottelson theorem may not be exactly valid as the Coulomb forces have not been included in the formation of the nuclear field.

P.E. NEMIROVSKY: Have you taken into account in your calculations the interaction of the N and N+2 shells in the oscillator model? This interaction seems to be rather considerable, as was shown by our calculations from the Woods-Saxon model. This may result in a decrease of the level energy by 1 MeV.

Z. SZYMANSKI: The quadrupole coupling between the N and N+2 shells is taken into account by using the Nilsson 'stretched' coordinates. The rest of the coupling caused by the P_4 term has also been included and it seems to be quite important for the potential energy. We have also included the N, N+2 matrix elements in the calculation of the mass parameter B and we find it also essential.

K.A. BRUECKNER: The prediction of nuclear properties far from observed nuclei depends on a knowledge of the effective field and liquid drop parameters. These cannot be predicted by extrapolation but must be calculated from realistic forces in a correlated Hartree-Fock calculation. The problems, for example, of higher order terms in surface energy, the surface symmetry energy, may be important and cannot be determined without use of realistic forces and calculation of the effective potential field.

Z. SZYMANSKI: I agree completely with your comment. I can only add that up to now the liquid-drop model has been used almost exclusively in the explanation of fission phenomena. The approach I have attempted to present here consists mostly in the application of the simplest nuclear potential such as, for example, the harmonic oscillator. The next step would be to introduce a more realistic potential (perhaps Saxon-Woods). In the following step one should try a self-consistent Hartree-Fock approach that I believe would improve the results.

Krishna KUMAR: In connection with Professor Brueckner's remarks, I would like to say that of course it is better to use realistic forces and Hartree-Fock methods. But there are two serious limitations, especially when one tries to calculate large deformations of heavy nuclei. Only a limited number of states near the Fermi surface are considered, and time-dependence of deformation is neglected. Such calculations with a very large number of single-particle states are quite impractical when realistic forces are used.

J.R. NIX: Your potential-energy contour map for ^{242}Pu indicates that the potential energy diverges to infinity at large deformations. This occurs for all nuclei in the actinide region, even when the potential energy is calculated by using the Strutinsky method, which is the best method that can be used at present. This divergence of the potential energy is primarily the result of not taking into account a sufficient number of degrees of freedom to describe the large deformations encountered beyond the saddle point. As a method for including more degrees of freedom we recommend using a parameterization of the nuclear shape defined in terms of smoothly joined portions of three quadratic surfaces of revolution (e.g. two spheroids connected by a hyperboloidal neck) rather than continuing to add more

degrees of freedom of the Legendre-polynomial type. This parameterization is appropriate for the calculation of the potential energy by using methods other than the Strutinsky method, for example the Hartree-Fock method. If the Strutinsky method is used, we recommend using a realistic Woods-Saxon potential well rather than a harmonic-oscillator potential well, since the oscillator potential is itself ill-behaved at large deformations.

A.V. IGNATYUK: Could you comment on the dependence of the saddle-point deformation on the methods of calculating equilibrium deformations and pairing interaction constants? In the interpretation of the data on the angular distribution of fission fragments there is a considerable spread of the correlation function Δ, which is often explained by the increase of the pairing interaction constant for the saddle point.

Z. SZYMANSKI: We have used a constant pairing-force strength G. However, I agree that one should also investigate the possible influence of the variation in that parameter. It may affect quite appreciably the mass parameter B, for example.

M. VENERONI: About the problem of improving the calculations by using the Saxon-Woods potential instead of a harmonic oscillator, it seems to me that one should seriously think about the non-locality of the Hartree-Fock well which is a crucial ingredient for getting the right wave-functions and, more important, right single-particle energies.

A. BOHR: Rather than attempt a detailed Hartree-Fock calculation of the strongly deformed nuclei, it would seem preferable to concentrate efforts in this direction on the analysis of the parameters which enter into the more phenomenological calculations in an important manner. Of special significance is the symmetry term in the surface energy on which there is only a small amount of empirical evidence. Another problem to be further explored is the extent to which the surface deformation parameter is equal to the parameters determined from the nuclear mass formula.

A. SOBICZEWSKI reported briefly on the results of calculations performed at JINR, Dubna, concerning the equilibrium deformations of the ground and the lowest one-or two-quasiparticle excited states of even, odd-mass and odd nuclei in the $50 < Z, N < 82$ region. The calculations have been performed by D.A. Arseniev, L.A. Malov, V.V. Pashkevich, A. Sobiczewski and V.G. Soloviev and some of their results are presented as Contributions Nos. 92 and 93 to this Symposium.

K.F. ALEXANDER (JINR, Dubna) presented Contribution No. 18 to this Symposium, on the experimental indication for an oblate shape of the nucleus ^{129}La.

L. GRODZINS: The evidence presented shows clearly that in ^{129}La there exists an E3 and an M1 transition. From this point one uses a very uncertain theory to obtain essentially unequivalent assertions about spins, Nilsson levels, and about the deformation. In my opinion such conclusions are completely unwarranted. One is tempted to ask, why do the experiment if such meagre evidence is 'strong evidence' for the state parameters?

R.K. SHELINE: I feel perhaps the last comment of Dr. Grodzins was a bit unfair. It is difficult to establish a new region of oblate deformation and I feel the results of Alexander are highly suggestive of his conclusion. Of course, still more definitive data are highly desirable. It is possible

that C,e values determined from the $^{130}Ba(d,t)^{129}Ba$ reaction would help define a region of oblate deformation. These experiments should be possible.

R. ARLT: I would like to make a comment which confirms the identification of the isomer state just in the nucleus of ^{129}La. We have investigated this nucleus from the decay of a short-lived isotope of ^{129}Ce, and observed the 67 keV energy gamma-transition which also arises from the isomer cascade transition in ^{129}La.

NUCLEAR COLLECTIVE HAMILTONIAN AND DEFORMATIONS

KRISHNA KUMAR
THE NIELS BOHR INSTITUTE,
UNIVERSITY OF COPENHAGEN,
COPENHAGEN, DENMARK

Abstract — Аннотация

NUCLEAR COLLECTIVE HAMILTONIAN AND DEFORMATIONS. The scope and limitations of a recently developed treatment of collective quadrupole motion of even-even nuclei are reviewed. This method is based on Bohr's collective Hamiltonian and the pairing-plus-quadrupole model. With an exact, numerical treatment of the couplings between the five components of quadrupole motion, the theory is able to explain and predict many trends in the low-lying levels and electromagnetic moments of nuclei in the W-Os-Pt region. The zero-point quantal motion plays an important role in spreading the nuclear wave-function in the β-γ plane so that the nucleus is affected essentially by the behaviour of the collective Hamiltonian away from the equilibrium shape. The γ-dependence of the Hamiltonian, especially the prolate-oblate difference term of the potential function, plays a crucial role in the splitting of the $2'^{+}$and 4^{+} states and the non-zero quadrupole moments of $I \neq 0$ states, which can occur even if the equilibrium shape is spherical or completely asymmetric with $\gamma = 30°$. The anharmonicities of the six inertial functions of Bohr's Hamiltonian cause β-γ band-mixing in the W isotopes, reduce the ground-β-γ band-mixing in the Os isotopes, and counteract the prolate-oblate difference term so that the spectrum of the calculated ^{196}Pt appears to be vibrational. The calculation for ^{196}Pt gives a large, oblate quadrupole moment of the first 2^{+} state as well as a small cross-over transition from the ground state to the second 2^{+} state. However, the calculated $2'^{+}$ states of $^{192-196}$Pt are too high by 0.1-0.2 MeV, and the calculated B(E2; $2 \rightarrow 2'$) values for the region are too large by about a factor of two. Some possible ways of improvement are indicated.

ЯДЕРНЫЙ КОЛЛЕКТИВНЫЙ ГАМИЛЬТОНИАН И ДЕФОРМАЦИИ. Рассматриваются возможности и ограничения недавно развитой трактовки коллективного квадрупольного движения в четно-четных ядрах. Этот метод основан на коллективном гамильтониане Бора и модели с парным и квадрупольным взаимодействием. С помощью численного подбора величины связей между пятью компонентами квадрупольного движения теория может объяснить и предсказывать многие тенденции низколежащих уровней и электромагнитных переходов в области W – Os – Pt. Нулевые колебания играют важную роль в размытии волновой функции ядра в плоскости $\beta - \gamma$, так что поведение ядра существенно зависит от поведения коллективного гамильтониана вдали от равновесной формы. Зависимость гамильтониана от γ, и особенно члена в потенциале, отвечающего за разницу вытянутой и сплюснутой формы, играет решающую роль в расщеплении 2_{+}^{1} и 4_{+}^{1} состояний и в состояниях $I \neq 0$, с квадрупольными моментами, неравными нулю и имеющими место даже в случае сферической равновесной формы или полностью ассимметричной с $\gamma \approx 30°$. Ангармоничность шести инерционных функций гамильтониана Бора вызывает смешивание β-γ полос в протонах W, уменьшает β- γ-смешивание в изотопах Os и нейтрализует различие в потенциале вытянутой и сплюснутой формы. Таким образом, рассчитанный спектр ^{196}Pt оказался колебательным. Расчеты для ^{196}Pt дают как достаточно большой отрицательный квадрупольный момент первого 2_{+} состояния, так и малую вероятность прямого перехода из основного состояния на второе 2_{+} состояние. Однако, рассчитанные 2_{+}^{1} состояния $^{192-196}$Pt находятся на 0,1 – 0,2 Мэв выше. Величины B(E2; $2 \rightarrow 2'$), рассчитанные для этой области, больше наблюдаемых приблизительно раза в два. Указываются некоторые возможные пути совершенствования методики.

INTRODUCTION

The subject of my paper is rather broad and has already been touched upon at this Symposium by Professors Sorensen, Vogel, Davydov, Szymański and others. As I understand it, my task is to outline the scope and limitations of the program developed during the past five years under the leadership of Professor Michel Baranger. This treatment is based on the collective Hamiltonian developed by Professor Aage Bohr in 1952 [1], and on the pairing-plus-quadrupole model worked out by Bohr, Mottelson and Belyaev around 1958 [2]. These two models have been applied and developed in numerous papers of the past few years [3].

The main new element in the present program [4, 5] is an exact, numerical treatment of the couplings between the five components of quadrupole motion, that is the rotation-vibration coupling in the language of the rotational model or the phonon mixing in the language of the vibrational model. Instead of making a perturbation expansion around the equilibrium nuclear shape, a detailed microscopic calculation is performed for each point on a β-γ mesh and the complete β-γ dependence of the potential and kinetic energy functions is determined. A numerical method of solving Bohr's collective Hamiltonian is then used to calculate the energy levels and wave-functions. The same method is applied to spherical as well as deformed nuclei. The transitional nuclei such as those of the osmium region are treated in a natural way as those lying in between the two limits of quadrupole motion. The main limitations of this program come from the assumptions made in the pairing-plus-quadrupole model.

Because of limitations of time and knowledge, this report is very sketchy. We shall briefly discuss the physical assumptions in part I and some results and conclusions in part II.

I. PHYSICAL ASSUMPTIONS

I.1. Bohr's collective Hamiltonian and its solutions

In tensor notation, the Hamiltonian is written as

$$H_c = V(\vec{\beta}) + \tfrac{1}{2}\dot{\vec{\beta}} \cdot B(\vec{\beta}) \cdot \dot{\vec{\beta}} \qquad (1)$$

where $\vec{\beta}$ is the quadrupole deformation vector with five components and $V(\vec{\beta})$ is the potential energy or the total instantaneous energy of the nucleus. The second term in H_c is the kinetic energy of collective quadrupole motion or the second-order time-dependent correction to the instantaneous energy. In the limit of zero deformation, the inertial function matrix $B(\vec{\beta})$ approaches a simple, harmonic form and depends on a single constant [1]. In general, it is a 5×5 matrix with $\vec{\beta}$-dependent elements which can, however, be reduced to six $\vec{\beta}$-dependent functions on choosing the axes to coincide with those of the principal moments of inertia and on making use of the rotational and time-reversal invariance of H_c. Thus, in general, Bohr's collective Hamiltonian contains seven functions of deformation which are completely arbitrary, except for certain symmetry requirements [1, 5].

The collective variable method has three main advantages over the pure shell-model method. (1) It is not limited by the degree of configuration mixing. Each collective state of an even-even nucleus represents

a linear combination of zero, two, four, and higher quasi-particle states. (2) It is not limited by the number of particles. In fact, the method works better when the number is large. (3) A large number of single-particle states can be included in the microscopic part of the calculation and thus it is comparatively easier to include the off-the-energy-shell matrix elements.

In its usual form, this method has three main limitations. (1) It is assumed that the collective quadrupole mode is separated from all other modes of motion. While this is not really an assumption for the most important nuclear matrix elements connecting the 0^+ and 2^+ states, this is probably the most severe limitation of the method. (2) The adiabatic assumption is made that the collective motion is slow and, hence, higher than second-order terms in the velocity $\dot{\beta}$ can be neglected. This assumption is necessary for the quantization of the Hamiltonian. (3) It is assumed that the nucleus performs small, harmonic vibrations around the equilibrium shape which is determined in a phenomenological treatment by fitting the experimental data and in a microscopic treatment by looking for the lowest minimum of $V(\beta)$.

The calculation of equilibrium nuclear shapes, reviewed in the preceding talk by Szymański [6], provides a very useful test of the microscopic theory. However, it is not a sufficient test, since the nuclear spectra are in general sensitive to the variation of the potential and inertial functions away from the lowest minimum. If the variation of the potential energy is slow, as in the transitional nuclei, then the amplitude of zero-point vibrations is large and causes rotation-vibration coupling or phonon mixing. If this variation is rapid as in the closed-shell nuclei or strongly deformed nuclei, then the energy of zero-point motion is large. In either case, the anharmonicities or the deviations of the potential function from a parabola around the equilibrium shape and those of the inertial functions from the harmonic form can be important.

The limitation of small, harmonic vibrations is removed in the numerical method [4, 5]. The total nuclear wave-function is written as

$$\Psi_{IM} = |0(\beta,\gamma)\rangle \sum_K C_{IK}(\beta,\gamma)\mathscr{D}^I_{MK}(\theta,\varphi,\psi) \qquad (2)$$

where β, γ represent the shape of the nuclear quadrupole in the intrinsic system and the Euler angles θ, φ, ψ give its orientation with respect to the laboratory axes. The intrinsic or zero quasi-particle wave-function $|0(\beta,\gamma)\rangle$ is coupled to the vibrational wave-function C_{IK} through the dynamic variables β, γ. The degree of coupling of the vibrational wave-function and the rotational $\mathscr{D}$-matrix depends on K, which is not a good quantum number in general. The Hamiltonian H_c (Eq. (1)) is quantized and the Schrödinger equation $H_c\Psi = E\Psi$ is constructed. On using the standard $\mathscr{D}$-matrices, the problem is reduced to a set of coupled partial-differential equations in β and γ, whose degree of coupling depends on the number of K components. These equations are then solved by using numerical methods, and values of C_{IK} are determined at each point of a β-γ mesh (Fig. 1).

This method is quite general and can be used for spherical nuclei, deformed nuclei, and also transitional nuclei. It is also independent of the method of determination of the seven functions of Bohr's Hamiltonian. For example, in case of small deviations from the vibrational and rotational limits, one can make an analytical expansion and study the effects of different anharmonic terms. However, such a method has limited value.

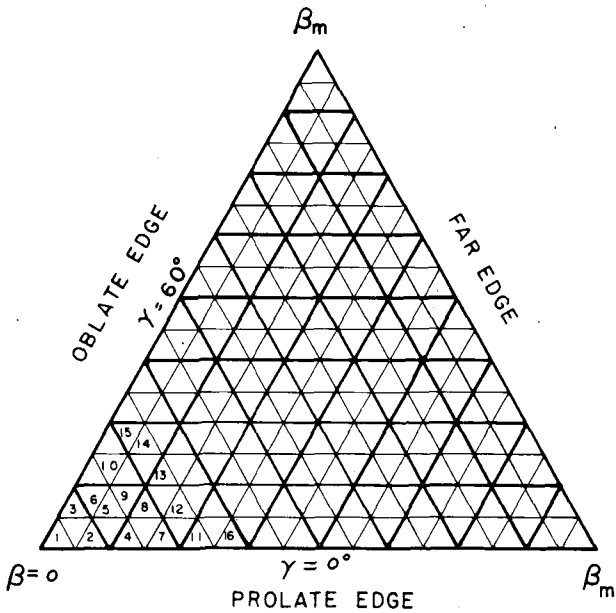

FIG. 1. The β-γ mesh used for numerical solution.

Anharmonic terms appear in the potential as well as inertial functions. Hence, a large number of parameters would be required for a complete treatment. Also, the anharmonic terms are in general quite large and the convergence is not rapid [4, 7]. Therefore, most of our work has been performed with a microscopic determination of the numerical values of the seven functions at each point of the β-γ mesh.

I. 2. The pairing-plus-quadrupole model and the determination of the twelve functions of β and γ

The model Hamiltonian consists of three parts: a spherical, shell-model part whose eigenvalues are the empirical single-particle energies and whose eigenvectors are approximated by the harmonic oscillator wave-functions; a pairing part which represents the $J = 0$, $T = 1$ component of the residual two-body interaction and whose strength is determined by fitting the odd-even mass differences; and a quadrupole part which represents the $J = 2$, $T = 0$ component of the residual interaction and whose strength is determined by fitting the static deformations of well-deformed nuclei.

Aside from the neglect of higher-order components of the residual interaction, two assumptions are made in this model: (1) the pairing matrix elements are state-independent, and (2) the radial form of the quadrupole operator is r^2. These two assumptions have been tested by making a comparison with the pairing-type and the quadrupole-type components of several "realistic" forces [8, 9]. The model is quite good within the major shell near the Fermi surface but gets worse as we include states away from the Fermi surface.

Using this model, the seven functions of Bohr's Hamiltonian are calculated. In addition, two electric quadrupole moment functions and three gyromagnetic ratio functions are computed. The method of calculation is similar to the Nilsson model plus pairing plus cranking model [3]. The main difference is that the condition of volume conservation and the method of summing over the occupied Nilsson levels are not used. Instead, a self-consistent time-dependent Hartree-Bogolyubov [10] type of calculation is done. Thus, the uncertainty due to the condition of volume conservation as discussed by Strutinsky [11] never enters this program. Also, the self-consistency condition that the wave-function and potential deformation are equal at equilibrium provides a useful check of the calculation.

There are several other differences which could in principle be incorporated in a Nilsson calculation but usually are not. (1) The complete β-γ dependence of the twelve functions is determined. (2) The contributions of time-dependent or deformation-dependent changes in the pairing field to the inertial functions are included. Such contributions were first discussed by Bès [12]. (3) The assumption of uniform charge distribution is not made. Instead, the electric quadrupole moment of the intrinsic wave-function is determined by summing over the quadrupole moments of the single particle orbits. This procedure has one unpleasant aspect, namely, since we sum over only the nucleons outside the core, an effective charge has to be used. But there is also a pleasant aspect. Higher-order terms in $\beta^2, \beta^3, \ldots$ which are responsible for part of the anharmonicity are automatically included. (4) The assumption of a constant g-value (independent of $\vec{\beta}$ and direction) is not made; therefore the B(M1) values do not vanish trivially.

II. SOME RESULTS AND CONCLUSIONS

II.1. Some results

Energy levels calculated [13] for the W-Os-Pt region are compared with experiment in Fig. 2. Trends of various levels are given correctly. But the calculated $2'^+$ state of the Pt isotopes is too high by 0.1-0.2 MeV. Some of the untested predictions are: strong β-γ band mixing in tungsten, and β-phonon plus two γ-phonon mixing in the osmium isotopes.

Figure 3 has been taken from the work of Casten et al. [14], who have performed some beautiful Coulomb excitation measurements in the Os isotopes. While the theory [13] gives the trends correctly, the too sharp decrease in $B(E2; 0 \rightarrow 2')$ and the factor of about 2 in the $B(E2; 2 \rightarrow 2')$ values are challenging problems.

Figure 4 has been taken from the work of Glenn and Saladin [15] who have measured the quadrupole moments of the platinum isotopes. It is encouraging that the measured value and sign (which corresponds to an oblate shape) are in good agreement with theory [13]. The measurements of the remaining Q_{2^+} values would provide further useful tests.

Detailed comparisons between theory and experiment are given elsewhere [13-16]. We shall now discuss these results in terms of the nuclear collective Hamiltonian.

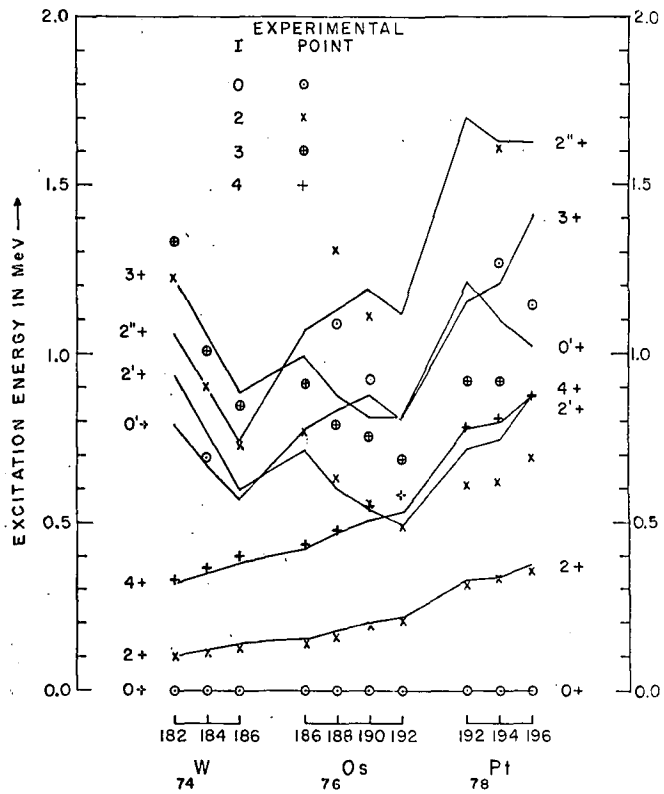

FIG. 2. Energy levels of tungsten, osmium and platinum nuclei.

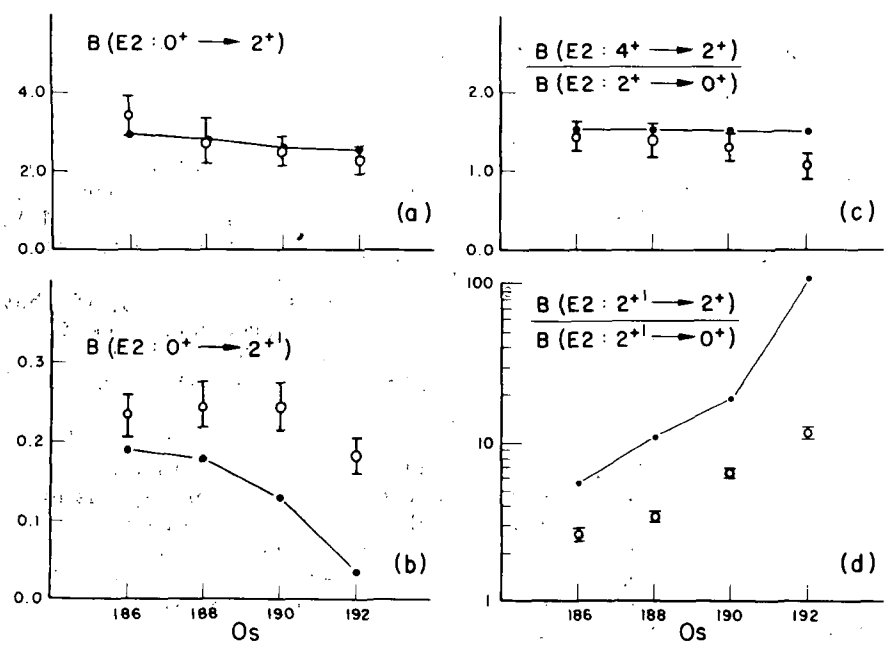

FIG. 3. Electric quadrupole transitions in the osmium nuclei. Figure taken from Casten et al. [14].

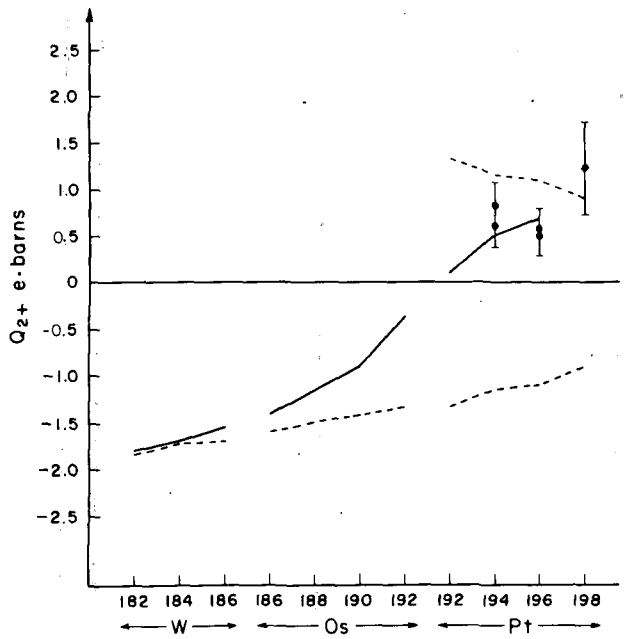

FIG.4. Quadrupole moment values of tungsten, osmium and platinum nuclei. The dashed curves give the rotational values. The solid curves give the theoretical values from Ref. [13]. Experimental values and the figure are from Glenn and Saladin [15].

The equilibrium nuclear shape gives us our most important clue about the collective behaviour of a nucleus. However, it is not enough. We also need to know the relationship of this *minimum* to other possible minima, maxima or saddlepoints of the potential surface. In this connection, the zero-point motion, the γ-dependence of the potential function, and the anharmonicities of the inertial functions play crucial roles. Effects of these three intermingle and cannot be separated out completely. With this reservation in mind, we shall now discuss the major effects of each.

II. 2. Zero-point motion

The energy of zero-point motion ξ_0 is just the difference between the energy of the ground-state solution of the Hamiltonian and the energy of the lowest potential minimum. In the vibrational limit of the five-dimensional quadrupole motion, it is given by $(5/2)\hbar\omega$. If the equilibrium shape is to be stable against zero-point motion, two conditions must be satisfied:

$$\xi_0 \ll E_s \tag{3}$$

$$\xi_0 \ll E_{p0} \tag{4}$$

where E_s is the energy of deformation compared to the spherical shape, and E_{p0} is the energy of prolate-oblate difference at $\beta = \beta_{r.m.s.}$. Additional stationary points of V would require more conditions.

These conditions are obviously satisfied by the nuclei in the middle of the deformed region, but are not always satisfied by the potential

functions used to describe these nuclei! The conditions are obviously not satisfied by the spherical nuclei since $E_s = 0$, but this simply means that the r.m.s. value of deformation is non-zero and differs from the static, zero value. In the transitional region, these conditions are not satisfied (Table I). Hence, the nuclear wave-functions are spread in the β-γ plane instead of being concentrated at the equilibrium shape [4, 13]. The extent of the spreading is directly proportional to the degree of violation of these two conditions and therefore increases as we go from W to Os to Pt nuclei.

II. 3. The γ-dependence of the potential function

Since the potential energy is a scalar, it can be written as

$$V = a + b(\vec{\beta} \cdot \vec{\beta})_0 + c(\vec{\beta} \cdot \vec{\beta} \cdot \vec{\beta})_0 + \ldots \qquad (5)$$

where $\vec{\beta}$ is the deformation tensor of rank 2 and the symbol $(\ )_0$ signifies that the tensors inside the brackets are coupled to $J = 0$. When such

TABLE I. EFFECTS OF ZERO-POINT MOTION AND PROLATE-OBLATE DIFFERENCE

Experimental values are given in parentheses

	Col. 2	3	4	5	6	7	8
	β_s	γ_s	E_s (MeV)	E_{p0} (MeV)	ξ_0 (MeV)	$\frac{E_{2^+} - E_4}{E_2}$	$\frac{Q_{2+}}{Q_R}$
$^{172}_{70}$Yb	0.32	0.0	10.6	7.3	3.3	18.0 (15.4)[a]	1.0
$^{182}_{74}$W	0.25	0.0	4.3	1.5	1.9	7.2 (8.9)[a]	0.99
$^{190}_{76}$Os	0.22	30.0	3.0	0.1	1.1	0.15 (0.05)[a]	0.61
$^{196}_{78}$Pt	0.15	60.0	1.5	-0.7	1.6	0.0 (-0.53)[a]	-0.65 (-0.51 ± 19)[b]
$^{206}_{82}$Pb	0.0	0.0	0.0	-0.8	2.0	2.0 (-0.27)[a]	-1.0

Col. 2. Equilibrium shape deformation.
Col. 3. Equilibrium shape asymmetry.
Col. 4. Deformation energy.
Col. 5. Prolate-oblate difference energy calculated at $\beta = \beta_{r.m.s.} = 0.085$ for ^{206}Pb and $\beta = \beta_s$ for others.
Col. 6. Zero-point motion energy.
Col. 7. Splitting of 2^{+} and 4^{+} states.
Col. 8. Quadrupole moment of the first 2^+ state compared to the rotational value for a prolate shape, $Q_R = -\frac{2}{7}\left[\frac{16\pi}{5} B(E2; 0 \rightarrow 2)\right]^{\frac{1}{2}}$.

[a] 1967 Table of Isotopes [20]. [b] Glenn and Saladin [15].

products are written in terms of the intrinsic components, one finds that the only two basic invariants that can enter V are β^2 and $\beta^3 \cos 3\gamma$ [5, 17]. Thus, the γ-dependence of V can be expressed as

$$V(\beta, \gamma) = V_0(\beta^2) + V_1(\beta^2)\beta^3 \cos 3\gamma + V_2(\beta^2)\beta^6 \cos^2 3\gamma + \ldots \qquad (6)$$

where $V_0, V_1, V_2, \ldots$ are γ-independent functions of even powers of β. The V_1 term causes prolate-oblate difference and the V_2 term creates a ridge or a valley along $\gamma = 30°$.

The two main effects of the prolate-oblate difference term are : (1) the splitting of the $2'^+$ and 4^+ states, which belong to the γ-band and the ground band in the rotational limit and to the N = 2 phonon triplet in the vibrational limit; and (2) the non-zero quadrupole moments of $I \neq 0$ states.

The calculated prolate-oblate difference is about 7 MeV in ^{172}Yb and leads to ratios $(E_{2'} - E_4)/E_2 = 18.0$ and $Q_{2^+}/Q_R = 1.0$ (Table I). If this term had not been there, then the $2'^+$ state of the γ-band would have been degenerate with the 4^+ state of the ground band and this nucleus with a static deformation of 0.3 would look transitional rather than deformed! Hence, the condition (4) is really essential for a rotational nucleus.

As A is increased in the Yb-Pb region, the prolate-oblate difference decreases up to ^{190}Os where it passes through zero and builds up again in the negative direction. As can be seen from Table I, the ratios $(E_{2'} - E_4)/E_2$ and Q_{2^+}/Q_R follow this difference rather closely (the formed ratio depends on the magnitude only) except in the region of small E_{p0} where other anharmonicities become important.

The $\beta^6 \cos^2 3\gamma$ term of $V(\beta, \gamma)$ appears to be small since in most of the calculated nuclei the potential energy surface rises smoothly from the lowest minimum to the higher one. This term would have its best chance in a nucleus like ^{190}Os where the main γ-dependent term is vanishingly small near $\beta = \beta_s$. If V_2 had a substantial negative value, then a ridge along $\gamma = 30°$ would separate the prolate and oblate minima and there would be two sets of rotational bands. If V_2 had a substantial positive value, a valley along $\gamma = 30°$ would make the nucleus asymmetric. There is some evidence for the second possibility since the lowest minimum of ^{190}Os occurs at $\gamma = 30°$. However, this evidence must be considered very weak since the energy gained by making the nucleus asymmetric is only 0.1 MeV, while the energy of zero point motion is 1.1 MeV.

This calculation also indicates that a deformed equilibrium shape is not essential for a large Q_{2^+}/Q_R. In the calculated ^{206}Pb (Table I), the equilibrium shape is spherical, but the potential energy surface rises more rapidly on the prolate side than on the oblate side of $\beta = 0$. The nucleus has a substantial prolate-oblate difference of -0.8 MeV at $\beta = \beta_{r.m.s.} = 0.085$ and a large, oblate quadrupole moment of the first 2^+ state.

II.4. Anharmonicities of the six inertial functions

Since these functions are parts of a 5×5 matrix, their symmetry conditions and β-γ dependence [5] are considerably more complicated than those of the scalar potential function. A comparison of the calculated inertial functions with the harmonic forms shows that the anharmonicities have no marked trends with β and γ. With a suitable average over the

six B-functions, the average B-value changes over the entire β-γ mesh region by only $\pm 10\%$ in the W and Os isotopes, and $\pm 20\%$ in the Pt isotopes. However, the local variations by factors of two indicate a competition between several large terms of comparable magnitudes but opposite signs. Hence a perturbation expansion is not valid.

The main effects of these anharmonic terms are as follows. (1) The γ-band is pushed up and band mixing between the β-and γ-bands is caused in the W isotopes. The B(E2) values connecting these bands are quite large, and the spectroscopic quadrupole moments deviate strongly from the rotational values. For example, in ^{182}W the ratio $B(E2; 2' \rightarrow 2'')/B(E2; 0 \rightarrow 2)$ is 0.25 instead of zero and the ratios $Q_{2'}/Q_R$, $Q_{2''}/Q_R$ are 0.08, 0.17 instead of ± 1.0. Experimental measurements of these quantities would provide useful tests of this point. (2) Mixing between the ground, β- and γ-bands is reduced in the Os isotopes. Even though the equilibrium shape of ^{190,192}Os is asymmetric ($\gamma = 30°, 45°$), the quadrupole moment of the 2^+ state is negative (Fig. 4) instead of being zero in ^{190}Os and positive in ^{192}Os [18]. This happens partly because the anharmonicities of B favour prolate over oblate in this region and partly because the potential function at large β also favours prolate over oblate. These Q_{2^+} values remain to be tested, but the anharmonic terms of B play an essential role in lowering the $2'^+$ below the 4^+ state of ^{192}Os in agreement with experiment. (3) The main effect in the Pt isotopes is that the $2'^+$ state is lowered. If these anharmonic terms had been neglected, then the $2'^+$ state of ^{196}Pt would have been above 4^+ because of the substantial prolate-oblate difference. Thus, the anharmonicities of the inertial functions oppose those of the potential function and play a crucial role in giving us this picture of the calculated ^{196}Pt. The spectrum looks approximately vibrational (the $2'^+$ and 4^+ states are degenerate) but the first 2^+ state has a large quadrupole moment ($Q_{2^+}/Q_R = -0.65$). Also, the cross-over transition $0 \rightarrow 2'$ is small by a factor of 65 compared to $0 \rightarrow 2$ and by a factor of 14 compared to $2 \rightarrow 2'$. This is strongly suggestive of the situation in ^{114}Cd [19], but more experimental checks for ^{196}Pt and theoretical checks for ^{114}Cd are needed.

II. 5. Main conclusions

It appears that, in its present form, the method of nuclear collective Hamiltonian and deformations is a powerful tool for studying the low-energy properties of even-even nuclei. The main virtues of this method are: (1) large amounts of configuration mixing can be included at a comparatively small price; (2) time-dependence or quantal fluctuations are taken into account and nuclear wave-functions are constructed without confrontation with the problems of non-conservation of angular momentum or non-conservation of particle number; and (3) the same method is applied to spherical and deformed nuclei, so that the transitional nuclei are treated in a natural way as those lying in between the two limits.

In its present form the method has the following limitations. (1) The numerical accuracy of the method of solving Bohr's collective Hamiltonian is limited by the fact that the matrix size is proportional to the number of points in the β-γ mesh. Also, the matrix size is proportional to the number of K components, hence the method is limited to states with $I \leqslant 4$. A modified method based on analytic expansions is being investigated. (2)

Interactions between states away from the Fermi surface, for example the $\Delta N = 2$ mixing, are not described correctly by the pairing-plus-quadrupole model based on the harmonic oscillator well. A modification based on the Woods-Saxon well is being investigated in collaboration with B. Sørensen. (3) Higher modes of nuclear motion, such as octupole vibrations (essential for negative parity and 1^+ states) and pairing vibrations (important for high lying 0^+ states) have been neglected. The present technique is being applied to the problem of pairing vibrations in collaboration with R. Broglia. At a later stage, we hope to treat the coupling between pairing and quadrupole vibrations. (4) The present treatment is limited to even-even nuclei. Its extension to odd nuclei poses a challenging problem.

REFERENCES

[1] BOHR, A., Mat. Fys. Medd. Dan. Vid. Selsk. 26 14 (1952).

[2] MOTTELSON, B.R., The Many-body Problem, lectures given at the summer school in Les Houches, 1958, Wiley, N.Y. (1959); BELYAEV, S.T., Mat. Fys. Medd. Dan. Vid. Selsk. 31 11 (1959).

[3] NATHAN, O., NILSSON, S.G., Alpha-, Beta- and Gamma-Ray Spectroscopy, (SIEGBAHN, K., Ed.) North-Holland, Amsterdam (1965); also see several papers in these Proceedings.

[4] KUMAR, K., Ph. D. thesis, Carnegie Institute of Technology (1963); BARANGER, M., KUMAR, K., Perspectives in Modern Physics. (MARSHAK, R.A., Ed.) Wiley-Interscience, N.Y. (1966).

[5] KUMAR, K., BARANGER, M., Nucl. Phys. 92 (1967) 608.

[6] SZYMANSKI, Z., Equilibrium deformations of the ground and excited states, these Proceedings.

[7] KERMAN, A.K., SHAKIN, C.M., Phys. Lett. 1 (1962) 151; BRINK, D.M., DE TOLEDO, PIZA, A.F.R., KERMAN, A.K., Phys. Lett. 19 (1965) 413; SØRENSEN, B., Nucl. Phys. A 97 (1967) 1, and private communication.

[8] BARANGER, M., KUMAR, K., Nucl. Phys. A110 (1968) 490.

[9] BROWN, G.E., KUO, T.T.S., International Nuclear Physics Conference, Gatlinburg, Tennessee, 1966, (BECKER, R.L., Ed.) Academic Press, N.Y. (1967).

[10] BELYAEV, S.T., Nucl. Phys. 64 (1965) 17; BARANGER, M., Cargèse Lectures in Theoretical Physics, (LEVY, M., Ed.) Benjamin, N.Y. (1963); BARANGER, M., KUMAR, K., submitted to Nucl. Phys.

[11] STRUTINSKY, V.M., Nucl. Phys. A 95 (1967) 420.

[12] BES, D.R., Mat. Fys. Medd. Dan. Vid. Selsk. 33 2 (1961).

[13] KUMAR, K., BARANGER, M., Phys. Rev. Lett. 17 (1966) 1146, and submitted to Nucl. Phys.

[14] CASTEN, R.F., GREENBERG, J.S., BURGINYON, G.A., BROMLEY, D.A., Phys. Rev. Lett. 18 (1967) 912; CASTEN, R.F., Ph. D. thesis, Yale University (1967).

[15] GLENN, J.E., SALADIN, J.X., Preprint (University of Pittsburgh) (1968)

[16] McGOWAN, F.K., STELSON, P.H., (Oak Ridge) private communication.

[17] NOACK, C.C., Nucl. Phys. A 108 (1968) 493.

[18] DAVYDOV, A.S., OVCHARENKO, V.I., Preprint ITF-67-14, Kiev (1967).

[19] DE BOER, J., STOCKSTAD, R.G., SYMONS, G.D., WINTHER, A., Phys. Rev. Lett. 14 (1965) 564; BROMLEY, D.A., WENESER, J., Comments Nucl. Particle Phys. 1 (1967) 75.

[20] LEDERER, C.M., HOLLANDER, J.M., PERLMAN, I., Table of Isotopes, 6th Ed., Wiley, N.Y. (1967).

DISCUSSION

R.V. JOLOS: It seems to me that when you consider nuclei with the small deformation or transition nuclei as Os and Pt isotopes it is not evident that you can use the Hartree-Fock method because it does not take into account the fluctuations of the deformation which are large in these cases.

With the help of another method, which is based essentially on the boson expansion method proposed by S.T. Belyaev and V.G. Zelevinsky, and takes into account the fluctuations of the deformation I get another picture for the potential energy. Instead of one maximum at $\beta = 0$ and minimum at $\beta \neq 0$ (the usual picture for the Hartree calculations) there are two minima at $\beta = 0$ and at $\beta \neq 0$. The second minimum becomes deeper and deeper when it goes from spherical to deformed nuclei. And only in the case of strongly deformed nuclei do we get the same picture as in the Hartree-Fock calculations.

D.F. ZARETSKY: Dr. Kumar, does it follow from your calculations that the existence of a shape isomer stable against γ-deformation is possible?

Krishna KUMAR: In all our calculations, the potential energy rises or falls smoothly from $\gamma = 0°$ to $60°$ without a barrier in the middle. In fact, the γ-dependence is very similar to that shown by Prof. Szymanski. The reason is that the main γ-dependence comes from the $\beta^3 \cos 3\gamma$ term in accordance with general invariance properties of the potential energy function.

INTERMEDIATE STATES IN FISSION

V.M. STRUTINSKY* AND S. BJØRNHOLM
THE NIELS BOHR INSTITUTE,
UNIVERSITY OF COPENHAGEN,
COPENHAGEN, DENMARK

Abstract — Аннотация

INTERMEDIATE STATES IN FISSION. Consequences of the presence of a second, intermediate equilibrium state at large deformations in some fissioning nuclei (two-humped fission barrier) are discussed. The most important effects related to such states are: (1) spontaneously fissioning isomers, (2) grouping of neutron-induced fission resonances, related to intrinsic states in the second potential well, (3) vibration-mode resonances in the fission cross-section, and (4) moderation of the channel structure in fission fragment anisotropies for fission near the barrier. An attempt is made to summarize the evidence obtained from various experiments.

ПРОМЕЖУТОЧНЫЕ СОСТОЯНИЯ ДЕЛЕНИЯ. Обсуждаются последствия наличия второго промежуточного равновесного состояния при больших деформациях в некоторых делящихся ядрах (двугорбный барьер деления). Наиболее существенными эффектами, относящимися к этим состояниям, являются следующие: 1) наличие спонтанно делящихся изомеров, 2) группировка вызванного нейтронами резонансов деления, относящихся к внутренним состояниям во второй потенциальной яме, 3) вибрационные резонансы в сечении деления и 4) отклонения от обычной модели каналов в анизотропии осколков деления при делении около барьера. Анализируются данные, полученные в различных экспериментах.

INTRODUCTION

Non-uniformities in the energy distribution of single nucleons in the nuclear binding field influence the stability of heavy nuclei against fission in a very important way. When the nucleus is deformed, such as in fission, compression of the single-nucleon levels near the Fermi energy alternates with a thinning-out (a shell), and this leads to modulations in the liquid drop (LDM) energy of the nucleus (see Fig. 1).

Minima in the deformation energy, arising from shell effects, correspond to stationary deformations of the nucleus.

The possible appearance of shells in deformed nuclei was discussed in, for example, the paper by Geilikman [1]. However, the conclusions were so uncertain that it was commonly assumed that the shells are characteristic only for the spherical shape and disappear when the nucleus is slightly deformed.

The presence of shells is a rather regular feature, which is not related to the sphericity of the average field. The minimum at the smallest deformation corresponds to the ground-state deformation, spherical or deformed. Important shell effects are present also at larger deformations and, in some cases, these can give rise to a second minimum in the deformation energy with which spontaneously fissioning isomers, discovered in Dubna some years ago [2], are possibly related.

The shell phenomena are accounted for by the method of shell-energy corrections [3]. With this method the equilibrium deformations as well as

---

* On leave from the I.V. Kurchatov Institute for Atomic Energy, Moscow, USSR.

the shell energy corrections to the semi-empirical mass formulae can be evaluated, and they can be immediately compared with experiment (see Fig. 2).

The agreement is good and the calculations show that the results are rather insensitive to the specific single-particle model; this is, of course, important for extrapolations to larger deformations or new regions of nuclei.

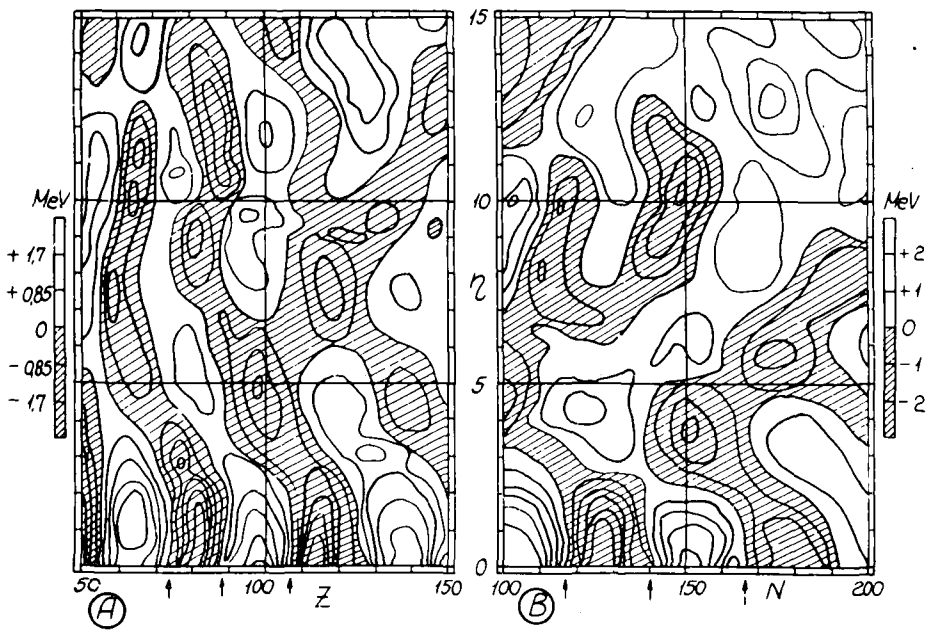

FIG. 1. Contour map of the shell energy correction to the LDM deformation energy; η is Nilsson's deformation parameter, calculated from the Nilsson level schemes suggested for the protons Z > 82 and neutrons (left) N > 126. The low-density "shell" regions, where δU is negative, are shaded. (From Ref. [3]).

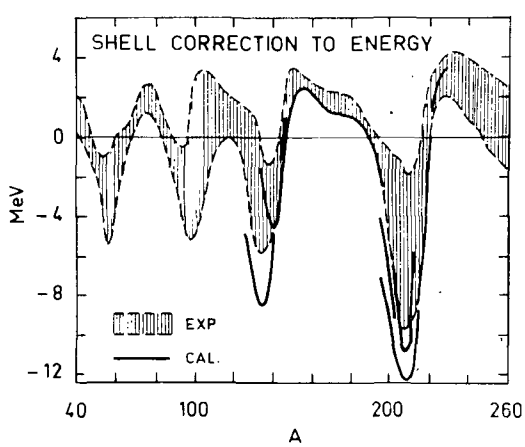

FIG. 2. Calculated total shell cross-sections for the nuclear ground-state masses compared with the experimental deviations from the smooth LDM mass law. (From Ref. [3]).

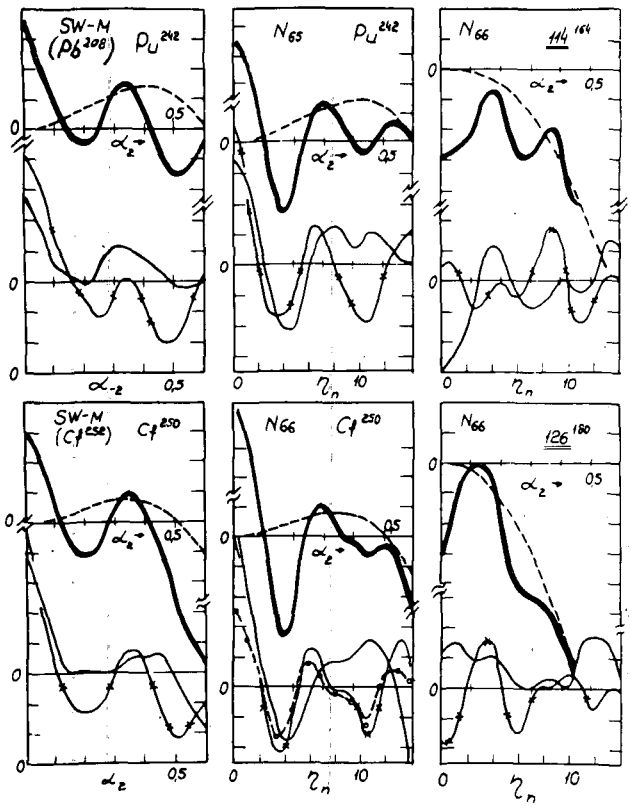

FIG. 3. Examples of the deformation energies (heavy lines) calculated with the perturbation theory Saxon-Woods level schemes (^{242}Pu, ^{250}Cf, left side) and the Nilsson schemes. Dashed lines are liquid drop deformation energies, thin lines the shell corrections for protons and neutrons (the latter are denoted by crosses). For the energy scale one division is 2 MeV. (From Ref. [3]).

At the same time, the calculations show that equilibrium states, corresponding to a second energy minimum on the way towards fission, may be important for a number of heavy elements, where the second minimum is found just a few MeV above the ground state. The energy difference between the two minima depends strongly on the effective surface energy of the LDM and is therefore, in general, larger for lighter nuclei, where the Coulomb field is weaker. The second minimum appears at a deformation, which is 2 to 2.5 times larger than the ground-state deformation. This corresponds approximately to the LDM saddle shapes in nuclei, such as uranium and plutonium. The LDM predicts here a long and flat portion in the diagram of energy versus deformation, i.e. a flat top of the fission barrier. For these nuclei, the shell corrections are therefore particularly likely to produce a pronounced second minimum.

As a result, one obtains fission barriers such as those shown in Fig. 3, depending somewhat on the single-particle model used.

Many experiments are insensitive to the presence of a second well. Single-particle transfer reactions, scattering and γ-transitions, for example, involve only excitations of states in the first well. For nuclear fission,

however, the second minimum is very important. During fission, the nucleus passes over the second minimum and its presence strongly influences the observed features of the process.

It was felt that the existence of the spontaneously fissioning isomers was suggestive evidence for the fact that the fission barrier could have two humps with a rather deep minimum between them.

Since then, several new developments have increased our belief in these ideas; thus, today we plan to start directly talking about the two-humped barrier. New calculations gave additional proofs that the presence of the second minimum is a rather general feature. It was obtained in all models known at present, including the finite-depth Woods-Saxon potential [4]; it is stable to some most important deformations, like Y_4-type or non-axial γ-deformations [4], and its features are rather insensitive to the model. The experimental evidences are: (a) fission isomers, (b) narrow sub-barrier fission resonance groups of compound type, (c) broad sub-barrier fission resonances of vibrational type, and (d) some evidence from studies of channel effects in near-the-barrier fission.

We shall try to discuss here some of the theoretical consequences of the two-humped barrier in relation to the experimental situation.

I

In hot nuclei, a fast dissipation of the collective motion normally takes place and, as a result, the nucleus takes a shape which corresponds to one or the other of the two energy minima. In the collective, as well as in each of the one-particle degrees of freedom, a relatively small amount of energy of the order of the nuclear temperature T is collected. If T is smaller than the depth of the potential well, the nucleus maintains its equilibrium shape for a relatively long time. Thus, there are two intermediate equilibrium states present in the compound nucleus, each with its own temperature, spectrum, etc. (see Fig. 4). For reactions produced by monochromatic neutrons, one may expect structures related to the states in the second potential well; particularly in the distribution of fission resonances, the fission width must be especially large, with capture resonances which are close in energy to these states [5]. The fission cross-section is modulated by this structure, and the energy width of these modulations corresponds to the spreading width (γ_2^t) of the quasi-equilibrium states in the second well. The structure in the fission cross-section is shown qualitatively in Fig. 5, where the different widths relevant to this case are indicated. The figure illustrates schematically the cross-section for fission induced in ^{240}Pu by sub-barrier neutrons, as described by Migneco and Theobald [6]. The quantity Γ_t is the total width of the compound nucleus formed in the neutron capture reaction; Fig. 5 corresponds to a case where γ_2^t is larger than Γ_t, but smaller than the spacing between the internal levels in the second well. The area of each resonance determines, as usual, the fission width Γ_f. Indices 1 and 2 correspond to the states in the first and second potential wells (class I and II states, respectively, according to the denotation given by J. E. Lynn) and quantities without these indices, denoted by Γ, refer to the compound nucleus as a whole. In general, these are different from the analogous quantities for the two states individually, but one may deduce simple relationships for the average widths, valid for the case which we consider here, i.e. when

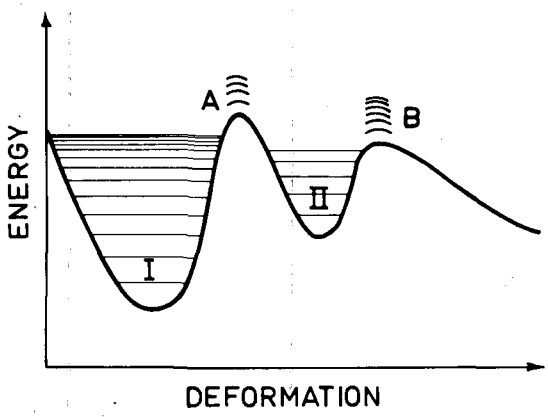

FIG. 4. Intrinsic excitations in the two potential wells and at the two barriers.

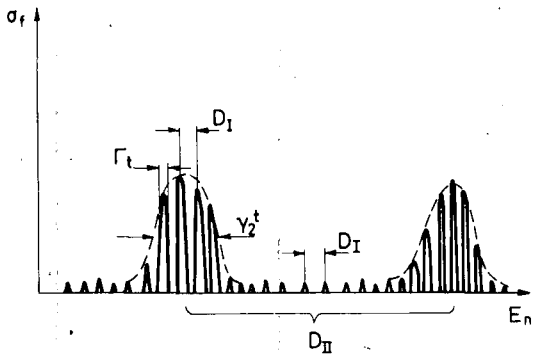

FIG. 5. Schematic representation of the fission cross-section observed for fission of ^{240}Pu by sub-barrier resonance neutrons. The quantities discussed in the text are shown on the figure.

the nucleus is hot in both states and a simple statistical model can be used. Later, we consider the case when the nucleus is cold in the second well and the statistical picture becomes irrelevant.

Let $n_1(\tau)$ and $n_2(\tau)$ be the populations of the first and the second potential wells at the time τ. We assume that the nucleus was formed at $\tau = 0$ in the first well, i.e.

$$n_1(0) = 1$$
$$n_2(0) = 0 \qquad (1)$$

For $\tau > 0$, the following equations hold:

$$\frac{\partial n_1}{\partial \tau} = -\gamma_1^t n_1 + \overleftarrow{\gamma}_2 n_2$$
$$\frac{\partial n_2}{\partial \tau} = \vec{\gamma}_1 n_1 - \gamma_2^t n_2 \qquad (2)$$

The symbols $\vec{\gamma}$ denote the widths of the internal non-radiative transitions from the first well to the second ($\vec{\gamma}_1$), and backward ($\vec{\gamma}_2$); γ_1^t and γ_2^t are the total widths of the states in the first and the second wells, respectively, which include the decay widths for all partial decays which are energetically possible. The rate of any partial decay of the compound nucleus as well as the probability for specific excitations in the second well (yield of the spontaneous fission isomers [7]) may be found from these equations. Thus the fission rate is determined by the equation

$$\frac{\partial n_f}{\partial \tau} = \vec{\gamma}_2 n_2(\tau), \qquad n_f(\tau) = \vec{\gamma}_2 \int_0^\tau n_2(\tau)\, d\tau \tag{3}$$

where n_f is the integrated number of fissions at the time τ. We find that the average number of fissions per compound nucleus formed is

$$n_f(\infty) = \int_0^\infty \vec{\gamma}_2 n_2(\tau)\, d\tau = \vec{\gamma}_1 \vec{\gamma}_2 / (\gamma_1^t \gamma_2^t - \vec{\gamma}_1 \overleftarrow{\gamma}_2). \tag{4}$$

This can be identified with the average branching ratio for fission, i.e. the ratio of the average fission width to the average total width of the nucleus $\langle \Gamma_f \rangle / \langle \Gamma_t \rangle$. Simple expressions for the widths of the compound nucleus are obtained for the case of a weak coupling with the second well or for a strong coupling when at least one of the two non-radiative transition widths $\vec{\gamma}_1$ or $\overleftarrow{\gamma}_2$ is larger than the decay widths γ_1^d and γ_2^d. The expression for the average fission width for the weak coupling case is

$$\langle \Gamma_f \rangle = \vec{\gamma}_1 \vec{\gamma}_2 / \gamma_2^t \tag{5}$$

Quantitative estimates can be obtained for an important practical case, when the spreading width γ_2^t of the state in the second well is larger than the average distance between the levels in the first well, so that each of the class II states overlaps with many states in the first well, as was illustrated in Fig. 3. In this case, the Bohr-Wheeler formula for average widths $\vec{\gamma}_1$, $\overleftarrow{\gamma}_2$ and $\vec{\gamma}_2$ may be used. In the case of ^{240}Pu, the spreading width γ_2^t is of the order of tens of keV, and it is clear that it is essentially a sum of $\overleftarrow{\gamma}_2$ and $\vec{\gamma}_2$:

$$\gamma_2^t \approx \frac{1}{2\pi\rho_2} [N(A)+N(B)] \tag{6}$$

The average fission width, in the region of the second well resonance, is

$$\langle \Gamma_f \rangle = \vec{\gamma}_1 \vec{\gamma}_2 / \gamma_2^t \approx \frac{1}{2\pi\rho_1} \frac{N(A)\,N(B)}{[N(A)+N(B)]} \tag{7}$$

The spreading width γ_2^t as well as $\langle \Gamma_f \rangle$ and the densities ρ_1 and ρ_2 are immediately obtained from experiment and, therefore, N(A) and N(B) may

be found. However, from these data it cannot be decided which of the two numbers is related to the barrier A and which to B, since Eqs (6) and (7) are symmetric in these two quantities. For the ^{240}Pu experiment we obtain N(A) or N(B) equal to 0.5 and N(B) (or N(A)) equal to 0.003.

These numbers show that the energy is slightly below one of the barriers and appreciably below the other. The large difference between the two numbers N(A) and N(B) is not surprising because of their exponentially strong dependence on the heights of the barriers.

At higher energies, the total width γ_2^t of the states in the second well approaches, or is larger than, the level spacing $1/\rho_2$ and no clear structure is to be seen. It might be expected, however, that in this case the influence of the second well may be disclosed by studying the autocorrelation in the fission cross-section, as in the case of Erikson's fluctuation. Evidence of this type, related possibly to the closed 4-fission channel in ^{235}U+n, has recently been reported by the Geel group; in ^{233}U, on the other hand, no autocorrelation effects could be found.

II

In discussing these results, it has been assumed that the motion in the fission direction, i.e. the separate stretching degree of freedom, is completely damped, completely distributed in a statistical way on the compound nuclear states in both wells. If the second minimum is not very deep, this assumption may not be true. The other extreme, no damping, is illustrated in Fig. 6. In this case, the penetration function will have spikes at energies corresponding to vibration state in the second well [8] (see Fig. 7).

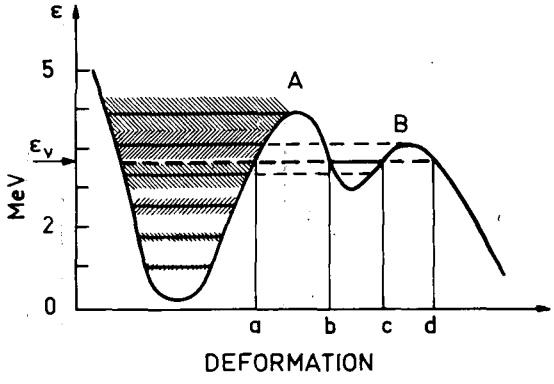

FIG. 6. Model of the vibrational states in the two-well model. Heavy lines represent the regions where the vibrational wave functions are concentrated, the energy ϵ_ν corresponds to a resonance in the second well. Damping is indicated with hatched lines. Because of larger damping, vibrations in the first well form almost a continuum at higher energies.

Perhaps this happens [9] in ^{230}Th+n (see Fig. 8) and, who knows, it may also have been observed in ^{239}Pu (d, pf) (see Fig. 9). The maximum at 4.9 MeV excitation energy, which is below the neutron binding energy, cannot be explained as a channel structure (A. Bohr's theory predicts

plateaus, not maxima), and may therefore represent another example of a resonance. If this is true, the plateaus, which are observed in the fission probability, might as well be weakly pronounced maxima and correspond to internal states in the second potential well. The true fission barrier, which corresponds to the top of the higher of the barriers A or B, would then lie at a higher energy than hitherto assumed. It seems that the existing experimental evidence does not rule out such a possibility, which deserves to be studied more carefully.

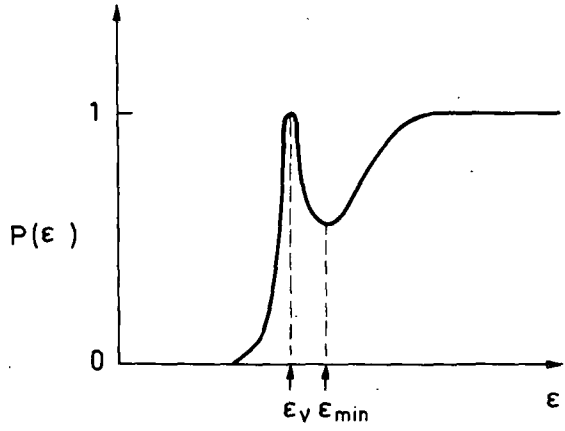

FIG. 7. Penetration function for vibrational motion in the fission direction for the two-humped potential, shown in Fig. 6.

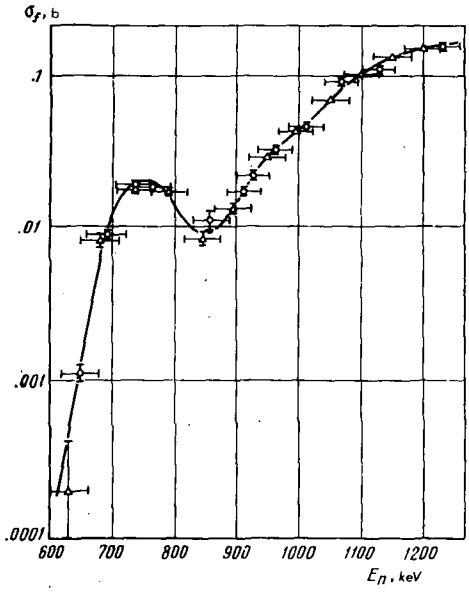

FIG. 8. Possible example of the vibration-mode resonance: cross-section for fission of ^{230}Th with neutrons. (From Ref. [9]).

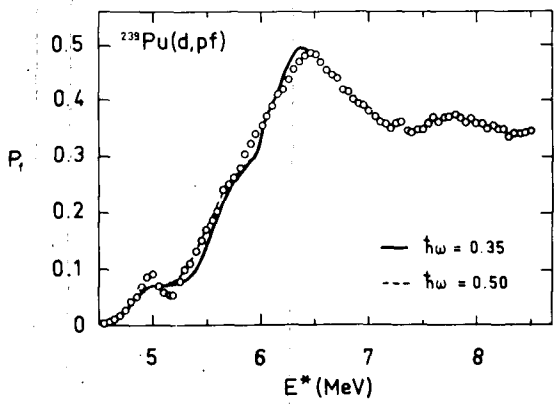

FIG. 9. Probability of fission as a function of the excitation energy of the compound nucleus, as obtained in Ref. [10] from the ^{239}Pu(d, pf) reaction.

It is interesting that the resonance maximum in $P(\epsilon)$ has a very peculiar form. Near the resonance

$$P(\epsilon) = \theta^2(\epsilon)/[\theta^2(\epsilon)+(\epsilon - \epsilon_{res})^2] \qquad (8)$$

where $\theta(\epsilon)$ is the escape width from the second well, the half-width of the resonance becomes exponentially small when ϵ decreases. However, owing to a very strong dependence of θ on the energy ϵ, the width of the resonance maximum in its lower part remains of the order of the frequency of vibrations in the second well, i.e. the resonance is very thin at the top and broad at the bottom. The observed value of $P(\epsilon_{res})$ will always be less than unity, both because of the poor energy resolution in the experiments and damping of the vibrational motion in the second well. Another condition for observing the maximum resonance in the fission cross-section is that the width θ must be less than the spacing between the intrinsic excitations (the fission channels). Otherwise, a plateau will be seen instead, when the sum over different fission channels is taken.

III

Another consequence of a two-humped barrier is that it affects the angular distribution of fission fragments. Looking at Fig. 3, we see that the nucleus may forget its orientation because it stays in the second well for a time long enough for coriolis forces to redistribute the angular momentum projection K with which the nucleus passed over the first barrier. Thus, the channel structure observed in angular anisotropy experiments must correspond to the second barrier B, if the second well is deep enough. Now, if the second barrier lies lower than the first, many channels will be open there and a weak, statistical-type angular anisotropy will result even in the near-barrier (i.e. near the barrier A) fission. This is important because, in the usual picture of channel effects, the channel structure must invariably be present near the barrier.

Even for some even target nuclei, such as ^{238}U and ^{240}Pu, the near-barrier neutron-induced fission is rather structureless (see Fig.10). In contrast to the lighter nuclei, the fission cross-section is peaked in the forward-backward direction and it changes smoothly with angle so that essentially only a P_2-component is necessary to describe the angular distribution. It also does not depend significantly on energy, and there is no pronounced channel structure in the integral fission cross-section.

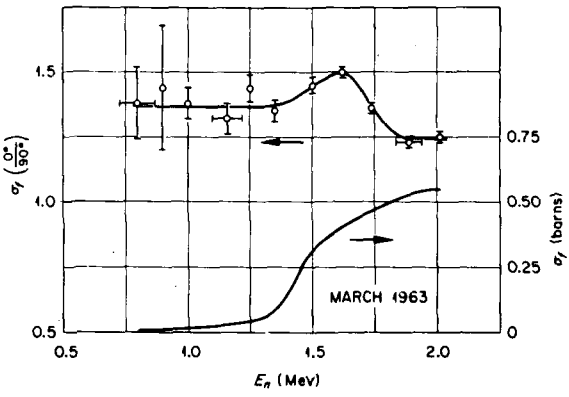

FIG.10. Fission fragment anisotropy and the cross-section for fission of ^{238}U. (From Ref. [11]).

So far, there seems to be no good explanation for it [11]. In some other cases, where a strong channel structure is observed, one may also see some effects of the second minimum, as in the case [11] of $^{234}U(n,f)$. Here, strong channel effects are observed in parallel with a pronounced structure of the excitation function for fission.

We think that it is Lamphere [11] who has pointed out a difficulty with this "typical case" of channel structure. The excitation function has a spike and you make inelastic neutron competition responsible for the decrease beyond the maximum; now, the anisotropy also decreases despite the fact that fission still proceeds through the same channel. In the standard theory, we have to make very artificial assumptions to explain this: the neutrons have to carry away a specific part of the angular momentum to explain the decrease in anisotropy. Perhaps in effect we are concerned here with a sub-barrier vibration-type resonance, in which case the anisotropy should peak together with the cross-section.

The examples discussed here seem to indicate that, indeed, the fission barrier can have quite a complicated structure and, in a sense, we should be happy to have found a new degree of freedom, a new dimension in fission, for a better understanding of the data. But of course a number of consequences follow from the new theory and we would like to see their verification before we are convinced. The second minimum must develop and disappear very smoothly when we add neutrons or protons to the nucleus. According to the calculations, something like 10 protons or neutrons must be added to see the minimum develop and disappear again. Thus, all the effects we have discussed for particular nuclei must also be present in their immediate neighbours. It is comforting that an intensified search for isomers, for example, extending the measurements to nanosecond life-

times, has resulted in the discovery [12] of eight new isomers of Am, Pu, and U or Np with a variety of lifetimes, as one would have expected. The theory predicts that the deepest minimum should occur for N = 148, and the isomers really seem to cluster around this number. Additional attempts to find isomers in lighter nuclei, such as ^{232}Th+d/p ^{233,234}U+13 MeV d/p, have failed. More detailed up-to-date information about the spontaneously fissioning isomers is presented in the talks by Drs. S.M. Polikanov and J.E. Lynn at this Symposium.

Evidence for sub-barrier resonances also clusters in the same region of neutron numbers. So far so good, but we can go further in our demand for consistency of the data. The excitation energy of the second minimum E_{isomer} can be measured through a determination of the threshold in compound reactions (p, 2n) or (n, 2n) leading to the isomer. This number can, in principle, be compared to a determination based on the measurements of sub-barrier resonance groups: the distance between groups measures the level density in the second well, the distance between the individual resonances essentially measures the level density in the first well. From these, it is possible to derive excitation energies from the level densities and thus to find the difference in excitation energy in the two wells [5]. We feel some satisfaction that isomers and sub-barrier resonances really seem to occur generally in this region and in the one case where the two independently derived energies can be compared, in ^{242}Am, they agree. An aspect of the isomer lifetimes is puzzling: actually one would estimate the spontaneous lifetime of an isomer, situated in the second minimum 3 MeV higher than the first, to be 10^{-10} s and not 10^{-2} s, as observed for ^{242}Am. The resonance data predict lower-lying isomers in Pu, for example, but here the lifetimes are of the order of 10^{-7} s, i.e. shorter. However, this discrepancy may be overcome by varying the shape of the barrier.

It is certainly a legitimate objection to say: No wonder that you find these special effects for neutron numbers near 148; all fission studies are made with nuclei in this vicinity. More significant would be to identify a new region of isomerism, new magic numbers for saddle shape deformation. Calculations show that N = 118 and Z = 86 (Nilsson's Lysekil version in Fig. 1) are also magic. Well, that gives ^{204}Rn, which could be studied in the isotope separation on-line experiments at CERN, for example.

We feel that we are in the middle of a very promising development. You may say that it has been shown that, even at high excitation energies of the nucleus, the quantum states separate in two well-defined classes weakly coupled to one another; in this sense, a nice parallel to the isospin analogue states is presented. There is another prospect if we can substantiate our findings. We essentially measure the properties of the single-particle energy diagram at very large deformations and extrapolate from small to large deformations. This is intimately connected to extrapolation from a small to a large particle number N or Z and thus it is related to the reliability with which we can hope to predict the stability of superheavy elements. The shell effects in spherical and deformed nuclei are extremely important for this problem, and a better understanding of them may be obtained from studies of a broader range of problems, particularly related to nuclear fission.

On the other hand, it seems that the method of shell energy correction provides a reasonable basis for the theoretical study of these problems. Some calculations on the stability of hypothetical superheavy elements

were done recently in Dubna by Muzichka, Pashkevich and Strutinsky [13], and in Berkeley by Nilsson and his group [14]. Very interesting results, which promise exciting developments, were obtained.

REFERENCES

[1] GEILIKMAN, B.T., Proc. Int. Conf. Nuclear Structure, Kingston, Canada, 1960, Univ. of Toronto Press, Toronto, and North-Holland, Amsterdam (1960) p.874.
[2] POLIKANOV, S.M., Usp. Fiz. Nauk, 94 (1968) 44.
[3] STRUTINSKY, V.M., Yadernaya Fiz. 3 (1966) 614; Nucl. Phys. A95 (1967) 420; Nucl. Phys. (1968) in press.
[4] PASHKEVICH, V.V., Contribution No. 94 to this Symposium.
[5] WEIGMANN, H., Z. Phys. 214 (1968) 7; LYNN, J.E., to be published.
[6] MIGNECO, E., THEOBALD, J.P., Nucl. Phys. A112 (1968) 603.
[7] JUNGCLAUSSEN, H., Yadernaya Fiz. 7 (1968) 83.
[8] GOL'DMAN, I.I., KRIVCHENKO, V.D., Problems in Quantum Mechanics, Pergamon Press, London (1961) p.9.
[9] VOROTNIKOV, P.E., Yadernaya Fiz. 5 (1967) 415, 728.
[10] BRITT, H.C., RICKEY, F.A., Jr., HALL, W.S., Los Alamos Sc. Lab. preprint 2A-DC-9562.
[11] LAMPHERE, R.M., Physics and Chemistry of Fission (Proc. Symp. Salzburg, 1951) 1, IAEA, Vienna (1965) 63.
[12] LARK, N., SLETTEN, G., BJØRNHOLM, S., Contribution No.90 to this Symposium; LARK, N., short contribution to Discussion following paper by S.M. Polikanov, these Proceedings.
[13] MUZICHKA, Yu.A., PASHKEVICH, V.V., STRUTINSKY, V.M., Preprint JINR (Dubna) R7-3733 (1967).
[14] NILSSON, S.G., NIX, J.R., SOBICZEWSKI, A., SZYMANSKI, Z., WYCECH, S., GUSTAFSON, G., MØLLER, P., UCRL-18068 (1968).

DISCUSSION

V.A. KRAVTSOV: I have a question concerning the first part of the paper. In studying the energy surface of the nuclei developed on the basis of experimental data (mass tables by Mattauch, Wapstra et al.) one can discover the sub-shells of protons 66 and 70. They are seen as valleys along the lines on the diagrams for Dy($Z = 66$) and Yb($Z = 70$) isotopes, whereas their curvature exceeds the errors of experimental data several times. All this occurs in the deformed nuclear region limited by the lines of $N = 88$ and $N = 114$. Can your theory explain the presence of these sub-shells?

V.M. STRUTINSKY: In principle it should. But up to now only preliminary "experimental" calculations have been made which seem to be insufficiently accurate for the description of such details.

Z. SZYMANSKI: You have shown the results of the calculation of the position of the second minimum. My question is whether the inclusion of the hexadecapole deformation could be important in these calculations.

V.M. STRUTINSKY: The effect of the hexadecapole deformation was estimated. Relatively small corrections arise but they do not change the picture.

S.T. BELYAEV: As follows from the paper by Dr. Kumar, the collective Hamiltonian has a very complicated structure, not only the potential but also the kinetic energy being strongly dependent on β and γ. In this

case, the stability of a nucleus is not determined only by potential energy. Was this question investigated?

V.M. STRUTINSKY: Dr. Kumar has considered the problem of collective modes in the so-called transition nuclei, where shells do not arise. There a finer structure (about 0.5 - 1.0 MeV) is meant. The shell effects are much larger. Therefore, the question is reduced to the relation between the frequency of oscillations and the depth of the well. The ratio of these quantities is, probably, sufficiently small.

J.J. GRIFFIN: At the second minimum we know that the surface energy is greater and the Coulomb energy less than at the first minimum. One might expect, therefore, that in the deformed isomer the Z^{th} proton level lies considerably lower than the N^{th} neutron level so that the nucleus is unstable against β-decay. I wonder whether such β-decays are accessible experimentally, and whether the theory in its present form is able to provide any guidance to experimentalists as to where best to look for such events?

V.M. STRUTINSKY: The life-times in the second well can be estimated from the life-times of spontaneously fissioning isomers. In some cases, it is seconds, therefore the measurement of β-decay is in principle possible. We hope to calculate the masses of nuclei with respect to deformation and then, perhaps, we shall be able to give guidance to experimentalists.

Yu. P. POPOV: How may the nuclear deformations, which you consider, affect the velocities of the α-decay of the states excited during the neutron capture?

V.M. STRUTINSKY: As I said, the presence of the second well does not influence most of the nuclear processes. I think that this is valid for the α-decay too.

Yu.Ts. OGANESYAN: You have said that a similar situation in the form of nuclear potential energy appears in the rare earth region. Does this mean that when the fission cross-sections or angular distributions in the rare earth region are studied, then the effects characteristic of heavy nuclei will be observed? And if so, then how strongly?

V.M. STRUTINSKY: Although the second shell appears in the rare-earth region, it produces only a very shallow minimum (or none) at a rather high energy, about 15 or 20 MeV. Therefore, it can hardly influence the fission process there.

F.L. SHAPIRO: What do you think about the possibility of using the reaction inverse to fission, for example the reaction of the fusion of the nuclei of krypton and xenon, for the study of nuclear states at large deformations, in particular those associated with the second well?

V.M. STRUTINSKY: I have not thought about this, but it should be done.

J.O. RASMUSSEN: I wish to comment on the alpha decay rate question. For decay of the highly deformed isomer, it might at first appear that alpha decay rates could be very fast, both because of increased decay energy and because of a thinner barrier at the poles of the spheroid. However, alpha decay to ground might be highly inhibited by a large shape change. For alpha decay to the deformed isomer of the daughter, the decay energy would be similar to ground-to-ground decay. Whether or not there is some small speed-up due to the thinner barrier depends on the type of Nilsson orbitals near the Fermi energy. If they are of low Ω value (projection of angular momentum), then alpha decay may exploit the thin

barrier and there would be a speed-up. On the other hand, if most orbitals have high Ω then there will be no speed-up from the thinner barrier because the alphas are formed at the nuclear equator where the barrier is thicker. We must look at a Nilsson level diagram for the region of the isomer to decide better. Finally, a question for Dr. Strutinsky. Does the double-humped barrier occur also in the region of ^{210}Po?

V.M. STRUTINSKY: Yes, it does, at least in the calculations which have been done so far.

R.L. HAHN: We have discussed alpha and beta decay. I wish now to ask about gamma decay. You show well-defined level structure in your well number II. Should not one expect to see gamma transitions between these levels? So far as I know, people have not seen any gamma rays from the spontaneously fissioning isomers.

V.M. STRUTINSKY: I believe that it would be rather difficult to do this.

S.A. KARAMYAN: Could you comment on the influence of the two-humped fission barrier on the mass, charge and energy distributions of fragments at induced fission?

V.M. STRUTINSKY: It is intended to look into this problem.

D.F. ZARETSKY: At present it cannot be stated that the shape isomer corresponding to the oblate deformation does not exist. If this is so, it may be assumed that the main data, namely the existence of an isomer for spontaneous fission and the anomaly in the cross-sections (n,f), maybe qualitatively explained by the hypothesis mentioned. The presence of isomers corresponding to the oblate shape can be discovered by studying delayed coincidences in the cascade of γ-quanta which occur after the neutron capture by nuclei. What is your opinion?

V.M. STRUTINSKY: The oblate shape minima which we obtained in the calculation were all unstable towards γ-deformations. I think that such an explanation would meet with other essential difficulties.

V.G. SOLOVIEV: The calculations of the deformation dependence of the total energy made by Arseniev, Malov and others showed that for the nuclei of the transuranium region the protruded rotational ellipsoid is an equilibrium shape. The energy minimum corresponds to the nuclear oblate shape.

Yu.P. POPOV: Did you obtain in your calculations the cases when the ratio of I and II maxima is inverse, i.e. the second one is below the first, and how will this affect the properties of fissioning nuclei?

V.M. STRUTINSKY: The second barrier is lower than the first essentially because of the Coulomb energy, when it strongly decreases in nuclei with a large value of Z^2/A. Therefore the second barrier must be higher than the first in lighter nuclei. The well is shallower there, too.

T.E.O. ERICSON: Various people have suggested looking for β, α and γ transitions from the second minimum. I am ignorant of these questions, and wonder how long the nucleus stays in the second minimum. This time is highly relevant for there are sum-rules of weak interactions, for example, which say that even a fully allowed β-decay cannot go faster than $\sim 10^{-4}$ sec^{-1} or so.

V.M. STRUTINSKY: My answer to Dr. Griffin applies here.

B.T. GEILIKMAN: In the calculations which I reported at the Kingston Conference on Nuclear Structure in 1960 it was shown that there exist shells for large nuclear deformations in the simple one-particle Nilsson model

and an ellipsoidal square well. In the anisotropical oscillation model the physical meaning of the secondary shells is especially clear. The energy levels of such an oscillator are of the form

$$E = \hbar\omega_x(n_\perp+1) + \hbar\omega_z(n_z+\tfrac{1}{2}); \qquad n_\perp = n_x+n_y; \quad \omega_x = \omega_y$$

or

$$E = \hbar\omega_z\left(n_z + n_\perp\frac{\omega_x}{\omega_z}\right) + E_0; \quad \text{if } \frac{\omega_x}{\omega_z} = 2, 3, 4$$

Then

$$E = \hbar\omega_z(n+mn_\perp) \equiv \hbar\omega_z n'$$

where $m = 1, 2, 3$ and n' is an integer, i.e. the energy degeneration appears again as in the spherical nucleus, i.e. some shells occur. If we introduce the deformation parameter ϵ according to

$$\omega_x = \omega_0(\epsilon)\left(1+\frac{\epsilon}{3}\right); \quad \omega_z = \omega_0(\epsilon)\left(1-\frac{2\epsilon}{3}\right)$$

then it is easy to see that shells appear at $\epsilon \equiv \epsilon_m = m/[1+(2m/3)] = 0.6; 6/7; 1$, and so on. Of especial importance is the shell for $\epsilon = 0.6$, i.e. $n' = n+n_\perp$. The following shells become denser and the magic numbers for them become closer to each other, i.e. the shell effects disappear when m increases. For $\epsilon = 0.6$ the magic numbers (corresponding to $n' = 0, 1, 2, \ldots$) are $2, 4, 6, 10, 16, 28, 40, 60, 80, 110, \ldots$ The introduction of the spin-orbital coupling and the transition to the Nilsson Hamiltonian change the magic numbers but conserve the same qualitative picture of secondary shells. Professor Strutinsky has made more detailed calculations.

The presence of the maxima on the curve $F_f(E)$ may also be explained without the assumption about two wells. Indeed, in the well for the nuclear potential energy as a function of the deformation parameter α there must exist quasi-stationary levels. The fission probability should be proportional to the square of the ψ function amplitude $\psi(\alpha)$ inside the well a(E) which is especially large for quasi-stationary levels. It is known that

$$a^2(E) \simeq \frac{\Delta E_i^2 \cdot p(E)}{(E-E_i)^2 + (\Delta E_i)^2 \cdot p^2(E)}$$

Then

$$\Gamma_f \approx \hbar\omega \cdot W(E) \cdot a^2(E) \cdot p(E)$$

Here $\Delta E_i \equiv E_i - E_{i-1}$ is the scattering between two quasi-stationary levels; $p(E) = \exp(-G)$ is the barrier penetrability; $G = \frac{2}{\hbar}\int_{\alpha_1}^{\alpha_2}\sqrt{2B[U(\alpha)-E]\hbar}\cdot d\alpha$; B is

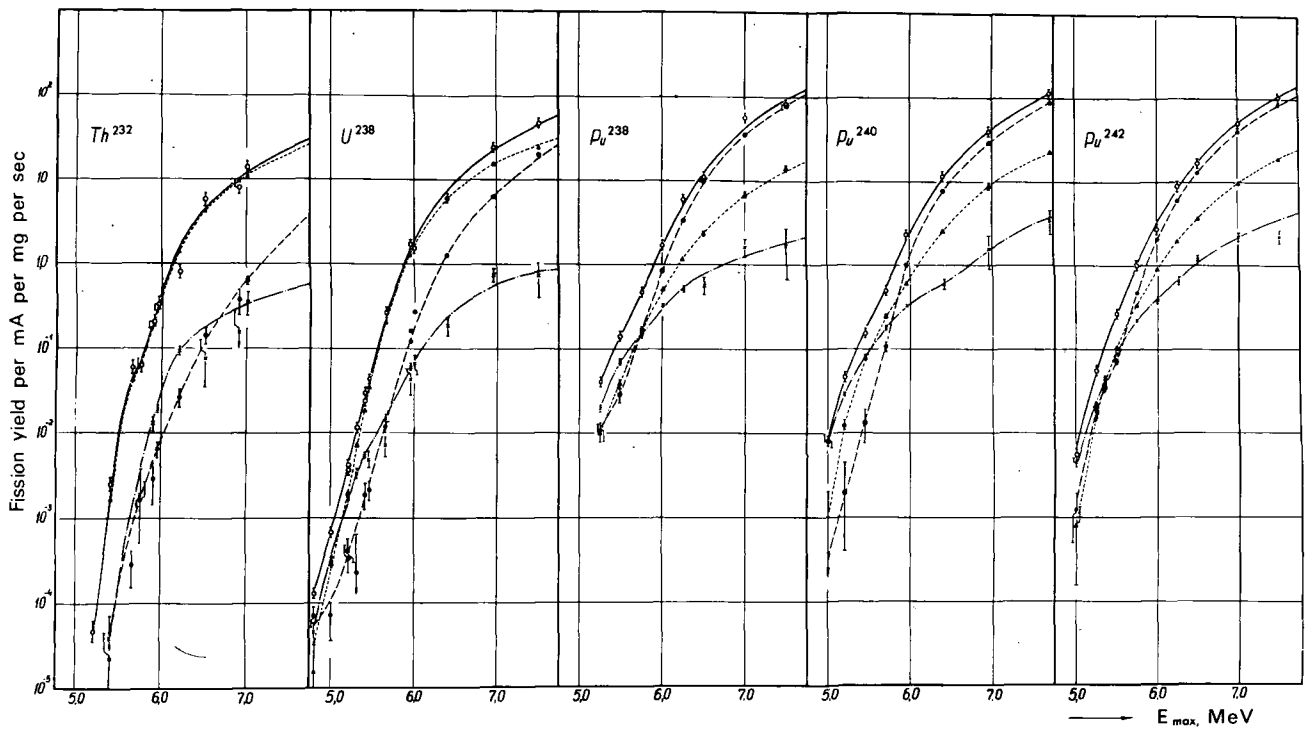

FIG. A. Fission yield per μA, per mg, per sec.
——— total fission yield
---------- dipole fission yield through the channel K = 0
– – – – – – dipole fission yield through the channel K = 1
-·-·-·-·- quadrupole fission yield

the mass coefficient and W(E) is the probability of the thermal fluctuation corresponding to the concentration of the energy E on the degrees of freedom α. All the factors except $a^2(E)$ depend smoothly on E; a^2 has the character of the dispersion formula. The levels E_i become closer to each other near the barrier top and ΔE_i may be very small there. These levels form a second system of levels in addition to the usual system of nucleon levels.

L.N. USACHEV: Owing to new concepts on the fission two-humped barrier, I would like to draw your attention to some experimental results on the photo-fission of even-even nuclei ^{232}Th, ^{238}U, ^{238}Pu, ^{240}Pu and ^{242}Pu on the bremsstrahlung spectra whose boundary energies are varied within 5-8 MeV.

The method of measurement and the main results have been published in some papers by N.S. Rabotnov, G.N. Smirenkin, A.S. Soldatov, L.N. Usachev (Institute of Physics and Power Engineering, Obninsk), S.P. Kapitza and Yu.M. Tsipeniuk (S.I. Vavilov Institute for Physical Problems, Moscow).

I shall mention only that the 12 MeV microtron of the Institute for Physical Problems and the glass technique have been used. The yield of fission fragments at each energy has been expanded into three components differing in their angular distribution: quadrupole, dipole with angular distribution $\cos^2\theta$, and the isotropic ones. The isotropic component is related by us to dipole gamma-quanta fission through the K = 1 fission channel, whereas the component $\cos^2\theta$ is due to fission through the K = 0 channel.

Consider Fig. A, where the curves have the meanings given in the caption. The aim of my comment is to compare the relative energy dependence of fission through the channels K = 0 and K = 1.

In the case of Th and U the K = 1 component does not reach the K = 0 component. Such behaviour does not contradict the old concept of the one-hump fission barrier and fission channels in the saddle-point developed by Professor A. Bohr in 1955.

However, the overtaking of the K = 0 component by the K = 1 component, occurring for all three Pu isotopes far below the fission barrier, cannot be explained from the point of view of the old concept of the fission barrier.

At the same time, the concept of the two-humped barrier having the first maximum higher allows one to explain the observed phenomenon.

As to the cases with Th and U, the observed behaviour of fission components is described on the basis of the two-humped potential curve having approximately similar heights of both the barriers or having a higher second barrier.

I.P. SELINOV: Professor Strutinsky's very interesting calculations are based mainly on experimental data on nuclide masses used for the determination of the shell correction. Thus, the dependence of the binding energy curve and the improvement of the shell model are of importance for the development of this method. The pairing energy curve that has been demonstrated has been drawn entirely on the basis of experimental data. It shows a sharp decrease of the binding energy after nuclides having the "magic" neutron numbers: $^{88}Sr_{50}$, $^{140}Ce_{82}$, $^{208}Pb_{126}$ etc., which, therefore, can be considered as "end" nuclides completing nuclear shells. In view of the regularities of this curve and of other nuclear properties, the principles of a new nuclear model construction (the so-called bihomonucleon version of the shell theory) have been formulated. This model,

which I have no possibility of discussing in detail here, can explain better than other models the structure of a number of beta-stable isotopes and all the mass peculiarities and some other properties. It also allows one to predict beta-stable isotopes of transactinides and to determine the region of longest-lived nuclides. One usually does not take into account that the 2 beta-stable line is of significance for the problem that has been discussed of the longest-lived isotopes of transactinides. As has been mentioned by the author, the half-lives in beta-transitions (T_β) are reduced on removal from the beta-stability region. Therefore, if there were nuclides having larger periods of spontaneous fission (T_0) far from the beta-stability region, this would not be important for their production since they would disintegrate rapidly by beta or alpha-decays before these decay chains had reached the longest-lived beta-stable isotopes (with considerably smaller number Z than the initial ones). These nuclides could decay by spontaneous fission in traversing the regions of short-lived spontaneously fissioning isotopes. Moreover, one can assume with great probability that these excess-proton nuclides (in the majority of reactions with multicharge ions) can be reduced by removing from the 2 beta-stability region, as this occurs for well-known isotopes. On this basis, as well as from the dependences of the binding energy and in the 2 beta-stable nuclide formations from p and n, one can predict that the longest-lived transactinide isotopes will be near the end nuclide (the nuclear analogue ^{208}Pb) according to the simple rule of $\Delta Z = 2n = 2 \times 6 = 12$, where n is the shell number, and also near the nuclear analogues of the longest-lived Th and U natural isotopes. It is most probable that the isotope $^{288}110_{178}$, $^{298}114_{184}$ or $^{300}114_{186}$ (but not the nuclide $^{276}106_{170}$ suggested earlier) will be the end nuclide. The long-lived nuclear analogue of ^{238}U will be the nuclide $^{336}126$ (with end nuclide $^{300}114$).

It would be of interest to know Professor Strutinsky's opinion on the possibility of continuing his interesting and picturesque diagram in the direction of removed transactinides in order to clarify whether these nuclides, having the largest values of T_0, are in the region of beta-stable isotopes near the nuclides $^{300}114$ and $^{336}126$.

V.M. STRUTINSKY: The calculation of hypothetical super-heavy nuclei is one of the main aims of the calculations by the shell correction method. This would, however, require a separate discussion.

In concluding the present discussion, I would first like to note that a better understanding of the role of the shells both in spherical and deformed nuclei would lead us to a better understanding of the whole problem of stability of the superheavy nuclei, which lie far from the beta-stability line.

Qualitatively, the distribution of shells in deformed nuclei can be easily understood by considering a simplified shell model. In nuclear deformation the splitting of 'shell' levels takes place, which results in the picture which is characterized by the deformation of the order of $A^{-1/3}$ and inhomogeneities in energy intervals of the order of $\hbar\omega \approx 6$-8 MeV. The oscillator is a very special case.

My third remark concerns the alternative interpretation of 'vibrational' resonances in the fission cross-section, which was suggested by Dr. Geilikman. Of course, it might be possible to associate them with the vibrational levels in the first well, but it seems to me that in this case a difficulty will arise since I think it should be assumed that vibrational level at a 5-7 MeV excitation energy has a width of the order of 100 keV.

SPONTANEOUSLY FISSIONING ISOMERS

S.M. POLIKANOV
JOINT INSTITUTE FOR NUCLEAR RESEARCH,
DUBNA, UNION OF SOVIET SOCIALIST REPUBLICS

Abstract — Аннотация

SPONTANEOUSLY FISSIONING ISOMERS. A review is given of the basic experimental data which permit some assumptions to be made about the nature of the spontaneously fissioning isomer. Recently, americium isomer production both by neutron radiative capture and stripping reactions with deuterons has been studied. An analysis of the data obtained provided the basis for suggesting "shape isomerism" in the case of the americium fissioning isomers.

Some possible experiments permitting a check on the validity of the suggested hypothesis are discussed.

СПОНТАННО ДЕЛЯЩИЕСЯ ИЗОМЕРЫ. Дается обзор основных экспериментальных данных, которые позволяют сделать некоторые предположения относительно природы спонтанно делящихся изомеров. Недавно было изучено образование изомера америция как при радиационном захвате нейтронов, так и в реакциях срыва на дейтонах. Анализ полученных данных дает основание сделать предположение "об изомерии формы" в случае спонтанно делящихся изомеров америция. Обсуждаются возможные эксперименты, позволяющие проверить справедливость сделанной гипотезы.

In recent years some new experimental data about spontaneously fissioning isomers of transuranium have appeared which permit us to assume that we are dealing with "shape isomerism".

There are also some theoretical foundations justifying the consideration of this hypothesis, i.e. the calculations made by Strutinsky [1] and Gustafson et al. [2], where conclusions as to the complex fission barrier shape were drawn and, in particular, the second minima of the potential energy at the saddle point.

Nevertheless, it is impossible now to draw only the conclusion that the deformation parameter is larger for the observed isomeric states than that for the ground state. The available experimental data, as we shall see later, only make it possible to state that they do not contradict this hypothesis but nothing more. Thus, serious work on the accumulation of new facts is needed.

Let us now analyse the most important experimental data.

First of all, the question arises as to how often the spontaneously fissioning isomers appear among transuranium elements.

Figure 1 shows the data on the half-lives of all isomers synthesized up to now. The surest are the points for americium isomers with masses 238, 240, 242 and 244.

There is no doubt that for these nuclei the observed effect is due to isomer fission with half-lives of 60 μs to 14 ms. All americium isomers shown have odd numbers of protons and neutrons. For a long time it was not clear why only odd-odd isomers were observed.

There were two possible reasons for this: either such isomers did not exist, or their half-lives were so short that it was impossible to observe such isomers with the help of the equipment used in earlier experiments.

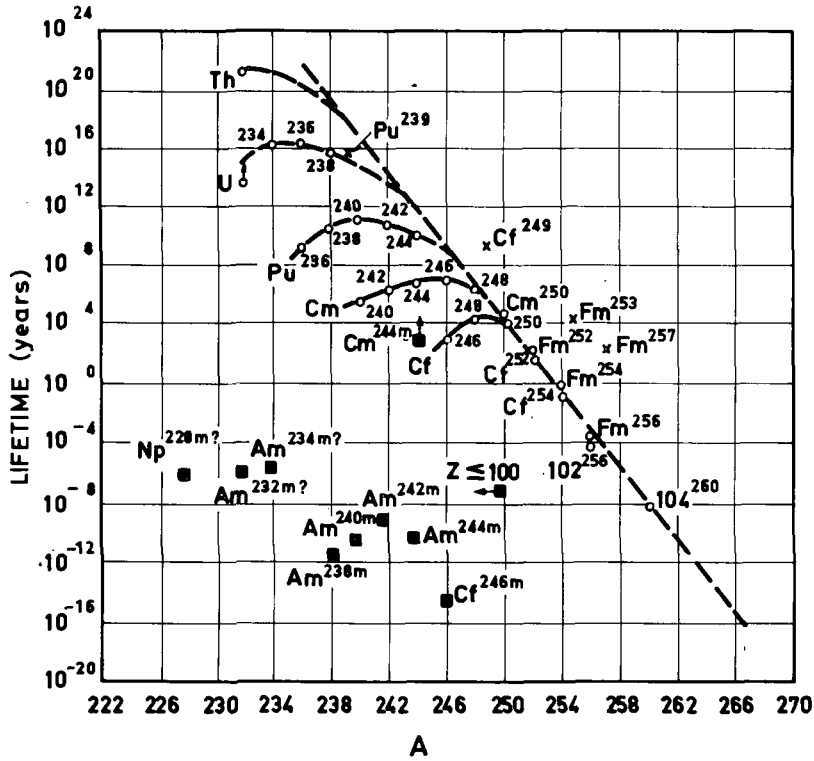

FIG.1. Systematics of spontaneous fission half-lives. ■ isomers, ○ even-even nuclei, x odd nuclei.

The only even-even isomer with a half-life of $\sim 10^{-7}$ s known up to now was ^{246}Cf produced in ^{238}U irradiation with ^{12}C [3].

At the Niels Bohr Institute, Bjørnholm et al. [4] recently observed new fissioning isomers with half-lives of 10-100 ns in experiments on ^{235}U, ^{239}Pu, ^{240}Pu, ^{241}Pu, and ^{242}Pu targets irradiated with deuterons. Apparently, in this case decay of isomers with even number of nucleons took place. However, it is not excluded that new odd-odd isomers were produced.

It can thus be seen that in the Am region the existence of a spontaneously fissioning isomer is rather the rule than the exception.

In the experiments with heavy ions some fissioning isomers with half-lives ~ 3 s and longer were produced; however, these isomers have not yet been identified and for this reason their properties cannot be discussed.

The fullest information obtained so far is related to americium isomers. The isomeric state energy values determined in threshold measurements for (p, 2n) and (n, 2n) reactions are given in Table I.

According to rough estimates, a change of 1 MeV in the fission barrier height corresponds to a barrier penetrability change by a factor $\sim 10^8$. Consequently, for the excited state with energy near 3 MeV we can expect the penetrability to increase 10^{24} times, on the assumption that the height of the fission barrier does not change and this agrees with experimental data.

TABLE I. ISOMERIC STATE ENERGY VALUES

Isomer	^{238}Am	^{240}Am	^{242}Am
Half-life (s)	6×10^{-5}	9×10^{-4}	1.4×10^{-2}
Excitation energy (MeV)	3-4	3.15 ± 0.25	2.9 ± 0.4

However, the question now is: Why is the electromagnetic transition from the isomeric state hindered?

Fig. 2 shows the level scheme for ^{242}Am calculated by Malov et al. [5]. We see that the levels with spin 12 ħ appear already at 1.2 MeV. To explain the large value of the hindrance factor ($\sim 10^{12}$) we suggest that the isomer spin is high, at least higher than 14 ħ.

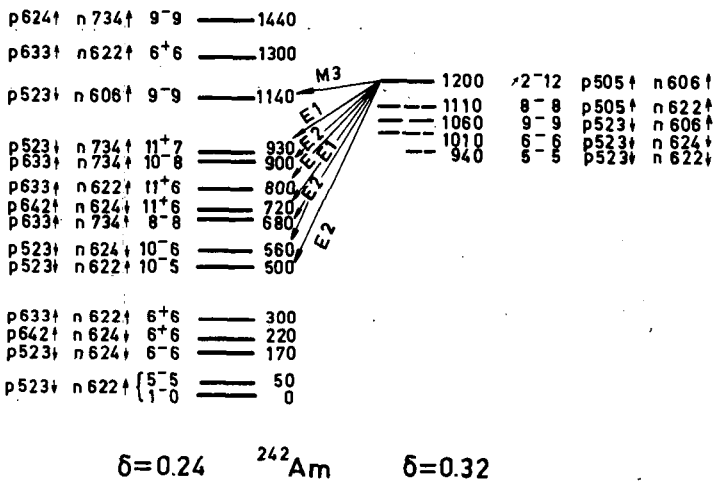

FIG. 2. Level scheme of ^{242}Am; δ is the deformation parameter.

Now there is only one possibility of obtaining some information concerning the spin value of spontaneously fissioning isomers. This follows from an analysis of experimental data on the main features of isomer formation in nuclear reactions.

A fact which attracts attention is that in the case of ^{242}Am the isomeric ratio, equal almost to 10^{-4}, in practice does not depend on the compound nucleus spin (Fig. 3).

At the same time, it is clear from Fig. 3 that the probability of formation of two quasiparticle isomers ^{196}Au and ^{190}Ir with spins 12 ħ and 11 ħ increases sharply with the increase of the compound-nucleus spin.

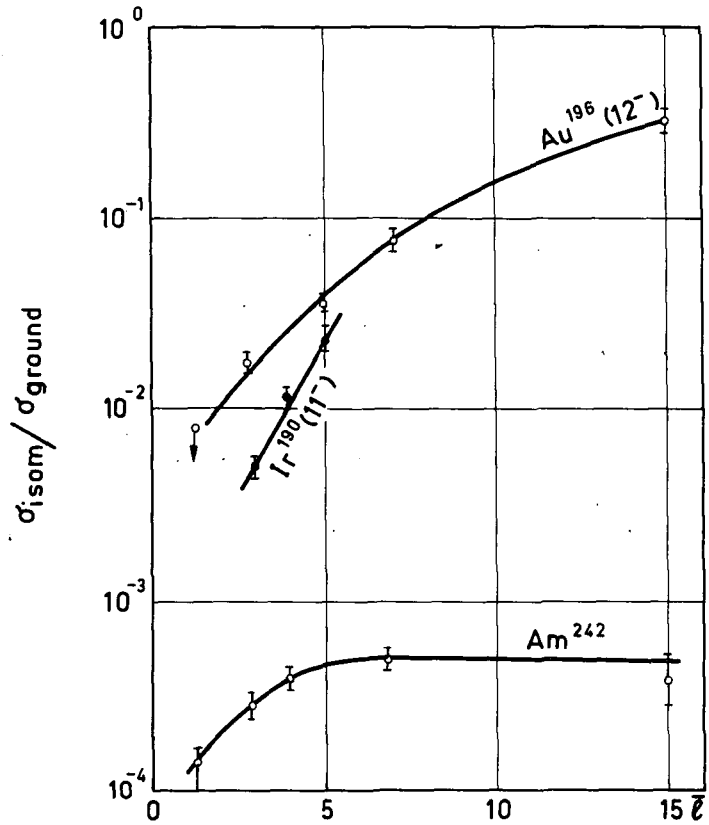

FIG.3. Dependence of isomeric ratio on averaged angular momentum $\bar{\ell}$.

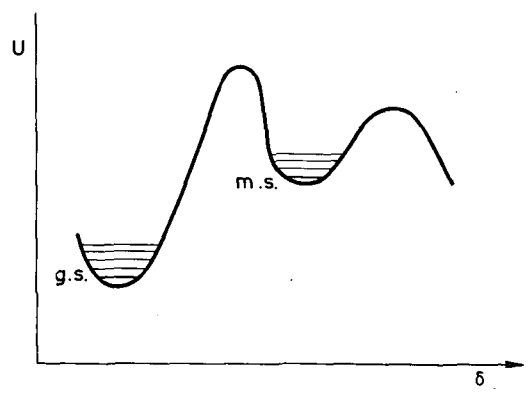

FIG.4. Fission barrier calculated with shell corrections [1].

This circumstance indicates that the spin of the ^{242}Au isomer does not differ greatly from that in the ground state, i.e. it is equal to some units of $\hbar$ only [6].

A very simple nuclear reaction leading to ^{242}Am isomer formation is the radiative capture of neutrons with ~1.5 MeV energy by ^{241}Am [7]. The cross-section of the spontaneously fissioning ^{242}Am isomer production is equal to 1.5×10^{-29} cm^2 with this neutron energy, i.e. only ten times less than for the ^{243}Am (n, 2n) ^{242}Am reaction although the partial cross-section of formation of a compound nucleus with spin more than 14 $\hbar$ is some orders less for the reaction of neutron radiative capture.

The experimental data hitherto available lead to the conclusion that the spin of the ^{242}Am isomer is apparently low. However, if the spin of the isomeric state is low it is difficult to understand the reason for the stability with respect to γ-emission.

In connection with this, some authors have suggested that the large hindrance factor is due to the large difference of the nucleus shape in the ground and the isomeric states [9].

In particular, it is possible that the isomeric state is the ground state in the second potential well obtained in Strutinsky's calculations (Fig. 4). The fission barrier for such a state is sharply decreased, and there are no difficulties in explaining the high probability of spontaneous fission.

At the same time, the potential barrier between the isomeric and the ground states will lead to a large retardation of the electromagnetic transition.

The estimates made by Baldin et al. [10] show that the necessary value of the hindrance factor may be obtained if the deformation parameter δ_m is near to 0.6 in the case of the isomer as well as when the ^{242}Am ground state is near to 0.3.

Fig. 5 shows the cross-section for the ^{242}Am isomer formation for neutron radiative capture depending on neutron energy. One can see that the shape of the curve obtained is unusual for neutron radiative capture reactions. Usually, a monotonic decrease of cross-section in the studied energy range is observed. But for the ^{242}Am isomer a rather sharp cross-section rise in the 0.5-1.5 MeV energy range is observed with neutron energy increase, the slope of the curve being just the same as that for neutron-induced fission.

Such a character for the curve can be understood if it is assumed that the isomeric state corresponds to a level in the second potential well, separated from the ground state by a barrier.

If we take this assumption into consideration, the increase of the isomer formation cross-section can be explained as the result of overcoming the barrier separating the two wells. For thermal neutron capture the probability of overcoming the barrier is low and for this reason the probability of both isomer production and fission is significantly less in comparison with radiative capture to the ground state of ^{242}Am [11].

The decrease of the cross-section for production of the ^{242}Am isomer at neutron energy higher than 1.5 MeV is evidently induced by the increase of inelastic neutron scattering.

Bjørnholm et al. [12] studied Am isomer formation in (d, p) and (d, t) reactions. Fig. 6 shows the cross-section obtained for the ^{242}Am and ^{244}Am isomers produced in (d, p) reaction. In the case of the (d, t) reaction the cross-section appeared to be too low to be observed.

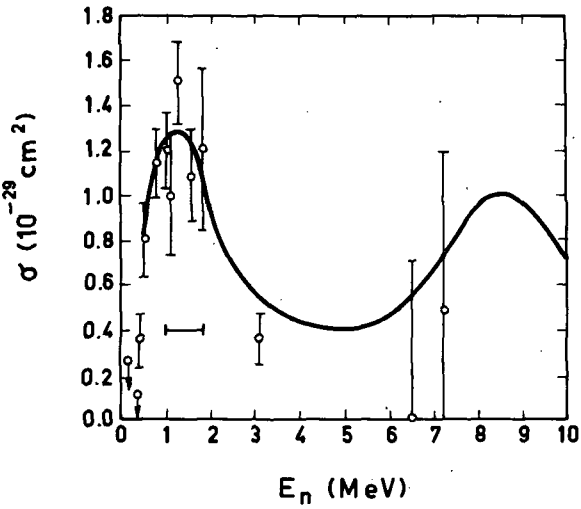

FIG. 5. Excitation function for the ^{242}Am spontaneously fissioning isomer resulting from neutron radiative capture.

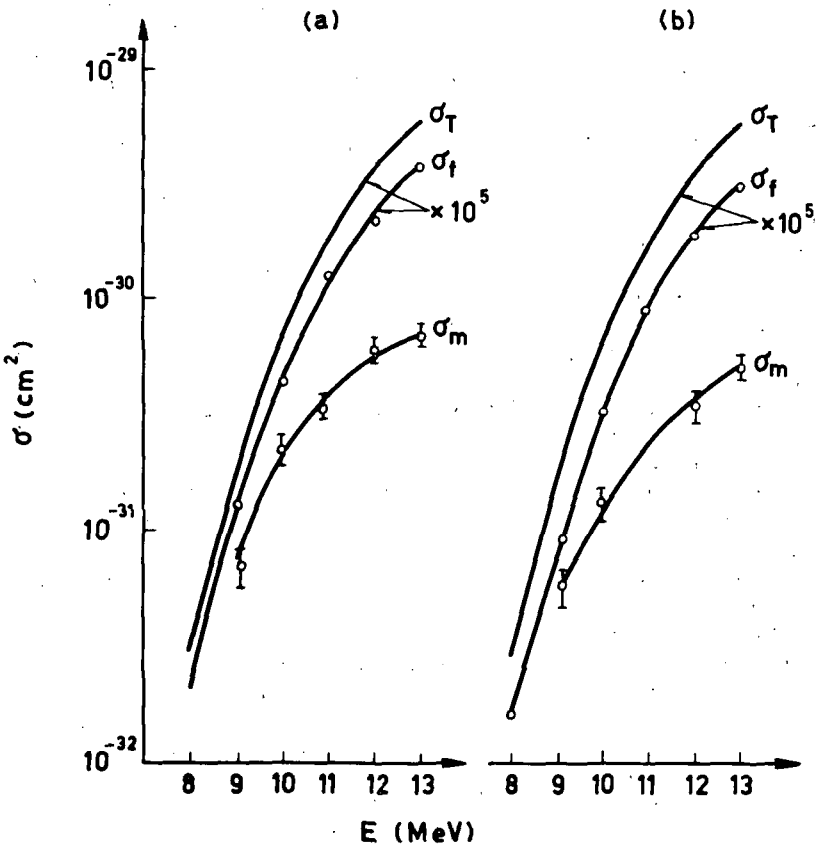

FIG. 6. Excitation functions for compound-nucleus formation (σ_T), induced fission (σ_f) and ^{241,243}Am (d, p) ^{242,244}Am (σ_m). (a) ^{241}Am, (b) ^{243}Am.

The experimental data analysis done by the authors on the basis of present ideas about the neutron stripping reaction mechanism led them to the conclusion that for isomer production the formation of ^{242}Am excited states proceeds at an energy higher than 6 MeV. This result is in good agreement with the data on the $^{241}Am(n,\gamma)^{242m}Am$ reaction and was explained by the authors as a possible indication of the fact that the observed isomers are "shape isomers".

Of course, we cannot exclude a different nature for spontaneously fissioning isomers, and further experiments are necessary to decide this problem.

In Refs [10, 13] some conclusions were given to the effect that if the Am isomers discussed are really strongly deformed it is possible to obtain some information on the deformation parameter by studying the radiative capture in a wide neutron energy range.

As a basis, the above-mentioned authors took the well-known experimental fact of giant resonance splitting into two peaks observed during photonuclear reaction studies. This splitting is explained as a result of two types of nucleus oscillations — along and perpendicular to the symmetry axis of the deformed nucleus.

The estimates show that this optical anisotropy of the solid line in Fig. 5 represents the result of the calculations [10] on the assumption that the deformation parameter of ^{242}Am in the isomeric state is equal to about 0.6.

In the framework of the model considered it was assumed that the appearance of a peak is connected with dipole transition when the excitation energy corresponds to the giant resonance.

In conclusion, let us consider some possible experiments which will extend our understanding of the nature of the spontaneously fissioning isomer.

It is interesting to extend the experiments on neutron radiative capture with ^{242m}Am formation. In experiments with neutron energies up to 10 MeV it is possible to check whether the second maximum for cross-section at $E_n \approx 8$ MeV exists.

It seems to be very important to increase the efficiency of the equipment and to measure the cross-section for ^{242m}Am production from the thermal energy of neutrons up to some eV where the cross-section for induced fission is about 3×10^{-24} cm^2. If ^{242m}Am is a nucleus "frozen" in the saddle point, then in the range from thermal energy up to 1.5 MeV the dependence of isomer formation on the neutron energy will be just the same as that for induced fission.

Finally, the discovery of short-lived isomers in Copenhagen permits us, in principle, to study the (d, pi) reaction with measurements of the energy spectra of the proton which accompanies the isomer formation.

REFERENCES

[1] STRUTINSKY, V.M., in Physics and Chemistry of Fission, (Proc. Symp. Salzburg, 1965) 1, IAEA Vienna (1965) 171.

[2] GUSTAFSON, C., LAMM, I.L., NILSSON, B., NILSSON, S.G., Ark. Fys. 36 (1967) 613.

[3] GANGRSKY, Y.P., MARKOV, B.N., POLIKANOV, S.M., CHARISOV, I.F., JUNGCLAUSSEN, G., Preprint JINR P7-3673, Dubna (1968).

[4] BJØRNHOLM, S., private communication.
[5] MALOV, L.A., POLIKANOV, S.M., SOLOVIEV, V.G., Yademaya Fiz. 4 (1966) 528.
[6] FLEROV, G.N., GANGRSKY, Y.P., MARKOV, B.N., PLEVE, A.A., POLIKANOV, S.M., JUNGCLAUSSEN, G., Yademaya Fiz. 6 (1967) 17.
[7] BOKA, I., MORTOLOGU, N., SEZON, M., VILKOV, I., VILKOV, N., FLEROV, G.N., PLEVE, A.A., POLIKANOV, S.M., TRETIAKOVA, S.P., Preprint JINR E15-3573, Dubna (1967).
[8] LINEV, A.F., MARKOV, B.N., PLEVE, A.A., POLIKANOV, S.M., Nucl. Phys. 63 (1965) 173.
[9] POLIKANOV, S.M., Usp. fiz. Nauk 94 (1968) 44.
[10] BALDIN, A.M., SEMENKO, S.F., TULUPOV, B.A., submitted to Yademaya Fiz.
[11] MARKOV, B.N., PLEVE, A.A., POLIKANOV, S.M., FLEROV, G.N., Yademaya Fiz. 3 (1966) 455.
[12] BJØRNHOLM, S., BORGGREEN, J., GANGRSKY, Y.P., SLETTEN, G., Preprint JINR P6-3744, Dubna (1968).
[13] GREINER, W., private communication.

DISCUSSION

Short Contribution

N. LARK: I should like to report the discovery of several new short-lived spontaneously fissioning isomers. This research has been done at the Niels Bohr Institute by G. Sletten, S. Bjørnholm and myself, with the collaboration of V.A. Druin during the early stages. I shall confine my report entirely to our own experimental procedures and results and leave general discussion and theoretical interpretation to other speakers on the program.

We have bombarded thin targets of the available enriched isotopes of Th, U, Np and Pu with protons and deuterons of 13 MeV energy. Fission fragments from the decay-in-flight of recoiling compound nuclei are registered in plastic detector foils which are placed so that they cannot be hit by fission fragments coming directly from the target. The plastic foils are 15 cm long, and the front edge is 5 mm from the target, so we can measure half-lives in the range of 15 ns to 1 μs.

The detector foils are 8 μm thick Makrofol, a polycarbonate plastic. After exposure, they are etched in sodium hydroxide, which makes microscopic holes through the foils by dissolving away the material which was damaged by the passage of the heavily ionizing fission fragments. Then a spark gap is used as a fast scanning device for finding the holes in the foil. The sparks enlarge the holes and also darken the rims of the holes, so that they become clearly visible to the unaided eye.

The analysis of our results is made difficult by the problems of absorption and scattering of the recoiling nuclei in the targets. Consequently, we have not yet completed our analyses, so that values which are quoted here must be considered very preliminary. Uncertainties may be as large as a factor of two in some cases. Cross-sections for producing the various isomers in reactions induced by 13 MeV protons and deuterons are consistently near 1 μb, while our limit of detectability is about 0.02 μb. Because of this consistency and our experimental uncertainties I will not consider most cross-sections in detail here.

The best studied of the new isomers are odd-mass Am isotopes. From the reactions ^{241}Pu+d and ^{242}Pu+p at 13 MeV we observe delayed fission with a lifetime of about 1.5 μs. The isomer is then very probably

^{241}Am. We have measured the excitation function for the (p, 2n) reaction and find the threshold is 2.5 MeV higher than the Q value for the reaction to the ground state. This difference probably represents the excitation energy of the isomeric state.

In an entirely parallel situation, we observe delayed fission with a half-life of 140 ns from the reactions ^{239}Pu+d and ^{240}Pu+p. From the threshold of the (p, 2n) reaction we infer that the excitation energy of the ^{239}Am isomer is 2.9 MeV.

In 13 MeV deuteron bombardments of ^{239}Pu, ^{240}Pu, ^{241}Pu and ^{242}Pu we observe delayed fission with half-lives of ~10, 35, 40 and 55 ns, respectively. These are in addition to the long-lived isomers of Am produced in each case. None of these short-lived isomers are seen from proton-induced reactions, so it is likely that the (d, p) reaction is responsible, and that the isomers are in ^{240,241,242,243}Pu.

In a similar way, we see delayed fission with a 105 ns half-life from bombardment of ^{235}U with deuterons, but find nothing from proton bombardment of ^{234,235,236}U or deuteron bombardment of ^{234}U or ^{236}U. Our best guess is then that we are producing an isomer of ^{236}U from a (d, p) reaction.

From the reactions ^{238}U+d and ^{237}Np+d we see a half-life of about 120 ns. Apparently, the product here is an isomer of ^{238}Np, produced through (d, 2n) and (d, p) reactions.

Finally, we have observed an isomer with a 30 ns half-life from proton bombardment of ^{237}Np. It seems most likely that this is in ^{236}Pu, but our evidence is not at all conclusive.

In closing, I would like to emphasize again the preliminary and tentative nature of our results. Some of our isotopic assignments may well be incorrect and many of the numerical values will be changed as we refine our analysis and extend our measurements. However, this does not affect our main conclusion: that the existence of spontaneously fissioning isomers is quite widespread and that this will require a general and systematic theoretical interpretation.

H. JUNGCLAUSSEN: After the discovery of the spontaneous fission of nuclei in isomer states, a large number of hypotheses were made as to the nature of these states. The history of experimental studies, about which Professor Polikanov has spoken, was in a sense the history of the rejection of one theory after another.

After the appearance of the calculations by Professor Strutinsky, about which he spoke in his paper, it was the turn of the hypothesis on shape isomerism in the case of spontaneously fissioning isotopes. This possibility has already been mentioned[1]. However, this hypothesis turned out to be vital while all the others dropped out. It did not bring about serious contradictions with experimental data; on the contrary, it helped to explain the main experimental facts which is difficult on the basis of other hypotheses. I shall dwell upon two peculiarities mentioned by Professor Polikanov, namely the dependence of the isomer ratio for the generation of an ^{242mf}Am isomer on the average orbital momentum of the compound nucleus (Fig. 3 in the paper) and the excitation functions of the same isomer state of the neutron radiative capture (Fig. 5). Both dependences can easily be obtained theoretically if one starts from the assumption about

[1] POLIKANOV, S.M. et al., Zh. eksp. teor. Fiz. 42 (1962) 1464.

which Professor Strutinsky spoke, namely that a sufficiently high excited nucleus, on going through the first potential barrier, forms a new compound nucleus with deformation corresponding to the second minimum of the deformation energy. This takes place if, in the nucleus being removed in the region of the second well, the energy, concentrated during the barrier transition to collective degrees of freedom, dissipates rapidly and is distributed among other degrees of freedom. Then the following calculational procedure is justified: (1) to associate the reaction cross-sections with the widths of all the processes taking part in this reaction, say, neutron widths in the first and second wells, widths of transitions over the first barrier in both directions, etc.; (2) to express the widths through the number of channels open for a given transition; (3) to calculate the number of open channels from the statistical model.

The results obtained in this way reproduce the experimental curves satisfactorily, i.e. the isomer ratio[2] and the excitation function of radiative capture[3]. From the value of the ratio of $\sigma_m/\sigma_f \approx 3 \times 10^{-5}$ (σ_m is the cross-section of the isomer generation) measured for the maximum of the excitation function, it follows that the second barrier is approximately 1 MeV lower than the first one. These results are a convincing argument in favour of the hypothesis of the shape isomerism. However, if one goes into details, a number of problems arise. One of them was indicated by Dr. Nix in an earlier comment. While the ratio of the lifetimes of the ground and isomer states to spontaneous fission, obtained theoretically from the two-humped shape of the fission barrier taking into account the energy difference of the ground and isomer state equal to 3 MeV, is consistent with experimental data, to obtain the absolute value of the lifetime of the ^{242mf}Am isomer the number of attempts of a nucleus to penetrate the barrier should be assumed to be equal to 10^{14} sec^{-1} in order of magnitude, i.e. several orders of magnitude lower than the frequency of zero oscillations.

–. SEMENKO: There are some basic reasons (e.g. Sommer-calculation for thermal neutrons) which allow one to consider the (n, γ) reaction with isomer formation to be of the one-stage type (a gamma-quantum is emitted). At higher neutron energies (about 1 MeV) when direct capture is predominant, this seems to be of special importance. In this case the applicability of only statistical considerations is not quite understandable.

The state from which the gamma-quantum is emitted has a different parity and different intrinsic structure from the isomeric ones. It is clear that it should be described with a different curve; one should not interpolate it as if it is within the isomeric potential well.

H. JUNGCLAUSSEN: The spin and parity of one or the other states can, of course, affect the probability of isomer production. However, if the basic assumption mentioned above is true, then this effect, primarily, is hardly related to the gamma width but rather to the fact that the barrier shape is spin-dependent and can vary for ground and isomeric spin states. The account of such effects requires a more developed theory.

N. VILCOV: Concerning Professor Polikanov's paper, our understanding of the mechanism of the formation and decay of spontaneously fissioning isomeric states has been considerably clarified in the last year. This is due to the application of the two-humped potential barrier to explain

[2] JUNGCLAUSSEN, H., Yadernaya Fiz. 5 (1967) 538.
[3] JUNGCLAUSSEN, H., PLEVE, A.A., Preprint P15-3618, Dubna (1967).

the experiments on fast neutron capture (of the reaction type $^{241}Am(n, \gamma)$ $^{242mf}Am$) as well as the experiments on sub-barrier resonances of induced fission. Unfortunately, the present theory is of a qualitative character, mainly because of the absence of data on nuclear parameters, e.g. the level density parameter for heavy nuclei at large deformations. In principle, the study of sub-barrier resonances and (d, p) experiments can provide information only on nuclear states in the second potential well. Taking into account the complexity of these experiments in the saddle-point, one arrives at the conclusion that the values of the statistical model parameters with respect to nuclear deformations can be obtained now only by means of calculations.

Some words on the 'undeservedly forgotten' spin. The isomeric state spin allows one to forget it until it is small. The experiments have shown that for the isomeric state of $^{242mf}Am$ this is the case, i.e. the spin is not likely to exceed a few units. But this refers to a single isomer. It is quite possible that, for example, the shift of the excitation functions of the $^{243}Am(n, \gamma)$ reaction obtained recently in Bucharest is due to a larger spin value of the $^{244mf}Am$ isomeric states. From this point of view the attempts to combine the two-humped barrier model with statistical calculations, taking into account angular momenta, seem to be of special interest.

J.R. NIX: For the classic ^{242}Am spontaneously fissioning isomer an inconsistency exists between the various types of experimental data if it is assumed that the isomeric state is the result of a secondary minimum in a one-dimensional potential barrier. The measured total half-life (i.e. the half-life for spontaneous fission through the second barrier, for gamma decay through the first barrier, for alpha and beta decay, etc.) is 14 ms for the isomeric state. The measured spontaneous-fission half-life from essentially the ground state is 10^{12} years, and the larger of the two barrier heights is 6.4 MeV. From these data one can compute that the energy of the secondary minimum can at most be about 1.5 MeV above the energy of the ground state, even if one permits a dependence of the inertial parameter upon deformation and a wide range of barrier shapes. This is substantially less than the value of (2.9 ± 0.4) MeV deduced from the excitation functions for producing the ground and isomeric states, or the value of 3.1 MeV deduced from fission cross-section resonance spacings. This inconsistency leads one to suggest that if these deduced values represent accurate measurements of the energy of the secondary minimum, then perhaps the position of the secondary minimum is in a direction in the multi-dimensional deformation space that is not along the direction through which spontaneous fission from the ground state proceeds.

For the one other nucleus for which the two half-lives, the barrier height, and the isomer excitation energy have been measured, namely ^{241}Am, this inconsistency is not present. However, the inconsistency for ^{242}Am means that we do not really have the entire explanation of spontaneously fissioning isomers in terms of a secondary minimum in a one-dimensional potential barrier.

J.J. GRIFFIN: I would like very briefly to give a possible basis for describing the mass asymmetry in nuclear fission. The description involves three essential elements:

(1) the assumption that the deformation from saddle point shape to scission shape proceeds mildly;

(2) the recognition that the collective potential energy for large rapid shape changes is not the same as the liquid drop potential surface,

(3) the use of the reflection symmetry property of nucleonic orbitals in reflection-symmetric nuclei to study the potential energy for rapid collective motion.

Hill and Wheeler have calculated[4] the probability that an occupied orbit, (++), remains occupied as the deformation is changed through a value, a_0, at which this orbit crosses an unfilled orbit (--). If $\dot{a}$ is small, then the system follows E_{low} and the probability of finding (++) occupied at large a is zero. For a deformation velocity large compared with $V_{12}/\hbar$, the probability that (++) remains occupied approaches 1.

This suggests a simple model for estimating the potential energy for rapid deformation as follows. Let each nucleon remain in the orbital which evolves continuously as the deformation proceeds, i.e. neglect the effect of residual two-body interactions, V_{12}, in scattering nucleons into other lower energy orbits. Then the total energy of all the nucleons occupying the orbits obtained in this way gives an estimate of the potential energy for rapid collective motion. We refer to this energy as the nucleon-configurational (or "N-C") energy surface.

For many nucleons contained in an infinite square well box of volume V and surface area S one can write down a statistical formula for the density of orbits, dN/dk. If, besides, the shape is reflection-symmetric, one can write down separately the densities of reflection-symmetric and anti-symmetric orbits (cf. Contribution No.166 to this Symposium). With such formulas we have studied the N-C surface which lies lowest at the saddle point along two edges of a two-parameter deformation space. One edge is the line of reflection-symmetric shapes, parameterized by the area, a, of the nuclear neck in the Z = 0 plane. The other edge is the line of scission shapes ($a \equiv 0$), parameterized by the asymmetry parameter, δ, chosen so that the volume ratio of the two fragments is $(1+\delta)/(1-\delta)$.

The results are as follows. For a given configuration, specified for reflection-symmetric shapes by the number, N_+, of filled reflection-symmetric orbits, the energy rises monotonically as the area, a, tends towards zero. Along the scission line, on the other hand, the lowest energy configuration which can be evolved continuously from this highly excited N_+ configuration has an energy which decreases with asymmetry, δ, until it touches the liquid drop surface at a value of δ given by

$$(1+\delta)/(1-\delta) = N_+/N_- = V_H/V_L \qquad (1)$$

One therefore infers that the sequence of symmetric shapes leading to symmetric scission is quite unfavourable energetically for rapid deformations. (Slow deformations, in contrast, would find this path the most favourable one on the L-D surface.) Rather, a sequence of shapes along which δ increases as 'a' decreases to zero, and which leads to an asymmetric scission with mass ratio given by Eq.(1), is preferred on the N-C potential surface.

Thus one comes to consider 'walk-run' fission in which slow motion over the L-D potential surface brings the nucleus to its saddle point shape, whence rapid motion occurs to a scission point with asymmetry defined in first approximation by the value of N_+/N_- at the saddle point.

[4] Phys. Rev. 89 (1953) 1102.

This asymmetry decreases with decreasing fissionability, x, in qualitative agreement with experimental fact.

Finally, we point out that the difference between the energy at the symmetric scission shape and that of the lowest energy asymmetric scission shape is a term of order of the nuclear volume, A, in contrast to the surface energy and shell corrections which are of order $A^{2/3}$. This result provides grounds for optimism that the major features of the description will still obtain when the nuclear model is made more realistic.

All in all, the results seem to recommend a careful study of the dynamical aspects of the collective problem, aimed at establishing the assumption of rapid motion which underlies the present description.

STRUCTURE EFFECTS IN NUCLEAR FISSION

J.E. LYNN
ATOMIC ENERGY RESEARCH ESTABLISHMENT,
UKAEA, HARWELL, BERKS, UNITED KINGDOM

Abstract — Аннотация

STRUCTURE EFFECTS IN NUCLEAR FISSION. Two kinds of structure in sub-threshold fission have been observed and are reviewed here. The first kind, called gross structure, are the peaks ranging over some tens of keV in width in the neutron cross-sections, averaged over energy intervals that include very many fine-structure resonances, for fission of many actinide nuclei. The second kind, called narrow intermediate structure, is spectacular, and is found in narrow groups of fine-structure resonances with anomalously high fission widths. The explanation for both these kinds of structure seems to be the Strutinsky potential energy curve for the prolate deformation of transuranic nuclei. This exhibits a secondary minimum before reaching the saddle-point. This secondary minimum, in which the compound nucleus has a low effective excitation energy, may be responsible for the weak-mixing of fission modes into the compound nucleus motion (gross structure), as well as for the appearance of a second class of 'compound nucleus states', with large fission widths, that are only very weakly coupled to the much denser 'normal' class of compound nucleus states (narrow intermediate structure).

ВЛИЯНИЕ РЕЗОНАНСНОЙ СТРУКТУРЫ НА ДЕЛЕНИЕ ЯДРА. Рассматриваются два типа структуры, которые были обнаружены в сечении подпорогового деления. Первый тип, называемый грубой структурой, представляет собой пики с шириной больше нескольких десятков кэв в нейтронном сечении, усредненном по энергетическому интервалу, включающему большое количество резонансов тонкой структуры, и наблюдается у многих актинидов. Второй тип, называемый узкой промежуточной структурой, виден непосредственно и обнаружен в узких группах резонансов с аномально большими делительными ширинами. Объяснение обоих этих видов структуры, видимо, дает кривая Струтинского для потенциальной энергии вытянутых деформированных ядер трансурановой области. Эта кривая имеет ниже седловой точки второй минимум. Этот второй минимум, где составное ядро имеет низкую эффективную энергию возбуждения, может отвечать как за слабое смешивание конфигураций различных типов деления и составного ядра (грубая структура), так и за появление другого класса "состояний составного ядра" с большой делительной шириной, очень слабо связанных с гораздо более плотными "нормальными" состояниями составного ядра (узкая промежуточная структура).

1. INTRODUCTION

It has long been believed that the fission mode of motion of an excited nucleus is one that is strongly damped; i.e. the elementary fission mode, a prolate shape vibration leading to division of the nucleus, is dissolved among the compound nucleus states over a very broad energy interval. Now, however, there is persuasive evidence that the strong damping mechanism breaks down, at least for sub-threshold fission, and that this breakdown is associated with the existence of metastable shapes of the nucleus. There are four main groups of evidence for this statement.

2. SPONTANEOUS FISSIONING ISOMERS

The first group of evidence is concerned with the existence of metastable shapes, and will only be dealt with very summarily here because it was the subject of the previous paper [1]. It starts from the discovery of

spontaneous fissioning isomers by Flerov and Polikanov [2] in 1964. Since the original discovery a number of these highly interesting isomeric states have been discovered and their properties investigated, mainly by Flerov and Polikanov's group in Russia and by Bjørnholm and his colleagues in Copenhagen. All those discovered up to the end of 1967 are in isotopes of americium. Their half-lives are of the order of milliseconds, and the principal mode of decay is spontaneous fission. The energies of these states have been found in a few cases to be about 3 MeV above the ground state of the respective isotope, thus showing that their peculiar property is not the decay by spontaneous fission, but the extraordinary inhibition of gamma-decay to lower states. Analysis of the shapes of the yield curves for formation of the isomers shows that their spins are not particularly high ($\approx 7\hbar$); the conventional explanation for isomerism (high multipolarity of all electromagnetic transitions in decay) cannot apply here.

3. DEFORMATION ENERGY OF NUCLEI: THE STRUTINSKY POTENTIAL

3.1. The source of the potential

The second line of research is a purely theoretical one. In an effort to explain the equilibrium deformations of non-magic nuclei as well as the heights and saddle-point deformations of fission barriers, Strutinsky [3] has adopted a combination of liquid-drop model, which provides the major component of the nuclear mass, and a Nilsson deformed shell-model; the latter provides a correction term to the liquid-drop energy. Minima in the shell-correction term occur where there are gaps in the single-particle level structure near the Fermi energy of the system. For spherical nuclei these minima are most pronounced at the magic numbers, but the important property of the Nilsson diagram that Strutinsky emphasizes is that other gaps occur at non-zero deformations, and such gaps recur with increasing deformation for a given nucleon number. Thus, according to the calculations, more than one minimum can occur in the potential energy of deformation of a nucleus, and such a secondary minimum is expected to be strongly pronounced in the transuranic nuclei.

This secondary minimum provides a possible explanation of the spontaneous fissioning isomers; such an isomer would be the lowest vibrational state of the secondary minimum. Its tunnelling towards decay by spontaneous fission would be less inhibited than usual while its gamma decay would be strongly reduced because of its small amplitude in the normal minimum.

3.2. Wave-functions in the Strutinsky potential

The Strutinsky potential is shown schematically in Fig. 1. The parameter β is the co-ordinate describing prolate deformation of the nucleus, through the saddle point in the potential energy surface of the nucleus as a function of deformation, leading eventually towards scission. Generally speaking, the one-dimensional wave-functions in this potential may be classified by their relative amplitudes in the two potential energy minima. We consider those eigenfunctions with the major part of their amplitudes in

the first, deeper minimum as "class I", and those with the major part of their amplitudes in the shallower minimum as "class II".

The relative amplitudes of a given eigenfunction in the two minima depend on the depth of the eigenfunction below the intermediate maximum (in an exponential manner) and on the eigenvalue separation of two neighbouring eigenfunctions of opposite class. It is possible (though not likely) that such neighbouring eigenstates are so close that they cannot be significantly classified by the shape quantum numbers given above: i.e. for each eigenfunction the relative amplitude c in the two minima is close to unity.

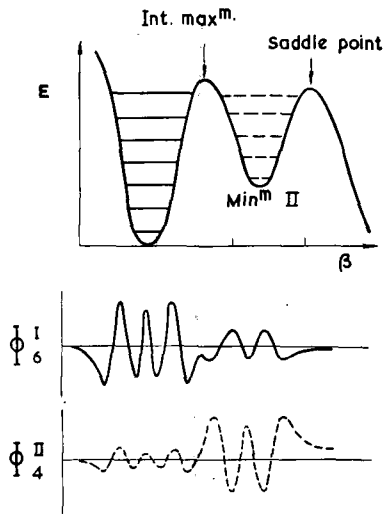

FIG.1. Schematic diagram of the Strutinsky potential as a function of prolate deformation of the nucleus. Class I (full line) and class II (broken line) vibrational levels and wave-functions are also shown.

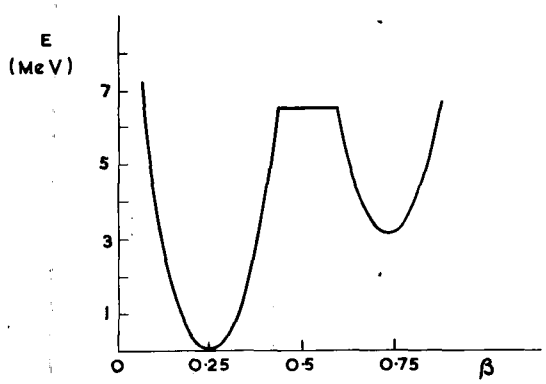

FIG.2. Actual potential used for calculations of tunnelling properties of class I and class II wave-functions. Mass parameter B = 2.84 × 10^{-46} g cm². Conditions are chosen to approximate those believed to appertain to ^{242}Am (except that the saddle point is not shown). Cut-off intermediate peak is to simplify numerical computation.

The approximate relationships governing the relative amplitude are given in Ref. [4] and are not repeated here. Instead we present a numerical example for a particular case, in which the secondary minimum lies 3.1 MeV above the primary minimum, and the intermediate maximum is 3.4 MeV above this. The relative values of the mass parameter and the restoring force constant are chosen to give a phonon energy of 0.8 MeV, and the separation of the two minima in β is approximately that suggested by Strutinsky's calculations. The absolute value of the mass parameter is then chosen to give a tunnelling parameter, $\hbar\omega_f$, in the Hill-Wheeler formula for the transmission coefficient through a parabolic barrier, of about 800 keV. The potential is shown in Fig. 2, and the approximate intensity c^2 of the subsidiary part of the wave-function relative to the major part is shown in Fig. 3 as a function of energy. In this, the class I-class II nearest neighbour eigenvalue separation is assumed to be about 100 keV.

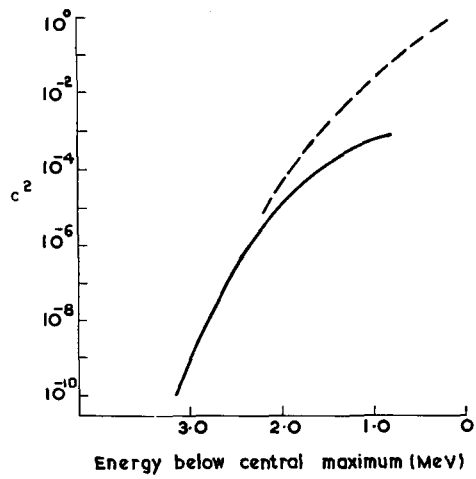

FIG. 3. Tunnelling intensity for wave-functions of potential in Fig. 2 as function of energy below intermediate maximum. Towards the top of this peak the calculation is expected to be unrealistically low. Physically one would expect c^2 to tend towards unity at the peak, and this extrapolation is roughly shown by the broken line.

4. GROSS STRUCTURE IN SUB-THRESHOLD FISSION

4.1. Data

The third group of evidence is mainly to do with the hypothesis of weak damping of sub-threshold fission modes. There is now ample evidence that the strong-mixing mechanism breaks down for such modes. It has long been known that the cross-sections for fast-neutron induced fission (up to about 2 MeV neutron energy) exhibit a certain amount of structure. The explanation that was usually advanced for this [5] is that the competition from neutron inelastic scattering causes the fission cross-section to fall following its increase with energy and eventual saturation as each new fission channel opens. Recent measurements and more careful analysis of such cross-sections and related phenomena show that this explanation is untenable in a number of cases at least. The individual cases are summarized below.

(a) ^{231}Th

The fast neutron induced fission cross-section of ^{230}Th [6] exhibits a peak less than 100 keV wide reaching a maximum value of 50 mb (under the available resolution of 20 keV) at 750 keV and falling to less than one-quarter of this value at 800 keV. Calculations [7, 8] show that this cannot be a result of inelastic scattering competition. The angular distribution of fission products from the same reaction shows [9, 10] that the fission channel associated with this peak has a K quantum number (projection of spin on the cylindrical symmetry axis) of $\frac{1}{2}$.

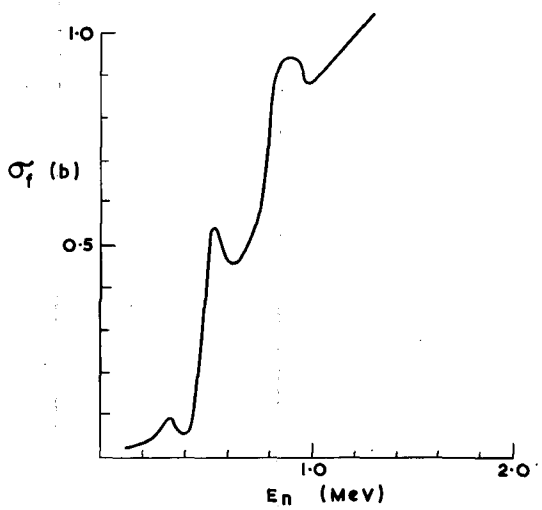

FIG. 4. Fast neutron-induced fission cross-section of ^{231}Pa.

(b) ^{232}Pa

Similar structure is observed in the cross-section of ^{231}Pa [11]. The first very marked peak is at 320 keV neutron energy and has a width of less than 80 keV. It falls to only half of its peak of 100 mb at 400 keV. There is a second peak to 530 keV, reaching 550 mb, with a rate of fall at higher energies that seems much too great to be due to competition (see Fig. 4).

(c) ^{233}Th

The neutron-induced fission cross-section of ^{232}Th shows marked peaks at 1.6 MeV and 1.7 MeV with widths of about 150 keV. Calculation and observation of neutron inelastic scattering [12] show that these structures cannot be a competition effect. There are also breaks far below threshold, at energies of 0.8 MeV and 1.05 MeV, which might be poorly resolved structure. The fission product angular distribution [13] indicates that these breaks are associated with $K = \frac{1}{2}$ channels, therefore high neutron angular momentum cannot be responsible for the low cross-sections. It follows that the breaks are truly sub-threshold and therefore cannot be competition effects.

(d) ^{235}U

The fission structure in this compound nucleus is revealed not so much by the neutron cross-section of ^{234}U as by the fission product angular distribution both from the $^{234}U(n, f)$ [10] and $^{234}U(d, pf)$ [14] reactions, which fluctuate quite strongly with changing excitation energy. There is a peak perhaps 200 to 300 keV wide at 840 keV and a break at 300 keV in the (n, f) cross-section. Both are associated with $K = \frac{1}{2}$ saddle-point channels.

(e) ^{239}U

The neutron-induced fission cross-section of ^{238}U is very smooth in the near-threshold region but breaks occur far below threshold at 630 keV, 950 keV and 1.2 MeV. Angular distribution data [10] indicate that all these are associated with $K = \frac{1}{2}$ saddle-point channels.

(f) ^{242}Am

At low neutron energies the fission cross-section of ^{241}Am is quite appreciable; even though the excitation energy is strongly sub-threshold (by about 900 keV). The shape of the average cross-section [15] shown in Fig. 5 is most unlike that of an s-wave neutron reaction cross-section, which is normally proportional to $1/\sqrt{E}$. On dividing out by the normal compound nucleus formation cross-section we find that $\overline{\Gamma}_{(f)}/\overline{\Gamma}$ has the energy dependence shown in Fig. 6. The fall above 15 keV cannot be accounted for by neutron scattering competition. The near-Lorentzian form of $\overline{\Gamma}_{(f)}$ is thus quite striking.

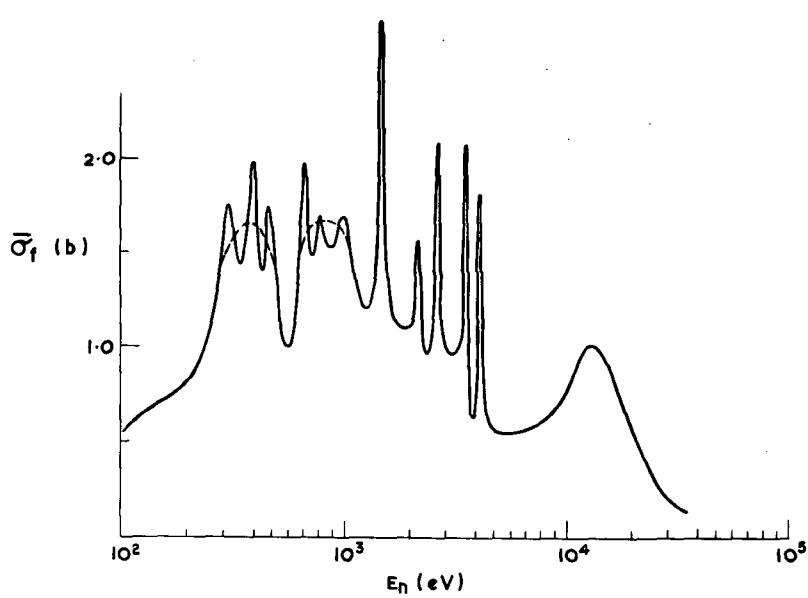

FIG. 5. Fission cross-section (locally averaged over groups of many fine-structure resonances) of ^{241}Am. This figure is a schematic diagram of the data rather than a truly quantitative representation.

The ratio $\bar{\Gamma}_f/\bar{\Gamma}$ for $^{241}Am + n$ under the assumption that the fission cross-section is entirely due to s-wave interactions.

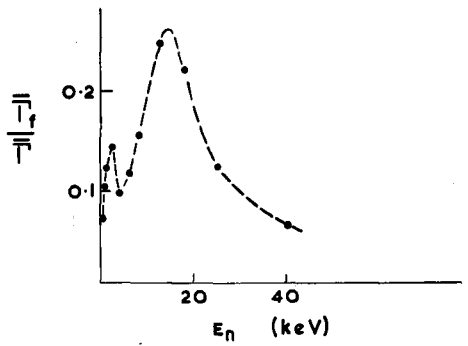

FIG.6. The ratio of $\bar{\Gamma}_{(f)}/\bar{\Gamma}$ for fine-structure resonances of $^{241}Am + n$, deduced from average fission cross-section.

4.2. Interpretation of gross structure

If it is accepted that the above cross-sections are all associated with processes that operate through the compound nucleus mechanism (and the neutron energies in these examples, particularly in the ^{242}Am case, are sufficiently low, and the cross-section in many cases sufficiently high, for only compound nucleus processes to seem valid) then it is clear that the structure is associated with the fission strength function $\bar{\Gamma}_{(f)}/\bar{D}$. This is because similar structure is not apparent in the total neutron cross-section, thus ruling out its association with the neutron strength function $\bar{\Gamma}_{(n)}/\bar{D}$.

A phenomenological interpretation of the gross structure can be provided in the form of a complex potential model for the fission mode [7]. The complex potential energy is a function of the prolate deformation β. In this model structure in the fission strength function will appear at energies of virtual states in the potential but not at energies much above the fission barrier. Structure below the barrier will only appear as well-defined peaks, however, if the imaginary component of the potential energy (the damping width) is very much less than the tunnelling parameter, $\hbar\omega_f$, of the Hill-Wheeler [16] saddle-point barrier. Such damping widths (less than about 100 keV) are, of course, very small, and a fundamental explanation of them is required.

Although no quantitative calculations have been made, it certainly seems plausible on qualitative reasoning that the Strutinsky potential is very important for such an explanation. Damping widths in general are expected to depend on the excitation energy available, and damping widths of harmonic vibrations, in particular, can be shown to depend linearly on the energy of the vibration as well as inversely on the restoring force constant of the potential. The fission mode will normally be associated with the highest energetically available vibration in the secondary minimum of the Strutinsky potential; because of the higher potential energy in this

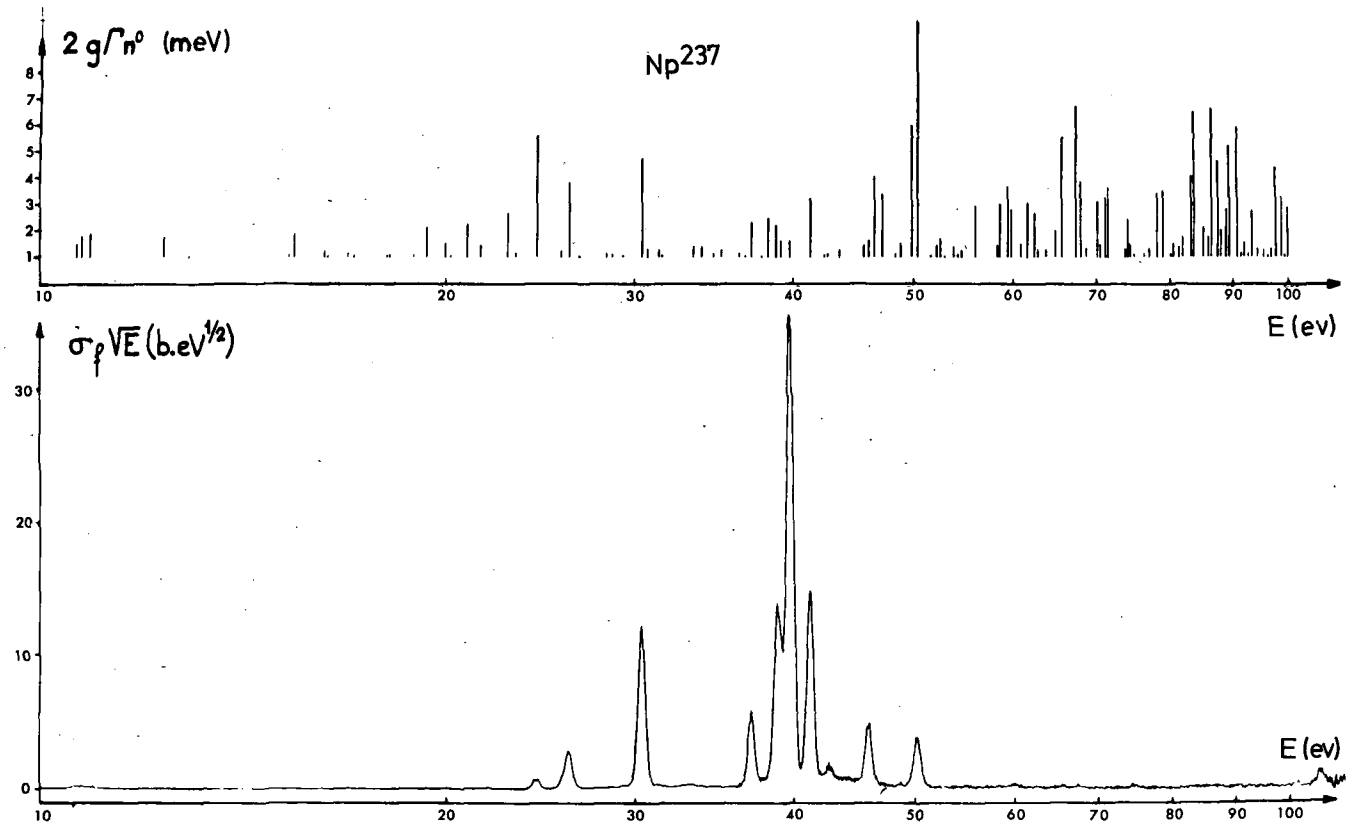

FIG. 7. Comparison of reduced neutron widths of resonances in the cross-section of ^{237}Np with the fission cross-section.

minimum, the 'excitation energy' available to the fission mode is much less than that of the proper excitation energy of the compound nucleus. The shape of the potential energy curve also implies that the restoring force constants in the two individual wells are considerably higher than that, say, for a conventional liquid drop potential energy curve. It is to be noted that when the vibrational energy of the fission mode is above the intermediate maximum in the potential energy curve the damping width ought to increase dramatically because the effective excitation energy of the fission mode rises to that of the compound nucleus, and the effective restoring force constant falls to a much lower value than that in the secondary minimum. This would explain the vital fact that strong-damping of the fission mode seems necessary to explain above-threshold fission, such as slow-neutron induced fission of ^{233}U [17].

5. NARROW INTERMEDIATE STRUCTURE IN SUB-THRESHOLD FISSION

5.1. Data

In the resonance region of neutron cross-sections it has now been discovered that fission can occur in narrow bands that include only a few resonances while in large intervening regions of neutron energy there is little or no observable fission. The observed examples of this (up to March 1968) are listed below.

(a) $^{237}Np + n$

In this cross-section, the first discovered example of the phenomenon, measured by the Saclay group [18], there is a cluster of fission resonances around 39 eV. The neutron widths and fission cross-section from 10 eV to about 100 eV are shown in Fig. 7; it is clear from this that the fission widths are responsible for the structure. The resonance at 39.9 eV has a fission width of 6 meV while its immediate neighbours have fission widths of about 0.5 meV. Far away from this group the fission widths are much smaller, about 0.03 meV at 25 eV, and 0.002 meV at a few eV. Measurements at higher energies with coarser resolution show that there are many more such groups of fission resonances (Fig. 8). The mean spacing of these bands is 54 eV, whereas the mean resonance spacing in the total cross-section is 0.67 eV.

(b) $^{240}Pu + n$

In the total cross-section of this reaction the mean resonance spacing is 13 eV. The lowest resonance at 1.04 eV has a fission width of 6 μeV and in the immediately higher resonances fission is not measurable. Band fission was first suspected in the cross-section by Weigmann and Schmid [19] on the basis of radiative capture anomalies, and fission measurements by Migneco and Theobald [20] revealed the dramatic fission cross-section shown in Fig. 9. Analysis of the data shows that in the first group the resonance at 782 eV has a fission width of about 130 meV, while its immediate neighbours at 750 eV and 791 eV have fission widths of only about

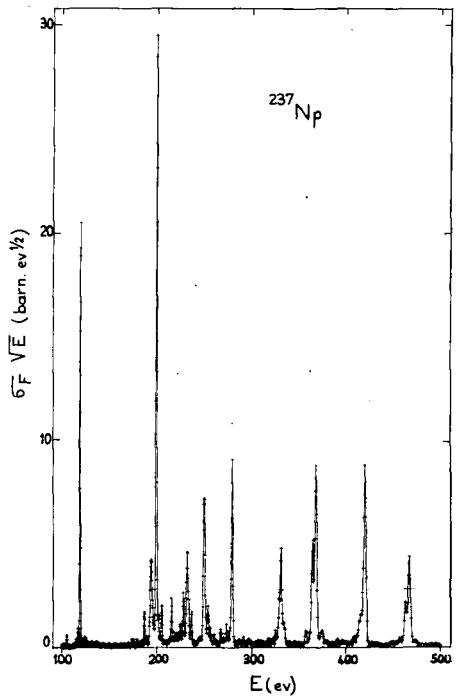

FIG. 8. Coarser resolution measurements of the fission cross-section of ^{237}Np showing intermediate structure groups.

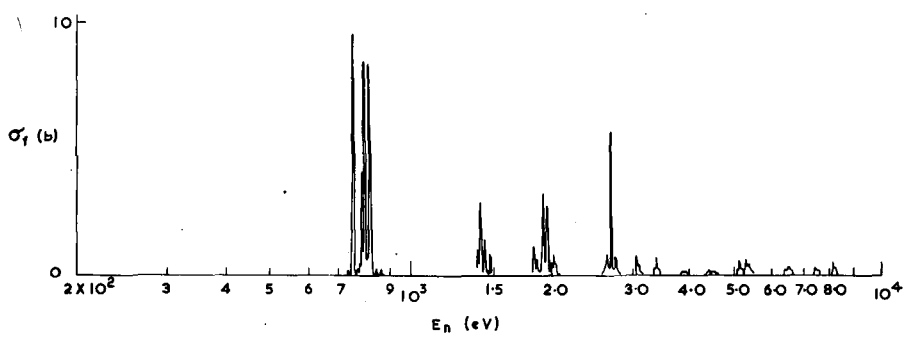

FIG. 9. Neutron-induced fission cross-section of ^{240}Pu showing narrow groups of resonances with appreciable fission.

10 meV. On the other hand, the neutron width of the 782 eV resonance is much smaller than its neighbours, and it shows up in the fission cross-section as only a relatively minor peak in the group at 780 eV. The higher groups, at 1400 eV and 1900 eV, also show one or two resonances to have much larger fission widths than their neighbours. The mean spacing of the fission bands is 720 eV.

(c) $^{241}Am + n$

The lowest resonances in the ^{241}Am cross-section have a mean spacing of 0.56 eV and exhibit quite considerable sub-threshold fission ($\overline{\Gamma}_{(f)} \approx 0.2$ meV) [21]. No special feature emerges in the resolved fine structure resonances. In the coarser resolution measurements [15] at higher energies, however, there are suggestions of spikes at energies of 1.6 keV, 2.3 keV, 2.8 keV, 3.5 keV and 4.3 keV (i.e. with a mean spacing of about 1 keV) as well as broader structure at, for example, 400 eV (see Fig.5).

(d) $^{234}U + n$

The fission cross-section of ^{234}U up to about 15 keV has been measured at Harwell by James and Rae [22]. The cross-section is shown in Fig.10. There is a group with a half-width of about 250 eV, centred at 500 eV, in which the resonances show fission. Thereafter no fission is observable up to about 7 keV, where there is a distinct band of fission, although the individual resonances within it are not resolved, and at 13.9 keV. Lesser structure is indicated at 7.3 and 9.1 keV. The cross-section areas within these groups are reported to be 95 b.eV (500 eV group), 47 b.eV (8.3 keV group) and 35 b.ev (13.9 keV group). The mean fine structure resonance spacing is 14 eV.

5.2. General interpretation of narrow intermediate structure

The interpretation presented here is a summary of that given in Ref.[4]. The eigenvalues and eigenfunctions of the vibrational states in the Strutinsky potential are denoted by E_ν^{I}, $\Phi_\nu^{(I)}$, E_ν^{II}, $\Phi_\nu^{(II)}$ for class I and class II states, respectively. The eigenvalues and eigenfunctions for the dynamical motion of the nucleus in all the other degrees of freedom, i.e. intrinsic nucleonic motion, rotational motion and collective vibration in modes other than that of spheroidal elongation, are denoted by E_μ, χ_μ. These "intrinsic" states are defined for a fixed prolate deformation, β_0, say. In the first place all these states are assumed discrete, either by imagining the barriers in each decay channel to be raised so that the channels are closed, or by imposing suitable boundary conditions in the open channels. The simple product functions $\Phi_\nu\chi_\mu$ with energy $E_\nu + E_\mu$ may now be used as a basis for diagonalizing the nuclear Hamiltonian, there being a residual term of this, H", describing interplay of the β-vibrational and other degrees of freedom, that has not been used in defining either the vibrational states Φ_ν or the "intrinsic" states χ_μ. It is possible to diagonalize separately the two sub-matrices, one referring only to basic states with class I vibrations, and the other referring only to basic states with class II vibrations. In this way we obtain two sets of eigenstates; the one, $X_{\lambda_I}^{(I)}$, with eigenvalues E_λ^{I}, may be called compound states of class I with vibrational motion in the first minimum, and the other, $X_{\lambda_{II}}^{(II)}$, with eigenvalues E_λ^{II}, may be called compound states of class II. There is a residual interaction between these two sets, the matrix elements for which are given by

$$\langle \lambda_I | H'' | \lambda_{II} \rangle = \sum_{\nu^I\mu ; \nu^{II}\mu'} \langle \lambda_I | \nu^I \mu \rangle \langle \nu^I \mu | H'' | \nu^{II} \mu' \rangle \langle \nu^{II} \mu' | \lambda_{II} \rangle \qquad (1)$$

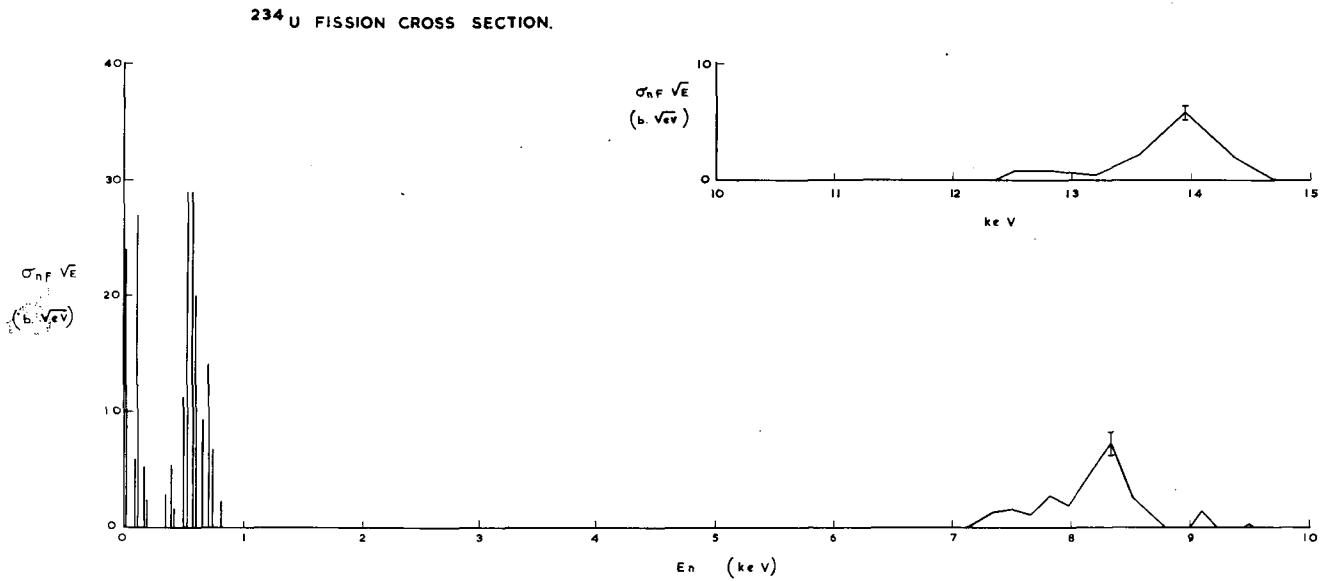
234 U FISSION CROSS SECTION.
σnF √E
(b. √eV)
40
30
20
10
0
0
1
2
3
4
5
6
7
8
9
10
En (ke V)
σnF √E
(b. √eV)
10
0
10
11
12
13
14
15
ke V

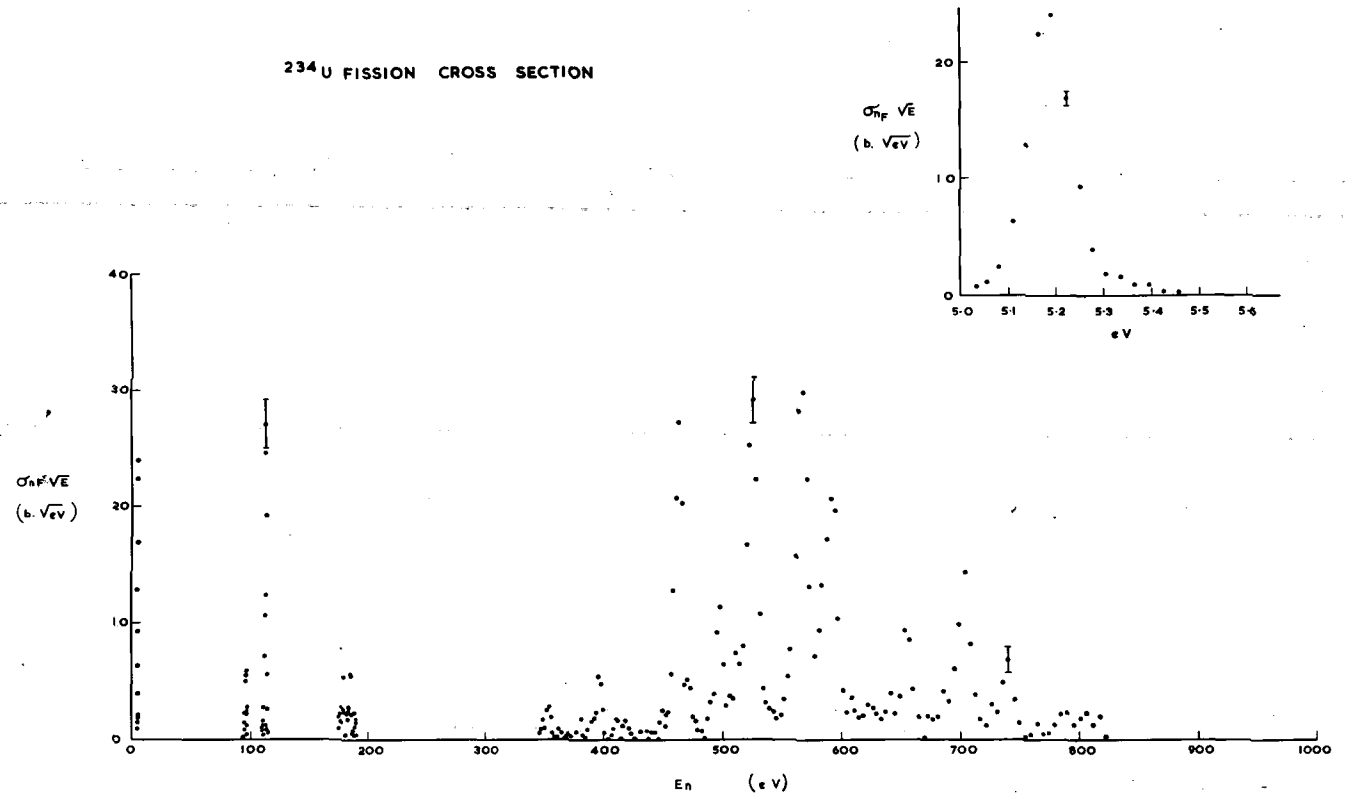

FIG.10. Neutron-induced fission cross-section of ^{234}U, showing a group of resolved resonances around 500 eV and unresolved groups at 6.5 keV and 13.5 keV.

If the excitation energy of the compound nucleus is sufficiently far below the top of the first maximum, vibrational states that only tunnel weakly through this barrier are involved in the right-hand side of Eq. (1). Consequently, the overlap of class I and class II vibrational states is very small, and it follows that the residual interaction matrix element is also small.

A very rough semi-quantitative estimate of this matrix element can be made. Retaining only the terms with highest, appreciably mixed vibrational components in Eq. (1) we have, approximately

$$\overline{\langle \lambda_I | H^n | \lambda_{II} \rangle^2} \approx c^2 \left\{ \overline{\langle \lambda_I | \nu^I \mu \rangle^2} \, \overline{\langle \nu^{II} \mu | H^n | \lambda_{II} \rangle^2} + \overline{\langle \nu^{II} \mu' | \lambda_{II} \rangle^2} \, \overline{\langle \lambda_I | H^n | \nu^I \mu' \rangle^2} \right\} \tag{2}$$

where c is the relative amplitude of a vibrational wave-function of given class in the potential minimum of the opposite class. Numerical estimates of it have already been given in Section 3.2. The coefficients and matrix elements on the right-hand side of Eq. (2) are related to damping widths W_I, W_{II} of the vibrational modes and the mean spacings $\overline{D}_I$, $\overline{D}_{II}$ of class I and class II compound states. Introduction of these relations (with certain assumptions) leads to

$$\overline{\langle \lambda_I | H^n | \lambda_{II} \rangle^2} \approx \frac{\overline{D}_I \overline{D}_{II} c^2}{\pi^2} \left[\frac{W_{II}}{W_I} + \frac{W_I}{W_{II}} \right] \tag{3}$$

Numerically, this gives for ^{242}Am at its neutron separation energy, if assumed to be 900 keV below the intermediate maximum, a value of about 10^{-2} eV^2. This could be in error by two or three orders of magnitude because of the various assumptions made in the calculations, but nevertheless it shows how weak the coupling between class I and class II states may be within the framework of the Strutinsky potential.

The density of the class II compound states at a given energy will normally be considerably lower than the density of class I states, owing to the greater amount of energy tied up in deformation in the former case. The properties of the two classes will be very different. The fission width amplitudes associated with the class II levels are related to the amplitude of the highest admixed class II vibrational state together with an attenuation factor for tunnelling through the saddle-point barrier. Fission-width amplitudes of the class I levels will be much smaller because they depend on the amplitude of a class I vibrational wave-function within the secondary minimum, as well as on the saddle-point tunnelling factor. The difference in relative fission widths is further increased by the level density difference between the two classes (coefficients for admixture of elementary modes are proportional to the level spacing of the compound states). The neutron widths (elastic scattering) will have opposite behaviour; because the residual nucleus has to be left in its ground state, the vibrational wave-function of which is the zero-point vibration of the first minimum, the class II levels are associated with zero neutron width. Radiation properties are also quite different. The cascade of gamma-rays from a state of particular class will mostly be through lower levels of the same class. Qualitatively, the gamma-ray spectra of class II levels will be character-

ized by widely-spaced transitions (enhanced relative to the class I transitions by the difference in initial level density) at comparatively low gamma-ray energies.

On the other hand, so long as the compound nucleus excitation energy is at least 2 or 3 MeV greater than the energy of the lowest class II state (the spontaneous fissioning isomer) it is to be expected that the more general statistical properties of the two classes of compound states will be similar. Thus, for a given total angular momentum and parity, the spacings of the class II states should have a Wigner distribution, while their fission widths, for a single saddle-point channel, should have a Porter-Thomas distribution. The fluctuation about zero mean of the expansion coefficients $\langle \lambda \,|\, \nu\mu \rangle$ that is responsible for the Porter-Thomas distribution also suggests a bivariate Porter-Thomas distribution for the squared matrix elements $\langle \lambda_I | H'' | \lambda_{II} \rangle^2$.

The interpretation of the narrow intermediate structure in the fission strength is now clear. Each group of fissile resonances corresponds to a class II compound state. The latter is revealed in the neutron cross-section by the coupling with class I compound states (having non-zero neutron widths). This coupling causes the admixture of some of the class II compound state wave-functions with neighbouring class I states giving them anomalous fission widths.

From the ratio of the density of class II states (the fissile groups) to the density of class I states (very nearly the normal resonance density), standard level density formulae, such as that of Lang and Le Couteur [23], enable us to estimate the difference in effective excitation energy, or potential energy difference, in the two minima. For the cases described in Section 5.1 we find the following energy differences:

^{241}Pu, 1.9 MeV; ^{235}U, 2.4 MeV; ^{238}Np, 2.3 MeV; ^{242}Am, 3.1 MeV.

The last is particularly interesting because the measured energy of the spontaneous fissioning isomer [24] above the ground state gives us a direct estimate of this difference; it is 2.9 ± 0.4 MeV.

5.3. Coupling conditions in the intermediate structure

The different coupling conditions between the class I and class II compound states may be classified as follows.

(a) Very weak coupling

If the residual interaction $\langle \lambda_I | H'' | \lambda_{II} \rangle^2$, averaged over the states λ_I for a given class II state λ_{II}, is small compared with the class I level spacing, then, generally speaking, perturbation theory may be applied to obtain the properties of the ultimate compound states λ of the system. One compound state remains predominantly class II, and the others remain predominantly class I. The fission width of the first state predominates over all the others in the group, while its neutron width can be shown to have one of a limited set of values that depend on the neutron and fission widths of all the neighbouring states.

It can also happen that one class I state is accidentally degenerate with the class II state, in which case there are two ultimate compound states with comparable fission widths much larger than those of their neighbours.

The fissile groups of the ^{240}Pu cross-section appear to provide examples of very weak coupling. Analysis of the resonance parameter data reveals that the neutron width of the strongest fission resonance in each group is related to the remaining parameters within the rather broad limits allowed by the experimental errors. This is also true of the lowest fissile group in the ^{237}Np cross-section. It cannot be ruled out, however, that there is not a resonance with even greater fission width present in each group, but with such a small ratio of neutron to fission width that it has not been observed in the cross-section. In this case the coupling strength $\overline{\langle\lambda_I|H''|\lambda_{II}\rangle^2}$ will be rather smaller than the value of ≈ 100 eV^2 deduced from the ^{240}Pu data. For a class II fission width $\overline{\Gamma}_{\lambda_{II}(f)} \approx 0.5$ eV it will be about 20 eV^2, for $\overline{\Gamma}_{\lambda_{II}(f)} \approx 3.0$ eV it will be about 3 eV^2.

For class II fission widths that approach or exceed the order of magnitude of the class I level spacing we can no longer regard the coupling of the discrete compound states to the channels as being a minor perturbation. Proper consideration of the coupling to the continuum, through the R-matrix technique, for example, shows that in the former case ($\overline{\Gamma}_{\lambda_{II}(f)} \approx \overline{D}_I$) even accidental degeneracy of a class I and class II state results in a quasi-resonance the narrow component of which has small fission and appreciable neutron width,

$$\Gamma_{1(f)} \approx \frac{4\langle\lambda_I|H''|\lambda_{II}\rangle^2}{(\Gamma_{\lambda_{II}(f)} - \Gamma_{\lambda_I(n)})^2} \cdot \Gamma_{\lambda_{II}(f)} \tag{4}$$

$$\Gamma_{1(n)} \approx \Gamma_{\lambda_I(n)} \tag{5}$$

while the broad component will probably be undetectable by virtue of its small neutron width:

$$\Gamma_{2(f)} \approx \Gamma_{\lambda_{II}(f)} \tag{6}$$

$$\Gamma_{2(n)} \approx \frac{4\langle\lambda_I|H''|\lambda_{II}\rangle^2}{(\Gamma_{\lambda_{II}(f)} - \Gamma_{\lambda_I(n)})^2} \cdot \Gamma_{\lambda_I(n)} \tag{7}$$

This situation could also correspond to the ^{240}Pu data, yielding a residual coupling strength of the order of 1 eV^2, for $\overline{\Gamma}_{\lambda_{II}(f)} \approx 10$ eV.

In the second case ($\overline{\Gamma}_{\lambda_{II}(f)} \gg \overline{D}_I$) it can be shown by the R-matrix technique that the original class I states become resonances with fission widths

$$\Gamma_{\lambda(f)} \approx \frac{\langle\lambda_I|H''|\lambda_{II}\rangle^2 \Gamma_{\lambda_{II}(f)}}{(E_\lambda - E_{\lambda_{II}})^2 + \frac{1}{4}\Gamma^2_{\lambda_{II}(f)}} \tag{8}$$

(a result demonstrated by Weigmann [25] in a different way) while a very weak background term underlying these resonances will carry most of the fission width.

(b) Weak coupling

We use this term to describe the situation in which the class II compound state is spread effectively over many of the ultimate resonances but

yet over an energy region that is much smaller than the class II level spacing. It can be shown that the profile of the fission widths is Lorentzian

$$\overline{\Gamma}_{\lambda(f)} \approx \frac{\overline{\langle \lambda_I | H'' | \lambda_{II} \rangle^2}\ \Gamma_{\lambda_{II}(f)}}{(E_\lambda - E_{\lambda_{II}})^2 + W^2} \qquad (9)$$

where $W \approx \pi\ \overline{\langle \lambda_I | H'' | \lambda_{II} \rangle^2} / \overline{D}_I$. There will be strong individual fluctuations about this envelope of course. The ^{234}U cross-section data seem to provide an example of this behaviour. The lowest group of resonances has a half-width $2W \approx 250$ eV, giving us a value of about 500 eV^2 for $\overline{\langle \lambda_I | H'' | \lambda_{II} \rangle^2}$. From the cross-section area of this group we find that $\Gamma_{\lambda_{II}(f)} \approx 20$ meV. It is tempting to speculate that the break at 300 keV in the fast neutron fission cross-section of ^{234}U is the centre of the nearest "giant resonance" in the $K^\pi = \frac{1}{2}^+$ fission mode (the angular distribution data certainly support this assignment of k and perhaps of parity also). With a saddle-point height of between 600 keV and 1 MeV above neutron threshold and a saddle-point tunnelling parameter $\hbar\omega_f \approx 800$ keV, this class II fission width would indicate a giant resonance damping width W of the order of 1 to 10 keV. In the light of the evidence presented in Section 4.1 this would seem quite reasonable.

However, the ^{234}U resonance data could also be an example of the extreme case of very weak coupling to a very broad class II level (Eq. (8)). In this case it is found that $\Gamma_{\lambda_{II}(f)} \approx 250$ eV and $\overline{\langle \lambda_I | H'' | \lambda_{II} \rangle^2} \approx 0.1$ eV^2. This result for $\Gamma_{\lambda_{II}(f)}$ would signify that the saddle-point is close to or below the neutron threshold. Such a low saddle-point would render structure in the fast-neutron cross-section most improbable [26].

(c) Moderately weak coupling

When the spreading of the class II fission widths over the compound states approaches the order of magnitude of the class II level spacing we may describe the coupling as moderately weak. Many of the existing resonance fission data will have to be analysed most carefully to establish whether or not this condition is fulfilled. There is some hint that it may occur in the slow neutron cross-section of ^{239}Pu. In ^{240}Pu it is known that the fission threshold of 1^+ states lies some 100 or 200 keV above neutron threshold. If this threshold is due to the intermediate maximum then moderately weak coupling is possible. The fission cross-section data [27] as well as the ratio of locally-averaged (over 100 eV intervals) capture to fission cross-section [28] show signs of structure.

6. INTERPRETATION OF FISSION DATA ON THE COMPOUND NUCLEUS ^{242}Am

In the low-energy neutron cross-section of ^{241}Am we have an example of the detailed interplay of resonance fine structure, narrow intermediate structure and gross structure. Furthermore, we have some data on the lowest, or 'ground', of the class II set of states, the spontaneous fissioning isomer [24], as well as data on the excitation of this isomer by neutron bombardment of ^{241}Am [29]. All these data enable us to make some deductions about coupling strengths and barrier heights in ^{242}Am.

First of all, the fission cross-section data suggest that the lowest class II resonance is at about 400 eV with a width W (either coupling or fission) of about 300 eV (see Fig. 5); there may be a second broad class II resonance at about 1 keV, and another is at 1600 eV with a width less than about 100 eV. There are two sets of s-wave resonances in the cross-section of ^{241}Am, having total angular momentum and parity 2^-, 3^- and we do not know to which set to ascribe the above class II resonances, nor indeed do we know these quantum numbers for the fine structure resonances, or anything about class II states below the neutron threshold. All this introduces some uncertainty into the analysis.

The thermal neutron capture cross-section for excitation of the spontaneous fission isomer is less than 5×10^{-7} of that for formation of the ground state of ^{242}Am [29]. Thus, the total radiation width for transitions from a compound state λ (of nearly pure class I character) to a lower class II state (these assumed to be essentially unmixed with lower class I states) is

$$\Gamma_{\lambda(\gamma\to II)} \approx \frac{\langle\lambda_I|H''|\lambda_{II}\rangle^2\,\Gamma_{\lambda_{II}(\gamma)}}{(E_\lambda - E_{\lambda_{II}})^2 + \frac{1}{4}\mathscr{W}^2} \lesssim 5\times10^{-7}\,\Gamma_{\lambda(\gamma\to I)} = 2\times10^{-8}\text{eV} \tag{10}$$

where the 'normal' radiation width $\Gamma_{\lambda(\gamma\to I)}$ of a resonance to all lower class I states is assumed to be 40 meV. From this, with $E_\lambda \approx 0$, we find that $\langle\lambda_I|H''|\lambda_{II}\rangle^2$ is less than 0.1 eV^2 (assuming $E_{\lambda_{II}} \approx 400$ eV), or less than 1.6 eV^2 (if $E_{\lambda_{II}} \approx 1600$ eV). In the first case ($E_{\lambda_{II}} \approx 400$ eV) we conclude that the width $\mathscr{W}$ is essentially the class II state fission width ($\Gamma_{\lambda_{II}(f)} \approx 300$ eV); this is a case of very weak coupling to a broad class II level (see Section 5.3). From Eq. (8) we deduce in turn that the fission width of a resonance near zero ($E_\lambda \approx 0$) is about 0.2 meV, which agrees with observation. The second assumption ($E_{\lambda_{II}} \approx 1600$ eV) together with the values of the observed fission widths near zero suggests a class II fission width of about 300 eV, which is greater than the observed width of this class II state.

We can obtain more information by considering the value of the integrated fission cross-section (from zero to about 40 keV) in Fig. 5, or, more precisely, $\int dE\,\sigma_f(E)\sqrt{E}$; the experimental value is about 2.2×10^6 b.eV$^{3/2}$. If it is assumed that this cross-section is mainly due to s-wave neutron bombardment, its theoretical value is

$$\int dE\,\sigma_f\sqrt{E} = \sum 2\pi^2\lambda\!\!\!^{-2}_0\,\Gamma^{(0)}_{\lambda(n)}\,\Gamma_{\lambda(f)}/\Gamma_\lambda \approx 2\pi^2\lambda\!\!\!^{-2}_0\,\frac{\Gamma^{(0)}_{\lambda(n)}}{\Gamma_\lambda}\sum_\lambda \Gamma_{\lambda(f)} \tag{11}$$

where $\lambda\!\!\!^{-}_0$ and $\Gamma^{(0)}_{\lambda(0)}$ are the de Broglie wavelength and neutron width reduced to 1 eV. Using

$$\Gamma_{\lambda(f)} \approx \frac{\langle\lambda_I|H''|\lambda_{II}\rangle^2\,\Gamma_{\lambda_{II}(f)}}{(E_\lambda - E_{\lambda_{II}})^2 + \frac{1}{4}\mathscr{W}^2} \tag{12}$$

we find

$$\sum_\lambda \Gamma_{\lambda(f)} \approx \sum_{\lambda_{II}} \frac{2\pi\,\overline{\langle\lambda_I|H''|\lambda_{II}\rangle^2}\,\Gamma_{\lambda_{II}(f)}}{\mathscr{W}\,\overline{D}_I} \tag{13}$$

The information deduced on the 400 eV class II resonance suggests that $\mathscr{W} \approx \Gamma_{\lambda_{II}(f)}$, and, therefore, that σ_F averaged over each class II resonance is dependent, not on $\Gamma_{\lambda_{II}(f)}$, but on the coupling matrix element. If the latter, then, is assumed to have the Lorentzian behaviour shown in Fig. 6, i.e.

$$\overline{\langle \lambda_I | H'' | \lambda_{II} \rangle^2} \approx \frac{\overline{D}_{II}}{\pi} \cdot \frac{w H_0''^2}{(E_{\lambda_{II}} - E_H)^2 + w^2} \tag{14}$$

we have $\sum_{\lambda_{II}} \overline{\langle \lambda_I | H'' | \lambda_{II} \rangle^2} \approx H_0''^2$, and hence,

$$\sum_{\lambda} \Gamma_{\lambda(f)} \approx \frac{2\pi}{\overline{D}_I} \cdot H_0''^2 \tag{15}$$

$$\int dE\, \sigma_f \sqrt{E} \approx 4\pi^3 \lambda_0^2 \frac{\overline{\Gamma}_{\lambda(n)}^{(0)}}{\overline{\Gamma}_\lambda} \cdot \frac{H_0''^2}{\overline{D}_I} \tag{16}$$

Using this in conjunction with the experimental value, we find $H_0''^2 \approx 30$ eV^2. With this value, $E_H \approx 15$ keV and $w \approx 7.5$ keV, we also find that $\overline{\langle \lambda_I | H'' | \lambda_{II} \rangle^2}$ for a class II level near zero neutron energy should be of the order of 0.25 eV^2, close to the value deduced for the 400 eV class II resonance.

Comparison with Eq. (1) suggests the predominance of a single mode $|\nu\mu\rangle$ at 15 keV neutron energy in the expression for the matrix element. Its narrow spread suggests that it is a class II mode, most likely with high vibrational quantum number ν_{II}. It can probably be identified with the fission mode, in which case we can deduce the tunnelling factor T_f through the saddle-point barrier from the spreading width, 15 keV, the fission width, 300 eV, of the 400 eV class II resonance, and the theoretical fission width of a pure vibrational state, $(\hbar\omega/2\pi)T_f$. This turns out to be about 0.25, implying that the saddle-point barrier is only very slightly higher than the neutron threshold in ^{242}Am. The value of $H_0''^2$ can be interpreted to indicate that c^2, the squared amplitude of the supposed fission mode within the first minimum, is of the order of 0.01. This is in not too bad agreement with Fig. 3, provided that we remember all the limitations of that calculation, and supports the idea, deduced from the energy dependence of the neutron capture cross-section for excitation of the spontaneous fission isomer [30], that the intermediate maximum is nearly 1 MeV above the neutron threshold.

REFERENCES

[1] POLIKANOV, S. M., these Proceedings.

[2] FLEROV, G. N., POLIKANOV, S. M., Comptes Rendus du Congrès International de Physique Nucléaire, Paris, 1964, Vol. 1, Editions du Centre National de la Recherche Scientifique, Paris (1964) 407.

[3] STRUTINSKY, V. M., Nucl. Phys. A95 (1967) 420; see also Ref. [26].

[4] LYNN, J. E., to be published; also Theory of Neutron Resonance Reactions, Clarendon Press, Oxford (1968) 461.

[5] WHEELER, J. A., Physica 22 (1956) 1103.

[6] EVANS, J. E., JONES, G. A. (1965) (Harwell) private communication.

[7] LYNN, J. E., Nuclear Data for Reactors (Proc. Conf. Paris, 1966) 2, IAEA, Vienna (1967) 89.

[8] VOROTNIKOV, P. E., DUBROVINA, S. M., OSTROSHCHENKO, G. A., SHIGIN, V. A., Sov. J. nucl. Phys. 5 (1967) 207.
[9] GOKHBERG, B. M., OSTROSHCHENKO, G. A., SHIGIN, V. A., Dokl. Akad. Nauk. SSSR 128 (1959) 1157.
[10] LAMPHERE, R. W., Physics and Chemistry of Fission (Proc. Symp. Salzburg, 1965) 1, IAEA, Vienna (1965) 63.
[11] DUBROVINA, S. M., SHIGIN, V. A., Dokl. Akad. Nauk. SSSR 157 (1964) 561.
[12] HOLMBERG, M. et al. (1967) (Studsvik, Sweden) private communication.
[13] ERMAGENBETOV, S. B., KUZNETSOV, V. F., SMIRENKIN, G. N., Sov. J. Nucl. Phys. 5 (1967) 181.
[14] VANDENBOSCH, R., UNIK, J. P., HUIZENGA, J. R., Physics and Chemistry of Fission (Proc. Symp. Salzburg, 1965) 1, IAEA, Vienna (1966) 547.
[15] SEEGER, P. A., HEMMENDINGER, A., DIVEN, B. C., Nucl. Phys. A96 (1967) 605.
[16] HILL, D. L., WHEELER, J. A., Phys. Rev. 89 (1953) 1102.
[17] LYNN, J. E., Nuclear Structure Study with Neutrons, North-Holland, Amsterdam (1966) 125.
[18] PAYA, D., DERRIEN, H., FUBINI, A., MICHAUDON, A., RIBON, P., Nuclear Data for Reactors (Proc. Conf. Paris, 1966) 2, IAEA, Vienna (1967) 128.
PAYA, D., BLONS, J., DERRIEN, H., FUBINI, A., MICHAUDON, A., RIBON, P., Journal de Physique 29 (1968) Suppl. 1, 159; see also PAYA, D., BLONS, J., MICHAUDON, A., Short Contribution in the following Discussion, these Proceedings.
MICHAUDON, A., Invited paper, 2nd Conf. Neutron Cross-section Technology, Washington (March 1958).
FUBINI, A., et al., Phys. Rev. Lett. 20 (1968) 1373.
[19] WEIGMANN, H., SCHMID, A., J. nucl. Energy (1968), to be published.
[20] MIGNECO, E., THEOBALD, J. P., Nucl. Phys. A112 (1968) 603.
[21] BOWMAN, C. D., COOPS, M. S., AUCHAMPAUGH, G. F., FULTZ, S. C., Phys. Rev. 137 (1965) B326.
[22] JAMES, G. D., RAE, E. R. (Harwell) private communication.
[23] LANG, J. M. B., LE COUTEUR, K. J., Proc. phys. Soc. A67 (1953) 586.
[24] FLEROV, G. N., PLEVE, A. A., POLIKANOV, S. M., TRETYAKOVA, S. P., MARTALOGU, N., POENARÚ, D., SEZON, M., VILCOV, I., VILCOV, N., Nucl. Phys. A97 444.
[25] WEIGMANN, H., Z. Phys., submitted for publication.
[26] STRUTINSKY, V. M., BJØRNHOLM, S., these Proceedings.
[27] MICHAUDON, A. (1967) private communication.
JAMES, G. D., ENDACOTT, D., AERE Report PR/6.
[28] SCHOMBERG, M. G., SOWERBY, M. G., EVANS, F. W. (1968) (Harwell) private communication.
[29] MARKO, B. N., PLEVE, A. A., POLIKANOV, S. M., FLEROV, G. N., Sov. J. nucl. Phys. 3 (1966) 329.
[30] FLEROV, G. N., PLEVE, A. A., POLIKANOV, S. M., TRETYAKOVA, S. P., BREA, I., SEZON, M., VILCOV, I., VILCOV, N., Nucl. Phys. A102 (1967) 443.

DISCUSSION

H. MELDNER: I would like to ask Dr. Lynn for a comment on the structure explanation via the one-dimensional Strutinsky potential versus the suggestion of Dr. Nix of two minima in, say, a two-dimensional plot of the energy surface.

J. E. LYNN: Dr. Nix's suggestion of an alternative, more direct route to fission in such a two-dimensional plot of the energy surface may certainly provide an explanation of the relative lifetimes for spontaneous fission of the 'shape isomer' and the ground state of ^{242}Am. A high narrow barrier in the direct route and a low, rather wide barrier in the saddle point from the secondary minimum would achieve an explanation of the lifetimes without appreciably affecting the one-dimensional explanation of the slow-neutron-induced fission cross-sections.

D. F. ZARETSKY: (1) Did you estimate the radiation half-life of the isomer? (2) The wave-functions of two-system levels will differ in the case of an oblate isomer form. Is there any experimental approach for distinguishing these forms?

J. E. LYNN: (1) I made an estimate of the radiation half-life of the isomer of ^{242}Am. With the assumptions that the intermediate barrier has a penetrability given by the Hill-Wheeler formula with a tunnelling parameter $\hbar\omega_f$ of the order of 0.8 MeV, and that this barrier extends to 1 MeV above the neutron separation energy, a rough calculation indicates that this half-life should be of the order of 20 ms. This is consistent with the observed half-life of the isomer in the sense that it is greater.

(2) I think the ^{241}Am neutron cross-section data are certainly inconsistent with the hypothesis of an oblate secondary minimum. The fission width associated with the vibrational mode mixed into the class II states evident in this cross-section is about 30 keV, indicating a penetrability of the order of 0.25. This is much too high for a vibrational mode in an oblate minimum separated by a high barrier from the normal minimum.

N. VILCOV: By deducing the energy of the ground state in the second potential well from the underbarrier resonances data you have used the same 'a' parameter in both wells. (a) Is it correct to use the Fermi-gas model level density for vibrational states in the second potential well? (b) Is it correct to use the same 'a' parameter at very different deformations and energies?

J. E. LYNN: The compound states associated with the second well are built up from combinations of the many 'intrinsic' states X of the many degrees of freedom of the nucleus and the few vibrational states. The intrinsic states are expected to be approximately, so far as their density goes, of independent particle character, and this is why we use an independent particle model.

To the second part of your question, I would answer that the minima in the Strutinsky potential are associated with high single-particle density at the Fermi energy while the maxima are associated with low single-particle density. To a first approximation, therefore, we assume that the single-particle densities, and therefore the 'a' parameters, are similar for the two minima. The energy dependence of level density laws is not very well known, and this is a point that will certainly need more attention.

P. AXEL: In those cases which involve mixing of class II states among several class I states, are all of the class I states seen? If not, is the number of detectable class I states consistent with reasonable assumptions about the mixing matrix elements?

J. E. LYNN: In at least one case, the 1900 eV group in the cross-section of ^{240}Pu, not all the resonances seem to be observed. The reason seems to be partly experimental resolution and partly the effect of the Porter-Thomas statistical distribution of the coupling matrix elements.

Short Contribution

A. F. MICHAUDON (Centre d'Etudes Nucléaires de Saclay, Gif-sur-Yvette, France): I should like to present a short report on the subject of the intermediate structure observed in the fission cross-sections of ^{237}Np and possibly of ^{239}Pu. This work has been done by D. Paya, J. Blons, A. Fubini and A. Michaudon.

The ^{237}Np nucleus is not fissionable by slow neutrons because the fission barrier in ^{238}Np is 650 keV above the neutron binding energy. Nevertheless, the penetration of this fission barrier leads to a small sub-threshold fission

cross-section which can be measured using the intense neutron sources now available.

The interaction of resonance neutrons with ^{237}Np has been studied with the Saclay linear accelerator used as a pulsed neutron source in order to obtain more information on the fission barrier and the mechanism of sub-threshold fission induced by slow neutrons.[1,2]

The total cross-section is very similar to those of odd-A nuclei with mass numbers close to 237.

On the contrary, the behaviour of the fission cross-sections is radically different from that of the total cross-section. Since it has an unusual behaviour it has been measured several times. The first measurement was carried out with a gas scintillator. A grouping effect of resonances was clearly observed and reported at the Paris conference in 1966.[3] This was confirmed by a second measurement carried out in 1967 with an ionization chamber.[4] In Figs A and B the same cross-section is shown, measured in much better conditions[1,5] with an improved gas scintillator and an overall resolution of 18 ns/m at 100 eV.

Instead of showing a regular pattern, the fission cross-section is composed of several peaks or 'structures' (which may contain several resonances) at definite energies: 40 eV, 118 eV, 198 eV, etc. The mean level spacing of these 'structures' is about 60 eV, which is roughly 100 times as great as the spacing of the compound nucleus resonances observed in transmission. Between the peaks, the cross-section is almost too small to be measured. Such a cross-section is incompatible with resonance parameters distributed at random, as has been checked by means of Monte Carlo calculations.

The intermediate structure that is observed cannot be caused by complicated 'doorway states' in the entrance channel since the total cross-section does not show any anomaly. Rather, it appears that only the coupling of the compound nucleus states to the fission exit channels is more intense at some discrete energies (40 eV, 118 eV, etc.). It has been suggested[6-8] that the compound nucleus states could be coupled to intermediate stationary states situated between the two humps of a double-humped fission barrier.[9] Consequently, all the large fission resonances belonging to one of the observed 'structures' should have the same spin and parity. The need to measure the spins of the resonances in the first 'structure' at 40 eV is therefore obvious.

Other cases of intermediate structure in sub-threshold fission were found later in other nuclei.[5-7] So it seems that this is a general phenomenon in this mass region. If true, it may be observed also in the fission cross-section of fissile nuclei when the contribution of transition states above

---

[1] FUBINI, A., et al., Phys. Rev. Lett. 20, Nb 4, 1373.

[2] RAE, E.R., in Physics and Chemistry of Fission (Proc. Symp. Salzburg, 1965) 1, IAEA, Vienna (1965) 187.

[3] PAYA, D., et al., in Nuclear Data for Reactors (Proc. Conf. Paris, 1966) 2, IAEA, Vienna (1966) 128.

[4] PAYA, D., et al., Proc. Conf. Medium-Mass and Heavy Nuclei, Bordeaux 1967, Journal de Physique, Suppl. No.1 (1968)159.

[5] MICHAUDON, A.F., Invited paper, 2nd Conf. Neutron Cross-sections, Washington, March 1964.

[6] LYNN, J.E., these Proceedings; also private communication.

[7] STRUTINSKY, V.M., these Proceedings.

[8] WEIGMANN, H., private communication.

[9] STRUTINSKY, V.M., Nucl. Phys. 95A (1967) 420.

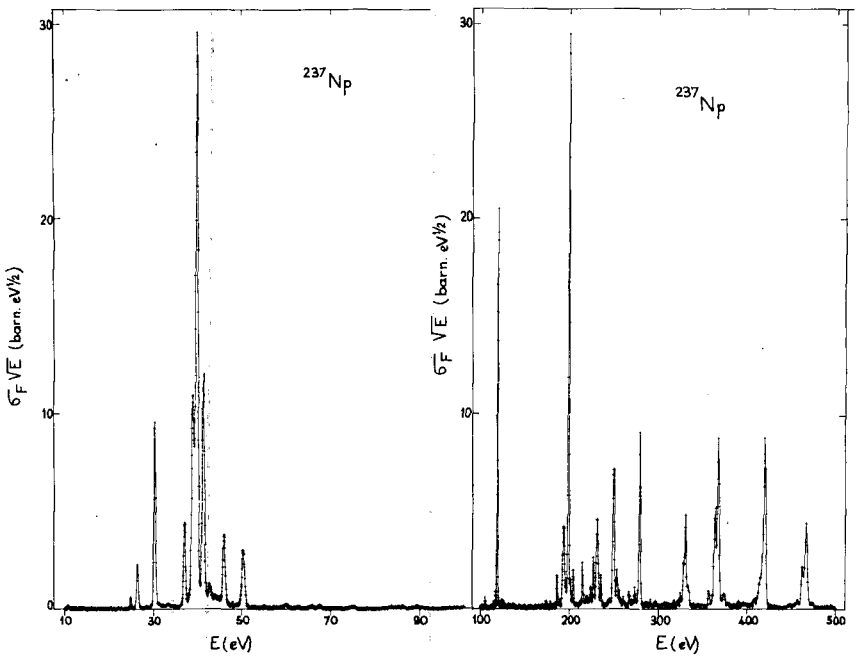

FIG. A. Fission cross-section of ^{237}Np from 10 eV to 500 eV.

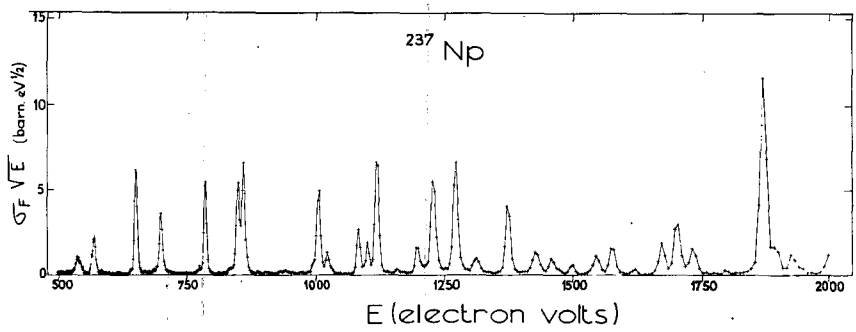

FIG. B. Fission cross-section of ^{237}Np from 500 eV to 2000 eV.

the neutron binding energy is of some importance.[5] This is probably the case for the 4$^-$ transition state in ^{235}U where auto-correlations have been found in the fission cross-section.[5] In ^{239}Pu the 1$^+$ transition state is about 200 keV above the neutron binding energy. In Fig. C is shown the fission cross-section of ^{239}Pu, recently measured at Saclay[10] with samples cooled down to the liquid nitrogen temperature and with a nominal resolution of 1 ns/m. This cross-section shows some structures at 500 eV, 950 eV,

[10] BLONS, J. et al., C.r. hebd. Séanc. Acad. Sci., Paris, to be published.

etc. with a mean level spacing of about 350 eV, which is roughly 100 times as great as the spacing of the compound nucleus resonances. These 'structures' could be due to an intermediate structure in the cross-section for sub-threshold fission through the 1^+ transition state.

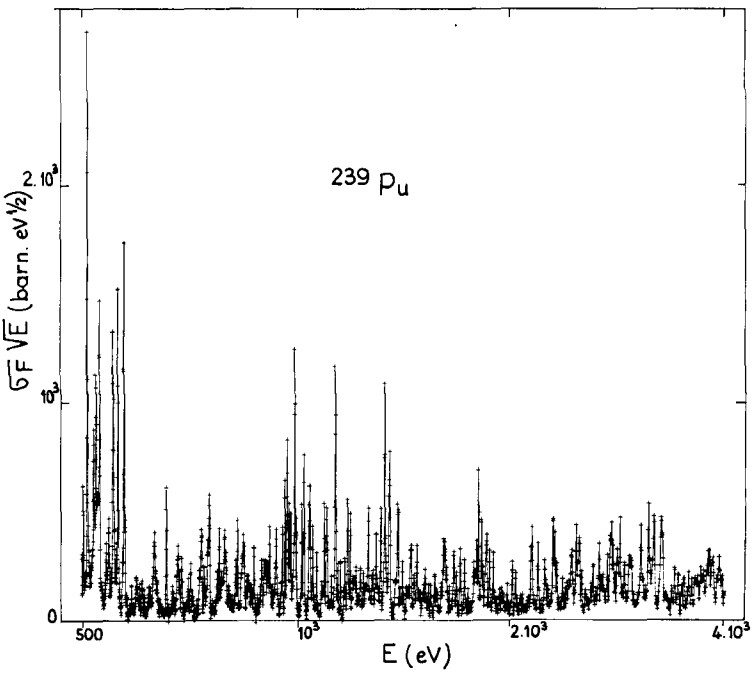

FIG.C. Fission cross-section of ^{239}Pu from 500 eV to 4000 eV.

L. B. PIKELNER: Did you perform the analysis of the distribution of spaces between maxima of the intermediate structure in the case of ^{237}Np? If so, is there agreement with the Wigner distribution?

A. F. MICHAUDON: The 'structures' which show up in the fission cross-section of ^{237}Np are supposed to be coupled to excited states in the second well having spin and parity 2^+ or 3^+. Therefore, the level spacing distribution of these 'structures' should obey a distribution obtained from the random superposition of two Wigner distributions. In fact, the observed level spacing distribution of the 'structures' is in agreement with a Wigner distribution corresponding to one single family as if all the 'structures' were coupled to one spin state only. Nevertheless, this result should not be considered as definite because of the difficulty of correctly identifying different structures in the fission cross-section.

Short Contribution

M. PETRASCU (Institute for Atomic Physics, Bucharest, Romania): I should like to present a short report on mechanisms of plutonium-239 fission induced by muons.

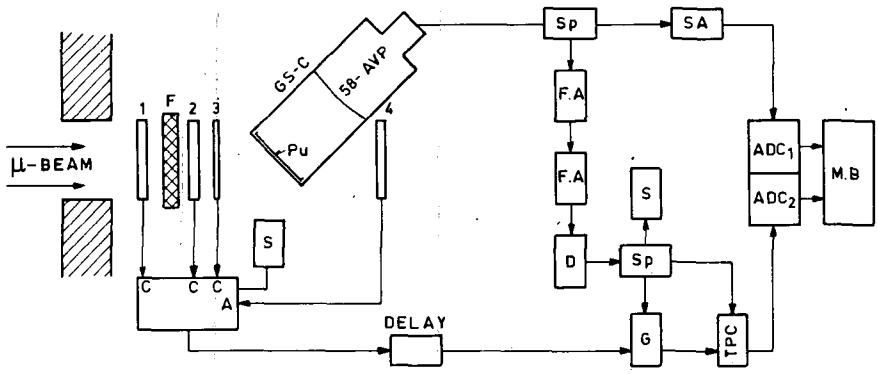

FIG.(i). Block diagram of the experiment. 1, 2, 3, 4: scintillation counters; GSC: gaseous scintillation counter; F: filter; CCCA: coincidence-anticoincidence scheme; Sp: split; FA: fast amplifier; D: discriminator; G: gate; TPC: time to pulse height converter; SA: slow amplifier; $ADC_{1,2}$: double analogue to digital converter; MB: 4096 memory block.

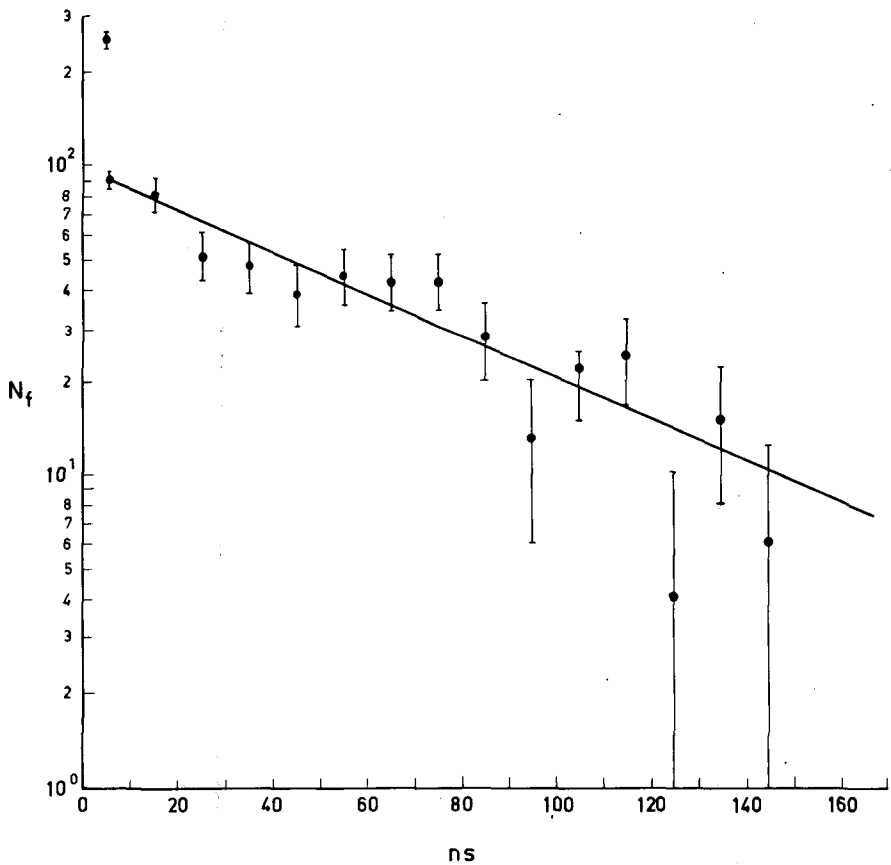

FIG.(ii). Time distribution of the fission fragments.

There are two mechanisms which are assumed to contribute to the fission of heavy mu-mesic atoms. One mechanism consists in the excitation of the nucleus due to muon capture through the reaction $\mu^- + p \rightarrow n + \nu$. Fissions due to this reaction appear with the lifetime of the muon in a specific mesic atom. The other mechanism was theoretically investigated by Zaretsky and consists in the direct transfer to the nucleus of the 2p-1s transition energy of the mesic atom. Fissions induced by this mode of excitation are present. Due to this difference in time characteristics one can separate the two mechanisms by measuring the time at which the fissions occur, the origin of the time scale being given by the stopping of the muon in the target.

A group of us from Romania (A. Butā, N. Grama, V. Hulubei, L. Marinescu, G. Voiculescu and myself) together with M. Omelianenko from Dubna have just finished a two parameter (time and pulse-height selection) investigation of the fissions induced by muons in plutonium-239. Fig. (i) shows the general layout of the experiment together with the electronics used for time and pulse-height selection. Fig. (ii) represents on a semilogarithmic scale the time distribution obtained; excluding the first time interval, one obtains by applying the method of Peierls the value 67 ± 8 ns for the muon lifetime in plutonium-239. In the first interval one can see a significant effect due to direct excitation of the nucleus by the non-radiative 2p-1s transition, confirming our previous results. If one calculates the ratio of the fissions by this mechanism to the fissions from muon capture one obtains the value 0.28 ± 0.04. Now if one compares this result with those obtained by Diaz et al. and by Bielovitsky and by us for uranium one gets an increase by an order of magnitude of the non-radiative mechanism contribution in the case of plutonium. Perhaps this is connected, as suggested by Zaretsky, with a modification of the fission barrier due to the presence of the muon in the 1s shell. This modification of the fission barrier according to the theoretical calculations is smaller for plutonium than for uranium.

FISSION OF EXCITED NUCLEI

Yu.Ts. OGANESYAN
JOINT INSTITUTE FOR NUCLEAR RESEARCH,
DUBNA, UNION OF SOVIET SOCIALIST REPUBLICS

Abstract — Аннотация

FISSION OF EXCITED NUCLEI. Nuclear fission at excitation energy more than 50 MeV has been investigated. It is shown that the statistical theory determines a nuclear state at the saddle-point rather well, but appears to be inapplicable for describing the process at the scission point. This conclusion is based on the experiments on mass and charge distributions of fission fragments for nuclei in the wide Z^2/A range.

ДЕЛЕНИЕ ВОЗБУЖДЕННЫХ ЯДЕР. Рассматривается деление ядер при энергии возбуждения свыше 50 Мэв. Показано, что статистическая теория деления хорошо определяет состояние ядра в седловой точке и неприменима для описания процесса в токе разделения осколков. Этот вывод следует из опытов по измерению массовых и зарядовых распределений осколков при делении ядер в широком диапазоне Z^2/A.

I

Since the discovery of uranium fission, the study of the fission mechanism has been one of the most important and interesting problems of nuclear physics. A lot of work is devoted to the investigation of this phenomenon; to explain experimental data various nuclear structure models are used, such as the liquid drop model, the shell model and statistical theory. It is natural that the range of application of a model is very limited and there is as yet no consistent theoretical interpretation of this complicated nuclear process.

The well-known mass distribution of fission fragments of ^{235}U with thermal neutrons is sometimes explained from positions little compatible with one another. It is probably because of this that a great deal of effort is made to explain the mechanism of low-energy or spontaneous nuclear fission.

However, it has been established experimentally that with increasing nuclear temperature the picture changes: at an excitation energy higher than 50 MeV, fission actually becomes symmetrical [1, 2]. It may be supposed that this energy increase does not radically alter the mechanism of this complicated nuclear transformation. At the same time the field of the experimental study of nuclear fission is considerably extended.

Indeed, for the investigation of spontaneous fission or fission on thermal neutrons, only nuclei from uranium to californium can be used while in the highly excited state all nuclei with $Z^2/A > 25$ undergo fission [3]. Of course, data obtained for a heated nucleus cannot be directly used for explaining all fission regularities near the threshold. However, facts such as nuclear shape at the saddle point, the mechanism of nuclear motion from saddle to scission point, the character of separation, etc. are common and important for the fission problem as a whole.

Thus, in what follows we shall consider nuclei at an excitation energy higher than 50 MeV; at these energies the structure features of low-energy fission are completely absent.

We note, however, that the quantitative study of the excited nucleus fission meets with serious difficulties. When the projectile energy increases, the number of reaction channels also increases and the initial state of a fissioning system is uncertain. Experiments with relativistic protons may serve as an example of this; here, after the fast cascade emission of nucleons, quite a number of nuclei with a wide excitation spectrum undergo fission [4, 5].

From this point of view, heavy ions have some advantages since at an energy lower than 10 MeV per atomic mass unit the main mode of interaction of complex nuclei is complete fusion with the production of a highly excited compound nucleus. On the one hand, this defines unambiguously the nuclear state just before fission; on the other hand, it allows a large number of nuclei to be investigated in a wide range of Z^2/A.

Below we shall discuss the experimental data on fission induced by heavy ions from ^{12}C to ^{40}Ar.

II

It appears that in the fission process the nucleus passes through a transition state – the saddle point – which corresponds to the fission barrier. It is assumed that at the saddle point the nucleus is in thermal equilibrium. This state is essentially an initial state for all further fission processes.

If such a situation occurs, then according to statistical theory the angular distribution of the fragments is unambiguously related to the effective moment of inertial I_{eff} which characterizes the nuclear shape at the saddle point [7-9].

$$\frac{1}{I_{eff}} = \frac{1}{I_{\parallel}} - \frac{1}{I_{\perp}}$$

where $I_{\perp}$ and $I_{\parallel}$ are the moments of inertia of the transition state nucleus at the saddle deformation about an axis perpendicular and parallel to the axis of symmetry, respectively.

The experimental data on I_{eff} calculated from the angular anisotropies for heavy ion-induced fission in various target nuclides are given in Fig. 1.

It should be noted that, within experimental accuracy, I_{eff} does not depend on the mode of production, the excitation energy and the angular momentum of a fissioning nucleus [10, 12], but is only a function of Z^2/A.

Now it is interesting to compare the experimental data with the calculated results for I_{eff} using the usual liquid drop model [10, 11]. A noticeable lack of agreement for large Z^2/A values is seen in Fig. 1, which indicates that the deformation at the saddle point is small as compared with the shape obtained by means of the liquid drop model.

However, this disagreement is practically eliminated if, as before in the framework of the liquid drop model, the distribution of the nucleon density of the nucleus is correctly taken into account and the surface tension as a function of the curvature of the effective surface is introduced in calculating I_{eff} [13].

It is very important that the calculated results agree with the experimental ones.

This provides evidence that the liquid drop model is a good approximation in calculating the potential energy and the nuclear shape at the saddle point. At the same time the assumption of the statistical nuclear equilibrium on the top of the barrier is valid with great accuracy for all investigated nuclei.

Hence, it follows that the deformed nucleus is really for a long time in an intermediate state corresponding to the saddle point.

Note that the extreme point at $Z^2/A = 43.5$ (Fig. 1) obtained from the angular distribution of ^{140}La nuclei in the fission of ^{238}U by the ^{40}Ar ions corresponds to $I_{sph}/I_{eff} = 0.1$. Because of this, it is possible to determine accurately from experiments the main parameter of the liquid drop model, $(Z^2/A)_{crit}$, which defines the stability limit of nuclear matter against fission. The extrapolation $1/I_{eff} \to 0$ (nuclei with spherical shape at the saddle point) gives $(Z^2/A)_{crit} = 45 \pm 1$.

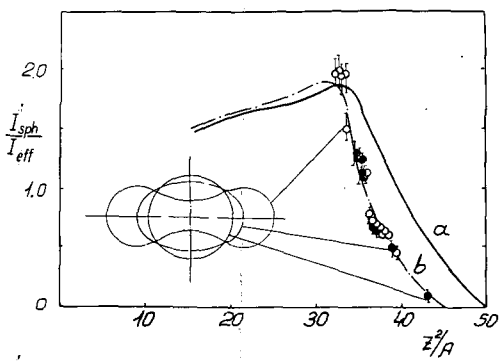

FIG. 1. Dependence of the effective moment of inertia at the saddle point on the fission parameter Z^2/A. The curves are the results of calculation using the liquid drop model: (a) for a nucleus with sharp edge, (b) taking into account the nucleon density distribution in the surface layer. The experimental points: open circles are the data from experiments on deuterons and alpha particles [10, 11]; full circles, experiments on heavy ions. The figures correspond to the nucleus shape at the saddle point on the assumption of axial symmetry.

It is shown above that the main characteristics of the nucleus in the quasi-stationary state near the barrier top can be determined fairly accurately. Further motion of the nucleus from saddle to scission point is very complicated whereas the appropriate information may be obtained only at the initial moment (the barrier top) and in the very last stage (division into two fragments). Thus the charge and mass distributions of fragments, the total kinetic energy and fluctuations of the fragment kinetic energy are essentially the only data which reflect the fission mechanism.

It is obvious that this information is not explicit enough to describe a complicated nuclear system with many degrees of freedom. Therefore, to describe the phenomenon one or other of the models is used which supposes a priori a certain regularity in the development of the process.

When a fissioning nucleus is highly excited it is assumed that the energy exchange between different degrees of freedom proceeds far more rapidly compared to the rate of the deformation change. This allows one to consider the nucleus as an isolated system in thermodynamic

equilibrium in all the stages of motion from saddle to scission point [14-17]. Thus, the whole process may be considered in the very last stage, that is at the scission point, and the statistical theory may be applied to describe the main fission regularities.

This approach seems to be justified for fission from excited states for general reasons [14, 18], so an experimental check of the applicability of statistical theory is important here.

The statistical model has been used for explaining many experimental data [19-21] on the fission of excited nuclei. However, until recently only a small number of light nuclei with Z^2/A from 31 to 35 have been systematically investigated.

We give below the results of measurements of the mass and charge distributions of fission fragments [22, 23] for nuclei with Z^2/A from 37.5 to 43.5.

When bombarding ^{209}Bi and ^{238}U thin targets with the ^{16}O, ^{20}Ne and ^{40}Ar ions, fragments of the rare-earth group and, in some cases, heavy fragments from gold to polonium were separated by the radiochemical method [24].

Further, using a Ge(Li)-gamma spectrometer, the gamma radioactivity of fragments was measured and the spectrum obtained was analysed with the aim of identifying the isotopes and determining their yield. This technique was fairly reliable and the yield was determined with an error not greater than 15%.

To plot the mass distributions the following assumptions were made about the charge distribution of fragments, which were then checked experimentally:

(1) For each fragment mass A_f the yield of isobars with Z differing from the most probable values of Z_p was described by the Gaussian distribution

$$W(Z - Z_p) = \frac{1}{(\pi c)^{1/2}} \exp\left[-\frac{(Z - Z_p)^2}{c}\right]$$

(2) The dependence of Z_p on A_f was calculated under the following hypothesis:
   (i) constant charge density of fragments
   (ii) equal charge displacement [25]
   (iii) the charge distribution from the minimum of the potential energy of fragments [16].

It was also assumed that neutrons were evaporated from fragments [25] ($\Gamma_n/\Gamma_f \ll 1$) in a number proportional to the fragment mass $\nu_f = (\nu/A_0)A_f$.

With the aid of an electronic computer, using the least squares method, the parameters ν and $\langle c \rangle$ were chosen for different dependences $Z_p(A)$, giving the smallest deflection of the experimental points from the smooth curve which, as expected, was well described by the Gaussian distribution:

$$P(A_f) = \frac{1}{(\pi \sigma^2)^{1/2}} \exp\left[-\frac{\left(A_f - \frac{A_0}{2}\right)^2}{\langle \sigma \rangle^2}\right]$$

with one parameter $\langle \sigma \rangle^2$.

TABLE I. EXPERIMENTAL DATA ON HEAVY-ION INDUCED FISSION [23]. The $\langle c \rangle_{exp}$ values are given for rare-earth fragments.

	$\frac{Z^2}{A}$	E_t(MeV)	$\langle\sigma\rangle^2$	$\bar{\nu}$	$\langle c \rangle$	$\langle c \rangle_{exp}$
^{209}Bi(^{20}Ne, f)	37.7	100	710	10.8	0.56	
^{238}U(^{12}C, f)	38.4	42				0.7 ± 0.2
^{238}U(^{16}O, f)	39.4	81	1280	11.2	1.7	
^{238}U(^{20}Ne, f)	40.5	120	2280	12.6	3.3	
		95	1660	11.5	2.9	
		65	1130	8.9	2.7	2.6 ± 0.2
^{209}Bi(^{40}Ar, f)	41.0	115	2200	9.5	2.75	
^{238}U(^{40}Ar, f)	43.5	110	2790	13.3	3.0	
		75	1980	10.6	2.9	2.8 ± 0.2

When using such a method, preference is not given to any one hypothesis on the charge distribution of fragments; this follows from the best fit of the experimental points on the mass curve.

The experimental data are given in Table I. It was found for all reactions that the worst agreement is obtained when the charge is assumed to be proportional to the fragment mass (Fig. 2) while for the other two cases the results practically coincide.

The mass spectra for fission fragments are given in Fig. 3. Using the dependence of the mass distribution width on the nuclear temperature we obtain $\langle\sigma\rangle^2$ as a function of the parameter Z^2/A for a fixed excitation energy. As is seen from Fig. 4 at $Z^2/A > 38$ a strong enlargement of the mass curve is observed.

Now it is interesting to compare the experimental data with the calculations performed using the statistical theory. Several methods of such calculations are known. Here we use the method suggested in Ref. [16], which is the most convenient and exact.

In the framework of the statistical theory the fission probability for a given ratio of fragment masses is

$$P(A) \sim \exp\left[-\frac{(A-\bar{A})^2}{\bar{A}^2\langle\Delta\delta\rangle^2}\right]$$

where

$$\bar{A} = \frac{A_0}{2}, \quad \delta = \frac{1}{2}\left(1 - \frac{2A_f}{A_0}\right), \quad \langle\Delta\delta\rangle^2 = T\left[\frac{1}{2}\frac{\partial^2 w}{\partial \delta^2}\bigg|_{\delta=\bar{\delta}}\right]^{-1}.$$

Here T is the nucleus temperature.

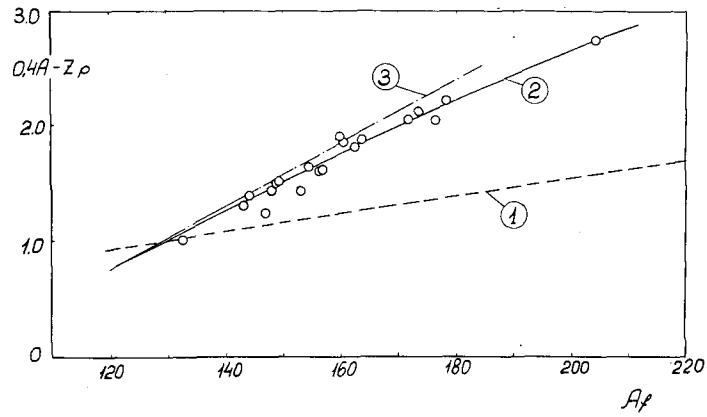

FIG. 2. $(0.4A - Z_p)$ as a function of the fragment mass A_f for the reaction $^{238}U(^{22}Ne, f)$. The curves are the predictions of the hypotheses: (1) constant charge density of the fragments, proportionality of the charge to the fragment mass, (2) equal charge displacement, (3) the charge distribution according to the minimum of potential energy at the scission point [16].

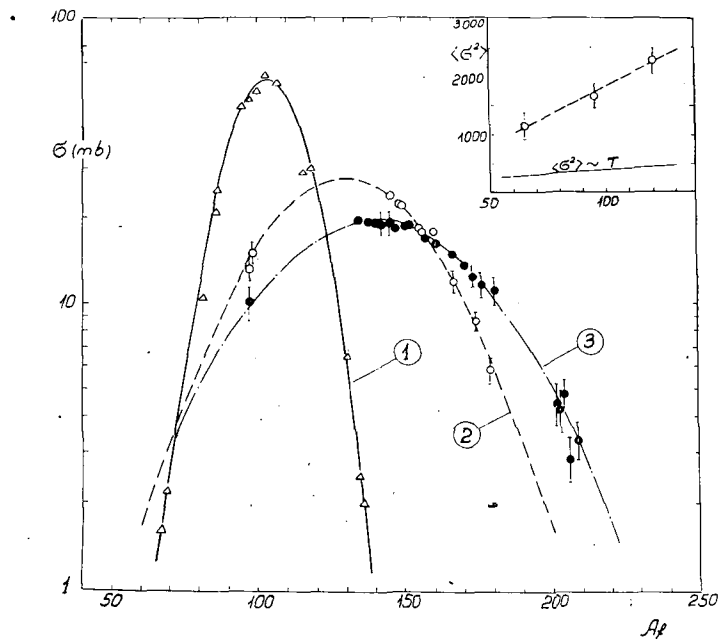

FIG. 3. Mass distribution of the fission fragments. Curve 1: $^{197}Au(^{12}C, f)$ [20], excitation energy 105 MeV; curve 2: $^{238}U(^{20}Ne, f)$ [23], excitation energy 95 MeV; curve 3: $^{238}U(^{40}Ar, f)$ [23], excitation energy 110 MeV. The upper diagram is the dependence of $\langle\sigma\rangle^2$ on the excitation energy of a fissioning nucleus $^{238}U(^{20}Ne, f)$.

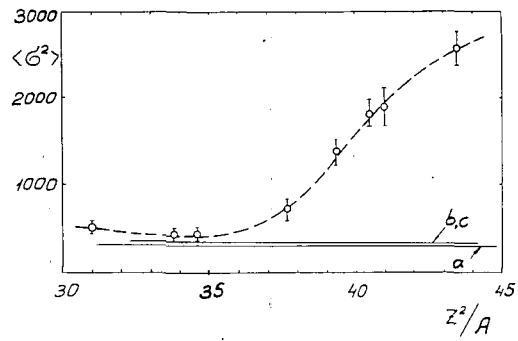

FIG.4. Mass distribution width $\langle\sigma\rangle^2$ as a function of the parameter Z^2/A at an excitation energy of about 100 MeV. The dotted line is drawn through the experimental points. The continuous lines are the predictions of the statistical theory obtained for different mass formulas: (a) Cameron [28], (b) Green[25], (c) Myers and Swiatecki [29].

$\partial^2 w/\partial\delta^2$ is the second derivative of the total potential nucleus energy which, according to Ref. [16], can be presented as:

$$\frac{\partial^2 w}{\partial \delta^2} = \alpha_1 \Delta E_s + \alpha_2 \Delta E_c - \alpha_3 \overline{E} - \alpha_4 E_{ds} + \alpha_5 E_{dc} - \alpha_6 A_0^{7/3}$$

where $\alpha_1, \alpha_2, \ldots \alpha_6$ are the constant coefficients. ΔE_s and ΔE_c are the differences in the surface and Coulomb energy for the initial (spherical) nucleus and two (spherical) fragments. E_{ds}, E_{dc} are the surface and Coulomb energies of the fragment deformation at the scission moment. $\overline{E}$ is the energy for the Coulomb interaction of fragments which is equal to the total kinetic energy, the latter being determined accurately from the experimental dependence [27]

$$\overline{E} = 0.1065 \frac{Z_0^2}{A_0^{1/3}} + 20.1 \text{ MeV}$$

In calculating the potential nucleus energy different mass formulas were used [25, 28, 29]. Comparison of the theoretical and experimental data in Fig. 4 shows that agreement is obtained only for a very narrow region of light nuclei, while for $Z^2/A > 38$ there is an essential disagreement, considerably exceeding the errors. Thus, the large disagreement can be eliminated by not varying the model parameters, within reasonable limits.

It is also seen from experiments that the dependence of $\langle\sigma\rangle^2$ on the excitation energy is stronger than the theory predicts.

However, it seems to us that the strictest criterion of the validity of the statistical approach is the fluctuation of the fragment charge for a given mass ratio (or the mass fluctuation for a given charge ratio).

Indeed, according to Ref. [16], in calculating the isobar or isotopic curves, only the well-known term of the mass formula $\sim (A-2Z)^2/A$ is used, which takes into account the affinity of the protons and neutrons in the nucleus.

In this connection, we nave measured the isotopic distributions of fragments near the maximum of the mass curve for nuclei with different Z^2/A. It is seen from Fig. 5 that the charge (or isotopic) curves are well described by the Gaussian distribution and the parameter $\langle c \rangle$ agrees with the data of Table I.

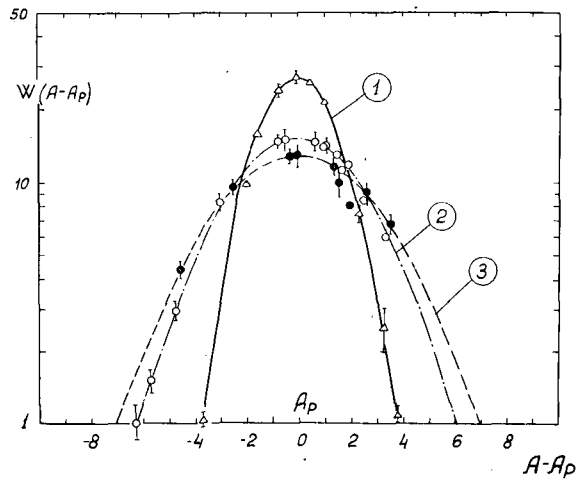

FIG. 5. Isotopic distributions of the fission fragments. Curve 1: ^{197}Au(^{12}C, f) [20]; curve 2: ^{238}U (^{20}Ne, f) [23]; curve 3: ^{238}U (^{40}Ar, f) [23]. Parameter Z^2/A is 34.5, 40.5 and 43.5 respectively. The charge distribution widths $\langle c \rangle_{exp}$ for this reaction are presented in Table I.

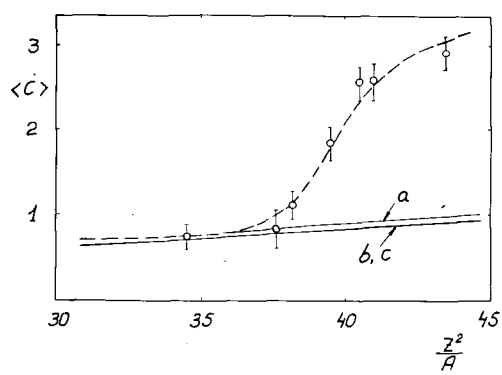

FIG. 6. Charge distribution width $\langle c \rangle$ as a function of the parameter Z^2/A at an excitation energy of about 80 MeV. The dotted line is drawn through the experimental points. The curves a, b and c are the theoretical calculations (see Fig. 4).

The experimental dependence of the charge distribution width $\langle c \rangle$ on Z^2/A (Fig. 6) agrees with the theoretical one in the range of light nuclei only, and disagrees strongly for $Z^2/A > 38$.

The isotopic distributions in different places of the mass curve were measured for the reaction ^{238}U (^{40}Ar, f). The $\langle c \rangle$ values obtained from these data as a function of the mass asymmetry (Fig. 7) indicate that the charge distribution width is not constant for all the masses, as is usually assumed when calculating the mass distributions of fragments.

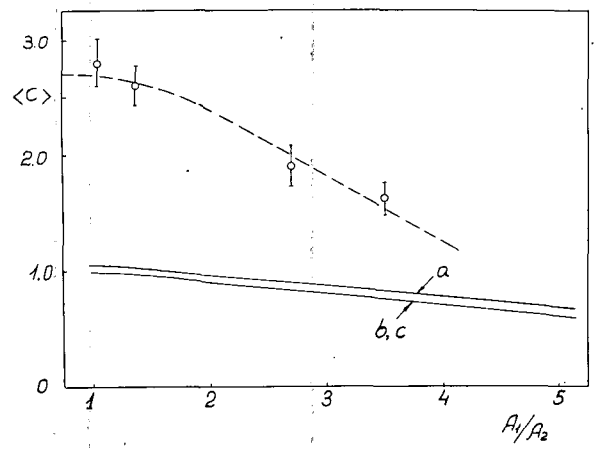

FIG. 7. Dependence of $\langle c \rangle$ on the asymmetry of ^{238}U fission with ^{40}Ar ions. The dotted line is drawn through the experimental points. The curves a, b and c are the theoretical calculations (Fig. 4).

III

The main cause of the disagreement between the experimental data and the theoretical predictions of the statistical model lies, it seems to us, in the fact that unjustified assumptions have been made concerning the fission mechanism.

The existence of thermodynamic equilibrium at the scission point, which is used for the calculation of the nuclear potential energy and of all other quantities, seems to be doubtful for the following reasons.

The statistical approach is valid only in the case when the relaxation time of the nucleus is far shorter than the time of the deformation change. However, the rate of the deformation change is minimum at the barrier and maximum at the scission point. In the latter case it may be the same as or even larger than the rate of the nucleus relaxation [30].

This fact contradicts the assumptions of the statistical theory.

A correct description of the phenomenon may be obtained only by taking into account the dynamics of the process, which needs additional assumptions regarding the kinetic properties of the fission process.

Let us try to explain qualitatively the experimental data.

For different Z^2/A the starting figures (saddle point) may be essentially different (Fig. 1), therefore the number of configurations along the whole path up to the scission point is also different. Taking into account the accelerative character of the motion, it should be assumed that most of the time the nucleus has a deformation which differs strongly from the figure at the scission point. This means that the fate of the separation was at stake long before the moment when the nucleus was ready to assume the shape of two separate fragments. In the process of change of deformation, each figure has a certain stability against the asymmetrical variations of the shape [31].

For such an approach the fluctuation of the mass and charge of fragments depends on the rate of the deformation change and on the initial shape of the nucleus.

However, the exact calculation is a matter of some difficulty but, with some simplifications of the problem, the dependence of the mass distribution width $\langle\sigma\rangle^2$ may be obtained close to the experimental one.

It should be noted that the good agreement of the experimental points (Figs 4 and 6) with the calculations using the statistical theory in the range of light nuclei ($Z^2/A = 31 - 34$) is accounted for by the fact that the nuclear shapes at the scission moment and at the saddle point differ little from each other. Since the second stage of the process is practically absent, the assumption of thermodynamic equilibrium at the scission point is essentially related to the saddle point; this is quite justified and agrees well with experimental results.

IV

A noticeable enlargement of the mass curve with increasing Z^2/A gives rise to an interesting phenomenon: "cascade fission" of the nucleus with the production of three fragments of about equal masses [32].

The essence of this phenomenon is that in some cases an excited compound nucleus undergoes a strong asymmetrical fission.

If the excitation energy of a heavy fragment is higher than its fission barrier, then it can disintegrate once again into two parts. The cross-section of this process depends on the mass distribution in the first stage of fission (the yield of large masses) and on the fission probability for the heavy fragment. This mechanism explains clearly the experimental data on the fission of nuclei into three fragments in heavy-ion induced reactions [33, 34].

Note also that the fission of heavy excited nuclei may be a good method for synthesizing new isotopes [35]. It seems to us that fission induced by ions heavier than argon is very promising for obtaining nuclei far off the stability line [36].

REFERENCES

[1] COLBY, L.J., COBBLE, J.W., Phys. Rev. 121 (1961) 1410.
[2] UNIK, J.P., HUIZENGA, J.R., Phys. Rev. 134 (1964) B90.
[3] OBUKHOV, A.I., PERFILOV, N.A., Yadernaya Fiz. 3 (1966) 979.
[4] RUDSTAM, G., SØRENSEN, G., J. inorg. Chem. 28 (1965) 771.
[5] HAGEBØ, E., J. inorg. nucl. Chem. 29 (1967) 2515.
[6] BOHR, A., Int. Conf. peaceful Uses atom. Energy (Proc. Conf. Geneva, 1955) 2, UN, New York (1956) 151.
[7] STRUTINSKY, V.M., Zh. eksp. teor. Fiz. 30 (1956) 606.
[8] STRUTINSKY, V.M., Atomnaya Energia 2 (1957) 508.
[9] HALPERN, I., STRUTINSKY, V.M., Int. Conf. peaceful Uses atom. Energy (Proc. Conf. Geneva, 1958) 15, UN, New York (1958) 408.
[10] CHAUDHRY, R., VANDENBOSCH, R., HUIZENGA, J.R., Phys. Rev. 126 (1962) 220.
[11] BATE, G.L., CHAUDHRY, R., HUIZENGA, J.R., Phys. Rev. 131 (1963) 722.
[12] KARAMYAN, S.A., KUZNETSOV, I.V., MUZYCKA, Yu.A., OGANESYAN, Yu. Ts., PENIONZKEVICH, Yu.E., PUSTYLNIK, B.I., Yadernaya Fiz. 6 (1967) 494.
[13] STRUTINSKY, V.M., Yadernaya Fiz. 2 (1965) 821.
[14] FONG, P., Phys. Rev. 102 (1956) 434.
[15] NEWTON, T.D., Proc. Symp. Physics of Fission, Chalk River, Ontario (1956).
[16] PIK-PICHAK, G.A., STRUTINSKY, V.M., Nuclear Fission, Atomizdat, Moscow (1962).
[17] NIX, J.R., Preprint UCRL-11338 (1964).
[18] HILL, D.L., WHEELER, J.A., Phys. Rev. 89 (1953) 1102.
[19] BURNETT, D.S., GATTI, R.C., PLASIL, F., PRICE, P.B., SWIATECKI, W.J., THOMPSON, S.G., Report UCRL-11079 (1963).

[20] VIOLA, V.E., BLANN, H.M., THOMAS, T.D., Proc. 2nd Conf. Reactions Between Complex Nuclei, New York (1960).
[21] PLASIL, F., Report UCRL-11193 (1963).
[22] KARAMYAN, S.A., LIPTAC, I., OGANESYAN, Yu. Ts., PENIONZKEVICH, Yu.E., URBANEC, J., Atomnaya Energia 23 (1967) 564.
[23] KARAMYAN, S.A., NORMURATOV, F., OGANESYAN, Yu. Ts., PENIONZKEVICH, Yu.E., PUSTYLNIK, B.I., FLEROV, G.N., Preprint JINR P7-3732 (1968).
[24] KUZNETSOV, I.V., MALTSEVA, N.S., OGANESYAN, Yu. Ts., SUKHOV, A.M., SHOHEGOLEV, V.A., Preprint JINR P7-3710 (1968).
[25] GREEN, A.E.S., Phys. Rev. 95 (1954) 1006.
[26] SIKKELAND, T., Preprint UCRL-16348 (1965).
[27] TERRELL, J., Phys. Rev. 113 (1959) 527.
[28] CAMERON, Q.G.W., Can. J. Phys. 35 (1957) 1021.
[29] MYERS, W.D., SWIATECKI, W.J., Preprint UCRL-11980 (1965).
[30] NIX, J.R., Contributions to Int. Conf. Nuclear Structure, Tokyo (1967).
[31] STRUTINSKY, V.M., Zh. eksp. teor. Fiz. 45 (1963) 1900.
[32] MUZYCKA, Yu.A., OGANESYAN, Yu. Ts., PUSTYLNIK, B.I., FLEROV, G.N., Yadernaya Fiz. 6 (1967) 306.
[33] PRICE, P.B., FLEISCHER, R.L., WALKER, R.M., Proc. 3rd Conf. Reactions Between Complex Nuclei, University of California Press (1963).
[34] KARAMYAN, S.A., KUZNETSOV, I.V., OGANESYAN, Yu. Ts., PENIONZKEVICH, Yu.E., Yadernaya Fiz. 5 (1967) 959.
[35] FLEROV, G.N., Nucleonika 12 (1967) 1081.
[36] FLEROV, G.N., Preprint JINR D7-3623, Dubna (1967).

V

GENERAL PROPERTIES OF NUCLEI

Chairmen	Secretaries
A. HRYNKIEWICZ	Z. STAHURA
G. ALAGA	V.V. BABIKOV
V.G. SOLOVIEV	R.V. JOLOS

THE INCONSTANCY OF MEAN RADII OF NUCLEAR STATES IN ROTATIONAL BANDS*

L. GRODZINS
MASSACHUSETTS INSTITUTE OF TECHNOLOGY,
CAMBRIDGE, MASS., UNITED STATES OF AMERICA

Abstract — Аннотация

THE INCONSTANCY OF MEAN RADII OF NUCLEAR STATES IN ROTATIONAL BANDS. The difference, $\Delta\langle R^2\rangle$, in the mean square radius of the first 2^+ state with respect to the 0^+ ground state of rotational bands has now been measured for a number of deformed nuclei using Mössbauer and muonic isomer shift techniques. The results of both types of measurements are reviewed. The derivation of $\Delta\langle R^2\rangle$ from Mössbauer data still contains up to 50% uncertainty in the evaluation of $|\psi(0)|^2$. The muonic data are superficially more reliably analysed. There are, however, large corrections for energy shifts resulting from asymmetries in the decay of the magnetically split nuclear transition. And there are further ambiguities in evaluating polarization effects. Considering the overall uncertainties, the results of the two techniques are in good accord. On the other hand the theoretical predictions of $\Delta\langle R^2\rangle$ are uniformly several times larger than the experimental values. Even more interesting is that recent experiments indicate that the mean radius of first 2^+ states become smaller than the mean radius of the respective ground state in the W - Os region.

НЕПОСТОЯНСТВО СРЕДНИХ РАДИУСОВ ЯДЕРНЫХ СОСТОЯНИЙ В РОТАЦИОННЫХ ПОЛОСАХ. Разница $\Delta\langle R^2\rangle$ для средне-квадратичного радиуса первого 2^+ состояния относительно 0^+ основного состояния полос вращения была измерена для ряда деформированных ядер с использованием методики Мессбауэра и мюонного изомерного сдвига. Дается обзор результатов обоих типов измерений. Получение $\Delta\langle R^2\rangle$ из Мессбауэровских данных содержит все же 50% неопределенности в расчетах $|\psi(0)|^2$. Мюонные данные проанализированы намного надежнее. Однако, имеются большие поправки на сдвиги по энергии в результате асимметрии в распаде для ядерного перехода с расщепленного магнитным полем состояния. Есть и другие неясности в оценке эффектов поляризации. При учете всех неопределенностей, результаты двух методик можно считать находящимися в хорошем согласии. С другой стороны, теоретические предсказания $\Delta\langle R^2\rangle$ постоянно превышают экспериментальные значения в 7 раз. Последние эксперименты указывают, что средний радиус первых 2^+ состояний становится меньше среднего радиуса соответствующего основного состояния в области W-Os.

INTRODUCTION

The study of nuclear radii remains one of the classic approaches to the understanding of nuclear structure with the preponderance of such investigations being concerned with radial distributions of ground states. The development of techniques to accurately compare the radius of a ground state with that of an isomer [1, 2] has allowed the isolation of specific effects of the nuclear configuration. The measurements are carried out by comparing the transition energy between excited (e) and ground state (g) in two electronic environments. The difference in energy, observed as a velocity Doppler shift of the centre of gravity

* This work is supported in part through funds provided by the U.S. Atomic Energy Commission Contract AT (30-1)-2098.

of the source (S) line with respect to the absorber (A) is given by [3] (see Fig. 1),

$$\Delta E = \frac{2\pi}{5} Ze^2R^2 \left[|\Psi_A(0)|^2 - |\Psi_S(0)|^2 \right] \left[\frac{\langle R_e^2 \rangle - \langle R_g^2 \rangle}{\langle R^2 \rangle} \right] \quad (1)$$

The isomer shift measurements were first carried out between states of widely different configurations such as are found in ^{57}Fe, but it was realized quite early that one of the important applications of such measurements would be to the study of rotational states in order to directly examine the non-adiabatic effects in rotational bands of deformed nuclei. Unfortunately the very similarity of the nuclear configurations within a band makes the observation difficult. For this reason the early searches were carried out on transition nuclei at the edges of the deformed region where the configurations were expected to be most different. The first unambiguous measurement of a finite isomer shift was observed [4] on the 100 keV transition of ^{182}W. This measurement was not, however, amenable to unambiguous abstraction of the radial change, owing to very uncertain calculations of the s-electron wave-functions, $|\Psi(0)|^2 = \rho(0)$ at the W nuclei. (Gross uncertainties in $\rho(0)$ are still the rule rather than the exception; for example the recent calculations of the value of $\Delta\langle R^2\rangle/\langle R^2\rangle$ for the 14.4 keV transition of ^{57}Fe differ by a factor of three [5].)

To reduce these uncertainties investigators concentrated on the more amenable rare earth nuclei where the unfilled but well-shielded 4f shell, the reliable hyperfine and isotope shift data, and the theoretical understanding, make for reasonably reliable estimates of $\rho(0)$. The entire subject has been reviewed recently by Kienle [11], who, in collaboration with Brix, Hüfner and Quitmann laid the foundation for much of the precise calibrations

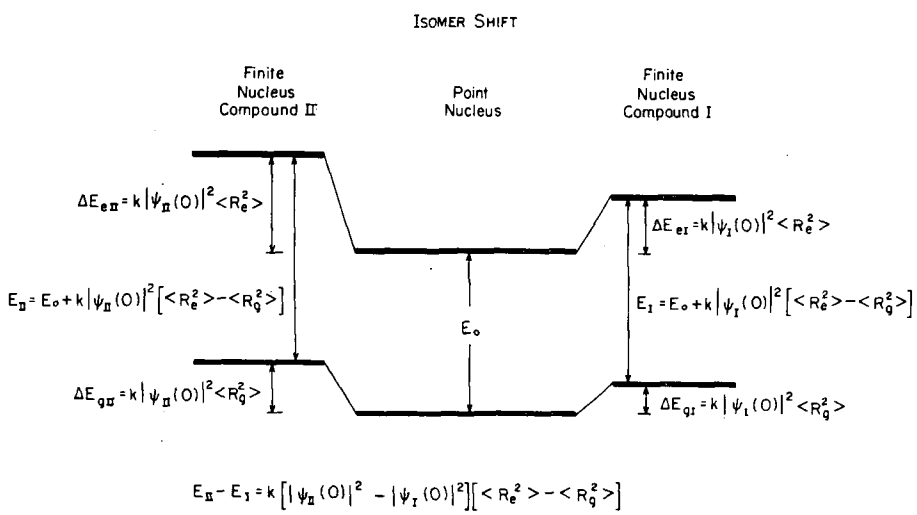

FIG. 1. Schematic representation of the isomer energy shifts due to the interaction of the atomic electrons with the nucleus of finite size.

in this field [6]. In the present paper we will discuss selected points with reference to the Mössbauer experiments on deformed nuclei. Much of the data is collated in Table IA (Even-Even Nuclei) and IB (Odd-A Nuclei).

The second portion of this paper will be concerned with the nuclear energy shift data observed in the presence of the muon following μ-meson capture. This effect, first observed in 1966 by Bernow et al. [7] following an idea of Devons [8], has now been investigated with great care in a number of deformed nuclei by Wu [9] and collaborators. A main contribution to the energy shift is due to the change in nuclear radius. There are, however, additional contributions to the observed energy shift, one of which arises from the hyperfine interaction and can be fairly reliably calculated, while others, arising from polarization effects, can at best be estimated.

As we shall see, the values obtained through Mössbauer investigations are in reasonable accord with μ-mesic results. Moreover, all results are consistent with the interpretation that in even-even nuclei, from ^{152}Sm to ^{182}W, $\langle R_e^2 \rangle$ is greater than $\langle R_g^2 \rangle$.

The final section discusses the implications of these results for the theory of nuclear structure. It is shown that so far there is no theoretical calculation which fits the experimental results in a systematic way; most calculations predict $\Delta\langle R^2 \rangle$ values which are several times greater than observed. Furthermore the theoretical predictions available at this time do not explain the trend of $\Delta\langle R^2 \rangle$ towards negative values in the W–Os region.

MÖSSBAUER ISOMER SHIFT

The methodology and technology of the Mössbauer effect is too well-known to need repetition here. Moreover the search for small line shifts has long been one of the most stimulating of investigations. One only need cite the investigation of the gravitational red shift [10] where a line shift of a few per cent of the line width was measured to an uncertainty of a few per cent. The ^{57}Fe study however involved a Mössbauer absorption effect greater than 50% while the transitions of interest here yield Mössbauer effects of 1% or less. The search for small line shifts under the latter conditions is made even more difficult if, as is generally the case, one must work at liquid helium temperatures where relaxation effects are pronounced, where one investigates a rare earth whose compounds are often magnetic and where nuclei have large quadrupole moments. For these reasons the following experimental points appear pertinent.

(1) It is important that the empirical line be free from hyperfine interactions. Ideally one desires a single line of natural line width in both the source and the absorber, yet with a finite and calculable difference in the values of $|\Psi(0)|^2$. These conditions are almost never attained in practice so that one must accept the possibilities of pseudo-isomer shifts arising from polarization effects, relaxation effects, crystal anisotropies, etc., as well as the practical difficulties of measuring centres of gravity in the presence of weak lines of uncertain width and position.

(2) To obviate questions of uncertain electronic environments in the radioactive sources, which in most cases involve a transmutation process,

TABLE I. MÖSSBAUER ISOMER SHIFTS OF ROTATION BAND TRANSITIONS

Isotope	E_0 (keV)	Spins	Cmpd I	Cmpd II	Δv (mm/sec)	$\Delta\langle R^2\rangle/\langle R^2\rangle \times 10^4$	$\Delta\langle R^2\rangle/\langle R^2\rangle \times 10^4$ (Ref. [43])	Ref. to Exp.
A. Even-Even Nuclei								
^{152}Sm	122	$2^+ - 0^+$	Eu in CaF_2	Sm_2O_3	1.65(15)	3.7	19.7	[24]
			Eu in CaF_2	Sm_2O_3	1.65(9)	3.7	19.7	[25]
			Gd_2O_3	$SmCl_2$	1.60(10)	3.7	19.7	[26]
^{154}Gd	123	$2^+ - 0^+$	Eu in CaF_2	Gd_2O_3	0.16(7)	---	8.8	[22]
			EuF_3	$GdFe_2$	0.92(26)	3.90		[50]
^{156}Gd	89	$2^+ - 0^+$	Sm_2O_3	metal	0.26(9)	0.84	1.5	[22]
			$Sm_{05}Al_{95}$	metal	0.16(3)	0.64		[23]
^{170}Yb	84	$2^+ - 0^+$	$TmAl_2$	YbOOH	0.12(3)	0.42	1.26	[48]
			$YbAl_2$	$YbSO_4$	0.39(7)	1.2		[51]
^{182}W	100	$2^+ - 0^+$	W	WCl_{5-6}	0.21(2)	---	2.45	[4]
			W	$Na_2WO_4 \cdot 2H_2O$	0.156(8)	---		[50]
			W	$Na_2WO_4 \cdot 2H_2O$	-0.0479(177)	---	2.88	[50]
B. Odd-A Nuclei								
^{153}Eu	83.4	7/2 - 5/2	Eu_2O_3	EuB_6	-0.37(8)	-1.1(3)		[15]
			Eu_2O_3	$EuSO_4$	-0.80(20)	-2.6(6)		[16]
			Eu_2O_3	$EuSO_4$	-0.21(6)	-0.68(11)		[17]
^{169}Tm	8.42	3/2 - 1/2	Tm	TmES	-1.18(13)	-0.09		[47,11]
^{171}Yb	66.7	3/2 - 1/2	ErAl	Yb_2O_3	0.23(2)	0.45		[48,11]

one tries to compare the shift observed between two quiescent absorbers [4] rather than between source and absorber. Kienle and co-workers [11] have developed a method using three sources on a single drive rod to diminish instrumental effects.

(3) Temperature dependent energy shifts [12, 13] must be considered in special cases though such shifts are quite small at the low temperatures needed for most Mössbauer transitions of interest.

(4) One method of checking the overall consistency of the experimental results is to compare the isomer shift, for different transitions in the same element, for different absorber combinations. The ratio of isomer shifts should be unchanged on changing the absorber [14]. Kienle and co-workers [11] have applied this technique extensively in order to establish a reliability judgement on the data.

Some of the problems are illustrated by the following examples.

The isomer shift results for ^{182}W in Ta metal versus a tungsten absorber and versus a WCl_6 absorber [4] have eluded successful repetition, possibly because of the unstable nature of WCl_6. It seems likely that the successful compound was a mixture of chlorides. In this first experiment the qualitative rather than the quantitative aspects were most relevant since, as stressed by Cohen et al. [4], the electronic factors were not known anyway to be better than a factor of two, if that.

The fluctuations which can occur in measuring small shifts are illustrated by the isomer shift investigations of the 83.4 keV ($7/2^+ \rightarrow 5/2^+$) rotational transition in ^{153}Eu. Schnidman et al. [15] used a Coulomb excited source to compare the shifts between two quiescent absorbers. Ansaldo et al. [16], Atzmony et al. [17] and Kienle et al. [18] used radioactive ^{153}Sm as a source. Some results of the Ansaldo work are shown in Figs 2-4. Figure 2 shows the gamma-ray spectrum from the source; the inset presents the pertinent nuclear levels. Two of the levels fed from ^{153}Sm show a Mössbauer effect. The velocity spectra obtained with oxide sources and absorbers for the 103 keV and 83 keV levels are exhibited in Fig. 3. Each is centered at zero relative velocity. When the absorber compound was changed to the $EuSO_4$ the results were dramatically different as shown in Fig. 4. The 103 keV line shows the well-known large shift [6, 19, 20] of 17 mm/sec, produced as a result of the substantial difference in the nuclear radii of these different intrinsic states, the 103 keV state having the smaller radius. The shift of the 83 keV state is more than an order of magnitude smaller but in the same direction as the shift observed for the 103 keV transition. The mean radius of the 83 keV state is therefore smaller than that of the ground state. On this point all groups agree. There is, however, no agreement at this time as to the magnitude of the effect; Refs [15-18] report shifts of Eu_2O_3 relative to $EuSO_4$ of 0.40 ± 0.10, 0.80 ± 0.15, 0.22 ± 0.07, and 0.65 ± 0.22 mm/sec respectively. The cleanest of the experiments is probably that of Schnidman et al. [15] who observe a 2% absorption effect, though probably the safest statement is that computer fits to data do not necessarily yield the true value or errors in the experiment.

Another illuminating example is the investigations of the isomer shift [21-23] of the 89 keV, $2^+ \rightarrow 0^+$, transition in ^{156}Gd. Measurable and interpretable isomer shifts have been observed between the trivalent Gd compounds and the Gd metal, but unfortunately Gd metal has a significant

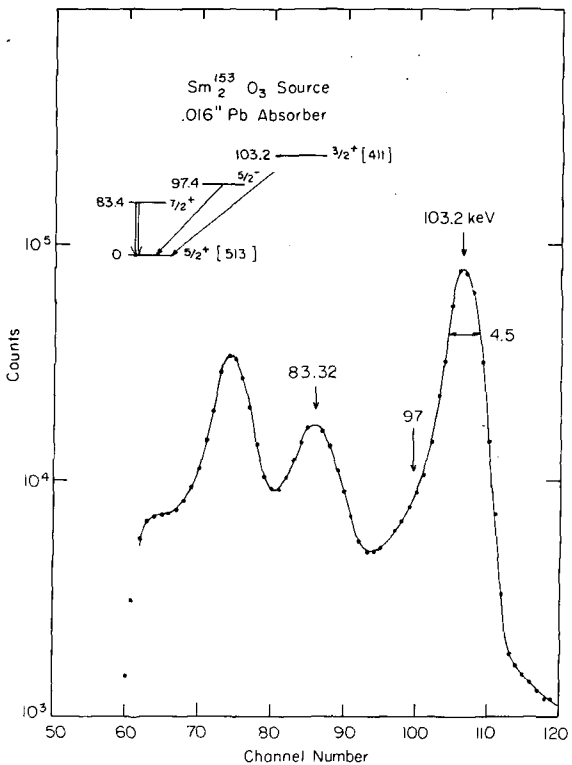

FIG.2. Gamma ray spectrum of ^{153}Sm observed with a Pb critical absorber. The inset diagram shows the pertinent Mössbauer levels in ^{153}Eu. Figure taken from Ref. [16].

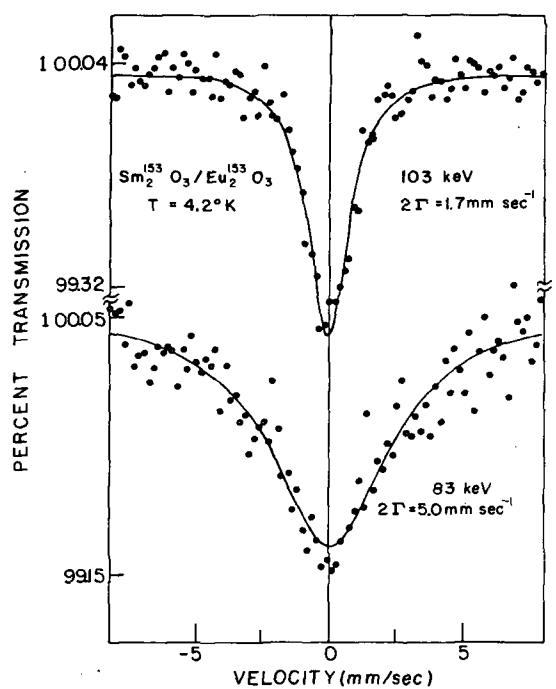

FIG.3. Mössbauer absorption spectra for the 83.4 and 103 keV transitions of ^{153}Eu using similar sourceabsorber compounds. Figure taken from Ref. [16].

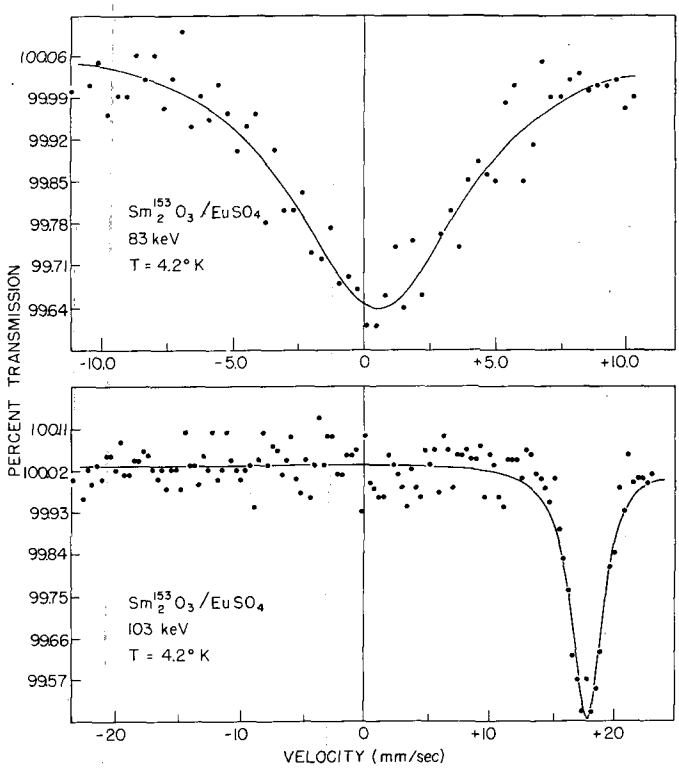

FIG.4. Mössbauer absorption spectra for the 83.4 and 103 keV transitions of ^{153}Eu using a trivalent Eu source and a divalent Eu absorber. Note that the isomer shift of the 83 keV line is the same direction as is the isomer shift of the 103 keV line. Figure taken from Ref. [16].

magnetic hyperfine interaction and is not cubic, so that the quadrupole interaction can lead to spurious energy shifts.

Typical spectra are shown in Fig. 5 for two different absorbers. (Note the change in velocity scale.) Experimentalists agree reasonably well on the apparent value of the Doppler shift. Nevertheless, the empirical line width Fig. 5a is about six times the natural line width and under these circumstances it is the author's opinion that the shift should be considered more as a limit than as a definitive number.

As a final example we consider the important case of the 122 keV ($2^+ - 0^+$) transition in ^{152}Sm. The isomer shift results of Yeboah-Amankwah [24] are shown in Fig. 6. The unambiguous energy shift, 0.165 ± 0.015 cm/sec, has been confirmed within a few per cent by Steiner et al. [25] and by Atzmony et al. [26]. Despite this agreement there is considerable disagreement in the values of $|\Psi(0)|^2 = \rho(0)$ necessary to evaluate $\Delta\langle R^2\rangle/\langle R^2\rangle$ (Eq.(1)). The essentials of the argument are sketched below.

The effect of $\rho(0)$ due to the difference between a $4f^5$ and a $4f^6$ configuration is indirect, arising mainly from the change in the shielding of the closed shell s electrons. There are two interrelated ways of determining the relevant different $[\rho(0)(4f^5) - \rho(0)(4f^6)]$. One is via the

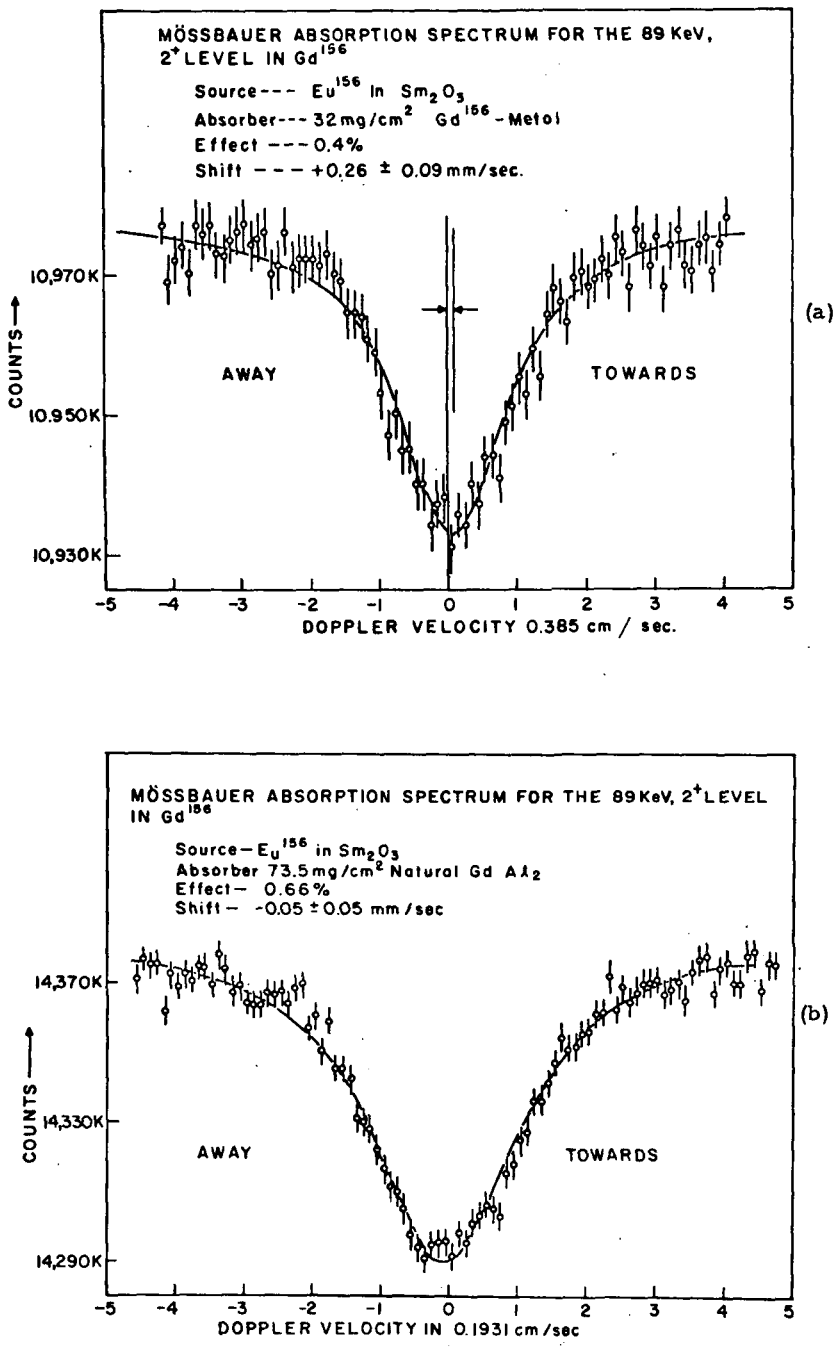

FIG. 5. Mössbauer spectra observed for the 89 keV transition of ^{156}Gd. Note the different velocity scales. Figure taken from Ref. [21].

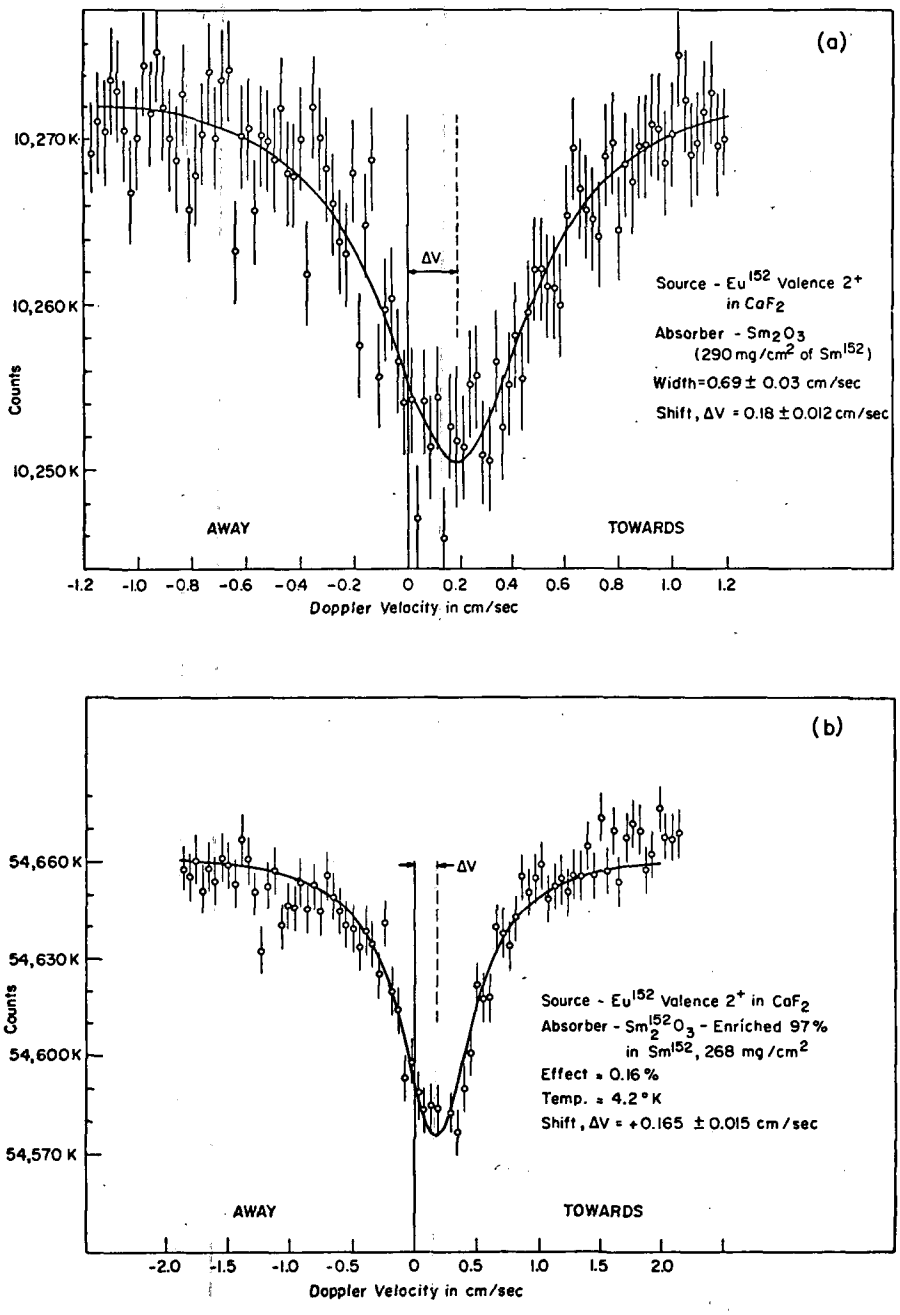

FIG. 6. (a) Mössbauer absorption resonance in the 122 keV, $2^+ \rightarrow 0^+$ transition in ^{152}Sm, for a ^{152}Eu 2^+ source in CaF_2 and a $^{152}Sm_2O_3$ absorber. (b) Same as (a), but covering a wider velocity range. Figure taken from Ref. [24].

hyperfine interaction; the other through the isotope shift. In the Yeboah-Amankwah [24] work, both approaches were presented since they yielded results which differed by a factor of two.

The resolution of the difference [56] lies in taking account of the specific mass effects in the isotope shift data. As Hüfner et al. [20] have shown, based on the method of King [27], the isotope shift data in Sm of Striganov et al. [28] can be interpreted as containing a mass contribution of about 50%. If one accepts this interpretation, which requires that a specific mass term be invoked which is an order of magnitude larger than the Bohr mass term, then one finds that

$$\left.\frac{\Delta\langle R^2\rangle}{\langle R^2\rangle}\right|_{^{152}\mathrm{Sm}} = 7.3 \times 10^{-4}$$

There is now strong additional evidence that such an effect exists. Wu [29] has shown that if one plots the values of the electronic isotope shift versus the corresponding values obtained from μ-mesic work then the resultant straight line does not intercept the origin but gives strong evidence for a volume-independent term of about 50% of the observed isotope effect. We therefore assume the calibration of Brix et al. [6] for analysis of the data.

There is still another uncertainty. The interpretations above are based on free atom data, and isomer shift experiments in solids [30] indicate that one should increase the free atom values of $\rho(0)$ by a factor of two for applications to solids.

Thus though all investigators agree on the experimental Mössbauer Doppler shifts in ^{152}Sm there is a wide divergence on the final value of $\Delta\langle R^2\rangle/\langle R^2\rangle$. The two values for ^{152}Sm given in Fig. 10 are based on the isotope shift and the hyperfine interpretations assuming in both cases the above compression factor of two. The other rare earth results in Fig. 10 are based on the Kienle [6, 11, 20] choice of calibration. No error is assigned to the crudely known tungsten result.

We turn now to μ-mesic experiments which give one hope that many of the above difficulties may be circumvented.

ISOMER SHIFTS IN THE PRESENCE OF THE MUON[1]

Wilets [31] and Jacobsen [32] showed some years ago that the muonic transitions in an atom can lead to excitation of the nucleus levels, especially low-lying states of large quadrupole moments. In 1960, Devons [8] pointed out that the presence of the muon in the $1s_{1/2}$ state could affect the energy of the excited nucleus in observable ways. At his suggestion in 1963, Wilets and Chinn [33] calculated the polarization effects of the muon arising from the nuclear compression in the muon-nuclear potential of the muon. A similar and independent calculation was performed at this time by Hüfner [34]. To observe the small effect predicted one should look directly at the nuclear de-excitation rather than the muonic X-ray and this the Columbia group did in an elegant experiment [7] on the $2^+ \rightarrow 0^+$ transition in ^{152}Sm. An energy shift of the transition

[1] This section is based on work done with A. Gal and J. Hüfner.

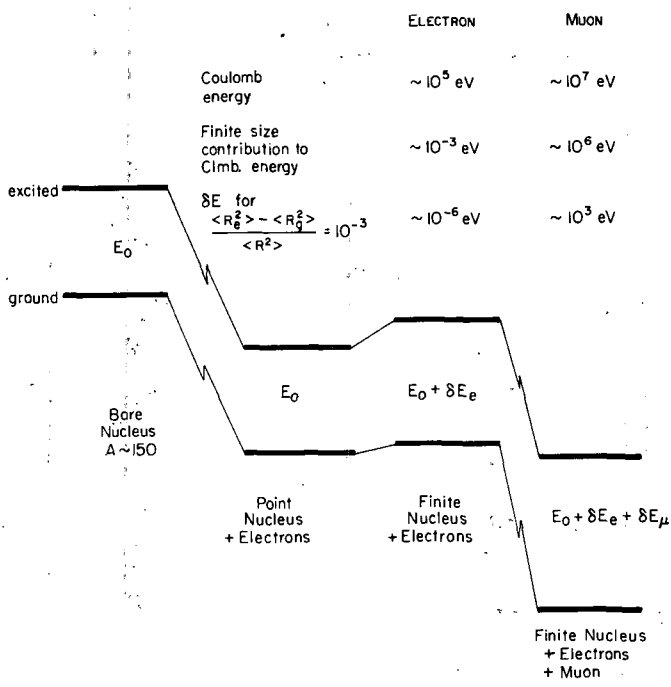

FIG. 7. Schematic representation of the energy shift of the nuclear transition under the influence of the atomic electrons and the muon.

of the order of 1 keV was observed by comparison with the same transition from a radioactive source of ^{152}Eu. The latest data on this transition are shown in Fig. 8.

It was realized however that the effect of the change of nuclear radius on the transition energy would be a significant contribution to the energy shift and indeed Telegdi [57] showed that the polarization effect suggested by Devons was zero due to the similarity of the rotational band members. The observed energy shift was then interpreted as arising wholly from a change in radius. And this agreement between the result for $\Delta\langle R^2\rangle/\langle R^2\rangle$ from Mössbauer [24] and muonic experiments [7] on ^{152}Sm was gratifying and gave confidence in the explanation.

The nuclear energy shifts arising from the Coulomb interaction of the electrons and the muon with the finite nucleus are shown schematically in Fig. 7. Muonic investigations of the nuclear isomer shift have significant advantages over Mössbauer experiments. The low-lying rotational states are readily excited by the muon. The isomer shift is measured directly in terms of the energy of the state in the absence of the muon. The calculation of the $\rho(0)$ factor enters into other muonic phenomena such as μ-capture and can be calculated reliably from the finite size effect. These advantages, coupled with the importance of the results for the theory of nuclear structure, led to a concentrated attack on isomer shift investigations both by the Columbia and CERN-Darmstadt groups.

The first experiments of the Columbia group, following their ^{152}Sm work, were to the study of the $2^+ \rightarrow 0^+$ transitions of ^{182,184,186}W. They

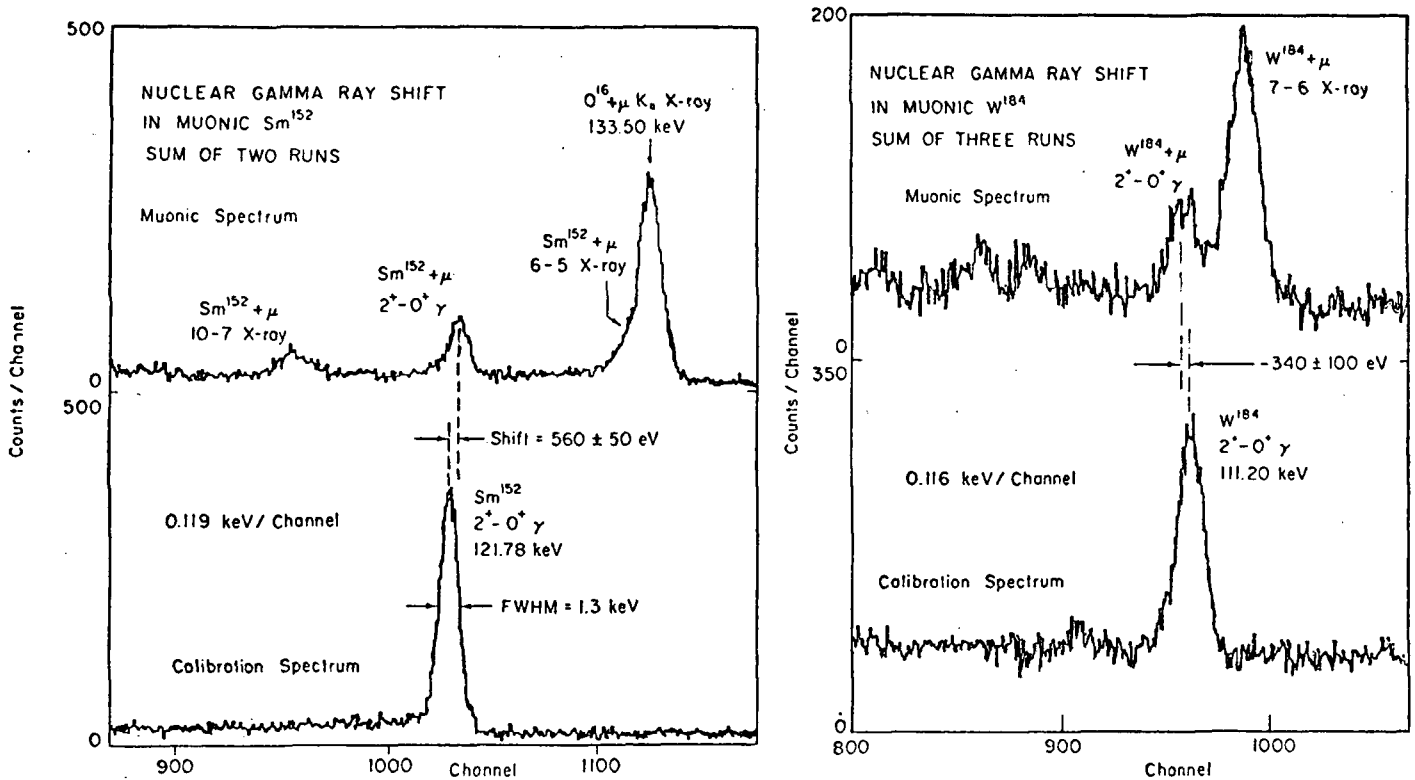

FIG. 8. Muonic energy spectra for ^{152}Sm and ^{184}W displaying the nuclear de-excitation in the presence of the muon. Lower spectra are obtained concurrently using appropriate radioactive source. Figure taken from Ref. [38].

immediately encountered the startling observation (Fig. 8) that the energy of the $2^+ - 0^+$ transition in ^{182}W was smaller in the presence than in the absence of the muon [9], implying that $\langle R_e^2 \rangle$ was less than $\langle R_g^2 \rangle$, a result hard to understand for a good rotor such as ^{182}W.

These negative shifts have been shown by Gal, Hüfner and Grodzins [35] to result principally from asymmetries in the observed hyperfine spectra. Polarization contributions cannot be excluded, however, and may yet turn out to be significant. The following remarks on the hyperfine asymmetries are based on Ref. [35].

The isomer shift between two nuclear states Ψ_α and Ψ_β is defined as the energy difference.

$$\Delta E^{ISOMER}_{\alpha,\beta} = \left\langle \Psi_\alpha,\ 1s_{\frac{1}{2}} \middle| H^C \middle| \Psi_\alpha,\ 1s_{\frac{1}{2}} \right\rangle - \left\langle \Psi_\beta,\ 1s_{\frac{1}{2}} \middle| H^C \middle| \Psi_\beta,\ 1s_{\frac{1}{2}} \right\rangle \qquad (2)$$

where $1s_{1/2}$ denotes the spectator muon, and H^C is the appropriate Coulomb interaction.

For precise comparison with experiment one must solve Eq. (2) exactly for different nuclear potentials. It is useful however to cast it in a form analogous to Eq. (1) by applying the Ehrlich et al. [36] prescription for obtaining $|\Psi(0)|^2$ values from the μ-capture calculations of Ford and Wills [37]. Thus one replaces

$$\left|\Psi(0)\right|^2 = Z_{eff}^4/Z \ \frac{1}{\pi a_{o\mu}^3} \qquad (3)$$

where Z_{eff} is tabulated in Ref. [37], and $a_{o\mu}$ is the muon Bohr radius. One then obtains

$$\Delta E^{ISOMER} = 6.0 \times 10^{-2}\ A^{2/3}\ Z_{eff}^4\ \frac{\left[\langle R_e^2 \rangle - \langle R_g^2 \rangle\right]}{\langle R^2 \rangle} \quad \text{e V} \qquad (4)$$

The constant has been arbitrarily normalized upwards by a factor of 1.2 from the value of Eq. (3) in order that ΔE^{ISOMER} agree with more precise calculations [38].

Each nuclear state Ψ_α with spin $I_\alpha \neq 0$ also exhibits a hyperfine splitting which originates from the interaction of the nucleus with the magnetic moment of the 1s-muon. The splitting is given in first order by

$$\Delta E^M_\alpha = \left\langle \Psi_\alpha,\ 1s_{\frac{1}{2}};\ F = I_\alpha + \tfrac{1}{2} \middle| H^M \middle| \Psi_\alpha,\ 1s_{\frac{1}{2}};\ F = I_\alpha + \tfrac{1}{2} \right\rangle - \left\langle \Psi_\alpha,\ 1s_{\frac{1}{2}};\ F = I_\alpha - \tfrac{1}{2} \middle| H^M \middle| \Psi_\alpha,\ 1s_{\frac{1}{2}};\ F = I_\alpha - \tfrac{1}{2} \right\rangle \qquad (5)$$

Again we can use the above prescription to cast Eq.(5) into the useful form.

$$\Delta E^M = 2.5 \times 10^{-2} \mu_I \frac{2I+1}{I} \frac{Z_{eff}^4}{Z} \quad eV \qquad (6)$$

The numerical constant has been normalized to the value of ΔE^M for the ground state of ^{209}Bi [36] and we have assumed that the average of $\rho(0)$ is the same for the magnetic as for the electronic form factors.

The muon hyperfine interaction is illustrated in Fig. 9 for the case of an even-even nucleus. If the F = 5/2 and F = 3/2 levels are fed statistically, and if the inter-doublet transition shown in Fig. 9 can be neglected then one would observe a doublet c and b (resolved or not) with centre of gravity at E_0 and a splitting given by Eq.(6). (The magnetic splitting for several first 2^+ states is given in Table II, column 2. The nuclear g-factors have been taken from references cited therein.) However, neither of the two assumptions is even approximately correct for the cases of interest. We take them up in turn.

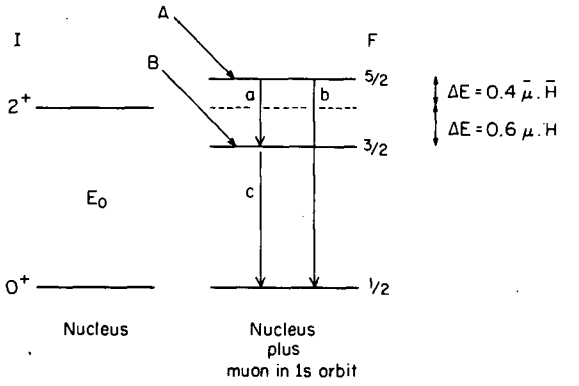

FIG. 9. Schematic representation of hyperfine interaction of $1s_{1/2}$ muon with an even-even nucleus in the 2^+ state.

The components of the hyperfine doublet built on the nuclear rotational state are not populated statistically, i.e. proportionally to (2F+1). Their feeding depends on the mechanism by which these rotational states are excited and varies from one nucleus to another. While each case must be treated separately, as was done for the values in column 3, the following limits may be useful.

If the $p_{3/2}$-$p_{1/2}$ muonic fine splitting is much less than the $2^+ \rightarrow 0^+$ transition energy, then the feeding $R = [1(F5/2)/1(F3/2)] \simeq 4$. ^{152}Sm approximates this situation: R = 5. When the converse is true, e.g. for ^{238}U, then R = 1/4.

A more dominant factor is the effect of the M1 hyperfine transition which depopulates the upper state. (A similar effect of the strong inter-doublet transition has been shown to be important for μ^- capture by Winston and Telegdi [39].)

The M1, spin flip transition probability is given by $\Gamma(M1) = \Gamma_\gamma(M1)[1+\alpha(M1)]$. The values $\Gamma_\gamma(M1)$ are calculated from

$$\Gamma_\gamma(M1) = 3/2(2F_f + 1)\begin{Bmatrix} F_j & F_f & 1 \\ 1/2 & 1/2 & J_c \end{Bmatrix}^2 \alpha_1 \Delta E_M^3 (g_c - g_\mu)^2 \qquad (7)$$

where J_c is the nuclear (core) spin, $F_{j,f}$ are the initial and final spin values of the doublet, ΔE_M is in keV, $g_{c,\mu}$ are in units of nuclear magnetons, and $\alpha_1 = 4.2 \times 10^3$ keV^{-3} sec^{-1}. For the doublet built on the 2^+ level, Eq.(10) takes on the simple form

$$\Gamma_\gamma(M1) = 5.35 \times 10^5 \ \Delta E_M^3 \ \text{sec}^{-1} \qquad (8)$$

where the small contribution of g_c has been neglected.

The calculation of $\alpha(M1)$ for the 400 to 800 eV transitions contains the major uncertainty in evaluating the relative transition probabilities. Estimates of N_I and O_I shell coefficients for a transition in element Z were obtained by extrapolating the low energy K, L, and M shell values for Z - 1 calculated recently by Hager and Seltzer [40, 41]. The resulting internal conversion coefficients are given in column 5 of Table II. The estimated values have been confirmed to within 20% by the recent calculations of Pauli [42] of N_I and O_I internal conversion coefficients based on self-consistent solutions of the electron wave-functions.

There are, however, further sources of ambiguity. The values of ΔE^M are close to the values of the N_I threshold energies so that effects of the nuclear magnetic form factor, which can produce 10% changes in ΔE^M, and the changes in the electron binding energies due to the presence of the muon and to the atomic environment, assume an amplified importance, particularly for the states in tungsten. (Of course, these difficulties become advantages when the effects themselves are to be studied.)

The branching ratio b : a (Fig. 9) is then readily calculated using the known lifetimes of the nuclear states. Values are given in column 6, Table II.

The intensities of the observed transitions from the doublet to the ground states

$$I\left(\frac{F_f - g_r}{F_j - g_r}\right) = \frac{a}{b} + R_F\ (3/2 : 5/2)\ \left(\frac{a}{b} + 1\right) \qquad (9)$$

are given in column 7, Table II.

The calculated centre-of-gravity shift of the hyperfine doublet, given in column 8, Table II, is of the order of the reported energy shifts, column 9.

After correcting for the hyperfine centre-of-gravity shift, the positive energy shift observed in ^{152}Sm is seen to increase, leading to values of

TABLE II. HYPERFINE CENTRE-OF-GRAVITY SHIFT FOR E2 TRANSITIONS IN SEVERAL EVEN-EVEN DEFORMED NUCLEI

Isotope 2^+ Energy (keV)	ΔE^M (eV)	Feeding $R_F \frac{3}{2}:\frac{5}{2}$	Electron binding energy[f] (eV)	M1-Int. conv. coeff. $\times 10^{-4}$	Branch. ratio $R_T \frac{M1}{E2}$	$I\frac{3}{2}\rightarrow$g.s.) / $I\frac{5}{2}\rightarrow$g.s.)	Cent.-of-grav. shift (eV)	Experimental shifts (eV)
^{152}Sm	740[a]	0.18	333(N_I)	1.7	7	8.5	-360	+560 ± 50[g]
(122)	490[b]			5.4	7	8.5	-240	
^{166}Er	570[c]	0.54	435(N_I)	6	15	24	-320	-350 ± 100[h]
(81)								
^{170}Yb	615[d]	0.55	471(N_I)	6	16	26	-350	
(84)								
^{182}W	495[e]	0.48	565(N_I)	24	30	45	-290	-320 ± 100[h]
(100)			71(O_I)	4	5	8	-240	
^{184}W	550[e]	0.38	565(N_I)	16	24	34	-315	-340 ± 100[h]
(111)			71(O_I)	3	5	7	-250	
^{186}W	580[e]	0.31	565(N_I)	13	20	25	-340	-360 ± 100[h]
(122)			71(O_I)	2.5	4	5	-250	

a) Using $g_{2+}(^{152}\mathrm{Sm}) = 0.416 \pm 0.025$: ATZMONY, U., BAUMINGER, E.R., FROINDLICH, D., OFER, S., Phys. Lett. 26B (1968) 81.

b) Using $g_{2+}(^{152}\mathrm{Sm}) = 0.277 \pm 0.028$: WOLFE, P.J., SCHARENBERG, R.P., Phys. Rev. 160 (1967) 866.

c) Using $g_{2+}(^{166}\mathrm{Er}) = 0.312 \pm 0.006$: DOBLER, H., PETRICH, G., HÜFNER, S., KIENLE, P., WIEDEMANN, W., EICHER, H., Phys. Lett. 10 (1964) 319.

d) Using $g_{2+}(^{170}\mathrm{Yb}) = 0.335 \pm 0.005$: HÜLLER, A., WIEDEMANN, W., KIENLE, P., HÜFNER, S., Phys. Lett. 15 (1965) 269.

e) Using $g_{2+}(^{182}\mathrm{W}) = 0.266 \pm 0.009$; $g_{2+}(^{184}\mathrm{W}) = 0.295 \pm 0.010$; $g_{2+}(^{186}\mathrm{W}) = 0.312 \pm 0.011$: PERSSON, B., BLUMBERG, H., AGRESTI, D., Hyperfine Structure and Nuclear Radiations (MATTHIAS, E., SHIRLEY, D.A., Eds) North-Holland, Amsterdam (1968) 268.

f) Taken from HAGSTRÖM, S., NORDLING, C., SIEGBAHN, K., Alpha-, Beta-, and Gamma-Ray Spectroscopy (SIEGBAHN, K., Ed.) North-Holland, Amsterdam (1965) 845.

g) Ref. [7] of text.

h) BERNOW, S., DEVONS, S., DUERDOTH, I., HITLIN, D., KAST, J.W., LEE, P.W.Y., MACAGNO, E.R., RAINWATER, J., WU, C.S., Bull. Am. phys. Soc. 13 (1968) 678.

TABLE III. ISOMER SHIFT DATA

Isotope	$2^+ \rightarrow 0^+$ Energy (keV)	Exp. energy shift ΔE_{obs} (eV) Ref. [38]	Centre-of-gravity shift $\Delta E_{c.g.}$ (eV) (Table II)	ΔE_{isomer} (eV)	$\frac{\Delta\langle r^2\rangle}{\langle r^2\rangle} \times 10^4$	$\frac{\Delta\langle R^2\rangle}{\langle R^2\rangle} \times 10^4$	$\frac{\Delta\langle r^2\rangle}{\langle r^2\rangle} \times 10^4$
					Muonic	Mössbauer	Marshalek [55]
$^{150}_{60}Nd$	130.17	+570 ± 120	-270	+840 ± 120	+5.8 ± 0.8	No measurement	
$^{152}_{62}Sm$	121.78	+560 ± 60	-360 -240	+920 ± 70 +800 ± 70	+5.9 ± 0.4 +5.1 ± 0.4	+3.7	19.7
$^{154}_{64}Gd$	123.07	+670 ± 150	-310	+980 ± 150	+5.9 ± 0.8	No measurement	8.8
$^{166}_{66}Er$	80.56	-350 ± 150	-320	- 30 ± 150	-0.16 ± 0.8	No measurement	0.51
$^{182}_{74}W$	100.10	-320 ± 100	-290 -240	- 30 ± 100 - 80 ± 100	-0.13 ± 0.5 -0.33 ± 0.5	(+0.15) (+1.2)	2.45
$^{184}_{74}W$	111.20	-340 ± 100	-315 -250	- 25 ± 100 - 90 ± 100	-0.11 ± 0.5 -0.40 ± 0.5		2.88
$^{186}_{74}W$	122.57	-350 ± 100	-340 -250	- 10 ± 100 -100 ± 100	-0.04 ± 0.5 -0.50 ± 0.5		5.5

$\Delta\langle r^2\rangle$ in closer agreement with Mössbauer results. The negative energy shifts (which imply that the excited state radius is smaller than that of the ground state) become smaller and may reverse sign.

The situation in odd-A nuclei is more complex since magnetic splitting occurs in both the ground and excited nuclear states. For example in the μ-mesic isomer shift study of ^{181}Ta this splitting was taken into account [43] and shown to lead to an apparent energy shift of 25 eV. It was assumed that the feeding, R_F, was statistical and that the spin-flip inter-doublet transition probability is negligible. Neither assumption is valid in this case, yet neither phenomenon measurably affects the apparent shift of 25 eV.

The isomer shift data of Bernow et al. [38] are summarized in Table III. The only meaningful comparison between muonic and Mössbauer results for the same state is for ^{152}Sm and here the difference is on the edge of the stated errors. Polarization effects can produce energy shifts and splittings of the nuclear levels in a muonic atom through second-order effects of the term $H^C + H^M$. Certain specific polarization contributions have been estimated and shown to be small [35, 44-46] but some polarization effects have not yet been evaluated. It remains to be seen whether such effects will be significant contributions.

The muonic and Mössbauer results of $\Delta\langle R^2\rangle/\langle R^2\rangle$ for $2^+ \rightarrow 0^+$ transitions in even-even nuclei are plotted in Fig.10. Keeping in mind the uncertainties which still plague the results one has the impression that both methods are giving positive values of $\Delta\langle R^2\rangle/\langle R^2\rangle$ in fair agreement with each other.

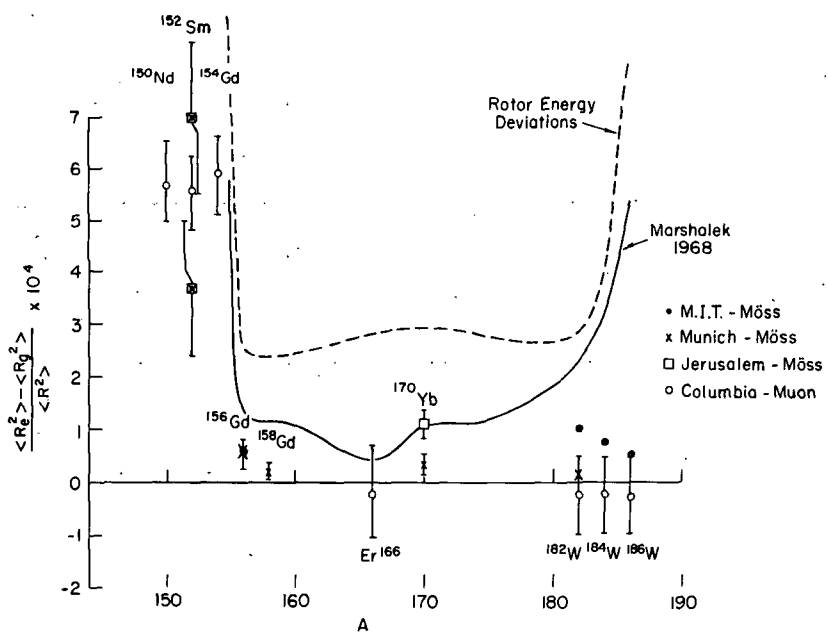

FIG.10. Summary of $\Delta\langle R^2\rangle/\langle R^2\rangle$ data for even-even rotational transitions. The two Mössbauer points for ^{152}Sm result from two possible methods of calculating $\Delta|\psi(0)|^2$; the lower value should be taken as being most correct (see text). The open-circle points are taken from Ref. [38]. The solid and dashed curves are theoretical predictions (see text).

(Note added: Many of the muonic results of the Columbia group have recently been repeated and extended by the Darmstadt-CERN collaboration of H. Backe et al. [58]. Their results and interpretation for ^{152}Sm, ^{182,184,186}W are similar to those present here and in Ref. [35] and [38]. Their results for the even-even osmium isotopes indicate that $\langle r_e^2 \rangle$ is smaller than $\langle r_g^2 \rangle$. Magnetic effects do not change this conclusion. It should be emphasized, however, that polarization effects have not been included in the analysis. And it is just in this region that one expects polarization to be significant since osmium nuclei are "soft" and presumably more readily polarized than in the other cases.)

DISCUSSION

The isomer shift of rotational transitions in odd-A nuclei have been investigated in ^{153}Eu [15-18], ^{169}Tm [47], ^{171}Yb [11,48], ^{181}Ta [43], and ^{183}W [11]. $[\langle R_{ex}^2 \rangle - \langle R_{gr}^2 \rangle]$ is positive in the last three cases but negative in the first two. Negative values are readily rationalized [16,17,47] by invoking coriolis coupling between intrinsic bands [49]. However, since the observed change in nuclear radius is the sum of several terms in addition to such mixing, it is not clear how quantitative any explanation of $\Delta\langle R^2 \rangle$ values can be at this time. We therefore by-pass these questions to discuss the case of even-even rotors where coriolis mixing may be expected to be negligible.

Isomer shift measurements in even-even nuclei are now available at the beginning [22, 24-26, 38], middle [38, 48, 51] and end of the deformed region. The phenomenological description of the energy of rotational states,

$$E = AI(I + 1) + BI^2(I + 1)^2 + \ldots . \qquad (10)$$

can be used to relate the relative change of nuclear deformation $\Delta\beta/\beta$, to deviations of the ground state rotational band energies from that of a pure rotor. If one assumes an incompressible, axially symmetric nucleus with moment of inertia proportional to β^2 then

$$\Delta\beta/\beta = -I(I + 1)\, B/A \qquad (11)$$

The values of $\Delta\langle R^2 \rangle/\langle R^2 \rangle$ derived from Eq.(11) are shown in Fig.10 by a dashed line. The predicted values are uniformly much higher than the experimental values and indicate that deviations from the rotor energies are not primarily the result of centrifugal stretching.

One can carry the above argument a step further by considering the specific rotational-vibration contribution of the mixing of the β-band with the ground state; the contribution of the γ-band is negligible. One can estimate the contribution of the β-band mixing to $\Delta\langle R^2 \rangle/\langle R^2 \rangle$ in a nearly model-independent way obtaining [24]

$$\frac{\Delta\langle R^2 \rangle}{\langle R^2 \rangle} = \frac{10}{3}\, \epsilon I(I + 1)\rho/Z \qquad (12)$$

where ϵ is the β band mixing parameter and

$$\rho = \left\langle I_{gr} \left| \left(\sum_p \frac{r_p^2}{R^2} \right) \right| I_\beta \right\rangle$$

defined by Church and Weneser [52]. (An error of 5/3 in Ref. [24] has been corrected in Eq. (12)).

The parameters ϵ and ρ are known [53] for ^{152}Sm (and ^{154}Eu), though with large errors. Using the best available numbers one finds $\Delta\langle R^2\rangle/\langle R^2\rangle \approx (2 \text{ to } 5) \times 10^{-4}$ for ^{152}Sm; i.e. about the measured value. Thus β-band mixing, which does not account for the deviations of the energy levels from that of a pure rotor, may account for the radius change. We emphasize however that the values of ϵ and ρ are not yet well fixed.

Finally, there have been microscopic, and basically not dissimilar, calculations of $\Delta\beta/\beta$ [54] and $\Delta\langle R^2\rangle/\langle R^2\rangle$ directly [55]. Marshalek's calculations [55] are extensive and detailed, exposing the contributions from centrifugal stretching and coriolis anti-pairing. His results are given in Tables I and III and plotted in Fig. 10. Again one sees that theory predicts larger values than observed, the disagreement being worse at the ends of the rotational band.

Whether the persistent discrepancy between experiment and theory augurs the importance of a new effect or is simply the consequence of inadequacies in the calculation is unclear. In either case further experimental work is called for.

One may hope to test for polarization terms in muonic isomer shift investigations by comparing several such shifts in a given element with the corresponding Mössbauer isomer shifts.

Another open question is the spin dependence of the isomer shift. The centrifugal stretching model predicts an I(I+1) dependence which might be observable in odd-A nuclei investigations.

The empirical radial changes are not even proportional to the theoretical predictions at the upper end of the rotational region. The values of $\Delta\langle R^2\rangle/\langle R^2\rangle$ for the tungsten isotopes may be crossing to negative values. Moreover, the values of ΔE for osmium isotopes, obtained by the CERN-Darmstadt collaboration, indicate negative values of $\Delta\langle R^2\rangle/\langle R^2\rangle$ (see above).

The systematics of these effects, the measurements to even greater precision, as well as the resolution of remaining discrepancies will be a central concern of experimentalists. We may also expect that other techniques, most particularly multiple Coulomb excitation with heavy ions, will join this front of investigation so that the present somewhat foggy picture will be clarified.

ACKNOWLEDGEMENTS

It is a pleasure to thank A. Gal and J. Hüfner for their assistance with the section dealing with isomer shifts in the presence of the muon, and for their generous insight generally. I would also like to thank C.S. Wu and V. L. Telegdi for many clarifying conversations, A.C. Pauli for communi-

cating his results on internal conversion coefficients, and W. Henning, P. Kienle, H. Körner and F. Wagner for communicating results on isomer shift data.

REFERENCES

[1] MELISSINOS, A.C., DAVIS, S.P., Phys. Rev. 115 (1959) 130.
[2] KISTNER, O.C., SUNYAR, A.W., Phys. Rev. Lett. 4 (1960) 412.
[3] SHIRLEY, D.A., Rev. mod. Phys. 36 (1964) 339.
[4] COHEN, S.G., BLUM, N.A., CHOW, Y.W., FRANKEL, R.B., GRODZINS, L., Phys. Rev. Lett. 16 (1966) 322.
[5] KIENLE, P., KALVIUS, G.M., RUBY, S.L., Hyperfine Structure and Nuclear Radiations (MATTHIAS, E., SHIRLEY, D., Eds) North-Holland, Amsterdam (1968) 971.
[6] BRIX, P., HÜFNER, S., KIENLE, P., QUITMANN, D., Phys. Lett. 13 (1964) 140.
[7] BERNOW, S., DEVONS, S., DUERDOTH, I., HITLIN, D., KAST, J.W., MACAGNO, E.R., RAINWATER, J., RUNGE, K., WU, C.S., Phys. Rev. Lett. 18 (1967) 787.
[8] DEVONS, S., Proc. of the Rutherford Jubilee International Conf., Manchester, 1961 (BIRKS, J., Ed.) Academic Press, New York, p.624.
[9] WU, C.S., Hyperfine Structure and Nuclear Radiations (MATTHIAS, E., SHIRLEY, D., Eds) North-Holland, Amsterdam (1968) 46.
[10] POUND, R.V., REBKA, G.A., Jr., Phys. Rev. Lett. 4 (1960) 337.
[11] KIENLE, P., Hyperfine Structure and Nuclear Radiations (MATTHIAS, E., SHIRLEY, D., Eds) North-Holland, Amsterdam (1968) 27.
[12] POUND, R.V., REBKA, G.A., Jr., Phys. Rev. Lett. 4 (1960) 274.
[13] JOSEPHSON, B.D., Phys. Rev. Lett. 4 (1960) 341.
[14] STEICHELE, E., Z. Phys. 201 (1967) 331.
[15] SCHNIDMAN, R., LEE, Y.K., WALKER, J.C., Bull. Am. phys. Soc. 12 (1967) 1065.
[16] ANSALDO, E., GRODZINS, L., FRANKEL, R.B., Bull. Am. phys. Soc. 13 (1968) 174.
[17] ATZMONY, U., BAUMINGER, E.R., FROINDLICH, D., HESS, J., OFER, S., Phys. Lett. 26B (1968) 613.
[18] KIENLE, P., HENNING, W., WAGNER, F., private communication.
[19] STEICHELE, E., HÜFNER, S., KIENLE, P., Phys. Lett. 21 (1964) 220.
[20] HÜFNER, S., KIENLE, P., QUITMANN, D., BRIX, P., Z. Phys. 187 (1965) 67.
[21] FINK, J., KIENLE, P., Phys. Lett. 17 (1965) 326.
[22] YEBOAH-AMANKWAH, D., GRODZINS, L., FRANKEL, R.B., Bull. Am. phys. Soc. 12 (1967) 580.
[23] HENNING, W., HEUNEMANN, D., KIENLE, P., KÖRNER, H.J., Hyperfine Structure and Nuclear Radiations (MATTHIAS, E., SHIRLEY, D., Eds) North-Holland, Amsterdam (1968) 256.
[24] YEBOAH-AMANKWAH, D., GRODZINS, L., FRANKEL, R.B., Phys. Rev. Lett. 18 (1967) 791.
[25] STEINER, P., GERDAU, E., KIENLE, P., KÖRNER, H.J., Phys. Lett. 24 (1967) B515.
[26] ATZMONY, U., BAUMINGER, E.R., HESS, J., OFER, S., in Hyperfine Structure and Nuclear Radiations (MATTHIAS, E., SHIRLEY, D., Eds) North-Holland, Amsterdam (1968).
[27] KING, W.H., J. opt. Soc. Am. 53 (1963) 638.
[28] STRIGANOV, A.R., KATALIN, V.A., ELISEEV, V.V., Opt. Spectry (USSR) 12 (1962) 91.
[29] WU, C.S., these Proceedings.
[30] GRABMAIER, J., HÜFNER, S., ORLICH, E., PELZL, J., Phys. Lett. 24 (1967) A580.
[31] WILETS, L., Dan. Mat. Fys. Medd. 29 3 (1954).
[32] JACOBSEN, B., Phys. Rev. 96 (1954) 1637.
[33] WILETS, L., CHINN, L., unpublished.
[34] HÜFNER, JÖRG, Nucl. Phys. 60 (1964) 427.
[35] GAL, A., GRODZINS, L., HÜFNER, JÖRG, Phys. Rev. Lett., to be published.
[36] EHRLICH, R.D., FRYBERGER, D., JENSEN, D.A., NISSIM-SABAT, C., POWERS, R.J., SHERWOOD, B.A., TELEGDI, V.L., Phys. Rev. Lett. 16 (1966) 425.
[37] FORD, K.W., WILLS, J.G., Nucl. Phys. 35 (1962) 295.
[38] BERNOW, S., DEVONS, S., DUERDOTH, I., HITLIN, D., KAST, J.W., LEE, W.Y., MACAGNO, E.R., RAINWATER, J., WU, C.S., Phys. Rev. Lett. 21 (1968) 457.
[39] WINSTON, R., TELEGDI, V.L., Phys. Rev. Lett. 7 (1961) 104. WINSTON, R., Phys. Rev. 129 (1963) 2766.
[40] HAGER, R.S., SELTZER, E.C., Internal Conversion Tables CALT-63-60 (1967).

[41] O'CONNELL, R.F., CARROLL, C.O., Internal Conversion Processes (HAMILTON, J.H., Ed.) Academic Press, New York (1966) 333.
[42] PAULI, A.C., private communication.
[43] BACKE, H., BACKENSTOSS, G., DANIEL, H., ENGFER, R., KANKELEIT, E., POELZ, G., SCHMITT, H., TAUSCHER, L., WIEN, K., submitted to Int. Conf. Hyperfine Interactions Detected by Nuclear Radiation, Asilomar, California (1967).
[44] SCHECK, F., Z. Phys. 172 (1963) 239.
[45] PIEPER, W., GREINER, W., Nucl. Phys. A109 (1968) 539.
[46] CHEN, M.Y., Ph.D. Thesis, Princeton University (1968).
[47] SCHALLER, H., KAINDL, G., WAGNER, F., KIENLE, P., Phys. Lett. 24 (1967) B397.
[48] KIENLE, P., HENNING, W., KAINDL, G., KÖRNER, A.J., SCHALLER, H., WAGNER, F., Proc. Int. Conf. Nucl. Structure, Tokyo (1967) 195.
[49] KERMAN, A.K., Mat. Fys. Medd Dansk Vid Selsk 30 15 (1956).
[50] KIENLE, P., WAGNER, F., HENNING, W., RICHTER, M., KÖRNER, H., to be published.
[51] ATZMONY, U., BAUMINGER, E.R., HESS, I., MUSTACHI, A., OFER, S., Phys. Rev. Lett. 18 (1967) 1061.
[52] CHURCH, E.L., WENESER, J., Phys. Rev. 103 (1956) 1035.
[53] YOSHIZAWA, Y., ELBEK, B., HERSKIND, B., OLESEN, M.C., Nucl. Phys. 73 (1965) 273; SEAMAN, G.G., GREENBERG, J.G., BROMLEY, D.A., McGOWAN, F.K., Phys. Rev. 149 (1966) 925.
[54] UDAGAWA, T., SHELINE, R.K., Phys. Rev. Lett. 16 (1966) 325.
[55] MARSHALEK, E.R., Phys. Rev. Lett. 20 (1968) 214.
[56] KIENLE, P., private communication.
[57] TELEGDI, V.L., private communication.
[58] BACKE, H., ENGFER, R., KANDELEIT, E., SCHRÖDER, U., WALTER, H.K., WIEN, K., to be published.

DISCUSSION

Krishna KUMAR: I would like to suggest a qualitative reason for the smallness of the measured nuclear stretching. This is due to a cancellation of two effects. The centrifugal barrier tends to increase the nuclear deformation. On the other hand, the potential energy function tends to decrease it since this function rises in most calculations more rapidly on the larger β side of the equilibrium deformation.

C.S. WU: A word of caution concerning the isomer shift from the muonic X-ray data should be mentioned here. In our calculations the difference in nuclear polarization between the 2^+ and 0^+ states has been neglected, although it has been shown by our theoretician M.Y. Chen that in the simple rotational model the nuclear polarization corrections to the 2^+ and 0^+ states are nearly identical. However, this conclusion applies only to the rotational model which, in general, is probably not expected to hold to better than a few percent. In the absence of any reliable estimates, we have neglected this possible contribution to the observed shifts.

G.K. BACKENSTOSS: I would like to point out that work on isomer shift is also being done at CERN. At the Asilomar Conference measurements on ^{181}Ta were reported; these were recently remeasured and reconfirmed, the shift being about + 100 eV. Furthermore, there are measurements by a group from Darmstadt, Germany, working at CERN on numerous nuclei, such as Os and Ir. Negative shifts were observed for Os and positive shifts for Ir. But there is a recent paper by H. Daniel in Naturwissenschaften, who discusses the corrections necessary as a consequence of the spin flip transition pointed out by Professor Grodzins.

L. GRODZINS: Do the negative values in Os remain after correcting for magnetic splitting?

G.K. BACKENSTOSS: I do not know the exact answer as to whether the Os-shifts remain still slightly negative after correction. However, since one can only estimate the spread of the spin flip transition and one does not know exactly the intensity of the hyperfine components, one should be cautious about drawing conclusions as long as the hyperfine splitting cannot be resolved.

L. GRODZINS: First, it is interesting that in ^{181}Ta the spin flip considerations as well as the deviations from statistical feeding do not affect the result (see the text). Second, the negative values for the Os results are most interesting since a shift, as preliminary reports indicate, of -500 eV, cannot be cancelled by the magnetic interaction which can at most account for about 350 eV, and is probably considerably smaller. Thus, if there are no further major corrections, such large energy shifts in osmium would mean that $\langle r_e^2 \rangle$ is less than $\langle r_g^2 \rangle$, in strong disagreement with theory.

V.S. SHPINEL: A variation of the nuclear charge radius in electromagnetic transition is an important property of the nucleus and a sensitive proof of nuclear models. To determine this quantity from the observed isomeric chemical shift of the γ-line, one should know the variation of electron density for the nucleus in different chemical compounds. Theoretical calculations of electron density depend on a number of inaccurately determined parameters and therefore the values of $\delta R/R$ obtained by different authors are in disagreement, sometimes even in the sign of the values.

To obtain more exact information about $\delta R/R$ it is worthwhile measuring the relative values of $\delta R/R$ for different γ-transitions. If these transitions occur in the same isotope or different isotopes of the same element, the electron factor can be reduced. To determine the relative values of $\delta R/R$ in different nuclei we chose nuclei of atoms neighbouring in the Z number: ^{119}Sn, ^{121}Sb and ^{125}Te. Atoms of these elements form a number of isostructural compounds, which facilitates an interpretation of isomeric shifts. In Fig. 3 of a recent paper[1] the results are shown of isomeric shifts δE for γ-rays of 23.8 keV in ^{119}Sn, 37.2 keV in ^{121}Sb and 35.6 keV in ^{125}Te for octahedral complexes of the $SnΓ_6$, $SbΓ_6$ and $TeΓ_6$ type ($Γ$ = F, Cl, Br, I). The figure shows the linear dependence of δE on a difference in electronegativity ($\Delta\chi$), Sn-Γ, Sb-Γ and Te-Γ. From the sign of the slopes of these lines it follows that the sign of nuclear charge variation for the considered transitions in ^{119}Sn and ^{125}Te nuclei is the same, while that in the ^{121}Sb nucleus is the opposite. The data of relative values of $\delta R/R$ can be used to check the $\delta R/R$ values calculated from the electron density. The experimental values of $\delta R/R$ in ^{119}Sn and ^{125}Te are in good agreement with those calculated by Uher and Sorensen. These calculations give satisfactory agreement in a number of other cases. The $\delta R/R$ value in the ^{121}Sb nucleus, however, as measured by us and simultaneously in the USA by Ruby et al. is higher by two orders of magnitude than the theoretical value. It is an interesting fact that the $\delta R/R$ values for $7/2^+ \rightarrow 5/2^+$ gamma transitions in the ^{127}I and ^{129}I isotopes, analogous to the discussed transition in ^{121}Sb, are also in agreement with the calculated value.

---

[1] BRUKHANOV, V.A., et al., Zh. eksp. teor. Fiz. 53 (1967) 1582; Soviet Physics JETP 26 (1968) 912.

STUDIES ON THE CHANGES OF NUCLEAR CHARGE RADII USING THE EFFECT OF X-RAY LINE ISOTOPE SHIFT

O.I. SUMBAEV
A.F. IOFFE PHYSICAL-TECHNICAL INSTITUTE,
LENINGRAD, UNION OF SOVIET SOCIALIST REPUBLICS

Abstract — Аннотация

STUDIES ON THE CHANGES OF NUCLEAR CHARGE RADII USING THE EFFECT OF X-RAY LINE ISOTOPE SHIFT. The effect of the X-ray volume isotope shift in ordinary atoms is discussed as a new experimental method for determining the differences between the nuclear charge radii ($\Delta \langle r^2 \rangle$) of isotopes.

The core of the subject, which deals with the possibility of sufficiently accurate ($\lesssim 5\%$) transition from the measured ΔE shifts to $\Delta \langle r^2 \rangle$ for the nuclei of the isotopes compared, is described.

A summary of the experimental data, obtained by using the method considered, is presented. It is evident from these data that the experimental errors can be at present reduced down to a few percent from the value of the shift, i.e. they do not exceed the errors due to the transition from ΔE to $\Delta \langle r^2 \rangle$ ($\lesssim 5\%$).

The comparison of the values of $\Delta \langle r^2 \rangle$ obtained by the X-ray I.S. methods for ordinary and mumesic atoms and by the optical I.S. method reveals satisfactory agreement. However, the X-ray data on the absolute values of $\Delta \langle r^2 \rangle$ are considerably more accurate and reliable than the optical shift data.

A comparison *is made* of the experimental results and the data calculated within the framework of Migdal's finite Fermi-systems theory.

In conclusion, the new experimental data on $\Delta \langle r^2 \rangle$ for Ba isotopes, which confirm the presence of anomalies, similar to the known case $^{40-48}$Ca, are discussed.

ИССЛЕДОВАНИЯ ИЗМЕНЕНИЙ ЗАРЯДОВЫХ РАДИУСОВ ЯДЕР С ПОМОЩЬЮ ЭФФЕКТА ИЗОТОПИЧЕСКОГО СДВИГА РЕНТГЕНОВСКИХ ЛИНИЙ. Рассмотрен эффект объемного изотопического сдвига рентгеновских линий в обычных атомах как новый экспериментальный метод определения зарядовых радиусов ядер ($\Delta \langle r^2 \rangle$) изотопов. Изложена принципиальная сторона вопроса, заключающегося в возможности достаточно точного ($\leq 5\%$) теоретического перехода от измеряемых сдвигов линий ΔE к $\Delta \langle r^2 \rangle$ ядер сравниваемых изотопов. Приводится свод экспериментальных данных, полученных с помощью рассматриваемого метода, показывающий, что в настоящее время экспериментальные ошибки удается снизить от величин сдвигов до нескольких процентов, т.е. они сравнимы с точностью ($\leq 5\%$) теоретического пересчета ΔE в $\Delta \langle r^2 \rangle$. Сопоставление значений $\Delta \langle r^2 \rangle$, полученных методами рентгеновского изотопического сдвига в обычных и μ-мезоатомах и изотопического сдвига оптических линий, обнаруживает удовлетворительное согласие. Однако, рентгеновские данные об абсолютных значениях $\Delta \langle r^2 \rangle$ обладают существенно большей точностью и надежностью по сравнению с оптическими. Приводится сравнение экспериментальных результатов с расчетами в рамках теории Мигдалла о конечных Ферми-системах. В заключение обсуждаются новые экспериментальные данные о $\Delta \langle r^2 \rangle$ у изотопов бария, подтверждающие наличие аномалий, аналогичных известному случаю $^{40-48}$ Ca.

INTRODUCTION

The theory of the effect of the so-called volume isotope shift of spectral lines due to the changes of nuclear charge radii was formulated in the early 1930s [1-4]. For optical lines this effect was discovered

experimentally even earlier [5], has gained recognition and is used extensively at present to study the changes of charge radii ($\Delta\langle r^2\rangle$) in the isotopes of relatively heavy elements ($Z \gtrsim 35$) (see Refs [6-9]).

After the first theoretical studies an analogous effect could be assumed in principle in X-ray and, following the discovery of mesic atoms, in mu-mesonic atom spectra. The radical advantage of the two latter effects (as compared to optical shift), consisting in the practical one-electron nature of the X-ray and mu-mesonic atom problems, particularly with respect to transitions between innermost atomic levels, was also apparent. The latter circumstance made it possible to believe that sufficiently accurate theoretical solutions, relating line shifts (ΔE) to be measured experimentally to the parameters specifying the distribution of nuclear electric charges (e.g. $\Delta\langle r^2\rangle$) to be studied, can be obtained.

For the case of X-ray spectra such solutions were found not long ago (1955-1963) in the studies of Wertheim and Igo [10], Schawlow and Townes [11] and Babushkin [12].

However, despite repeated attempts [13-16], an experimental detection of the X-ray isotope shift[1] was not successful for a long time and the X-ray shift in ordinary atoms was observed even a little later than a similar effect in mu-mesonic atoms [17]. A report on a preliminary result of the first successful experimental observation of the X.I.S. of the K_{α_1} line for uranium isotopes was made by Brockmeier, Boehm and Hatch (California Institute of Technology, USA) in 1964 [18]:

$$E^{U233} - E^{U238} = +1.3 \pm 0.5 \text{ eV}$$

Sumbaev and Mesentsev (A.F. Ioffe Physico-Technical Institute, Academy of Sciences, USSR) reported on their observation of the isotope shift of the K_{α_1} line for molybdenum isotopes in 1965 [19]:

$$E^{Mo92} - E^{Mo100} = +0.030 \pm 0.004 \text{ eV}$$

The final result obtained by Brockmeier et al. was published a little later [20]:

$$E^{U233} - E^{U238} = +1.8 \pm 0.2 \text{ eV}$$

The experimental procedure developed in Ref. [19] made it possible not only to detect the effect, but also to carry out systematic measurements for most relatively heavy elements ($Z \gtrsim 35$). This opened up possibilities for using the X.I.S. effect as an experimental means for studies on the changes of nuclear charge radii. In subsequent investigations conducted at the Physico-Technical Institute [21] and the California Institute of Technology [22] the new technique was used to advantage

[1] X.I.S. denotes the X-ray isotope shift, O.I.S. the optical isotope shift and μ.I.S. the mu-mesonic atom isotope shift.

for the isotopes of a number of elements, with relative accuracy of the shift determination within a view (2 to 10) per cent [22] approaching that of the pertinent theoretical solutions ($\lesssim 5\%$) relating ΔE to $\Delta\langle r^2\rangle$ [10, 12].

PHYSICS OF THE EFFECT AND THE PRINCIPLES UNDERLYING ITS USE AS A METHOD FOR DETERMINING $\Delta\langle r^2\rangle$

The dependence of the Coulomb potential V for a point nucleus and for Z; A, A + n isotopes with a finite region of the electrical charge distribution upon r (solid and dashed lines respectively) is shown on the left-hand side of Fig. 1. The electron energy levels whose wave-functions do not become zero within the nucleus region (Fig. 1, top left) will depend on the behaviour of V(r) over this region. To take an example: in the case of a nucleus with a finite region of the charge distribution, the level $1s_{1/2}$ will be located higher (with a smaller binding energy) than that in the case of a point nucleus (Fig. 1, at the right).

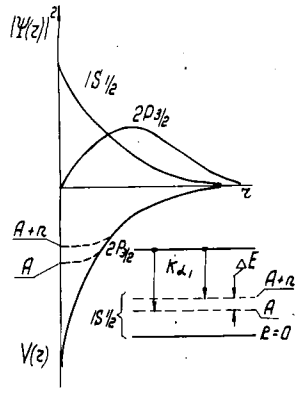

FIG. 1. Explanation of the physical nature of the isotopic X-ray shift effect (X.I.S. -effect).

Deviations of the potential from the Coulomb point potential are more pronounced the larger the charge radius of the respective nucleus and thus, generally speaking, for a heavier isotope than those under comparison one would expect, owing, for instance, to the drop dependence

$$R = R_0 A^{1/3}, \qquad (1)$$

larger deviations V(r) and, consequently, larger level shifts. The level energy difference ΔE of isotopes under comparison will thus be specific for the difference of their charge radii. For instance, if the transition $K_{\alpha_1}\ 2p_{3/2} \to 1s_{1/2}$, whose higher level is not subject to the influence of the isotope effect involved because of $|\Psi(0)_{p_{3/2}}|^2$ being equal to zero, is chosen, the experimentally measured difference in the energies of the line ($\Delta E_{K_{\alpha_1}}$) being studied for the isotopes under comparison will be a measure of the change in charge radii ($\Delta\langle r^2\rangle$). The effect described is referred to as the volume isotope shift of X-ray lines.

When solving the problem concerning the relation between $\Delta E_{K_{\alpha_1}}$ and $\Delta\langle r^2\rangle$ in this effect, Babushkin [12] found for the line shift[2]

$$\Delta E_{K_{\alpha_1}} = \frac{2}{3} Z^2 hc R_\infty \left(\frac{2Z}{a_0}\right)^{2\rho} \frac{L - \epsilon_0 M}{(1-\rho)L - (1+\rho)\epsilon_0 M} \frac{2\rho+3}{\Gamma(2\rho)} \Delta\langle r^2\rangle \qquad (2)$$

where

$$a_0 = \frac{\hbar}{me^2}; \quad \rho = \sqrt{1-\alpha^2 Z^2}; \quad \epsilon_0 = \sqrt{\frac{1-\epsilon}{1+\epsilon}};$$

$$L = \alpha Z \left(\frac{2}{5} - \frac{14}{315}\alpha^2 Z^2\right); \quad M = 1 - \frac{17}{60}\alpha^2 Z^2;$$

R_∞ is the Rydberg constant; $\epsilon = E/mc^2$ is the total energy of $1s_{1/2}$ electron in terms of mc^2. Solution (2) was obtained for the one-electron problem. However, a special analysis [10] has shown that the presence of the rest of the atomic electrons (shielding of the $1s_{1/2}$-electron by them and the change in their contribution to density on the nucleus in the X-ray transition) results in corrections not over $\approx 4\%$ within $40 \lesssim Z \lesssim 92$.

The practical one-electron nature of the problem concerning the X.I.S. determines a small magnitude of the so-called specific mass shift effect (known from the O.I.S.) which is essentially a many-electron effect due to correlations in the motion of electrons, is difficult to calculate and introduces an additional uncertainty when utilizing optical line shifts. Recent calculations [22] have shown that for the K_{α_1}-line this shift does not exceed -1/3 of the ordinary one-electron mass effect:

$$\frac{\Delta E}{E} = \frac{m}{m_n} \frac{\Delta A}{A_1 A_2} \qquad (3)$$

This result seems natural because a K_{α_1}-transition can be treated as a one-vacancy transition; that is, the problem is rather close to a single particle one. Thus, the total mass effect can be allowed for in the case of X.I.S. from the relation

$$\frac{\Delta E}{E} \approx \frac{2}{3}\left(\frac{1}{1836} \frac{\Delta A}{A_1 A_2}\right), \qquad (4)$$

generally accounting for a small part of the volume effect over the range.

Among other corrections, the effect related to the magnetic moment interaction of an electron moving within the nuclear electric field [25] should be pointed out. The correction factor

$$\epsilon = 1 - \frac{\alpha Z(2\rho+1)(2\rho+3)}{8\pi r_0(\rho+1)} \qquad (5)$$

[2] The ratio $\Delta R/R$ in Babushkin's original relation is expressed in Eq. (2) via $\Delta\langle r^2\rangle$, the only parameter upon which the effect under measurement is dependent both in the X.I.S. and O.I.S. cases [23, 24].

where

$$r_0 = 1.2 \times 10^{-13} A^{1/3} \Big/ \frac{e^2}{mc^2}$$

slightly dependent upon Z, equals 0.940 ± 0.005.

The corrections are covered in more detail in Ref. [22]. Table I, taken from this work, gives an indication of their values. A factor, termed in Table I the dynamic nuclear polarizability factor, practically equals unity and allows essentially for the change in energy of the $1s_{1/2}$ electronic level attributed to non-absolute rigidity of a nucleus [25a]. In the general case, such factors can occur due to the contribution of more complicated diagrams (of the type shown in Fig. 2(b)) to the Coulomb e-A interaction (Fig. 2(a)) allowing for intranuclear degrees of freedom. A small magnitude of such corrections determined in the case of X.I.S. is of advantage. Generally speaking, for more informative methods dealing with μ.I.S. and fast electron scattering (experiments of the type carried out by Hofstadter) there are no a priori reasons for expecting that these corrections would turn out to be small. Meanwhile, an accurate calculation of the corrections apparently involves an intimate knowledge of the intranuclear structure. Lack of this uncertainty in the effect of the X-ray line volume isotope shift for an ordinary atom is apt to make the X.I.S. the most reliable method for determining $\Delta\langle r^2 \rangle$.

TABLE I. CORRECTION FACTORS WHICH SHOULD BE INTRODUCED INTO THE EXPERIMENTAL DATA WHEN DETERMINING $\Delta\langle r^2 \rangle$ [22]

Isotope pair	Screening by transition electron	Nuclear polarization	Magnetic moment interaction
$^{116-124}$Sn	0.96	1.00	0.944
$^{148-154}$Sm	0.97	0.980	0.942
$^{182-184}$W	0.98	1.015	0.937
$^{184-186}$W	0.98	1.002	0.937

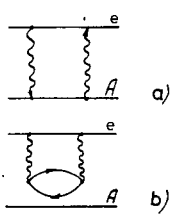

FIG. 2. Discussion of a correction to the dynamic polarizability of the nucleus.

TABLE II. PUBLISHED EXPERIMENTAL DATA OBTAINED BY THE X.I.S. METHOD (GOLUMNS 2, 3, 7) AND THEIR COMPARISON WITH THEORY (COLUMNS 4, 5, 6) AND DATA OBTAINED BY THE O.I.S. AND μ.I.S. METHODS (COLUMNS (8, 9)

	Isotope pair	ΔE_{exp} (meV)		ΔE_{theor} (meV)			$\gamma \equiv \Delta E_{exp}/\Delta E_{std}$		
		total	volume	[12]	[29]	[30]	X.I.S.	O.I.S.	μ.I.S.
	1	2	3	4	5	6	7	8	9
Mo	92 - 100	30 ± 5 [19]	35 ± 5	34.3	24.2	-	1.02 ± 0.15	1.21 ± 0.24 [37]	1.58 ± 0.18 [40]
	94 - 100	27 ± 8	31 ± 8	25.6	17.6	-	1.21 ± 0.31	1.13 ± 0.22	1.49 ± 0.17
Sn	116 - 124	29.9 ± 1.2 [22]	35.0 ± 1.2	76.9	31.4	63	0.46 ± 0.02	0.33 ± 0.06 [7]	0.66 ± 0.01 [41] 0.41 ± 0.15 [42]
Ba	134 - 135	-6.9 ± 2.0 [27]	-6.3 ± 2.0	17.1	13.7	-	-0.37 ± 0.12	-0.41 [7,31]	-
	134 - 136	-4.7 ± 2.0	-3.4 ± 2.0	34.2	15.2	25.2	-0.10 ± 0.06	+0.12 ± 0.05 0.45 ± 0.09 [34]	-
	136 - 137	-0.8 ± 2.0	-0.2 ± 2.0	17.0	13.7	2.7	-0.01 ± 0.12	-0.36	-
	136 - 138	7.7 ± 2.0	+9.0 ± 2.0	34.0	27.5	25.7	+0.26 ± 0.06	+0.15 ± 0.05 0.69 ± 0.14 [34]	-
Nd	144 - 146	63 ± 11 [22]	64 ± 11	49.3	-	67	1.29 ± 0.22	1.30 ± 0.24 [7,38]	1.11 ± 0.16 [42]
	146 - 148	65 ± 10	66 ± 10	49.1	-	67	1.34 ± 0.20	1.56 ± 0.29	-
	148 - 150	110 ± 13	111 ± 13	48.8	-	67	2.27 ± 0.27	2.15 ± 0.40	-
	144 - 150	238 ± 13 216.8 ± 3.5 [26]	242 ± 13 220.6 ± 3.5	147	-	201	1.65 ± 0.09 1.50 ± 0.02	1.67 ± 0.31	-

TABLE II. (cont.)

	Isotope pair	ΔE_{exp} (meV)		ΔE_{theor} (meV)			$\gamma \equiv \Delta E_{exp} / \Delta E_{std}$		
		total	volume	[12]	[29]	[30]	X.I.S.	O.I.S.	μ.I.S.
	1	2	3	4	5	6	7	8	9
Sm	144 - 148	136 ± 24 [21]	139 ± 24	119	-	158	1.16 ± 0.20	1.34 ± 0.27 [7,39]	-
	148 - 150	101 ± 15	102 ± 15	59.3	-	79	1.72 ± 0.25	1.66 ± 0.33	-
	150 - 152	109 ± 16	110 ± 16	59.0	-	79	1.86 ± 0.27	2.44 ± 0.49	-
	148 - 154	271.6 ± 3.5 [22]	275.4 ± 3.5	177	-	-	1.56 ± 0.02	1.76 ± 0.35	-
Gd	155 - 156	33.6 ± 5.4 [26]	34.2 ± 5.4	35.2	-	-	0.97 ± 0.15	-	-
	156 - 160	100.0 ± 4.6	102.5 ± 4.6	140	-	-	0.73 ± 0.03	0.79 ± 0.13 [7]	-
	155 - 160	133.6 ± 4.2	136.7 ± 4.2	175	-	-	0.78 ± 0.02	-	-
W	182 - 184	90.9 ± 10.5 [22]	92.2 ± 10.5	152	-	-	0.61 ± 0.07	0.40 ± 0.10 [7]	0.59 ± 0.13 [42]
	184 - 186	58.5 ± 8.0	59.8 ± 8.0	151	-	-	0.40 ± 0.05	0.35 ± 0.09	0.47 ± 0.13
	182 - 186	149.4 ± 10.0	151.9 ± 10.0	303	-	-	0.50 ± 0.03	0.37 ± 0.09	0.53 ± 0.09
Hg	200 - 204	252 ± 37 [26]	255 ± 37	551	406	367	0.46 ± 0.07	0.63 ± 0.07 [7]	-
Pb	206 - 208	166 ± 25 [26]	167 ± 25	326	240	334	0.51 ± 0.08	0.64 ± 0.07 [7]	0.55 ± 0.08 [43]
U	233 - 238	1800 ± 200 [20]	1803 ± 200	-	-	-	-	-	-

CORRELATION BETWEEN DATA ON $\Delta\langle r^2\rangle$ OBTAINED BY DIFFERENT METHODS. SOME PHYSICAL CONCLUSIONS

The effect of the isotope shift of X-ray lines was discovered experimentally in 1964-1965 (see above). Up to now only a few of the objects (isotope pairs) amongst those accessible for investigation in the present state of the method have been studied. Nevertheless, some data correlation can be made and the initial physical results discussed.

The experimental data known to the author which have been obtained up to data by the X.I.S. method are given in Table II. Column 2 lists the experimental values of total shifts; column 3 the same values corrected for mass shift (from relation (3)). Column 4 gives the values ΔE calculated from Eq.(2) under an elementary assumption of uniformly charged spherical nucleus with $R = 1.2 \times 10^{-13} A^{1/3}$ [12]; columns 5 and 6 present the theoretical values obtained in the calculation of $\Delta\langle r^2\rangle$ within the framework of the Migdal theory of finite Fermi-systems [28-30][3]. The values $\Delta E_{R\sim A^{1/3}} \equiv \Delta E_{std}$ are generally accepted as standard theoretical values offering a convenient unit for measuring isotope shifts. Columns 7-9 give the values of the γ effects (in terms of such standard shifts) obtained by the X.I.S., O.I.S. and μ.I.S. methods[4].

The fairly satisfactory general agreement between the values of γ obtained by different methods should be primarily noted.

However, the results vary substantially as to the magnitude and nature of errors [21]. The O.I.S. data exhibit the largest errors, caused completely by the uncertainties associated with the many-electron nature of the optical problem (uncertainties of shielding corrections and distortions of inner shells). The errors inherent in the X.I.S. are smaller (particularly in later studies [22, 26, 27]) and basically due to statistical errors of the experimental data.

Despite generally satisfactory agreement between the X.I.S. and O.I.S. data, there are discrepancies in a number of cases that are slightly beyond the limits of the errors specified by the authors (for instance, $^{116\text{-}124}$Sn, $^{200\text{-}204}$Hg). Since the X.I.S. data are more dependable with respect to their absolute values, they are likely to be used for normalizing the optical data.

The X.I.S. and μ.I.S. data agree within relatively small errors,[5] but are insufficient for revealing systematic divergencies likely to be present. It may be inferred, however, that corrections for intranuclear degrees of freedom which might cause concern in the μ.I.S. (see above) apparently do not exceed $\approx 20\%$ of the values of the effects concerned.

As to the theoretical values of the effect listed in Table II, the results of the study [12] (column 4) were obtained, as previously mentioned, under an elementary assumption regarding the dependence of the nuclear radius upon the number of neutrons ($R \sim A^{1/3}$) and for a uniform charge

---

[3] Values of K_{α_1}-shifts in columns 5, 6 are recalculated from isotope shift constants C (10^{-3} cm^{-1}) by the relation $\Delta E \approx CZ^2hc$ (see Ref. [30]).

[4] Babushkin's values (column 4) are taken as standard values without any additional corrections.

[5] Molybdenum, whose μ.I.S. values were obtained by recalculating $\Delta E_{exp}^{Mo\ 96\text{-}98}$ [40] using the relative shifts from the O.I.S. [37], is an exception to this.

distribution over the nuclear volume. Hence, from a nuclear point of view these data are not intended to convey any fine effects.

From this viewpoint the results of the calculations made according to Migdal's theory of finite Fermi-systems are of substantially greater interest in these calculations. Account is taken explicitly of the quantum characteristics of the states in which neutrons added to a nucleus turn out to be. Hence, when choosing a version for optimum agreement with the experimental data, it may be hoped in principle that information on the order of shell filling in even-even nuclei will be obtained. The results of these calculations from the qualitative standpoint are in satisfactory agreement with experiment, but cannot apparently be taken, as yet, for a strict quantitative agreement. (This is evident even from the comparison of the results from the two studies given in Table II).

Figure 3 presents a well-known graph (e.g. see Ref. [8]) of the dependence of γ on the neutron number N, constructed on the basis of optical data. Isotopes differing by two neutrons are compared and points are plotted opposite the neutron numbers corresponding to heavier isotopes in pairs. Triangles represent the X.I.S. values from Table II, squares the μ.I.S. values. The graph illustrates the aforesaid satisfactory agreement between the data obtained by different methods. The physical effects determining its major features have been repeatedly discussed elsewhere (e.g. see Refs [6-9, 21, 26]). The coincidence mentioned above makes further discussion unnecessary. Therefore, in conclusion, I would like to dwell on anomalously low points over the region N (neutron number) = 70-80. Specifically, barium and tellurium isotopes for which the O.I.S. data are available, even on the negative values of the effects [8, 31, 32], are located within this region. These data might possibly mean that the addition of a neutron causes a decrease in the mean square charge radius similarly to the well-known case of $^{40\text{-}48}$Ca [33]. However, another interpretation, based on the assumption that the anomalies are due to the presence in the O.I.S. of the specific mass shift effect whose sign is the reverse of the volume effect, was thought to be more probable [8, 34].

In the case of the X.I.S. the specific mass shift is negligibly small (see relation (3) above) and thus the detection of similar anomalies with this method would unambiguously mean anomalies in $\Delta\langle r^2\rangle$.

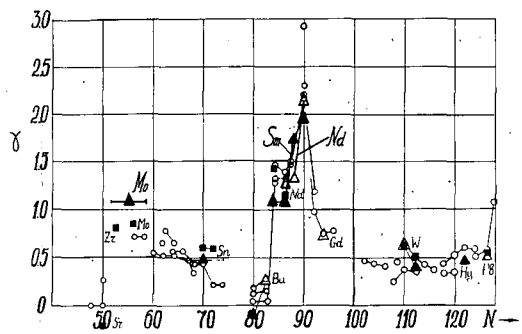

FIG. 3. Comparison of the variations of the nuclear charge radii $\gamma \equiv \dfrac{\Delta\langle r^2\rangle_{exp}}{\Delta\langle r^2\rangle_{std}\,(R\sim A^{1/3})}$ measured by means of the following effects: I.S. of the optical lines (O.I.S.-circles); I.S. X-ray lines (X.I.S.-triangles); I.S. mu-mesonic lines (μ I.S.-squares). The abscissa is the number of neutrons of a heavier isotope of the compared pair (A, A+2).

The preliminary results of the study carried out recently by the Ioffe Physical-Technical Institute group [27] and its final results given in Table II ($^{134-138}$Ba) and in part in Fig. 3 show that such anomalies do take place. They are particularly prominent when adding the 79th and 81st neutrons. It was supposed that the anomalies could be attributed to a decrease in the distortion of isotope nuclei when approaching the magic $^{138}Ba_{82}$ (e.g. see Refs [32, 35]), but other data on the deformations [36] do not seem to reveal the abrupt changes necessary for such an explanation and this intriguing problem thus still remains to be solved.

REFERENCES

[1] BARTLETT, J.H., Nature, Lond. 128 (1931) 408.
[2] PAULI, W., PEIERLS, R., Phys. Z. 32 (1931) 670.
[3] RACAH, G., Nature, Lond. 129 (1932) 723.
[4] ROSENTHAL, J., BREIT, G., Phys. Rev. 41 (1932) 459.
[5] MERTON, T.R., Nature, Lond. 104 (1919) 406.
[6] BREIT, G., Rev. mod. Phys. 30 (1958) 505.
[7] BRIX, P., KOPFERMAN, H., Rev. mod. Phys. 30 (1958) 517.
[8] KOPFERMAN, H., "Kernmomente", Akad. Verlag, Frankfurt (1956).
[9] MACK, J.E., ARROE, O.H., A. Rev. nucl. Sci. 6 (1956) 117.
[10] WERTHEIM, M.S., IGO, G., Phys. Rev. 98 (1955) 1.
[11] SCHAWLOW, A.L., TOWNES, C.H., Phys. Rev. 100 (1955) 1273.
[12] BABUSHKIN, F.A., Zh. eksp. teor. Fiz. 42 (1962) 1604; Optika spektrosk. 15 (1963) 721.
[13] RICHTMAYER, F.K., BARNES, S.W., Phys. Rev. 37 (1931) 1965.
[14] WILLIAMS, J.H., Phys. Rev. 37 (1931) 1431.
[15] FRILLAY, M., GOHKALE, B., VOLODARES, M., C.r.hebd. Séanc. Acad. Sci., Paris 233 (1951) 1183.
[16] ROGOSA, G.L., SCHWARZ, G., Phys. Rev. 92 (1953) 1434.
[17] ANDERSON, H.L., JOHNSON, C.S., HINCKS, E.P., RABOY, S., TRAIL, C.C., Phys. Lett. 4 (1963) 261;
BJORKLAND, J.A., RABOY, S., TRAIL, C.C., EHRLICH, R.D., POWERS, R.J., Phys. Rev. 136 (1964) B340.
[18] BROCKMEIER, R., BOEHM, F., HATCH, E.N., Papers from Symposium on Crystal Diffraction of Nuclear Gamma Rays, June 1964, Athens.
[19] SUMBAEV, O.I., MESENTSEV, A.F., Zh. eksp. teor. Fiz. 49 (1965) 459.
[20] BROCKMEIER, R., BOEHM, F., HATCH, E.N., Phys. Rev. Lett. 15 (1965) 132.
[21] SUMBAEV, O.I., PETROVITCH, E.V., ZIKOV, V.S., RIL'NIKOV, A.S., GRUSHKO, A.I., Yadernaya Fiz. 5 (1967) 544.
[22] CHESLER, R.B., BOEHM, F., BROCKMEIER, R.T., Phys. Rev. Lett. 18 (1967) 953.
[23] BODMER, A.R., Nucl. Phys. 9 (1958/59) 371.
[24] FRADKIN, E.E., Zh. eksp. teor. Fiz. 42 (1962) 787.
[25] BREIT, G., CLENDENIN, W.W., Phys. Rev. 85 (1952) 689;
BREIT, G., Rev. mod. Phys. 30 (1958) 507.
[25a] REINER, A.S., WILETS, L., Nucl. Phys. 36 (1962) 457.
[26] CHESLER, R.B., BOEHM, F., Research and Development Report CALT-63-67 (1967).
[27] SUMBAEV, O.I., MESENTSEV, A.F., MARUSHENKO, V.I., RILNIKOV, A.S., IVANOV, G.A., Contribution No. 179 to this Symposium.
[28] MIGDAL, A.B., "Teoriya konetchnykh Fermi-system i svoistva atomnykh yader", Moscow, Nauka (1965).
[29] BOUNATIAN, G.A., Yadernaya Fiz. 4 (1966) 707.
[30] KRAINOV, V.P., MIKULINSKY, M.A., Yadernaya Fiz. 4 (1966) 927.
[31] ARROE, O.H., Handb. Phys. 38 1 (1958) 117 (Fig. 9); and Phys. Rev. 79 (1950) 836.
[32] WILETS, L., Handb. Phys. 38 1 (1958) 115.
[33] HOFSTADTER, R., NOLDEKE, G.K., van OOSTRUM, K.J., SUELZLE, L., YEARIAN, M.R., CLARK, B.C., HERMAN, R., RAVENHALL, D.G., Phys. Rev. Lett. 15 (1965) 758.

[34] KALITIEVSKY, N.I., FRADKIN, E.E., TCHAIKA, N.P., Izv. Akad. Nauk SSSR, Ser. fiz. 25 (1961) 1178.
[35] WILETS, L., HILL, D., FORD, K., Phys. Rev. 91 (1953) 1488.
[36] MANFREDI, V.R., RICCI, R.A., Nuovo Cim. 53B (1968) 210.
[37] DONTSOV, Yu.P., Optika Spektrosk. 8 (1960) 446.
[38] DONTSOV, Yu.P., MOROZOV, V.A., STRIGANOV, A.R., Optika Spektrosk. 8 (1960) 741.
[39] STRIGANOV, A.R., KATULIN, V.A., ELISSEYEV, A.R., Optika Spektrosk. 12 (1962) 171.
[40] CHESMAN, C., RISTINEN, R.A., COHEN, R.C., DEVONS, S., NISSIM-SABAT, C., Phys. Rev. Lett. 14 (1965) 171.
[41] EHRLICH, R.D., FRYBERGER, D., JENSEN, D.A., NISSIM-SABAT, C., POWERS, R.L., TELEGDI, V.L., HARDGROVE, C.K., Phys. Rev. Lett. 18 (1967) 959.
[42] BARDIN, T.T., BARRETT, R.C., COHEN, R.C., DEVONS, S., HITLIN, D., MACAGNO, E., NISSIM-SABAT, C., REINWATER, J., RUNGE, K., WU, C., Phys. Rev. Lett. 16 (1966) 718.
[43] ANDERSON, H.L., McKEE, R.J., HARDGROVE, C.K., HINCKS, E.P., Phys. Rev. Lett. 16 (1966) 434.

DISCUSSION

C.S. WU: I have two remarks to make. First, our new isotope shift analysis is actually based on the shift of the binding energy of 1s levels and not the energy shift of K_{α_1} lines. Second, since the 1s muon wave-function is not constant over the nuclear volume, the binding energy of the 1s muon depends on finer details of the charge distribution. In other words, one must estimate the shift due to the change of all higher moments terms as well as the term due to the r.m.s. radius $\langle r^2 \rangle$.

F.H. BOEHM: I am presenting some recent results on the variations of mean square charge radii which were obtained from our atomic K-X-ray isotope shift work. In a figure to be published in the Physical Review, is presented a survey of the observed charge radii in terms of those of a homogeneous sphere for even-even nuclei. We have just recently obtained results for $^{178\text{-}180}$Hf for which we find $\delta\langle r^2\rangle_{exp} / \delta\langle r^2\rangle_{A^{1/3}} = 0.59 \pm 0.04$ and for $^{162\text{-}164}$Dy with $\delta\langle r^2\rangle_{exp} / \delta\langle r^2\rangle_{A^{1/3}} = 0.66 \pm 0.05$. Several interesting trends can be seen, notably in the Sn isotopes and in Nd. As an example, let us briefly discuss the case of Nd. Another figure to be published in the Physical Review shows a pictorial presentation of the charge radius based on that of ^{142}Nd. Also shown for comparison is a curve giving the radius from the $A^{1/3}$ law. We notice a pronounced even-odd staggering effect. For the even-even isotopes the variations of the radii are compared with other experimental results in Fig. 1 of a recent paper[1]. The agreement between K-X-ray, optical and μ- mesic data is good. The size of the radius increase for the case where two neutrons are added to the closed neutron shell of ^{142}Nd is in excellent agreement with a calculation based on the Migdal model. For the addition of subsequent neutron pairs the agreement is less good. Also shown are results from calculations by Uher and Sorensen based on a quadrupole and pairing model.

P. von BRENTANO: I would like to point out that there are now very accurate measurements of Coulomb displacement energies in the series of Nd isotopes done by Dr. Wurm and of the series of Ba isotopes done by Dr. Morrison at Argonne and it should be interesting to compare these data with yours. This comparison raises a problem, namely that

[1] BHATTACHERJEE, S.K., BOEHM, F., LEE, P., Phys. Rev. Lett. 20 (1968) 1295.

the Coulomb displacement energy depends not only on the r.m.s. charge radius but also on the r.m.s. radius of the excess neutrons. A method for calculating these energies has, however, recently been proposed in a very interesting paper by Nolen and Shiffer. Thus one might do a similar analysis on these nuclei as well.

G.K. BACKENSTOSS: It appears that there are three major methods for measuring charge radii and/or isotope shifts: electron scattering, μ-X-rays and now this new X-ray work. The accuracy of μ-X-rays increases with increasing Z, being better than for electron scattering for $Z \geq 11$. Now it appears from your measurements that the accuracy does not depend on Z. Could you measure lighter nuclei and what would be the accuracy you could achieve there?

F.H. BOEHM: Our present set-up limits us to $Z \geq 40$. However, I see no reason why one could not extend the range down to $Z = 30$, possibly replacing the transmission diffraction crystal by a reflection set-up.

Short Contribution

N.G. SHEVCHENKO (Physical-Technical Institute, Kharkov, USSR): I should like to report on work on the scattering of electrons on ^{58,60,64}Ni and ^{112,118}Sn isotopes, done by V.M. Khvastunov, N.G. Afanas'ev, N.G. Shevchenko, I.V. Andreeva, G.A. Savicky, I.S. Gulkarov, V.D. Afanas'ev, and A.A. Khomich.

We have measured the elastic scattering of electrons with an energy of 225 MeV on these isotopes in order to determine the effect of additional neutrons upon the distribution of charge density (half-density radius C, surface layer thickness t and the equivalent uniform distribution radius R). The theoretical calculation was performed using the high-energy approximation for the Fermi distribution of the charge[1].

TABLE A. ELECTRON SCATTERING RESULTS ON Ni AND Sn ISOTOPES

Nuclei	C(fm)	t(fm)	R(fm)	
^{58}Ni	4.140 ± 0.017	2.46 ± 0.02	4.940 ± 0.020	
^{112}Sn	5.375 ± 0.026	2.46 ± 0.045	6.009 ± 0.029	
	ΔC(fm)	Δt(fm)	ΔR(fm)	γ
^{60}Ni - ^{58}Ni	0.062 ± 0.018	0.000 ± 0.023	0.051 ± 0.014	0.88 ± 0.26
^{64}Ni - ^{60}Ni	0.044 ± 0.016	0.026 ± 0.020	0.055 ± 0.021	0.51 ± 0.19
^{64}Ni - ^{58}Ni	0.095 ± 0.018	0.045 ± 0.021	0.106 ± 0.020	0.62 ± 0.12
^{118}Sn - ^{112}Sn	0.021 ± 0.020	0.00 ± 0.03	0.031 ± 0.030	0.18 ± 0.17

[1] PETKOV, I.Zh., LUKYANOV, V.K., POL, Yu.S., Yadernaya Fiz. 4 (1966) 57.

Table A presents the quantity γ, characterizing a deviation from the $A^{1/3}$ law (we put $R = r_0 A^{\gamma/3}$). It was observed that the addition of the first two neutrons to the ^{58}Ni nucleus gives $\gamma \approx 1$, while the addition of the next four neutrons gives $\gamma \approx 0.5$. This can be interpreted as follows: the first two neutrons are plunged completely into the volume occupied by protons and the next neutrons only by halves. The first two neutrons have the orbital momentum lower ($\ell_n = 1$) than and the next four equal ($\ell_n = 3$) to the orbital momentum of peripheral protons ($\ell_p = 3$).

In the isotope ^{118}Sn we have an addition of neutrons with $\ell_n \approx 5$ while $\ell_p = 4$, and we observe $\gamma = 0$. This can be interpreted as an indication that added neutrons are practically on the surface of the nucleus. In this way a connection between a variation of a charge radius and orbital momenta of neutrons filling the nuclear shells is observed.

THE METHOD OF QUASIPARTICLES IN THE THEORY OF THE NUCLEUS

A. MIGDAL
I.V. KURCHATOV INSTITUTE OF ATOMIC ENERGY,
MOSCOW, UNION OF SOVIET SOCIALIST REPUBLICS

Abstract — Аннотация

THE METHOD OF QUASIPARTICLES IN THE THEORY OF THE NUCLEUS. The results of the application of Green's function to the theory of the nucleus are analysed. It is shown that the large number of observed phenomena (quadrupole and magnetic moments, probabilities and transition rates, isotopic shifts, etc.) can be expressed by some constants identical for all medium and heavy nuclei.

МЕТОД КВАЗИЧАСТИЦ В ТЕОРИИ ЯДРА. Анализируются результаты применения к теории ядра метода функций Грина. Показано, что большое число наблюдаемых явлений (квадрупольные и магнитные моменты, вероятности и частоты переходов, изотопическое смещение и т.д.) могут быть выражены через небольшое число констант, одинаковых для всех средних и тяжелых ядер.

In an ideal physical theory there should be no constants determined from experiment: all dimensionless quantities such as m/M, g^2/hc, etc. should be determined from the theory itself.

A theory of this kind belongs to the remote future. It will be constructed when a lark has made her nest on a ram's back, to quote an Eastern proverb.

For the time being the goal of the theory is much more modest: to obtain relations between quantities observed, introducing a minimum number of empirical constants. Thus, masses and constants determining the interaction between particles are introduced in the dispersion theory of elementary particles, whereupon the relations between the observed quantities are obtained. Similar methods can be applied in the theory of the nucleus.

A consistent application of the field theory methods to a finite system of strongly interacting particles in the spirit of the Landau-Fermi liquid theory makes it possible to introduce quasiparticles correctly and yields, similarly to the dispersion theory of elementary particles, the relations between the quantities observed at the price of the introduction of constants characterizing the interaction.

We shall begin with a schematic outline of the structure of this theory.

It can be rigorously shown that the first excited states of Fermi systems have a very simple nature even when the particle-particle interaction is strong. These are either single-particle excitations, which can be described as the origin of quasiparticles and quasi-holes, or collective excitations which can be interpreted as bound quasiparticle and quasi-hole states.

A few quasiparticles are involved in nearly all essential nuclear processes. Therefore, quasiparticles can be regarded as gas, i.e. the cases when more than two quasiparticles collide simultaneously can be neglected.

Since the quasiparticle is a particle moving in a dense medium, its properties may differ considerably from those of a free particle. The effective mass of quasiparticles and "charge" with respect to an external field differ from the corresponding quantities for free particles. Thus, the interaction with a magnetic field changes: moving in the nucleus, the neutron acquires orbital magnetism.

A medium introduces still more essential changes into the interaction between particles. Comparison of theory with experiment shows that attraction may be replaced by repulsion in some cases; and analysis, based on the Green's function method, indicates that all quantities describing the motion of quasiparticles can be divided into two groups: (1) local quantities which are determined by the properties of nuclear matter at each point of the nucleus; these quantities include the depth of the potential well, the nuclear radius, the local charge of quasiparticles, the constants describing the local interaction between quasiparticles, etc., and (2) quantities describing the motion and interaction of quasiparticles over distances of the order of the nuclear radius; these quantities include the scattering amplitude of quasiparticles in the nucleus, the effective (and not local) charge of quasiparticles, the effective interaction between quasiparticles in an unfilled shell, etc.; it is through these quantities that all nuclear processes observed are expressed, such as nuclear moments, the intensities and frequencies of electromagnetic transitions, changes in the distribution of nucleons with excitation and addition of particles, nuclear mass differences, etc.

The quantities of the first kind can only be found with the aid of some approximate methods assuming that the interaction is small in some sense, for which there are no sufficient grounds in the nucleus. Therefore, it is reasonable, having rejected the calculation of these quantities, to describe them by a minimum number of parameters determined from experiment. This approach is exemplified by the shell model of the nucleus for which the depth, radius and width of the transitional layer of the potential well are taken from the comparison of single-particle energies with mass differences of magic and near-magic nuclei.

As for the quantities of the second kind, they can be calculated comparatively after the local quantities have been introduced. As a result, we have relations between different physical processes.

It should be emphasized that those approximate models which are usually used are quite sufficient for a qualitative study of nearly all nuclear processes. What we are discussing is the possibility of obtaining quantitative relations. However, below we cite several processes which cannot be interpreted correctly without a rigorous approach.

For homogeneous infinite Fermi systems such a program was carried out by Landau in his Fermi-liquid theory.

Thus, the idea of the method proposed is the same as in the dispersion theory of elementary particles: constants describing the motion and interaction of quasiparticles are introduced, whereupon we can calculate in principle all nuclear processes for energies low compared with the Fermi energy (40 MeV).

Let us enumerate the peculiarities of the theory which distinguish it from other approaches.

(1) First of all, the theory may be consecutively evolved in more accurate terms. All omitted terms may be evaluated. In the theory there

is a parameter of smallness $A^{-1/3}$, the expansion in which may be found (for most processes the corrections begin from $A^{-2/3}$).

(2) A minimum number of constants is introduced, or, more accurately, only those constants are introduced which cannot be calculated without the assumption that the interaction in the nucleus is small.

(3) The theory makes it possible to introduce unambiguously the parameters characterizing the interaction between quasiparticles, taking into account the finiteness of the range of forces, without introducing arbitrary functions (like the Gaussian dependence of forces on the distance). The natural assumption that we can confine ourselves to a small number of harmonics in the expansion of the amplitude in scattering angles is made for this purpose. The relations between amplitude harmonics, following from isotopic invariance and the Pauli principle, are used. Possibly, we may confine ourselves to the S, P, D harmonics (not coinciding, of course, with their analogue for free nucleons of the same energy).

(4) The fact that the parameters of interaction outside the nucleus essentially differ from their counterparts inside the nucleus is taken into account and proves to be quite important. External interaction constants may be connected with the scattering amplitude of two nucleons in vacuum. For quasiparticles with energies near the Fermi surface the interaction amplitude passes into the two-nucleon scattering amplitude extrapolated into a region of negative energy equal in absolute value to the doubled binding energy in two-neutron cases or to the doubled difference between the nucleon barrier and the Fermi energy in two-proton cases.

It can be calculated that the scattering amplitude, into which the internal interaction amplitude should pass, has the following form

$$\mathscr{F} = -\frac{4\pi}{\kappa + \sqrt{|E|}} \cdot \frac{1}{1+\frac{1}{x}e^{-x}}$$

Here $x = 2\sqrt{|E|}(r-R)$, $(r-R) > r_0$; at $x \gg 1$ the limit value corresponding to the scattering amplitude of two free nucleons with negative energy $-|E|$ is attained; the second factor in $\mathscr{F}$ arises due to reflection from the edge of the nucleus.

This expression results from the solution of the Schrödinger equation for two nucleons with δ-type interaction and with boundary conditions, taking into account the potential well.

Thus, outside the nucleus there is considerable attraction between quasiparticles leading to an effective extension of the well. In this way the process explains why the density radius is appreciably smaller than the radius of the potential well.

Since the quantity E differs appreciably for two neutrons and two protons, the effective extension of the well will be different for neutrons and protons.

Let us elucidate the well extension mechanism without taking into account the differences in interaction for neutrons and protons.

Let R be the density distribution radius determined in the Hofstadter experiments.

Then, schematically, the nucleon potential near the edge of the nucleus is given in the gas approximation by the expression

$$U(r) = n(r)\mathcal{F}(r)$$

Let us assume that $\mathcal{F}(r)$ is determined by the same interpolation formula as n(r)

$$n(r) = \frac{n(0)}{1+e^{\alpha\xi}}, \quad \mathcal{F} = \mathcal{F}_\infty + \frac{\mathcal{F}_0 - \mathcal{F}_\infty}{1+e^{\alpha\xi}}$$

where $\xi = r - R$.

The expression U(r) can be represented in approximate terms as

$$U(r) = \frac{U(0)}{1+e^{\alpha\xi - \alpha\delta}}$$

where δ is the effective increase of the radius. In the first order in δ we have

$$U(r) = \frac{U(0)}{1+e^{\alpha\xi}} + \frac{U(0)e^{\alpha\xi}}{(1+e^{\alpha\xi})^2}\,\alpha\delta$$

Comparing it with the expression

$$U(r) = \frac{n(0)\mathcal{F}_0}{1+e^{\alpha\xi}} - \frac{n(0)(\mathcal{F}_0 - \mathcal{F}_\infty)e^{\alpha\xi}}{(1+e^{\alpha\xi})^2}$$

we obtain

$$\alpha\delta = \frac{(\mathcal{F}_0 - \mathcal{F}_\infty)n(0)}{U(0)}$$

The result is a reasonable quantity for δ.

(5) The effective interaction and effective charge in an unfilled shell are expressed by constants of the theory. This dispenses with the need for introducing the constants of different interactions ($\kappa_2 QQ$, $\kappa_3 v_3 v_3$, $\kappa_0 v_0 v_0$, etc.).

(6) It has been found that quasiparticles possess local "charges" differing from the "charge" of a particle: the external field should be multiplied by an additional factor depending on the type of field (moreover, the field obviously undergoes non-local changes connected with

the polarizability of quasiparticles which is simply expressed via interaction constants). The relations between local charges have been obtained for different fields. Thus, the local charge, by which the pseudovector constant of beta decay in the nucleus is multiplied, is connected with the factor of the spin magnetic moment of nucleons.

Comparison of the theory with experiment proves conclusively enough, it seems to us, that the approach proposed is sensible. Many widely different processes can thus be brought into agreement at the expense of the introduction of a minimum number of constants.

The interaction constants, introduced in the theory, have been determined very roughly so far. Moreover, the behaviour of interaction constants near the surface of the nucleus should be specified and the effect of finiteness of the effective interaction range be taken into account. All these drawbacks can be eliminated after a sufficiently extensive comparison with experiment.

Of essential importance is the comparison with experiment of the calculations by the frequencies and intensities of collective transitions, calculations by the first levels of twice magic nuclei, etc.

It is of considerable interest to explain the Hofstadter experiments in the scattering of electrons on calcium isotopes and in general to predict theoretically the experiments of this kind.

An explanation of the negative isotopic shift in Sr, Ba would be a major success of the theory.

Calculations of this kind are being made at present.

It is also of interest to calculate the average quadrupole moments in excited states. Estimates yield values of quadrupole moments exceeding by several times the single-particle values. The physical cause is a stronger quadrupole field owing to the influence of the low-lying 2^+ level. Quantitative calculations are now in progress.

Research has started in terms of the proposed approach to explain quantitatively the processes connected with analogue states.

Useful information will also come from dipole photo-absorption calculations under the assumption that the initial reaction is the single-particle excitation of the nucleus which is then redistributed over more complex excitations. Thus, this example will enable us to trace the whole mechanism of initial reactions.

It is of great interest to consider the unified model of the nucleus in terms of the approach proposed.

Of special interest is the calculation of the processes involved in the transition from a spherical to a deformed state.

Apart from local interaction, in deformed nuclei there is another mechanism of interaction of quasiparticles, namely exchange in rotational nuclear excitations. This mechanism can also be taken into account in terms of the theory proposed.

A considerable range of problems is connected with the interaction with the nucleus of a μ-meson lying on the K-shell, since the former causes a strong electric and magnetic polarization of the nucleus. Of the problems of this range, only the problem of the isotopic shift in the μ-atom has been solved.

Finally, it would be extremely important to develop a method of calculating the constants of the theory via the interaction of nucleons in vacuum.

Though there is no small parameter in the nucleus, it may appear that some method of calculation will give satisfactory results owing to a good convergence of series. If the results of these calculations yield the correct values of those constants of the theory which have already been found, other results of such calculations can also be trusted.

I would like to reconcile contradictory approaches to the theory of the nucleus by recounting the following fairy-tale. Once a father tried to find his son in a crowd of dirty children by washing them. But he had to give up his idea, saying: "It's easier to give birth to a new baby than to wash all this crowd." Thus, in view of the variety of approaches and papers on nuclear structure, it seems easier to develop a new theory than to study all those that already exist.

DISCUSSION

G.E. BROWN: I am reluctant to criticize Professor Migdal, since I remember the time when I was on a walk with my father and we came to a stream. In order to cross it, we took off our shoes. I looked at his feet and remarked "your feet are dirtier than mine". My father said, "I'm older than you are."

When it comes right down to what people do with the Migdal theory, this amounts, at the moment, to using a density-dependent δ-interaction such as

$$f(\rho)\,\delta(\vec{r}_1 - \vec{r}_2)\{f + g\vec{\sigma}_1 \cdot \vec{\sigma}_2 + \ldots\}$$

Migdal and his group have shown that a strong density dependence is necessary, especially for effects such as the isotope shift. The zero range is clearly a rather crude approximation, and will have to be extended when more spectra and other effects are fitted.

K.A. BRUECKNER: The method of quasiparticles is particularly useful since exact relationships are maintained by the exact structure of the theory. The method is, however, useful if a simple parameterization is adequate. It is known that the nuclear forces acting over the energy range of nuclear collisions must be described by 30-40 parameters and that six parameters are sufficient only over a few MeV range at very low energy. It therefore seems probable that the need for higher accuracy in nuclear spectra will lead to many more parameters in the effective force. These will describe, for example, force range, strength, shape, non-central terms, velocity dependence ($L \cdot S$).

It is possible to calculate these parameters by perturbation methods since nuclei are dilute weakly interacting systems.

S.T. BELYAEV: I would like to comment on the hierarchy and the division of the "spheres of influence" of various approaches. The use of simple model interactions (pairing, Q-Q interaction, etc.) permits a very simple and fruitful search for new phenomena in nuclear structure and clarification of the qualitative picture of phenomena. However, in so doing, one should not take the quantitative description into account. For this purpose, a more consistent approach of the Fermi-liquid theory should be used. Certainly, in the framework of the latter a simplified parameterization of the effective interaction can be used, but it may be made successively more complicated if required.

A. BOHR: As Professor Migdal reported, one can understand the order of magnitude of the static quadrupole moments of the 2^+ states on the basis of the graphs shown, and by including the polarization factor $(1 + \chi)$, where χ, for example, for ^{144}Cd is about 20. It is also interesting, as has been pointed out by Professor Mottelson, that the frequency dependence of χ can give some understanding of why the cross-over transition $Z' \to 0$ from the second 2^+ state to the ground state is relatively weak; in fact

$$\chi(\omega = E(2') - E(0)) = -\frac{1}{3}\chi(\omega = 0)$$

It must be stressed, however, that such estimates are only qualitative, since for the rest of the nuclei considered the particle-vibration coupling is strong; we are in the transition region between spherical and deformed nuclei, and more general methods are needed for a quantitative description of these spectra.

A. B. MIGDAL: It seems to me that it is possible to create a theory which takes into account the effect of the 2^+ level in the adiabatic approximation. But, independently of this, there is a wide region of nuclei with a not very low 2^+ level, where the influence of anharmonicity can be studied by the perturbation theory.

V. V. BALASHOV: You have emphasized the particular importance of the study of the negative isotopic shift. Don't you think that nuclear cluster states and especially nuclear surface should be taken into account when discussing this effect?

A. B. MIGDAL: It seems to me that the negative isotopic shift is connected with the properties of the potential and the nuclear surface, and possibly with clusters near the nuclear surface.

Krishna KUMAR: In a deformed system the single-particle angular momentum is not conserved in the intrinsic system. In your theory, how do you avoid this problem and construct states of good angular momentum?

A. B. MIGDAL: In a deformed nucleus the eigenfunctions of the deformed field $\widetilde{\varphi}_\lambda$, through which new Green's functions can be expressed, should be introduced. The Green's function $G_{\lambda\lambda'}(\epsilon)$ near the Fermi surface is diagonal on the new integrals of motion λ: $G_{\lambda\lambda'}(\epsilon) = G_\lambda(\epsilon)\,\delta_{\lambda\lambda'}$.

B. L. BIRBRAIR: What is the number of parameters in your theory now?

A. B. MIGDAL: The number of empirical constants of the interaction was considerably reduced due to the calculation of the interaction outside the nucleus. Five constants are practically sufficient for the majority of phenomena.

B. L. BIRBRAIR: We have recently attempted to calculate the quadrupole moments of the first 2^+ levels, taking into account all the effects you mentioned in your report. The qualitative result is as follows: the quadrupole moments appeared to be large in absolute value but the numerical results are strongly dependent upon the details of the single-particle scheme. By changing the scheme of single-particle levels one can obtain any number desired. This agrees with the results of analogous calculations by Balbutsev and Jolos.

A. B. MIGDAL: The analysis with the help of diagram techniques shows that the result is stable. For this purpose the Ward identity is used, after which the results are practically independent of single-particle states.

M. G. URIN: I should like to dwell on a single and, at the same time, practically important application of the Migdal theory, namely, the calculation of the value and radial dependence of the $V_1(r)$ function in the well-known Lane potential

$$V_L(r) = \frac{4}{A} V_1(r) \vec{t}\vec{T}$$

This potential describes in particular the excitation of the analogous states in direct (p, n) reactions. In the excitation of analogous states any excess neutron is transformed into a proton state with the same quantum numbers. These transformations result in a change of the density of quasiparticles $\delta\rho(r)$, and, consequently, in accordance with the Migdal theory, in the appearance of the charge-exchange field

$$V_1(r) \sim \hat{F}\, \delta\rho$$

where $\hat{F}$ is the charge-exchange part of the scattering amplitude. In heavy nuclei, where $\delta\rho \approx (N-Z)/V$ (V is the nucleus volume):

$$V_1 = \frac{1}{2} \frac{A}{V} F$$

For the value of the force constant F (its dimensionless value is $f \simeq 1.3$) assumed in the Migdal theory $V_1 \cong 29$ MeV, which is in satisfactory agreement with the average experimental value.

If the density of the excess neutrons $\delta\rho(r)$ markedly varies within the nucleus volume, then it should be found from the integral equation taking into account the core N = Z polarization effect in the excitation of the analogous state. When applied to other problems, this equation was solved numerically by M. Troitsky. In the quasi-classical approximation one can obtain a simple analytical expression for $\delta\rho(r)$:

$$\delta\rho(r) = \frac{1}{1+f}\left[\delta\rho_0(r) + f\,\frac{N-Z}{V}\right] \qquad (r < R)$$

where $\delta\rho_0(r)$ is the density of excess neutrons in the shell model. Thus, the microscopic approach allows the dependence of the Lane potential on the shell effects to be found.

EFFECTIVE FORCE FOR NUCLEAR RANDOM PHASE APPROXIMATION (RPA)

I.N. MIKHAILOV
JOINT INSTITUTE FOR NUCLEAR RESEARCH,
DUBNA, UNION OF SOVIET SOCIALIST REPUBLICS

Abstract — Аннотация

EFFECTIVE FORCE FOR NUCLEAR RANDOM PHASE APPROXIMATION (RPA). The theoretical evaluation of the effective force operators for nuclear structure models is achieved within different approximate schemes. Some of the matrix elements of the force result from the study of the association energies of nucleons, which involves various assumptions of nuclear coupling. Further information on the effective force is obtained by solving equations for the reaction-matrix - a reliable operator substituting the realistic inter-nucleon force - and also from the data available on the nuclear-matter properties. When comparing this information with 'experiment' it should be remembered that each of the models is characterized by its own effective force evaluated from appropriate equations.

Much attention is given to the precise definition of the effective force for a particular model - the random phase approximation (RPA) - and the relationship is established between the effective force operator and the reaction-matrix, on the one hand, and the scattering amplitude in the Fermi-liquid theory, on the other.

Some estimates for the zero-range effective force are given. These are obtained from the data on the density dependence of the local part of the nuclear self-consistent potential. The resulting operator depends on the density itself.

ЭФФЕКТИВНЫЕ СИЛЫ ДЛЯ ЯДЕРНОГО ВАРИАНТА МЕТОДА СЛУЧАЙНОЙ ФАЗЫ. Проблема теоретического определения параметров эффективных сил для моделей структуры ядра рассматривается в настоящее время с различных точек зрения. Отдельные матричные элементы сил удается вычислить по энергии отделения нуклонов от ядра, используя при этом предположения о характере связи нуклонов ядра. Для дальнейшего расширения знаний об эффективных силах применяются методы вычисления матрицы реакции – оператора с хорошими аналитическими свойствами, заменяющего реалистический потенциал межнуклонного взаимодействия, а также используются данные о свойствах ядерной материи. При сопоставлении этих данных с "экспериментом" следует учитывать, что каждой модели структуры ядра должна соответствовать своя эффективная сила, вычисленная из соответствующих уравнений. Подробно рассматриваются вопросы строгого определения эффективного взаимодействия для данной модели ядра, а именно для метода случайной фазы. С одной стороны, найдена связь этого оператора с матрицей реакции, а с другой стороны - с амплитудой рассеяния квазичастиц в соответствии с теорией жидкости Ферми. Даны оценки величины эффективных сил в приближении оператором нулевого радиуса действия. Оценки получены по данным о зависимости локальной части потенциала самосогласованного поля ядра от плотности нуклонов. Оператор эффективных сил, полученный таким образом, также зависит от плотности нуклонов в ядре.

1. INTRODUCTION

Some relationship must exist between the parameters used in nuclear structure models and those describing the scattering of free nucleons, unless the nuclear field affects the collision process too much. The nuclear matter calculations indicate that the effect of the nuclear field on the inter-nuclear force is not great. But the nuclear-matter calculations are concerned only with the gross properties of nuclei and it is interesting therefore to establish this relationship by studying the nuclear structure. To achieve this aim one will have to deal with the problem of evaluation of the effective force for nuclear models.

Another reason for the theoretical evaluation of the effective force lies in the large number of nuclear models [1]. In these models the equations describing physical processes differ essentially in the choice of the effective force and effective charges [2-4]. Thus, in practice, the model whose parameters can be calculated from first principles must be considered preferable.

Some calculations of the force using the Brueckner technique [5-7] have been already performed. In Ref. [8] the matrix elements of the effective force are related in a simple way to Brueckner's reaction-matrix. There are indications, however, that not all the important renormalization processes are taken into account in these papers. For instance, the force calculated in Ref. [8] fails to reproduce the available experimental data on the muon capture rates [9] in ^{16}O.

Another approach to the problem is suggested in Ref. [10]. Here the effective force is defined as a second variational derivative of the energy in the density-matrix (as in the Fermi-liquid theory [11, 12]). Some data on the nuclear binding energy are used in Ref. [10] to evaluate the zero-range effective force.

The two approaches used in the calculation of the effective force for the nuclear random phase approximation (RPA) – one in Refs [5-8] and the other in Ref. [10] – are rather different. For practical reasons the first approach is restricted to nuclei with few nucleons outside the closed shells. Detailed information on the effective force is obtained here in the framework of the simple version of the Brueckner theory.

The second approach is based on the recent nuclear-matter calculations, taking into account three-body clusters and using the most up-to-date force between free nucleons. However, the information on nuclear matter is used here in conjunction with the variational technique which makes the theory strikingly different from that in Refs [5-8] on the one hand and introduces unpredictable errors in it on the other.

Thus both approaches have their advantages and drawbacks. It is justifiable, then, to try to find an unambiguous definition of the effective force which is general enough to link them. This definition is given in Section 2. In Section 3 the relationship between the variational procedure and the diagrammatic representation of the force is established. In Section 4 the estimates of Ref. [10] are recapitulated.

2. GENERAL EXPRESSION FOR EFFECTIVE FORCE

The objective of RPA is to describe nuclear transitions, for example, between states $|0\rangle$ and $|1\rangle$, and this is achieved by writing equations for the transition operator b^+. The latter is such that

$$|1\rangle = b^+ |0\rangle \tag{1}$$

Equations for b^+ are based on a number of assumptions, two of which are relevant to what follows:

(i) It is assumed that the matrix elements of b^+ between eigenstates $|i\rangle$ are close to the matrix elements between states of a very simple

structure. One of the states includes no correlations at all (in nuclei without pairing) or only pairing correlations in other nuclei. In some cases the uncorrelated states represent the ground states of nuclei. Such functions may be written in the form

$$|K\rangle = \prod_{\nu \leq \nu_F} a_\nu^+ \; || \; 0 \; \rangle\rangle \tag{2}$$

where a^+ is a creation operator of a single-particle state $\varphi(x)$, $|| \; 0 \; \rangle\rangle$ is a vacuum state. In Eq.(2) K is defined by the one-particle density-matrix:

$$K(x, x') = \sum_{\nu \leq \nu_F} \varphi_\nu^* (x) \, \varphi_\nu (x') \tag{3}$$

(ii) One assumes a relatively simple structure of the transition operator b^+

$$b^+ = \int dx dx' \quad (x \, |b^+| x') \, \psi^+ (x) \, \psi (x') \tag{4}$$

Here $\psi(x)$ is a field operator

$$\psi (x) = \sum_\nu \varphi_\nu (x) \, a_\nu \tag{5}$$

Because of the repulsion between nucleons at small distances each state (2) is practically orthogonal to any of the nuclear eigenstates. Indeed the mean value $\langle K | H | K \rangle$ of a realistic Hamiltonian H exceeds the energy of a nucleus in all of the states considered in nuclear spectroscopy. Therefore one takes a model Hamiltonian

$$\begin{aligned} H = &\int dx \, dx' \quad (x \, |h| x') \psi^+ (x) \psi (x') \\ &+ \tfrac{1}{4} \int dx_1 \, dx_1', \, dx_2 dx_2' \, (x_1 \, x_2 \, |V| x_1' \quad x_2') \, \psi^+ (x_1) \, \psi^+ (x_2) \, \psi (x_2') \, \psi (x_1') \end{aligned} \tag{6}$$

with a potential included in h and a smooth force V.

The physical meaning of the above assumptions and the relation of the model Hamiltonian to the realistic many-body operator can be understood by introducing a truncated space (m) of many-body configurations [8, 14]. To define it we write the Hamiltonian in the form

$$H = H_0 + V \tag{7}$$

where H_0 is a one-body Hamiltonian such that its lowest N-nucleon configuration gives a correct density distribution in (even) nuclei with N-nucleons and the sequence of eigenvalues resembles the spectra of neighbouring (odd) nuclei. The configurations of H_0 may be used as basic functions in the expansions for the eigenfunctions of H.

Let us split the set of single-particle functions $|\Psi\rangle$ into two parts so that one of them will include only relatively low-lying states, as is shown in Fig.1. The truncated (model) space of N-particle configurations is then defined as the manifold of all configurations with N particles occupying single-particle states below the wavy line in Fig.1.

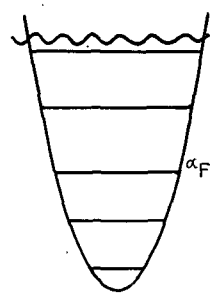

FIG.1. Definition of the model space of configurations. Orbitals up to α_F are occupied in the shell-model ground-state function.

The true nuclear wave-function may be found in the following way. First one finds an operator $\Omega(z)$ satisfying the equation

$$\Omega(z) = 1 + \frac{1 - p_m}{z - H_0} V \Omega(z) \tag{8}$$

with the projection operator p_m which projects on states of the model space (m).

Then the model Hamiltonian H_m is evaluated

$$H_m(z) = H_0 + V\Omega(z) = H_0 + V_m(z) = H_m^+(z^*) \tag{9}$$

The Hamiltonian H_m operates in (m) only.

One finds eigenstates of the model Hamiltonian

$$H_m(z) |\phi_m\rangle = E_m(z) |\phi_m\rangle \tag{10}$$

After this is done, one finds the true eigenfunctions and energies of the system from the equations

$$E_m(E) = E \tag{11}$$

$$|\Psi\rangle = \Omega(z) |\phi_m\rangle \tag{12}$$

If only one pair of quantities $E_m = E_0$, $|\phi_m\rangle = |0\rangle$ is known, and this corresponds, for example, to the ground state, it is possible to write an equation for the transition operator b^+

$$H_m(E_0 + \hbar\omega)b^+ - b^+ H_m(E_0) = \hbar\omega\, b^+ + \pi \tag{13}$$

or

$$[\mathscr{H}_0, b^+] = \hbar\omega \left\{ 1 - \mathscr{H}'_0 - \tfrac{1}{2}\hbar\omega\, \mathscr{H}''_0 + \ldots \right\} b^+ + \pi \tag{14}$$

$$\left(\pi |0\rangle = 0,\ \mathscr{H}_0^{(i)} = \left(\partial^i H_m(z)/\partial z^i\right)_{z=E_0}\right)$$

From Refs [3,4] it is known how the equations of the RPA are obtained starting with Eqs (13), (14) when H_m is given by Eq. (6).

In order to calculate the effective force operator we assume that the quantities entering the RPA equations are those which should be used in a Schrödinger equation for the model functions $|\phi_m\rangle$. More particularly, we suppose that in the model space (m) an uncorrelated function K_0 can be found which satisfies the conditions

$$\pi |K_0\rangle \approx \pi^+ |K_0\rangle \approx 0 \tag{15}$$

where π is the operator on the r.h.s. of Eqs (13), (14). Further, Eq. (4) with the appropriately chosen weighting function $(x|b^+|x')$ is assumed to be a good approximation to the transition operator. All these assumptions seem to be reasonable, because the exclusion of the high-lying configurations from (m) results in greatly reduced short-range correlations in $|\phi\rangle$. However, due to the operator $\Omega(z)$, the model Hamiltonian H_m has a very complicated structure. The truncation of the configuration space leads to changes in the matrix elements of H_m taken between the two-particle states. As a result of the truncation there appear three- and more-particle components of H_m (see examples in Fig.2).

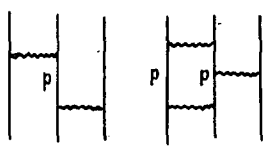

FIG.2. Some three-body components of $H_m(z)$. The label p denotes orbitals which are not included in (m).

In what follows two problems are considered: (i) How are the components of $H_m(z)$ evaluated ? and (ii) In what way do the many-particle components of H_m affect the equations of RPA?

A simple solution of the second problem is obtained by using the definition of a normal product of several field operators [12, 15]. For two operators the definition reads

$$:\psi(x)\,\psi(x'):\; = \psi(x)\,\psi(x')$$
$$:\psi^{+}(x)\,\psi(x'):\; = \psi^{+}(x)\,\psi(x') - K(x', x) \tag{16}$$

where $K(x', x)$ is the density-matrix. The normal product of more than two operators is given by the Wick theorem with the contractions defined as in Eq. (16).

Let us write the model Hamiltonian in the form

$$H_m(z) = h_0(z) + \sum_{n=1,2\ldots} (1/n!)^2 \int dx_1 \ldots dx'_n\; h_n(z; x_1 \ldots x'_n)$$
$$\times :\psi^{+}(x_1) \ldots \psi(x'_n): \tag{17}$$

From the definition of a normal product one has

$$h_0(z) = \langle K_0 | H_m(z) | K_0 \rangle \tag{18}$$

The other coefficients in Eq. (17) are connected with h_0 by the equation

$$h_n = \frac{\delta h_{n-1}}{\delta K(x_n, x'_n)} = \ldots = \frac{\delta^n h_0}{\delta K_1 \ldots \delta K_n} \tag{19}$$

Eq. (19) *is obtained by varying* $K(x, x')$ *within* (m).

To see the role of coefficients h_n in the equations for the transition operator b^{+} we write the matrix element of Eq. (14) between the states $|K_0\rangle$ and $\langle K_0 | \psi^{+}(x_0)\,\psi(x'_0)$

$$\langle K_0 | \psi^{+}(x_0)\,\psi(x'_0) \left\{ H_m(E_0 + \hbar\omega)\, b^{+} - b^{+} H_m(E_0) - \hbar\omega b^{+} \right\} | K_0 \rangle = 0 \tag{20}$$

It is easily found that the components h_n with $n \geqslant 3$ do not contribute to the matrix element (20) provided that b^{+} is given by Eq. (4). Indeed, a typical term of Eq. (4) *containing* h_3 has the form

$$\int dx_1 \ldots dx'_4\, h_3(x_1, \ldots x'_3)\, (x_4 | b^{+} | x'_4)$$
$$\times \langle K_0 | \psi^{+}(x_0)\,\psi(x'_0) : \psi^{+}(x_1) \ldots \psi(x'_3) : \psi^{+}(x_4)\,\psi(x'_4) | K_0 \rangle \tag{21}$$

When evaluating the bracket in Eq. (21) with the help of the Wick theorem it should be remembered that the six operators $\psi(x)$ associated with h_3 stand in the normal order, so that no contraction involving any pair of

them can appear. But the four remaining operators are not sufficient to form a C-number out of the product inside the bracket. Thus, the bracket is equal to zero. For the same reason all the other terms with $n > 3$ vanish as well.

If the z-dependence of $H_m(z)$ is weak, then for transitions with small excitation energies Eq. (21) and its analogue with bra and ket exchanging places are reduced to the ordinary equations of the RPA. Writing the model Hamiltonian (6) in normal products it becomes evident that the self-consistent Hamiltonian and effective force operators are given by the following terms of $H_m(z)$ respectively

$$H^{s.c.} = \int d\,x\,d\,x' \frac{\delta h_0}{\delta K(x'\,x)} : \varphi^+(x)\,\psi(x') :$$

$$F = \tfrac{1}{4} \int d\,x_1 d\,x_2 d\,x'_1\,d\,x'_2 \frac{\delta^2 h_0}{\delta K(x'_1\,x_1)\,\delta K(x'_2\,x_2)} : \psi^+(x_1)\,\psi(x'_1)\psi^+(x_2)\psi(x'_2): \tag{22}$$

Eq. (22) is in agreement with the postulates in the Fermi-liquid theory. But the precise definition of the quantities entering Eq. (22), given above, is necessary if the parameters of the effective force are to be evaluated. Moreover, the above derivation suggests that in principle it is possible to go beyond the RPA limits.

3. RENORMALIZATION OF THE FORCE

In accordance with Eqs (18), (22) the self-consistent field and the effective force operators are given by the variational derivatives of the functional

$$E_{pot} = \langle K \left| \left\{ V + V \frac{1 - p_m}{E - H_0} V + V \frac{1 - p_m}{E - H_0} V \frac{1 - p_m}{E - H_0} V + \ldots \right\} \right| K \rangle \tag{23}$$

where $|K\rangle$ is an uncorrelated state belonging to (m), and $V = H - H_0$ includes the interaction potential between free nucleons. We suppose that the matrix elements $\langle K|\psi^+(x)\psi(x')\,V\,|K\rangle$ are finite (but possibly arbitrarily large).

In a particular case, when (m) contains only one configuration (say $|K_0\rangle$), Eq. (23) represents the perturbation series for the energy in a stationary state $|\Psi\rangle = \Omega|K_0\rangle$. Such a limited model space makes it impossible to study transitions, and the above formalism cannot be applied in this case.

The states which are considered in nuclear models are rather numerous and include configurations of one or more shells lying close to the open shell. Accordingly, we assume that the model Hamiltonian H_m is defined in a sufficiently large space of configurations.

Because of the projection operator p_m a number of matrix elements of V do not appear in Eqs (8), (23). This makes it possible to simplify the evaluation of E_{pot} for a many-body system with forces displaying a strong

repulsion at small distances. To show this, we split the interaction potential into short (V_s) and long-range (V_ℓ) parts

$$V = V_s + V_\ell \equiv V\chi(d - r) + V\chi(r - d)$$
$$\chi(\xi) = \begin{cases} 0 & \xi < 0 \\ 1 & \xi \geqslant 0 \end{cases} \tag{24}$$

If the separation distance d is sufficiently small the contribution of V_s to the energy E_{pot} may be found by means of the expansion in powers of the mean nuclear density. Further, for any value of d the number of states included in (m) may be fixed so as to ensure a good convergency of the expansion for E_{pot} in powers of V_ℓ. It is obvious that this number tends to decrease when d is increased. But if d is too large the low-density expansion for the contribution of V_s becomes inapplicable. Thus it is logical to look for such a value of d and definition of (m) that make the evaluation of E_{pot} simple without overcomplicating the diagonalization of H_m owing to the necessity to take into account a great number of configurations.

The nuclear-matter calculations indicate that E_{pot} does not depend on the choice of (m) critically (some remarks on this may be found in Ref. [8]). Thus one may try to estimate the effective force from the data on E_{pot} obtained by using the Brueckner technique.

The effective mass of a quasiparticle in the shell-model Hamiltonian usually coincides with the mass of a bare nucleon. This explains the label of the quantity on the right-hand side of Eq. (23), as here V does not involve the kinetic energy operator. Thus in this case the kinetic energy is not renormalized and, being linear in $K(x, x')$, does not contribute to the effective force

$$F_{12} = \frac{\delta^2 h_0}{\delta K_1 \delta K_2} = \frac{\delta^2 E_{pot}}{\delta K_1 \delta K_2} \tag{25}$$

The relationship between the reaction-matrix and an operator in Eq. (25) may be established by studying the Feynmann diagrams for E_{pot}. It is easy to show that each hole line in a diagram contributes a density-matrix $K(x, x')$, and that variation in K leads to diagrams which are obtained by cutting one of the hole lines in the varied diagram in all possible ways.

Let us define the reaction-matrix G as the sum of all ladder diagrams in which at least one of the two intermediate particle states does not belong to (m). When the density is low the diagrams with only a few hole lines give the largest contribution to E_{pot}. These diagrams are considered in the nuclear-matter calculations and some examples are shown in Fig.3. For instance, diagram 3a is the low-density limit of E_{pot}. Its second variational derivative in K is equal to G. The other diagrams for E_{pot} lead to additional renormalization of the force and make it different from the reaction-matrix.

The renormalization due to many-body processes which are shown in Fig.4 does not coincide with that considered by Brown [1, 8]. Brown takes into account only that process which is specific for a case when

the model space is composed of configurations with the same harmonic-oscillator principal quantum number. This process (see Fig.4d) is connected with the long-range part of the potential. If the orbitals included in (m) belong to more than one major shell this renormalization may be small but there remains another renormalization due to V_s, corresponding to the diagrams b, c, in Fig.4.

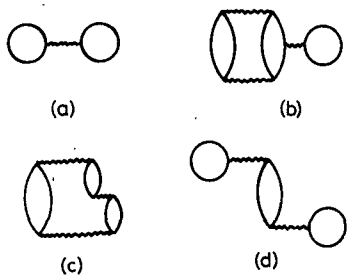

FIG.3. Diagrams for E_{pot}: (a) low-density limit, (b) and (c) three-body terms associated with V_s, (d) a diagram associated with V_ℓ.

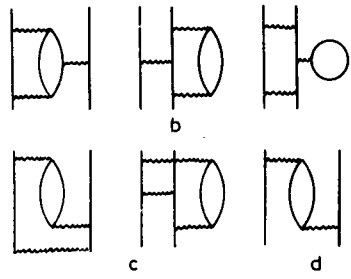

FIG.4. Renormalization of the effective force. Diagrams b, c, d are obtained by cutting two hole lines in the respective diagrams of Fig.3.

The renormalization affects the multipole structure of the force. The diagrams in Fig.3 determine the so-called rearrangement energy. The substantial contribution of the rearrangement effects to the single-particle potential suggests that some of the multipole components of the force may become noticeably changed as a result of the renormalization processes indicated above. The contribution of the rearrangement effects to the low multipole components of the force is now calculated.

4. EFFECTIVE δ-FORCE

One may apply Eqs (23), (25) to determine the parameters of an effective δ-force using the available data on the saturation energy and compressibility in nuclear matter [10]. This force is connected with the local term in the nuclear self-consistent potential

$$F_{loc} = \frac{\partial U_{loc}}{\partial \rho}\,\delta(\vec{r}_1 - \vec{r}_2) = \frac{\partial^2 \epsilon}{\partial \rho^2}\,\delta(\vec{r}_1 - \vec{r}_2) \qquad (26)$$

Here U_{loc} and ϵ are respectively the local potential and binding energy per unit volume in nuclear matter, and ρ is the particle density.

The density dependence of saturating potentials $U_{loc}(\rho)$ causes the coefficient at the δ-function in Eq. (26) to depend on the density too. In this sense the force (26) resembles the scattering amplitude in the Migdal theory [2]. Indeed one of the coefficients of the scattering amplitude includes the term which is linear in ρ. One obtains this dependence if

$$\epsilon_{pot} = -a\rho^2 + b\rho^3. \tag{27}$$

In Eq. (27) two constants a and b may be chosen so that Eq. (27) would give correct values of the saturation density (ρ_0) and the binding energy $\epsilon_{pot}(\rho_0)$. Parameters of the force corresponding to this choice are given in Table I together with some other data on the force.

The application of the Thomas-Fermi method in evaluating the nuclear potential [16] shows that unlocal terms in E_{pot} are important in the description of the surface. According to Ref. [16]

$$\epsilon_{pot} = -a_1\rho^2 + a_2\rho^{8/3} + a_3(\nabla\rho)^2 \tag{28}$$

where a_i are empirical parameters. The last term in Eq. (28) gives rise to a velocity-dependent term in the effective force. If the nuclear transition is described in terms of the Time-dependent Hartree-Fock (TDHF) theory one may conclude that each of the two states is characterized

TABLE I. ZERO-RANGE EFFECTIVE FORCE

	Col.	1	2	3
f_0	external	-3	-2.5	-1.4
	internal	1	0.45	0.15
g_0	external	0.5	-	0.3
	internal	0.5	-	0.1
f_0'	external	0	-	-0.22
	internal	0.3	-	0.62
g_0'	external	0.5	-	-0.05
	internal	0.5	-	0.45

The parameters of the force

$$F = \delta(\vec{r}_1 - \vec{r}_2)\{f_0 + g_0\vec{\sigma}_1\cdot\vec{\sigma}_2 + [f_0' + g_0'\vec{\sigma}_1\cdot\vec{\sigma}_2]\vec{\tau}_1\cdot\vec{\tau}_2\}$$

from Ref. [2] (column 1) are compared with the estimates in Ref. [10]. In column 2 the values are given which correspond to $E_{pot}(\rho)$ in Eq. (27) and saturation conditions E_{bind} = 15 MeV/nucl. T_F = 35 MeV. The force in column 3 is obtained by using the nuclear-matter calculations in Ref. [17] with the Bressel-Kerman force between free nucleons. The force in column 3 acts in the relative S-wave of the colliding particles only. The quantities are given in units of $2/3\,(T_F/\rho_0)$ = 320 MeV fm^3.

by a functional dependence $(\nabla\rho)^2 = f(\rho)$. Now, if the function $f(\rho)$ is the same for both states, then the force corresponding to Eq. (28) may be written in the form

$$F = \delta(\vec{r}_1 - \vec{r}_2)\left\{-2a_1 + \frac{40}{9}a_2\rho^{2/3} + f''(\rho)\right\} \qquad (29)$$

In Ref. [10], $f(\rho)$ is such that the radial distribution $\rho(r)$ is given by the Saxon-Woods formula $\rho = \rho_0\{1+\exp[(r-R)/b]\}^{-1}$. Figure 5 shows the radial dependence of the coefficient in the effective δ-force obtained in this way.

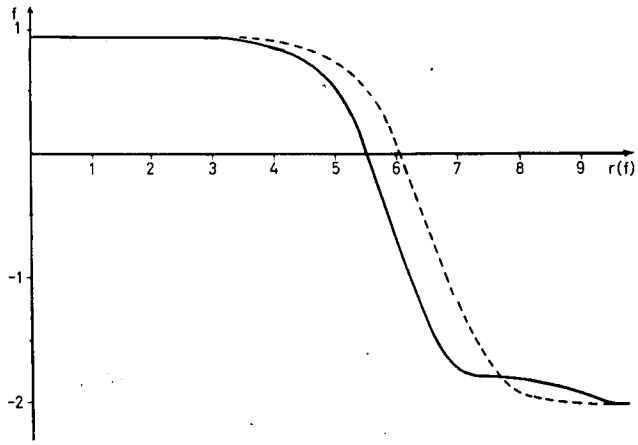

FIG.5. Radial dependence of the zero-range effective force for ^{208}Pb. Normalization as in Table I.

The spin-isospin dependence of the force can be determined if the contribution of different S, T states of colliding particles to E_{pot} is known. This information can be found, for example, in Ref. [17]. The values of the force corresponding to these data are given in Table I.

The force in Ref. [10], although somewhat similar to the scattering amplitude in Ref. [2], differs from it in many details. If applied to the muon capture in ^{16}O and ^{40}Ca this force leads to satisfactory capture rates in states 0^- and 1^- of the daughter nuclei [9]. However, the calculated capture rate in state 2^- is more than twice as big as the experimental value. Thus the estimates of Ref. [10] should be corrected. It may be noted here that the failure to describe this particular transition is common to some other approaches which use the force calculated from the data on the scattering of free nucleons.

5. CONCLUDING REMARKS

The detail which distinguishes the formalism described in Sections 2 and 3 from that used in the Brueckner theory is that a number of states are excluded from the equations for the reaction-matrix and E_{pot}. Apparently, the changes in these quantities due to the exclusion are negligible. But the

new definition simplifies the establishment of relations between two-nucleon scattering data and parameters in nuclear-structure models.

The above discussion is concerned with nuclei having no pairing correlations. Pairing effects may be accounted for by anomalous contractions $\mu = \langle BCS | \psi(x)\, \psi(x') | BCS \rangle$ in the definition of a normal product. This modification of the theory makes it possible to study transitions in which a pair of nucleons is transferred to or from a nucleus. The frequencies of such transitions are determined by the variational derivatives of h_0 in μ. The second derivative in μ defines a force which is much closer to the operator considered in Ref. [8] than the force which describes transitions in a particular nucleus.

ACKNOWLEDGEMENTS

This paper has been the subject of many useful discussions which I have had with Drs. Z. Bochnacki and W. Rybarska, and also with E.B. Balbutzev and I.M. Holban, to whom I am glad to acknowledge my sincere gratitude.

REFERENCES

[1] BROWN, G., Unified Theory of Nuclear Models and Forces, North-Holland, Amsterdam (1967).
[2] MIGDAL, A.B., these Proceedings; see also Quasiparticles in Nuclear Theory, Enrico Fermi Summer School, Varenna (1965).
[3] LANE, A.M., Nuclear Theory, Benjamin, New York-Amsterdam, (1964). (Russian transl., Moscow, 1967).
[4] ROWE, D.J., Microscopic collective theories, Fundamentals in Nuclear Theory, IAEA, Vienna (1967) 531.
[5] BROWN, G.E., these Proceedings.
[6] MOSZKOWSKI, S.A., these Proceedings.
[7] KALLIO, A., KOLTVEIT, K., Nucl. Phys. 53 (1964) 87.
[8] KUO, T., BROWN, G.E., Nucl. Phys. 85 (1966) 40; A92 (1967) 481.
[9] RHO, M., Muon Capture in Nuclei and Migdal Theory, Lectures at the Summer School, McGill Univ., Canada (1967).
[10] BOCHNACKI, Z., HOLBAN, I.M., MIKHAILOV, I.N., Nucl. Phys. A97 (1967) 33.
[11] LANDAU, L.D., Zh. eksp. teor. Fiz 30 (1956) 1058; 32 (1957) 59.
[12] ABRIKOSOV, A.A., GORKOV, A.P., DZYALOSHINSKY, I.E., Methods of Quantum Field Theory in Statistical Physics, Fiz. Mat. GIZ, Moscow, 1962.
[13] MIKHAILOV, I.N., Preprints JINR P4-3873, P4-3849, Dubna, (1968).
[14] BLOCH, C., HOROWITZ, J., Nucl. Phys. 8 (1958) 91.
[15] THOULESS, D., Quantum Mechanics of Many-Body Systems, Pergamon Press (1962). (Russian transl. Moscow, 1964).
[16] KUMAR, K., COUNTEUR, K.H., ROY, M.K., Nucl. Phys. 42 (1963) 529; 60 (1964) 634.
[17] BHARGAVA, P.C., SPRUNG, P.W.L., Ann. Phys. 42 (1967) 222.

DISCUSSION

C.F. CLEMENT: I would like to make a comment concerning the effective δ-function interaction shown by Professor Mikhailov. Such a form for the interaction is often used in nuclear reaction theories, particularly at high energies. From comparison with experiments there is a considerable amount of information in the literature on the values of the parameters of the interaction.

D.J. ROWE: I should like to comment that regardless of the nature of the true effective interaction it is sometimes justifiable to replace it with a single schematic interaction. For example, consider the static Hartree-Fock problem: the self-consistent field may be written

$$u_0(r) = \int V(r, r')\rho_0(r')\, d\vec{r},$$

$$\propto u_0(r) \int u_0(r')\, \rho_0(r')\, d\vec{r}'$$

where ρ_0 is the static density. Thus we see that, for the Hartree-Fock problem, we could make the substitution

$$V(r, r') \propto u_0(r)\, u_0(r')$$

Of course, both u_0 and V should be non-local, and one can make them so, thereby including exchange and everything else.

The useful application of this concept comes when we apply it to the RPA (*Random Phase Approximation*). Since the RPA is equivalent to Time-Dependent Hartree-Fock theory, all interactions which generate the same time-dependent self-consistent field are equivalent. Writing the time-dependent part of the field

$$u(r;t) = \int V_{res}(r, r')\, \rho_1(r';t)\, d\vec{r}'$$

we again find that the residual interaction V_{res} can be represented as a separable interaction. If we suppose that the <u>field</u> oscillation is volume conserving, we obtain

$$V_{res}(1, 2) = \chi\, r_1 \frac{du_0}{dr}(1) \cdot r_2 \frac{du_0}{dr}(2) \sum_{\lambda\mu} y^*_{\lambda\mu}(\theta_1) \cdot y_{\lambda\mu}(\theta_2)$$

$$= \chi\, r_1 \frac{du_0}{dr}(1) \cdot r_2 \frac{du_0}{dr}(2) \quad \delta(\Omega_{12})$$

Let us consider two possibilities. (1) If the static field u_0 is approximated by a harmonic oscillation potential

$$r \frac{du_0}{dr} \propto r^2$$

and the $\lambda = 2$ component of the above interaction becomes the often used $P^{(2)}$ force. (2) If u_0 is approximated by a square well, then

$$r \frac{du_0}{dr} \propto \delta (r - R_0)$$

and we have the SDI (Surface-Delta Interaction). For a more realistic well, such as a Woods-Saxon potential, we obtain a radial dependence intermediate between those of the $P^{(2)}$ and SDI interactions, i.e. peaking at the nuclear surface but with a finite width.

EFFECTIVE NUCLEAR FORCES

G.E. BROWN
STATE UNIVERSITY OF NEW YORK AT STONY BROOK,
STONY BROOK, LONG ISLAND, N.Y.,
UNITED STATES OF AMERICA

Abstract — Аннотация

EFFECTIVE NUCLEAR FORCES. Calculation of effective forces in nuclei from the Hamada-Johnston potential is described. This work begins from the theories of Brueckner and Bethe and applies them to finite systems. Various renormalizations of the force are discussed. The density dependence of the effective forces is considered in detail. Arguments for the partial breakdown of the shell model in heavy nuclei are given.

ЭФФЕКТИВНЫЕ ЯДЕРНЫЕ СИЛЫ. Дается описание расчета эффективных сил в ядрах с потенциалом Хамады-Джонстона. Работа берет начало от теории Бракнера и Бэтэ, которая применяется к конечным системам. Обсуждаются различные перенормировки сил. Подробно рассматривается зависимость плотности эффективных сил. Даются аргументы для различного нарушения оболочечной модели в тяжелых ядрах.

1. INTRODUCTION

The calculation of effective forces in nuclei from the nucleon-nucleon force is one of the most fundamental problems in nuclear physics. In past years, it has received considerable attention, and I shall review the results of those investigations based on the theory of Brueckner and Bethe. Quite frankly, I shall cover mainly the work of Dr. T.T.S. Kuo and myself. Other groups have put parts of the calculations into more aesthetic forms, but they have not, in general, made such complete calculations.

Let me say, at the outset, that we believe that we can calculate directly the effective force between nucleons in the nucleus from the force between two isolated nucleons. The effective force is, of course, different from the latter. It contains effects from the Pauli Principle, many-body effects, and those from polarization of the nucleus. We believe these to be calculable to a reasonable accuracy.

In philosophy, this approach is nearly the opposite of that of Professor Migdal and his co-workers. We have no adjustable parameters. The procedure used was set down in detail by Kuo and Brown [1] for ^{18}O and ^{18}F and, as regards the effective particle-particle interaction, has not been changed since. The theory is, however, by no means closed, and it is not clear that higher-order terms are negligible. Bethe's work [2] on the theory of nuclear matter shows that the expansion is in powers of a parameter

$$\kappa = \rho \int \chi^2 \, d\tau \qquad (1)$$

where ρ is the density and $\int \chi^2 \, d\tau$ is the volume of the "hole" made in the wave-function by the two-body interaction. For two-body forces in current

use, $\kappa \simeq 0.2$, so that the expansion should be good. However, in many cases, the lowest-order term nearly vanishes, so that the correction of next order changes the results drastically. In a sense, one simply has to use the theory, see where it works, see where higher-order terms are important.

In practice, how we describe nuclear phenomena is not much different from the way in which Migdal and his collaborators describe them and, in fact, not much different from the way people have been describing them for years. We arrive at a relatively short-range, bare interaction, not unlike Migdal's effective interaction, and we obtain P_2-forces from polarization of the medium, as does Migdal and his group. We differ in one important respect, which I shall discuss later; namely, our interaction in singlet states is almost independent of density, whereas Migdal's is extremely density-dependent. Finally, we differ in the amount of work we have to do; undoubtedly our approach requires much more computation. But we feel that this is a fundamental problem, and that it is well worth letting the computers grind a bit in order to try to solve it.

2. DEVELOPMENT

In Fig. 1, I show my characterization of the development of a theory of effective forces. This consists of many links, not one of which (with the possible exception of "experiment") is in really good shape, yet all seem to hang together.

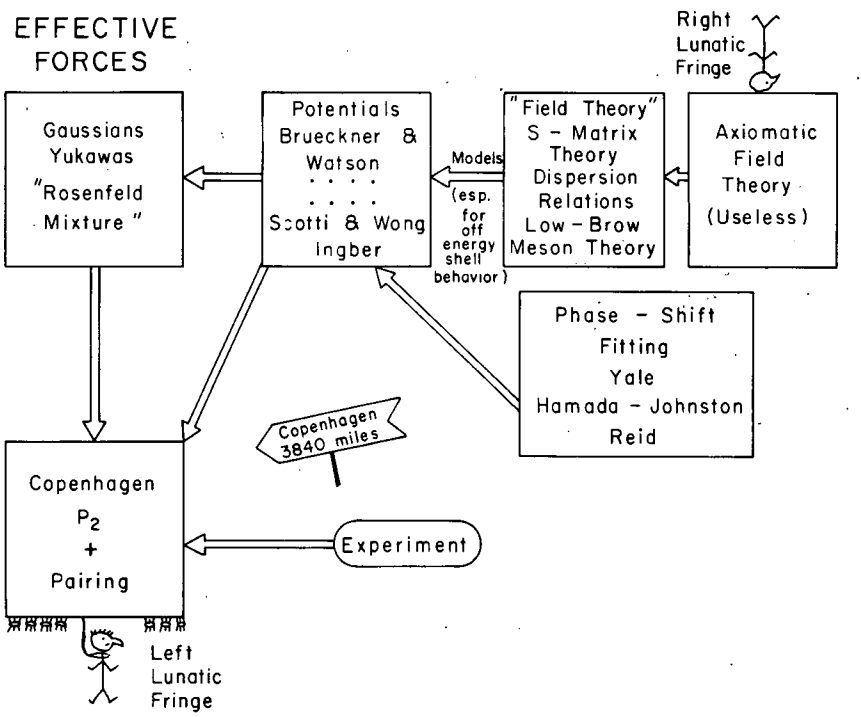

FIG. 1. Characterization of the calculation of effective forces.

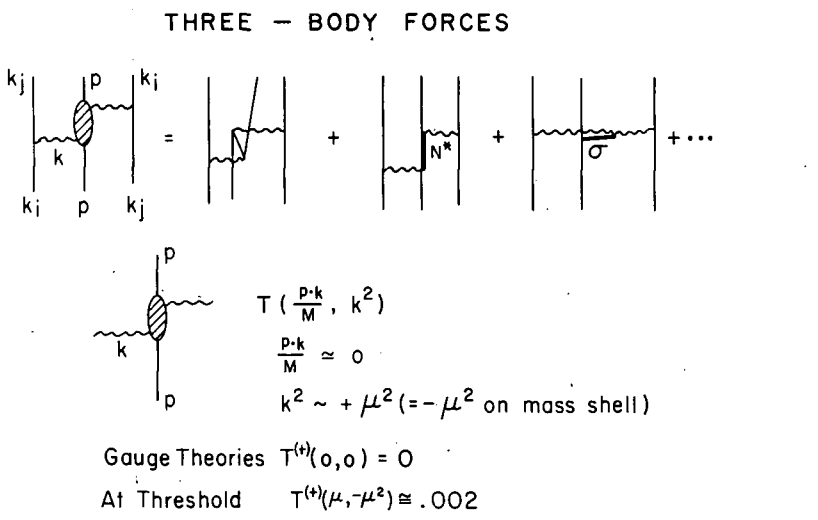

FIG. 2. Treatment of three-body forces. The process by which the virtual pion excites the middle nucleon to an excited state (N^*, σ, etc.) or creates a virtual pair can be viewed as the scattering of a virtual pion off its mass shell. The low-energy external nucleons constrain the energy of this pion ($p \cdot k/M$ in terms of four-vectors) to be $\cong 0$. Typical values of k are $|\mathbf{k}| \cong \mu c$, $k_0 \cong 0$ giving $k^2 \sim \mu^2$ in nuclear matter.

The question of whether there are large three-body forces in nuclei has received a somewhat definite "no" as an answer in the past year. As shown in Fig. 2, the long-range part of the three-body force can be visualized as arising from the scattering of a virtual meson, involving the excitation of an intermediate nucleon to an isobar, etc. We have learned from PCAC and gauge theories of pion interactions that the isospin symmetric part of that scattering amplitude must vanish for particular values of the two invariants involved. These values are not far from those of interest in nuclear matter and in the nucleus. Furthermore, there are good indications that this scattering amplitude extrapolates smoothly to the values required in the three-body problem [3]. Although more work needs to be done, I feel that the three-body forces cannot be large, on the basis of these arguments.

In Fig. 3 is shown the general scheme of calculation in the Brueckner-Bethe method. The two-nucleon potential has a hard core, so that one must use some scheme to "regularize" it. This scheme is based on the method of Moszkowski and Scott [4], who recognized that the short-range part of the potential will act in nuclear matter or in nuclei very much as it does between two isolated particles. The potential in this region is so strong, that only high-lying intermediate states are involved, of energy $E \sim 300 - 500$ MeV, so that the Pauli Principle is just not important. The reaction matrix G can then be written in a series involving the reaction matrix G_s for the short-range part of the potential, and the long-range part of the potential V_ℓ. The separation is made so that in zeroth approximation, G_s does not contribute to the matrix elements. Now V_ℓ is determined pretty well by the nucleon-nucleon scattering data. Where off-the-energy-shell information comes in, is the so-called dispersion correction. This is not large, of the order of 10% in typical matrix elements for forces used

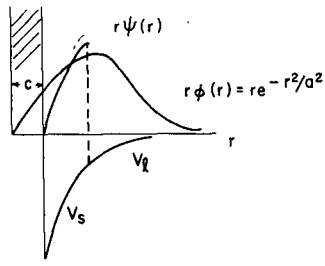

$$G = V_\ell + G_S - 2V_\ell \frac{Q}{e} G_S - V_\ell \frac{Q}{e} V_\ell - \cdots$$

$$G_S = V_S - V_S \frac{Q}{e} G_S$$

$$G_S^{(0)} = V_S - V_S \frac{1}{e^{(0)}} \cdot G_S^{(0)}$$

Dispersion Correction

$$(\phi, G_S^{(0)} \left(\frac{Q}{e^{(0)}} - \frac{Q}{e}\right) G_S \phi) = \boxed{2\bar{u}\int (\phi - \psi)^2 d\tau}$$

Minimal Relativity

Waste Basket

FIG.3. Scheme of calculation with the G-matrix. Off-energy shell effects come almost completely in the dispersion correction, which is ~ 10% of the main term for typical potentials used. Introducing relativistic phase-space factors into the theory seems to cut it down even more.

HAMADA-JOHNSTON POTENTIAL

$$V = V_c + V_T S_{12} + V_{LS} (L \cdot S) + V_{LL} L_{12}$$

$$L_{12} = (\sigma_1 \cdot \sigma_2) L^2 - \frac{1}{2} \left\{ (\sigma_1 \cdot L)(\sigma_2 \cdot L) + (\sigma_2 \cdot L)(\sigma_1 \cdot L) \right\}$$

$$V_c = 0.08 \left(\frac{1}{3}\mu\right)(\tau_1 \cdot \tau_2)(\sigma_1 \cdot \sigma_2)\, Y(x) \quad [1 + a_c Y(x) + b_c Y^2(x)]$$

$$V_T = 0.08 \left(\frac{1}{3}\mu\right)(\tau_1 \cdot \tau_2)\, Z(x) \quad [1 + a_T Y(x) + b_T Y^2(x)]$$

$$V_{LS} = \mu G_{LS} Y^2(x) \quad [1 + b_{LS} Y(x)]$$

$$V_{LL} = \mu G_{LL} x^{-2} Z(x) \left[1 + a_{LL} Y(x) + b_{LL} Y^2(x) \right]$$

$$Y(x) = e^{-x}/x\,, \quad Z(x) = (1 + 3/x + 3/x^2)\, Y(x)$$

FIG.4. Hamada-Johnston potential [5]. Here μ is the pion mass, $x = \mu r$ is the radial coordinate measured in units of the pion Compton wavelength. The values of the parameters can be found in the paper.

P_2 Force

$$V_{12} = -\chi_\lambda \frac{\gamma^\lambda}{(2n+\ell+\frac{3}{2})^\lambda} r_1^2 r_2^2 P_2 (\cos\theta_{12})$$

Pairing

$$((j_a j_b)^J \mid V_{pair} \mid (j_c j_d)^J) = -\delta_{J0} \sqrt{2j_a+1}\sqrt{2j_c+1} \frac{G}{2}$$

FIG. 5. Definition of P_2 and pairing fa$\sqrt{2j_a+1}\sqrt{2j_c+1}$

so far. In fact, we have an argument that if one puts in a "minimum" amount of relativity (to ensure relativistic unitarity along the elastic cut), then this correction will be even smaller. This correction is the only strongly model-dependent part of the problem; the other parts are determined well by the nucleon-nucleon scattering and by the properties of the deuteron. But this correction can vary quite a bit if, for example, one changes from a force with a hard core to one with a soft core.

Fig. 4 shows the Hamada-Johnston potential used in our calculations. The parameters entering into it are fitted so as to reproduce the nucleon-nucleon scattering data as best possible. Had we used the Yale potential, or other current potentials, our results would not have been much different, as we checked in some isolated cases.

The traditional P_2 plus Pairing forces are shown in Fig. 5. As is well known, with just these two effective interactions, and with coefficients which vary in a reasonable way throughout the periodic table, it is possible to give not only a qualitative, but also a semiquantitative description of most nuclear spectra. Our job is, then, to show how effective forces of this nature arise from a rather complicated two-nucleon potential, like the Hamada-Johnston one which we displayed.

Of course, the bare G-matrix interaction, when expanded in multipoles, has some P_2 component. Baranger and Kumar [6] have analysed this and find the amount of P_2 force here to be about one half of that required to fit the data. We have found [7] that the renormalization (Fig. 6) of the inter-

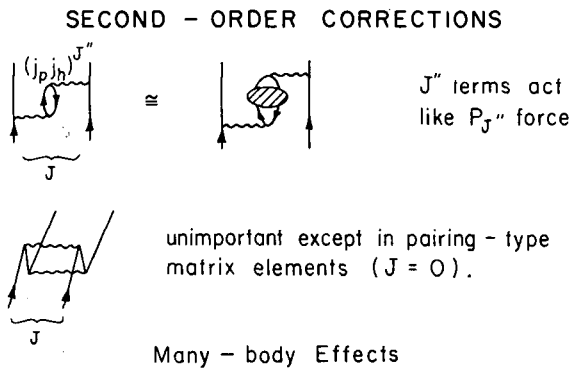

FIG. 6. Second-order contributions to the effective interaction.

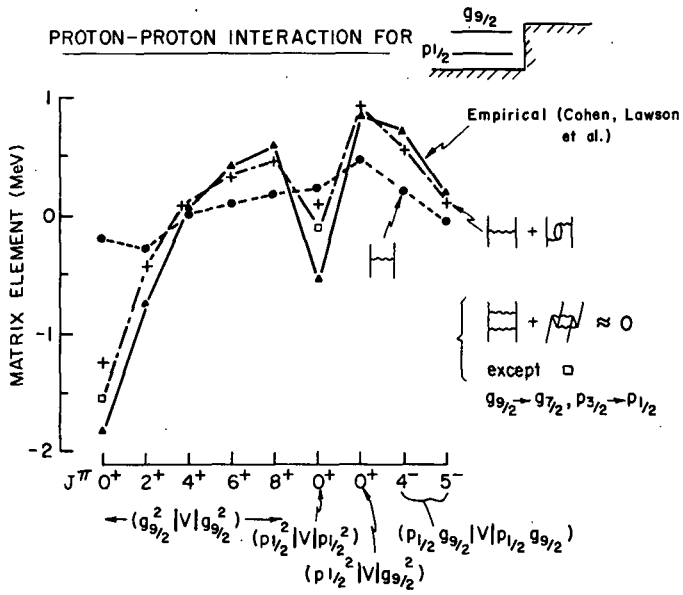

FIG. 7. Comparison of calculated and empirical proton-proton matrix elements in the Zr region. Empirical matrix elements were obtained in Ref. [9].

action through polarization of the medium contributes a large part of the P_2 force, as we shall discuss. This is a situation in which one of the particles excites a particle out of the core, which de-excites in interaction with the second particle. All particle-hole excitations of unperturbed energy $2\hbar\omega$, where $\hbar\omega$ is the oscillator splitting, are included here. Krainov and Malov [8] come to similar conclusions within the generalized

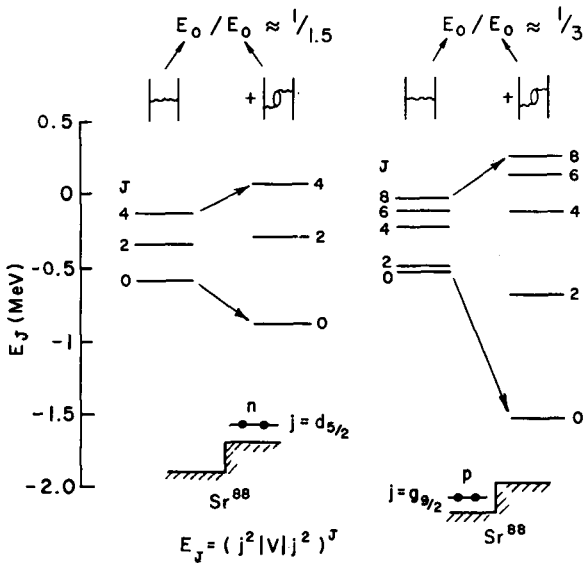

FIG. 8. Effects of the core polarization for nuclei in the Zr region.

framework of the Migdal theory. In this theory, although one begins with a zero-range phenomenological interaction, introduction of polarization processes such as shown in Fig. 6 leads to long-range components in the effective force, the main one being the P_2 component.

In Fig. 7 we show how the inclusion of the polarization improves the agreement between calculated effective matrix elements and the data. Other second-order corrections are rather smaller than that from core polarization. In Fig. 8 we see, in a typical case, that the inclusion of the core polarization "opens out" the spectra, pushing the 0^+ level down, the levels of highest angular momenta up. This latter effect is extremely important in the spectra of systems with many valence particles, since

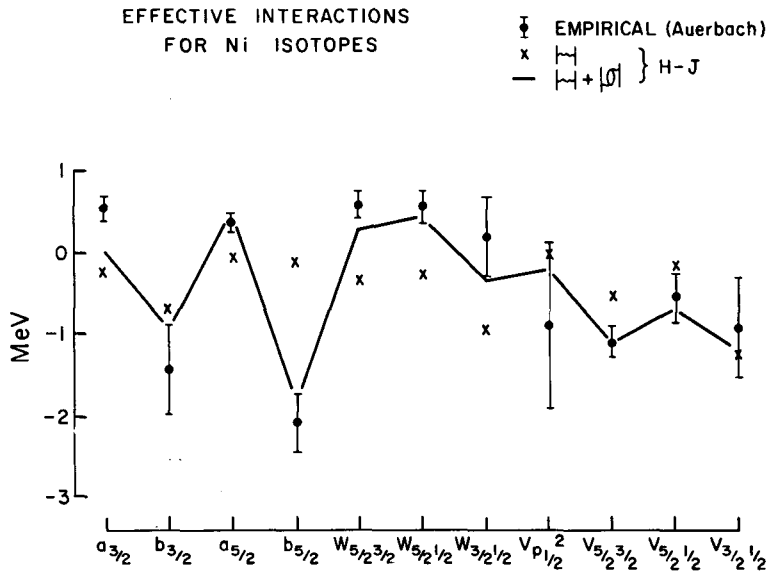

FIG. 9. Comparison of calculated and empirical matrix elements in the Ni isotopes. The $a_{3/2}$, $b_{3/2}$, etc. are combinations of matrix elements which Auerbach [11] found convenient to use in parameterizing the spectrum.

the E_J tend to enter here with a statistical factor of (2J+1). Talmi has emphasized for years (see, for example, Ref. [10]) that the coefficient of n(n-1) in the expression for the ground-state energy of a system of identical particles filling a given subshell is repulsive. Such a repulsive term emerges from the calculations only after inclusion of the core polarization.

In Fig. 9 we show the comparison between calculated matrix elements and empirical ones, derived directly from known energies of levels in the Ni isotopes. In Fig. 10, the contribution of the core-polarization with J" = 2, that part contributing to the P_2 force, to various matrix elements is shown and compared with the contribution from the P_2 force chosen by Kisslinger and Sorensen [12]. In Fig. 11 we tabulate the strengths of P_2 and P_4 multipole forces which would give the same matrix elements as those found in the core-polarization contribution. It is seen that they correspond quite well to the value of 125/A, that usually chosen for the

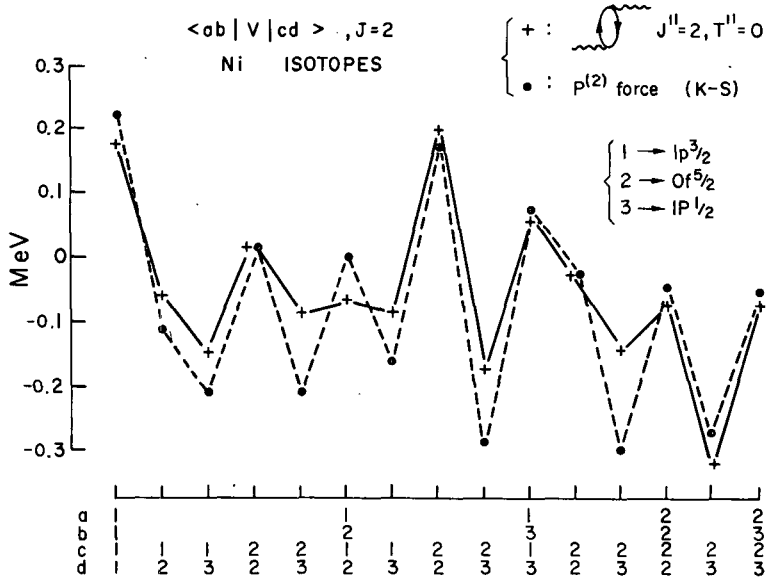

FIG.10. Comparison of the contribution of the "bubbles" in which the particle and hole are coupled to J" = 2, T" = 0 matrix elements in the Ni region with that from the P_2 force used by Kisslinger and Sorensen [12].

empirical P_2 force. In fact, we are a bit embarrassed by a surfeit of P_2 force, since this represents only the contribution from the core polarization, and inclusion of the P_2 component of the bare interaction would increase the total P_2 force by ~50%.

In Fig. 12 we show that our calculations give a large pairing component. After inclusion of the core polarization it is larger, in general, than the pairing interaction chosen by Kisslinger and Sorensen.

Calculated Strengths Of Equivalent Multipole Forces

$$H_\lambda = -X_\lambda \frac{\gamma^\lambda}{(2n+\ell+3/2)^\lambda} r_1^\lambda r_2^\lambda P_\lambda(\cos\theta_{12})$$

Nucleus	j	X_2	125/A	X_4
O^{18}	$0d_{5/2}$	4.24	6.95	2.48
Ca^{42}	$0f_{7/2}$	3.14	2.98	2.44
Ni^{58}	$1P_{3/2}$	1.82	2.15	0
	$0f_{5/2}$	3.88		3.60
Zr^{92}	$1d_{5/2}$	1.13	1.36	.94

FIG.11. Strengths of P_2 and P_4 forces which would give the same contributions to matrix elements $((j^2)^J | V_{eff} | (j^2)^J)$ for various j.

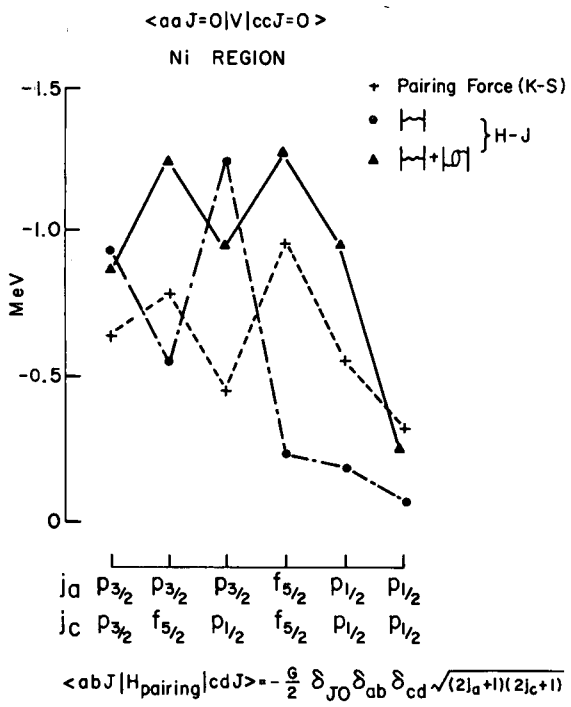

FIG. 12. Comparison of calculated pairing components with those obtained from the pairing force used by Kisslinger and Sorensen [12].

Just to show how well the calculated matrix elements fit the empirical energy levels in "good" cases, we show in Fig. 13 the results of a complete diagonalization in the s-d shell for ^{20}Ne by Flores and Perez [13].

In the calculations summarized above, the effective force employed was that calculated for an average density, and it was then used as a density-independent force. Since matrix elements between nodeless shell-model states were the most important ones, in general, this seemed to be an adequate approximation. Clearly it would be disastrous to use such forces for calculating nuclear saturation, or effects connected with the nuclear compressibility, however.

One such effect is the isotope shift. The main contributions to this come from protons making a virtual transition through interaction with the added neutron from an initial nodeless state, denoted by p_i in Fig. 14, to a final state with one node. Because of this node, contributions from inner and outer regions of the nucleus tend to cancel. One can say that when the added neutron is in the interior, it tends to pull protons in; when on the surface, it tends to pull them out. Whereas the latter should predominate, to produce the observed isotope shift, with a density-independent force the effect either vanishes, or goes in the wrong direction.

To get the right magnitude for this effect, Migdal and collaborators used an interaction with such a density dependence that it was repulsive in the interior of the nucleus and attractive on the surface [14].

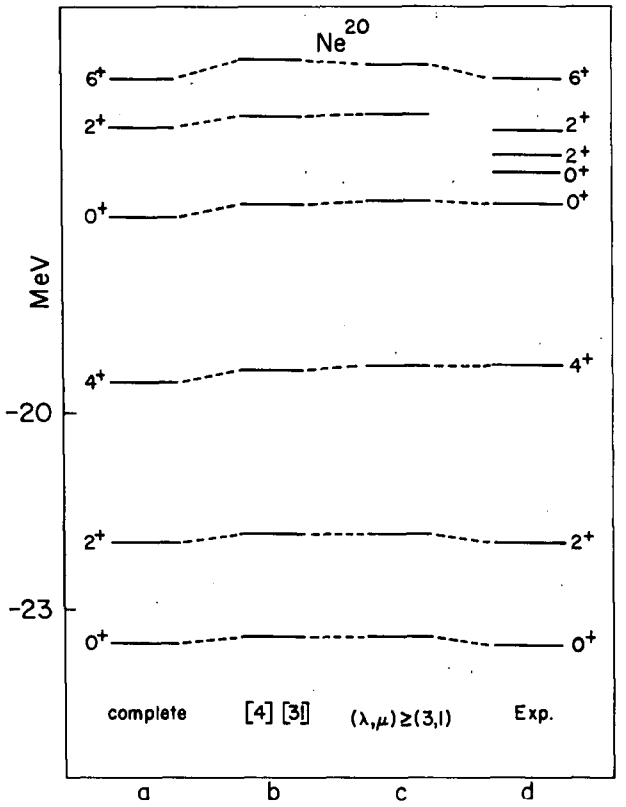

FIG. 13. Comparison with experiment of the results of a complete diagonalization in the s-d shell using the Kuo-Brown forces [1]. The [4], [31] and (λ, μ) are U(4) and SU(3) quantum numbers, respectively. The second column was obtained when the U(4) symmetry was restricted to [4] and [31] and the third column was obtained under the restriction in SU(3) quantum numbers shown.

Such effects have led to a more detailed consideration of the density dependence within the framework of the Brueckner-Bethe theory. This density dependence comes from various sources, but mainly from the term

$$V_\ell \frac{Q}{e} V_\ell$$

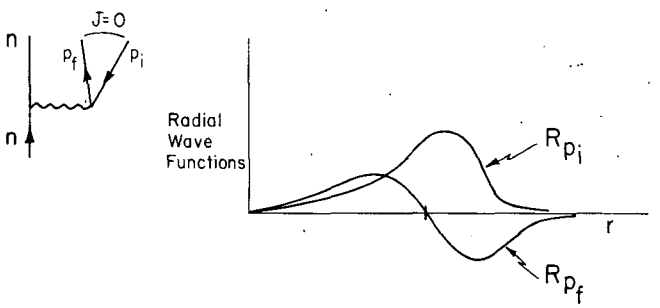

FIG. 14. Characterization of the matrix element entering into the isotope shift.

in the G-matrix, almost the entire contribution coming here from the long-range part of the two-body tensor force. Bethe [15] has suggested that the entire density dependence could be mocked up in a particularly simple way, by using

$$G = \beta_S \left[1 - \alpha_S \rho^{2/3}(R)\right] V_\ell(r)$$

for the G-matrix. Here r is the relative coordinate of the two interacting particles; R is the centre-of-mass coordinate; α_S and β_S are constants, determined separately for S = 0 and S = 1 states, so as to reproduce the singlet and triplet contributions to the binding energy of nuclear matter at various densities, as calculated from more elaborate forces; V_ℓ is a central force, similar to the V_ℓ defined in Fig. 3. The above approximation to G is used only in relative S-states.

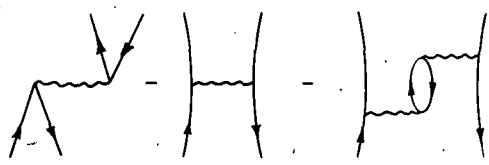

FIG. 15. Particle-hole interaction inclusive of the "bubble" term.

Fits to the binding energy from forces such as the Hamada-Johnston, or newer potentials, give large values for α_1, the coefficient relevant to the triplet case, mirroring the large density dependence produced by the tensor force [15]. However, α_0 is small, and here is a major difference between this approach and that of Migdal, who has the same density dependence in triplet and singlet states. When rearrangement terms are included, it looks like the above density dependence is adequate to account for the isotope shift [17].

Does the general success in calculating effective interactions reviewed above mean that everything is in order? Not exactly. One runs into trouble, of quite a general nature, in calculating vibrations in which protons move against neutrons in heavy nuclei. In ^{208}Pb, for example, the calculated giant dipole state comes out at ~11 MeV, whereas empirically it occurs at ~14 MeV. That the calculated state came too low was already found by Gillet, Green and Sanderson [18] who used a phenomenological finite-range interaction, the parameters of which were determined from fits to levels in light nuclei. Our calculations with the G-matrix give roughly the same results as theirs. One might think that this failure of ours is due to poor convergence of our expansion for the effective force. Dr. Kuo has carried out the dipole state calculation with the "bubble" term included in the interaction, as shown in Fig. 15. This additional term is known as the "self-screening of the exchange term" in the case of the electron gas. Such a calculation involves 175 000 matrix elements of the bare G-matrix, when all particle-hole states of unperturbed energy $2\hbar\omega$ are included in the "bubble"! The inclusion of such higher-order terms changes the calculated distribution of dipole strength only negligibly.

Well, one could say that we are completely on the wrong track and that the calculation of effective forces just fails here. However, Petersen and Veje [19] show in a simple and straightforward way that if one schematizes the interaction involved here as

$$\frac{1}{2}\sum_{i,j}(\kappa_0+4\kappa_1 t(i)\cdot t(j))\sum_{\mu} r_i Y_{1\mu}(i)\, r_j Y_{1\mu}{}^*(j),$$

i.e. represents it as a dipole-dipole interaction, then one needs a ratio $a=-\kappa_1/\kappa_0=2$, a surprisingly large value, to get the dipole state at the right energy. If one assumes the oscillating dipole field to be of the same isospin structure as the central nuclear field, one finds $a\simeq 0.5$.

On the other hand, the two-fluid model of Steinwedel and Jensen [20] obtains a reasonable energy for the dipole excitation. In this model, one considers oscillations in the proton fluid $\delta\rho_p$, the restoring force being the symmetry energy. Now, Steinwedel and Jensen use the boundary condition $\delta\rho_p(R)=0$, where R is the nuclear radius. This is a completely different situation from that of the RPA description, where protons oscillate rather freely back and forth over neutrons in the nuclear surface. Bohr and Mottelson have pointed out that the success of the Steinwedel-Jenson model may indicate that protons and neutrons are glued together somewhat more strongly in the surface than in the shell-model description. Clustering into α-particles could produce this sort of situation. There is further evidence on this point from the small isospin admixture in low-lying 2^+ and 3^- vibrations [21].

In any case, when our calculation fails so badly as in the case of the giant dipole state in ^{208}Pb, we are led to reassess the model. Of course, if one were using a phenomenological force, one might be able to just crank up the strength until the dipole state was brought high enough, and various people have done this with zero-range forces. However, I believe our way of calculating effective forces to be well founded and fairly accurate, giving bare G-matrix elements to an accuracy of ~10-15%, and I see no way of running them up a factor of 2. If one did, all sorts of other disagreements would appear, especially in lighter elements.

In summary, I believe that the derivation of effective forces in nuclei from the nucleon-nucleon force is a basic problem which we have gone some way towards solving. If one knows the effective forces, one eliminates one major source of ambiguity and can concentrate on sorting out which configurations or models to use.

REFERENCES

[1] KUO, T.T.S., BROWN, G.E., Nucl. Phys. 85 (1966) 40.
[2] BETHE, H.A., Phys. Rev. 138B (1965) 804; see also BRANDOW, B.H., Rev. mod. Phys. 39 (1967) 771.
[3] BROWN, G.E., GREEN, A.M., GERACE, W.J., Nucl. Phys. (to be published).
[4] MOSZKOWSKI, S.A., SCOTT, B.L., Ann. Phys. 11 (1960) 65.
[5] HAMADA, T., JOHNSTON, I.D., Nucl. Phys. 34 (1962) 382.
[6] BARANGER, M., KUMAR, K., Nucl. Phys. A110 (1968) 490.
[7] BROWN, G.E., KUO, T.T.S., Nucl. Phys. A92 (1967) 481.
[8] KRAINOV, V.P., MALOV, V.V., Yadernaya Fiz. 6 (1967) 252.

[9] COHEN, S., LAWSON, R.D., MACFARLANE, M.H., SOGA, M., Phys. Lett. 10 (1964) 195.
[10] TALMI, I., Rev. mod. Phys. 34 (1962) 704.
[11] AUERBACH, N., Nucl. Phys. 76 (1966) 321.
[12] KISSLINGER, L., SORENSEN, R.A., Mat. Fys. Medd. Dan. Vid. Selsk. 32 9 (1960); Rev. mod. Phys. 35 (1963) 853.
[13] FLORES, J., PÉREZ, R., Phys. Lett. 26B (1967) 55.
[14] BUNATYAN, G.G., MIKULINSKII, M.A., Yadernaya Fiz. 1 (1965) 38; KRAINOV, V.P., MIKULINSKII, M.A., Yadernaya Fiz. 4 (1966) 928.
[15] BETHE, H.A., Proc. Int. Conf. Nuclear Physics, Gatlinburg, Tennessee (1966).
[16] GREEN, A.M., Phys. Lett. 24B (1967) 384.
[17] LANDE, A., MOLINARI, A., BROWN, G.E., Nucl. Phys. (to be published).
[18] GILLET, V., GREEN, A.M., SANDERSON, E.A., Nucl. Phys. 88 (1966) 321.
[19] PETERSEN, D.F., VEJE, C.J., Phys. Lett. 24B (1967) 449.
[20] STEINWEDEL, H., JENSEN, J.H.D., Z. Naturf. 5A (1950) 413.
[21] VEJE, C.J., private communication.

DISCUSSION

K.A. BRUECKNER: The problem of the dipole resonance in lead is related to the proper prediction of the symmetry energy. Does the Hamada-Johnson potential as evaluated in your approximation give the correct symmetry energy? The correct prediction requires inclusion of rearrangement effects which may be omitted in your treatment of the problem.

G.E. BROWN: We took into account the rearrangement terms of second order, and we find that the third-order terms only cut the interaction down further.

I. ÚLEHLA: How large is the dependence of the calculated effective interaction on the space of the wave-functions of the model?

G.E. BROWN: The effective interaction depends sensitively on the precise model space chosen; often changing the latter by two or three levels will change the matrix elements by ~ 20%. Thus, when comparing with empirical matrix elements, one must be careful to use precisely the same model space from which these were deduced.

D.J. ROWE: I would like to enquire about the use of unperturbed particle-hole energies for the core-polarization corrections. If the interaction at all resembles a $P^{(\lambda)}$ force, which is a field force and which would preferentially excite vibrational core excitations, then, since the low-lying vibrational states tend to lie at about half the energy of the lowest particle-hole energies, one might expect your core-polarization corrections to be underestimated by something like a factor of two.

G.E. BROWN: Of course, the T = 0 vibrations go down in energy, but the T = 1 ones go up. Although they move up less than the T = 0 ones move down, there are three times as many of them. In ^{16}O Kuo constructed the normal modes by the RPA and checked that their exchange gave the same result as perturbation theory; that is, summing the bubbles to all orders did not change the results.

L.A. SLIV: From the theoretical point of view a more favourable way of investigating the nuclear properties is one in which a nucleus is considered as a system of A nucleons, interacting by the "realistic forces". This is the method of Professor Brown, with which he obtained very interesting results. But it should be remembered that at small distances

we know very little about the two-particle potential and it is this part of the potential which makes the main contribution to the effective interaction. Moreover, the realistic forces are very complicated and the methods of the many-body theories, which we use in calculating the complicated realistic forces, require using an approximation which is not always justified. This is the reason why, in order to obtain good data on the effective interaction in nuclei, it is necessary to introduce the effective interaction with a parameter which can be determined from experimental data very sensitive to the given parameter.

It is possible to show that the selection of the parameter can be performed uniquely enough.

Ya. A. SMORODINSKY: It should be mentioned that it is impossible to get an effective 2-body potential from 2-body data. When you add even the one particle when going to the T or ^{3}He system, you have to add new information concerning the potential at small distances (going, say, from the wave-zone into a static one). If you add more particles you have again to add information for each particle added. The question is whether the limit of this process (which gives the effective potential) can be obtained from first principles. Up to now, in my opinion, this limiting potential has been considered on a semi-empirical basis.

GENERAL NUCLEAR PROPERTIES WITH EFFECTIVE INTERACTIONS*

S.A. MOSZKOWSKI
UNIVERSITY OF CALIFORNIA, LOS ANGELES, CALIF.,
UNITED STATES OF AMERICA

Abstract — Аннотация

GENERAL NUCLEAR PROPERTIES WITH EFFECTIVE INTERACTIONS. This report deals with the use of some effective interactions in calculating properties of closed shell nuclei and of the nuclear surface. Closed shell nuclei have been investigated by several groups; the work of three of these groups is discussed here. Davies, Baranger et al. use a momentum-dependent Gaussian effective interaction whose parameters are adjusted to fit the binding energy and density of nuclear matter using first-order perturbation theory and also match at least the low-energy nucleon-nucleon scattering phase shifts. Pearson and Saunier use quite similar interactions except that instead of fitting low-energy scattering data, they insist that the long range part must be of the one-boson exchange form, at least in $^1S_0$ states. Brink and Boeker study various interactions which fit nuclear matter and the alpha particle binding energy. For ^{16}O, these groups obtain somewhat too low a binding energy.

Bethe has worked out a theory of the nuclear surface, which uses a quite simple effective interaction derived from a realistic interaction. Bethe uses the Thomas-Fermi approximation and obtains an analytic form for the particle density distribution at the nuclear surface. He also calculates the nuclear surface energy and surface thickness and obtains good agreement with empirical values.

The nuclear surface problem has also been studied by other authors who do not make the Thomas-Fermi approximation. In particular, if one uses a simple effective interaction of the form suggested by Skyrme, with the same criteria as Brink and Boeker, then the surface energy comes out in good agreement with empirical values. In addition, this effective interaction can be used to assess the accuracy of the Thomas-Fermi approximation. This approximation underestimates the surface energy by only $1\frac{1}{2}$ MeV.

ОБЩИЕ ЯДЕРНЫЕ СВОЙСТВА С ПРОСТЫМИ ЭФФЕКТИВНЫМИ ВЗАИМОДЕЙСТВИЯМИ. Рассматривается использование некоторых эффективных взаимодействий в вычислении свойств магических ядер и ядерной поверхности. Ядра с замкнутыми оболочками исследовались несколькими группами авторов. Обсуждаются результаты исследований трех групп. Девис, Баранжер и другие используют зависящее от скорости гауссовское эффективное взаимодействие, параметры которого выбираются так, чтобы с помощью теории возмущений первого порядка получить правильные значения энергии связи и плотность ядерной материи, а также сдвиги фаз нуклон-нуклонного рассеяния при низких энергиях. Пирсон и Сонье используют почти такие же взаимодействия, но вместо подгонки данных по рассеянию при низких энергиях они исходят из предположения, что дальнодействующая часть должна иметь вид, соответствующий однобозонному обмену хотя бы в $^1S_0$ состояниях. Бринк и Бекер изучают различные взаимодействия для получения плотности ядерной материи и энергии связи α-частиц. Для ^{16}O эти группы получили несколько заниженное значение энергии связи. Бете предложил теорию ядерной поверхности, которая использует простое эффективное взаимодействие, полученное из реального взаимодействия. Бете использует приближение Томаса-Ферми и получает распределение плотности частиц на ядерной поверхности в аналитическом виде. Он также вычисляет энергию и толщину ядерной поверхности и получает хорошее согласие с эмпирическими значениями этих величин. Проблема ядерной поверхности изучалась также другими авторами, не использующими приближение Томаса-Ферми. В частности, если использовать простое эффективное взаимодействие, предложенное Скирмом, с тем же критерием, что и при взаимодействии Бринка и Бекера, энергия связи получается в хорошем согласии с эмпирическими значениями. К тому же, это эффективное взаимодействие может быть использовано для оценки точности приближения Томаса-Ферми. Это приближение дает энергию связи только на $1\frac{1}{2}$ Мэв ниже наблюдаемой.

* Work supported in part by the National Science Foundation.

1. INTRODUCTION

In the last few years, much progress has been made in relating some nuclear properties such as the binding energy and density of nuclear matter and energy level spectra of light nuclei, to realistic nucleon-nucleon interactions. By "realistic" is generally meant an interaction which fits two-body nucleon-nucleon phase shifts and also the properties of the deuteron. However, the required calculations are quite complicated, owing to both the short-range repulsion and tensor interaction. Until about 5 to 10 years ago, it was hoped that low-energy nuclear properties of interest could be accounted for by a simple "effective" interaction which does not necessarily fit nucleon-nucleon results. However, it now appears that this is probably not possible. Nevertheless, with effective interactions, one can gain insight into at least some nuclear properties as I will discuss.

Actually, the concept of effective interactions dates back to the early days of nuclear physics. At that time, Rosenfeld [1] proposed that the interaction contains a large repulsion in odd states of relative motion, which counterbalances the attractive interaction in even states, so as to yield saturation of nuclear matter. Such an interaction has been widely used, even recently, in shell model calculations.

In this paper I discuss several kinds of effective interactions as applied to some general nuclear properties; namely,

(1) Ground-state properties of light closed shell nuclei.

(2) Theory of the nuclear surface.

Other nuclear properties, especially applications in the shell model, have already been discussed in this conference by Drs. Migdal [2], Mikhailov [3] and Brown [4].

2. CLOSED SHELL NUCLEI WITH EFFECTIVE INTERACTIONS

First let us define an effective interaction more precisely. Such an interaction is generally taken to:

(a) fit binding energy (-16 MeV/A) and density of nuclear matter $\rho_0 \sim (1/6)$ nucleon/Fm^3 in first-order perturbation theory. (This density, presumably equal to the density at the centre of finite nuclei, is deduced from electron scattering cross-sections with the additional assumption that neutrons and protons occupy the same volume. It is equivalent to a Fermi momentum $k_F = 1.36\,Fm^{-1}$);

(b) be non-singular enough to make first-order perturbation theory applicable;

(c) fit at least some free space nucleon-nucleon results.

This paper mentions the applications of effective interactions used by three different groups.

2.A. Interactions used by Davies, Baranger and co-workers

An early version of the interaction used by Davies, Baranger and co-workers [5] was taken to be a sum of a central Gaussian interaction $V_c(r)$ and a momentum-dependent repulsion of the form $p^2 w(r) + w(r)p^2$ (where p denotes the momentum operator) studied by Green [6], and w(r) is a short-range Gaussian interaction. This interaction was assumed to act only in

S states, i.e. zero relative orbital angular momentum. (The interaction was, however, taken to be stronger in the $^3S_1$ state than in the $^1S_0$ state.) The parameters were chosen so as to fit both the binding energy and density of nuclear matter in first order and the nucleon-nucleon scattering lengths and effective ranges in both the $^3S_1$ and $^1S_0$ state.

Davies et al. [5] found that the second-order energy in nuclear matter was only about 2 MeV. They also studied the energy, radius and single-particle energies of closed shell nuclei using the Hartree-Fock method. They obtained rough agreement with experimental results. However, their binding energy of ^{16}O per nucleon is only 5 MeV as contrasted with the empirical 8 MeV.

Recently, Nestor et al. [7] developed a somewhat more realistic interaction which acts in all two-particle states, odd as well as even [7]. This interaction is chosen so as to fit not only low-energy scattering properties, but also the binding energy, and quadrupole moment of the deuteron and roughly the triplet odd state phase shifts. This requires the introduction of two-body tensor and spin orbit coupling terms. The former is written as

$$V^T(r) = -A[3(\vec{\sigma}_1\cdot\vec{r})(\vec{\sigma}_2\cdot\vec{r}) - (\vec{\sigma}_1\cdot\vec{\sigma}_2)r^2]e^{-r^2/2\alpha^2}$$

which makes it tractable in Hartree-Fock calculations using oscillator wavefunctions. Again the nuclear matter properties are fitted. The second-order energy of nuclear matter is larger than before, about 3 MeV/A. This is due to the presence of odd state interactions. The symmetry energy of nuclear matter was also calculated. The result, 40 MeV, is somewhat larger than the 30.6 MeV obtained by a recent analysis of empirical nuclear masses [8]. Also the $^1S_0$ nucleon-nucleon phase shifts at medium energies are not reproduced, for example at 150 MeV (laboratory energy) the empirical phase shift [9] is 15° while the interaction chosen gives close to 0°.

Tarbutton and Davies [10] used the above interactions to study the properties of closed shell nuclei, from ^{16}O to ^{208}Pb. Again they obtain too small binding energies, i.e. 5 MeV/A in ^{16}O and ^{208}Pb. However, their calculated root-mean-square radii have reasonable values, i.e.

$$\sqrt{\langle r^2\rangle} = 2.67 \text{ Fm (expt. value} = 2.62) \text{ for } ^{16}O$$

$$= 5.14 \text{ Fm (expt. value} = 5.52) \text{ for } ^{208}Pb$$

Davies et al. actually assumed a slightly larger nuclear matter density, with $k_F = 1.45$ Fm^{-1}. This is roughly consistent with the slightly smaller calculated r.m.s. radius for ^{208}Pb. Also the energy of bound single particle states comes out quite well. Thus, for $1s_{1/2}$, $1p_{3/2}$ and $1p_{1/2}$, the calculated single proton energies in ^{16}O are 44.4, 17.4 and 11.7 MeV respectively, while the energies determined from (p, 2p) reactions [11] are 44, 19, and 12 MeV.

2.B. Interaction used by Pearson et al.

A slightly different kind of effective interaction was developed by Pearson and Saunier [12] at Montreal. Their interaction is again required to fit the binding energy and density of nuclear matter, and give

small second-order energy. It is also required to match the realistic interaction at interparticle distances > 1 Fm, in other words, the long-range part of the interaction should be realistic. This statement has to be qualified somewhat. The authors neglect any spin dependence, spin orbit interaction and tensor force. Thus their idea of "long-range conformity" requires that the interaction in the $^1S_0$ state agrees with the predictions of a one-boson exchange model. The latter should be fairly realistic down to about 1 Fm. Pearson and Saunier use the one-boson exchange potential (OBEP) proposed by Bryan and Scott [13], which includes contributions from exchange of π, ρ, ω and a hypothetical σ (scalar) meson which is meant to reproduce approximately the effect of the two-pion exchange interaction. More accurate OBEP potentials with momentum-dependent terms have become available recently [14, 15]. Such a long range potential, cut off below 1 Fm, should, in fact, reproduce roughly the same S-wave phase shift at low energies as a reasonable S-state potential with a repulsive core of radius ~0.4 Fm and attraction outside. Stated in other words, an S state interaction which fits at least the $^1S_0$ phase shift reasonably well has a separation distance [16] of about 1 Fm at low momenta. The short-range potential including core and some attraction gives no phase shift at low momenta, but it acts like a repulsion at higher momenta. However, the exact form of the S state nucleon-nucleon interaction below about 1 Fm is still somewhat uncertain, as it is possible to fit phase shifts up to 300 MeV equally well with hard core [17], soft core [18] and momentum-dependent core potentials [14]. Also the OBEP model may well fail at distances less than 1 Fm. Thus Pearson and Saunier [19] introduce a phenomenological momentum-dependent short-range interaction of the same form as discussed before [5]. (They also treat an interaction [20] in which the momentum-dependent part is $p^2e^{-p^2s^2}\cdot w(r)$, but this does not lead to significantly different conclusions.)

The short-range interaction

(1) must essentially vanish at $r > 1$ Fm,
(2) can be treated in first order perturbation theory, and
(3) together with the long-range potential gives the empirical binding energy and density of nuclear matter.

Using this combined interaction, together with a spin-independent long-range interaction in odd states, Pearson and Saunier calculated the binding energy and radius of ^{16}O and ^{40}Ca. They use oscillator radial wave-functions and merely minimized the energy as a function of oscillator spacing $\hbar\omega$. This procedure has been shown to be almost as accurate as a Hartree-Fock calculation of the best radial wave-functions [21]. They also varied the ranges of the components of the short-range interaction. The second-order energy came out only ~1 to 2 MeV per particle. The calculated energy and radius of ^{16}O and ^{40}Ca turns out to be nearly independent of the assumed nuclear interaction and close to the experimental values (i.e. calculated E of ^{16}O = 6.5 MeV/A), as long as it satisfies the three criteria mentioned above. If the short-range interaction has too large a range, then it "spills over" into the long-range region. In this case ^{16}O and ^{40}Ca become underbound and their radius gets too large.

Altogether, the idea of separating the nucleon-nucleon interaction into a realistic long-range and a phenomenological short-range part may turn out to be very promising for future nuclear structure applications.

2.C. Interactions treated by Brink and Boeker

Brink and Boeker [22] studied various effective, spin-independent interactions in both even and odd states, i.e. different exchange mixtures. They include a sum of two Gaussians, Gaussian plus delta-interaction and a velocity-dependent interaction. Again one of the criteria is to fit nuclear matter binding energy and density; however, instead of matching the low-energy nucleon-nucleon data, they fit the empirical binding energy and radius of the alpha particle. Brink and Boeker then calculate, for each of the interactions, the binding energy and mean square radius of ^{16}O. For most of them, ^{16}O is again underbound by 1 to 2 MeV per particle. The main application of these interactions is in Hartree-Fock calculations for non-closed shell nuclei and excited states. Thus Brink and Boeker calculated the ground state intrinsic energies of ^{8}Be and ^{12}C using an anisotropic oscillator basis for the single particle wave-functions. In all cases, they obtain too little binding.

It seems that all the effective interactions discussed here do not give enough binding energy for ^{16}O and also for other closed shell nuclei. This discrepancy can perhaps be removed in part by inclusion of the ground-state correlation energy as calculated by Brown and Wong [23] and possibly also by a density dependence of the effective interaction such as used by Green [24]. One such calculation was made by Krieger, Baranger and Davies [21], who used an interaction of the type discussed in Section 2.A, and an additional density-dependent repulsive delta interaction (cf. Section 3). Their results were very close to those obtained in Ref. [5].

3. THE NUCLEAR SURFACE

3.A. Bethe's Thomas-Fermi Theory

Recently, Bethe [25] has derived the properties of the nuclear surface, that is, its thickness and shape and the surface energy. He assumed N = Z and did not take into account the Coulomb effect. Bethe, like most previous authors studying the nuclear surface, assumed the validity of the Thomas-Fermi approximation. This appears to be a good approximation for nuclei, and it greatly simplifies the calculation. Bethe shows, using a simple form of reaction matrix theory, how to convert the complicated realistic interaction to a much less singular effective interaction from which the energy of a finite nucleus can be obtained in first order. Bethe uses the following approximate and very simple effective interaction:

$$V_L(r)[1+P_r] + G_S(\rho)\delta(r)$$

where $v_L(r)$ is the long-range [16] part of the realistic S state interaction in the separation method and P_r is the Majorana space exchange operator. Thus the first part of the effective interaction acts only in spatially even states. The second part of the interaction denotes a density-dependent δ-function. This arises from the following two sources.

(1) The short-range part of the interaction containing a repulsive core and part of the attractive well does not contribute to the energy at low density, i.e. the energies due to the repulsive and attractive inter-

actions cancel. However, at nuclear density, the repulsion becomes relatively more important. Since the short-range correlations are nearly momentum-independent, we can replace the extra effective repulsion term by a delta interaction.

(2) The tensor force contributes to the binding of nuclear matter only in second and higher order. Very roughly, its effect in nuclear matter can be simulated by an attractive interaction which becomes weaker with increasing density. This term can be only very roughly represented by a delta interaction. Altogether $G_S(\rho)$ can be approximated [25] by a constant times $\rho^{2/3}$.

The total energy of the nucleus can then be expressed in terms of densities:

$$E = \frac{3}{8}\int\int V_L(r_{12})\left[\rho(r_1)\rho(r_2) + (\rho(r_1,r_2))^2\right] d^3r_1\, d^3r_2 + \frac{1}{2}\int G_S(\rho(r))\rho^2(r)\, d^3(r) + \int T(r)\, d^3r \qquad (1)$$

where $\rho(r_1, r_2)$ is the mixed density

$$\rho(r_1, r_2) = \sum_n \phi_n(r_1)\phi_n^*(r_2)$$

summed over all occupied states. T(r) is the kinetic energy density.

In the Thomas-Fermi approximation, the mixed density is given by the following simple expression: [26]

$$\rho(r_1, r_2) = \rho(R)\, j(k_F(R)\cdot r_{12}) \quad \text{where} \quad R = \frac{1}{2}(r_1 + r_2)$$

and $j(x) = 3(\sin x - x\cos x)/x^3$. Thus the mixed density has the same form as for nuclear matter with density corresponding to $k_F(R)$. Substituting this result into the equation for E we obtain for the second term of Eq. (1):

$$\int \rho^2(R)\, \Phi(\rho(R))\, d^3R$$

where

$$\Phi(\rho(R)) = \frac{3}{8}\int V_L(r_{12})\, j^2(k_F(R)\cdot r_{12})\, d^3r_{12}$$

The expression for the energy becomes:

$$E = \int\left\{\rho^2(R)\left[-V_0 + \frac{1}{2}G_S(\rho(R)) + \Phi(\rho(R))\right] + T(\rho(R))\right\} d^3R \qquad (2)$$

where

$$V_0 = -\frac{3}{8}\int V_L(r_{12})\, d^3r_{12}$$

The quantity in brackets is the total energy density. It is related to the energy per particle at constant density $W(\rho)$ by $\{\ \} = \rho W(\rho)$. The energy

per particle as function of density can be taken from nuclear matter calculations without having to treat the individual terms V_0, G_S or Φ in detail.[1]

Now, taking into account the spatial dependence of the density, and rewriting Eq. (2), we obtain:

$$E = \int \rho(R) W(\rho(R))\, d^3R + \frac{3\varphi}{8} \int \rho(r_1)[\rho(r_2) - \rho(r_1)]\, v_L(r_{12})\, d^3r_1 d^3r_2 \qquad (3)$$

The second term is the only one which depends upon variations in the nuclear density (for constant density it vanishes). The factor φ is a correction due to the fact that for part of the time, each nucleon is thrown out of the Fermi sea of nuclear matter by virtue of the short-range repulsion. When out of the Fermi sea a nucleon feels practically no binding due to other nucleons in bound states. This is just another way of saying that the one-body potential is assumed to vanish in intermediate states [27]. The factor φ is then just the probability that the interacting particles at r_1 and r_2 are both inside the Fermi sea. Calculations [28] give $\varphi = 0.75$ to 0.8.

Next, Bethe expands $\rho(r_2) - \rho(r_1)$ in powers of r_{12}. Since the density is slowly varying compared with the range of the nuclear forces, it may be a good approximation to keep only derivatives of ρ up to the second. This makes it possible to obtain a differential equation for the density. Next the form of $\rho(r)$ in Eq. (3) is varied subject to the condition that $\int \rho(r) d^3r = A$ is a constant. Finally, Bethe assumes a plane nuclear surface. Then the surface energy is given by:

$$E_S = \frac{3}{r_0}\left[\int_{-\infty}^{\infty} (W(\rho) - W_0)\hat{\rho}\, dz + \frac{1}{2} B \int_{-\infty}^{\infty} \left(\frac{d\hat{\rho}}{dz}\right)^2 dz\right] \qquad (4)$$

where $\hat{\rho} = \rho/\rho_0$

ρ_0 = nuclear matter density

$B = -\frac{\rho_0 \varphi}{8} \int v_L(r_{12}) r_{12}^2\, d^3r_{12}$

r_0 = nuclear radius constant = 1.12 Fm.

According to Eq. (4), the surface energy depends only on $W(\rho)$, the binding energy of nuclear matter vs. density, and $\int v_L(r_{12}) r_{12}^2\, d^3r_{12}$, the second moment of the long-range interaction. Using the calculus of variations it is readily shown that the density function which minimizes the surface energy obeys the differential equation

$$\frac{1}{2} B \left(\frac{d\hat{\rho}}{dz}\right)^2 = \hat{\rho}\,(W(\hat{\rho}) - W_0) \qquad (5)$$

[1] It has to be mentioned that nucleon-nucleon interactions which accurately fit nucleon-nucleon scattering phase shifts and have a static repulsive core (infinite or finite) give only 8 to 10 MeV (per particle) binding in nuclear matter [38].

In order to use a realistic interaction in nuclear matter or at the surface, perhaps the best procedure is the one suggested by Bethe [25], which is simply to increase the calculated potential energy of nuclear matter due to the realistic interaction by about 20%, which will then yield the empirical nuclear matter energy.

It is not yet established if one can get the correct nuclear matter binding energy with a realistic interaction possessing a velocity dependent repulsion. This problem is being studied by L. Ingber, who uses an OBE potential.

A quite accurate representation of $W(\hat{\rho})$ is [25]:

$$W(\hat{\rho})/W_0 = -1 + 4\hat{\rho}^{1/2} - 2\hat{\rho}$$

This leads to a nuclear compression modulus

$$K = -9W_0 - 144 \text{ MeV}$$

The differential equation has the exact solution:

$$\hat{\rho}(z) = (1 - e^{z/a})^2 \qquad \text{for } z < 0$$

where $a = \left(\frac{B}{-W_0}\right)^{1/2}$.

The density function $\hat{\rho}(z)$ is plotted in Fig. 1. As can be seen, its point of most rapid falloff occurs at a density only 25% of the central value. The calculated surface thickness, defined as a reciprocal of the maximum slope, is $b = 2a$. Assuming a reasonable value for $b \sim$ say 2.4 Fm, then $a = 1.2$ Fm, which implies that $B = 23$ MeV. Actually, using this simplified interaction, Bethe's calculated b is much too large. The surface energy is

$$E_S = \frac{3}{r_0} \times \frac{B}{3a} = 17 \text{ MeV}$$

in quite good agreement with the most recent empirical value [8].

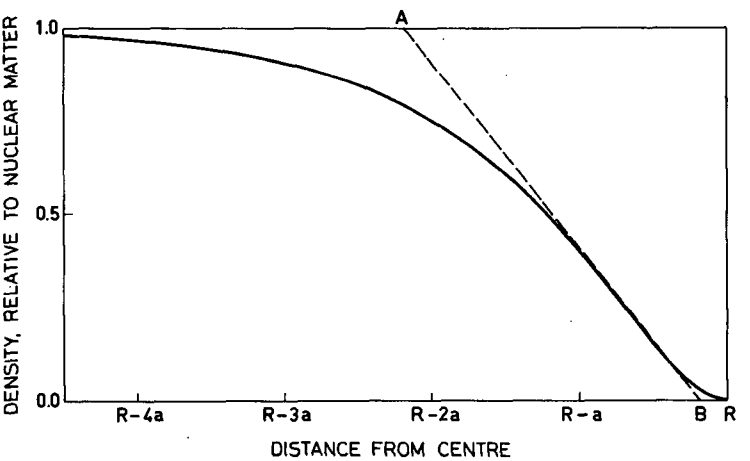

FIG.1. Theoretical density distribution from differential theory versus r. AB is the tangent drawn at the point of steepest slope, the distance $r_B - r_A$ is $b = 2a$. (From Ref. [25]).

An alternative procedure is to drop the assumption that the density varies slowly. In this case, Bethe obtains an integral equation for $\rho(r)$; namely

$$\frac{1}{3}K(\hat{\rho}(r_1) - 1) + \frac{3}{4}\rho_0 \varphi \int v_L(r_{12})[\hat{\rho}(r_2) - \hat{\rho}(r_1)]\, d^3 r_2 = 0$$

This equation (as well as more complicated ones resulting from the inclusion of strong S state and tensor forces), was solved by Nemeth [29] and the resulting density distribution turns out to be of the form:

$$\hat{\rho}(x) = 1 - e^{-\alpha x} \qquad \text{if } \alpha x \gg 1$$

where x is the distance from the nuclear surface ($\alpha \sim 0.7$ Fm). This density approaches the nuclear matter value somewhat more slowly than the density derived from the differential equation. Furthermore, use of this integral equation yields a reasonable value of the surface thickness.

3.B. Some other theoretical treatments

I should like to briefly mention some other recent theoretical studies of the nuclear surface. Buchler, Lombard, Jorna and Brueckner [30] have calculated the density distribution of some finite closed shell nuclei, using a method quite similar to Bethe's. Thus they also assume the validity of the Thomas-Fermi approximation and N = Z, and they write the expression for the surface energy so that it depends essentially only on the energy density relation of nuclear matter and on the inhomogeneity terms $(\nabla\rho)^2$. Unlike Bethe, these authors take into account the curvature of the nuclear surface.

Some of the other nuclear surface studies have not assumed the validity of the Thomas-Fermi approximation. Thus Swiatecki [31], in one of the earliest works on the nuclear surface, used a Rosenfeld potential. He found much too small values, i.e. surface thickness b = 1.6 Fm and E_S = 10 MeV. However, we now know that the Rosenfeld interaction does not describe nucleon-nucleon scattering phase shifts at other than very low energies.

Another recent investigation of interest is the one by Tabakin and Amos [32]. These authors used various effective two-nucleon interactions and did not make the Thomas-Fermi approximation. With a velocity-dependent potential which reproduces the saturation properties of nuclear matter, but not the two-body data, they find: $E_S \simeq 28$ MeV, b = 3.5 Fm. This same interaction also gives too little binding and too much surface diffuseness in Hartree-Fock calculations of closed shell nuclei. On the other hand, with an interaction which fits two-body results but not nuclear matter, they obtain more reasonable values E_S = 22 MeV and B = 2.1 Fm, quite close to the empirical values.

3.C. Use of a simple effective interaction

It was pointed out by Bethe [25] that the Thomas-Fermi approximation is accurate to within 10% in the region where the density is more than 15% of the nuclear matter value. It would, however, be of interest to study in more detail the accuracy of this approximation especially for the nuclear surface energy. This is difficult to do for a realistic nucleon-nucleon interaction such as Bethe used. Instead, I have used a greatly simplified effective interaction of the form suggested by Skyrme [33] some years ago.

Consider a short-range interaction v(r) acting in S states only. Then the diagonal matrix element of v for relative momentum k is given by

$v(k,k) = \int v(r)\, j_0^2(kr)\, d^3r$. For low momentum, or a very short-range interaction, we can expand in powers of k^2 to obtain

$$V(k,k) = \int v\, d^3r - \frac{1}{3}k^2 \int v r^2 d^3r + \frac{2}{45}k^4 \int v r^4 d^3r \ldots .$$

Our approximation is to drop the k^4 term or we may suppose that the interaction is so short-ranged that $\int v r^4 d^3r$ and higher moments can be neglected.

In coordinate space, this new interaction can be written as

$$V(p,r) = \int v\, d^3r\, \delta(r) - \frac{1}{6}\int v r^2 d^3r \left[p^2 \delta(r) + \delta(r) p^2\right]$$

where p is the momentum operator. The first term is a conventional delta interaction. In addition we add a density-dependent delta interaction to simulate the effect of the short-range repulsion just as was done in Section 3.A. Thus the complete interaction, which we call a modified delta interaction, can be written as

$$V(p,r) = -\alpha_0 \delta(r) + \alpha_1 k_F^2(R)\, \delta(r) + \frac{1}{2}\beta\left[p^2 \delta(r) + \delta(r) p^2\right] \qquad (6)$$

where the Fermi momentum is related to the density ρ by

$$\rho(R) = \frac{2}{3\pi^2} k_F^3(R)$$

We can easily obtain an analytic expression for the energy of nuclear matter as a function of density.

$$W = \frac{3}{10}\frac{\hbar^2}{m} k_F^2 + \frac{k_F^3}{3\pi^2}\left[-\frac{3}{4}\alpha_0 + \left(\frac{3}{4}\alpha_1 + \frac{9}{40}\beta\right) k_F^2\right]$$

Now the interaction has three arbitrary parameters. Following Brink and Boeker [22], we fit these parameters to yield the correct binding energy and density of nuclear matter and the binding energy of the α-particle, the latter in the harmonic oscillator approximation. This yields

$$\alpha_0 = 1160 \text{ MeV Fm}^3, \quad \alpha_1 = 71 \text{ MeV Fm}^5, \quad \beta = 756 \text{ MeV Fm}^5$$

(We have not taken into account any spin dependence of the interaction.) As a test for the interaction we calculated the nuclear matter symmetry energy, including a small correction for spin dependence. The result is 35 MeV. This should be compared with the empirical value 31 MeV for the volume symmetry energy [8] and with the results of calculations by Brueckner and Dabrowski [34] (32 MeV) and by Nemeth [35] (32 MeV). Also, the calculated binding energy of ^{16}O agrees well with empirical results.

Next, we use the modified delta interaction to calculate the properties of the nuclear surface, assuming N = Z. The calculation can be done either

without or with the Thomas-Fermi approximation. We neglect the curvature of the surface, then the one-particle wave-function can be written as

$$\psi_i(k,z) = e^{i(k_x x + k_y y)}\phi(k_z,z)$$

where ϕ is the solution to the one-dimensional Schroedinger equation. We chose a Woods-Saxon type one-body potential to generate the ϕ function $u = -u_0[1+\exp(z/z_0)]$. For a modified delta interaction, the energy density is a function of particle density ρ and reduced kinetic energy density τ alone.

$$\tau = -\frac{1}{2}\sum \psi_i^* \nabla^2 \psi_i + \frac{1}{2}(\nabla\psi_i)^2$$

Both ρ and τ can easily be evaluated either exactly or in the Thomas-Fermi approximation. In either case, the surface energy E_S is given by the following expression:

$$E_S = \frac{3}{z_0}\left\{\frac{3}{10}\frac{\hbar^2}{m}k_F^2 J_k + \frac{k_F^3}{3\pi^2}\left[-\frac{3}{4}\alpha_0 J_0 + \frac{3}{4}\alpha_1 k_F^2 J_1 + \frac{9}{40}\beta k_F^2 J_2 + \frac{3}{16}\beta \bar{I}_g\right]\right\}$$

Each of the integrals J is of the form:

$$J = \int_{-\infty}^{\infty}\left(\frac{f(z)}{f_0} - \hat{\rho}(z)\right)dz$$

f = τ for J_k, ρ^2 for J_0, $\rho^{8/3}$ for J , $\rho\tau$ for J_2,

f_0 = nuclear matter value

$$\bar{I}_g = \int_{-\infty}^{\infty}\left(\frac{d\hat{\rho}}{dz}\right)^2 dz$$

The surface energy was minimized with respect to the diffuseness parameter z_0 of the generating potential, with V_0 = 50 MeV, and maximum Fermi energy E_F = - 12.5 MeV, and was found to have a minimum close to z_0 = 0.7 F both in the Thomas-Fermi approximation and the exact calculation. The kinetic and potential energy terms are respectively about 5% and 10% larger than the Thomas-Fermi values, while the density gradient term is 10% smaller. We obtain E_S = 20.9 (22.3) MeV in the Thomas-Fermi (exact) calculation. The resultant particle density is quite close to the Woods-Saxon form, with an effective surface thickness of 2.5 Fm. The Thomas-Fermi and exact particle densities agree rather closely down to densities $\hat{\rho} \sim 0.15$. This is illustrated in Fig. 2, which also shows that the generating potential U(z) extends further out than the density distribution does. Finally it is noted that the potential is slightly more diffuse than the particle density.

It will be very interesting to extend the calculations of this section to finite nuclei where N > Z and the Coulomb effect is included. This is especially so since there is now considerable evidence of a neutron-rich outer surface in heavy nuclei [36].

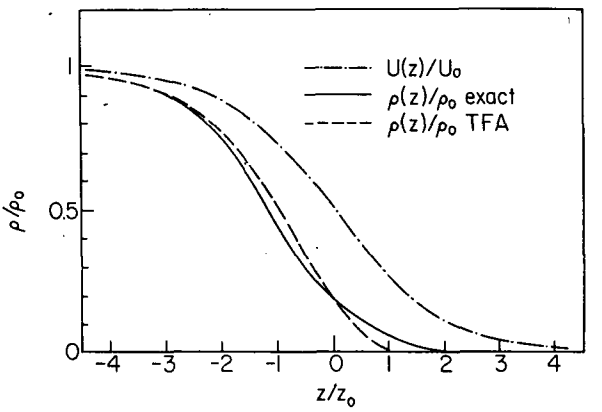

FIG.2. Theoretical distribution of potential (Woods-Saxon) and resulting particle density at the nuclear surface. Also shown is the Thomas-Fermi distribution.

In this connection, I feel it would be appropriate to close by saying a few words about the contribution to this symposium of Dr. M.A. Naqvi, who as you all know, drowned here so tragically last week.

Dr. Naqvi, in collaboration with Dr. Donelly, estimated the various terms in the nuclear mass formula excluding pairing and shell corrections

$$B.E. = a_v A = a_{sym} I^2 A - a_{surf} A^{2/3} + a_{surf\text{-}sym} I^2 A^{2/3} + \text{Coulomb energy.}$$

$$I = (N - Z)/A$$

They assumed a momentum-dependent nucleon-nucleon interaction similar to that used by Davies, Baranger et al., described in Section 2.A. The parameters in the interaction were fixed by fitting the low-energy two-nucleon data and the saturation properties of nuclear matter. Their calculated symmetry energy is 30 MeV, close to the empirical and theoretical value. A large value for the surface symmetry energy was already obtained in a recent study by Myers [37].

REFERENCES

[1] ROSENFELD, L., Nuclear Forces, North Holland, Amsterdam (1949).
[2] MIGDAL, A.B., these Proceedings.
[3] MIKHAILOV, I.N., these Proceedings.
[4] BROWN, G.E., these Proceedings.
[5] DAVIES, K.T.R., KRIEGER, S.J., BARANGER, M., Nucl. Phys. 84 (1966) 545.
[6] GREEN, A.M., Nucl. Phys. 33 (1962) 218.
[7] NESTOR, C.W., DAVIES, K.T.R., KRIEGER, S.J., BARANGER, M., Preprint, Oak Ridge, and Carnegie Mellon Univ. (These authors actually studied several interactions with slightly different values of the parameters.)
[8] SEEGER, P.A., PERISHO, R.C., Los Alamos Report LA-3751 (Sept. 1967).
[9] ARNDT, R.A., MacGREGOR, M.H., Phys. Rev. 141 (1966) 873.
[10] TARBUTTON, R.M., DAVIES, K.T.R., Preprint, Oak Ridge.
[11] ELTON, L.R.B., SWIFT, A., Nucl. Phys. A94 (1967) 52.
[12] SAUNIER, G.O., PEARSON, J.M., Phys. Rev. 160 (1967) 740.
[13] BRYAN, R.A., SCOTT, B.L., Phys. Rev. 135 (1964) B434.
[14] GREEN, A.E.S., SAWADA, T., Nucl. Phys. B2 (1967) 267; BRYAN, R.A., SCOTT, B.L., Phys. Rev. 164 (1967) 1215; INGBER, L., Preprint, Univ. of California, San Diego.

[15] For an excellent review of the present status of nuclear forces, including the one-boson exchange model, see supplement to Progress in Theoretical Physics, Vol.39 (1967).
[16] MOSZKOWSKI, S., SCOTT, B.L., Ann. Phys. 11 (1960) 65.
[17] HAMADA, T., JOHNSTON, I.D., Nucl. Phys. 34 (1962) 382.
[18] BRESSEL, C., Ph.D. thesis, Massachusetts Institute of Technology (1965); REID, R.V., Ph.D. thesis, Cornell Univ. (1967); TAMAGAKI, R., Proc. Int. Conf. Nuclear Structure, Tokyo, Japan (1967) 27-43.
[19] PEARSON, J.M., SAUNIER, G., Preprint, Univ. of Montreal, Canada.
[20] TABAKIN, F., DAVIES, K.T.R., Phys. Rev. 150 (1966) 793.
[21] KRIEGER, S.J., BARANGER, M., DAVIES, K.T.R., Phys. Lett. 22 (1966) 607.
[22] BRINK, D.M., BOEKER, E., Nucl. Phys. A91 (1967) 1.
[23] BROWN, G.E., WONG, C.W., Nucl. Phys. A100 (1967) 241.
[24] GREEN, A.M., Phys. Lett. 24 (1967) 384.
[25] BETHE, H.A., Phys. Rev. 167 (1968) 879.
[26] SLATER, J.C., Phys. Rev. 81 (1951) 385.
[27] RAJARAMAN, R., BETHE, H.A., Rev. mod. Phys. 39 (1967) 745.
[28] DAHLBLOM, T. (private communication to H.A. Bethe) calculates a related quantity K where $\zeta = (1+2K)^{-1}$ and obtains K = 0.14.
[29] NEMETH, J., BETHE, H.A., ITP Report 226, University, Budapest.
[30] BUCHLER, J.R., LOMBARD, R.J., JORNA, S., BRUECKNER, K.A., Preprint, Univ. of California, San Diego.
[31] SWIATECKI, W.J., Proc. phys. Soc. 64A (1951) 226.
[32] TABAKIN, F., AMOS, K., Nucl. Phys. A100 (1967) 574.
[33] SKYRME, T.H.R., Phil. Mag. 1 (1956) 1043; Nucl. Phys. 9 (1968) 615.
[34] BRUECKNER, K.A., DABROWSKI, J., Phys. Rev. 134B (1964) 722.
[35] NEMETH, J., (University, Budapest) private communication.
[36] GREENLEES, G.W., PYLE, G.J., TANG, Y.C., Phys. Rev. Lett. 17 (1966) 33 and Preprint, Univ. of Minnesota, USA; BURHOP, E.H.S., Nucl. Phys. B1 (1967) 438.
[37] MYERS, W.D., Ph. D. Thesis, Univ. of California (1968).
[38] SPRUNG, D., Proc. Int. Conf. Nuclear Masses, Winnipeg, Canada (August 1967).

DISCUSSION

P.E. NEMIROVSKY: We have calculated the radius of nuclear density and the radius of the self-consistent potential. The results obtained are in good agreement with the experimental data if we assume that the nuclear density is a weaker source of nuclear forces in the central part of a nucleus in comparison with the nuclear surface.

S.A. MOSZKOWSKI: Indeed, the interaction I mentioned is stronger at the surface of a nucleus.

J. NÉMETH: I would like to point out that the introduction of non-local density-dependent terms into the effective interaction might be very important. In our Thomas-Fermi calculation it changed the surface thickness about 20% and the surface energy a few MeV.

VI

CLOSING REMARKS

Chairman

V.G. SOLOVIEV

CLOSING REMARKS

In the closing session of the symposium, under the chairmanship of Professor V. G. Soloviev, short statements were made by Professors A. Bohr, P. Huber, M. Sakai and J. O. Rasmussen. The closing remarks of Professor Bohr are included here.

A. BOHR: I should like to give expression to the gratitude which the participants of the symposium feel towards our hosts for their generous hospitality and to congratulate the organizers for a very successful meeting. Indeed, our symposium has been very impressive in registering advances over a broad front. We have heard about tests and consolidations of our picture of nuclear structure, of important progress in our understanding, and, not least, the explorers on the different frontiers have reported exciting new phenomena that pose challenging problems. The theorists, I believe, leave the symposium with much food for thought and plenty of homework. Professor Rasmussen has mentioned some of the developments on the experimental side; I should like to make a few general remarks on trends and perspectives on the theoretical side.

One of the main themes of the symposium has been the elementary modes of excitation in the nucleus. We have had valuable new information on the spectrum and properties of the single particle or quasiparticle excitations in the spherical and deformed nuclei. But one is eager to understand these excitations much better because of the basic role they play in the nuclear dynamics. For example, the velocity dependence or non-locality is still a very open question and it would be very significant to have a better understanding of the more specific level shifts depending on the configuration involved, either through Hartree-Fock calculations or by other approaches. This is of importance not least for the extrapolation into new regions of nuclei.

We have learned a great deal about the collective modes, have had more detailed information about previously established modes, as well as evidence on new collective modes. But we can rather confidently expect that a wealth of interesting phenomena are awaiting the hunters in this field. Thus, the exploration of excitations involving charge exchange and pairing is only just beginning; we still know very little about the spin modes, and are almost in the dark about the compression modes, which represent another important aspect of the nuclear dynamics, related to the electric monopole phenomena on which we have heard many new and puzzling results.

The microscopic theory of collective motion has made it possible to tie together many features of the elementary excitations and of the nuclear deformations, but there is need for further developments in many directions. Thus, there is the subtle problem of the effective interactions which generate the collective motion. Much of the successful work has been based on the assumption that the nucleonic interactions can be represented by a coupling of the nucleons to the static and time-dependent nuclear potentials (for example, in the pairing and multipole models); one tries, as it were, to represent the four-field nucleon coupling by a three-field coupling, and this

appears to be at least an important aspect of the collective motion. But we need much more information about the coupling, i.e. on the relation between density and potential, due to the many field components which may occur and also due to the special conditions which occur in the surface region. Indeed, the structure of the surface is becoming a more and more acute problem. There is a need to combine approaches on many levels of phenomenology, from the studies based on the nucleon-nucleon interaction to the direct determination of the coupling parameters from inelastic scattering processes or from the interaction of bound nucleons with the vibrational motion.[1]

The nucleus offers the opportunity for penetrating deeply into the structure of collective motion in a many-body system. Theory makes very detailed predictions concerning the microstructure of the collective modes and the many phenomena associated with their coupling to other excitations, and these can be tested by the great arsenal of probes which are becoming available and the many different reactions which can give pertinent information. We have heard about many of the promising developments in this direction.

Important general problems are connected with the anharmonicity of the collective motion, which becomes especially strong in the region of the transitions from spherical to deformed nuclei and from normal to superfluid nuclei. This is a field of great activity and new promising results have been presented. Still, the problems remain of great challenge and the phenomena can have considerable structure. Much guidance can be obtained by the exploration of simple models. There is an intimate relation to the phase transitions in infinite systems which is at present an area in the focus of interest of solid state physicists; the nucleus may elucidate new features of such phenomena, since it is possible to study the spectrum of individual quantum states of the collective modes associated with the phase transitions.

Another theme at the symposium has been the study of nuclear spectra in the region of high-level density where many degrees of freedom can be excited and where the individual quantum states may acquire great complexity. We have heard about considerable gains in the statistical analysis of level densities and partial widths for various types of processes, and many phenomena can be understood on this basis, i.e. by assuming a randomness in the partition of the energy on the different degrees of freedom. However, many trustworthy explorers have reported findings that suggest more specific structure. We have only the first indications, but one has the feeling that we are coming to a very interesting stage of development on this frontier. The field is a huge one and one can envisage an enormous variety of correlations and new types of collective behaviour, but it is as yet quite unclear what will be the most relevant phenomena, what are the questions to be asked and the concepts needed. We are dealing with matter in a form which has never been studied at the level of detail to which the nucleus is now being subjected.

Professor Rasmussen has talked about the fission process, for which this symposium is a landmark. The exciting developments brought about by experimental discoveries and advances in the theory open up many new prospects. Fission is joining up much more intimately than before with nuclear spectroscopy, and the study of this extraordinary collective mode is likely to bring out new aspects of nuclear dynamics. We can also foresee

---

[1] It may be more simple to drag a hippopotamus out of a swamp than to synthesize one in the laboratory, though the ingredients are readily available.

that the study of heavy ion reactions will give new insight into the behaviour of nuclear matter under novel and more violent conditions. After all, in the usual reactions, we are just tickling the nucleus.

I should like to conclude by stressing the richness of the nuclear phenomena, as so well illustrated by this symposium. In the theoretical description, the richness is reflected in the many levels of phenomenology on which the analysis is carried forward, from the description based on interacting nucleons, or even deeper levels of phenomenology in the description of hadrons, at the one extreme, to the analysis based on general symmetry principles applying to the nucleus as a whole and to its modes of excitation, at the other extreme. The total picture must be a unified one, but the efforts at the different levels complement each other and together give the subject its special flavour and conceptual content.

The game of pushing forward at many levels of phenomenology is characteristic of quantal physics dealing with systems with many degrees of freedom and is a common theme for nuclear physics and our neighbouring fields, which deal with quanta with higher and smaller energies than those governing the nuclear dynamics. The importance of cultivating the connection between the various domains of quantal physics has been stressed by several speakers, and we have heard of new effects and approaches which combine methods from different fields. The nuclear physicists, being so to speak in the centre of the spectrum of quantal physicists, have the opportunity to play an important role in promoting these connections, which can be expected to be very fruitful for the development of physics as a whole.

LIST OF CONTRIBUTIONS*

I. BOUND STATES OF COMPLEX NUCLEI

1. FOWLER, J.L., JOHNSON, C.H., HAAS, F.X.: Resonant states of doubly closed shell plus one neutron nuclei.

2. BRUGE, G., BUSSIÈRE, A., FARAGGI, H., KOSSANYI-DEMAY, P., LOISEAUX, J.M., ROUSSEL, P., VALENTIN, L.: Spectroscopy of the N=27 odd-odd nuclei through the (^{3}He, t) reaction.

3. GASTEBOIS, J., KUZMINSKI, J., LAGET, J.M., NATHAN, O.: Study of the ^{52}Cr (^{3}He, p) ^{54}Mn reaction at E(^{3}He) = 18 MeV.

4. LAGET, J.M., GASTEBOIS, J.: Study of the ^{54}Fe(^{3}He, p) ^{56}Co reaction at E(^{3}He) = 18 MeV.

5. FANGER, U., SCHMIDT, H., MICHAELIS, W.: Level structure investigation of Fe^{58}.

6. BRODA, R., HRYNKIEWICZ, A.Z., KISIELEWSKI, J., STYCZEN, J., SZEGLOWSKI, Z., WALUS, W.: Directional correlations of gamma cascades in ^{75}As.

7. RUITER, A.P. de, VERHEUL, H.: The decay of $^{70}_{33}As_{37}$

8. GAL'PERIN, L.N., ILYASOV, A.Z., LEMBERT, I.Kh., FIRTSANOV, G.A.: Coulomb excitation of the nuclear levels of ^{53}Cr, ^{57}Fe, ^{59}Co, ^{61}Ni, ^{91}Zr, ^{92}Zr, ^{94}Zr, ^{111}Cd and ^{123}Te (in Russian).

9. BRUGE, G., BUSSIÈRE, A., FARAGGI, H., LOISEAUX, J.M., ROUSSEL, P., TESTONI, J., VALENTIN, L.: Nuclear structure study in the f-p shell through (α, ^{3}H) and (α, ^{3}He) reactions.

10. ARLT, R., KRACÍK, B., LOSHCHILOV, M., MUSIOL, G., STRUSNY, H., TRAN THANH MINH, ZAITSEVA, N.G.: On the decay of ^{87}Zr.

11. CONJEAUD, M., HARAR, S., THURIÈRE, E.: (^{3}He, d) reaction on the even cadmium isotopes.

12. SUBOTOWICZ, M., KURANC, J., SARZYŃSKI, J., CHLEBOWSKA, M.: Measurements of the beta-gamma directional correlations in some allowed beta transitions in ^{22}Na, ^{110}Ag, ^{134}Cs, ^{154}Eu and ^{160}Tb.

13. SYCHIKOV, G.I., KOVRIGIN, O.D.: Study of internal conversion electrons and gamma rays of In^{108} (in Russian).

14. SYCHIKOV, G.I., KOVRIGIN, O.D.: Study of internal conversion electrons and gamma rays of In^{109} and In^{110m} (in Russian).

15. CONJEAUD, M., HARAR, S., THURIÈRE, E.: Study of the odd indium isotopes with the (d, ^{3}He) reaction.

16. VALLOIS, G., BEER, O., BEHAY, A.El, LOPATO, P., TERRIEN, Y., SETH, K.: Even tin spectroscopy by scattering pp' at 24.5 MeV.

17. ZHELEV, Zh., ZAITSEVA, N.G., LOSCHILOV, M.G., NAZAROV, U.K., SABIROV, S.S., URBANEC, J.: The ^{124}J → ^{124}Te decay.

18. ALEXANDER, K.F., NEUBERT, W.: Experimental indication for an oblate shape of the nucleus ^{129}La.

19. ŘEZANKA, I., ŠPALEK, A., FRAŇA, J.: Spectroscopic study of odd-mass nuclei with A ≈ 130.

20. BRINCKMANN, H.F., HEISER, C., FROMM, W.D., HAGEMANN, U.: The decay of the high-excited isomeric state in ^{132}Xe.

21. BADICA, T., MOROZOV, V.A., MUMINOV, T.M.: Half-lives of 108.8 keV excited states in ^{136}Pr and 113.8 keV in ^{139}Pr.

---

* These contributions, each about 400 words long, were issued before the meeting by the Joint Institute for Nuclear Research, Dubna, as Dubna publication D-3893. Each contribution fills one page, and is here given the number of that page. A few contributions which for various reasons could not be published in D-3893 are marked at the end of each section here with a dagger (†).

22. ZHELEV, Zh., KALINNIKOV, V.G., LEBEDEV, N.A.: On the identification of the ^{137}Nd and ^{136}Nd isotopes.

23. ARLT, R., BEYER, G., MUSIOL, G., PFREPPER, G., STRUSNY, H.: The decay of ^{145}Gd; the energy interval between $2d_{3/2}$ and $3s_{1/2}$ levels in odd nuclei with $Z \geq 50$ and N=67-81.

24. ADAM, I., TOTH, K.S., ROCHE, M.F.: Decay of ^{145}Eu to levels in ^{145}Sm.

25. ADAM, I., ŻYLICZ, J., TOTH, K.S., NIELSEN, O.B.: The decay of ^{146}Eu.

26. GŌNŌ, Y., ISHIHARA, M., SAKAI, M.: The levels of ^{150}Sm and ^{152}Gd.

27. GOLOVKOV, N.A., SO KI HWANG, CHUMIN, V.G.: On alpha decay of Er, No and Dy isotopes (in Russian).

28. MEYER, R.A.: Band properties of even-even nuclei with small deformations.

29. SUJKOWSKI, Z., UNGRIN, J.: Low energy levels in ^{155}Eu.

30. WIDEMANN, F., SEBILLE, C.: Experimental study of ^{155}Eu levels. A possible border effect within a deformation zone.

31. HRYNKIEWICZ, A.Z., KISIELEWSKI, J., STACHURA, Z., STYCZEN, J., SZAWLOWSKI, M., WALUS, W.: Directional correlations of gamma cascades in ^{155}Gd.

32. ABDURAZAKOV, A.A., GROMOV, K.Ya., NAZAROV, U.K., SABIROV, S.S., STYCZEŃ, J., ZHELEV, Zh.T.: Rotational bands of gamma and beta vibrational states in ^{156}Dy.

33. HRYNKIEWICZ, A.Z., STYCZÉN, J., SZEGLOWSKI, Z., WALUŚ, W.: Directional correlations of gamma cascades in ^{160}Dy.

34. GROMOV, K.Ya., ZHELEV, Zh., KALINNIKOV, V.G., KONDRAT, E.T., LEBEDEV, N.A., MALEK, Z., NENOFF, N., PFREPPER, G., STYCZEŃ, B., HRISTOV, D., STRUSNY, H.: New short-lived activities ^{163}Yb, ^{165m}Tm, ^{163m}Tm and ^{159}Tm.

35. BUNKER, M.E., BERZINS, G., STARNER, J.W.: State mixing in ^{165}Ho.

36. BONDARENKO, V., MANFRASS, P., PROKOFJEV, P.: The Coriolis coupling in ^{165}Dy.

37. MICHAELIS, W., WELLER, F., SCHMIDT, H., MARKUS, G., FANGER, U.: Band mixing effects in deformed odd-mass nuclei.

38. FUNKE, L., ANDREJTSCHEFF, W., GRABER, H., HAGEMANN, U., KAUN, K.-H., KEMNITZ, P., MEILING, W., SODAN, H., STARY, F., WINTER, G.: Levels in ^{167}Er.

39. ROZKOŠ, M., ŠTĚRBA, F., ŠTĚRBOVÁ, J., ELBEK, B., TJØM, P.O.: The study of the Er-167 isotope by the (d, d') process.

40. ARLT, R., MALEK, Z., MUSIOL, G., PFREPPER, G., STRUSNY, H.: The decay of 7 min ^{168}Lu.

41. ARLT, R., MALEK, Z., MUSIOL, G., PFREPPER, G., STRUSNY, H.: New isotopes ^{169}Hf, ^{167}Hf, ^{166}Hf; the new ^{166m}Lu isomer.

42. BONCH-OSMOLOVSKAYA, N.A., PLOCHOCKI, A., PREBISZ, Z., ZGLIŃSKI, A.: Coincidence study of the ^{170}Lu → ^{170}Yb decay.

43. BONCH-OSMOLOVSKAYA, N.A., GRIGORIEV, E.P., LIPTAK, J., URBANEC, J.: The ^{170}Lu decay scheme and the 0^+, 0^- states.

44. GRAHAM, R.L., GEIGER, J.S., JOHNS, M.W.: The level structure of ^{171}Tm.

45. NADJAKOV, E., BOCHEV, B., PFREPPER, G., RAICHEV, H., KUTSAROVA, T., NENOFF, N., FOMINICH, W.I., FOMINICH, M.I., BAKARDJIEV, S.: New rhenium activities obtained by irradiating with heavy ions.

46. FOMINIKH, W.I., MOLNAR, J., NENOFF, N., STYCZEŃ, B., ZVOLSKÝ, J.: On the decay of ^{176}Ta and ^{175}Ta.

47. BODDENDIJK, H.G., KLEIMEER, G., VERHEUL, H.: The γ-ray decay of ^{176}Ta.

48. ŻUK, W., KRUPA, E., ORZECHOWSKI, A., TAŃSKA, W.: Gamma-gamma and electron-gamma angular correlation in ^{177}Lu decay.

49. WAHLBORN, S.: Properties of the retarded, parity-impure dipole transitions in ^{181}Ta and ^{175}Lu.

50. GALAN, P., GALANOVA, T., MALEK, Z., VOINOVA, N., ADAMOVICZ, B., PREIBISZ, Z., STRYCZNIEWICZ, K.: The decay of the 13-hour isomer of ^{182}Re.

51. BĂDICĂ, T., GELBERG, A., PROTOP, C., SĂLĂGEANU, S.: Lifetime and angular correlation measurements in ^{193}Ir.

52. ALVÈS, R., SAMOUR, C., JULIEN, J., MORGENSTERN, J.: Level schemes and transition intensities following resonance neutron capture for several nuclei.

53. REID, P.G.E., SOTT, M., STONE, M.J.: Nuclear orientation study of ^{192}Ir and ^{194}Ir.

54. GOLOVKOV, N.A., IVANOV, R.B., NORSEYEV, Yu.V., SO KI HWANG, KHALKIN, V.A., CHUMIN, V.G.: Determination of the energy of main alpha groups of short-living Po and At isotopes (in Russian).

55. BRENTANO, P. von, RICHARD, P., WHARTON, W.: States in ^{208}Pb with a $(d_{5/2}, p_{1/2}^{-1})$ configuration.

56. GOLOVKOV, N., GUETH, L., GUETH, S., DAROCZY, E., DZHELEPOV, B., NORSEYEV, Yu., KHALKIN, V., CHUMIN, V.: Measurement of the fine structure of the alpha-spectra of ^{211}At, ^{210}At and ^{209}At.

57. HARADA, Kichinosuke: Alpha decay of the high-spin isomer of ^{212}Po.

58. HAHN, R.L., ROCHE, M.F., TOTH, K.S.: New neptunium isotopes, ^{229}Np and ^{230}Np.

59. CHWASZCEWSKA, J., KACZAROWSKI, R., RUDZIŃSKA, J., KURCEWICZ, W., ŻYLICZ, J.: Possible $K^{\pi} = 2^-$ and $K^{\pi} = 1^-$ octupole bands in ^{232}U.

60. ŠTĚRBA, G., ŠTĚRBOVÁ, J.: The inelastic scattering of deuterons by the U233 and U235.

61. ERSKINE, J.R., FRIEDMAN, A.M., BRAID, T.H., CHASMAN, R.R.: Survey of single-particle and collective states of the actinides by use of transfer reactions.

62. KERN, J., STRUBLE, G.L.: On the validity of quasi-particle descriptions for N=83 odd-odd isotopes.

63. BOGDAN, D., FUIA, H., PROTOP, C., VÂȚĂ, I.: Woods-Saxon superfluid corrections for some β transitions of deformed nuclei.

64. HERBUT, F., VUJIČIĆ, M.: New methods for solution of Hartree-Bogolyubov dynamical equations.

65. CHASMAN, R.R.: A new approach to pairing forces: the intermediate state method.

66. GMITRO, M., RIMINI, A., SAWICKI, J., WEBER, T.: Two- and four-quasiparticle theories of even tin isotopes and Yale-Shakin nucleon-nucleon potentials.

67. GILLET, V., RAYNAL, J.: Competition between stretch and seniority schemes.

68. FAESSLER, A., SAUER, P.U., WOLTER, H.H.: Competition between selfconsistency and pairing as causes of the energy gap.

69. KAMLAH, A.: A quantum mechanical derivation of the cranking model.

70. BECK, R., MANG, H.J., RING, P.: Application of the cranking model to odd mass nuclei.

71. HAMAMOTO, I., UDAGAWA, T.: Rotational constant of $I^2(I+1)^2$ corrections to "rotational spectra in odd-A nuclei".

72. FRAUENDORF, S., YANSSEN, D., MÜNCHOW, L.: Rotations and non-adiabatical corrections to the ground state.

73. KULIEV, A.A., PYATOV, N.I.: Magnetic dipole interactions in deformed nuclei.

74. MARUMORI, T., YAMAMURA, M., MIYANISHI, Y., NISHIYAMA, S.: A new microscopic approach to the collective motion.

75. HEHL, K., RIEDEL, C., BROGLIA, R.A., UDAGAWA, T.: Nuclear collectivity in two-nucleon transfer reactions.

76. LAGET, J.M., GASTEBOIS, J.: On the calculation of the form factor in two-nucleon transfer reactions.

77. KORNEICHUK, A.A., MALOV, L.M., SOLOVIEV, V.G., FEDOTOV, S.I., SCHULZ, H.: Quadrupole 2^+ states in the region $150 \leq A \leq 174$.

78. MALOV, L.A., SOLOVIEV, V.G., FAINER, U.M.: Quadrupole and octupole states in the range $174 \leq A \leq 188$.

79. PARIKH, J.C., ROWE, D.J.: An investigation of ground state correlations in vibrational nuclei.

80. BIRBRAIR, B.L., EROKHINA, K.I., LEMBERG, I.Kh.: First levels 2^+ and 3^- of spherical nuclei (in Russian).

81. GILLET, V., GIRAUD, B., RHO, M.: Core effects on vibrational states of spherical nuclei.

82. CHOUDHURY, D.C., CLEMENS, J.T., BAILEY, F.G.: Application of intermediate-coupling unified nuclear model to several odd-mass nuclei.

83. ZIELIŃSKA-PFABÉ, M.: γ-vibrations of nuclei with the new single particle scheme.

84. (Number not used).

† JOHNSON, N.R., RIEDINGER, L.L., HAMILTON, J.H.: Mixing of the β - and γ-vibrational bands in ^{152}Sm and ^{154}Gd.

† GOWOREK, T., KLISZCZEWSKA, K., WAWRYSZCZUK, J.: Quantum characteristics of levels and transitions in ^{147}Eu to ^{147}Sm decay.

† GOWOREK, T., KLISZCZEWSKA, K., WAWRYSZCZUK, J.: On the existence of new transitions in ^{140}Ba to ^{140}La decay.

II. NUCLEAR EQUILIBRIUM DEFORMATIONS AND FISSION

85. NIX, J.R.: Further results from the liquid-drop theory of nuclear fission.

86. NILSSON, S.G., NIX, J.R.: Estimates of the spontaneous-fission half lives of $Z = 114$ nuclei.

87. ALBINSSON, H., HIGBIE, J., LINDOW, L.: Prompt gamma radiation from fission fragments.

88. RYABOV, Yu.V., SO DON SICK, CHICKOV, N., IANEVA, N.: Variations of the yield of the average number of prompt fission neutrons for U-235 and Pu-239 in the resonance neutron energy region.

89. BŁOCKI, J., CHWASZCZEWSKA, J., DAKOWSKI, M., KROGULSKI, T., PIASECKI, E., PIEKARZ, H., SOWIŃSKI, M., STEGNER, A., TYS, J.: Emission of light charged particles in thermal neutron fission of ^{235}U.

90. LARK, N., SLETTEN, G., BJØRNHOLM, S.: New spontaneously fissioning isomers with nanosecond lifetimes.

91. WAKAI, M., HARADA, K., OHNISHI, N.: On the existence of shape isomers.

92. ARSENIEV, D.A., MALOV, L.A., PASHKEVICH, V.V., SOBICZEWSKI, A., SOLOVIEV, V.G.: Equilibrium deformations of nuclei in the region $50 < Z < 82$, $50 < N < 82$.

93. ARSENIEV, D.A., MALOV, L.A., SOBICZEWSKI, A., SOLOVIEV, V.G.: Equilibrium deformations of quasi-particle nuclear states in the region $Z > 50$, $N < 82$.

94. PASHKEVICH, V.V.: The energy of nonaxial deformation of heavy nuclei.

95. BERLOVICH, E.Ye.: On the shape of the atomic nuclei in transition regions.

96. KLUGE, Gy., LAJTAI, A.: Average number and energy of prompt neutrons from fission.

97. RAMANNA, R., RAMAMURTHY, V.S.: Mass and charge division in fission.

98. BANG, J., JENSEN, A.S.: Coulomb energy of deformed nuclei.

† NAQVI, M.A.: The liquid drop mass formula.

III. QUASIBOUND STATES OF COMPLEX NUCLEI

99. DOLINSZKY, T.: A unified theory of the compound and the intermediate resonances.

100. ZHIVOPISTZEV, F.A., MOSKOVKIN, V.M., NAGAR, N.El, SHITIKOVA, K.V., YUDIN, N.P.: Effect of lowest collective states of negative parity on the dipole resonance structure (in Russian).

101. TOMASELLI, G., MEHNERT, R., OTTO, G.: Investigation of level shift parameters and resonance widths of isobaric analogue resonances (IAR).

102. CASSAGNOU, Y., FOISSEL, P., GASTEBOIS, J., LÉVI, C., MITTIG, W., PAPINEAU, L.: Coulomb displacement energies from isobaric analogue state studies in deformed nuclei.

103. GIPPNER, P., GERSCH, H.U., RUDOLPH, W.: Comparison of (d,p) and (n,γ) reactions on ^{63}Cu and ^{65}Cu.

104. GERSCH, H.U., RUDOLPH, W.: The influence of doorway states in the $^{51}V(n,\gamma)^{52}V$ reaction.

105. NILSSON, L., STARFELT, N., BERGQVIST, I., LUNDBERG, B.: Radiative capture of neutrons in the MeV region.

106. CASSAGNOU, Y., FOISSEL, P., GASTEBOIS, J., LÉVI, C., MITTIG, W., PAPINEAU, L.: Effect of vibrational admixtures to rotational states from analogue state studies.

107. ISMATOV, E.I.: On excitation of analogue states of nuclei in the scattering of ^{3}He (in Russian).

108. CVELBAR, F., HUDOKLIN, A., MIHAILOVIC, M.V., NAJZER, M., PETRISIC, M.: Gamma-ray spectra from the radiative capture of fast neutrons and the direct-semidirect capture mechanism.

109. FEIFRLIK, V., RIZEK, J., VOGEL, P.: Dipole states in deformed nuclei.

110. (Number not used)

† METHA, M.K., SEKHARAN, K.K.: Absolute total cross section for the reaction $^{Si}V(p,n)^{Si}Cr$ over the isobaric analogue resonance near 2.340 MeV.

IV. COMPOUND STATES AND PARAMETERS OF OPTICAL POTENTIAL

111. PETKOV, I.Zh., POL, Yu.S.: A model of elastic scattering of electrons on nuclei (in Russian).

112. ZIMÁNYI, J., GYARMATI, B.: Charge-exchange in (d,p) stripping reaction.

113. GYARMATI, B., ZIMÁNYI, J.: On the shape of the symmetry potential.

114. COHEN, B.L., MAY, E.C., O'KEEFE, T.M., FINK, C.L.: (p,p'n), (p,p'γ) and (p,np') reactions in Sn^{119} and Ni^{61}.

115. BUDZANOWSKI, A., DUDEK, A., DYMARZ, R., GROTOWSKI, K., JARCZYK, L., NIEWODNICZAŃSKI, H., STRZAŁKOWSKI, A.: Optical model analysis of the nuclear glory effect.

116. BOBROWSKA, A., BUDZANOWSKI, A., GROTOWSKI, K., JARCZYK, L., MICEK, S., NIEWODNICZÁNSKI, H., STRZAŁKOWSKI, A., WRÓBEL, Z.: Nuclear glory effect in the elastic scattering of alpha particles on ^{27}Al, ^{28}Si, ^{32}S, ^{39}K, ^{40}Ca, Ti and ^{59}Co nuclei.

117. BOLLINGER, L.M., THOMAS, G.E.: Nuclear spectroscopy with average spectra from neutron-resonance capture.

118. MORGENSTERN, J., ALVÈS, R., JULIEN, J., SAMOUR, C.: Examples of time-of-flight methods to determine neutron resonance parameters and values of strength functions (S_0 and S_1), total radiative width Γγ and mean level spacing D as a function of mass number and spin value.

119. SAMOUR, C., ALVÈS, R., JACKSON, H., JULIEN, J., MORGENSTERN, J.: A study of partial radiative widths at and between neutron resonances.

120. JULIEN, J., ALVÈS, R., MORGENSTERN, J., SAMOUR, C.: Distribution of neutron resonance spacings and correlation factors between next nearest spacings, next nearest neutron reduced width, and partial radiative width with total radiative width.

121. GOFMAN, Yu.V., ZAIKA, N.I., KIBKALO, Yu.I., MOCHNACH, A.V., NEMETS, O.F., SHMARIN, P.L., YASNOGORODSKY, A.M.: Deuteron polarization in elastic scattering.

122. ALEXEYEV, V.V., NEMETS, O.F., SIMONOV, I.N., TERENETSKY, K.O., TOKAREVSKY, V.V.: Unique optical potential parameter set for 27.2 MeV alpha particles interaction with medium weight nuclei.

123. NEMETS, O.F., PUGACH, V.M., SOKOLOV, M.V., STRUZHKO, B.G.: Some features of 13.6 MeV deuterons break-up on medium nuclei.

124. CHERNOV, I., NEMETS, O., SOKOLOV, L., TOKAREVSKY, V., VERESHCHAGIN, A., YATIS, A.: About anomalies in deuteron elastic scattering by nuclei.

125. MALECKI, H., PIKELNER, L.B., SALAMATIN, I.M., SHARAPOV, E.I.: Radiative capture and neutron total cross sections for selenium isotopes.

126. ADAM, A., DEAK, F., IEKI, L., KISHSH, A., KEVESHI, Zh., PALLA, G., KHRASHKO, P.: Anomalous forward scattering of 14 MeV neutrons on uranium (in Russian).

127. ABBOUD, A., DECOWSKI, P., GROCHULSKI, W., MARCINKOWSKI, A., SIWEK, K., WILHELMI, Z.: Isomeric ratios and total cross sections for the (n, 2n) reactions in the vicinity of closed shells.

128. D'AURIA, J., JODOGNE, J.C., KOWALSKI, L., MILLER, J.M.: Measurements of the cross sections for formation of compound nuclei in heavy-ion reactions.

129. RAYNAL, J.: An iterative procedure for coupled channel calculations.

130. GLASHAUSSER, C., GOUDERGUES, J., LOMBARD, R.M., MAYER, B., THIRION, J., VAGANOV, P.: Scattering of 20.3 MeV polarized protons by ^{90}Zr, ^{92}Zr and ^{92}Mo.

131. BRZOSKO, J.S., GIERLIK, E., SOŁTAN, A., WILHELMI, Z.: Neutron induced reactions on ^{181}Ta.

132. (Number not used)

† CHRIEN, R.E., WASSON, O.A., BHAT, M.R., BEER, M., LONE, M.A., MUGHABGHAB, S.F., GARBER, D.I.: Resonant and non-resonant neutron capture experiments at the high flux beam reactor.

† ESWARAN, M.A., ISMAIL, M., RAGOOWANSI, N.L., MITZA, P.C.: Proton-gamma ray angular correlation study of 3.067-MeV state of ^{29}Si in the reaction $^{28}Si(d,p\gamma)^{29}Si$.

V. LIGHT NUCLEI

133. ERAMZHYAN, R.A., KUDEJAROV, Yu.A.: Nucleon clusters in nuclei Li^6 and He^6 from the data on various reactions at high energies.

134. ŠLAUS, I., VALKOVIĆ, V.: Multiparticle reactions and the spectroscopy of lightest nuclei.

135. BLANK, J., ŰLEHLA, I.: The ground state properties of the He^4 nucleus.

136. VASHAKIDZE, I.Sh., ELIAVA, A.T.: Application of the non-local factorizing potential in the determination of the spectrum of nuclei with A=12 in the approximation of particle-hole excitation (in Russian).

137. ROTTER, I.: On reactions with transfer of two particles.

138. GORODETZKY, S., GALLMANN, A., HAAS, F., HEUSCH, B.: Electromagnetic properties of the N^{14} bond states.

139. EKEDA, K., HORIUCHI, H.: A molecule-like structure of atomic nuclei of $^{16}O^*$ and ^{20}Ne.

140. GOODMAN, A., STRUBLE, G., BAR-TOUV, J., GOSWAMI, A.: Generalized pairing correlations in the s-d shell.

141. PANDYA, S.P., KULKARNI, D.R.: SU_3 symmetry and s-state interactions in s-d shell.

142. IOSIFESCU, M., STANCU, F.: SU_3 spectroscopical calculations on Ne^{21}.

143. HULUBEI, H., NEAMU, I., TEODORESCU, C.M., SCINTEI, N., MARTALOGU, N., BERINDE, A.: Angular correlations $^{22}Ne(p,p_1\gamma)^{22}Ne$.

144. HULUBEI, H., NEAMU, I., VLĂDUCĂ, G., SCINTEI, N., MARTALOGU, N., TEODORESCU, C.M., IVAŞCU, M., BERINDE, A.: Elastic and inelastic scattering of protons on ^{22}Ne.

145. KRUG, H., PAPINEAU, A.: Vectorial and tensorial asymmetries in $^{12}C(d, p)^{13}C$ with different transfer momentum by polarized deuterons at 21.8 MeV.

146. FULBRIGHT, H.W., BLANN, H.M., FLEMING, D., ROBBINS, J.A., PLENDL, H.S.: The structure of oxygen 16.

147. VERRALL, R.I., BELL, R.E.: Delayed protons following the decay of ^{40}Sc.

148. PIRÈS, P., TOURREIL, R. de, VAUTHERIN, D., VÉNÉRONI, M.: Hartree-Fock spectra and densities of ^{40}Ca and ^{48}Ca isotopes.

149. DELAUNAY, J., TELLEZ, A., BALLINI, R., CINDRO, N., FOUAN, J.P.: Gamma decay of levels of ^{40}Ca and ^{48}Ca.

150. SOTONA, M., PLUHAŘ, Z., TRLIFAJ, L., GMITRO, M.: Structure of A = 21 nuclei.

151. TURKEVICH, I.M., TURKEVICH, Ya., CHEPURCHENKO, I.A., FRYSHKIN, B.: γ-dependence of the angular distribution of protons from the reaction $^{6}Li(d, p)^{7}Li$ (in Russian).

152. DAVYDOV, V.V., OGLOBLIN, A.A., SAKUTA, S.B., CHIEV, V.I.: The reaction (Li^{6}, d) and alpha-particle states of nuclei of the 2s-1d shell (in Russian).

153. ARTEMOV, K.P., GOLDBERG, V.Z., DAVYDOV, V.V., OGLOBLIN, A.A., RUDAKOV, V.P., SAKUTA, S.B., CHIEV, V.I.: Excitation of O^{16} and Ne^{20} levels in alpha-particle transfer reaction (in Russian).

154. *(Number not used)*

† VAN LEUVEN, P.: On the form factor for electron scattering from the first excited state of Li^{6}.

† ARDITI, M., DOUBRE, H., FRASCARIA, N., GARRON, J.P., RIOU, M., ROYER, D.: (d, He^{3}) reactions on light nuclei at 82 MeV.

VI. GENERAL PROPERTIES OF NUCLEI

155. KHANNA, F.C.: Short-range nucleon-nucleon correlations and elastic scattering of high energy electrons.

156. TOEPFFER, Ch., GREINER, W.: Dispersion effects in electron scattering.

157. BABIKOV, V.V.: A peculiar Thomas-Fermi equation for the nucleus.

158. MIHAILOVIC, M.V., ROSINA, M.: A variational method for the ground state density matrix.

159. AMUSYA, M.Ya., CHERELKOV, N.A.: A specific application of the many-body theory for the description of bound systems consisting of a finite number of particles (in Russian).

160. MELDNER, H.: Nuclear orbital rearrangement energy and self-consistent field models.

161. GMITRO, M., RIMINI, A., SAWICKI, J., WEBER, T.: Effective charge operator and realistic nucleon-nucleon potentials.

162. LAW, J.B., SPRUNG, D.W.L.: A note on the single particle spin-orbit force.

163. BAND, I.M., GUMAN, V.N., SLIV, L.A., KHARITONOV, Yu.I.: Residual particle interaction (in Russian).

164. CLEMENT, C.F.: Widths of nuclear single particle states.

165. DABROWSKI, J., SKŁADANOWSKI, Z.: Binding energy of a Λ particle in nuclear matter.

166. GRIFFIN, J.J.: "Walk-run" fission and mass asymmetry.

167. ARVIEU, R., BOHIGAS, O., LORAZO, B., QUESNE, C.: Seniority breaking of two-body forces and accuracy of the BCS method.

168. (Number not used)

† DANOS, M., HUBER, M.G.: Shell model treatment of the short-range correlations.

† NÉMETH, J., BETHE, H.A.: Symmetry and rearrangement energy in nuclear matter.

† RAMANNA, R.: Differential forms and nuclear structure.

VII. NEW TRENDS IN NUCLEAR STRUCTURE STUDIES AND UNCLASSIFIED CONTRIBUTIONS

169. GOL'DANSKY, V.I.: Direct observation of gigantic magnetic fields induced by the K-shell hole (in Russian).

170. GOL'DANSKY, V.I., LARKIN, A.I.: Analogue of the G-effect in nuclear transformations (in Russian).

171. FOSSAN, D.B., OLNESS, J.W., POLETTI, A.R., WARBURTON, E.K.: Experimental studies of excited-state magnetic moments.

172. BURKE, D.G., ALFORD, W.P.: Studies of (^{3}He, α) reactions on heavy nuclei.

173. STEFFEN, R.M.: The determination of G-factors of short-lived excited states using magnetic sources.

174. BURSON, S.B.: Measurement of internal-conversion coefficients of neutron-capture gamma rays with a super-conducting spectrometer.

175. COHEN, B.L., MAY, E.C., O'KEEFE, T.M., FINK, C.L.: Singlet deuterons ($\bar{d}$) from (p, $\bar{d}$) reactions.

176. VINDUŠKA, M.: A computer (Gier-Algol) program for computing electron and positron wave functions.

177. BATKIN, I.S., ZON, B.A., RAPOPORT, L.P.: Coulomb corrections to the neutron asymmetry coefficient in μ-capture (in Russian).

178. SUBOTOWICZ, M.: Experimental verification of the higher order effects and nuclear structure factors in the allowed beta transitions.

179. SUMBAEV, O.I., MESENTSEV, A.F., MARUSHENKO, V.I., RILNIKOV, A.S., IVANOV, G.A.: Anomalous I.S. of nuclear charge radii in isotopes of Ba.

180. BACKENSTOSS, G., CHARALAMBUS, S., DANIEL, H., KOCH, H., KRELL, M., POELZ, G., SCHMITT, H., TAUSCHER, L.: Nuclear structure studies with π-mesic atoms.

181. McINTYRE, J.A., RAMCHONDRAN, S., MICHALK, V.E.: Measurement of electromagnetic properties of nuclei using neutron-capture gamma rays.

182. BOEHM, F., BHATTACHERJEE, S.K.: Isotope shift of K X-rays and variations of nuclear charge radii.

APPENDIX

183. GRIN, Yu.T., PAVLICHENKOV, I.M.: Change of the quadrupole moment of deformed nuclei due to rotation (in Russian).

184. BARANOV, S.A., SHATINSKY, V.M., KULAKOV, V.M., SHUBKO, V.M.: Radium-255 levels from the alpha decay of thorium-229 (in Russian).

185. NEMIROVSKY, GORODKOV, S.S.: On the inverse connection between nuclear matter density and the potential of the shell model (in Russian).

186. KARADZHEV, K.V., MANKO, V.M., CHUKREEV, F.E.: Alpha particle structure levels in ^{32}S (in Russian).

187. GROSHEV, L.V., DVORETSKY, V.N., DEMIDOV, A.M., PAKHIMOV, A.S.: De-excitation of barium nuclei after thermal neutron capture (in Russian).

LIST OF SEMINAR PAPERS

I. THE INTERACTION OF HIGH-ENERGY PARTICLES WITH NUCLEI

1. G.K. Backenstoss
   Nuclear structure studies with π-mesic atoms

2. T.E.O. Ericson and M. Locher
   Nucleon-nucleus forward dispersion relations

3. A.I. Akhiezer
   Interaction of pions with nuclear matter

4. V.M. Kolybasov and N.Ya. Smorodinskaya
   Nucleon-nucleus interaction at high energies

II. NEW APPROACHES TO OLD PROBLEMS

1. T. Marumori
   A new microscopic approach to the collective motion

2. R.R. Chasman
   A new approach to pairing forces: the intermediate state method

3. A. Faessler
   Competition between pairing and self-consistency as causes of the energy gap

4. S. Szpikowski
   Preliminary remark on the common symmetry of pairing and quadrupole forces

5. M.V. Mihailovic
   Transition amplitudes as variational parameters for the ground state

III. HIGHLY EXCITED NUCLEAR STATES; NEUTRON RESONANCES

1. R.E. Chrien
   Resonant and non-resonant neutron-capture experiments

2. G. Samour
   A study of partial radiative widths at and between neutron resonances

3. L.M. Bollinger
   Neutron spectroscopy with average spectra from neutron-resonance capture

4. L.R. Nilsson
Radiative capture of neutrons in the MeV region

5. G. Longo
Calculations on dipole radiative capture of 5-50 MeV nucleons

6. J.L. Fowler
Resonant states of doubly closed shell plus one neutron nuclei

7. R. Alves
Strength functions, radiation widths and level spacings as a function of A and J

8. J.A. McIntyre
Study of highly excited states using the resonance fluorescence process

IV. THE INTERACTION OF HIGH-ENERGY ELECTRONS WITH NUCLEI

1. N.G. Afanasiev
The elastic and non-elastic scattering of 100-200 MeV electrons with 2s - 1d shell nuclei and quasi-elastic scattering of 500-1000 MeV electrons with ^{12}C.

2. N.G. Shevchenko
The elastic scattering of 200 MeV electrons with Ni and Sn isotopes

3. F.K. Hann
Short-lived nucleon-nucleon correlation and the scattering of fast electrons

4. P.E. Nemirovsky
Self-consistent calculation of charge density distribution from the data on elastic scattering of electrons

5. V.K. Lukyanov, I.Z. Petkov, Yu.S. Pol
The scattering of fast electrons by nuclei with arbitrary distribution of charge density

V. THE INTERACTION OF HEAVY IONS WITH NUCLEI; THE PROPERTIES OF TRANSURANIUM ELEMENTS

1. J.R. Nix, P.E. Nemirosvky, I.P. Selinov et al.
Discussion on the new region of stable superheavy elements

2. R.L. Hahn
New neptunium isotopes ^{230}Np, ^{237}Np

3. Yu.Ts. Oganesyan, A. Winther, U. Lemberg, Yu.T. Grin
Coulomb excitation of nuclei induced by heavy ions

4. A.A. Ogloblin
   Study of nuclear reactions induced by lithium ions

5. M. Riou
   $^{12}C + {}^{12}C$ reactions at 87 MeV

6. V.I. Goldansky
   Analogue of the Josefson effect in nuclear transformations

VI. INVESTIGATIONS OF THE RADIOACTIVE DECAY OF NUCLEI

1. G. Musiol
   Nuclear spectroscopy on the beam of the Dubna synchrocyclotron

2. C.M. Lederer
   On beam gamma-ray spectroscopy of nuclei in the region of ^{90}Zr

3. R. Foucher
   Some results on new rubidium isotopes

4. W. Michaelis
   Band mixing in deformed odd-A nuclei

5. M.E. Bunker
   State mixing in ^{165}Ho

6. P.G. Hansen
   The E2 + M1 decay of the 2^+ beta vibrational state in ^{178}Hf

7. F. Wideman
   Experimental study of ^{155}Eu levels

8. C.W. Reich
   Decay of a long-lived isomeric state in ^{178}Hf with $K = 16$

9. J.W. Mihelich
   New results on the decay of ^{158}Tb (long-lived isomers)

10. H. Verheul
    Study of the decay scheme of ^{176}Ta

11. M. Šott
    Nuclear orientation study of ^{192}Ir and ^{194}Ir

12. A. Gelberg
    Life-time and angular correlation measurements in ^{193}Ir

13. M.F. Subotowicz
    Investigation of the highly retarded allowed beta-transitions

14. L.A. Malov
    Equilibrium deformations in the region $50 \leq Z \leq 82$, $50 \leq N \leq 82$

15. K.F. Alexander
Experimental indication of the oblate shape of the nucleus ^{129}La

16. I. Řezanka
Spectroscopic study of odd-A nuclei

17. V.I. Goldansky
Way to the direct observation of gigantic magnetic fields produced on nuclei by the K-shell hole

18. J. Kern
On the validity of quasiparticle descriptions of N = 83 odd-odd isotopes

VII. ANALOGUE STATES IN NUCLEI

1. M.G. Urin, D.F. Zaretsky
Microscopical description of resonance reactions with excitation of analogue states

2. S.I. Drozdov
The width of analogue states

3. J. Zimanyi, B. Gyarmati
On the shape of the symmetry potential

4. M.V. Mihailovic
Gamma-ray spectra from the radiative capture of fast neutrons and the direct-semidirect capture mechanism

VIII. NUCLEAR FORCES AND NUCLEAR MATTER; THE STRUCTURE OF LIGHT ELEMENTS

1. K.A. Brueckner
Nuclear forces and nuclear matter

2. A.B. Migdal
Interactions between quasiparticles outside the nucleus

3. I. Ulehla
Ground state properties of the ^{4}He nucleus

4. G.F. Filippov
Vibrational and rotational states in systems containing several particles

5. R.A. Eramzhyan, Yu.A. Kudejarov, V.G. Neudachin
Nucleon clusters in light nuclei

IX. THE BOUND STATES OF COMPLEX NUCLEI

1. T. Udagawa
   Nuclear collectivity in two-nucleon transfer reactions

2. B.L. Birbrair
   2^+ and 3^- states of spherical nuclei

3. G.L. Struble
   Generalized pairing correlations in the s-d shell

4. N.P. Yudin
   The interaction of the single-particle and vibrational degrees of freedom

5. E.E. Berlovich
   On the shape of the atomic nuclei in transition regions

ORGANIZING COMMITTEE

Chairman

N. N. BOGOLYUBOV

Vice-Chairman

V. G. SOLOVIEV

Scientific Secretary

I. N. MIKHAILOV

Members

K. F. ALEXANDER
R. A. ERAMZHYAN
G. N. FLEROV
I. M. FRANK
A. HRYNKIEWICZ
F. JANOUCH
V. L. KARPOVSKY
M. M. LEBEDENKO
O. S. LUPANDIN
V. L. MIKHEEV
V. S. SHVANEV
N. SODNOM
V. V. VOLKOV
B. N. ZAKHARIEV
I. S. ZARUBINA
Zh. ZHELEV

Scientific Consultants

A. BOHR
B. S. DZHELEPOV
H. NIEWODNICZAŃSKI
J. O. RASMUSSEN
M. SAKAI

Editors

L. A. SELF
H. KACZEROVA

CHAIRMEN AND SECRETARIES OF SESSIONS

Session	Chairmen	Secretaries
1	N. N. BOGOLYUBOV	V. V. VOLKOV
2	H. NIEWODNICZAŃSKI	V. G. CHUMIN
3	J. SCHINTLMEISTER	R. ARLT
4	R. F. BELL	V. K. LUKYANOV
5	B. S. DZHELEPOV	M. ADAM
6	N. SODNOM	V. A. KARNAUKHOV
7	A. S. DAVYDOV	B. N. KALINKIN
8	Zh. ZHELEV	I. Z. PETKOV
9	G. RASMUSSEN	S. REVAI
10	P. HUBER	V. I. FURMAN
11	J. URBANEC	F. BEČVÁŘ
12	I. M. FRANK	N. IANEVA
13	A. BOHR	L. A. MALOV
14	S. GORODETZKY	V. V. PASHKEVICH
15	G. N. FLEROV	V. A. DRUIN
16	L. N. USACHEV	Yu. P. GANGRSKY
17	A. HRYNKIEWICZ	Z. STAHURA
18	G. ALAGA	V. V. BABIKOV
19	V. G. SOLOVIEV	R. V. JOLOS
20	V. G. SOLOVIEV	

LIST OF PARTICIPANTS

NAME	PRESENT ADDRESS	NATIONALITY
Abdurazakov, A.A.	Tashkent State University, Tashkent	Union of Soviet Socialist Republics
Adam, J.	Joint Institute for Nuclear Research, Dubna, USSR (Head P.O. Box 79, Moscow)	Czechoslovakia
Afanasiev, N.G.	Physical-Technical Institute, Yumovski tupik, Kharkov	Union of Soviet Socialist Republics
Agnew, L.	International Atomic Energy Agency, Kärntner Ring 11, 1010, Vienna, Austria	United States of America
Akhiezer, A.I.	Physical-Technical Institute, Yumovski tupik, Kharkov	Union of Soviet Socialist Republics
Alaga, G.	Institut "Ruder Bošković", Bijanička 54, Zagreb	Yugoslavia
Alexander, J.M.	State University of New York, Stony Brook, N.Y. 11790	United States of America
Alexander, K.F.	Joint Institute for Nuclear Research, Dubna, USSR (Head P.O. Box 79, Moscow)	German Democratic Republic
Alexeev, V.L.	A.F. Ioffe Physical-Technical Institute, ul. Politekhnicheskaya 26, Leningrad	Union of Soviet Socialist Republics
Alves, R.	Orme des Merisiers GP/ALS, B.P.2, 91 Gif-sur-Yvette, France	Brasil
Andreeff, A.	Zentralinstitut für Kernforschung, Rossendorf, 8051 Dresden, Postfach 19	German Democratic Republic
Andreev, V.N.	Institute of Theoretical and Experimental Physics, ul.B. Cheremushkinskaya 89, Moscow M-259	Union of Soviet Socialist Republics
Arlt, R.	Joint Institute for Nuclear Research, Dubna, USSR (Head P.O. Box 79 Moscow)	German Democratic Republic
Asfour, F.	Joint Institute for Nuclear Research, Dubna, USSR (Head P.O. Box 79, Moscow)	United Arab Republic
Axel, P.	Physics Dept, University of Illinois, Urbana, Illinois 61801.	United States of America

NAME	PRESENT ADDRESS	NATIONALITY
Azhgirey, L.S.	Joint Institute for Nuclear Research, Dubna USSR (Head P.O. Box 79, Moscow)	Union of Soviet Socialist Republics
Babikov, V.V.	Joint Institute for Nuclear Research, Dubna USSR (Head P.O. Box 79, Moscow)	Union of Soviet Socialist Republics
Backenstoss, G.K.	CERN, 1211 Geneva 23, Switzerland	German Federal Republic
Balashov, V.V.	Institute of Nuclear Physics, Moscow State University, Moscow 234	Union of Soviet Socialist Republics
Balbutsev, E.B.	Joint Institute for Nuclear Research, Dubna USSR (Head P.O. Box 79, Moscow)	Union of Soviet Socialist Republics
Baldeweg, F.	Zentralinstitut für Kernforschung, Rossendorf, 8051 Dresden, Postfach 19	German Democratic Republic
Baldin, A.M.	Joint Institute for Nuclear Research, Dubna, USSR (Head P.O. Box 79, Moscow)	Union of Soviet Socialist Republics
Bang, J.	Niels Bohr Institute, 17 Blegdamsvej, Copenhagen	Denmark
Baranov, S.A.	I.V. Kurchatov Institute of Atomic Energy, ul. Kurchatova 46, Moscow D-182	Union of Soviet Socialist Republics
Barkan, S.H.	Scottish Research Reactor Centre, East Kilbride, Glasgow, United Kingdom	Turkey
Bartholomew, G.A.	Atomic Energy of Canada Ltd., Chalk River, Ontario	Canada
Bečvář, F.	Joint Institute for Nuclear Research, Dubna, USSR (Head P.O. Box 79, Moscow)	Czechoslovakia
Begzhanov, R.B.	Institute of Nuclear Physics, p. Ulugbek 4, Tashkent	Union of Soviet Socialist Republics
Bell, R.E.	Foster Radiation Laboratory, McGill University, Montreal 2	Canada
Belovitsky, G.E.	P.N. Lebedev Physical Institute, Leninsky Prospect 53, Moscow	Union of Soviet Socialist Republics
Belyaev, S.T.	Novosibirsk State University, Novosibirsk	Union of Soviet Socialist Republics

NAME	PRESENT ADDRESS	NATIONALITY
Belyaev, V.B.	Joint Institute for Nuclear Research, Dubna, USSR (Head P.O. Box 79, Moscow)	Union of Soviet Socialist Republics
Bencze, Gy.	Central Research Institute for Physics, P.O. Box 49, Budapest 114	Hungary
Benzi, V.	CNEN, Via Mazzini 2, Bologna	Italy
Beregi, P.	Central Research Institute for Physics, P.O. Box 49, Budapest 114	Hungary
Berlovich, E.E.	A.F. Ioffe Physical-Technical Institute, ul. Polytekhnicheskaya 26, Leningrad	Union of Soviet Socialist Republics
Birbrair, B.L.	A.F. Ioffe Physical-Technical Institute, ul. Polytekhnicheskaya 26, Leningrad	Union of Soviet Socialist Republics
Blomqvist, J.E.	Research Institute for Physics, Stockholm 50	Sweden
Bochev, B.	Physical Institute, V.I. Lenin bul. 72, Sofia	Bulgaria
Bochnacki, Z.	Institute of Nuclear Physics, ul. Radzikowskiego, Cracow 23	Poland
Boehm, F.H.	California Institute of Technology, Physics Dept, Pasadena, California 91109	United States of America
Bogolyubov, N.N.	Joint Institute for Nuclear Research, Dubna USSR (Head P.O. Box 79, Moscow)	Union of Soviet Socialist Republics
Bohr, A.	Niels Bohr Institute Blegdamsvej 17, Copenhagen	Denmark
Bollinger, L.M.	Argonne National Laboratory, Argonne, Illinois 60439	United States of America
Bonch-Osmolovskaya, N.A.	Joint Institute for Nuclear Research, Dubna USSR (Head P.O. Box 79, Moscow)	Union of Soviet Socialist Republics
Bondarenko, V.A.	Institute of Physics, Riga	Union of Soviet Socialist Republics
Bonchev, C.	Sofia University, Anton Ivanov 1, Sofia	Bulgaria
Brabec, V.	Nuclear Research Institute, Řež near Prague	Czechoslovakia

NAME	PRESENT ADDRESS	NATIONALITY
Bravin, A.V.	Saratov State University, Saratov	Union of Soviet Socialist Republics
Brentano, P. von	Max-Planck Institute for Nuclear Physics, Saupfercheckweg 69 Heidelberg	German Federal Republic
Broder, D.L.	Physical-Technical Institute, Obninsk	Union of Soviet Socialist Republics
Brown, G.E.	State University of New York, Stony Brook, N.Y. 11790	United States of America
Brueckner, K.A.	University of California, San Diego, La Jolla, California	United States of America
Bruge, G.L.	Centre d'Etudes Nucléaires de Saclay, B.P. No.2, 91-Gif-sur-Yvette	France
Brussard, P.	Physics Laboratory of the State University, Bijlhouwerstraat 6, Utrecht	Holland
Budzanowski, A.	Institute of Nuclear Physics, ul. Radzikowskiego, Cracow 23	Poland
Bunker, M.E.	Los Alamos Scientific Laboratory, P.O. Box 1663, Los Alamos, New Mexico 87544	United States of America
Burke, D.	McMaster University, Hamilton, Ontario	Canada
Burson, S.B.	Argonne National Laboratory, Argonne, Illinois 60439	United States of America
Butsev, V.S.	Joint Institute for Nuclear Research, Dubna, USSR (Head P.O. Box 79, Moscow)	Union of Soviet Socialist Republics
Chasman, R.R.	Argonne National Laboratory, Argonne, Illinois 60439	United States of America
Cherenkov, P.A.	P.N. Lebedev Physical Institute, Leninsky Prospect 53, Moscow	Union of Soviet Socialist Republics
Chojnacki, S.	Joint Institute for Nuclear Research, Dubna, USSR (Head P.O. Box 79, Moscow)	Union of Soviet Socialist Republics
Choudhury, D.C.	Polytechnic Institute of Brooklyn, 333 Jay St., Brooklyn, N.Y. 11201	United States of America

NAME	PRESENT ADDRESS	NATIONALITY
Chrien, R.E.	Brookhaven National Laboratory, Dept. of Physics, Bldg. 510A, Upton, N.Y. 11973	United States of America
Chultem, D.	Mongolian State University, Ulanbator 46/473	Mongolia
Chumin, V.G.	Joint Institute for Nuclear Research, Dubna, USSR (Head P.O. Box 79, Moscow)	Union of Soviet Socialist Republics
Clement, C.F.	Theoretical Physics Division 8.9, UKAEA, AERE Harwell, Didcot, Berks	United Kingdom
Clementel, E.	CNEN and Institute of Physics, Via Mazzini 2, Bologna	Italy
Cohen, B.	University of Pittsburg, Pittsburg, Pennsylvania	United States of America
Csikai, J.	Institute of Experimental Physics, University I.M.L. Kossuth, Bem. 18/a, Debrecen	Hungary
Dabrowski, J.	Theoretical Division, Institute for Nuclear Research, Hoza 69, Warsaw	Poland
Dakowski, M.	Institute for Nuclear Research, 1 A Division, Swierk	Poland
Danilyan, G.V.	Institute for Theoretical and Experimental Physics, B. Cheremushkinskaya 89, Moscow M-259	Union of Soviet Socialist Republics
Davydov, A.S.	Institute for Theoretical Physics, Kiev	Union of Soviet Socialist Republics
Davydov, A.V.	Institute for Theoretical and Experimental Physics, Kiev B. Cheremushkinskaya 89, Moscow M-259	Union of Soviet Socialist Republics
Deberth, K.	Institute for Atomic Physics, P.O. Box 35, Bucharest	Rumania
Decowski, P.	University of Warsaw, Institute of Experimental Physics, Hoza 69, Warsaw	Poland
Delaunay, J.	Centre d'Etudes Nucléaires de Saclay, B.P.2, 91-Gif-sur-Yvette	France
Demidov, A.M.	I.V. Kurchatov Institute of Atomic Energy, ul. Kurchatova 46, Moscow-D-182	Union of Soviet Socialist Republics

NAME	PRESENT ADDRESS	NATIONALITY
Dermendzhiev, E.	Joint Institute for Nuclear Research, Dubna, USSR (Head P.O. Box 79. Moscow)	Union of Soviet Socialist Republics
Devare, H.G.	Tata Institute of Fundamental Research, Colaba, Bombay 5	India
Dietrich, F.S.	Niels Bohr Institute, Blegdamsvej 17, Copenhagen, Denmark	United States of America
Dolbilkin, B.S.	P.N. Lebedev Institute of Physics, Leninsky Prospect 53, Moscow	Union of Soviet Socialist Republics
Dorokhov, V.V.	Physical-Technical Institute, Sukhumi n/o 14	Union of Soviet Socialist Republics
Dragnev, T.N.	Physical Institute, V.I. Lenin bul. 72, Sofia	Bulgaria
Dranitsina, G.F.	Library of Academy of Sciences USSR, Birzhevaya liniya 1, Leningrad	Union of Soviet Socialist Republics
Droste, Ch.	Joint Institute Nuclear Research, Dubna, USSR (Head P.O. Box 79, Moscow)	Poland
Druin, V.A.	Joint Institute Nuclear Research, Dubna, USSR (Head P.O. Box 79, Moscow)	Union of Soviet Socialist Republics
Dzhelepov, B.S.	V.G. Khlopin Institute of Radium, ul. Roentgena 1, Leningrad	Union of Soviet Socialist Republics
Efimov, V.N.	Joint Institute Nuclear Research, Dubna, USSR (Head P.O. Box 79, Moscow)	Union of Soviet Socialist Republics
Eramzhyan, R.A.	Joint Institute Nuclear Research, Dubna, USSR (Head P.O. Box 79, Moscow)	Union of Soviet Socialist Republics
Ericson, T.E.O.	CERN, 1211 Geneva 23, Switzerland	Sweden
Erskine, J.R.	Argonne National Laboratory, Argonne, Illinois 60439	United States of America
Estulin, I.V.	Institute of Physics, Moscow State University, Moscow	Union of Soviet Socialist Republics
Evseyev, V.S.	Joint Institute Nuclear Research, Dubna, USSR (Head P.O. Box 79, Moscow)	Union of Soviet Socialist Republics

NAME	PRESENT ADDRESS	NATIONALITY
Faessler, A.	University of Muenster, Dept of Physics, Muenster 44	German Federal Republic
Fedotov, S.I.	Joint Institute Nuclear Research, Dubna, USSR (Head P.O. Box 79, Moscow)	Union of Soviet Socialist Republics
Fenin, Yu.M.	Joint Institute Nuclear Research, Dubna, USSR (Head P.O. Box 79, Moscow)	Union of Soviet Socialist Republics
Feoktistov, A.I.	Institute of Physics, B. Kitayevskaya 144, Kiev 28	Union of Soviet Socialist Republics
Filippov, G.F.	Institute of Physics, B. Kitayevskaya 144, Kiev 28	Union of Soviet Socialist Republics
Flerov, G.N.	Joint Institute for Nuclear Research, Dubna, USSR (Head P.O. Box 79, Moscow)	Union of Soviet Socialist Republics
Fossan, D.B.	Physics Dept, State University of New York, Stony Brook, N.Y. 11790	United States of America
Foucher, R.	Institut de Physique Nucléaire, B.P. No.1, 91-Orsay	France
Fowler, J.L.	Oak Ridge National Laboratory, P.O.B. x, Oak Ridge, Tennessee 37830	United States of America
Frank, I.M.	Joint Institute for Nuclear Research, Dubna, USSR (Head P.O. Box 79, Moscow)	Union of Soviet Socialist Republics
Fulbright, H.W.	University of Rochester, Rochester, N.Y. 14627	United States of America
Fülle, R.	Zentralinstitut für Kernforschung, Rossendorf, 8051 Dresden, Postfach 19	German Democratic Republic
Furman, V.I.	Joint Institute for Nuclear Research, Dubna, USSR (Head P.O. Box 79, Moscow)	Union of Soviet Socialist Republics
Gabrakov, S.I.	Joint Institute for Nuclear Research, Dubna, USSR (Head P.O. Box 79, Moscow)	Bulgaria
Gadǧakov, B.	Institute of Physics, University of Sofia, Sofia	Bulgaria

NAME	PRESENT ADDRESS	NATIONALITY
Galan, P.	Joint Institute for Nuclear Research, Dubna, USSR (Head P.O. Box 79, Moscow)	Czechoslovakia
Gallmann, A.	Université de Strasbourg, B.P. 16, CR 67-Strasbourg 3	France
Gangrsky, Yu.P.	Joint Institute for Nuclear Research, Dubna, USSR (Head P.O. Box 79, Moscow)	Union of Soviet Socialist Republics
Geilikman, B.T.	I.V. Kurchatov Institute of Atomic Energy, ul. Kurchatova 46, Moscow D-182	Union of Soviet Socialist Republics
Gelberg, A.	Institute for Atomic Physics, P.O. Box 35, Bucharest	Romania
Gillet, V.	Service de Physique théorique, Centre d'Etudes Nucléaires de Saclay, B.P. No.2, 91-Gif-sur-Yvette	France
Glendenning, N.K.	Lawrence Radiation Laboratory, Berkeley, California	Canada
Gmitro, M.	Nuclear Research Institute, Řež near Prague	Czechoslovakia
Goldansky, V.I.	Institute of Chemical Physics, Vorobyevskoe Shosse 2, Moscow B-334	Union of Soviet Socialist Republics
Golovkov, N.A.	Joint Institute for Nuclear Research, Dubna, USSR (Head P.O. Box 79, Moscow)	Union of Soviet Socialist Republics
Gorbunov, A.N.	P.N. Lebedev Institute of Physics, Leninsky Prospect 53, Moscow	Union of Soviet Socialist Republics
Gorodetzky, S.	Institut de Recherches nucléaires de l'Université de Strasbourg, B.P.16, 67-Strasbourg-Cronenbourg	France
Grabowski, J.	Institute of Nuclear Physics, ul. Radzikowskiego, Cracow 23	Poland
Graham, R.L.	Chalk River Nuclear Laboratory, Atomic Energy of Canada Ltd., Chalk River, Ontario	Canada
Gridnev, K.A.	Leningrad State University Universitetskaya nab.7/9, Leningrad B-164	Union of Soviet Socialist Republics
Griffin, J.J.	Dept of Physics, University of Maryland, College Park, Maryland, 20742	United States of America

NAME	PRESENT ADDRESS	NATIONALITY
Grigoriev, E.L.	Joint Institute for Nuclear Research, Dubna, USSR (Head P.O. Box 79, Moscow)	Union of Soviet Socialist Republics
Grigoriev, E.P.	Physical Institute, Leningrad State University, Universitetskaya nab.7/9, Leningrad B-164	Union of Soviet Socialist Republics
Grin, Yu.T.	I.V. Kurchatov Institute of Atomic Energy, ul. Kurchatova 46, Moscow D-182	Union of Soviet Socialist Republics
Grodzins, L.	Massachusetts Institute of Technology, Physics Dept, Cambridge, Mass. 02139	United States of America
Gromov, K.Ya.	Joint Institute for Nuclear Research, Dubna, USSR (Head P.O. Box 79, Moscow)	Union of Soviet Socialist Republics
Guiasu, I.N.	Institute for Atomic Physics, P.O. Box 35, Bucharest	Romania
Guzhovsky, B.Ya.	I.V. Kurchatov Institute of Atomic Energy, ul. Kurchatova 46, Moscow D-182	Union of Soviet Socialist Republics
Gyarmati, B.	Nuclear Research Institute, P.O. Box 51, Debrecen	Hungary
Hahn, R.L.	Transuranium Laboratory, Oak Ridge National Laboratory, Oak Ridge, Tennessee	United States of America
Hamamoto-Kuroda, I.	Niels Bohr Institute Blegdamsvej 17, Copenhagen	Denmark
Hanna, S.S.	Physics Dept, Stanford University, Stanford, California 94305	United States of America
Hansen, P.G.	Institute of Physics, University of Aarhus, 8000 Aarhus	Denmark
Hänsgen, H.R.	Technische Universität Dresden, Pratzschwitzer Str. 15, Pirna	German Democratic Republic
Harada, K.	Nuclear Physics Laboratory, Japan Atomic Energy Research Institute, Tokai-mura, Iberaki-ken	Japan
Harar, S.	Centre d'Etudes Nucléaires de Saclay, B,P.2, 91-Gif-sur-Yvette	France
Herbut, F.E.	Institute "Boris Kidrič" P.O. Box 522, Belgrade-Vinča	Yugoslavia

NAME	PRESENT ADDRESS	NATIONALITY
Herrlander, C.J.	Research Institute for Physics, Stockholm 50	Sweden
Hnatowicz, V.	Nuclear Research Institute, Řež near Prague	Czechoslovakia
Hornshøj, P.	Institute of Physics, University of Aarhus, 8000 Aarhus	Denmark
Hrynkiewicz, A.	Joint Institute for Nuclear Research, Dubna, USSR (Head P.O. Box 79, Moscow)	Poland
Huber, M.G.	Institute for Theoretical Physics, Department of Physics, Robert Mayer Str. 10, 6 Frankfurt a.M.	German Federal Republic
Huber, P.	Physics Dept, University of Basel, Klingelstr. 82, Basel	Switzerland
Ianeva, N.	Joint Institute for Nuclear Research, Dubna, USSR (Head P.O. Box 79, Moscow)	Bulgaria
Ikeda, K.	Joint Institute for Nuclear Research, Dubna, USSR (Head P.O. Box 79, Moscow)	Japan
Iljuschenko, V.I.	Joint Institute for Nuclear Research, Dubna, USSR (Head P.O. Box 79, Moscow)	Union of Soviet Socialist Republics
Inopin, E.V.	Physical-Technical Institute, Yumovski tupik, Kharkov	Union of Soviet Socialist Republics
Ismatov, E.I.	Institute of Nuclear Physics, p. Ulukbek 4, Tashkent	Union of Soviet Socialist Republics
Janouch, F.	Nuclear Research Institute, Řež near Prague	Czechoslovakia
Jarczyk, L.I.	Uniwersytet jagiellónski ul. Roymonta 4, Cracow	Poland
Jean, M.	Institut de Physique nucléaire, D.Ph.Th., B.P.1, 91-Orsay	France
Jéki, L.	Central Research Institute for Physics, P.O. Box 49, Budapest 114	Hungary
Jibuti, R.I.	Institute of Physics, Guramishvili 6, Tbilisi	Union of Soviet Socialist Republics

NAME	PRESSENT ADDRESS	NATIONALITY
Johnson, N.	Oak Ridge National Laboratory, P.O.B. x, Oak Ridge, Tennessee 37830	United States of America
Jolos, R.V.	Joint Institute for Nuclear Research, Dubna, USSR (Head P.O. Box 79, Moscow)	Union of Soviet Socialist Republics
Jungclaussen, H.	Joint Institute for Nuclear Research, Dubna, USSR (Head P.O. Box 79, Moscow)	German Democratic Republic
Kalinkin, B.N.	Joint Institute for Nuclear Research, Dubna, USSR (Head P.O. Box 79, Moscow)	Union of Soviet Socialist Republics
Kalinnikov, V.G.	Joint Institute for Nuclear Research, Dubna, USSR (Head P.O. Box 79, Moscow)	Union of Soviet Socialist Republics
Kaminker, D.M.	A.F. Ioffe Physical-Technical Institute, ul. Politekhnicheskaya 26, Leningrad	Union of Soviet Socialist Republics
Kantele, J.	Dept of Physics, University of Jyväskylä Nisulankatu 78, Jyväskylä	Finland
Karamyan, S.A.	Joint Institute for Nuclear Research, Dubna, USSR (Head P.O. Box 79, Moscow)	Union of Soviet Socialist Republics
Karnaukhov, V.A.	Joint Institute for Nuclear Research, Dubna, USSR (head P.O. Box 79, Moscow)	Union of Soviet Socialist Republics
Karpovsky, V.L.	Joint Institute for Nuclear Research, Dubna, USSR (Head P.O. Box 79, Moscow)	Union of Soviet Socialist Republics
Kashukeev, N.T.	Physical Institute, V.1. Lenin bul. 72, Sofia	Bulgaria
Kaun, K.H.	Zentralinstitut für Kernforschung, Rossendorf, 8051 Dresden, Postfach 19	German Democratic Republic
Kerman, A.K.	Massachusetts Institute of Technology, Cambridge, Mass. 02139	United States of America
Kern, J.	Physics Dept, University of Fribourg, CH-1700, Fribourg	Switzerland
Khanna, F.Ch.	Atomic Energy of Canada Ltd, Chalk River, Ontario	Canada
Kholnov, Yu.V.	V.G. Khlopin Institute of Radium, ul. Roentgena 1, Leningrad	Union of Soviet Socialist Republics

NAME	PRESENT ADDRESS	NATIONALITY
Khristov, I.D.	Joint Institute for Nuclear Research, Dubna, USSR (Head P.O. Box 79, Moscow)	Bulgaria
Khristov, Kh.	Physical Institute, V.I. Lenin bul. 72, Sofia	Bulgaria
Klimentovskaya, M.V.	Institute of Physics, Moscow State University, Moscow-234	Union of Soviet Socialist Republics
Klimov, Yu.G.	State Atomic Energy Committee, Moscow	Union of Soviet Socialist Republics
Klucherev, A.P.	Physical Technical Institute, ul. Gudanova 2, Kharkov	Union of Soviet Socialist Republics
Kluge, Gy.	Central Research Institute for Physics, P.O. Box 49, Budapest 114	Hungary
Knapp, V.	Institute Ruder Boškovič, Bijenička 54, Zagreb	Yugoslavia
Koch, H.	University of Jena, Technical-Physical Institut, Helmholzweg 3, Jena	German Democratic Republic
Kolybasov, V.M.	Institute of Theoretical and Experimental Physics, B. Cheremushkinskaya 89, Moscow M-259	Union of Soviet Socialist Republics
Komarov, V.V.	Institute of Nuclear Physics, Moscow State University, Moscow 234	Union of Soviet Socialist Republics
Kopaleyshvili, T.I.	Tbilisi State University, Tbilisi	Union of Soviet Socialist Republics
Korin, V.I.	P.N. Lebedev Physical Institute, Leninsky-Prospect 53, Moscow	Union of Soviet Socialist Republics
Kormicki, J.	Institute of Nuclear Physics, ul. Radzikowskiego, Cracow 23	Poland
Kovrigin, O.D.	Institute of Nuclear Physics, Alma-Ata 82	Union of Soviet Socialist Republics
Kracík, B.	Joint Institute for Nuclear Research, Dubna, USSR (Head P.O. Box 79, Moscow)	Czechoslovakia
Kraev, M.M.	Physical Institute, V.I. Lenin bul. 72, Sofia	Bulgaria

NAME	PRESENT ADDRESS	NATIONALITY
Kravtsov, V.A.	M.I. Kalinin Polytechnical Institute, ul. Politekhnicheskaya 29, Leningrad	Union of Soviet Socialist Republics
Křemenek, J.	Nuclear Research Institute, Řež near Prague	Czechoslovakia
Krjukova, L.H.	Institute of Physics, Moscow State University, Moscow 234	Union of Soviet Socialist Republics
Krogulski, T.	Nuclear Research Institute, Swierk	Poland
Kühn, B.	Zentralinstitut für Kernforschung, Rossendorf 8051, Dresden, Postfach 19	German Democratic Republic
Kulakov, V.M.	I.V. Kurchatov Institute of Atomic Energy, ul. Kurchatova 46, Moscow D-182	Union of Soviet Socialist Republics
Kumar, Krishna	Niels Bohr Institute, Blegdamsvej 17, Copenhagen	Denmark
Kuperin, A.B.	P.N. Lebedev Physical Institute, Leninsky Prospect 53, Moscow	Union of Soviet Socialist Republics
Kuzin, L.A.	State Atomic Energy Committee, Moscow	Union of Soviet Socialist Republics
Kuznetsova, M.Ya.	Joint Institute for Nuclear Research, Dubna, USSR (Head P.O. Box 79, Moscow)	Union of Soviet Socialist Republics
Kuznetsov, V.I.	Joint Institute for Nuclear Research, Dubna, USSR (Head P.O. Box 79, Moscow)	Union of Soviet Socialist Republics
Kuznetsova, M.Ya.	Joint Institute for Nuclear Research, Dubna, USSR (Head P.O. Box 79, Moscow)	Union of Soviet Socialist Republics
Lark, N.	Niels Bohr Institute, 17 Blegdamsvej, Copenhagen Denmark	United States of America
Latyshev, G.D.	Institute of Physics, B. Kitčevskaj 144, Kiev-28	Union of Soviet Socialist Republics
Lavrukhina, A.K.	GEOKHI, Moscow	Union of Soviet Socialist Republics
Leachman, R.B.	Kansas State University, Physics Dept, Manhattan, Kansas 66502	United States of America

NAME	PRESENT ADDRESS	NATIONALITY
Lebank Suong	Hanoi	Vietnam
Lederer, C.M.	Chemistry Division, Lawrence Radiation Laboratory, Berkeley, California 94720	United States of America
Lefterov, D.	Physical Institute, V.I. Lenin bul.72, Sofia	Bulgaria
Lemberg, I.Kh.	A.F. Ioffe Physical Technical Institute, Politekhnicheskaya 26, Leningrad	Union of Soviet Socialist Republics
Leuven, P. van	S.C.K.-C.E.N., Mol, Belgium	Belgium
Listengarten, M.A.	Institute of Physics, Leningrad State University, Leningrad B-164	Union of Soviet Socialist Republics
Lobanov, Yu.V.	Joint Institute for Nuclear Research, Dubna, USSR (Head P.O. Box 79, Moscow)	Union of Soviet Socialist Republics
Lobashov, V.M.	I.F. Ioffe Physical Technical Institute, Politekhnicheskaya 26, Leningrad	Union of Soviet Socialist Republics
Locher, M.	CERN, 1211 Geneva 23	Switzerland
Lombard, R.M.	Collège de France, Laboratoire de physique atomique et moléculaire, 11 Place Marcellin Bertholt, Paris V^{e}	France
Longo, G.	CNEN, Via Mazzini 2, Bologna	Italy
Lovas, I.	Joint Institute for Nuclear Research, Dubna, USSR (Head P.O. Box 79, Moscow)	Hungary
Lukyanov, V.K.	Joint Institute for Nuclear Research, Dubna, USSR (Head P.O. Box 79, Moscow)	Union of Soviet Socialist Republics
Lupandin, O.S.	State Atomic Energy Committee, Moscow	Union of Soviet Socialist Republics
Lynn, J.E.	Nuclear Physics Division, UKAEA, AERE Harwell, Didcot, Berks	United Kingdom
Macharadze, T.S.	Institute of Physics of the Academy of Sciences of the Georgian SSR, Guramishvili 6, Tbilisi 77	Union of Soviet Socialist Republics
Małecki, H.	Joint Institute for Nuclear Research, Dubna, USSR (Head P.O. Box 79, Moscow)	Poland

NAME	PRESENT ADDRESS	NATIONALITY
Malov, L.A.	Joint Institute for Nuclear Research, Dubna, USSR (Head P.O. Box 79, Moscow)	Union of Soviet Socialist Republics
Mamasakhlisov, V.I.	Tbilisi State University, p.I. Chavchavadze 1, Tbilisi 28	Union of Soviet Socialist Republics
Mang, H.J.	Physik Department der Technischen Hochschule, Theoretisches Teilinstitut, 8 München 2	German Federal Republic
Manko, V.I.	I.V. Kurchatov Institute of Atomic Energy, ul. Kurchatova 46, Moscow D-182	Union of Soviet Socialist Republics
Marinkov, L.	Institute Boris Kidrič, P.O. Box 522, Beograd-Vinča	Yugoslavia
Markov, B.N.	Joint Institute for Nuclear Research, Dubna, USSR (Head P.O. Box 79, Moscow)	Union of Soviet Socialist Republics
Martalogu, N.	Institute for Atomic Physics, P.O.Box 35, Bucharest	Romania
Marumori, T.	Dept of Physics, Kyushu University, Fukuoka	Japan
Maximov, B.M.	Moscow Physical Engineering Institute, Kashirskoe sh. 1, Moscow B-409	Union of Soviet Socialist Republics
McIntyre, J.A.	Cyclotron Institute, Texas A@M University, College Station, Texas	United States of America
Meldner, H.	Theoretical Physics, FU Berlin, 1 Berlin 33	German Federal Republic
Meyer, R.A.	Lawrence Radiation Laboratory L233, P.O. Box 808, Livermore, California 94550	United States of America
Michaelis, W.	Nuclear Research Centre, 75 Karlsruhe, P.O. Box 3640	German Federal Republic
Michaudon, A.F.	Centre d'Etudes Nucléaires de Saclay, B.P.No 2, 91-Gif-sur-Yvette	France
Middleton, R.	University of Pennsylvania, Dept of Physics, 209S 33rd Street, Philadelphia 19104	United Kingdom
Migdal, A.	I.V. Kurchatov Inst. of Atomic Energy, ul. Kurchatova 46, Moscow D-182	Union of Soviet Socialist Republics
Mihailović, M.V.	Nuclear Institute "J. Stefan", Ljubljana 199/IV	Yugoslavia

NAME	PRESENT ADDRESS	NATIONALITY
Mihelich, J.W.	Dept of Physics, University of Notre Dame, Indiana 46556	United States of America
Mikhailov, I.N.	Joint Institute for Nuclear Research, Dubna, USSR (Head P.O. Box 79, Moscow)	Union of Soviet Socialist Republics
Mikhailov, V.M.	Physical Faculty, Leningrad State University, Leningrad	Union of Soviet Socialist Republics
Mikhaleva, T.N.	Institute of Nuclear Physics, Moscow State University, Moscow B-234	Union of Soviet Socialist Republics
Mikheev, V.L.	Joint Institute for Nuclear Research, Dubna, USSR (Head P.O. Box 79, Moscow)	Union of Soviet Socialist Republics
Misharin, V.	Joint Institute for Nuclear Research, Dubna, USSR (Head P.O. Box 79, Moscow)	Union of Soviet Socialist Republics
Morozov, V.A.	Joint Institute for Nuclear Research, Dubna, USSR (Head P.O. Box 79, Moscow)	Union of Soviet Socialist Republics
Moszkowski, S.A.	University of California, Los Angeles, California	United States of America
Motz, H.T.	Los Alamos Scientific Laboratory, P.O. Box 1663, Los Alamos, New Mexico, 87544	United States of America
Müller, K.H.	Zentralinstitut für Kernforschung, Rossendorf, 8051 Dresden, Postfach 19	German Democratic Republic
Münchow, L.	Zentralinstitut für Kernforschung, Rossendorf, 8051 Dresden, Postfach 19	German Democratic Republic
Münnich, F.	CERN, 1211 Geneva 23, Switzerland	German Federal Republic
Musiol, G.	Joint Institute for Nuclear Research, Dubna, USSR (Head P.O. Box 79, Moscow)	German Democratic Republic
Nadzhakov, E.	Physical Institute, V.I. Lenin bul. 72, Sofia	Bulgaria
Naqvi, M.A., obiit	Institute of Physics, University of Islamabad, Rawalpindi, Pakistan	Pakistan
Nathan, O.	Niels Bohr Institute 17 Blegdamsvej, Copenhagen	Denmark

NAME	PRESSENT ADDRESS	NATIONALITY
Németh-Dörnyei, J.	Theoretical Physics Institute, Eotvös University, Puskin U 5-7, Budapest	Hungary
Nemets, O.F.	Institute of Physics, Ukraine Academy of Sciences, B. Kitaevskaya 144, Kiev	Union of Soviet Socialist Republics
Nemirovsky, P.E.	I.V. Kurchatov Institute of Atomic Energy, ul. Kurchatova 46, Moscow D-182	Union of Soviet Socialist Republics
Nenov, N.	Joint Institute for Nuclear Research, Dubna, USSR (Head P.O. Box 79, Moscow)	Bulgaria
Neubert, W.	Joint Institute for Nuclear Research, Dubna, USSR (Head P.O. Box 79, Moscow)	German Democratic Republic
Neudachin, V.G.	Moscow State University, Moscow B-234	Union of Soviet Socialist Republics
Nguyen-Cong-Khanh	Joint Institute for Nuclear Research, Dubna, USSR (Head P.O. Box 79, Moscow)	Vietnam
Nguyen Long-Den	Institut de Physique Nucléaire, B.P.1, Orsay, France	Vietnam
Niewodniczański, H.	Institute of Nuclear Physics, ul. Radzikowskiego, Cracow 23	Poland
Nilsson, L.R.	AB Atomenergi, Fack 61101, Nyköping	Sweden
Nix, J.R.	Group T-9, Los Alamos Scientific Laboratory, Los Alamos, New Mexico 87544	United States of America
Oehler, H.	Joint Institute for Nuclear Research, Dubna, USSR (Head P.O. Box 79, Moscow)	German Democratic Republic
Oganesyan, Yu.Ts.	Joint Institute for Nuclear Research, Dubna, USSR (Head P.O. Box 79, Moscow)	Union of Soviet Socialist Republics
Ogloblin, A.A.	I.V. Kurchatov Institute of Atomic Energy, ul. Kurchatova 46, Moscow D-182	Union of Soviet Socialist Republics
Osetinsky, G.M.	Joint Institute for Nuclear Research, Dubna, USSR (Head P.O. Box 79, Moscow)	Union of Soviet Socialist Republics

NAME	PRESENT ADDRESS	NATIONALITY
Otroschenko, G.A.	I.V. Kurchatov Institute of Atomic Energy, ul. Kurchatova 46, Moscow D-182	Union of Soviet Socialist Republics
Ovcharenko, V.I.	Institute of Theoretical Physics, Kiev	Union of Soviet Socialist Republics
Palla, G.	Central Research Institute for Physics, P.O. Box 49, Budapest 114	Hungary
Pancheva, N.	Physical Institute, V.I. Lenin bul. 72, Sofia	Bulgaria
Pandya, S.	Physical Research Laboratory, Ahmedabad 9	India
Panteleev, C.	Physical Institute, V.I. Lenin bul. 72, Sofia	Bulgaria
Papineau, A.	Centre d'Etudes Nucléaires de Saclay, B.P. No.2, 91-Gif-sur-Yvette	France
Pasechnik, M.V.	Institute of Physics, Kiev	Union of Soviet Socialist Republics
Pashkevich, V.V.	Joint Institute for Nuclear Research, Dubna, USSR (Head P.O. Box 79, Moscow)	Union of Soviet Socialist Republics
Pavlichenkov, I.M.	I.V. Kurchatov Institute of Atomic Energy, ul. Kurchatova 46, Moscow-182	Union of Soviet Socialist Republics
Peker, L.K.	D.I. Mendeleev Institute of Metrology, Moskowski Prospect 19, Leningrad-5	Union of Soviet Socialist Republics
Penionshkevich, Yu.E.	Joint Institute for Nuclear Research, Dubna, USSR (Head P.O. Box 79, Moscow)	Union of Soviet Socialist Republics
Petkov, I.Z.	Joint Institute for Nuclear Research, Dubna, USSR (Head P.O. Box 79, Moscow)	Bulgaria
Petrascu, M.	Institute for Atomic Physics, P.O. Box 35, Bucharest	Romania
Petrov, E.	Joint Institute for Nuclear Research, Dubna, USSR (Head P.O. Box 79, Moscow)	Union of Soviet Socialist Republics
Petrov, L.A.	Joint Institute for Nuclear Research, Dubna, USSR (Head P.O. Box 79, Moscow)	Union of Soviet Socialist Republics

NAME	PRESENT ADDRESS	NATIONALITY
Petrov, N.I.	Joint Institute for Nuclear Research, Dubna, USSR (Head P.O. Box 79, Moscow)	Union of Soviet Socialist Republics
Petrova, N.S.	Joint Institute for Nuclear Research, Dubna, USSR (Head P.O. Box 79, Moscow)	Union of Soviet Socialist Republics
Pikelner, L.B.	Joint Institute for Nuclear Research, Dubna, USSR (Head P.O. Box 79, Moscow)	Union of Soviet Socialist Republics
Plajner, Z.	Nuclear Research Institute, Řež near Prague	Czechoslovakia
Pleve, A.A.	Joint Institute for Nuclear Research, Dubna, USSR (Head P.O. Box 79, Moscow)	Union of Soviet Socialist Republics
Pol, Yu.S.	Joint Institute for Nuclear Research, Dubna, USSR (Head P.O. Box 79, Moscow)	Union of Soviet Socialist Republics
Polikanov, S.M.	Joint Institute for Nuclear Research, Dubna, USSR (Head P.O. Box 79, Moscow)	Union of Soviet Socialist Republics
Popov, A.B.	Joint Institute for Nuclear Research, Dubna, USSR (Head P.O. Box 79, Moscow)	Union of Soviet Socialist Republics
Popov, V.I.	P.N. Lebedev Physical Institute, Leninsky Prospect 53, Moscow	Union of Soviet Socialist Republics
Popov, Yu.P.	Joint Institute for Nuclear Research, Dubna, USSR (Head P.O. Box 79, Moscow)	Union of Soviet Socialist Republics
Preston, M.A.	McMaster University, Hamilton, Ontario	Canada
Prikhodtseva, V.P.	V.G. Khlopin Institute of Radium, ul. Roentgena 1, Leningrad	Union of Soviet Socialist Republics
Prokof'ev, P.T.	Institute of Physics, Riga	Union of Soviet Socialist Republics
Pyatov, N.I.	Joint Institute for Nuclear Research, Dubna, USSR (Head P.O. Box 79, Moscow)	Union of Soviet Socialist Republics
Rapoport, L.P.	Voronezh State University, Voronezh	Union of Soviet Socialist Republics
Rasmussen, J.O.	Latimer Hall, University of California, Berkeley, California	United States of America

NAME	PRESENT ADDRESS	NATIONALITY
Raychev, P.P.	Sofia University, Anton Ivanov 1, Sofia	Bulgaria
Reich, C.W.	National Reactor Testing Station, Idaho Nuclear Corp., Idaho Falls, Idaho	United States of America
Reif, R.	Zentralinstitut für Kernforschung, Rossendorf, 8051 Dresden, Postfach 19	German Democratic Republic
Revai, J.	Joint Institute for Nuclear Research, Dubna, USSR (Head P.O. Box 79, Moscow)	Hungary
Řezanka, I.	Nuclear Research Institute, Řež near Prague	Czechoslovakia
Riedel, C.	Zentralinstitut für Kernforschung, Rossendorf, 8051 Dresden, Postfach 19	German Democratic Republic
Riou, M.	Institut de Physique Nucléaire, B.P.1, 91-Orsay	France
Ripka, G.	Centre d'Etudes Nucléaires de Saclay, B.P. No.2, 91-Gif-sur-Yvette	France
Rohoziński, S.G.	Joint Institute for Nuclear Research, Dubna, USSR (Head P.O. Box 79, Moscow)	Poland
Romanovsky, E.A.	Institute of Nuclear Physics, Moscow State University, Moscow-234	Union of Soviet Socialist Republics
Rotter, I.	Joint Institute for Nuclear Research, Dubna, USSR (Head P.O. Box 79, Moscow)	German Democratic Republic
Rowe, D.J.	Physics Dept, University of Toronto, Toronto, Canada	United Kingdom
Rudolph, W.	Zentralinstitut für Kernforschung, Rossendorf, 8051 Dresden, Postfach 19	German Democratic Republic
Ruskov, T.	Physical Institute, V.1. Lenin bul .72, Sofia	Bulgaria
Rybarska, W.	Institute for Theoretical Physics, Wroclaw University, ul.Cybulskiego 36, Wroclaw 2	Poland
Ryde, H.	Research Institute for Physics, Stockholm 50	Sweden

NAME	PRESENT ADDRESS	NATIONALITY
Safarov, R. Kh.	Institute of Nuclear Physics, p. Ulugbek 4, Tashkent	Union of Soviet Socialist Republics
Sakai, M.	Institute for Nuclear Study, University of Tokyo, Tanashi-shi, Kitatama-gun, Tokyo	Japan
Salamatin, I. M.	Joint Institute for Nuclear Research, Dubna, USSR (Head P.O. Box 79, Moscow)	Union of Soviet Socialist Republics
Samour, G.	Centre d'Etudes Nucléaires de Saclay, B.P. 2, 91-Gif-sur-Yvette	France
Scherbakov, Yu. A.	Joint Institute for Nuclear Research, Dubna, USSR (Head P.O. Box 79, Moscow)	Union of Soviet Socialist Republics
Schintlmeister, J.	Zentralinstitut für Kernforschung, Rossendorf, 8051 Dresden, Postfach 19	German Democratic Republic
Schirmer, G.	Joint Institute for Nuclear Research, Dubna, USSR (Head P.O. Box 79, Moscow)	German Democratic Republic
Schulz, G.	Joint Institute for Nuclear Research, Dubna, USSR (Head P.O. Box 79, Moscow)	German Democratic Republic
Selinov, I. P.	Academy of Sciences, Moscow	Union of Soviet Socialist Republics
Sergeev, V. G.	Physical Faculty, Leningrad State University, Leningrad	Union of Soviet Socialist Republics
Shapiro, F. L.	Joint Institute for Nuclear Research, Dubna, USSR (Head P.O. Box 79, Moscow)	Union of Soviet Socialist Republics
Shapiro, I. S.	Institute of Theoretical and Experimental Physics, B. Cheremushkinskaya 89, Moscow	Union of Soviet Socialist Republics
Sharapov, I. S.	Joint Institute for Nuclear Research, Dubna, USSR (Head P.O. Box 79, Moscow)	Union of Soviet Socialist Republics
Sheline, R. K.	Nuclear Research Bldg., Florida State University, Tallahassee, Florida	United States of America
Shestopalova, S. A.	D. I. Mendeleev Institute of Metrology, Moscowski Prospect 19, Leningrad-5	Union of Soviet Socialist Republics

NAME	PRESENT ADDRESS	NATIONALITY
Shevchenko, N.G.	Physical-Technical Institute, Yumovski tupik, Kharkov	Union of Soviet Socialist Republics
Shevchenko, V.G.	Institute of Nuclear Physics, Moscow State University, Moscow-234	Union of Soviet Socialist Republics
Shpinel, V.S.	Institute of Nuclear Physics, Moscow State University, Moscow-234	Union of Soviet Socialist Republics
Sidorov, V.M.	Joint Institute for Nuclear Research, Dubna, USSR (Head P.O. Box 79, Moscow)	Union of Soviet Socialist Republics
Siksin, V.S.	Rostov State University, Engels-105, Rostov	Union of Soviet Socialist Republics
Sitenko, A.G.	Institute of Physics, Kiev	Union of Soviet Socialist Republics
Siwek-Wilczynska, K.	University of Warsaw, Institute of Experimental Physics, Hoza, 69, Warsaw	Poland
Sizanov, I.V.	Joint Institute for Nuclear Research, Dubna, USSR (Head P.O. Box 79, Moscow)	Union of Soviet Socialist Republics
Šlaus, I.	Institute "Ruder Bošković", Bijenička 54, Zagreb	Yugoslavia
Slavov, -.	Physical Institute, I.V. Lenin bul. 72, Sofia	Bulgaria
Sliv, L.A.	A.F. Ioffe Physical-Technical Institute, ul. Politekhnicheskaya 26, Leningrad	Union of Soviet Socialist Republics
Smirnov, Yu.F.	Institute of Nuclear Physics, Moscow State University, Moscow-234	Union of Soviet Socialist Republics
Smith, P.B.	University of Groningen, Westersingel 34, Groningen, Holland	United States of America
Smorodinsky, Ya.A.	Joint Institute for Nuclear Research, Dubna, USSR (Head P.O. Box 79, Moscow)	Union of Soviet Socialist Republics
Sobiczewski, A.	Joint Institute for Nuclear Research, Dubna, USSR (Head P.O. Box 79, Moscow)	Poland
Sodnom, N.	Joint Institute for Nuclear Research, Dubna, USSR (Head P.O. Box 79, Moscow)	Mongolia

NAME	PRESENT ADDRESS	NATIONALITY
So-Don-Sick	Joint Institute for Nuclear Research, Dubna, USSR (Head P.O. Box 79, Moscow)	Korea
So-Ki-Hwang	Joint Institute for Nuclear Research, Dubna, USSR (Head P.O. Box 79, Moscow)	
Soloviev, V.G.	Joint Institute for Nuclear Research, Dubna, USSR (Head P.O. Box 79, Moscow)	Union of Soviet Socialist Republics
Sorensen, R.A.	Carnegie-Mellon University, Pittsburg, Pennsylvania 15213	United States of America
Sotona, M.	Nuclear Research Institute, Řež near Prague	Czechoslovakia
Šott, M.	Nuclear Research Institute, Řež near Prague	Czechoslovakia
Sprung, D.	McMaster University, Hamilton, Ontario	Canada
Stachura, Z.	Joint Institute for Nuclear Research, Dubna, USSR (Head P.O. Box 79, Moscow)	Poland
Stavisky, Yu. Ya.	Physical-Technical Institute, Obninsk	Union of Soviet Socialist Republics
Štěrba, F.	Mathematical-Physical Faculty, Charles University, Prague 1	Czechoslovakia
Stiller, G.	Zentralinstitut für Kernforschung, Rossendorf, 8051 Dresden, Postfach 19	German Democratic Republic
Struble, G.L.	Chemistry Dept, University of California, Berkeley, California 94720	United States of America
Strussny, G.	Joint Institute for Nuclear Research, Dubna, USSR (Head, P.O. Box 79, Moscow)	German Democratic Republic
Strutinsky, V.M.	Niels Bohr Institute, Blegdamsvej 17, Copenhagen	Union of Soviet Socialist Republics
Styczeń, J.	Joint Institute for Nuclear Research, Dubna, USSR (Head, P.O. Box 79, Moscow)	Poland
Subotowicz, M.F.	Dept of Experimental Physics, M. Curie-Skłodowska University, ul. Nowotki 8, Lublin	Poland

NAME	PRESENT ADDRESS	NATIONALITY
Sukhoruchkin, S.I.	Institute of Theoretical and Experimental Physics, B. Cheremushkinskaya 89, Moscow	Union of Soviet Socialist Republics
Sujkowski, Z.	Institute for Nuclear Research, Swierk	Poland
Sumbaev, O.I.	A.F. Ioffe Physical-Technical Institute, ul. Politekhnicheskaya 26, Leningrad	Union of Soviet Socialist Republics
Sunyar, A.W.	Brookhaven National Laboratory, Upton, N.Y. 11973	United States of America
Szpikowski, S.	Dept of Theoretical Physics, M. Curie-Skłodowska University, ul. Nowotki 8, Lublin	Poland
Szymański, Z.	Institute for Nuclear Research, Hoza 69, Warsaw	Poland
Tamura, T.	Oak Ridge National Laboratory P.O.B. x, Oak Ridge, Tennessee 37830, USA	Japan
Tarantin, N.I.	Joint Institute for Nuclear Research, Dubna, USSR (Head P.O. Box 79, Moscow)	Union of Soviet Socialist Republics
Teillac, J.	Institut de Physique Nucléaire, B.P.No.1, 91-Orsay	France
Temmer, G.M.	Dept of Physics, Rutgers, The State University, New Brunswick, New Jersey 08903	United States of America
Teplov, I.B.	Institute of Nuclear Physics, Moscow State University, Moscow-234	Union of Soviet Socialist Republics
Tjapin, A.S.	I.V. Kurchatov Institute of Atomic Energy, ul. Kurchatova 46, Moscow D-182	Union of Soviet Socialist Republics
Tokarevsky, V.V.	Institute of Physics, ul. B. Kitayevskaya 144, Kiev 28	Union of Soviet Socialist Republics
Toktarov, K.A.	Institute of Nuclear Physics, Alma-Ata 82	Union of Soviet Socialist Republics
Tomaselli, G.	Physical Institute, Karl-Marx-University, Leipzig, Linnestr.5, 701 Leipzig	German Democratic Republic

NAME	PRESENT ADDRESS	NATIONALITY
Toth, K.S.	Oak Ridge National Laboratory, Bldg 6000, Oak Ridge, Tennessee 37830	United States of America
Tran-Thanh-Minh	Joint Institute for Nuclear Research, Dubna, USSR (Head P.O. Box 79, Moscow)	Vietnam
Trlifaj, L.	Nuclear Research Institute, Řež near Prague	Czechoslovakia
Tulupov, B.A.	P.N. Lebedev Physical Institute, Leninsky Prospect 53, Moscow	Union of Soviet Socialist Republics
Tumbaev, G.	Institute of Physics, Sofia	Bulgaria
Turkiewicz, J.	Institute for Nuclear Research, Hoza 69, Warsaw	Poland
Tys, J.	Institute for Nuclear Research, Swierk	Poland
Udagawa, T.	Nordita, Copenhagen, Denmark	Japan
Úlehla, I.	Mathematical-Physical Faculty, Charles University, Myslikova 7, Prague 1	Czechoslovakia
Urbanec, J.	Nuclear Research Institute, Řež near Prague	Czechoslovakia
Urin, M.G.	Moscow Physical Engineering Institute, Kashirskoe sh.1, Moscow B-409	Union of Soviet Socialist Republics
Usachev, L.N.	Physical-Technical Institute, Obninsk	Union of Soviet Socialist Republics
Valentin, J.	University of Grenoble, Rue des Martyrs, I.S.N., 38-Grenoble	France
Vashakidze, I.Sh.	Tbilisi State University, pr. Chavchavadze 3, Tbilisi	Union of Soviet Socialist Republics
Vasiliev, S.S.	Institute of Nuclear Physics, Moscow State University, Moscow-234	Union of Soviet Socialist Republics
Vasiliev, V.A.	State Atomic Energy Committee of the USSR, Moscow	Union of Soviet Socialist Republics
Veje, C.J.	Niels Bohr Institute Blegdamsvej 17, Copenhagen	Denmark

NAME	PRESENT ADDRESS	NATIONALITY
Vénéroni, M.	Institut de Physique Nucléaire, B.P. No.1, 91-Orsay	France
Verheul, H.	Natuurkundig Laboratorium, Vrije Universiteit de Boelelaan 1081, Amsterdam-Buitenveldert	Holland
Vervier, J.	Centre d'Etude de l'Energie Nucléaire, 200 Boeretang, Mol-Donk	Belgium
Vilcov, N.	Institute for Atomic Physics, P.O.35, Bucharest	Romania
Vilov, C.	Physical Institute, V.1. Lenin bul.72, Sofia	Bulgaria
Vinduška, M.	Nuclear Research Institute, Řež near Prague	Czechoslovakia
Vlasov, N.A.	I.V. Kurchatov Institute of Atomic Energy, ul. Kurchatova 46, Moscow D-182	Union of Soviet Socialist Republics
Vogel, P.	Nuclear Research Institute, Řež near Prague	Czechoslovakia
Voinova, N.A.	A.F. Ioffe Physical-Technical Institute, ul. Polytekhnicheskaya 26, Leningrad	Union of Soviet Socialist Republics
Volkov, V.V.	Joint Institute for Nuclear Research, Dubna, USSR (Head P.O. Box 79, Moscow)	Union of Soviet Socialist Republics
Vorobiev, E.D.	Joint Institute for Nuclear Research, Dubna, USSR (Head P.O. Box 79, Moscow)	Union of Soviet Socialist Republics
Wahlborn, S.	Research Institute for Physics, Stockholm 50	Sweden
Wapstra, A.H.	Instituut voor Kernphysisch, Onderzoek, Oosterringdijk 18, Amsterdam	Holland
Weisskopf, V.F.	Massachussetts Institute of Technology, Physics Dept, Cambridge, Massachusetts	United States of America
Weneser, J.	Brookhaven National Laboratory, Dept of Physics, Upton, N.Y. 11973	United States of America
Whineray, S.	Niels Bohr Institute, Blegdamsvej 17, Copenhagen, Denmark	New Zealand

NAME	PRESENT ADDRESS	NATIONALITY
Wiebicke, H.J.	Joint Institute for Nuclear Research, Dubna, USSR (Head P.O. Box 79, Moscow)	German Democratic Republic
Widemann, F.	Centre de Spetrométrie nucléaire, B.P. No.1, 91-Orsay	France
Wilczyński, J.	Joint Institute for Nuclear Research, Dubna, USSR (Head P.O. Box 79, Moscow)	Poland
Wildermuth, K.	Institut für Theoretische Physik, University of Tübingen, Gartenstr. 47, 74 Tübingen	German Federal Republic
Wilhelm, I.	Joint Institute for Nuclear Research, Dubna, USSR (Head P.O.Box 79, Moscow)	German Federal Republic
Wilhelmi, Z.	Institute of Nuclear Physics, ul. Radzikowskiego, Cracow 23	Poland
Wilkinson, D.H.	Nuclear Physics Laboratory, Oxford	United Kingdom
Winther, A.	Niels Bohr Institute, Blegdamsvej 17, Copenhagen	Denmark
Wu, C.S.	Dept of Physics, Columbia University, N.Y. 10027	United States of America
Yoshizawa, Y.	Faculty of Science, Osaka University, Toyonaka, Osaka Fu	Japan
Yudin, N.P.	Institute of Nuclear Physics, Moscow State University, Moscow-234	Union of Soviet Socialist Republics
Yutlandov, I.A.	Joint Institute for Nuclear Research, Dubna, USSR (Head P.O. Box 79, Moscow)	Union of Soviet Socialist Republics
Zaikin, D.A.	P.N. Lebedev Physical Institute, Leninsky Prospect 53, Moscow	Union of Soviet Socialist Republics
Zakhariev, B.N.	Joint Institute for Nuclear Research, Dubna, USSR (Head P.O. Box 79, Moscow)	Union of Soviet Socialist Republics
Zámori, Z.	Central Research Institute for Physics, P.O. Box 49, Budapest 114	Hungary
Zaretsky, D.F.	I.V. Kurchatov Institute of Atomic Energy, ul. Kurchatova 46, Moscow D-182	Union of Soviet Socialist Republics

Zelenkov, A.G.	I.V. Kurchatov Institute of Atomic Energy, ul. Kurchatova 46, Moscow D-182	Union of Soviet Socialist Republics
Zelevinsky, V.G.	Institute of Nuclear Physics, Novosibirsk 90	Union of Soviet Socialist Republics
Zhelev, Zh.	Joint Institute for Nuclear Research, Dubna, USSR (Head P.O. Box 79, Moscow)	Bulgaria
Zhukovsky, N.N.	V.G. Khlopin Institute of Radium, ul. Roentgena 1, Leningrad	Union of Soviet Socialist Republics
Zimanyi, J.	Central Research Institute for Physics, P.O. Box 49, Budapest 114	Hungary
Zolotavin, A.V.	Leningrad State University, Universitetskaya nab. 7/9, Leningrad B-164	Union of Soviet Socialist Republics
Zvára, I.I.	Joint Institute for Nuclear Research, Dubna, USSR (Head P.O. Box 79, Moscow)	Czechoslovakia
Zvolská, V.	Joint Institute for Nuclear Research, Dubna, USSR (Head P.O. Box 79, Moscow)	Czechoslovakia
Zvolský, I.	Joint Institute for Nuclear Research, Dubna, USSR (Head P.O. Box 79, Moscow)	Czechoslovakia
Žuk, Z	M. Curie-Skłodowska University, ul. Nowotki 8, Lublin	Poland
Žylicz, J.	Institute for Nuclear Research, Swierk	Poland

AUTHOR INDEX

(including Participants in Discussions)

The numbers underlined indicate the first page of a paper by an author. Other numbers denote the page numbers of discussion comments. Literature references are not indexed.

IAEA SALES AGENTS

Orders for Agency publications can be placed with your bookseller or any of our sales agents listed below:

ARGENTINA
Comisión Nacional de
Energía Atómica
Avenida del Libertador
General San Martin 8250
Buenos Aires - Suc. 29

AUSTRALIA
Hunter Publications,
23 McKillop Street
Melbourne, C.1

AUSTRIA
Georg Fromme & Co.
Spengergasse 39
A-1050, Vienna V

BELGIUM
Office international de librairie
30, avenue Marnix
Brussels 5

BRAZIL
Livraria Kosmos Editora
Rua do Rosario, 135-137
Rio de Janeiro

Agencia Expoente Oscar M. Silva
Rua Xavier de Toledo, 140-1° Andar
(Caixa Postal No. 5.614)
São Paulo

BYELORUSSIAN SOVIET SOCIALIST REPUBLIC
See under USSR

CANADA
The Queen's Printer
Ottawa, Ontario

CHINA (Taiwan)
Books and Scientific Supplies
Service, Ltd.,
P.O. Box 83
Taipei

CZECHOSLOVAK SOCIALIST REPUBLIC
S.N.T.L.
Spolena 51
Nové Mĕsto
Prague 1

DENMARK
Ejnar Munksgaard Ltd.
6 Nörregade
Copenhagen K

FINLAND
Akateeminen Kirjakauppa
Keskuskatu 2
Helsinki

FRANCE
Office international de
documentation et librairie
48, rue Gay-Lussac
F-75, Paris 5e

GERMANY, Federal Republic of
R. Oldenbourg
Rosenheimer Strasse 145
8 Munich 8

HUNGARY
Kultura
Hungarian Trading Co. for Books
and Newspapers
P.O.B. 149
Budapest 62

ISRAEL
Heiliger and Co.
3 Nathan Strauss Street
Jerusalem

ITALY
Agenzia Editoriale Internazionale
Organizzazioni Universali (A.E.I.O.U.)
Via Meravigli 16
Milan

JAPAN
Maruzen Company Ltd.
6, Tori Nichome
Nihonbashi
(P.O. Box 605)
Tokyo Central

MEXICO
Librería Internacional
Av. Sonora 206
Mexico 11, D.F.

NETHERLANDS
N.V. Martinus Nijhoff
Lange Voorhout 9
The Hague

NEW ZEALAND
Whitcombe & Tombs, Ltd.
G.P.O. Box 1894
Wellington, C.1

NORWAY
Johan Grundt Tanum
Karl Johans gate 43
Oslo

PAKISTAN
Karachi Education Society
Haroon Chambers
South Napier Road
(P.O. Box No. 4866)
Karachi 2

POLAND
Ośrodek Rozpowszechniana
Wydawnictw Naukowych
Polska Akademia Nauk
Pałac Kultury i Nauki
Warsaw

ROMANIA
Cartimex
Rue A. Briand 14-18
Bucarest

SOUTH AFRICA
Van Schaik's Bookstore (Pty) Ltd.
Libri Building
Church Street
(P.O. Box 724)
Pretoria

SPAIN
Librería Bosch
Ronda de la Universidad 11
Barcelona

SWEDEN
C.E. Fritzes Kungl. Hovbokhandel
Fredsgatan 2
Stockholm 16

SWITZERLAND
Librairie Payot
Rue Grenus 6
1211 Geneva 11

TURKEY
Librairie Hachette
469, Istiklâl Caddesi
Beyoğlu, Istanbul

UKRAINIAN SOVIET SOCIALIST REPUBLIC
See under USSR

UNION OF SOVIET SOCIALIST REPUBLICS
Mezhdunarodnaya Kniga
Smolenskaya-Sennaya 32-34
Moscow G-200

UNITED KINGDOM OF GREAT BRITAIN AND NORTHERN IRELAND
Her Majesty's Stationery Office
P.O. Box 569
London, S.E.1

UNITED STATES OF AMERICA
National Agency for
International Publications, Inc.
317 East 34th Street
New York, N.Y. 10016

VENEZUELA
Sr. Braulio Gabriel Chacares
Gobernador a Candilito 37
Santa Rosalía
(Apartado Postal 8092)
Caracas D.F.

YUGOSLAVIA
Jugoslovenska Knjiga
Terazije 27
Belgrade

IAEA publications can also be purchased retail at the United Nations Bookshop at United Nations Headquarters, New York, at the news-stand at the Agency's Headquarters, Vienna, and at most conferences, symposia and seminars organized by the Agency.

In order to facilitate the distribution of its publications, the Agency is prepared to accept payment in UNESCO coupons or in local currencies.

Orders and inquiries from countries where sales agents have not yet been appointed may be sent to:

Distribution and Sales Group, International Atomic Energy Agency,
Kärntner Ring 11, A-1010, Vienna I, Austria

INTERNATIONAL
ATOMIC ENERGY AGENCY
VIENNA, 1968

PRICE: US $15.00
Austrian Schillings 388,-
(£6.5.0; F.Fr. 73,50; DM 60,-)